frontiers | Research Topics

Plasticity of monocytes/macrophages: Phenotypic changes during disease progression

Edited by
Ruoxi Yuan, Chao Yang, Yanan Ma and Liwu Li

Published in
Frontiers in Immunology

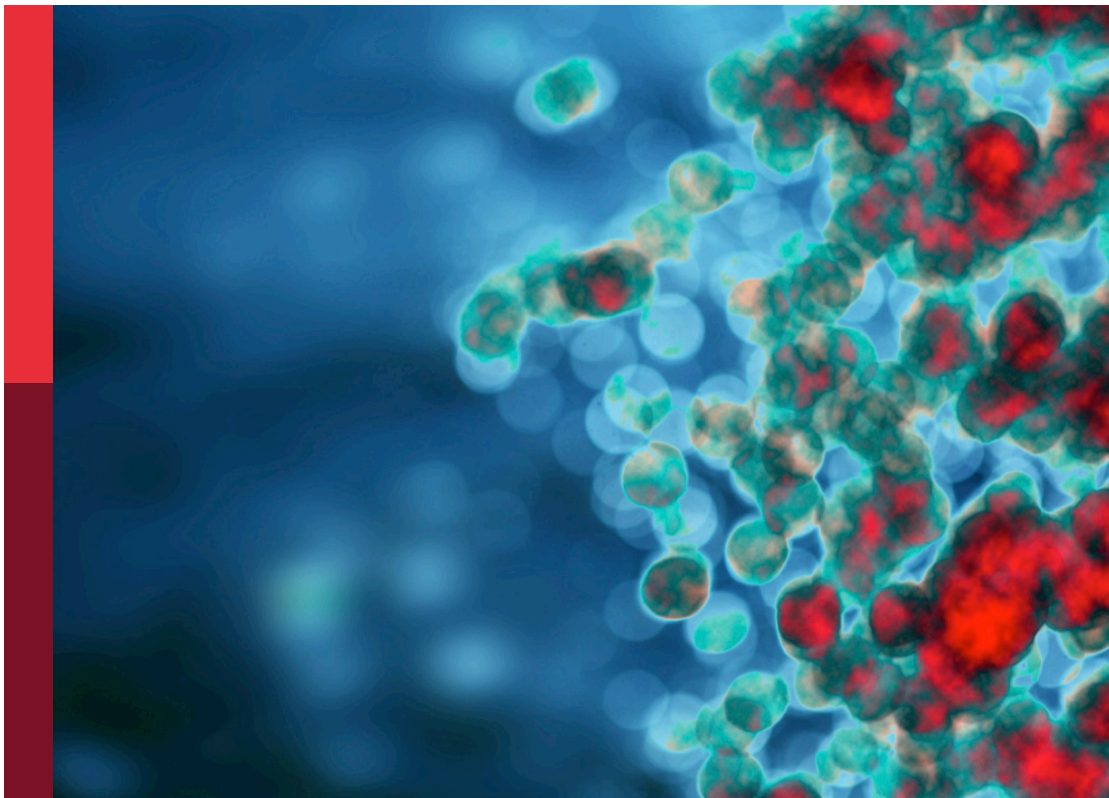

ISSN 1664-8714
ISBN 978-2-8325-4011-4
DOI 10.3389/978-2-8325-4011-4

About Frontiers

Frontiers is more than just an open access publisher of scholarly articles: it is a pioneering approach to the world of academia, radically improving the way scholarly research is managed. The grand vision of Frontiers is a world where all people have an equal opportunity to seek, share and generate knowledge. Frontiers provides immediate and permanent online open access to all its publications, but this alone is not enough to realize our grand goals.

Frontiers journal series

The Frontiers journal series is a multi-tier and interdisciplinary set of open-access, online journals, promising a paradigm shift from the current review, selection and dissemination processes in academic publishing. All Frontiers journals are driven by researchers for researchers; therefore, they constitute a service to the scholarly community. At the same time, the *Frontiers journal series* operates on a revolutionary invention, the tiered publishing system, initially addressing specific communities of scholars, and gradually climbing up to broader public understanding, thus serving the interests of the lay society, too.

Dedication to quality

Each Frontiers article is a landmark of the highest quality, thanks to genuinely collaborative interactions between authors and review editors, who include some of the world's best academicians. Research must be certified by peers before entering a stream of knowledge that may eventually reach the public - and shape society; therefore, Frontiers only applies the most rigorous and unbiased reviews. Frontiers revolutionizes research publishing by freely delivering the most outstanding research, evaluated with no bias from both the academic and social point of view. By applying the most advanced information technologies, Frontiers is catapulting scholarly publishing into a new generation.

What are Frontiers Research Topics?

Frontiers Research Topics are very popular trademarks of the *Frontiers journals series*: they are collections of at least ten articles, all centered on a particular subject. With their unique mix of varied contributions from Original Research to Review Articles, Frontiers Research Topics unify the most influential researchers, the latest key findings and historical advances in a hot research area.

Find out more on how to host your own Frontiers Research Topic or contribute to one as an author by contacting the Frontiers editorial office: frontiersin.org/about/contact

Plasticity of monocytes/macrophages: Phenotypic changes during disease progression

Topic editors

Ruoxi Yuan — Hospital for Special Surgery, United States
Chao Yang — The First Affiliated Hospital of Xi'an Jiaotong University, China
Yanan Ma — Memorial Sloan Kettering Cancer Center, United States
Liwu Li — Virginia Tech, United States

Citation

Yuan, R., Yang, C., Ma, Y., Li, L., eds. (2023). *Plasticity of monocytes/macrophages: Phenotypic changes during disease progression*. Lausanne: Frontiers Media SA. doi: 10.3389/978-2-8325-4011-4

Table of contents

05 Editorial: Plasticity of monocytes/macrophages: phenotypic changes during disease progression
Ruoxi Yuan, Yanan Ma, Chao Yang and Liwu Li

07 Engineered M2a macrophages for the treatment of osteoarthritis
Chi Liang, Song Wu, Guang Xia, Junjie Huang, Zi Wen, Wenxiu Zhang and Xu Cao

23 The roles of long noncoding RNA-mediated macrophage polarization in respiratory diseases
Xin Qiao, Yuxiao Ding, Dasen Wu, Anle Zhang, Yan Yin, Qiuyue Wang, Wei Wang and Jian Kang

39 Placental macrophages present distinct polarization pattern and effector functions depending on clinical onset of preeclampsia
Monika Horvat Mercnik, Carolin Schliefsteiner, Herbert Fluhr and Christian Wadsack

56 Programmed cell death and lipid metabolism of macrophages in NAFLD
Zhun Xiao, Minghao Liu, Fangming Yang, Guangwei Liu, Jiangkai Liu, Wenxia Zhao, Suping Ma and Zhongping Duan

74 High aspect ratio nanomaterial-induced macrophage polarization is mediated by changes in miRNA levels
Johanna Samulin Erdem, Táňa Závodná, Torunn K. Ervik, Øivind Skare, Tomáš Hron, Kristine H. Anmarkrud, Anna Kuśnierczyk, Julia Catalán, Dag G. Ellingsen, Jan Topinka and Shan Zienolddiny-Narui

91 Deciphering the sequential changes of monocytes/macrophages in the progression of IDD with longitudinal approach using single-cell transcriptome
Weihang Li, Yingjing Zhao, Yongchun Wang, Zhijian He, Linyuan Zhang, Bin Yuan, Chengfei Li, Zhuojing Luo, Bo Gao and Ming Yan

110 Macrophage: Key player in the pathogenesis of autoimmune diseases
Shuang Yang, Ming Zhao and Sujie Jia

125 Nur77 and PPARγ regulate transcription and polarization in distinct subsets of M2-like reparative macrophages during regenerative inflammation
Éva Garabuczi, Nastaran Tarban, Éva Fige, Andreas Patsalos, László Halász, Tímea Szendi-Szatmári, Zsolt Sarang, Róbert Király and Zsuzsa Szondy

139 Macrophages in aseptic loosening: Characteristics, functions, and mechanisms
Yehao Cong, Yi Wang, Tao Yuan, Zheng Zhang, Jianxun Ge, Qi Meng, Ziqing Li and Shui Sun

156 Identification of biomarkers co-associated with M1 macrophages, ferroptosis and cuproptosis in alcoholic hepatitis by bioinformatics and experimental verification
Shasha Hou, Dan Wang, Xiaxia Yuan, Xiaohuan Yuan and Qi Yuan

170 MicroRNA: role in macrophage polarization and the pathogenesis of the liver fibrosis
Wen Yu, Shu Wang, Yangyang Wang, Hui Chen, Hao Nie, Lian Liu, Xiaoting Zou, Quan Gong and Bing Zheng

183 The generation, activation, and polarization of monocyte-derived macrophages in human malignancies
Paul Chaintreuil, Emeline Kerreneur, Maxence Bourgoin, Coline Savy, Cécile Favreau, Guillaume Robert, Arnaud Jacquel and Patrick Auberger

202 A potential therapeutic approach for ulcerative colitis: targeted regulation of macrophage polarization through phytochemicals
Ke Wang, Tangyou Mao, Xinyu Lu, Muyuan Wang, Yifei Yun, Zeyu Jia, Lei Shi, Haoxi Jiang, Junxiang Li and Rui Shi

217 NOD2 in monocytes negatively regulates macrophage development through TNFalpha
Camille Chauvin, Daniel Alvarez-Simon, Katarina Radulovic, Olivier Boulard, William Laine, Myriam Delacre, Nadine Waldschmitt, Elodie Segura, Jérome Kluza, Mathias Chamaillard and Lionel F. Poulin

237 Macrophages and fibrosis: how resident and infiltrating mononuclear phagocytes account for organ injury, regeneration or atrophy
Hao Long, Julia Lichtnekert, Joachim Andrassy, Barbara U. Schraml, Paola Romagnani and Hans-Joachim Anders

248 Roles of microglia in adult hippocampal neurogenesis in depression and their therapeutics
Shaoyi Fang, Zhibin Wu, Yali Guo, Wenjun Zhu, Chunmiao Wan, Naijun Yuan, Jianbei Chen, Wenzhi Hao, Xiaowei Mo, Xiaofang Guo, Lili Fan, Xiaojuan Li and Jiaxu Chen

frontiers | Frontiers in Immunology

TYPE Editorial
PUBLISHED 13 November 2023
DOI 10.3389/fimmu.2023.1328382

OPEN ACCESS

EDITED AND REVIEWED BY
Pietro Ghezzi,
University of Urbino Carlo Bo, Italy

*CORRESPONDENCE
Ruoxi Yuan
yuanr@hss.edu

RECEIVED 26 October 2023
ACCEPTED 27 October 2023
PUBLISHED 13 November 2023

CITATION
Yuan R, Ma Y, Yang C and Li L (2023) Editorial: Plasticity of monocytes/macrophages: phenotypic changes during disease progression.
Front. Immunol. 14:1328382.
doi: 10.3389/fimmu.2023.1328382

Editorial: Plasticity of monocytes/macrophages: phenotypic changes during disease progression

Ruoxi Yuan[1]*, Yanan Ma[2], Chao Yang[3] and Liwu Li[4]

[1]HSS Research Institute and David Z. Rosensweig Genomics Research Center, Hospital for Special Surgery, New York, NY, United States, [2]Memorial Sloan Kettering Cancer Center, New York, NY, United States, [3]Center for Immunological and Metabolic Diseases, Med-X Institute, First Affiliated Hospital of Xi'an Jiaotong University, Xi'an Jiaotong University, Xianyang, Shaanxi, China, [4]Department of Biological Sciences, Virginia Tech, Blacksburg, VA, United States

KEYWORDS

macrophage heterogeneity, monocytes polarization, innate immunity, inflammation, therapeutic targets

Editorial on the Research Topic
Plasticity of monocytes/macrophages: phenotypic changes during disease progression

Monocytes and macrophages, with their inherent heterogeneity, manifest a spectrum of phenotypes and functions finely tuned by their surrounding microenvironments. These versatile immune sentinels exhibit a remarkable capacity to adapt their responses within distinct pathological contexts, thus positioning them as central characters in various medical conditions. In summarizing the recent advances in our understanding of monocyte and macrophage heterogeneity in regulating disease progression and maintaining tissue homeostasis, we have compiled research articles encompassing various aspects of macrophage polarization and its impact within this specific Research Topic.

A more comprehensive understanding of the molecular mechanisms governing the generation, activation, and polarization of macrophages is imperative as a fundamental requirement for devising innovative therapeutic approaches to modulate macrophage functions within pathological contexts. Our Research Topic includes three reviews, each approaching this subject from distinct angles, focusing on autoimmune diseases (Yang et al.), adult hippocampal neurogenesis (Fang et al.), and human malignancies (Chaintreuil et al.). Additionally, it is noteworthy that advancements in cutting-edge technologies, such as single-cell RNA sequencing, which has also been utilized by papers under this topic as well, have paved the way for significant breakthroughs in the field of monocytes and macrophages.

Cong et al. summarized the advanced awareness of the multifaceted roles played by macrophages in the regulation of aseptic loosening (AL) pathogenesis. AL, the most common complication of total joint arthroplasty, is associated with activated macrophages that produce proinflammatory mediators, subsequently triggering the activation of osteoclasts, leading to bone breakdown. Additionally, macrophages, present in both homeostatic and injured skeletal muscle tissues, encompass heterogeneous functional subtypes that perform diverse roles in maintaining homeostasis and facilitating injury

repair. Li et al. identified five distinct monocyte/macrophage subpopulations during intervertebral disk degeneration (IDD) using a single-cell RNAseq dataset spanning early to late degenerative stages of the intervertebral disk (IVD). The authors suggested that selectively removing regulatory macrophages in the early stage and oxidative stress (OS)-related macrophages in the late stage could alleviate angiogenesis and promote IDD recovery. Furthermore, genetic engineering of macrophages has been highly appreciated in numerous therapeutic approaches. Liang et al. utilized engineered L-M2a macrophages displaying a typical anti-inflammatory phenotype akin to M2 macrophages *in vitro*, resulting in markedly enhanced therapeutic outcomes for osteoarthritis (OA) by effectively addressing inflammation, reinstating tissue homeostasis, and promoting cartilage regeneration. Garabuczi et al. unveiled the pivotal roles of PPARg and Nur77 in shaping distinct macrophage subsets during skeletal muscle injury in a cardiotoxin–induced injury model.

The role of non-coding RNAs (ncRNAs), including long non-coding RNAs (lncRNAs) and microRNAs (miRNAs), in the regulation of macrophage polarization is an emerging field of interest, as comprehensively reviewed by Qiao et al. and Yu et al. The potential of lncRNAs as both biomarkers and therapeutic targets for modulating macrophage polarization during disease development is increasingly recognized. For example, Erdem et al. demonstrated the pivotal role of these small RNA molecules in finely tuning macrophage responses, particularly in inducing epigenetic modifications and miRNA levels changes upon exposure to cellulose nanocrystals (CNF) and multiwalled carbon nanotubes (MWCNT). Inhalation of nanomaterials has been associated with the induction of inflammation in the lungs. These nanomaterials prompt phenotypic alterations in alveolar macrophages, with CNF exposure enhancing the M1 phenotype and MWCNT promoting the M2 phenotype. The manipulation of ncRNA expression emerges as a novel approach to regulate macrophage polarization, thus influencing inflammation, fibrosis, immune responses, and even tumorigenesis.

Macrophages play a pivotal role in the delicate balance of immune regulation in the context of Inflammatory Bowel Disease (IBD), and their dysregulation can lead to inflammation and tissue damage. Wang et al. summarized updated therapeutic approaches targeting macrophage polarization in Ulcerative Colitis, and concurrently, Chauvin et al. conducted original research demonstrating that NOD2 negatively regulates a macrophage developmental program through a feed-forward loop. This finding offers promise for addressing resistance to anti-TNF therapy in Crohn's Disease.

Although monocytes and macrophages that migrate to sites of injury or inflammation have received significant attention in research, it's equally important to acknowledge that tissue-resident macrophages like Kupffer cells, microglia, and Hofbauer cells are subjected to environment-mediated polarization as well. These resident macrophages are intricately involved in local inflammation and reparative processes within their respective tissues. Mercnik et al. showed that the inflammatory environment of preeclampsia (PE) causes the phenotypic changes observed between early and late PE Hofbauer cells (HBCs). Furthermore, the role of Kupffer cells in Non-alcoholic fatty liver disease (NAFLD) was also well documented in reviews by Xiao et al. and Yu et al. Microglia, the sole macrophage population within the central nervous system, holds the remarkable capability to modulate adult hippocampal neurogenesis in the context of depression. The findings summarized by Fang et al. underscore the potential for pharmaceutical interventions to specifically target microglia as a promising strategy for the treatment of depression.

As highlighted in this discussion, this Research Topic encompasses a wide array of seminal articles delving into the intricate mechanisms governing the shift of macrophage phenotypes at various stages of disease progression. It offers a comprehensive overview of potential therapeutic targets and approaches for modulating macrophage behavior in the treatment of these conditions.

Author contributions

RY: Writing – original draft. YM: Writing – review & editing. CY: Writing – review & editing. LL: Writing – review & editing.

Funding

The author(s) declare that no financial support was received for the research, authorship, and/or publication of this article.

Acknowledgments

We express our gratitude to all contributing authors and research groups who contributed to this Research Topic, as well as the diligent reviewers and editors who dedicated their efforts to evaluating the submitted manuscripts. Additionally, we extend our thanks to the Frontiers Editorial Office for their valuable assistance throughout this endeavor.

Conflict of interest

The authors declare that the research was conducted in the absence of any commercial or financial relationships that could be construed as a potential conflict of interest.

The author(s) declared that they were an editorial board member of Frontiers, at the time of submission. This had no impact on the peer review process and the final decision.

Publisher's note

frontiers | Frontiers in Immunology

TYPE Original Research
PUBLISHED 13 December 2022
DOI 10.3389/fimmu.2022.1054938

OPEN ACCESS

EDITED BY
Yanan Ma,
Memorial Sloan Kettering Cancer Center, United States

REVIEWED BY
Mingxin Shi,
Washington State University, United States
Shiping Lu,
Tulane University, United States
Poonam Dhillon,
University of Pennsylvania, United States

*CORRESPONDENCE
Xu Cao
hughcaoxu@hotmail.com

SPECIALTY SECTION
This article was submitted to Inflammation, a section of the journal Frontiers in Immunology

RECEIVED 27 September 2022
ACCEPTED 30 November 2022
PUBLISHED 13 December 2022

CITATION
Liang C, Wu S, Xia G, Huang J, Wen Z, Zhang W and Cao X (2022) Engineered M2a macrophages for the treatment of osteoarthritis.
Front. Immunol. 13:1054938.
doi: 10.3389/fimmu.2022.1054938

Engineered M2a macrophages for the treatment of osteoarthritis

Chi Liang[1], Song Wu[1], Guang Xia[1], Junjie Huang[1,2], Zi Wen[1], Wenxiu Zhang[1] and Xu Cao[1,2]*

[1]Department of Orthopaedics of the 3rd Xiangya Hospital, Central South University, Changsha, China, [2]Institute of Basic Medicine and Cancer (IBMC), Chinese Academy of Sciences, Changsha, China

Background: Macrophage is a central regulator of innate immunity. Its M2 subsets, such as interstitial synovial macrophages, have been found to play critical roles in suppressing chronic inflammation and maintaining homeostasis within the joint. These macrophages have great potential as a disease-modifying cell therapy for osteoarthritis (OA). However, this has not yet been studied.

Methods: Macrophages were isolated from the bone marrow of rats. We constructed a stable macrophage that "locked" in anti-inflammatory and pro-regenerative M2a polarity (L-M2a) by simultaneously knocking out tumor necrosis factor receptor 1 (TNFR1) and overexpressing IL-4 using Cas9-ribonuclear proteins (Cas9-RNP) and electroporation. *In vitro*, these L-M2a macrophages were treated with OA synovial fluid or co-cultured with OA chondrocytes or fibroblast-like synoviocytes (FLS). *In vivo*, L-M2a macrophages were injected intra-articularly to evaluate their homing and engrafting abilities and therapeutic effects on OA progression using a rat model.

Results: L-M2a macrophages displayed a typical anti-inflammatory phenotype similar to that of M2 macrophages *in vitro*. In OA microenvironment, L-M2a macrophages maintained a stable anti-inflammatory phenotype, whereas unmodified M2 macrophages lost their phenotype and switched to M1 polarity. L-M2a macrophages demonstrated a potent anti-inflammatory effect in crosstalk with OA-FLSs and an anti-degenerative effect in crosstalk with senescent OA chondrocytes. *In vivo*, compared with M2 macrophages and exosomes, L-M2a macrophages exhibited significantly superior therapeutic effects in OA by successfully resolving inflammation, restoring tissue homeostasis, and promoting cartilage regeneration.

Conclusion: The engineered L-M2a macrophages maintained a superior anti-inflammatory and pro-regenerative capacity in the inflammatory OA microenvironment and represents an ideal new strategy for the disease-modifying therapy of OA.

KEYWORDS

macrophages, Cas9-ribonuclear proteins, cell therapy, tumor necrosis factor receptor 1, osteoarthritis

Introduction

Osteoarthritis (OA) is viewed as a multifactorial disorder affecting the entire joint, in which persistent low-grade inflammation plays a central role. Due to the interaction between immune system and various factors (including damage associated molecules and metabolic dysfunction), this long-term inflammation is initiated in the early stage of OA, leading to cartilage loss and progressive joint degeneration (1). Although disease-modifying OA drugs targeting this pathomechanism have been developed in recent years, no drug has yet achieved satisfactory results capable of delaying the clinical progression of OA (2).

Macrophage (Mφ) is a primary immunomodulator of the innate immune system and critical regulator of chronic inflammation and tissue homeostasis. Based on the activation pattern, Mφs have been typically dichotomized into two phenotypes: M1-polarized Mφs ('classically' activated) are pro-inflammatory with the release of interleukin (IL)-1β, IL-6, IL-12, IL-23, and TNF-α, while M2-polarized Mφs ('alternatively' activated) are anti-inflammatory and pro-regenerative, secreting IL-4, IL-10, and TGF-β, etc (3). Specific Mφ phenotypes differentially modulate the inflammation and regeneration responses of multiple cell types during the onset or progression of OA (4). M1 Mφs stimulate the production of inflammatory cytokines and matrix-degrading enzymes, promoting hypertrophic differentiation of chondrocytes and cartilage destruction (5). In contrast, M2 Mφs are characterized by pro-chondrogenic genes expression, which improves cartilage health (6). Recently, studies have observed a subpopulation of RELMα$^+$ interstitial synovial macrophages (ISMφ) with a stable M2a phenotype in the sub-lining layer of synovium (7). These M2a ISMφs release resolvins to switch fibroblasts from a proinflammatory to a reparative state to restore homeostasis, and were proposed to act as critical cellular checkpoints and off switches for intra-articular inflammation (8). In OA, an increase in M1 and a corresponding decrease in M2 Mφ have been observed to be directly related to OA severity (5, 9).

M2 Mφ possesses potent anti-inflammatory and pro-regenerative properties, and intrinsic 'homing' ability to migrate to sites of injury or inflammation (10). Therefore, it has great potential as an ideal seed cell for disease-modifying cell therapy for OA. However, to our knowledge, transplantation of M2 Mφ has not been studied in the treatment of OA. A major obstacle hindering the application of exogenous Mφ in regenerative medicine lies in the plasticity of its polarity. The polarization of Mφs is not fixed and characterized by high adaptability and plasticity in the microenvironment (11). Studies have found that the new environment is sufficient to reprogram well-polarized Mφs after transplantation (12, 13). This may lead to the loss of phenotype and expected function of the delivered Mφs. For example, Qi et al. observed the polarization loss of M2 Mφs in the inflammatory environment after transplantation, which impaired their protective effect against renal inflammatory injury (12). Thus, constructing M2 Mφs with a stable or 'locked' phenotype will provide a great opportunity for the treatment of inflammatory diseases including OA.

As tumor necrosis factor (TNF) is a major anti-M2 (pro-M1) factor in the chronic inflammatory microenvironment, such as OA, and IL-4 is a major pro-M2a factor (3), we proposed a stable Mφ that, like ISMφ, is 'locked' in M2a phenotype by knocking out TNFR1 and overexpressing IL-4 using Cas9-ribonuclear protein (Cas9-RNP) complexes and electroporation. In this study, we attempted to treat OA by intra-articular delivery of exogenous M2a Mφs for the first time and investigated the effect of this 'locked M2a-like Mφ' (L-M2a Mφ) on restoring the homeostasis of OA cartilage and synovium. We concluded that this L-M2a Mφ successfully maintained a stable phenotype in OA environment and significantly alleviated inflammation, promoted regeneration and delayed progression of OA in animal models.

Materials and methods

All experiments involving human tissues and animals were performed in accordance with guidelines approved by the Institutional Review Board (IRB). The source and identifier of reagents in this study are showed in Supplementary Table S1.

Isolation and polarization of bone marrow derived Mφ

All the Sprague-Dawley (SD) rats used in this study were provided by the Department of Laboratory Animals of the Central South University (Changsha, China). The bone marrow was harvested from the tibia and femurs of the rats. Red blood cells were lysed with ammonium-chloride-potassium lysis buffer. The remaining bone marrow cells were plated in RPMI-1640 medium with 10% FCS and 100 U/100 μg/ml penicillin/streptomycin supplemented with 50 ng/ml M-CSF at a density of 1×10^6 cells/ml for 5 days to obtain M0 Mφs. Subsequently, the Mφ cells were treated with IFNγ (20 ng/ml) and LPS (100 ng/ml), or IL-4/IL-13 (each 10 ng/ml) for 24 h to obtain M1 and M2 Mφ, and the cytokine secretion of M0, M1, and M2 were examined.

Construction of LM2a Mφ

EasyEdit sgTNFR1 and NLS-Cas9-EGFP nuclease proteins were purchased from GenScript (Nanjing, China). The pCDNA-IL-4 plasmid was purchased from Tsingke Biotechnology Co. Ltd (Shanghai, China). LM2a Mφ with nucleofection was

constructed according to the manufacturers and a previous study's instructions (14). Briefly, day 4 BMDMs were resuspended in 100 μL nucleofection solutions at a density of 1×10^6 cells per reaction in and mixed with 1 Cas9-RNP (25 μM Cas9 protein premixed with 100 μM sgRNA at a ratio of 1:3 for 10 min) and 2 μg IL-4 plasmid. The suspension was transferred into a certified cuvette and inserted into Nucleofector® Cuvette Holder using the Nucleofector® Program Y-001.

Nucleofected Mφs were cultured in prewarmed RPMI medium supplemented with 10% FBS for 48 h and treated with IL-4/IL-13 (each 10 ng/ml) for 24 h. LM2a Mφs were assessed using flow cytometry, DNA cleavage assay, and western blotting.

DNA cleavage assay

gDNA was extracted from LM2a and M2 Mφs using QuickExtract solution, following the manufacturer's instructions. DNA primers were generated upstream and downstream of the sgRNA target editing site (sequences are presented in Supplementary Table S2). PCR was run for 30 cycles following the manufacturer's instructions, and the products were determined with 1% agarose gel electrophoresis and analyzed using Gelation imaging system (ImageQuant350, GE, USA).

Flow cytometry analysis

Polarized and constructed Mφs were suspended in flow cytometry staining buffer (phosphate-buffered saline with 1% fetal calf serum). Cells were treated with CD86 (1:100) rabbit, CD206 (1:100) mouse, and IgG isotype control (1:100) primary antibody, and then stained with Alexa Fluor 488 anti-Rabbit IgG antibody (1: 500) and Alexa Fluor 405 anti-Mouse IgG antibody (1: 500) respectively. All samples were detected by Becton Dickinson FACScan (BD Biosciences) and analyzed with FlowJo10. The gating strategy was showed in Supplementary Figure S1B.

In vitro stimulation assay

Human OA synovial fluid (OASF) was aspirated from the knee joints of five patients with OA at the Third Xiangya Hospital of the Central South University and used to mimic the joint microenvironment of OA. Detailed clinical information and Kellgren–Lawrence gradation of all participants was presented in Supplementary Table S3. OASF was further purified by centrifugation at 3000 rpm for 15 min, and the supernatants were harvested. M2, and L-M2a Mφs were cultured in RPMI1640 or diluted OASF (50%) for 3 days. Polarized and inflammatory phenotypes were detected by RNA-sequencing, western blotting, RT-qPCR, immunofluorescence, and flow cytometry.

Co-culture assay

A co-culture system was established using six-well transwell plates. OA chondrocytes and FLS were isolated and cultured using a previously described method from a rat OA model (15), which was established by Hulth's surgery. FLS (1×10^6) or chondrocytes (1×10^6) were cultured in the lower compartments, and 1×10^6 M2a or LM2a Mφs were cultured in the upper compartments in RPMI 1640 with 10% FBS. FLS, chondrocytes, M2a, or LM2a Mφs were cultured alone as controls. Co-cultures were maintained for 1 or 7 days before evaluation. The anti-inflammatory factors and polarization markers of M2a and LM2a were analyzed using western blotting and RT-qPCR. The inflammatory factors and invasion ability of FLS were evaluated using western blotting, RT-qPCR, and invasion assays. The degenerative indicators of chondrocytes were determined using western blotting and RT-qPCR. The number of senescent chondrocytes was evaluated by RT-qPCR using $p16^{INK4a}$ and $p21^{Cip1}$ and SA-β-gal staining kits. Chondrocyte apoptosis rates were analyzed by annexin V-FITC/propidium iodide (PI) double staining according to the manufacturer's instructions. Co-cultures were conducted in technical triplicate for each assay, and five random fields of each well were selected for evaluation.

Mφ tracing *in vivo*

Hulth's surgery was performed on the right joints of 12-week-old male rats to establish an OA model (16). Overall, 20 μl 1×10^6/ml M2 or LM2a (n= 6 for each group) were labelled with CellTracker CM-Dil according to the manufacturer's protocol and then injected intra-articularly at 4 weeks after surgery. Mφ viability was examined using an *in vivo* imaging system (IVIS Lumina II, Caliper Life Science, USA) at 1, 2, and 4 weeks after injection. At 1 and 4 weeks after the injection, the rats were sacrificed. The samples were decalcified in JYBL I for 48 h, cut into frozen sections, and stained by immunofluorescence for CD206, which was detected by fluorescence microscopy (Leica TCS-SP5, DM6000-CFS).

Histological evaluation

For the histological evaluation, 20μl PBS (OA group), 1×10^6/ml M2a, LM2a, or M2a exosomes derived from equal Mφs (n= 5 for each group) were injected intra-articularly 4 weeks after the Hulth's surgery. The sham operation group was

used as control. After 8 weeks, the rats were sacrificed. Joint samples were collected and fixed in 4% paraformaldehyde for 48 h. The samples derived from the rats were detected using magnetic resonance imaging (7.0T MRI Biospoin GmbH, BRUKER) and graded using the MOAKS score. Synovial samples were collected from each group for western blot analysis. All samples were decalcified in 0.5M EDTA for 4 weeks, embedded in paraffin, and cut into sections (6 μm). Immunohistochemistry and immunofluorescence were performed using anti-MMP13, anti-IL-6, and anti-Col I antibodies. Secondary antibodies were detected using a fluorescent secondary antibody or rabbit streptavidin-biotin detection system kit according to the manufacturer's protocol. Slices of rat knee joints were stained with safranin O/fast green. The Osteoarthritis Research Society International (OARSI) scoring system was used to evaluate OA cartilage pathology.

Western blot analysis

Total proteins obtained from the cells and tissues were subjected to SDS–PAGE, transferred to PVDF membranes, and blocked in 5% skimmed milk for 30 min. The membranes were incubated overnight at 4°C with primary antibodies against CD206 (1:1000), CD86 (1:1000), iNOS (1:1000), TNFR1 (1:1000), IL-4 (1:1000), MMP13 (1:1000), IL-6 (1:1000), Col I (1:1000), Col II (1:1000), Col X (1:1000), ACAN (1:1000), p-STAT6 (1:500), STAT6 (1:1000), N-cadherin (1:1000), and GAPDH (1:8000). The membranes were incubated with HRP-conjugated secondary antibodies (1:10000) at temperature for 1 h and developed using electrochemiluminescence western blot reagents. Then the membranes were analyzed using a UVP Chem studio PLUS 815 (Analytik Jena, Germany).

RT-qPCR

Total RNA was isolated from the synovium or cells using TRIzol reagent and the consentration was measured by a NanoPhotometer spectrophotometer (IMPLEN, CA). RNA was then converted to cDNA according to the manufacturer's instructions. ChamQ Universal SYBR qPCR Master Mix was used for qPCR. Gene transcription levels were normalized to those of GAPDH. The primer design is shown in Supplementary Table S2.

Immunofluorescence assay

Mφ or slices were fixed in 4% paraformaldehyde. BSA (4%) was used to block non-specific binding. The cells were then incubated with CD86, CD206, and CD4 primary antibodies overnight. Fluorescent secondary antibodies were used, and the samples were subsequently stained with 4,6-diamidino-2-phenylindole (DAPI) for 5 min. The cells or slices were observed under a confocal fluorescence microscope.

RNA sequencing

Total RNA was extracted using Trizol reagent (thermofisher, 15596018) following the manufacturer's procedure. After total RNA was extracted, mRNA was purified from total RNA (5ug) using Dynabeads Oligo (dT) (Thermo Fisher, CA, USA) with two rounds of purification. Following purification, the mRNA was fragmented into short fragments using divalent cations under elevated temperature (Magnesium RNA Fragmentation Module (NEB, cat.e6150, USA) under 94°C 5-7min). Then the cleaved RNA fragments were reverse-transcribed to create the cDNA by SuperScript™ II Reverse Transcriptase (Invitrogen, cat.1896649, USA), which were next used to synthesise U-labeled second-stranded DNAs with E. coli DNA polymerase I (NEB, cat.m0209, USA), RNase H (NEB, cat.m0297, USA) and dUTP Solution (Thermo Fisher, cat.R0133, USA). An A-base was then added to the blunt ends of each strand, preparing them for ligation to the indexed adapters. Each adapter contained a T-base overhang for ligating the adapter to the A-tailed fragmented DNA. Dual-index adapters were ligated to the fragments, and size selection was performed with AMPureXP beads. After the heat-labile UDG enzyme (NEB, cat.m0280, USA) treatment of the U-labeled second-stranded DNAs, the ligated products were amplified with PCR. At last, we performed the 2×150bp paired-end sequencing (PE150) on an Illumina Novaseq™ 6000 following the vendor's recommended protocol.

Genes differential expression analysis was performed by DESeq2 software between two different groups (and by edgeR between two samples). The genes with the parameter of false discovery rate (FDR) below 0.05 and absolute fold change ≥ 2 were considered differentially expressed genes. Differentially expressed genes were then subjected to enrichment analysis of GO functions and KEGG pathways. Principal component analysis (PCA) and correlation analysis were performed with princomp function of R (http://www.r-project.org/).

Statistical analysis

All experiments were repeated at least three times, and the data are presented mean with 95% confidence intervals (CI) by individual dot plots. A one-way analysis of variance (ANOVA) was used for comparisons across multiple groups including phenotypic identification and *in vivo* experiments, while Dunnett's test was used for *post-hoc* multiple comparisons. Comparisons of M2 and L-M2a Mφs *in vitro* were calculated using a two-way ANOVA followed by Tukey's multiple comparisons test. All data analyses were performed using the GraphPad Prism 8.

Results

Construction and phenotypic evaluation of genome edited L-M2a Mφ

Our CRISPR-Cas9 genome editing strategy for Mφ is outlined in Figure 1A. The knockout efficiency of TNFR1 was shown to be more than 60% by flow cytometry (Figure 1B), DNA cleavage assay (Figure 1C), and western blot (Figure 1D), while the overexpression efficiency of IL-4 is shown in Figure 1D. The feasibility of this editing strategy was also verified with human-derived primary Mφs (Supplementary Figure S1A). We examined the phenotype of Mφs *in vitro* using immunofluorescence and flow cytometry. In contrast to M0 and M1 Mφ, which variably express the M1 marker CD86, both M2 and genome-edited L-M2a Mφs were characterized by low expression of CD86 and high expression of the M2 marker CD206 *in vitro* (Figures 1E, F). From the aspect of morphology, M1 Mφ showed the characteristic changes of flattening and a lot of pseudopodia (Figure 1F). Western blotting suggested lower CD86 levels in L-M2a Mφs than in M2 Mφs (Figure 1G). L-M2a Mφs displayed a typical anti-inflammatory phenotype similar to that of M2 Mφs *in vitro*, with high expression of IL-4, IL-10, TGF-β, and Arginase-1, and low expression of IL-1β, IL-6, TNFα, iNOS, NF-κB, and VEGF (Figures 1G, H). In addition, the same gene editing strategy in M1 Mφs can not be sufficient to reverse the M1 phenotype (Figure S3B).

L-M2a Mφ maintains a stable polarized phenotype in the OA microenvironment

To investigate whether L-M2a Mφs had a more stable phenotype in the OA microenvironment, we analyzed the transcriptome changes of M2 and L-M2a Mφs treated with OA synovial fluid (OASF) by RNA-sequencing (2A, B, S1C). We found that under the treatment of OASF, M2 Mφs exhibited up-regulation of a variety of pro-inflammatory cytokines and chemokines (Il1b, Il6, Tnfa, Ccl5, Ccl2, Ccl9, Cxcl2), while down-regulation of M2 polarization markers (Mrc1, Arg1) and anti-inflammatory cytokines (Il10, Il4). In contrast, L-M2a Mφs showed obvious resistance to OASF and remained a more stable expression of M2 polarization markers and anti-inflammatory cytokines (Figure 2A). Meanwhile, we used the number of differentially expressed genes (DEGs) in macrophages to reflect the extent to which they were affected by OASF. Compared with the 3419 DEGs of M2 Mφs, L-M2a Mφs only had 865 DEGs after OASF treatment, which indicated a more stable phenotype of L-M2a Mφs in OA microenvironment (Figure 2B). Western blot and RT-qPCR verified that the expression of CD86 and CD206 in L-M2a Mφs was almost unaffected, whereas it was significantly changed in M2 Mφs (Figures 2C, D, S3F). Similarly, the ratio of CD206hi cells remained stable in L-M2a Mφs (from 40.5%–32.6%), whereas it decreased dramatically in M2 (from 43.1%–4.7%) Mφs (Figures 2E, F). OA-SF induced the expression of pro-inflammatory factors (IL-1β, IL-6, TNF-α and iNOS) and inhibited the activation of anti-inflammatory IL-4/STAT6 signaling in M2 Mφs. In contrast, L-M2a Mφs were less affected and maintained an anti-inflammatory phenotype (Figure 2). However, L-M2a Mφs didn't show the same stability against the stimulation of LPS+IFNγ (Figure S3C).

L-M2a Mφs have potent anti-inflammatory effects in crosstalk with OA-FLS

We established a transwell co-culture system *in vitro* for M2/L-M2a Mφs and OA-FLS (Figure 3A). After co-culture with OA-FLS, M2 Mφs showed a trend of transition to the M1 phenotype, with decreased polarization markers of M2 (CD206, ARG1). This trend was more pronounced with prolonged coculture. On day 7, M2 Mφ shifted to an obvious pro-inflammatory state (TNFα and IL-β expression) and M1-polarized phenotype (CD86 and CD206 expression). In contrast, L-M2a Mφs showed a more stable anti-inflammatory state and polarization marker expression in co-culture with OA-FLS (Figures 3B, C). Moreover, M2 Mφs exhibited a limited ameliorative effect on the pro-inflammatory and destructive phenotype of OA-FLS, with only mild inhibition of IL-1β and N-cadherin expression and FLS invasion at day 7. In contrast, L-M2a Mφ significantly inhibited the pro-inflammatory factors (IL-1β, IL-6 and TNFα) expression and invasive activity (MMP1 and transwell invasion) of OA-FLS (Figures 3D–F).

L-M2a Mφ exhibits anti-degenerative effects through crosstalk with OA chondrocytes

We established an *in vitro* transwell co-culture system for M2/L-M2a Mφs and OA-derived chondrocytes (OA-Cho) (Figure 4A). The changing trend in the phenotype of Mφs was similar to that observed in the OA-FLS co-culture described above (Supplementary Figures S2A, B). For OA-Chos, M2 Mφs exhibited only a slight ameliorative effect on several degenerative indicators (Col I, Col X, and ACAN). In contrast, L-M2a Mφs markedly improved the degenerative phenotype of OA-Chos (increased hyaline cartilage marker Col II and ACAN, and decreased fibrocartilage marker Col I and hypertrophic marker Col X) and alleviated cellular senescence (decreased p16INK4a and p21Cip1 expression and SA-β-Gal staining) (Figures 4B,–D) and apoptosis (decreased Annexin V positive cells) (Figure 4E) in the co-culture system.

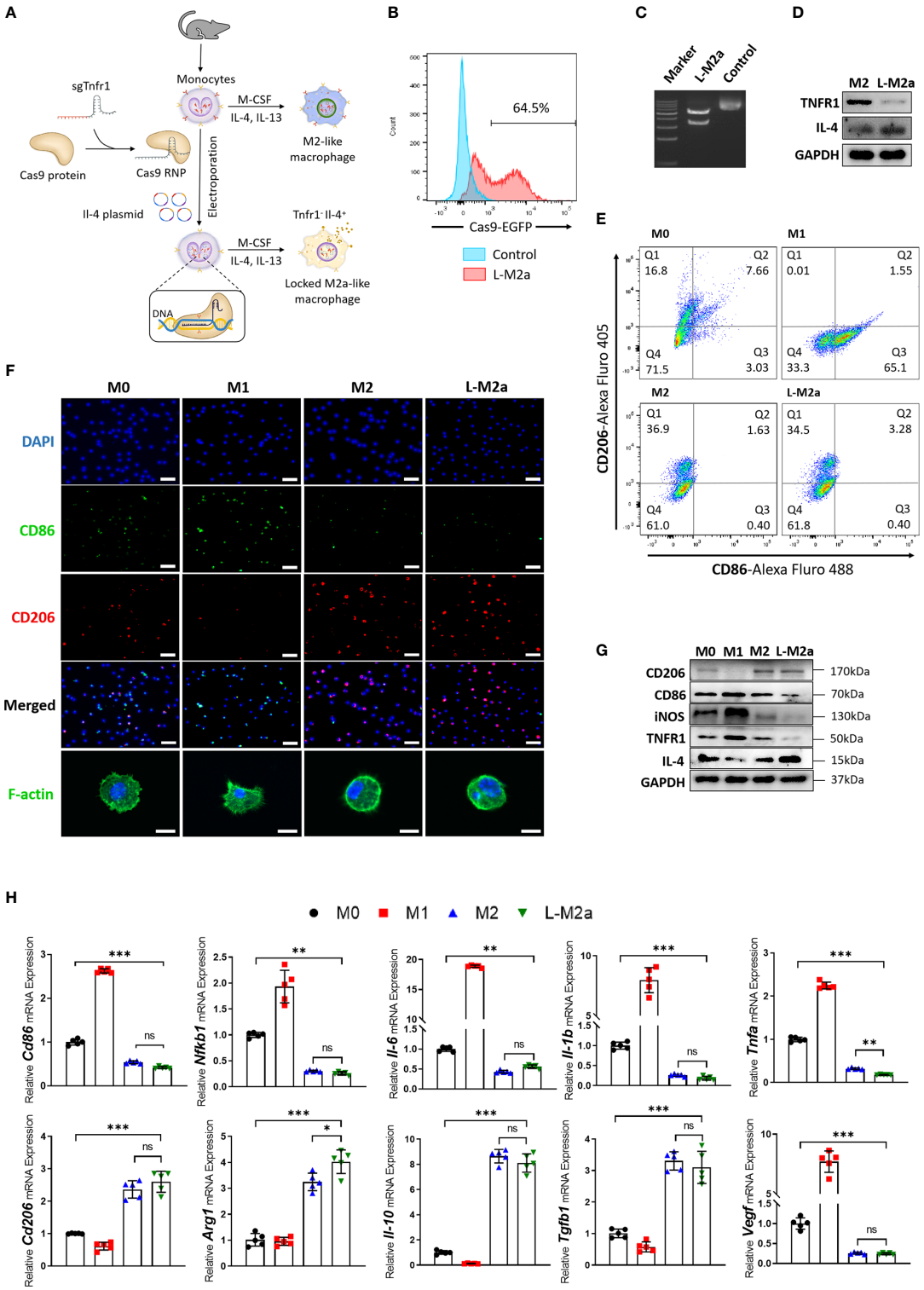

FIGURE 1
Construction and identification of L-M2a Mφ. **(A)** Illustration of the polarization of M0, M1, M2 Mφ and construction of L-M2a Mφ. **(B-D)** Validation of knockout efficiency of sgTNFR1-EGFP-Cas9-RNP and overexpression of pCDNA -IL-4 using flow cytometry **(B)**, DNA cleavage assay **(C)** and western blot **(D)**. **(E-H)** Polarized phenotype, inflammatory phenotype and morphological differences among M0, M1, M2a, L-M2a Mφ by western blot (E, n=3), immunofluorescence (F, upper part, bar= 100 μm), confocal (F, bottom part, bar=10 μm), flow cytometry **(G)** and RT-qPCR (H, n=5). $*p < 0.05$; $**p < 0.01$; $***p < 0.001$. ns, no significance; Mφ, macrophage; L-M2a Mφ, locked M2a macrophage.

10.3389/fimmu.2022.1054938

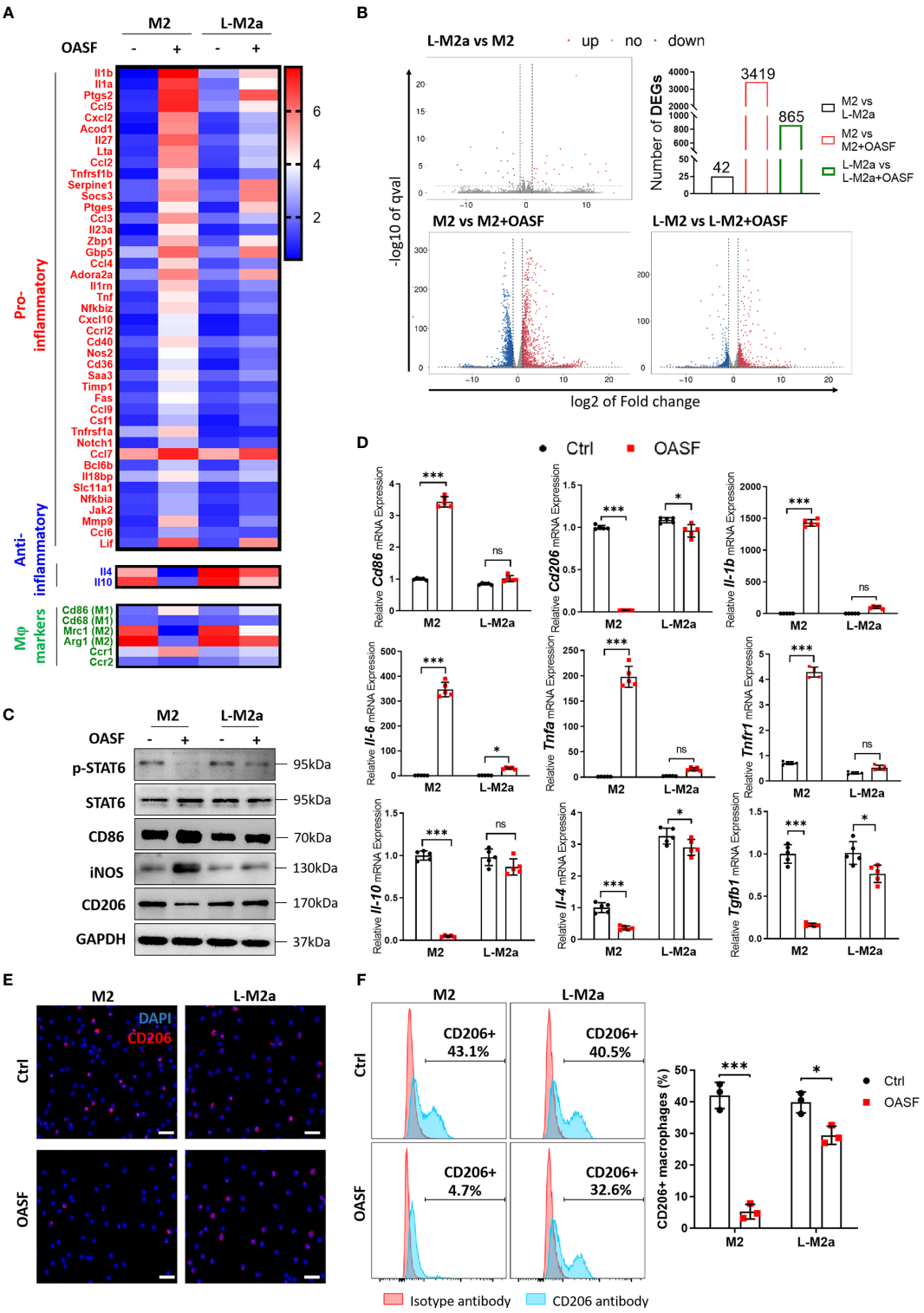

FIGURE 2
L-M2a Mφs maintained a more stable polarization in the presence of OASF *in vitro*. **(A, B)** A heatmap about inflammatory related transcriptome changes **(A)** and number of differentially expressed genes **(B)** among M2 and L-M2a macrophages treated with or without OASF by RNA sequencing (n=3). **(C, D)** Validation of expression level of saveral typical genes in **(A)** using western blot (C, n=3) and RT-qPCR (D, n=5). **(E, F)** Expression of M2 maker CD206 in M2, and L-M2a Mφ when stimulated with or without OASF by immunofluorescence (E, bar= 100μm) and flow cytometry **(F)**. ∗p < 0.05; ∗∗∗p < 0.001. ns, no significance; Mφ, macrophage; L-M2a Mφ, locked M2a macrophage; OASF, OA synovial fluid.

10.3389/fimmu.2022.1054938

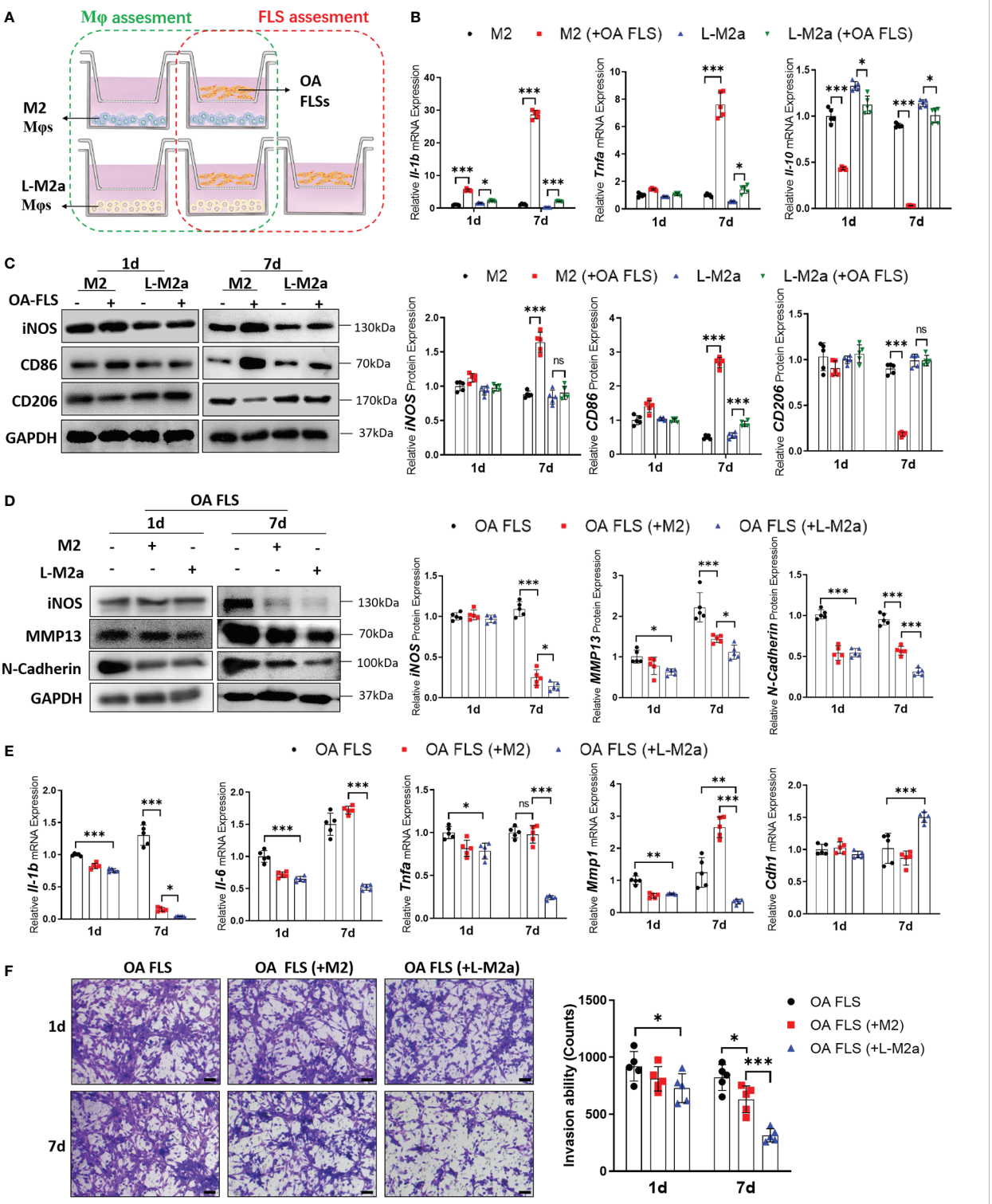

FIGURE 3
L-M2a Mφ had potent anti-inflammatory effects in crosstalk with OA-FLS. **(A)** Illustration of transwell co-culture system of Mφs and OA FLSs. **(B, C)** Polarized phenotype and inflammatory phenotype of M2 and L-M2a Mφ co-cultured with or without OA FLS for 1 or 7 days using RT-qPCR (B, n=5) and Western blot (C, n=3). **(D, F)** Assessment of EMT markers **(D)**, inflammation factors **(D, E)** and invasion activity (F, bar= 100μm) in OA-FLS co-cultured with control, M2 or L-M2a Mφ. ∗p < 0.05; ∗∗p < 0.01; ∗∗∗p < 0.001. ns, no significance; Mφ, macrophage; L-M2a Mφ, locked M2a macrophage; FLS, fibroblast-like synoviocyte.

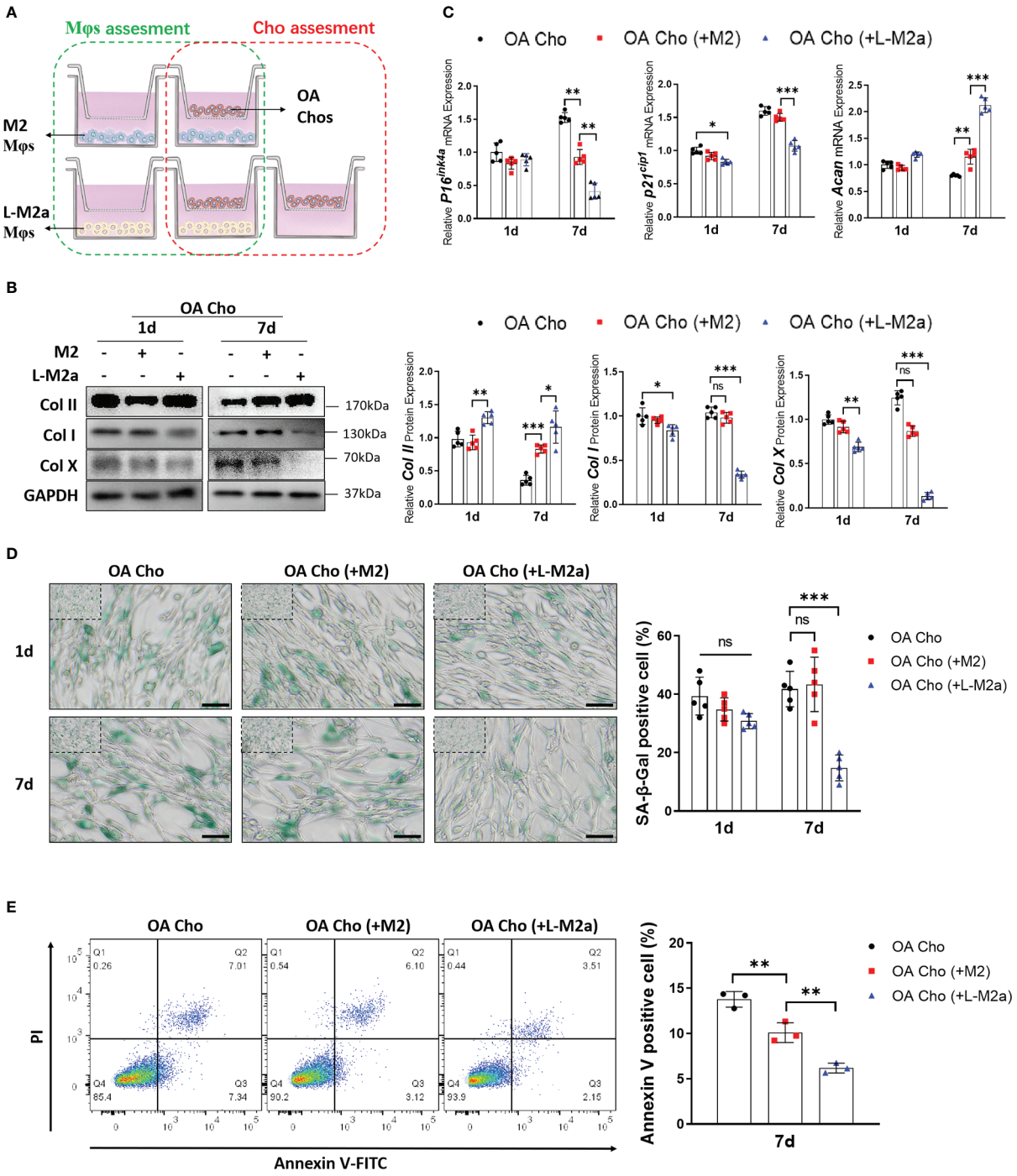

FIGURE 4
L-M2a Mφs exhibited anti-degenerative effects in crosstalk with OA-chondrocytes. **(A)** Illustration of transwell co-culture system of Mφs and OA chondrocytes. **(B, C)** Assessment of collagen synthesis ability **(B)**, inflammation factors and senescence markers **(C)** in OA chondrocytes co-cultured with control, M2 or L-M2 cells for 1 and 7 days. **(D)** Staining of SA-β-Gal (green, bar= 100μm) in OA chondrocytes co-cultured with control, M2 or L-M2a Mφs for 1 and 7 days. **(E)** Apoptosis rates for different Mφ-stimulated OA chondrocytes after 7 days coculture were analyzed by flow cytometry using annexin V-FITC/PI apoptosis analysis. ∗p < 0.05; ∗∗p < 0.01; ∗∗∗p < 0.001. ns, no significance; Mφ, macrophage; L-M2a Mφ, locked M2a macrophage; Cho, chondrocyte.

L-M2a Mφ restored tissue homeostasis and promoted cartilage regeneration in a rat OA model

We used the Hulth's method to establish an OA model in SD rats. M2 or L-M2a Mφ (labelled with CM-Dil) was injected intra-articularly 4 weeks after surgery. *In vivo* imaging systems (IVIS) showed strong fluorescence intensity in the knee joints 4 weeks after injection, whereas there was no statistical difference between M2 and L-M2a Mφs (Figure 5A). At week 1 after injection, Mφs in both groups homed to the OA synovium and maintained the M2 phenotype (CD206). However, M2 Mφs rapidly lost their M2 phenotype within 4 weeks, while L-M2a Mφs maintained a high positivity for CD206 (Figure 5B).

Histological evaluation of OA was performed 8 weeks after surgery. OA modeling induced immune cell ($CD4^+$ T cells and $CD86^+$ M1 Mφs) infiltration (Figure 6A) and MMP13 and IL-6 expression in the OA synovium (Figure 6B). Typical cartilage degeneration (Col I expression, cartilage thinning, and proteoglycan loss) was evident 8 weeks after surgery (Figures 6C-F). Overall, M2 Mφs failed to alleviate degenerative progression, with only slight improvement in synovial inflammation. In contrast L-M2a Mφs significantly reduced immune cell infiltration and MMP13/IL-6 expression in the OA synovium (Figures 6B, C), reduced Col I expression (Figure 6D), and restored tissue integrity, joint space width (Figure 6F), and safranin O staining in the cartilage (Figure 6E).

We also extracted exosomes from the same number of M2 Mφs (Supplementary Figure 2C) to treat OA. However, the overall therapeutic effect was not as obvious as that of L-M2a Mφs (Figure 6).

Discussion

In the past decades, studies on stem cell therapy for OA have been performed globally to evaluate their safety and efficacy and have yielded positive results. They improved the pain, physical function, stability of cartilage defect, and thickening of articular cartilage of OA patients (17). The desired mode of cell therapy in OA involves engraftment of injected stem cells on the chondral defect and repair of cartilage by direct chondrogenic differentiation (18, 19). However, accurate homing and directional differentiation of stem cells are challenging (20). In addition, injected stem cells usually perish rapidly in the joint cavity and are undetectable 14–50 days post-infusion (21, 22). Other studies have shown that the positive effects of therapies involving stem cells are mediated by the secretion of molecules that act in a paracrine manner to restore tissue homeostasis and regulate local immunity (23). It has been proved that the existence of stem cells leads to the production of anti-inflammatory cytokines (such as IL-10 and TGFβ) and TNFα-stimulated gene/protein 6 (TSG-6), which leads to the inhibition of the toll-like receptors-2 (TLR2)/nuclear factor κ-light-chain-enhancer of activated B cells (NFκB) signaling pathway, followed by the downregulation of inflammatory mediators, such as nitric oxide, TNFα, and IL-1β (24, 25). Similarly, upregulation of prostaglandin E2 (PGE-2) and (2,3-dioxygenase) IDO by MSCs leads to the inhibition of IFN-γ, inducing the differentiation of M1-type Mφs to M2-type Mφs (26, 27). However, the immune and inflammatory regulation of stem cells is not as strong as that of immune cells, which makes them insufficient to counteract the long-term chronic inflammatory environment of OA. Moreover, aging and tumorigenicity caused by excessive proliferation and difficulties in obtaining primary stem cells are challenging problems (28, 29).

Recently, Mφs which is a key cell composition of innate immunity and have a powerful role in regulating immunity and maintaining tissue homeostasis have emerged as a novel candidate for cell-based therapy in cancer and regenerative medicine (30). Mφs exhibit numerous potential advantages in the treatment of inflammatory diseases, including OA. First, unlike tissue-resident Mφs, Mφs for therapeutic purposes are based on differentiating a collection of monocytes from blood or extracted bone marrow, which means a stable acquisition method and a sufficient number. Moreover, Mφs, as terminally differentiated and non-proliferative cells, do not have the possibility of reproductive senescence and tumorigenesis during treatment. Furthermore, as a major immunoregulatory cell, Mφs are characterized by an intrinsic and powerful immune and inflammatory regulatory capacity (31). Thus, Mφs are promising seed cells for OA treatment. Based on this, we used Mφ in this study for the first time for OA treatment and obtained encouraging preliminary results, although there are still some limitations and problems that need to be addressed by further studies.

In contrast to M1-based therapy, which is commonly used in antitumor fields, M2-based cell therapy is used in anti-inflammatory and regenerative fields. M2 Mφs show diverse gene expression signatures, and distinct M2a, M2b, M2c, and M2d Mφs subpopulations have been identified using transcriptome analysis (Figures S3D, E). It is recognized that M2a Mφs, which are stimulated by IL-4 and characterized by the expression of CD206 and arginase (ARG)-1, present a potent anti-inflammatory function by producing IL-10, IL-1Rα, CCL18, and TGF-β, and pro-regenerative factors such as TGF-β, IGF, and FGF (32, 33). Therefore, in recent years, cell transplantation of M2a Mφ has been used to treat several inflammatory and traumatic conditions with satisfactory results. In a phase 2B clinical trial of 125 patients with dilated cardiomyopathy, compared with the placebo group, intracardiac administration of the mixture of M2 Mφs and mesenchymal stem cells resulted in a decrease in cardiac adverse events (34). Lu et al. also showed that in the mouse model of chronic

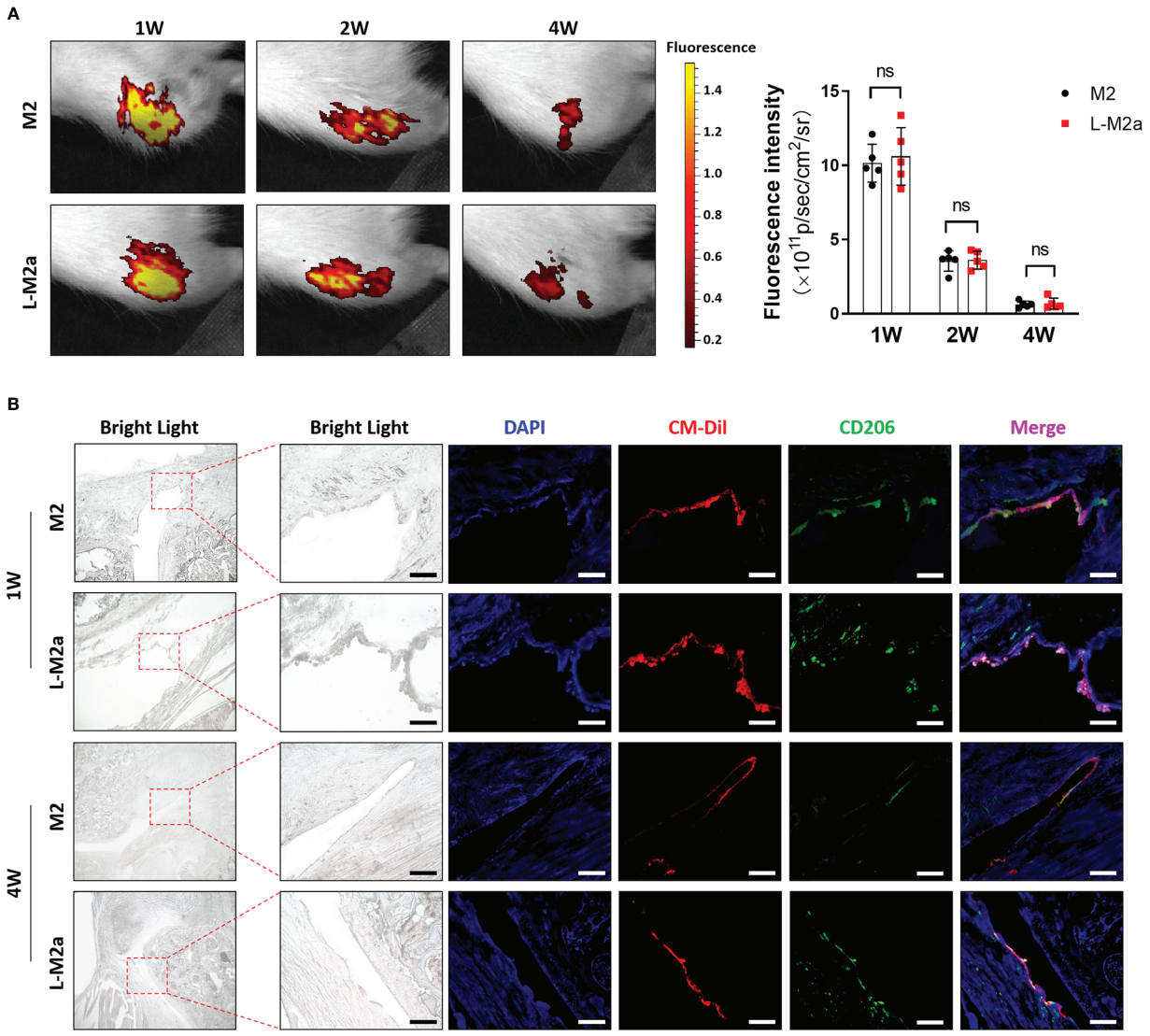

FIGURE 5
Tracing of L-M2a Mφ *in vivo*. **(A)** The fluorescence intensity of CM-Dil labelled M2 or L-M2a Mφ at 1, 2, and 4 weeks after intra-articular injection by IVIS. **(B)** The bright light, DAPI staining (blue), CM-Dil labelled M2 or L-M2a Mφ (red), CD206 immunofluorescence (green) and merge vision of joints at 1 and 4 weeks after intra-articular injection. bar= 100μm. ns, no significance; Mφ, macrophage; L-M2a Mφ, locked M2a macrophage.

nephropathy induced by adriamycin, M2a Mφs was injected into tail vein once after 5 days, which prevented kidney injury after 28 days, but inactivated Mφs had no effect. They also revealed that M2a Mφs inhibited effector T cells through the anti-inflammatory effects of cytokines IL-10 and TGF-β, resulting in less tissue damage and inflammation and less fibrosis (35). Although promising results have been observed in other studies, Mφ transplantation did not produce a sufficient therapeutic effect or even aggravated the damage *in vivo*. In an independent study of patients who received the following treatment, intramyocardial delivery of unamplified autologous bone marrow mononuclear Mφs did not show clinical improvement of ischemic cardiomyopathy (36). Moreover, wound administration of mouse Mφs activated IL-4 or IL-10 *in vitro* into the M2-like phenotype damaged skin wound healing in a diabetic mouse model (37). Additionally, adoptive metastasis-inhibitory BM-M2 Mφs could not prevent inflammatory kidney injury (12). It is believed that the poor curative effect in these studies is more likely due to the plasticity of Mφs, leading to a short M2 anti-inflammatory phenotype maintenance *in vivo*. In this study, we observed that unmodified M2 Mφs could not maintain its anti-inflammatory phenotype *in vivo* and even transformed into pro-inflammatory M1 Mφs in an OA environment, which largely compromised its therapeutic

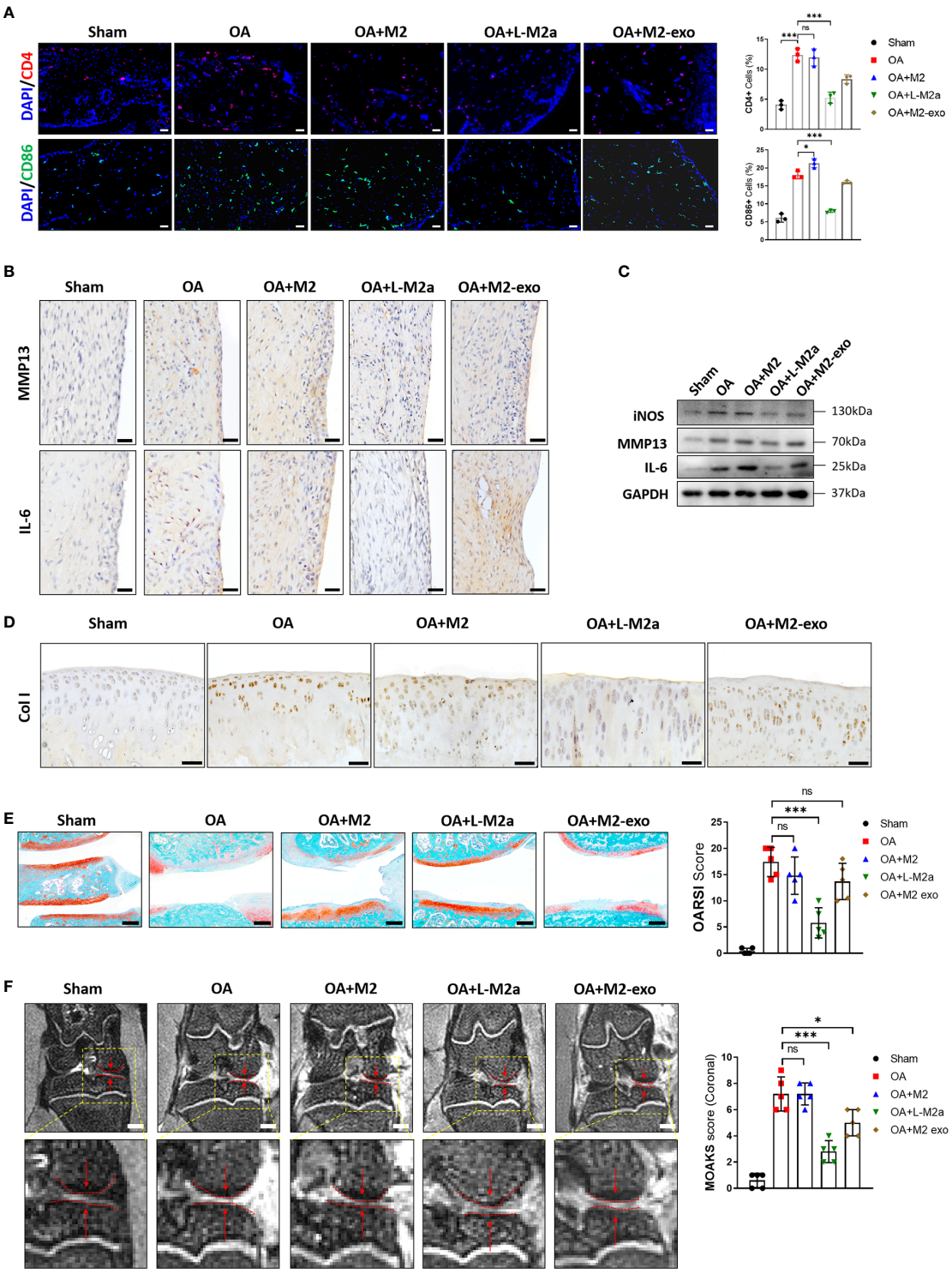

FIGURE 6
L-M2a Mφs promoted OA repair in a rat OA model. **(A)** Immunofluorescence of CD4+ (red) and CD86+ (green) cells and DAPI staining (blue) in Sham, OA, M2, L-M2a, and M2-exo groups at 4 weeks after injection (n=3, bar= 100μm). **(B, C)** Immunohistochemical staining (B, bar= 100μm) and western blot **(C)** of IL-6, MMP13, and iNOS in synovium of rat joints. **(D)** Immunohistochemical staining of Col I in cartilage of rat joints. bar= 100μm. **(E)** Safranin O/fast green staining of cartilage (left) and OARSI score (right) (n=5, bar=500μm). **(F)** Medial joint space (left, red arrow between two dotted lines) in coronal position of total knee and MOAKS score (right) by magnetic resonance imaging. (n=5, bar=1000μm). ∗p < 0.05; ∗∗∗p < 0.001. ns, no significance; Mφ, macrophage; L-M2a Mφ, locked M2a macrophage; M2-exo, M2 macrophage exosomes.

effects for OA. Therefore, it is essential to modify Mφs to obtain a stable *in vivo* phenotype.

Based on this, reprogramming of Mφ polarization has become the focus of research. Reprogramming intra-articular Mφs from M1 to M2 by local or systemic delivery of bioactive factors was confirmed to be able to improve the microenvironment of OA to some extent (38, 39). The traditional method of Mφ reprogramming involves changing the polarity of signaling molecules (such as cytokines, receptor agonists, and inhibitory antibodies). For example, Mφ pretreated with LPS + IFN-γ can reduce fibrosis formation after trauma or ischemic injury (40). However, such reprogramming is often transient and insufficient to resist the chronic inflammatory environment *in vivo*. In contrast, genome editing can achieve the long-term effect of complete or partial inhibition of a specific gene by forming stable modifications. Ad5f35, a chimeric adenoviral vector, synergizes with chimeric antigen receptor (CAR) activity, activates the Mφ inflammasome, and provided a beneficial proinflammatory priming signal, which renders CAR-Mφ locked into an M1 phenotype (41). Using this strategy, the selection of target genes is the first step in gene editing. A network typing based on the Mφ phenotype transcriptome found that, unlike the classic M1 Mφ phenotype activated by LPS or IFNγ signaling in acute inflammation, TNF is the key signal that induces Mφs to polarize towards M1 in a chronic inflammatory environment (42). Moreover, TNF is recognized as the most potent factor against the M2 phenotype because of its direct effects on Mφs and the indirect inhibitory effects of TNF on IL-4 and IL-13 production by other innate cell types. Furthermore, IL-4/STAT6 is considered the most important pathway of M2a polarization, and the absence of IL-4, IL-4R, and STAT6 leads to the complete loss of the M2a phenotype (3). In addition, in this study, we also compared TNFR knock-out with IL-4 over-expression and their synergy in pre-experiment, and found that the combination of these two editing was more resistant to OASF (Figure S3A). Therefore, it is reasonable to 'lock' Mφ in an M2a phenotype in a chronic inflammatory environment by simultaneously knocking-out TNFR1 and up-regulating IL-4.

Appropriate editing method is an important factor in gene editing. Primary immune cells such as monocytes and Mφs have low replication ability and high sensitivity to foreign nucleic acids and viruses. This makes conventional editing methods, such as transfection or lentivirus infection difficult (43). The direct delivery of Cas9 protein and its related single instruction RNA (sgRNA, together comprising the CRISPR-Cas9-RNP) complex provides an attractive alternative method for genome editing based on CRISPR. Protein-mediated strategies are short-lived, thus limiting genome exposure to editing mechanisms, which may lead to unnecessary off-target editing. Transient protein delivery also reduces the risk of immunogenicity in the host due to the continuous expression of active Cas9 (44, 45). Recent studies showed that the efficiency of the Cas9-RNP editing strategy was far superior to that of the traditional method in myeloid cells. They proved that the delivery of Cas9-RNP complex usually produces single or multiple target genes with > 90% KO, so that it is possible to quickly evaluate the functionally deficient genes of donors or cells from a predetermined genetic background without damaging the normal cell function. This process produces genetically edited Mφs, which retains transcripts and protein markers of myeloid differentiation and phagocytic function (14, 46).

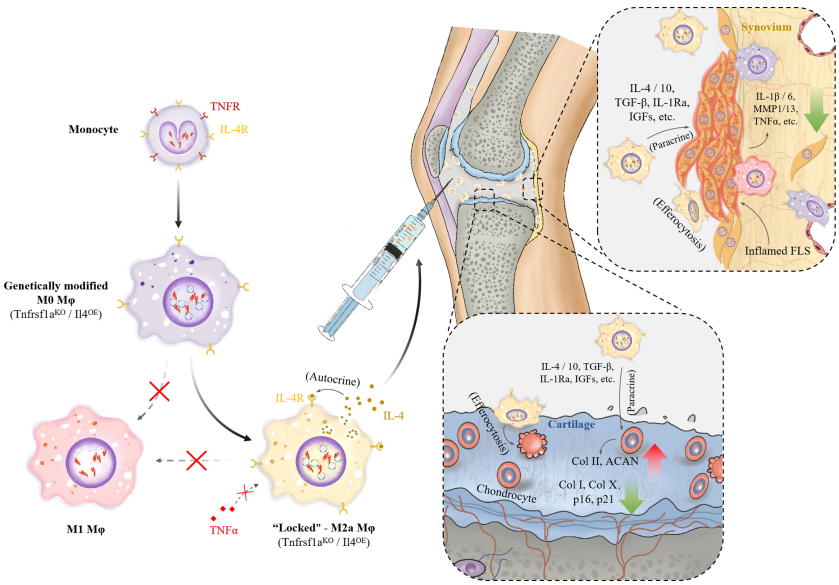

FIGURE 7
Diagram of construction of L-M2a Mφs and mechanism of its function in joints.

In conclusion, in this study, we constructed locked M2a Mφs with TNFR1 knockout and IL-4 overexpression for OA treatment. We found that it maintained a more stable M2a polarization and anti-inflammatory phenotypes in an inflammatory environment *in vitro* and in a rat OA model. Moreover, an intra-articular injection of L-M2a Mφ delayed the process of OA (Figure 7). This study provides insights into the treatment of inflammatory joint diseases including OA.

Data availability statement

The original contributions presented in the study are included in the article/Supplementary Material. Further inquiries can be directed to the corresponding author.

Ethics statement

The studies involving human participants were reviewed and approved by Institutional Review Board (IRB) of the Third Xiangya Hospital, Central South University (No. 2020-S221). The patients/participants provided their written informed consent to participate in this study.The animal study was reviewed and approved by Department of Laboratory Animals of the Central South University (Changsha, China).

Author contributions

CL contributed to conception, design, data acquisition, analysis, and interpretation. SW, GX, JH, ZW and WZ contributed to the data interpretation, critically revised the manuscript. XC contributed to conception, design, and data interpretation, drafted the manuscript. All authors read and approved the final manuscript.

Funding

This work was supported by the National Natural Science Foundation of China (82072501); Science and Technology Innovation Leading Plan of High-Tech Industry in Hunan Province (2020SK2011); Youth Fund Project of Natural Science Foundation of Hunan Province (2020JJ5848) and Medical Research Development Fund Project (WS865C).

Acknowledgments

The authors thank Editage Service (www.editage.cn) for the English language editing and review services.

Conflict of interest

The authors declare that the research was conducted in the absence of any commercial or financial relationships that could be construed as a potential conflict of interest.

Publisher's note

Supplementary material

The Supplementary Material for this article can be found online at: https://www.frontiersin.org/articles/10.3389/fimmu.2022.1054938/full#supplementary-material

SUPPLEMENTARY FIGURE 1
(A) Validation of knockout efficiency of sgTNFR1-EGFP-Cas9-RNP and overexpression of pCDNA -IL-4 in human-derived macrophages by flow cytometry, DNA cleavage assay and Western blot. (B) The isotype controls and gating strategy of flow cytometry in Fig 1E. (C) The PCA plot (left) and Pearson correlation (right) among M2 (A group), M2+OASF (B group), L-M2a (C group), L-M2a+OASF (D group). Mφ: macrophage; L-M2a Mφ: locked M2a macrophage; OASF: OA synovial fluid.

SUPPLEMENTARY FIGURE 2
(A-B) Polarized phenotype and inflammatory phenotype of M2 and L-M2a Mφ co-cultured with or without OA chondrocytes for 1 or 7 days using western bolt (A, n=3) and RT-qPCR (B, n=5). (C) Nanoparticle Analysis of M2 macrophage exosomes.

SUPPLEMENTARY FIGURE 3
(A) Comparison of polarized phenotype and inflammatory phenotype among M2 Mφs constructed with Tnfrsf1a knockout and Il4 stimulation ($Tnfrsf1a^{KO}$ group), Il4 overexpression ($Il4^{OE}$) or Tnfrsf1a knockout and Il4 overexpression ($Tnfrsf1a^{KO}Il4^{OE}$) when stimulated with or without OASF by RT-qPCR. (B) Comparison of polarized phenotype among M1, M2 and $Tnfrsf1a^{KO}Il4^{OE}$ M1 Mφs by Western blot. (C) Expression of CD86 and CD206 in M0, M2, and L-M2a Mφ when stimulated with or without LPS +IFNγ by Western blot. (D) A heatmap of anti-inflammatory and pro-regenerative cytokines expression of M0, M1, M2a, M2b, M2c Mφs by RT-qPCR. (E) Expression of inflammatory factors of chondrocytes co-cultured among with M0, M1, M2a, M2b, M2c Mφs. (F) The expression of CD86 and CD206 in M1, M2 and macrophages treated with OASF. KO: knockout; OE: overexpression; Mφ: macrophage; OASF: OA synovial fluid.

SUPPLEMENTARY TABLE 1
The source and identifier of reagents used in this study.

SUPPLEMENTARY TABLE 2
The rat primer sequence for RT-PCR.

SUPPLEMENTARY TABLE 3
Basic information (gender, age, K/L grade) of 5 OA patients for OASF. K/L grade: Kellgren & Lawrence grade.

References

1. Robinson WH, Lepus CM, Wang Q, Raghu H, Mao R, Lindstrom TM, et al. Low-grade inflammation as a key mediator of the pathogenesis of osteoarthritis. *Nat Rev Rheumatol* (2016) 12(10):580–92. doi: 10.1038/nrrheum.2016.136

2. Latourte A, Kloppenburg M, Richette P. Emerging pharmaceutical therapies for osteoarthritis. *Nat Rev Rheumatol* (2020) 16(12):673–88. doi: 10.1038/s41584-020-00518-6

3. Murray PJ. Macrophage polarization. *Annu Rev Physiol* (2017) 79:541–66. doi: 10.1146/annurev-physiol-022516-034339

4. Sica A, Mantovani A. Macrophage plasticity and polarization: *in vivo* veritas. *J Clin Invest* (2012) 122(3):787–95. doi: 10.1172/JCI59643

5. Zhang H, Lin C, Zeng C, Wang Z, Wang H, Lu J, et al. Synovial macrophage M1 polarisation exacerbates experimental osteoarthritis partially through r-spondin-2. *Ann Rheum Dis* (2018) 77(10):1524–34. doi: 10.1136/annrheumdis-2018-213450

6. Dai M, Sui B, Xue Y, Liu X, Sun J. Cartilage repair in degenerative osteoarthritis mediated by squid type II collagen *via* immunomodulating activation of M2 macrophages, inhibiting apoptosis and hypertrophy of chondrocytes. *Biomaterials* (2018) 180:91–103. doi: 10.1016/j.biomaterials.2018.07.011

7. Culemann S, Grüneboom A, Nicolás-Ávila JÁ, Weidner D, Lämmle KF, Rothe T, et al. Locally renewing resident synovial macrophages provide a protective barrier for the joint. *Nature* (2019) 572(7771):670–5. doi: 10.1038/s41586-019-1471-1

8. Kemble S, Croft AP. Critical role of synovial tissue-resident macrophage and fibroblast subsets in the persistence of joint inflammation. *Front Immunol* (2021) 12:715894. doi: 10.3389/fimmu.2021.715894

9. Liu B, Zhang M, Zhao J, Zheng M, Yang H. Imbalance of M1/M2 macrophages is linked to severity level of knee osteoarthritis. *Exp Ther Med* (2018) 16(6):5009–14. doi: 10.3892/etm.2018.6852

10. Sun Y, Zuo Z, Kuang Y. An emerging target in the battle against osteoarthritis: Macrophage polarization. *Int J Mol Sci* (2020) 21(22):8513. doi: 10.3390/ijms21228513

11. Locati M, Curtale G, Mantovani A. Diversity, mechanisms, and significance of macrophage plasticity. *Annu Rev Pathol* (2020) 15:123–47. doi: 10.1146/annurev-pathmechdis-012418-012718

12. Cao Q, Wang Y, Zheng D, Sun Y, Wang C, Wang XM, et al. Failed renoprotection by alternatively activated bone marrow macrophages is due to a proliferation-dependent phenotype switch in vivo. *Kidney Int* (2014) 85(4):794–806. doi: 10.1038/ki.2013.341

13. Lavin Y, Winter D, Blecher-Gonen R, David E, Keren-Shaul H, Merad M, et al. Tissue-resident macrophage enhancer landscapes are shaped by the local microenvironment. *Cell* (2014) 159(6):1312–26. doi: 10.1016/j.cell.2014.11.018

14. Freund EC, Lock JY, Oh J, Maculins T, Delamarre L, Bohlen CJ, et al. Efficient gene knockout in primary human and murine myeloid cells by non-viral delivery of CRISPR-Cas9. *J Exp Med* (2020) 217(7):e20191692. doi: 10.1084/jem.20191692

15. Cao X, Cui Z, Ding Z, Chen Y, Wu S, Wang X, et al. An osteoarthritis subtype characterized by synovial lipid metabolism disorder and fibroblast-like synoviocyte dysfunction. *J Orthop Translat* (2022) 33:142–52. doi: 10.1016/j.jot.2022.02.007

16. Liang Y, Chen S, Yang Y, Lan C, Zhang G, Ji Z, et al. Vasoactive intestinal peptide alleviates osteoarthritis effectively *via* inhibiting NF-κB signaling pathway. *J BioMed Sci* (2018) 25(1):25. doi: 10.1186/s12929-018-0410-z

17. Loo SJQ, Wong NK. Advantages and challenges of stem cell therapy for osteoarthritis (Review). *BioMed Rep* (2021) 15(2):67. doi: 10.3892/br.2021.1443

18. Mak J, Jablonski CL, Leonard CA, Dunn JF, Raharjo E, Matyas JR, et al. Intra-articular injection of synovial mesenchymal stem cells improves cartilage repair in a mouse injury model. *Sci Rep* (2016) 6:23076. doi: 10.1038/srep23076

19. Mokbel AN, El Tookhy OS, Shamaa AA, Rashed LA, Sabry D, El Sayed AM. Homing and reparative effect of intra-articular injection of autologus mesenchymal stem cells in osteoarthritic animal model. *BMC Musculoskelet Disord* (2011) 12:259. doi: 10.1186/1471-2474-12-259

20. Im GI. Perspective on intra-articular injection cell therapy for osteoarthritis treatment. *Tissue Eng Regener Med* (2019) 16(4):357–63. doi: 10.1007/s13770-018-00176-6

21. ter Huurne M, Schelbergen R, Blattes R, Blom A, de Munter W, Grevers LC, et al. Antiinflammatory and chondroprotective effects of intraarticular injection of adipose-derived stem cells in experimental osteoarthritis. *Arthritis Rheum* (2012) 64(11):3604–13. doi: 10.1002/art.34626

22. von Bahr L, Batsis I, Moll G, Hägg M, Szakos A, Sundberg B, et al. Analysis of tissues following mesenchymal stromal cell therapy in humans indicates limited long-term engraftment and no ectopic tissue formation. *Stem Cells* (2012) 30(7):1575–8. doi: 10.1002/stem.1118

23. Mancuso P, Raman S, Glynn A, Barry F, Murphy JM. Mesenchymal stem cell therapy for osteoarthritis: The critical role of the cell secretome. *Front Bioeng Biotechnol* (2019) 7:9. doi: 10.3389/fbioe.2019.00009

24. Choi H, Lee RH, Bazhanov N, Oh JY, Prockop DJ. Anti-inflammatory protein TSG-6 secreted by activated MSCs attenuates zymosan-induced mouse peritonitis by decreasing TLR2/NF-κB signaling in resident macrophages. *Blood* (2011) 118(2):330–8. doi: 10.1182/blood-2010-12-327353

25. Prockop DJ, Oh JY. Mesenchymal stem/stromal cells (MSCs): role as guardians of inflammation. *Mol Ther* (2012) 20(1):14–20. doi: 10.1038/mt.2011.211

26. François M, Romieu-Mourez R, Li M, Galipeau J. Human MSC suppression correlates with cytokine induction of indoleamine 2,3-dioxygenase and bystander M2 macrophage differentiation. *Mol Ther* (2012) 20(1):187–95. doi: 10.1038/mt.2011.189

27. Németh K, Leelahavanichkul A, Yuen PS, Mayer B, Parmelee A, Doi K, et al. Bone marrow stromal cells attenuate sepsis *via* prostaglandin E(2)-dependent reprogramming of host macrophages to increase their interleukin-10 production. *Nat Med* (2009) 15(1):42–9. doi: 10.1038/nm.1905

28. Marks PW, Witten CM, Califf RM. Clarifying stem-cell therapy's benefits and risks. *N Engl J Med* (2017) 376(11):1007–9. doi: 10.1056/NEJMp1613723

29. Prockop DJ, Brenner M, Fibbe WE, Horwitz E, Le Blanc K, Phinney DG, et al. Defining the risks of mesenchymal stromal cell therapy. *Cytotherapy* (2010) 12(5):576–8. doi: 10.3109/14653249.2010.507330

30. Biswas SK, Mantovani A. Macrophage plasticity and interaction with lymphocyte subsets: cancer as a paradigm. *Nat Immunol* (2010) 11(10):889–96. doi: 10.1038/ni.1937

31. Spiller KL, Koh TJ. Macrophage-based therapeutic strategies in regenerative medicine. *Adv Drug Delivery Rev* (2017) 122:74–83. doi: 10.1016/j.addr.2017.05.010

32. Das A, Sinha M, Datta S, Abas M, Chaffee S, Sen CK, et al. Monocyte and macrophage plasticity in tissue repair and regeneration. *Am J Pathol* (2015) 185(10):2596–606. doi: 10.1016/j.ajpath.2015.06.001

33. Shapouri-Moghaddam A, Mohammadian S, Vazini H, Taghadosi M, Esmaeili SA, Mardani F, et al. Macrophage plasticity, polarization, and function in health and disease. *J Cell Physiol* (2018) 233(9):6425–40. doi: 10.1002/jcp.26429

34. Patel AN, Henry TD, Quyyumi AA, Schaer GL, Anderson RD, Toma C, et al. Ixmyelocel-T for patients with ischaemic heart failure: a prospective randomised double-blind trial. *Lancet* (2016) 387(10036):2412–21. doi: 10.1016/S0140-6736(16)30137-4

35. Lu J, Cao Q, Zheng D, Sun Y, Wang C, Yu X, et al. Discrete functions of M2a and M2c macrophage subsets determine their relative efficacy in treating chronic kidney disease. *Kidney Int* (2013) 84(4):745–55. doi: 10.1038/ki.2013.135

36. Perin EC, Willerson JT, Pepine CJ, Henry TD, Ellis SG, Zhao DX, et al. Effect of transendocardial delivery of autologous bone marrow mononuclear cells on functional capacity, left ventricular function, and perfusion in chronic heart failure: the FOCUS-CCTRN trial. *Jama* (2012) 307(16):1717–26. doi: 10.1001/jama.2012.418

37. Jetten N, Roumans N, Gijbels MJ, Romano A, Post MJ, de Winther MP, et al. Wound administration of M2-polarized macrophages does not improve murine cutaneous healing responses. *PloS One* (2014) 9(7):e102994. doi: 10.1371/journal.pone.0102994

38. Siebelt M, Korthagen N, Wei W, Groen H, Bastiaansen-Jenniskens Y, Müller C, et al. Triamcinolone acetonide activates an anti-inflammatory and folate receptor-positive macrophage that prevents osteophytosis in vivo. *Arthritis Res Ther* (2015) 17:352. doi: 10.1186/s13075-015-0865-1

39. Choi K, Lee H, Kim D, Lee H, Kim M, Lim C-L, et al. Invossa™ (TISSUEGENE-c) induces an anti-inflammatory environment in the arthritic knee joints *via* macrophage polarization. *Osteoarthritis Cartilage* (2017) 25:S157. doi: 10.1016/j.joca.2017.02.267

40. Novak ML, Weinheimer-Haus EM, Koh TJ. Macrophage activation and skeletal muscle healing following traumatic injury. *J Pathol* (2014) 232(3):344–55. doi: 10.1002/path.4301

41. Klichinsky M, Ruella M, Shestova O, Lu XM, Best A, Zeeman M, et al. Human chimeric antigen receptor macrophages for cancer immunotherapy. *Nat Biotechnol* (2020) 38(8):947–53. doi: 10.1038/s41587-020-0462-y

42. Xue J, Schmidt SV, Sander J, Draffehn A, Krebs W, Quester I, et al. Transcriptome-based network analysis reveals a spectrum model of human macrophage activation. *Immunity* (2014) 40(2):274–88. doi: 10.1016/j.immuni.2014.01.006

43. Lee S, Kivimäe S, Dolor A, Szoka FC. Macrophage-based cell therapies: The long and winding road. *J Control Release* (2016) 240:527–40. doi: 10.1016/j.jconrel.2016.07.018

44. Kleinstiver BP, Pattanayak V, Prew MS, Tsai SQ, Nguyen NT, Zheng Z, et al. High-fidelity CRISPR-Cas9 nucleases with no detectable genome-wide off-target effects. *Nature* (2016) 529(7587):490–5. doi: 10.1038/nature16526

45. Slaymaker IM, Gao L, Zetsche B, Scott DA, Yan WX, Zhang F. Rationally engineered Cas9 nucleases with improved specificity. *Science* (2016) 351(6268):84–8. doi: 10.1126/science.aad5227

46. Hiatt J, Cavero DA, McGregor MJ, Zheng W, Budzik JM, Roth TL, et al. Efficient generation of isogenic primary human myeloid cells using CRISPR-Cas9 ribonucleoproteins. *Cell Rep* (2021) 35(6):109105. doi: 10.1016/j.celrep.2021.109105

frontiers | Frontiers in Immunology

TYPE Review
PUBLISHED 05 January 2023
DOI 10.3389/fimmu.2022.1110774

OPEN ACCESS

EDITED BY
Ruoxi Yuan,
Hospital for Special Surgery,
United States

REVIEWED BY
Rui Dong,
Massachusetts General Hospital and Harvard Medical School, United States
Enchao Qiu,
Thomas Jefferson University,
United States

*CORRESPONDENCE
Yan Yin
yinyan1b@126.com

SPECIALTY SECTION
This article was submitted to Inflammation, a section of the journal Frontiers in Immunology

RECEIVED 29 November 2022
ACCEPTED 16 December 2022
PUBLISHED 05 January 2023

CITATION
Qiao X, Ding Y, Wu D, Zhang A, Yin Y, Wang Q, Wang W and Kang J (2023) The roles of long noncoding RNA-mediated macrophage polarization in respiratory diseases.
Front. Immunol. 13:1110774.
doi: 10.3389/fimmu.2022.1110774

The roles of long noncoding RNA-mediated macrophage polarization in respiratory diseases

Xin Qiao, Yuxiao Ding, Dasen Wu, Anle Zhang, Yan Yin*, Qiuyue Wang, Wei Wang and Jian Kang

Department of Pulmonary and Critical Care Medicine, The First Hospital of China Medical University, Shenyang, China

Macrophages play an essential role in maintaining the normal function of the innate and adaptive immune responses during host defence. Macrophages acquire diverse functional phenotypes in response to various microenvironmental stimuli, and are mainly classified into classically activated macrophages (M1) and alternatively activated macrophages (M2). Macrophage polarization participates in the inflammatory, fibrotic, and oncogenic processes of diverse respiratory diseases by changing phenotype and function. In recent decades, with the advent of broad-range profiling methods such as microarrays and next-generation sequencing, the discovery of RNA transcripts that do not encode proteins termed "noncoding RNAs (ncRNAs)" has become more easily accessible. As one major member of the regulatory ncRNA family, long noncoding RNAs (lncRNAs, transcripts >200 nucleotides) participate in multiple pathophysiological processes, including cell proliferation, differentiation, and apoptosis, and vary with different stimulants and cell types. Emerging evidence suggests that lncRNAs account for the regulation of macrophage polarization and subsequent effects on respiratory diseases. In this review, we summarize the current published literature from the PubMed database concerning lncRNAs relevant to macrophage polarization and the underlying molecular mechanisms during the occurrence and development of respiratory diseases. These differentially expressed lncRNAs are expected to be biomarkers and targets for the therapeutic regulation of macrophage polarization during disease development.

KEYWORDS

macrophages, M1/M2 polarization, long noncoding RNAs, respiratory diseases, lung cancer

1 Introduction

Respiratory diseases are responsible for a significant proportion of serious morbidity and premature death worldwide (1). The Global Burden of Diseases (GBD) Study 2017 data showed that there were 3.2 million deaths due to COPD and 495,000 deaths due to asthma (2). Lung cancer is the deadliest of nearly all cancers, with 5-year survival rates of 4-17% depending on stage and regional differences (3). In addition, the COVID-19 pandemic has claimed more than 5.7 million lives within a year, mostly from respiratory causes (4). A number of other conditions, including interstitial disease diagnosed as IPF, noninfectious granulomatous lung diseases such as sarcoidosis, and infectious lung diseases such as tuberculosis, also contribute to a significant global burden. Therefore, early diagnosis and precise therapy are especially crucial. Despite considerable advancements in fundamental research and clinical practice that have shed light on the pathophysiology of these diseases in recent decades, challenges remain in exploring molecular mechanisms.

Macrophages play an essential role in maintaining the normal function of the innate and adaptive immune responses during host defence (5). Macrophages acquire diverse functional phenotypes in response to various microenvironmental stimuli, which are mainly classified into classically activated macrophages (M1) and alternatively activated macrophages (M2) (6). Exposure to interferon-γ (IFN-γ) or lipopolysaccharide (LPS) stimulates M1 macrophage polarization with the ability to produce proinflammatory cytokines such as IL-1β, IL-6, IL-12, and TNFα, leading to pathogen clearance and tissue damage (7). In contrast, M2-polarized macrophages are further classified into four subsets based on their *in vitro* responses to stimuli: M2a macrophages (characterized by the expression of CD206 receptors on the cell surface and that can be induced by IL-4 and IL-13), which promote type II immune responses and fibrogenesis; M2b macrophages (characterized by the expression of CD86 receptors on the cell surface and that can be induced by immune complexes), which are immunoregulatory; M2c macrophages (characterized by the expression of CD163 receptors on the cell surface and that can be induced by IL-10 and transforming growth factor-β (TGF-β), which are anti-inflammatory and initiators of tissue remodelling; and M2d macrophages, also known as tumour-associated macrophages (TAMs), which are the major inflammatory component of the tumour microenvironment (TME) (7–11). The pathogenic process of most respiratory diseases has been proposed to be regulated by macrophage plasticity (M1/M2 polarization) (12). For example, the activation of M1 macrophage polarization is important for inflammation formation, while the activation of M2 macrophage polarization is important for fibrosis, inflammation solution and tumorigenesis (12, 13). In this scenario, targeting the balance of macrophage phenotypes may be a key step in respiratory disease management.

In recent decades, with the advent of broad-range profiling methods such as microarrays and next-generation sequencing, the discovery of RNA transcripts that do not encode proteins termed "noncoding RNAs (ncRNAs)" has become more easily accessible. NcRNAs are generally classified into two groups, housekeeping and regulatory ncRNAs, according to their regulatory effects. As one major member of the regulatory ncRNA family, long noncoding RNAs (transcripts >200 nucleotides) participate in multiple pathophysiological processes, including cell proliferation, differentiation and apoptosis, which vary with different stimulants and cell types (14, 15). Many studies have reported that the lncRNA profiles in patients with respiratory disease differ from those in healthy people (16–18). In addition, emerging evidence suggests that dysregulated lncRNAs account for the pathogenesis and progression of several lung diseases, including COPD, asthma, and ALI, due to their roles in regulating macrophage polarization (19–21). In this review, we will summarize recent findings regarding lncRNA-mediated macrophage polarization in four categories of respiratory conditions: chronic airway disease (asthma, COPD, and cystic fibrosis), interstitial lung disease (IPF, CTD-ILD, and sarcoidosis), infectious lung disease (TB, pneumonia, and acute lung injury/acute respiratory distress syndrome), and lung cancer, providing a theoretical basis for the use of lncRNAs as noninvasive diagnostic biomarkers and therapeutic targets for respiratory diseases.

2 LncRNA expression profiles in M1/M2 macrophage polarization

A number of studies have analysed the expression profiles of lncRNAs in human- and murine-derived macrophages under various polarized conditions. Zhang et al. (22) used murine bone marrow-derived macrophages (BMDMs) to determine lncRNA expression in M1 and M2 polarizing conditions. In this study, M1-polarised conditions in BMDMs were induced by LPS plus IFN-γ treatment, whereas M2 polarization was stimulated by IL-4. The lncRNA-microarray results identified 33,231 lncRNAs, of which 627 lncRNAs were enriched in M1 macrophages and 624 lncRNAs were enriched in M2 macrophages with the selection criteria of >2-fold differentially expressed changes and FDR adjusted P values < 0.05 (22). Using qRT–PCR, they confirmed that in M1 polarized macrophages, *lncAK048798* and *lncAK153212* were downregulated, whereas *lncAK085865* and *lncAK083884* were upregulated in comparison to levels in M2 polarized conditions (22). Luo and his colleague (23) used microarray analyses to analyse the expression of lncRNAs in the process of M2 to M1 macrophage polarization in human monocytic U937 cells. Specifically, stimulation of U937 cell cultures with PMA, IL-4, and IL-13 induced the M2 phenotype, while a switch from the M2 to the M1 phenotype

was promoted by LPS and IFN-γ stimulation. They uncovered 26,276 differentially expressed lncRNAs between M1 and M2 phenotypes of U937 macrophages. Pearson correlation analysis was used to verify the agreement between microarray data and qRT−PCR examination. Although the qRT−PCR results of some lncRNAs were inconsistent with the microarray results, the majority of lncRNAs analysed were congruent in both assays. On the other hand, Ito et al. (24) stimulated mouse BMDMs into various phenotypes with IFN-γ (M1), IL-4 (M2a), LPS and immobilized IgG (M2b), and IL-10 (M2c). The qRT−PCR results showed that lncRNA growth arrest specific 5 (*GAS5*) is not expressed by M2b cells, but M0, M1, M2a, and M2c cells express it. Additionally, BMDMs overexpressing *GAS5* RNA after *GAS5* gene transduction did not switch to the M2b phenotype after stimulation with LPS and IC in combination.

In summary, profiling lncRNA expression in polarized macrophages with techniques such as microarray and RT −qPCR arrays yields large amounts of dysregulated lncRNAs. For the most part, the therapeutic potential of such dysregulated lncRNAs through regulating macrophage polarization is worth exploring. In the following sections, we summarize the broad spectrum of lncRNAs involved in macrophage polarization along with their target proteins and their possible roles in the regulation of respiratory diseases. An overview of these lncRNAs is given in Table 1 and Figure 1.

3 LncRNA-based regulation of macrophage polarization in chronic airway disease

Chronic airway diseases, characterized by airway inflammation and airway remodelling, are increasing as a cause of morbidity and mortality for all age groups and races across the world. The underlying molecular mechanisms involved in chronic inflammatory airway diseases have not been fully explored. Recently, accumulative evidence has shown that the novel regulatory mechanism underlying the action between lncRNAs and polarized macrophages plays a critical role in the pathophysiological processes of chronic airway diseases, particularly chronic obstructive pulmonary disease (COPD) and asthma.

3.1 Asthma

Asthma, characterized by reversible airflow limitation, airway inflammation and airway hyperresponsiveness, is mainly divided into two phenotypes: Th2 and non-Th2 (36, 37). Th2-asthma (i.e., eosinophilic asthma) is well established to play a leading role in asthma development, as more than half of asthma cases have a Th2 phenotype, where M2 macrophages predominantly secrete high levels of IL-13 and chemokines (e.g., CCL-17 and CCL-18), inducing airway eosinophil infiltration and mucus hypersecretion and contributing to lung function impairment and airway remodelling (38, 39). Non-Th2 asthma (i.e., neutrophilic asthma), by contrast, is characterized by neutrophil dominance airway inflammation that can be driven by M1 macrophages or Th1/Th17 lymphocytes and by the production of high levels of proinflammatory Th1 cytokines (e.g., IL-6, IL-1β, and TNF-α) and chemokines (e.g., CCL2 and CCL5) (36, 38, 40). Thus, patients with neutrophilic asthma have a poor response to corticosteroids and tend to develop severe or refractory asthma (41, 42). These results indicate that regulating the M1 and M2 macrophage phenotype balance would guide individualized therapy for different types of asthma. To date, several lncRNAs have been proven to play an important role in the pathogenesis of asthma by regulating M1/M2 macrophage polarization balance (Figure 2). We discuss them below.

Pei and his colleagues (20) found that there was high expression of lncRNA *AK085865* in BAL cells and lung tissues from dermatophagoides farinae protein 1 (Der f1)-induced asthmatic mice compared with PBS-induced mice. LncRNA *AK085865* expression was upregulated during the M1 to M2 transition (20). Upon *AK085865* knockdown, IgE-mediated eosinophilic airway inflammation and M2 macrophages were both decreased in asthmatic mice, which proved that *AK085865* knockout protected against allergic inflammation in mice by inhibiting M2 polarization. Furthermore, *AK085865* could promote the differentiation of innate lymphoid cells progenitor (ILCP) into type II innate immune lymphoid cells (ILC2s) and then augment type 2 inflammation (20). Therefore, knockout of the lncRNA *AK085865* may guide novel treatment for type 2 asthma. Xia et al. (17) conducted a differential lncRNA expression profile and found that lnc-*BAZ2B* was upregulated and that its expression was correlated with BAZ2B expression in the PBMCs of children with asthma. In addition, *lnc-BAZ2B* knockdown significantly inhibited the M2-specific marker expression of THP1-derived macrophages *in vitro*. Further mechanistic investigation showed that *lnc-BAZ2B* was an upstream regulator of BAZ2B and positively regulated the expression of BAZ2B by stabilizing its pre-mRNA, which promoted the transcription of IRF4 by binding H3K14ac-modified sites within the IRF4 gene and thus influenced the activation of M2 macrophages (17). This observation was consistent with a cockroach allergen extract (CRE)-induced asthma model, where BAZ2B knockdown inhibited pulmonary inflammation and mucus secretion by inhibiting M2 macrophage polarization *via* IRF4 (17). Taken together, we speculate that inactivation of *lnc-BAZ2B* could help prevent Th2 asthma aggravation. Another lncRNA reported to be upregulated during IL-4–induced M2 macrophage activation is *PTPRE-AS1* (25). Knockdown of *PTPRE-AS1* expression promoted transcription of M2 marker genes by targeting receptor-type tyrosine protein phosphatase (PTPRE), which promoted IL-4–induced activation of MAPK/ERK 1/2 signalling (25). Moreover, *PTPRE-AS1* plays a

TABLE 1 LncRNAs regulate M1/M2 polarization through targeting various adaptor proteins and transcription factors in respiratory diseases.

Type of diseases	LncRNAs	Cell types	Polarization	Targets	Function	Reference
Asthma	*AK085865*	Primary macrophages in the BALF from mouse	Promote M2	None	*AK085865* knockout ameliorates asthmatic airway inflammation.	Pei et al. (20)
	PTPRE-AS1	Bone marrow-derived macrophages (BMDMs) and RAW 264.7	Suppress M2	PTPRE/ ERK1/2	Protects against allergic inflammation.	Han et al. (25)
	Lnc-BAZ2B	PMA-induced human monocyte THP-1 cells	Promote M2	BAZ2B/ IRF4	Enhances the disease severity of allergic asthma.	Xia et al. (17)
Chronic obstructive pulmonary disease (COPD)	*MIR155HG*	GM-CSF induced peripheral blood mononuclear cells (PBMCs)	Promote M1, suppress M2	NF- κB/p65	Enhance pro-inflammatory cytokine release.	Li et al. (19)
Idiopathic Pulmonary Fibrosis (IPF)	*H19*	THP-1 macrophages and BMDMs	Promote M2	let-7a/c-Myc	Promotes myofibroblast differentiation.	Xiao et al. (26)
Pulmonary tuberculosis	*XIST*	RAW264.7 cells and human monocyte-derived macrophages (hMDMs)	Suppress M1	miR-125b-5p/A20/NF-κB	*XIST* downregulation suppress preexisting MTB infection.	Luo et al. (27)
	MIR99AHG	PBMCs, monocyte-derived macrophages (MDMs), BMDMs	Promote M2	hnRNPA2/ B1	Promote MTB growth.	Gcanga et al. (28)
Pneumonia	*GAS5*	HMDMs and PBMCs	Promote M1	miR-455-5p/SOCS3/ JAK2/ STAT3	Protect against childhood pneumonia.	Chi et al. (29)
Acute lung injury (ALI)/ Acute respiratory distress syndrome (ARDS)	*LincRNA-p21*	MH-S	Promote M1	NF-κB/p65	*LincRNA-p21* inhibition may protect against ALI.	Zhang et al. (21)
	MALAT1	Mouse BMDMs, human PBMCs and THP-1 macrophages and mouse alveolar macrophages	Promote M1	Clec16a	*Malat1* knockout ameliorated LPS-induced pulmonary inflammation and injury but led to severe lung fibrosis.	Cui et al. (30)
Lung cancer	*GNAS-AS1*	PMA-induced human monocyte THP-1 cells	Promote M2	miR-4319/ NECAB3	Facilitating the progression of NSCLC.	Li et al. (31)
	LARRPM	PMA-induced human monocyte THP-1 cells	Suppress M2 Promote M1	*LINC00240*/ CSF1	Suppressed LUAD cell proliferation, migration and invasion, and promoted apoptosis.	Li et al. (32)
	LINC01094	PMA-induced human monocyte THP-1 cells	Promote M2	SPI1/CCL7	Facilitating the progression of LUAD.	Wu et al. (33)
	PCAT6	PMA-induced human monocyte THP-1 cells	Promote M2	miR-326/ KLF1	Promoted metastasis and EMT process of NSCLC cells.	Chen et al. (34)
	SNHG7	THP-1 macrophages	Promote M2	CUL4A/ PTEN/ PI3K/Akt	Enhanced docetaxel resistance of LUAD cells.	Zhang et al. (35)

positive role in the regulation of PTPRE expression and protects against allergic inflammation by inhibiting M2 macrophage polarization, whether in a mouse model or in PBMCs from asthmatic patients, whereas it promotes M1-associated colitis functionally (25). Additionally, *PTPRE-AS1* can be used to distinguish asthma patients from normal individuals by receiver operating curve (ROC) analysis, implying that *PTPRE-AS1* exhibits potential as a biomarker in childhood asthma (25). During M2 macrophage activation, *PTPRE-AS1* directly bound to WDR5, regulating PTPRE-dependent signalling by modulating the

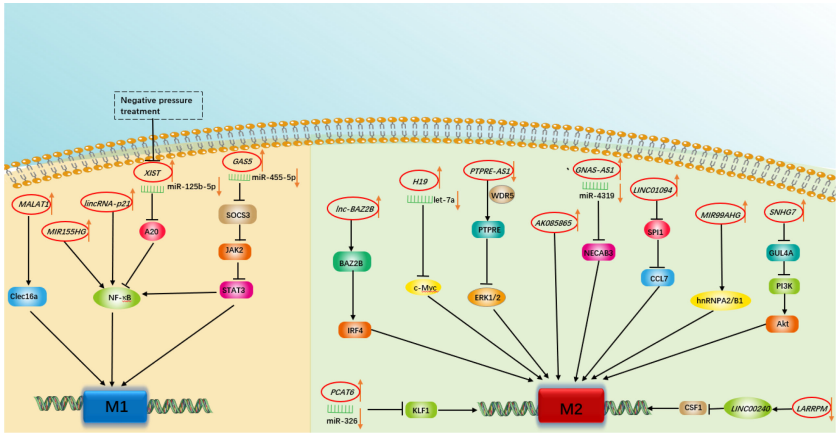

FIGURE 1
A schematic summary of the role of various long non-coding RNAs in modulating macrophage polarization involved in respiratory diseases.

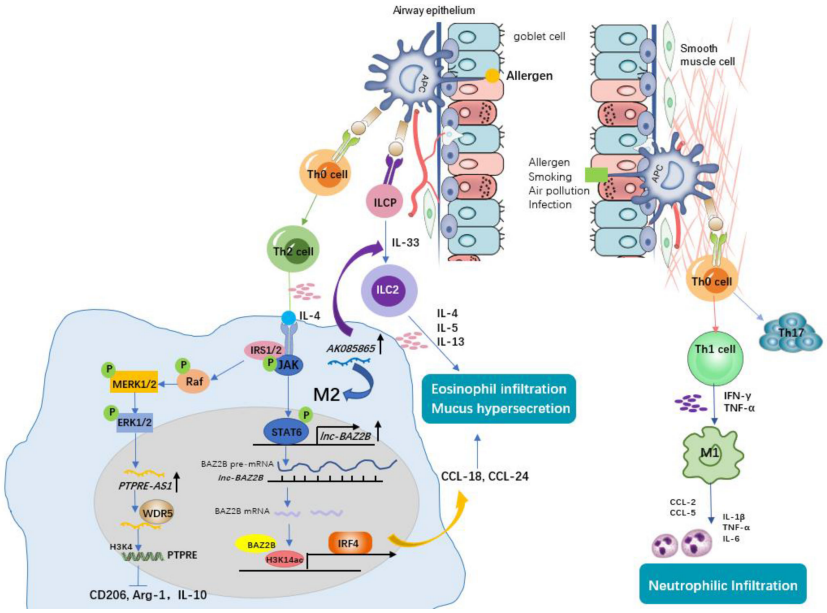

FIGURE 2
The role of macrophages and associated lncRNAs in allergic asthma. Antigen-presenting cells (APCs) identify allergens and initiate the allergic response. Under this condition, naïve CD4+ T cells differentiate into Th2 cells. Th2 cells secreting IL-4 induce M2 macrophage polarization. *Lnc-BAZ2B* promotes M2 macrophage activation by stabilizing BAZ2B pre-mRNA, thereby promoting IRF4 expression and chemokines secretion, leading to mucus hypersecretion and eosinophil infiltration in allergic children. *PTPRE-AS1* is selectively expressed in IL-4–stimulated M2 macrophages. *PTPRE-AS1* binds WDR5 directly, modulating H3K4me3 of the PTPRE promoter to regulate PTPRE-dependent signaling during M2 macrophage activation and protects against pulmonary allergic inflammation. LncRNA *AK085865* promotes M2 macrophages activation and M2 macrophages promote the differentiation of innate lymphoid cells progenitor (ILCP) into type II innate lymphoid cells (ILC2s), thus aggravate Type 2 immune response. Non-Th2 asthma (i.e., neutrophilic asthma), by contrast, is driven by M1 macrophages or Th1/Th17 lymphocytes through the production of high levels of proinflammatory Th1 cytokines (e.g., IL-6, IL-1β, and TNF-α) and chemokines (e.g., CCL2 and CCL5), contributing to neutrophilic infiltration and airway inflammation.

PTPRE promoter's H3K4me3. These results provide evidence to support the potential of lncRNA *PTPRE-AS1* to serve as a biomarker for type 2 inflammation remission.

Taken together, these data show that lncRNAs possess wonderful capability as biomarkers and therapeutic targets for asthma. This potential, however, remains far from being completely assessed. For example, most published lncRNAs are focused on regulating M2 macrophage-mediated type 2 inflammation, and identifying those lncRNA profiles that can regulate M1 macrophages is essential for confirming the potential of lncRNAs to identify asthma phenotype and determine the optimal treatment for each patient. Therefore, there are many opportunities for further research.

3.2 COPD

COPD is a preventable and treatable condition characterized by persistent airflow restriction and chronic airway inflammation (43). Cigarette smoking (CS) is the largest known risk factor for COPD (43). The phenotypic transformation of macrophages induced by CS or cigarette smoking extract (CSE) has been demonstrated in *in vivo* and *in vitro* studies of COPD (44–47). In addition to CS exposure, biomass ambient particulate matter (PM) has been indicated to be crucial for COPD pathogenesis by numerous epidemiological studies. Recent studies have shown that biomass fuel smoke (BMF) and PM2.5 facilitate macrophage polarization and activation *in vitro* (48, 49). Consistently, M1 and M2 macrophages have been detected in the lungs of COPD patients (46). Functionally, M1 macrophage-induced iNOS, IL-1β, IL-6, IL-8, and TNF-α contribute to oxidative stress and airway inflammation, while M2 macrophage-induced TGF-β facilitates epithelial–mesenchymal transition (EMT)-based small airway remodelling in COPD (46, 47, 50). In addition, M2 macrophage-induced TGF-β, Fizz1 and Ym1 are both involved in extracellular matrix dynamics, and arginine accelerates collagen synthesis, which leads to fibrosis (51). Therefore, the functional differentiation of macrophages is important for the specific pathology observed in COPD (Figure 3).

The MIR155 host gene (*MIR155HG*), an endogenous lncRNA located at chromosome 21q2 within a 13-kb length, is upregulated in M1 macrophages (52, 53), but *MIR155HG* promoter activity could be inhibited by M2 macrophage-secreted IL-10 in a STAT3-dependent manner (signal transducer and activator of transcription 3) *via* its Ets1 transcription factor-binding site (54). Li and his colleagues (19) recently found that *MIR155HG* was highly expressed in peripheral blood mononuclear cells of COPD patients compared with normal controls, and *MIR155HG* overexpression resulted in a significantly increased percentage of M1 macrophages accompanied by enhanced proinflammatory cytokine release (TNF-α, IL-1β and IL-12) as well as decreased M2 macrophage levels, whereas interference with *MIR155HG* expression reduced the ratio of M1/M2 macrophages (19).

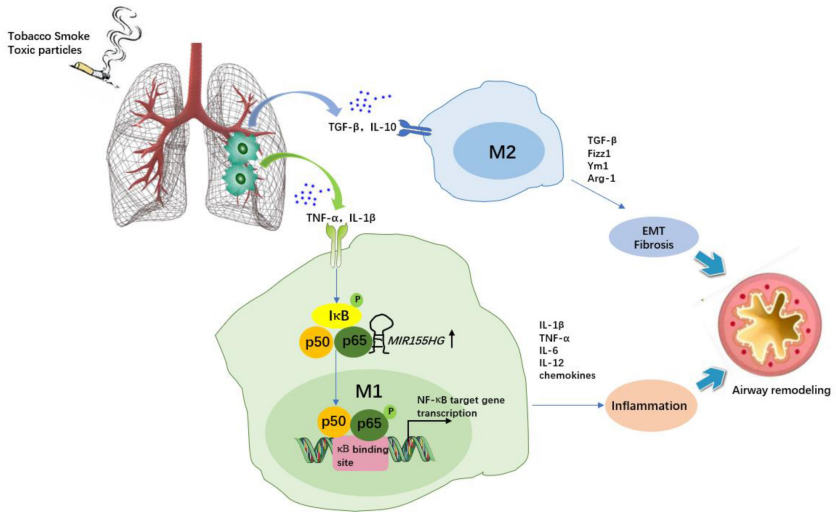

FIGURE 3
The role of macrophages and *MIR155HG* in chronic obstructive pulmonary disease (COPD). Tobacco smoke or toxic particles cause airway inflammation and airway remodelling. Macrophage polarization plays a key role. M1 macrophages secrete inflammatory cytokines and chemokines, promoting neutrophil recruitment and augmenting airway inflammation. *MIR155HG* indirectly regulate NF-κB signaling activity by interacting with the p65-p50 complex, resulting in M1 macrophages activation accompanied by enhanced proinflammatory cytokine release (TNF-α, IL-1β and IL-12). M2 macrophage-induced TGF-β, Fizz1 and Ym1 are involved in epithelial mesenchymal transformation (EMT) and extracellular matrix dynamics, and arginine accelerates collagen synthesis, which leads to fibrosis.

Mechanistically, the NF-κB protein p65 could combine with the upstream transcription site of *MIR155HG*, suggesting that *MIR155HG* was a direct NF-κB target gene contributing to airway inflammation in COPD (Figure 3). Another report also showed increased expression of *MIR155HG* in lung tissues of smokers with non-COPD or COPD compared to healthy controls, particularly in COPD patients (55). Therefore, targeting *MIR155HG* to reduce M1 differentiation may be beneficial for COPD relief. On the other hand, *MIR155HG* is also known for promoting cell migration, proliferation, and invasion in multiple cancers, including non-small cell lung cancer (NSCLC), where M2d macrophages (TAMs) play a key role in tumorigenesis (56, 57). This might contradict the regulatory role of *MIR155HG* in COPD. The exact effect of targeting *MIR155HG* to shift the macrophage phenotype in COPD complicated with lung cancer should be considered. Indeed, macrophage polarization is a complex and dynamic evolutionary process that is affected by various environmental stimuli. These findings offer multiple chances to further explore the role of *MIR155HG* in respiratory diseases.

3.3 Cystic fibrosis

CF is a major disease associated with bronchiectasis and is caused by a mutation in a gene called cystic fibrosis transmembrane conduction regulator (CFTR), whose dysfunction gives rise to mucus retention, chronic infection, and airway inflammation (58). Human monocytes, alveolar macrophages, and monocyte-derived macrophages (MDMs) express CFTR protein, and CFTR dysfunction in macrophages is related to augmented airway inflammation, increased mucus cells and mucus blockage, and increased lethal pneumonia, emphasizing the critical role of macrophages in promoting CF (59–61). Most importantly, Tarique et al. (62) reported that the polarization of anti-inflammatory, alternately activated M2 macrophages is CFTR dependent. In addition, MDMs from healthy controls treated with a CFTR inhibitor (CFTRInh-172) were incapable of polarizing into anti-inflammatory M2 macrophages, suggesting that understanding the link between CFTR dysfunction and M2 polarization may provide new therapeutic targets for CF (62). On the other hand, growing evidence supports that lncRNAs regulate CF. For example, McKiernan et al. (63) found that X inactivation-specific transcript (*XIST*) and *MALAT1* are differentially expressed in bronchial brushings of CF patients. Balloy et al. (64) also found that in *Pseudomonas aeruginosa* (PA)-infected CF bronchial epithelial cells, the expression of several lncRNAs, such as maternal expression gene 9 (*MEG9*) and bladder cancer-associated transcription 1 (*BLACAT1*), was downregulated. In addition, lncRNA *BGas* has been shown to be associated with CF by targeting and regulating CFTR directly (65). Unfortunately, current studies on the roles of lncRNA-mediated macrophage polarization in CF are limited and require further investigation. If macrophage function can be recovered by rectifying CFTR dysfunction *via* lncRNAs, lncRNAs will be promising in the control of the onset and progression of CF.

4 LncRNA-based regulation of macrophage polarization in interstitial lung disease

4.1 Idiopathic pulmonary fibrosis

IPF is a lethal, chronic, progressive interstitial lung disease characterized by the deposition of fibroblasts and collagen in the lung interstitum, resulting in destruction and fibrotic remodelling of lung tissue (66). M2 macrophages induce the differentiation of the myofibroblast phenotype by releasing the fibrogenic cytokine TGF-β1, contributing to the deposition of extracellular matrix, suggesting a key role in IPF (51, 67). A recent study showed that decreased M2 macrophage infiltration in the lung significantly protected mice from bleomycin-induced lung injury and fibrosis. These IPF pathogenic factors were further reported to be related to lncRNAs. For instance, Xiao et al. (26) found elevated *H19* expression levels and decreased let-7a expression levels in lung tissues from arsenite-induced pulmonary fibrosis mice. Mechanistically, *H19* acts as a ceRNA for let-7a regulating c-Myc, resulting in lower expression of M2 macrophage markers (CD206, Arg1, and TGF-β1) and lower fibrosis-related markers (p-SMAD2/3, SMAD4, α-SMA and collagen I) (26). Similarly, in the sera of arseniasis patients, *H19* levels were higher and let-7a levels were lower than those in healthy controls (26). These observations elucidate the possible mechanism of pulmonary fibrosis induced by arsenic exposure and provide a theoretical basis for its treatment. In addition to the TGF-β/Smad pathways, the macrophage-based pathways implicated in fibrosis also include Wnt/beta-catenin and PI3K-AKT-mTOR, which can be regulated by a number of lncRNAs, such as *GAS5* and *LOC102551149* (68–70), in other fibrosis-related diseases. Obviously, more investigations are required to understand whether these lncRNAs are pivotal regarding the regulation of macrophage polarization in IPF.

4.2 Sarcoidosis

Sarcoidosis is a granulomatous disease of unknown aetiology. Macrophages and CD4+ T cells play a key role in granuloma formation (71). A previous study showed that the proportion of M1 macrophages (defined as CD40 cell surface expression) in the pulmonary lumen of patients with sarcoidosis is significantly increased, while the proportion of M2 macrophages (defined as CD163 cell surface expression) tends

to increase in nonspecific interstitial pneumonia (NSIP), IPF, and hypersensitivity pneumonia (HP) (72). In contrast, Shamaei and his colleagues reported enhanced CD163 staining in granulomas of patients with sarcoidosis compared with tuberculous granulomas (73). Using a one-sided M2 phenotype marker and different sample types may explain the contradiction between the above two studies. The mechanism of transition from acute inflammation (granuloma) to the fibrotic stage is particularly complex. Increasing evidence suggests that granuloma formation is supported by Th1/M1 immune polarization due to exaggerated TNF-α and INF-γ. In contrast to the acute phase of sarcoidosis, the chronic fibrotic disease state is associated with M2/Th2 polarization (74, 75). Thus, a key point in sarcoidosis therapeutics is restoring the M1/Th1 (inflammation) and M2/Th2 (fibrosis) balance. To date, the expression profile and functional studies of lncRNAs in sarcoidosis remain unknown. Considering the ability of lncRNAs to regulate macrophage polarization and participate in immune regulation, the diagnostic and therapeutic role of lncRNAs in sarcoidosis might be an important area of research.

4.3 Connective tissue disease-associated ILD

Approximately one-third of individuals with ILD have associated connective tissue disease (CTD) (76). The CTD demonstrating features of ILD include rheumatoid arthritis (RA), systemic lupus erythematosus (SLE), dermatomyositis (DM) and polymyositis (PM), systemic sclerosis (SSc), Sjogren's syndrome (SS), and mixed connective tissue disease (MCTD) (77). RA-ILD is the most common type (78). RA is a chronic inflammatory autoimmune disease characterized by massive immune cell infiltration, pannus formation and destruction of cartilage and bone. Macrophages play a crucial role in the pathogenesis of RA, and the degree of synovial macrophage infiltration, particularly elevated M1 macrophages, correlates with clinical disease activity and severity in RA patients (79–81). Zhu et al. (82) found that lncRNA *H19* is upregulated in RA patients and arthritic mice. Additionally, *H19* overexpression promoted M1 macrophage polarization along with increased expression of M1 macrophage-related factors and aggravated arthritis in mice by upregulating KDM6A expression (82). Therefore, targeting *H19* may develop into a novel therapy for RA by inhibiting M1 macrophage polarization. As described previously, *H19* promotes myofibroblast differentiation in PF by regulating M2 polarization (26). It remains to be known whether *H19* is involved in the progression of pulmonary manifestations in RA by altering the macrophage phenotype.

In addition, the role of macrophage polarization and plasticity in SLE and DM/PM development has also been explored in several studies (83–85). Despite the emerging role of lncRNAs in autoimmune diseases, whether their regulatory role in these diseases is through the induction of macrophage polarization remains less understood and requires further exploration.

5 LncRNA-based regulation of macrophage polarization in infectious lung disease

5.1 Tuberculosis

Tuberculosis (TB) continues to be a major public health problem, with over 10 million new cases and 1.5 million deaths annually (86). *Mycobacterium tuberculosis* (MTB) is the most common pathogen causing TB and has high drug resistance (87). Macrophages play a crucial role in the host immune response and infection outcome post-TB infection (88). In addition, antibacterial activity and cytokine production during the formation of tuberculosis granuloma are usually concomitant with the transformation of the macrophage phenotype from M1 to M2 (88). Accordingly, MTB inhibit the development of the M1 phenotype and reprogram macrophages towards the M2 phenotype for better survival in the host, resulting in increased occurrence and development of pulmonary TB (89). It was proven that the fusion of lysosomes with TB-containing phagosomes and the upregulation of iNOS were caused by M1 polarization (90). Additionally, the TLR2/MyD88 signalling pathway associated with M1 macrophage activation plays a key role in host defence during MTB infection (91). Thus, inhibition of the intracellular survival of MTB may be orchestrated by M1 macrophage activation, which would facilitate pathogen clearance. Additionally, the protective effect of proinflammatory/M1 macrophages on MTB infection has been confirmed in many clinical studies (92). Although the administration of antibiotics has been widely used to prevent and treat TB, the persistence of latent infections and the emergence of resistance urgently require the development of new drugs and treatments. Therefore, controlling macrophage polarization is expected to improve TB progression.

Recent studies have identified ncRNA profiles and explored the functional role of lncRNAs such as *MEG3* and *NEAT1* during MTB infection, further implicating their potential in the immune response (93–95). Two lncRNAs are functionally related to polarized macrophages during MTB infection. For example, Luo et al. (27) discovered that *XIST* expression was upregulated in RAW264.7 cells and human monocyte-derived macrophages (hMDMs) after MTB infection and that its expression was regulated by ESAT-6, an important determinant of MTB virulence. Functionally, *XIST* serves as a competing endogenous RNA targeting miR-125b-5p, a miRNA that promotes M1 macrophage polarization by modulating A20/NF-κB signalling. A previous study also supported the conclusion that the expression of A20 was upregulated in MTB-infected

macrophages, thereby inhibiting the NF-κB pathway and regulating the immune response after MTB infection (96). The regulatory network of the *XIST*/miR-125b-5p/A20/NF-κB axis has also been proven to be a molecular mechanism of negative pressure treatment for MTB infection (27). Another recent study reported that *MIR99AHG* is upregulated in M2 (IL-4/IL-13)-polarized mouse and human macrophages but downregulated after clinical MTB HN878 strain infection and in PBMCs from active TB patients (97). Knockdown of *MIR99AHG* using antisense oligonucleotides (ASOs) significantly reduced intracellular MTB growth, necrosis, and proinflammatory cytokine production in mouse and human macrophages, as well as reduced mycobacterial burden in the lungs of mice (28). Thus, as an addition to existing antibiotics, *MIR99AHG* may be a potential target for host-directed TB drug therapy.

5.2 Pneumonia

Pneumonia is the leading cause of death for children under the age of 5 (98). Particularly, after the outbreak of severe acute respiratory syndrome coronavirus type 2 (SARS-CoV-2) in Wuhan in December 2019, approximately 20-30% of patients hospitalized for COVID-19-associated pneumonia required intensive care for respiratory support (99, 100). At present, there are still difficulties in clinical treatment. Given that morbidity and mortality are associated with excessive inflammation, it is necessary to better understand the immunological basis of pneumonia in patients to better identify therapeutic targets. It has been shown that macrophages play an important role in pneumonia and polarize into different phenotypes when responding to various pathogens. For instance, macrophages are polarized towards an M1 phenotype in the early stage of bacterial infection and serve as a prompt to eliminate pathogens (101). As described by Li et al. (102), the M1 phenotype ($iNOS^+$) was increased and the M2 phenotype ($CD206^+$) was decreased after *Klebsiella pneumoniae*-induced pneumonia. High expression of IL-10 and a high population of M2-polarized macrophages play important roles in the production of lung consolidation in *Mycoplasma hyopneumoniae* infection (103). In SARS-CoV-2 infection, M1 macrophage-derived inflammatory cytokines, such as TNF-α and IL-1β, have been confirmed in the respiratory tract and are closely correlated with increased disease severity. M2 macrophages are thought to play an important role in the process of fibrosis (104–106). In addition, Shibata et al. reported that alveolar macrophages could acquire the M2 phenotype at Day 8 after RSV infection (107). During cryptococcal infection, the polarization status of pulmonary macrophages changed with time: at 1 week after infection, the pulmonary M2 macrophages were strongly polarized, but at 3 and 4 weeks after infection, the overall polarization of the macrophages shifted to M1. These studies suggest that the polarization of macrophages is phenotypic and functional plasticity shifts in response to changes in external stimuli. Targeting macrophage polarization and reinforcing phenotypic adaptation to the microenvironment may hold great promise for the treatment of pneumonia.

lncRNAs that regulate macrophage polarization may affect pneumonia. As an example, Chi et al. (29) found that *GAS5* mRNA expression was significantly decreased in hMDMs from children with pneumonia and this is accompanied by increased M2 phenotype macrophages compared with the control group, and *GAS5* overexpression promoted macrophage polarization from M2 to M1 in children with pneumonia *via* the miR-455-5p/SOCS3/JAK2/STAT3 axis, indicating its protective role in pneumonia in children. Indeed, the role of *GAS5* in the pathogenesis of pneumonia has been confirmed by emerging evidence (108–110). In addition, downregulation of lncRNA *GAS5* can decrease ACE2 expression by increasing miR-200c-3p and promote apoptosis of A549 cells, thus promoting the progression of acute respiratory distress syndrome (ARDS) (28, 111). It would be exciting if overexpressing lncRNA *GAS5* reduces the chance of death in severe viral pneumonia patients caused by ARDS.

5.3 ALI/ARDS

Acute lung injury (ALI) is a typical pathological feature of ARDS, and is characterized by the secretion of high levels of proinflammatory factors and the triggering of the inflammatory cascade, where alveolar macrophages (AMs), especially M1 macrophages, have been shown to be the major component (112, 113). Pulmonary fibrosis is the advanced stage of ALI/ARDS and is caused by fibroblast proliferation and excessive collagen deposition (12). In this phase, M2 phenotype macrophage-derived TGF-β and IL-10 play a leading role. Therefore, controlling macrophage polarization is expected to ameliorate the progression of ALI/ARDS. Several lncRNAs have been shown to be involved in inflammation-triggered ALI (Figure 4). For example, *lincRNA-p21* levels were highly expressed in AMs from LPS-induced ARDS mice in a time-independent manner, and *lincRNA-p21* inhibition reversed LPS-induced M1 activation and attenuated LPS-induced lung injury (21). Further experiments showed that *lincRNA-p21* overexpression promoted p65 nuclear translocation and NF-κB activity, indicating the underlying application of *lncRNA-p21* for ADRS therapy *via* NF-κB/p65-mediated pathways. Similar to *lincRNA-p21*, lncRNA *MALAT1* has the capacity to promote proinflammatory M1 activation and inhibit alternative M2 activation (30). Knocking out *MALAT1* reduced LPS-induced systemic and pulmonary inflammation and injury, but more severe bleomycin-induced pulmonary fibrosis and M2 alveolar macrophage augmentation were observed in mice (30). Mechanistically, *MALAT1* knockdown may promote

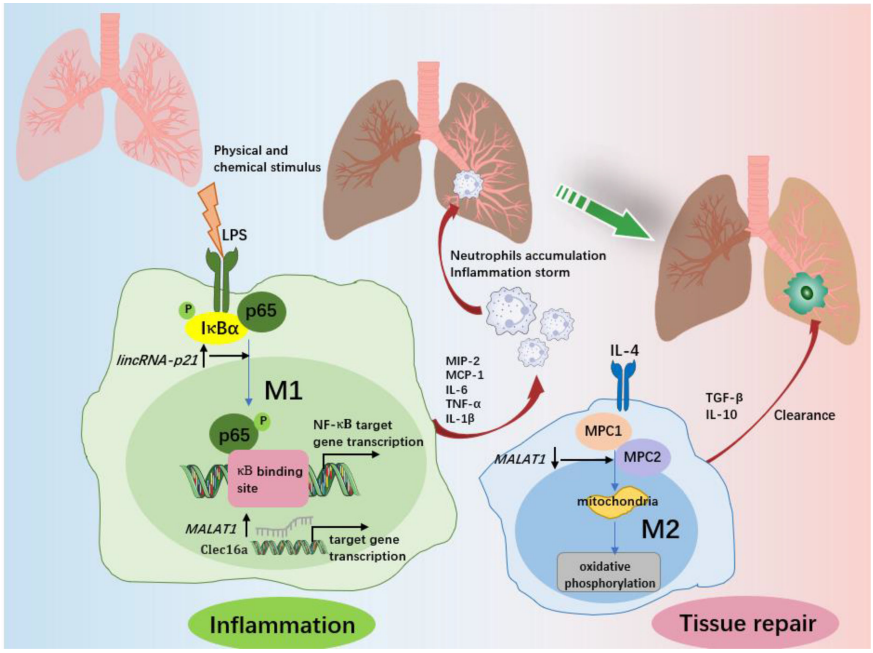

FIGURE 4
The role of macrophages and associated lncRNAs in ALI/ARDS. In response to various physicochemical stimuli, M1 macrophages release various proinflammatory cytokines at the site of inflammation and then recruit neutrophils from the circulation into the lung and alveolar spaces. Excess accumulation of proinflammatory factors and neutrophils promotes the progression of inflammation and lung injury. *LincRNA-p21* contributes to LPS-induced M1 activation by promoting the ubiquitination of IκBα, activating NF-κB as well as promoting p65 nuclear translocation. *MALAT1* promotes the expression of C-type lectin domain family 16, member A (Clec16a) in nucleus, which is required for the proinflammatory activation of M1 macrophages. After the elimination of the trigger, macrophages changed from the M1 to the M2 phenotype, and ALI/ARDS entered the recovery stage. M2 macrophages play an important role in inflammation resolution and lung tissue repair by limiting the levels of proinflammatory cytokines and enhancing the production of anti-inflammatory cytokines. *MALAT1* regulation of M2 activation of macrophages is dependent on glucose metabolism. Both mitochondrial pyruvate carriers (MPC)1 and MPC2 are upregulated by IL-4. IL-4 downregulates *MALAT1* expression, and *MALAT1* knockdown enhances the expression of MPC1 and MPC2, therefore regulating glucose-derived mitochondrial oxidative phosphorylation (OxPhos), which is essential to M2 macrophage polarization.

mitochondrial pyruvate carriers (MPCs) and their mediated glucose-derived oxidative phosphorylation (OxPhos) induced by IL-4, thereby enhancing the M2 macrophage phenotype (114). This finding supports the role of *MALAT1* in promoting the progression of ALI. In addition, the silencing of *MALAT1* can reduce the inflammatory response in lung injury as well as the prevalence of cytokine storms in SARS-CoV-2 patients (115). It would be promising if targeting lncRNA *MALAT1* expression lowers the risk of COVID-19-related ARDS.

6 LncRNA-based regulation of macrophage polarization in lung cancer

Lung cancer, the most common cancer and the leading cause of cancer-related deaths, is mainly divided into two types: non-small cell lung cancer (NSCLC) and small cell lung cancer (SCLC) (116). NSCLC accounts for approximately 85% of lung cancer and is classified by histopathology as adenocarcinoma, squamous cell carcinoma and large cell carcinoma (117). Although molecular targeted therapies and immunotherapies are available for lung cancer patients, recurrence and progression due to drug resistance remain persistent problems (118). Currently, the modulation of immune responses in lung cancer has not been fully elucidated. Tumour-associated macrophages (TAMs), which are most likely of the M2 phenotype and have anti-inflammatory properties, play an important role in stimulating tumour cell proliferation and invasion as well as inducing tumour angiogenesis and lymphangiogenesis (119). Furthermore, M1 macrophages also play a key role in tumorigenesis. In the chronic inflammatory environment, M1 macrophages can not only induce the carcinogenic process by secreting proinflammatory mediators for a long time but also directly kill tumour cells and antagonize the growth of established tumours by stimulating the antitumour immune response (120). In this context, driving TAM polarization to modulate immune responses could be a novel therapeutic approach for lung cancer. A recent study discovered the functional relevance of lncRNAs in cancer immune

regulation and TME, contributing to the progression and clinical outcome of a variety of cancers, including lung cancer (121, 122). Here, we discuss specific lncRNAs that regulate polarized TAMs in lung cancer.

Li et al. (31) reported that lncRNA *GNAS-AS1* was highly expressed in TAMs, human NSCLC cell lines and tumour tissues. Moreover, high *GNAS-AS1* expression predicts lower overall survival and metastasis-free survival of NSCLC patients (31). The oncogenic effect of *GNAS-AS1* is achieved by promotion of M2 polarization *via* directly inhibiting miR-4319, which can target the expression of N-terminal EF-hand calcium binding protein 3 (NECAB3) (31). Downregulation of NECAB3 in tumour cells has been shown to suppress tumorigenicity and play a crucial role in cancer development (123).

LncRNA *SNHG7* was highly expressed in docetaxel-resistant cells, and exosomal SNHG7 enhanced docetaxel resistance in lung adenocarcinoma (LUAD) cells by inducing autophagy and promoting M2 macrophage polarization (35). It was shown that lncRNA *SNHG7* activated the PI3K/AKT pathway by recruiting CUL4A to promote PTEN ubiquitination and thereby mediating macrophage M2 polarization (35). These discoveries implied that *SNHG7* may be a promising target for alleviating docetaxel resistance in LUAD.

Chen et al. (34) observed a higher expression of lncRNA *PCAT6* in human NSCLC cells, and siRNA-mediated knockdown of *PCAT6* inhibited the viability, migration, and invasion of NSCLC cells. A direct interaction was revealed by luciferase reporter assays between miR-326 and *PCAT6*. Kruppel-like Factor 1 (KLF1), an important participant in the process of macrophage polarization (124), is a direct target of miR-326. Consequently, *PCAT6* can activate KLF1 by sponging miR-326, induce macrophage M2 polarization and further promoting metastasis and EMT in NSCLC cells.

Wu et al. (33) demonstrated that CCL7 was abundantly expressed in LUAD and was associated with increased TAM infiltration. Additionally, CCL7 knockdown suppresses chemotactic migration and M2 macrophage polarization. Employing RNA immunoprecipitation and RNA pull-down assays, we found that *LINC01094* binds to SPI1 and promotes its nuclear translocation and that a luciferase reporter assay revealed an interaction between SPI1 and CCL7 (33). Therefore, *LINC01094* may be the cause of the aggregation of M2 macrophages and the spread of tumour cells caused by the upregulation of CCL7 in LUAD. However, the exact role of *LINC01094* in macrophage infiltration and LUAD development requires further investigation.

Another assessed lncRNA in lung cancer is lncRNA *LARRPM*. Li et al. (32) reported lower expression of *LARRPM* in LUAD tissues, which was negatively associated with poor survival and advanced stage in patients with LUAD. Further experiments showed that *LARRPM* could inhibit the proliferation, migration and invasion of LUAD cells, promote cell apoptosis, and inhibit M2 polarization and infiltration of macrophages by epigenetically regulating *LINC00240* and CSF1 (32). These results provide evidence of the potential utility of *LARRPM* as a prognostic biomarker and a therapeutic target for LUAD.

Collectively, these studies not only underscore the role of lncRNA-based TAM polarization in the pathogenesis of lung cancer but also identify lncRNAs as biomarkers for designing individualized treatment for patients with lung cancer.

7 Discussion

Macrophage polarization has functional significance in respiratory diseases, including nonneoplastic conditions and neoplastic conditions, by regulating inflammation, fibrosis, immune response, and tumorigenesis. Targeting macrophage phenotypic transformation may be a potential therapeutic strategy for respiratory diseases. With the rapid development of bioinformatics and high-throughput sequencing, diverse significant functional roles of lncRNAs in human diseases have been gradually revealed. A large number of studies have illustrated that lncRNAs are fundamental factors in genomic imprinting, chromatin modification, posttranscriptional regulation and transcription, splicing and modification and are involved in gene expression regulation at almost every stage in various diseases (125, 126). Recently, different lncRNAs have emerged as key regulators in the regulation of M1/M2 polarization. Given the important role of macrophage polarization in the development of respiratory diseases, the use of lncRNA-mediated M1/M2 polarization opens up new possibilities for the control of respiratory diseases.

Macrophage polarization plays a significant role in respiratory diseases, which are heterogeneous and dynamically evolving. For instance, M1 macrophages cause pulmonary inflammation in the early stages of ALI/ARDS, and M2 macrophages induce tissue repair and pulmonary fibrosis in the late stages. Th2-asthma is related to augmented M2 macrophages, while non-Th2 asthma is related to M1 macrophages. As described above, differentially expressed lncRNAs have the potential to serve as diagnostic or prognostic biomarkers of various respiratory diseases due to their abilities to regulate macrophage polarization. For example, several lncRNAs, including *AK085865*, *PTPRE-AS1*, and *lnc-BAZ2B*, have been demonstrated to be biomarkers for M2 macrophage-mediated Th2-asthma. *LARRPM* expression in lung tissues is negatively associated with advanced stage and poor survival in patients with lung cancer due to its ability to inhibit M2 polarization. Thus, lncRNAs that regulate macrophage polarization may be helpful indicators of respiratory disease stage and progression.

M1/M2 macrophage polarization is mediated by lncRNAs which directly target or sponge miRNAs to affect identified macrophage regulators and mediate respiratory disease

development; therefore, targeting lncRNAs may become an effective therapeutic tool. For instance, the use of siRNA targeting *MIR155HG* reduced proinflammatory cytokines by shifting PBMCs of COPD patients from the M1 to the M2 phenotype. CRISPR/Cas9-mediated deletion of lncRNA *AK085865* ameliorates airway inflammation in asthmatic mice by inhibiting M2 macrophage polarization. The use of ASOs to knock out *MIR99AHG* inhibited the activation of M2 macrophages and significantly reduced the growth of MTB as well as the production of proinflammatory cytokines in the lungs of mice. In lung cancer, exosomal SNHG7 enhances docetaxel resistance in LUAD cells by inducing autophagy and promoting the polarization of M2 macrophages, which may provide clues for ways to reduce the likelihood of chemotherapy failure in lung cancer. In other words, using siRNA to downregulate *SNHG7* expression in exosomes that promote drug resistance is conducive to maintaining or recovering the sensitivity of cancer cells to chemotherapy drugs. To date, the role of lncRNA-mediated macrophage polarization in CF, sarcoidosis and CTD-ILD has not been explored. This could be a promising target for future exploration and verification.

Currently, RNA-based drugs have been approved for a variety of disease conditions, and many miRNA drug candidates are in clinical trials (i.e., TargomiR, an miR-16 mimic tested in mesothelioma, and Miravirsen, an miR-122 antagonist tested in HCV infection) (127–129). However, lncRNA-based therapy is still in its infancy, whether in animal studies or clinical trials. Direct delivery of lncRNA drugs to the lungs by inhalation is the most effective way to reduce systemic adverse effects. Gu et al. (126) demonstrated that intranasal delivery of shRNA lentivirus against *TUG1* blocks CS-induced inflammation and remodelling in a COPD mouse model. However, the stability of lncRNAs and delivery systems continues to present clinical challenges (130). In addition, the same lncRNA may mediate various biological processes by regulating multiple genes concurrently in response to different stimuli. The worry is that such indirect and complicated regulatory mechanisms make it difficult to target lncRNAs for therapeutic purposes. As an example, lncRNA *H19* promotes M1 macrophage polarization and aggravates arthritis by upregulating KDM6A expression (82), which contradicts the role of *H19* in promoting M2 polarization through the *H19*-miR let-7a/c-Myc axis in IPF. But for patients with rheumatoid arthritis complicated with IPF, targeting *H19* seems beneficial for disease progression. Therefore, compared with strategies targeting macrophage regulators or miRNAs, lncRNA-targeted therapy acting on polarization seems to be more difficult to implement and requires special precautions to minimize off-target adverse effects. Applying lncRNAs to drive effective reprogramming of macrophage polarization under specific disease conditions requires more effort. Most importantly, altering macrophage polarization might benefit a particular disease but exacerbate other coexisting diseases due to its heterogeneity and plasticity. For instance, *MALAT1*-mediated M1 polarization is involved in different pulmonary processes and plays opposite roles in lung injury and pulmonary fibrosis. *PTPRE-AS1* deficiency exacerbates CRE allergen–induced lung inflammation and attenuates colitis in an acute DSS model by promoting M2 macrophages.

Despite promising in indicating the diagnosis, prognosis, or treatment of respiratory diseases, there are several obstacles to overcome regarding the clinical application. First, some lncRNAs such as *MIR155HG*, *lnc-BAZ2B*, and *LARRPM* studied in asthma, COPD, and lung cancer studies are based on a small sample size at present. Validation studies on larger sample numbers from multi-centers are required to identify those lncRNAs that could identify different disease stages and phenotypes of diseases, which might improve current disease diagnostic strategies and achieve individualized treatment. Furthermore, lncRNAs with therapeutic potential for certain respiratory diseases such as MTB, ALI/ARDS, and IPF are only being studied in animal models or cell lines. Further research is required to determine whether lncRNA can be effectively used in clinical settings. Second, as the disease progresses, the polarization of macrophages changes dynamically. For example, M1 macrophages cause pulmonary inflammation in the early stages of ALI/ARDS, and M2 macrophages induce tissue repair and pulmonary fibrosis in the late stages. Currently, we have only a very limited understanding of the regulation mechanisms between lncRNAs and highly heterogeneous macrophages. More studies should be done to clarify the role of lncRNAs in the progression of respiratory diseases *via* macrophage polarization. Third, the stability of lncRNAs in specimens needs more attention as it may be affected by the detection environment and specimen quality, storage time, and temperature. Besides the stability of lncRNAs, it is also imperative to address off-target adverse effects in order to optimize their efficacy. Finally, lncRNAs' economic benefits and broad applicability should also be considered.

Conclusion

The present study suggests that manipulation of lncRNA expression can be used as a novel modality to regulate macrophage polarization, thereby regulating inflammation, fibrosis, immune response, and tumorigenesis in the respiratory system. Accumulating evidence has demonstrated that lncRNAs have the potential to become diagnostic or prognostic biomarkers and therapeutic targets in COPD, asthma, lung cancer, IPF, pneumonia, and ALI/ARDS. However, explorations of the roles of lncRNAs related to macrophage polarization in CF, sarcoidosis, and CTD-ILD are still lacking. Further confirmatory studies are essential to broaden the lncRNA horizon for the proper elucidation of novel lncRNAs that are likely to emerge as important regulators of macrophage polarization in broad respiratory diseases. Hopefully, lncRNA discovery will complement macrophage-

centered diagnostic and therapeutic strategies allowing them to be used in the clinic more quickly.

Author contributions

YY, WW, QW, and JK designed, supervised, and critically revised the manuscript. XQ drafted the manuscript. YD, DW and AZ did the reference collection. All authors contributed to the article and approved the submitted version.

Funding

This study was supported by the National Natural Science Foundation of China (Grant number: 82270046).

Conflict of interest

The authors declare that the research was conducted in the absence of any commercial or financial relationships that could be construed as a potential conflict of interest.

Publisher's note

All claims expressed in this article are solely those of the authors and do not necessarily represent those of their affiliated organizations, or those of the publisher, the editors and the reviewers. Any product that may be evaluated in this article, or claim that may be made by its manufacturer, is not guaranteed or endorsed by the publisher.

References

1. Levine SM, Marciniuk DD. Global impact of respiratory disease: What can we do, together, to make a difference? *Chest* (2022) 161(5):1153–54. doi: 10.1016/j.chest.2022.01.014

2. GBD 2017 Causes of Death Collaborators. Global, regional, and national age-sex-specific mortality for 282 causes of death in 195 countries and territories, 1980–2017: A systematic analysis for the global burden of disease study 2017. *Lancet* (2018) 392:1736–88. doi: 10.1016/S0140-6736(18)32203-7

3. Hirsch FR, Scagliotti GV, Mulshine JL, Kwon R, Curran WJ, Wu YL, et al. Lung cancer: Current therapies and new targeted treatments. *Lancet* (2017) 389 (10066):299–311. doi: 10.1016/S0140-6736(16)30958-8

4. WHO. *Coronovirus (COVID-19) dashboard*. World Health Organization (Accessed February 9, 2022).

5. Ross EA, Devitt A, Johnson JR. Macrophages: The good, the bad, and the gluttony. *Front Immunol* (2021) 12:708186(undefined). doi: 10.3389/fimmu.2021.708186

6. Mosser DM, Edwards JP. Exploring the full spectrum of macrophage activation. *Nat Rev Immunol* (2008) 8(12):958–69. doi: 10.1038/nri2448

7. Tarique AA, Logan J, Thomas E, Holt PG, Sly PD, Fantino E. Phenotypic, functional, and plasticity features of classical and alternatively activated human macrophages. *Am J Respir Cell Mol Biol* (2015) 53(5):676–88. doi: 10.1165/rcmb.2015-0012OC

8. Kittan NA, Allen RM, Dhaliwal A, Cavassani KA, Schaller M, Gallagher KA, et al. Cytokine induced phenotypic and epigenetic signatures are key to establishing specific macrophage phenotypes. *PloS One* (2013) 8(10):e78045. doi: 10.1371/journal.pone.0078045

9. Gordon S, Martinez FO. Alternative activation of macrophages: mechanism and functions. *Immunity* (2010) 32(5):593–604. doi: 10.1016/j.immuni.2010.05.007

10. Shapouri-Moghaddam A, Mohammadian S, Vazini H, Taghadosi M, Esmaeili SA, Mardani F, et al. Macrophage plasticity, polarization, and function in health and diseases. *J Cell Physiol* (2018) 233(9):6425–40. doi: 10.1002/jcp.26429

11. Mantovani A, Sozzani S, Locati M, Allavena P, Sica A. Macrophage polarization: tumor-associated macrophages as a paradigm for polarized M2 mononuclear phagocytes. *Trends Immunol* (2002) 23(11):549–55. doi: 10.1016/s1471-4906(02)02302-5

12. Arora S, Dev K, Agarwal B, Das P, Syed MA. Macrophages: Their role, activation and polarization in pulmonary diseases. *Immunobiology* (2018) 223(4-5):383–96. doi: 10.1016/j.imbio.2017.11.001

13. Sedighzadeh SS, Khoshbin AP, Razi S, Keshavarz-Fathi M, Rezaei N. A narrative review of tumor-associated macrophages in lung cancer: Regulation of macrophage polarization and therapeutic implications. *Transl Lung Cancer Res* (2021) 10(4):1889–916. doi: 10.21037/tlcr-20-1241

14. Ransohoff JD, Wei YN, Khavari PA. The functions and unique features of long intergenic non-coding RNA. *Nat Rev Mol Cell Biol* (2018) 19(3):143–57. doi: 10.1038/nrm.2017.104

15. Qiao X, Hou G, He YL, Song DF, An Y, Altawil A, et al. The novel regulatory role of the lncRNA-miRNA-mRNA axis in chronic inflammatory airway diseases. *Front Mol Biosci* (2022) 9:927549(undefined). doi: 10.3389/fmolb.2022.927549

16. Tang W, Shen Z, Guo J, Sun SH. Screening of long non-coding RNA and TUG1 inhibits proliferation with TGF-β induction in patients with COPD. *Int J Chron Obstruct Pulmon Dis* (2016) 11(undefined):2951–64. doi: 10.2147/COPD.S109570

17. Xia L, Wang X, Liu LJ, Fu JR, Xiao WF, Liang QY, et al. Lnc-BAZ2B promotes M2 macrophage activation and inflammation in children with asthma through stabilizing BAZ2B pre-mRNA. *J Allergy Clin Immunol* (2021) 147(3):921–932.e9. doi: 10.1016/j.jaci.2020.06.034

18. Pardo A, Gibson K, Cisneros J, Richards TJ, Yang YK, Becerril C, et al. Up-regulation and profibrotic role of osteopontin in human idiopathic pulmonary fibrosis. *PloS Med* (2005) 2(9):e251. doi: 10.1371/journal.pmed.0020251

19. Li NN, Liu Y, Cai JF. LncRNA MIR155HG regulates M1/M2 macrophage polarization in chronic obstructive pulmonary disease. *BioMed Pharmacother* (2019) 117(undefined):109015. doi: 10.1016/j.biopha.2019.109015

20. Pei WY, Zhang YY, Li XQ, Luo MS, Chen TB, Zhang MY, et al. LncRNA AK085865 depletion ameliorates asthmatic airway inflammation by modulating macrophage polarization. *Int Immunopharmacol* (2020) 83(undefined):106450. doi: 10.1016/j.intimp.2020.106450

21. Zhang XY, Chen ZC, Zhang LX, Li XS, Guo YL, Tian CJ, et al. LincRNA-p21 promotes classical macrophage activation in acute respiratory distress syndrome by activating NF-κB. *Exp Lung Res* (2020) 46(6):174–84. doi: 10.1080/01902148.2020.1758246

22. Zhang YY, Li XQ, Wang C, Zhang MY, Yang H, Lv K, et al. lncRNA AK085865 promotes macrophage M2 polarization in CVB3-induced VM by regulating ILF2-ILF3 complex-mediated miRNA-192 biogenesis. *Mol Ther Nucleic Acids* (2020) 21(undefined):441–51. doi: 10.1016/j.omtn.2020.06.017

23. Luo HL, Luo T, Liu JJ, Wu FX, Bai T, Ou C, et al. Macrophage polarization-associated lnc-Ma301 interacts with caprin-1 to inhibit hepatocellular carcinoma metastasis through the Akt/Erk1 pathway. *Cancer Cell Int* (2021) 21(1):422. doi: 10.1186/s12935-021-02133-1

24. Ito I, Asai A, Suzuki S, Kobayashi M, Suzuki F. M2b macrophage polarization accompanied with reduction of long noncoding RNA GAS5. *Biochem Biophys Res Commun* (2017) 493(1):170–5. doi: 10.1016/j.bbrc.2017.09.053

25. Han X, Huang SH, Xue P, Fu J, Liu L, Zhang CY, et al. PTPRE-AS1LncRNA modulates M2 macrophage activation and inflammatory diseases by epigenetic promotion of PTPRE. *Sci Adv* (2019) 5(12):eaax9230. doi: 10.1126/sciadv.aax9230

26. Xiao T, Zou ZL, Xue JC, Syed BM, Sun J, Dai XY, et al. LncRNA H19-mediated M2 polarization of macrophages promotes myofibroblast differentiation in pulmonary fibrosis induced by arsenic exposure. *Environ pollut* (2021) 268(Pt A):115810. doi: 10.1016/j.envpol.2020.115810

27. Luo XB, Li LT, Xi JC, Liu HT, Liu Z, Yu L, et al. Negative pressure promotes macrophage M1 polarization after mycobacterium tuberculosis infection *via* the lncRNA XIST/microRNA-125b-5p/A20/NF-κB axis. *Ann N Y Acad Sci* (2022) 1514(1):116–31. doi: 10.1111/nyas.14781

28. Channappanavar R, Perlman S. Pathogenic human coronavirus infections: Causes and consequences of cytokine storm and immunopathology. *Semin Immunopathol* (2017) 39(5):529–39. doi: 10.1007/s00281-017-0629-x

29. Chi XW, Ding BC, Zhang LJ, Zhang JW, Wang JM, Zhang W. lncRNA GAS5 promotes M1 macrophage polarization *via* miR-455-5p/SOCS3 pathway in childhood pneumonia. *J Cell Physiol* (2019) 234(8):13242–51. doi: 10.1002/jcp.27996

30. Cui HC, Banerjee S, Guo SJ, Xie N, Ge J, Jiang DY, et al. Long noncoding RNA Malat1 regulates differential activation of macrophages and response to lung injury. *JCI Insight* (2019) 4(4):e124522. doi: 10.1172/jci.insight.124522

31. Li ZX, Feng CJ, Guo JH, Hu XF, Xie D. GNAS-AS1/miR-4319/NECAB3 axis promotes migration and invasion of non-small cell lung cancer cells by altering macrophage polarization. *Funct Integr Genomics* (2020) 20(1):17–28. doi: 10.1007/s10142-019-00696-x

32. Li Y, Chen C, Liu HL, Zhang ZF, Wang CL. LARRPM restricts lung adenocarcinoma progression and M2 macrophage polarization through epigenetically regulating LINC00240 and CSF1. *Cell Mol Biol Lett* (2022) 27 (1):91. doi: 10.1186/s11658-022-00376-y

33. Wu Z, Bai X, Lu ZB, Liu SJ, Jiang HF. LINC01094/SPI1/CCL7 axis promotes macrophage accumulation in lung adenocarcinoma and tumor cell dissemination. *J Immunol Res* (2022) 2022(undefined):6450721. doi: 10.1155/2022/6450721

34. Chen Y, Hong CJ, Qu J, Chen JJ, Qin ZQ. Knockdown of lncRNA PCAT6 suppresses the growth of non-small cell lung cancer cells by inhibiting macrophages M2 polarization *via* miR-326/KLF1 axis. *Bioengineered* (2022) 13 (5):12834–46. doi: 10.1080/21655979.2022.2076388

35. Zhang K, Chen J, Li C, Yuan Y, Fang S, Liu WF, et al. Exosome-mediated transfer of SNHG7 enhances docetaxel resistance in lung adenocarcinoma. *Cancer Lett* (2022) 526(undefined):142–54. doi: 10.1016/j.canlet.2021.10.029

36. Sze E, Bhalla A, Nair P. Mechanisms and therapeutic strategies for non-T2 asthma. *Allergy* (2020) 75(2):311–25. doi: 10.1111/all.13985

37. Reddel HK, Bateman ED, Becker A, Boulet LP, Cruz AA, Drazen JM, et al. A summary of the new GINA strategy: A roadmap to asthma control. *Eur Respir J* (2015) 46(3):622–39. doi: 10.1183/13993003.00853-2015

38. Saradna A, Do DC, Kumar S, Fu QL, Gao P. Macrophage polarization and allergic asthma. *Transl Res* (2018) 191(undefined):1–14. doi: 10.1016/j.trsl.2017.09.002

39. Hammad H, Lambrecht BN. The basic immunology of asthma. *Cell* (2021) 184(9):2521–2. doi: 10.1016/j.cell.2021.04.019

40. Choy DF, Hart KM, Borthwick LA, Shikotra A, Nagarkar DR, Siddiqui S, et al. TH2 and TH17 inflammatory pathways are reciprocally regulated in asthma. *Sci Transl Med* (2015) 7(301):301ra129. doi: 10.1126/scitranslmed.aab3142

41. Heffler E, Madeira LNG, Ferrando M, Puggioni F, Racca F, Malvezzi L, et al. Inhaled corticosteroids safety and adverse effects in patients with asthma. *J Allergy Clin Immunol Pract* (2018) 6(3):776–81. doi: 10.1016/j.jaip.2018.01.025

42. Choi JS, Jang AS, Park JS, Park SW, Paik SH, Park JS, et al. Role of neutrophils in persistent airway obstruction due to refractory asthma. *Respirology* (2012) 17(2):322–9. doi: 10.1111/j.1440-1843.2011.02097.x

43. Vogelmeier CF, Criner GJ, Martinez FJ, Anzueto A, Barnes PJ, Bourbeau J, et al. Global strategy for the diagnosis, management, and prevention of chronic obstructive lung disease 2017 report. *GOLD Executive Summary Am J Respir Crit Care Med* (2017) 195(5):557–82. doi: 10.1164/rccm.201701-0218PP

44. Feng H, Yin Y, Ren Y, Li ML, Zhang D, Xu MT, et al. Effect of CSE on M1/M2 polarization in alveolar and peritoneal macrophages at different concentrations and exposure in vitro. *In Vitro Cell Dev Biol Anim* (2020) 56(2):154–64. doi: 10.1007/s11626-019-00426-4

45. Feng H, Yin Y, Zheng R, Kang J. Rosiglitazone ameliorated airway inflammation induced by cigarette smoke *via* inhibiting the M1 macrophage polarization by activating PPARγ and RXRα. *Int Immunopharmacol* (2021) 97 (undefined):107809. doi: 10.1016/j.intimp.2021.107809

46. Eapen MS, Hansbro PM, McAlinden K, Kim RY, Ward C, Hackett TL, et al. Abnormal M1/M2 macrophage phenotype profiles in the small airway wall and lumen in smokers and chronic obstructive pulmonary disease (COPD). *Sci Rep* (2017) 7(1):1–12. doi: 10.1038/s41598-017-13888-x

47. He SY, Chen DN, Hu MY, Zhang L, Liu C, Traini D, et al. Bronchial epithelial cell extracellular vesicles ameliorate epithelial-mesenchymal transition in COPD pathogenesis by alleviating M2 macrophage polarization. *Nanomedicine* (2019) 18(undefined):259–71. doi: 10.1016/j.nano.2019.03.010

48. Jiang Y, Zhao YF, Wang QL, Chen H, Zhou X. Fine particulate matter exposure promotes M2 macrophage polarization through inhibiting histone deacetylase 2 in the pathogenesis of chronic obstructive pulmonary disease. *Ann Transl Med* (2020) 8(20):1303. doi: 10.21037/atm-20-6653

49. Wang SL, Chen YH, Hong W, Li B, Zhou Y, Ran P, et al. Chronic exposure to biomass ambient particulate matter triggers alveolar macrophage polarization and activation in the rat lung. *J Cell Mol Med* (2022) 26(4):1156–68. doi: 10.1111/jcmm.17169

50. Daldegan MB, Teixeira MM, Talvani A. Concentration of CCL11, CXCL8 and TNF-alpha in sputum and plasma of patients undergoing asthma or chronic obstructive pulmonary disease exacerbation. *Braz J Med Biol Res* (2005) 38 (9):1359–65. doi: 10.1590/s0100-879x2005000900010

51. Murthy S, Larson-Casey JL, Ryan AJ, He C, Kobzik L, Carter AB, et al. Alternative activation of macrophages and pulmonary fibrosis are modulated by scavenger receptor, macrophage receptor with collagenous structure. *FASEB J* (2015) 29(8):3527–36. doi: 10.1096/fj.15-271304

52. Zhang HR, Xue CY, Wang Y, Shi JT, Zhang X, Li WJ, et al. Deep RNA sequencing uncovers a repertoire of human macrophage long intergenic noncoding RNAs modulated by macrophage activation and associated with cardiometabolic diseases. *J Am Heart Assoc* (2017) 6(11):e007431. doi: 10.1161/JAHA.117.007431

53. McCoy CE, Sheedy FJ, Qualls JE, Doyle SL, Quinn SR, Murray PJ, et al. IL-10 inhibits miR-155 induction by toll-like receptors. *J Biol Chem* (2010) 285 (27):20492–8. doi: 10.1074/jbc.M110.102111

54. Elton TS, Selemon H, Elton SM, Parinandi NL. Regulation of the MIR155 host gene in physiological and pathological processes. *Gene* (2013) 532(1):1–12. doi: 10.1016/j.gene.2012.12.009

55. Song J, Wang Q, Zong L. LncRNA MIR155HG contributes to smoke-related chronic obstructive pulmonary disease by targeting miR-128-5p/BRD4 axis. *Biosci Rep* (2020) 40(3). doi: 10.1042/BSR20192567. undefined.

56. Ren XY, Han YD, Lin Q. Long non-coding RNA MIR155HG knockdown suppresses cell proliferation, migration and invasion in NSCLC by upregulating TP53INP1 directly targeted by miR-155-3p and miR-155-5p. *Eur Rev Med Pharmacol Sci* (2020) 24(9):4822–35. doi: 10.26355/eurrev_202005_21171

57. Murray LA, Dunmore R, Camelo A, Silva CAD, Gustavsson MJ, Habiel DM, et al. Acute cigarette smoke exposure activates apoptotic and inflammatory programs but a second stimulus is required to induce epithelial to mesenchymal transition in COPD epithelium. *Respir Res* (2017) 18(1):82. doi: 10.1186/s12931-017-0565-2

58. Elborn JS. Cystic fibrosis. *Lancet* (2016) 388(10059):2519–31. doi: 10.1016/S0140-6736(16)00576-6

59. Porto PD, Cifani N, Guarnieri S, Domenico EGD, Mariggiò MA, Spadaro F, et al. Dysfunctional CFTR alters the bactericidal activity of human macrophages against pseudomonas aeruginosa. *PloS One* (2011) 6(5):e19970. doi: 10.1371/journal.pone.0019970

60. Tarique AA, Sly PD, Cardenas DG, Luo L, Stow JL, Bell SC, et al. Differential expression of genes and receptors in monocytes from patients with cystic fibrosis. *J Cyst Fibros* (2019) 18(3):342–348. doi: 10.1016/j.jcf.2018.07.012

61. Sorio C, Buffelli M, Angiari C, Ettorre M, Johansson J, Vezzalini M, et al. Defective CFTR expression and function are detectable in blood monocytes: development of a new blood test for cystic fibrosis. *PloS One* (2011) 6(7):e22212. doi: 10.1371/journal.pone.0022212

62. Tarique AA, Sly PD, Holt PG, Bosco A, Ware RS, Logan J, et al. CFTR-dependent defect in alternatively-activated macrophages in cystic fibrosis. *J Cyst Fibros* (2017) 16(4):475–82. doi: 10.1016/j.jcf.2017.03.011

63. McKiernan PJ, Molloy K, Cryan Sally A, McElvaney NJ, Greene CM. Long noncoding RNA are aberrantly expressed *in vivo* in the cystic fibrosis bronchial epithelium. *Int J Biochem Cell Biol* (2014) 52(undefined):184–91. doi: 10.1016/j.biocel.2014.02.022

64. Balloy V, Koshy R, Perra L, Corvol H, Chignard M, Guillot L, et al. PseudomonasaeruginosaBronchial epithelial cells from cystic fibrosis patients express a specific long non-coding RNA signature upon infection. *Front Cell Infect Microbiol* (2017) 7:218(undefined). doi: 10.3389/fcimb.2017.00218

65. Saayman SM, Ackley A, Burdach J, Clemson M, Gruenert DC, Tachikawa K, et al. Long non-coding RNA bgas regulates the cystic fibrosis transmembrane conductance regulator. *Mol Ther* (2016) 24(8):1351–7. doi: 10.1038/mt.2016.112

66. Richeldi L, Collard HR, Jones MG. Idiopathic pulmonary fibrosis. *Lancet* (2017) 389(10082):1941–52. doi: 10.1016/S0140-6736(17)30866-8

67. Hou JW, Shi JY, Chen L, Lv ZY, Chen X, Cao HH, et al. M2 macrophages promote myofibroblast differentiation of LR-MSCs and are associated with pulmonary fibrogenesis. *Cell Commun Signal* (2018) 16(1):89. doi: 10.1186/s12964-018-0300-8

68. Fan Y, Zhao XX, Ma JF, Yang LN. LncRNA GAS5 competitively combined with miR-21 regulates PTEN and influences EMT of peritoneal mesothelial cells *via* wnt/β-catenin signaling pathway. *Front Physiol* (2021) 12:654951. doi: 10.3389/fphys.2021.654951

69. Dong ZH, Li S, Wang XH, Si LG, Ma RL, Bao LD, et al. lncRNA GAS5 restrains CCl-induced hepatic fibrosis by targeting miR-23a through the PTEN/PI3K/Akt signaling pathway. *Am J Physiol Gastrointest Liver Physiol* (2019) 316(4): G539–50. doi: 10.1152/ajpgi.00249.2018

70. Dong ZH, Li S, Si LG, Ma RL, Bao LD, Bo A. Identification lncRNA LOC102551149/miR-23a-5p pathway in hepatic fibrosis. *Eur J Clin Invest* (2020) 50(6):e13243. doi: 10.1111/eci.13243

71. Patterson KC, Chen ES. The pathogenesis of pulmonary sarcoidosis and implications for treatment. *Chest* (2018) 153(6):1432–42. doi: 10.1016/j.chest.2017.11.030

72. Wojtan P, Mierzejewski M, Osińska I, Domagała-Kulawik J. Macrophage polarization in interstitial lung diseases. *Cent Eur J Immunol* (2016) 41(2):159–64. doi: 10.5114/ceji.2016.60990

73. Shamaei M, Mortaz E, Pourabdollah M, Garssen J, Tabarsi P, Velayati A, et al. Evidence for M2 macrophages in granulomas from pulmonary sarcoidosis: a new aspect of macrophage heterogeneity. *Hum Immunol* (2018) 79(1):63–9. doi: 10.1016/j.humimm.2017.10.009

74. Zissel G, Muller-Quernheim J. Cellular players in the immunopathogenesis of sarcoidosis. *Clin Chest Med* (2015) 36(4):549–60. doi: 10.1016/j.ccm.2015.08.016

75. Timmermans WM, van Laar JA, van Hagen PM, van Zelm MC. Immunopathogenesis of granulomas in chronic autoinflammatory diseases. *Clin Transl Immunol* (2016) 5(12):e118. doi: 10.1038/cti.2016.75

76. Barnes H, Holland AE, Westall GP, Goh NS, Glaspole IN. Cyclophosphamide for connective tissue disease-associated interstitial lung disease. *Cochrane Database Syst Rev* (2018) 1(1):CD010908. doi: 10.1002/14651858.CD010908.pub2

77. Yoo H, Hino T, Han J, Franks TJ, Im Y, Hatabu H, et al. Connective tissue disease-related interstitial lung disease (CTD-ILD) and interstitial lung abnormality (ILA): Evolving concept of CT findings, pathology and management. *Eur J Radiol Open* (2020) 8:100311. doi: 10.1016/j.ejro.2020.100311

78. Kwon BS, Choe J, Chae EJ, Hwang HS, Kim YG, Song JW. Progressive fibrosing interstitial lung disease: Prevalence and clinical outcome. *Respir Res* (2021) 22(1):282. doi: 10.1186/s12931-021-01879-6

79. Haringman JJ, Gerlag DM, Zwinderman AH, Smeets TJ, Kraan MC, Baeten D, et al. Synovial tissue macrophages: A sensitive biomarker for response to treatment in patients with rheumatoid arthritis. *Ann Rheum Dis* (2005) 64(6):834–8. doi: 10.1136/ard.2004.029751

80. Wijbrandts CA, Vergunst CE, Haringman JJ, Gerlag DM, Smeets TJ, Tak PP. Absence of changes in the number of synovial sublining macrophages after ineffective treatment for rheumatoid arthritis: Implications for use of synovial sublining macrophages as a biomarker. *Arthritis Rheum* (2007) 56(11):3869–71. doi: 10.1002/art.22964

81. Zhu W, Li X, Fang SH, Zhang XL, Wang Y, Zhang TS, et al. Anti-citrullinated protein antibodies induce macrophage subset disequilibrium in RA patients. *Inflammation* (2015) 38(6):2067–75. doi: 10.1007/s10753-015-0188-z

82. Zhu XD, Zhu Y, Ding C, Zhang WT, Guan HL, Li CM, et al. LncRNA H19 regulates macrophage polarization and promotes freund's complete adjuvant-induced arthritis by upregulating KDM6A. *Int Immunopharmacol* (2021) 93:107402. doi: 10.1016/j.intimp.2021.107402

83. Matsuda S, Kotani T, Ishida T, Fukui K, Fujiki Y, Suzuka T, et al. Exploration of pathomechanism using comprehensive analysis of serum cytokines in polymyositis/ dermatomyositis-interstitial lung disease. *Rheumatol (Oxford)* (2020) 59(2):310–8. doi: 10.1093/rheumatology/kez301

84. Ahamada MM Jia Y, Wu XC. Macrophage polarization and plasticity in systemic lupus erythematosus. *Front Immunol* (2021) 12:734008. doi: 10.3389/fimmu.2021.734008

85. Li F, Zhu XH, Yang YS Huang L, Xu JH. TIPE2 alleviates systemic lupus erythematosus through regulating macrophage polarization. *Cell Physiol Biochem* (2016) 38(1):330–9. doi: 10.1159/000438633

86. Pai M, Behr MA, Dowdy D, Dheda K, Divangahi M, Boehme CC, et al. Tuberculosis. *Nat Rev Dis Primers* (2016) 2:16076. doi: 10.1038/nrdp.2016.76

87. Hmama Z, Peña-Díaz S, Joseph S, Av-Gay Y. Immunoevasion and immunosuppression of the macrophage by mycobacterium tuberculosis. *Immunol Rev* (2015) 264(1):220–32. doi: 10.1111/imr.12268

88. Marino S, Cilfone NA, Mattila JT, Linderman JJ, Flynn JL, Kirschner DE. Macrophage polarization drives granuloma outcome during mycobacterium tuberculosis infection. *Infect Immun* (2015) 83(1):324–38. doi: 10.1128/IAI.02494-14

89. Khan A, Singh VK, Hunter RL, Jagannath C. Macrophage heterogeneity and plasticity in tuberculosis. *J Leukoc Biol* (2019) 06(2):275–82. doi: 10.1002/JLB.MR0318-095RR

90. Sica A, Invernizzi P, Mantovani A. Macrophage plasticity and polarization in liver homeostasis and pathology. *Hepatology* (2014) 59(5):2034–42. doi: 10.1002/hep.26754

91. Lim YJ, Yi MH, Choi JA, Lee J, Han JY, Jo SH, et al. Roles of endoplasmic reticulum stress-mediated apoptosis in M1-polarized macrophages during mycobacterial infections. *Sci Rep* (2016) 6(undefined):37211. doi: 10.1038/srep37211

92. Benoit M, Desnues B, Mege JL. Macrophage polarization in bacterial infections. *J Immunol* (2008) 181(6):3733–9. doi: 10.4049/jimmunol.181.6.3733

93. Li MY, Cui JW, Niu WY, Huang J, Feng TJ, Sun B, et al. Long non-coding PCED1B-AS1 regulates macrophage apoptosis and autophagy by sponging miR-155 in active tuberculosis. *Biochem Biophys Res Commun* (2019) 509(3):803–9. doi: 10.1016/j.bbrc.2019.01.005

94. Kundu M, Basu J. The role of microRNAs and long non-coding RNAs in the regulation of the immune response to mycobacterium tuberculosis infection. *Front Immunol* (2021) 12:687962(undefined). doi: 10.3389/fimmu.2021.687962

95. Huang SY, Huang ZK, Luo Q, Qing C. The expression of lncRNA NEAT1 in human tuberculosis and its antituberculosis effect. *BioMed Res Int* (2018) 2018 (undefined):9529072. doi: 10.1155/2018/9529072

96. Kumar M, Sahu SK, Kumar R, Subuddhi A, Maji RK, Jana K, et al. MicroRNA let-7 modulates the immune response to mycobacterium tuberculosis infection *via* control of A20, an inhibitor of the NF-κB pathway. *Cell Host Microbe* (2015) 17(3):345–56. doi: 10.1016/j.chom.2015.01.007

97. Gcanga L, Tamgue O, Ozturk M, Pillay S, Jacobs R, Chia JE, et al. Host-directed targeting of LincRNA-MIR99AHG suppresses intracellular growth of mycobacterium tuberculosis. *Nucleic Acid Ther* (2022) 32(5):421–37. doi: 10.1089/nat.2022.0009

98. *The world health organization the united nations children's fund global action plan for prevention and control of pneumonia (GAPP)*. Available at: http://www.who.int/maternal_child_adolescent/documents/fch_cah_nch_09_04/en/ (Accessed Jan 16, 2018).

99. Chen NS, Zhou M, Dong X, Qu JM, Gong FY, Han Y, et al. Epidemiological and clinical characteristics of 99 cases of 2019 novel coronavirus pneumonia in wuhan, China: a descriptive study. *Lancet* (2020) 395(10223):507–13. doi: 10.1016/S0140-6736(20)30211-7

100. Huang CL, Wang YM, Li XW, Ren LL, Zhao JP, Hu Y, et al. Clinical features of patients infected with 2019 novel coronavirus in wuhan, China. *Lancet* (2020) 395(10223):497–506. doi: 10.4049/jimmunol.181.6.3733

101. Benoit M, Desnues B, Mege JL. Macrophage polarization in bacterial infections. *J Immunol* (2008) 181(6):3733–9. doi: 10.4049/jimmunol.181.6.3733

102. Li QR, Tan SR, Yang L, He W, Chen L, Shen FX, et al. Mechanism of chlorogenic acid in alveolar macrophage polarization in klebsiella pneumoniae-induced pneumonia. *J Leukoc Biol* (2022) 112(1):9–21. doi: 10.1002/JLB.3HI0721-368R

103. Nueangphuet P, Suwanruengsri M, Fuke N, Uemura R, Hirai T, Yamaguchi R. Neutrophil and M2-polarized macrophage infiltration, expression of IL-8 and apoptosis in mycoplasma hyopneumoniae pneumonia in swine. *J Comp Pathol* (2021) 189(undefined):31–44. doi: 10.1016/j.jcpa.2021.09.004

104. Chua RL, Lukassen S, Trump S, Hennig BP, Wendisch D, Pott F, et al. COVID-19 severity correlates with airway epithelium-immune cell interactions identified by single-cell analysis. *Nat Biotechnol* (2020) 38(8):970–9. doi: 10.1038/s41587-020-0602-4

105. Hojyo S, Uchida M, Tanaka K, Hasebe R, Tanaka Y, Murakami M, et al. How COVID-19 induces cytokine storm with high mortality. *Inflammation Regener* (2020) 40(undefined):37. doi: 10.1186/s41232-020-00146-3

106. Gracia-Hernandez M, Sotomayor EM, Villagra A. Targeting macrophages as a therapeutic option in coronavirus disease 2019. *Front Pharmacol* (2020) 11:577571(undefined). doi: 10.3389/fphar.2020.577571

107. Shibata T, Makino A, Ogata R, Nakamura S, Ito T, Nagata K, et al. Respiratory syncytial virus infection exacerbates pneumococcal pneumonia *via* Gas6/Axl-mediated macrophage polarization. *J Clin Invest* (2020) 130(6):3021–37. doi: 10.1172/JCI125505

108. Wang XP, Guo P, Tian JH, Li J, Yan N, Zhao X, et al. LncRNA GAS5 participates in childhood pneumonia by inhibiting cell apoptosis and promoting SHIP-1 expression *via* downregulating miR-155. *BMC Pulm Med* (2021) 21(1):362. doi: 10.1186/s12890-021-01724-y

109. Chi XW, Guo YN, Zhang LJ, Zhang JW, Du YM, Zhao WC, et al. Long non-coding RNA GAS5 regulates Th17/Treg imbalance in childhood pneumonia by targeting miR-217/STAT5. *Cell Immunol* (2021) 364(undefined):104357. doi: 10.1016/j.cellimm.2021.104357

110. Yang LK, Zhang XF, Liu XF. Long non-coding RNA GAS5 protects against mycoplasma pneumoniae pneumonia by regulating the microRNA-222-3p/TIMP3 axis. *Mol Med Rep* (2021) 23(5):380. doi: 10.3892/mmr.2021.12019

111. Li HB, Zi PP, Shi HJ, Gao M, Sun RQ. Role of signaling pathway of long non-coding RNA growth arrest-specific transcript 5/microRNA-200c-3p/angiotensin converting enzyme 2 in the apoptosis of human lung epithelial cell A549 in acute respiratory distress syndrome. *Zhonghua Yi Xue Za Zhi* (2018) 98 (41):3354–9. doi: 10.3760/cma.j.issn.0376-2491.2018.41.013

112. Matute-Bello G, Frevert CW, Martin TR. Animal models of acute lung injury. *Am J Physiol Lung Cell Mol Physiol* (2008) 295(3):L379–99. doi: 10.1152/ajplung.00010.2008

113. Frank JA, Wray CM, McAuley DF, Schwendener R, Matthay MA. Alveolar macrophages contribute to alveolar barrier dysfunction in ventilator-induced lung

injury. *Am J Physiol Lung Cell Mol Physiol* (2006) 291(6):L1191–8. doi: 10.1152/ajplung.00055.2006

114. Huang SC, Smith AM, Everts B, Colonna M, Pearce EL, Schilling JD, et al. Metabolic reprogramming mediated by the mTORC2-IRF4 signaling axis is essential for macrophage alternative activation. *Immunity* (2016) 45(4):817–30. doi: 10.1016/j.immuni.2016.09.016

115. Vishnubalaji R, Shaath H, Alajez NM. Protein coding and long noncoding RNA (lncRNA) transcriptional landscape in SARS-CoV-2 infected bronchial epithelial cells highlight a role for interferon and inflammatory response. *Genes (Basel)* (2020) 11(7):760. doi: 10.3390/genes11070760

116. Bray F, Ferlay J, Soerjomataram I, Siegel RL, Torre LA, Jemal A. Global cancer statistics 2018: GLOBOCAN estimates of incidence and mortality worldwide for 36 cancers in 185 countries. *CA Cancer J Clin* (2018) 68(6):394–424. doi: 10.3322/caac.21492

117. Molina JR, Yang P, Cassivi SD, Schild SE, Adjei AA. Non-small cell lung cancer: epidemiology, risk factors, treatment, and survivorship. *Mayo Clin Proc* (2008) 83(5):584–94. doi: 10.4065/83.5.584

118. Rothschild SI, Gautschi O, Haura EB, Johnson FM. Src inhibitors in lung cancer: current status and future directions. *Clin Lung Cancer* (2010) 11(4):238–42. doi: 10.3816/CLC.2010.n.030

119. Solinas G, Germano G, Mantovani A, Allavena P. Tumor-associated macrophages (TAM) as major players of the cancer-related inflammation. *J Leukoc Biol* (2009) 86(5):1065–73. doi: 10.1189/jlb.0609385

120. Sica A, Larghi P, Mancino A, Rubino L, Porta C, Totaro MG, et al. Macrophage polarization in tumour progression. *Semin Cancer Biol* (2008) 18 (5):349–55. doi: 10.1016/j.semcancer.2008.03.004

121. Denaro N, Merlano MC, Lo Nigro C. Long noncoding RNAs as regulators of cancer immunity. *Mol Oncol* (2019) 13(1):61–73. doi: 10.1002/1878-0261.12413

122. Mei JD, Xiao ZL, Guo CL, Pu Q, Ma L, Liu CW, et al. Prognostic impact of tumor-associated macrophage infiltration in non-small cell lung cancer: A systemic review and meta-analysis. *Oncotarget* (2016) 7(23):34217–28. doi: 10.18632/oncotarget.9079

123. Nakaoka HJ, Hara T, Yoshino S, Kanamori A, Matsui Y, Shimamura T, et al. NECAB3 promotes activation of hypoxia-inducible factor-1 during normoxia and enhances tumourigenicity of cancer. *Cells Sci Rep* (2016) 6(undefined):22784. doi: 10.1038/srep22784

124. Mukherjee K, Xue L, Planutis A, Gnanapragasam MN, Chess A, Bieker JJ. EKLF/KLF1 expression defines a unique macrophage subset during mouse erythropoiesis. *Elife* (2021) 10(undefined):e61070. doi: 10.7554/eLife.61070

125. Zhao S, Lin CY, Yang T, Qian XY, Lu JJ, Cheng J. Expression of long non-coding RNA LUCAT1 in patients with chronic obstructive PulmonaryDisease and its potential functions in regulating cigarette smoke extract induced 16HBE cell proliferation and apoptosis. *J Clin Lab Anal* (2021) 35:e23823. doi: 10.1002/jcla.23823

126. Gu WC, Yuan YP, Wang LX, Yang H, Li SS, Tang ZJ, et al. Long non-coding RNA TUG1 promotes airway remodelling by suppressing the miR-145-5p/DUSP6 axis in cigarette smoke-induced COPD. *J Cell Mol Med* (2019) 23 (11):7200–9. doi: 10.1111/jcmm.14389

127. Rüger J, Ioannou S, Castanotto D, Stein CA. Oligonucleotides to the (Gene) rescue: FDA approvals 2017-2019. *Trends Pharmacol Sci* (2020) 41(1):27–41. doi: 10.1016/j.tips.2019.10.009

128. Reid G, Kao SC, Pavlakis N, Brahmbhatt H, MacDiarmid J, Clarke S, et al. Clinical development of TargomiRs, a miRNA mimic-based treatment for patients with recurrent thoracic cancer. *Epigenomics* (2016) 8(8):1079–85. doi: 10.2217/epi-2016-0035

129. Ottosen S, Parsley TB, Yang L, Zeh K, van Doorn LJ, van der Veer E, et al. *In vitro* antiviral activity and preclinical and clinical resistance profile of miravirsen, a novel anti-hepatitis c virus therapeutic targeting the human factor miR-122. *Antimicrob Agents Chemother* (2015) 59(1):599–608. doi: 10.1128/AAC.04220-14

130. Mei D, Tan WSD, Tay Y, Mukhopadhyay A, Wong WSF. Therapeutic RNA strategies for chronic obstructive pulmonary disease. *Trends Pharmacol Sci* (2020) 41(7):475–86. doi: 10.1016/j.tips.2020.04.007

frontiers | Frontiers in Immunology

TYPE Original Research
PUBLISHED 12 January 2023
DOI 10.3389/fimmu.2022.1095879

OPEN ACCESS

EDITED BY
Ruoxi Yuan,
Hospital for Special Surgery, United States

REVIEWED BY
Poonam Dhillon,
University of Pennsylvania, United States
Xinjun Wu,
University of North Carolina at Chapel Hill, United States

*CORRESPONDENCE
Christian Wadsack
christian.wadsack@medunigraz.at

SPECIALTY SECTION
This article was submitted to Inflammation, a section of the journal Frontiers in Immunology

RECEIVED 11 November 2022
ACCEPTED 28 December 2022
PUBLISHED 12 January 2023

CITATION
Mercnik MH, Schliefsteiner C, Fluhr H and Wadsack C (2023) Placental macrophages present distinct polarization pattern and effector functions depending on clinical onset of preeclampsia.
Front. Immunol. 13:1095879.
doi: 10.3389/fimmu.2022.1095879

Placental macrophages present distinct polarization pattern and effector functions depending on clinical onset of preeclampsia

Monika Horvat Mercnik[1], Carolin Schliefsteiner[1], Herbert Fluhr[1] and Christian Wadsack[1,2]*

[1]Department of Obstetrics and Gynaecology, Medical University of Graz, Graz, Austria, [2]BioTechMed-Graz, Graz, Austria

Hofbauer cells (HBCs) are resident macrophages of the human placenta, regulating immune tolerance and tissue homeostasis. HBCs of a normal placenta (CTR) exhibit mainly an anti-inflammatory M2 phenotype. Under exaggerated chronic inflammation during pregnancy, as in preeclampsia (PE), a phenotypic switch towards M1 polarization has been proposed. PE, defined as maternally derived syndrome can be distinguished into two different entities: early-onset (EO) preeclampsia and late-onset (LO) preeclampsia. Although the clinical presenting characteristics overlap, both can be identified by biochemical markers, heritability, and different maternal and fetal outcomes. To date, no study has specifically investigated polarization and phenotype of EO- and LO-PE HBCs and looked at possible changes in HBC functionality. Primary HBCs were isolated from CTR and PE placentae. First, *in vitro* morphological differences were observed between CTR and PE HBCs, with both PE groups exhibiting features of M1 macrophages alongside M2 forms. Interestingly, a different polarization pattern was observed between EO- and LO-PE HBCs. EO-PE HBCs develop a tissue remodeling M2 phenotype that is strongly shifted toward M1 polarization and showed a significant upregulation of CD86, TLR4, and HLA-DR. Furthermore, this pro-inflammatory signature is corroborated by higher expression of IRF5 and of *NOS2* ($p \leq 0.05$). However, their M2 characteristics is reflected by significant TGF-β secretion and *ARG1* expression. In contrast, LO-PE HBCs developed a phagocytic CD209-low M2 phenotype in which the M1 pattern was not as pronounced as they downregulated the *NOS2* gene, but expressed increased levels of pro-inflammatory CD80 and TLR1 ($p \leq 0.05$). The enhanced phagocytosis and MMP-9 secretion alongside the increased secretion of anti-inflammatory IL -4, IL -13 and TGF-β in both EO- and LO-PE HBCs suggests their adaptive role and plasticity in resolving inflammation and tissue homeostasis.

KEYWORDS

hofbauer cell, preeclampsia, polarization, early onset preeeclampsia, late onset preeclampsia, inflammation, macrophage, human placenta

1 Introduction

Preeclampsia is a maternally derived inflammatory syndrome, affecting 4-5% of pregnancies worldwide. It is a leading cause of preterm delivery and intrauterine growth restriction, mainly due to the insufficient nutrient supply across the placenta and chronic hypoxia exposure of the fetus (1, 2). PE is clinically defined as *de novo* onset of hypertension (≥140/90 mmHg) accompanied by one or more of the following new-onset conditions: proteinuria, thrombocytopenia, renal failure, impaired liver function, pulmonary edema, neurological complications, or uteroplacental dysfunction, occurring after 20 weeks of gestation (1–3). Depending on the time of diagnosis, this syndrome can be divided into two subgroups, namely before (early-onset, EO) or after (late-onset, LO) 34 weeks of gestation (4–6). PE is a complex and heterogeneous disorder whose pathophysiological mechanisms are still not fully understood (7). Of note, different aetiology of EO- and LO-PE has been suggested. Briefly, EO-PE is associated with placental dysfunction and is more likely to affect the fetus (8, 9), whereas LO-PE is mediated by maternal factors, therefore more favourable for successful fetal outcome (10). The placenta in PE is characterized by profound morphological and functional alterations (11), due to poor placentation and placental ischemia (12, 13). In addition, placental dysfunction has been associated with an imbalanced immune function, excessive inflammation accompanied with increased production of pro-inflammatory factors, and simultaneously a decrease in the number of regulatory immune cells and anti-inflammatory cytokines, all together contributing to the development and progress of PE (14–16).

Both the maternal and feto-placental immune system play a crucial role in the development of pregnancy (16). Hence, in contrast to normal pregnancy, where the immune systems contribute to the maintenance of feto-maternal tolerance and placental development, a pro-inflammatory environment leads to excessive activation of innate immune cells and consequently to placental dysfunction and/or poor maternal vascular adaptation (16–19). Macrophages represent a diverse group of innate immune cells, vital for the regulation of inflammation, tissue homeostasis, and defence (20). Due to their remarkable plasticity that allows them fast and direct response to the stimuli and to the adaptive capability of their micro-environmental milieu (21), they are important key players in the progression of pregnancy and could be involved in the development and progression of PE (16, 19). Macrophages are keen to develop a broad spectrum of phenotypes along the M1 and M2 axis, which allows to divide the cells into defined classical M1 and M2 polarized groups (22, 23) The balance between the different polarization states often plays an important role in the resolution or progression of inflammation (24, 25). Their phenotypic heterogeneity is also reflected in their effector functions. In general, M1 macrophages are thought to be pro-inflammatory, while M2 macrophages limit inflammation and promote tissue repair, angiogenesis and homeostasis (26, 27).

Hofbauer cells (HBCs) are placental macrophages residing from day 18 after conception (28) in the chorionic villi of the human placenta (29). In a normal pregnancy HBCs are M2 polarized (26, 30–33) long spindled cells with large vacuoles (34). Due to their phenotypic heterogeneity, HBCs fulfil a variety of functions (35). As placental immune cells, they exhibit micro-biocidal activity (36, 37) and promote maternal tolerance towards the fetus (38). They are known to engage in tight and specific interactions with surrounding placental cells, therefore promoting trophoblast function (39, 40), tissue remodeling (36) and angiogenesis (26, 36, 41, 42). Perturbations in the homeostatic functions of HBCs are often associated with inflammation (43–46) and infection (47). Despite their crucial role in placental tissue, knowledge about the role of HBCs in PE is still lacking. A deeper understanding of HBC function offers the potential for therapeutical immune manipulation during compromised pregnancies in relation to gestational age, which determines both maternal and perinatal outcomes.

This study aimed to investigate polarization and phenotypic differences of primary human HBCs isolated from normal and PE placentae. In addition, we tested whether changes of the HBC phenotype might be linked to altered functionality, specifically to phagocytosis, tissue remodeling and the ability of macrophages to activate feto-placental endothelial cells (fpEC). Further, as gestational age has been identified as the most important clinical variable, we hypothesized that stratification of PE (EO-PE vs LO-PE) may account for the observed functional changes of HBCs within each group. These findings, while somewhat preliminary (due to case numbers), demonstrate that the inflammatory placental environment of EO-PE alters the immunoregulatory phenotype of HBCs with an increased pro-inflammatory M1 signature. Interestingly, LO-PE HBCs remained M2 polarized cells, but with a different polarization pattern as controls.

2 Materials and methods

2.1 Study population

In this study preeclampsia was defined according to the guidelines of the American College of Obstetricians and Gynaecologists as already mentioned above (1, 2). The institutional ethics committee of the Medical University of Graz (29-319 ex 16/17) approved the study. Subjects included in the study signed an informed consent form before participation, the characteristics of which are shown in the Table 1. Included placentae from singleton pregnancies were used within 30 minutes of caesarean section or vaginal delivery. PE was defined as a sustained blood pressure of 140/90 mm Hg or greater (on two occasions at least 4 hours apart) occurring after 20 weeks of gestation in a woman with previously normal blood pressure, accompanied by one or more of the following new onset conditions: proteinuria, thrombocytopenia, renal insufficiency, impaired liver function, pulmonary edema, neurological complications or uteroplacental dysfunction. Onset of PE was defined as early (EO, delivered and detected before 34 weeks of gestation) or late (LO, delivered and detected after 34 weeks of gestation) (1). Placentae from normal pregnancies served as controls.

2.2 Isolation of HBCs

Primary HBCs were isolated according to a modified protocol as described by Tang et al. (48). To avoid contamination with decidual macrophages, the decidual membrane was removed before isolating

10.3389/fimmu.2022.1095879

TABLE 1 Subject characteristics of women and their offspring included in the study.

	CTR (n=22)	EO-PE (n=8)	LO-PE (n=6)
Age	29.4 ± 3.5	34.4 ± 3.6 **	34.4 ± 4.0 †
BMI before pregnancy (kg/m2)	22.5 ± 2.9	21.0 ± 2.1	23.4 ± 3.2
Week of gestation	38.7 ± 1.5	34.2 ± 1.1 ****	37.7 ± 1.1
Mode of the delivery	SP 10/CS 12	CS 8	SP 3/CS 3
Fetal sex	8♀ 14♂	4♀, 4♂	2♀, 4♂
Umbilical cord blood Arterial, pH	7.30 ± 0.06	7.31 ± 0.03	7.25 ± 0.09
Umbilical cord blood Venous, pH	7.37 ± 0.06	7.36 ± 0.02	7.34 ± 0.05
Placental weight (g)	616.7 ± 123.0	425.7 ± 63.7	506.7 ± 82.8
Birth weight (g)	3345 ± 398	1996 ± 404.7 ****	2955 ± 288.9
Birth weight percentile	49.2 ± 21.2	24.0 ± 18.7 **	34.3 ± 11.3
Systolic blood pressure (mmHg)	115.1 ± 6.9	162 ± 12.1****	153.2 ± 20.9 ††††
Diastolic blood pressure (mmHg)	72.9 ± 10.2	94.3 ± 8***	103 ± 13.3 ††††
sFlt-1 [pg/mL]	/	14472 ± 5083 ‡	8257 ± 2881
PlGF [pg/mL]	/	66.2 ± 24.3	81.6 ± 13.02
sFlt-1/PlGF [pg/mL]	/	248.7 ± 118.1	105.5 ± 51.9
Platelets [109/L]	218.3 ± 63.1	221.9 ± 106.3	191.8 ± 60.8
Uric acid [mg/dL]	/	6.3 ± 1.4	5.9 ± 0.7
AST [U/L]	/	21.0 ± 6.3	21.2 ± 4.2
ALT [U/L]	/	17.4± 5.6	12.7 ± 4.8

BMI, body-mass index; SP, spontaneous delivery; CS, caesarean section; All data are shown as mean ± SD. Statistical significance was assessed by one-way ANOVA with Tukey's *post-hoc* test. If normality testing failed, Kruskal-Wallis test with Dunn's *post-hoc* test was used. When comparing two groups' Students t-test was used. **p ≤ 0.01, ***p ≤ 0.001 and ****p ≤ 0.0001; whereas *CTR vs EO-PE. †p ≤ 0.05 and † † † †p ≤ 0.0001; whereas †CTR vs LO-PE. ‡ represents comparison between EO-PE vs LO-PE; whereas ‡ p ≤ 0.05.

HBCs. The villous tissue was dissected, washed in 0.4% saline solution (Fresenius, Cat #C924228), and finely minced. Between 60 and 100 g of the minced tissue was stored overnight at 4°C in 1 x phosphate buffered saline (PBS, Medicado, Cat #09-9400-100). On the next day, the tissue was digested with trypsin (0.25%, Sigma Aldrich, Cat #T4549) and DNase I (0.08 mg/ml; Roche, Cat #10104159001), followed by digestion with collagenase A (1 mg/ml; Roche, Cat #10103586001) and DNase I (0.08 mg/ml, Roche, Cat #10104159001). The cell suspension containing the HBCs was applied to a Percoll gradient (20-40%, Sigma Aldrich, Cat #P4937) and centrifuged unrestrained at 1000 g for 30 min. At this point, the HBCs appearing as bands between 30 and 35% gradient layers were aspirated and purified by negative selection using Dynabeads (Invitrogen, Cat #11033) coated with antibodies against epithelial growth factor receptor (EGFR, Santa Cruz, Cat #sc-120) and CD10 (Sigma Aldrich, Cat #SAB4700440). After immunopurification, cells were seeded in macrophage medium (MaM, ScienCell, Cat #SC1921) containing 5% FBS (ScienCell, Cat #SC1921), PenStrep (ScienCell, Cat #SC1921) and macrophage growth supplements (ScienCell, Cat #SC1921) at a cell density of $1x10^6$ cells/ml. Cells were cultured at 21% oxygen and 37°C. Quality control of the isolated HBCs was performed on the fixed cells after 6 days by immunocytochemistry for CD163 (Thermo Fischer Scientific, Cat #MA1-82342), CD90 (Dianova, Cat # DIA100), CD80 (Abcam, Cat #ab86473), CD68 (Dako, Cat #GA613), CD86 (Abcam, Cat #ab270719), CD206 (Novus, Cat #H00004360), CD209 (R&D Systems, Cat #MAB1621), and isotype control (Dako, Cat #X0931) as previously described by Schliefsteiner et al. (31). Cell culture images were obtained using brightfield microscope with a SC50 Olympus camera and CellSens software.

2.3 Immunohistochemistry

Tissue sections were taken from four different areas of placenta (reaching from chorionic plate to the decidual side and a central region of the placental disk) and fixed overnight in 4% neutral buffered paraformaldehyde solution. After paraffin embedding, tissue sections with a thickness of 5µm were mounted on glass slides. The paraffin was then removed with xylene and rehydrated in an ethanol dilution series. Antigen retrieval was performed using a citrate buffer (Gatt, Cat #403139070) adjusted to pH 6.0. UltraVision LP detection system (Thermo Fischer Scientific, Cat #TL125HL) was used for histochemical immunostaining. Tissue was incubated with Hydrogen Peroxide Block (Thermo Fischer Scientific, Cat #TL125HL) for 15 minutes and washed in TBE buffer (Gatt, Cat #403211370),

followed by a 5-minute incubation with Ultra V protein block (Thermo Fischer Scientific, Cat #TL125HL). The primary antibody isotype control (1:200, Dako, Cat #X0931) and CD163 (1:200, Thermo Fischer Scientific, Cat #MA1-82342) were diluted in antibody diluent (Agilent, Dako, Cat #S0809) and incubated overnight at 4°C in a humidified chamber. After washing step, primary antibody enhancer (Thermo Fischer Scientific, Cat #TL125HL) was applied for 20 minutes. After another washing step samples were incubated with Large HRP Polymer (Thermo Fischer Scientific, Cat #TL125HL) solution for 30 minutes, followed by intensive washing and incubation with AEC Chromogen Solution (Abcam, Cat #64252) for 10 minutes. The tissue was counterstained with Haematoxylin (Gatt-Koller Cat #401296170) for 1 minute and mounted with embedding medium. Images were acquired using CellSens Standard software and an Olympus BX53 light microscope with an Olympus UC90 camera. Per slide, images of 5-10 different areas were taken and quantified with Qupath software (49).

2.4 Fluorescence assisted cell sorting (FACS)

FACS was performed to quantify the cell populations expressing M1 and M2 polarization markers of HBCs. On the fifth day after isolation, cells were harvested using accutase (Thermo Fischer Scientific, Cat #00-4555-56) and gentle scraping. Viability and number of cells after scraping was determined using a CASY cell counter model TT (Innovatis, Bielefeld). At least $1x10^5$ viable cells per tube were used for the experiment. Cells were resuspended in 3% FCS - HBSS solution for 10 min at room temperature to block Fc-receptors and reduce non-specific binding. For surface staining, cells were incubated with a fluorochrome-conjugated antibody in the amount indicated in the Supplementary Table 1 for 20 minutes at 4°C in the dark. Cells were washed with staining buffer [PBS containing 0.1% BSA (Sigma Aldrich, Cat #A2153) and 2mM EDTA (Thermo Fischer Scientific, Cat #15575020)], centrifuged at 300 g for 5 minutes and resuspended in 200 µL staining buffer. For detection of surface molecules, a minimum of 10000 live events per sample were counted. In order to identify expression of surface markers, cells were separated by size using forward and size scatter (FSC and SSC, respectively), followed by doublet discrimination. In the next step, cells were discriminated into live and dead cells using the 7-AAD dye (BD Biosciences, Cat #559925) by plotting it against the SSC area. In the fourth step cells were plotted for the respective marker against the SSC area. For staining of intracellular molecules, cells were fixed and permeabilized with BD Cytofix/Cytoperm kit (BD Biosciences, Cat #554714). Staining was performed according to the manufacturer's instructions. A minimum of 10000 events per sample were counted. To investigate the expression of intracellular polarization markers cells were separated by size using forward and size scatter (FSC and SSC, respectively), followed by doublet discrimination and gating against SSC-area and respective marker. The same gating strategy was employed on CTR and PE macrophages. Surface molecules were compensated by individual staining on OneComp eBeadsTM Compensation Beads (Thermo Fischer Scientific, Cat #01-1111-42). Isotype controls corresponding to each fluorochrome in the experiment were used to detect non-specific positive signals. Antibodies used for FACS analysis and their corresponding dilutions are listed in the Supplementary Table 1. Cell sorting was performed using a CytoFLEX flow cytometer (Beckman Coulter, Brea, CA, USA) and analysed with FlowJoTM v10.8 software for gate setting and data analysis.

2.5 Multiplex ELISA-on-bead Assay

Inflammation 20-Plex Human ProcartaPlex™ Panel (Invitrogen, Thermo Fischer Scientific, Cat #EPX200-12185-901) was used to quantify the secretion of pro- and anti-inflammatory molecules. Human TIMP Magnetic Luminex Performance Assay 4- Plex Kit (R&D Systems, Cat #LKTM003) was used to analyse TIMP secretion. HBCs were cultured in MaM for 5-6 days before supernatants were collected and centrifuged at 4000 rpm, 4°C for 15 minutes. MaM medium processed under the same conditions as the samples served as a blank. Multiplex assays were performed according to the manufacturer's instructions. Cytokines reaching the detection limits were normalized to total protein content in the supernatant using the Pierce BCA kit (Thermo Fischer Scientific, Cat #23225).

2.6 Enzyme- linked immunosorbent assay (ELISA)

TGF-beta 1 Quantikine ELISA kit for human/mouse/rat/porcine/rabbit (R&D Systems, Cat #DB100B) was used for the detection of TGF-β1. Next, to quantify secretion of IL-8, human IL -8/CXCL8 Quantikine ELISA kit (R&D Systems, Cat #D8000C) was used. Both ELISA kits were performed according to the manufacturers' instructions. To quantify the amount of secreted TGF-β1 and IL-8, cells were cultured in MaM for 5-6 days before collection of the supernatants. MaM medium processed under the same conditions as the samples, but without cells served as a blank. Cytokine levels were normalized to the total protein content in the supernatant measured with the Pierce BCA kit (Thermo Fischer Scientific, Cat #23225), in order to account for deviating volume concentrations.

2.7 Quantitative Real-Time PCR (RT-qPCR)

HBCs were washed twice with ice cold Hanks' salt balanced solution (HBSS, Thermo Fischer Scientific, Cat #14175-053) and harvested in 700 µL QIazol Lysis Reagent (Quiagen, Cat #79306). Total RNA content was isolated using miRNeasy Mini Kit (Quiagen, Cat #217004). Reverse transcription was performed using 1 µg of RNA and Luna Script RT SuperMix Kit (New England BioLabs, Cat #M3010). For qPCR analysis, SYBR Green Luna Universal qPCR Master Mix (New England BioLabs, Cat #M3003) and CFX-384 Touch Real time PCR detection system (Bio-Rad) were used. Expression of target genes was normalized to the following housekeeping genes (*18S*, *RPL30* and *HPRT*) using $2^{(-\Delta\Delta Ct)}$ method. Primer sequences used for qPCR analysis are listed in the Supplementary Table 2.

2.8 Phagocytosis assay measured with FACS

Phagocytosis Assay Kit (Abcam, Cat #ab234053) was used according to the manufacturer's instructions. For detection of phagocytic activity 1 x 10^6 cells/ml were used. On the fifth day post isolation HBCs were treated with zymosan slurry and incubated for 3 hours at 21% oxygen and 37°C. After washing steps, cells were detached using accutase (Thermo Fischer Scientific, Cat #00-4555-56) and careful scraping, followed by a washing step with staining buffer containing PBS with 0.1% BSA (Sigma Aldrich, Cat #A2153) and 2mM EDTA (Thermo Fischer Scientific, Cat #15575020). Afterwards measurements were performed in the FITC channel. Untreated cells served as controls. Cells were separated by size using FSC-A and SSC-A, followed by doublet discrimination gating the area and height of FSC. Lastly, the FITC fluorescent signal was determined using histograms. Cell sorting was performed on a CytoFLEX flow cytometer (Beckman Coulter, Brea, CA, USA) using FlowJoTM v10.8software for gate setting and data analysis.

2.9 Phagocytosis assay with high-content confocal screening microscope

Phagocytosis Assay Kit (Abcam, Cat #ab234053) was used according to the manufacturer's instructions. HBCs were seeded at the density of 0.5 x 10^6 cells/ml in 24-well black/clear bottom plates. 5 µL of zymosan slurry was added to the cells and incubated at 21% oxygen and 37°C for 3 hours, followed by a washing step. Next, cells were fixed in a plate containing 4% neutral buffered paraformaldehyde solution, followed by an intensive wash step with TBE buffer containing 1x TBE and 0.1% Tween (Thermo Fischer Scientific, Cat #003005). HBCs were incubated with Protein Block (Thermo Fischer Scientific, Cat #TL125HL) for 20 minutes. Cells were then counterstained with CD163 (1:100, Thermo Fischer Scientific, Cat #MA1-82342), diluted to working concentration in Antibody diluent (Agilent, Dako, Cat #S0809) and incubated overnight at 4°C. After serial washing steps, the plate was incubated with the secondary antibody Dylight633 (goat versus mouse 1:200, Thermo Fischer Scientific, Cat #35512) for 2 h at room temperature. To stain the nuclei, the plate was counterstained with DAPI (1:1000, Sigma Aldrich, Cat #D9542) diluted in antibody diluent for 10 min. After intensive washing, 300 µL of PBS was added to each well and stored at 4°C. Image acquisition was performed using a Nikon microscope with the Zyla sCMON camera. All statistical analysis was carried out on 25 different locations per well using 20x magnification. For better visualization of phagocytosis shown images in the Figures 4C–E were taken with 40x magnification. The number of FITC labelled beads was counted within the cells positive for CD163 and DAPI staining using Nis Elements viewer version 5.20.01 software. Cell surface area was measured using the measuring tool provided within the software.

2.10 Gelatin zymography

HBCs supernatants were collected on the fifth day post isolation. The supernatants were centrifuged at 4000 rpm for 15 minutes at 4°C. Total protein concentration was determined using Pierce BCA kit (Thermo Fischer Scientific, Cat #23225) according to the manufacturer's guidelines. A total of 15 µg of protein sample was diluted with Tris-Glycine SDS sample buffer (Thermo Fisher Scientific, Cat # LC2676) and loaded onto 10% Tris-Glycine gels containing 0.1% gelatin (Thermo Fisher Scientific, Cat #ZY00105BOX) and separated for 135 min at 125 V, 35 mA. After electrophoresis, the gels were incubated in 1x Zymogram Renaturating buffer (Thermo Fisher Scientific, Cat #LC2670) at room temperature with gentle agitation. Followed by 30 minutes incubation with 1x Zymogram developing buffer (Thermo Fisher Scientific, Cat #LC2671). Fresh developing buffer was added and the gels were stored overnight at 37°C. Next day, gels were stained with Coomassie Brilliant Blue (Sigma Aldrich, Cat #1.15444) for 50 minutes and decolorized in 50% distilled water (Fresenius, Cat #C920928): 40% methanol (Sigma Aldrich, Cat #322415): 10% acetic acid (Roth, Cat #3738.5) solution for 10 minutes. Protease activity appearing as a clear band on the dark background was visualized with the ChemiDoc™Touch Imaging System (Bio-Rad). Band densitometry was determined using Image Lab Software Version 6.1 (Bio-Rad).

2.11 Statistical analysis

SPSS (IBM SPSS Statistics version 26) was used for statistical calculations. Next, graphs were generated using Graph Pad Prism 9.3.1 software (GraphPad Software Inc.). To test normal distribution Shapiro-Wilk test was used. Skewed data were transformed using natural logarithm (ln) before applied to statistical analysis and re-transformed for the graphical presentation. To assess statistical significance of the patient characteristics (Table 1) one-way ANOVA with Tukey's *post-hoc* test was used. If normality testing failed, Kruskal-Wallis test with Dunn's *post-hoc* test was performed. Next, to compare differences between three groups (CTR; EO-PE and LO-PE) ANCOVA with adjustment for gestational age and Sidak's *post-hoc* test was used. Equal variances of variables were verified by Levene´s test. When comparing the effect of HBCs conditioned medium on fpECs without adjustment for gestational age (Supplementary Figure 5) two-way ANOVA with Sidak's *post-hoc* test was used. All values are given as mean ± S.E.M. p-values ≤ 0.05 were considered statistically significant.

3 Results

3.1 The number and morphology of HBCs is affected by PE

The characteristics of the study population are shown in Table 1. Women who developed early (EO, n=8) and late onset (LO, n=6) PE were included in this pilot study. Advanced maternal age, high pre-pregnancy BMI, nulliparity, gestational diabetes, chronic hypertension are some of the risk factors for the development of PE (1). Women in PE groups were significantly older as those in CTR group and their pre-pregnancy BMI ranged from 19.6 to 25.4 kg/m2. As expected, systolic and diastolic blood pressure levels differed

significantly between the CTR and PE groups. Gestational age of EO-PE group was significantly lower than of CTR and LO-PE group. Consequently, early gestational age of the EO-PE group is directly related to placental- and fetal weight, both of which were significantly lower than in CTRs. Since development of the placenta depends on gestational age (50), we adjusted the (normally distributed) data for that respective factor. We found a significant difference in the levels of sFlt between EO- and LO-PE group, while there were no significant differences between other clinical parameters (PlGF, platelets, uric acid, AST and ALT).

To study polarization, we first examined the distribution and number of HBCs in placental tissue using immunohistochemistry approach. Since HBCs have been shown to be strongly positive for CD163, we stained 5 µm serial sections of CTR (n=5), EO-PE (n=6) and LO-PE (n=6) placental tissue, mouse IgG served as a negative control. CD163 is used as a marker used for placenta resident macrophages, and if combined with other markers (e.g. Folate receptor-β, CD206, CD209) is often associated with M2 polarization (26, 30, 31, 51). HBCs positive for CD163 were found in the villous stroma, moreover in stem, intermediate and terminal villi of CTR, EO- and LO- PE placentae (Figure 1A). Furthermore, quantification of CD163-positive cells revealed a significantly decreased number of stained (Figure 1B) cells per mm^2 in both PE groups, indicating reduced number of HBCs in respective groups. Next, we adjusted the number of isolated HBCs to the wet weight (grams) of placental tissue used for isolation. Consistent with immunohistochemical analysis, we found significantly reduced number of primary LO-PE HBCs. Reduction of HBCs was also observed in the EO-PE group, however, did not reach significance compared to the CTRs (Figure 1C).

In vitro, cell morphology of HBCs isolated from CTR, EO- and LO-PE placentae showed substantial differences (Supplementary Figure S1). Normally, directly after isolation, HBCs are round shaped cells with many vacuoles in the cytosol. Within 48-72 hours after isolation, cells differentiate and develop different shapes. Usually, M2 characterized macrophages exhibit an elongated, spindle-shaped morphology, whereas M1 polarized cells form a round, dendritic cell-like morphology with large filopodia (52, 53). CTR HBCs developed typical M2 features (Supplementary Figure 1A), whereas within isolations of EO- and LO-PE HBCs more of round shaped cells with larger filopodia next to M2 morphologies were found (Supplementary Figures 1B, C).

3.2 EO- and LO-PE HBCs are characterized by different expression of polarization markers

Basal expression of surface and intracellular M1 and M2 markers was determined by FACS (Tables 2 and 3) on primary isolated CTR (n=12), EO-PE (n=6) and LO-PE (n=5) HBCs. The gating strategy is shown in Supplementary Figure 2. FACS analysis revealed distinct expression of M1 and M2 markers in EO- and LO- PE HBCs (Table 2). EO-PE HBCs tend to express higher levels of pro-inflammatory CD11b, CD11c, CD40 ($p=0.09$) and TLR4 ($p \leq 0.05$), whereas expression of listed markers was similarly distributed

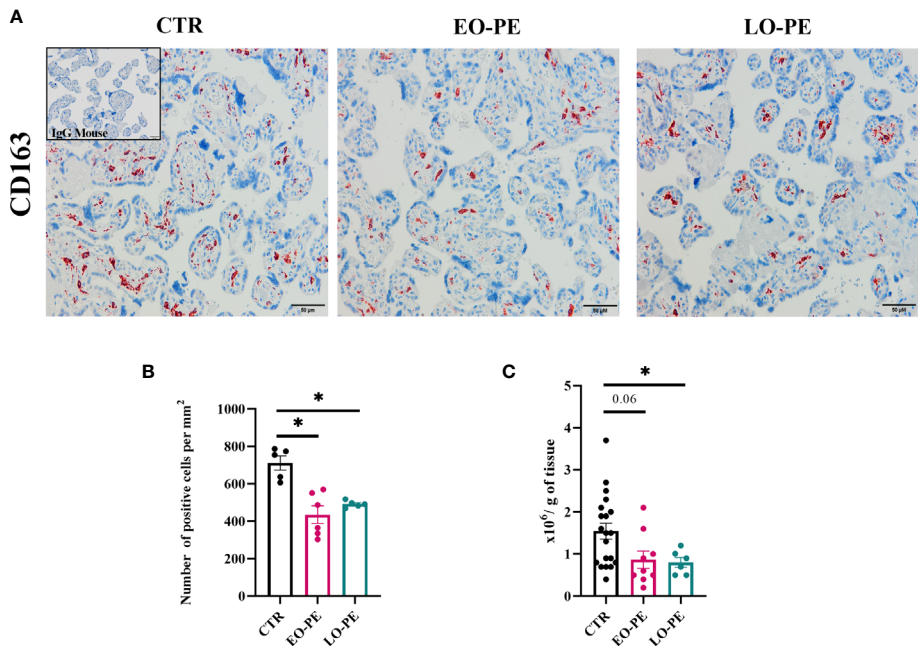

FIGURE 1
Immunohistochemical assessment of CD163 in placental tissue. **(A)** Representative images of serial sections of CTR (n=5), EO- (n=6) and LO-PE (n=6) are shown. Insert in the top right corner of CTR image depicts negative control stainings (blue). Images were taken at 20x magnification, scale bar represents 50µm. **(B)** Quantification of cells positive for CD163 in CTR, EO- and LO-PE group. Cells were quantified by using Quapath software. **(C)** Average yield of HBCs, adjusted to the wet weight (in grams) of minced tissue for each respective isolation, CTR (n=22), EO-PE (n=8), LO-PE (n=6). Data on **(B)** in **(C)** graphs are presented as mean ± S.E.M, ANCOVA with adjustment for gestational age, followed by Sidak's *post-hoc* test to examine statistical significance, *$p \leq 0.05$.

10.3389/fimmu.2022.1095879

TABLE 2 Percentage of live cells positive for respective surface polarization markers within the CTR (n=12), EO- (n=6) and LO-PE (n=5) groups.

Surface polarization marker	CTR (% of live cells)	EO-PE (% of live cells)	LO-PE (% of live cells)
CD11B	22.2 ± 9.6	38.7 ± 16.5	28.8 ± 17.0
CD11C	45.1 ± 14.3	69.9 ± 17.8	51.9 ± 11.8
CD40	17.1 ± 5.9	38.9 ± 12.6	22.6 ± 10.9
CD80	2.9 ± 1.8	6.5 ± 3.5	10.5 ± 8.9
CD86	25.0 ± 10.3 *	41.7 ± 3.6 ‡	21.6 ± 6.8
CD163	89.4 ± 3.9	82.0 ± 4.5	81.8 ± 6.8
CD206	47.6 ± 9.8	33.5 ± 6.5	38.2 ± 13.3
CD209	53.3 ± 6.9 †††	43.7± 12.1 ‡‡	22.1 ± 5.2
TLR1	5. 9 ± 6.2 †	9.5 ± 6.2	18.8 ± 13.6
TLR2	6.1 ± 3.9 *	1.2 ± 1.5	5.4 ± 4.5
TLR4	37.3 ± 12.3 *	79.7 ± 19.9	54.2 ± 18.8
HLA-DR	33.8 ± 14.1 ***	77.9 ± 12.6 ‡‡	44.3 ± 18.7
FR-β	79.2 ± 10.0	77.6 ± 20.7	68.4 ± 15.3

Data are presented as mean ± SD. Statistical significance is represented with *p ≤ 0.05, ***p ≤ 0.001; whereas *CTR vs EO-PE; †p ≤ 0.05, †††p ≤ 0.001; whereas †CTR vs LO-PE; ‡ p ≤ 0.05, ‡‡p ≤ 0.01; whereas ‡EO-PE vs LO-PE, by ANCOVA with Sidak's post-hoc test and adjustment for gestational age.

between LO-PE and CTR HBCs, except for CD209 ($p \leq 0.001$). Furthermore, we found significant increase of the major histocompatibility class (MHC) II molecule HLA-DR within the EO-PE group compared to the CTR group ($p \leq 0.001$). Interestingly, the HLA-DR expression was significantly different between EO- and LO-PE HBCs ($p \leq 0.01$) as well. Among the M1 markers only expression of CD80 ($p=0.05$) and TLR1 ($p \leq 0.05$) were elevated in LO-PE group. Notably, expression of CD80 and TLR1 was elevated in EO-PE group as well, but only by trend. Interestingly, surface expression of TLR2 was reduced in both EO- ($p \leq 0.05$) and LO-PE group. Next, we investigated the expression levels of CD86. Since CD86 can serve as M1 or M2b marker (54, 55), the secretion profile and expression of other markers should be taken into account when interpreting its expression. We found significant induction of the expression of the respective marker in EO-PE HBCs ($p \leq 0.05$) compared to the CTR ($p \leq 0.05$) or LO-PE ($p \leq 0.05$) group. In LO-PE HBCs the expression of CD86 did not differ from the control. In contrast to the increase of pro-inflammatory markers in EO-PE HBCs, a slight decrease in the anti-inflammatory markers CD206 and folate receptor β (FR-β) was observed. Expression pattern of CD206 and FR-β was similar in LO-PE HBCs as well. Expression of CD163 on primary isolated HBCs was evenly distributed between all investigated groups, confirming that CD163 can be used rather as a reliable tissue resident marker (Figures 1A, B) than a direct indicator of M2 phenotype. Next, M2 marker CD209 was suppressed in the LO-PE group ($p \leq 0.001$). Its expression was only minimally decreased by 10% in EO-PE HBCs group. Interestingly, we found a significant difference in the expression of CD209 between EO- and LO-PE HBCs ($p \leq 0.01$).

In addition to the investigation of surface polarization markers, we studied intracellular markers (Table 3). Next to the pan-macrophage marker CD68, two important regulators of TLR-Myd88 signaling (56, 57), IRF4 and IRF5 were investigated. Noteworthy, IRF4/IRF5 axis is involved in the initiation control of a specific M1/M2 polarization program. IRF5 as a positive regulator of Myd88 induces the expression of pro-inflammatory genes and establishment of M1 phenotype (58). Whereas IRF4, as a negative regulator of Myd88, leads to the activation of anti-inflammatory genes and initiation of M2 polarization (56, 59).We found the highest expression of IRF5 in EO-PE group and the lowest in CTRs. Expression of IRF4 the regulator of M2 polarization was evenly distributed between CTR and LO-PE group. Importantly, expression of IRF4 in EO-PE HBCs was reduced. Moreover, balance in favour of IRF5 together with higher expression of other surface M1 markers (Table 2) indicates possible phenotypic switch towards M1 polarization of EO-PE HBCs.

TABLE 3 Percentage of positive CTR (n=12), EO-PE (n=5) and LO-PE (n=4) HBCs for respective intracellular polarization markers.

Intracellular polarization marker	CTR (% of positive cells)	EO-PE (% of positive cells)	LO-PE (% of positive cells)
CD68	84.0 ± 9.8	70.4 ± 9.1	87.5 ± 5.4
IRF4	91.6 ± 8.0	85.7 ± 11.8	96.2 ± 2.0
IRF5	73.1 ± 12.8	91.5 ± 10.8	85.2 ± 12.0

Data are presented as mean ± SD. Statistical significance was tested by ANCOVA with Sidak's post-hoc test and adjustment for gestational age.

3.3 HBC secretion profile of cytokines and adhesion molecules differs in PE

Polarized macrophages are known to secrete specific patterns of cytokines, chemokines, and growth factors, allowing us to characterize polarization states (60). Using multiplex ELISA-on-bead technology, we determined the secretion profile of cytokines and chemokines secreted by CTR (n=8), EO-PE (n=6) and LO-PE (n=4) HBCs (Figure 2, Supplementary Figure 3). Moreover, secretion of IL-8 was determined using ELISA, since its secretion excided the detection limit of the multiplex ELISA (CTR n=10, EO-PE n=5, LO-PE n= 5; Figure 2J). Notably, TGF-β1 was measured with ELISA (CTR n=12, EO-PE n=6, LO-PE n=6, Figure 2K) since the sample preparation requires acidification of the samples for binding of TGF-β epitopes.

Secretion profile of EO- and LO-PE HBCs differs from the CTR group. First, among pro-inflammatory cytokines, we discovered a trend of an increased secretion of IL-6, IL-12p70 and P-Selectin by

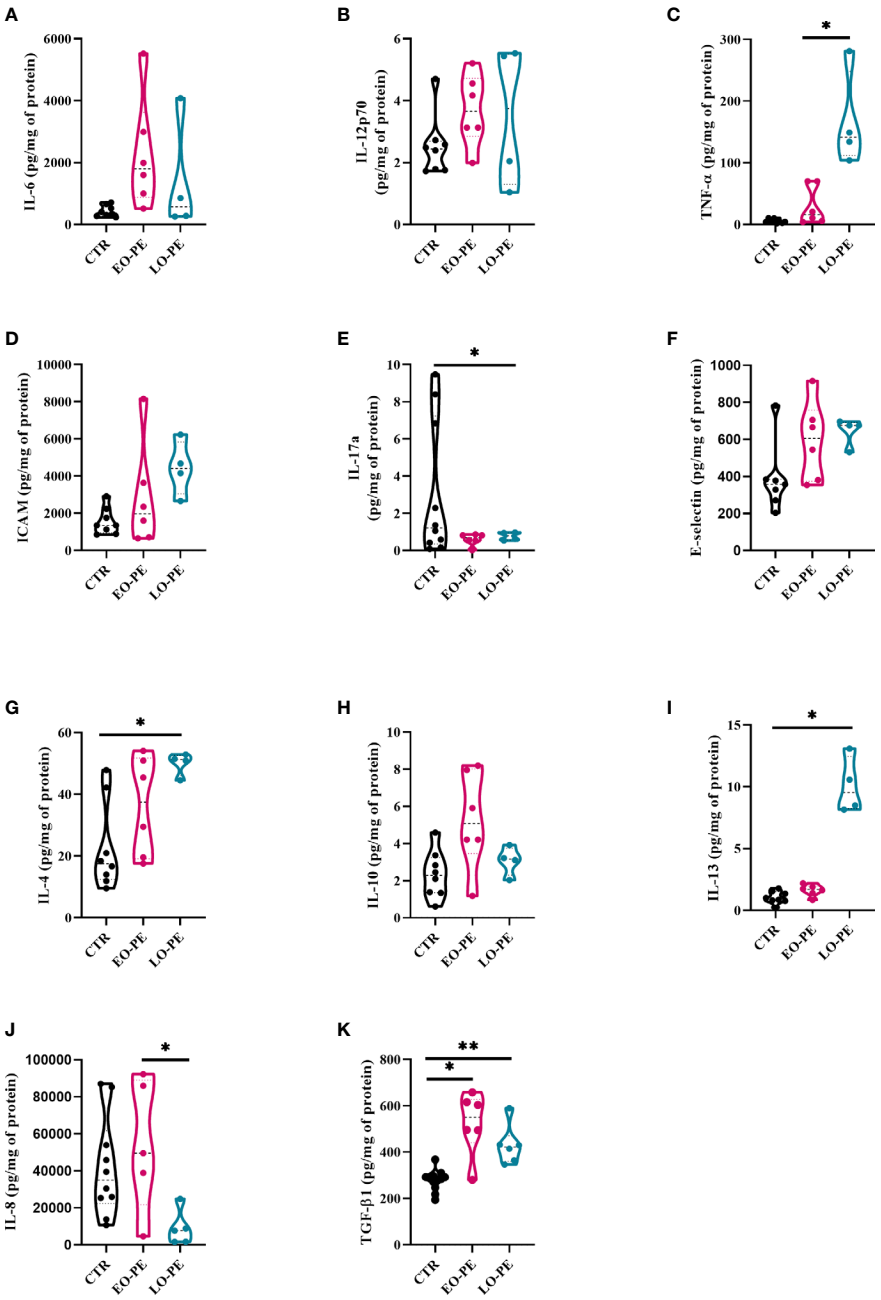

FIGURE 2
Secretion of cytokines and adhesion molecules by CTR (n=8), EO- (n=6) and LO-PE (n=4) HBCs. Multiplex-ELISA-on-beads assay for followed pro-inflammatory and anti-inflammatory cytokines **(A)** IL-6, **(B)** IL-12p-70, **(C)** TNF-α, **(D)** ICAM, **(E)** IL-17a, **(F)** E-selectin, **(G)** IL-4, **(H)** IL-10 and **(I)** IL-13, respectively. Multiplex was performed in duplicates. **(J)** ELISA against IL-8 performed in duplicates (CTR n=10, EO-PE n=5 and LO-PE n=5). **(K)** ELISA assay against TGF-β1 performed in duplicates (CTR n=12, EO-PE n=6 and LO-PE n=6). Secretion of respective cytokines was normalized to the total protein content measured in the cell culture supernatants. Statistical significance was tested using ANCOVA with adjustment for gestational age followed by Sidak's *post-hoc* test. *p ≤ 0.05, **p ≤0.01.

EO-PE HBCs (Figures 2A, B; Supplementary Figure 3A). Contrary, to the EO-PE HBCs where secretion of TNF-α was unchanged, LO-PE released higher amounts of TNF-α as CTRs or EO-PE HBCs ($p \leq 0.05$) (Figure 2C). LO-PE HBCs secreted higher amounts of ICAM, but only by trend (Figure 2D). Moreover, both PE groups secreted less IL-17a compared to CTRs (Figure 2E). Although, release of E-Selectin was higher in both PE groups, we did not find any differences in the production of other pro-inflammatory cytokines, such as: IL-1α, IL-1 β, CCL-3, CCL-4, IFN- α, and IFN-γ between investigated groups (Figure 2F, Supplementary Figures 3B–H). A decrease of IL-8, measured by ELISA was detected in LO-PE HBC group, whereas unchanged between CTR HBCs and EO-PE group. Interestingly, we found a significant difference in the release of IL-8 between EO- and LO-PE HBCs ($p \leq 0.05$) (Figure 2J).

Next, we examined the secretion of anti-inflammatory cytokines namely, IL-4, IL-10, IL-13, and TGF-β1, which serve as important drivers of M2 polarization (53, 61). We did not find any differences in the secretion of IL-13; however, secretion of IL-4 and IL-10 was increased, but only by trend in EO-PE HBCs. LO-PE HBCs secreted significantly higher levels of IL-4 ($p \leq 0.05$) and IL-13 ($p \leq 0.05$) compared to CTR HBCs (Figures 2G–I). Interestingly, both PE groups released significantly higher amounts of anti-inflammatory TGF-β1, which was even more pronounced in the LO-PE group ($p \leq 0.01$) (Figure 2K).

Noteworthy, some of the secreted pro-inflammatory cytokines are not reliable identifiers of a specific phenotype, since they are expressed by both M1 and M2 macrophages. E.g. IL-6 is a pro-inflammatory cytokine produced by both M1- and M2a-polarized macrophages (62). In addition, secretion of ICAM is mediated by NF-κB, but can serve as both an M1 and M2 cytokine due to its pro-angiogenic nature (63). The observed changes in the secretion profile indicate a switch in the phenotype and possible protective mechanisms of PE HBCs in an attempt to reduce the extent of inflammation by increasing the production of anti-inflammatory cytokines.

3.4 Preeclampsia triggers transcriptional changes of HBC-genes involved in inflammation

Macrophages are capable of responding to the local stimuli and acquiring different phenotypes and functions to meet changing physiological needs (64). Next, we examined transcriptional changes in HBCs that may be triggered by PE. Basal gene expression of CTR (n=12), EO- (n=5) and LO-PE (n=5) HBCs was determined on the fifth day after isolation. We analysed selected genes associated with phenotype and functionality of macrophages undergoing inflammation (Figure 3). Dynamic changes in gene expression were observed between the PE subgroups EO and LO. First, we found -as expected - an upregulation of *NFKB1* in both EO- and LO-PE groups ($p \leq 0.05$) (Figure 3A). Among the inflammatory pathways involved in M1 polarization, NF-κB plays an important role and regulates the expression of pro-inflammatory genes such as cytokines, adhesion molecules and growth factors (65). Next, the expression of *HIF1*, another M1-associated gene was upregulated in the LO-PE group ($p \leq 0.05$), whereas its expression was surprisingly decreased in EO-PE group ($p \leq 0.05$) (Supplementary Figure 4). In line with the increased secretion of *ICAM* (Figure 2H), mRNA of the respective gene was upregulated in the both PE groups (Supplementary Figure 4). In contrast to the expression of *ICAM, VCAM* was downregulated in EO-PE, whereas in LO-PE group remained on the level of CTRs (Supplementary Figure 4). Consistent with secretion of IL-8 (Figure 2J), higher fold change of *IL8* was detected in CTR group (Supplementary Figure 4). The expression of *TGFB1*, which acts as important M2 inducer (66), was significantly elevated in both, EO- and LO-PE HBCs ($p \leq 0.05$) (Figure 3B). Although, the differences in the secretion of CCL-4 (Supplementary Figure 3H) were not noticeable, higher expression was detected in the CTR group by RT-qPCR. In contrast to the secretion profile of IL -6 and IL -10, which was higher in the PE group (Figures 2A, H), qPCR analysis revealed downregulation of respective cytokines in the EO- and LO-PE groups (Supplementary Figure 4), possibly due to the tight post-transcriptional gene regulation of these cytokines in particular (67). As polarized macrophages metabolise L-arginine differently, M2 *via* arginase-1 and M1 macrophages *via* nitric oxide synthase (iNOS) (68), we looked at expression of *ARG1* gene, encoding arginase-1, and *NOS2*, encoding iNOS (68). Interestingly, *ARG1* expression was increased in both PE groups (Figure 3C). However, expression of *NOS2* was strongly upregulated in EO-PE ($p \leq 0.05$); whereas expression of the respective gene in LO-PE HBCs was even lower as in CTR HBCs (Figure 3D). In addition to the metabolism of L-arginine, regulation of reactive oxygen species (ROS), represents an important link between M1 and M2 polarization (69). M1 macrophages produce higher amounts of ROS and consequently downregulate antioxidant enzymes such as *CAT* encoding catalase, or *SOD* encoding superoxide dismutase (70), whereas, M2 macrophages are thought to produce lower levels of ROS and express higher levels of *CAT* or *SOD* (71). The expression of the genes *CAT* and *SOD*, was significantly attenuated in both, EO- and LO-PE groups (Figure 3E, F). Next in respect to observed TGF-β1 differences, we looked at the expression of genes involved in tissue remodeling and adhesion. Importantly, we found upregulation of *MMP*9 in both PE groups (Figure 3G). The expression of other genes involved in tissue remodeling (*MMP2, MMP12, TIMP1, TIMP2*), did not differ between groups (Supplementary Figure 4). Adhesion molecules, such as *CDH2* has been downregulated in both EO-PE ($p \leq 0.05$) and LO-PE HBCs (Figure 3H). Similarly, as *CDH2* we identified reduced expression of *CDH5* in both, EO- and LO- PE HBCs (Figure 3I).

In the healthy placenta, HBCs are often found in close proximity to feto-placental endothelial cells (fpEC), and M2 macrophages have the ability to regulate placental angiogenesis by secretion of pro-angiogenic factors (26). To gain insight into their role in angiogenesis, HBCs were examined for the expression of *FLT, VEGFA, KDR*, and *EGFR*; which were all downregulated in EO- and LO-PE group (Supplementary Figure 4).

Furthermore, EO-PE and CTR fpECs were treated with conditioned medium (CM) collected from CTR and EO-PE HBCs. In order to further investigate the influence of HBCs on the fpEC, metabolic activity of fpECs using the MTS assay (Supplementary Figure 5A) and the proliferation of the fpEC by incorporation of BrDU (Supplementary Figure 5B) were measured. CM of CTR HBCs increased the NAD(P)H dehydrogenase activity of CTR fpEC,

10.3389/fimmu.2022.1095879

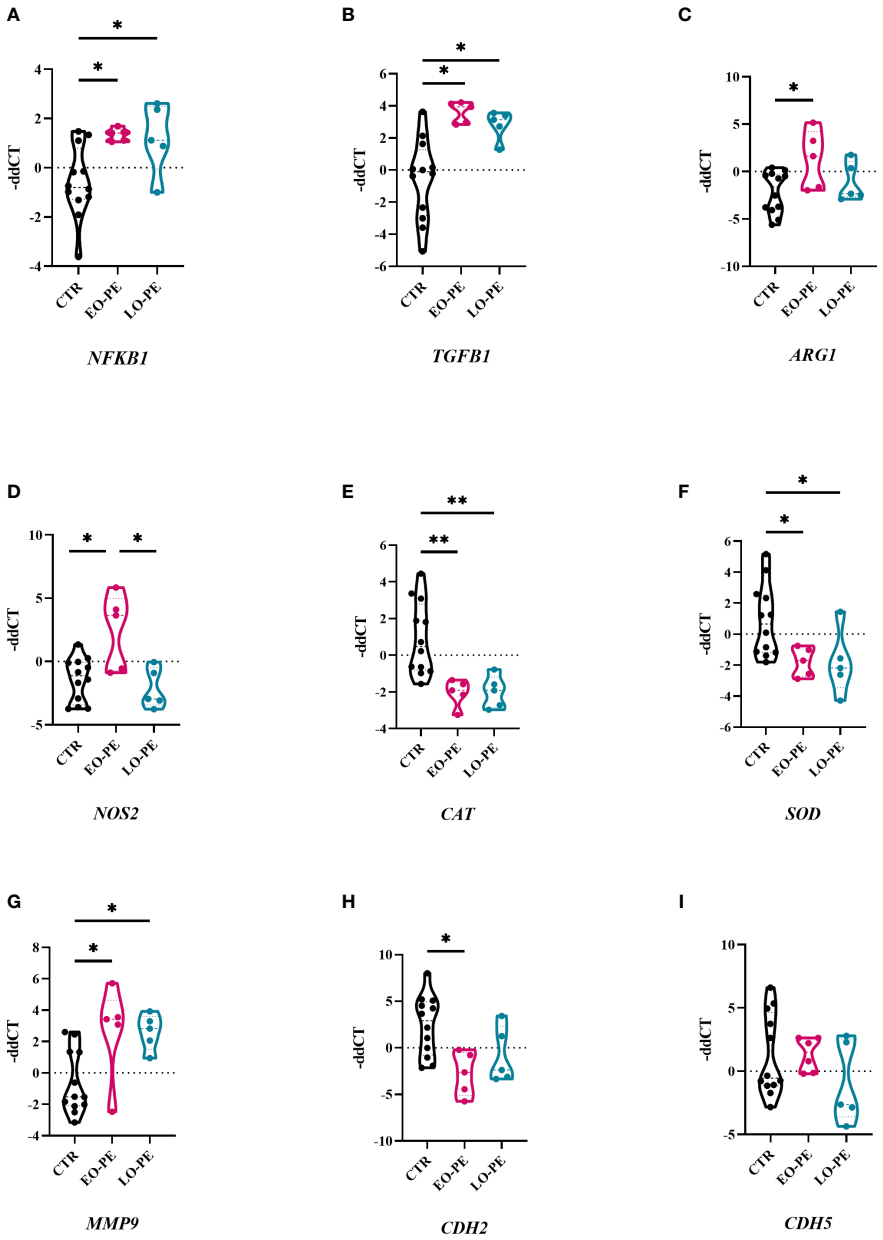

FIGURE 3
Preeclampsia alters inflammatory related gene expression in HBCs. **(A)** Total RNA of cultivated HBCs was harvested on the fifth day post isolation and analysed by RT-qPCR. **(A)** *NFKB1*, **(B)** *TGFB1*, **(C)** *ARG1*, **(D)** *NOS2*, **(E)** *CAT*, **(F)** *SOD*, **(G)** *MMP9*, **(H)** *CDH2*, **(I)** *CDH5*. In total 12 CTR, 5 EO-PE and 5 LO-PE HBCs isolations in three technical replicates were used. Expression of target genes was normalized to the following housekeeping genes (*18S*, *RPL30* and *HPRT1*) using $2^{\Delta\Delta Ct}$ method. Statistical significance was tested using ANCOVA with adjustment for gestational age followed by Sidak's *post-hoc* test. *p ≤ 0.05 and **p ≤ 0.01.

whereas PE CM had no effect on the activity of PE fpEC (Supplementary Figure 5A). A similar effect was observed when the proliferation of CTR fpEC was measured (Supplementary Figure 5B).

3.5 Phagocytosis of HBCs is altered in PE

Macrophages, as professional phagocytes eliminate pathogens and apoptotic cells. The elimination of apoptotic cells plays an important regulatory role regarding the reduction of the inflammatory burden (72). Phagocytosis was measured and visualised using two different approaches. First, it was assessed by FACS (CTR n=10, EO-PE n=5, LO-PE n=5), where median fluorescence intensity (MFI) was used to quantify the phagocytic activity. PE HBC showed significantly higher phagocytic activity ($p \leq 0.01$) than CTRs (Figures 4A, B). Second, we analysed phagocytic activity using HCS (Figures 4C–E). For better visualisation cells were stained with HBCs tissue resident marker CD163. Analysis of CTR (n=7) and PE (n=5, EO n=3, LO n=2) confirmed higher (though not significant) phagocytosis of PE HBCs (Figure 4F). Furthermore, visualisation of phagocytosis allowed us to analyse morphology of the cells, calculating cell size - surface area (μM^2), which was lower in EO- and LO-PE groups, when compared to the surface area (μM^2) of CTRs (Supplementary Figure 6) confirming *in vitro* observations of smaller round cell morphologies of PE HBC (Supplementary Figures 1A–C).

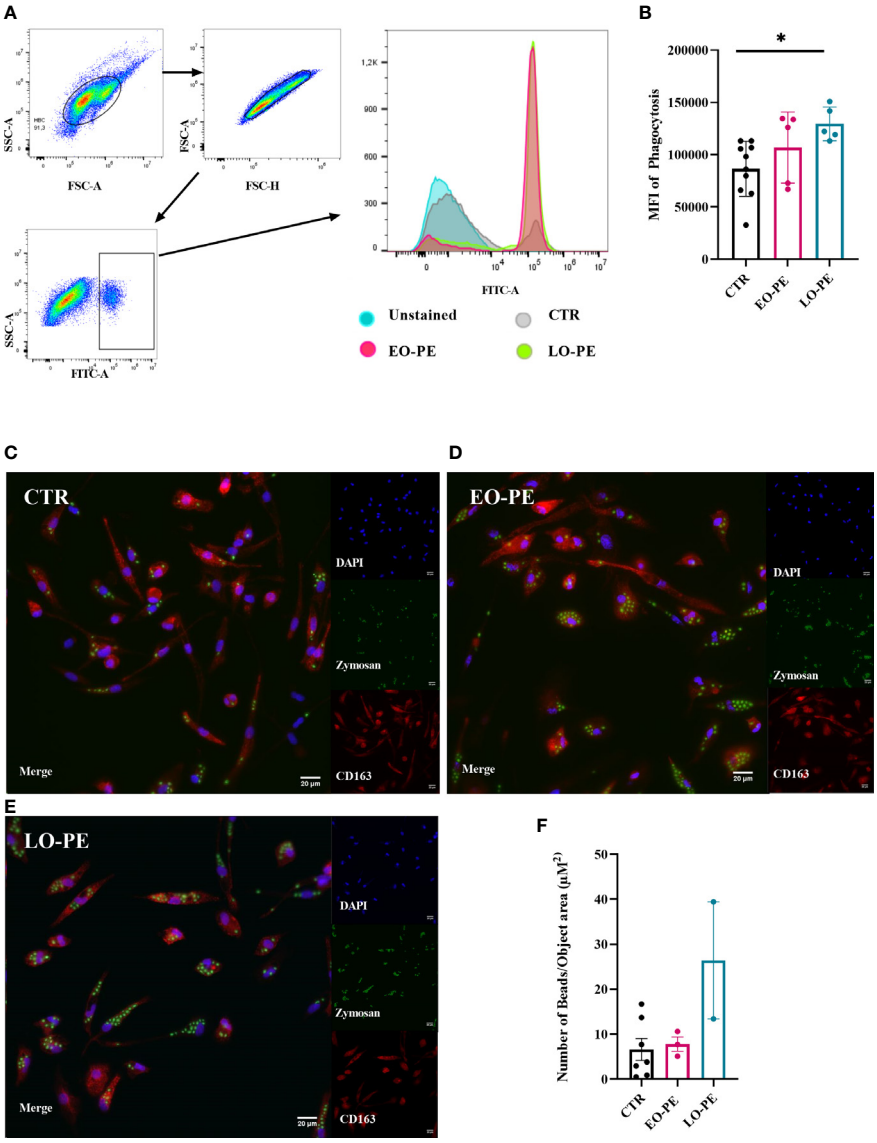

FIGURE 4
PE HBCs possess a higher phagocytic capacity. **(A)** Gating strategy cells for the measurement of phagocytosis. Cells were separated by size using forward and size scatter (FSC and SSC, respectively), followed by doublet discrimination and gating against SSC-area and FITC -A fluorescent signal. Histograms of one representative experiment are shown, in total 10 CTR, 5 EO-PE and 5 LO-PE HBCs were used. **(B)** Quantification of median fluorescence intensity (MFI) of phagocytosis measured with FACS. **(C)** Visualization of phagocytosis with high content screening microscopy (HCS). HBCs were treated with zymosan beads (green) and co-stained with CD163 (red), DAPI was used to stain nuclei. Representative images of individual experiments are shown. To visualize phagocytosis CTR (**C**, n=7), EO-PE (**D**, n=3) and LO-PE (**E**, n=2) isolations were used. Scale bar represents 20µM. **(F)** Quantification of the phagocytosis measured with high content screening. Analysis was carried out with NisViewer Software, analyzing the number of beads within the CD163 positive HBC cell. All data in **(B, F)** are presented as mean ± S.E.M, ANCOVA with adjustment for gestational age with Sidak's *post-hoc* test was used for to test statistical significance. *p ≤ 0.05.

3.6 PE attenuates MMP-9 activity of HBCs

In a normal placenta M2-polarized HBCs contribute to tissue remodeling and repair (73). To confirm strong upregulation of *MMP9* (Figure 3G), we additionally performed gelatin zymography to assess the activity of MMP-2 and MMP-9 (Figure 5A). As shown with *MMP2* mRNA expression (Supplementary Figure 4), detectable MMP-2 activity (Figure 5A) did not differ between studied groups (Figure 5B). In line with upregulation of *MMP9*, EO-PE HBCs displayed significantly ($p \leq 0.05$) higher MMP-9 activity as CTR. LO-PE HBCs MMP-9 activity was increased, but only by trend (Figure 5C).

Expression and production of MMPs are usually tightly regulated within the complex network of their four different tissue inhibitors of metalloproteinases 1-4 (TIMP). HBCs secretion of TIMP- (1, 2, 74, 75) was assessed using a multiplex ELISA-on-bead assay (Figure 5D). Production of TIMP-1, TIMP-2, TIMP-3 was unchanged in EO-PE group, we noticed a decreased production of TIMP-4 in the respective group. Furthermore, LO-PE HBCs secretion of TIMP-1 was significantly decreased, followed by trend in the reduced production of TIMP-2. Interestingly, release of TIMP-3 in LO-PE group was similar as in CTR. LO-PE HBCs production of TIMP-4 was elevated, but only by trend. To further explore the gelatinolytic activity of HBCs, the ratio between mRNA expression of *MMP2/TIMP1*,

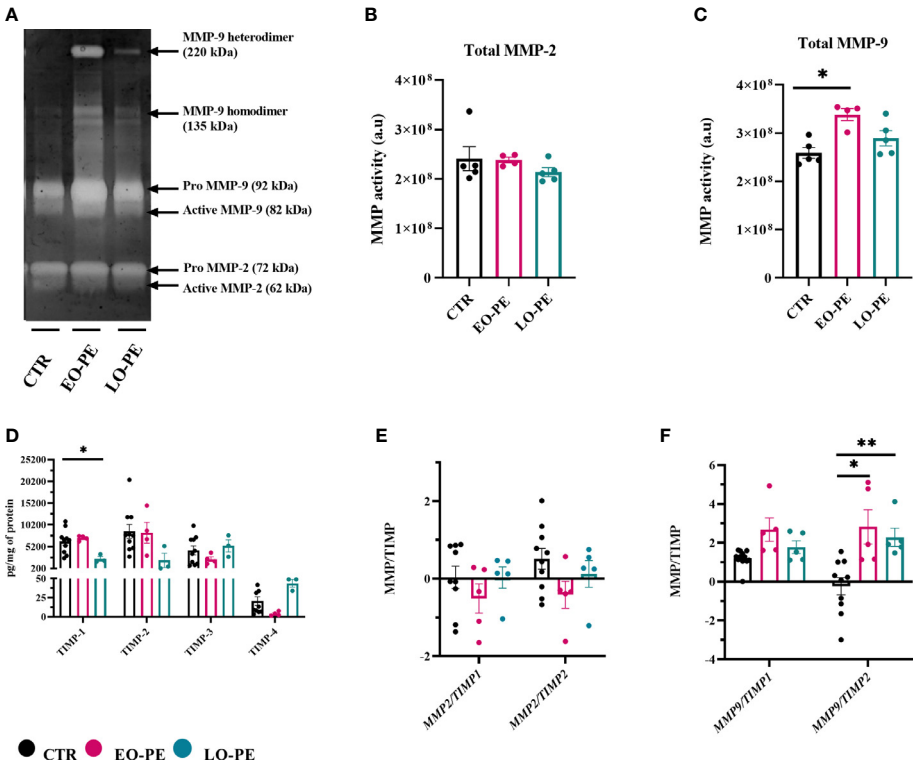

FIGURE 5
Gelatin zymography demonstrating gelatinolytic activity of HBCs. **(A)** A representative zymogram gel showing MMP-9 and MMP-2 activity of CTR (n=5), EO- (n=4) and LO-PE (n=5) HBCs. Activity was examined in the supernatants collected from CTR and PE HBCs on the 5th day post isolation. In total 15µg of protein measured in supernatants were loaded onto gelatin gels, respectively. To generate the comparable gelatinolytic bands, gelatin zymography was repeated twice. White bands of gelatinase activity observed at 92 and 82kDa are pro- and active form of MMP-9. Moreover, white bands at the size of 72 and 62kDa represents pro- and active form of MMP-2. Quantification of total (pro and active) form of MMP-9 **(B)** and MMP-2 **(C)** was performed as densitometric analysis of respective bands. **(D)** TIMP-1, TIMP-2, TIMP-3 and TIMP-4 levels measured in the cell culture supernatants using multiplex assay. In total CTR (n=10), EO- (n=4) and LO-PE (n=3) HBCs were used in technical duplicates. Secretion of respective TIMPs was normalized to the total protein content measured in the cell culture supernatants. **(E)** mRNA ratio between *MMP2* and *TIMP1* and *TIMP2*. **(F)** mRNA ratio between *MMP9* and *TIMP1* and *TIMP2*. mRNA ratio was calculated from the -ddCT values normalized to the corresponding housekeeping genes (*18S*, *RPL30* and *HRPT1*). The results are showed as a mean ± S.E.M of technical triplicates. Statistical significance was assessed using ANCOVA with adjustment for gestational age followed by Sidak's *post-hoc* test. *p ≤ 0.05. **p ≤ 0.01.

MMP2/TIMP2, *MMP9/TIMP1*, and *MMP9/TIMP2* was calculated. Normally, TIMPs regulate inhibition of MMPs by binding in 1:1 reversible complex with the MMPs (76, 77). The shift in MMP/TIMP balance in favor of MMPs reflects as increased extracellular matrix (ECM) proteolysis, or if in favor of TIMP as decreased proteolysis and protection of the ECM (78–80). In CTR, EO- and LO- PE HBCs the ratio between *MMP2* and *TIMP1* or *TIMP2* (Figure 5E) stayed unchanged. Similar *MMP9/TIMP1* ratio of investigated groups, was favoring the gelatinolytic activity, indicating that MMP-9 is the main gelatinase produced by HBCs. However, significant differences were demonstrated in *MMP-9/TIMP-2* of EO- and LO-PE HBCs, confirming higher gelatinolytic activity shown with gelatin zymography (Figures 5A, C, F).

4 Discussion

Hofbauer cells, play a pivotal but also a diverse role in placental physiology by maintaining tissue homeostasis and the tolerogenic environment (26, 36, 41, 81). HBCs plasticity is well characterized by an unique phenotype expressing both, M2 and M1 polarization markers (26, 30, 31). Preeclampsia is an inflammatory condition, accompanied by activation of both the innate and adaptive immune system. These alterations may directly influence the phenotype of HBCs and contribute to placental dysfunction (82). Due to the presumed distinct pathophysiological origins of EO- and LO-PE and the resulting different inflammatory burden within the PE placenta (5, 8, 9, 83), we aimed to determine the phenotypic and functional alterations between different HBCs. One of the more significant findings to emerge from this study is that both, EO- and LO-PE HBCs maintain a profound anti-inflammatory phenotype in the human placenta. In addition to HBCs general adaptive response to inflammatory stimuli, EO-PE HBCs cope differently with signals from their microenvironment.

The EO-PE placenta has been linked to placental malperfusion (84), leading to oxygen deficiency, increased inflammation and oxidative stress which all together deteriorate the mechanisms of placentation early in pregnancy. In contrast, LO-PE placenta has been linked to changes of systemic blood pressure in the mother leading to maternal endothelial dysfunction and oxidative stress, resulting in placental dysfunction (85, 86). Consequently, both subtypes of PE are characterized by excessive inflammation caused by oxidative stress and a hypoxic microenvironment, which affects the appearance and phenotypic composition of immune cells, particularly macrophages

(87). To investigate whether the number of HBCs differs between CTR and PE placenta, we first quantified the cells *in situ* using specific markers for tissue-resident macrophages. In agreement, with the findings of Tang et al., where they investigated CD163 positive HBCs in PE placentae (51), we found a decreased number of CD163 - positive macrophages in both EO- and LO-PE placentae. Similarly, Yang et al. observed a significantly reduced number of CD14-positive HBCs in PE (87). In addition, Broekhuizen et al., used combined staining for CD68 and CD163 and observed a significant decrease in double-positive HBCs in EO-PE, whereas the number of double-positive HBCs in LO-PE remained unchanged (18). We verified our immunohistochemical findings by analyzing the yield of primary isolated HBCs *in vitro*. Similar to *in situ*, we obtained a decreased number of primary HBCs isolated from EO- and LO-PE placental tissues. As PE placenta is characterized by an increased number of apoptotic trophoblasts (88, 89), it is likely that HBCs may undergo a similar apoptosis cascade, leading to a decreased number of vital HBCs in culture. According to our results, PE may exacerbate the participation of initial stages of apoptosis in placental tissue which in turn leads to a reduced anti-inflammatory and immunoregulatory capability of remaining HBCs.

Macrophage polarization is a complex process controlled by several factors and mechanisms (90). It is noteworthy that a subpopulation identified with the same markers may have different functions in different tissues and pathologies, adding to the complexity of defining phenotypes (27). At baseline, HBCs express M1 and M2 polarization markers (30, 31). Moreover, HBCs retain alternative M2 polarization in inflammatory complications such as in gestational diabetes mellitus (31), chorioamnionitis (91), or upon *in vitro* stimulation (30). Contrary to expectations, we observed differences in the expression pattern of polarization markers between EO- and LO-PE HBCs. In EO- HBC markers involved in M1 polarization such as TLR4, HLA-DR, CD40, CD80 and CD86 were upregulated, suggesting M1 phenotype. In contrast, in LO-PE HBCs the expression of before mentioned markers was either reduced or similar to CTRs. The anti-inflammatory phenotype of LO-PE HBCs is strongly underpinned by high expression of IRF4, which exerts important function in controlling local cytokine milieu thereby polarization (92). TLR signaling has been proposed as an important link between activation of innate immune system and PE, known to modulate the inflammatory responses (18, 93). Interestingly, Young et al. demonstrated the maintenance of the M2 phenotype of HBCs despite pro-inflammatory treatment and upregulation of TLR4 and increased secretion of pro-inflammatory cytokines (IL-6, IL-8) (37). We demonstrated an upregulation of TLR4 and its downstream mediators *NFKB1* and TNF-α in EO-PE, implying they give up M2 polarization and a shift towards M1. A change of phenotype toward M1 polarization is also suggested by increased expression of IRF5 and *NOS2*. IRF4 and IRF5, both regulators of the Myd88 pathway are crucial for the expression of M1/M2 genes (94). In particular, IRF5 regulates the expression of pro-inflammatory factors such as: TNF-α, IL-6, IL-12p70, CD86 (58). IRF4, on the other hand, is known to compete with IRF5 for interaction with Myd88 to activate the M2 program (56, 92). Its expression has been shown to be induced by anti-inflammatory IL-4 (92, 95). Interestingly, EO-PE HBCs, although favoring IRF5 activation, express IRF4 and consequently secrete both pro- and anti-inflammatory cytokines. A dysbalance of intracellular IRF4 and IRF5 regulating factors may control different phenotypes and the associated contributions to tissue inflammation.

It has been reported that in PE placentae CD163 and FR–β, expression is decreased (51). Although a reduction of CD163 on tissue levels could be confirmed, no differences of CD163 and FR-β expression on the primary isolated HBCs were detected. This inconsistency can be explained because CD163 is used as a tissue-resident marker for placental macrophages rather than only as an M2 marker. Among anti-inflammatory M2 markers, CD209 serves as one of the major M2 markers, moreover, CD209-positive HBCs have been shown to produce IL -10 an immunosuppressive cytokine one of the drivers of immunoregulatory M2 polarization (96). Our results suggest differential expression patterns of CD209 between EO- and LO-PE HBCs. Interestingly, the expression of CD209 was unchanged in CTRs and in the EO-PE group, whereas it was significantly reduced in the LO-PE group. In line, LO-PE HBCs tend to secrete lower levels of IL-10 supporting the notion that this polarization pattern favors regulatory properties of these cells. Yang et al. also reported lower numbers of CD209-positive HBCs in PE placental tissues, but they did not distinguish between onsets of PE (96)

Cytokines are important coordinators that likely promote phenotypic and functional changes of immune cells in inflammation (90, 97). We have shown that both, EO- and LO-PE HBCs produce different regulators of M2 polarization: IL-4, IL-10, IL-13 and TGF-β. Interestingly, whereas in EO-PE an increased production of TGF-β and IL-10 was observed, LO-PE HBCs secreted higher amounts of IL-4, IL-13, and TGF-β. IL-10 and IL-4, have been recognized as inducers of *ARG1*, which represents a hallmark of M2 polarization (97–100) IL-10 is a cytokine produced mainly by M2 macrophages (58) and its anti-inflammatory effect has been demonstrated by reduced production of pro-inflammatory cytokines such as TNF-α, IL-6, and IL-12 (101, 102). Moreover, although pro-inflammatory M1 marker - IRF5 has been shown to inhibit transcription of IL-10 and TGF-β (58, 103), this regulation may be impaired in EO-PE, where basal secretion of IL-10 and TGF-β levels were increased. Enhanced expression of M1 polarization markers, upregulation of both M1 *NOS2* and M2 *ARG1*, accompanied by secretion of anti-inflammatory cytokines, indicate a development of a specific M1 and M2 phenotype of EO-PE HBCs. On the other hand, LO-PE HBCs downregulate *NOS2* and express *ARG1* at the same level as CTRs HBCs, suggesting their anti-inflammatory phenotype.

Phenotypic plasticity enables macrophages to perform a variety of functions required for maintenance of homeostasis and rapid termination of inflammation in their microenvironment (66). The resolution of acute inflammation is a well-orchestrated synergistic process and can be divided into three phases on the way back to cell homeostasis. First, inflammation is downregulated by the temporal switching of secreted lipid mediators, then the clearance of debris and apoptotic cells by phagocytically active macrophages, and finally, tissue repair and angiogenesis are stimulated by the pro-resolving phenotype of macrophages (20, 24, 54, 104). We demonstrated a higher phagocytic capacity of EO- and LO-PE compared to normal HBCs, with concomitantly significantly higher levels of TGF-β produced by both groups. Interestingly, TGF-β in monocytes and macrophages is known for its role in maintaining the resolution of inflammation by increasing

phagocytosis and restoring tissue integrity (105–107). The increased phagocytosis and production of anti-inflammatory cytokines (90) may indicate one of the regulatory mechanisms that determine M2 phenotype of EO- and LO-PE HBCs by preventing a direct switch to M1 polarization.

Following clearance of cell-debris, M2 macrophages initiate events that are critical for tissue repair. These include the production of extracellular matrix (ECM), MMPs and the promotion of angiogenesis (108). Furthermore, MMPs make an important contribution to ECM repair (108), and macrophages require active MMP-9 for migration during an inflammatory response (109). TGF-β acts as a regulator of ECM production, reflecting its role in the tissue remodeling (110). We have shown compared to normal HBCs that both EO- and LO-PE HBCs secrete higher levels of MMP-9 and TGF-β. Interestingly, one of the many functions of MMP-9 is also to activate the inactive form of TGF-β (111), suggesting a possible mechanism driving polarization toward M2. MMP-9 is regulated by the expression of TIMPs, which has been shown to have pro-angiogenic features and is unique to M2 macrophages (112). Although the MMP9/TIMP2 ratio of EO- and LO-PE HBCs favors M2 polarization, we have shown that EO-PE HBCs were unable to stimulate proliferation of endothelial cells. Ability to enhance endothelial proliferation and consequently angiogenesis is one of the traits of M2 macrophages in the process of resolution of inflammation (104). The unsuccessful activation of proliferation of endothelial cells reveals another aspect of the pro-inflammatory M1 signature of EO-PE HBCs. It is more likely that they contribute to endothelial dysfunction instead of positive pro-angiogenic endothelial activation, but further investigation is needed.

Knowledge about the function of macrophages in PE is still insufficient. Our study focused on the *in vitro* polarization and functionality of EO- and LO-PE HBCs. Our results suggest that EO-PE HBCs develop a strong M1 signature, but despite the M1 features and PE inflammatory microenvironment, they still attempt to resolve inflammation by upregulating M2 anti-inflammatory factors and functions. Based on the fact that the expression of CD209 in EO-PE HBCs is at basal levels as in CTR HBCs, and expression of CD86 and secretion of TGF-β are increased, they might develop an immunoregulatory M2b and a tissue remodeling M2a phenotype with features of M1 polarization based on the increased expression of TLR4, HLA-DR, and IRF5. In contrast, LO-PE HBCs tend to develop a phagocytic M2 phenotype with increased production of IL-4, IL-13, and TGF-β. However, the higher expression of TLR1, TLR4, and CD80 and increased production of TNF-α indicate a specific pro-inflammatory pattern distinct from typical M2 polarization (Figure 6). Given the strength of our study, namely the use of a large number of clinically well-characterized samples from EO- and LO-PE placenta, there are some apparent limitations. First, macrophage polarization is a dynamic process, and therefore the choice of polarization markers included may vary among investigators. Because characterization of macrophage phenotype using polarization markers and cytokine release is rather descriptive, we chose to use functional assays to determine the relevant physiological functions of macrophages in addition to their phenotype. Second, primary HBCs might develop a different polarization pattern than *in vivo* because of the sensitivity of

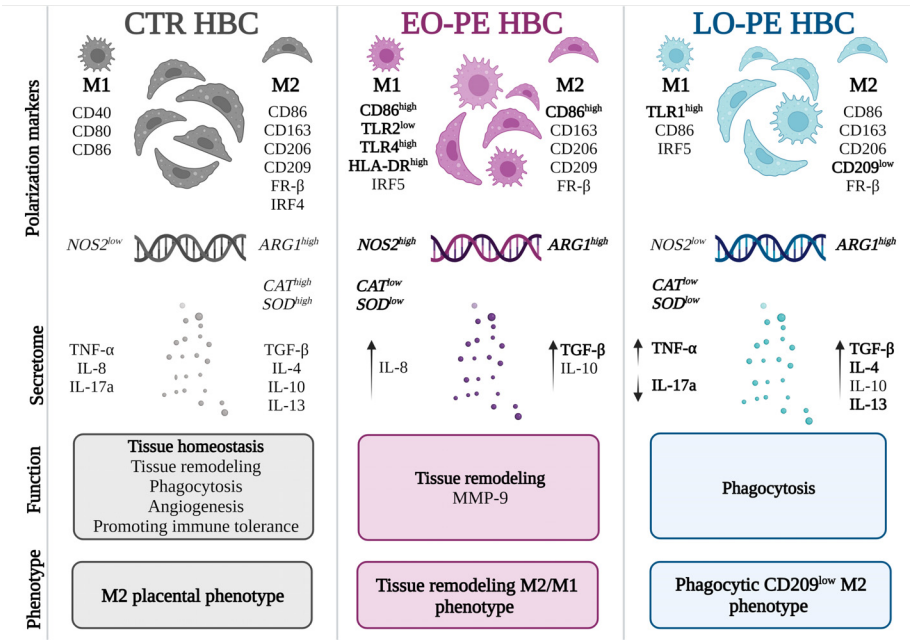

FIGURE 6
Different polarization patterns of CTR, EO - and LO-PE HBCs. HBCs isolated from CTR placenta develop a specific placental phenotype and express both M1 and M2 polarization markers. In CTR placenta, their M2 nature is reflected by increased expression of *ARG1*, *CAT*, and *SOD*, where HBCs promote tissue repair, angiogenesis, and homeostasis. Our results suggest that EO-PE HBCs develop an M2 phenotype that is strongly shifted toward M1 polarization. Their M2 phenotype is reflected in the upregulation of *ARG1*, secretion of TGF-β, and tissue remodeling function, whereas features of M1 polarization are seen in the increased expression of TLR4, HLA-DR, IRF5, and *NOS2*. In contrast, LO-PE HBCs tend to develop a phagocytic $CD209^{low}$ M2 phenotype with increased production of IL-4, IL-13, and TGF-β. However, the higher expression of TLR1 and increased production of TNF-α indicate a specific pro-inflammatory pattern that differs from the typical M2 polarization. The figure was generated using BioRender. Differences that were significant different between the groups studied are printed in bold.

primary HBCs to the *in vitro* environment. However, we and others have shown that Hofbauer cells have a very stable phenotype *in vitro* that is difficult to alter and correlates with the phenotype in tissue *in vivo* (30, 37).

In conclusion, to the best of our knowledge, this is the first study to show a pivotal difference of the polarization pattern between EO - and LO-PE HBCs *in vitro*. We demonstrated that the inflammatory environment of PE causes the phenotypic changes observed between early and late PE HBCs. The changes in polarization patterns indicate different etiologies of PE, as EO-PE is associated with inflammation on the placental side, whereas LO-PE results from a maternal inflammatory response. Furthermore, since placental immune cells responds differently to the source of inflammation, PE could be identified as different entities with a common phenotype rather than a single disorder.

Data availability statement

The original contributions presented in the study are included in the article/Supplementary Material. Further inquiries can be directed to the corresponding author.

Ethics statement

The studies involving human participants were reviewed and approved by Institutional ethics committee of the Medical University of Graz (29-319 ex 16/17). The patients/participants provided their written informed consent to participate in this study.

Author contributions

MHM and CW conceived the study and designed the experiments. MHM performed the experiments and analysed the data. Reviewing and editing was done by CS and HF. MHM and CW wrote the original draft manuscript. All authors contributed to the article and approved the submitted version.

Funding

MHM is supported through the PhD program Inflammatory Disorders in Pregnancy (DP-iDP) by the Austrian Science Fund FWF (Doc 31-B26) and the Medical University of Graz, Austria.

Acknowledgments

The authors thank Markus Absenger Novak from the Imaging core facility at the Center for Medical Research (ZMF) for advice on HCS set-up and analysis. The authors thank Renate Michlmaier for continuous technical support and Bettina Amtmann for patient acquisition.

Conflict of interest

The authors declare that the research was conducted in the absence of any commercial or financial relationships that could be construed as a potential conflict of interest.

Publisher's note

Supplementary material

The Supplementary Material for this article can be found online at: https://www.frontiersin.org/articles/10.3389/fimmu.2022.1095879/full#supplementary-material

References

1. Gestational hypertension and preeclampsia: ACOG practice bulletin, number 222. *Obstet Gynecol* (2020) 135:e237–60. doi: 10.1097/AOG.0000000000003891

2. Practice Bulletin No ACOG. 203: Chronic hypertension in pregnancy. *Obstet Gynecol* (2019) 133:e26–50. doi: 10.1097/AOG.0000000000003020

3. Brown MA, Magee LA, Kenny LC, Karumanchi SA, McCarthy FP, Saito S, et al. Hypertensive disorders of pregnancy. *Hypertension* (2018) 72:24–43. doi: 10.1161/HYPERTENSIONAHA.117.10803

4. Wójtowicz A, Zembala-Szczerba M, Babczyk D, Kołodziejczyk-Pietruszka M, Lewaczyńska O, Huras H. Early-and late-onset preeclampsia: A comprehensive cohort study of laboratory and clinical findings according to the new ISHHP criteria. *Int J Hypertens* (2019) 2019:4108271. doi: 10.1155/2019/4108271

5. von Dadelszen P, Magee LA, Roberts JM. Subclassification of preeclampsia. *Hypertens Pregnancy* (2003) 22:143–8. doi: 10.1081/PRG-120021060

6. Tranquilli AL, Brown MA, Zeeman GG, Dekker G, Sibai BM. The definition of severe and early-onset preeclampsia. statements from the international society for the study of hypertension in pregnancy (ISSHP). *Pregnancy Hypertension: Int J Women's Cardiovasc Health* (2013) 3:44–7. doi: 10.1016/J.PREGHY.2012.11.001

7. Huppertz B. Placental origins of preeclampsia: Challenging the current hypothesis. *Hypertension* (2008) 51:970–5. doi: 10.1161/HYPERTENSIONAHA.107.107607

8. Li XL, Guo PL, Xue Y, Gou WL, Tong M, Chen Q. An analysis of the differences between early and late preeclampsia with severe hypertension. *Pregnancy Hypertension: Int J Women's Cardiovasc Health* (2016) 6:47–52. doi: 10.1016/J.PREGHY.2015.12.003

9. Nelson DB, Ziadie MS, McIntire DD, Rogers BB, Leveno KJ. Placental pathology suggesting that preeclampsia is more than one disease. *Am J Obstet Gynecol* (2014) 210:66. doi: 10.1016/J.AJOG.2013.09.010

10. Stergiotou I, Crispi F, Valenzuela-Alcaraz B, Bijnens B, Gratacos E. Patterns of maternal vascular remodeling and responsiveness in early- versus late-onset preeclampsia. *Am J Obstet Gynecol* (2013) 209:558. doi: 10.1016/J.AJOG.2013.07.030

11. del Gaudio I, Sasset L, di Lorenzo A, Wadsack C. Sphingolipid signature of human feto-placental vasculature in preeclampsia. *Int J Mol Sci* (2020) 21(3):1019. doi: 10.3390/ijms21031019

12. Murthi P, Pinar AA, Dimitriadis E, Samuel CS. Inflammasomes–a molecular link for altered immunoregulation and inflammation mediated vascular dysfunction in preeclampsia. *Int J Mol Sci* (2020) 21:1406. doi: 10.3390/IJMS21041406

13. Borzychowski AM, Sargent IL, Redman CWG. Inflammation and pre-eclampsia. *Semin Fetal Neonatal Med* (2006) 11:309–16. doi: 10.1016/J.SINY.2006.04.001

14. Sharma A, Satyam A, Sharma JB. Leptin, IL-10 and inflammatory markers (TNF-α, IL-6 and IL-8) in pre-eclamptic, normotensive pregnant and healthy non-pregnant women. *Am J Reprod Immunol* (2007) 58:21–30. doi: 10.1111/J.1600-0897.2007.00486.X

15. Vishnyakova P, Poltavets A, Nikitina M, Muminova K, Potapova A, Vtorushina V, et al. Preeclampsia: inflammatory signature of decidual cells in early manifestation of disease. *Placenta* (2021) 104:277–83. doi: 10.1016/j.placenta.2021.01.011

16. Aneman I, Pienaar D, Suvakov S, Simic TP, Garovic VD, McClements L. Mechanisms of key innate immune cells in early- and late-onset preeclampsia. *Front Immunol* (2020) 11:1864/XML/NLM. doi: 10.3389/FIMMU.2020.01864/XML/NLM

17. Han X, Ghaemi MS, Ando K, Peterson LS, Ganio EA, Tsai AS, et al. Differential dynamics of the maternal immune system in healthy pregnancy and preeclampsia. *Front Immunol* (2019) 10:1305/BIBTEX. doi: 10.3389/FIMMU.2019.01305/BIBTEX

18. Broekhuizen M, Hitzerd E, van den Bosch TPP, Dumas J, Verdijk RM, van Rijn BB, et al. The placental innate immune system is altered in early-onset preeclampsia, but not in late-onset preeclampsia. *Front Immunol* (2021) 12:780043/BIBTEX. doi: 10.3389/FIMMU.2021.780043/BIBTEX

19. Ma Y, Ye Y, Zhang J, Ruan CC, Gao PJ. Immune imbalance is associated with the development of preeclampsia. *Med (United States)* (2019) 98(14):e15080. doi: 10.1097/MD.0000000000015080

20. Atri C, Guerfali FZ, Laouini D. Role of human macrophage polarization in inflammation during infectious diseases. *Int J Mol Sci* (2018) 19(6):1801. doi: 10.3390/IJMS19061801

21. Shapouri-Moghaddam A, Mohammadian S, Vazini H, Taghadosi M, Esmaeili SA, Mardani F, et al. Macrophage plasticity, polarization, and function in health and disease. *J Cell Physiol* (2018) 233:6425–40. doi: 10.1002/jcp.26429

22. Xue J, Schmidt SV, Sander J, Draffehn A, Krebs W, Quester I, et al. Transcriptome-based network analysis reveals a spectrum model of human macrophage activation. *Immunity* (2014) 40:274. doi: 10.1016/J.IMMUNI.2014.01.006

23. Takiguchi H, Yang CX, Yang CWT, Sahin B, Whalen BA, Milne S, et al. Macrophages with reduced expressions of classical M1 and M2 surface markers in human bronchoalveolar lavage fluid exhibit pro-inflammatory gene signatures. *Sci Rep* (2021) 11:1–11. doi: 10.1038/s41598-021-87720-y

24. Porcheray F, Viaud S, Rimaniol A-C, Léone C, Samah B, Dereuddre-Bosquet N, et al. Macrophage activation switching: an asset for the resolution of inflammation. *Clin Exp Immunol* (2005) 142:481. doi: 10.1111/J.1365-2249.2005.02934.X

25. Oshi M, Tokumaru Y, Asaoka M, Yan L, Satyananda V, Matsuyama R, et al. M1 macrophage and M1/M2 ratio defined by transcriptomic signatures resemble only part of their conventional clinical characteristics in breast cancer. *Sci Rep* (2020) 10:1–12. doi: 10.1038/s41598-020-73624-w

26. Loegl J, Hiden U, Nussbaumer E, Schliefsteiner C, Cvitic S, Lang I, et al. Hofbauer cells of M2a, M2b and M2c polarization may regulate feto-placental angiogenesis. *Reproduction* (2016) 152:447–55. doi: 10.1530/REP-16-0159

27. Martinez FO, Gordon S. The M1 and M2 paradigm of macrophage activation: time for reassessment. *F1000Prime Rep* (2014) 6:13. doi: 10.12703/P6-13

28. Turco MY, Moffett A. Development of the human placenta. *Development* (2019) 146(22):dev163428. doi: 10.1242/DEV.163428

29. Reyes L, Wolfe B, Golos T. "Hofbauer cells: Placental macrophages of fetal origin". In: *Results Problems Cell Differentiation* (2017) 62:45–60. doi: 10.1007/978-3-319-54090-0_3

30. Schliefsteiner C, Ibesich S, Wadsack C. Placental hofbauer cell polarization resists inflammatory cues *In vitro*. *Int J Mol Sci* (2020) 21(3):736. doi: 10.3390/ijms21030736

31. Schliefsteiner C, Peinhaupt M, Kopp S, Lögl J, Lang-Olip I, Hiden U, et al. Human placental hofbauer cells maintain an anti-inflammatory M2 phenotype despite the presence of gestational diabetes mellitus. *Front Immunol* (2017) 8:888. doi: 10.3389/fimmu.2017.00888

32. Tang Z, Niven-Fairchild T, Tadesse S, Norwitz ER, Buhimschi CS, Buhimschi IA, et al. Glucocorticoids enhance CD163 expression in placental hofbauer cells. *Endocrinology* (2013) 154:471–82. doi: 10.1210/EN.2012-1575

33. Kim SY, Romero R, Tarca AL, Bhatti G, Kim CJ, Lee J, et al. Methylome of fetal and maternal monocytes and macrophages at the feto-maternal interface. *Am J Reprod Immunol* (2012) 68:8–27. doi: 10.1111/J.1600-0897.2012.01108.X

34. Goldstein J, Braverman M, Salafia C, Buckley P. The phenotype of human placental macrophages and its variation with gestational age(1988) (Accessed November 5, 2021).

35. Zulu MZ, Martinez FO, Gordon S, Gray CM. The elusive role of placental macrophages: The hofbauer cell. *J Innate Immun* (2019) 11:447–56. doi: 10.1159/000497416

36. Thomas JR, Appios A, Zhao X, Dutkiewicz R, Donde M, Lee CYC, et al. Phenotypic and functional characterization of first-trimester human placental macrophages, hofbauer cells. *J Exp Med* (2020) 218(1):e20200891. doi: 10.1084/JEM.20200891

37. Young OM, Tang Z, Niven-Fairchild T, Tadesse S, Krikun G, Norwitz ER, et al. Toll-like receptor-mediated responses by placental hofbauer cells (HBCs): A potential pro-inflammatory role for fetal M2 macrophages. *Am J Reprod Immunol* (2015) 73:22–35. doi: 10.1111/aji.12336

38. Svensson-Arvelund J, Mehta RB, Lindau R, Mirrasekhian E, Rodriguez-Martinez H, Berg G, et al. The human fetal placenta promotes tolerance against the semiallogeneic fetus by inducing regulatory T cells and homeostatic M2 macrophages. *J Immunol* (2015) 194:1534–44. doi: 10.4049/JIMMUNOL.1401536

39. Cervar M, Blaschitz A, Dohr G, Desoye G. Paracrine regulation of distinct trophoblast functions *in vitro* by placental macrophages. *Cell Tissue Res* (1999) 295:297–305. doi: 10.1007/S004410051236

40. Khan S, Katabuchi H, Araki M, Nishimura R, Okamura H. Human villous macrophage-conditioned media enhance human trophoblast growth and differentiation. *In Vitro Biol Reprod* (2000) 62:1075–83. doi: 10.1095/BIOLREPROD62.4.1075

41. Anteby EY, Natanson-Yaron S, Greenfield C, Goldman-Wohl D, Haimov-Kochman R, Holzer H, et al. Human placental hofbauer cells express sprouty proteins: a possible modulating mechanism of villous branching. *Placenta* (2005) 26:476–83. doi: 10.1016/J.PLACENTA.2004.08.008

42. Seval Y, Korgun ET, Demir R. Hofbauer cells in early human placenta: possible implications in vasculogenesis and angiogenesis. *Placenta* (2007) 28:841–5. doi: 10.1016/J.PLACENTA.2007.01.010

43. ben Amara A, Gorvel L, Baulan K, Derain-Court J, Buffat C, Vérollet C, et al. Placental macrophages are impaired in chorioamnionitis, an infectious pathology of the placenta. *J Immunol* (2013) 191:5501–14. doi: 10.4049/jimmunol.1300988

44. Vinnars M-TN, Rindsjö E, Ghazi S, Sundberg A, Papadogiannakis N. The number of CD68+ (Hofbauer) cells is decreased in placentas with chorioamnionitis and with advancing gestational age. *Pediatr Dev Pathol* (2010) 13:300–4. doi: 10.2350/09-03-0632-OA.1

45. Toti P, Arcuri F, Tang Z, Schatz F, Zambrano E, Mor G, et al. Focal increases of fetal macrophages in placentas from pregnancies with histological chorioamnionitis: Potential role of fibroblast monocyte chemotactic protein-1. *Am J Reprod Immunol* (2011) 65:470–9. doi: 10.1111/j.1600-0897.2010.00927.x

46. Kim JS, Romero R, Kim MR, Kim YM, Friel L, Espinoza J, et al. Involvement of hofbauer cells and maternal T cells in villitis of unknown aetiology. *Histopathology* (2008) 52:457–64. doi: 10.1111/j.1365-2559.2008.02964.x

47. Quicke KM, Bowen JR, Johnson EL, McDonald CE, Ma H, O'Neal JT, et al. Zika virus infects human placental macrophages. *Cell Host Microbe* (2016) 20:83–90. doi: 10.1016/J.CHOM.2016.05.015

48. Tang Z, Tadesse S, Norwitz E, Mor G, Abrahams VM, Guller S. Isolation of hofbauer cells from human term placentas with high yield and purity. *Am J Reprod Immunol* (2011) 66:336–48. doi: 10.1111/j.1600-0897.2011.01006.x

49. Bankhead P, Loughrey MB, Fernández JA, Dombrowski Y, McArt DG, Dunne PD, et al. QuPath: Open source software for digital pathology image analysis. *Sci Rep* (2017) 7:1–7. doi: 10.1038/s41598-017-17204-5

50. Moldenhauer JS, Stanek J, Warshak C, Khoury J, Sibai B. The frequency and severity of placental findings in women with preeclampsia are gestational age dependent. *Am J Obstet Gynecol* (2003) 189:1173–7. doi: 10.1067/S0002-9378(03)00576-3

51. Tang Z, Buhimschi IA, Buhimschi CS, Tadesse S, Norwitz E, Niven-Fairchild T, et al. Decreased levels of folate receptor-β and reduced numbers of fetal macrophages (Hofbauer cells) in placentas from pregnancies with severe pre-eclampsia. *Am J Reprod Immunol* (2013) 70:104–15. doi: 10.1111/AJI.12112

52. McWhorter FY, Wang T, Nguyen P, Chung T, Liu WF. Modulation of macrophage phenotype by cell shape. *Proc Natl Acad Sci* (2013) 110:17253–8. doi: 10.1073/PNAS.1308887110

53. Porta C, Riboldi E, Ippolito A, Sica A. Molecular and epigenetic basis of macrophage polarized activation. *Semin Immunol* (2015) 27:237–48. doi: 10.1016/J.SMIM.2015.10.003

54. Wang Lx, Zhang S, Wu Hj, Rong X, Guo J. M2b macrophage polarization and its roles in diseases. *J Leukoc Biol* (2019) 106:345–58. doi: 10.1002/JLB.3RU1018-378RR

55. Martinez FO, Sica A, Mantovani A, Locati M. Macrophage activation and polarization. *Front Bioscience* (2008) 13:453–61. doi: 10.2741/2692/PDF

56. Negishi H, Ohba Y, Yanai H, Takaoka A, Honma K, Yui K, et al. Negative regulation of toll-like-receptor signaling by IRF-4. *Proc Natl Acad Sci* (2005) 102:15989–94. doi: 10.1073/PNAS.0508327102

57. Takaoka A, Yanai H, Kondo S, Duncan G, Negishi H, Mizutani T, et al. Integral role of IRF-5 in the gene induction programme activated by toll-like receptors. *Nature* (2005) 434:243–9. doi: 10.1038/nature03308

58. Krausgruber T, Blazek K, Smallie T, Alzabin S, Lockstone H, Sahgal N, et al. IRF5 promotes inflammatory macrophage polarization and TH1-TH17 responses. *Nat Immunol* (2011) 12:231–8. doi: 10.1038/ni.1990

59. Honma K, Udono H, Kohno T, Yamamoto K, Ogawa A, Takemori T, et al. Interferon regulatory factor 4 negatively regulates the production of proinflammatory cytokines by macrophages in response to LPS. *Proc Natl Acad Sci* (2005) 102:16001–6. doi: 10.1073/PNAS.0504226102

60. Raggi F, Pelassa S, Pierobon D, Penco F, Gattorno M, Novelli F, et al. Regulation of human macrophage M1–M2 polarization balance by hypoxia and the triggering receptor expressed on myeloid cells-1. *Front Immunol* (2017) 0:1097. doi: 10.3389/FIMMU.2017.01097

61. Makita N, Hizukuri Y, Yamashiro K, Murakawa M, Hayashi Y. IL-10 enhances the phenotype of M2 macrophages induced by IL-4 and confers the ability to increase eosinophil migration. *Int Immunol* (2015) 27:131–41. doi: 10.1093/INTIMM/DXU090

62. Fernando MR, Reyes JL, Iannuzzi J, Leung G, McKay DM. The pro-inflammatory cytokine, interleukin-6, enhances the polarization of alternatively activated macrophages. *PloS One* (2014) 9:e94188. doi: 10.1371/JOURNAL.PONE.0094188

63. Frank PG, Lisanti MP. ICAM-1: role in inflammation and in the regulation of vascular permeability. *Am J Physiol Heart Circ Physiol* (2008) 295:H926. doi: 10.1152/AJPHEART.00779.2008

64. Hu G, Su Y, Kang BH, Fan Z, Dong T, Brown DR, et al. High-throughput phenotypic screen and transcriptional analysis identify new compounds and targets for macrophage reprogramming. *Nat Commun* (2021) 12:1–14. doi: 10.1038/s41467-021-21066-x

65. Liu T, Zhang L, Joo D, Sun S-C. NF-κB signaling in inflammation. *Signal Transduction Targeted Ther* (2017) 2:1–9. doi: 10.1038/sigtrans.2017.23

66. Murray PJ, Allen JE, Biswas SK, Fisher EA, Gilroy DW, Goerdt S, et al. Macrophage activation and polarization: Nomenclature and experimental guidelines. *Immunity* (2014) 41:14–20. doi: 10.1016/J.IMMUNI.2014.06.008

67. Palanisamy V, Jakymiw A, van Tubergen EA, D'Silva NJ, Kirkwood KL. Control of cytokine mRNA expression by RNA-binding proteins and microRNAs. *J Dent Res* (2012) 91:651. doi: 10.1177/0022034512437372

68. Rath M, Müller I, Kropf P, Closs EI, Munder M. Metabolism *via* arginase or nitric oxide synthase: Two competing arginine pathways in macrophages. *Front Immunol* (2014) 0:532. doi: 10.3389/FIMMU.2014.00532

69. Zhang Y, Choksi S, Chen K, Pobezinskaya Y, Linnoila I, Liu Z-G. ROS play a critical role in the differentiation of alternatively activated macrophages and the occurrence of tumor-associated macrophages. *Cell Res* (2013) 23:898–914. doi: 10.1038/cr.2013.75

70. Rendra E, Riabov V, Mossel DM, Sevastyanova T, Harmsen MC, Kzhyshkowska J. Reactive oxygen species (ROS) in macrophage activation and function in diabetes. *Immunobiology* (2019) 224:242–53. doi: 10.1016/J.IMBIO.2018.11.010

71. Griess B, Mir S, Datta K, Teoh-Fitzgerald M. Scavenging reactive oxygen species selectively inhibits M2 macrophage polarization and their pro-tumorigenic function in part, *via* Stat3 suppression. *Free Radic Biol Med* (2020) 147:48–60. doi: 10.1016/J.FREERADBIOMED.2019.12.018

72. Klöditz K, Fadeel B. Three cell deaths and a funeral: macrophage clearance of cells undergoing distinct modes of cell death. *Cell Death Discov* (2019) 5:1–9. doi: 10.1038/s41420-019-0146-x

73. Reyes L, Golos TG. Hofbauer cells: Their role in healthy and complicated pregnancy. *Front Immunol* (2018) 9:2628. doi: 10.3389/fimmu.2018.02628

74. Raguema N, Moustadraf S, Bertagnolli M. Immune and apoptosis mechanisms regulating placental development and vascularization in preeclampsia. *Front Physiol* (2020) 11:98. doi: 10.3389/fphys.2020.00098

75. Phipps EA, Thadhani R, Benzing T, Karumanchi SA. Pre-eclampsia: pathogenesis, novel diagnostics and therapies. *Nat Rev Nephrol* (2019) 15:275–89. doi: 10.1038/s41581-019-0119-6

76. Brew K, Nagase H. The tissue inhibitors of metalloproteinases (TIMPs): An ancient family with structural and functional diversity. *Biochim Biophys Acta* (2010) 1803:55. doi: 10.1016/J.BBAMCR.2010.01.003

77. Cataldo DD, Gueders M, Munaut C, Rocks N, Bartsch P, Foidart J-M, et al. Matrix metalloproteinases and tissue inhibitors of matrix metalloproteinases mRNA transcripts in the bronchial secretions of asthmatics. *Lab Invest* (2004) 84:418–24. doi: 10.1038/labinvest.3700063

78. Visse R, Nagase H. Matrix metalloproteinases and tissue inhibitors of metalloproteinases. *Circ Res* (2003) 92:827–39. doi: 10.1161/01.RES.0000070112.80711.3D

79. Gardner K, Arnoczky SP, Caballero O, Lavagnino M. The effect of stress-deprivation and cyclic loading on the TIMP/MMP ratio in tendon cells: An in vitro experimental study. *Disabil Rehabil* (2008). 30(20–22):1523–9. doi: 10.1080/09638280701785395

80. Arpino V, Brock M, Gill SE. The role of TIMPs in regulation of extracellular matrix proteolysis. *Matrix Biol* (2015) 44–46:247–54. doi: 10.1016/J.MATBIO.2015.03.005

81. Svensson J, Jenmalm MC, Matussek A, Geffers R, Berg G, Ernerudh J. Macrophages at the fetal–maternal interface express markers of alternative activation and are induced by m-CSF and IL-10. *J Immunol* (2011) 187:3671–82. doi: 10.4049/JIMMUNOL.1100130

82. Rana S, Lemoine E, Granger J, Karumanchi SA. Preeclampsia: Pathophysiology, challenges, and perspectives. *Circ Res* (2019) 124:1094–112. doi: 10.1161/CIRCRESAHA.118.313276/FORMAT/EPUB

83. Ren Z, Gao Y, Gao Y, Liang G, Chen Q, Jiang S, et al. Distinct placental molecular processes associated with early-onset and late-onset preeclampsia. *Theranostics* (2021) 11:5028–44. doi: 10.7150/THNO.56141

84. Kovo M, Schreiber L, Ben-Haroush A, Gold E, Golan A, Bar J. The placental component in early-onset and late-onset preeclampsia in relation to fetal growth restriction. *Prenat Diagn* (2012) 32:632–7. doi: 10.1002/PD.3872

85. Sohlberg S, Mulic-Lutvica A, Lindgren P, Ortiz-Nieto F, Wikström AK, Wikström J. Placental perfusion in normal pregnancy and early and late preeclampsia: A magnetic resonance imaging study. *Placenta* (2014) 35:202–6. doi: 10.1016/J.PLACENTA.2014.01.008

86. Marín R, Chiarello DI, Abad C, Rojas D, Toledo F, Sobrevia L. Oxidative stress and mitochondrial dysfunction in early-onset and late-onset preeclampsia. *Biochim Biophys Acta (BBA) - Mol Basis Dis* (2020) 1866:165961. doi: 10.1016/J.BBADIS.2020.165961

87. Saito S, Shiozaki A, Nakashima A, Sakai M, Sasaki Y. The role of the immune system in preeclampsia. *Mol Aspects Med* (2007) 28:192–209. doi: 10.1016/J.MAM.2007.02.006

88. DiFederico E, Genbacev O, Fisher SJ. Preeclampsia is associated with widespread apoptosis of placental cytotrophoblasts within the uterine wall. *Am J Pathol* (1999) 155:293–301. doi: 10.1016/S0002-9440(10)65123-1

89. He G, Xu W, Chen Y, Liu X, Xi M. Abnormal apoptosis of trophoblastic cells is related to the up-regulation of CYP11A gene in placenta of preeclampsia patients. *PloS One* (2013) 8:e59609. doi: 10.1371/JOURNAL.PONE.0059609

90. Mor G, Abrahams VM. Potential role of macrophages as immunoregulators of pregnancy. *Reprod Biol Endocrinol* (2003) 1:1–8. doi: 10.1186/1477-7827-1-119/FIGURES/4

91. Joerink M, Rindsjö E, van Riel B, Alm J, Papadogiannakis N. Placental macrophage (Hofbauer cell) polarization is independent of maternal allergen-sensitization and presence of chorioamnionitis. *Placenta* (2011) 32:380–5. doi: 10.1016/J.PLACENTA.2011.02.003

92. Satoh T, Takeuchi O, Vandenbon A, Yasuda K, Tanaka Y, Kumagai Y, et al. The Jmjd3-Irf4 axis regulates M2 macrophage polarization and host responses against helminth infection. *Nat Immunol* (2010) 11:936–44. doi: 10.1038/ni.1920

93. Yeon MK, Romero R, Seo YO, Chong JK, Kilburn BA, Armant DR, et al. Toll-like receptor 4: A potential link between "danger signals," the innate immune system, and preeclampsia? *Am J Obstet Gynecol* (2005) 193:921.e1–8. doi: 10.1016/J.AJOG.2005.07.076

94. al Mamun A, Chauhan A, Qi S, Ngwa C, Xu Y, Sharmeen R, et al. Microglial IRF5-IRF4 regulatory axis regulates neuroinflammation after cerebral ischemia and impacts stroke outcomes. *Proc Natl Acad Sci USA* (2020) 117:1742–52. doi: 10.1073/PNAS.1914742117/-/DCSUPPLEMENTAL

95. el Chartouni C, Schwarzfischer L, Rehli M. Interleukin-4 induced interferon regulatory factor (Irf) 4 participates in the regulation of alternative macrophage priming. *Immunobiology* (2010) 215:821–5. doi: 10.1016/J.IMBIO.2010.05.031

96. Yang SW, Cho EH, Choi SY, Lee YK, Park JH, Kim MK, et al. DC-SIGN expression in hofbauer cells may play an important role in immune tolerance in fetal chorionic villi during the development of preeclampsia. *J Reprod Immunol* (2017) 124:30–7. doi: 10.1016/J.JRI.2017.09.012

97. Deng B, Wehling-Henricks M, Villalta SA, Wang Y, Tidball JG. IL-10 triggers changes in macrophage phenotype that promote muscle growth and regeneration. *J Immunol* (2012) 189:3669–80. doi: 10.4049/JIMMUNOL.1103180

98. Sulahian TH, Högger P, Wahner AE, Wardwell K, Goulding NJ, Sorg C, et al. Human monocytes express cd163, which is upregulated by il-10 and identical TO p155. *Cytokine* (2000) 12:1312–21. doi: 10.1006/CYTO.2000.0720

99. Gray MJ, Poljakovic M, Kepka-Lenhart D, Morris SM. Induction of arginase I transcription by IL-4 requires a composite DNA response element for STAT6 and C/EBPβ. *Gene* (2005) 353:98–106. doi: 10.1016/J.GENE.2005.04.004

100. Wu WK, Georgiadis A, Copland DA, Liyanage S, Luhmann UFO, Robbie SJ, et al. IL-4 regulates specific arg-1+ macrophage sFlt-1–mediated inhibition of angiogenesis. *Am J Pathol* (2015) 185:2324–35. doi: 10.1016/J.AJPATH.2015.04.013

101. Lang R, Patel D, Morris JJ, Rutschman RL, Murray PJ. Shaping gene expression in activated and resting primary macrophages by IL-10. *J Immunol* (2002) 169:2253–63. doi: 10.4049/JIMMUNOL.169.5.2253

102. Schottelius AJG, Mayo MW, Balfour Sartor R, Baldwin AS. Interleukin-10 signaling blocks inhibitor of κB kinase activity and nuclear factor κB DNA binding *. *J Biol Chem* (1999) 274:31868–74. doi: 10.1074/JBC.274.45.31868

103. Dalmas E, Toubal A, Alzaid F, Blazek K, Eames HL, Lebozec K, et al. Irf5 deficiency in macrophages promotes beneficial adipose tissue expansion and insulin sensitivity during obesity. *Nat Med* (2015) 21:610–8. doi: 10.1038/nm.3829

104. Mosser DM, Hamidzadeh K, Goncalves R. Macrophages and the maintenance of homeostasis. *Cell Mol Immunol* (2020) 18:579–87. doi: 10.1038/s41423-020-00541-3

105. A-Gonzalez N, Bensinger SJ, Hong C, Beceiro S, Bradley MN, Zelcer N, et al. Apoptotic cells promote their own clearance and immune tolerance through activation of the nuclear receptor LXR. *Immunity* (2009) 31:245–58. doi: 10.1016/J.IMMUNI.2009.06.018

106. Kourtzelis I, Hajishengallis G, Chavakis T. Phagocytosis of apoptotic cells in resolution of inflammation. *Front Immunol* (2020) 11:553/BIBTEX. doi: 10.3389/FIMMU.2020.00553/BIBTEX

107. Gong D, Shi W, Yi S, Chen H, Groffen J, Heisterkamp N. TGFβ signaling plays a critical role in promoting alternative macrophage activation. *BMC Immunol* (2012) 13:1–10. doi: 10.1186/1471-2172-13-31

108. Oishi Y, Manabe I. Macrophages in inflammation, repair and regeneration. *Int Immunol* (2018) 30:511–28. doi: 10.1093/INTIMM/DXY054

109. Hanania R, Sun HS, Xu K, Pustylnik S, Jeganathan S, Harrison RE. Classically activated macrophages use stable microtubules for matrix metalloproteinase-9 (MMP-9) secretion. *J Biol Chem* (2012) 287:8468–83. doi: 10.1074/JBC.M111.290676/ATTACHMENT/13099993-EBF4-49E0-A71C-77C3089A9E06/MMC1.PDF

110. Xu X, Zheng L, Yuan Q, Zhen G, Crane JL, Zhou X, et al. Transforming growth factor-β in stem cells and tissue homeostasis. *Bone Res* (2018) 6:1–31. doi: 10.1038/s41413-017-0005-4

111. Kobayashi T, Kim HJ, Liu X, Sugiura H, Kohyama T, Fang Q, et al. Matrix metalloproteinase-9 activates TGF-β and stimulates fibroblast contraction of collagen gels. *Am J Physiol Lung Cell Mol Physiol* (2014) 306:L1006. doi: 10.1152/AJPLUNG.00015.2014

112. Zajac E, Schweighofer B, Kupriyanova TA, Juncker-Jensen A, Minder P, Quigley JP, et al. Angiogenic capacity of M1- and M2-polarized macrophages is determined by the levels of TIMP-1 complexed with their secreted proMMP-9. *Blood* (2013) 1122(25):4054–67. doi: 10.1182/BLOOD-2013-05-501494

frontiers | Frontiers in Immunology

TYPE Review
PUBLISHED 18 January 2023
DOI 10.3389/fimmu.2023.1118449

OPEN ACCESS

EDITED BY
Chao Yang,
Zhejiang University, China

REVIEWED BY
Jingbo Pang,
University of Illinois at Chicago, United States
Feng He,
Stanford University, United States
Bojie Zhang,
Regeneron Pharmaceuticals, Inc., United States

*CORRESPONDENCE
Suping Ma
masuping@163.com
Zhongping Duan
duan2517@163.com

†These authors have contributed equally to this work and share first authorship

SPECIALTY SECTION
This article was submitted to Inflammation, a section of the journal Frontiers in Immunology

RECEIVED 07 December 2022
ACCEPTED 06 January 2023
PUBLISHED 18 January 2023

CITATION
Xiao Z, Liu M, Yang F, Liu G, Liu J, Zhao W, Ma S and Duan Z (2023) Programmed cell death and lipid metabolism of macrophages in NAFLD.
Front. Immunol. 14:1118449.
doi: 10.3389/fimmu.2023.1118449

Programmed cell death and lipid metabolism of macrophages in NAFLD

Zhun Xiao[1†], Minghao Liu[1†], Fangming Yang[1], Guangwei Liu[1], Jiangkai Liu[1], Wenxia Zhao[1], Suping Ma[1*] and Zhongping Duan[2*]

[1]Department of Digestive Diseases, The First Affiliated Hospital of Henan University of Chinese Medicine, Zhengzhou, China, [2]Beijing Institute of Hepatology, Beijing Youan Hospital Capital Medical University, Beijing, China

Non-alcoholic fatty liver disease (NAFLD) has now become the leading chronic liver disease worldwide with lifestyle changes. This may lead to NAFLD becoming the leading cause of end-stage liver disease in the future. To date, there are still no effective therapeutic drugs for NAFLD. An in-depth exploration of the pathogenesis of NAFLD can help to provide a basis for new therapeutic agents or strategies. As the most important immune cells of the liver, macrophages play an important role in the occurrence and development of liver inflammation and are expected to become effective targets for NAFLD treatment. Programmed cell death (PCD) of macrophages plays a regulatory role in phenotypic transformation, and there is also a certain connection between different types of PCD. However, how PCD regulates macrophage polarization has still not been systematically elucidated. Based on the role of lipid metabolic reprogramming in macrophage polarization, PCD may alter the phenotype by regulating lipid metabolism. We reviewed the effects of macrophages on inflammation in NAFLD and changes in their lipid metabolism, as well as the relationship between different types of PCD and lipid metabolism in macrophages. Furthermore, interactions between different types of PCD and potential therapeutic agents targeting of macrophages PCD are also explored.

KEYWORDS

non-alcoholic fatty liver disease, inflammation, macrophages, programmed cell death, lipid metabolism

1 Introduction

Non-alcoholic fatty liver disease (NAFLD) is currently the most common liver disease, and affects approximately one-third of the world's population (1). According to the severity and the pathological phase, NAFLD can be divided into non-alcoholic fatty liver (NAFL), non-alcoholic fat hepatitis (NASH), liver fibrosis and cirrhosis. Although NAFL has no clinically significant, there is evidence suggests that approximately 25% of patients with NAFL progress to NASH (2). The presence of NASH promotes the progression of liver pathology and increases the incidence of adverse outcomes compared to NAFL. In recent

years, the global proportion of NAFLD-associated hepatocellular carcinoma (HCC) has increased year by year and may gradually become the main cause of HCC (3). Therefore, it is important to find effective therapeutic agents to block the pathological progression of NAFLD, especially NASH. The transition from NAFL to NASH is the result of a complex multifactorial effect, which involves a complex liver cell population (both parenchymal and non-parenchymal cells) as well as pathological signals from visceral fat and intestine. The pathogenesis of NAFLD was considered to be the "two-hit hypothesis" (4). Lipid accumulation in hepatocytes represents the "first hit", while other factors such as oxidative stress are referred to as the "second hit". However, recent studies have suggested that NAFLD progression may be influenced by various factors such as environment, metabolism, gut microbiota, and genetic factors (5, 6). The simultaneous changes of insulin resistance, genetic and epigenetic factors, mitochondrial dysfunction, endoplasmic reticulum stress, microbiota, chronic low-grade inflammation, etc. led to the progress of NAFLD, which was named "multiple parallel hits hypothesis" (7).

The main sources of lipid deposition in the liver include adipose tissue lipolysis, hepatic *de novo* lipogenesis (DNL), and diet, with the former accounting for the majority (8). Excess fatty acids are taken up and intracellularly transported in the liver by hepatocytes, macrophages, and other liver cells. When excess free fatty acids (FFAs) exceed the antioxidant capacity of the body, inflammation occurs. These mechanisms have been well summarized in previous reviews (9, 10). Macrophages are an important component of innate immunity. Macrophages in the liver mainly include tissue-resident Kupffer cells (KCs), monocyte-derived macrophages (MoMFs) and subcapsular macrophages discovered in recent years (11). Subcapsular macrophages play a major role in the defense against infectious agents from the abdominal cavity and are not the topic of this article. KCs are the most abundant tissue-resident macrophages in the mammalian body, accounting for 80-90% of all tissue-resident macrophages (12). KCs are mainly localized in the reticuloendothelial system and sense risk factors from the intestine and adipose tissue as well as multiple signals from the liver microenvironment. KCs constitute the hepatic immune homeostasis and alert when the balance is disturbed. When inflammation is induced, numerous monocytes are recruited to the liver (13). This may contribute to the chronic low-grade inflammation in NAFLD. Considering the important impact of macrophages on hepatic inflammation and their ability to process lipids, they play an important role in the pathological progression of NAFLD. Programmed cell death (PCD) of macrophages is closely associated with the development of inflammation (14). This paper mainly focuses on the effects of lipid metabolism and PCD on the phenotype of macrophages in NAFLD and the relationship between them. The possibility of targeting PCD of macrophages in the treatment of NAFLD has also been explored.

2 Effect of macrophages on the inflammatory response in NAFLD

Inflammation is a major pathological factor in the progression of NAFLD, and hepatocyte death is one of the crucial triggers of liver inflammation (15). Macrophages play an important role in the inflammatory response in NAFLD due to their ability to clear pathogens and recruit circulating inflammatory cells (2). Typically, macrophages can be classified into two phenotypes, the classically activated M1 type and the alternatively activated M2 type (Figure 1). M1 macrophages are induced by lipopolysaccharide (LPS) and Th1 cytokines such as interferon-γ (IFN-γ) and granulocyte-macrophage colony-stimulating factor (GM-CSF) alone or in combination to secrete pro-inflammatory factors such as interleukin 1β (IL-1β), IL-6 and tumor necrosis factor-α (TNF-α), while M2 macrophages are induced by Th2 cytokines such as IL-4 and IL-13 to secrete anti-inflammatory factors such as IL-10 and transforming growth factor-β (TGF-β) (16). The balance of M1 and M2 macrophages is an important determinant of the pathological changes in the liver under inflammatory conditions. However, the M1 and M2 classification cannot describe macrophages accurately due to the heterogeneity and functional diversity of macrophages. More specific markers of different macrophage phenotypes are needed.

KCs are liver-resident macrophages and account for 15% of all liver cells (17). It is now clear that KCs originate from yolk-sac-derived erythro-myeloid progenitors expressing colony stimulating factor 1 receptor (CSF1R) (18). In the context of NAFLD, KCs are the major source of cytokines and chemokines (19). For example, KCs promote steatosis and insulin resistance by secreting IL-1β to downregulate peroxisome proliferative activated receptor α (PPARα) expression in hepatocytes (20). A previous study has demonstrated that consumption of KCs attenuates high fat or high sucrose diet-induced NASH in rats (21). On the one hand, portal vein-derived LPS can bind to toll-like receptor 4 (TLR4) on the surface of KCs to induce their polarization toward M1 pro-inflammatory phenotype and enhance pro-inflammatory cytokines including monocyte chemoattractant protein-1 (MCP1, also known as C-C motif chemokine ligand 2, CCL2), TNF-α and IL-6 expression *via* yes-associated Protein (YAP) (22). On the other hand, KCs can also promote hepatocyte apoptosis and inflammatory progression by producing TNF, TNF-related apoptosis-inducing ligand (TRAIL) and factor associated suicide (Fas) ligand through phagocytosis of apoptotic bodies (23). In addition, lipotoxic hepatocytes can release mitochondrial DNA (mtDNA) to induce nuclear factor kappa-light-chain-enhancer of activated B cells (NF-κB) dependent inflammation by binding to transmembrane protein 173 (TMEM173 or STING) on the surface of KCs (24), while KCs themselves can activate the NOD-like receptor thermal protein domain associated protein 3 (NLRP3) inflammasome *via* mtDNA released from mitochondria thereby promoting the progression of NASH (25).

MoMFs are recruited to the liver under inflammatory conditions and transformed to different phenotypes in response to stimulation by complex cytokines. Recent studies have confirmed that lipotoxic hepatocytes can secrete extracellular vesicles rich in MicroRNA 192-5p (26), C-X-C Motif Chemokine Ligand 10 (CXCL10) (27), ceramide (28) to promote M1 polarization of MoMFs and secrete pro-inflammatory cytokines. Meanwhile, extracellular vesicles can also promote the recruitment of MoMFs through an integrin β1 (ITGβ1)-dependent pathway (29). Except for CXCL10, various chemokines including CCL2 played important roles in the infiltration of MoMFs and M1 polarization, while inhibition or knockdown of CXCL10 and CCL2 showed inhibition of liver macrophage infiltration and improvement of inflammation in the mouse model of NASH

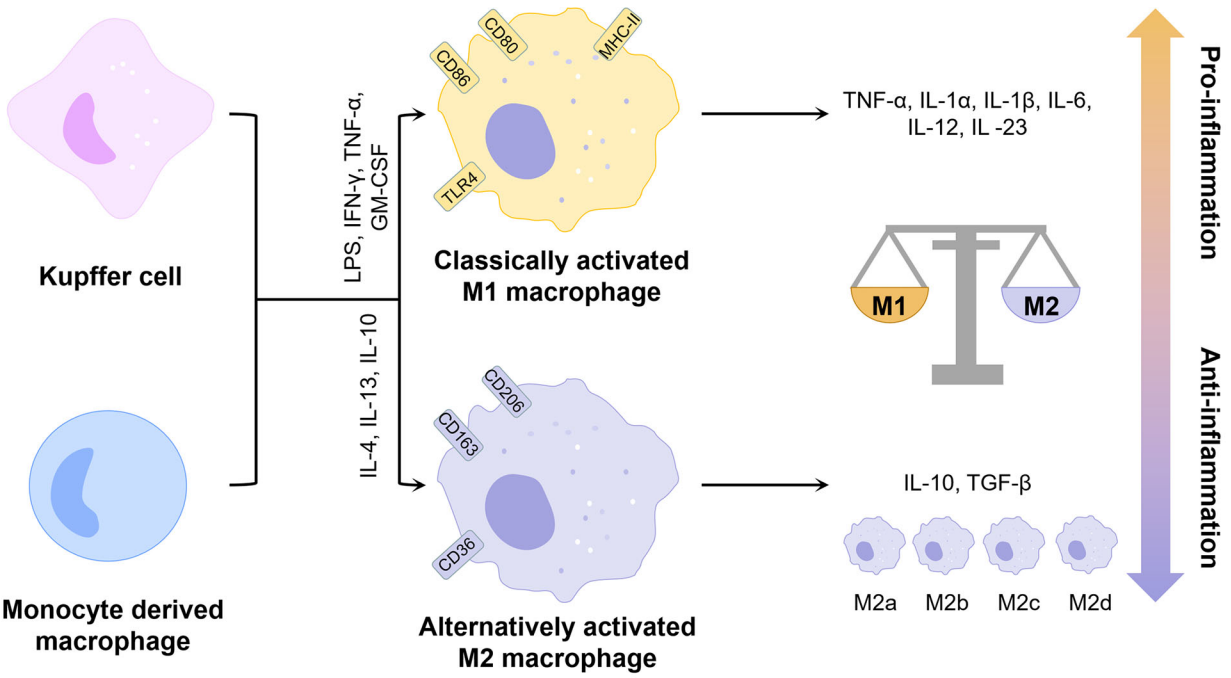

FIGURE 1
Phenotype and function of liver macrophages. KCs and monocyte-derived macrophages can be polarized by different factors into two distinct phenotypes, classically activated M1 and alternatively activated M2. M2 macrophages can be further classified into multiple phenotypes. Overall, M1 exhibits pro-inflammatory properties and M2 exhibits anti-inflammatory properties. The balance between the two determines the direction of liver inflammation. GM-CSF, granulocyte-macrophage colony-stimulating factor; IFN-γ, interferon-γ; IL, interleukin; LPS, lipopolysaccharide; MHC-II, major histocompatibility complex class IITGF-β, transforming growth factor-β; TLR4, toll-like receptor 4; TNF-α, tumor necrosis factor-α.

(30, 31). Lymphocyte antigen 6C (Ly6C) is a marker of mouse monocytes, which divides circulating monocytes into two major subpopulations, Ly6C^{hi} and Ly6C^{lo} (32). The Ly6C^{lo} subgroup shows anti-inflammatory properties, while the Ly6C^{hi} subgroup exhibits pro-inflammatory properties and constitutes the main pathological mechanism of NASH progression. Ly6C^{hi} MoMFs can be converted to Ly6C^{lo} MoMFs after the clearance of apoptotic hepatocytes (33). A dual C-C Motif Chemokine Receptor 2 (CCR2)/CCR5 antagonist, cenicriviroc (CVC), demonstrated improvement in NASH-related liver fibrosis and inhibition of steatohepatitis progression in a completed phase II clinical trial enrolling 289 patients with NASH (34). A study in a mouse model of NASH showed that CVC inhibited Ly6C^{hi} MoMFs infiltration and fibrosis progression, but had no direct effect on macrophage polarization (35).

Due to the immune tolerance characteristic of the liver, KCs are mainly involved in maintaining inflammatory homeostasis, while MoMFs play a major role in acute and chronic liver inflammation (32). Under homeostatic conditions, the hepatic macrophage population contains only a small amount of MoMFs. KCs could directly inhibit the inflammatory response of MoMFs by secreting miR-690-containing exosomes, whereas miR-690 of KCs showed low expression during the progression of NASH (36), which might promote the recruitment and pro-inflammatory transformation of MoMFs. In addition, activated KCs can promote the recruitment of Ly6C^{hi} MoMFs by secreting CCL2 (31). KCs proliferate for self-renewal in the liver, but the mechanism of renewal is impaired during NASH. When KCs are depleted, some Ly6C^{hi} MoMFs are even able to convert to KCs to replenish the hepatic KCs pool under specific factors (37). However, compared with embryo-derived KCs, monocyte-derived KCs do not effectively promote hepatic triglyceride storage and exhibit pro-inflammatory properties in the liver, thereby exacerbating liver injury in NASH (38).

3 Lipid metabolism in macrophages

Macrophages require a lot of energy to maintain their function in inflammation. Metabolic reprogramming has an important role in regulating the function of immune cells, and macrophages of different phenotypes usually exhibit different metabolic profiles (39). Macrophages possess lipid-processing function and play an important role in lipid metabolism. Intracellular lipid metabolism involves a series of complex enzymatic reactions (Figure 2). FFAs taken up by fatty acid transport proteins (e.g. CD36) and fatty acid binding proteins (FABPs) are transformed to acyl-coenzyme A (acyl-CoA) by the action of acyl-CoA synthase (ACS). Acyl-CoA can not only participate in the synthesis of triglycerides, but also converted to acyl-carnitine by carnitine palmitoyltransferase-1 (CPT1). Subsequently, acyl-carnitine is transported into the mitochondria *via* carnitine-acylcarnitine translocase (CACT) and CPT2 for fatty acid oxidation (FAO) and increases the production of nicotinamide adenine dinucleotide (NADH)/1,5-dihydroflavin adenine dinucleotide (FADH2) thereby promoting oxidative phosphorylation (OXPHOS). The acetyl-CoA produced during this process participates in the TCA cycle and

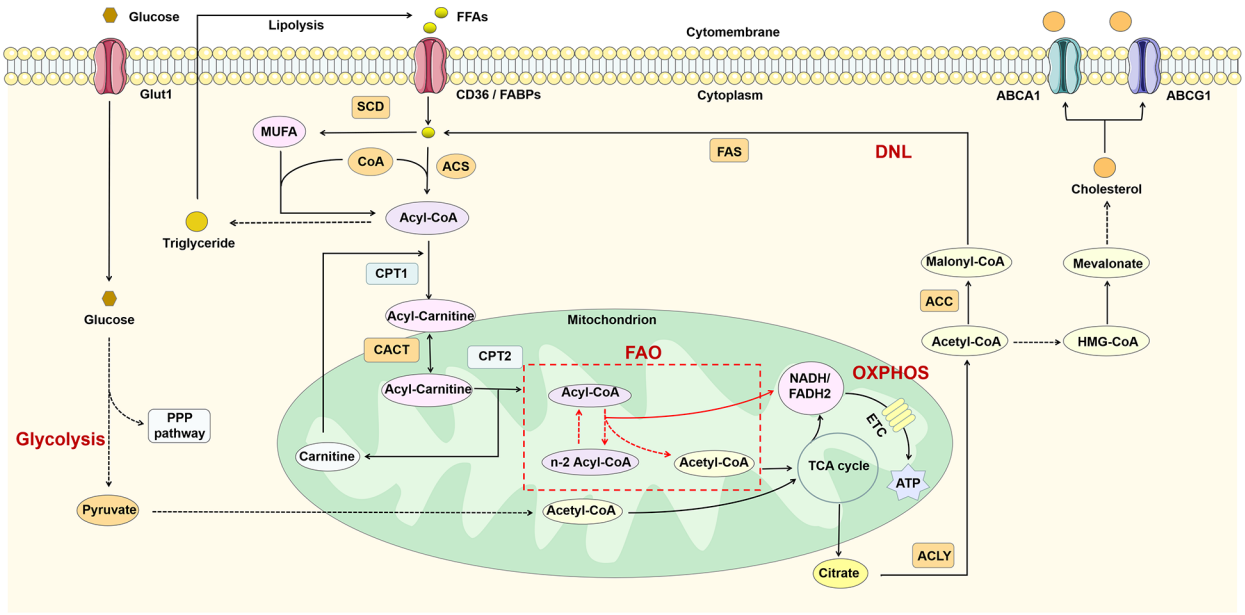

FIGURE 2
Lipid metabolism in macrophages. FFAs are catabolized to acyl-CoA by the action of ACS and thus participate in triglyceride synthesis and FAO. FAO can participate in the TCA cycle by producing acetyl-CoA and also promote OXPHOS by increasing NADH/FADH2 production. In addition, glucose can also produce acetyl-CoA through glycolysis. The citrate generated by the TCA cycle is reconverted to acetyl-CoA in the cytoplasm by ACL, thus participating in DNL and cholesterol synthesis. ABCA1, ATP-binding cassette sub-family A member 1; ABCG1, ATP-binding cassette sub-family G member 1; ACC, acetyl-CoA carboxylase; ACLY, ATP-citrate lyase; ACS, acyl-CoA synthetase; CACT, carnitine-acylcarnitine translocase; CoA, coenzyme A; CPT1, carnitine palmitoyl transferase 1; DNL, *de novo* lipogenesis; ETC, electron transport chain; FAO, fatty acid oxidation; FAS, fatty acid synthase; FFAs, free fatty acids; Glut1, glucose transporterisoform 1; MUFA, monounsaturated fatty acid; OXPHOS, oxidative phosphorylation; PPP pathway, pentose phosphate pathway; SCD, stearoyl-coenzyme A desaturase; TCA, tricarboxylic acid.

ultimately promotes the production of citrate. Glucose can be converted to pyruvate through glycolysis and then also participate in the TCA cycle through conversion to acetyl-CoA (40). Citrate can be converted back to acetyl-CoA by the action of ATP-citrate lyase (ACLY). Acetyl-CoA is not only involved in *de novo* lipogenesis (DNL), but also in cholesterol synthesis. The excess fatty acids are used for the synthesis of triglycerides and other complex lipids (41), while cholesterol is transported out of the cell under the regulation of ATP-binding cassette sub-family A member 1 (ABCA1) and ATP-binding cassette sub-family G member 1 (ABCG1) (42).

In M1 macrophages, increased glycolysis not only provides ATP more rapidly, but also promotes the TCA cycle and acetyl-CoA production (43). Sterol regulatory element-binding proteins (SREBPs) and fatty acid synthase (FAS), both key regulators of fatty acid synthesis, not only promote lipid biosynthesis in macrophages, but have also been shown to be critical for the induction of M1 polarization of macrophages (44–46). Different from M1, M2 macrophages possess an intact TCA cycle and enhanced mitochondrial OXPHOS, which depends on fatty acid uptake and FAO (43). CPT1 is involved in the production and mitochondrial transport of fatty acid-derived acyl-carnitine. Inhibition of CPT1 blocks mitochondrial FAO and has been shown to inhibit IL-4-mediated M2 polarization of macrophages (47). Thus, classical LPS/IFN-γ-activated pro-inflammatory M1 macrophages *in vitro* exhibit enhanced glucose uptake and anaerobic glycolysis, whereas anti-inflammatory M2 macrophages induced by IL-4/IL-13 exhibit enhanced FAO and OXPHOS (Figure 3). Lipid metabolism in M1 macrophages favors lipid synthesis and proinflammatory factor expression, whereas M2 macrophages receive their energy supply through FAO (48, 49). It has been shown that inhibition of FAO inhibits M2 polarization in macrophages (50), while LPS in combination with IFNγ inhibits IL-4-induced M2 repolarization by suppressing OXPHOS in macrophages (51). Due to the high plasticity, macrophages can be phenotypically "repolarized" or "reprogrammed" when induced by the corresponding signals (16). Thus, metabolic regulation may be central to the functional plasticity of macrophages, and FAO plays an essential role in inflammatory and metabolism-mediated phenotypic changes in immune cells.

4 Effect of lipid metabolic reprogramming of macrophages on NAFLD

The liver is an important organ of lipid metabolism. Based on the close relationship between macrophage lipid metabolism and inflammation, dysregulated lipid metabolism in NAFLD may promote the progression of inflammation by affecting macrophage function. Modulation of lipid metabolism may have potential therapeutic implications for the progression of inflammation in NAFLD by reshaping the M1/M2 balance. Therefore, it is necessary to further clarify the changes in lipid metabolism of macrophages in NAFLD. KCs express receptors such as MSR1, CD36, and TIM4, which recognize and remove membrane lipid components of apoptotic cells and circulating oxidized low-density lipoproteins (ox-LDL). Subsequently, these lipids are degraded to FFAs and cholesterol by lysosomal acid lipase (LAL), which is involved in HDL synthesis (52). This function of KCs is

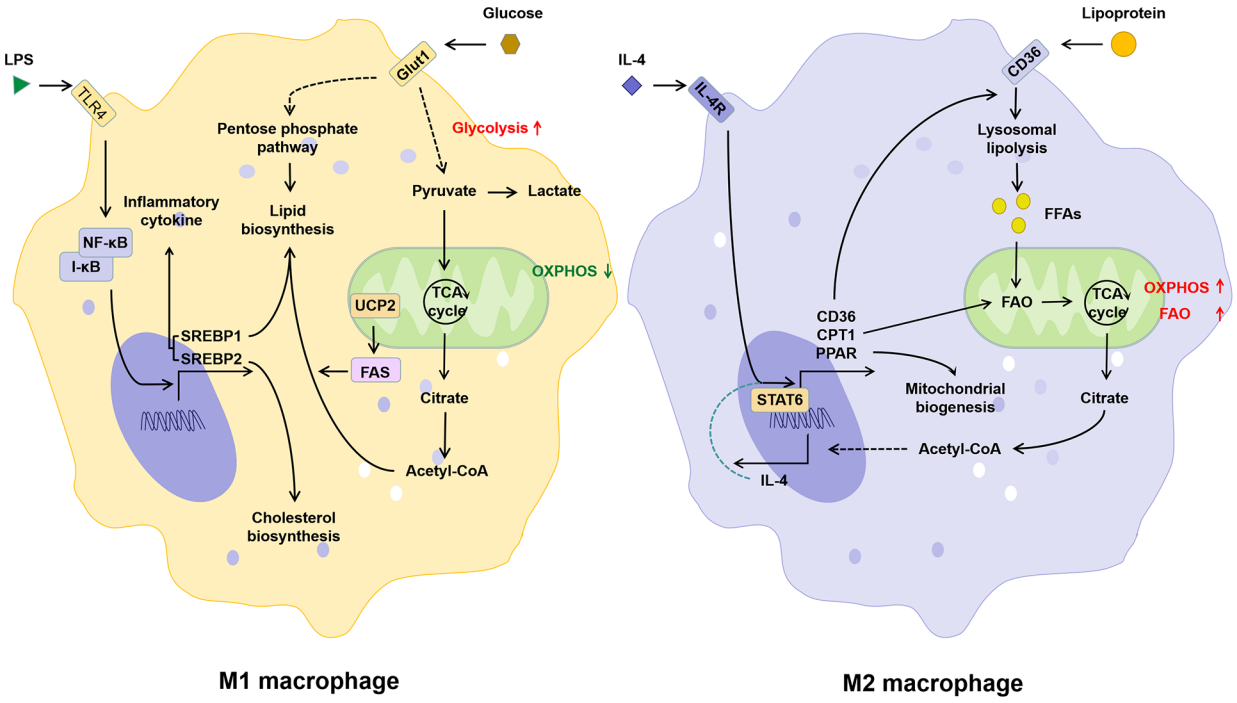

FIGURE 3
The relationship between lipid metabolism and phenotype of macrophages. Activation of the TLR signaling pathway induced by LPS promotes M1 polarization of macrophages, which is manifested by increased glucose uptake, glycolysis, lipid biosynthesis and decreased OXPHOS. The IL-4 induced M2 polarization of macrophages is manifested as the increase in lipid intake, FAO, and OXPHOS. IL-4, interleukin-4; IL-4R, interleukin-4 receptor; I-κB, inhibitor of NF-κB; LPS, lipopolysaccharide; NF-κB, nuclear factor kappa-light-chain-enhancer of activated B cells; PPAR, peroxisome proliferative activated receptor; SREBP, sterol-regulatory element binding protein; STAT6, signal transducer and activator of transcription 6; TLR4, toll-like receptor 4; UCP2, uncoupling protein 2.

highly conserved in several species (53), and their expression of genes related to lipid metabolism are more abundant than in other tissue-resident macrophages (54). Given the role of KCs in hepatic immune homeostasis, they may maintain specific functions, particularly tissue-specific functions, dependent on certain metabolites or nutrients (55). Imbalance of lipid homeostasis may lead to pro-inflammatory polarization of KCs thereby inducing inflammation in NAFLD. Improvement of NASH by KCs elimination provides evidence for its driving effect on early NASH (20). $CD11c^+$ macrophages may be an important subset driving hepatocyte death-induced inflammation and fibrosis, which promotes disease progression from steatosis to NASH, while KCs are a major source of $CD11c^+$ macrophages (56). Macrophage scavenger receptor 1 (MSR1, CD204) mediates lipid uptake and accumulation in KCs and correlates with the degree of steatosis and steatohepatitis in patients with NAFLD. In a fatty acid-rich environment, MSR1 induces a pro-inflammatory response through the JNK signaling pathway, and its blockade inhibits lipid accumulation in KCs, thereby suppressing their pro-inflammatory polarization and the release of cytokines such as TNF-α (57). Similarly, the knockdown of myeloid forkhead box O1 (FoxO1) induced a shift in macrophage polarization from a pro-inflammatory M1 to an anti-inflammatory M2 phenotype and reduced liver macrophage infiltration in a mouse model of high-fat diet-induced NASH (58). At least for now, it seems that lipid overload may promote M1 polarization of KCs and MoMFs through MSR1 and FoxO1, respectively.

Nuclear receptors, including PPARs and liver X receptor (LXR), are ligand-dependent transcription factors and involved in the regulation of lipid and glucose metabolism genes and inflammation-regulated genes (59). This provides another link between macrophage lipid metabolism and inflammation. The three isoforms of PPARs, PPARα, β/δ, and γ, play different but complementary regulatory roles in lipid metabolism and inflammation in the liver (48). The current studies have confirmed the promotion and necessity of PPARγ and PPARβ/δ on M2 polarization of macrophages (60, 61). And LXR can also induce the anti-inflammatory phenotype of MoMFs by inhibiting TLR2, TLR4 and TLR9 and related pathways (62). Interestingly, although LXR was expressed in both hepatocytes and macrophages, an LXRα agonist, DMHCA, selectively activated LXRα in macrophages (63), suggesting the feasibility of targeting LXR in macrophages. In addition, retinoic acid-related orphan nuclear receptor alpha (RORα) is also thought to regulate M2 polarization in macrophages in NAFLD (64). However, the significance of RORα-specific deletion in macrophages for NASH progression remains controversial (65). In addition to regulating lipid metabolism and inflammation, nuclear receptors can also act as redox sensors to sense metabolic stress and thus prevent oxidative damage (66). Due to the important role of oxidative stress in promoting lipid metabolism disorders and inflammation, targeting nuclear receptors may improve NASH progression by regulating macrophage phenotype through antioxidant, anti-inflammatory, and regulating lipid metabolism.

Although the current study confirms the importance of lipid metabolism reprogramming on the pro-inflammatory phenotype of macrophages, changes in the phenotype and lipid metabolism of

hepatic macrophage subsets need to be further explored. A recent study showed that depletion of a subset of CD206^{hi} ESAM^{+} KCs or silencing of their fatty acid transporter protein CD36 reversed obesity and steatosis in mice (67). CD36 and CD206 are both commonly considered to be M2 markers (68). These conflicting results further demonstrate the complexity of macrophage function. Furthermore, the role of lipid metabolism in macrophage polarization remains controversial, although it is now generally accepted that glycolysis defines M1 macrophages and FAO defines M2 (43). Glycolysis, OXPHOS and FAO may determine phenotypic shifts through complex interactions rather than a single pathway, which remains to be elucidated.

5 Different types of PCD and lipid metabolism in macrophages

Cells may die from accidental cell death (ACD) or regulatory cell death (RCD). RCD is a strictly regulated form of cell death induced by complex molecular mechanisms, and it is also known as PCD when it occurs in the absence of external environmental interference (69). PCD plays an important role in host defense against pathogens and maintenance of body homeostasis, while its over-activation or tolerance leads to the development of disease. Several types of PCD have been identified including autophagy, apoptosis, necroptosis, pyroptosis, and ferroptosis (Figure 4). We focused on these types of PCD in macrophages in the NASH phase of NAFLD.

5.1 Autophagy

Autophagy is a catabolic process that degrades damaged organelles and abnormally accumulated proteins *via* lysosomes (70). Autophagy can be classified as macroautophagy, chaperone-mediated autophagy (CMA), and microautophagy according to the pathways of cytoplasmic materials into lysosomes (71). In addition, autophagy can be further classified into selective and non-selective autophagy according to the specificity of degradation substrates. Physiological autophagy is essential for maintaining cellular homeostasis, and its regulation of macrophage function is widely recognized (72). It has been demonstrated that autophagy is impaired in human livers with steatosis or NASH and that promoting autophagy inhibits the pro-inflammatory activation of human macrophage cell lines (73). Typically, autophagy of macrophages in most NAFLD-related studies refers to macroautophagy, the lack of which amplifies hepatic steatosis and/or liver injury through overactivation of the innate immune response. Macrophage-specific deletion of macroautophagy-dependent autophagy-associated proteins such as autophagy protein 5 (ATG5) was shown to increase IL1α and IL1β secretion thereby exacerbating liver inflammation and fibrosis in mice (74). It is suggested that autophagy contributes to the down-regulation of macrophage-induced inflammatory responses, whereas insufficient autophagy may lead to macrophage polarization toward pro-inflammatory M1. Dysbiosis of intestinal flora and increased intestinal permeability in

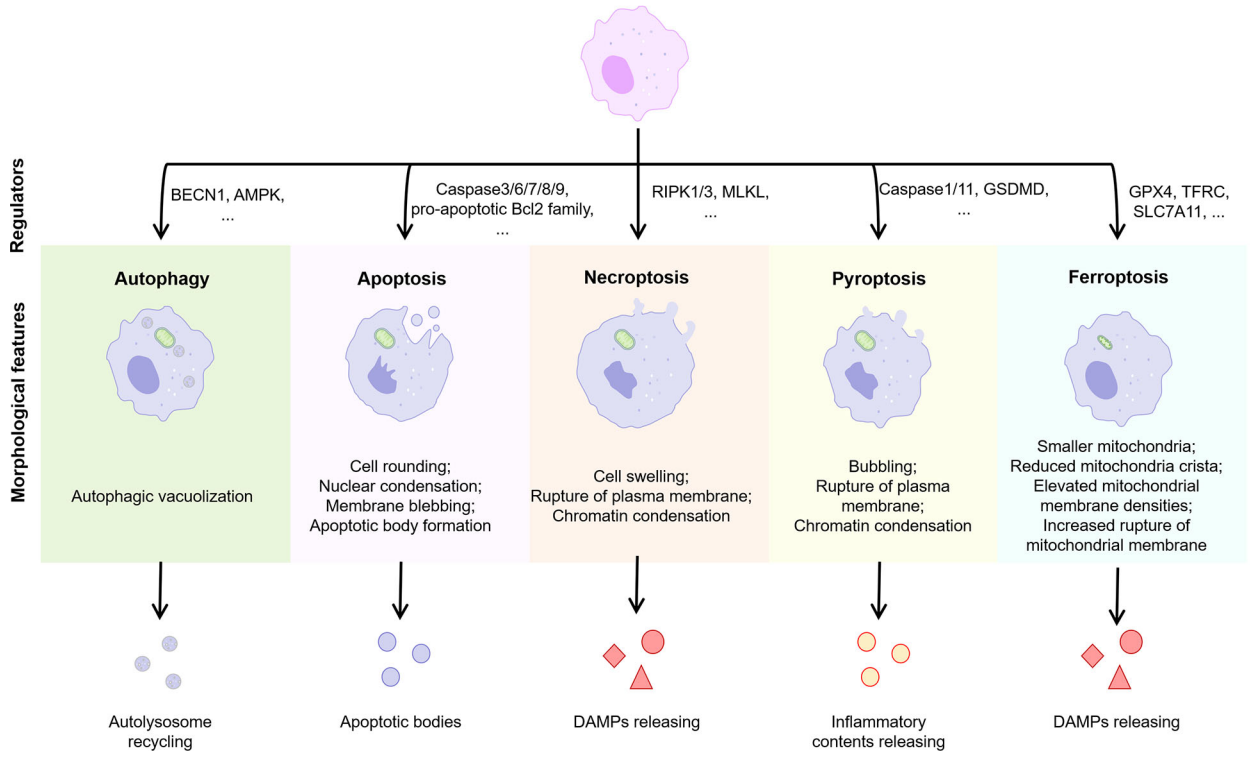

FIGURE 4
Features of different types of PCD. Normal cells are induced to different forms of death by different stimuli or signals, including autophagy, apoptosis, necroptosis, pyroptosis, and ferroptosis. Different PCD types exhibit different morphological features and play an important regulatory role in the progression of inflammation. BECN1, beclin 1; AMPK, adenosine 5'-monophosphate (AMP)-activated protein kinase; RIPK, receptor-interacting protein kinase; MLKL, mixed lineage kinase domain-like; GSDMD, gasderminD; DAMPs, damage associated molecular patterns; GPX4, glutathione peroxidases 4; TFRC, transferrin receptor; SLC7A11, solute carrier family 7 member 11.

NAFLD patients lead to elevated serum LPS levels, which induce increased secretion of pro-inflammatory factors and reactive oxygen species (ROS) through binding to TLR4, a pattern recognition receptor on the membrane surface of macrophages (75). High concentrations of ROS activated the oxidative stress regulatory switch nuclear factor erythroid 2-related factor 2 (Nrf2) and further induced transcription of antioxidant genes and sequestosome 1 (SQSTM1, also known as p62), thereby inducing p62-dependent selective autophagy in macrophages (76). In contrast, autophagy-deficient hepatic macrophages promoted liver inflammation and fibrosis by enhancing the mitochondrial ROS (mtROS)/NF-κB/IL-1α/β pathway (77).

As a cellular energy sensor, adenosine 5'-monophosphate (AMP)-activated protein kinase (AMPK) can promote macrophage M2 polarization through mitochondrial autophagy (78). However, both free fatty acids and hyperglycemia can lead to autophagy deficiency through the inhibition of AMPK, thereby inhibiting macrophage M2 polarization (79, 80). A study based on liver-specific SQSTM1 knockout mice showed that SQSTM1 induces hepatocyte autophagy by promoting the interaction between AMPK and unc-51 Like Autophagy Activating Kinase 1 (ULK1) and further activates the kelch-1ike ECH- associated protein 1 (Keap1)-Nrf2 signaling pathway to protect the liver from lipotoxicity in mice (81). As an important regulator of nutrient perception, growth, and metabolism, the mammalian target of rapamycin complex (mTORC) phosphorylates ULK1 to inhibit the interaction between AMPK and ULK1 (82), exhibiting a regulatory role in autophagy in contrast to SQSTM1. In addition, AMPK can also inhibit mTORC1 function by phosphorylating Raptor in the mTORC1 complex (83). These studies suggest an antagonism between AMPK and mTORC1 on the regulatory function of autophagy. However, previous studies have demonstrated that SQSTM1 also interacts with Raptor to activate mTORC1 (84). Persistent deficiency of mTORC1 in macrophages has also been shown to inhibit their M2 polarization by inducing lysosomal dysfunction (85). The role of mTORC1 in the regulation of macrophage autophagy and phenotype remains puzzling.

Lipid deposition in the liver impairs local oxygen homeostasis, followed by tissue hypoxia-induced adaptive responses that ultimately affect the homeostasis of hepatic lipid metabolism (86). Since oxygen is transported through the blood, hypoxia means impaired blood microcirculation. Therefore, hypoxia and nutritional disorders occur simultaneously. Nutrient depletion caused by hypoxia activates AMPK and simultaneously inactivates mTORC1 thereby inducing autophagy to maintain cell survival. As a key regulator of hypoxia, Hypoxia-inducible factor 1 subunit alpha (HIF-1α) can broadly regulate the expression of hypoxia-inducible genes and the activation of various signaling pathways (87). A study based on methionine and choline-deficient L-amino acid diet (MCD)-fed mice and NASH patients showed that HIF-1α expression in hepatic macrophages was induced by palmitic acid, thereby reducing autophagic flux and targeting inflammasomes to increase IL-1β production (88). Although HIF-1α and AMPK/mTORC1 regulate macrophage autophagy and phenotypic transformation as important links of hypoxia and energy regulation, respectively, their interactions are still not systematically elucidated.

Currently, studies on HIF-1α and AMPK regulation of lipid metabolism in NAFLD are mainly carried out in hepatocytes (89, 90). The mechanisms by which lipid metabolism reprogramming in macrophages regulates autophagy are still poorly understood. Monoacylglycerol lipase (MAGL), the rate-limiting enzyme in the degradation of monoacylglycerols, not only degrades triacylglycerols to free fatty acids and glycerol, but also metabolizes endogenous cannabinoid receptor ligand 2-arachidonyl acid glycerol to arachidonic acid (91). During chronic liver injury, MAGL inhibited macrophage autophagy to promote inflammation and fibrosis, whereas inhibition of MAGL reduced the number of Ly-6C^{hi} macrophages and increased the number of Ly-6C^{lo} macrophages in an autophagy-dependent manner (92). In high-fat diet-induced obese mice, MAGL deletion also exhibited improved inflammation and insulin resistance in adipose tissue and reduced triglyceride levels in the liver (93). This provides evidence for a link between macrophage autophagy and lipid metabolism reprogramming. In addition, macrophage autophagy reduces programmed death ligand 1 (PD-L1) expression and thus inhibits hepatocellular carcinogenesis, while defective autophagy induces its immunosuppressive phenotype and thus promotes hepatocellular carcinoma progression (94). Given the increased incidence of NAFLD-associated HCC, regulation of macrophage autophagy may be valuable in reducing NAFLD-associated HCC.

5.2 Apoptosis

Apoptosis is a Caspase-dependent cell death that includes intrinsic pathways induced by DNA damage, ROS accumulation, and endoplasmic reticulum stress (also known as the mitochondrial pathway) as well as exogenous apoptotic pathways initiated by the binding of other cellular soluble or cell surface ligands including TNF, FasL, or TRAIL to death receptors (95). The Caspase family is a family of evolutionarily conserved cysteine-dependent endonucleases that are primarily involved in cell death and inflammatory responses. Caspases involved in apoptosis are divided into two main categories: initiating Caspases (Caspases-2, 8, 9 and 10) and effector Caspases (Caspases-3, 6 and 7) (96). Current studies have amply demonstrated that Caspases-3, 6, 7, 8, and 9 promote the progression of NASH (97). Among them, Caspases-8 is mainly involved in the exogenous apoptotic pathway, while Caspases-9 is mainly involved in the endogenous apoptotic pathway. Increased positivity of the terminal deoxynucleotidyl transferase-mediated dUTP nick end labeling (TUNEL) assay in liver tissue of NASH patients demonstrates the involvement of apoptosis in the progression of NASH (98). Most of the current studies on apoptosis have been conducted on hepatocytes and few on macrophages. A study based on a high-fat diet-induced mouse model of NAFLD and primary KCs demonstrated that IL-4-activated M2 KCs could release IL-10 to promote apoptosis of M1 KCs thereby reducing liver inflammation and hepatocyte injury in NAFLD (99). This study suggests an intrinsic regulatory mechanism for the balance of M1 and M2 macrophages, i.e., M2 macrophages induce protective apoptosis of M1 macrophages and their dysfunction leads to the accumulation of M1 macrophages in the liver and the progression of inflammation.

Endoplasmic reticulum stress is significantly associated with lipotoxicity and NASH (100). C/EBP homologous protein (CHOP) is a transcription factor downstream of protein kinase RNA-

activated-like ER kinase. CHOP is induced by endoplasmic reticulum stress and its deletion prevents apoptosis induced by endoplasmic reticulum stress (101). As endoplasmic reticulum stress can induce TRAIL receptors and activate Caspase-8 (102), this may string endogenous apoptotic and exogenous apoptotic pathways together. Early studies demonstrated that CHOP deficiency promotes macrophage resistance to lipotoxicity and the progression of inflammation in NAFLD (103). Therefore, CHOP may have the effect of inducing apoptosis of M1 macrophages and thus regulating hepatic macrophage homeostasis to protect the liver from steatohepatitis. The role of LXRα in promoting M2 polarization in hepatic macrophages has been discussed above. Paradoxically, a peritoneal macrophage-based study demonstrated that LXRα can inhibit the CHOP pathway induced by endoplasmic reticulum stress and thus inhibit macrophage apoptosis (104). The relationship between CHOP and LXRα in M1 macrophages in the liver obviously needs to be further explored.

The suppressor of cytokine signaling (SOCS) family is a class of proteins with negative feedback regulation on cytokine signaling pathways, including eight members of SOCS1 to SOCS7 and cytokine-inducible SH2-containing protein (CIS) (105). Currently, SOCS1, SOCS2 and SOCS3 are the most studied in macrophages. IL-4-induces SOCS2 expression, IFN-γ induces SOCS3 expression, while SOCS1 can be induced by both (106). Differently, induction of SOCS1 by IL-4 is signal transducer and activator of transcription 6 (STAT6) dependent, whereas induction of SOCS1 by IFN-γ is STAT1 dependent. At the same time, IL-4 induced SOCS1 can inhibit the expression of STAT6 and form a negative feedback signal. A recent study showed that SOCS2 expression in macrophages was negatively correlated with the degree of NASH (107). The study also found that SOCS2 plays a role in inhibiting inflammation and apoptosis *via* NF-κB and inflammasome signaling pathway in macrophages during NASH. In addition, SOCS1 and SOCS3 have been shown to inhibit the exogenous apoptotic pathway in other cell lines such as renal tubular epithelial cells and prostate cancer cells, respectively (108, 109). Overall, SOCS2 may promote M2 polarization and inhibit apoptosis in macrophages, while SOCS1 and SOCS3 may promote M1 polarization and inhibit apoptosis. The three are induced by different signals to inhibit exogenous apoptosis in macrophages of the corresponding phenotype thereby regulating the progression of NASH. Notably, both SOCS1 and SOCS3 have been shown to have inhibitory effects on FAO (110–112). Although these studies were not performed in macrophages, the mechanisms all involved inhibition of the Janus kinase (JAK)/STAT pathway. Different from SOCS1 and SOCS3, the effect of SOCS2 on lipid metabolism has received rarely attention. Although it has been shown to prevent hepatic steatosis due to high-fat diet (113), some studies suggest that it does not promote the increase of FAO in the liver (114). In conclusion, it remains to be clarified whether the SOCS family is involved in the regulation of macrophage polarization and apoptosis by inhibiting FAO through the JAK/STAT pathway.

5.3 Necroptosis

Necroptosis is a caspase-independent necrotic cell death program regulated by receptor interacting serine/threonine kinase 1 (RIPK1) and RIPK3. It can be triggered by extracellular stimuli that activate inflammation and cell death. Various innate immune signaling pathways such as TNFR, TLR and interferon receptors (IFNRs) can induce the binding of RIPK1 and RIPK3, which then leads to phosphorylation and translocation of mixed lineage kinase domain-like pseudokinase (MLKL) to the cell membrane, ultimately leading to necroptosis and release of damage-associated molecular patterns (DAMPs) (115). Precisely, RIPK1 induces apoptosis rather than necroptosis when Caspase-8 is present. When Caspase-8 is inhibited, deubiquitinated RIPK1 does not bind to complex 2, but to RIPK3, forming a necrosome complex and subsequently recruiting and activating MLKL (116). Thus, inhibition of Caspase-8 is as important as activation of RIPK3 for necroptosis. In contrast, RIPK1, although involved in the induction of necroptosis, may not be necessary for necroptosis. Depletion of nicotinamide adenine dinucleotide (NAD+) is sufficient to trigger necroptosis in a RIPK3- and MLKL-dependent manner (117), which provides a non-classical necroptotic pathway.

Necroptosis plays an important role in macrophage polarization and inflammation. A study based on aged mice showed that aging led to increased necroptosis in liver macrophages and release of pro-inflammatory factors including TNFα, IL-6 and IL-1β, while necrostatin-1s, a necroptosis inhibitor, significantly reduced M1 macrophages and improved inflammation (118). This study suggests that necroptosis promotes M1 polarization of macrophages. O-acetylglucosamine glycosylation modification (O-GlcNAcylation) is a specific glycosylation modification of intracellular proteins that can affect the localization, function and stability of substrate proteins (119). LPS-activated M1 macrophages exhibit attenuated hexose biosynthetic pathway and protein O-GlcNAcylation, while O-GlcNAc transferase (OGT) mediated O-GlcNAcyclization of RIPK3 prevented the hetero interaction and homo interaction of RIPK3-RIPK1, thereby inhibiting macrophage necroptosis (120). A study based on patients with NASH and choline-deficient L-amino acid-defined diet (CDAA)-induced NAFLD models in mice showed that hepatic RIPK3 correlated with NAFLD severity in humans and mice and RIPK3 deficiency ameliorated CDAA-induced inflammation, fibrosis and carcinogenesis in mice (121). Even though RIPK3 has now emerged as one of the promising targets for the treatment of NASH, the mechanism by which necroptosis regulates macrophage polarization has not been systematically elucidated. Studies based on the RIP3-deficient mouse model demonstrated that RIPK3 promotes the TLR4-NF-κB pathway *via* Rho-associated coiled-coil-containing protein kinase (ROCK)1 and thereby induces M1 polarization of macrophages in the liver (122). The effect of necroptosis on M1 macrophage activation and pro-inflammation may also be paracrine-related. Interestingly, M1 but not M2 macrophages exhibited higher RIPK3 and MLKL expression when BMDMs were intervened with necroptosis inducers (123). In contrast, another study expressed a different result. Blockade of TAK1, the RIPK1 inhibitor, induced more intense necroptosis in M2 but not M1 peripheral blood monocyte-derived macrophages in the context of Caspase inhibition (124). The mechanisms underlying these different results are still unclear. Necroptosis may be involved in both depletion of M2 macrophages and activation of M1 to promote the progression of inflammation in NASH.

There may be a correlation between the necroptosis of macrophages and their lipid metabolism reprogramming. RIPK3 was downregulated in macrophages in HCC and promoted FAO

via the ROS-Caspase1-PPAR pathway, which induced the reprogramming of fatty acid metabolism and ultimately induced M2 polarization in tumor-associated macrophages (125). An atherosclerosis-based study found that MLKL deficiency exacerbated lipid accumulation despite reducing the occurrence of necroptosis in macrophages (126). Another study based on the high-fat diet-induced NAFLD model in mice also showed that RIPK3 deficiency inhibited inflammation while exacerbating hepatic steatosis (127). These studies suggest that the inhibition of necroptosis may promote increased lipid uptake or *de novo* synthesis of fatty acids. Therefore, the relationship between necroptosis and the reprogramming of lipid metabolism in macrophages remains to be further clarified.

5.4 Pyroptosis

Pyroptosis is a form of PCD mediated by inflammasome activation, which is manifested by continuous cellular distension until the cell membrane ruptures, thereby releasing cellular contents to activate an intense inflammatory response. Classical pyroptosis is regulated by the inflammasome composed of NLRP3, apoptosis-associated speck-like protein containing a CARD (ASC), pro-Caspase-1 and gasdermin D (GSDMD) (128). Various exogenous and endogenous signals including LPS and ATP can induce inflammasome formation followed by activation of Caspase-1. Activated Caspase-1 cleaves pro-IL-1β and pro-IL-18 to mature IL-1β and IL-18, while cleaving the pyroptotic substrate GSDMD and forming membrane pores to induce pyroptosis and releasing IL-1β and IL-18 (129). The non-classical pyroptosis pathways are cytoplasmic LPS-mediated activation of Caspase-4/5/11 and cleavage by GSDMD (130). Xu et al. (131) showed that GSDMD and its fragment GSDMD-N protein expression, which induce pyroptosis, were significantly increased in liver tissues of NAFLD/NASH patients and correlated with NAFLD activity score and fibrosis. In contrast, MCD-fed GSDMD$^{-/-}$ mice were free from steatohepatitis and fibrosis, demonstrating the role of GSDMD-mediated pyroptosis in promoting NASH. In addition to GSDMD, most members of the gasdermin family can also induce pyroptosis (132), but their role in NAFLD still needs further evaluation.

Most studies on pyroptosis have focused on hepatocytes, but inflammasomes are mainly expressed in immune cells, especially macrophages (133). As an important regulator of anti-inflammation and antioxidant, Nrf2 is downregulated in the liver of NASH patients (134). Macrophage-specific Nrf2 knockdown promotes ROS and IL-1β production *via* a YAP-NLRP3-dependent manner thereby exacerbating NASH progression (135), suggesting the promotion of macrophage pyroptosis on NASH progression. Meanwhile, the gasdermin family may also induce mtROS release by targeting the mitochondrial membrane, thereby triggering NLRP3 inflammasome activation (136, 137). These studies suggest that pyroptosis may promote NASH progression by inducing ROS release and thus amplifying the cascade of pyroptosis and inflammation. Given the regulation of pyroptosis by the NLRP3 inflammasome, inhibition of the NLRP3 inflammasome may attenuate the inflammatory response of liver tissue by inhibiting macrophage pyroptosis (138). NLRP3 blockade also shows improvement in liver inflammation and fibrosis in atherogenic diet-fed foz/foz mice with NASH (139). In addition to the NLRP3 inflammasome, other inflammasome complexes, such as the NLR family CARD domain containing 4 (NLRC4) inflammasome, can also be involved in NAFLD inflammatory progression by promoting macrophage pyroptosis (140). In conclusion, inflammasome activation induces macrophage pyroptosis on the one hand and mediates macrophage polarization on the other. This provides evidence for a close relationship between liver macrophage pyroptosis and pro-inflammatory polarization in NASH.

As mentioned above, macrophage polarization is regulated by disorders of lipid metabolism. Previous studies have demonstrated that lipids released from dead hepatocytes in NASH activate macrophages to overexpress NLRP3 inflammasome and Caspase-1 (141). Therefore, macrophage pyroptosis may be associated with lipid metabolism. Bile acids are endogenous ligands for nuclear receptors that regulate lipid and energy metabolism (142). As a bile acid receptor, G protein-coupled bile acid receptor 1 (GPBAR1, also known as TGR5)-mediated bile acid signaling plays a key role in integrating glucose, lipid and energy metabolism (143). TGR5 activates PPARα and PPAR-γ coactivator 1 alpha (PGC-1α) to increase mitochondrial oxidative phosphorylation and energy metabolism and inhibit NF-κB-mediated pro-inflammatory cytokine production (144, 145), which is important for the metabolic reprogramming of M2 macrophages. Shi et al. (146) found that TGR5 expression was significantly reduced in the liver tissue of NASH patients and mouse models, while TGR5 knockdown exacerbated liver injury and inflammation and promoted macrophage M1 polarization in mice. Mechanistically, TGR5 signaling inhibits NLRP3-mediated macrophage M1 polarization thereby ameliorating hepatic steatosis and inflammation. Although the available evidence suggests an association between macrophage pyroptosis and lipid metabolism, the regulatory mechanisms are still poorly understood.

5.5 Ferroptosis

Ferroptosis is a form of iron-dependent cell death mediated by lipid peroxidation, whose main biochemical features are iron deposition and lipid peroxidation (147). Both increased iron uptake and decreased iron excretion may lead to iron overload, which in turn leads to excessive ROS production and lipid peroxidation through Fenton reaction and enzymatic oxygenation, subsequently triggering ferroptosis. The liver is one of the most important organs for iron storage and metabolism. Due to the abnormal lipid deposition in the liver of NASH patients, this may promote the development of ferroptosis. The correlation between disease progression and liver iron overload in NAFLD patients has been demonstrated (148). A bioinformatics study showed that the grading of liver steatosis was associated with 8 iron death-related genes including *ACSL3*, *ACSL4*, *AKR1C1*, *AKR1C2*, *CS*, *FADS2*, *GSS* and *PGD* (149). Another study also showed that the expression of *SLC11A2*, *CP*, *SLC40A1*, and *ACSL5* was downregulated in the livers of NASH patients compared to healthy livers, while the expression of *FTL*, *FTH1*, *ACSL4*, and *ACSL6* was upregulated (150). Actually, targeted ferroptosis has been shown to improve inflammation in both MCD and choline-deficient, ethionine-supplemented (CDE) diet-induced NASH models in mice

(151, 152). Current studies on the role of ferroptosis in NAFLD progression have focused on hepatocytes and HSCs (153). Since liver iron is mainly distributed in hepatocytes and reticuloendothelial system (macrophages), iron deposition in macrophages may play a role in NASH. An earlier multicenter study that included 849 patients with NAFLD has also demonstrated that iron deposition in macrophages is associated with severe NASH and advanced liver histological features (154).

Previous studies have confirmed that iron chelation in M1 macrophages may contribute to the development of chronic inflammation, while iron export from M2 macrophages may promote the growth of adjacent cells in the microenvironment (155), suggesting that macrophage polarization is associated with altered iron metabolism. A study based on BMDMs showed that iron overload increased the levels of M1 products (e.g. IL-6, TNF-α and IL-1β), promoting their polarization to the M1 type while exacerbating steatohepatitis and liver fibrosis (156). This study also showed that iron overload inhibited M2 polarization in BMDMs in the presence of IL-4. This differential performance may be associated with higher expression of Hamp and ferritin heavy chain (FTH)/ferritin light chain (FTL) and lower expression of ferroportin (FPN1, also known as SLC40A1) and iron regulatory proteins 1/2 (IRP1/2) in M1 macrophages compared to M2 (157). Moreover, the stronger antioxidant capacity of M1 macrophages enhanced their resistance to iron overload (158). Thus, under the same conditions, M2 macrophages may be induced to die, while the M1 type survives. As iron may be involved in the regulation of energy production and amino acid catabolism, the regulation of iron metabolism in polarized macrophages may alter the macrophage phenotype. For example, anti-inflammatory M2 macrophages in the tumor microenvironment can be converted to pro-inflammatory M1 macrophages *via* ferroptosis (159, 160). However, whether macrophages have this property in NASH remains to be elucidated. Notably, a study based on human monocytic leukemia THP-1 cell-derived macrophages showed that macrophages exhibit M2 polarization rather than M1 in response to chronic iron overload (161), but this may be related to metabolic changes in tumor-associated macrophages.

There is also a connection between ferroptosis and lipid metabolism, which has been well summarized in a recent review (162). Ferroptosis is characterized by iron-dependent peroxidation with phospholipids containing polyunsaturated fatty acyl (PUFA) chains as substrates. Monounsaturated fatty acids (MUFAs), as inhibitor of iron death (163), can be synthesized *de novo* in cells and participate in membrane lipid composition. Lipid metabolism may control the composition of membrane lipid by regulating the balance of PUFAs and MUFAs.Interestingly, sterol-regulatory element binding protein 1 (SREBP-1), which regulates MUFAs synthesis, is upregulated in M1 macrophages. One possible explanation is that ferroptosis signaling induces M1 polarization in macrophages, while reprogramming of lipid metabolism increases their resistance to ferroptosis. Similarly, not only fatty acid β-oxidation is increased in M2 macrophages, but also lipid transport proteins such as CD36 are upregulated. Given that fatty acid β-oxidation reduces the accumulation of PUFAs and thus inhibits lipid peroxidation (164), and that CD36-mediated lipid uptake increases susceptibility to ferroptosis (165), the ferroptosis-mediated shift in macrophage phenotype may ultimately depend on the disruption of the balance between PUFAs and MUFAs.

6 Interaction of signals of different types of PCD in macrophages

Due to the complex signal environment in the body, there is significant crosstalk between different types of PCD (Figure 5). As one of the main inducing pathways of exogenous apoptosis, the TNF signaling pathway also induces necroptosis. The difference is that necroptosis is RIPK3-dependent MLKL activation, while apoptosis is manifested as activation of Caspase-8. A study based on the mouse NASH model induced by MCD showed that Caspase-8 could balance the over-activation of RIPK3-dependent necroptosis, suggesting the mutual inhibition of RIPK3 and Caspase-8 (166). However, the study was performed based on hepatocytes rather than macrophages. Increased autophagy inhibits necroptosis by upregulating ATG16L1 (167) and inhibits apoptosis by inhibiting Caspase-8 activity (168). MLKL, another key regulator of necrotic apoptosis, has been demonstrated to participate in autophagy inhibition in a RIPK3-independent manner in FFC diet (high in fat, fructose and cholesterol) induced NASH mice and palmitic acid treated primary mouse hepatocytes (169). These studies suggest that Caspase-8 is a key node in balancing apoptosis and necroptosis, while MLKL may be an essential node in balancing autophagy and necroptosis. In addition to Caspase-8, Caspase-6 has also been shown to be involved in the interaction between autophagy and apoptosis. As an important participant in autophagy, AMPK can also inhibit apoptosis by phosphorylating Caspase-6 to inhibit its function (170), suggesting an antagonistic mechanism between autophagy and endogenous apoptosis. Notably, the relationship between autophagy and necroptosis is not merely antagonistic. For example, a recent study showed that RIPK3 can directly bind and activate AMPK (171). Considering the mutual inhibition of AMPK and mTOR to regulate autophagic signaling in the downstream, this may be an important link in the balance of autophagy and necroptosis. As an upstream regulator of RIPK3, RIPK1 regulates apoptosis and necroptosis through Caspase-8 and RIPK3, respectively (115). Caspase-8 has been shown to cleave GSDMD to induce pyroptosis (172). These studies all illustrate the complex interaction network among pyroptosis, apoptosis and necroptosis. In experimental and clinical NASH, RIPK1 is phosphorylated and activated mainly in liver macrophages, especially in BMDMs (173). As mentioned above, palmitic acid-induced a decrease in autophagic flux of macrophages (88). However, palmitic acid also induced the activation of RIPK1 (173). Thus, fatty acid-induced inflammatory activation of macrophages was accompanied by an inhibition of autophagy and an increase in apoptosis, necroptosis, and pyroptosis, while the predominant PCD type may be associated with different inducing factors and cytokine expression.

Activation of the NLRP3 inflammasome is not only the initiating link of classical scorch death, but also leads to other types of PCD, including apoptosis, necroptosis, and ferroptosis (132). Prostaglandin-endoperoxide synthase 2 (PTGS2), one of the markers of iron death, regulates the synthesis of cyclooxygenase-2

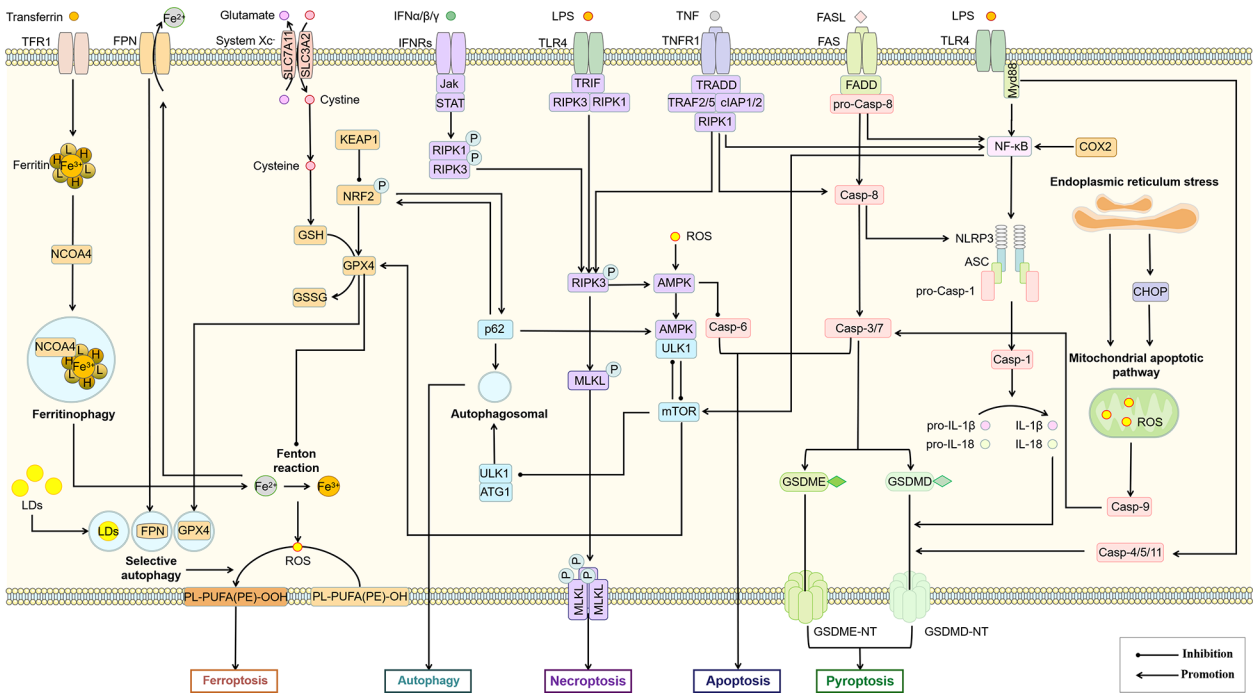

FIGURE 5
Association of different types of PCD in macrophages. The interaction between different PCD constitutes a complex regulatory network for survival or death of macrophages. AMPK, mTOR, Casp-8, RIPK3, Bcl-2 and p62 may be important nodes in the interaction of autophagy, apoptosis, necroptosis, pyroptosis and ferroptosis in this cell death network. ASC, apoptosis-associated speck-like protein; Casp, Caspase; CHOP, C/EBP homologous protein; cIAP, cellular inhibitor of apoptosis protein; COX-2, cyclooxygenase-2; FADD, Fas-associating protein with a novel death domain; FASL, Fas Ligand; FPN, ferroportin; GSDME, gasdermin E; GSH, glutathione; GSSG, glutathiol; IFN, interferon; Jak, janus kinase; KEAP1, kelch-1like ECH-associated protein 1; LDs, lipid droplets; mTOR, mammalian target of rapamycin; Myd88, myeloid differentiation primary response 88; NCOA4, nuclear receptor coactivator 4; NLRP3, NOD-like receptor thermal protein domain associated protein 3; NRF2, nuclear factor erythroid 2-related factor 2; ROS, reactive oxygen species; SLC3A2, solute carrier family 3 member 2; TFR1, transferrin receptor 1; TNFR1, tumor necrosis factor receptor 1; TRADD, TNFR1-associated death domain protein; TRAF, TNF-receptor associated factor.

(COX-2). However, COX-2 increases pro-IL-1β and NLRP3 expression through NF-κB activation and mediates NLRP3 inflammasome activation by enhancing Caspase-1 activation through promoting mitochondrial damage and ROS production (174), which may lead to an increase in pyroptosis. As a major member of the antioxidant system and an important regulator of ferroptosis, glutathione peroxidases 4 (GPX4) also showed the function of inhibiting macrophage pyroptosis (175). Therefore, pyroptosis and ferroptosis may promote each other and thus regulate macrophage pro-inflammatory polarization. The relationship between selective autophagy and ferroptosis has also been widely demonstrated (176). Autophagy promotes ferroptosis through selective degradation of ferritin (177), GPX4 (178), SLC40A1 (179), aryl hydrocarbon receptor nuclear translocator-like (ARNTL) (180), and lipid droplets (181). As a widely recognized inhibitor of autophagy, mTORC1 has also been shown to inhibit ferroptosis by regulating GPX4 synthesis (182). Since DAMPs including proteoglycan decorin (DCN) secreted by ferroptotic cells can bind to advanced glycosylation end-product-specific receptor (AGER) on macrophages and further trigger the production of pro-inflammatory cytokines in an NF-κB-dependent manner. Macrophage-selective autophagy and ferroptosis may promote each other and induce the formation of the NASH inflammatory microenvironment (183). Interestingly, although both pyroptosis and selective autophagy can promote the occurrence of ferroptosis, they do not promote each other. The inhibition of macrophage autophagy has been previously mentioned to be associated with increased pyroptosis. The inhibition of macrophage autophagy has been previously mentioned to be associated with increased pyroptosis. A recent study also confirmed that Tim-4, a phosphatidylserine (PS) receptor, activates liver kinase B1 (LKB1)/AMPKα-mediated autophagy to inhibit NLRP3 inflammasome activation, thereby improving the release of IL-1β and IL-18 from macrophages (184), suggesting that Tim-4$^+$ macrophages may inhibit the onset of pyroptosis through autophagy. On the other hand, peritoneal Tim-4 macrophages could inhibit CD8$^+$ T proliferation (185), while activated CD8$^+$ T cells could release granzyme B to induce increased macrophage pyroptosis and promote NAFLD progression (186). Thus, Tim-4-mediated macrophage autophagy not only directly inhibits pyroptosis, but also indirectly inhibits macrophage pyroptosis by suppressing CD8$^+$ T cell activation, suggesting an antagonistic relationship between autophagy and pyroptosis.

It is now generally accepted that the progression of NAFLD is caused by liver lipotoxicity. Possible mediators of lipotoxicity include free cholesterol, saturated free fatty acids, diacylglycerol, lysophosphatidylcholine, sphingolipids, and ceramides (187). Lipotoxic mediators not only induce damage and death of hepatocytes thereby recruiting macrophages, but also directly induce M1 polarization of macrophages. Mitochondria serve as important sites of energy metabolism and regulate liver lipid

metabolism and oxidative stress. Changes in mitochondrial metabolism and physiology may underlie the corresponding phenotypes of macrophage activation induced by various signals, including alterations in oxidative metabolism, mitochondrial membrane potential and tricarboxylic acid cycle, as well as the release of mtROS and mtDNA and alterations in mitochondrial ultrastructure (188). Excess ROS attacks biological membranes leading to lipid peroxidation, which not only direct damages phospholipids but also acts as a cell death signal to induce PCD. Numerous studies have confirmed that mitochondrial ROS can induce a variety of PCD in macrophages including pyroptosis (189), autophagy (190), apoptosis (191), necroptosis (192), and ferroptosis (193), suggesting that macrophage polarization and death are closely related to disturbed energy metabolism and oxidative stress. However, it is poorly understood that how dysregulated lipid metabolism in the complex *in vivo* environment leads to different types of PCD in macrophages. Mitochondria play an important role as the energy center in different types of PCD (164), and the development of single cell omics and mitochondriomics may provide valuable information. This aspect is still poorly understood and requires continuous and intensive research.

7 Potential drugs targeting PCD of macrophages

As drivers of hepatic steatosis, inflammation, fibrosis and important players in hepatic lipid metabolism, macrophages are attractive therapeutic targets for the treatment of NAFLD. The main strategies currently used to target macrophages include inhibition of monocyte infiltration and inhibition of pro-inflammatory macrophage polarization (194). The improvement of liver inflammation by inhibition of MoMFs infiltration has been well supported by evidence in preclinical studies. A randomized, double-blind, multinational phase 2b study showed that canicriviroc, a dual chemokine receptor CCR2/CCR5 inhibitor, doubled the proportion of patients with at least 1 stage of fibrosis improvement after 1 year despite no improvement in liver inflammation (34). The nuclear receptor family mediates anti-inflammatory polarization of macrophages, thus providing a link between inflammation and lipid metabolism and may be a promising target for NAFLD treatment. Drugs targeting nuclear receptors for the treatment of NAFLD including pan-PPAR agonist (Lanifibranor), PPAR-α/δ agonists (elafibranor), PPAR-α/γ agonist (Saroglitazar) and FXR agonist (Obecholic acid) have been well summarised (48). These drugs may have the effect of modulating both lipid metabolism and phenotypes of macrophages, but more evidence is needed.

PCD is involved in the regulation of the pro-inflammatory polarization of macrophages. Although apoptosis does not induce intense inflammation, apoptosis inhibition has also been considered a therapeutic strategy for NAFLD. As mentioned above, the Caspase family plays an important role in M1 polarization and apoptosis of macrophages. A double-blind, placebo-controlled clinical trial demonstrated that 28 days of treatment with the pan-Caspase inhibitor emricasan significantly reduced ALT and Caspase-3/7 activation in patients with NAFLD (195). However, another clinical study showed that 72 weeks of emricasan treatment did not improve liver histology in patients with NASH fibrosis and may have worsened fibrosis and ballooning (196). Similarly, apoptosis signal-regulated kinase 1 (ASK1) promotes the mitochondrial apoptotic pathway. A multicenter phase 2 clinical trial showed that 24 weeks of treatment with Selonsertib, an ASK1 inhibitor, had no effect on histological inflammation or ballooning despite a reduction in liver fibrosis (197). As the pro-inflammatory properties of hepatocytes and hepatic stellate cells are also regulated by PCD, it is difficult to identify which type or types of liver cells are targeted by these drugs *in vivo*. Multiple types of PCD may act in combination to induce the pro-inflammatory polarization of macrophages. These targeted drugs may have induced other types of PCD and thus failed to improve liver inflammation. Inhibition of Caspases, particularly Caspase-8, may lead to a bias towards necroptosis. Necroptosis of monocytes induced by LPS and pan-Caspase inhibitors increased CXCL1/2, TNF-α and IL-6 expression, whereas inhibition of RIPK3 resulted in a decrease in CXCL1 and CXCL2 and an increase in TNF-α (127). This result suggests that inhibition of a single type of PCD does not resolve inflammation completely. In addition, some natural drugs and their active ingredients have extremely strong anti-inflammation and anti-oxidation capabilities (198), which help regulate the death of macrophages, and are also potential therapeutic drugs for NAFLD. Licochalcone B (LicoB), a main component of the traditional medicinal herb licorice, is a specific inhibitor of the NLRP3 inflammasome which directly binds to never in mitosis A-related kinase 7 (NEK7) and inhibits the interaction between NLRP3 and NEK7 (199). Glycyrrhetinic acid, another active ingredient of licorice, can also improve the damaged autophagy flux and reduce the excessive production of inflammatory cytokines such as TNF-α, IL-6 and IL-1β by regulating the STAT3-HIF-1 pathway of macrophages (200). Curcumin and berberine, two of the most studied natural products for the treatment of NAFLD, have shown positive results in several clinical trials (201, 202). Mechanistic studies have also demonstrated the effect of both on macrophage polarization (203, 204). However, whether regulation of PCD is involved remains unclear.

Given the possible relationship between PCD-regulated macrophage polarization and lipid metabolism, drugs that regulate lipid metabolism may also improve NAFLD by modulating PCD of macrophages and thereby inhibiting the pro-inflammatory polarization. For example, Ezetimibe blocks the NLRP3 inflammasome-IL-1β pathway in macrophages in an autophagy dependent manner, and regulates the interaction between hepatocytes and macrophages through extracellular vesicles (73). In addition, sodium dependent glucose transporters 2 (SGLT2) inhibitors not only control blood glucose by inhibiting the reabsorption of glucose by the proximal tubules of the kidney, but also show regulatory effects on lipid metabolism, such as lipid synthesis and FAO (205). Empagliflozin, one of the SGLT2 inhibitors, also shows the role of regulating the AMPK/mTOR signal pathway to enhance autophagy of liver macrophages in T2DM mouse models with NAFLD (206). The therapeutic strategy of targeting lipid metabolism and PCD for the treatment of NAFLD is gradually being emphasized, and the research progress and clinical trials of inhibitors of the relevant targets are well summarized in a recent review (207). However, it is unclear whether these inhibitors target hepatic macrophages. In Table 1, we briefly summarize

TABLE 1 Potential small molecule drugs that regulate macrophage death to improve NAFLD.

Agent	Model	Target/pathway	PCD	Function	Ref
Antcin A	Mouse, high-fat diet; LPS and Nigericin stimulated mouse liver Kupffer cell line	NLRP3	Pyroptosis	Inhibition	(138)
Benzyl isothiocyanate	Mouse, HFCCD diet; LPS with or without cholesterol crystals stimulated primary mouse Kupffer cells,	NLRP3	Pyroptosis	Inhibition	(208)
CpG ODN	T-BHP stimulated RAW264.7 cells	ERK1/2 and Akt signaling pathway	Apoptosis	Inhibition	(209)
Scoparone	Mouse, MCD diet; LPS stimulated RAW264.7 cells	ROS/P38/Nrf2 axis and PI3K/AKT/mTOR pathway	Autophagy	Promotion	(210)
Ezetimibe	Mouse, MCD diet; LPS and palmitate stimulated THP-1 cells	NLRP3 inflammasone-IL1β pathway	Autophagy	Promotion	(73)
Empagliflozin	Mouse, high-fat diet and streptozotocin intraperitoneally injected	AMPK/mTOR pathway	Autophagy	Promotion	(206)
Glycyrrhetinic acid	Mouse, high-fat diet and drinking water containing fructose; Palmitic acid stimulated RAW264.7 and Kupffer cells	STAT3-HIF-1α pathway	Autophagy	Promotion	(200)

MCD, methionine-choline deficient; HFCCD, high-fat diet containing cholesterol and cholic acid; LPS, lipopolysaccharide.

potential small molecule drugs that may improve NAFLD by regulating PCD of macrophages. The safety and efficacy of these small molecule drugs still need to be supported by more clinical evidence.

8 Discussion

Lipid metabolism disorders are an important factor in the development of NAFLD. Lipid deposition is not the main inducement of cell damage, but it makes cells more vulnerable to the influence of internal and external environments and aggravates cell damage (211). Once the fuse is ignited, disordered lipid metabolism can rapidly exacerbate the hepatic inflammatory cascade. Compared to other liver disease, NAFLD is more likely to be susceptible to severe damage from lipid peroxidation. This may be part of the reason that NAFLD can progress to HCC without the stage of liver cirrhosis. As an important regulator of hepatic inflammatory homeostasis, the M1/M2 imbalance in macrophages leads to the development and progression of inflammation. Based on the important role and huge number of macrophages in liver immune cells, targeting macrophages is of great significance to improve the development and progression of inflammation in NAFLD. Lipids, as key metabolites in macrophage polarization, are closely associated with macrophage function. Conventional opinion suggests that M1 macrophages are dependent on glycolysis for energy while M2 macrophages are dependent on FAO. However, this view has been challenged by some data in recent years, which demonstrate the complexity of macrophage metabolism. Therefore, it remains difficult to answer whether intervention in the lipid metabolic reprogramming of macrophages can improve NASH, and the metabolic profile of different phenotypes of macrophages still needs to be further clarified.

PCD is closely related to the polarization of macrophages. Compared with M2 macrophages, M1 macrophages may be more tolerant to various types of PCD, which leads to its survival in inflammation. At present, most studies targeting macrophages to treat NAFLD only focus on different types of PCD. As mentioned above, various types of PCD crosstalk with each other, which makes it difficult to obtain satisfactory results by blocking a single type of PCD. Other types of PCD can continue to promote the progress of inflammation as a complementary or alternative way. Therefore, elucidating the relationship between different types of PCD and the main regulatory factors will help to effectively regulate the proinflammatory polarization of macrophages. Regulation of macrophage polarization by targeting key regulators of specific macrophage populations to inhibit the pro-inflammatory PCD may be a promising therapeutic strategy for NAFLD. Most studies only provided preliminary evidence for the correlation between PCD and lipid metabolism of macrophages. Based on the regulation of lipid metabolism reprogramming on macrophage polarization, exploring the relationship between PCD and lipid metabolism may help to clarify how PCD regulates the phenotypic transformation of macrophages, and provide a basis for the strategy of targeting macrophages in the treatment of NAFLD.

A suitable animal model is important for mechanistic studies and pre-clinical evaluation of drugs. The pathology of NAFLD is extremely complex. Animal models of NAFLD, whether induced by high-fat, MCD, CDAA diets or specific gene deletions, are only partially reflect the characteristics of NAFLD in humans. This may have led to frustration in clinical trials of numerous drugs that performed well in pre-clinical studies. In addition, the majority of pre-clinical studies were conducted on mice. Species differences lead to inconsistent expression of phenotypic, inflammation, and metabolism-related genes in human and mouse macrophages. The elucidation of the epigenetic and metabolic characteristics of human macrophages is particularly important for the translation from pre-clinical studies to clinical applications. Further exploration of the links between various types of PCD in macrophages and the links between PCD and lipid metabolism may help to identify specific markers of macrophages. This will not only contribute to the development of drugs targeting macrophages for the treatment of NAFLD, but will also be important for the non-invasive diagnosis and assessment of the degree of liver inflammation and disease progression.

Author contributions

ZX wrote the manuscript. ML involved with project concept. FY, GL, JL and WZ performed data collection. SM and ZD revised the manuscript and were responsible for final approval. All authors contributed to the article and approved the submitted version.

Funding

This work is supported by National Natural Science Foundation of China (No. 82104772, 81904154, 82205208), China Postdoctoral Science Foundation (No. 2022M721067), The Science and Technology Research Program of Henan Province (No. 222102310502), Key Research and Promotion Project of Henan Province (No. 202102310168), Special Project of Traditional Chinese Medicine Scientific Research of Henan Province (No. 2018JDZX004) and Traditional Chinese Medicine Science Research Project of Henan Province (No. 2022ZY2008).

Conflict of interest

The authors declare that the research was conducted in the absence of any commercial or financial relationships that could be construed as a potential conflict of interest.

Publisher's note

References

1. Eslam M, Valenti L, Romeo S. Genetics and epigenetics of NAFLD and NASH: Clinical impact. *J Hepatol* (2018) 68:268–79. doi: 10.1016/j.jhep.2017.09.003

2. Orci LA, Kreutzfeldt M, Goossens N, Rubbia-Brandt L, Slits F, Hammad K, et al. Tolerogenic properties of liver macrophages in non-alcoholic steatohepatitis. *Liver Int* (2020) 40:609–21. doi: 10.1111/liv.14336

3. Huang DQ, El-Serag HB, Loomba R. Global epidemiology of NAFLD-related HCC: Trends, predictions, risk factors and prevention. *Nat Rev Gastroenterol Hepatol* (2021) 18:223–38. doi: 10.1038/s41575-020-00381-6

4. Ma KL, Ruan XZ, Powis SH, Chen Y, Moorhead JF, Varghese Z. Inflammatory stress exacerbates lipid accumulation in hepatic cells and fatty livers of apolipoprotein e knockout mice. *Hepatology* (2008) 48:770–81. doi: 10.1002/hep.22423

5. Younossi Z, Anstee QM, Marietti M, Hardy T, Henry L, Eslam M, et al. Global burden of NAFLD and NASH: Trends, predictions, risk factors and prevention. *Nat Rev Gastroenterol Hepatol* (2018) 15:11–20. doi: 10.1038/nrgastro.2017.109

6. Friedman SL, Neuschwander-Tetri BA, Rinella M, Sanyal AJ. Mechanisms of NAFLD development and therapeutic strategies. *Nat Med* (2018) 24:908–22. doi: 10.1038/s41591-018-0104-9

7. Caturano A, Acierno C, Nevola R, Pafundi PC, Galiero R, Rinaldi L, et al. Non-alcoholic fatty liver disease: From pathogenesis to clinical impact. *Processes (Basel)* (2021) 9:135. doi: 10.3390/pr9010135

8. Donnelly KL, Smith CI, Schwarzenberg SJ, Jessurun J, Boldt MD, Parks EJ. Sources of fatty acids stored in liver and secreted *via* lipoproteins in patients with nonalcoholic fatty liver disease. *J Clin Invest* (2005) 115:1343–51. doi: 10.1172/JCI23621

9. Arab JP, Arrese M, Trauner M. Recent insights into the pathogenesis of nonalcoholic fatty liver disease. *Annu Rev Pathol* (2018) 13:321–50. doi: 10.1146/annurev-pathol-020117-043617

10. Pierantonelli I, Svegliati-Baroni G. Nonalcoholic fatty liver disease: Basic pathogenetic mechanisms in the progression from NAFLD to NASH. *Transplantation* (2019) 103:e1–13. doi: 10.1097/TP.0000000000002480

11. Sierro F, Evrard M, Rizzetto S, Melino M, Mitchell AJ, Florido M, et al. A liver capsular network of monocyte-derived macrophages restricts hepatic dissemination of intraperitoneal bacteria by neutrophil recruitment. *Immunity* (2017) 47:374–88. doi: 10.1016/j.immuni.2017.07.018

12. Bouwens L, Baekeland M, De Zanger R, Wisse E. Quantitation, tissue distribution and proliferation kinetics of kupffer cells in normal rat liver. *Hepatology* (1986) 6:718–22. doi: 10.1002/hep.1840060430

13. Devisscher L, Scott CL, Lefere S, Raevens S, Bogaerts E, Paridaens A, et al. Non-alcoholic steatohepatitis induces transient changes within the liver macrophage pool. *Cell Immunol* (2017) 322:74–83. doi: 10.1016/j.cellimm.2017.10.006

14. Robinson N, Ganesan R, Hegedus C, Kovacs K, Kufer TA, Virag L. Programmed necrotic cell death of macrophages: Focus on pyroptosis, necroptosis, and parthanatos. *Redox Biol* (2019) 26:101239. doi: 10.1016/j.redox.2019.101239

15. Ibrahim SH, Hirsova P, Gores GJ. Non-alcoholic steatohepatitis pathogenesis: Sublethal hepatocyte injury as a driver of liver inflammation. *Gut* (2018) 67:963–72. doi: 10.1136/gutjnl-2017-315691

16. Shapouri-Moghaddam A, Mohammadian S, Vazini H, Taghadosi M, Esmaeili SA, Mardani F, et al. Macrophage plasticity, polarization, and function in health and disease. *J Cell Physiol* (2018) 233:6425–40. doi: 10.1002/jcp.26429

17. Mirshafiee V, Sun B, Chang CH, Liao YP, Jiang W, Jiang J, et al. Toxicological profiling of metal oxide nanoparticles in liver context reveals pyroptosis in kupffer cells and macrophages versus apoptosis in hepatocytes. *ACS Nano* (2018) 12:3836–52. doi: 10.1021/acsnano.8b01086

18. Gomez PE, Klapproth K, Schulz C, Busch K, Azzoni E, Crozet L, et al. Tissue-resident macrophages originate from yolk-sac-derived erythro-myeloid progenitors. *Nature* (2015) 518:547–51. doi: 10.1038/nature13989

19. Krenkel O, Tacke F. Liver macrophages in tissue homeostasis and disease. *Nat Rev Immunol* (2017) 17:306–21. doi: 10.1038/nri.2017.11

20. Stienstra R, Saudale F, Duval C, Keshtkar S, Groener JE, van Rooijen N, et al. Kupffer cells promote hepatic steatosis *via* interleukin-1beta-dependent suppression of peroxisome proliferator-activated receptor alpha activity. *Hepatology* (2010) 51:511–22. doi: 10.1002/hep.23337

21. Huang W, Metlakunta A, Dedousis N, Zhang P, Sipula I, Dube JJ, et al. Depletion of liver kupffer cells prevents the development of diet-induced hepatic steatosis and insulin resistance. *Diabetes* (2010) 59:347–57. doi: 10.2337/db09-0016

22. Song K, Kwon H, Han C, Chen W, Zhang J, Ma W, et al. Yes-associated protein in kupffer cells enhances the production of proinflammatory cytokines and promotes the development of nonalcoholic steatohepatitis. *Hepatology* (2020) 72:72–87. doi: 10.1002/hep.30990

23. Canbay A, Feldstein AE, Higuchi H, Werneburg N, Grambihler A, Bronk SF, et al. Kupffer cell engulfment of apoptotic bodies stimulates death ligand and cytokine expression. *Hepatology* (2003) 38:1188–98. doi: 10.1053/jhep.2003.50472

24. Yu Y, Liu Y, An W, Song J, Zhang Y, Zhao X. STING-mediated inflammation in kupffer cells contributes to progression of nonalcoholic steatohepatitis. *J Clin Invest* (2019) 129:546–55. doi: 10.1172/JCI121842

25. Pan J, Ou Z, Cai C, Li P, Gong J, Ruan XZ, et al. Fatty acid activates NLRP3 inflammasomes in mouse kupffer cells through mitochondrial DNA release. *Cell Immunol* (2018) 332:111–20. doi: 10.1016/j.cellimm.2018.08.006

26. Liu XL, Pan Q, Cao HX, Xin FZ, Zhao ZH, Yang RX, et al. Lipotoxic hepatocyte-derived exosomal MicroRNA 192-5p activates macrophages through Rictor/Akt/Forkhead box transcription factor O1 signaling in nonalcoholic fatty liver disease. *Hepatology* (2020) 72:454–69. doi: 10.1002/hep.31050

27. Ibrahim SH, Hirsova P, Tomita K, Bronk SF, Werneburg NW, Harrison SA, et al. Mixed lineage kinase 3 mediates release of c-X-C motif ligand 10-bearing chemotactic extracellular vesicles from lipotoxic hepatocytes. *Hepatology* (2016) 63:731–44. doi: 10.1002/hep.28252

28. Dasgupta D, Nakao Y, Mauer AS, Thompson JM, Sehrawat TS, Liao CY, et al. IRE1A stimulates hepatocyte-derived extracellular vesicles that promote inflammation in mice with steatohepatitis. *Gastroenterology* (2020) 159:1487–503. doi: 10.1053/j.gastro.2020.06.031

29. Guo Q, Furuta K, Lucien F, Gutierrez SL, Hirsova P, Krishnan A, et al. Integrin beta1-enriched extracellular vesicles mediate monocyte adhesion and promote liver inflammation in murine NASH. *J Hepatol* (2019) 71:1193–205. doi: 10.1016/j.jhep.2019.07.019

30. Tomita K, Freeman BL, Bronk SF, LeBrasseur NK, White TA, Hirsova P, et al. CXCL10-mediates macrophage, but not other innate immune cells-associated inflammation in murine nonalcoholic steatohepatitis. *Sci Rep* (2016) 6:28786. doi: 10.1038/srep28786

31. Baeck C, Wehr A, Karlmark KR, Heymann F, Vucur M, Gassler N, et al. Pharmacological inhibition of the chemokine CCL2 (MCP-1) diminishes liver macrophage infiltration and steatohepatitis in chronic hepatic injury. *Gut* (2012) 61:416–26. doi: 10.1136/gutjnl-2011-300304

32. Guillot A, Tacke F. Liver macrophages: Old dogmas and new insights. *Hepatol Commun* (2019) 3:730–43. doi: 10.1002/hep4.1356

33. Wang H, Mehal W, Nagy LE, Rotman Y. Immunological mechanisms and therapeutic targets of fatty liver diseases. *Cell Mol Immunol* (2021) 18:73–91. doi: 10.1038/s41423-020-00579-3

34. Friedman SL, Ratziu V, Harrison SA, Abdelmalek MF, Aithal GP, Caballeria J, et al. A randomized, placebo-controlled trial of cenicriviroc for treatment of nonalcoholic steatohepatitis with fibrosis. *Hepatology* (2018) 67:1754–67. doi: 10.1002/hep.29477

35. Krenkel O, Puengel T, Govaere O, Abdallah AT, Mossanen JC, Kohlhepp M, et al. Therapeutic inhibition of inflammatory monocyte recruitment reduces steatohepatitis and liver fibrosis. *Hepatology* (2018) 67:1270–83. doi: 10.1002/hep.29544

36. Gao H, Jin Z, Bandyopadhyay G, Cunha ERK, Liu X, Zhao H, et al. MiR-690 treatment causes decreased fibrosis and steatosis and restores specific kupffer cell functions in NASH. *Cell Metab* (2022) 34:978–90. doi: 10.1016/j.cmet.2022.05.008

37. Scott CL, Zheng F, De Baetselier P, Martens L, Saeys Y, De Prijck S, et al. Bone marrow-derived monocytes give rise to self-renewing and fully differentiated kupffer cells. *Nat Commun* (2016) 7:10321. doi: 10.1038/ncomms10321

38. Tran S, Baba I, Poupel L, Dussaud S, Moreau M, Gelineau A, et al. Impaired kupffer cell self-renewal alters the liver response to lipid overload during non-alcoholic steatohepatitis. *Immunity* (2020) 53:627–40. doi: 10.1016/j.immuni.2020.06.003

39. Viola A, Munari F, Sanchez-Rodriguez R, Scolaro T, Castegna A. The metabolic signature of macrophage responses. *Front Immunol* (2019) 10:1462. doi: 10.3389/fimmu.2019.01462

40. Yan J, Horng T. Lipid metabolism in regulation of macrophage functions. *Trends Cell Biol* (2020) 30:979–89. doi: 10.1016/j.tcb.2020.09.006

41. Song Z, Xiaoli AM, Yang F. Regulation and metabolic significance of *De novo* lipogenesis in adipose tissues. *Nutrients* (2018) 10:1383. doi: 10.3390/nu10101383

42. Yvan-Charvet L, Wang N, Tall AR. Role of HDL, ABCA1, and ABCG1 transporters in cholesterol efflux and immune responses. *Arterioscler Thromb Vasc Biol* (2010) 30:139–43. doi: 10.1161/ATVBAHA.108.179283

43. Batista-Gonzalez A, Vidal R, Criollo A, Carreno LJ. New insights on the role of lipid metabolism in the metabolic reprogramming of macrophages. *Front Immunol* (2019) 10:2993. doi: 10.3389/fimmu.2019.02993

44. Oishi Y, Spann NJ, Link VM, Muse ED, Strid T, Edillor C, et al. SREBP1 contributes to resolution of pro-inflammatory TLR4 signaling by reprogramming fatty acid metabolism. *Cell Metab* (2017) 25:412–27. doi: 10.1016/j.cmet.2016.11.009

45. Guo C, Chi Z, Jiang D, Xu T, Yu W, Wang Z, et al. Cholesterol homeostatic regulator SCAP-SREBP2 integrates NLRP3 inflammasome activation and cholesterol biosynthetic signaling in macrophages. *Immunity* (2018) 49:842–56. doi: 10.1016/j.immuni.2018.08.021

46. Carroll RG, Zaslona Z, Galvan-Pena S, Koppe EL, Sevin DC, Angiari S, et al. An unexpected link between fatty acid synthase and cholesterol synthesis in proinflammatory macrophage activation. *J Biol Chem* (2018) 293:5509–21. doi: 10.1074/jbc.RA118.001921

47. Malandrino MI, Fucho R, Weber M, Calderon-Dominguez M, Mir JF, Valcarcel L, et al. Enhanced fatty acid oxidation in adipocytes and macrophages reduces lipid-induced triglyceride accumulation and inflammation. *Am J Physiol Endocrinol Metab* (2015) 308:E756–69. doi: 10.1152/ajpendo.00362.2014

48. Puengel T, Liu H, Guillot A, Heymann F, Tacke F, Peiseler M. Nuclear receptors linking metabolism, inflammation, and fibrosis in nonalcoholic fatty liver disease. *Int J Mol Sci* (2022) 23:2668. doi: 10.3390/ijms23052668

49. Nomura M, Liu J, Rovira II, Gonzalez-Hurtado E, Lee J, Wolfgang MJ, et al. Fatty acid oxidation in macrophage polarization. *Nat Immunol* (2016) 17:216–17. doi: 10.1038/ni.3366

50. Huang SC, Everts B, Ivanova Y, O'Sullivan D, Nascimento M, Smith AM, et al. Cell-intrinsic lysosomal lipolysis is essential for alternative activation of macrophages. *Nat Immunol* (2014) 15:846–55. doi: 10.1038/ni.2956

51. Van den Bossche J, Baardman J, Otto NA, van der Velden S, Neele AE, van den Berg SM, et al. Mitochondrial dysfunction prevents repolarization of inflammatory macrophages. *Cell Rep* (2016) 17:684–96. doi: 10.1016/j.celrep.2016.09.008

52. Guilliams M, Scott CL. Liver macrophages in health and disease. *Immunity* (2022) 55:1515–29. doi: 10.1016/j.immuni.2022.08.002

53. Guilliams M, Bonnardel J, Haest B, Vanderborght B, Wagner C, Remmerie A, et al. Spatial proteogenomics reveals distinct and evolutionarily conserved hepatic macrophage niches. *Cell* (2022) 185:379–96. doi: 10.1016/j.cell.2021.12.018

54. Scott CL, Guilliams M. The role of kupffer cells in hepatic iron and lipid metabolism. *J Hepatol* (2018) 69:1197–99. doi: 10.1016/j.jhep.2018.02.013

55. Wculek SK, Dunphy G, Heras-Murillo I, Mastrangelo A, Sancho D. Metabolism of tissue macrophages in homeostasis and pathology. *Cell Mol Immunol* (2022) 19:384–408. doi: 10.1038/s41423-021-00791-9

56. Itoh M, Suganami T, Kato H, Kanai S, Shirakawa I, Sakai T, et al. CD11c+ resident macrophages drive hepatocyte death-triggered liver fibrosis in a murine model of nonalcoholic steatohepatitis. *JCI Insight* (2017) 2:e92902. doi: 10.1172/jci.insight.92902

57. Govaere O, Petersen SK, Martinez-Lopez N, Wouters J, Van Haele M, Mancina RM, et al. Macrophage scavenger receptor 1 mediates lipid-induced inflammation in non-alcoholic fatty liver disease. *J Hepatol* (2022) 76:1001–12. doi: 10.1016/j.jhep.2021.12.012

58. Lee S, Usman TO, Yamauchi J, Chhetri G, Wang X, Coudriet GM, et al. Myeloid FoxO1 depletion attenuates hepatic inflammation and prevents nonalcoholic steatohepatitis. *J Clin Invest* (2022) 132:e154333. doi: 10.1172/JCI154333

59. Dixon ED, Nardo AD, Claudel T, Trauner M. The role of lipid sensing nuclear receptors (PPARs and LXR) and metabolic lipases in obesity, diabetes and NAFLD. *Genes (Basel)* (2021) 12:645. doi: 10.3390/genes12050645

60. Luo W, Xu Q, Wang Q, Wu H, Hua J. Effect of modulation of PPAR-gamma activity on kupffer cells M1/M2 polarization in the development of non-alcoholic fatty liver disease. *Sci Rep* (2017) 7:44612. doi: 10.1038/srep44612

61. Lefere S, Puengel T, Hundertmark J, Penners C, Frank AK, Guillot A, et al. Differential effects of selective- and pan-PPAR agonists on experimental steatohepatitis and hepatic macrophages. *J Hepatol* (2020) 73:757–70. doi: 10.1016/j.jhep.2020.04.025

62. Ito A, Hong C, Rong X, Zhu X, Tarling EJ, Hedde PN, et al. LXRs link metabolism to inflammation through Abca1-dependent regulation of membrane composition and TLR signaling. *Elife* (2015) 4:e8009. doi: 10.7554/eLife.08009

63. Muse ED, Yu S, Edillor CR, Tao J, Spann NJ, Troutman TD, et al. Cell-specific discrimination of desmosterol and desmosterol mimetics confers selective regulation of LXR and SREBP in macrophages. *Proc Natl Acad Sci U.S.A.* (2018) 115:E4680–89. doi: 10.1073/pnas.1714518115

64. Han YH, Kim HJ, Na H, Nam MW, Kim JY, Kim JS, et al. RORalpha induces KLF4-mediated M2 polarization in the liver macrophages that protect against nonalcoholic steatohepatitis. *Cell Rep* (2017) 20:124–35. doi: 10.1016/j.celrep.2017.06.017

65. L'Homme L, Sermikli BP, Molendi-Coste O, Fleury S, Quemener S, Le Maitre M, et al. Deletion of the nuclear receptor RORalpha in macrophages does not modify the development of obesity, insulin resistance and NASH. *Sci Rep* (2020) 10:21095. doi: 10.1038/s41598-020-77858-6

66. Hong T, Chen Y, Li X, Lu Y. The role and mechanism of oxidative stress and nuclear receptors in the development of NAFLD. *Oxid Med Cell Longev* (2021) 2021:6889533. doi: 10.1155/2021/6889533

67. Bleriot C, Barreby E, Dunsmore G, Ballaire R, Chakarov S, Ficht X, et al. A subset of kupffer cells regulates metabolism through the expression of CD36. *Immunity* (2021) 54:2101–16. doi: 10.1016/j.immuni.2021.08.006

68. Orecchioni M, Ghosheh Y, Pramod AB, Ley K. Macrophage polarization: Different gene signatures in M1(LPS+) vs. classically and M2(LPS-) vs. alternatively activated macrophages. *Front Immunol* (2019) 10:1084. doi: 10.3389/fimmu.2019.01084

69. Galluzzi L, Vitale I, Aaronson SA, Abrams JM, Adam D, Agostinis P, et al. Molecular mechanisms of cell death: Recommendations of the nomenclature committee on cell death 2018. *Cell Death Differ* (2018) 25:486–541. doi: 10.1038/s41418-017-0012-4

70. Gual P, Gilgenkrantz H, Lotersztajn S. Autophagy in chronic liver diseases: the two faces of janus. *Am J Physiol Cell Physiol* (2017) 312:C263–73. doi: 10.1152/ajpcell.00295.2016

71. Wang L, Klionsky DJ, Shen HM. The emerging mechanisms and functions of microautophagy. *Nat Rev Mol Cell Biol* (2022). doi: 10.1038/s41580-022-00529-z

72. Wu MY, Lu JH. Autophagy and macrophage functions: Inflammatory response and phagocytosis. *Cells* (2019) 9:70. doi: 10.3390/cells9010070

73. Kim SH, Kim G, Han DH, Lee M, Kim I, Kim B, et al. Ezetimibe ameliorates steatohepatitis *via* AMP activated protein kinase-TFEB-mediated activation of autophagy and NLRP3 inflammasome inhibition. *Autophagy* (2017) 13:1767–81. doi: 10.1080/15548627.2017.1356977

74. Lodder J, Denaes T, Chobert MN, Wan J, El-Benna J, Pawlotsky JM, et al. Macrophage autophagy protects against liver fibrosis in mice. *Autophagy* (2015) 11:1280–92. doi: 10.1080/15548627.2015.1058473

75. Dornas W, Lagente V. Intestinally derived bacterial products stimulate development of nonalcoholic steatohepatitis. *Pharmacol Res* (2019) 141:418–28. doi: 10.1016/j.phrs.2019.01.026

76. Fukushima H, Yamashina S, Arakawa A, Taniguchi G, Aoyama T, Uchiyama A, et al. Formation of p62-positive inclusion body is associated with macrophage polarization in non-alcoholic fatty liver disease. *Hepatol Res* (2018) 48:757–67. doi: 10.1111/hepr.13071

77. Sun K, Xu L, Jing Y, Han Z, Chen X, Cai C, et al. Autophagy-deficient kupffer cells promote tumorigenesis by enhancing mtROS-NF-kappaB-IL1alpha/beta-dependent inflammation and fibrosis during the preneoplastic stage of hepatocarcinogenesis. *Cancer Lett* (2017) 388:198–207. doi: 10.1016/j.canlet.2016.12.004

78. Tsai ML, Tsai YG, Lin YC, Hsu YL, Chen YT, Tsai MK, et al. IL-25 induced ROS-mediated M2 macrophage polarization *via* AMPK-associated mitophagy. *Int J Mol Sci* (2021) 23:3. doi: 10.3390/ijms23010003

79. Wen H, Gris D, Lei Y, Jha S, Zhang L, Huang MT, et al. Fatty acid-induced NLRP3-ASC inflammasome activation interferes with insulin signaling. *Nat Immunol* (2011) 12:408–15. doi: 10.1038/ni.2022

80. Wang Q, Wei S, Zhou S, Qiu J, Shi C, Liu R, et al. Hyperglycemia aggravates acute liver injury by promoting liver-resident macrophage NLRP3 inflammasome activation *via* the inhibition of AMPK/mTOR-mediated autophagy induction. *Immunol Cell Biol* (2020) 98:54–66. doi: 10.1111/imcb.12297

81. Lee DH, Park JS, Lee YS, Han J, Lee DK, Kwon SW, et al. SQSTM1/p62 activates NFE2L2/NRF2 *via* ULK1-mediated autophagic KEAP1 degradation and protects mouse liver from lipotoxicity. *Autophagy* (2020) 16:1949–73. doi: 10.1080/15548627.2020.1712108

82. Kim J, Kundu M, Viollet B, Guan KL. AMPK and mTOR regulate autophagy through direct phosphorylation of Ulk1. *Nat Cell Biol* (2011) 13:132–41. doi: 10.1038/ncb2152

83. Gwinn DM, Shackelford DB, Egan DF, Mihaylova MM, Mery A, Vasquez DS, et al. AMPK phosphorylation of raptor mediates a metabolic checkpoint. *Mol Cell* (2008) 30:214–26. doi: 10.1016/j.molcel.2008.03.003

84. Duran A, Amanchy R, Linares JF, Joshi J, Abu-Baker S, Porollo A, et al. p62 is a key regulator of nutrient sensing in the mTORC1 pathway. *Mol Cell* (2011) 44:134–46. doi: 10.1016/j.molcel.2011.06.038

85. Liu W, Ye C, Cheng Q, Zhang X, Yao L, Li Q, et al. Macrophage raptor deficiency-induced lysosome dysfunction exacerbates nonalcoholic steatohepatitis. *Cell Mol Gastroenterol Hepatol* (2019) 7:211–31. doi: 10.1016/j.jcmgh.2018.09.011

86. Lefere S, Van Steenkiste C, Verhelst X, Van Vlierberghe H, Devisscher L, Geerts A. Hypoxia-regulated mechanisms in the pathogenesis of obesity and non-alcoholic fatty liver disease. *Cell Mol Life Sci* (2016) 73:3419–31. doi: 10.1007/s00018-016-2222-1

87. Fu ZJ, Wang ZY, Xu L, Chen XH, Li XX, Liao WT, et al. HIF-1alpha-BNIP3-mediated mitophagy in tubular cells protects against renal ischemia/reperfusion injury. *Redox Biol* (2020) 36:101671. doi: 10.1016/j.redox.2020.101671

88. Wang X, de Carvalho RM, Iracheta-Vellve A, Lowe P, Ambade A, Satishchandran A, et al. Macrophage-specific hypoxia-inducible factor-1alpha contributes to impaired autophagic flux in nonalcoholic steatohepatitis. *Hepatology* (2019) 69:545–63. doi: 10.1002/hep.30215

89. Fang C, Pan J, Qu N, Lei Y, Han J, Zhang J, et al. The AMPK pathway in fatty liver disease. *Front Physiol* (2022) 13:970292. doi: 10.3389/fphys.2022.970292

90. Isaza SC, Del PE, Dominguez-Alcon L, Elbouayadi L, Gonzalez-Rodriguez A, Garcia-Monzon C. Hypoxia and non-alcoholic fatty liver disease. *Front Med (Lausanne)* (2020) 7:578001. doi: 10.3389/fmed.2020.578001

91. Tardelli M. Monoacylglycerol lipase reprograms lipid precursors signaling in liver disease. *World J Gastroenterol* (2020) 26:3577–85. doi: 10.3748/wjg.v26.i25.3577

92. Habib A, Chokr D, Wan J, Hegde P, Mabire M, Siebert M, et al. Inhibition of monoacylglycerol lipase, an anti-inflammatory and antifibrogenic strategy in the liver. *Gut* (2019) 68:522–32. doi: 10.1136/gutjnl-2018-316137

93. Taschler U, Radner FP, Heier C, Schreiber R, Schweiger M, Schoiswohl G, et al. Monoglyceride lipase deficiency in mice impairs lipolysis and attenuates diet-induced insulin resistance. *J Biol Chem* (2011) 286:17467–77. doi: 10.1074/jbc.M110.215434

94. Deust A, Chobert MN, Demontant V, Gricourt G, Denaes T, Thiolat A, et al. Macrophage autophagy protects against hepatocellular carcinogenesis in mice. *Sci Rep* (2021) 11:18809. doi: 10.1038/s41598-021-98203-5

95. Izadi M, Ali TA, Pourkarimi E. Over fifty years of life, death, and cannibalism: A historical recollection of apoptosis and autophagy. *Int J Mol Sci* (2021) 22:12466. doi: 10.3390/ijms222212466

96. Kesavardhana S, Malireddi R, Kanneganti TD. Caspases in cell death, inflammation, and pyroptosis. *Annu Rev Immunol* (2020) 38:567–95. doi: 10.1146/annurev-immunol-073119-095439

97. Shojaie L, Iorga A, Dara L. Cell death in liver diseases: A review. *Int J Mol Sci* (2020) 21:9682. doi: 10.3390/ijms21249682

98. Feldstein AE, Canbay A, Angulo P, Taniai M, Burgart LJ, Lindor KD, et al. Hepatocyte apoptosis and fas expression are prominent features of human nonalcoholic steatohepatitis. *Gastroenterology* (2003) 125:437–43. doi: 10.1016/s0016-5085(03)00907-7

99. Wan J, Benkdane M, Teixeira-Clerc F, Bonnafous S, Louvet A, Lafdil F, et al. M2 kupffer cells promote M1 kupffer cell apoptosis: A protective mechanism against alcoholic and nonalcoholic fatty liver disease. *Hepatology* (2014) 59:130–42. doi: 10.1002/hep.26607

100. Maiers JL, Malhi H. Endoplasmic reticulum stress in metabolic liver diseases and hepatic fibrosis. *Semin Liver Dis* (2019) 39:235–48. doi: 10.1055/s-0039-1681032

101. Zinszner H, Kuroda M, Wang X, Batchvarova N, Lightfoot RT, Remotti H, et al. CHOP is implicated in programmed cell death in response to impaired function of the endoplasmic reticulum. *Genes Dev* (1998) 12:982–95. doi: 10.1101/gad.12.7.982

102. Iurlaro R, Munoz-Pinedo C. Cell death induced by endoplasmic reticulum stress. *FEBS J* (2016) 283:2640–52. doi: 10.1111/febs.13598

103. Malhi H, Kropp EM, Clavo VF, Kobrossi CR, Han J, Mauer AS, et al. C/EBP homologous protein-induced macrophage apoptosis protects mice from steatohepatitis. *J Biol Chem* (2013) 288:18624–42. doi: 10.1074/jbc.M112.442954

104. Che X, Xiao Q, Song W, Zhang H, Sun B, Geng N, et al. Protective functions of liver X receptor alpha in established vulnerable plaques: Involvement of regulating endoplasmic reticulum-mediated macrophage apoptosis and efferocytosis. *J Am Heart Assoc* (2021) 10:e18455. doi: 10.1161/JAHA.120.018455

105. Yoshimura A, Ito M, Mise-Omata S, Ando M. SOCS: Negative regulators of cytokine signaling for immune tolerance. *Int Immunol* (2021) 33:711–16. doi: 10.1093/intimm/dxab055

106. Dickensheets H, Vazquez N, Sheikh F, Gingras S, Murray PJ, Ryan JJ, et al. Suppressor of cytokine signaling-1 is an IL-4-inducible gene in macrophages and feedback inhibits IL-4 signaling. *Genes Immun* (2007) 8:21–7. doi: 10.1038/sj.gene.6364352

107. Li S, Han S, Jin K, Yu T, Chen H, Zhou X, et al. SOCS2 suppresses inflammation and apoptosis during NASH progression through limiting NF-kappaB activation in macrophages. *Int J Biol Sci* (2021) 17:4165–75. doi: 10.7150/ijbs.63889

108. Horndasch M, Culig Z. SOCS-3 antagonizes pro-apoptotic effects of TRAIL and resveratrol in prostate cancer cells. *Prostate* (2011) 71:1357–66. doi: 10.1002/pros.21353

109. Du C, Yao F, Ren Y, Du Y, Wei J, Wu H, et al. SOCS-1 is involved in TNF-alpha-induced mitochondrial dysfunction and apoptosis in renal tubular epithelial cells. *Tissue Cell* (2017) 49:537–44. doi: 10.1016/j.tice.2017.06.005

110. Luo B, Zou T, Lu N, Chai F, Ye X, Wang Y, et al. Role of suppressor of cytokine signaling 3 in lipid metabolism: Analysis based on a phage-display human liver cDNA library. *Biochem Biophys Res Commun* (2011) 416:39–44. doi: 10.1016/j.bbrc.2011.10.129

111. Vila L, Roglans N, Alegret M, Sanchez RM, Vazquez-Carrera M, Laguna JC. Suppressor of cytokine signaling-3 (SOCS-3) and a deficit of serine/threonine (Ser/Thr) phosphoproteins involved in leptin transduction mediate the effect of fructose on rat liver lipid metabolism. *Hepatology* (2008) 48:1506–16. doi: 10.1002/hep.22523

112. Dai Z, Wang H, Jin X, Wang H, He J, Liu M, et al. Depletion of suppressor of cytokine signaling-1a causes hepatic steatosis and insulin resistance in zebrafish. *Am J Physiol Endocrinol Metab* (2015) 308:E849–59. doi: 10.1152/ajpendo.00540.2014

113. Zadjali F, Santana-Farre R, Vesterlund M, Carow B, Mirecki-Garrido M, Hernandez-Hernandez I, et al. SOCS2 deletion protects against hepatic steatosis but worsens insulin resistance in high-fat-diet-fed mice. *FASEB J* (2012) 26:3282–91. doi: 10.1096/fj.12-205583

114. LaPensee CR, Lin G, Dent AL, Schwartz J. Deficiency of the transcriptional repressor b cell lymphoma 6 (Bcl6) is accompanied by dysregulated lipid metabolism. *PloS One* (2014) 9:e97090. doi: 10.1371/journal.pone.0097090

115. Silke J, Rickard JA, Gerlic M. The diverse role of RIP kinases in necroptosis and inflammation. *Nat Immunol* (2015) 16:689–97. doi: 10.1038/ni.3206

116. Sun L, Wang H, Wang Z, He S, Chen S, Liao D, et al. Mixed lineage kinase domain-like protein mediates necrosis signaling downstream of RIP3 kinase. *Cell* (2012) 148:213–27. doi: 10.1016/j.cell.2011.11.031

117. Pajuelo D, Gonzalez-Juarbe N, Tak U, Sun J, Orihuela CJ, Niederweis M. NAD(+) depletion triggers macrophage necroptosis, a cell death pathway exploited by mycobacterium tuberculosis. *Cell Rep* (2018) 24:429–40. doi: 10.1016/j.celrep.2018.06.042

118. Mohammed S, Thadathil N, Selvarani R, Nicklas EH, Wang D, Miller BF, et al. Necroptosis contributes to chronic inflammation and fibrosis in aging liver. *Aging Cell* (2021) 20:e13512. doi: 10.1111/acel.13512

119. Chang YH, Weng CL, Lin KI. O-GlcNAcylation and its role in the immune system. *J BioMed Sci* (2020) 27:57. doi: 10.1186/s12929-020-00648-9

120. Li X, Gong W, Wang H, Li T, Attri KS, Lewis RE, et al. O-GlcNAc transferase suppresses inflammation and necroptosis by targeting receptor-interacting Serine/Threonine-protein kinase 3. *Immunity* (2019) 50:576–90. doi: 10.1016/j.immuni.2019.01.007

121. Afonso MB, Rodrigues PM, Mateus-Pinheiro M, Simao AL, Gaspar MM, Majdi A, et al. RIPK3 acts as a lipid metabolism regulator contributing to inflammation and carcinogenesis in non-alcoholic fatty liver disease. *Gut* (2021) 70:2359–72. doi: 10.1136/gutjnl-2020-321767

122. Wei S, Zhou H, Wang Q, Zhou S, Li C, Liu R, et al. RIP3 deficiency alleviates liver fibrosis by inhibiting ROCK1-TLR4-NF-kappaB pathway in macrophages. *FASEB J* (2019) 33:11180–93. doi: 10.1096/fj.201900752R

123. Hao Q, Kundu S, Kleam J, Zhao ZJ, Idell S, Tang H. Enhanced RIPK3 kinase activity-dependent lytic cell death in M1 but not M2 macrophages. *Mol Immunol* (2021) 129:86–93. doi: 10.1016/j.molimm.2020.11.001

124. Varga Z, Molnar T, Mazlo A, Kovacs R, Jenei V, Kerekes K, et al. Differences in the sensitivity of classically and alternatively activated macrophages to TAK1 inhibitor-induced necroptosis. *Cancer Immunol Immunother* (2020) 69:2193–207. doi: 10.1007/s00262-020-02623-7

125. Wu L, Zhang X, Zheng L, Zhao H, Yan G, Zhang Q, et al. RIPK3 orchestrates fatty acid metabolism in tumor-associated macrophages and hepatocarcinogenesis. *Cancer Immunol Res* (2020) 8:710–21. doi: 10.1158/2326-6066.CIR-19-0261

126. Rasheed A, Robichaud S, Nguyen MA, Geoffrion M, Wyatt H, Cottee ML, et al. Loss of MLKL (Mixed lineage kinase domain-like protein) decreases necrotic core but increases macrophage lipid accumulation in atherosclerosis. *Arterioscler Thromb Vasc Biol* (2020) 40:1155–67. doi: 10.1161/ATVBAHA.119.313640

127. Saeed WK, Jun DW, Jang K, Ahn SB, Oh JH, Chae YJ, et al. Mismatched effects of receptor interacting protein kinase-3 on hepatic steatosis and inflammation in non-alcoholic fatty liver disease. *World J Gastroenterol* (2018) 24:5477–90. doi: 10.3748/wjg.v24.i48.5477

128. Coll RC, Schroder K, Pelegrin P. NLRP3 and pyroptosis blockers for treating inflammatory diseases. *Trends Pharmacol Sci* (2022) 43:653–68. doi: 10.1016/j.tips.2022.04.003

129. de Carvalho RM, Szabo G. Role of the inflammasome in liver disease. *Annu Rev Pathol* (2022) 17:345–65. doi: 10.1146/annurev-pathmechdis-032521-102529

130. Kayagaki N, Wong MT, Stowe IB, Ramani SR, Gonzalez LC, Akashi-Takamura S, et al. Noncanonical inflammasome activation by intracellular LPS independent of TLR4. *Science* (2013) 341:1246–49. doi: 10.1126/science.1240248

131. Xu B, Jiang M, Chu Y, Wang W, Chen D, Li X, et al. Gasdermin d plays a key role as a pyroptosis executor of non-alcoholic steatohepatitis in humans and mice. *J Hepatol* (2018) 68:773–82. doi: 10.1016/j.jhep.2017.11.040

132. Huang Y, Xu W, Zhou R. NLRP3 inflammasome activation and cell death. *Cell Mol Immunol* (2021) 18:2114–27. doi: 10.1038/s41423-021-00740-6

133. Gan C, Cai Q, Tang C, Gao J. Inflammasomes and pyroptosis of liver cells in liver fibrosis. *Front Immunol* (2022) 13:896473. doi: 10.3389/fimmu.2022.896473

134. Azzimato V, Jager J, Chen P, Morgantini C, Levi L, Barreby E, et al. Liver macrophages inhibit the endogenous antioxidant response in obesity-associated insulin resistance. *Sci Transl Med* (2020) 12:w9709. doi: 10.1126/scitranslmed.aaw9709

135. Wang P, Ni M, Tian Y, Wang H, Qiu J, You W, et al. Myeloid Nrf2 deficiency aggravates non-alcoholic steatohepatitis progression by regulating YAP-mediated NLRP3 inflammasome signaling. *Iscience* (2021) 24:102427. doi: 10.1016/j.isci.2021.102427

136. Platnich JM, Chung H, Lau A, Sandall CF, Bondzi-Simpson A, Chen HM, et al. Shiga Toxin/Lipopolysaccharide activates caspase-4 and gasdermin d to trigger mitochondrial reactive oxygen species upstream of the NLRP3 inflammasome. *Cell Rep* (2018) 25:1525–36. doi: 10.1016/j.celrep.2018.09.071

137. Rogers C, Erkes DA, Nardone A, Aplin AE, Fernandes-Alnemri T, Alnemri ES. Gasdermin pores permeabilize mitochondria to augment caspase-3 activation during apoptosis and inflammasome activation. *Nat Commun* (2019) 10:1689. doi: 10.1038/s41467-019-09397-2

138. Ruan S, Han C, Sheng Y, Wang J, Zhou X, Guan Q, et al. Antcin a alleviates pyroptosis and inflammatory response in kupffercells of non-alcoholic fatty liver disease by targeting NLRP3. *Int Immunopharmacol* (2021) 100:108126. doi: 10.1016/j.intimp.2021.108126

139. Mridha AR, Wree A, Robertson A, Yeh MM, Johnson CD, Van Rooyen DM, et al. NLRP3 inflammasome blockade reduces liver inflammation and fibrosis in experimental NASH in mice. *J Hepatol* (2017) 66:1037–46. doi: 10.1016/j.jhep.2017.01.022

140. Chen Y, Ma K. NLRC4 inflammasome activation regulated by TNF-alpha promotes inflammatory responses in nonalcoholic fatty liver disease. *Biochem Biophys Res Commun* (2019) 511:524–30. doi: 10.1016/j.bbrc.2019.02.099

141. Ioannou GN, Subramanian S, Chait A, Haigh WG, Yeh MM, Farrell GC, et al. Cholesterol crystallization within hepatocyte lipid droplets and its role in murine NASH. *J Lipid Res* (2017) 58:1067–79. doi: 10.1194/jlr.M072454

142. Chiang J, Ferrell JM. Bile acids as metabolic regulators and nutrient sensors. *Annu Rev Nutr* (2019) 39:175–200. doi: 10.1146/annurev-nutr-082018-124344

143. Chiang J, Ferrell JM. Bile acid receptors FXR and TGR5 signaling in fatty liver diseases and therapy. *Am J Physiol Gastrointest Liver Physiol* (2020) 318:G554–73. doi: 10.1152/ajpgi.00223.2019

144. Fiorucci S, Mencarelli A, Palladino G, Cipriani S. Bile-acid-activated receptors: Targeting TGR5 and farnesoid-x-receptor in lipid and glucose disorders. *Trends Pharmacol Sci* (2009) 30:570–80. doi: 10.1016/j.tips.2009.08.001

145. Wang YD, Chen WD, Yu D, Forman BM, Huang W. The G-protein-coupled bile acid receptor, Gpbar1 (TGR5), negatively regulates hepatic inflammatory response through antagonizing nuclear factor kappa light-chain enhancer of activated b cells (NF-kappaB) in mice. *Hepatology* (2011) 54:1421–32. doi: 10.1002/hep.24525

146. Shi Y, Su W, Zhang L, Shi C, Zhou J, Wang P, et al. TGR5 regulates macrophage inflammation in nonalcoholic steatohepatitis by modulating NLRP3 inflammasome activation. *Front Immunol* (2020) 11:609060. doi: 10.3389/fimmu.2020.609060

147. Dixon SJ, Lemberg KM, Lamprecht MR, Skouta R, Zaitsev EM, Gleason CE, et al. Ferroptosis: An iron-dependent form of nonapoptotic cell death. *Cell* (2012) 149:1060–72. doi: 10.1016/j.cell.2012.03.042

148. Britton LJ, Subramaniam VN, Crawford DH. Iron and non-alcoholic fatty liver disease. *World J Gastroenterol* (2016) 22:8112–22. doi: 10.3748/wjg.v22.i36.8112

149. Dai X, Zhang R, Wang B. Contribution of classification based on ferroptosis-related genes to the heterogeneity of MAFLD. *BMC Gastroenterol* (2022) 22:55. doi: 10.1186/s12876-022-02137-9

150. Day K, Seale LA, Graham RM, Cardoso BR. Selenotranscriptome network in non-alcoholic fatty liver disease. *Front Nutr* (2021) 8:744825. doi: 10.3389/fnut.2021.744825

151. Li X, Wang TX, Huang X, Li Y, Sun T, Zang S, et al. Targeting ferroptosis alleviates methionine-choline deficient (MCD)-diet induced NASH by suppressing liver lipotoxicity. *Liver Int* (2020) 40:1378–94. doi: 10.1111/liv.14428

152. Tsurusaki S, Tsuchiya Y, Koumura T, Nakasone M, Sakamoto T, Matsuoka M, et al. Hepatic ferroptosis plays an important role as the trigger for initiating inflammation in nonalcoholic steatohepatitis. *Cell Death Dis* (2019) 10:449. doi: 10.1038/s41419-019-1678-y

153. Wang S, Liu Z, Geng J, Li L, Feng X. An overview of ferroptosis in non-alcoholic fatty liver disease. *BioMed Pharmacother* (2022) 153:113374. doi: 10.1016/j.biopha.2022.113374

154. Nelson JE, Wilson L, Brunt EM, Yeh MM, Kleiner DE, Unalp-Arida A, et al. Relationship between the pattern of hepatic iron deposition and histological severity in nonalcoholic fatty liver disease. *Hepatology* (2011) 53:448–57. doi: 10.1002/hep.24038

155. Recalcati S, Cairo G. Macrophages and iron: A special relationship. *Biomedicines* (2021) 9:1585. doi: 10.3390/biomedicines9111585

156. Handa P, Thomas S, Morgan-Stevenson V, Maliken BD, Gochanour E, Boukhar S, et al. Iron alters macrophage polarization status and leads to steatohepatitis and fibrogenesis. *J Leukoc Biol* (2019) 105:1015–26. doi: 10.1002/JLB.3A0318-108R

157. Marques L, Negre-Salvayre A, Costa L, Canonne-Hergaux F. Iron gene expression profile in atherogenic Mox macrophages. *Biochim Biophys Acta* (2016) 1862:1137–46. doi: 10.1016/j.bbadis.2016.03.004

158. Kapralov AA, Yang Q, Dar HH, Tyurina YY, Anthonymuthu TS, Kim R, et al. Redox lipid reprogramming commands susceptibility of macrophages and microglia to ferroptotic death. *Nat Chem Biol* (2020) 16:278–90. doi: 10.1038/s41589-019-0462-8

159. Hao X, Zheng Z, Liu H, Zhang Y, Kang J, Kong X, et al. Inhibition of APOC1 promotes the transformation of M2 into M1 macrophages *via* the ferroptosis pathway and enhances anti-PD1 immunotherapy in hepatocellular carcinoma based on single-cell RNA sequencing. *Redox Biol* (2022) 56:102463. doi: 10.1016/j.redox.2022.102463

160. Li LG, Peng XC, Yu TT, Xu HZ, Han N, Yang XX, et al. Dihydroartemisinin remodels macrophage into an M1 phenotype *via* ferroptosis-mediated DNA damage. *Front Pharmacol* (2022) 13:949835. doi: 10.3389/fphar.2022.949835

161. Kao JK, Wang SC, Ho LW, Huang SW, Lee CH, Lee MS, et al. M2-like polarization of THP-1 monocyte-derived macrophages under chronic iron overload. *Ann Hematol* (2020) 99:431–41. doi: 10.1007/s00277-020-03916-8

162. Liang D, Minikes AM, Jiang X. Ferroptosis at the intersection of lipid metabolism and cellular signaling. *Mol Cell* (2022) 82:2215–27. doi: 10.1016/j.molcel.2022.03.022

163. Magtanong L, Ko PJ, To M, Cao JY, Forcina GC, Tarangelo A, et al. Exogenous monounsaturated fatty acids promote a ferroptosis-resistant cell state. *Cell Chem Biol* (2019) 26:420–32. doi: 10.1016/j.chembiol.2018.11.016

164. Bock FJ, Tait S. Mitochondria as multifaceted regulators of cell death. *Nat Rev Mol Cell Biol* (2020) 21:85–100. doi: 10.1038/s41580-019-0173-8

165. Ma X, Xiao L, Liu L, Ye L, Su P, Bi E, et al. CD36-mediated ferroptosis dampens intratumoral CD8(+) T cell effector function and impairs their antitumor ability. *Cell Metab* (2021) 33:1001–12. doi: 10.1016/j.cmet.2021.02.015

166. Gautheron J, Vucur M, Reisinger F, Cardenas DV, Roderburg C, Koppe C, et al. A positive feedback loop between RIP3 and JNK controls non-alcoholic steatohepatitis. *EMBO Mol Med* (2014) 6:1062–74. doi: 10.15252/emmm.201403856

167. Matsuzawa-Ishimoto Y, Shono Y, Gomez LE, Hubbard-Lucey VM, Cammer M, Neil J, et al. Autophagy protein ATG16L1 prevents necroptosis in the intestinal epithelium. *J Exp Med* (2017) 214:3687–705. doi: 10.1084/jem.20170558

168. Hou W, Han J, Lu C, Goldstein LA, Rabinowich H. Autophagic degradation of active caspase-8: A crosstalk mechanism between autophagy and apoptosis. *Autophagy* (2010) 6:891–900. doi: 10.4161/auto.6.7.13038

169. Wu X, Poulsen KL, Sanz-Garcia C, Huang E, McMullen MR, Roychowdhury S, et al. MLKL-dependent signaling regulates autophagic flux in a murine model of non-alcohol-associated fatty liver and steatohepatitis. *J Hepatol* (2020) 73:616–27. doi: 10.1016/j.jhep.2020.03.023

170. Zhao P, Sun X, Chaggan C, Liao Z, In WK, He F, et al. An AMPK-caspase-6 axis controls liver damage in nonalcoholic steatohepatitis. *Science* (2020) 367:652–60. doi: 10.1126/science.aay0542

171. Wu W, Wang X, Sun Y, Berleth N, Deitersen J, Schlutermann D, et al. TNF-induced necroptosis initiates early autophagy events *via* RIPK3-dependent AMPK activation, but inhibits late autophagy. *Autophagy* (2021) 17:3992–4009. doi: 10.1080/15548627.2021.1899667

172. Gram AM, Booty LM, Bryant CE. Chopping GSDMD: Caspase-8 has joined the team of pyroptosis-mediating caspases. *EMBO J* (2019) 38:e102065. doi: 10.15252/embj.2019102065

173. Tao L, Yi Y, Chen Y, Zhang H, Orning P, Lien E, et al. RIP1 kinase activity promotes steatohepatitis through mediating cell death and inflammation in macrophages. *Cell Death Differ* (2021) 28:1418–33. doi: 10.1038/s41418-020-00668-w

174. Hua KF, Chou JC, Ka SM, Tasi YL, Chen A, Wu SH, et al. Cyclooxygenase-2 regulates NLRP3 inflammasome-derived IL-1beta production. *J Cell Physiol* (2015) 230:863–74. doi: 10.1002/jcp.24815

175. Kang R, Zeng L, Zhu S, Xie Y, Liu J, Wen Q, et al. Lipid peroxidation drives gasdermin d-mediated pyroptosis in lethal polymicrobial sepsis. *Cell Host Microbe* (2018) 24:97–108. doi: 10.1016/j.chom.2018.05.009

176. Zhou B, Liu J, Kang R, Klionsky DJ, Kroemer G, Tang D. Ferroptosis is a type of autophagy-dependent cell death. *Semin Cancer Biol* (2020) 66:89–100. doi: 10.1016/j.semcancer.2019.03.002

177. Hou W, Xie Y, Song X, Sun X, Lotze MT, Zeh HR, et al. Autophagy promotes ferroptosis by degradation of ferritin. *Autophagy* (2016) 12:1425–28. doi: 10.1080/15548627.2016.1187366

178. Wu Z, Geng Y, Lu X, Shi Y, Wu G, Zhang M, et al. Chaperone-mediated autophagy is involved in the execution of ferroptosis. *Proc Natl Acad Sci U.S.A.* (2019) 116:2996–3005. doi: 10.1073/pnas.1819728116

179. Li J, Liu J, Xu Y, Wu R, Chen X, Song X, et al. Tumor heterogeneity in autophagy-dependent ferroptosis. *Autophagy* (2021) 17:3361–74. doi: 10.1080/15548627.2021.1872241

180. Liu J, Yang M, Kang R, Klionsky DJ, Tang D. Autophagic degradation of the circadian clock regulator promotes ferroptosis. *Autophagy* (2019) 15:2033–35. doi: 10.1080/15548627.2019.1659623

181. Bai Y, Meng L, Han L, Jia Y, Zhao Y, Gao H, et al. Lipid storage and lipophagy regulates ferroptosis. *Biochem Biophys Res Commun* (2019) 508:997–1003. doi: 10.1016/j.bbrc.2018.12.039

182. Zhang Y, Swanda RV, Nie L, Liu X, Wang C, Lee H, et al. mTORC1 couples cyst(e)ine availability with GPX4 protein synthesis and ferroptosis regulation. *Nat Commun* (2021) 12:1589. doi: 10.1038/s41467-021-21841-w

183. Liu J, Zhu S, Zeng L, Li J, Klionsky DJ, Kroemer G, et al. DCN released from ferroptotic cells ignites AGER-dependent immune responses. *Autophagy* (2022) 18:2036–49. doi: 10.1080/15548627.2021.2008692

184. Liu W, Bai F, Wang H, Liang Y, Du X, Liu C, et al. Tim-4 inhibits NLRP3 inflammasome *via* the LKB1/AMPKalpha pathway in macrophages. *J Immunol* (2019) 203:990–1000. doi: 10.4049/jimmunol.1900117

185. Chow A, Schad S, Green MD, Hellmann MD, Allaj V, Ceglia N, et al. Tim-4(+) cavity-resident macrophages impair anti-tumor CD8(+) T cell immunity. *Cancer Cell* (2021) 39:973–88. doi: 10.1016/j.ccell.2021.05.006

186. Zhang Q, Wang J, Huang F, Yao Y, Xu L. Leptin induces NAFLD progression through infiltrated CD8+ T lymphocytes mediating pyroptotic-like cell death of hepatocytes and macrophages. *Dig Liver Dis* (2021) 53:598–605. doi: 10.1016/j.dld.2020.10.025

187. Farrell GC, Haczeyni F, Chitturi S. Pathogenesis of NASH: How metabolic complications of overnutrition favour lipotoxicity and pro-inflammatory fatty liver disease. *Adv Exp Med Biol* (2018) 1061:19–44. doi: 10.1007/978-981-10-8684-7_3

188. Wang Y, Li N, Zhang X, Horng T. Mitochondrial metabolism regulates macrophage biology. *J Biol Chem* (2021) 297:100904. doi: 10.1016/j.jbc.2021.100904

189. Wang Y, Shi P, Chen Q, Huang Z, Zou D, Zhang J, et al. Mitochondrial ROS promote macrophage pyroptosis by inducing GSDMD oxidation. *J Mol Cell Biol* (2019) 11:1069–82. doi: 10.1093/jmcb/mjz020

190. Luo Q, Song Y, Kang J, Wu Y, Wu F, Li Y, et al. mtROS-mediated Akt/AMPK/mTOR pathway was involved in copper-induced autophagy and it attenuates copper-induced apoptosis in RAW264.7 mouse monocytes. *Redox Biol* (2021) 41:101912. doi: 10.1016/j.redox.2021.101912

191. Du S, Li C, Lu Y, Lei X, Zhang Y, Li S, et al. Dioscin alleviates crystalline silica-induced pulmonary inflammation and fibrosis through promoting alveolar macrophage autophagy. *Theranostics* (2019) 9:1878–92. doi: 10.7150/thno.29682

192. Zhang Y, Su SS, Zhao S, Yang Z, Zhong CQ, Chen X, et al. RIP1 autophosphorylation is promoted by mitochondrial ROS and is essential for RIP3 recruitment into necrosome. *Nat Commun* (2017) 8:14329. doi: 10.1038/ncomms14329

193. Jiang JJ, Zhang GF, Zheng JY, Sun JH, Ding SB. Targeting mitochondrial ROS-mediated ferroptosis by quercetin alleviates high-fat diet-induced hepatic lipotoxicity. *Front Pharmacol* (2022) 13:876550. doi: 10.3389/fphar.2022.876550

194. Krenkel O, Tacke F. Macrophages in nonalcoholic fatty liver disease: A role model of pathogenic immunometabolism. *Semin Liver Dis* (2017) 37:189–97. doi: 10.1055/s-0037-1604480

195. Shiffman M, Freilich B, Vuppalanchi R, Watt K, Chan JL, Spada A, et al. Randomised clinical trial: emricasan versus placebo significantly decreases ALT and caspase 3/7 activation in subjects with non-alcoholic fatty liver disease. *Aliment Pharmacol Ther* (2019) 49:64–73. doi: 10.1111/apt.15030

196. Harrison SA, Goodman Z, Jabbar A, Vemulapalli R, Younes ZH, Freilich B, et al. A randomized, placebo-controlled trial of emricasan in patients with NASH and F1-F3 fibrosis. *J Hepatol* (2020) 72:816–27. doi: 10.1016/j.jhep.2019.11.024

197. Loomba R, Lawitz E, Mantry PS, Jayakumar S, Caldwell SH, Arnold H, et al. The ASK1 inhibitor selonsertib in patients with nonalcoholic steatohepatitis: A randomized, phase 2 trial. *Hepatology* (2018) 67:549–59. doi: 10.1002/hep.29514

198. Arulselvan P, Fard MT, Tan WS, Gothai S, Fakurazi S, Norhaizan ME, et al. Role of antioxidants and natural products in inflammation. *Oxid Med Cell Longev* (2016) 2016:5276130. doi: 10.1155/2016/5276130

199. Li Q, Feng H, Wang H, Wang Y, Mou W, Xu G, et al. Licochalcone b specifically inhibits the NLRP3 inflammasome by disrupting NEK7-NLRP3 interaction. *EMBO Rep* (2022) 23:e53499. doi: 10.15252/embr.202153499

200. Fan Y, Dong W, Wang Y, Zhu S, Chai R, Xu Z, et al. Glycyrrhetinic acid regulates impaired macrophage autophagic flux in the treatment of non-alcoholic fatty liver disease. *Front Immunol* (2022) 13:959495. doi: 10.3389/fimmu.2022.959495

201. Ngu MH, Norhayati MN, Rosnani Z, Zulkifli MM. Curcumin as adjuvant treatment in patients with non-alcoholic fatty liver (NAFLD) disease: A systematic review and meta-analysis. *Complement Ther Med* (2022) 68:102843. doi: 10.1016/j.ctim.2022.102843

202. Koperska A, Wesolek A, Moszak M, Szulinska M. Berberine in non-alcoholic fatty liver disease-a review. *Nutrients* (2022) 14:3459. doi: 10.3390/nu14173459

203. Tong C, Wu H, Gu D, Li Y, Fan Y, Zeng J, et al. Effect of curcumin on the non-alcoholic steatohepatitis *via* inhibiting the M1 polarization of macrophages. *Hum Exp Toxicol* (2021) 40:S310–17. doi: 10.1177/09603271211038741

204. Wang Y, Zhou X, Zhao D, Wang X, Gurley EC, Liu R, et al. Berberine inhibits free fatty acid and LPS-induced inflammation *via* modulating ER stress response in macrophages and hepatocytes. *PloS One* (2020) 15:e232630. doi: 10.1371/journal.pone.0232630

205. Szekeres Z, Toth K, Szabados E. The effects of SGLT2 inhibitors on lipid metabolism. *Metabolites* (2021) 11:87. doi: 10.3390/metabo11020087

206. Meng Z, Liu X, Li T, Fang T, Cheng Y, Han L, et al. The SGLT2 inhibitor empagliflozin negatively regulates IL-17/IL-23 axis-mediated inflammatory responses in T2DM with NAFLD *via* the AMPK/mTOR/autophagy pathway. *Int Immunopharmacol* (2021) 94:107492. doi: 10.1016/j.intimp.2021.107492

207. Xu X, Poulsen KL, Wu L, Liu S, Miyata T, Song Q, et al. Targeted therapeutics and novel signaling pathways in non-alcohol-associated fatty liver/steatohepatitis (NAFL/NASH). *Signal Transduct Target Ther* (2022) 7:287. doi: 10.1038/s41392-022-01119-3

208. Chen HW, Yen CC, Kuo LL, Lo CW, Huang CS, Chen CC, et al. Benzyl isothiocyanate ameliorates high-fat/cholesterol/cholic acid diet-induced nonalcoholic steatohepatitis through inhibiting cholesterol crystal-activated NLRP3 inflammasome in kupffer cells. *Toxicol Appl Pharmacol* (2020) 393:114941. doi: 10.1016/j.taap.2020.114941

209. Qu Y, Yang C, Li X, Luo H, Li S, Niu M, et al. CpG-oligodeoxynucleotides alleviate tert-butyl hydroperoxide-induced macrophage apoptosis by regulating mitochondrial function and suppressing ROS production. *Oxid Med Cell Longev* (2020) 2020:1714352. doi: 10.1155/2020/1714352

210. Liu B, Deng X, Jiang Q, Li G, Zhang J, Zhang N, et al. Scoparone improves hepatic inflammation and autophagy in mice with nonalcoholic steatohepatitis by regulating the ROS/P38/Nrf2 axis and PI3K/AKT/mTOR pathway in macrophages. *BioMed Pharmacother* (2020) 125:109895. doi: 10.1016/j.biopha.2020.109895

211. Machado MV, Diehl AM. Pathogenesis of nonalcoholic steatohepatitis. *Gastroenterology* (2016) 150:1769–77. doi: 10.1053/j.gastro.2016.02.066

frontiers | Frontiers in Immunology

TYPE Original Research
PUBLISHED 27 January 2023
DOI 10.3389/fimmu.2023.1111123

OPEN ACCESS

EDITED BY
Yanan Ma,
Memorial Sloan Kettering Cancer Center, United States

REVIEWED BY
Binglong Zhang,
Memorial Sloan Kettering Cancer Center, United States
Yuhao Chen,
Washington University in St. Louis, United States
Junchao Xu,
University of Pennsylvania, United States
Chuanbin Su,
University of Pennsylvania, United States

*CORRESPONDENCE
Johanna Samulin Erdem
Johanna.Samulin-Erdem@stami.no

SPECIALTY SECTION
This article was submitted to Inflammation, a section of the journal Frontiers in Immunology

RECEIVED 29 November 2022
ACCEPTED 16 January 2023
PUBLISHED 27 January 2023

CITATION
Erdem JS, Závodná T, Ervik TK, Skare Ø, Hron T, Anmarkrud KH, Kuśnierczyk A, Catalán J, Ellingsen DG, Topinka J and Zienolddiny-Narui S (2023) High aspect ratio nanomaterial-induced macrophage polarization is mediated by changes in miRNA levels.
Front. Immunol. 14:1111123.
doi: 10.3389/fimmu.2023.1111123

High aspect ratio nanomaterial-induced macrophage polarization is mediated by changes in miRNA levels

Johanna Samulin Erdem[1]*, Táňa Závodná[2], Torunn K. Ervik[1], Øivind Skare[1], Tomáš Hron[3], Kristine H. Anmarkrud[1], Anna Kuśnierczyk[4,5], Julia Catalán[6,7], Dag G. Ellingsen[1], Jan Topinka[2] and Shan Zienolddiny-Narui[1]

[1]National Institute of Occupational Health, Oslo, Norway, [2]Department of Genetic Toxicology and Epigenetics, Institute of Experimental Medicine, the Czech Academy of Sciences, Prague, Czechia, [3]Institute of Molecular Genetics, Academy of Sciences of the Czech Republic, Prague, Czechia, [4]Department of Clinical and Molecular Medicine, Norwegian University of Science and Technology, Trondheim, Norway, [5]Proteomics and Modomics Experimental Core Facility and St. Olavs Hospital Central Staff, Trondheim, Norway, [6]Department of Work Safety, Finnish Institute of Occupational Health, Helsinki, Finland, [7]Department of Anatomy, Embryology and Genetics, University of Zaragoza, Zaragoza, Spain

Introduction: Inhalation of nanomaterials may induce inflammation in the lung which if left unresolved can manifest in pulmonary fibrosis. In these processes, alveolar macrophages have an essential role and timely modulation of the macrophage phenotype is imperative in the onset and resolution of inflammatory responses. This study aimed to investigate, the immunomodulating properties of two industrially relevant high aspect ratio nanomaterials, namely nanocellulose and multiwalled carbon nanotubes (MWCNT), in an alveolar macrophage model.

Methods: MH-S alveolar macrophages were exposed at air-liquid interface to cellulose nanocrystals (CNC), cellulose nanofibers (CNF) and two MWCNT (NM-400 and NM-401). Following exposure, changes in macrophage polarization markers and secretion of inflammatory cytokines were analyzed. Furthermore, the potential contribution of epigenetic regulation in nanomaterial-induced macrophage polarization was investigated by assessing changes in epigenetic regulatory enzymes, miRNAs, and rRNA modifications.

Results: Our data illustrate that the investigated nanomaterials trigger phenotypic changes in alveolar macrophages, where CNF exposure leads to enhanced M1 phenotype and MWCNT promotes M2 phenotype. Furthermore, MWCNT exposure induced more prominent epigenetic regulatory events with changes in the expression of histone modification and DNA methylation enzymes as well as in miRNA transcript levels. MWCNT-enhanced changes in the macrophage phenotype were correlated with prominent downregulation of the histone methyltransferases *Kmt2a* and *Smyd5* and histone deacetylases *Hdac4*, *Hdac9* and *Sirt1* indicating that both histone methylation and acetylation events may be critical in the Th2 responses to MWCNT. Furthermore, MWCNT as well as CNF exposure led to altered miRNA levels, where miR-155-5p, miR-16-1-3p, miR-25-3p, and miR-27a-5p were significantly regulated by both materials. PANTHER pathway analysis of the

identified miRNA targets showed that both materials affected growth factor (PDGF, EGF and FGF), Ras/MAPKs, CCKR, GnRH-R, integrin, and endothelin signaling pathways. These pathways are important in inflammation or in the activation, polarization, migration, and regulation of phagocytic capacity of macrophages. In addition, pathways involved in interleukin, WNT and TGFB signaling were highly enriched following MWCNT exposure.

Conclusion: Together, these data support the importance of macrophage phenotypic changes in the onset and resolution of inflammation and identify epigenetic patterns in macrophages which may be critical in nanomaterial-induced inflammation and fibrosis.

KEYWORDS

macrophage, polarization, nanomaterials, inflammation, fibrosis, epigenetic, miRNA

1 Introduction

Environmental and occupational pulmonary exposures may lead to inflammation and fibrosis in the lung. Understanding the cellular and molecular mechanisms regulating the onset of acute inflammatory responses and development of chronic inflammation and fibrosis is important. In these processes macrophages play pivotal roles as they are involved not only in the onset but also the resolution of inflammatory responses. The macrophage population is highly heterogeneous and has a high phenotypic plasticity in response to environmental cues. The intricate population of macrophages cannot be easily characterized, and while it is generally accepted that the phenotype is dynamic, the traditional M1/M2 phenotype classification is still commonly used as an outline to assess inflammatory responses (1). Similar to environmental pollutants, inhaled nanomaterials may lead to inflammatory responses in the lung and if left unresolved, poorly soluble and biopersistent materials, e.g., high aspect ratio nanofibers, may bioaccumulate and induce chronic inflammation and fibrosis in the lung and pleura (2, 3). In the resolution and transition of immune responses, a timely alteration of macrophage phenotypes is imperative. Albeit various nanomaterials have been shown to possess immunomodulating properties, the involvement of macrophage polarization in nanomaterial-induced pulmonary inflammation and fibrosis is not well understood. The transition of macrophage phenotypes is tightly controlled by transcriptional and metabolic changes and is fine-tuned by epigenetic regulation (1, 4, 5). The epigenetic regulation occurs through histone modifications (e.g., methylation and acetylation mostly at lysine residues), DNA (5mC) and RNA modifications (e.g., m6A, m5C, m1A, 2'-O-Me, and Y), and non-coding RNAs. Together these epigenetic events allow alterations in gene transcription and translation by changing the promoter accessibility and destabilizing target transcripts important for macrophage functions. In the reprogramming of macrophages in response to external stimuli, histone modifications have been most extensively studied, and histone modifications at enhancers or promoters of inflammation-related genes are heavily altered by epigenetic enzymes (6). These enzymes, i.e., histone methyltransferases (HMTs) and demethylases (HDMs), acetyltransferases (HATs) and deacetylases (HDACs), are responsible for adding and removing histone modifications and therefore dictate the magnitude and type of immune response. Methylation of histones can result in either gene activation or repression depending on the site. Methylation of histones H3K4, H3K36, and H3K79 are commonly associated with gene activation while H3K9, H3K27, and H4K20 marks indicate gene silencing. HMTs are commonly associated with M2 macrophage activation by repressing M1 genes and promoting M2 gene transcription, while HDMs are generally linked to induction of M1 phenotype (5). Furthermore, certain histone acetylation marks have been shown to contribute to macrophage phenotypes. H3 acetylation, specifically H3K9 and H3K14, is important for M1 phenotypes. These sites are modified by HAT and HDAC activity, and while the role of HATs has not been thoroughly investigated, extensive evidence suggest a role of HDACs in macrophage polarization (7, 8).

There is also compelling evidence that non-coding RNAs play pivotal roles in the fine-tuning of macrophage phenotypes and resolution of inflammation. Non-coding RNAs e.g., miRNAs exert transcriptional and post-transcriptional regulation of inflammatory pathways. Several studies have confirmed that many different miRNAs affect macrophage polarization (reviewed in 9, 10). Furthermore, recent RNome work by Ma et al. identified several miRNAs differentially expressed during M1 and M2 polarization (9). Although, the regulation is complex and affected by many factors such as species differences, macrophage population and surrounding microenvironment, miR-21, miR-26a, miR-27a and b, miR-155 as well as miR-125a, miR-146a and b, and let-7c have been identified as critical regulators of M1 and M2 polarization (9–11). The involvement of DNA and RNA modifications in the regulation of macrophage polarization is less well known. While DNA methylation may influence macrophage activity and the DNA methyltransferases DNMT1 and DNMT3b, are important in the regulation of macrophage polarization (12–14), the role of RNA modifications is unstudied. As the biologic roles of RNA modifications are starting to emerge, it is however becoming increasingly evident that these dynamic modifications represent a new layer of control of genetic information.

Although changes in macrophage polarization have been implicated in the inflammatory and fibrotic responses to nanomaterials, the regulation of their immunomodulating properties needs further investigation. As such nanocellulose (NC) materials are both inflammogenic and immunomodulating, and NC exposure induces inflammation in the lung (15–21), increases the secretion of proinflammatory cytokines and chemokines, e.g., IL1B, IL1RA, IL6, IL8, TNFA, MCP1, CCL3, CCL4, CSF2, and GCF3 (22–26), and enhances M1 macrophage phenotype (27). However, the inflammatory response is timely resolved, and NC exposure does not result in pulmonary fibrosis (17, 28). In contrast, multi-walled carbon nanotubes (MWCNT) may, like asbestos fibers, induce pulmonary fibrosis and mesothelioma in exposed animals (2, 3). The onset of MWCNT-induced fibrosis is characterized by Th2-type responses following the initial acute inflammation, which is manifested as an induction in e.g., IL4, IL5 and IL13 in the BAL and the lung of exposed animals (29–33) as well as elevated levels of IL4 and IL5 in sputum of MWCNT-exposed workers (34), and is suggested to involve macrophage phenotypic changes (35–38). To evaluate the immunomodulatory effects of these two classes of industrially relevant nanomaterials, we here utilized a murine alveolar macrophage model which was exposed to cellulose nanocrystals (CNC), cellulose nanofibers (CNF) and two MWCNT under air-liquid interphase conditions. Furthermore, the potential contribution of epigenetic regulation in nanofiber-induced macrophage polarization was investigated by assessing the regulation of epigenetic regulatory enzymes, miRNAs, and rRNA modifications following exposure.

2 Materials and methods

2.1 Particle preparation and characterization

CNC (12.1%) was purchased from University of Maine Process Development Centre, ME, USA. CNF (1.0%) produced at Aalto University, Finland, was a kind gift from Prof. H. Norppa, Finnish Institute of Occupational Health, Finland. In addition, the two JRC MWCNT materials NM-400 (JRCNM04000a) and NM-401 (JRCNM04001a) were used. NC dispersions were prepared in sterile ultrapure water and the MWCNT were dispersed in 0.05% Bovine Serum Albumin (BSA; m/v in H_2O). CNC dispersions were vortexed for 30 s and CNF and MWCNT dispersions were sonicated using a probe sonicator at 10% amplitude (Sonifier 450S, Branson Ultrasonics, Danbury, CT, USA) for 16 min. Prior to nebulization, MWCNT dispersions were passed through a 40 µm filter to remove large agglomerates. Endotoxin levels were assessed by kinetic chromogenic limulus amebocyte lysate (LAL) assay according to the manufacturer's instructions (Lonza, Basel, Switzerland). Endotoxin levels of CNC and MWCNT particles were below the detection limit of 0.005 EU/ml. Endotoxin content in CNF was measured to 0.14 EU/ml. Hydrodynamic diameter was measure for the crystalline particle (CNC) by dynamic light scattering (DLS) (ZetaSizer Nano ZS, Malvern Instruments Ltd, Malvern, UK). Scanning electron microscope (SEM) specimens of nebulized samples were prepared on newly cleaved poly-L-lysine-coated mica, essentially as previously described (27). In brief, the specimens were sputter-coated with 2.4 nm platinum in a Cressington 208HR (Cressington Scientific Instruments, Watford, UK) sputter coater and analyzed with a Hitachi SU 6600 (Hitachi High-Technologies Corporation, Tokyo, Japan) field emission scanning electron microscope (FE-SEM). The instrument was operated under the following conditions: accelerating voltage of 15-20 kV and a working distance of 10 mm. High resolution images of the particles were obtained by acquiring at slow scanning speed. Length and diameter of the nanomaterials were measured using ImageJ software (39). At least 150 fibers/particles were measured for each material. Curved nanofibers were measured using the Simple Neurite Tracer plugin in Image J (40).

2.2 Air-liquid interface cell exposure

Murine alveolar macrophages, MH-S (CRL-2019, ATCC, Rockville, MD, USA) were maintained in ATCC-formulated RPMI-1640 medium (Gibco, ThermoFisher Scientific, MA, USA) supplemented with 10% ultra-low endotoxin FBS (Biowest, Nuaillé - France), and 50 µM β-mercaptoethanol (Gibco, ThermoFisher Scientific) in 5% CO_2 at 37°C. MH-S cells were seeded in Falcon cell culture inserts (PET membranes, 4.2 cm^2 growth area, 0.4 µm pore size, 1.6×10^6 pores/cm^2; Corning, NY, USA) at a concentration of $1.0E^6$ cells/well. The cells were allowed to attach overnight and were air-lifted immediately prior to exposure. Air-lifted cell cultures were exposed at air-liquid interface (ALI) using Cloud 6 (Vitrocell, Waldkirch, Germany) to nanoparticles at concentrations C1: 0.15 µg/cm^2 and C2: 2.7 µg/cm^2. Cells exposed to the dispersant were used as controls. Exposure experiments were performed in duplicates and repeated three times. Aerosol generation was performed by Aeroneb 4.0 - 6.0 µm nebulizers for CNC and Aeroneb 10 µm nebulizers for CNF and MWCNT dispersions. Shortly, the dispersions were adjusted with 0.01% NaCl to optimize nebulization efficiency, and 200-1000 µl dispersion was nebulized to obtain the desired deposited doses measured by the Quartz Crystal Microbalance (QCM). The measured deposited doses were 0.20 ± 0.04 µg/cm^2 and 2.4 ± 0.3 µg/cm^2 for CNC, 0.19 ± 0.04 µg/cm^2 and 2.5 ± 0.1 µg/cm^2 for CNF, 0.14 ± 0.03 µg/cm^2 and 2.8 ± 0.3 µg/cm^2 for NM-400, and 0.14 ± 0.03 µg/cm^2 and 2.8 ± 0.4 µg/cm^2 for NM-401. After exposure, cells were transferred to i) culture media (M0), ii) media with IFNG (20 ng/ml; PeproTech, NJ, USA), or iii) media with IL4 and IL13 (20 ng/ml each; PeproTech). IFNG-stimulated and IL4/IL13 stimulated cells are hereafter denoted as M1 and M2 cells, respectively. Polarized MH-S macrophages have been previously thoroughly characterized (27). M1 (IFNG) and M2 (IL4/L13) polarization was confirmed on air-lifted MH-S cells, Supplementary Figure 1. A simplified classification of macrophage M1 and M2 phenotype was performed by analyzing the expression of classical M1 and M2 makers by qPCR. The classical M1 markers assessed included the proinflammatory cytokine (*Il6*), nitric oxide synthase (*Nos2*), and Th1-cell attracting chemokines (*Cxcl9* and *Cxcl10*). The M2 phenotype was characterized by assessing the expression of receptors required for phagocytosis and scavenging of mannose (*Mrc1*, encoding CD206), markers involved in the arginase pathway (*Arg1*), as well as Th-2 cell response chemokines (*Ear11*). Four and 24h post-exposure, aliquots of cell media were collected for analysis of cytokine/chemokine and LDH release, and 24h post-exposure cells were collected for nanoparticle uptake, viability analysis and RNA extraction.

2.3 Uptake and cell viability

Uptake of nanomaterials was analyzed by transmission electron microscopy (TEM) at the Electron Microscopy Lab, Oslo University, Norway. In short, 24h after exposure cells were fixed with double strength PHEM fix (41), postfixed in 1% OsO_4 (Electron Microscopy Sciences, PA, USA) and stained with 1% UA (Electron Microscopy Sciences). The specimens were dehydrated in an ethanol series, embedded in EPON (Sigma Aldrich, MO, USA) which was polymerized at 60°C and ultrathin sections (80 nm) were made with a Leica ultramicrotome (Leica Microsystems, Wetzlar, Germany). For visualization of NC materials, the sections were labeled with a biotinylated carbohydrate binding module (CBM) of β-1,4-glycanase (EXG : CBM) which was a kind gift from Dr H. Wolff (Finnish Institute of Occupational Health, Finland) and Prof. U. Vogel (National Research Centre for Work Environment, Denmark) (42). In brief, the sections were incubated with 1% fish skin gelatin for 30 min and washed twice with 0.1% BSA-PBS. The NC materials were stained using the biotinylated EXG : CBM protein at 1:500 dilution in 1% BSA-PBS for 30 min. Samples incubated with 1% BSA-PBS for 30 min instead of the EXG : CBM protein were used as negative controls. The EXG : CBM protein was visualized by immunogold labeling. Accordingly, the washed sections were incubated with a rabbit anti-biotin antibody (ab53494, Abcam, Cambridge, UK) at 1:300 dilution in 1% BSA-PBS for 30 min, followed by repeated washing in 0.1% BSA-PBS and incubation with 10 nm protein A gold (Cell Microscopy Core, UMC Utrecht, the Netherlands) at 1:50 dilution for 30 min. The stained sections were washed and allowed to air dry. All incubations were performed at room temperature. Images were taken in a JEOL 1400plus TEM equipped with a Ruby camera at 120 kV (JEOL Ltd., Tokyo, Japan). Cell viability and proliferation were assessed by acridine orange DAPI live dead discrimination using Via1-Cassette on a NucleoCounter NC-200 instrument (ChemoMetec, Allerod, Denmark), and cell membrane leakage was analyzed by CyQUANT™ LDH Cytotoxicity Assay (ThermoFisher Scientific), according to the manufacturer's instructions. In the LDH analysis, lysed cells were included as a positive control indicating the maximum LDH release (100% LDH release), furthermore, a negative control for the spontaneous release of LDH was included corresponding to 0% LDH release. These controls were utilized in the calculation of LDH release according to the manufacturer's recommendations.

2.4 RNA extraction and RT-qPCR analysis

Total RNA was extracted using RNA/DNA Purification Kit and RNase-Free DNase I Kit (Norgen Biotek Corp., Ontario, Canada). Purity and concentration were assessed by Nanodrop 2000 spectrophotometer and Qubit fluorometric measurement (ThermoFisher Scientific). Gene expression was analyzed by RT-qPCR using SYBR Green I technology on a QuantStudio 5 Real-Time PCR System (Applied Biosystems, ThermoFisher Scientific). For assessment of macrophage polarization, RNA was reverse transcribed using qScript cDNA synthesis kit, according to the manufacturer's instructions (Quanta BioSciences, MA, USA). Primer sequences (KiCqStart™ Primers, Sigma Aldrich) are available in Supplementary Table 1. Expression of genes encoding epigenetic modification enzymes was assessed by a custom RT2 array (Qiagen, Hilden, Germany), order information is available upon request. Expression was normalized to the geometric mean of *Ubc* and *Hprt* (for individual assays) and *Hprt*, *Tbp* and *Ubc* (for the RT2 array). Expression was assessed using the ddCt method.

2.5 Analysis of cytokine and chemokine secretion

Concentrations of mouse cytokines/chemokines were measured in culture media by Bio-Plex Pro™ Mouse Cytokine 23-plex, according to manufacturer's instructions (Bio-Rad Laboratories Ltd, CA, USA). CCL3 was excluded from the analysis as the samples fell outside of the standard curve.

2.6 miRNA sequencing and differential expression analysis

miRNA libraries were prepared using QIAseq miRNA library kit (Qiagen) and QIAseq miRNA NGS 96 Index IL according to the manufacturer's instructions. Library concentrations were measured by Qubit 4.0 fluorometer using dsDNA HS assay kit (Invitrogen, ThermoFisher Scientific). The size and purity of the libraries were evaluated on Agilent 5200 Fragment Analyzer System using HS NGS Fragment Kit (1–6000 bp) (Agilent Technologies, CA, USA). For sequencing, the libraries were pooled at an equimolar concentration and denatured according to the standard Illumina NextSeq Library pooling guide. Sequencing was performed on Illumina NextSeq 550 system using NextSeq™ 500/550 High Output Kit v2.5 (75 cycles) (Illumina, CA, USA) following the manufacturer's instructions. For detection and quantification of miRNAs in sequencing data the miARma-Seq v1.7.2 toolset was used (43). Specifically, adapters were trimmed from raw reads using CutAdapt and sequences between 18-26 bp and average quality >25 Phread score were included in further analysis. The sequences were mapped to the mouse reference genome (GRCm38) using Bowtie1 with the following parameters: –seedlen 19 –seedmms 0 –best –nomaqround. Reads mapped to miRNA regions annotated in miRBase Release 22.1 were counted using the featureCounts tool (44). Differential expression analysis of detected miRNAs was performed with the DEseq2 v1.36.0 tool using default parameters (45). miRNAs with less than 10 reads in total across all samples were excluded. CNF and NM-401-treated samples were compared to control groups for M1 and M2 cells respectively. Differentially expressed miRNAs with False Discovery Rate, FDR < 0.1 were considered as statistically significant. Variance stabilizing transformation was performed on raw count data prior Principal Component Analysis. Heatmaps were generated using a heatmap tool included in NMF v0.17.6 R package. Before plotting, raw count data were RPKM-normalized and log-transformed. Color scale in heatmaps represents row-normalized Z-scores. Volcano plots were generated using the EnhancedVolcano v1.14.0 R package (46). In the volcano plots a cutoff of FDR ==0.1 were utilized, this corresponds to the plotted uncorrected p-values of -log10(p-value) ==2.5 and to -log10(p-value)==2.0 in M1 and M2 cells, respectively. mRNA targets of differentially expressed known miRNAs were

estimated using miRDB v6 web service (47, 48). Only validated sets of functional miRNAs (the FuncMir Collection in miRDB) were considered. Genes with target prediction score <60 or more than 2000 predictions were excluded. Predicted target genes of significantly differentially expressed miRNAs were then used for statistical overrepresentation test in PANTHER Pathways v17.0 (49). It should be noted that the results obtained from the pathway analysis relies both on the prediction of differentially expressed miRNAs, and on the consequent miRNA target prediction. To minimize potential accumulative error effects, previously outlined filtering thresholds were applied in each step. Whole set of mouse genes was used as a reference set for Fisher's Exact test. Results with False discovery rate < 0.05 were plotted using the ggplot2 R package.

2.7 Quantification of RNA modifications by LC-MS/MS

rRNA was extracted from total RNA using an Agilent 1260 Infinity II Analytical-Scale LC-UV Purification System with a Bio SEC-3 300 Å, 2.1 x 300 mm column (Agilent Technologies) chromatographed isocratically with 100 mM ammonium acetate pH 7 at 0.280 ml/min and 40°C for 20 min. Chromatograms were recorded at 260 nm and peaks corresponding to 18S and 28S rRNA were collected, lyophilized and solved in 30 µl of water. The rRNA was enzymatically hydrolyzed to ribonucleosides by 20 U benzonase (Santa Cruz Biotech, TX, USA) and 0.2 U nuclease P1 (Sigma Aldrich) in 10 mM ammonium acetate pH 6.0 and 1 mM magnesium chloride at 40 °C for 1h, then added ammonium bicarbonate to 50 mM, 0.002 U phoshodiesterase I and 0.1 U alkaline phosphatase (Sigma Aldrich) and incubated further at 37 °C for 1h. The hydrolysates were added 3 volumes of acetonitrile and centrifuged (16,000 g, 30 min, 4 °C). The supernatants were lyophilized and dissolved in 50 µl water for LC-MS/MS analysis of modified and canonical ribonucleosides. Chromatographic separation was performed using an Agilent 1290 Infinity II UHPLC system with an ZORBAX RRHD Eclipse Plus C18 150 x 2.1 mm ID (1.8 µm) column protected with an ZORBAX RRHD Eclipse Plus C18 5 x 2.1 mm ID (1.8 µm) guard column (Agilent Technologies). The mobile phase consisted of water and methanol (both added 0.1% formic acid) run at 0.23 ml/min, for modifications starting with 5% methanol for 0.5 min followed by a 2.5 min gradient of 5-15% methanol, a 3 min gradient of 15-95% methanol and 4 min re-equilibration with 5% methanol. A portion of each sample was diluted for the analysis of unmodified ribonucleosides which was chromatographed isocratically with 20% methanol. Mass spectrometric detection was performed using an Agilent 6495 Triple Quadrupole system with electrospray ionization, monitoring the mass transitions 268.1-136.1 (A), 284.1-152.1 (G), 244.1-112.1 (C), 245.1-113.1 (U), 282.1-150.1 (m^6A and m^1A), 282.1-136.1 (Am), 258.1-126.1 (m^5C), 286.1-154.1 (ac^4C), 298.1-166.1 (m^7G and m^2G), 296.1-164.1 ($m^{6,6}A$), 259.1-127.1 (m^3U), 258.1-112-1 (Cm), 298.1-152.1 (Gm), 259.1-113.1 (Um), and 245.1-155.1 (Y) in positive ionization mode.

2.8 Statistics

Gene expression and cytokine/chemokine secretion data were analyzed by linear mixed effects models using the lmer function in the lme4 package for R 4.0.3. For analysis of gene expression, observations, where the standardized residual was larger than 3 in absolute values, were considered outliers and excluded from the analysis. Nested random effects were included for treatment (i.e., nanomaterial), concentration and experiment number, (concentration was nested in treatment, and treatment was nested in experiment number). For statistical analysis of cytokine secretion, treatment and experiment number were combined in to one variable and then included as a random effect. For assessment of the combined inflammatory potential, random effects were included for exposure (i.e., treatment and experiment number combined) and protein level, with protein level nested in exposure. p-values were adjusted with the Benjamini & Hochberg (BH) step-up FDR-controlling procedure. Cell viability data was analyzed by one-way ANOVA and Dunnett's test. p-values <0.05 were considered significant. Venn diagrams were created using http://bioinformatics.psb.ugent.be/webtools/Venn/. If not stated otherwise, graphs were created using GraphPad Prism 9.4.1 and multipaneled figures were created in GIMP 2.10.4.

3 Results

3.1 Characterization of nanomaterials

Physicochemical characterization of NC and MWCNT materials is presented in Figure 1. Size distribution of nebulized nanomaterials was determined by SEM analysis, with averages of 202 ± 73 nm in length and 15 ± 3 nm in width for CNC, Figure 1A, and long fibers of 2.63 ± 1.39 µm in length and 20 ± 10 nm in width for CNF, Figure 1B. Nebulized NM-400 fibers had an average length of 0.77 ± 0.50 µm and a width of 18 ± 4 nm, Figure 1C, and NM-401 had longer fibers of an average length of 4.10 ± 2.90 µm and a width of 93 ± 26 nm, Figure 1D. DLS measurements showed that CNC was well dispersed and had a hydrodynamic diameter of 119 ± 1 nm (polydispersity index: 0.14). The materials had calculated aspect ratios of 13.5 (CNC), 131.5 (CNF), 42.8 (NM-400), and 44.1 (NM-401), indicating that the fibrous particles included in this study are high aspect ratio nanomaterials.

3.2 Cellular uptake and effects on cell viability

Cellular uptake of nanomaterials was investigated by TEM or immuno-TEM. Cellular uptake 24h post-exposure was not affected by polarization status, Supplementary Figure 2. Representative images of cellular uptake of nanomaterials in M1 macrophages are shown in Figure 2. M1 macrophages exposed to dispersion media only (control cells), Figure 2A. CNC was highly taken up by all three macrophage phenotypes and was found predominantly within endosomes, as exemplified in M1 cells, Figure 2B. It should be noted that the uptake of nanocellulose materials were identified using immuno-TEM. Thus, the signal emanates from the gold labelled antibody used to detect the EXG-CNC complex and does not give any information to the size or shape of the particles taken up. CNF particles were not observed within exposed cells, Figure 2C. However, while CNF was not taken up, exposed cells had a high prevalence of lysosomal structures in the cytoplasm compared to controls, Figure 2C. In NM-400-exposed cells,

fibers were found both within endosomes and in the extracellular space between adjacent cells, Figure 2D. NM-401-exposed cells showed fibers within endosomal structures but also partially in the cytoplasm, Figure 2E. Acridine orange staining, showed that nanomaterial exposure did not induce cytotoxicity at the investigated doses, Supplementary Figure 3. Altogether, these data show that CNC, NM-400 and NM-401 particles were taken up, whereas CNF particles were not phagocytosed by MH-S macrophages. Moreover, cells exposed to NM-401 had an increased dose-dependent leakage of LDH to the medium after 24h of exposure suggesting that NM-401 fibers may penetrate the cell membrane leading to LDH leakage, Figure 2F. This increase was not evident after 4h of NM-401 exposure nor in cells exposed to NC and NM-400, data not shown.

3.3 Effects of nanomaterial exposure on macrophage polarization markers

Effects of nanomaterial exposure on macrophage phenotype were assessed based on the expression of classical M1 and M2 markers. CNF exposure led to an enhanced M1 polarization with increased expression of *Cxcl9, Cxcl10, Il6* and *Nos2* in M1 cells, Figure 3A. On contrary, MWCNT exposure led to an increase in M2 markers. Both NM-400 and NM-401 induced the expression of the *Ear11* independent of dose, Figure 3B. Furthermore, NM-401 increased the expression of *Arg1* and *Mrc1* independent of dose, while NM-400 increased *Mrc1* expression only at the high dose (C2) in M2 macrophages, Figure 3B. Similarly, NM-400 (C1) treatment gave a 2.3-fold increase in *Mrc1* expression as well as a 0.4-fold decrease in *Cxcl10* expression in unpolarized M0 cells (p=0.010 and p=0.012, respectively), Supplementary Table 2. Exposure with CNC at the assessed doses did not affect the expression of macrophage polarization markers, Figures 3A, B. These data indicate that CNF induces the expression of common M1 markers, whereas NM-400 and NM-401 induce the expression of M2 macrophage markers at the tested doses.

3.4 Effects of nanomaterial exposure on cytokine and chemokine levels

Secretion of a panel of predominantly pro-inflammatory cytokines and chemokines were quantified after 4h and 24h of nanomaterial exposure at the high dose (C2). Nanomaterial exposure led to an induction in the secretion of several cytokines and chemokines. This effect was especially prominent for M0 but also M1 cells, which both had similar response patterns at 4h,

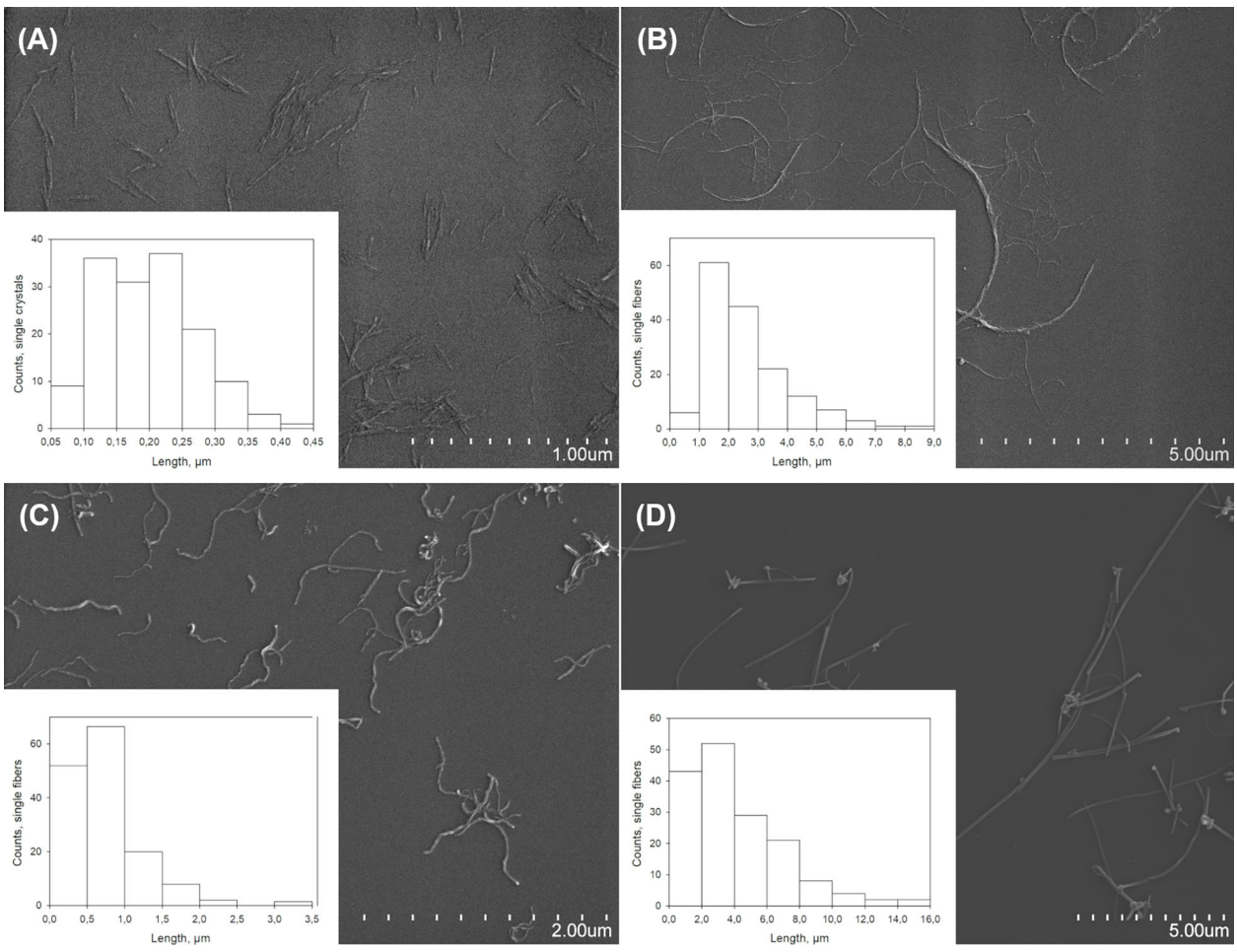

FIGURE 1
Characterization of nanomaterials. Representative SEM images and length measurements in µm of **(A)** CNC, **(B)** CNF, **(C)** NM-400, and **(D)** NM-401.

Supplementary Figure 4. Furthermore, NC materials induced stronger effects than MWCNT. At 4h, NC exposure induced the secretion of CCL2, CCL5, IL10 and IL1A independent of polarization phenotypes, while IL5, IL12p70 and TNF secretion was induced only in M0 cells. Interestingly, in M1 cells, the largest effects of exposure was observed at 4h, while in M2 cells the number of proteins affected were higher at 24h, Figure 4A. Analysis of the effects of treatment on the total cytokine release rather than on each individual cytokine separately (used as an estimation of inflammatory potential) showed that CNF exposure had the most pronounced overall effect on cytokine release in M1 macrophages at both 4 and 24h of exposure, whereas responses in M2 cells by both CNF and CNC exposure was delayed and evident only after 24h, Figure 4B. In M1 cells the largest effect of CNF exposure was observed in CCL2 (3.4-fold, p=0.017) and CCL5 (7.0-fold, p<0.001) at 4h, and in IL6 (14.3-fold, p<0.001) at 24h, Figure 4C. While MWCNT gave overall lower changes in the measured cytokine levels, an early response to MWCNT were observed in M2 cells, Figure 4B, where CCL5 levels were induced (2.4-fold, p=0.049) and IFNG levels reduced (0.4-fold, p=0.047) following 4h of NM-401 exposure, Figure 4C. Notably, CCL5 secretion was uniformly increased in both phenotypes and by both NC and MWCNT materials.

3.5 Epigenetic regulation of nanomaterial-modulated macrophage polarization

3.5.1 Genes regulating epigenetic modifications

The expression of genes regulating histone methylation (*Prt1*, *Smyd2*, *Smyd3*, *Smyd5*, *Kmt2a*, *Ezh1*, *Ezh2*, *Suv39h2*, *Dot1l*, *Wdr5*, *Ash1l*, *Setd7*, *Kdm1a*, and *Kdm6b*), histone acetylation (*Hdac2*, *Hdac3*, *Hdac4*, *Hdac9*, *Sirt1*, *Sirt2*, *Kat3a*, *Kat3b/Ep300*, *Kat5*, *Kat6a*, and *Kat6b*), and DNA methylation (*Dnmt1*, *Dnmt3a*, and *Dnmt3b*), was assessed in M0, M1 and M2 macrophages exposed to nanomaterials for 24h, Figure 5A, Supplementary Table 3. MWCNT exposure resulted in more alterations in the analyzed markers compared to NC, which only showed trends to an increase in *Kdm6b* and a reduction in *Hdac9* expression, Figure 5A. MWCNT exposure reduced the expression of several genes regulating DNA methylation and histone modifications. Although the overall effects of nanomaterial exposure on the expression of epigenetic regulators were moderate, the most prominent effect was observed in M2 cells exposed to NM-401 high dose (C2), where 12 genes were found to be differentially regulated, Figure 5B. Of these, 7 genes (*Dnmt1*, *Dnmt3a*, *Ezh1*, *Dot1l*, *Hdac4*, *Hdac9*, and *Sirt1*) were exclusively regulated by NM-401, whereas 5 genes (*Dnmt3b*, *Kdm6b*, *Kmt2a*, *Smyd5*, and *Ep300*) were regulated by both MWCNT materials, Figures 5C, D. Only *Kmt2a* and *Smyd5* were regulated by both MWCNT in both cell types, Figures 5C, D. Exposure at the low dose resulted in similar trend in effect as the high doses for each nanomaterial, Figure 5A, Supplementary Table 3.

3.5.2 miRNAs

The involvement of miRNA regulation in CNF and NM-401-induced macrophage polarization was assessed by miRNA NGS. CNF and NM-401 were selected based on their observed ability to enhance M1 polarization (CNF) and M2 polarization (NM-401). Nanomaterial exposure altered the expression (FDR < 0.1) of 11 and 52 miRNA in CNF-exposed M1 macrophages and NM-401-exposed M2 macrophages, respectively. Of these, 4 miRNAs were

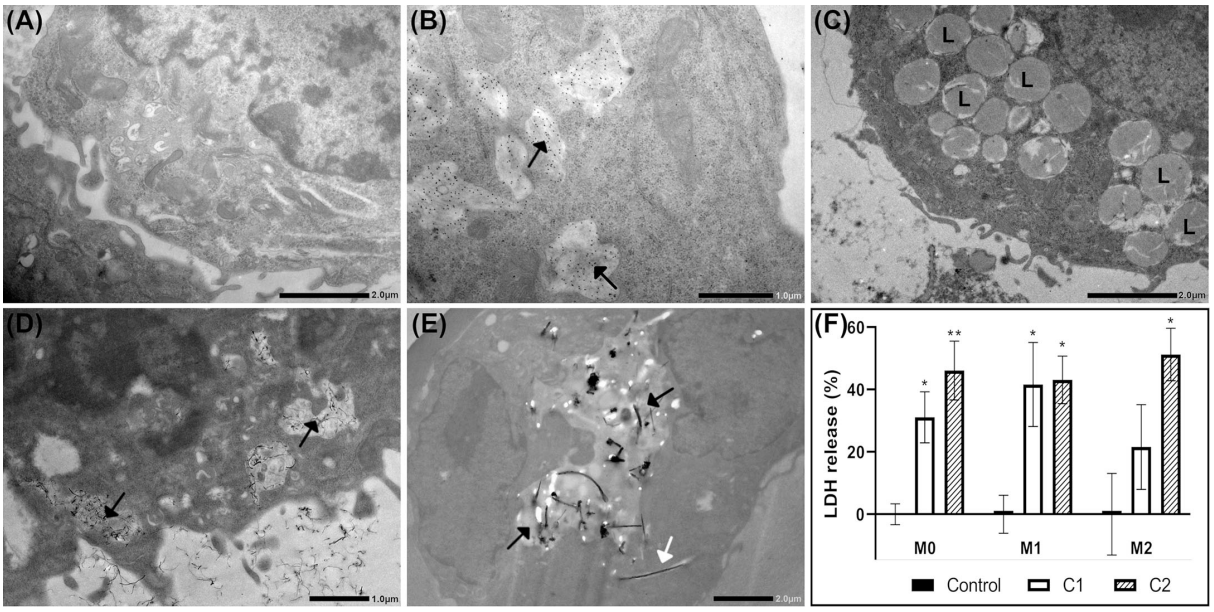

FIGURE 2
Cellular uptake and effects on membrane permeability at 24h post-exposure. Uptake of nanomaterials was investigated by TEM or immuno-TEM in M1 macrophages. Representative images of **(A)** Control, **(B)** CNC, **(C)** CNF, **(D)** NM-400, and **(E)** NM-401-exposed cells. C1: 0.15 µg/cm^2 and C2: 2.7 µg/cm^2. The experiment was repeated twice. Black arrows indicate endosomal structures with nanomaterials. White arrows indicate fibers in cell cytoplasm. L indicates lysosomal structures. **(F)** Membrane leakage as measured by medium lactate dehydrogenase (LDH) release following NM-401 exposure. Data indicate mean ± SD, (n=3-5), *p<0.05, **p<0.01.

significantly regulated in CNF-exposed M1 cells and 11 miRNAs were significantly regulated in NM-401 exposed M2 cells, (FDR < 0.1, p<0.05), Figures 6A, B. Figure 6C shows heatmap and clustering analysis of the identified miRNAs. Moreover, six miRNAs (miR-26a-2-3p, miR-26a-1-3p, miR16-1-3p, miR155-5p, miR-27a-5p and miR-25-3p) were regulated by both nanomaterials indicating that these miRNAs may be common regulators of macrophage phenotypic alterations following nanofiber exposure, Figure 6D. CNF led to a >2-fold increase in the expression of miR-122-5p and >2-fold reduction in miR-16-1-3p and miR-27a-5p expression in M1 macrophages. Of the 52 miRNAs regulated following NM-401 exposure, miR-511-3p, miR-677-3p, miR-5121 and the unverified miRNAs miR-6238, miR-6239 and miR-6240 were >2-fold upregulated whereas let-7c-1-3p, miR-708-5p, miR-26a-2-3p and miR27a-5p were >2-fold downregulated. Fold changes and adjusted p-values are available in Supplementary Data Sheet 1. Predicted mRNA targets for the differentially expressed miRNAs, Figure 6E, Supplementary Data Sheet 2, were used for statistical overrepresentation test in PANTHER Pathways. Pathway analysis showed that targets of the regulated miRNAs were enriched in growth factor (PDGF, EGF and FGF), RAS/MAPK, CCKR, GNRHR, integrin, and endothelin signaling pathways, Figures 6F, G. These pathways are

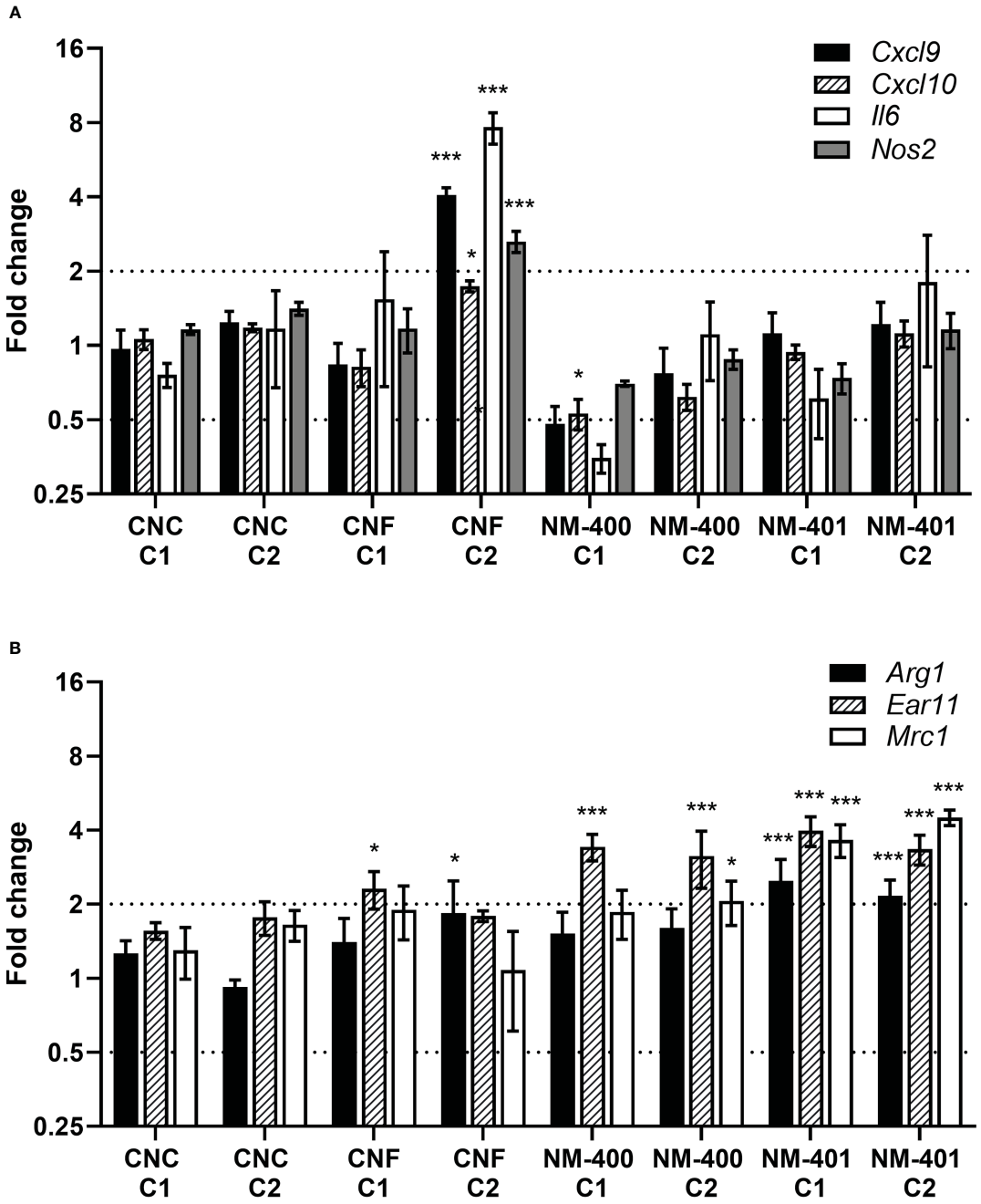

FIGURE 3
Effects of nanomaterial exposure on the expression of common macrophage polarization markers. Changes in gene expression were assessed by qPCR following exposure to CNC, CNF, NM-400 and NM-401 in **(A)** M1 and **(B)** M2 macrophages. C1: 0.15 µg/cm^2 and C2: 2.7 µg/cm^2. Expression was related to the mean expression in unexposed control cells which was set to 1. Data represent mean ± SE, (n=5), *p<0.05, ***p<0.001.

important in inflammation or in the activation, polarization, migration, and regulation of the phagocytic capacity of macrophages. In addition, pathways involved in interleukin, WNT and TGFB signaling were highly enriched for the NM-401 differentially expressed miRNAs, Figure 6G.

3.5.3 rRNA modifications

To assess the potential involvement of epitranscriptomic regulation on nanomaterial-induced macrophage polarization, posttranscriptional base modifications of rRNA were assessed. CNF and NM-401 were selected based on their observed ability to enhance M1 polarization (CNF) and M2 polarization (NM-401). The confirmed rRNA modifications (50): m^1A, m^6A, $m^{6,6}A$, m^5C, ac^4C, m^7G, m^2G, Y, m^3U, and the 2'-O-Me (Am, Cm, Gm, and Um) were analyzed. Exposure to CNF and NM-401 did not induce changes in the analyzed rRNA modifications, Supplementary Table 4.

4 Discussion

Inhalation of high aspect ratio nanomaterials evokes inflammatory responses in the lung, which if left unresolved may evolve into pulmonary fibrosis and cancer (18, 29, 51–54). It is well documented that the inhalation of persistent NC leads to acute pulmonary inflammation which is gradually time-dependently alleviated and does not result in fibrosis (15, 17–20, 28). In accordance with previous studies (23, 26, 27), we here show that NC materials trigger proinflammatory responses and enhance macrophage M1 phenotype. CNF alone did not alter the expression of the analyzed macrophage polarization markers in M0 cells, however induced the secretion of the proinflammatory cytokines IL5, IL12 and TNF. Furthermore, CNF exposure enhanced the expression of the M1 markers *Cxcl9*, *Cxcl10*, *Il6*, and *Nos2* in IFNG-activated M1 macrophages, and resulted in a marked increased secretion of e.g., CCL5 and IL6 after 4h exposure. Thus, CNF exposure highly induced the expression of IL6 both on mRNA and protein level. Similarly, NC exposure enhances both CXCL9 mRNA and protein expression (27). CNC did not affect the expression of macrophage polarization markers at the doses investigated. We have previously shown that CNC enhanced M1 phenotype and trigged secretion of proinflammatory cytokines at higher doses (15 ug/cm^2) (27). Interestingly, CNC materials typically induce more pronounced inflammation than CNF materials in exposed animals. Concurrently, CNC is rapidly internalized by macrophages and found within endosomes in the cell cytoplasm at 24h of exposure. We have previously demonstrated that CNC particles are taken up through phagocytosis/micropinocytosis *via* actin and PI3K-dependent mechanisms already after 2h of exposure

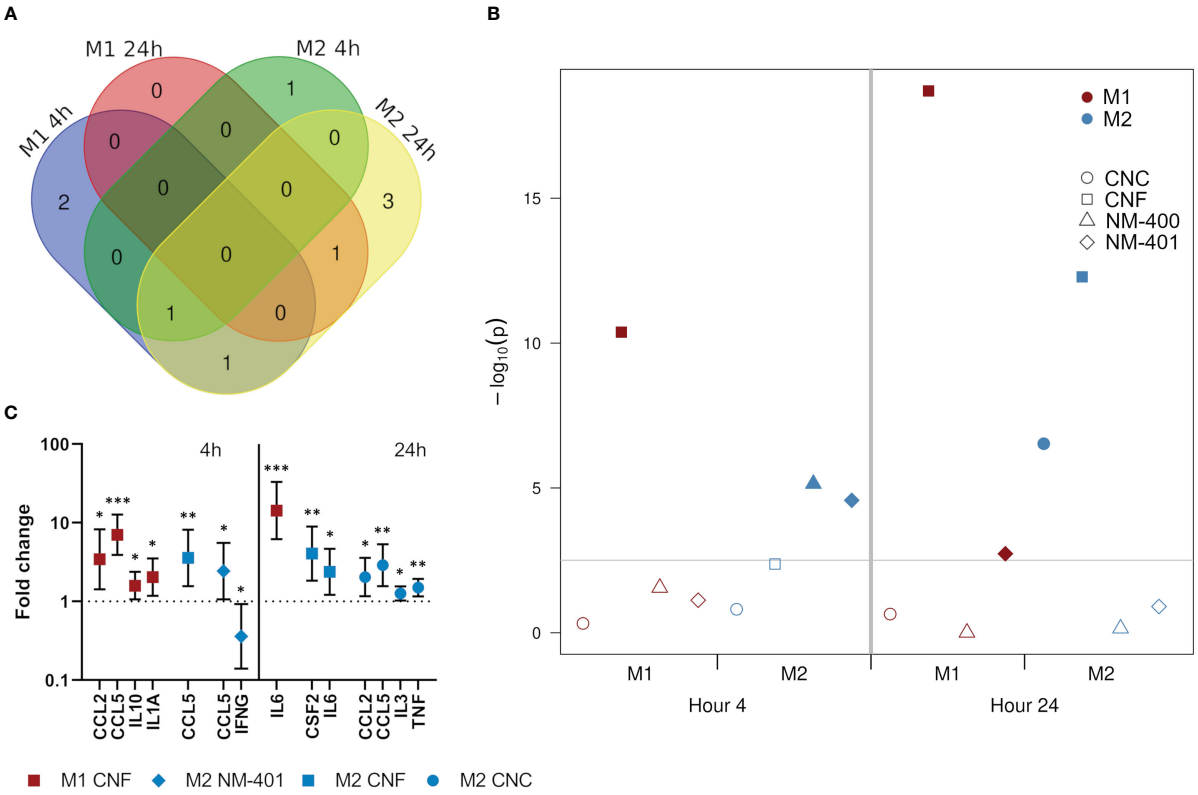

FIGURE 4
Effects on the secretion of cytokines and chemokines following exposure to CNC, CNF, NM-400 and NM-401 (high C2 dose). **(A)** Venn diagram illustrates the temporal differences in affected cytokines and chemokines in exposed M1 and M2 cells. **(B)** The combined inflammatory potential of nanomaterial exposure was illustrated by the p–values ($-\log_{10}$) of treatment effects for the deregulated proteins. The cutoff line indicates the significance level corrected for multiple testing. Filled symbols indicate values above the cutoff line where the exposure significantly affected the total secretion of cytokines in the specified macrophage subclass. **(C)** Cytokines and chemokines with significant changes in their secretion in M1 cells and M2 cells at 4 and 24h of exposure compared to controls. Data indicate mean ± CI, (n=4), *p<0.05, **p<0.01, ***p<0.001.

(27). CNF on contrary, is not effectively internalized by alveolar macrophages *in vitro* as demonstrated here by immuno-TEM analysis, however exposed cells showed an increased presence of lysosomal structures. These findings are supported by previous studies showing increased presence of vacuoles in the cytoplasm of CNF exposed cells despite low or no particle uptake (24, 55). Previous studies also suggest that CNF may absorb to the plasma membrane resulting in limited uptake and that its effects may involve receptor-mediated mechanisms (23, 56, 57). Thus, these findings indicate that the pulmonary inflammation induced by CNC and CNF materials may involve different cellular mechanisms. Furthermore, the different shape and physical characteristics of these two materials likely influence their effects and the fiber shape of CNF may contribute to the stronger pro-inflammatory effects observed. Indeed, it is well acknowledged that fibers and high aspect nanomaterials may induce prominent sustained inflammation upon inhalation and may even result in pulmonary fibrosis or cancer (58).

Despite the high aspect ratio of CNF materials, their toxic pulmonary responses differ from that caused by MWCNT and asbestos (18, 28). Contrary to NC, MWCNT, similarly to asbestos, are inefficient cleared and retained in the lung resulting in chronic inflammation, fibrotic lesions, lung cancer and mesothelioma in long-term exposed animals (51, 59–64). In addition to differences in chemical composition, CNF particles are also highly coiled and branched, affecting their uptake. It is generally acknowledged that high rigidity of particles highly influences their clearance and the physiological responses upon inhalation, as they may induce damage to endosomes and phagosomes or directly pierce the cells leading to prolonged and more prominent inflammatory responses (65–68). For MWCNT, a progression from acute inflammation to chronic fibrotic changes suggests that a resolution of inflammation involving Th2 responses may underlie the fibrotic events (38). It is also evident that long and rigid MWCNT typically induce more prominent inflammation and fibrotic responses than shorter coiled MWCNT (61, 64, 69). In agreement, this study showed that the long and rigid NM-401 fibers gave more severe effects on macrophage markers, as illustrated by increased M2 markers *Arg1*, *Ear11*, and *Mrc1*, and cytokine secretion, compared to the shorter and more coiled NM-400

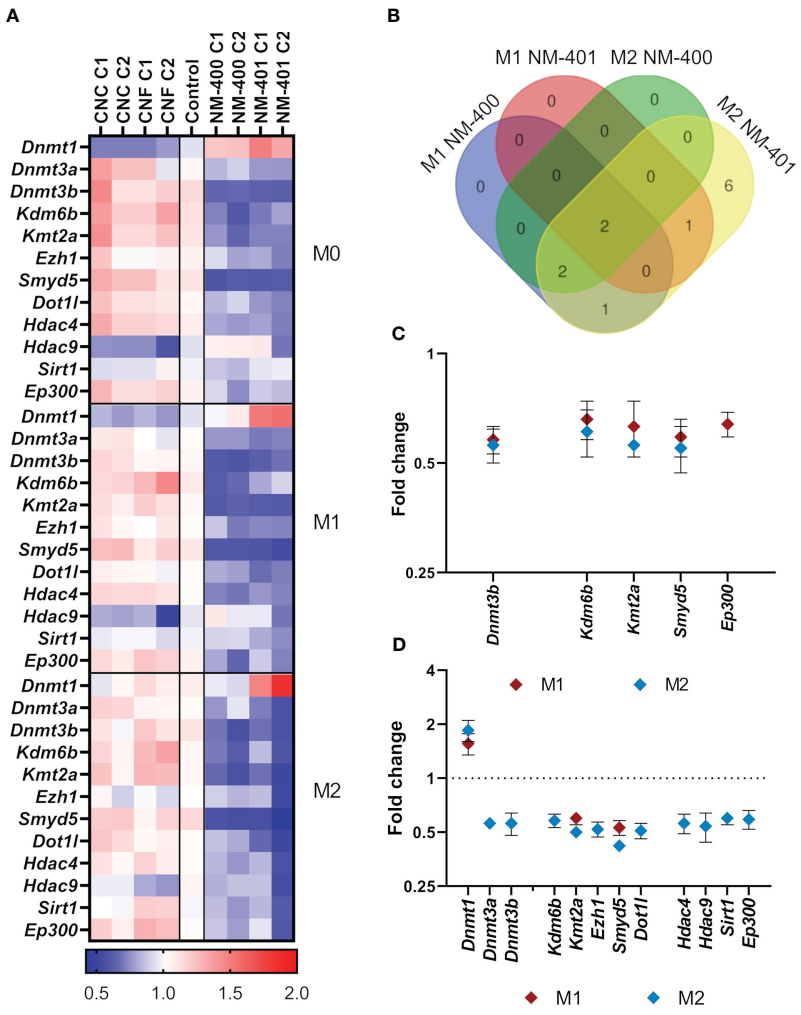

FIGURE 5
Effects on the expression of genes regulating epigenetic modifications. Changes in gene expression were assessed by qPCR following exposure to CNC, CNF, NM-400 and NM-401. C1: 0.15 μg/cm^2 and C2: 2.7 μg/cm^2. **(A)** Heatmap of the mean fold changes in regulated genes following 24h of nanomaterial exposure in M0, M1 and M2 macrophages. **(B)** Venn diagram illustrates commonly regulated genes in M1 and M2 cells after NM-400 and NM-401 exposure. **(C)** Genes significantly regulated following exposure to NM-400. **(D)** Genes significantly regulated following exposure to NM-401. Data represent mean ± SD, (n=5), $p<0.05$.

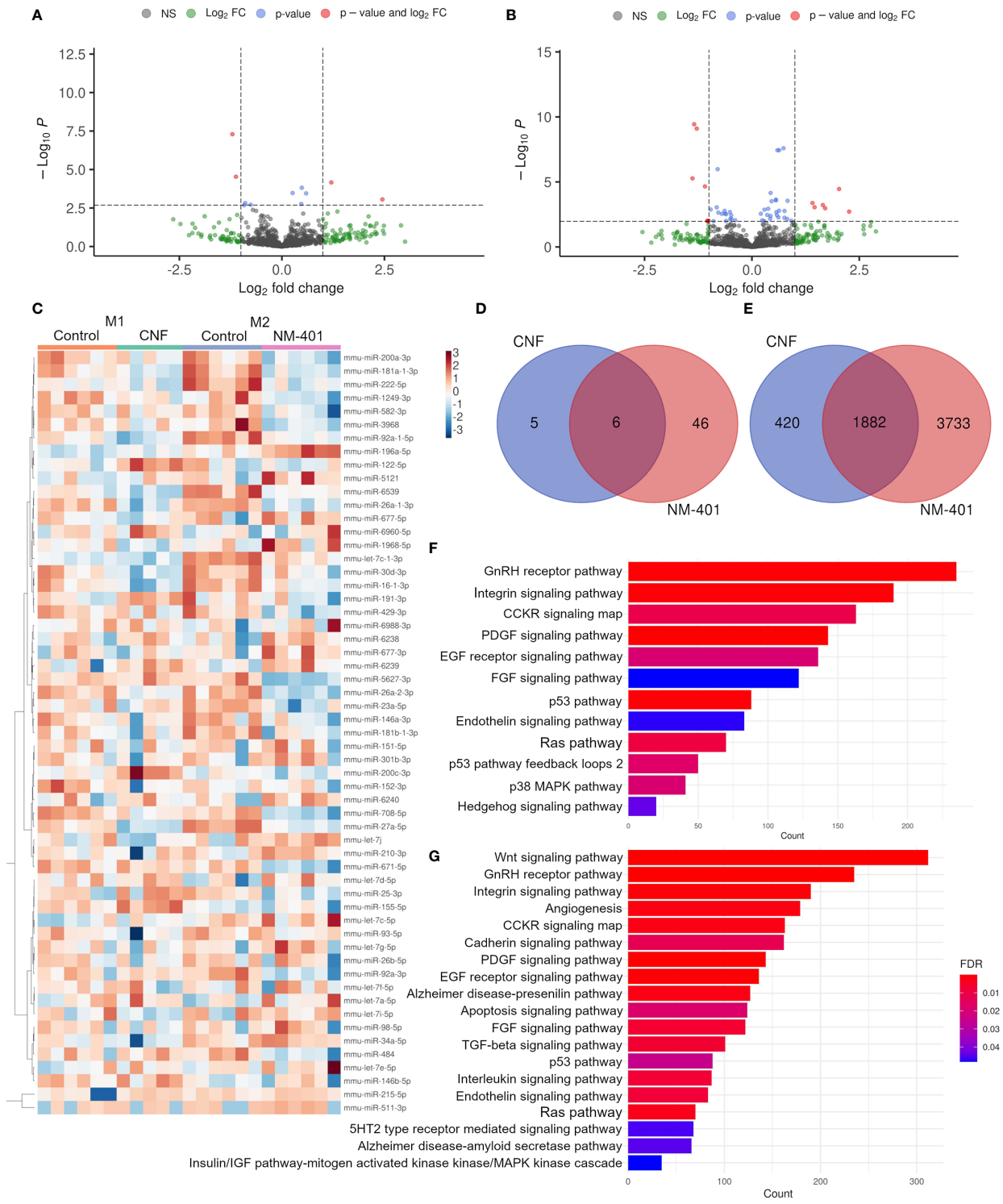

FIGURE 6
CNF and NM-401 exposure induced changes in miRNA expression. **(A)** Volcano plot of differentially expressed known miRNAs in CNF-exposed M1 cells. **(B)** Volcano plot of differentially expressed known miRNAs in NM-401-exposed M2 cells. Y-axes show negative decadic logarithm of uncorrected p-values (-log10 P), x-axes show the binary logarithm of fold changes (log2 fold change). Log2 fold change cutoff = 1, and FDR cutoff = 0.1 are indicated. **(C)** Clustering heat map of differentially expressed miRNAs -$\log_{10}$(CPM). **(D)** Venn diagrams of differentially expressed miRNAs and **(E)** their predicted target genes. PANTHER analyzes of the target genes of differentially expressed miRNA in **(F)** CNF- and **(G)** NM-401-exposed macrophages, (n=5-6).

fibers. As both materials have similar aspect ratios (NM-400: 42.8 and NM-401: 44.1), these differences could possibly to some extent be attributed to the rigidity of the materials. It is well described that rod-like CNT may induce more severe fibrotic responses (61, 64) and may disrupt macrophage function due to unsuccessful uptake resulting in frustrated phagocytoses and damage of surrounding tissues (58, 67). Analyzes of cellular uptake showed that although both NM-400 and NM-401 were internalized and found within endosomes in alveolar

macrophages, NM-401 fibers were also found in the cytoplasm after 24h of exposure. Previous studies have demonstrated that MWCNT may be taken up by macrophages already after 1h of exposure (70). Further analyzes indicated that NM-401-exposed cells showed signs of membrane leakage at the sub-toxic concentrations tested. This may suggest that the more rigid NM-401 fibers induce cellular membrane damage which may contribute to the enhanced effects observed by these fibers. In agreement with our findings, a grouping effort of MWCNT for risk assessment (69) conclude that NM-400 occurs as tangled agglomerates which are not able to induce frustrated phagocytosis (65), while NM-401 cause lysosomal disruption, intracellular 'vesicle escape' (66) and frustrated phagocytosis in macrophages both *in vitro* and *in vivo* (65). As several studies have demonstrated that MWCNT-induced fibrosis is Th2-type response mediated (reviewed in 38), the involvement of M2 polarization events has been suggested (35–37). Our data confirm an enhanced M2 phenotype following MWCNT exposure, which is more prominent for long rigid fibers. This further supports the involvement of M2 macrophage phenotype in the onset of MWCNT-induced lung fibrosis.

The involvement of epigenetic events in the observed fine-tuning of macrophage phenotype in response to nanofiber exposure has not been clarified. Here we demonstrate that the enhanced M1 phenotype observed after CNF exposure did not involve histone or DNA modification events. However, the MWCNT-induced M2 phenotype showed regulation of several histone and DNA modifying enzymes which may be of importance in fibrosis onset following MWCNT exposure. The epigenetic regulation of M1 macrophage phenotypes has been extensively studied and involves KDM6B (previously known as JMJD3), KMT6, several HDACs and DNMT1 (6). However, fever studies have focused on the role of histone and DNA modifying enzymes in M2 macrophage polarization (71–74). In murine macrophages, alternative M2 phenotype is mediated by the histone H3K27 demethylase *Kdm6b* which may regulate the expression of e.g., *Irf4*, *Chi3l3*, *Retn1a*, and *Arg1* (71, 74). Furthermore, *Kdm6a* deficient mice show enhanced M2 macrophage polarization (75). These findings indicate that the KDM6 family is important in regulating the M2 phenotype. Interestingly, in this study, both MWCNT decreased the expression of *Kdm6b* in M2 cells, supporting a potential role of H3K27 methylation in the regulation of macrophage phenotype associated with increased expression of *Arg1*, *Mrc1*, and *Ear11* following MWCNT exposure. Furthermore, the expression of the H3K4 methyltransferases *Kmt2a* (previously known as *Mll*) and *Smyd5* mRNA was reduced by MWCNT in both M1 and M2 macrophages, while the *Ezh1* and *Dot1l* mRNA were downregulated exclusively by NM-401 in M2 macrophages. The HMT family members hold diverse roles in macrophage polarization as they regulate the expression of inflammatory genes. In general, HMTs promote M2 phenotype by repressing the expression of pro-inflammatory cytokines e.g., *Tnf*, *Il1b*, *Il6*, and *Cxcl10* (76, 77). On the other hand, KMT2A is required for M1 macrophage polarization as it leads to enhanced *Cxcl10* expression (72). In addition to alterations in HMT expression, we also observed a reduction in the expression of *Hdac4*, *Hdac9* and *Sirt1* as well as the HAT *Kat3b (Ep300)* in M2 cells following NM-401 exposure. HDACs are recognized as important regulators of polarization as their inhibition results in altered levels of cytokines, chemokines and macrophage activation markers (5, 78). Accordingly, *Hdac9* deficiency has been shown to exaggerate M2 macrophage polarization in mouse and human macrophages by upregulating M2 markers e.g., *Mrc1* (also known as *Cd206*) and *Pparg* and repressing markers involved in M1 polarization e.g., *TNF*, *IL6* and *CXCL10* (79, 80). Similarly, HDAC4 inhibits NFKB signaling and increase *Tnf* and *Il6* expression in M1 cells (81). On contrary, SIRT1 represses M1 phenotype by reducing the expression of IKK/NFKB and JNK regulated inflammatory target genes e.g., *Tnf, Il1b, Il6, Il12, Nos2*, and *Mcp1* (82, 83).

While histone modifications are important in the regulation of macrophage polarization and their involvement in nanomaterial-induced pulmonary effects is evident (84, 85), the role of histone modifications during macrophage phenotypic changes in response to nanomaterial exposure has not been previously explored. Thus, while it is difficult to infer the direct effects the epigenetic regulatory enzymes have on the genetic profiles of activated macrophages it is evident that they are important in the fine-tuning of macrophages' responses to MWCNT exposure. For the MWCNT-enhanced changes in macrophage phenotype our data emphasize the role of the HMTs *Kmt2a* and *Smyd5* as their expression is universally downregulated by both MWCNT and shows the largest effect of all modifying enzymes investigated in this study. In support of our data, it is well known that KMT2A is essential for M1 polarization and its downregulation by MWCNT may be important for the triggering of an enhanced M2 phenotype. SMYD5 is a relatively unknown member of the SMYD family proteins. To date, there is only one study proposing a role of SMYD5 and H4K20me3 in the repression of TLR4 target genes in macrophages (76). However, our data indicate that SMYD5 may also have a role in the regulation of the alternative M2 phenotype. Thus, the downregulation of HMTs observed in our study suggests that their activity is important in MWCNT-induced macrophage polarization and that methylation of H3K4, H3K27 and H3K79 may be critical in modifying macrophage phenotypes in response to nanomaterial exposure. Furthermore, our data support a role of HDACs in nanomaterial-induced inflammation and more specifically our findings indicate that histone acetylation events regulated by HDAC4, HDAC9 and SIRT1 may be critical in the Th2 responses to MWCNT.

The interplay between histone modifications and other epigenetic mechanisms such as nucleotide modifications may add further complexity and may be critical for macrophages' ability to adjust and reprogram to changes in their environment. It has been shown that MWCNT induce changes in DNA methylation in the lungs of exposed animals (86–88), as well as in MWCNT-exposed workers (89). Furthermore, NM-400-exposure of monocytes induces DNA hypomethylation of inflammation-related genes and genes involved in macrophage polarization, e.g., the JAK-STAT pathway (90). In this study changes in DNA methylation were not directly measured, however, a deregulation of the expression of DNA methyltransferases was observed following MWCNT exposure, where MWCNT induced *Dnmt1* and reduced *Dnmt3a* and *Dnmt3b* expression in M2 macrophages. DNMT1 and DNMT3B are important in the regulation of macrophage polarization as their overexpression usually results in induced expression of proinflammatory cytokines and concurrent M1 polarization, whereas their depletion leads to enhanced M2 macrophage polarization (12–14). Altogether, these

finding support a potential role of DNA methylation events in MWCNT induced M2 polarization.

A well-recognized level of epigenetic regulation is exerted by non-coding RNAs, which affect the expression of various genes involved in macrophage polarization. In this study, both CNF and NM-401 exposure induced changes in miRNA transcript levels. The target genes of the differentially expressed miRNA were involved in several different signaling pathways, e.g., growth factor, Ras/MAPK, CCKR, GnRH-R, and integrin signaling, which are important for inflammation and for the activation, polarization, and function of macrophages. More specifically, CNF exposure resulted in a 2-fold upregulation of miR-122-5p and downregulation of miR-16-1-3p, and miR-27a-5p expression in M1 cells. Recent studies suggest a role of miR-122-5p in pulmonary inflammation and in the regulation of pro-inflammatory cytokine expression e.g., TNF, IL1B, IL6, and MCP1 (91, 92). Furthermore, miR-122-5p may induce M1 polarization (93). While the role of miR-16-1-3p in macrophage polarization has not been investigated, it is suggested to modulate the IL6-JAK-STAT3 signaling pathway (94). On contrary, more targets are described for miR-16-5p which has been suggested as a promotor of M2 polarization (95). These finding are consistent with our data showing that miR-122-5p is highly upregulated and miR-16-1-3p downregulated following CNF exposure, which is associated with increased secretion of IL6, CCL2, and CCL5 and an enhanced M1 phenotype. Interestingly, a 0.4-fold change in miR-27a-5p expression levels was observed for both CNF and NM-401. The role of miR-27a-5p in macrophage polarization is not well understood, as different studies have demonstrated induced expression of miR-27a-5p in both M1 and M2 polarization (96, 97). Furthermore, miR-27a is suggested to suppress PPARG signaling which is involved in the control of inflammatory responses by repressing pro-inflammatory signaling pathways such as JUN (previously known as AP-1), NFKB and STAT3, consequently enhancing M1 polarization (98). Thus, while it is evident that this miRNA is important in macrophage polarization more studies are needed to understand the exact regulation it exerts. Moreover, while the role of miR27-a has not been previously demonstrated in nanofiber-induced macrophage polarization, TiO_2 exposure decreases the expression of miR-27a-5p in murine macrophages (99). Furthermore, miR-155-5p and miR-25-3p were also regulated by both CNF and NM-401 exposure in this study. Especially, miR-155 is recognized as a major regulator of inflammation and macrophage polarization and has several known target mRNAs involved in cytokine signaling. miR-155 alters macrophage phenotype through various signaling pathways including the STAT6 and JNK pathways (100–102). In addition, CEBPB is a direct target of miR-155 (103). MWCNT exposure has previously been shown to reduce the expression of miR-155-5p in BEAS-2B cells (104). Moreover, both polystyrene and TiO_2 nanomaterials reduce the expression of miR-155-5p in THP1 monocytes (105). Together these data indicate that miR-27a-5p and miR-155-5p may be common regulators of macrophage phenotypes in response to various nanomaterial exposures.

NM-401 exposure also led to a prominent upregulation of miR-511-3p and miR-677-3p and a downregulation of miR-708-5p, miR-26a-2-3p and let-7c-1-3p. While very little information is available on the function of miR-677-3p, miR-708-5p, miR-26a-2-3p and let-7c-1-3p in macrophage polarization, they have been indicated roles in immune responses. Accordingly, miR-708 has been suggested as a suppressor of TNF/IL1B signaling leading to reduced IL6 levels in pulmonary cells (106). Furthermore, let-7c-1-3p is induced in M2 macrophages and both let-7c-1-3p and miR-26a-2-3p are involved in cytokine-cytokine receptor interactions (97). Accordingly, let-7c-1-3p targets immune response genes e.g., *Ccr9*, *Il15*, *Cxcl10* and *Ccl2*, whereas miR-26a-2-3p targets e.g., *Il15ra*, *Ccl7*, *Cx3cl1*, *Cxcl11* and *Il1b* (97). On contrary, miR-511-3p is acknowledged as regulator of M2 polarization. miR-511 is a putative positive regulator of Toll-like receptor 4 in macrophages and is involved in the Th cell polarization through modulation of *MRC1* expression (107, 108). Moreover, downregulation of miR-511-3p alters PPARG activity leading to downregulation of pro-inflammatory cytokine production in dendritic cells (109). In accordance, MRC1 has been shown to regulate macrophage polarization through miR-511-3p in mice. MRC1 depletion resulted in reduced miR-511-5p levels and enhanced M1 polarization whereas, enhanced miR-511-3p levels resulted in M2-driven anti-inflammatory responses (110). Furthermore, miR-511 has been shown to be highly expressed in IL4-stimulated (M2a) macrophages (111). Thus, while the contribution of miR-677-3p, miR-708-5p, miR-26a-2-3p and let-7c-1-3p on MWCNT-enhanced M2 polarization need further investigation, the increased miR-511-3p expression levels observed in this study could suggest a role of miR-511-3p in the enhanced M2 macrophage phenotype observed following MWCNT exposure.

Finally, RNA modifications have been recently suggested as an additional level of epigenetic regulation in response to various environmental stimuli. For instance, air pollution and PM2.5 exposure has been shown to affect the global N6-methyladenosine (m^6A) and mRNA 5-methylcytidine (m^5C) levels (112, 113). Moreover, RNA modifications, specifically m^6A, have critical roles in immune cell function and immune responses, and have been implicated in various aspects of macrophage biology, including macrophage polarization (114–116). Considering this, RNA modifications could contribute to adjustment of macrophage responses to various nanomaterials. However, our data show that CNF and MWCNT did not induce any changes in the levels of known rRNA modifications.

Altogether, this study demonstrates that CNF exposure enhances M1 macrophage, while MWCNT exposure enhances M2 macrophage polarization, congruent with the observed effects of these materials in triggering inflammation and fibrosis, respectively, in exposed animals. These data support the importance of macrophage phenotypic changes in the onset and resolution of nanofiber-induced inflammation and fibrosis and emphasize the importance of epigenetic regulation in the fine-tuning of macrophages. In correspondence with its stronger immunogenic effects, the MWCNT-induced changes in macrophage polarization involved more prominent epigenetic regulatory events i.e., histone modifications, DNA methylation and miRNAs. Whilst, epigenetic modifications are often investigated separately, there is substantial cross talk between mechanisms to establish the epigenetic landscape. In light of this, our study provides important novel evidence illustrating the intricacy of the epigenetic regulation in macrophages in response to environmental changes. Further, identifying epigenetic patterns in macrophages which may be important in nanofiber-induced inflammation and fibrosis.

Data availability statement

The datasets presented in this study can be found in online repositories. The names of the repository/repositories and accession number(s) can be found below: PRJNA902122 (SRA).

Author contributions

Conceptualization: JE, DE, JT and SZ-N. Methodology: JE, TZ, TE, KA, AK and JC. Bioinformatics and statistics: TZ, ØS and TH. Data curation: JE, ØS and TH. Writing – original draft: JE, TZ and TE. Writing – reviewing and editing: JE, TZ, JC, JT and SZ-N. All authors contributed to the article and approved the submitted version.

Funding

This work was supported by the National Institute of Occupational Health, Oslo, Norway (Grant number: 201600262). Mass spectrometry-based analyses were performed by the Proteomics and Modomics Experimental Core (PROMEC), Norwegian University of Science and Technology (NTNU) and The Central Norway Regional Health Authority. This facility is a member of the National Network of Advanced Proteomics Infrastructure (NAPI), which is funded by the Research Council of Norway INFRASTRUKTUR-program (project number: 295910). The authors also acknowledge the assistance provided by the Research Infrastructures NanoEnviCz (Project No. LM2015073), supported by the Ministry of Education, Youth, and Sports of the Czech Republic and the project Pro-NanoEnviCz (Reg. No. CZ.02.1.01/0.0/0.0/16_013/0001821) supported by the Ministry of Education, Youth, and Sports of the Czech Republic and the European Union—European Structural and Investments Funds in the frame of Operational Program Research Development and Education.

Acknowledgments

We wish to thank Ulla Vogel at the National Research Centre for Work Environment, Copenhagen, Denmark and Henrik Wolff at the Finnish Institute of Occupational Health, Helsinki, Finland for their kind gift of EXG : CBM protein. Hannu Norppa at the Finnish Institute of Occupational Health, Helsinki, Finland is acknowledged for the kind gift of CNF material. We also thank Antje Hofgaard at the Electron Microscopy Lab, Oslo University, Norway for her assistance with TEM analysis. Thilde Nygård, Mayes Alswady-Hoff and Tiril Schjølberg are acknowledged for excellent technical support.

Conflict of interest

The authors declare that the research was conducted in the absence of any commercial or financial relationships that could be construed as a potential conflict of interest.

Publisher's note

Supplementary material

The Supplementary Material for this article can be found online at: https://www.frontiersin.org/articles/10.3389/fimmu.2023.1111123/full#supplementary-material

References

1. Murray PJ. Macrophage polarization. *Annu Rev Physiol* (2017) 79(1):541–66. doi: 10.1146/annurev-physiol-022516-034339

2. Donaldson K, Murphy F, Schinwald A, Duffin R, Poland CA. Identifying the pulmonary hazard of high aspect ratio nanoparticles to enable their safety-by-Design. *Nanomed (London)* (2011) 6(1):143–56. doi: 10.2217/nnm.10.139

3. Sanchez VC, Pietruska JR, Miselis NR, Hurt RH, Kane AB. Biopersistence and potential adverse health impacts of fibrous nanomaterials: What have we learned from asbestos? *Wiley Interdiscip Rev Nanomed Nanobiotechnol* (2009) 1(5):511–29. doi: 10.1002/wnan.41

4. Natoli G, Pileri F, Gualdrini F, Ghisletti S. Integration of transcriptional and metabolic control in macrophage activation. *EMBO Rep* (2021) 22(9):e53251. doi: 10.15252/embr.202153251

5. Kapellos TS, Iqbal AJ. Epigenetic control of macrophage polarisation and soluble mediator gene expression during inflammation. *Mediators Inflammation* (2016) 2016:6591703. doi: 10.1155/2016/6591703

6. Chen S, Yang J, Wei Y, Wei X. Epigenetic regulation of macrophages: From homeostasis maintenance to host defense. *Cell Mol Immunol* (2020) 17(1):36–49. doi: 10.1038/s41423-019-0315-0

7. de Groot AE, Pienta KJ. Epigenetic control of macrophage polarization: Implications for targeting tumor-associated macrophages. *Oncotarget* (2018) 9 (29):20908–27. doi: 10.18632/oncotarget.24556

8. Daskalaki MG, Tsatsanis C, Kampranis SC. Histone methylation and acetylation in macrophages as a mechanism for regulation of inflammatory responses. *J Cell Physiol* (2018) 233(9):6495–507. doi: 10.1002/jcp.26497

9. Ma D, Zhou X, Wang Y, Dai L, Yuan J, Peng J, et al. Changes in the small noncoding rnaome during M1 and M2 macrophage polarization. *Front Immunol* (2022) 13:799733. doi: 10.3389/fimmu.2022.799733

10. Curtale G, Rubino M, Locati M. Micrornas as molecular switches in macrophage activation. *Front Immunol* (2019) 10:799. doi: 10.3389/fimmu.2019.00799

11. Kishore A, Petrek M. Roles of macrophage polarization and macrophage-derived mirnas in pulmonary fibrosis. *Front Immunol* (2021) 12:678457. doi: 10.3389/fimmu.2021.678457

12. Qin W, Spek CA, Scicluna BP, van der Poll T, Duitman J. Myeloid DNA Methyltransferase3b deficiency aggravates pulmonary fibrosis by enhancing profibrotic macrophage activation. *Respir Res* (2022) 23(1):162. doi: 10.1186/s12931-022-02088-5

13. Wang X, Cao Q, Yu L, Shi H, Xue B, Shi H. Epigenetic regulation of macrophage polarization and inflammation by DNA methylation in obesity. *JCI Insight* (2016) 1(19): e87748. doi: 10.1172/jci.insight.87748

14. Yang X, Wang X, Liu D, Yu L, Xue B, Shi H. Epigenetic regulation of macrophage polarization by DNA methyltransferase 3b. *Mol Endocrinol* (2014) 28(4):565–74. doi: 10.1210/me.2013-1293

15. Catalán J, Rydman E, Aimonen K, Hannukainen K-S, Suhonen S, Vanhala E, et al. Genotoxic and inflammatory effects of nanofibrillated cellulose in murine lungs. *Mutagenesis* (2017) 32(1):23–31. doi: 10.1093/mutage/gew035

16. Hadrup N, Knudsen KB, Berthing T, Wolff H, Bengtson S, Kofoed C, et al. Pulmonary effects of nanofibrillated celluloses in mice suggest that carboxylation lowers the inflammatory and acute phase responses. *Environ Toxicol Pharmacol* (2019) 66:116–25. doi: 10.1016/j.etap.2019.01.003

17. Ilves M, Vilske S, Aimonen K, Lindberg HK, Pesonen S, Wedin I, et al. Nanofibrillated cellulose causes acute pulmonary inflammation that subsides within a month. *Nanotoxicology* (2018) 12(7):729–746. doi: 10.1080/17435390.2018.1472312

18. Park E-J, Khaliullin TO, Shurin MR, Kisin ER, Yanamala N, Fadeel B, et al. Fibrous nanocellulose, crystalline nanocellulose, carbon nanotubes, and crocidolite asbestos elicit disparate immune responses upon pharyngeal aspiration in mice. *J Immunotoxicol* (2018) 15(1):12–23. doi: 10.1080/1547691X.2017.1414339

19. Shvedova AA, Kisin ER, Yanamala N, Farcas MT, Menas AL, Williams A, et al. Gender differences in murine pulmonary responses elicited by cellulose nanocrystals. *Part Fibre Toxicol* (2016) 13(1):28. doi: 10.1186/s12989-016-0140-x

20. Yanamala N, Farcas MT, Hatfield MK, Kisin ER, Kagan VE, Geraci CL, et al. *In vivo* evaluation of the pulmonary toxicity of cellulose nanocrystals: A renewable and sustainable nanomaterial of the future. *ACS Sustain Chem Eng* (2014) 2(7):1691–8. doi: 10.1021/sc500153k

21. Song LY, Wu YZ, Pei XX, Li R, Chen HT, Sun XZ. Pulmonary toxicity and rna sequencing analyses of mouse in response to exposure to cellulose nanofibrils. *Inhal Toxicol* (2020) 32(9-10):388–401. doi: 10.1080/08958378.2020.1831112

22. Catalán J, Ilves M, Järventaus H, Hannukainen K-S, Kontturi E, Vanhala E, et al. Genotoxic and immunotoxic effects of cellulose nanocrystals in vitro. *Environ Mol Mutagen* (2015) 56(2):171–82. doi: 10.1002/em.21913

23. Lopes VR, Sanchez-Martinez C, Strømme M, Ferraz N. *In vitro* biological responses to nanofibrillated cellulose by human dermal, lung and immune cells: Surface chemistry aspect. *Part Fibre Toxicol* (2017) 14:1. doi: 10.1186/s12989-016-0182-0

24. Menas AL, Yanamala N, Farcas MT, Russo M, Friend S, Fournier PM, et al. Fibrillar vs crystalline nanocellulose pulmonary epithelial cell responses: Cytotoxicity or inflammation? *Chemosphere* (2017) 171:671–80. doi: 10.1016/j.chemosphere.2016.12.105

25. Yanamala N, Kisin ER, Menas AL, Farcas MT, Khaliullin TO, Vogel UB, et al. *In vitro* toxicity evaluation of lignin-(Un)Coated cellulose based nanomaterials on human A549 and thp-1 cells. *Biomacromolecules* (2016) 17(11):3464–73. doi: 10.1021/acs.biomac.6b00756

26. Bhattacharya K, Kiliç G, Costa PM, Fadeel B. Cytotoxicity screening and cytokine profiling of nineteen nanomaterials enables hazard ranking and grouping based on inflammogenic potential. *Nanotoxicology* (2017) 11(6):809–26. doi: 10.1080/17435390.2017.1363309

27. Samulin Erdem J, Alswady-Hoff M, Ervik TK, Skare Ø, Ellingsen DG, Zienolddiny S. Cellulose nanocrystals modulate alveolar macrophage phenotype and phagocytic function. *Biomaterials* (2019) 203:31–42. doi: 10.1016/j.biomaterials.2019.02.025

28. Aimonen K, Hartikainen M, Imani M, Suhonen S, Vales G, Moreno C, et al. Effect of surface modification on the pulmonary and systemic toxicity of cellulose nanofibrils. *Biomacromolecules* (2022) 23(7):2752–66. doi: 10.1021/acs.biomac.2c00072

29. Park E-J, Roh J, Kim S-N, M-s K, Han Y-A, Kim Y, et al. A single intratracheal instillation of single-walled carbon nanotubes induced early lung fibrosis and subchronic tissue damage in mice. *Arch Toxicol* (2011) 85(9):1121–31. doi: 10.1007/s00204-011-0655-8

30. Dong J, Ma Q. *In vivo* activation of a T helper 2-driven innate immune response in lung fibrosis induced by multi-walled carbon nanotubes. *Arch Toxicol* (2016) 90(9):2231–48. doi: 10.1007/s00204-016-1711-1

31. Park EJ, Cho WS, Jeong J, Yi J, Choi K, Park K. Pro-inflammatory and potential allergic responses resulting from b cell activation in mice treated with multi-walled carbon nanotubes by intratracheal instillation. *Toxicology* (2009) 259(3):113–21. doi: 10.1016/j.tox.2009.02.009

32. Rydman EM, Ilves M, Koivisto AJ, Kinaret PA, Fortino V, Savinko TS, et al. Inhalation of rod-like carbon nanotubes causes unconventional allergic airway inflammation. *Part Fibre Toxicol* (2014) 11:48. doi: 10.1186/s12989-014-0048-2

33. Labib S, Williams A, Yauk CL, Nikota JK, Wallin H, Vogel U, et al. Nano-risk science: Application of toxicogenomics in an adverse outcome pathway framework for risk assessment of multi-walled carbon nanotubes. *Part Fibre Toxicol* (2016) 13:15. doi: 10.1186/s12989-016-0125-9

34. Fatkhutdinova LM, Khaliullin TO, Vasil'yeva OL, Zalyalov RR, Mustafin IG, Kisin ER, et al. Fibrosis biomarkers in workers exposed to mwcnts. *Toxicol Appl Pharmacol* (2016) 299:125–31. doi: 10.1016/j.taap.2016.02.016

35. Dong J, Ma Q. Macrophage polarization and activation at the interface of multi-walled carbon nanotube-induced pulmonary inflammation and fibrosis. *Nanotoxicology* (2018) 12(2):153–68. doi: 10.1080/17435390.2018.1425501

36. Lim CS, Porter DW, Orandle MS, Green BJ, Barnes MA, Croston TL, et al. Resolution of pulmonary inflammation induced by carbon nanotubes and fullerenes in mice: Role of macrophage polarization. *Front Immunol* (2020) 11:1186. doi: 10.3389/fimmu.2020.01186

37. Beyeler S, Steiner S, Wotzkow C, Tschanz SA, Adhanom Sengal A, Wick P, et al. Multi-walled carbon nanotubes activate and shift polarization of pulmonary macrophages and dendritic cells in an in vivo model of chronic obstructive lung disease. *Nanotoxicology* (2020) 14(1):77–96. doi: 10.1080/17435390.2019.1663954

38. Dong J, Ma Q. Type 2 immune mechanisms in carbon nanotube-induced lung fibrosis. *Front Immunol* (2018) 9:1120. doi: 10.3389/fimmu.2018.01120

39. Schneider CA, Rasband WS, Eliceiri KW. Nih image to imagej: 25 years of image analysis. *Nat Methods* (2012) 9(7):671–5. doi: 10.1038/nmeth.2089

40. Longair MH, Baker DA, Armstrong JD. Simple neurite tracer: Open source software for reconstruction, visualization and analysis of neuronal processes. *Bioinformatics* (2011) 27(17):2453–4. doi: 10.1093/bioinformatics/btr390

41. Schliwa M, van Blerkom J. Structural interaction of cytoskeletal components. *J Cell Biol* (1981) 90(1):222–35. doi: 10.1083/jcb.90.1.222

42. Knudsen KB, Kofoed C, Espersen R, Højgaard C, Winther JR, Willemoës M, et al. Visualization of nanofibrillar cellulose in biological tissues using a biotinylated carbohydrate binding module of β-1,4-Glycanase. *Chem Res Toxicol* (2015) 28(8):1627–35. doi: 10.1021/acs.chemrestox.5b00271

43. Andrés-León E, Núñez-Torres R, Rojas AM. Miarma-seq: A comprehensive tool for mirna, mrna and circrna analysis. *Sci Rep* (2016) 6(1):25749. doi: 10.1038/srep25749

44. Kozomara A, Birgaoanu M, Griffiths-Jones S. Mirbase: From microrna sequences to function. *Nucleic Acids Res* (2018) 47(D1):D155–D62. doi: 10.1093/nar/gky1141

45. Love MI, Huber W, Anders S. Moderated estimation of fold change and dispersion for rna-seq data with Deseq2. *Genome Biol* (2014) 15(12):550. doi: 10.1186/s13059-014-0550-8

46. Blighe K, Sharmila R, Lewis M. *Enhancedvolcano: Publication-ready volcano plots with enhanced colouring and labeling* (2022). Available at: https://github.com/kevinblighe/EnhancedVolcano.

47. Chen Y, Wang X. Mirdb: An online database for prediction of functional microrna targets. *Nucleic Acids Res* (2019) 48(D1):D127–D31. doi: 10.1093/nar/gkz757

48. Liu W, Wang X. Prediction of functional microrna targets by integrative modeling of microrna binding and target expression data. *Genome Biol* (2019) 20(1):18. doi: 10.1186/s13059-019-1629-z

49. Mi H, Thomas P. Panther pathway: An ontology-based pathway database coupled with data analysis tools. *Methods Mol Biol* (2009) 563:123–40. doi: 10.1007/978-1-60761-175-2_7

50. Taoka M, Nobe Y, Yamaki Y, Sato K, Ishikawa H, Izumikawa K, et al. Landscape of the complete rna chemical modifications in the human 80s ribosome. *Nucleic Acids Res* (2018) 46(18):9289–98. doi: 10.1093/nar/gky811

51. Alswady-Hoff M, Erdem JS, Aleksandersen M, Anmarkrud KH, Skare Ø, Lin F-C, et al. Multiwalled carbon nanotubes induce fibrosis and telomere length alterations. *Int J Mol Sci* (2022) 23(11):6005. doi: 10.3390/ijms23116005

52. Arnoldussen YJ, Skaug V, Aleksandersen M, Ropstad E, Anmarkrud KH, Einarsdottir E, et al. Inflammation in the pleural cavity following injection of multi-walled carbon nanotubes is dependent on their characteristics and the presence of il-1 genes. *Nanotoxicology* (2018) 12(6):522–38. doi: 10.1080/17435390.2018.1465139

53. Barbarino M, Giordano A. Assessment of the carcinogenicity of carbon nanotubes in the respiratory system. *Cancers* (2021) 13(6):1318. doi: 10.3390/cancers13061318

54. Sargent LM, Porter DW, Staska LM, Hubbs AF, Lowry DT, Battelli L, et al. Promotion of lung adenocarcinoma following inhalation exposure to multi-walled carbon nanotubes. *Part Fibre Toxicol* (2014) 11(1):3. doi: 10.1186/1743-8977-11-3

55. Aimonen K, Imani M, Hartikainen M, Suhonen S, Vanhala E, Moreno C, et al. Surface functionalization and size modulate the formation of reactive oxygen species and genotoxic effects of cellulose nanofibrils. *Part Fibre Toxicol* (2022) 19(1):19. doi: 10.1186/s12989-022-00460-3

56. Čolić M, Tomić S, Bekić M. Immunological aspects of nanocellulose. *Immunol Lett* (2020) 222:80–9. doi: 10.1016/j.imlet.2020.04.004

57. Li J, Wang X, Chang CH, Jiang J, Liu Q, Liu X, et al. Nanocellulose length determines the differential cytotoxic effects and inflammatory responses in macrophages and hepatocytes. *Small* (2021) 17(38):2102545. doi: 10.1002/smll.202102545

58. Donaldson K, Murphy FA, Duffin R, Poland CA. Asbestos, carbon nanotubes and the pleural mesothelium: A review of the hypothesis regarding the role of long fibre retention in the parietal pleura, inflammation and mesothelioma. *Part Fibre Toxicol* (2010) 7(1):5. doi: 10.1186/1743-8977-7-5

59. Kasai T, Umeda Y, Ohnishi M, Mine T, Kondo H, Takeuchi T, et al. Lung carcinogenicity of inhaled multi-walled carbon nanotube in rats. *Part Fibre Toxicol* (2016) 13(1):53. doi: 10.1186/s12989-016-0164-2

60. Pauluhn J. Subchronic 13-week inhalation exposure of rats to multiwalled carbon nanotubes: Toxic effects are determined by density of agglomerate structures, not fibrillar structures. *Toxicol Sci* (2009) 113(1):226–42. doi: 10.1093/toxsci/kfp247

61. Poulsen SS, Jackson P, Kling K, Knudsen KB, Skaug V, Kyjovska ZO, et al. Multi-walled carbon nanotube physicochemical properties predict pulmonary inflammation and genotoxicity. *Nanotoxicology* (2016) 10(9):1263–75. doi: 10.1080/17435390.2016.1202351

62. Saleh DM, Alexander WT, Numano T, Ahmed OHM, Gunasekaran S, Alexander DB, et al. Comparative carcinogenicity study of a thick, straight-type and a thin, tangled-type multi-walled carbon nanotube administered by intra-tracheal instillation in the rat. *Part Fibre Toxicol* (2020) 17(1):48. doi: 10.1186/s12989-020-00382-y

63. Suzui M, Futakuchi M, Fukamachi K, Numano T, Abdelgied M, Takahashi S, et al. Multiwalled carbon nanotubes intratracheally instilled into the rat lung induce development of pleural malignant mesothelioma and lung tumors. *Cancer Sci* (2016) 107(7):924–35. doi: 10.1111/cas.12954

64. Xu J, Alexander DB, Futakuchi M, Numano T, Fukamachi K, Suzui M, et al. Size- and shape-dependent pleural translocation, deposition, fibrogenesis, and mesothelial proliferation by multiwalled carbon nanotubes. *Cancer Sci* (2014) 105(7):763–9. doi: 10.1111/cas.12437

65. Di Ianni E, Erdem JS, Møller P, Sahlgren NM, Poulsen SS, Knudsen KB, et al. *In vitro*-in vivo correlations of pulmonary inflammogenicity and genotoxicity of mwcnt. *Part Fibre Toxicol* (2021) 18(1):25. doi: 10.1186/s12989-021-00413-2

66. Købler C, Poulsen SS, Saber AT, Jacobsen NR, Wallin H, Yauk CL, et al. Time-dependent subcellular distribution and effects of carbon nanotubes in lungs of mice. *PloS One* (2015) 10(1):e0116481. doi: 10.1371/journal.pone.0116481

67. Murphy FA, Schinwald A, Poland CA, Donaldson K. The mechanism of pleural inflammation by long carbon nanotubes: Interaction of long fibres with macrophages stimulates them to amplify pro-inflammatory responses in mesothelial cells. *Part Fibre Toxicol* (2012) 9:8–. doi: 10.1186/1743-8977-9-8

68. Nagai H, Okazaki Y, Chew SH, Misawa N, Yamashita Y, Akatsuka S, et al. Diameter and rigidity of multiwalled carbon nanotubes are critical factors in mesothelial injury and carcinogenesis. *Proc Natl Acad Sci* (2011) 108(49):E1330–E8. doi: 10.1073/pnas.1110013108

69. Murphy F, Jacobsen NR, Di Ianni E, Johnston H, Braakhuis H, Peijnenburg W, et al. Grouping mwcnts based on their similar potential to cause pulmonary hazard after inhalation: A case-study. *Part Fibre Toxicol* (2022) 19(1):50. doi: 10.1186/s12989-022-00487-6

70. Hamilton RFJr., Xiang C, Li M, Ka I, Yang F, Ma D, et al. Purification and sidewall functionalization of multiwalled carbon nanotubes and resulting bioactivity in two macrophage models. *Inhal Toxicol* (2013) 25(4):199–210. doi: 10.3109/08958378.2013.775197

71. Ishii M, Wen H, Corsa CA, Liu T, Coelho AL, Allen RM, et al. Epigenetic regulation of the alternatively activated macrophage phenotype. *Blood* (2009) 114 (15):3244–54. doi: 10.1182/blood-2009-04-217620

72. Kittan NA, Allen RM, Dhaliwal A, Cavassani KA, Schaller M, Gallagher KA, et al. Cytokine induced phenotypic and epigenetic signatures are key to establishing specific macrophage phenotypes. *PloS One* (2013) 8(10):e78045. doi: 10.1371/journal.pone.0078045

73. Mullican SE, Gaddis CA, Alenghat T, Nair MG, Giacomin PR, Everett LJ, et al. Histone deacetylase 3 is an epigenomic brake in macrophage alternative activation. *Genes Dev* (2011) 25(23):2480–8. doi: 10.1101/gad.175950.111

74. Satoh T, Takeuchi O, Vandenbon A, Yasuda K, Tanaka Y, Kumagai Y, et al. The Jmjd3-Irf4 axis regulates M2 macrophage polarization and host responses against helminth infection. *Nat Immunol* (2010) 11(10):936–44. doi: 10.1038/ni.1920

75. Kobatake K, Ikeda KI, Nakata Y, Yamasaki N, Ueda T, Kanai A, et al. Kdm6a deficiency activates inflammatory pathways, promotes M2 macrophage polarization, and causes bladder cancer in cooperation with P53 dysfunction. *Clin Cancer Res* (2020) 26 (8):2065–79. doi: 10.1158/1078-0432.Ccr-19-2230

76. Stender JD, Pascual G, Liu W, Kaikkonen MU, Do K, Spann NJ, et al. Control of proinflammatory gene programs by regulated trimethylation and demethylation of histone H4k20. *Mol Cell* (2012) 48(1):28–38. doi: 10.1016/j.molcel.2012.07.020

77. Xu G, Liu G, Xiong S, Liu H, Chen X, Zheng B. The histone methyltransferase Smyd2 is a negative regulator of macrophage activation by suppressing interleukin 6 (Il-6) and tumor necrosis factor α (Tnf-α) production. *J Biol Chem* (2015) 290(9):5414–23. doi: 10.1074/jbc.M114.610345

78. Yang H, Sun Y, Li Q, Jin F, Dai Y. Diverse epigenetic regulations of macrophages in atherosclerosis. *Front Cardiovasc Med* (2022) 9:868788. doi: 10.3389/fcvm.2022.868788

79. Cao Q, Rong S, Repa JJ, St Clair R, Parks JS, Mishra N. Histone deacetylase 9 represses cholesterol efflux and alternatively activated macrophages in atherosclerosis development. *Arterioscler Thromb Vasc Biol* (2014) 34(9):1871–9. doi: 10.1161/atvbaha.114.303393

80. Liu Y, Du M, Lin HY. Histone deacetylase 9 deficiency exaggerates uterine M2 macrophage polarization. *J Cell Mol Med* (2021) 25(16):7690–708. doi: 10.1111/jcmm.16616

81. Luan B, Goodarzi MO, Phillips NG, Guo X, Chen YD, Yao J, et al. Leptin-mediated increases in catecholamine signaling reduce adipose tissue inflammation *Via* activation of macrophage Hdac4. *Cell Metab* (2014) 19(6):1058–65. doi: 10.1016/j.cmet.2014.03.024

82. Schug TT, Xu Q, Gao H, Peres-da-Silva A, Draper DW, Fessler MB, et al. Myeloid deletion of Sirt1 induces inflammatory signaling in response to environmental stress. *Mol Cell Biol* (2010) 30(19):4712–21. doi: 10.1128/mcb.00657-10

83. Yoshizaki T, Schenk S, Imamura T, Babendure JL, Sonoda N, Bae EJ, et al. Sirt1 inhibits inflammatory pathways in macrophages and modulates insulin sensitivity. *Am J Physiol Endocrinol Metab* (2010) 298(3):E419–28. doi: 10.1152/ajpendo.00417.2009

84. Pogribna M, Hammons G. Epigenetic effects of nanomaterials and nanoparticles. *J Nanobiotechnol* (2021) 19(1):2. doi: 10.1186/s12951-020-00740-0

85. Zhang W, Liu S, Han D, He Z. Engineered nanoparticle-induced epigenetic changes: An important consideration in nanomedicine. *Acta Biomater* (2020) 117:93–107. doi: 10.1016/j.actbio.2020.09.034

86. Brown TA, Lee JW, Holian A, Porter V, Fredriksen H, Kim M, et al. Alterations in DNA methylation corresponding with lung inflammation and as a biomarker for disease development after mwcnt exposure. *Nanotoxicology* (2016) 10(4):453–61. doi: 10.3109/17435390.2015.1078852

87. Cole E, Ray JL, Bolten S, Hamilton RFJr., Shaw PK, Postma B, et al. Multiwalled carbon nanotubes of varying size lead to DNA methylation changes that correspond to lung inflammation and injury in a mouse model. *Chem Res Toxicol* (2019) 32(8):1545–53. doi: 10.1021/acs.chemrestox.9b00075

88. Scala G, Delaval MN, Mukherjee SP, Federico A, Khaliullin TO, Yanamala N, et al. Multi-walled carbon nanotubes elicit concordant changes in DNA methylation and gene expression following long-term pulmonary exposure in mice. *Carbon* (2021) 178:563–72. doi: 10.1016/j.carbon.2021.03.045

89. Ghosh M, Öner D, Poels K, Tabish AM, Vlaanderen J, Pronk A, et al. Changes in DNA methylation induced by multi-walled carbon nanotube exposure in the workplace. *Nanotoxicology* (2017) 11(9-10):1195–210. doi: 10.1080/17435390.2017.1406169

90. Öner D, Moisse M, Ghosh M, Duca RC, Poels K, Luyts K, et al. Epigenetic effects of carbon nanotubes in human monocytic cells. *Mutagenesis* (2017) 32(1):181–91. doi: 10.1093/mutage/gew053

91. Li J, Zeng X, Wang W. Mir-122-5p downregulation attenuates lipopolysaccharide-induced acute lung injury by targeting Il1rn. *Exp Ther Med* (2021) 22(5):1278. doi: 10.3892/etm.2021.10713

92. Wang H, Zhang C, Zhang C, Wang Y, Zhai K, Tong Z. Microrna-122-5p regulates coagulation and inflammation through Masp1 and ho-1 genes. *Infect Genet Evol* (2022) 100:105268. doi: 10.1016/j.meegid.2022.105268

93. Zhao Z, Zhong L, Li P, He K, Qiu C, Zhao L, et al. Cholesterol impairs hepatocyte lysosomal function causing M1 polarization of macrophages *Via* exosomal mir-122-5p. *Exp Cell Res* (2020) 387(1):111738. doi: 10.1016/j.yexcr.2019.111738

94. Servais FA, Kirchmeyer M, Hamdorf M, Minoungou NWE, Rose-John S, Kreis S, et al. Modulation of the il-6-Signaling pathway in liver cells by mirnas targeting Gp130, Jak1, and/or Stat3. *Mol Ther Nucleic Acids* (2019) 16:419–33. doi: 10.1016/j.omtn.2019.03.007

95. Talari M, Kapadia B, Kain V, Seshadri S, Prajapati B, Rajput P, et al. Microrna-16 modulates macrophage polarization leading to improved insulin sensitivity in myoblasts. *Biochimie* (2015) 119:16–26. doi: 10.1016/j.biochi.2015.10.004

96. Graff JW, Dickson AM, Clay G, McCaffrey AP, Wilson ME. Identifying functional micrornas in macrophages with polarized phenotypes. *J Biol Chem* (2012) 287(26):21816–25. doi: 10.1074/jbc.M111.327031

97. Lu L, McCurdy S, Huang S, Zhu X, Peplowska K, Tiirikainen M, et al. Time series mirna-mrna integrated analysis reveals critical mirnas and targets in macrophage polarization. *Sci Rep* (2016) 6(1):37446. doi: 10.1038/srep37446

98. Yao F, Yu Y, Feng L, Li J, Zhang M, Lan X, et al. Adipogenic mir-27a in adipose tissue upregulates macrophage activation *Via* inhibiting pparγ of insulin resistance induced by high-fat diet-associated obesity. *Exp Cell Res* (2017) 355(2):105–12. doi: 10.1016/j.yexcr.2017.03.060

99. Sui J, Fu Y, Zhang Y, Ma S, Yin L, Pu Y, et al. Molecular mechanism for mir-350 in regulating of titanium dioxide nanoparticles in macrophage Raw264.7 cells. *Chem Biol Interact* (2018) 280:77–85. doi: 10.1016/j.cbi.2017.12.020

100. Zhang Y, Zhang M, Li X, Tang Z, Wang X, Zhong M, et al. Silencing microrna-155 attenuates cardiac injury and dysfunction in viral myocarditis *Via* promotion of M2 phenotype polarization of macrophages. *Sci Rep* (2016) 6(1):22613. doi: 10.1038/srep22613

101. O'Connell RM, Taganov KD, Boldin MP, Cheng G, Baltimore D. Microrna-155 is induced during the macrophage inflammatory response. *Proc Natl Acad Sci U.S.A.* (2007) 104(5):1604–9. doi: 10.1073/pnas.0610731104

102. Martinez-Nunez RT, Louafi F, Sanchez-Elsner T. The interleukin 13 (Il-13) pathway in human macrophages is modulated by microrna-155 *Via* direct targeting of interleukin 13 receptor Alpha1 (Il13ralpha1). *J Biol Chem* (2011) 286(3):1786–94. doi: 10.1074/jbc.M110.169367

103. He M, Xu Z, Ding T, Kuang DM, Zheng L. Microrna-155 regulates inflammatory cytokine production in tumor-associated macrophages *Via* targeting C/Ebpbeta. *Cell Mol Immunol* (2009) 6(5):343–52. doi: 10.1038/cmi.2009.45

104. Ballesteros S, Vales G, Velázquez A, Pastor S, Alaraby M, Marcos R, et al. Micrornas as a suitable biomarker to detect the effects of long-term exposures to nanomaterials. *Stud Tio2np Mwcnt. Nanomater* (2021) 11(12):3458. doi: 10.3390/nano11123458

105. Hu M, Palić D. Role of micrornas in regulation of DNA damage in monocytes exposed to polystyrene and Tio2 nanoparticles. *Toxicol Rep* (2020) 7:743–51. doi: 10.1016/j.toxrep.2020.05.007

106. Monteleone NJ, Lutz CS. Mir-708 negatively regulates Tnfα/Il-1β signaling by suppressing nf-κb and arachidonic acid pathways. *Mediators Inflammation* (2021) 2021:5595520. doi: 10.1155/2021/5595520

107. Tserel L, Runnel T, Kisand K, Pihlap M, Bakhoff L, Kolde R, et al. Microrna expression profiles of human blood monocyte-derived dendritic cells and macrophages reveal mir-511 as putative positive regulator of toll-like receptor 4. *J Biol Chem* (2011) 286 (30):26487–95. doi: 10.1074/jbc.M110.213561

108. Awuah D, Alobaid M, Latif A, Salazar F, Emes RD, Ghaemmaghami AM. The cross-talk between mir-511-3p and c-type lectin receptors on dendritic cells affects dendritic cell function. *J Immunol* (2019) 203(1):148–157. doi: 10.4049/jimmunol.1801108

109. Awuah D, Ruisinger A, Alobaid M, Mbadugha C, Ghaemmaghami AM. Microrna-511-3p mediated modulation of the peroxisome proliferator-activated receptor gamma (Pparγ) controls lps-induced inflammatory responses in human monocyte derived dcs. *bioRxiv* (2020), 369967. doi: 10.1101/2020.11.05.369967. 2020.11.05.

110. Zhou Y, Do DC, Ishmael FT, Squadrito ML, Tang HM, Tang HL, et al. Mannose receptor modulates macrophage polarization and allergic inflammation through mir-511-3p. *J Allergy Clin Immunol* (2018) 141(1):350–64.e8. doi: 10.1016/j.jaci.2017.04.049

111. Cobos Jiménez V, Bradley EJ, Willemsen AM, van Kampen AH, Baas F, Kootstra NA. Next-generation sequencing of micrornas uncovers expression signatures in polarized macrophages. *Physiol Genomics* (2014) 46(3):91–103. doi: 10.1152/physiolgenomics.00140.2013

112. Han X, Liu H, Zhang Z, Yang W, Wu C, Liu X, et al. Epitranscriptomic 5-methylcytosine profile in Pm2.5-induced mouse pulmonary fibrosis. *Genom Proteom Bioinform* (2020) 18(1):41–51. doi: 10.1016/j.gpb.2019.11.005

113. Kupsco A, Gonzalez G, Baker BH, Knox JM, Zheng Y, Wang S, et al. Associations of smoking and air pollution with peripheral blood rna N6-methyladenosine in the

Beijing truck driver air pollution study. *Environ Int* (2020) 144:106021. doi: 10.1016/j.envint.2020.106021

114. Du J, Liao W, Liu W, Deb DK, He L, Hsu PJ, et al. N(6)-adenosine methylation of Socs1 mrna is required to sustain the negative feedback control of macrophage activation. *Dev Cell* (2020) 55(6):737–53.e7. doi: 10.1016/j.devcel.2020.10.023

115. Tong J, Wang X, Liu Y, Ren X, Wang A, Chen Z, et al. Pooled crispr screening identifies M6a as a positive regulator of macrophage activation. *Sci Adv* (2021) 7(18): eabd4742. doi: 10.1126/sciadv.abd4742

116. Yu R, Li Q, Feng Z, Cai L, Xu Q. M6a reader Ythdf2 regulates lps-induced inflammatory response. *Int J Mol Sci* (2019) 20(6):1323. doi: 10.3390/ijms20061323

frontiers | Frontiers in Immunology

TYPE Original Research
PUBLISHED 01 February 2023
DOI 10.3389/fimmu.2023.1090637

OPEN ACCESS

EDITED BY
Chao Yang,
Zhejiang University, China

REVIEWED BY
Chongming Jiang,
Baylor College of Medicine, United States
Siyang Hao,
Bristol Myers Squibb, United States
Ning Zhang,
Zhejiang University, China

*CORRESPONDENCE
Ming Yan
yanming_spine@163.com
Bo Gao
gaobofmmu@hotmail.com
Zhuojing Luo
Zjluo@fmmu.edu.cn

†These authors have contributed equally to this work and share first authorship

SPECIALTY SECTION
This article was submitted to Inflammation, a section of the journal Frontiers in Immunology

RECEIVED 05 November 2022
ACCEPTED 12 January 2023
PUBLISHED 01 February 2023

CITATION
Li W, Zhao Y, Wang Y, He Z, Zhang L, Yuan B, Li C, Luo Z, Gao B and Yan M (2023) Deciphering the sequential changes of monocytes/macrophages in the progression of IDD with longitudinal approach using single-cell transcriptome. *Front. Immunol.* 14:1090637. doi: 10.3389/fimmu.2023.1090637

Deciphering the sequential changes of monocytes/macrophages in the progression of IDD with longitudinal approach using single-cell transcriptome

Weihang Li[1†], Yingjing Zhao[2†], Yongchun Wang[3†], Zhijian He[4], Linyuan Zhang[5], Bin Yuan[6], Chengfei Li[3], Zhuojing Luo[1*], Bo Gao[1*] and Ming Yan[1*]

[1]Department of Orthopedic Surgery, Xijing Hospital, Air Force Medical University, Xi'an, China, [2]Department of Critical Care Medicine, Nanjing First Hospital, Nanjing Medical University, Nanjing, Jiangsu, China, [3]Department of Aerospace Medical Training, School of Aerospace Medicine, Air Force Medical University, Xi'an, China, [4]Department of Sports Teaching and Research, Lanzhou University, Lanzhou, China, [5]Department of Nursing, Air Force Medical University, Xi'an, China, [6]Department of Spine Surgery, Daxing Hospital, Xi'an, Shaanxi, China

Intervertebral disk degeneration (IDD) is a chronic inflammatory disease with intricate connections between immune infiltration and oxidative stress (OS). Complex cell niches exist in degenerative intervertebral disk (IVD) and interact with each other and regulate the disk homeostasis together. However, few studies have used longitudinal approach to describe the immune response of IDD progression. Here, we conducted conjoint analysis of bulk-RNA sequencing and single-cell sequencing, together with a series of techniques like weighted gene co-expression network analysis (WGCNA), immune infiltration analysis, and differential analysis, to systematically decipher the difference in OS-related functions of different cell populations within degenerative IVD tissues, and further depicted the longitudinal alterations of immune cells, especially monocytes/macrophages in the progression of IDD. The OS-related genes CYP1A1, MMP1, CCND1, and NQO1 are highly expressed and might be diagnostic biomarkers for the progression of IDD. Further landscape of IVD microenvironment showed distinct changes in cell proportions and characteristics at late degeneration compared to early degeneration of IDD. Monocytes/macrophages were classified into five distinct subpopulations with different roles. The trajectory lineage analysis revealed transcriptome alterations from effector monocytes/macrophages and regulatory macrophages to other subtypes during the evolution process and identified monocytes/macrophage subpopulations that had rapidly experienced the activation of inflammatory or anti-inflammatory responses. This study further proposed that personalized therapeutic strategies are needed to be formulated based on specific monocyte/macrophage subtypes and degenerative stages of IDD.

KEYWORDS

intervertebral disk degeneration, monocytes/macrophage subtypes evolution, oxidative stress, trajectory lineage analysis, single-cell transcriptome landscape, longitudinal approach

Introduction

Low back pain (LBP) has continuously been the major cause of disability in human adults, affecting almost 80% of the population worldwide, leading to heavy socioeconomic burden (1, 2). There are lots of triggers of LBP, and intervertebral disk degeneration (IDD) is considered as one of the common reasons (3). IDD progression is a commonly seen musculoskeletal disorder, accompanied by gradual structure alteration with several metabolic homeostasis process, spinal stenosis, disk herniation, lumbar spondylolisthesis, spinal segmental instability, nerve root compression, etc. (4, 5). Consequently, a better understanding of the potential pathological mechanisms has continuously been a research hotspot, which may help to promote the knowledge of IDD progression and finally find novel biological treatments.

Increasing evidence has reported that despite multifactorial etiology like loading changes, smoking, senescence, and poor nutrient supply, genetic factor is the essential risk of IDD, which accounts for more than 70% of the risks (2). Meanwhile, as the largest avascular organ within body, IVD consists of the middle nucleus pulposus (NP), surrounding annulus fibrosis (AF), and cartilage endplate (CEP) on the inferior and superior sides. This special structure makes it an immune-privilege organ and avoids infiltration by immune and inflammatory factors (6, 7). When IDD occurs, the blood vessels infiltrate and inflammatory factors aggregate at the IVD tissue, destroying the homeostasis of IVD (8).

Redox homeostasis is a pivotal process for the physiological maintenance of many cellular activities; the dysregulation of redox homeostasis is tightly related to diversity pathological conditions that influence human health, including different kinds of neoplasms and degenerative skeletal disease (9–13). Oxidative stress (OS) is regarded as the imbalanced state of redox homeostasis with higher reactive oxygen species (ROS) production; OS also plays essential roles in the progression of IDD (12, 14). It has been elucidated that OS could induce autophagy, apoptosis, and calcification of CEP chondrocytes (15–17). Existing studies also reported that the excessive accumulation of ROS would cause OS reaction and injure the normal functions and integrity of NP cells, thereby triggering inflammatory reactions and promoting IDD progression (18, 19).

Recent advanced techniques in single-cell RNA sequencing (scRNA-seq) have provided powerful algorithm for exploring and analyzing the interactive roles and functional heterogeneity of different cell populations (20–22). These methods have been widely performed in different fields like transcriptomic atlas construction and novel populations identification, which have revolutionized studies of gene expression (23, 24). Existing studies have already depicted the transcriptomic atlas for the IVD tissue based on scRNA-seq, which discovered and defined different or new cell subpopulations, providing comprehensive interpretations and novel insights in cellular heterogeneity of IVD, including physiological and degenerative states (25–29).

Immune cells, especially monocytes/macrophages, are reported to produce ROS and promote the onset of OS, causing severe metabolic disorders and even cell death; ROS could also activate transcriptional factors and pro-inflammatory factors and further accelerate inflammation reactions (30). Consequently, identifying functional OS-related immune cells can increase our understanding of OS mechanisms and provide novel antioxidative avenues in the treatment of IDD. However, due to the intrinsic limitations that most scRNA studies have in providing cell atlas in a specific tissue without lucubrating the cell subtypes, the current available transcriptomic analyses of immune cells are from cross-sectional studies, with rare longitudinal description of the immune response. This study performed conjoint analysis of bulk RNA-seq and scRNA-seq to analyze OS functions in different cell populations from early to late degenerative IDD patients. This is the first such landscape to depict the longitudinal alterations of NP cells and monocytes/macrophages heterogeneity in the progression of IDD. Importantly, we revealed the evolution process of monocytes/macrophages, identified different subtypes based on their unique gene expression patterns, and described their temporal transcriptome changes from early to late degenerative IVD tissue. Intriguingly, the highly dynamic populations, effector monocyte/macrophages, and regulatory macrophages were mainly enriched in early degenerative stage, while the homeostatic and activated tissue macrophages were more like terminal differentiated populations that increased during disease progression, which could provide reference for monocyte/macrophage targeted therapy at different stages of IDD.

Materials and methods

Data collection and preprocessing

Microarray datasets were retrieved and downloaded from Gene Expression Omnibus (GEO, https://www.ncbi.nlm.nih.gov/geo/) database. Bulk RNA-seq data GSE70362 was obtained for OS functional analysis between different degenerative stages, which contained 48 IDD patients with Pfirrmann grade from I to V; grade <3 was considered as early degenerative, and grade ≥3 was late degenerative stage (31). GSE147383 was applied to evaluate OS functional levels and immune infiltration situation and construct weighted gene co-expression network analysis (WGCNA) of degenerative IVD tissues (32). Then, GSE165722 series data were used for scRNA-seq analysis to analyze the OS functional levels between different cell populations and depict transcriptome atlas during different degenerative stages, which included eight patients with degenerative stages from II to V. Only NP tissues were harvested, following a standard surgical protocol. No AF tissues and blood were contaminated the into NP tissue upon collection (25). This study included multiple datasets for analysis to avoid the bias from the same dataset and make the results more convincing.

Identification of differentially expressed OS genes

According to Pfirrmann grade, bulk RNA-seq data (GSE70362) totally contained 16 early degenerative samples and 32 late degenerative samples. This study divided patients into two groups and further screened differentially expressed genes (DEGs) with "limma" package (3.50.0) in R, followed by a cutoff threshold with adjusted p-value < 0.05 and |FC| (fold change) > 1.5, which was considered as statistically significant. To identify DEOSGs, we further

extracted 824 OS-associated protein domains from GeneCards database (https://www.genecards.org/) with a relevance score ≥ 7 (see in Supplementary Table S1); then, DEOSGs were screened by taking the intersection of DEGs and OS-related genes to generate a more accurate result, based on Venn plot analysis ("VennDiagram" package in R, 1.7.1).

Immune infiltration analysis

The proportions of the 22 types of immune cells in IVD tissues were estimated using "CIBERSORT" algorithm (33). The proportions and contents of immune cell members from mixed IVD tissues were assessed through gene expression profiles, followed by correlation heatmap and differential expression patterns between different groups. Immune infiltration analysis demands strict requirements on data; only high contents of estimated immune cells are appropriate for analysis. After evaluation of the immune cells components, GSE147383 possessed the highest quality, which was conducted for immune infiltration to analyze the potential existing immune cells, which contained eight samples.

Construction of weighted gene co-expression network and immune-related DEOSGs identification

The top 5,000 most variable genes were included for WGCNA ("WGCNA" package in R, 1.71) construction, based on their median absolute deviation (MAD) values according to official introduction (34). Hierarchical clustering analysis was performed to detect outliers of these tissues, and the soft threshold power (β) was calculated to build a scale-free network. Weighted gene co-expression network was constructed based on β-value; then, co-expression modules were identified according to the heterogeneity of different genes. The relationships between each module and differentially infiltrating immune cells were then calculated and visualized. As Li et al. described, the module with the highest correlation coefficient was considered as the candidate module, which was compared horizontally to discover the most essential genes targeting specific immune cell (35). The intersection of DEGs, OS-related genes, and genes in the interested module was considered as the most related genes (hub genes) for the progression of IDD.

Hub genes validation by principal component analysis and gene expression detection

Principal component analysis (PCA) was used to reduce the dimension of these hub genes from high dimension into three dimensions (PC1, PC2, and PC3), to observe the separating ability between early and late degenerative IVD tissues, based on "prcomp" and "princomp" functions in R. The results were visualized in three-dimensional coordinate system ("scatterplot3d," "ggplot2," and "rgl" packages in R, 3.3.5). Human primary NP cells were obtained from iCellbioscience (HUM-iCell-s012) and were maintained in Dulbecco's modified Eagle's medium (DMEM)/F12 (1:1) (DF12; Gibco, Grand Island, NY, United States) with 10 fetal bovine serum (FBS; Invitrogen, Carlsbad, CA, United States) and 1% antibiotics (penicillin/streptomycin) (Gibco) in an incubator at 5% CO_2 and 37°C (36, 37). Tert-butyl hydroperoxide (TBHP) was purchased from Sigma-Aldrich (St. Louis, MO, United States), to trigger oxidative stress and thus simulate high-ROS environment, which is a stable form of hydrogen peroxide and widely used as an *in vitro* model to induce extracellular matrix (ECM) degeneration and the apoptosis of NP cells (38). To establish the apoptosis and degenerative model of NP cells, complete culture media with different concentrations (0, 50, and 100 μM) of TBHP were added for 24 h (38). Then, the expression levels of those hub genes under different conditions of degenerative NP cells were detected by quantitative real-time PCR (qRT-PCR). The primers of corresponding genes were listed as follows (5–3′): CCND1, (F) GATGCCAACCTCCTCAACGA and (R) ACTTCTGTT CCTCGCAGACC; CYP1A1, (F) CAAGGGGCGTTGTGTCTTTG and (R) GTCGATAGCACCATCAGGGG; MMP1, (F) TG TGGTGTCTCACAGCTTCC and (R) CGCTTTTCAACTTGC CTCCC; and NQO1, (F) TTTGGAGTCCCTGCCATTCT and (R) TTGCAGAGAGTACATGGAGCC.

Single-cell RNA data integration and processing

The raw scRNA-seq data of NP tissues (Pfirrmann grade II–V) stages were retrieved and obtained (based on GSE165722). After the whole data were read and presented in R, filtering criteria were followed by rigorous procedure, and low-quality cells were removed as follows: cells had fewer than 200 expressed genes and mitochondria UMI counts rate >20%.

After quality control, we created Seurat objects from scRNA-seq data based on each tissue according to "Seurat" package in R (4.1.0) (39). Then, RPCA algorithm wrapped in "Seurat" package was applied to integrate the expression matrix of each tissue and correct batch effects among different tissues; "FindIntegrationAnchors" function was used to merge samples with common anchors among variables (dims = 1:30, k.anchors=10). Then, the integrated matrix was followed by cell normalization and scale. In brief, the top 2,000 highly variable features were analyzed after normalization, which were selected for downstream analysis. Then, PCA was constructed using "RunPCA" function based on the scaled data with the top 2,000 highly variable genes, and the top 30 principles were further chosen for uniform manifold approximation and projection (UMAP) and t-distributed stochastic neighbor embedding (tSNE) dimensional reduction. The unsupervised cells were clustered together by "FindClusters" and "FindNeighbors" functions based on the top 30 PCA principles, to cluster the similar types of cell populations together, with resolution setting as 0.3. The marker genes of each cell cluster were detected by "FindAllMarkers" function with the following criteria: min.pct > 0.1, logfc.threshold > 0.25 and p-value < 0.01. Immune cells were further extracted out and conducted for subsets subdivided, followed by re-tSNE and re-UMAP dimensional reduction.

GSVA algorithm assessed the OS functional levels

To evaluate the differences in OS-related functions in different degenerative grade samples, we retrieved and downloaded GO BP terms from the MsigDB database (Molecular Signatures Database, https://www.gsea-msigdb.org/gsea/msigdb/) to screen the required OS-related functional items (40). "Single sample GSEA (ssGSEA)" algorithm was conducted in R ("GSVA" package, 1.42.0) to calculate functional scores in each sample. Higher scores indicated higher levels of the functional item in each sample. We obtained the following items to fully assess the OS-related functions in IVD tissues: "GO_RESPONSE_TO_OXIDATIVE STRESS," "GO_REGULATION_OF_RESPONSE_TO_OXIDATIVE_STRESS," "GO_CELL_DEATH_IN_RESPONSE_TO_OXIDATIVE_STRESS," and "GO_CELLULAR_OXIDANT_DETOXIFICATION," as Yu et al. described (41). OS-related scores of different cell populations were calculated to evaluate these OS functions.

Differentially gene expression analysis

"FindMarkers" function was applied to detect DEGs among different groups or cell populations within scRNA-seq data, followed by the following criteria: Wilcox rank sum test algorithm, min.pct > 0.1, logfc.threshold > 0.25, p-value < 0.01, and only.pos = TRUE.

Functional and pathway enrichment analysis of DEGs and sub-populations

DEGs and marker genes of each cell population were analyzed by R ("clusterProfiler" package, 4.2.1) and DAVID database (https://david.ncifcrf.gov/) to get understanding of functional annotations and interpretations, including Gene Ontology (GO) and Kyoto Encyclopedia Genes and Genomes (KEGG) results. p-value < 0.05 and false discovery rate (FDR) < 0.25 were considered as significantly enriched. For each cell population, the top 50 genes (prioritized by fold change when comparing each cluster with the rest) were conducted to the enrichment analysis, and ontology terms with near-duplicated terms were eliminated using custom script. The exclusion criteria of GO terms were "POSITIVE," "NEGATIVE," "EOSINOPHIL," "T_HELPER," or "T_CELL," as Lee described (42).

Monocytes/macrophages evolvement analysis

To analyze the evolvement procedure of monocytes/macrophages, this study applied CytoTRACE analysis to decode the relative evolutionary states of different subtypes, which was one of the computational methods for depicting the states of cell fate without any prior information (43). The monocytes/macrophages evolvement process was thus analyzed by CytoTRACE with the default parameter.

Differentiation trajectory of monocytes/macrophages by pseudotime analysis

The trajectory analysis of monocytes/macrophages was performed by Monocle2 algorithm (44). After the calculation of size factor and dispersions estimation, DEGs along the trajectory branch were further identified. Seurat clustering results and raw expression counts matrix of cells were prepared before monocle analysis, followed by "DDR-Tree" method and other default parameters to reduce dimensions. Based on pseudotime results, evolvement procedure of monocytes/macrophages were conducted by branch expression analysis modeling (BEAM) analysis.

Cell–cell interaction analysis

To investigate cellular interactive communications among different cell populations, this study conducted CellPhoneDB (based on Python 3.7) and CellChat to get a systematic understanding for cell–cell communication molecules (45, 46). CellPhoneDB and CellChat were public databases for ligands, receptors, and their interactions, where the membrane and secreted and peripheral proteins of the clusters were annotated. The normalized cell expression matrix was prepared by Seurat normalization; the significant mean and cell communication significance were calculated based on each interactive role, setting as p-value < 0.05.

Transcription factor network inference

To further decode the gene regulatory network of different monocyte/macrophage subtypes, we performed single cell regulatory network inference and clustering (SCENIC) algorithm to identify specific regulons involved in different cell subpopulations (based on pySCENIC and R-SCENIC) (47). After extraction of count expression matrix, the transcription factor (TF) activities (AUCell) for each cell were calculated through motif library (version "mc9nr"), and the TF regulation strength was assessed using the 20,000 motifs database according to RcisTarget and GRNboost.

Statistical analysis

Data statistical analysis and visualization in this study was achieved by R (version 4.1.3, based on different packages and algorithms mentioned above) and GraphPad Prism (version 8.3.0). One-way ANOVA analysis was chosen flexibly to compare three or more groups, and Student's t-test was used for statistical analysis between two groups. The difference of p< 0.05 was considered as statistically significant.

Results

Oxidative stress levels increased gradually with degenerative stages

The human body is always within a balanced state between the oxidant and antioxidant system. The imbalance refers to

overexpression of ROS and reduction in antioxidant capacity. Thus, we compared and analyzed the OS functional levels of IVD tissues under different degenerative stages, based on GSE70362 and GSE147383.

According to the relevant functional items retrieved from MsigDB database, we performed GSVA algorithm to score each different degenerative IVD tissue from Pfirrmann grades I–V. We evaluated the OS-related functions like "GO_RESPONSE_TO_OXIDATIVE STRESS," "GO_REGULATION_OF_RESPONSE_TO_OXIDATIV E_STRESS," and "GO_CELL_DEATH_IN_RESPNSE_TO_OXID ATIVE_STRESS." Results illustrated that the OS-related levels in severe degenerative IVD tissues were significantly higher than that in early degenerative tissues among different datasets (Figure 1A). Then, we analyzed the OS-related scores in each degenerative stage. Results revealed that the OS levels elevated with the degenerative stage, and OS levels in grades IV and V were significantly higher than that in grade I, which demonstrated the close correlations of OS reactions with the progression of IDD, as shown in Figure 1B.

Identifying DEOSGs related with the OS functions during IDD progression

This study divided the total gene expression matrix of GSE70362 into two groups (early and late degenerative group), followed by linear model fitting and Bayes detection. With cutoff criteria setting as adjusted $p < 0.05$ and $|FC| > 1.5$, 259 DEGs were totally screened, with 124 upregulated and 135 downregulated genes. The volcano plot visualized the distribution of these DEGs between early and late degenerative IVD tissues (Figure 1C). Then, the DEOSGs were

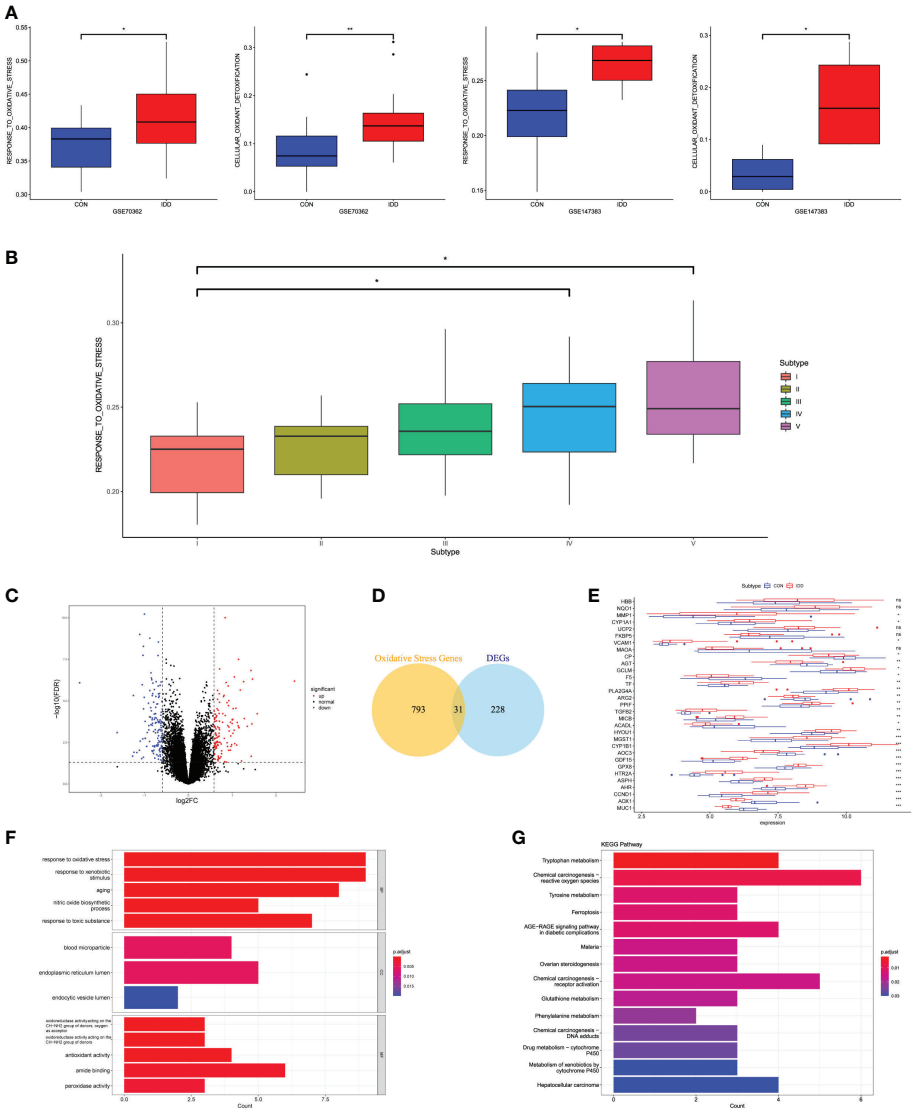

FIGURE 1
(A) Differences in cellular oxidative stress response in GSE70362 and GSE147383, respectively. **(B)** OS-related functional scores in each degenerative stage. The higher the score, the more active function. **(C)** Volcano plot of the identified DEGs. **(D)** Venn diagram indicating 31 genes were commonly expressed as DEOSGs. **(E)** The expression situations of these 31 DEOSGs in CON and IDD groups. **(F, G)** Representative analysis of GO, KEGG categories showing different functions of the screened 31 DEOSGs. "CON" group represented "early degenerative patients," and "IDD" group represented "late degenerative patients", *p < 0.05, **p < 0.01, ***p < 0.0001, ns: none significance, which were the same as below.

further identified by the intersection of 259 DEGs and 824 OS-related genes. Altogether, 31 genes were filtered as DEOSGs, which were associated with the progression of IDD (Figure 1D). We further analyzed the gene expression values of each DEOSG, as shown in Figure 1E.

Functional enrichment analysis was further applied to understand the roles in the progression of IDD. GO analysis suggested that the upregulated DEOSGs were primarily correlated with biological functions like "response to oxidative stress," "response to xenobiotic stimulus," "response to toxic substance," "peroxidase activity," "oxidoreductase activity," and "aging"; besides, the cellular components were mainly located in the endoplasmic reticulum lumen (Figure 1F). These results indicated the essential roles of OS in the progression of IDD. The KEGG pathway illustrated that these DEOSGs were mainly involved in "chemical carcinogenesis production-ROS," "DNA adducts," "receptor activation," "ferroptosis," "tryptophan and tyrosine metabolism," and "metabolism of xenobiotics by cytochrome P450" (Figure 1G).

Immune-infiltrating cell analysis

To understand the compositions of immune cells between normal and degenerative IVD tissues, this study applied "CIBERSORT" method from GSE147383 to discover the correlated immune cells involved in the progression of IDD. The "CIBERSORT" method was designed to estimate the relative proportion of different types of immune cells *via* deconvolution algorithm. Figure 2A and Supplementary Figures S1E, F displayed the enrichment fraction of immune-infiltrating cells in IVD tissue. Results illustrated that T-cells regulatory (Tregs), plasma cells, and monocytes/macrophages were significantly activated and T-cell follicular helper (Tfhs) were significantly inhibited in late degenerative IVD tissues, as shown in Figure 2B, which suggested the potential regulatory roles of these immune cells in the progression of IDD.

Construction of co-expression network and identification of interested modules

After samples heterogeneity detection, all samples were included in the WGCNA workflow, together with their immune cells' information (Figure 2C). Soft threshold power was determined as 18 based on the scale-free network construction (Figure 2D). Then, hierarchical clustering tree analysis was performed based on the mutual genes' co-expression; altogether, 20 modules were generated, and each module had unique gene expression patterns (Figure 2E). Furthermore, the relationships between modules and clinical traits (infiltrating immune cells) was demonstrated in Figure 3A. The genes in these generated modules are associated with the progression of IDD, the color depth, and correlation coefficient, and the p-value is correlated with the weights of IDD occurrence. Since the immune infiltration analysis algorithm was developed based on gene expression, the real monocytes/macrophages subtypes could not be analyzed accurately. Results discovered several interested modules like pink, yellow, and green yellow modules targeting macrophages M0 (Cor = 0.89, p = 0.003), monocytes (Cor = 0.88, p = 0.004), plasma cells (Cor = 0.91, p = 0.002), and Tregs (Cor = 0.93, p = 9e−04), respectively. Pink and yellow modules were further merged together as essential modules of monocytes/macrophages and conducted for further analysis to avoid the loss of gene information.

Identification of differentially expressed immune-related oxidative stress genes and hub genes validation

The differentially expressed immune-related OS genes, namely, hub genes, were finally identified by Venn plot analysis; the intersection of the three parts included screened 259 DEGs, 824 OS-related genes, and genes in pink and yellow modules. Totally, four genes were obtained: CYP1A1, MMP1, CCND1, and NQO1 (Figure 3B).

Then, the robustness of these four genes was validated by PCA dimensional reduction analysis among different databases. PCA was performed to reduce the dimension of these hub genes into three principal components PC1, PC2, and PC3, where each dot plot indicated each sample in the three-dimensional coordinate system. Based on the gene expression matrix of each database, these dot plots showed significantly distinguishment ability in spatial distribution (Figure 3C).

Based on the four genes identified in this study, we further conducted ROC curve analysis to assess the predictive ability of each feature to observe their diagnostic ability of IDD. As shown in Figure 3D, results indicated high area under curve (AUC) value of each gene among different datasets. The AUC of CYP1A1 was 0.63, 0.66; AUC of MMP1 was 0.73, 0.66; AUC of CCND1 was 1.00, 0.89, 0.82; and AUC of NQO1 was 0.75, 0.76, respectively. Meanwhile, the PCR results further validated that these four hub genes were significantly upregulated in degenerative NP cells with the concentration of TBHP, which further proved the essential roles of these genes in the progression of IDD. Consequently, these four genes were determined as hub genes in this study, which had the most connections with the progression of IDD.

Single-cell profiles landscape revealed the immune cellular heterogeneity within different degenerative stages of IVD tissues

In the above analysis, we found that some immune cells like Tregs, plasma cells, and monocytes/macrophages were upregulated aberrantly in IDD groups. Therefore, we further depicted immune cells heterogeneity atlas within IVD tissues at single-cell level (based on GSE165722). After rigorous quality control workflow to eliminate cells with low gene detection (<200 genes) and high mitochondrial gene content (>20%), a total of 42,960 cells with 18,142 expressed genes were included for subsequent analysis (Figure 4A). The number of the detected genes was significantly correlated with the sequencing depth, and mitochondria UMI rate of each cell was lower than 20% (Figure 4B). The variance analysis revealed the top 2,000 highly variable genes of each sample, and PCA method was performed to identify available dimensions based on these principals; dot plots and

10.3389/fimmu.2023.1090637

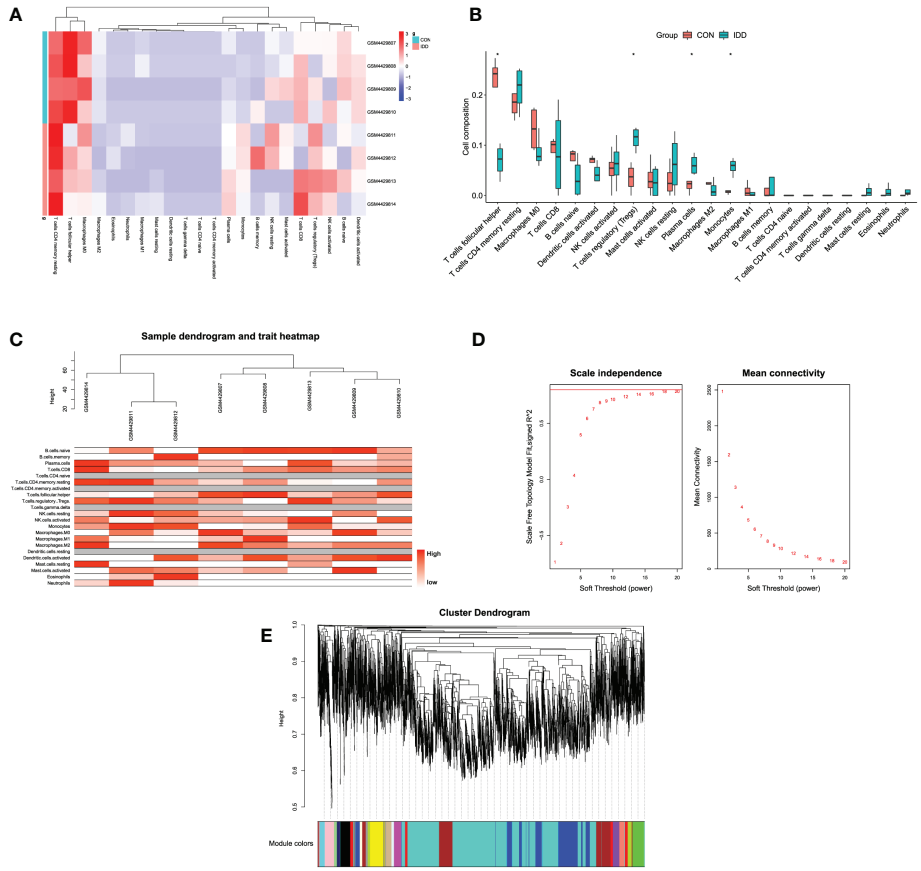

FIGURE 2
(A) Heatmap displaying the distribution of 22 types of immune cells in different groups. **(B)** The relationships of immune infiltration levels between different groups. **(C)** Cluster dendrogram of samples to detect outliers. The color is from white to red; the redder color represented higher contents of immune cells. **(D)** Selection of the soft threshold power value. The left panel represents scale-free model fit index; the right panel represents the mean connectivity of these values. **(E)** Cluster dendrogram of genes enriched based on dissimilarity measure and assignment modules.

heatmap also displayed the significant correlated genes for cell clustering (Supplementary Figures S1A–C). After elimination of different samples by RPCA integration algorithm, PCA and UMAP scatter plot suggested a high overlap of these cells, whether by grades or patients, indicating good integration result (Figure 4C and Supplementary Figure S1D). Then, the top 50 PCs were calculated based on the top 2,000 genes, and the top 30 PCs with the lowest p-values were chosen for subsequent dimensional reduction analysis.

Unsupervised dimensional reduction method was performed for cell subtype clustering by UMAP algorithm; totally, 18 cell clusters were generated in the NP tissue, and according to marker genes detection of each cluster, different cell populations showed high heterogeneity with each other (Figure 4D). The detailed types of cell clusters were referenced by singleR, combined with the existing literatures and databases (48). The heterogeneity of different cell clusters was classified by gene expression (Figure 4E), and 11 clear separations of cell subtypes were annotated, including six types of immune cells and the rest types of NP-related cells. The representative gene expression patterns of specific markers are shown in Figures 4F, G: the core genes encoding anabolic metabolism like COL2A1 and ACAN were highly expressed in NP cells, together with highly expressed SOX9 gene (25, 29); PDGFRA and PRRX1 were mainly expressed in NP progenitor cells (NPPCs), which were the two mesenchymal progenitor markers (28); stromal cells highly expressed COL1A1 and COL3A1 genes (27); endothelial cells mainly included specific marker genes of CDH5 and PECAM1 (49); erythroblast cells consist of CA1, HBB, GYPA, ALAS2, and AHSP; in terms of immune cells, monocytes/macrophages were identified by CD14, CD163, CD86 and MRC1 (50); B cells were identified with MS4A1 and IGKC (49); NK/T cells were identified with TRAC, TRBC2 and SPOCK2; neutrophils mainly expressed FCGR3B and CXCL8 (51); granulocytic myeloid-derived suppressor cells (G-MDSC) highly expressed marker genes of ITGAM and ARG1 (52, 53); and granulocyte macrophage progenitor (GMP) cells were identified by marker genes of ELANE, MPO, and MS4A3 (54, 55). The distribution of distinct cell populations between different degenerative stages is shown in Figures 4H, I.

Oxidative stress levels among different cell populations of IDD

Based on the classified cell populations, we also performed "GSVA" algorithm to calculate the scores of OS-related functions for each single cell and observed the OS levels in real IVD microenvironment. The results of single cells in IDD were

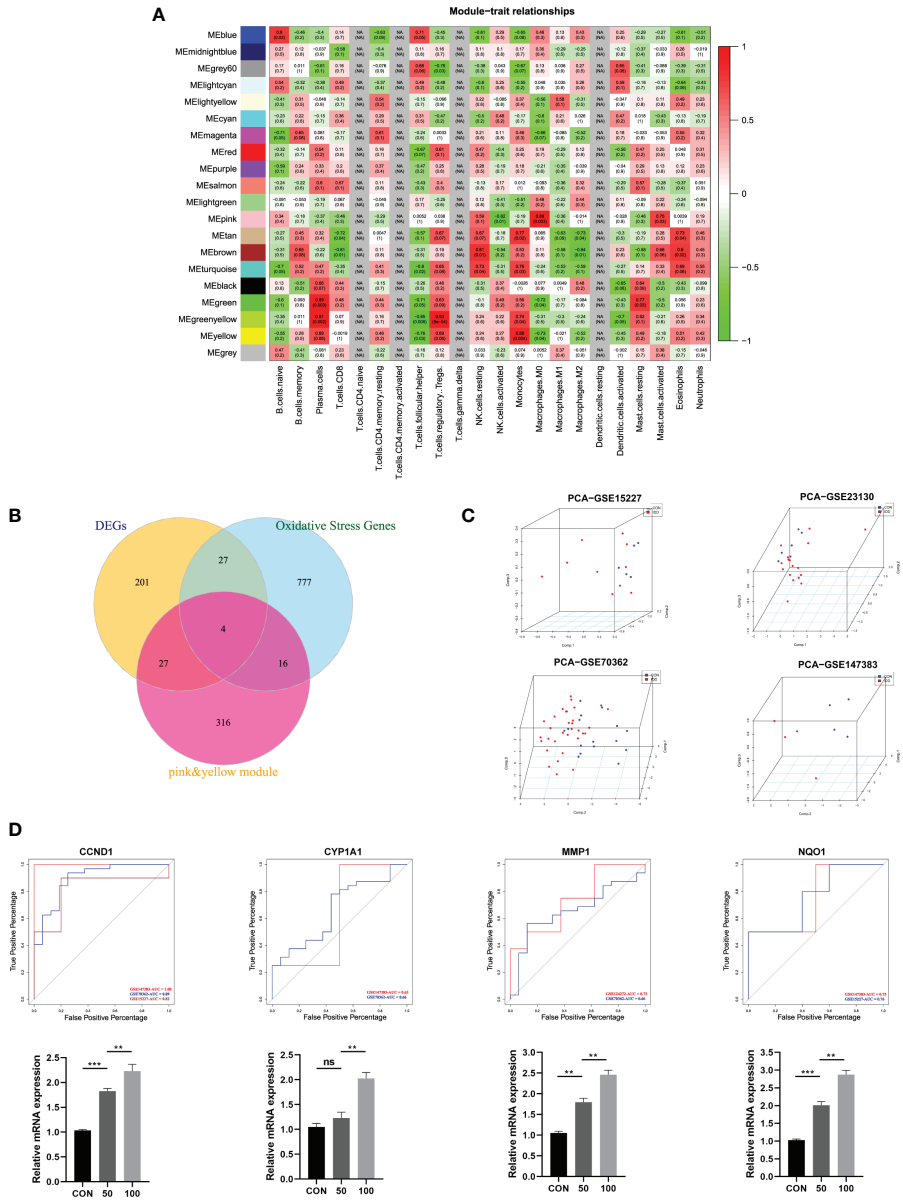

FIGURE 3
(A) Module−trait relationships between different clustered modules and immune infiltration cells. Green represents negative correlation, and red represents positive correlation; the darker colors indicated higher weights. Each square also contained corresponding correlation (first line) and p-value (second line), which were consistent with the shade of the color. **(B)** Venn diagram showing the hub genes among three parts. **(C)** 3D scatter plot after PCA dimensional reduction in these hub genes in different datasets. **(D)** ROC curve analysis for predicting IDD in different datasets; qRT-PCR was used to detect the mRNA expression of CCND1, CYP1A1, MMP1, NQO1 in human NP cells treated with TBHP for different concentrations.

consistent with the bulk-RNA seq, in that the OS-related functions in late degenerative IVD tissues were significantly higher than that in early degenerative tissues (Figure 5A). Moreover, we evaluated the OS-related functions for each cell subtype. Results illustrated that the NP and NPPC cells had the highest OS-related scores. As for immune cells, monocytes/macrophages were shown as the most correlated immune cells with OS-related functions. Intriguingly, we also observed high OS levels in endothelial cells (Figures 5B, C). We next observed the OS-related functions among different cell subtypes between early and late degenerative IDD. Results suggested that most cell populations had higher OS-related levels in late degenerative IVD tissues except GMP and G-MDSC, as shown in Figure 5D and Supplementary Figure S2, which may behave protective roles to ameliorate IDD progression, at least by reducing OS levels.

Sequential alterations of monocyte/macrophage populations during IDD

In immune cells, monocytes/macrophages possessed the highest OS-related functions in degenerative IVD tissues, whether by bulk-RNA-seq or scRNA-seq analysis. We next analyzed monocyte/macrophage-specific features that dynamically changed during IDD. Therefore, we extracted and performed re-clustering analysis of the

10.3389/fimmu.2023.1090637

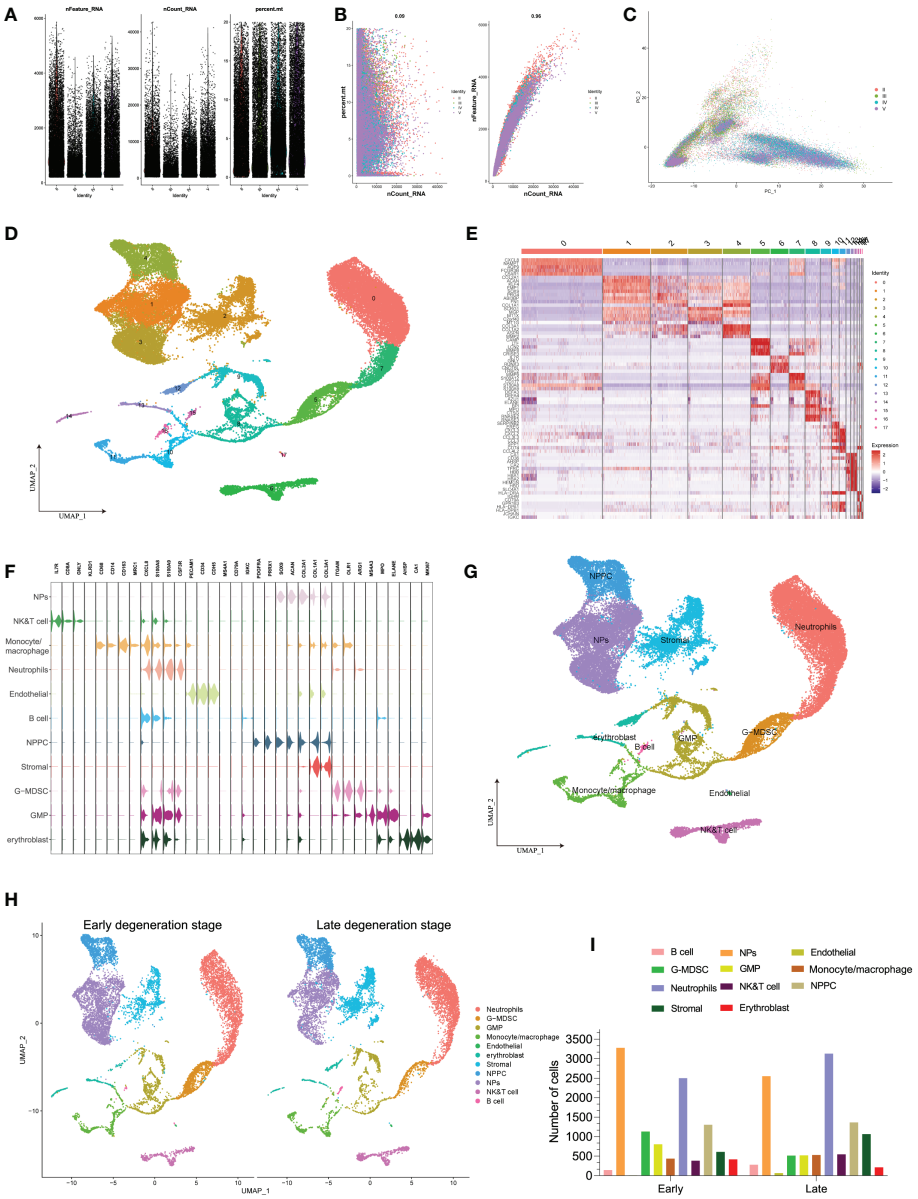

FIGURE 4
(A) Scatter plot after quality control and filtering of cells. **(B)** The left panel indicates that the mitochondria were the same with sequencing depth; the right panel suggests that the numbers of the detected genes were significantly related to the sequencing depth. **(C)** PCA scatter plot displayed the dot distribution after sample integration. **(D)** UMAP visualization of degenerative IVD, which identified 17 cell clusters. **(E)** The heatmap displays the top 5 genes of the identified markers genes of each cluster. **(F)** The violin plot shows the mean expression of the selected marker genes used for annotation in each cell cluster. **(G)** UMAP visualization after annotation for each cell cluster. **(H)** UMAP visualization of cell populations distribution between early and late degeneration stage. **(I)** The numbers of each cell type in different degeneration stage.

monocyte/macrophage population through UMAP dimensional reduction method. Totally, we analyzed 1,824 monocyte/macrophage cells based on variable genes and identified six different sub-clusters (Supplementary Figure S3A). Based on the distinct gene signatures, we identified the following five monocyte/macrophage subtypes with distinct biological significance for downstream analysis: OS related macrophages ($EREG^+$ $IL1A^+$ macrophages), activated tissue macrophages ($APOC1^+$ CLU^- macrophages), effector monocytes/macrophages ($CTGF^+$ $COL3A1^+$ monocytes/macrophages), regulatory macrophages ($AZU1^+$ $ELANE^+$ macrophages), and homeostatic macrophages ($CTSL^+$ $MRC1^+$ macrophages) (shown in Figures 6A, B; Supplementary Figure S3B). Supplementary Figure S3D also displayed the normalized expression levels of representative marker genes for each subtype.

Although there were no significant number changes in monocytes/macrophages as a whole during early and late stages, we observed an interesting trend of subtypes after monocytes/macrophages re-clustering. The proportion of each subtype underwent distinct changes during IDD: the subpopulation of effector monocytes/macrophages and regulatory macrophages was dominant at grade II but was drastically decreased from grade III; with the progression of degenerative grade, we observed increased proportions of OS related macrophages, activated tissue macrophages, and homeostatic macrophages, while effector

10.3389/fimmu.2023.1090637

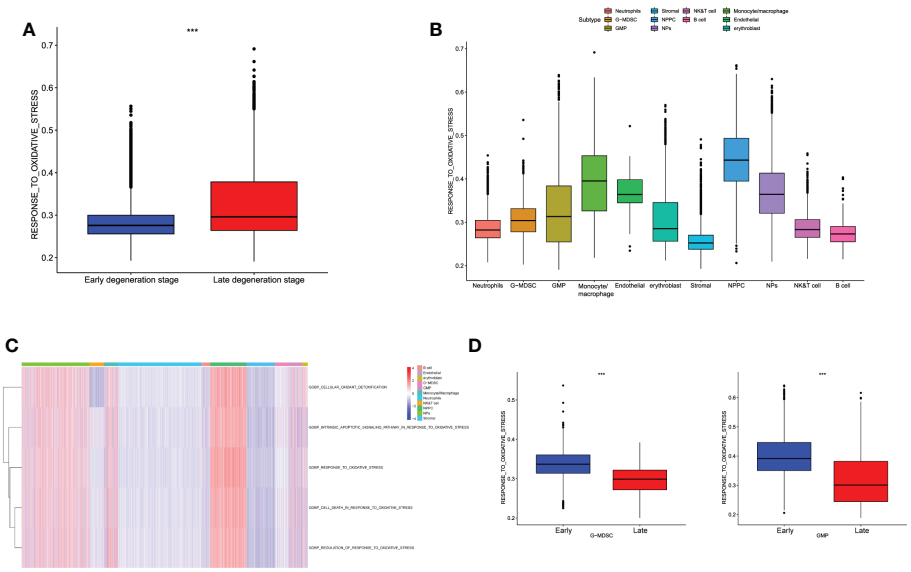

FIGURE 5
(A) Differences in cellular oxidative stress response of different groups at the single-cell level. **(B)** The OS-related functions among different cell populations. **(C)** The heatmap shows each OS-related function among different cell populations. **(D)** Comparison of OS-related functions between early and late stage in G-MDSC and GMP.

monocytes/macrophages and regulatory macrophages barely existed (Figures 6C, D). Dynamic changes in the proportions of the subtypes are summarized on UMAP plot in Supplementary Figure S3C.

To characterize the subtypes of monocytes/macrophages in detail, we identified DEGs for each subtype, and the top 50 DEGs of each subtype were analyzed by GO biological functions (Figure 6E). DEGs of OS-related macrophages (the dominant population in late degenerative IVD tissues) were enriched in functions like "acute inflammatory response," "ROS metabolic process," and "response to oxidative stress"; besides, they mainly expressed markers of M1 (IL1A, IL1B, TLR4, and IL6), which were considered to act roles like M1. Activated tissue macrophages had DEGs that were mainly associated with activated inflammatory response like "response to lipopolysaccharide" and "regulation of inflammatory response." As expected, DEGs of homeostatic macrophages and effector monocytes/macrophages were chiefly enriched in protective functions like "tissue remodeling" and "collagen binding;" meanwhile, both two subtypes highly expressed M2 markers (CSF1R, MRC1, C1QB, and C1QC), which may behave roles like M2, and effector monocytes/macrophages also highly expressed monocytes marker (CD14) and proliferative markers (CTGF and PCNA) (56, 57). As for regulatory macrophages, they were mainly involved in functions of regulating effects, such as "cytoplasmic translation" and "humoral immune response" (Figure 6F; Supplementary Figure S3D). Overall, we totally defined five distinct subtypes of monocytes/macrophages, which suggested extensive heterogeneity with each other in different degenerative stages of IDD.

Evolution lineage trajectory of different monocyte/macrophage subtypes in IDD

We next performed the CytoTRACE analysis to further evaluate the evolutionary dynamics of the monocyte/macrophage subtypes, which could reveal the direction of evolution and predict cell lineage trajectories using gene counts and expression (43). Few kinetics were observed in activated tissue macrophages, while regulatory and effector monocytes/macrophages formed complex kinetics during IDD (Figure 7A). To quantify the kinetic dynamics of CytoTRACE results, we calculated the scores of each cell in Figure 7B, which represent the evolutionary ability. Regulatory macrophages had the highest levels of dynamics. In contrast, activated tissue macrophages and homeostatic macrophages both had low levels of dynamics, which were consistent with the findings from UMAP embedding (shown in Figure 7A). The results suggested that regulatory and effector monocytes/macrophages contributed to the formation of the rest macrophages during IDD.

To investigated the dynamic transcriptome changes of these subtypes, we next constructed monocle pseudo-time trajectory analysis. The trace displayed that effector monocytes/macrophages that accumulated at the root of the trajectory, homeostatic, and activated tissue macrophages were distributed alongside different branches from the root, while regulatory and OS-related macrophages accumulated together at the tail end of the track (Figures 7C, E). The pseudo-time tree branch diagram further demonstrated the detailed evolution process of these monocyte/macrophage subtypes (Figure 7D). Results illustrated that effector monocytes/macrophages were located at the father node, which further divided into homeostatic and activated tissue macrophages. Regulatory and OS-related macrophages clustered together at the end of child nodes, which were consistent with the trajectory evolution results. These data indicated that separate trajectories of these subtypes were useful to depict their distinct evolution pathways; effector monocytes/macrophages could evolve into homeostatic and activated tissue macrophages, while regulatory macrophages could evolve into OS-related macrophages.

For the trajectory towards OS-related macrophages (OS route) (Figure 7F), we defined three distinctive clusters showing different

10.3389/fimmu.2023.1090637

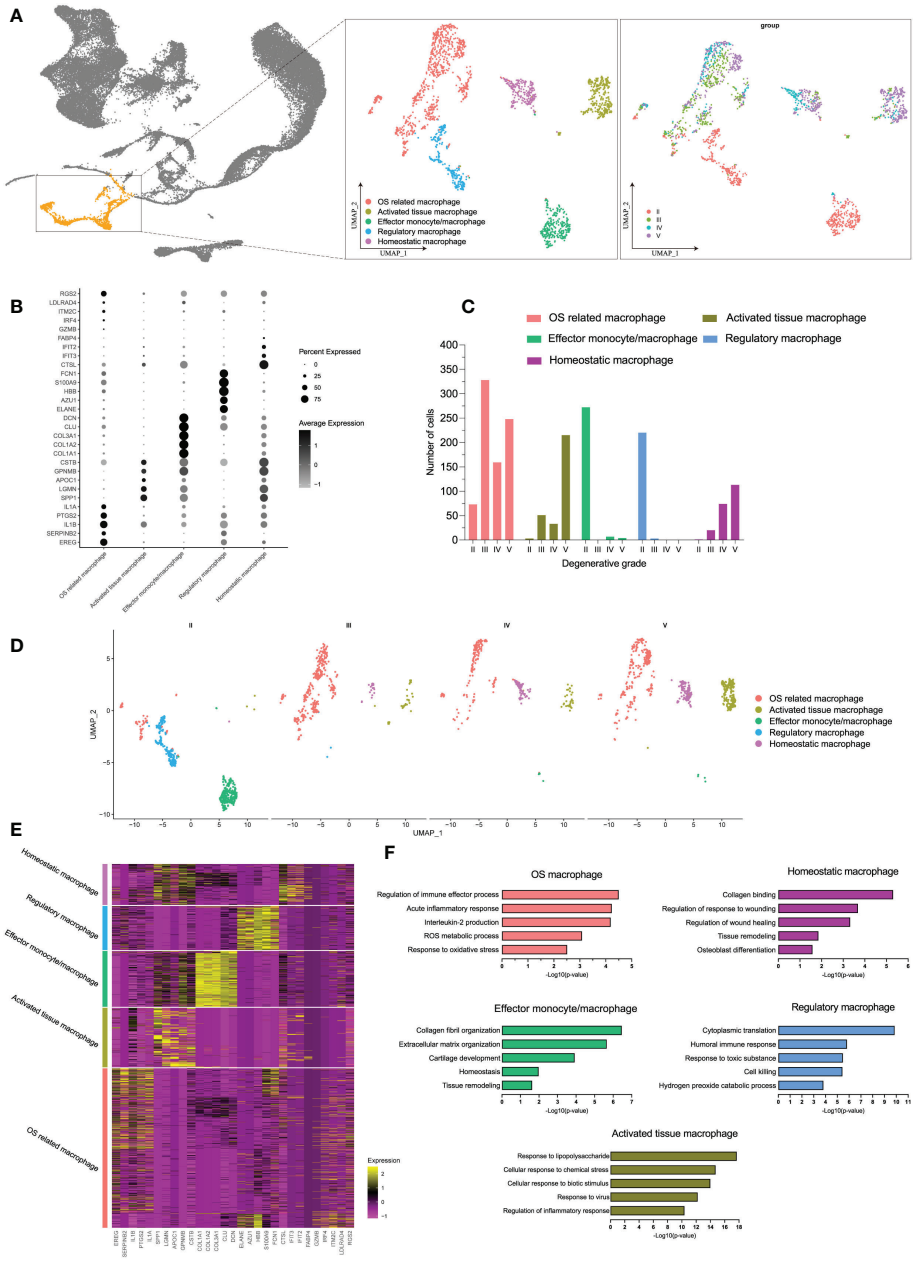

FIGURE 6
(A) The distribution of macrophages among all cell populations and the further re-clustering of macrophages with UMAP visualization. **(B)** Five different macrophage subtypes and their specific marker gene expression levels, with brightness indicating log-normalized average expression, and circle size representing the percent expressed. **(C)** The number cells of macrophage subtypes in different degeneration stage. **(D)** UMAP visualization of macrophage subtypes in different degeneration stage. **(E)** Heatmap of the top 5 of cluster-specific DEGs for each macrophage subtype; the color indicated the relative gene expression. **(F)** Bar plots showing the –log10 (p-value) from enrichment analysis of representative GO biological functions among different macrophage subtypes.

modular gene expression alterations. We summarized the top 5 GO biological functions in Figure 7G; notably, clusters 1 and 2 of the OS-related macrophages route (which was exclusively expressed in highly activated OS-related macrophages) suggested increased expression of IL1B and IFN. In addition, highly activated OS-related macrophage clusters displayed predominant enrichment of pro-inflammatory mediators like IL1A, IL1B, CXCL8, and TNF (Supplementary Table S2). These findings pointed that the specific subpopulation that derived from regulatory macrophages had experienced IDD-dependent activation of macrophage inflammatory responses.

As for the trajectory from effector monocytes/macrophages, we performed BEAM analysis for branch fate-determined gene analysis according to node 1, branch heatmap visualized significant gene expression alterations in different subtypes, cell type I represented the smaller state ID (namely activated tissue macrophages), and cell type II indicated bigger state ID (namely, homeostatic macrophages), as shown in Figures 8A, B. We totally defined six distinct clusters and analyzed their biological functions. Results suggested that genes in cluster 4 became highly expressed in activated tissue macrophages, with their biological functions associating with immune response,

10.3389/fimmu.2023.1090637

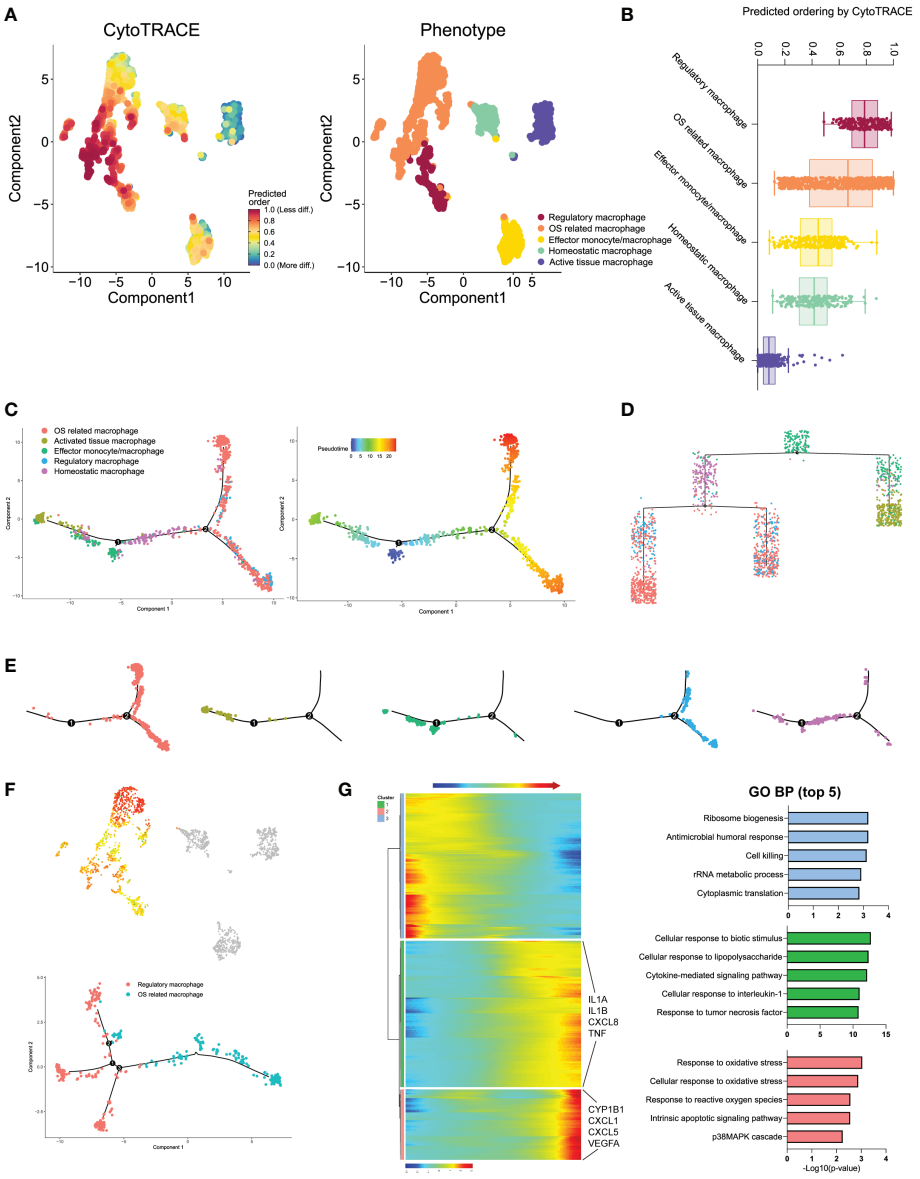

FIGURE 7
(A) Plot of the CytoTRACE pseudo-time order for the macrophage subtypes. **(B)** Calculation of CytoTRACE scores of each macrophage cell according to predicted order. **(C)** Monocle pseudo-time analysis revealed the macrophage subtypes lineage progression. The left panel displays the different macrophage subtypes along lineage progression; the right panel indicates the pseudo-time results of these subtypes. **(D)** Tree branch diagram of the macrophage subtypes; the legend of macrophage subtypes is the same as in panel **(C)**. **(E)** The detailed location of different macrophage subtypes along the lineage progression. **(F)** Pseudo-time trajectory initiated from regulatory macrophages toward OS-related macrophages. **(G)** The left panel shows the alterations of relative expression patterns of representative genes along the pseudo time. The right panel analyzed the GO biological functions in clusters 1–3, as defined in the left panel.

including cellular response to oxidative response and inflammatory response. In contrast, genes in the rest clusters were mainly overexpressed in homeostatic macrophages, with their biological enrichment with protective functions like regulation of cell proliferation, collagen fibril organization, and extracellular matrix organization; they also showed increased expression of C1QA and TGFB2, which were known to be key genes of well-differentiated M2 macrophages (42).

In brief, the monocyte/macrophage subpopulations experienced time-dependent and subtypes-specific alterations during IDD progression. These subpopulations exhibited a continuous spectrum changes at the transcriptome level, which mainly began with effector monocyte/macrophages and regulatory macrophages from early degenerative stage.

Signaling network for the intercellular crosstalk regulating the homeostasis of NP Cells

To seek further insights about the critical factors and the pathways that contribute to the activation or homeostasis of NP cells, especially between different monocyte/macrophage subtypes and NP cells, we investigated the signaling network in the whole

10.3389/fimmu.2023.1090637

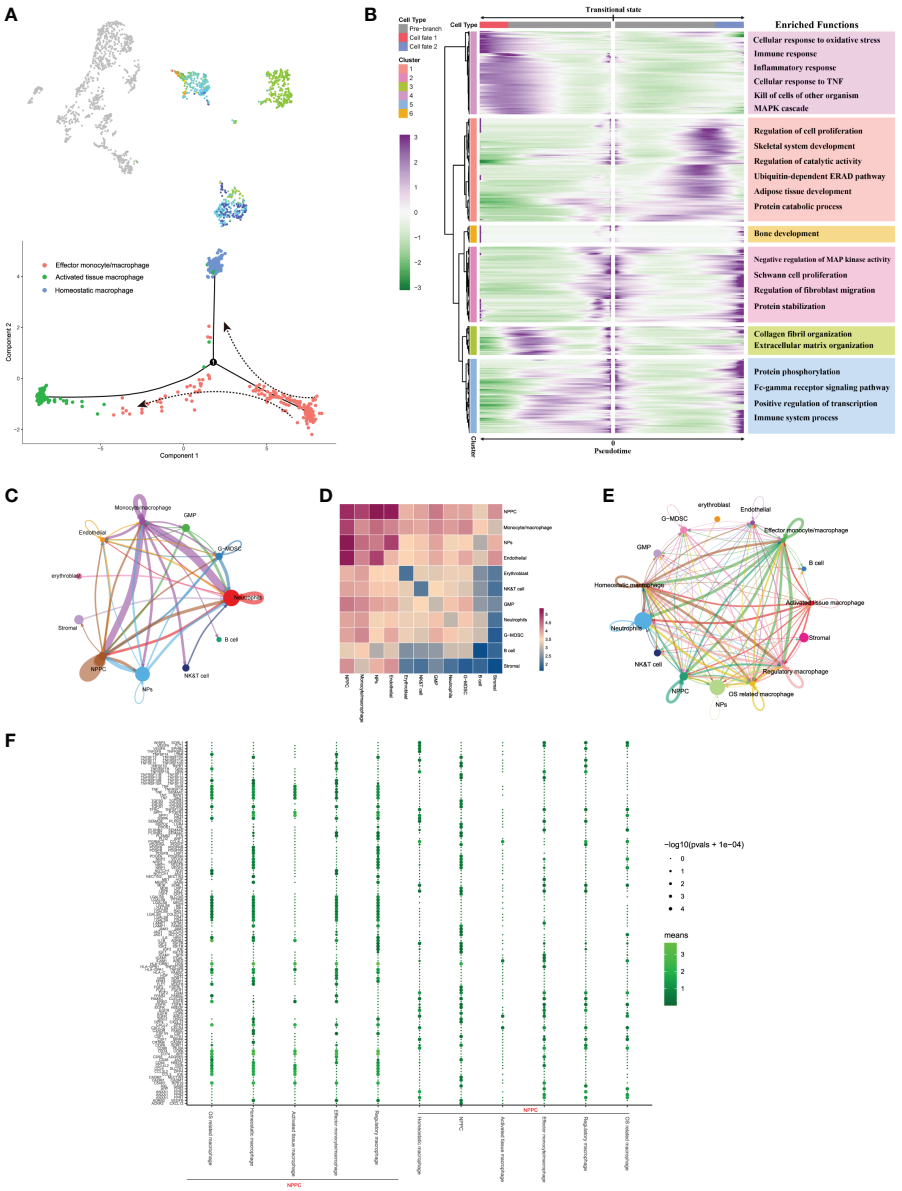

FIGURE 8
(A) Pseudo-time trajectory initiated from effector monocytes/macrophages toward activated tissue and homeostatic macrophages. **(B)** Branch trajectory heatmap of the DEGs revealed gene expression alterations under different lineage progression directions, together with the main functions of these genes in each cluster displayed. **(C–E)** Overview of the cellular inter-regulatory network and the correlation among different cell populations. **(F)** The bubble plot shows each statistically significant ligand–receptor pair between NPPC and macrophage subtypes.

cell populations based on CellphoneDB and Cellchat analysis. Results displayed highly regulated cellular communications from the bidirectional interactions among those cell populations; the more and thicker lines indicated more participated signaling pathways and more interaction weights, and the size of circles represented the numbers of each cell population (Figure 8C). Communication correlation heatmap quantified the numbers or weights among different cell populations, which demonstrated that the NPPC, NPs, and monocytes/macrophages had actively regulated roles (Figure 8D); thus, monocytes/macrophages were determined as the essential immune niche components in degenerative IVD tissues. We further divided monocytes/macrophages into distinct subtypes, and regulatory network indicated that each subtype had distinct active interactions with other cell populations (Figure 8E). The detailed signaling communication results between different subtypes and other cell populations are shown in Figure 8F.

Notably, only regulatory and OS-related macrophages were involved in vascular endothelial growth factor (VEGF) signaling pathway through autocrine, which also served as receiver of VEGF signals, while NPs and NPPC functioned as the main regulators of the communication (Figure 9A). The SPP1 pathway had significant changes in NPPC, NP cells, NK/T cells, and endothelial cells, which were especially participated by monocytes/macrophages (except regulatory and OS-related macrophages subtypes) (Figure 9B). Moreover, the tumor growth factor beta (TGF-β) pathway was modulated by regulatory macrophages and NPPC, mainly through autocrine or paracrine mediation by TGFB1-TGFBR1 or TGFB1-ACVR1 interactions. Intriguingly, the OSM signaling pathway was

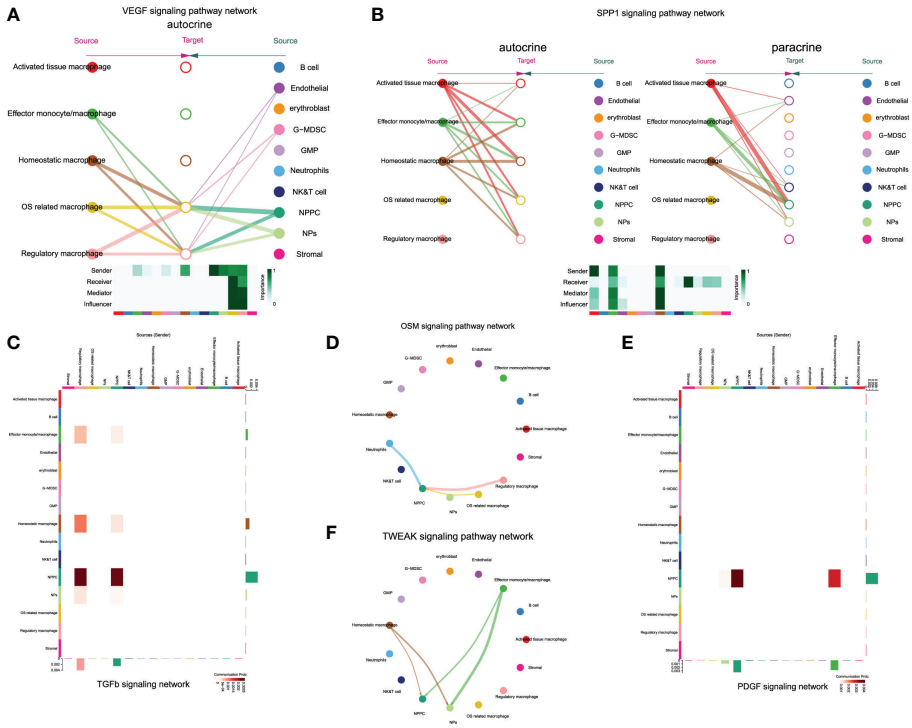

FIGURE 9
The enrichment situation of VEGF **(A)**, SPP1 **(B)**, TGFβ **(C)**, OSM **(D)**, TWEAK **(E)** and PDGF **(F)** signaling pathways respectively.

mainly observed in regulatory and OS-related macrophages through paracrine, targeting NPPC. In the platelet-derived growth factor (PDGF) signaling network, the effector monocytes/macrophages acted as critical contributions by secreting PDGFA, PDGFB, and PDGFC ligands, leading to the paracrine from effector monocytes/macrophages to NPPC and NP cells. In addition, the TWEAK signaling pathway was mainly mediated by effector monocytes/macrophages and homeostatic macrophages through paracrine targeting NPPC and NP cells; the detailed information of these activated signaling pathways is shown in Figures 9C–F. These findings could also advance the intervention targeting potential signaling pathways to ameliorate IDD.

Transcription factors regulatory network among monocytes/macrophage subtypes

To explore the gene regulatory networks that determined cell fate in the monocyte/macrophage subtypes, we performed SCENIC analysis to decipher the regulatory activity (regulons) from the co-expression of transcription factors (TFs). Totally, we discovered 357 regulons that were used to discriminate the different monocytes/macrophage subtypes (Figure 10A). After the calculation of regulon specificity score (RSS), totally, 25 regulons were further determined as the core regulons that modulate the downstream functions. As shown in Figures 10B, C, results illustrated that different subtypes upregulated the expression of different TF regulatory networks. The highly enriched regulons in activated macrophages included RXRB, HOXA3, ZNF559, ZNF285 and MGA. The SIX4, SOX8, SOX9, ZIC1, and TEF TFs were specific to effector monocytes/macrophages. Homeostatic macrophages exhibited strong enrichment of MTA3, GTF3C2, MYC, ZNF567, and peroxisome proliferator- activated receptor gamma (PPARG) TFs. OS-related macrophages were enriched in regulons such as ERG, GATA2, HOXA9, TAL1, and SOHLH2. As for regulatory macrophages, they mainly overexpressed MZF1, HES6 CEBPE, FLI1, and POU3F1 TFs. The representative motifs of each monocyte/macrophage subtype are illustrated in Figure 10C. These identified TFs helped researchers further realize the gene regulatory network by monocytes/macrophages and made it possible for cell therapies to mitigate the IDD.

Discussion

The cellular heterogeneity of IVD tissues has been a long-debated controversy due to the complexity of IDD (28). Although recent studies have reported several single-cell transcriptomes of physiological or degenerative IVD tissues, none have used a longitudinal approach along with the natural disease course. Inflammatory responses are closely related to oxidative stress and immune processes (58), while few studies have focused on the aberrantly expressed biomarkers associated with immune infiltration and oxidative stress in degenerative IVD tissues.

Herein, based on the differential analysis, WGCNA, and immune infiltration results, we finally determined four hub genes, namely, CYP1A1, MMP1, CCND1, and NQO1, which suggested tight associations with the progression of IDD. The functional enrichment annotations of DEOSGs further helped us realize the potential mechanisms of IDD that oxidative stress responses, xenobiotic stimulus, ferroptosis, and metabolism of cytochrome

10.3389/fimmu.2023.1090637

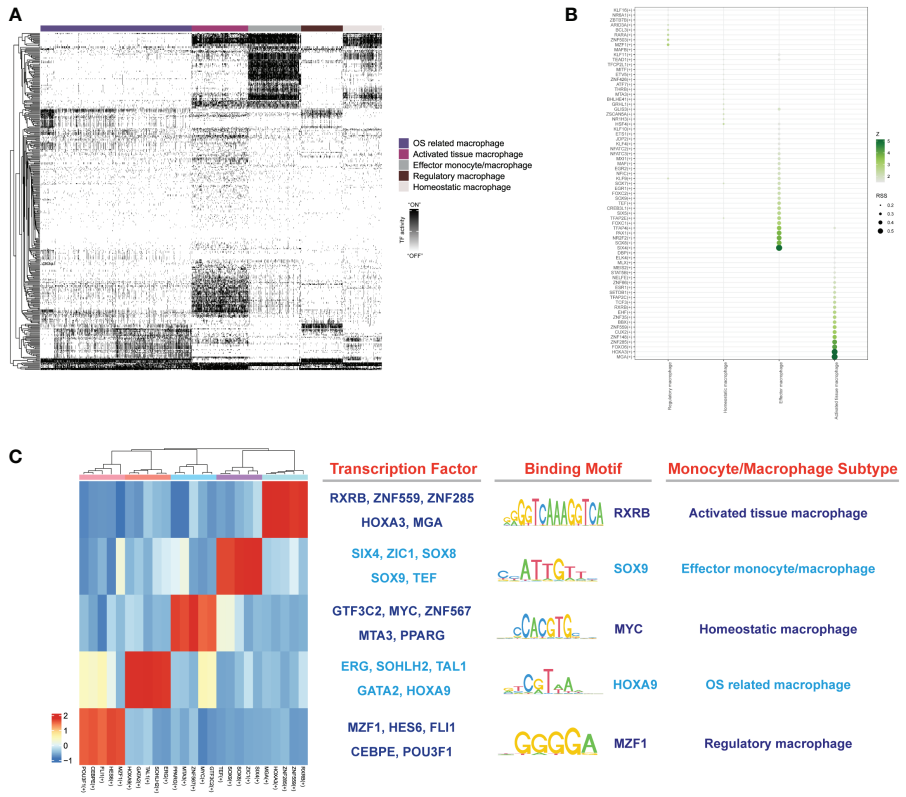

FIGURE 10
(A) The heatmap reveals binary regulon activities analyzed with SCENIC in each subtype of macrophage; "ON" indicated active regulons and "OFF" indicated inactive regulons. **(B)** Hub TFs calculated by calcRSS algorithm. **(C)** The heatmap displays the identified regulon modules for each macrophage subtype, along with representative transcription factors, corresponding binding motifs, and associated cell types.

P450 were mainly involved in the pathological processes of IDD. We previously discovered that lipid-metabolism gene CYP1B1 from blood tissues could promote the development of IDD through immune infiltration (59); this study further found that CYP1A1 behaved OS-related functions in IDD. The characteristic feature of cytochrome P450 (CYPs) enzyme could produce H_2O_2 directly or indirectly *via* superoxide anions, which were also known as "NADPH oxidase" activity. H_2O_2 produced by CYPs could lead to the accumulation of cytotoxic ROS, which thereby impairs cell functions and causes tissue damage (60). This is the first time that the essential roles of CYPs family with oxidative stress and immune responses were connected with the pathological process of IDD, which were worth of subsequent in-depth research. Existed studies have reported the essential roles of MMPs family and their inhibitors screening in the progression of IDD, among which MMP1 may participate partially through OS-related functions and inflammatory reactions (61, 62). NQO1 served as antioxidant genes and played essential roles in ameliorating inflammatory responses, reticulum stress, and apoptosis of degenerative NP cells, which were partially regulated by the antioxidant transcription factor Nrf2 (14, 63).

According to the immune infiltration analysis based on bluk-RNA seq, Tregs, plasma cells, and monocytes/macrophages were aberrantly activated in the progression of IDD. The results of the significant changes in immune cells by immune infiltration analysis could give us evidence in the following focused research by scRNA-seq. The immune infiltration analysis is a developed algorithm based on gene expression. The 22 immune cell types have already been determined since the algorithm was developed. Thus, single-cell results further verified the above findings that different immune cell infiltrations occurred in the early stage of IDD.

The number of neutrophils increased with the degenerative stages, which also played essential roles in OS-related functions. This study further intuitively demonstrated the importance of neutrophils infiltration in mediating the development of IDD from the single-cell level, which confirmed our previous deduction that neutrophils could arrive and accumulate in degenerative IVD through blood vessels and acted directly on NP cells by releasing inflammatory factors, thereby undermining the immune privilege of IVD (59). G-MDSC was widely defined as immature neutrophils, with immunosuppressive functions that inhibit T-cell activation and ROS production, which has been widely studied in neoplasms, acting as a suppressor of anti-tumor immune response (64–67). The numbers of G-MDSC were found to be decreased in late degenerative IVD, and the potential protective roles of G-MDSC have been reported by Tu et al. in IDD (25). This study further determined that this protective process may be achieved by reducing the levels of oxidative stress. In addition, GMP also possessed low levels of OS-related functions, and the numbers were found to be decreased in late degenerative IVD, which may behave similar protective roles with immunosuppressive functions to ameliorate IDD as G-MDSC did. Moreover, we observed that endothelial cells also possessed high OS scores except monocytes/macrophages in

IDD. Endothelial cells are vascular, non-conventional immune cells that participated in angiogenesis, homeostasis, and the regulation of vascular tone; they are also essential and active components of immune responses (68, 69). Existing studies have reported the OS functions of endothelial cells in different diseases like sepsis, acute inflammation, and neurovascular defects of the retina, and that OS activated endothelial cells, changed multiple endothelial cells functions, and promoted pro-inflammatory, pro-coagulant, and pro-adhesive phenotype (70, 71). Our findings further indicated the essential connections between endothelial cells and the progression of IDD on OS levels.

The inaccurate classification of monocytes/macrophages subtypes by immune infiltration analysis resulted in the module difference in WGCNA network. Based on the high levels of OS-related functions of monocytes/macrophages in degenerative IVD, we further extracted monocytes/macrophages to explore the longitudinal alterations of distinct phenotypes during the different degenerative stages. Monocytes/macrophages are heterogeneous, and their phenotypes and functions are regulated by the surrounding microenvironment. The detailed classification of monocytes/macrophages could help better understand the different roles in the progression of diseases. Lee et al. have conducted longitudinal approach based on scRNA-seq to reveal the sequential changes of macrophages during severe acute respiratory syndrome coronavirus 2 (SARS-CoV-2) infection, which classified nine distinct macrophage subtypes and exhibited exciting results in the progression of SARS-CoV-2 infection (42). In our study, we have provided the evidence that monocytes/macrophages infiltration occurred in the early degenerative stage of IVD. Importantly, we depicted the longitudinal alterations of monocytes/macrophages and NP cells heterogeneity within degenerative IVD tissue based on single-cell level. We discovered and annotated five different subpopulations among monocytes/macrophages, with their sequential and subtypes alterations from early to late degenerative IVD. There remained complex monocyte/macrophage subtypes in early degenerative IVD, with different pro- or anti-inflammation functions. We also observed distinctive and stepwise evolution lineage among those subtypes. The predominant dynamic changes in the transcriptome mainly involved effector monocytes/macrophages and regulatory macrophages, which drastically decreased at degenerative grade III, suggesting that these populations experienced shift of transcriptome features towards other populations. Based on the CytoTRACE and pseudo-time trajectory analysis, we could infer that OS-related macrophage clusters were derived from regulatory macrophage clusters, which also indicated that OS-related macrophages increased with degenerative stages, while with insufficient infiltration at early stage. The effector monocytes/macrophages could further shift into two subtypes of homeostatic and activated tissue macrophages with distinctive functions, demonstrating that although inflammation-related macrophages increased in severe degenerative IVD, protective macrophages also existed against inflammation.

Increasing studies have reported not only that blood cells are composed of endothelial cells but also that vascular-like structures could be generated by non-endothelial cells (18, 72). Macrophages are reported to regulate blood vessels growth, the new blood vessels could serve as passage for macrophages into ECM, and the interactions between macrophages and NP cells are potentially proangiogenic in degenerative IVD (73–76). Notably, Barnett et al. have demonstrated the significant finding that macrophages could form vascular mimicry channels in tumors or other hypoxic environments the same as cancer stem cells did (77). In intercellular crosstalk signaling network, we found that regulatory and OS-related macrophages mainly participated in VEGF signaling pathway, which may behave similar functions in degenerative IVD tissues, to form vascular mimicry channels themselves. The identification of this novel type of channels may help understand the development of IDD. Targeted clearance of regulatory macrophages from early stage and OS-related macrophages from late stage could reduce the angiogenesis. In addition, we also analyzed and reported other regulatory pathways between different monocyte/macrophage subtypes and NPPC or NP cells. These potential signaling pathways may provide personalized treatment targeting different subtypes through certain interactions.

Finally, a group of specific TFs were identified with distinct functions in different monocyte/macrophage subtypes, together with their corresponding binding motifs. Some TFs were reported to behave different functions to modulate the homeostasis of NP cells. SOX9 played essential roles in chondrocytes differentiation. Existing study demonstrated that the deletion of SOX9 could cause severe IDD characterized by apoptosis and matrix remodeling (78, 79). PPARG was reported to regulate osteoclast and osteoblast differentiation. Baroi et al. have already reported its essential roles in the treatment of osteoporosis (80). MTA3 is a latest identified member in the MTA family. It usually downregulates the expression of SNAIL, a major regulator of epithelium–mesenchymal transition, and subsequently inhibits the invasion and migration of tumor cells (81). More relationships between MTA3 and IDD are worth discovering. Zhang et al. have confirmed the negative correlations of HOXA9 and IDD, in which HOXA9 played pivotal roles in FAS-mediated apoptosis of NP cells and HOXA9 could serve as potential therapeutic target in the treatment of IDD (82). FLI1 belongs to the Ets transcription factor family and is highly expressed in activated immune cells, which modulates the development of monocytes/macrophages by the C-terminal transcriptional activation domain. In addition, FLI1 also participated in affecting the function of immune cells by regulating cytokines and chemokines (83, 84). These identified TFs made it possible for cell therapies to mitigate the IDD. Through the TFs, we can definitely advance the development of NP cell homeostasis by combining the potential TFs and downstream therapeutic targets in specific monocyte/macrophage subtypes, within the degenerative IVD microenvironment.

Collectively, this study combined transcriptome and single-cell sequencing results to systematically decipher the difference in OS-related functions of different cell populations within degenerative IVD tissues and further depicted the longitudinal alterations of immune cells, especially monocytes/macrophages in different degenerative stages of IDD. These findings further enhanced the understanding of the distinct functions of monocyte/macrophage subtypes during IDD progression. This study proposed that specific therapy strategies need to be formulated on different stages of IDD, thereby providing personalized treatment based on specific monocyte/macrophage subtypes.

Data availability statement

The original contributions presented in the study are included in the article/Supplementary Material. Further inquiries can be directed to the corresponding authors.

Author contributions

This study was completed with teamwork. Each author had made corresponding contribution to the study. Conceived the idea: WL, MY, BG, and ZL. Manuscript draft: WL, and YZ. Technical support on analysis: WL, YZ, ZH and CL. Downloaded and collected data: WL, YZ, BG, MY, ZH, LZ and BY. Analyzed the data: WL, YZ, BG, MY, and ZL. Prepared figures: WL, YZ, ZH, LZ, and YW. Redressed the manuscript: all authors. All authors contributed to the article and approved the submitted version.

Funding

This study was supported by grants from the National Natural Science Foundation of China (NSFC, 82072475, 82172475, 82260443); "the National Science Fund for Excellent Young Scholars" (NSFC, 82222046); and Flow Station of Principal Investigator Program (2022HYPI06, 2021HYPI05).

Acknowledgments

We thank Dr. Jiangming Zeng (University of Macau) and all the members of his bioinformatics team, biotrainee, for generously sharing their experiences and codes. We also thank the "Xiyoucloud" Supercomputing Technology Co. Ltd for providing the cloud supercomputing server.

Conflict of interest

The authors declare that the research was conducted in the absence of any commercial or financial relationships that could be construed as a potential conflict of interest.

Publisher's note

Supplementary material

The Supplementary Material for this article can be found online at: https://www.frontiersin.org/articles/10.3389/fimmu.2023.1090637/full#supplementary-material

SUPPLEMENTARY FIGURE 1
(A) PCA heatmap illustrated expression patterns of the top 30 significantly correlated genes in each component. Colors represented gene expression levels and PC_1 to PC_10 were displayed. **(B)** Dot plots illustrated the significantly correlated genes in each component, and PC_1 to PC_4 were displayed. **(C)** Red dots represented highly variable genes and black dots represented non-variable genes. The top 10 most variable genes were marked. **(D)** UMAP plot displayed the dot distribution after samples integration. **(E)** The expression components situation of each immune cell. **(F)** The enrichment fraction of 22 types of immune infiltrating cells in each sample.

SUPPLEMENTARY FIGURE 2
The Comparison of OS-related functions between early and late stage in different cell populations.

SUPPLEMENTARY FIGURE 3
(A) UMAP plot of macrophage subtypes, colored according to clusters. **(B)** Proportion of each macrophage population at different degeneration stages. **(C)** UMAP plot with color density reflecting distribution of macrophage subpopulations at different degeneration stages. **(D)** UMAP plot illustrating normalized expression of markers of macrophage subtypes.

SUPPLEMENTARY TABLE 1
The OS-related genes obtained from GeneCards database.

SUPPLEMENTARY TABLE 2
The DEGs that were identified for lineage progression from regulatory macrophage toward OS related macrophage.

References

1. Andersson GB. Epidemiological features of chronic low-back pain. *Lancet* (1999) 354(9178):581–5. doi: 10.1016/S0140-6736(99)01312-4

2. Li W, Zhang S, Wang D, Zhang H, Shi Q, Zhang Y, et al. Exosomes immunity strategy: A novel approach for ameliorating intervertebral disc degeneration. *Front Cell Dev Biol* (2021) 9:822149. doi: 10.3389/fcell.2021.822149

3. Rigal J, Léglise A, Barnetche T, Cogniet A, Aunoble S, Le Huec JC. Meta-analysis of the effects of genetic polymorphisms on intervertebral disc degeneration. *Eur Spine J* (2017) 26(8):2045–52. doi: 10.1007/s00586-017-5146-z

4. Francisco V, Pino J, González-Gay MÁ, Lago F, Karppinen J, Tervonen O, et al. A new immunometabolic perspective of intervertebral disc degeneration. *Nat Rev Rheumatol* (2022) 18(1):47–60. doi: 10.1038/s41584-021-00713-z

5. Yang S, Zhang F, Ma J, Ding W. Intervertebral disc ageing and degeneration: The antiapoptotic effect of oestrogen. *Ageing Res Rev* (2020) 57:100978. doi: 10.1016/j.arr.2019.100978

6. Le Maitre CL, Pockert A, Buttle DJ, Freemont AJ, Hoyland JA. Matrix synthesis and degradation in human intervertebral disc degeneration. *Biochem Soc Trans* (2007) 35(Pt 4):652–5. doi: 10.1042/BST0350652

7. Sun Z, Liu B, Luo Z-J. The immune privilege of the intervertebral disc: Implications for intervertebral disc degeneration treatment. *Int J Med Sci* (2020) 17(5):685–92. doi: 10.7150/ijms.42238

8. Vergroesen PPA, Kingma I, Emanuel KS, Hoogendoorn RJW, Welting TJ, van Royen BJ, et al. Mechanics and biology in intervertebral disc degeneration: A vicious circle. *Osteoarthritis Cartilage.* (2015) 23(7):1057–70. doi: 10.1016/j.joca.2015.03.028

9. Akanji MA, Rotimi DE, Elebiyo TC, Awakan OJ, Adeyemi OS. Redox homeostasis and prospects for therapeutic targeting in neurodegenerative disorders. *Oxid Med Cell Longev* (2021) 2021:9971885. doi: 10.1155/2021/9971885

10. Nandi A, Yan L-J, Jana CK, Das N. Role of catalase in oxidative stress- and age-associated degenerative diseases. *Oxid Med Cell Longev* (2019) 2019:9613090. doi: 10.1155/2019/9613090

11. Ramkumar V, Mukherjea D, Dhukhwa A, Rybak LP. Oxidative stress and inflammation caused by cisplatin ototoxicity. *Antioxidants (Basel).* (2021) 10(12):1919. doi: 10.3390/antiox10121919

12. Shiau J-P, Chuang Y-T, Tang J-Y, Yang K-H, Chang F-R, Hou M-F, et al. The impact of oxidative stress and AKT pathway on cancer cell functions and its application to natural products. *Antioxidants (Basel)* (2022) 11(9):1845. doi: 10.3390/antiox11091845

13. Zhao Y, Li W, Zhang K, Xu M, Zou Y, Qiu X, et al. Revealing oxidative stress-related genes in osteoporosis and advanced structural biological study for novel natural material discovery regarding MAPKAPK2. *Front Endocrinol* (2022) 13:1052721. doi: 10.3389/fendo.2022.1052721

14. Xiang Q, Zhao Y, Lin J, Jiang S, Li W. The Nrf2 antioxidant defense system in intervertebral disc degeneration: Molecular insights. *Exp Mol Med* (2022) 54(8):1067–75. doi: 10.1038/s12276-022-00829-6

15. Kang L, Liu S, Li J, Tian Y, Xue Y, Liu X. Parkin and Nrf2 prevent oxidative stress-induced apoptosis in intervertebral endplate chondrocytes *via* inducing mitophagy and anti-oxidant defenses. *Life Sci* (2020) 243:117244. doi: 10.1016/j.lfs.2019.117244

16. Zhang Z, Lin J, Tian N, Wu Y, Zhou Y, Wang C, et al. Melatonin protects vertebral endplate chondrocytes against apoptosis and calcification *via* the Sirt1-autophagy pathway. *J Cell Mol Med* (2019) 23(1):177–93. doi: 10.1111/jcmm.13903

17. Tang P, Chen W-X, Gao H-L, Dai J-Y, Gu Y, Xie Z-A, et al. Small molecule inhibitor of TAK1 ameliorates rat cartilaginous endplate degeneration induced by oxidative stress *in vitro* and in vivo. *Free Radic Biol Med* (2020) 148:140–50. doi: 10.1016/j.freeradbiomed.2020.01.002

18. Seol D, Coleman MC, Martin JA, Song I, Jaidev LR, Salem AK, et al. Targeting oxidative stress with amobarbital to prevent intervertebral disc degeneration: Part i. *in vitro* and ex vivo studies. *Spine J* (2021) 21(6):1021–30. doi: 10.1016/j.spinee.2021.02.008

19. Feng C, Yang M, Lan M, Liu C, Zhang Y, Huang B, et al. ROS: Crucial intermediators in the pathogenesis of intervertebral disc degeneration. *Oxid Med Cell Longev* (2017) 2017:5601593. doi: 10.1155/2017/5601593

20. Navin NE. The first five years of single-cell cancer genomics and beyond. *Genome Res* (2015) 25(10):1499–507. doi: 10.1101/gr.191098.115

21. Tanay A, Regev A. Scaling single-cell genomics from phenomenology to mechanism. *Nature.* (2017) 541(7637):331–8. doi: 10.1038/nature21350

22. Ziegenhain C, Vieth B, Parekh S, Reinius B, Guillaumet-Adkins A, Smets M, et al. Comparative analysis of single-cell RNA sequencing methods. *Mol Cell* (2017) 65(4):331–8. doi: 10.1016/j.molcel.2017.01.023

23. Morgan DM, Shreffler WG, Love JC. Revealing the heterogeneity of CD4 T cells through single-cell transcriptomics. *J Allergy Clin Immunol* (2022) 150(4):748–55. doi: 10.1016/j.jaci.2022.08.010

24. van der Wijst MGP, Brugge H, de Vries DH, Deelen P, Swertz MA, Franke L. Single-cell RNA sequencing identifies celltype-specific cis-eQTLs and co-expression QTLs. *Nat Genet* (2018) 50(4):493–7. doi: 10.1038/s41588-018-0089-9

25. Tu J, Li W, Yang S, Yang P, Yan Q, Wang S, et al. Single-cell transcriptome profiling reveals multicellular ecosystem of nucleus pulposus during degeneration progression. *Adv Sci (Weinh).* (2022) 9(3):e2103631. doi: 10.1002/advs.202103631

26. Ling Z, Liu Y, Wang Z, Zhang Z, Chen B, Yang J, et al. Single-cell RNA-seq analysis reveals macrophage involved in the progression of human intervertebral disc degeneration. *Front Cell Dev Biol* (2021) 9:833420. doi: 10.3389/fcell.2021.833420

27. Li W, Zhang S, Zhao Y, Wang D, Shi Q, Ding Z, et al. Revealing the key MSCs niches and pathogenic genes in influencing CEP homeostasis: A conjoint analysis of single-cell and WGCNA. *Front Immunol* (2022) 13:933721. doi: 10.3389/fimmu.2022.933721

28. Gan Y, He J, Zhu J, Xu Z, Wang Z, Yan J, et al. Spatially defined single-cell transcriptional profiling characterizes diverse chondrocyte subtypes and nucleus pulposus progenitors in human intervertebral discs. *Bone Res* (2021) 9(1):37. doi: 10.1038/s41413-021-00163-z

29. Gao B, Jiang B, Xing W, Xie Z, Luo Z, Zou W. Discovery and application of postnatal nucleus pulposus progenitors essential for intervertebral disc homeostasis and degeneration. *Adv Sci (Weinh).* (2022) 9(13):e2104888. doi: 10.1002/advs.202104888

30. Wójcik P, Gęgotek A, Žarković N, Skrzydlewska E. Oxidative stress and lipid mediators modulate immune cell functions in autoimmune diseases. *Int J Mol Sci* (2021) 22(2):723. doi: 10.3390/ijms22020723

31. Kazezian Z, Gawri R, Haglund L, Ouellet J, Mwale F, Tarrant F, et al. Gene expression profiling identifies interferon signalling molecules and IGFBP3 in human degenerative annulus fibrosus. *Sci Rep* (2015) 5:15662. doi: 10.1038/srep15662

32. Tam V, Chen P, Yee A, Solis N, Klein T, Kudelko M, et al. DIPPER, a spatiotemporal proteomics atlas of human intervertebral discs for exploring ageing and degeneration dynamics. *Elife* (2020) 9:e64940. doi: 10.7554/eLife.64940

33. Newman AM, Steen CB, Liu CL, Gentles AJ, Chaudhuri AA, Scherer F, et al. Determining cell type abundance and expression from bulk tissues with digital cytometry. *Nat Biotechnol* (2019) 37(7):773–82. doi: 10.1038/s41587-019-0114-2

34. Langfelder P, Horvath S. WGCNA: An r package for weighted correlation network analysis. *BMC Bioinf* (2008) 9:559. doi: 10.1186/1471-2105-9-559

35. Li M, Xin S, Gu R, Zheng L, Hu J, Zhang R, et al. Novel diagnostic biomarkers related to oxidative stress and macrophage ferroptosis in atherosclerosis. *Oxid Med Cell Longev* (2022) 2022:8917947. doi: 10.1155/2022/8917947

36. Zheng Y, Liu C, Ni L, Liu Z, Mirando AJ, Lin J, et al. Cell type-specific effects of notch signaling activation on intervertebral discs: Implications for intervertebral disc degeneration. *J Cell Physiol* (2018) 233(7):5431–40. doi: 10.1002/jcp.26385

37. Xu X, Wang D, Zheng C, Gao B, Fan J, Cheng P, et al. Progerin accumulation in nucleus pulposus cells impairs mitochondrial function and induces intervertebral disc degeneration and therapeutic effects of sulforaphane. *Theranostics.* (2019) 9(8):2252–67. doi: 10.7150/thno.30658

38. Wang D, He X, Wang D, Peng P, Xu X, Gao B, et al. Quercetin suppresses apoptosis and attenuates intervertebral disc degeneration *via* the SIRT1-autophagy pathway. *Front Cell Dev Biol* (2020) 8:613006. doi: 10.3389/fcell.2020.613006

39. Butler A, Hoffman P, Smibert P, Papalexi E, Satija R. Integrating single-cell transcriptomic data across different conditions, technologies, and species. *Nat Biotechnol* (2018) 36(5):411–20. doi: 10.1038/nbt.4096

40. Subramanian A, Tamayo P, Mootha VK, Mukherjee S, Ebert BL, Gillette MA, et al. Gene set enrichment analysis: A knowledge-based approach for interpreting genome-wide expression profiles. *Proc Natl Acad Sci USA* (2005) 102(43):15545–50. doi: 10.1073/pnas.0506580102

41. Yu W, Chen G, Yan J, Wang X, Zhu Y, Zhu L. Single-cell sequencing analysis reveals gastric cancer microenvironment cells respond vastly different to oxidative stress. *J Transl Med* (2022) 20(1):250. doi: 10.1186/s12967-022-03411-w

42. Lee JS, Koh J-Y, Yi K, Kim Y-I, Park S-J, Kim E-H, et al. Single-cell transcriptome of bronchoalveolar lavage fluid reveals sequential change of macrophages during SARS-CoV-2 infection in ferrets. *Nat Commun* (2021) 12(1):4567. doi: 10.1038/s41467-021-24807-0

43. Gulati GS, Sikandar SS, Wesche DJ, Manjunath A, Bharadwaj A, Berger MJ, et al. Single-cell transcriptional diversity is a hallmark of developmental potential. *Science.* (2020) 367(6476):405–11. doi: 10.1126/science.aax0249

44. Haghverdi L, Büttner M, Wolf FA, Buettner F, Theis FJ. Diffusion pseudotime robustly reconstructs lineage branching. *Nat Methods* (2016) 13(10):845–8. doi: 10.1038/nmeth.3971

45. Vento-Tormo R, Efremova M, Botting RA, Turco MY, Vento-Tormo M, Meyer KB, et al. Single-cell reconstruction of the early maternal-fetal interface in humans. *Nature.* (2018) 563(7731):347–53. doi: 10.1038/s41586-018-0698-6

46. Jin S, Guerrero-Juarez CF, Zhang L, Chang I, Ramos R, Kuan C-H, et al. Inference and analysis of cell-cell communication using CellChat. *Nat Commun* (2021) 12(1):1088. doi: 10.1038/s41467-021-21246-9

47. Aibar S, González-Blas CB, Moerman T, Huynh-Thu VA, Imrichova H, Hulselmans G, et al. SCENIC: Single-cell regulatory network inference and clustering. *Nat Methods* (2017) 14(11):1083–6. doi: 10.1038/nmeth.4463

48. Aran D, Looney AP, Liu L, Wu E, Fong V, Hsu A, et al. Reference-based analysis of lung single-cell sequencing reveals a transitional profibrotic macrophage. *Nat Immunol* (2019) 20(2):163–72. doi: 10.1038/s41590-018-0276-y

49. Giordani L, He GJ, Negroni E, Sakai H, Law JYC, Siu MM, et al. High-dimensional single-cell cartography reveals novel skeletal muscle-resident cell populations. *Mol Cell* (2019) 74(3):609–21. doi: 10.1016/j.molcel.2019.02.026

50. Thornton S, Tan R, Sproles A, Do T, Schick J, Grom AA, et al. A multiparameter flow cytometry analysis panel to assess CD163 mRNA and protein in monocyte and macrophage populations in hyperinflammatory diseases. *J Immunol* (2019) 202(5):1635–43. doi: 10.4049/jimmunol.1800765

51. Meknache N, Jönsson F, Laurent J, Guinnepain M-T, Daëron M. Human basophils express the glycosylphosphatidylinositol-anchored low-affinity IgG receptor FcgammaRIIIB (CD16B). *J Immunol* (2009) 182(4):2542–50. doi: 10.4049/jimmunol.0801665

52. Condamine T, Dominguez GA, Youn J-I, Kossenkov AV, Mony S, Alicea-Torres K, et al. Lectin-type oxidized LDL receptor-1 distinguishes population of human polymorphonuclear myeloid-derived suppressor cells in cancer patients. *Sci Immunol* (2016) 1(2):aaf8943. doi: 10.1126/sciimmunol.aaf8943

53. Perez C, Botta C, Zabaleta A, Puig N, Cedena M-T, Goicoechea I, et al. Immunogenomic identification and characterization of granulocytic myeloid-derived suppressor cells in multiple myeloma. *Blood.* (2020) 136(2):199–209. doi: 10.1182/blood.2019004537

54. Karamitros D, Stoilova B, Aboukhalil Z, Hamey F, Reinisch A, Samitsch M, et al. Single-cell analysis reveals the continuum of human lympho-myeloid progenitor cells. *Nat Immunol* (2018) 19(1):85–97. doi: 10.1038/s41590-017-0001-2

55. Liu Z, Gu Y, Chakarov S, Bleriot C, Kwok I, Chen X, et al. Fate mapping *via* Ms4a3-expression history traces monocyte-derived cells. *Cell* (2019) 178(6):1509–25. doi: 10.1016/j.cell.2019.08.009

56. Chamcheu JC, Adhami VM, Esnault S, Sechi M, Siddiqui IA, Satyshur KA, et al. Dual inhibition of PI3K/Akt and mTOR by the dietary antioxidant, delphinidin, ameliorates psoriatic features *In vitro* and in an imiquimod-induced psoriasis-like disease in mice. *Antioxid Redox Signal* (2017) 26(2):49–69. doi: 10.1089/ars.2016.6769

57. Riley KG, Pasek RC, Maulis MF, Dunn JC, Bolus WR, Kendall PL, et al. Macrophages are essential for CTGF-mediated adult β-cell proliferation after injury. *Mol Metab* (2015) 4(8):584–91. doi: 10.1016/j.molmet.2015.05.002

58. Guzik TJ, Touyz RM. Oxidative stress, inflammation, and vascular aging in hypertension. *Hypertension.* (2017) 70(4):660–7. doi: 10.1161/HYPERTENSIONAHA.117.07802

59. Li W, Ding Z, Zhang H, Shi Q, Wang D, Zhang S, et al. The roles of blood lipid-metabolism genes in immune infiltration could promote the development of IDD. *Front Cell Dev Biol* (2022) 10:844395. doi: 10.3389/fcell.2022.844395

60. Song Y-S, Annalora AJ, Marcus CB, Jefcoate CR, Sorenson CM, Sheibani N. Cytochrome P450 1B1: A key regulator of ocular iron homeostasis and oxidative stress. *Cells.* (2022) 11(19):2930. doi: 10.3390/cells11192930

61. Vo NV, Hartman RA, Yurube T, Jacobs LJ, Sowa GA, Kang JD. Expression and regulation of metalloproteinases and their inhibitors in intervertebral disc aging and degeneration. *Spine J* (2013) 13(3):331–41. doi: 10.1016/j.spinee.2012.02.027

62. Chen Q, Tang Y, Deng H, Liang B, Li H, Li Z, et al. Curcumin improves keratinocyte proliferation, inflammation, and oxidative stress through mediating the SPAG5/FOXM1 axis in an model of actinic dermatitis by ultraviolet. *Dis Markers.* (2022) 2022:5085183. doi: 10.1155/2022/5085183

63. Feng Y, Cui R, Li Z, Zhang X, Jia Y, Zhang X, et al. Methane alleviates acetaminophen-induced liver injury by inhibiting inflammation, oxidative stress, endoplasmic reticulum stress, and apoptosis through the Nrf2/HO-1/NQO1 signaling pathway. *Oxid Med Cell Longev* (2019) 2019:7067619. doi: 10.1155/2019/7067619

64. Srivastava MK, Sinha P, Clements VK, Rodriguez P, Ostrand-Rosenberg S. Myeloid-derived suppressor cells inhibit T-cell activation by depleting cystine and cysteine. *Cancer Res* (2010) 70(1):68–77. doi: 10.1158/0008-5472.CAN-09-2587

65. Veglia F, Perego M, Gabrilovich D. Myeloid-derived suppressor cells coming of age. *Nat Immunol* (2018) 19(2):108–19. doi: 10.1038/s41590-017-0022-x

66. Bronte V, Brandau S, Chen S-H, Colombo MP, Frey AB, Greten TF, et al. Recommendations for myeloid-derived suppressor cell nomenclature and characterization standards. *Nat Commun* (2016) 7:12150. doi: 10.1038/ncomms12150

67. Haile LA, von Wasielewski R, Gamrekelashvili J, Krüger C, Bachmann O, Westendorf AM, et al. Myeloid-derived suppressor cells in inflammatory bowel disease: A new immunoregulatory pathway. *Gastroenterology* (2008) 135(3):871–81. doi: 10.1053/j.gastro.2008.06.032

68. Joffre J, Hellman J, Ince C, Ait-Oufella H. Endothelial responses in sepsis. *Am J Respir Crit Care Med* (2020) 202(3):361–70. doi: 10.1164/rccm.201910-1911TR

69. Sturtzel C. Endothelial cells. *Adv Exp Med Biol* (2017) 1003:71–91. doi: 10.1007/978-3-319-57613-8_4

70. Joffre J, Hellman J. Oxidative stress and endothelial dysfunction in sepsis and acute inflammation. *Antioxid Redox Signal* (2021) 35(15):1291–307. doi: 10.1089/ars.2021.0027

71. Lenin R, Thomas SM, Gangaraju R. Endothelial activation and oxidative stress in neurovascular defects of the retina. *Curr Pharm Des* (2018) 24(40):4742–54. doi: 10.2174/1381612825666190115122622

72. Yorimitsu E, Chiba K, Toyama Y, Hirabayashi K. Long-term outcomes of standard discectomy for lumbar disc herniation: A follow-up study of more than 10 years. *Spine (Phila Pa 1976).* (2001) 26(6):652–7. doi: 10.1097/00007632-200103150-00019

73. Koike Y, Uzuki M, Kokubun S, Sawai T. Angiogenesis and inflammatory cell infiltration in lumbar disc herniation. *Spine (Phila Pa 1976).* (2003) 28(17):1928–33. doi: 10.1097/01.BRS.0000083324.65405.AE

74. Martin P, Gurevich DB. Macrophage regulation of angiogenesis in health and disease. *Semin Cell Dev Biol* (2021) 119:101–10. doi: 10.1016/j.semcdb.2021.06.010

75. Huang M, Lin Y, Wang C, Deng L, Chen M, Assaraf YG, et al. New insights into antiangiogenic therapy resistance in cancer: Mechanisms and therapeutic aspects. *Drug Resist Updat.* (2022) 64:100849. doi: 10.1016/j.drup.2022.100849

76. Andreucci E, Peppicelli S, Ruzzolini J, Bianchini F, Calorini L. Physicochemical aspects of the tumour microenvironment as drivers of vasculogenic mimicry. *Cancer Metastasis Rev* (2022) 41(4):935–51. doi: 10.1007/s10555-022-10067-x

77. Barnett FH, Rosenfeld M, Wood M, Kiosses WB, Usui Y, Marchetti V, et al. Macrophages form functional vascular mimicry channels in vivo. *Sci Rep* (2016) 6:36659. doi: 10.1038/srep36659

78. Tsingas M, Ottone OK, Haseeb A, Barve RA, Shapiro IM, Lefebvre V, et al. Sox9 deletion causes severe intervertebral disc degeneration characterized by apoptosis, matrix remodeling, and compartment-specific transcriptomic changes. *Matrix Biol* (2020) 94:110–33. doi: 10.1016/j.matbio.2020.09.003

79. Haseeb A, Kc R, Angelozzi M, de Charleroy C, Rux D, Tower RJ, et al. SOX9 keeps growth plates and articular cartilage healthy by inhibiting chondrocyte dedifferentiation/osteoblastic redifferentiation. *Proc Natl Acad Sci USA* (2021) 118(8):e2019152118. doi: 10.1073/pnas.2019152118

80. Baroi S, Czernik PJ, Chougule A, Griffin PR, Lecka-Czernik B. PPARG in osteocytes controls sclerostin expression, bone mass, marrow adiposity and mediates TZD-induced bone loss. *Bone.* (2021) 147:115913. doi: 10.1016/j.bone.2021.115913

81. Ma L, Yao Z, Deng W, Zhang D, Zhang H. The many faces of MTA3 protein in normal development and cancers. *Curr Protein Pept Sci* (2016) 17(8):726–34. doi: 10.2174/1389203717666160401150122

82. Zhang DAY, Wang Z-J, Yu Y-B, Zhang Y, Zhang X-X. Role of microRNA-210 in human intervertebral disc degeneration. *Exp Ther Med* (2016) 11(6):2349–54. doi: 10.3892/etm.2016.3176

83. Suzuki E, Williams S, Sato S, Gilkeson G, Watson DK, Zhang XK. The transcription factor fli-1 regulates monocyte, macrophage and dendritic cell development in mice. *Immunology.* (2013) 139(3):318–27. doi: 10.1111/imm.12070

84. He Y-S, Yang X-K, Hu Y-Q, Xiang K, Pan H-F. Emerging role of Fli1 in autoimmune diseases. *Int Immunopharmacol.* (2021) 90:107127. doi: 10.1016/j.intimp.2020.107127

frontiers | Frontiers in Immunology

TYPE Review
PUBLISHED 14 February 2023
DOI 10.3389/fimmu.2023.1080310

OPEN ACCESS

EDITED BY
Yanan Ma,
Memorial Sloan Kettering Cancer Center, United States

REVIEWED BY
Mengmeng Jin,
Rutgers, The State University of New Jersey, United States
Shiping Lu,
Tulane University, United States
Siyang Hao,
Bristol Myers Squibb, United States

*CORRESPONDENCE
Sujie Jia
sujiejia@126.com

SPECIALTY SECTION
This article was submitted to Inflammation, a section of the journal Frontiers in Immunology

RECEIVED 26 October 2022
ACCEPTED 09 January 2023
PUBLISHED 14 February 2023

CITATION
Yang S, Zhao M and Jia S (2023) Macrophage: Key player in the pathogenesis of autoimmune diseases. *Front. Immunol.* 14:1080310. doi: 10.3389/fimmu.2023.1080310

Macrophage: Key player in the pathogenesis of autoimmune diseases

Shuang Yang[1], Ming Zhao[1,2,3] and Sujie Jia[4]*

[1]Dapartment of Dermatology, Hunan Key Laboratory of Medical Epigenomics, The Second Xiangya Hospital, Central South University, Changsha, Hunan, China, [2]Institute of Dermatology, Chinese Academy of Medical Sciences and Peking Union Medical College, Nanjing, China, [3]Key Laboratory of Basic and Translational Research on Immune-Mediated Skin Diseases, Chinese Academy of Medical Sciences, Nanjing, China, [4]Department of Pharmacy, Chinese Academy of Medical Sciences and Peking Union Medical College, Nanjing, China

The macrophage is an essential part of the innate immune system and also serves as the bridge between innate immunity and adaptive immune response. As the initiator and executor of the adaptive immune response, macrophage plays an important role in various physiological processes such as immune tolerance, fibrosis, inflammatory response, angiogenesis and phagocytosis of apoptotic cells. Consequently, macrophage dysfunction is a vital cause of the occurrence and development of autoimmune diseases. In this review, we mainly discuss the functions of macrophages in autoimmune diseases, especially in systemic lupus erythematosus (SLE), rheumatic arthritis (RA), systemic sclerosis (SSc) and type 1 diabetes (T1D), providing references for the treatment and prevention of autoimmune diseases.

KEYWORDS

macrophage, systemic lupus erythematosus, rheumatic arthritis, systemic sclerosis, type 1 diabetes

1 Introduction

According to whether tissues and organs are targeted by the damaging immune response, autoimmune diseases classified into systemic autoimmune disease, such as systemic lupus erythematosus (SLE) and systemic sclerosis (SSc) and rheumatoid arthritis (RA), or organ-specific autoimmune diseases, such as thyroid disease, type 1 diabetes (T1D), myasthenia gravis and multiple sclerosis (1, 2). The autoimmune diseases are clinically diverse but share a fundamental etiology: the form of self-reactive antibodies, presence of self-reactive T cells, and activation of the innate immune system (3). Although the exact pathogenesis remains unclear, it is interesting to note that genetic, immunological, hormonal and environmental factors are important triggers for autoimmune diseases (4).

However, it is difficult to precisely inhibit the abnormal immunity activation triggered by pathogenic factors. The current treatment of autoimmune diseases is limited and relatively conservative, which mainly depends on the overall inhibition of the immune response.

However, blindly suppressing the immune response can cause inevitable side effects such as infection. Therefore, there is an urgent need to understand the pathological mechanism that causes the initiation and development of autoimmune diseases so as to provide new ideas for the prevention and treatment of autoimmune diseases.

The innate immune system exerts immune function independently of antigens, which form the body's immune defense system interacting with the adaptive immune system. Abnormal innate immune response is a significant reason for the breakdown of autoimmune tolerance, which is closely related to the occurrence and development of autoimmune diseases (5). Macrophage is a crucial part of the innate immune system and participates in almost every biological process such as tissue homeostasis, resisting infection, repairing after infection, metabolism and inflammation, affecting the body's development and immune response (6, 7). This review summarizes the impaired functions and abnormal macrophage activation and their roles in the pathogenesis of autoimmune diseases showed in Figure 1, especially in SLE, RA, SSc and T1D. In addition, the potential value of macrophages in the treatment and prevention of autoimmune diseases is also summarized.

2 Macrophage

2.1 The origin of macrophages

It has been universally accepted that macrophages in tissues are differentiated from monocytes that originate in bone marrow (8). However, studies in recent years have found that monocytes are not the only source of macrophages. Tissue macrophages are also derived from the yolk sac and fetal liver, which have self-renewal properties independent of monocyte recruitment (9, 10). According to the tissue distribution, macrophages can be divided into alveolar macrophages, intestinal macrophages, osteoclasts in bone, microglia in the brain, Kupffer cells in the liver, Langerhans cells in the epidermis (10). Secondary lymphoid organs also have distinct macrophages, including marginal zone macrophages (MZMs) and metallophilic macrophages in the spleen, which involved in clearance of apoptotic cell and tolerance to auto-antigens (11). It is worth noting that microglia and partial Langerhans cells are derived from yolk sac progenitor cells as shown by pedigree tracing experiments. In contrast, macrophages in other tissues, such as intestinal lamina propria and dermis, are mainly derived from hematopoietic stem cells (12–16). Macrophages are, therefore, key tissue sentinel cells that react to tissue-specific signals, while retaining the ability to execute physiological functions such as phagocytes. During chronic inflammation such as autoimmune diseases, tissue-resident macrophages fail to solve aggravated inflammation that leads to immune system abnormal activation and damage. And peripheral monocytes are recruited and differentiated into macrophages non-homeostatically in combination with injury-associated signals including pro-inflammatory cytokines, which are further activated and participated in the body's immune responses (17, 18). The tissue-resident macrophages participate jointly in protecting tissue homeostasis, and form the first line of defense against invading pathogens. Miriam. et al. considered that embryonically derived and monocyte-derived tissue-resident macrophages are likely to promote the development of the disease through the maintenance of tissue homeostasis through phagocytosis of cell fragments, resistance to pathogen invasion, while recruited monocyte-derived macrophages by disease-associated signals drives disease progression (19). Similarly, recruited monocyte-derived macrophage also plays an important role in autoimmune related diseases. For example, infiltrated macrophages, especially proliferating macrophages was seen in glomerulonephritis from patients with lupus, which may be a potential diagnostic and prognostic indicator for renal injury (20).

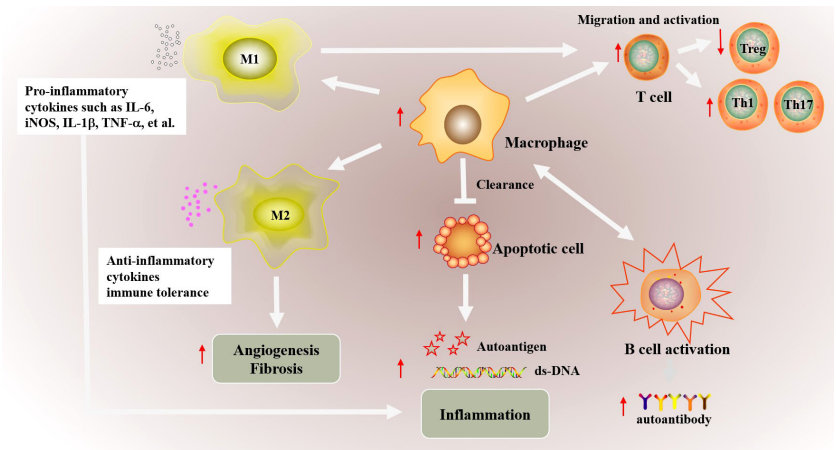

FIGURE 1
The possible abnormal macrophage activation in autoimmune diseases. The phagocytic function of macrophages is weakened in autoimmune diseases, which inhibits the clearance of apoptotic cells. Increased apoptotic cells promotes the production of autoimmune antigens and antibody, and further exacerbates inflammatory inflammation. In addition, macrophages promote the migration and abnormal activation of T cells including increased Th1/Th17 differentiation and downregulated Treg differentiation, and ultimately cause abnormal activation of B cells. Besides, the imbalance of M1/M2 macrophages also involved in autoimmune. Abnormal M1 macrophage activation promotes the production of proinflammatory cytokines such as IL-6, iNOS, TNF-α and IL-1β, which promote inflammation in targeted organs. Decreased M2 polarization inhibited the production of anti-inflammatory cytokines and the immune tolerance. Besides, abnormal M2 macrophage polarization also affects vascular proliferation, fibrosis in autoimmune disease such as SSc.

Ly6C is a marker for circulating monocytes in mice. Different monocyte subpopulations Ly6C^{hi} and Ly6C^{lo} exist in mice, which express different adhesion molecule and chemokine receptor and gene expression profile. Response to inflammatory signals Ly6C^{hi} monocytes could rapidly infiltrate in inflamed tissues mostly dependent on chemokine receptors C-C motif chemokine receptor 2 (CCR2), CCR6 and CCR8 and results in enhanced liver fibrosis (21). Inhibiting migration of blood monocyte into liver alleviated macrophage infiltration in liver, and decreased pro-inflammatory cytokines such as interferon gamma (IFNγ), IL-6 expression in chronic hepatic injury (22). Besides, inhibiting monocyte recruitment by blocking C-C motif chemokine ligand 24 (CCL24) or CCL2 may be an appealing novel therapy to limit fibrotic manifestations of SSc (23).

The complex origin of macrophages has caused great difficulties in the study of macrophage functions in autoimmune diseases. Although the construction of mice with myeloid knockout has brought a lot of convenience for the study of macrophages *in vivo*, it also has certain limitations. On one hand, there are many kinds of myeloid cells, and it is difficult to accurately study the function of a single macrophage. On the other hand, macrophages in different tissue are heterogeneous and plastic, showing different morphologies and surface molecules. With the development of scientific research, especially in flow cytometry and single cell sequencing technology, the macrophage markers in different tissues are gradually discovered, and the research of macrophages ushers in new opportunities and challenges. At present, the studies about macrophage from different sources is limited, and mostly current studies focus on the abnormal function and mechanism of macrophages infiltrated in targeted organs and tissues. How to specifically distinguish unbalanced macrophages, specially manufacture macrophages that promote disease, and supplement and maintain tissue stable macrophages are the key and difficult points in autoimmune disease research.

2.2 Regulation in innate and adaptive immunity

Macrophages are vital participant of innate immunity, which recognize and effectively respond to invading pathogens, thus providing an early defense against external attack. Pattern recognition receptors (PRRs) on the surfaces of macrophage including toll-like receptors (TLRs) and the NOD-like receptors (NLRs) recognize pathogen-associated molecular patterns (PAMPs) and endogenous danger-associated molecular patterns (DAMPs) presented in the invaders and promote macrophage activation. Macrophages further release antimicrobial mediators to target the invading pathogen, chemokines to recruit immune cells to the inflammatory site, and pro-inflammatory cytokines to aggravate further inflammation, and even induce the adaptive immune response for the particular invading pathogen. Besides, macrophage forms a bridge connecting innate and adaptive immunity by presenting endogenous or exogenous antigen. It has been well known that antigen cross-presentation is crucial for initiating of adaptive immune responses against cancer, infection and immune tolerance. During this process, antigen-presenting cells (APCs) present intracellular and extracellular peptides derived from ingested antigens on primary histocompatibility complex class I (MHCI) protein complex to T lymphocytes (24). Although the cross-presentation of antigens by macrophages is not understood as well as that by dendritic cells (DCs), it is becoming clear that the cross-presentation by macrophages especially in spleen, liver and lymph nodes may help activate CD8$^+$ T lymphocytes (25).

Macrophage can participate in antigen presentation to Th1 cells and proliferation of T cells by surface co-expression molecules CD86 and MHCII, which indicate the significant role of the macrophage in the development of cancer, autoimmunity and viral infections (26–29). The CD8$^+$ T cells in mice with spontaneous autoimmune peripheral neuropathy (APN) exhibit an effector/memory phenotype required for the disease initiation. However, only effector/memory CD8$^+$ T (CD8$^+$ TEM) cells are not sufficient to induce autoimmune-mediated peripheral neuropathy and macrophages are additionally required (30). The early depletion of regulatory T cells (Tregs) in mice with acute cardiac injury enhances the inflammatory activation of macrophages by increasing the production of IFN-γ, which restrains muscle regeneration (31). Human macrophages activated by C1q can inhibit the T helper (Th) 17 and Th1 but promote Treg proliferation, orchestrating the adaptive immune system to avoid autoimmunity (32). Hence, the role of macrophage in connecting innate/adaptive immunity provides opportunities to prevent disease onset, reduce relapses and develop new therapeutic strategies. Intervening macrophage-T cell communication signals to prevent excessive activation of T cells may be an important research direction in the treatment of autoimmune diseases

2.3 Phagocytic, efferocytosis and secretory functions

Phagocytosis is an essential process for the uptake of particulate matter, including microbes and dying cells. Dying cells can expose and secrete signals that attract phagocytes and promote their phagocytosis. Several studies have shown that macrophage phagocytosis is affected by a variety of signaling pathways including TLRs (26). Reactive oxygen species (ROS) generated by the nicotinamide adenine dinucleotide phosphate oxidases (NADPH oxidase-2, also known as NOX2) in macrophages is dispensable for phagocytosis (33). The liver X receptors (LXRs) and the peroxisome proliferator-activated receptors (PPARs), nuclear receptor families that regulate genes involved in lipid metabolism and transport are important components of macrophage phagocytosis (34). The phagocytosis of dead and dying cells is a process known as efferocytosis, which is performed by macrophages, other immune phagocytes such as monocyte and DCs and non-phagocytes including epithelial cells. Efficient efferocytosis limits the release of intracellular PAMPs that drive inflammation and disrupting homeostatic efferocytosis can also lead to accumulation of uncleared apoptotic cells in autoimmune diseases. Efferocytosis mechanisms depends on the signaling programs depicted: chemoattractant-mediated recruitment of phagocytes, receptor-mediated recognition such as PtdSer receptor cell immunoglobulin mucin receptor 4 (TIM4), TAM family receptor tyrosine kinase receptor, engulfment of apoptotic cells, and the processing of engulfed cellular material (35). Disrupted

efferocytosis of macrophage promoted the accumulation of uncleared apoptotic or necroptosis cells in autoimmune, which is a universal feature of damaged tissues (36).

In response to exogenous danger signals or exogenous signals recognized by pattern-recognition receptors (PRRs), macrophages undergo physiological changes to initiate signal transduction cascades and result in abnormal production of chemokines, cytokines and toxic mediators, which can further enhance inflammation and contribute to autoimmune pathologies (37). The anti-inflammatory mediators by macrophages contribute to the dissolution of the inflammatory response. Cytokines such as tumor necrosis factor (TNF)-α, Interleukin (IL)-6, IL-1β, IL-12, IL-18, IL-23 and chemokines such as CXC chemokine ligands (CXCL)1, CXCL3 are secreted by macrophages, which are essential mediators and drivers of chronic inflammation and autoimmune diseases (38–40). Besides, macrophages contribute to angiogenesis by secreting proangiogenic proteases such as matrix metalloproteinases (MMP)-9 and MMP-12 (41–43). TNF-α occupies a pivotal position in RA pathogenesis. The TNF blockade reduced stromal cell activation, angiogenesis, and sustain regulatory pathways by mediating cytokine and chemokine and MMPs expression. And IL-6 signaling pathway promotes T cell activation and migration by regulating chemokine expression (44). In addition to clearing dead cells, macrophages significantly mediate wound healing and tissue homeostasis by producing anti-inflammatory molecules and tissue remodeling growth factors like IL-10 and transforming growth factor beta(TGF-β) (45). Cytokines including IL-6, IL-23, IL-10 and TGF-β all shaped Th17 cell differentiation placed at the center of autoimmune inflammation (46). IL-18 contributes to Th1/2 differentiation, participate in cytotoxic T cells (CTLs) and natural killer (NK) cells activation, and ultimately IgE production from B cells (47). Besides, tissue macrophages synthesize chemokines CXCL1/CXCL2 to increase neutrophil recruitment, which is an important early step in controlling tissue infections or injury (48). Islet-resident and islet-infiltrating macrophages can exacerbate β-cell destruction by synthesizing TNF-α, IL-12, IL-1β, and NOX2-derived ROS, which mature autoreactive CD4 and CD8 T cell effector responses (49).

2.4 Regulation in metabolic processes

Macrophages are also involved in a variety of metabolic processes, including arginine metabolism and glucose metabolism, which was indicated in Figure 2. The M1 macrophages express nitric oxide synthase (NOS) to metabolize arginine into NO and citrulline, which further promotes the synthesis of downstream active nitrogen, finally facilitating inflammatory response (50, 51). In addition, M2 macrophages regulate arginine metabolism and thus regulate cell proliferation, tissue repair and inhibited inflammation by medicating polyamine/proline synthesis (52). Macrophages maintain adaptive responses to oxygen gradients and hypoxia by regulating their glucose oxidative phosphorylation, glycolysis and fatty acid oxidation (53). Based on the demands for energy and the production of specific functional-associated factors, pro-inflammatory macrophages and anti-inflammatory macrophages opt for distinct metabolic pathways upon activation. Instead of M2 macrophage, M1 macrophages carry out glycolysis and rely on fatty acid biosynthesis, and increased glycolysis causes succinate accumulation and promote inflammation by ROS/(hypoxia-inducible factor-1α) HIF-1α/IL1β pathway (54, 55). On the other hand, M2 macrophages possess a high basal mitochondrial oxygen consumption rate (OCR), carry out oxidative phosphorylation (OXPHOS), and require the induction of fatty acid oxidation (55, 56). Different fatty acid metabolism, particularly mitochondrial fatty acid oxidation in macrophage modulates inflammatory signatures and macrophage phenotype, which indicated the vital function of macrophage in hyperlipidemia-associated autoimmune diseases include psoriasis, RA, and SLE. Programmed macrophages by setting metabolic commitment for

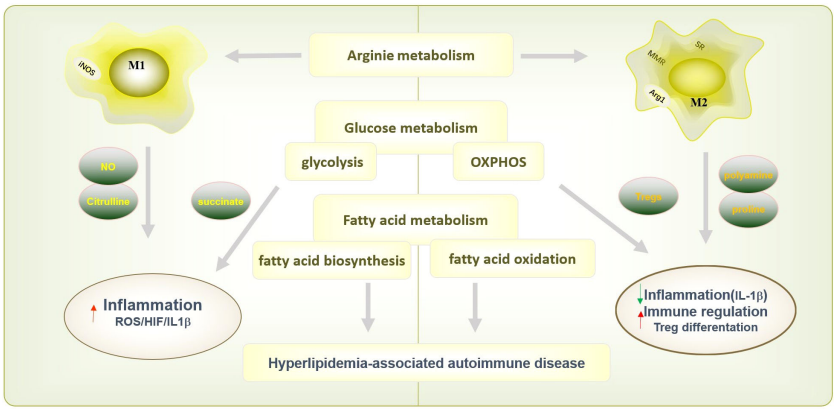

FIGURE 2
Macrophages polarization and function in metabolism processes. Macrophage are also involved in a variety of metabolic processes, including arginine metabolism glucose metabolism and fatty acid metabolism, to exert different immunological functions. The M1 macrophages express nitric oxide synthase (NOS) to metabolize arginine into NO and citrulline, which further promotes inflammatory response. Instead, M2 macrophages inhibited inflammation by medicating polyamine/proline synthesis. M1 macrophages carry out glycolysis, and causes succinate accumulation and promote inflammation by ROS/HIF-1α/IL1β pathway. And M2 macrophages carry out oxidative phosphorylation (OXPHOS) could decrease IL-1β after pro-inflammatory activation in macrophage, and promoted Treg differentiation to increase the regulatory function in immune system. M1 macrophage rely on fatty acid biosynthesis and M2 macrophage require fatty acid oxidation. The function of macrophage on fatty acid metabolism modulates inflammatory signatures and involved in hyperlipidemia-associated autoimmune diseases include psoriasis, RA, and SLE.

OXPHOS increased programmed death ligand 1 (PD-L1) expression, decreased IL-1β after pro-inflammatory activation in macrophage, and promoted Treg differentiation to increase the regulatory function in immune system (57). Moreover, macrophages resist parasite infection by regulating glutathione and redox metabolism and participate in tissue repair, tumor growth and anti-inflammatory response by regulating iron metabolism (58–60). Furthermore, the metabolites, in turn, mediate the macrophage response to inflammation. Recent study has found that citrulline levels in lipopolysaccharide (LPS) and IFNγ-stimulated macrophages are significantly reduced, which promotes inflammatory signals by activating Janus kinase 2 (JAK2)- signal transducer and activator of transcription 1 (STAT1) pathway (61). Citrulline can inhibit bacterial load in the spleen and liver of Listeria monocytogenes-infected mice by impeding pro-inflammatory macrophage activation (61).

2.5 Macrophage polarization

Macrophages display specific phenotypes and rapidly change their functions under the local microenvironment, called macrophage polarization (62). The phenotypes of macrophage polarization are generally divided into two types: one is classically activated macrophages (M1), which are pro-inflammatory and involved in the elimination of pathogens and resist infection. The other is alternative activation macrophages (M2) that are anti-inflammatory and involved in tissue repair and reconstruction (63). The Th1 cytokine, such as IFNγ or LPS, can induce M1 polarization, while Th2 cytokines, such as IL-4, can induce M2 polarization. Intracellular metabolite profiles of each macrophage activation state presented a unique metabolic signature. The 1D 1H NMR-based metabolomics identified increased adenosine triphosphate (ATP) and decreased intracellular nicotinamide adenine dinucleotide (NAD^+) in M1 macrophage, and increased adenosine diphosphate (ADP), guanosine triphosphate (GTP), adenosine monophosphate (AMP) in M2 macrophage (64). The M1 macrophages express high levels of pro-inflammatory cytokines, active nitrogen and oxygen intermediates, promote the responses of Th1 and Th17 by secreting IL12 and IL23, and have strong bactericidal and tumor-killing activity (63, 65). However, the M2 macrophages indicate high phagocytic activity and high expression of scavenger receptor (SR), macrophage mannose receptor (MMR), arginase-1(Arg-1), IL10, TGF-β, which are mainly involved in parasite containment, phagocytosis, promote tissue repair, wound healing, angiogenesis, fibrosis and immune regulation (66, 67). In fact, depending on induced agents, expressed markers, secreted mediators and functions, M2 macrophages are further classified as M2a, M2b, M2c, as well as M2d macrophages. The M2a macrophages induced by IL-4 or IL-13, also known as wound healing macrophages, can increase endocytosis activity and have immunity to parasites, tissue repair, collagen formation and fibrogenesis (68). M2b macrophages stimulated by immune complexes, TLR ligands or IL-1β, also known as regulatory macrophages, have strong anti-inflammatory and immunosuppressive effects (69). M2c macrophages induced by glucocorticoids, IL-10 or TGF-β promote phagocytosis and clearance of dead cells (70). M2d macrophages induced mainly by TLR antagonists, also known as tumor associated macrophages (TAM), can promote angiogenesis and tumor progression (71). However, M1 and M2 macrophages are the two extremes of the activation state of macrophages which cannot fully represent macrophages in the complex microenvironment *in vivo*. The dynamic balance of M1/M2 is crucial to maintain homeostasis. Response to foreign stimulation such as microbial infection or tumor, M1 macrophage is activated and promote inflammation to perform robust antimicrobial and anti-tumoral function. And to protect against the chronic inflammatory response, M1 macrophage is inhibited by regulatory mechanisms driven by anti-inflammatory function of enhanced M2 macrophages differentiation and promote tissue regeneration, angiogenesis and wound healing (72). And the imbalance contributes to the occurrence and development of many diseases including infection, tumor and autoimmune diseases (73–75). Fortunately, the high degree of plasticity allows macrophage switch from one phenotype to another depending on encountered micro-environment signals in each specific tissue, which providing a potential treatment target for autoimmune disease.

3 Macrophages in SLE

SLE is a chronic systemic autoimmune disease with diverse clinical manifestations characterized by immune system infiltration and inflammation in damaged organs covering skin, lungs, joints, kidneys and central nervous system (76). The abnormalities in the activation state of circulating and tissue macrophages in patients with SLE are crucial factors in the occurrence and development of the disease (77, 78). Depleting macrophage attenuated skin and kidney disease severity, which suggested the vital function in SLE pathogenesis (79, 80). The pro-inflammatory patrolling monocytes (PMOS) accumulated in the glomeruli in SLE patients and lupus mice are the main components of lupus glomerular or kidney inflammation (81). Emerging evidence has demonstrated that macrophage infiltration is associated with lupus nephritis in mice and humans (82, 83). Renal macrophage infiltration appears in spontaneous NZB/W nephritis and IFN-accelerated models of lupus nephritis (84). The function and numbers of MZMs are also reduced in autoimmune BXD2 mice (85). The absence of MZMs results in retention of apoptotic cell debris within the marginal zone and drives follicular Ag-transportation by marginal zone B (MZB) cells to stimulate an autoimmune response (85). The abnormal functions of macrophage in SLE are indicated in Figure 3.

The phagocytic ability of macrophages from SLE patients is weakened, which results in the production of autoantibodies and SLE-like autoimmune nephropahy (78, 85). Hence the dysfunction of macrophage phagocytosis may partly explain the gathering of apoptotic cells in the germinal center of lymph nodes in SLE patients (86). The mechanism response to the reduced clearance rate of macrophages has been widely demonstrated. It has been shown that the absence of PPARγ in macrophage cannot obtain an anti-inflammatory phenotype in the presence of apoptotic cells, finally resulting in glomerulonephritis and the autoantibodies production of nuclear Ags (87). The transcription factors Kruppel-like factor 2 (KLF2) and KLF4 also control apoptotic cells clearance program in tissue macrophage and maintain the homeostasis (88). Moreover, the increased autophagy and apoptosis in macrophage also contribute to the pathogenesis of SLE. The autophagy-related genes (*Atg5*, *Atg12* and *Beclin 1*) were significantly upregulated in the splenic and renal

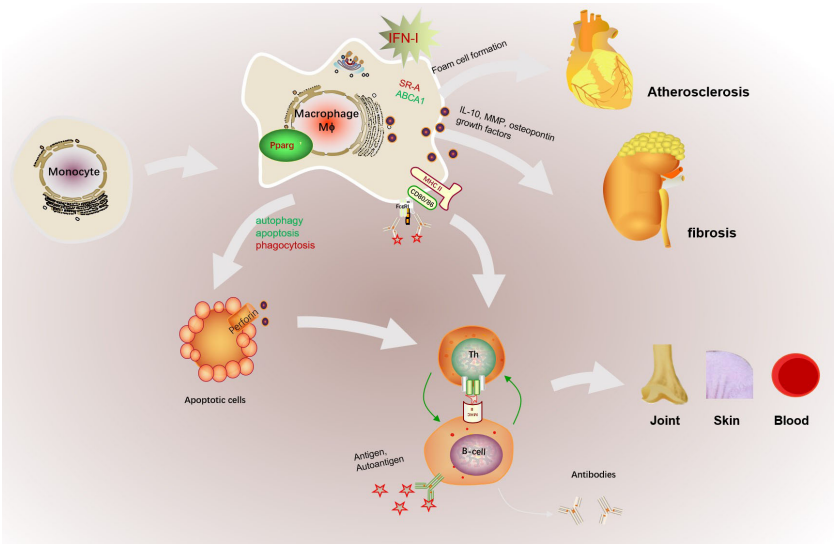

FIGURE 3
The abnormal activation of macrophage in SLE. The abnormal microenvironment in SLE patients, such as the high expressed IFN-I, promotes monocyte to recruit and differentiate into macrophages. In addition, increased antigen presentation of macrophage promotes B cell activation assisted with Th cells and further promotes the production of autoantibodies. Macrophages can also cause cardiovascular risk by promoting foam cell formation with increased SR-A and decreased ABCA1 expression. The dysfunction of macrophage phagocytosis may increase the gathered apoptotic cells and results in retention of apoptotic cell debris in SLE patients. Increased macrophage apoptosis and autophagy could contribute to autoantibody formation and organ damage by increased apoptotic load and impaired clearance of apoptotic material, finally exacerbated the production of autoantigens. Besides, macrophage infiltration the kidney promoted glomerular cell proliferation and early fibrosis by IL-10, MMP, osteopontin and growth factors. Besides, increased apoptotic cells serves as autoantigen to aggravate autoimmune reaction and may cause multiple targeted organs such as skin, joint, or blood.

macrophages in activated lymphocytes-derived DNA (ALD-DNA) induced lupus mice and in the peripheral blood mononuclear cells from SLE patients. And adoptive transfer of autophagy-suppressed macrophages alleviated lupus symptoms in SLE mice (89). Increased monocyte/macrophage apoptosis could contribute to autoantibody formation and organ damage by increased apoptotic load and impaired clearance of apoptotic material, finally exacerbated the autoimmune phenotype in NZB x SWR lupus-prone mice (90). Besides, research about lupus nephritis in NZB/W mice suggested that macrophage infiltration in the kidney promoted glomerular cell proliferation and early fibrosis by IL-10, MMP, osteopontin and growth factors (91).

SLE is a prototype autoimmune disease in which genetics play a major role. Researchers have identified many new loci which are attributed to the pathogenesis of SLE by genomewide association studies (GWAS). SLE susceptibility loci related to macrophages are mainly concentrated in genes that affect type I interferon (IFNI) signaling, NFκB activation, TLR signaling, phagocytosis and immune tolerance. Currently, more than 100 genetic risk sites related to SLE and more than half of them are closely related to the production or response of IFNI (92). IFNI promotes monocyte differentiation and the expression of MHCII and costimulatory molecules (such as CD40, CD80 and CD86) of macrophages to promote T cell activation (93, 94). Besides, increased IFNI levels in SLE patients can further promote the recruitment and adhesion of monocytes, and accumulation of macrophages in kidney and vascular lesions of SLE patients (95–97). In addition, IFNI enhances scavenger receptor SR-A and reduces ATP binding cassette subfamily A 1 (ABCA1) expression to promote cholesterol efflux, oxidation low lipoprotein (ox-LDL) uptake in macrophage and foam cell formation, which increasing the risk of cardiovascular diseases (96). Abnormal increased IFNI promotes the translocation of MZB cells to the follicular region of the spleen and disrupts the interaction between MZBs and MZMs, preventing clearance of apoptotic cells debris and follicular entry deterrence of apoptotic cells by MZMs (98, 99). The amplified TLR7 signaling in macrophage activation during antiviral responses and autoimmune diseases can occur product IFNI in turn by promoting phosphorylation and activation of MAP kinase p38 and transcription factor STAT1 (100). *TNIP1*(TNFAIP3-interacting protein 1, also known as ABIN1), a characteristic susceptibility gene for SLE identified by GWAS can regulate IFN-I production in DCs and macrophages through the TLR7 pathway (101). Large numbers of renal myeloid cells in patients with lupus nephritis, including macrophages, are activated. Almost all known susceptibility genes that affect innate immune signals may potentially affect the progression of lupus nephritis by activating myeloid cells in the kidney (102). Some genes such as *ITGAM* and *FCR* can potentially affect the recruitment of myeloid cells to the glomerular matrix by binding to the immune complexes in the glomerulus (103). DCs, macrophages and endothelial cells engulf C1q-coated apoptotic cells, and deficient in the complement protein C1q inhibit the clearance of apoptotic material and intensify lupus-like skin manifestations in mice and humans (100). *ITGAM* is an established SLE susceptibility locus, which impairs phagocytosis of complement-opsonized targets in monocytes, neutrophils and macrophages. In conclusion, these susceptible genes promote SLE pathogenesis through IFN-I-macrophage immune axis, and rebalancing macrophage functions may resist the damage of highly expressed IFN-I.

Abnormal macrophage polarization also has been identified in the occurrence and development of SLE. The overwhelming M1

macrophages promote the exposure of autoantigens and the occurrence of autoimmune reactions (104, 105). The gene expression profiles of myeloid cells from active SLE patients expressed higher M1-related genes and tend to promote inflammation. In comparison, myeloid cells from inactive SLE patients expressed higher M2-related genes and participated in immune repair (106). Aberrantly expanding M1 macrophages were dominating in MRL-Fas(Lpr) mice, hastened the onset of lupus nephritis, mediated defective renal repair and non-resolving inflammation (107). In the early stage of apoptosis, M2 macrophages can promote the production of anti-inflammatory factors and phagocytize apoptotic cells in an anti-inflammatory way called "bubble drink" (108, 109). Increased M2 macrophages reduced pro-inflammatory cytokines expression and increased the secretion of anti-inflammatory cytokines, which could be used for anti-inflammatory therapy in SLE (110). TIPE2 overexpression by AAV-TIPE2 induced M2 macrophage polarization, induced serum anti-dsDNA autoantibody and pathological renal damage, increased urine protein levels in the ALD-induced SLE mice (111). Adoptive transplantation of M2 macrophages or stimulating monocytes to differentiate into M2-like macrophages significantly reduced the severity of SLE, while M1 macrophage metastasis aggravated the development of SLE (112, 113). Virgin olive oil and its phenolic components have been shown to prevent various inflammatory and immune diseases, which may be related to inhibiting M1 and promoting M2 macrophage polarization (114, 115). The above studies show that the abnormal polarization of macrophages plays a vital role in SLE, which will be a potential target for SLE therapy.

Current therapies for SLE are designed to resolve inflammation with the goal of preventing permanent organ injury, and reduce clinical symptoms. Mycophenolate mofetil (MMF), an inhibitor of purine synthesis, inhibits the recruitment of monocytes and the production of nitric oxide and superoxide in activated macrophages to restrain tissue damage (116). The heterogeneity of disease mechanisms in SLE suggests that cell- and cytokine- or pathway-specific therapies for macrophage would be effective in treatment for SLE.

4 Macrophages in RA

RA is an autoimmune disease characterized by chronic inflammation that eventually results in joint damage and even joint dysfunction. It has been found that macrophage infiltration is positively correlated with the degree of joint erosion, and increased synovial macrophage infiltration in synovial tissue is an early sign of RA (117–119). Clodronate could reduce knee swelling, inflammation and joint destruction by eliminating synovial macrophages in rats with antigen-induced arthritis (AIA) (120). Various mechanisms generally lead to increased macrophage infiltration in inflammatory sites, such as facilitating the expression of chemokines and pro-inflammatory cytokines, local survival rate/reducing apoptosis (121). Inhibited macrophage infiltration in synovial tissue may be a protential target for RA treatment. Increased apoptosis of $Ly6C^+$ monocyte derived macrophages, reduced monocyte migration into the ankles and enhanced macrophage migration from the inflamed synovial tissue to the draining lymph nodes are responsible for the reduction of macrophages in synovial tissue after infliximab treatment alleviated disease progress in hTNF-Tg mice (122).

The infiltrated macrophage further mediated various inflammatory cell states, significantly contributing to the initiation and perpetuation of synovitis in RA by orchestrating cytokine network (123), as shown in Figure 4. Macrophages expedite inflammation by promoting the production of Th17 cells and stimulating osteoclast differentiation by secreting cytokines including IL-26 (124, 125). Besides, macrophages in synovial tissue and synovial fluid mediate the chemotaxis and proliferation of endothelial cells, promote the formation of pannus and infiltration of inflammatory cells, and further expand the inflammatory response in RA by producing vascular endothelial growth factor (VEGF) (126,

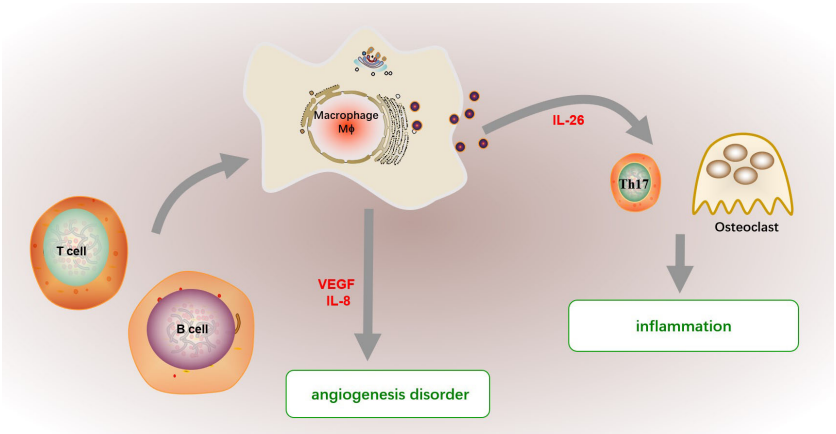

FIGURE 4
The function of macrophage in RA. The infiltrated macrophage further mediated various inflammatory cell states in synovitis by orchestrating cytokine network. Macrophages promote inflammation by promoting Th17 cell differentiation and stimulating osteoclast differentiation by secreting cytokines including IL-26. Besides, macrophages in synovial tissue and fluid mediate the chemotaxis and proliferation of endothelial cells, promote the formation of pannus and infiltration of inflammatory cells, and further expand the inflammation in RA by producing endothelial growth factor (VEGF). And macrophage-derived IL-8 also promote angiogenesis disorder in RA. The abnormally activated macrophage in RA patients show a proinflammatory profile, which may be supported by activated B or T cells.

127). And macrophage-derived IL-8 also promote angiogenesis disorder in RA (128). The mechanism of abnormal activation of macrophages is not clear at present. Burbano. et al. found that increased circulating microparticles (MP) forming immune complexes in SLE and RA patients favored the polarization of monocyte-derived macrophages into a proinflammatory profile, which promoted T and B cell activation, and B-cell survival (129). Transcriptome profiles of highly inflamed RA synovial tissue (RA-ST) also demonstrated that monocytes/macrophages show similar gene patterns induced by bacterial and fungal, and activated B or T cells also activate monocytes/macrophages (130).

Current conventional synthetic and biologic disease-modifying anti-rheumatic drugs (DMARDs) used in the clinic to treat of RA are related to adjusting macrophage activation and reducing synovial macrophage infiltration. Methotrexate, leflunomide or sulfasalazine reduces macrophage accumulation by promoting apoptosis and inhibiting Th1 response (123). Besides, the anti-TNF biological anti-rheumatic drugs such as etanercept, adalimumab decreased inflammatory cytokines production and increased phagocytosis in monocyte derived macrophages, which all alleviated inflammatory reactions (131). In addition, various monoclonal antibodies targeting biomolecules produced by macrophages are available for the therapeutic options of RA. The therapeutic efficacy of blocking granulocyte-macrophage colony stimulating factor receptor (GM-CSF) pathway like anti-GM-CSFR monoclonal antibody mavrilimumab is linked to inhibited production of pro-inflammatory mediators such as VICM (citrullinated and MMP degraded vimentin fragment) biomarker released by activated macrophages (132, 133). A monoclonal antibody to folate receptor β (FR-β) produced by macrophages specifically accumulates in inflamed lesions of murine RA and peritonitis disease models, facilitating immune cells, including T cells, B cells, neutrophils and DCs, to exit from the inflamed lesions and allative disease processes (134).

The imbalance of macrophage polarization also occurs in RA. The blood monocytes from RA patients had a propensity for preferential differentiate toward M1-like macrophages that contributed to synovial inflammation (135). Transcriptional omics study showed that synovial macrophages facilitate the expression of pro-inflammatory genes (*INHBA, FCER1A, SLC2A1, MMP12, EGLN3, NOS* and *CCR2*) but restrain anti-inflammatory genes (*IGF1, HTR2B, FOLR2* and *CD36*) expression (136, 137). Besides, M1 macrophages are characterized by decreased heme uptake and iron output but increased iron storage, which could partly explain the phenomenon of anemia in RA patients (138). The M1-to-M2 macrophage re-polarization can also serve as a promising treatment for RA. Targeted biologics that selectively regulate the function of macrophages have broad research prospects for the treatment of RA and also could solve the adverse effects of non-targeted drugs to a certain extent. Interfering with glycolytic pathways activated in M1 macrophages can reduce pro-inflammatory factors production and IgG antibodies, finally alleviating joint inflammation and damage in CIA mice (139). The administration of Wilforlide A reduced clinical scores, joint swelling and histological damage of collagen-induced RA mice by inhibiting the secretion of pro-inflammatory factors (MCP1, GM-CSF and M-CSF) and iNOS in the synovium (140). Angiotensin II type 2 receptor (AT2R) activation and a developed triamcinolone-gold nanoparticle (Triam-AuNP) complex promotes proinflammatory synovial macrophages to differentiate into the tolerogenic macrophage, finally attenuating the joint pathology in a rat model of collagen-induced RA (141, 142). The above studies have shown that M1 macrophages are dominant in RA synovium, regulating abnormal macrophage polarization is one of the important therapies of RA. Many new drug vectors and targets have been found to regulate macrophage function selectively. Encapsulated plasmid DNA encoding IL-10 and the chemotherapeutic drug betamethasone sodium phosphate (BSP) in biomimetic vector M2 exosomes derived from M2 macrophages, folate-modified triptolide liposomes (FA-TP-Lips) and folic acid modified silver nanoparticles(FA-AgNPs) all serve as a promising biocompatible drug to facilitate M2 macrophages polarization selectively, thereby treating RA safely and effectively (143–145). However, macrophages are incredibly heterogeneous. The focus and difficulty of RA drug development will be how to distinguish, identify and act on specific activated pathogenic macrophages.

5 Macrophages in SSc

Systemic sclerosis (SSc) is a chronic multi-system disease characterized by autoimmunity, immune cell infiltration and activation, fibrosis and vascular lesions, often accompanied by skin involvement and visceral dysfunction including heart and lungs caused by fibrosis (146, 147). Vascular complications such as pulmonary hypertension and scleroderma renal crisis have become the leading causes of disability and death of SSc (148, 149). The infiltrating inflammatory leukocytes in the new affected skin from SSc patients are mainly $CD14^+$ monocytes/macrophages (150). Transcriptomics analysis found that monocytes continuously migrated and differentiated into alveolar macrophages to promote fibrosis during pulmonary fibrosis and selectively targeting the differentiation of alveolar macrophages in the lung may improve fibrosis (151). These researches suggested that monocytes/macrophages play an essential role in the early pathogenesis of SSc, which was displayed in Figure 5.

Apoptotic cell clearance (efferocytosis) capacities of monocyte-induced macrophage from SSc patients are significantly lower than those in healthy donors, which partly explains the emergence of circulating nuclear antigens (152). Besides, macrophage is a main contributor for fibirosis. The $CD14^+$ monocytes and $CD14^+$ pulmonary macrophages in SSc patients have elevated profibrotic fibronectin production and are considered extracellular matrix producers (153). Activated macrophages produced a variety of cytokines, such as high levels of CCL18, CCL2, and CXCL8 but low IL-10 expression, which enriched in perivascular regions of highly fibrotic SSc skin to favor pro-inflammatory fibroblasts (154, 155). Additionally, the excessive production of CXCL13 and vascular VEGF by macrophages can also promote tissue fibrosis, immune activation and abnormal vascular morphology in SSc (156, 157). The formation mechanism of fibrogenic macrophages is still unclear. It has been demonstrated that fibrotic macrophage might be activated by a dysfunctional B cell in mice with bleomycin-induced SSc, and correlated with the severity of fibrosis in SSc patients (158). Besides, Dysregulation of TGF-β and IL-4 signaling may also be responsible for the pro-fibrotic function in SSc macrophages (159).

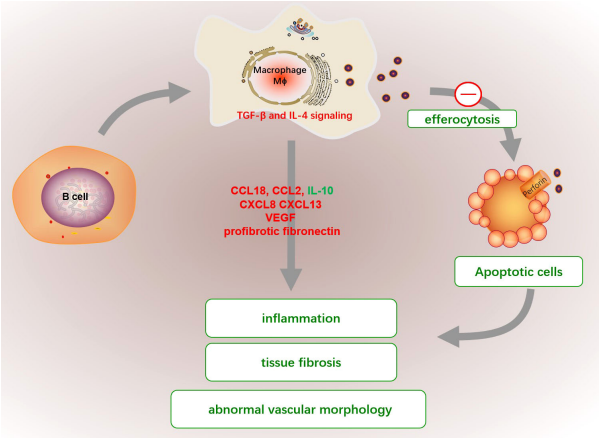

FIGURE 5
The abnormal functions of macrophage in SSc. The efferocytosis capacities of macrophage in SSc patients are significantly reduced, which cause the emergence of circulating nuclear antigens and promote proinflammatory fibroblasts. Activated macrophages produced a variety of cytokines, such as high levels of CCL18, CCL2, and CXCL8 but low IL-10 expression, which enriched in perivascular regions of highly fibrotic SSc skin to favor pro-inflammatory fibroblasts. Additionally, the excessive production of CXCL13, elevated profibrotic fibronectin and VEGF by macrophages can also promote tissue fibrosis, immune activation and abnormal vascular morphology in SSc. The fibrotic macrophage might be activated by a dysfunctional B cell or dysregulation of TGF-β and IL-4.

The abnormal polarization of macrophages in SSc is relatively complex. Studies have found that crystalline silica SiO or response gene to complement 32 (RGC32) can promote macrophages to form an M1-like phenotype and reduce M2 polarization, which caused the reduction of macrophages efferocytosis in SSc (160, 161). However, the gene expression profiles of affected skin, lung, esophagus and peripheral blood in patients with SSc showed that the expression of M2-related genes was significantly up-regulated in macrophages with pronounced fibrogenic effect (162). Infiltrated macrophages in skin lesions from SSc and local scleroderma were found to highly express CD163 (163–165), indicating that M2 macrophage may also involve in skin fibrosis. Besides, studies have found that some biological agents can inhibit the process of SSc by reversing the polarization of M2 macrophages. The PDE4 inhibition induced by nintedanib, rolipram and apremilast and glycyrrhizin all ameliorate the fibroblast activation by impeding M2 macrophage function in SSc-related mice (166–168). All the above studies indicate that M2 macrophage infiltration may be a target for SSc treatment. However, researchers had found the number of M1 and M2 macrophages in the skin of SSc patients was significantly increased, indicating that macrophages in different polarized states might synergistically promote the pathogenesis of SSc (169). Skin biopsy RNA examined by next-generation RNA sequencing suggested that most early diffuse SSc patients had a concomitant M1 and/or M2 macrophage signature, suggesting co-occurrence of dysregulated fibroblast and macrophage polarization (169). Studies about TLR signaling in fibrosis in SSC and other fibrotic diseases hinted that the conflicting results may be related to long-term inflammatory stimulation (170). Furthermore, macrophages can acquire memory-like characteristics to copy with antigen exposure, protection against re-infection and more efficient vaccine strategies. Recent research found that trained macrophage acquired memory-like characteristics in response to antigen exposure can be targeted to SSc treatment. Low-dose LPS training and adoptive transfer alleviated fibrosis and inflammation in SSc mice, while BCG-training aggravated disease in this model (171). The long-term and complex *in vivo* microenvironment may be an essential promoter of macrophage activation that is unique to SSc patients. However, the function and mechanism need to be further explored.

6 Macrophages in T1D

T1D is an autoimmune disease characterized by the continuous destruction of islet cells caused by islet leukocyte infiltration (172). The loss of pancreatic β cells can lead to uncontrolled blood glucose and various complications such as cardiovascular disease, nephropathy, retinopathy, heart attack and stroke, which require lifelong dependence on exogenous insulin (173). Islet inflammation is one of the main mechanisms of pancreatic β-cell injury and the development of T1D. In diabetes-prone biological breeding rats (DP-BB), it has been demonstrated that macrophages are the first immune cells to infiltrate into islets (174). Furthermore, there were no lymphocytes in the islets when macrophage infiltration was prevented (175), suggesting that lymphocyte recruitment in islets depends on the macrophage. In addition, the immunohistochemical results of pancreatic specimens from newly diagnosed T1D patients confirmed the presence of macrophages in early and advanced inflammation (176). Various research about spontaneous T1D animal models has shown that specific clearance of macrophages *in vivo* can significantly inhibit Th1 but increase Th2 immune response induced mainly by IL-12, and inhibited cytotoxic effector of $CD8^+$ T, even remaining selective acceleration of the recruitment of $CD8^+$ T cells into the islets (177–179). Depleting macrophage by liposomes containing clodronate also selectly abolished diabetogenic $CD4^+$ T cells induced diabetes even with inflammation existence (180).

The microenvironment in T1D pancreas promote the recruitment of macrophages and abnormal functions. It was found that islet resident macrophages of non-autoimmune mice had immunomodulatory phenotype and could promote Treg cell differentiation *in vitro* (181). Deficiency of immunomodulatory function in macrophages may be an essential mechanism of pathogenesis of T1D (181). In addition, the migration and phagocytosis to target inflammatory cells of macrophage in the streptozotocin (STZ) -induced T1D model weakened islet cell immune defense (182). Diabetgenic CD4 T cells produce a variety of inflammatory cytokines and chemokines such as CCL1, resulting in the recruitment of macrophages into pancreas (183). Reduced integrin-associated surface factor CD47 on islet cells promoted macrophage migration and phagocytosis of endogenous cells (182). Instead of clearing apoptotic cells silently without production of pro-inflammatory cytokines, macrophages in T1D secret inappropriately high amounts of IL-1β and TNF-α to contribute to the initiation or continuation of an immune attack towards the pancreatic beta-cells (184). Besides, previously research also showed that macrophages from non-obese diabetic (NOD) mice are activated and engulf apoptotic cells at a lower rate, which might result in secondary necrosis, inflammation and self-antigen presentation in T1D (185).

And increased macrophage-derived cytokines including IL-12, TNF-α and IL-1β selectively in spleen lymphocytes and pancreatic

islet are responsible for the inflammatory cascade of events leading to the destruction of pancreatic β cells (186). Macrophages are involved in regulating the infiltration and functions of immune cells in T1D. Recruited macrophages in the pancreas by diabetes-derived T cell produce IL-1β, TNF-α and NO, and express chemokine receptors CCR5, CXCR3 and CCR8 to further recruit and active other inflammatory cells (183). The interaction between inflammatory macrophages and β-cells promote the production of CXCR2 ligands (CXCL1 and CXCL2) in the pancreas of T1D mice, which further recruit diabetogenic $CXCR2^+$ neutrophils from the blood into the pancreatic islets (187). Autoreactive $CD4^+$ T cells destroyed β cells through a Fas-dependent mechanism that was assisted by cytokines IL-1α, IL-1β, and IFN-γ (188). Besides, macrophge derived IL-12 might contribute to the development and activation of β cell–cytotoxic Th1 and CD8 cells in NOD mice (189). And macrophages selectively traffick autoimmune cytotoxic T cells into the islets *via* IFN-I signaling even without entering the islets, and ablation of IFN-I signaling on macrophages limits the onset of T1D (190). The role of macrophage on the pathological process of T1D was shown in Figure 6.

Macrophage polarization may act as a potential therapeutic agent for T1D. M2 macrophages explicitly located in the inflammatory pancreas could significantly inhibit the proliferation of T cells and promote the survival of β cells after adoptive transfer into spontaneous T1D mice, resulting in resistance to T1D in non-obese resistant (NOR) mice (191). In addition, the survival of transplanted islets was partly dependent on the content of M2 macrophages (192, 193). The early glycosylation products (EGPs) produced in the first step of Maillard reaction/glycosylation alleviated insulin resistance and pancreatic immune infiltration by increasing the M2/M1 ratio (194). Macrophage-specific knockout ubiquitin coupling enzyme E2 can weaken the energy metabolism and M2 type polarization of macrophages, thus increasing the risk of diabetes T1D induced by STZ (195). Hence, promoting M2 but inhibiting M1 macrophage polarization may be an important target for preventing and treating T1D.

Macrophage-derived proinflammatory cytokines, chemokines and their receptors were identified the suitable targets for the therapeutic interventions of T1D. The TNF-α inhibitor infliximab could alleviate T1D, which might be related with the reduced presentation of islet antigen to both effector $CD4^+$ and $CD8^+$ T cells (196, 197). And IL-6 has also been suggested as a target for T1D treatment (198). Multiple strategies blocking the CXCR1/2 pathway main expressed in macrophage inhibited leucocyte recruitment and prevent inflammation and autoimmune mediated islet damage, which was new interventional approach for T1D (199).

7 Discussion

The possible functions of macrophages in autoimmune diseases as described in Table 1. In brief, the scavenging ability of macrophages was destroyed, leading to the accumulation of autoimmune complexes in local tissues. Besides, the abnormal macrophage activation induced a series of irrepressible pro-inflammatory responses, and promoted the activation and recruitment of

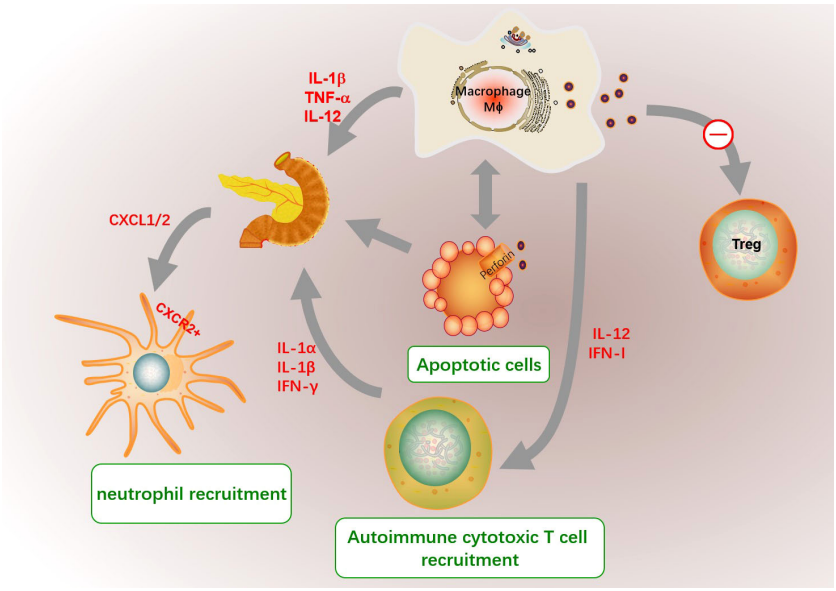

FIGURE 6
The role of macrophages in the pathogenesis of T1D. The microenvironment in T1D pancreas promote the recruitment of macrophages and abnormal functions. Islet resident macrophages in T1D had defected immunomodulatory phenotype and might inhibit Treg cell differentiation. In addition, the migration and phagocytosis to target inflammatory cells such as apoptotic cells of macrophage in T1D are decrease. And macrophage secret inappropriately high amounts of IL1β and TNFα to contribute to the initiation of an immune attack towards the pancreatic beta-cells. The unengulfed apoptotic cells might result in secondary necrosis, inflammation and self-antigen presentation in islet. And increased macrophage-derived cytokines including IL-12, TNF-α and IL-1β are responsible for the inflammatory cascade of events leading to the destruction of pancreatic β cells. The interaction between inflammatory macrophages and β-cells promote the production of CXCR2 ligands (CXCL1 and CXCL2), which further recruit diabetogenic $CXCR2^+$ neutrophils. Autoreactive $CD4^+$ T cells destroyed β cells assisted by cytokines IL-1α, IL-1β, and IFN-γ. Besides, macrophage derived IL-12 and IFN-I signaling might contribute to the development and activation of β cell–cytotoxic Th1 and CD8 cells.

TABLE 1 Possible function of macrophages in autoimmune diseases.

	Macrophage function	Macrophage polarization
SLE	• Increased autophagy of macrophage • Aggravating the inflammatory response • Reduced phagocytosis to apoptotic cells	↑ M1: Increasing secretion of pro-inflammatory cytokines ↓ M2: Reducing anti-inflammatory factors and phagocytize apoptotic cells
RA	• Increased anti-apoptosis • Increaed migration of macrophages to local tissues • Promoting Th17 differentiation and joint inflammation • Promoting the formation of pannus and causes further infiltration of inflammatory cells	↑ M1: Increasing iron storage and glycolysis, releasing pro-inflammatory cytokines to promote inflammation
SS	• Increased anti-apoptosis in macrophage • Reduced phagocytosis to apoptotic cell • Producing multiple cytokines to participate in fibrosis and angiogenesis	↑ M2: Increasing M2-related fibrotic phenotype
T1D	• Promoting the inflammatory response in islets • Mediating T cells recruitment and activation • Promoting immune cell infiltration and autoimmune response in islets	↓ M2: Insulin resistance and pancreatic immune infiltration are related to reduced M2 polarization

lymphocytes in local tissues, resulting in tissue damage. In addition, the aberrant polarization of macrophages has been identified to contribute to the pathogenesis of autoimmune diseases. However, due to the significant heterogeneity of macrophages, the polarization of macrophages varies significantly in different tissues and even in different phases of the same disease. Systematically and comprehensively understanding the polarization of macrophages in autoimmune diseases will conduce to the prevention and treatment of autoimmune diseases.

Currently anti-macrophage therapy in autoimmune diseases mainly focuses on down-regulation the production of abnormal macrophage-derived pro-inflammatory cytokines production, elimination of dysfunctional macrophage from the inflammatory regions such as inhibiting monocyte recruitment and differentiation, and upregulation of anti-inflammatory cytokines. In recent years, macrophage-derived extracellular vesicles composed of microvesicles and exosomes have aroused increased interest in the treatment for autoimmune disease. The macrophage-derived extracellular vesicles are considered as optimal delivery vehicles for the minimal toxicity and specific target effect. Macrophage-derived microvesicle-coated poly (lactic-co-glycolic acid) (PLGA) nanoparticles to encapsulate tacrolimus significant suppress the progression of RA in mice, which is an efficient biomimetic vehicle for RA targeted treatment (200). Besides, macrophage-derived extracellular vesicles efficiently delivered dexamethasone into inflamed kidney and effectively suppress inflammation and fibrosis in kidney (201).

Various new techniques such as single-cell sequencing, metabolomics and other multi-omics research methods have been applied in autoimmune diseases research and have achieved considerable achievements. A single-cell sequencing result of a mixed lung cell sample from bleomycin-induced lung injury mice found a group of disease-related transitional macrophages that specifically express CX3CR1 and PDGF-AA and are located in fibrotic scars to promote fibrosis (202). This study provides an effective target for preventing and treating pulmonary fibrosis-related diseases. In addition, single-cell pseudo-time analysis infer the transcription trajectory of macrophages when they gradually change their gene expression profile during autoimmunity, suggesting that we can find the molecular changes in the early stage of the disease and the most decisive target. The application of multi-omics methods at the single-cell level will provide an effective means for exploring the potential mechanisms of abnormal macrophage phenotypes and offer a solid theoretical basis for preventing and treating autoimmune diseases.

Author contributions

SY wrote the main manuscript. SJ, MZ revised the manuscript. SJ had primary responsibility for the final content. All authors agree to be accountable for the content of the work. All authors contributed to the article and approved the submitted version.

Funding

This work was supported by the Natural Science Foundation of Hunan province, China (Grant No.2020JJ4837), the Health Commission of Hunan province (Grant No.202202044436), the Project for leading talents in science and technology in Hunan province (2019RS3003) and National Natural Science Foundation of China (No. 82030097).

Conflict of interest

The authors declare that the research was conducted in the absence of any commercial or financial relationships that could be construed as a potential conflict of interest.

Publisher's note

References

1. Juarranz Y. Molecular and cellular basis of autoimmune diseases. *Cells.* (2021) 10 (2):474. doi: 10.3390/cells10020474

2. Marrack P, Kappler J, Kotzin BL. Autoimmune disease: why and where it occurs. *Nat Med* (2001) 7(8):899–905. doi: 10.1038/90935

3. Rose NR. Prediction and prevention of autoimmune disease in the 21st century: A review and preview. *Am J Epidemiol.* (2016) 183(5):403–6. doi: 10.1093/aje/kwv292

4. Molina V, Shoenfeld Y. Infection, vaccines and other environmental triggers of autoimmunity. *Autoimmunity.* (2005) 38(3):235–45. doi: 10.1080/08916930500050277

5. Saferding V, Blüml S. Innate immunity as the trigger of systemic autoimmune diseases. *J Autoimmun* (2020) 110:102382. doi: 10.1016/j.jaut.2019.102382

6. Pollard JW. Trophic macrophages in development and disease. *Nat Rev Immunol* (2009) 9(4):259–70. doi: 10.1038/nri2528

7. Wynn TA, Chawla A, Pollard JW. Macrophage biology in development, homeostasis and disease. *Nature.* (2013) 496(7446):445–55. doi: 10.1038/nature12034

8. van FR, Cohn ZA, Hirsch JG, Humphrey JH, Spector WG, Langevoort HL. The mononuclear phagocyte system: A new classification of macrophages, monocytes, and their precursor cells. *Bull World Health Organ* (1972) 46(6):845.

9. Ginhoux F, Guilliams M. Tissue-resident macrophage ontogeny and homeostasis. *Immunity.* (2016) 44(3):439–49. doi: 10.1016/j.immuni.2016.02.024

10. Gordon S, Taylor PR. Monocyte and macrophage heterogeneity. *Nat Rev Immunol* (2005) 5(12):953–64. doi: 10.1038/nri1733

11. Den Haan JM, Kraal G. Innate immune functions of macrophage subpopulations in the spleen. *J Innate Immun* (2012) 4(5-6):437–45. doi: 10.1159/000335216

12. Hoeffel G, Wang Y, Greter M, See P, Teo P, Malleret B, et al. Adult langerhans cells derive predominantly from embryonic fetal liver monocytes with a minor contribution of yolk sac-derived macrophages. *J Exp Med* (2012) 209(6):1167–81. doi: 10.1084/jem.20120340

13. Ginhoux F, Greter M, Leboeuf M, Nandi S, See P, Gokhan S, et al. Fate mapping analysis reveals that adult microglia derive from primitive macrophages. *Science.* (2010) 330(6005):841–5. doi: 10.1126/science.1194637

14. Sheng J, Ruedl C, Karjalainen K. Most tissue-resident macrophages except microglia are derived from fetal hematopoietic stem cells. *Immunity.* (2015) 43(2):382–93. doi: 10.1016/j.immuni.2015.07.016

15. Bain CC, Bravo-Blas A, Scott CL, Perdiguero EG, Geissmann F, Henri S, et al. Constant replenishment from circulating monocytes maintains the macrophage pool in the intestine of adult mice. *Nat Immunol* (2014) 15(10):929–37. doi: 10.1038/ni.2967

16. Tamoutounour S, Guilliams M, Montanana Sanchis F, Liu H, Terhorst D, Malosse C, et al. Origins and functional specialization of macrophages and of conventional and monocyte-derived dendritic cells in mouse skin. *Immunity.* (2013) 39(5):925–38. doi: 10.1016/j.immuni.2013.10.004

17. Wynn TA, Vannella KM. Macrophages in tissue repair, regeneration, and fibrosis. *Immunity.* (2016) 44(3):450–62. doi: 10.1016/j.immuni.2016.02.015

18. Gordon S, Plüddemann A, Martinez Estrada F. Macrophage heterogeneity in tissues: phenotypic diversity and functions. *Immunol Rev* (2014) 262(1):36–55. doi: 10.1111/imr.12223

19. Park MD, Silvin A, Ginhoux F, Merad M. Macrophages in health and disease. *Cell.* (2022) 185(23):4259–79. doi: 10.1016/j.cell.2022.10.007

20. Yang N, Isbel NM, Nikolic-Paterson DJ, Li Y, Ye R, Atkins RC, et al. Local macrophage proliferation in human glomerulonephritis. *Kidney Int* (1998) 54(1):143–51. doi: 10.1046/j.1523-1755.1998.00978.x

21. Tacke F. Functional role of intrahepatic monocyte subsets for the progression of liver inflammation and liver fibrosis In vivo. *Fibrogenesis Tissue Repair* (2012) 5(Suppl 1): S27. doi: 10.1186/1755-1536-5-S1-S27

22. Baeck C, Wehr A, Karlmark KR, Heymann F, Vucur M, Gassler N, et al. Pharmacological inhibition of the chemokine CCL2 (MCP-1) diminishes liver macrophage infiltration and steatohepatitis in chronic hepatic injury. *Gut.* (2012) 61 (3):416–26. doi: 10.1136/gutjnl-2011-300304

23. Lescoat A, Lecureur V, Varga J. Contribution of monocytes and macrophages to the pathogenesis of systemic sclerosis: recent insights and therapeutic implications. *Curr Opin Rheumatol* (2021) 33(6):463–70. doi: 10.1097/BOR.0000000000000835

24. Schuppan D. Current concepts of celiac disease pathogenesis. *Gastroenterology* (2000) 119(1):234–42. doi: 10.1053/gast.2000.8521

25. Fujiwara N, Kobayashi K. Macrophages in inflammation. *Curr Drug Targets Inflammation Allergy* (2005) 4(3):281–6. doi: 10.2174/1568010054022024

26. Celhar T, Pereira-Lopes S, Thornhill SI, Lee HY, Dhillon MK, Poidinger M, et al. TLR7 and TLR9 ligands regulate antigen presentation by macrophages. *Int Immunol* (2016) 28(5):223–32. doi: 10.1093/intimm/dxv066

27. Frascaroli G, Lecher C, Varani S, Setz C, van der Merwe J, Brune W, et al. Human macrophages escape inhibition of major histocompatibility complex-dependent antigen presentation by cytomegalovirus and drive proliferation and activation of memory CD4+ and CD8+ T cells. *Front Immunol* (2018) 9:1129. doi: 10.3389/fimmu.2018.01129

28. Wang J, Yang L, Mao X, Li Z, Lin X, Jiang C. Streptococcus salivarius-mediated CD8+ T cell stimulation required antigen presentation by macrophages in oral squamous cell carcinoma. *Exp Cell Res* (2018) 366(2):121–6. doi: 10.1016/j.yexcr.2018.03.007

29. Ulfig A, Bader V, Varatnitskaya M, Lupilov N, Winklhofer KF, Leichert LI. Hypochlorous acid-modified human serum albumin suppresses MHC class II - dependent antigen presentation in pro-inflammatory macrophages. *Redox Biol* (2021) 43:101981. doi: 10.1016/j.redox.2021.101981

30. Yang M, Shi XQ, Peyret C, Oladiran O, Wu S, Chambon J, et al. Effector/memory CD8+ T cells synergize with co-stimulation competent macrophages to trigger autoimmune peripheral neuropathy. *Brain Behav Immun* (2018) 71:142–57. doi: 10.1016/j.bbi.2018.04.001

31. Panduro M, Benoist C, Mathis D. Treg cells limit IFN-γ production to control macrophage accrual and phenotype during skeletal muscle regeneration. *Proc Natl Acad Sci U S A.* (2018) 115(11):E2585–93. doi: 10.1073/pnas.1800618115

32. Clarke EV, Weist BM, Walsh CM, Tenner AJ. Complement protein C1q bound to apoptotic cells suppresses human macrophage and dendritic cell-mediated Th17 and Th1 T cell subset proliferation. *J Leukoc Biol* (2015) 97(1):147–60. doi: 10.1189/jlb.3A0614-278R

33. Martinez J, Malireddi RK, Lu Q, Cunha LD, Pelletier S, Gingras S, et al. Molecular characterization of LC3-associated phagocytosis reveals distinct roles for Rubicon, NOX2 and autophagy proteins. *Nat Cell Biol* (2015) 17(7):893–906. doi: 10.1038/ncb3192

34. Boada-Romero E, Martinez J, Heckmann BL, Green DR. The clearance of dead cells by efferocytosis. *Nat Rev Mol Cell Biol* (2020) 21(7):398–414. doi: 10.1038/s41580-020-0232-1

35. Nishi C, Yanagihashi Y, Segawa K, Nagata S. MERTK tyrosine kinase receptor together with TIM4 phosphatidylserine receptor mediates distinct signal transduction pathways for efferocytosis and cell proliferation. *J Biol Chem* (2019) 294(18):7221–30. doi: 10.1074/jbc.RA118.006628

36. Kawano M, Nagata S. Efferocytosis and autoimmune disease. *Int Immunol* (2018) 30(12):551–8. doi: 10.1093/intimm/dxy055

37. Zhang X, Mosser DM. Macrophage activation by endogenous danger signals. *J Pathol* (2008) 214(2):161–78. doi: 10.1002/path.2284

38. Cuda CM, Pope RM, Perlman H. The inflammatory role of phagocyte apoptotic pathways in rheumatic diseases. *Nat Rev Rheumatol* (2016) 12(9):543–58. doi: 10.1038/nrrheum.2016.132

39. Udalova IA, Mantovani A, Feldmann M. Macrophage heterogeneity in the context of rheumatoid arthritis. *Nat Rev Rheumatol* (2016) 12(8):472–85. doi: 10.1038/nrrheum.2016.91

40. Jiang Z, Jiang JX, Zhang GX. Macrophages: a double-edged sword in experimental autoimmune encephalomyelitis. *Immunol Lett* (2014) 160(1):17–22. doi: 10.1016/j.imlet.2014.03.006

41. Giraudo E, Inoue M, Hanahan D. An amino-bisphosphonate targets MMP-9-expressing macrophages and angiogenesis to impair cervical carcinogenesis. *J Clin Invest.* (2004) 114(5):623–33. doi: 10.1172/JCI22087

42. Aurora AB, Porrello ER, Tan W, Mahmoud AI, Hill JA, Bassel-Duby R, et al. Macrophages are required for neonatal heart regeneration. *J Clin Invest.* (2014) 124 (3):1382–92. doi: 10.1172/JCI72181

43. Guan C, Xiao Y, Li K, Wang T, Liang Y, Liao G. MMP-12 regulates proliferation of mouse macrophages via the ERK/P38 MAPK pathways during inflammation. *Exp Cell Res* (2019) 378(2):182–90. doi: 10.1016/j.yexcr.2019.03.018

44. McInnes IB, Schett G. Pathogenetic insights from the treatment of rheumatoid arthritis. *Lancet.* (2017) 389(10086):2328–37. doi: 10.1016/S0140-6736(17)31472-1

45. Kim SY, Nair MG. Macrophages in wound healing: activation and plasticity. *Immunol Cell Biol* (2019) 97(3):258–67. doi: 10.1111/imcb.12236

46. Huang G, Wang Y, Chi H. Regulation of TH17 cell differentiation by innate immune signals. *Cell Mol Immunol* (2012) 9(4):287–95. doi: 10.1038/cmi.2012.10

47. Esmailbeig M, Ghaderi A. Interleukin-18: a regulator of cancer and autoimmune diseases. *Eur Cytokine Netw* (2017) 28(4):127–40. doi: 10.1684/ecn.2018.0401

48. De Filippo K, Dudeck A, Hasenberg M, Nye E, van Rooijen N, Hartmann K, et al. Mast cell and macrophage chemokines CXCL1/CXCL2 control the early stage of neutrophil recruitment during tissue inflammation. *Blood.* (2013) 121(24):4930–7. doi: 10.1182/blood-2013-02-486217

49. Feduska JM, Tse HM. The proinflammatory effects of macrophage-derived NADPH oxidase function in autoimmune diabetes. *Free Radic Biol Med* (2018) 125:81–89. doi: 10.1016/j.freeradbiomed.2018.04.581

50. Marletta MA, Yoon PS, Iyengar R, Leaf CD, Wishnok JS. Macrophage oxidation of l-arginine to nitrite and nitrate: nitric oxide is an intermediate. *Biochemistry.* (1988) 27 (24):8706–11. doi: 10.1021/bi00424a003

51. Palmer RM, Ashton DS, Moncada S. Vascular endothelial cells synthesize nitric oxide from l-arginine. *Nature.* (1988) 333(6174):664–6. doi: 10.1038/333664a0

52. Rath M, Müller I, Kropf P, Closs EI, Munder M. Metabolism *via* arginase or nitric oxide synthase: Two competing arginine pathways in macrophages. *Front Immunol* (2014) 5:532. doi: 10.3389/fimmu.2014.00532

53. Viola A, Munari F, Sánchez-Rodríguez R, Scolaro T, Castegna A. The metabolic signature of macrophage responses. *Front Immunol* (2019) 10:1462. doi: 10.3389/fimmu.2019.01462

54. Tannahill GM, Curtis AM, Adamik J, Palsson-McDermott EM, McGettrick AF, Goel G, et al. Succinate is an inflammatory signal that induces IL-1β through HIF-1α. *Nature.* (2013) 496(7444):238–42. doi: 10.1038/nature11986

55. Batista-Gonzalez A, Vidal R, Criollo A, Carreño LJ. New insights on the role of lipid metabolism in the metabolic reprogramming of macrophages. *Front Immunol* (2020) 10:2993. doi: 10.3389/fimmu.2019.02993

56. Huang SC, Smith AM, Everts B, Colonna M, Pearce EL, Schilling JD, et al. Metabolic reprogramming mediated by the mTORC2-IRF4 signaling axis is essential for macrophage alternative activation. *Immunity.* (2016) 45(4):817–30. doi: 10.1016/j.immuni.2016.09.016

57. Du L, Lin L, Li Q, Liu K, Huang Y, Wang X, et al. IGF-2 preprograms maturing macrophages to acquire oxidative phosphorylation-dependent anti-inflammatory properties. *Cell Metab* (2019) 29(6):1363–75. doi: 10.1016/j.cmet.2019.01.006

58. Biswas SK, Mantovani A. Orchestration of metabolism by macrophages. *Cell Metab* (2012) 15(4):432–7. doi: 10.1016/j.cmet.2011.11.013

59. Orihuela R, McPherson CA, Harry GJ. Microglial M1/M2 polarization and metabolic states. *Br J Pharmacol* (2016) 173(4):649–65. doi: 10.1111/bph.13139

60. Cairo G, Recalcati S, Mantovani A, Locati M. Iron trafficking and metabolism in macrophages: contribution to the polarized phenotype. *Trends Immunol* (2011) 32 (6):241–7. doi: 10.1016/j.it.2011.03.007

61. Mao Y, Shi D, Li G, Jiang P. Citrulline depletion by ASS1 is required for proinflammatory macrophage activation and immune responses. *Mol Cell* (2022) 82 (3):527–41. doi: 10.1016/j.molcel.2021.12.006

62. Sica A, Mantovani A. Macrophage plasticity and polarization: *in vivo* veritas[J]. *J Clin Invest* (2012) 122(3):787–95. doi: 10.1172/JCI59643

63. Murray PJ. Macrophage polarization. *Annu Rev Physiol* (2017) 79:541–66. doi: 10.1146/annurev-physiol-022516-034339

64. Fuchs AL, Schiller SM, Keegan WJ, Ammons MCB, Eilers B, Tripet B, et al. Quantitative 1H NMR metabolomics reveal distinct metabolic adaptations in human macrophages following differential activation. *Metabolites.* (2019) 9(11):248. doi: 10.3390/metabo9110248

65. Draijer C, Boorsma CE, Robbe P, Timens W, Hylkema MN, Ten Hacken NH, et al. Human asthma is characterized by more IRF5+ M1 and CD206+ M2 macrophages and less IL-10+ M2-like macrophages around airways compared with healthy airways. *J Allergy Clin Immunol* (2017) 140(1):280–283.e3. doi: 10.1016/j.jaci.2016.11.020

66. Gordon S, Martinez FO. Alternative activation of macrophages: mechanism and functions. *Immunity.* (2010) 32(5):593–604. doi: 10.1016/j.immuni.2010.05.007

67. Mantovani A, Sozzani S, Locati M, Allavena P, Sica A. Macrophage polarization: tumor-associated macrophages as a paradigm for polarized M2 mononuclear phagocytes. *Trends Immunol* (2002) 23(11):549–55. doi: 10.1016/s1471-4906(02)02302-5

68. Abdelaziz MH, Abdelwahab SF, Wan J, Cai W, Huixuan W, Jianjun C, et al. Alternatively activated macrophages; a double-edged sword in allergic asthma. *J Transl Med* (2020) 18(1):58. doi: 10.1186/s12967-020-02251-w

69. Wang LX, Zhang SX, Wu HJ, Rong XL, Guo J. M2b macrophage polarization and its roles in diseases. *J Leukoc Biol* (2019) 106(2):345–58. doi: 10.1002/JLB.3RU1018-378RR

70. Arora S, Dev K, Agarwal B, Das P, Syed MA. Macrophages: Their role, activation and polarization in pulmonary diseases. *Immunobiology.* (2018) 223(4-5):383–96. doi: 10.1016/j.imbio.2017.11.001

71. Wang Q, Ni H, Lan L, Wei X, Xiang R, Wang Y. Fra-1 protooncogene regulates IL-6 expression in macrophages and promotes the generation of M2d macrophages. *Cell Res* (2010) 20(6):701–12. doi: 10.1038/cr.2010.52

72. Shapouri-Moghaddam A, Mohammadian S, Vazini H, Taghadosi M, Esmaeili SA, Mardani F, et al. Macrophage plasticity, polarization, and function in health and disease. *J Cell Physiol* (2018) 233(9):6425–40. doi: 10.1002/jcp.26429

73. Tabas I, Bornfeldt KE. Macrophage phenotype and function in different stages of atherosclerosis. *Circ Res* (2016) 118(4):653–67. doi: 10.1161/CIRCRESAHA.115.306256

74. Biswas SK, Sica A, Lewis CE. Plasticity of macrophage function during tumor progression: regulation by distinct molecular mechanisms. *J Immunol* (2008) 180 (4):2011–7. doi: 10.4049/jimmunol

75. Funes SC, Rios M, Escobar-Vera J, Kalergis AM. Implications of macrophage polarization in autoimmunity. *Immunology.* (2018) 154(2):186–95. doi: 10.1111/imm.12910

76. Kaul A, Gordon C, Crow MK, Touma Z, Urowitz MB, van Vollenhoven R, et al. Systemic lupus erythematosus. *Nat Rev Dis Primers* (2016) 2:16039. doi: 10.1038/nrdp.2016.39

77. Li Y, Lee PY, Reeves WH. Monocyte and macrophage abnormalities in systemic lupus erythematosus. *Arch Immunol Ther Exp (Warsz).* (2010) 58(5):355–64. doi: 10.1007/s00005-010-0093-y

78. Katsiari CG, Liossis SN, Sfikakis PP. The pathophysiologic role of monocytes and macrophages in systemic lupus erythematosus: a reappraisal. *Semin Arthritis Rheumatol* (2010) 39(6):491–503. doi: 10.1016/j.semarthrit.2008.11.002

79. Ma WT, Gao F, Gu K, Chen DK. The role of monocytes and macrophages in autoimmune diseases: A comprehensive review. *Front Immunol* (2019) 10:1140. doi: 10.3389/fimmu.2019.01140

80. Chalmers SA, Chitu V, Herlitz LC, Sahu R, Stanley ER, Putterman C. Macrophage depletion ameliorates nephritis induced by pathogenic antibodies. *J Autoimmun* (2015) 57:42–52. doi: 10.1016/j.jaut.2014.11.007

81. Kuriakose J, Redecke V, Guy C, Zhou J, Wu R, Ippagunta SK, et al. Patrolling monocytes promote the pathogenesis of early lupus-like glomerulonephritis. *J Clin Invest.* (2019) 129(6):2251–65. doi: 10.1172/JCI125116

82. Hill GS, Delahousse M, Nochy D, Rémy P, Mignon F, Méry JP, et al. Predictive power of the second renal biopsy in lupus nephritis: significance of macrophages. *Kidney Int* (2001) 59(1):304–16. doi: 10.1046/j.1523-1755.2001.00492.x

83. Yoshimoto S, Nakatani K, Iwano M, Asai O, Samejima K, Sakan H, et al. Elevated levels of fractalkine expression and accumulation of CD16+ monocytes in glomeruli of active lupus nephritis. *Am J Kidney Dis* (2007) 50(1):47–58. doi: 10.1053/j.ajkd.2007.04.012

84. Schiffer L, Bethunaickan R, Ramanujam M, Huang W, Schiffer M, Tao H, et al. Activated renal macrophages are markers of disease onset and disease remission in lupus nephritis. *J Immunol* (2008) 180(3):1938–47. doi: 10.4049/jimmunol.180.3.1938

85. Li H, Wu Q, Li J, Yang P, Zhu Z, Luo B, et al. Cutting edge: defective follicular exclusion of apoptotic antigens due to marginal zone macrophage defects in autoimmune BXD2 mice. *J Immunol* (2013) 190(9):4465–9. doi: 10.4049/jimmunol.1300041

86. Gaipl US, Voll RE, Sheriff A, Franz S, Kalden JR, Herrmann M. Impaired clearance of dying cells in systemic lupus erythematosus. *Autoimmun Rev* (2005) 4(4):189–94. doi: 10.1016/j.autrev.2004.10.007

87. Roszer T, Menéndez-Gutiérrez MP, Lefterova MI, Alameda D, Núñez V, Lazar MA, et al. Autoimmune kidney disease and impaired engulfment of apoptotic cells in mice with macrophage peroxisome proliferator-activated receptor gamma or retinoid X receptor alpha deficiency. *J Immunol* (2011) 186(1):621–31. doi: 10.4049/jimmunol.1002230

88. Roberts AW, Lee BL, Deguine J, John S, Shlomchik MJ, Barton GM. Tissue-resident macrophages are locally programmed for silent clearance of apoptotic cells. *Immunity.* (2017) 47(5):913–27. doi: 10.1016/j.immuni.2017.10.006

89. Denny MF, Chandaroy P, Killen PD, Caricchio R, Lewis EE, Richardson BC, et al. Accelerated macrophage apoptosis induces autoantibody formation and organ damage in systemic lupus erythematosus. *J Immunol* (2006) 176(4):2095–104. doi: 10.4049/jimmunol.176.4.2095

90. Li B, Yue Y, Dong C, Shi Y, Xiong S. Blockade of macrophage autophagy ameliorates activated lymphocytes-derived DNA induced murine lupus possibly *via* inhibition of proinflammatory cytokine production. *Clin Exp Rheumatol* (2014) 32 (5):705–14.

91. Triantafyllopoulou A, Franzke CW, Seshan SV, Perino G, Kalliolias GD, Ramanujam M, et al. Proliferative lesions and metalloproteinase activity in murine lupus nephritis mediated by type I interferons and macrophages. *Proc Natl Acad Sci U S A.* (2010) 107(7):3012–7. doi: 10.1073/pnas.0914902107

92. Rönnblom L, Leonard D. Interferon pathway in SLE: one key to unlocking the mystery of the disease. *Lupus Sci Med* (2019) 6(1):e000270. doi: 10.1136/lupus-2018-000270

93. McNab F, Mayer-Barber K, Sher A, Wack A, O'Garra A. Type I interferons in infectious disease. *Nat Rev Immunol* (2015) 15(2):87–103. doi: 10.1038/nri3787

94. Bengtsson AA, Ronnblom L. Role of interferons in SLE. *Best Pract Res Clin Rheumatol* (2017) 31(3):415–28. doi: 10.1016/j.berh.2017.10.003

95. Tumurkhuu G, Montano E, Jefferies C. Innate immune dysregulation in the development of cardiovascular disease in lupus. *Curr Rheumatol Rep* (2019) 21(9):46. doi: 10.1007/s11926-019-0842-9

96. Boshuizen MC, de Winther MP. Interferons as essential modulators of atherosclerosis. *Arterioscler Thromb Vasc Biol* (2015) 35(7):1579–88. doi: 10.1161/ATVBAHA.115.305464

97. Crampton SP, Morawski PA, Bolland S. Linking susceptibility genes and pathogenesis mechanisms using mouse models of systemic lupus erythematosus. *Dis Model Mech* (2014) 7(9):1033–46. doi: 10.1242/dmm.016451

98. Li H, Fu YX, Wu Q, Zhou Y, Crossman DK, Yang P, et al. Interferon-induced mechanosensing defects impede apoptotic cell clearance in lupus. *J Clin Invest.* (2015) 125 (7):2877–90. doi: 10.1172/JCI81059

99. Wang JH, Li J, Wu Q, Yang P, Pawar RD, Xie S, et al. Marginal zone precursor b cells as cellular agents for type I IFN-promoted antigen transport in autoimmunity. *J Immunol* (2010) 184(1):442–51. doi: 10.4049/jimmunol.0900870

100. Ramirez-Ortiz ZG, Prasad A, Griffith JW, Pendergraft WF3rd, Cowley GS, Root DE, et al. The receptor TREML4 amplifies TLR7-mediated signaling during antiviral responses and autoimmunity. *Nat Immunol* (2015) 16(5):495–504. doi: 10.1038/ni.3143

101. Zhou J, Wu R, High AA, Slaughter CA, Finkelstein D, Rehg JE, et al. A20-binding inhibitor of NF-κB (ABIN1) controls toll-like receptor-mediated CCAAT/enhancer-binding protein β activation and protects from inflammatory disease. *Proc Natl Acad Sci U S A.* (2011) 108(44):E998–1006. doi: 10.1073/pnas.1106232108

102. Orme J, Mohan C. Macrophages and neutrophils in SLE-an online molecular catalog. *Autoimmun Rev* (2012) 11(5):365–72. doi: 10.1016/j.autrev.2011.10.010

103. Crispín JC, Hedrich CM, Tsokos GC. Gene-function studies in systemic lupus erythematosus. *Nat Rev Rheumatol* (2013) 9(8):476–84. doi: 10.1038/nrrheum.2013.78

104. Schaper F, de Leeuw K, Horst G, Bootsma H, Limburg PC, Heeringa P, et al. High mobility group box 1 skews macrophage polarization and negatively influences phagocytosis of apoptotic cells. *Rheumatol (Oxford).* (2016) 55(12):2260–70. doi: 10.1093/rheumatology/kew324

105. Hahn J, Euler M, Kilgus E, Kienhöfer D, Stoof J, Knopf J, et al. NOX2 mediates quiescent handling of dead cell remnants in phagocytes. *Redox Biol* (2019) 26:101279. doi: 10.1016/j.redox.2019.101279

106. Labonte AC, Kegerreis B, Geraci NS, Bachali P, Madamanchi S, Robl R, et al. Identification of alterations in macrophage activation associated with disease activity in systemic lupus erythematosus. *PloS One* (2018) 13(12):e0208132. doi: 10.1371/journal.pone.0208132

107. Iwata Y, Boström EA, Menke J, Rabacal WA, Morel L, Wada T, et al. Aberrant macrophages mediate defective kidney repair that triggers nephritis in lupus-susceptible mice. *J Immunol* (2012) 188(9):4568–80. doi: 10.4049/jimmunol.1102154

108. Vandivier RW, Henson PM, Douglas IS. Burying the dead: the impact of failed apoptotic cell removal (efferocytosis) on chronic inflammatory lung disease. *Chest.* (2006) 129(6):1673–82. doi: 10.1378/chest.129.6.1673

109. Poon IK, Lucas CD, Rossi AG, Ravichandran KS. Apoptotic cell clearance: basic biology and therapeutic potential. *Nat Rev Immunol* (2014) 14(3):166–80. doi: 10.1038/nri3607

110. Mohammadi S, Saghaeian-Jazi M, Sedighi S, Memarian A. Immunomodulation in systemic lupus erythematosus: induction of M2 population in monocyte-derived macrophages by pioglitazone. *Lupus*. (2017) 26(12):1318–27. doi: 10.1177/0961203317701842

111. Li F, Zhu X, Yang Y, Huang L, Xu J. TIPE2 alleviates systemic lupus erythematosus through regulating macrophage polarization. *Cell Physiol Biochem* (2016) 38(1):330–9. doi: 10.1159/000438633

112. Li F, Yang Y, Zhu X, Huang L, Xu J. Macrophage polarization modulates development of systemic lupus erythematosus. *Cell Physiol Biochem* (2015) 37(4):1279–88. doi: 10.1159/000430251

113. Horuluoglu B, Bayik D, Kayraklioglu N, Goguet E, Kaplan MJ, Klinman DM. PAM3 supports the generation of M2-like macrophages from lupus patient monocytes and improves disease outcome in murine lupus. *J Autoimmun* (2019) 99:24–32. doi: 10.1016/j.jaut.2019.01.004

114. Aparicio-Soto M, Montserrat-de la Paz S, Sanchez-Hidalgo M, Cardeno A, Bermudez B, Muriana FJG, et al. Virgin olive oil and its phenol fraction modulate monocyte/macrophage functionality: a potential therapeutic strategy in the treatment of systemic lupus erythematosus. *Br J Nutr* (2018) 120(6):681–92. doi: 10.1017/S0007114518001976

115. Aparicio-Soto M, Sánchez-Hidalgo M, Alarcón-de-la-Lastra C. An update on diet and nutritional factors in systemic lupus erythematosus management. *Nutr Res Rev* (2017) 30(1):118–37. doi: 10.1017/S0954422417000026

116. Allison AC. Mechanisms of action of mycophenolate mofetil. *Lupus* (2005) 14 Suppl 1:s2–8. doi: 10.1191/0961203305lu2109oa

117. Yoon BR, Yoo SJ, Choi Yh, Chung YH, Kim J, Yoo IS, et al. Functional phenotype of synovial monocytes modulating inflammatory T-cell responses in rheumatoid arthritis (RA). *PloS One* (2014) 9(10):e109775. doi: 10.1371/journal.pone.0109775

118. Yanni G, Whelan A, Feighery C, Bresnihan B. Synovial tissue macrophages and joint erosion in rheumatoid arthritis. *Ann Rheum Dis* (1994) 53(1):39–44. doi: 10.1136/ard.53.1.39

119. Patterson AM, Schmutz C, Davis S, Gardner L, Ashton BA, Middleton J. Differential binding of chemokines to macrophages and neutrophils in the human inflamed synovium. *Arthritis Res* (2002) 4(3):209–14. doi: 10.1186/ar408

120. Richards PJ, Williams AS, Goodfellow RM, Williams BD. Liposomal clodronate eliminates synovial macrophages, reduces inflammation and ameliorates joint destruction in antigen-induced arthritis. *Rheumatol (Oxford).* (1999) 38(9):818–25. doi: 10.1093/rheumatology/38.9.818

121. Hamilton JA, Tak PP. The dynamics of macrophage lineage populations in inflammatory and autoimmune diseases. *Arthritis Rheumatol* (2009) 60(5):1210–21. doi: 10.1002/art.24505

122. Huang QQ, Birkett R, Doyle R, Shi B, Roberts EL, Mao Q, et al. The role of macrophages in the response to TNF inhibition in experimental arthritis. *J Immunol* (2018) 200(1):130–8. doi: 10.4049/jimmunol.1700229

123. Boutet MA, Courties G, Nerviani A, Le Goff B, Apparailly F, Pitzalis C, et al. Novel insights into macrophage diversity in rheumatoid arthritis synovium. *Autoimmun Rev* (2021) 20(3):102758. doi: 10.1016/j.autrev.2021.102758

124. Corvaisier M, Delneste Y, Jeanvoine H, Preisser L, Blanchard S, Garo E, et al. IL-26 is overexpressed in rheumatoid arthritis and induces proinflammatory cytokine production and Th17 cell generation. *PloS Biol* (2012) 10(9):e1001395. doi: 10.1371/journal.pbio.1001395

125. Lee KA, Kim KW, Kim BM, Won JY, Min HK, Lee DW, et al. Promotion of osteoclastogenesis by IL-26 in rheumatoid arthritis. *Arthritis Res Ther* (2019) 21(1):283. doi: 10.1186/s13075-019-2070-0

126. Grabiec AM, Krausz S, de Jager W, Burakowski T, Groot D, Sanders ME, et al. Histone deacetylase inhibitors suppress inflammatory activation of rheumatoid arthritis patient synovial macrophages and tissue. *J Immunol* (2010) 184(5):2718–28. doi: 10.4049/jimmunol.0901467

127. Semerano L, Clavel G, Assier E, Denys A, Boissier MC. Blood vessels, a potential therapeutic target in rheumatoid arthritis? *Joint Bone Spine* (2011) 78(2):118–23. doi: 10.1016/j.jbspin.2010.06.004

128. Koch AE, Polverini PJ, Kunkel SL, Harlow LA, DiPietro LA, Elner VM, et al. Interleukin-8 as a macrophage-derived mediator of angiogenesis. *Science.* (1992) 258 (5089):1798–801. doi: 10.1126/science.1281554

129. Burbano C, Villar-Vesga J, Vásquez G, Muñoz-Vahos C, Rojas M, Castaño D. Proinflammatory differentiation of macrophages through microparticles that form immune complexes leads to T- and b-cell activation in systemic autoimmune diseases. *Front Immunol* (2019) 10:2058. doi: 10.3389/fimmu.2019.02058

130. Smiljanovic B, Grützkau A, Sörensen T, Grün JR, Vogl T, Bonin M, et al. Synovial tissue transcriptomes of long-standing rheumatoid arthritis are dominated by activated macrophages that reflect microbial stimulation. *Sci Rep* (2020) 10(1):7907. doi: 10.1038/s41598-020-64431-4

131. Degboé Y, Rauwel B, Baron M, Boyer JF, Ruyssen-Witrand A, Constantin A, et al. Polarization of rheumatoid macrophages by TNF targeting through an IL-10/STAT3 mechanism. *Front Immunol* (2019) 10:3. doi: 10.3389/fimmu.2019.00003

132. Crotti C, Biggioggero M, Becciolini A, Agape E, Favalli EG. Mavrilimumab: a unique insight and update on the current status in the treatment of rheumatoid arthritis. *Expert Opin Investig Drugs* (2019) 28(7):573–81. doi: 10.1080/13543784.2019.1631795

133. Mortensen JH, Guo X, De Los Reyes M, Dziegiel MH, Karsdal MA, Bay-Jensen AC, et al. The VICM biomarker is released from activated macrophages and inhibited by anti-GM-CSFRα-mAb treatment in rheumatoid arthritis patients. *Clin Exp Rheumatol* (2019) 37(1):73–80.

134. Hu Y, Wang B, Shen J, Low SA, Putt KS, Niessen HWM, et al. Depletion of activated macrophages with a folate receptor-beta-specific antibody improves symptoms in mouse models of rheumatoid arthritis. *Arthritis Res Ther* (2019) 21(1):143. doi: 10.1186/s13075-019-1912-0

135. Paoletti A, Rohmer J, Ly B, Pascaud J, Rivière E, Seror R, et al. Monocyte/Macrophage abnormalities specific to rheumatoid arthritis are linked to miR-155 and are differentially modulated by different TNF inhibitors. *J Immunol* (2019) 203(7):1766–75. doi: 10.4049/jimmunol.1900386

136. Soler Palacios B, Estrada-Capetillo L, Izquierdo E, Criado G, Nieto C, Municio C, et al. Macrophages from the synovium of active rheumatoid arthritis exhibit an activin a-dependent pro-inflammatory profile. *J Pathol* (2015) 235(3):515–26. doi: 10.1002/path.4466

137. Orecchioni M, Ghosheh Y, Pramod AB, Ley K. Macrophage polarization: Different gene signatures in M1(LPS+) vs. *Classically M2(LPS-) vs. Alternatively Activated Macrophages. Front Immunol* (2019) 10:1084. doi: 10.3389/fimmu.2019.01084

138. Yang X, Chang Y, Wei W. Emerging role of targeting macrophages in rheumatoid arthritis: Focus on polarization, metabolism and apoptosis. *Cell Prolif.* (2020) 53(7): e12854. doi: 10.1111/cpr.12854

139. Song G, Lu Q, Fan H, Zhang X, Ge L, Tian R, et al. Inhibition of hexokinases holds potential as treatment strategy for rheumatoid arthritis. *Arthritis Res Ther* (2019) 21 (1):87. doi: 10.1186/s13075-019-1865-3

140. Cao Y, Liu J, Huang C, Tao Y, Wang Y, Chen X, et al. Wilforlide a ameliorates the progression of rheumatoid arthritis by inhibiting M1 macrophage polarization. *J Pharmacol Sci* (2022) 148(1):116–24. doi: 10.1016/j.jphs.2021.10.005

141. Wang X, Tu J, Jiang J, Zhang Q, Liu Q, Körner H, et al. Angiotensin II type 2 receptor modulates synovial macrophage polarization by inhibiting GRK2 membrane translocation in a rat model of collagen-induced arthritis. *J Immunol* (2020) 205 (11):3141–53. doi: 10.4049/jimmunol.2000561

142. Park JY, Kwon S, Kim SH, Kang YJ, Khang D. Triamcinolone-gold nanoparticles repolarize synoviocytes and macrophages in an inflamed synovium. *ACS Appl Mater Interfaces.* (2020) 12(35):38936–49. doi: 10.1021/acsami.0c09842

143. Li H, Feng Y, Zheng X, Jia M, Mei Z, Wang Y, et al. M2-type exosomes nanoparticles for rheumatoid arthritis therapy *via* macrophage re-polarization. *J Control Release.* (2022) 341:16–30. doi: 10.1016/j.jconrel.2021.11.019

144. Guo RB, Zhang XY, Yan DK, Yu YJ, Wang YJ, Geng HX, et al. Folate-modified triptolide liposomes target activated macrophages for safe rheumatoid arthritis therapy. *Biomater Sci* (2022) 10(2):499–513. doi: 10.1039/d1bm01520f

145. Yang Y, Guo L, Wang Z, Liu P, Liu X, Ding J, et al. Targeted silver nanoparticles for rheumatoid arthritis therapy *via* macrophage apoptosis and re-polarization. *Biomaterials.* (2021) 264:120390. doi: 10.1016/j.biomaterials.2020.120390

146. Pattanaik D, Brown M, Postlethwaite BC, Postlethwaite AE. Pathogenesis of systemic sclerosis. *Front Immunol* (2015) 6:272. doi: 10.3389/fimmu.2015.00272

147. Brown M, O'Reilly S. The immunopathogenesis of fibrosis in systemic sclerosis. *Clin Exp Immunol* (2019) 195(3):310–21. doi: 10.1111/cei.13238

148. LeRoy EC. Systemic sclerosis. a vascular perspective. *Rheum Dis Clin North Am* (1996) 22(4):675–94. doi: 10.1016/s0889-857x(05)70295-7

149. Guiducci S, Giacomelli R, Cerinic MM. Vascular complications of scleroderma. *Autoimmun Rev* (2007) 6(8):520–3. doi: 10.1016/j.autrev.2006.12.006

150. Kräling BM, Maul GG, Jimenez SA. Mononuclear cellular infiltrates in clinically involved skin from patients with systemic sclerosis of recent onset predominantly consist of monocytes/macrophages. *Pathobiology.* (1995) 63(1):48–56. doi: 10.1159/000163933

151. Misharin AV, Morales-Nebreda L, Reyfman PA, Cuda CM, Walter JM, McQuattie-Pimentel AC, et al. Monocyte-derived alveolar macrophages drive lung fibrosis and persist in the lung over the life span. *J Exp Med* (2017) 214(8):2387–404. doi: 10.1084/jem.20162152

152. Ballerie A, Lescoat A, Augagneur Y, Lelong M, Morzadec C, Cazalets C, et al. Efferocytosis capacities of blood monocyte-derived macrophages in systemic sclerosis. *Immunol Cell Biol* (2019) 97(3):340–7. doi: 10.1111/imcb.12217

153. Rudnik M, Hukara A, Kocherova I, Jordan S, Schniering J, Milleret V, et al. Elevated fibronectin levels in profibrotic CD14+ monocytes and CD14+ macrophages in systemic sclerosis. *Front Immunol* (2021) 12:642891. doi: 10.3389/fimmu.2021.642891

154. Liakouli V, Cipriani P, Marrelli A, Alvaro S, Ruscitti P, Giacomelli R. Angiogenic cytokines and growth factors in systemic sclerosis. *Autoimmun Rev* (2011) 10(10):590–4. doi: 10.1016/j.autrev.2011.04.019

155. Laurent P, Lapoirie J, Leleu D, Levionnois E, Grenier C, Jurado-Mestre B, et al. Fédération hospitalo-universitaire ACRONIM and the centre national de référence des maladies auto-immunes systémiques rares de l'Est et du sud-ouest (RESO). interleukin-1β-Activated microvascular endothelial cells promote DC-SIGN-Positive alternatively activated macrophages as a mechanism of skin fibrosis in systemic sclerosis. *Arthritis Rheumatol* (2022) 74(6):1013–26. doi: 10.1002/art.42061

156. Taniguchi T, Miyagawa T, Toyama S, Yamashita T, Nakamura K, Saigusa R, et al. CXCL13 produced by macrophages due to Fli1 deficiency may contribute to the development of tissue fibrosis, vasculopathy and immune activation in systemic sclerosis. *Exp Dermatol* (2018) 27(9):1030–7. doi: 10.1111/exd.13724

157. Distler O, Distler JH, Scheid A, Acker T, Hirth A, Rethage J, et al. Uncontrolled expression of vascular endothelial growth factor and its receptors leads to insufficient skin angiogenesis in patients with systemic sclerosis. *Circ Res* (2004) 95(1):109–16. doi: 10.1161/01.RES.0000134644.89917.96

158. Numajiri H, Kuzumi A, Fukasawa T, Ebata S, Yoshizaki-Ogawa A, Asano Y, et al. B cell depletion inhibits fibrosis *via* suppression of profibrotic macrophage differentiation in a mouse model of systemic sclerosis. *Arthritis Rheumatol* (2021) 73(11):2086–95. doi: 10.1002/art.41798

159. Toledo DM, Pioli PA. Macrophages in systemic sclerosis: Novel insights and therapeutic implications. *Curr Rheumatol Rep* (2019) 21(7):31. doi: 10.1007/s11926-019-0831-z

160. Lescoat A, Ballerie A, Lelong M, Augagneur Y, Morzadec C, Jouneau S, et al. Crystalline silica impairs efferocytosis abilities of human and mouse macrophages: Implication for silica-associated systemic sclerosis. *Front Immunol* (2020) 11:219. doi: 10.3389/fimmu.2020.00219

161. Sun C, Chen SY. RGC32 promotes bleomycin-induced systemic sclerosis in a murine disease model by modulating classically activated macrophage function. *J Immunol* (2018) 200(8):2777–85. doi: 10.4049/jimmunol.1701542

162. Taroni JN, Greene CS, Martyanov V, Wood TA, Christmann RB, Farber HW, et al. A novel multi-network approach reveals tissue-specific cellular modulators of fibrosis in systemic sclerosis. *Genome Med* (2017) 9(1):27. doi: 10.1186/s13073-017-0417-1

163. Sun W, Yan S, Yang C, Yang J, Wang H, Li C, et al. Mesenchymal stem cells-derived exosomes ameliorate lupus by inducing M2 macrophage polarization and regulatory T cell expansion in MRL/lpr mice. *Immunol Invest.* (2022) 51(6):1785–803. doi: 10.1080/08820139.2022.2055478

164. Bielecki M, Kowal K, Lapinska A, Chyczewski L, Kowal-Bielecka O. Increased release of soluble CD163 by the peripheral blood mononuclear cells is associated with worse prognosis in patients with systemic sclerosis. *Adv Med Sci* (2013) 58(1):126–33. doi: 10.2478/v10039-012-0076-9

165. Higashi-Kuwata N, Makino T, Inoue Y, Takeya M, Ihn H. Alternatively activated macrophages (M2 macrophages) in the skin of patient with localized scleroderma. *Exp Dermatol* (2009) 18(8):727–9. doi: 10.1111/j.1600-0625.2008.00828.x

166. Maier C, Ramming A, Bergmann C, Weinkam R, Kittan N, Schett G, et al. Inhibition of phosphodiesterase 4 (PDE4) reduces dermal fibrosis by interfering with the release of interleukin-6 from M2 macrophages. *Ann Rheum Dis* (2017) 76(6):1133–41. doi: 10.1136/annrheumdis-2016-210189

167. Yamashita T, Asano Y, Taniguchi T, Nakamura K, Saigusa R, Miura S, et al. Glycyrrhizin ameliorates fibrosis, vasculopathy, and inflammation in animal models of systemic sclerosis. *J Invest Dermatol* (2017) 137(3):631–40. doi: 10.1016/j.jid.2016.08.037

168. Huang J, Maier C, Zhang Y, Soare A, Dees C, Beyer C, et al. Nintedanib inhibits macrophage activation and ameliorates vascular and fibrotic manifestations in the Fra2 mouse model of systemic sclerosis. *Ann Rheum Dis* (2017) 76(11):1941–8. doi: 10.1136/annrheumdis-2016-210823

169. Skaug B, Khanna D, Swindell WR, Hinchcliff ME, Frech TM, Steen VD, et al. Global skin gene expression analysis of early diffuse cutaneous systemic sclerosis shows a prominent innate and adaptive inflammatory profile. *Ann Rheum Dis* (2020) 79(3):379–86. doi: 10.1136/annrheumdis-2019-215894

170. Laurent P, Sisirak V, Lazaro E, Richez C, Duffau P, Blanco P, et al. Innate immunity in systemic sclerosis fibrosis: Recent advances. *Front Immunol* (2018) 9:1702. doi: 10.3389/fimmu.2018.01702

171. Jeljeli M, Riccio LGC, Doridot L, Chêne C, Nicco C, Chouzenoux S, et al. Trained immunity modulates inflammation-induced fibrosis. *Nat Commun* (2019) 10(1):5670. doi: 10.1038/s41467-019-13636-x

172. Anderson MS, Bluestone JA. The NOD mouse: a model of immune dysregulation. *Annu Rev Immunol* (2005) 23:447–85. doi: 10.1146/annurev.immunol

173. Burg AR, Tse HM. Redox-sensitive innate immune pathways during macrophage activation in type 1 diabetes. *Antioxid Redox Signal* (2018) 29(14):1373–98. doi: 10.1089/ars.2017.7243

174. O'Reilly LA, Hutchings PR, Crocker PR, Simpson E, Lund T, Kioussis D, et al. Characterization of pancreatic islet cell infiltrates in NOD mice: effect of cell transfer and transgene expression. *Eur J Immunol* (1991) 21(5):1171–80. doi: 10.1002/eji.1830210512

175. Hanenberg H, Kolb-Bachofen V, Kantwerk-Funke G, Kolb H. Macrophage infiltration precedes and is a prerequisite for lymphocytic insulitis in pancreatic islets of pre-diabetic BB rats. *Diabetologia.* (1989) 32(2):126–34. doi: 10.1007/BF00505185

176. Willcox A, Richardson SJ, Bone AJ, Foulis AK, Morgan NG. Analysis of islet inflammation in human type 1 diabetes. *Clin Exp Immunol* (2009) 155(2):173–81. doi: 10.1111/j.1365-2249.2008.03860.x

177. Oschilewski U, Kiesel U, Kolb H. Administration of silica prevents diabetes in BB-rats. *Diabetes* (1985) 34(2):197–9. doi: 10.2337/diab.34.2.197

178. Kolb H, Burkart V, Appels B, Hanenberg H, Kantwerk-Funke G, Kiesel U, et al. Essential contribution of macrophages to islet cell destruction *in vivo* and in vitro. *J Autoimmun* (1990) 3 Suppl 1:117–20. doi: 10.1016/s0896-8411(09)90020-8

179. Jun HS, Santamaria P, Lim HW, Zhang ML, Yoon JW. Absolute requirement of macrophages for the development and activation of beta-cell cytotoxic CD8+ T-cells in T-cell receptor transgenic NOD mice. *Diabetes.* (1999) 48(1):34–42. doi: 10.2337/diabetes.48.1.34

180. Calderon B, Suri A, Unanue ER. In CD4+ T-cell-induced diabetes, macrophages are the final effector cells that mediate islet beta-cell killing: studies from an acute model. *Am J Pathol* (2006) 169(6):2137–47. doi: 10.2353/ajpath.2006.060539

181. Thornley TB, Agarwal KA, Kyriazis P, Ma L, Chipashvili V, Aker JE, et al. Contrasting roles of islet resident immunoregulatory macrophages and dendritic cells in experimental autoimmune type 1 diabetes. *PloS One* (2016) 11(3):e0150792. doi: 10.1371/journal.pone.0150792

182. Zhang J, Tan SB, Guo ZG. CD47 decline in pancreatic islet cells promotes macrophage-mediated phagocytosis in type I diabetes. *World J Diabetes.* (2020) 11(6):239–51. doi: 10.4239/wjd.v11.i6.239

183. Cantor J, Haskins K. Recruitment and activation of macrophages by pathogenic CD4 T cells in type 1 diabetes: evidence for involvement of CCR8 and CCL1. *J Immunol* (2007) 179(9):5760–7. doi: 10.4049/jimmunol.179.9.5760

184. Stoffels K, Overbergh L, Giulietti A, Kasran A, Bouillon R, Gysemans C, et al. NOD macrophages produce high levels of inflammatory cytokines upon encounter of apoptotic or necrotic cells. *J Autoimmun* (2004) 23(1):9–15. doi: 10.1016/j.jaut.2004.03.012

185. Marée AF, Kublik R, Finegood DT, Edelstein-Keshet L. Modelling the onset of type 1 diabetes: can impaired macrophage phagocytosis make the difference between health and disease? *Philos Trans A Math Phys Eng Sci* (2006) 364(1842). doi: 10.1098/rsta.2006.1769

186. Chung YH, Jun HS, Kang Y, Hirasawa K, Lee BR, Van Rooijen N, et al. Role of macrophages and macrophage-derived cytokines in the pathogenesis of kilham rat virus-induced autoimmune diabetes in diabetes-resistant BioBreeding rats. *J Immunol* (1997) 159(1):466–71. doi: 10.4049/jimmunol.159.1.466

187. Diana J, Lehuen A. Macrophages and β-cells are responsible for CXCR2-mediated neutrophil infiltration of the pancreas during autoimmune diabetes. *EMBO Mol Med* (2014) 6(8):1090–104. doi: 10.15252/emmm.201404144

188. Amrani A, Verdaguer J, Thiessen S, Bou S, Santamaria P. IL-1alpha, IL-1beta, and IFN-gamma mark beta cells for fas-dependent destruction by diabetogenic CD4(+) T lymphocytes. *J Clin Invest.* (2000) 105(4):459–68. doi: 10.1172/JCI8185

189. Jun HS, Yoon CS, Zbytnuik L, van Rooijen N, Yoon JW. The role of macrophages in T cell-mediated autoimmune diabetes in nonobese diabetic mice. *J Exp Med* (1999) 189(2):347–58. doi: 10.1084/jem.189.2.347

190. Marro BS, Legrain S, Ware BC, Oldstone MB. Macrophage IFN-I signaling promotes autoreactive T cell infiltration into islets in type 1 diabetes model. *JCI Insight* (2019) 4(2):e125067. doi: 10.1172/jci.insight.125067

191. Parsa R, Andresen P, Gillett A, Mia S, Zhang XM, Mayans S, et al. Adoptive transfer of immunomodulatory M2 macrophages prevents type 1 diabetes in NOD mice. *Diabetes.* (2012) 61(11):2881–92. doi: 10.2337/db11-1635

192. Li Y, Ding X, Tian X, Zheng J, Ding C, Li X, et al. Islet transplantation modulates macrophage to induce immune tolerance and angiogenesis of islet tissue in type I diabetes mice model. *Aging (Albany NY).* (2020) 12(23):24023–32. doi: 10.18632/aging.104085

193. Barra JM, Kozlovskaya V, Kharlampieva E, Tse HM. Localized immunosuppression with tannic acid encapsulation delays islet allograft and autoimmune-mediated rejection. *Diabetes.* (2020) 69(9):1948–60. doi: 10.2337/db20-0248

194. Chen Y, Nagy T, Guo TL. Glycated whey proteins protect NOD mice against type 1 diabetes by increasing anti-inflammatory responses and decreasing autoreactivity to self-antigens. *J Funct Foods.* (2019) 56:171–81. doi: 10.1016/j.jff.2019.03.015

195. Wang F, Sun F, Luo J, Yue T, Chen L, Zhou H, et al. Loss of ubiquitin-conjugating enzyme E2 (Ubc9) in macrophages exacerbates multiple low-dose streptozotocin-induced diabetes by attenuating M2 macrophage polarization. *Cell Death Dis* (2019) 10(12):892. doi: 10.1038/s41419-019-2130-z

196. Timper K, Hruz P, Beglinger C, Donath MY. Infliximab in the treatment of crohn disease and type 1 diabetes. *Diabetes Care* (2013) 36(7):e90–1. doi: 10.2337/dc13-0199

197. Green EA, Flavell RA. Tumor necrosis factor-alpha and the progression of diabetes in non-obese diabetic mice. *Immunol Rev* (1999) 169:11–22. doi: 10.1111/j.1600-065x.1999.tb01302.x

198. Von Scholten BJ, Kreiner FF, Gough SCL, von Herrath M. Current and future therapies for type 1 diabetes. *Diabetologia.* (2021) 64(5):1037–48. doi: 10.1007/s00125-021-05398-3

199. Citro A, Cantarelli E, Piemonti L. The CXCR1/2 pathway: Involvement in diabetes pathophysiology and potential target for T1D interventions. *Curr Diabetes Rep* (2015) 15(10):68. doi: 10.1007/s11892-015-0638-x

200. Li R, He Y, Zhu Y, Jiang L, Zhang S, Qin J, et al. Route to rheumatoid arthritis by macrophage-derived microvesicle-coated nanoparticles. *Nano Lett* (2019) 19(1):124–34. doi: 10.1021/acs.nanolett.8b03439

201. Tang TT, Lv LL, Wang B, Cao JY, Feng Y, Li ZL, et al. Employing macrophage-derived microvesicle for kidney-targeted delivery of dexamethasone: An efficient therapeutic strategy against renal inflammation and fibrosis. *Theranostics.* (2019) 9(16):4740–55. doi: 10.7150/thno.33520

202. Aran D, Looney AP, Liu L, Wu E, Fong V, Hsu A, et al. Reference-based analysis of lung single-cell sequencing reveals a transitional profibrotic macrophage. *Nat Immunol* (2019) 20(2):163–72. doi: 10.1038/s41590-018-0276-y

frontiers | Frontiers in Immunology

TYPE Original Research
PUBLISHED 03 March 2023
DOI 10.3389/fimmu.2023.1139204

OPEN ACCESS

EDITED BY
Ruoxi Yuan,
Hospital for Special Surgery, United States

REVIEWED BY
Chao Ma,
Stanford University, United States
Mengmeng Jin,
Rutgers, The State University of New Jersey, United States
Xudong Wang,
University of Pennsylvania, United States

*CORRESPONDENCE
Zsuzsa Szondy
szondy@med.unideb.hu

SPECIALTY SECTION
This article was submitted to Inflammation, a section of the journal Frontiers in Immunology

RECEIVED 06 January 2023
ACCEPTED 22 February 2023
PUBLISHED 03 March 2023

CITATION
Garabuczi É, Tarban N, Fige É, Patsalos A, Halász L, Szendi-Szatmári T, Sarang Z, Király R and Szondy Z (2023) Nur77 and PPARγ regulate transcription and polarization in distinct subsets of M2-like reparative macrophages during regenerative inflammation. *Front. Immunol.* 14:1139204. doi: 10.3389/fimmu.2023.1139204

Nur77 and PPARγ regulate transcription and polarization in distinct subsets of M2-like reparative macrophages during regenerative inflammation

Éva Garabuczi[1], Nastaran Tarban[2], Éva Fige[3], Andreas Patsalos[4,5], László Halász[4,5], Tímea Szendi-Szatmári[6], Zsolt Sarang[7], Róbert Király[7] and Zsuzsa Szondy[7,8]*

[1]Department of Integrative Health Sciences, Institute of Health Sciences, Faculty of Health Sciences, University of Debrecen, Debrecen, Hungary, [2]Doctoral School of Molecular Cell and Immune Biology, Faculty of Medicine, University of Debrecen, Debrecen, Hungary, [3]Doctoral School of Dental Sciences, Faculty of Dentistry, University of Debrecen, Debrecen, Hungary, [4]Department of Medicine, Johns Hopkins University School of Medicine, Institute for Fundamental Biomedical Research, Johns Hopkins All Children's Hospital, St. Petersburg, FL, United States, [5]Department of Biological Chemistry, Johns Hopkins University School of Medicine, Institute for Fundamental Biomedical Research, Johns Hopkins All Children's Hospital, St. Petersburg, FL, United States, [6]Department of Biophysics and Cell Biology, Faculty of Medicine, University of Debrecen, Debrecen, Hungary, [7]Department of Biochemistry and Molecular Biology, Faculty of Medicine, University of Debrecen, Debrecen, Hungary, [8]Section of Dental Biochemistry, Department of Basic Medical Sciences, Faculty of Dentistry, University of Debrecen, Debrecen, Hungary

Macrophage polarization is a process whereby macrophages develop a specific phenotype and functional response to different pathophysiological stimuli and tissue environments. In general, two main macrophage phenotypes have been identified: inflammatory (M1) and alternatively activated (M2) macrophages characterized specifically by IL-1β and IL-10 production, respectively. In the cardiotoxin-induced skeletal muscle injury model bone marrow-derived macrophages (BMDMs) play the central role in regulating tissue repair. Bone marrow-derived monocytes arriving at the site of injury differentiate first to M1 BMDMs that clear cell debris and trigger proliferation and differentiation of the muscle stem cells, while during the process of efferocytosis they change their phenotype to M2 to drive resolution of inflammation and tissue repair. The M2 population is formed from at least three distinct subsets: antigen presenting, resolution-related and growth factor producing macrophages, the latest ones expressing the transcription factor PPARγ. Nuclear receptor subfamily 4 group A member 1 (NR4A1; also termed Nur77) transcription factor is expressed as an early response gene, and has been shown to suppress the expression of pro-inflammatory genes during efferocytosis. Here we demonstrate that (1) Nur77 null BMDMs are characterized by elevated expression of PPARγ resulting in enhanced efferocytosis capacity; (2) Nur77 and PPARγ regulate transcription in different subsets of M2 skeletal muscle macrophages during muscle repair; (3) the loss of Nur77 prolongs M1 polarization characterized by increased and

prolonged production of IL-1β by the resolution-related macrophages normally expressing Nur77; whereas, in contrast, (4) it promotes M2 polarization detected *via* the increased number of IL-10 producing CD206^{+} macrophages generated from the PPARγ-expressing subset.

KEYWORDS

macrophage, PPAR gamma, Nur77, polarization, cardiotoxin, skeletal muscle injury, efferocytosis

Introduction

Clearance of apoptotic cells (efferocytosis) by macrophages plays a central role in maintaining tissue homeostasis. During the efferocytosis process macrophages not only clear apoptotic cells and degrade them, but also release various biologically active signaling molecules the release of which is triggered by the apoptotic cell uptake itself. If these molecules are released in resting tissues, they provide local trophic support, as some of them are growth factors (1). In the thymus they contribute to the thymic selection processes by directing the formation of regulatory T cells (2), and by regulating the signalling threshold of negative selection (3). Following tissue injury, however, they drive the resolution of inflammation and tissue repair (4). Proper efferocytosis regulates the proper production of these engulfing macrophage-derived regulatory molecules. The efferocytosis process *in vivo* is initiated by finding the apoptotic cells by macrophages *via* the help of 'find me' signals released from the apoptotic cells (5). Macrophages then recognize the apoptotic cells *via* their characteristic cell surface changes. The most well-known cell surface change is the exposure of phosphatidylserine (PS), a key 'eat me' signal, on the surface of dying cells (6). Multiple receptors on the surface of macrophages such as Tim4, stabilin-2, or BAI1, recognize and bind to PS directly, whereas other receptors use bridging molecules to link the phagocytic receptor to PS (7). Bridging molecules are present in the serum but are also actively produced by the macrophages. One of them is milk fat globule-EGF-factor 8 (MFG-E8) which uses its RGD motif within its EGF-like domain to bind to various integrin receptors, such as β3 and β5 participating in the phagocytosis process, but also contains gamma carboxylated glutamate side chains to link the protein to PS (8, 9). In addition to using bridging molecules, integrin receptors also require coreceptors, such as Tim4 by integrin β1 (10) or transglutaminase 2 (TG2) and CD36 (11–13) by integrin β3, for their proper phagocytic function. Phagocytes in different tissues express different combinations of the various efferocytosis receptors, but all of the expressed ones assemble and function together in the phagocytic synapse to mediate tethering, and to initiate sufficient engulfment signaling once macrophages interact with the apoptotic cells (14). So far two efferocytosis signaling pathways have been identified that trigger the apoptotic cell uptake, and both lead to the activation of the small GTPase Rac1 (15). Nur77 (NR4a) is a transcription factor, which belongs to the steroid/thyroid hormone receptor superfamily, and is an orphan receptor for which no ligand is known (16). Besides forming a heterodimer with the retinoid X receptor to mediate retinoic acid-dependent transcription to reporters containing the DR5 regulatory element, it can also bind in monomeric form to promoters containing the Nur77 binding response element (17), as well as a homodimer to the Nur77 response element carrying ones (18). In addition, similar to other members of this transcription family, it is able to interact with other transcription factors, such as nuclear factor kappa-light-chain-enhancer of activated B cells (NF-κB) (19), and regulate their transcriptional activity. The activity of Nur77 was shown to be controlled through transcriptional regulation, posttranslational modifications, protein-protein interactions and subcellular localization (20, 21). Nur77 is abundantly expressed in various tissues including myeloid cells. Loss of Nur77 in macrophages has been reported to result in enhanced pro-inflammatory cytokine release following Toll like receptor 4 stimulation, and in an M1 type pro-inflammatory polarization in various atherosclerosis models. The effect has been linked to uncontrolled NF-κB activation leading to enhanced transcription of various inflammation-related genes (22). Recently the transcriptome of bone marrow-derived macrophages (BMDMs) from wild-type (WT) and Nur77-knockout (Nur77 KO) mice has been analyzed (23). In addition to the enhanced expression of a group of inflammation-related genes, IPA Upstream Regulator Analysis revealed Rac1 as an activated upstream regulator possibly mediating changes in gene expression induced by the loss of Nur77. Since enhanced Rac1 activity of BMDMs is known to be associated with enhanced efferocytosis capability, we decided to investigate phagocytosis of apoptotic cells mediated by the Nur77 KO macrophages. As phagocytosis of apoptotic cells plays a crucial role also in promoting formation of M2-like reparative macrophages which guide tissue repair during regenerative inflammation (24), we also followed the formation of reparative macrophages in the absence of Nur77 in the cardiotoxin–induced injury model of skeletal muscle.

Results

Nur77 KO bone marrow derived macrophages have enhanced efferocytosis capacity due to an increased integrin β3 and β5 signaling

Since previous studies indicated that Nur77 KO BMDMs have an enhanced Rac1 gene signature (23), and Rac1 is known to play a determining role also in efferocytosis by regulating lamellopodia

10.3389/fimmu.2023.1139204

formation (25), we checked whether Nur77 KO BMDMs have an altered efferocytosis capacity. As seen in Figure 1A, in line with the enhanced Rac1 gene signature, we also observed an increased efferocytosis capacity of BMDMs after a 45 min exposure to apoptotic cells. Loss of Nur77 resulted not only in an increase in the percentage of engulfing macrophages but also an increase in the number of engulfed apoptotic cells (Figure 1B) detected as an increased mean fluorescence within the engulfing macrophage population (415 ± 18 versus 482 ± 18 in the wild-type and knock out macrophages, respectively. Significantly different $p<0.05$). This enhancement was more pronounced, if macrophages engulfed apoptotic cells first for 6 h, and their efferocytosis capacity was determined 18 h later (Figure 1A). To check whether the observed difference in the efferocytosis capacity is related to a bridging molecule-driven efferocytosis pathway in Nur77 KO macrophages, their phagocytosis was also determined after washing the cultured medium away (Figure 1C). As compared to the efferocytosis capacity determined after 24 h in culture, the efferocytosis capacity of both types of macrophages decreased, if the culture medium was washed away (removal of the macrophage-produced bridging molecules), and phagocytosis was determined in the absence of fetal bovine serum (FBS) (removal of the serum-derived bridging molecules). What is more, the difference between the two types of macrophages completely disappeared. These data indicate that the enhanced efferocytic capacity of Nur77 KO macrophages is related either to enhanced production of a bridging molecule or to increased expression of a bridging molecule-dependent efferocytosis receptor. To determine, whether enhanced production of a bridging molecule is responsible for the observed effect, we compared the mRNA expression of each bridging molecule in the wild-type and Nur77 KO macrophages, and found that only that of MFG-E8 was increased, whereas no change in the mRNA expression of protein S, Gas6, C1qb or thrombospondin (THBS)-1 was found (Figure 1D). Next, we checked whether gene expression of the target efferocytosis receptors of the various bridging molecules is altered. However, we have not found a change in the expression of Axl, MerTK, or CD91, targets of Protein S, Gas6 or C1qb (Figure 1E). Since previous studies have shown that MFG-E8 binds to various integrin receptors *via* its RGD domain (8, 9), we also checked the mRNA expression of the various integrins and their coreceptors. While the mRNA expression of integrin β1 and β3, and that of Tim4 was not altered by the loss of Nur77 (Figure 1E), the basal gene expression of both CD36 and TG2 was significantly higher in the Nur77 KO macrophages, and we found a moderate increase in the expression of integrin β5 as well. Altogether, these data indicate that an enhanced integrin β3 and β5 signaling might be responsible for the enhanced efferocytosis capacity of Nur77 KO macrophages.

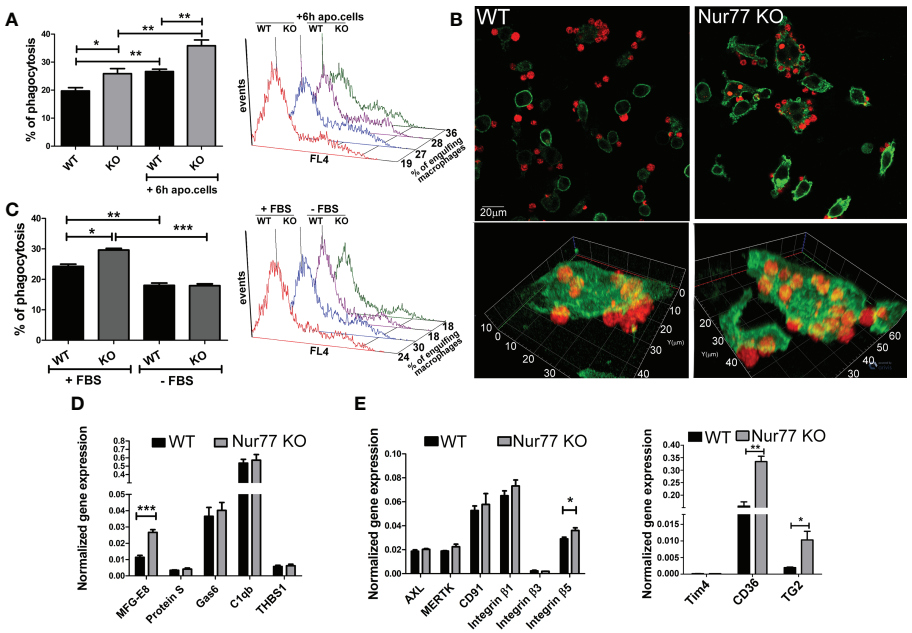

FIGURE 1
Loss of Nur77 in BMDMs leads to enhanced efferocytosis due to an increased integrin β3 and β5 signaling. **(A)** *In vitro* uptake of fluorescently-labeled apoptotic thymocytes by WT and Nur77 KO BMDMs following 24 h incubation after seeding the BMDMs or after 6h co-culture with non-labeled apoptotic thymocytes followed by additional 18 h incubation. The percentage of engulfing macrophages was determined by flow cytometry analysis. A representative histogram of each experimental setting is also shown. **(B)** One representative confocal image showing efferocytosis by wild-type and Nur77 KO BMDMs following 24h in culture. Alexa Fluor 488 conjugated anti-F4/80 antibody -labelled macrophages appear as green cells, while Deep Red dye-labelled apoptotic thymocytes appear as red cells. **(C)** Efferocytosis by WT or Nur77 KO BMDMs following 24h culture in 10% FBS containing DMEM or washing the culture medium away and using a fresh DMEM without FBS during the 45 min efferocytosis. A representative histogram of each experimental setting is also shown. **(D, E)** mRNA expressions of various bridging molecules and phagocytic receptors determined by qRT-PCR in WT and Nur77 KO BMDMs following 24 h in culture. β-actin was used as a reference gene. All the results are expressed as mean ± SEM (n = 3). Asterisks indicate statistical significance (*$P < 0.05$, **$P < 0.01$, *** $p < 0.001$).

Increased expression of PPARγ drives the enhanced phagocytic capacity of Nur77 KO BMDMs

How can the loss of Nur77 affect the expression of genes related to the integrin β3 and β5 signaling pathways? Previous studies have shown that engulfing macrophages are capable of increasing their efferocytosis capacity *via* activation of their lipid-sensing nuclear receptors (liver X receptor (LXR)α/β, PPARγ and δ). These transcription factors, in turn, induce the expression of various phagocytic receptors or bridging molecules (26–28). Since the difference in the efferocytosis capacity between WT and Nur77 KO macrophages was more pronounced, if macrophages have already engulfed apoptotic cells (Figure 1A) when the content of the engulfed apoptotic material triggers activation of these nuclear receptors, we checked their mRNA expression. While the mRNA expression of PPARδ and that of LXRα did not change (Figure 2A), the mRNA expression of PPARγ significantly increased in Nur77 KO macrophages. Enhanced PPARγ levels were detected in the Nur77 KO macrophages at the protein level as well (Figure 2B). In addition, the mRNA level of its known target gene, fatty acid binding protein (FABP) 4 (29), was also significantly elevated in the Nur77 KO cells (Figure 2C). Accordingly, inhibition of PPARγ transcriptional activity by GW9662 for 24 h decreased the efferocytic capacity of Nur77 KO macrophages (Figure 2D). What is more, in the presence of the inhibitor the difference in the efferocytosis capacity of the two types of macrophages disappeared. Altogether these data indicate that the difference in the efferocytic capacity of the Nur77 KO macrophages is related to an enhanced PPARγ transcriptional activity.

PPARγ induces the synthesis of retinoic acid to upregulate integrin signaling

Previous studies from our laboratory have demonstrated that engulfing macrophages produce retinoids that upregulate the expression of various phagocytic receptors (30, 31). This enhancement in the phagocytosis gene expressions was partially mediated *via* an LXR-dependent induction of retinaldehyde dehydrogenases (RALDHs), enzymes that are specifically involved in the synthesis of retinoic acids, and that of retinoic acid receptor (RAR)α, a nuclear receptor for which retinoic acids serve as ligands (31, 32). Since we have shown previously that rosiglitazone, a PPARγ agonist, was also capable of inducing RALDHs (30), we checked the mRNA and protein expression of RALDH2, the dominant RALDH in macrophages, and that of RARα. As seen Figures 3A, B, the expression of both RALDH2 and RARα was increased in Nur77 KO macrophages as compared to their wild-type counterparts at both mRNA and protein levels. Accordingly, Nur77 KO macrophages responded to all-trans retinoic acid (ATRA) treatment with a more significant increase in the efferocytosis capacity (Figure 3C). To determine whether PPARγ-regulated retinoid synthesis mediates the effect of the loss of Nur77 on the efferocytosis of macrophages, both WT and Nur77 KO macrophages were pre-treated for 24 h with the PPARγ antagonist GW9662, the RALDH inhibitor N,N-diethylaminobenzaldehyde (DEAB) or the pan-RAR antagonist AGN109, and their efferocytosis capacity was measured at the end of the treatments. These treatments decreased the efferocytosis capacity of both WT and Nur77 KO macrophages, and the efferocytosis capacity of Nur77 KO cells decreased to that of the WT ones (Figures 3D, E). Next we checked, how the above treatments

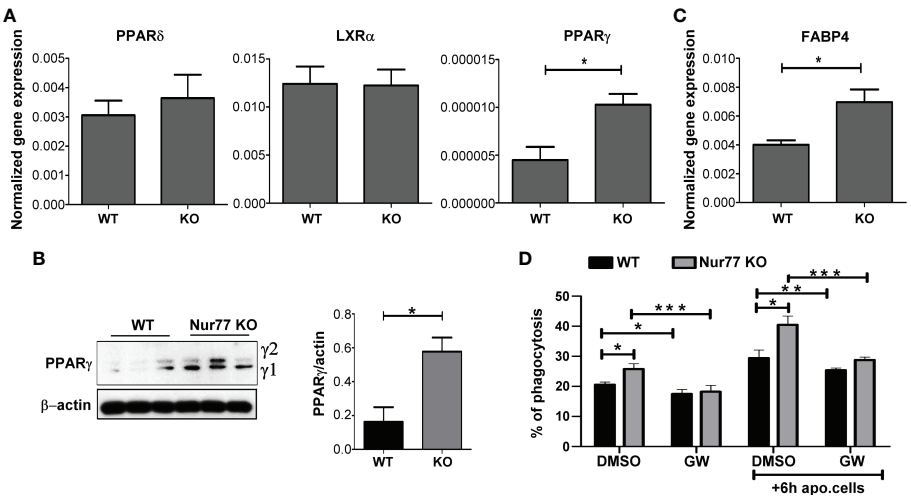

FIGURE 2
Loss of Nur77 leads to enhanced efferocytosis by BMDMs *via* upregulation of the PPARγ transcription factor. **(A)** mRNA expression levels of PPARδ, LXRα and PPARγ in WT and Nur77 KO BMDMs following 24h in culture determined by qRT-PCR. β-actin was used as a reference gene. **(B)** Protein levels of PPARγ in WT and Nur77 KO BMDMs under the same conditions determined by Western blot analysis. β-actin was used as a loading control. **(C)** mRNA expression levels of FABP4, a direct target gene of PPARγ, in WT and Nur77 KO BMDMs following 24h in culture detected by by qRT-PCR. β-actin was used as a reference gene. **(D)** Phagocytic capacity of WT and Nur77 KO BMDMs with or without pre-culture with non-labeled apoptotic thymocytes for 6 h, in the absence (DMSO control) or presence of PPARγ antagonist GW9662 (5μM) for 24 h determined by flow cytometry. All results are expressed as mean ± SEM (n = 3). Asterisks indicate statistical significance (*$P < 0.05$, **$P < 0.01$, ***$p < 0.001$).

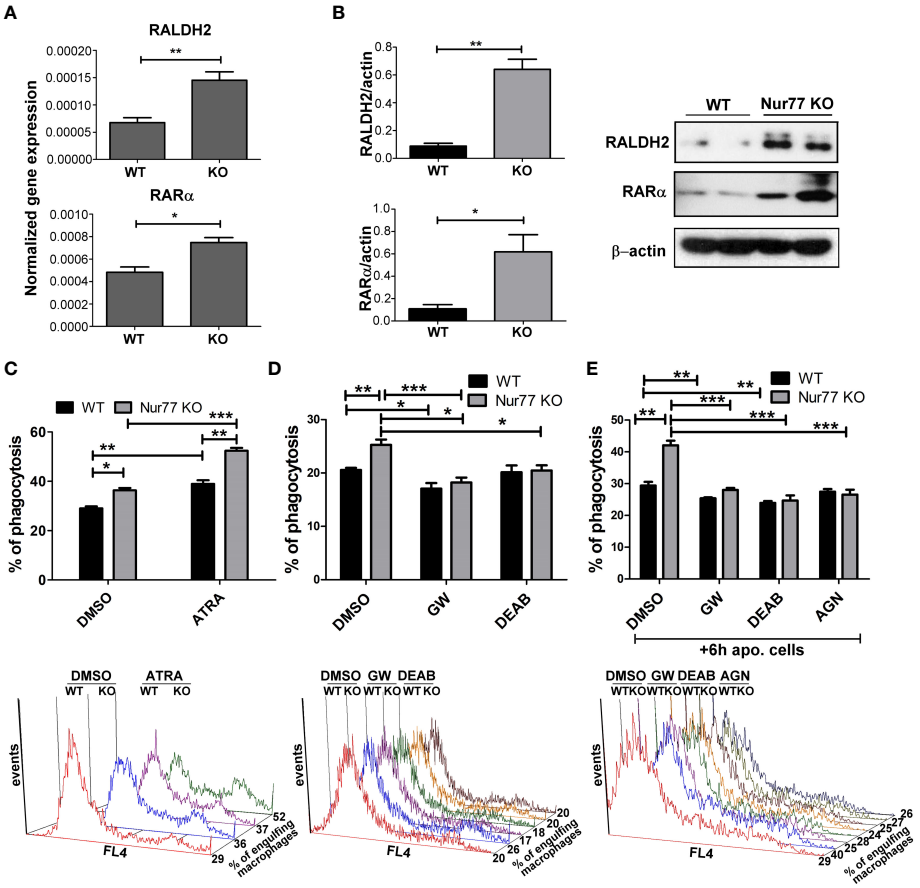

FIGURE 3
Elevated PPARγ expression leads to enhanced efferocytosis by Nur77 KO BMDMs *via* upregulating retinoic acid synthesis. **(A)** mRNA expression levels of RALDH2 and RARα of WT and Nur77 KO BMDMs following 24 h in culture determined by qRT-PCR. β-actin was used as a reference gene. **(B)** RALDH2 and RARα protein expression of WT and Nur77 KO BMDMs under the same conditions detected by Western blot analysis. β- actin was used as a loading control. **(C)** WT or Nur77 KO BMDMs were exposed to 300 nM ATRA or DMSO (vehicle) for 24 h, then the percentage of engulfing macrophages was determined by flow cytometry. A representative histogram of each experimental setting is also shown. **(D)** Wild-type and Nur77 KO BMDMs were exposed to GW9662 (5μM), a PPARγ antagonist, to DEAB (15 μM), an RALDH inhibitor, or to DMSO (vehicle) for 24h prior to determining their phagocytic capacity. The percentage of engulfing macrophages was detected by flow cytometry. A representative histogram of each experimental setting is also shown. **(E)** Wild-type or Nur77KO BMDMs were first exposed to non-fluorescent apoptotic thymocytes for 6 h together with GW9662 (5μM), with DEAB (15μM), or with the pan-RAR antagonist AGN193109 (1μM), then apoptotic cells were washed away and inhibitors was added again to BMDMs for additional 18 h prior to determining the percentage of macrophages engulfing apoptotic cells by flow cytometry. A representative histogram of each experimental setting is also shown. All results are expressed as mean ± SEM (n = 3). Asterisks indicate statistical significance (*$P < 0.05$, **$P < 0.01$, *** $p < 0.001$).

affect the mRNA expression of those three phagocytosis genes, which we found to be significantly altered by the loss of Nur77 (Figures 4A–C). The most dramatic change was seen in the gene expression of TG2, in accordance with the observation that its expression was enhanced most by the loss of Nur77. While these treatments hardly affected the basal levels of TG2 in the WT macrophages, each treatment reduced the TG2 mRNA expression of Nur77 KO cells to the wild-type level. CD36 mRNA expressions, on the other hand, were only partially dependent on the PPARγ/retinoid signaling pathway, despite of the fact that CD36 expression was shown to be affected by both PPARγ and retinoids (33). Finally, the elevated MFG-E8 expression was independent of $PPAR_{\gamma}$ indicating that Nur77 must suppress the expression MFG-E8 in WT cells *via* a different mechanism. Altogether, our data suggest that the enhanced PPARγ-dependent phagocytic capacity is largely dependent on the enhanced TG2 expression. TG2 was shown to facilitate integrin signaling and to promote efferocytosis added as a recombinant protein (11, 34). To determine whether addition of recombinant TG2 to WT macrophages could enhance their phagocytosis efficiency to the level of Nur77 KO cells, efferocytosis capacity of both cell types was determined after 24h in culture in the presence and absence of mouse recombinant TG2. As seen in Figures 4D, E, the addition of recombinant TG2 enhanced the phagocytic capacity of WT macrophages, but not that of the Nur77 KO cells. In addition, their phagocytic capacity was similar in the presence of recombinant TG2. These data provide further evidence for the TG2-dependence of the observed enhanced efferocytosis efficiency in Nur77 KO macrophages.

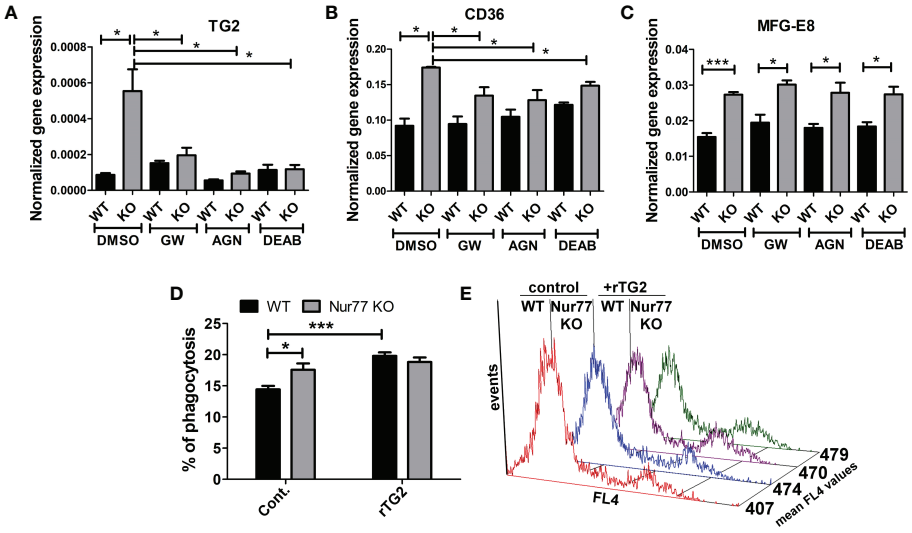

FIGURE 4
Increased efferocytosis capacity of Nur77 KO macrophages is strongly related to the enhanced TG2 expression. **(A-C)** mRNA expression levels of TG2, CD36 and MFG-E8 in wild-type and Nur77 KO BMDMs determined by qRT-PCR following a 24 h exposure to GW9662 (5 μM), DEAB (15 μM), AGN193109 (1 μM), or DMSO (vehicle). β-actin was used as a reference gene. **(D)** *In vitro* uptake of fluorescently-labeled apoptotic thymocytes by WT and Nur77 KO BMDMs after a 1 h exposure to recombinant mouse TG2 (rTG2) (10 μg/ml).The percentage of engulfing macrophages was determined by flow cytometry. **(E)** Mean fluorescence values of the engulfing macrophages in the above experiments indicating enhanced individual apoptotic cell uptake by the rTG2-exposed cells. Results are expressed as mean ± SEM (n = 3). Asterisks indicate statistical significance (*$P < 0.05$, **$P < 0.01$, ***p< 0.001).

Nur77 and PPARγ are expressed by distinct groups of M2 macrophages which drive skeletal muscle tissue repair following cardiotoxin injury

If Nur77 inhibits the expression of PPAR$_\gamma$, how is it possible that apoptotic cell uptake was shown to activate both transcription factors in BMDMs (27, 35)? Increasing evidence indicate that macrophages do not form one single group of cells, and even within their two main groups there is a big heterogeneity. The first group, the tissue resident macrophages are mainly derived from the yolk sac during embryogenesis (1, 36). They act as sentinels in the tissues, and play an essential role in tissue homeostasis by removing apoptotic cells generated during the normal tissue turnover, and by producing growth factors and other mediators that provide trophic support to the tissues in which they reside. The second group, the BMDMs are recruited to the tissues in response to tissue injury induced by infection, autoimmune disorders, or by various injuries, and are crucial drivers and regulators of inflammatory and tissue regenerative responses (4, 37). One model, in which the differentiation, phenotype change (polarization) and function of BMDMs can be studied *in vivo*, is the cardiotoxin-induced injury model of the tibialis anterior skeletal muscle (7). Cardiotoxin injection triggers apoptotic and necrotic skeletal muscle cell death (38). Within this model, one day after the cardiotoxin injury monocytes arrive at the injury site and differentiate into M1 macrophages, which clear dead cells and, additionally, trigger muscle stem cell proliferation *via* the pro-inflammatory cytokines formed by them. As a result of the interaction with apoptotic cells during efferocytosis, these M1 macrophages start their conversion into M2-like reparative macrophages from day 3, and they drive angiogenesis, myotube formation from myoblasts, and the resolution of inflammation. Recent work by Patsalos et al. revealed the generation of three functionally distinct (growth factor producing, resolution-related and antigen presenting) populations of these M2-like reparative macrophages by analyzing their mRNA expressions using single-cell RNA sequencing at day 4 following cardiotoxin-induced injury (39). Using these data, we demonstrate in Figure 5 that on a single cell level Nur77 and PPARγ are expressed by different groups of M2-like reparative macrophages, and even when they are co-expressed, the PPARγ levels are low. PPARγ-dominant expression characterizes the growth factor producing macrophage population, while Nur77 is mainly expressed by the resolution-related and antigen presenting cells. What is more, nearly all the PPARγ-expressing cells express TG2 or CD36 in the growth factor producing population (cluster 2), where the majority of high PPARγ-expressing macrophages were found, underlying our finding that PPARγ regulates their expression. However, only 24% of the PPARγ expressing macrophages express MFG-E8 (Figure 5), and only 11.2% of the MFG-E8-expressing cells express PPARγ (data not shown) in accordance with our *in vitro* finding that the increase in the MFG-E8 mRNA expression in Nur77 KO cells is largely PPARγ-independent.

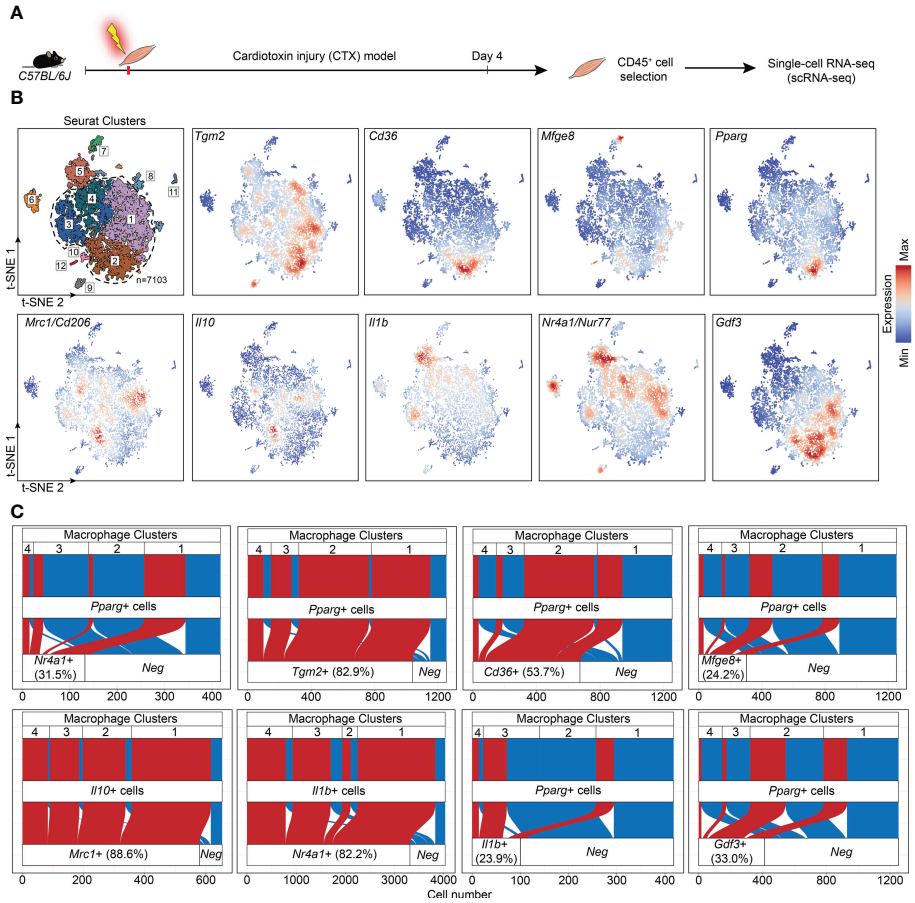

FIGURE 5
Immune single-cell transcriptomic map of regenerating murine skeletal muscle. **(A)** Workflow used for the isolation and analysis of previously published (39) single-cell RNAseq datasets from CD45$^+$ cells isolated at day 4 following cardiotoxin-induced injury (see also "Methods"). **(B)** Upper left panel: unsupervised clustering and t-SNE representation of CD45+ myeloid cells isolated from Day 4 post CTX injury (colored by 12 clusters defined using cluster resolution 0.4; dotted line indicates the four macrophage clusters 1-4; 1: Resolution-related, 2: Growth Factor-Expressing, 3: Pro-inflammatory, 4: Antigen-presenting macrophages). The rest of the panels indicate *Tgm2, Cd36, Mfge8, Pparg, Mrc1, Il10, Il1b, Nr4a1*, and *Gdf3* mRNA expression in the single-cell dataset. **(C)** Alluvial plots that simultaneously define the number of cells with single and double positive expression for indicated genes and for each macrophage cluster. Red indicates cells with double positive/detectable gene expression in the third layer).

Loss of Nur77 leads to enhanced PPARγ and TG2 expressions, and to an accelerated CD206$^+$ macrophage formation in day 4 skeletal muscle macrophages following cardiotoxin-induced injury

Our previous studies have demonstrated by studying macrophage polarization in the cardiotoxin-induced injury model of skeletal muscle that loss of TG2 not only affects the efficiency of the phagocytosis of dead cells, but also influences the expression levels of PPARγ, and the M1/M2 conversion of macrophages by significantly delaying the appearance of CD206$^+$ M2-like reparative macrophage subset (40). Using the same model, we tested how the loss of Nur77 affects the expression of PPARγ, and TG2, and the appearance of CD206$^+$ skeletal muscle macrophages following cardiotoxin-induced skeletal muscle injury. Simultaneously we also detected the disappearance of Ly6C, a marker, the disappearance of which allows us to follow the rate of M1/M2 macrophage conversion. As shown in Figures 6A, B, in Nur77 KO skeletal muscle-derived CD45$^+$ cells the expression of both PPARγ and TG2 was significantly higher. Accordingly, the number of CD206$^+$ macrophages was also significantly enhanced (Figure 6C). However, in line with a previous report (41), we did not find a difference in the rate of M1/M2 conversion of Nur77 KO skeletal muscle macrophages, if we followed it by the disappearance of the cell surface Ly6C molecule (Figure 6D). Interestingly, in TG2 null M2 macrophages the PPARγ expressions were found to be lower (40) indicating with the present data the existence of a positive autoregulatory loop that controls the expression of PPARγ or the number of PPARγ-expressing cells. PPARγ upregulates TG2, while the produced TG2 protein promotes either the stable expression of PPARγ mRNA or the better survival of the PPARγ-expressing macrophages. Altogether, our data indicate that the Ly6C$^-$ PPARγ+ TG2^{high} macrophages are the origin of at least one group of the Ly6C$^-$ CD206$^+$ macrophage population. Since TG2 acts as a coreceptor for integrins, our observations confirm that of others, who have demonstrated the

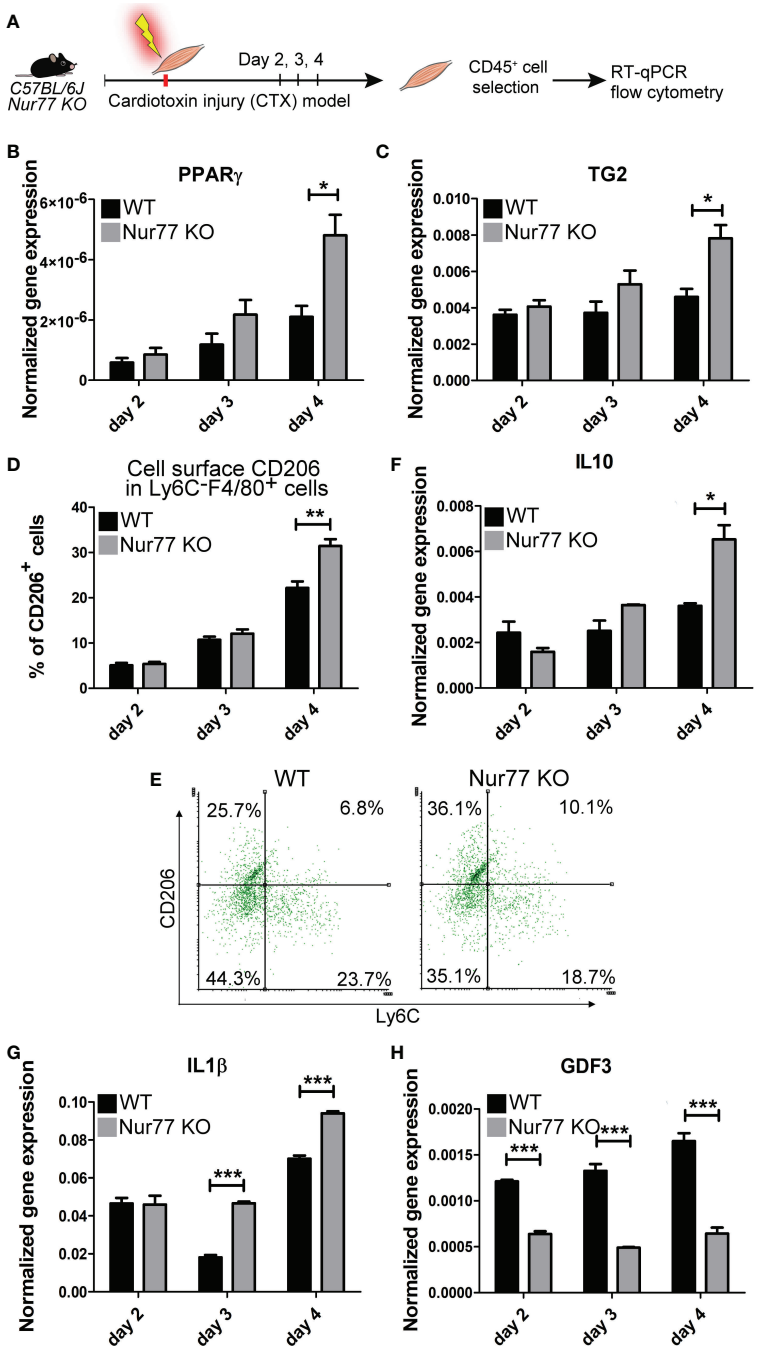

FIGURE 6
Contradicting M2 polarization of Nur77 KO skeletal muscle macrophages in the cardiotoxin-induced model of skeletal muscle injury. **(A)** Workflow used for the isolation and analysis of $CD45^+$ cells isolated at the indicated days following cardiotoxin-induced injury in the tibialis anterior muscle. **(B, C, F-H)** Time-dependent alterations in the mRNA expressions of PPARγ, TG2, IL-10, IL-1β and GDF3 of $CD45^+$ cells isolated from the tibialis anterior muscles determined by qRT-PCR at day 2, 3, and 4 post-injury (n= 4). β-actin was used as a reference gene. **(D)** Percent of $CD206^+$cells within the $Ly6C^-$ $F4/80^+$ macrophages and **(E)** representative scatter plots of $CD206^+$ and $Ly6C^+$ cells within the muscle-derived $F4/80^+$population determined at the indicated days following cardiotoxin-induced injury in the tibialis anterior muscles of wild-type and Nur77 KO mice (n= 3). Results are expressed as mean ± SEM. Asterisks indicate statistical significance (*$P < 0.05$, **$P < 0.01$, ***p< 0.001).

involvement of integrin signaling in the PPARγ-driven M2 conversion of macrophages (42, 43).

Loss of Nur77 results in conflicting production of pro- and anti-inflammatory cytokines by skeletal muscle macrophages following cardiotoxin-induced injury

M1 and M2 macrophages are characterized by the production of a different set of cytokines. While M1 macrophages produce pro-inflammatory cytokines, such as TNF-α, IL-1α, IL-1β, IL-6, IL-12, CXCL9, and CXCL10, M2 macrophages produce IL-10, TGF-β, CCL1, CCL17, CCL18, CCL22, and CCL24 (44). During M1/M2 conversion the production of pro-inflammatory cytokines gradually decreases, while that of anti-inflammatory cytokines or growth factors increases. Since Nur77 was shown to suppress the expression of IL-1β (45), while PPARγ to induce IL-10 production (46), both contributing this way to the M2-like polarization, we decided to follow the mRNA expression of these cytokines in the skeletal muscle $CD45^+$ cells following cardiotoxin-induced injury. As seen in Figure 6E, loss of Nur77 resulted in enhanced IL-10 production, a cytokine that plays a dominant role in promoting M2 conversion of the macrophages (47). Interestingly, we found that the producers of IL-10 are dominantly the $CD206^+$ macrophages (Figure 5) suggesting that the observed enhanced IL-10 production is the consequence of an enhanced conversion of Nur77 KO M1 macrophages into the $CD206^+$ direction by day 4. Altogether, these data demonstrate that PPARγ promotes IL-10 production by facilitating the formation of the IL-10-secreting $CD206^+$ macrophages. Surprisingly, while the IL-10 production increased indicating an enhanced M2 polarization of Nur77 KO macrophages in the cardiotoxin model of skeletal muscle injury, the IL-1β mRNA levels were also enhanced (Figure 6F). This later indicates a prolonged inflammatory M1 state. However, as shown in Figure 5, IL-1β is produced by separate populations of macrophages, which express dominantly Nur77. This observation supports the view that Nur77 acts as a suppressor of IL-1β production.

Loss of Nur77 results in decreased production of the growth differentiation factor 3

The way M2 macrophages are able to promote myoblast differentiation, myoblast fusion and myotube growth is that they produce various growth factors (39, 48, 49). Among them GDF3 was shown to be produced in a PPARγ-dependent manner (48). That is why we tested the expression of GDF3 in Nur77 KO skeletal muscle macrophages following cardiotoxin injury (Figure 6G). To our surprise, despite the higher expression of PPARγ, the expression of GDF3 was lower in Nur77 KO skeletal muscle macrophages (Figure 6G). Since the GDF3- and the PPARγ-expressing macrophage populations only partially overlap (Figure 5) (with 33% PPARγ-expressing cells expressing GDF3, and only 22.2% GDF3-expressing macrophages expressing PPARγ), our data indicate that Nur77 might contribute to the GDF3 expression in those $Nur77^+$ macrophages, which do not express PPARγ. Accordingly, Nur77 KO BMDMs also showed about a 55% decrease in the GDF3 mRNA expression (data not shown), as reported by others as well (23).

Discussion

In the present paper the effect of the loss of Nur77 transcription factor was investigated on the *in vitro* efferocytosis function, and on the *in vivo* polarization of BMDMs in the cardiotoxin-induced skeletal muscle injury model. Using this model, we have shown previously that efferocytosis and polarization of macrophages are strongly associated phenomena (40, 50). Previous studies have indicated that in macrophages the expression and the transcriptional activity of both PPARγ and Nur77 are increased following apoptotic cell uptake (27, 35). Here we found that Nur77 KO BMDMs express increased amount of PPARγ leading to enhanced efferocytosis capacity. Increasing evidence indicates that Nur77 can repress the expression of PPARγ (51), while PPARγ that of the Nur77 (52). These observations might explain why Nur77 KO BMDMs express more PPARγ, and why these two transcription factors are expressed in distinct M2-like reparative skeletal muscle macrophage subsets following cardiotoxin injury. While PPARγ was known to promote phagocytosis of apoptotic cells (27, 53) and to facilitate M1/M2 conversion of macrophages (42, 43, 54), here we have demonstrated for the first time that its efferocytosis-related effects are mediated partly by upregulating retinoid signaling. Nur77 is known to act as a negative regulator of the inflammatory response (19, 21, 45). This effect of Nur77 is mediated partly by controlling the mitochondrial metabolism (45), but also by interfering with the NF-κB-mediated pro-inflammatory signaling (19). Our data confirm these observations by demonstrating enhanced IL-1β production by the normally Nur77-expessing macrophage subset. In addition, our data also demonstrate that Nur77 contributes to M2 polarization not only by inhibiting pro-inflammatory cytokine production but also by promoting GDF3 expression, since GDF3 is not only a growth factor, but also acts as a suppressor of the pro-inflammatory macrophage phenotype (55). Thus, we should expect an enhanced M1 polarization in the absence of Nur77. However, the polarization detected in the absence of Nur77 is conflicting which is related to the upregulation of PPARγ which drives enhanced M2 polarization in a different reparative macrophage subset. These contradictory effects might explain why some investigators found that loss of Nur77 promotes M1 polarization (22), while others have not (56). Our data also questions, how well the disappearance of Ly6C reflects the true nature of macrophage M2 polarization, since it was not affected in the absence of Nur77. The novelty of our findings is that we demonstrate for the first time that PPARγ and Nur77 function in different subsets of macrophages, they appear in simultaneously differentiating macrophages in the cardiotoxin-induced skeletal muscle injury model, and their mutual antagonism makes sure that in one subtype the PPARγ-, while in

the other subtype the Nur77-mediated transcriptional events dominate. We also demonstrate for the first time that PPARγ-expressing cells are the precursors of at least one of the CD206$^+$ macrophage population, that dominantly the CD206$^+$ macrophages are responsible for the IL-10 production, and that the production of GDF3 is controlled by both Nur77 and PPARγ. What we did not investigate was whether the loss of Nur77 also alters the size of the different subsets within the M2-like reparative population. Thus, increased PPARγ expression could also mean an increase in the size of the PPARγ expressing macrophage subset. The increase in the size of CD206$^+$ macrophage population produced in a PPARγ-dependent manner indicates such a possibility. Still our data provide novel information about the heterogeneity of the bone marrow-derived macrophages, and about their polarization in a model of regenerative inflammation. Our results are summarized in Figure 7.

Materials and methods

Reagents

All reagents were obtained from Sigma-Aldrich (Budapest, Hungary) except when indicated otherwise.

Experimental animals

The experiments were carried out with 4-week-old C57BL/6 or 2- to 4-month-old Nur77$^{+/+}$ mice and their Nur77 deficient (57) littermates. Mice were maintained in specific pathogen-free condition in the Central Animal Facility, and all animal experiments were approved by the Animal Care and Use Committee of University of Debrecen (DEMÁB).

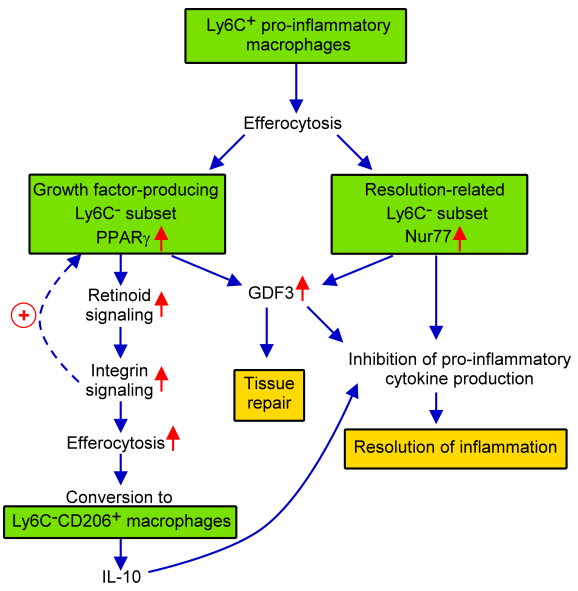

FIGURE 7
Schematic view of the events during conversion of M1 Ly6C$^+$ pro-inflammatory macrophages to M2-like reparative macrophages following cardiotoxin induced skeletal muscle injury.

Generation of apoptotic cells

Thymi from 4-week-old C57BL/6 mice were collected, and thymocytes were separated and incubated for 20 h (10^7 cells/ml) in RPMI 1640 media supplemented with 2 mM glutamine, 100 U/ml penicillin and 100 µg/ml streptomycin. This treatment results in approximately 80% annexin V positive cells (58). Apoptotic thymocytes were then stained by 0.5 µM CellTrackerTM Deep Red dye (Invitrogen, Carlsbad, CA, USA) for 30 min in the absence of serum to be used later as target cells to detect efferocytosis by BMDMs.

BMDM cell culture and treatments

2- to 4-month-old Nur77$^{+/+}$ and Nur77$^{-/-}$ mice were sacrificed by isoflurane overdose. Bone marrow progenitors were isolated from the femurs and tibiae by lavage with sterile physiological saline. Progenitor cells were differentiated to BMDMs in DMEM medium supplemented with 10% heat inactivated FBS, 20% conditioned medium derived from L929 cells, as a source for macrophage colony stimulating factor, 2 mM glutamine, 100 U/ml penicillin and 100µg/ml streptomycin for 5 days at 37°C in 5% CO_2. On the third day, non-adherent cells were washed away. Following the 5-day culturing period macrophages were plated on cell culture plates for various treatments. For long-term apoptotic cell phagocytosis experiments non-labeled apoptotic thymocytes in 5:1 (apoptotic cells: macrophage) ratio were added to BMDMs for 6 h, then apoptotic cells were washed away and efferocytosis was determined 18 h later. In some experiments BMDMs were treated for 24 h with 5 µM GW9662 (Tocris Bioscience, Bristol, UK), a selective PPARγ antagonist, 1 µM AGN193109 (Tocris Bioscience, Bristol, UK), a pan-RAR antagonist, 15 µM DEAB to block aldehyde dehydrogenase enzyme activities or for 1 h with 10 µg/ml mouse recombinant TG2 protein prior to determining the phagocytic capacity. The dose of these compounds was the same used for BMDMs in the literature. None of these compounds affected the viability of macrophages tested by the appearance of cell surface PS detected by Annexin V-FITC binding.

Western blot analysis

BMDMs were homogenized in ice-cold lysis buffer (10% v/v glycerol, 1% v/v Triton X-100, 1 mM EGTA, 20 mM Tris, pH 7.9, 100 µM β-glycerophosphate, 137 mM NaCl, 5 mM EDTA, 1.04 mM AEBSF, 0.8 µM aprotinin, 40 µM bestatin, 14 µM E-64, 20 µM leupeptin, and 15 µM pepstatin A). The protein content of the samples was determined by Bio-Rad Protein Assay Dye (Bio-Rad, Budapest, Hungary), and was diluted to 2 mg/ml, then the samples were boiled with an equal volume of Laemmli buffer. Electrophoresis was performed in 12% SDS-polyacrylamide gel.

Separated proteins were transferred to an Immobilion-P transfer membrane (Millipore, Budapest, Hungary) and were probed overnight at 4°C with anti-mouse PPARγ (81B8) (cat. #: 2443 Cell Signaling Technology, Beverly, MA, USA), RARα (sc-515796, Santa Cruz Biotechnology, Dallas, USA), RALDH2 (sc-393204, Santa Cruz Biotechnology, Dallas, USA) monoclonal antibodies in 1:1000 dilution, or monoclonal anti-β-actin antibody (A5441) in 1:5000 dilutions. After three washes with TBS-T, the membrane was incubated for 1 h with anti-mouse IgG (whole molecule)-peroxidase antibody produced in sheep or with goat-anti-rabbit IgG(H+L) HRP conjugate secondary antibody in 1:10000 dilutions followed by enhanced chemiluminescence (Advansta Inc., San Jose, CA, USA).

In vitro apoptotic cell phagocytosis

Stained apoptotic thymocytes were added to the BMDMs in 5:1 (apoptotic cells/macrophage) ratio for 45 min for flow cytometry analysis or for 120 min for confocal microscopy. After co-culture, non-engulfed cells were washed away extensively, and macrophages were detached by trypsinization. The percentage of engulfing cells was determined on a Becton Dickinson FACSCalibur flow cytometer (Becton Dickinson Company, Franklin Lakes, NJ, USA).

Confocal microscopy

For confocal microscopy, differentiated BMDMs were plated in 8-well chamber slides (8×10^5/well) (IBIDI GmbH, Gräfelfing, Germany).). Phagocytosis assays were carried out as described above. After coculture, apoptotic cells were washed away and macrophages were stained with Alexa Fluor 488 conjugated anti-F4/80 antibody (MF48020, Invitrogen, Carlsbad, USA) for confocal microscopy analysis. Macrophages were then washed and fixed in 1% paraformaldehyde. Fluorescence confocal images were taken by a Zeiss fluorescent microscope (Zeiss LSM 880 confocal microscope Göttingen, Germany). Images were analyzed with ZEN 2012 v.1.1.0.0 software (Carl Zeiss Microscopy GmbH, Göttingen, Germany).

Production of mouse recombinant TG2 protein

To obtain full-length recombinant N-terminally HIS_6-tagged mTg2 protein, the coding part of mouse transglutaminase 2 cDNA (BC016492, Dharmacon, GE, Boston, MA, USA) was amplified and cloned into pET-30 Ek/LIC vector (Merck, Darmstadt, Germany) based on the manufacturer instructions using HPLC-purified 5'-GAC GAC GAC AAG ATG AGA ATT CAG ACC ATG GCA GAG GAG CTG C-3' forward and 5'-GAG GAG AAG CCC GGT TGA ATT CGG TTA GGC CGG GCC GAT GAT AAC-3' reverse primers. The cloning was confirmed by restriction digestion and Sanger sequencing (Eurofins Genomics, Ebersberg, Germany). Recombinant mTG2 protein was expressed in Rosetta 2(DE3) bacterial cells (Novagen, Merck, Germany) and purified as described previously using the improved protocol (59).

Isolation of muscle-derived $CD45^+$ leukocytes from the tibialis anterior muscle following cardiotoxin-induced injury

WT or Nur77 KO mice were anesthetized with 2.5% isoflurane using a SomnoSuite device. After anesthesia, muscle damage was induced in the tibialis anterior (TA) muscle by injecting 50 µL of 12 µM cardiotoxin (Latoxan, Valence, France) in phosphate-buffered saline (PBS). Mice were sacrificed and muscles were collected on days 2, 3, and 4 post-injury and processed for cell and mRNA analysis. TA muscles were dissociated in RPMI containing 0.2% collagenase II (Thermo Fisher Scientific, Waltham, MA, USA) at 37°C for 1 h and filtered through a 100 µm and then a 40 µm filter. Muscle-derived $CD45^+$ cell isolation was carried out as described earlier (50). $CD45^+$ cells were separated using magnetic sorting (Miltenyi Biotec, Gladbach, Germany).

Single-cell RNA sequencing and analysis of muscle-derived $CD45^+$ cells

Single-cell gene expression barcode, feature, and count matrices from CD45+ cells isolated on day 4 following cardiotoxin-induced muscle injury were used from dataset GSE161467 (39). Downstream analysis was carried out with R version 4.2.2 (2022–10–31). Quality control, filtering, data clustering, marker gene analysis, and visualization were carried out using Seurat (v4.0.3) R package with some custom modifications to the standard pipeline (see below) (60).Genes expressed in less than 5 cells and cells with a number of detected genes within the lower quantile (q0.975) were removed from the gene expression matrix. We removed any single cell with > 5% UMIs mapped to mitochondrial genes as well as doublets and outliers with UMI counts in the upper quantile (q97.5). After log-normalizing the data, the expression of each gene was scaled, and PCA was performed on the top 1000 most variable genes. Unsupervised shared nearest neighbor (SNN) clustering was performed with a resolution of 0.35, and visualization was done using t-distributed stochastic neighbor embedding (t-SNE) from *SCpubr* (61). Feature plots were generated using the *Nebulosa* package (62). The alluvial plots were generated using the *ggalluvial* package (a *ggplot2* extension) (63).

Quantification of intramuscular immune cells by flow cytometry

The muscle-derived $CD45^+$ cells, separated from $Nur77^{+/+}$ or $Nur77^{-/-}$ mice, were stained with a combination of Alexa Fluor 488-conjugated anti-F4/80 (MF48020, Invitrogen, Carlsbad, USA), PerCP-Cy5.5-conjugated anti-Ly6C (128012, BioLegend, San Diego, USA) and PE-conjugated anti-CD206 (141705, BioLegend, San Diego, USA) antibodies at room temperature for 15 minutes. Fluorescent intensity was detected with a Becton Dickinson FACSCalibur. Cells were gated based on their forward- and side-scatter characteristics. Macrophages were gated as $F4/80^+$ cells. Fluorescent intensity was detected with a Becton Dickinson FACSCalibur.

Analysis of mRNA expression

Total RNA was isolated from BMDMs or muscle-derived $CD45^+$ cells by TRIzol (Invitrogen, Carlsbad, CA, USA) reagent according to the manufacturer's guidelines. Total RNA was reverse transcribed into cDNA using High Capacity cDNA Reverse Transcription Kit (Life Technologies, Budapest, Hungary)according to the manufacturer's instructions. Quantitative RT-PCR was carried out in triplicate using pre-designed FAM-labeled MGB assays (Life Technologies, Budapest, Hungary) on a Roche LightCycler LC 480 real-time PCR instrument. Relative mRNA levels were calculated using the comparative C_T method and were normalized to β-actin mRNA. Catalog numbers of the TaqMan assays used were the following: Actb Mm02619580_g1, integrin β1 Mm01253230_m1, integrin β3 Mm00443980_m1, integrin β5 Mm00439825_m1, CD36 Mm00432403_m1, MFG-E8 Mm00437836_m1, Protein S Mm01343426_m1, CD91 Mm00464608_m1, MERTK Mm00437221_m1, AXL Mm00500549_m1, transglutaminase 2 Mm00434920_m1, Thrombospondin-1 Mm00436979_m1, Tim4 Mm00449032_g1, CD14 Mm00432403_m1, PPARδ Mm00803184_m1, PPARγ Mm00440940_m1, LXRα Mm00443451_m1, RARα Mm01296312_m1, FABP4 Mm00445878_m1, RALDH2 Mm00501306_m1, GDF3 Mm00433563_m1, IL1 β Mm00434228_m1, and IL10 Mm01288386_m1.

Statistical analysis

All the data are representative of at least three independent experiments carried out with BMDMs originated from three different mice or with mice exposed to cardiotoxin-induced injury. Values are expressed as mean ± SEM. For differences between 2 groups two-tailed unpaired Student's t-test, for comparisons n > 2 groups one-way ANOVA (with Tukey's multiple comparisons test) was used. The equal variance of the samples was tested by F-test. All statistical analyses were performed using GraphPad Prism 6.01 and a P value <0.05 was considered as significant, and is indicated by asterisk (*).

Data availability statement

The datasets presented in this study can be found in online repositories. The names of the repository/repositories and accession number(s) can be found below:GSE161467 (GEO).

Ethics statement

The animal study was reviewed and approved by Review Board of Animal Care and Use Committee of the University of Debrecen (DEMÁB) with permission numbers 7/2016/DEMÁB and 7/2021/DEMÁB.

Author contributions

EG contributed to conception, design, data acquisition, analysis, and interpretation, EF, NT, TS-S, and ZSa, contributed to data acquisition, AP and LH contributed to data analysis, AP also critically revised the manuscript. RK provided material, ZSz contributed to conception, design and data interpretation, drafted the manuscript. All authors read and approved the final manuscript.

Funding

This study was supported by the National Research, Development, and Innovation Office-NKFI, Hungary (124244, 138162 and129139). Project no. [121174] has been implemented with the support provided by the Ministry of Culture and Innovation of Hungary from the National Research, Development and Innovation Fund, financed under the [PD_16] funding scheme.

Acknowledgments

Maintenance of the mouse colonies and the animal works were performed in the Laboratory Animal Facility, Life Science Building, University of Debrecen. The authors thank Professor László Nagy for providing the bioinformatic resources. The technical assistance of Anikó Nagy is gratefully acknowledged.

Conflict of interest

The authors declare that the research was conducted in the absence of any commercial or financial relationships that could be construed as a potential conflict of interest.

Publisher's note

References

1. Wu Y, Hirschi KK. Tissue-resident macrophage development and function. *Front Cell Dev Biol* (2020) 8:617879. doi: 10.3389/fcell.2020.617879

2. Konkel JE, Jin W, Abbatiello B, Grainger JR, Chen W. Thymocyte apoptosis drives the intrathymic generation of regulatory T cells. *Proc Natl Acad Sci USA* (2014) 111(4):E465–73. doi: 10.1073/pnas.1320319111

3. Sarang Z, Garabuczi É, Joós G, Kiss B, Tóth K, Rühl R, et al. Macrophages engulfing apoptotic thymocytes produce retinoids to promote selection, differentiation, removal and replacement of double positive thymocytes. *Immunobiology* (2013) 218 (11):1354–60. doi: 10.1016/j.imbio.2013.06.009

4. Vannella KM, Wynn TA. Mechanisms of organ injury and repair by macrophages. *Annu Rev Physiol* (2017) 79:593–617. doi: 10.1146/annurev-physiol-022516-034356

5. Ravichandran KS. Find-me and eat-me signals in apoptotic cell clearance: Progress and conundrums. *J Exp Med* (2010) 207(9):1807–17. doi: 10.1084/jem.20101157

6. Nagata S, Suzuki J, Segawa K, Fujii T. Exposure of phosphatidylserine on the cell surface. *Cell Death Differ* (2016) 23(6):952–61. doi: 10.1038/cdd.2016.7

7. Szondy Z, Al-Zaeed N, Tarban N, Fige E, Garabuczi E, Sarang Z. Involvement of phosphatidylserine receptors in skeletal muscle regeneration. therapeutic implications. *J Cachexia Sarcopenia Muscle* (2022) 13(4):1961–73. doi: 10.1002/jcsm.13024

8. Hanayama R, Tanak M, Miwa K, Shinohara A, Iwamatsu A, Nagata S. Identification of a factor that links apoptotic cells to phagocytes. *Nature* (2002) 417 (6885):182–87. doi: 10.1038/417182a

9. Nandrot EF, Anand M, Almeida D, Atabai K, Sheppard D, Finnemann SC. Essential role for MFG-E8 as ligand for alphavbeta5 integrin in diurnal retinal phagocytosis. *Proc Natl Acad Sci USA* (2007) 104(29):12005–10. doi: 10.1073/pnas.0704756104

10. Flannagan RS, Canton J, Furuya W, Glogauer M, Grinstein S. The phosphatidylserine receptor TIM4 utilizes integrins as coreceptors to effect phagocytosis. *Mol Biol Cell* (2014) 25(9):1511–22. doi: 10.1091/mbc.E13-04-0212

11. Tóth B, Garabuczi E, Sarang Z, Vereb G, Vámosi G, Aeschlimann D, et al. Transglutaminase 2 is needed for the formation of an efficient phagocyte portal in macrophages engulfing apoptotic cells. *J Immunol* (2009) 82(4):2084–92. doi: 10.4049/jimmunol.0803444

12. Savill J, Dransfield I, Hogg N, Haslett C. Vitronectin receptor-mediated phagocytosis of cells undergoing apoptosis. *Nature* (1990) 343(6254):170–73. doi: 10.1038/343170a0

13. Stern M, Savill J, Haslett C. Human monocyte-derived macrophage phagocytosis of senescent eosinophils undergoing apoptosis. mediation by alpha v beta 3/CD36/thrombospondin recognition mechanism and lack of phlogistic response. *Am J Pathol* (1996) 149(3):911–21.

14. Barth ND, Marvick JA, Vendrell M, Rossi AG, Dransfield I. "Phagocytic synapse" and clearance of apoptotic cells. *Front Immunol* (2017) 8:1708. doi: 10.3389/fimmu.2017.01708

15. Nakaya M, Kitano M, Matsuda M, Nagata S. Spatiotemporal activation of Rac1 for engulfment of apoptotic cells. *Proc Natl Acad Sci USA* (2008) 105(27):9198–203. doi: 10.1073/pnas.0803677105

16. Mangelsdorf DJ, Thummel C, Beato M, Herrlich P, Schütz G, Umesono K, et al. The nuclear receptor superfamily: The second decade. *Cell* (1995) 83(6):835–39. doi: 10.1016/0092-8674(95)90199-x

17. Wilson TE, Fahrner TJ, Milbrandt J. The orphan receptors NGFI-b and steroidiogenic factor 1 establish monomer binding as a third paradigm of nuclear receptor-DNA interaction. *Mol Cell Biol* (1993) 13(9):5794–804. doi: 10.1128/mcb.13.9.5794-5804.1993

18. Philips A, Lesage S, Gingras R, Maira M-H, Gauthier Y, Hugo P, et al. Novel dimeric nur77 signaling mechanism in endocrin and lymphoid cells. *Mol Cell Biol* (1997) 17(10):5946–51. doi: 10.1128/MCB.17.10.5946

19. Murphy EP, Crean D. Molecular interactions between NR4A orphan nuclear receptors and NF-κB are required for appropriate inflammatory responses and immune cell homeostasis. *Biomolecules* (2015) 5(3):1302–18. doi: 10.3390/biom5031302

20. Zhao Y, Bruemmer D. NR4A orphan nuclear receptors: Transcriptional regulators of gene expression in metabolism and vascular biology. *Arterioscler Thromb Vasc Biol* (2010) 30(8):1535–141. doi: 10.1161/ATVBAHA.109.191163

21. McMorrow JP, Murphy EP. Inflammation: A role for NR4A orphan nuclear receptors? *Biochem Soc Trans* (2011) 39(2):688–93. doi: 10.1042/BST0390688

22. Hanna RN, Shaked I, Hubbeling HG, Punt JA, Wu R, Herrley E, et al. NR4A1 (Nur77) deletion polarizes macrophages toward an inflammatory phenotype and increases atherosclerosis. *Circ Res* (2012) 110(3):416–27. doi: 10.1161/CIRCRESAHA.111.253377

23. Hamers AA, Argmann C, Moerland PD, Koenis DS, Marinković G, Sokolović M, et al. Nur77-deficiency in bone marrow-derived macrophages modulates inflammatory responses, extracellular matrix homeostasis, phagocytosis and tolerance. *BMC Genomics* (2016) 17:162. doi: 10.1186/s12864-016-2469-9

24. Chazaud B. Inflammation and skeletal muscle regeneration: Leave it to the macrophages. *Trends Immunol* (2020) 41(6):481–92. doi: 10.1016/j.it.2020.04.006

25. Tosello-Trampont AC, Brugnera E, Ravichandran KS. Evidence for a conserved role for CrkII and rac in engulfment of apoptotic cells. *J Biol Chem* (2001) 276 (17):13797–802. doi: 10.1074/jbc.M011238200

26. A-Gonzalez N, Bensinger SJ, Hong C, Beceiro S, Bradley MN, Zelcer N, et al. Apoptotic cells promote their own clearance and immune tolerance through activation of the nuclear receptor LXR. *Immunity* (2009) 31(2):245–58. doi: 10.1016/j.immuni.2009.06.018

27. Roszer T, Menéndez-Gutiérrez MP, Lefterova MI, Alameda D, Núñez V, Lazar MA, et al. Autoimmune kidney disease and impaired engulfment of apoptotic cells in mice with macrophage peroxisome proliferator-activated receptor gamma or retinoid X receptor alpha deficiency. *J Immunol* (2011) 186(1):621–31. doi: 10.4049/jimmunol.1002230

28. Mukundan L, Odegaard JI, Morel CR, Heredia JE, Mwangi JW, Ricardo-Gonzalez RR, et al. PPAR-delta senses and orchestrates clearance of apoptotic cells to promote tolerance. *Nat Med* (2009) 15(11):1266–72. doi: 10.1038/nm.2048

29. Tontonoz P, Spiegelman BM. Fat and beyond: the diverse biology of PPARgamma. *Annu Rev Biochem* (2008) 77:289–312. doi: 10.1146/annurev.biochem.77.061307.091829

30. Garabuczi E, Kiss B, Felszeghy S, Tsay GJ, Fésüs L, Szondy Z. Retinoids produced by macrophages engulfing apoptotic cells contribute to the appearance of transglutaminase 2 in apoptotic thymocytes. *Amino Acids* (2013) 44(1):235–44. doi: 10.1007/s00726-011-1119-4

31. Sarang Z, Joós G, Garabuczi E, Rühl R, Gregory CD, Szondy Z. Macrophages engulfing apoptotic cells produce non-classical retinoids to enhance their phagocytic capacity. *J Immunol* (2014) 192(12):5730–38. doi: 10.4049/jimmunol.1400284

32. Rébé C, Raveneau M, Chevriaux A, Lakomy D, Sberna AL, Costa A, et al. Induction of transglutaminase 2 by a liver X receptor/retinoic acid receptor alpha pathway increases the clearance of apoptotic cells by human macrophages. *Circ Res* (2009) 105(4):393–401. doi: 10.1161/CIRCRESAHA.109.201855

33. Han S, Sidell N. Peroxisome-proliferator-activated-receptor gamma (PPARgamma) independent induction of CD36 in THP-1 monocytes by retinoic acid. *Immunology* (2002) 106(1):56–9. doi: 10.1046/j.1365-2567.2002.01404.x

34. Johnson KA, Terkeltaub RA. External GTP-bound transglutaminase 2 is a molecular switch for chondrocyte hypertrophic differentiation and calcification. *J Biol Chem* (2005) 280(15):15004–12. doi: 10.1074/jbc.M500962200

35. Ipseiz N, Uderhardt S, Scholtysek C, Steffen M, Schabbauer G, Bozec A, et al. The nuclear receptor Nr4a1 mediates anti-inflammatory effects of apoptotic cells. *J Immunol* (2014) 192(10):4852–8. doi: 10.4049/jimmunol.1303377

36. Epelman S, LaVine KJ, Randolph GJ. Origin and functions of tissue macrophages. *Immunity* (2014) 41(1):21–35. doi: 10.1016/j.immuni.2014.06.013

37. Wynn TA, Vannella KM. Macrophages in tissue repair, regeneration, and fibrosis. *Immunity* (2016) 44(3):450–62. doi: 10.1016/j.immuni.2016.02.015

38. Fletcher JE, Hubert M, Wieland SJ, Gong QH, Jiang MS. Similarities and differences in mechanisms of cardiotoxins, melittin and other myotoxins. *Toxicon* (1996) 34(11-12):1301–11. doi: 10.1016/s0041-0101(96)00105-5

39. Patsalos A, Halasz L, Medina-Serpas MA, Berger WK, Daniel B, Tzerpos P, et al. A growth factor-expressing macrophage subpopulation orchestrates regenerative inflammation *via* GDF-15. *J Exp Med* (2022) 219(1):e20210420. doi: 10.1084/jem.20210420

40. Budai Z, Al-Zaeed N, Szentesi P, Halász H, Csernoch L, Szondy Z, et al. Impaired skeletal muscle development and regeneration in transglutaminase 2 knockout mice. *Cells* (2021) 10(11):3089. doi: 10.3390/cells10113089

41. Varga T, Mounier R, Gogolak P, Poliska S, Chazaud B, Nagy L. Tissue LyC6- macrophages are generated in the absence of circulating LyC6- monocytes and Nur77 in a model of muscle regeneration. *J Immunol* (2013) 191(11):5695–701. doi: 10.4049/jimmunol.1301445

42. Yao Q, Liu J, Zhang Z, Li F, Zhang C, Lai B, et al. Peroxisome proliferator–activated receptor γ (PPARγ) induces the gene expression of integrin $\alpha_V\beta_5$ to promote macrophage M2 polarization. *J Biol Chem* (2018) 293(43):16572–82. doi: 10.1074/jbc.RA118.003161

43. Shu Y, Qin M, Song Y, Tang Q, Huang Y, Shen P, et al. M2 polarization of tumor-associated macrophages is dependent on integrin β3 *via* peroxisome proliferator-activated receptor-γ up-regulation in breast cancer. *Immunology* (2020) 160(4):345–56. doi: 10.1111/imm.13196

44. Yao Y, Xu X-H, Jin L. Macrophage polarization in physiological and pathological pregnancy. *Front Immunol* (2019) 10:792. doi: 10.3389/fimmu.2019.00792

45. Koenis DS, Medzikovic L, van Loenen PB, van Weeghel M, Huveneers S, Vos M, et al. Nuclear receptor Nur77 limits the macrophage inflammatory response through transcriptional reprogramming of mitochondrial metabolism. *Cell Rep* (2018) 24 (8):2127–2140.e7. doi: 10.1016/j.celrep.2018.07.065

46. Kim SR, Lee KS, Park HS, Park SJ, Min KH, Jin SM, et al. Involvement of IL-10 in peroxisome proliferator-activated receptor gamma-mediated anti-inflammatory response in asthma. *Mol Pharmacol* (2005) 68(6):1568–75. doi: 10.1124/mol.105.017160

47. Chuang Y, Hung ME, Cangelose BK, Leonard JN. Regulation of the IL-10-driven macrophage phenotype under incoherent stimuli. *Innate Immun* (2016) 22(8):647–57. doi: 10.1177/1753425916668243

48. Varga T, Mounier R, Patsalos A, Gogolák P, Peloquin M, Horvath A, et al. Macrophage PPARγ, a lipid activated transcription factor controls the growth factor GDF3 and skeletal muscle regeneration. *Immunity* (2016) 45(5):1038–51. doi: 10.1016/j.immuni.2016.10.016

49. Dumont N, Frenette J. Macrophages protect against muscle atrophy and promote muscle recovery *in Vivo* and *in Vitro*. *Am J Pathol*. (2010) 76(5):2228–35. doi: 10.2353/ajpath.2010.090884

50. Al-Zaeed N, Budai Z, Szondy Z, Sarang Z. TAM kinase signaling is indispensable for the proper skeletal muscle regeneration process. *Cell Death Dis* (2021) 12(6):611. doi: 10.1038/s41419-021-03892-5

51. Duszka K, Bogner-Strauss JG, Hackl H, Rieder D, Neuhold C, Prokesch A, et al. Nr4a1 is required for fasting-induced down-regulation of PPARγ2 in white adipose tissue. *Mol Endocrinol* (2013) 27(1):135–49. doi: 10.1210/me.2012-1248

52. Yang PB, Hou PP, Liu FY, Hong WB, Chen HZ, Sun XY, et al. Blocking PPARγ interaction facilitates Nur77 interdiction of fatty acid uptake and suppresses breast cancer progression. *Proc Natl Acad Sci USA* (2020) 117(44):27412–22. doi: 10.1073/pnas.2002997117

53. Majai G, Sarang Z, Csomós K, Zahuczky G, Fésüs L. PPARgamma-dependent regulation of human macrophages in phagocytosis of apoptotic cells. *Eur J Immunol* (2007) 37(5):1343–54. doi: 10.1002/eji.200636398

54. Odegaard JI, Ricardo-Gonzalez RR, Goforth MH, Morel CR, Subramanian V, Mukundan L, et al. Macrophage-specific PPARγ controls alternative activation and improves insulin resistance. *Nature* (2007) 447(7148):1116–20. doi: 10.1038/nature05894

55. Wang L, Li Y, Wang X, Wang P, Essandoh K, Cui S, et al. GDF3 protects mice against sepsis-induced cardiac dysfunction and mortality by suppression of macrophage pro-inflammatory phenotype. *Cells* (2020) 9(1):120. doi: 10.3390/cells9010120

56. Chao LC, Soto E, Hong C, Ito A, Pei L, Chawla A, et al. Bone marrow NR4A expression is not a dominant factor in the development of atherosclerosis or macrophage polarization in mice. *J Lipid Res* (2013) 54(3):806–15. doi: 10.1194/jlr.M034157

57. Lee SL, Wesselschmidt RL, Linette GP, Kanagawa O, Russel JH, Milbrandt J. Unimpaired thymic and peripheral T cell death in mice lacking the nuclear receptor NGFI-b (Nur77). *Science* (1995) 269(5223):532–35. doi: 10.1126/science.7624775

58. Köröskényi K, Duró E, Pallai A, Sarang Z, Kloor D, Ucker DS, et al. Involvement of adenosine A2A receptors in engulfment-dependent apoptotic cell suppression of inflammation. *J Immunol* (2011) 186(12):7144–55. doi: 10.4049/jimmunol.1002284

59. Király R, Thangaraju K, Nagy Z, Nagy Z, Collighan R, Nemes Z, et al. Isopeptidase activity of human transglutaminase 2: Disconnection from transamidation and characterization by kinetic parameters. *Amino Acids* (2016) 48:31–40. doi: 10.1007/s00726-015-2063-5

60. Butler A, Hoffman P, Smibert P, Papalexi E, Satija R. Integrating single-cell transcriptomic data across different conditions, technologies, and species. *Nat Biotechnol* (2018) 36(5):411–20. doi: 10.1038/nbt.4096

61. Blanco-Carmona E. Generating publication ready visualizations for single cell transcriptomics using SCpubr. *bioRxiv* (2022). doi: 10.1101/2022.02.28.482303

62. Alquicira-Hernandez J, Powell JE. Recovers single-cell gene expression signals by kernel density estimation. *Bioinformatics* (2021) 37(16):2485–7. doi: 10.1093/bioinformatics/btab003

63. Brunson JC, Read QD. *Ggalluvial: Alluvial plots in 'ggplot2'* (2020). Available at: http://corybrunson.github.io/ggalluvial/.

frontiers | Frontiers in Immunology

TYPE Review
PUBLISHED 08 March 2023
DOI 10.3389/fimmu.2023.1122057

OPEN ACCESS

EDITED BY
Yanan Ma,
Memorial Sloan Kettering Cancer Center,
United States

REVIEWED BY
Wenjun Liu,
Amgen, United States
Xixi Zhang,
Dana–Farber Cancer Institute,
United States
Xinhe Shan,
Penn Medicine, United States
Jingkai Zhou,
City of Hope National Medical Center,
United States

*CORRESPONDENCE
Ziqing Li
liziqing@sdfmu.edu.cn
Shui Sun
sunshui@sdfmu.edu.cn

†These authors have contributed equally to this work

SPECIALTY SECTION
This article was submitted to Inflammation, a section of the journal Frontiers in Immunology

RECEIVED 12 December 2022
ACCEPTED 13 February 2023
PUBLISHED 08 March 2023

CITATION
Cong Y, Wang Y, Yuan T, Zhang Z, Ge J, Meng Q, Li Z and Sun S (2023) Macrophages in aseptic loosening: Characteristics, functions, and mechanisms.
Front. Immunol. 14:1122057.
doi: 10.3389/fimmu.2023.1122057

Macrophages in aseptic loosening: Characteristics, functions, and mechanisms

Yehao Cong[1,2†], Yi Wang[3†], Tao Yuan[3], Zheng Zhang[3], Jianxun Ge[3], Qi Meng[3], Ziqing Li[1,2*] and Shui Sun[1,2,3*]

[1]Department of Joint Surgery, Shandong Provincial Hospital Affiliated to Shandong First Medical University, Jinan, Shandong, China, [2]Orthopaedic Research Laboratory, Medical Science and Technology Innovation Center, Shandong First Medical University & Shandong Academy of Medical Sciences, Jinan, Shandong, China, [3]Department of Joint Surgery, Shandong Provincial Hospital, Shandong University, Jinan, Shandong, China

Aseptic loosening (AL) is the most common complication of total joint arthroplasty (TJA). Both local inflammatory response and subsequent osteolysis around the prosthesis are the fundamental causes of disease pathology. As the earliest change of cell behavior, polarizations of macrophages play an essential role in the pathogenesis of AL, including regulating inflammatory responses and related pathological bone remodeling. The direction of macrophage polarization is closely dependent on the microenvironment of the periprosthetic tissue. When the classically activated macrophages (M1) are characterized by the augmented ability to produce proinflammatory cytokines, the primary functions of alternatively activated macrophages (M2) are related to inflammatory relief and tissue repair. Yet, both M1 macrophages and M2 macrophages are involved in the occurrence and development of AL, and a comprehensive understanding of polarized behaviors and inducing factors would help in identifying specific therapies. In recent years, studies have witnessed novel discoveries regarding the role of macrophages in AL pathology, the shifts between polarized phenotype during disease progression, as well as local mediators and signaling pathways responsible for regulations in macrophages and subsequent osteoclasts (OCs). In this review, we summarize recent progress on macrophage polarization and related mechanisms during the development of AL and discuss new findings and concepts in the context of existing work.

KEYWORDS

macrophage, polarization, aseptic loosening, arthroplasty, inflammation

1 Introduction

Total joint arthroplasty (TJA) is an extensive and successful surgical therapy, which has been used in the treatment of severely traumatic or arthritic joint diseases. It helps in relieving arthralgia, rebuilding locomotor function, and improving living quality (1). Even so, the long-term survival of joint prosthesis reduces over time, which leads to implant failure, reduced locomotor ability, and heavy financial burden.

The main reason for the failure of TJA is that the joint interface continuously produces debris particles which induce a complex inflammatory response and leads to osteolysis and aseptic loosening (AL) (2–4). At present, the major pathogenesis of AL is the production of wear debris due to the mechanical strength of joints and biological interactions over time. On one hand, the debris induces functional changes in macrophages and promotes the release of cytokines to regulate the immune microenvironment in the bone-implant interface. On the other hand, by further affecting the bone remodeling process, the debris increases bone resorption, eventually resulting in AL (3–6).

Macrophages, the major population of tissue-resident mononuclear phagocytes, are a critical class of cells that have an effect on bacterial recognition and elimination, as well as in the process of innate and adaptive immunity (7). Macrophages have a variety of functions, exhibiting different phenotypes based on practical conditions and responding to microenvironmental signals. Two major phenotypes of macrophages include classically activated macrophages (M1) and alternatively activated macrophages (M2) (8–10). M1 macrophages have proinflammatory properties and are involved in initiating and maintaining the inflammatory state, whereas M2 macrophages have anti-inflammatory properties and take part in tissue homeostasis and repair (8–13).

During the development of inflammation, the polarized state of macrophage is in a dynamic equilibrium. In this regard, macrophages can distinctively adapt to the microenvironment, respectively (9). For example, the increased count of proinflammatory M1 macrophages induced by pathological stimulus leads to periprosthetic osteolysis, whereas anti-inflammatory M2 is favorable to shape an immunomodulatory environment towards osseointegration (14, 15). Therefore, it is essential to figure out the polarization of macrophages and associated regulatory mechanisms during the pathogenesis of AL.

At present, the understanding of macrophages is still limited to some extent. For the past few years, advancing awareness of the impact of macrophage polarization on the pathogenesis of AL has been recognized. This article reviewed interactions between the various receptors, ligands, signal transductions, and other factors related to functional changes of macrophage around the prosthesis. In addition, it cited the research conclusions and reviews regarding other macrophage-related inflammatory regulations, and also emphasized the importance of the functional changes and regulatory mechanisms of macrophages in the bone-implant interface microenvironment.

2 Overview of aseptic loosening

2.1 Clinical features

Harris et al. (16) described a phenomenon of extensive bone resorption leading to loosening without infection in four patients after receiving hip arthroplasty surgery, and this is the first detailed description of AL (16). In definition, AL can be generally described as a failure of the fixation of one or more prosthetic components without any infection (17). It may probably originate from inadequate initial fixation, mechanical loss of fixation over time, or biological loss of fixation, all of which are the leading causes of particles-induced osteolysis around the prosthesis (4, 17). Joint pain is the typical symptom of patients with AL, which always become worse when the affected joint carries out physical activity or bears weight. Impaired gait and restricted range of motion are often discovered in the physical exam of these patients (17).

As one of the major reasons for the failure of artificial joint implants, AL is the main cause of revision surgery (18–20). Due to the high complication rate, the requirement for complex technology, and the heavy economic burden brought by revision surgery (18), extensive studies have focused on the pathogenesis of AL in order to develop diagnostic and therapeutic avenues with more sensitivity and efficacy. The majority of published works reported that AL is mainly caused by wear particles-induced periprosthetic osteolysis (PPOL) (2–4).

2.2 Pathogenesis

Loosening of the prosthesis is a very complex process, involving many mechanical and biological aspects (21, 22). The main biological factor is the biological response of cells to a variety of wear particles (21), for example, wear particles can promote macrophage polarization to M1, and release proinflammatory cytokines and chemokines (23, 24). These cellular responses and subsequent activities are determined by many factors, such as the physical and chemical properties of the material, including the size, morphology, and composition of the material (23, 25–29). Moreover, the presence of endotoxin can also affect these cellular responses and activities (30–32). From the aspects of the disease host, patient-related risk factors, such as age, sex, obesity, smoking, and genetic variation, also play a role in AL pathogenesis (33–38). However, comorbidities affect the occurrence of AL even larger. Patients with hemophilia are reported to have a higher risk of AL (39). Elevated inflammatory activity will increase the risk of loosening after TJA in patients with rheumatoid arthritis (RA), thus the indication of arthroplasty for RA patients should be more strictly controlled (40).

2.3 Pathological feature

The chronic inflammation at the bone-implant interface, accompanied by osteolytic destruction in the surrounding bone, is the major pathological feature of AL (5, 6, 41, 42). Based on histopathological findings, there are numerous infiltrating CD68-positive mononuclear/macrophages, foreign body giant cells (sometimes organized as foreign body granulomas), and wear particles in the periprosthetic connective tissue (42, 43). Scattered fibroblasts and T cells can be observed in the surrounding area of infiltrating macrophage (42). In addition, endotoxin contamination is also present around the prosthesis (44, 45). Regarding the cytokines, there is a significant increase in the expression of proinflammatory factors in the tissue, including interleukin-1β (IL-1β), IL-2, IL-8, interferon-γ (IFN-γ), and tumor necrosis factor-α (TNF-α) (41). It was found that in the mice skull

implanted with titanium (Ti) particles, macrophages polarized into M1 macrophages in the early phase of the inflammatory responses, and partial tissue restoration was observed in the resolution of inflammation after 6 to 8 weeks (46). However, long-term chronic inflammation eventually leads to osteolytic destruction (6). Studies on the various polarization phenotypes of macrophages may help in further explaining the pathogenesis of AL.

3 Overview of macrophages in aseptic loosening

3.1 Origin of macrophages and wear particles

Monocytes/macrophages originally come from the hematopoietic stem cell (HSC) in the bone marrow and subsequently enter the peripheral blood. In responding to the local inflammation, circulating monocytes leave the bloodstream and mobilize into the local tissues. Upon stimulation by several growth factors, proinflammatory cytokines, or microbial products, circulating monocytes further differentiate into macrophages (11, 12). In addition to that, resident tissue macrophages recruited from the bone marrow are necessary drivers of inflammatory and tissue regenerative responses (47). The initial recruitment of inflammatory cells results from chemotactic factors produced by macrophages (48). When circulating macrophage or monocyte recruitment or activation is disrupted, the early inflammatory response is often diminished (49). Conclusively, the number of tissue-resident macrophages can increase exponentially, including locally proliferating macrophages and monocytes recruited from the bone marrow (50–52).

Due to the detection of ultra-high molecular weight polyethylene (UHMWPE) and various kinds of high-density material debris in tissue samples from patients, submicron-sized wear particles are usually considered potential causes of AL pathogenesis (53). During disease progress, macrophages play a crucial role in recognizing wear particles and releasing a large number of proinflammatory cytokines and chemokines, such as IL-1β, TNF-α, IL-6 (15, 23, 24, 26, 54–58). Diverse cytokines individually modulate the function of cells located at the interface between the prosthesis and the surrounding bone, and collectively affect other cells through diverse signaling mechanisms, ultimately leading to particles-induced inflammatory osteolysis. Detailed interactions between cytokines and cells are to be reviewed in section 4.

3.2 PAMPs and subclinical infection

Common pathogen-associated molecular patterns (PAMPs) include lipopolysaccharide (LPS) and lipoteichoic acid (LTA). LPS is a typical endotoxin and a major component of the outer cell wall of Gram-negative bacteria, whereas LTA is a cell wall polymer discovered in Gram-positive bacteria (59, 60). PAMPs regulate macrophage polarization through toll-like receptors (TLRs) and further promote the release of cytokines (61–63).

Previous studies have reported that some active bacteria or its structural components could be found in the tissues surrounding the loosened implant, even in the absence of any clinical or microbial evidence of infection (44, 45). In fact, subclinical infection is difficult to identify, and the probable cause of this is the growth pattern of biofilm. By firmly anchoring to the surface of the implanted prosthesis, biofilm may have protected inside microorganisms that are being infected from elimination, therefore it is reasonable to suspect these bacterial biofilms anchoring on the surface of the loosened implant as the latent source of endotoxin (45, 64). In addition, PAMPs may also originate from bacterial colonies residing in the gastrointestinal tract, the oral cavity, or even the wounds in the skin, where these bacteria and PAMPs are occasionally transferred to the circulating blood, in turn reaching the implant (65, 66). Evidenced by an *in vivo* experiment based on mouse balloon models, endotoxin in blood circulation could adhere to Ti particles and consequently induce macrophage aggregation (67).

3.3 Functional changes of macrophages

Macrophages are activated and alter their functions to defend against infections and present antigens to other immune cells, thereby regulating the immune responses (Figure 1) (68).

3.3.1 Proinflammatory and anti-inflammatory functions

Macrophages amplify the inflammatory process by releasing proinflammatory factors to remove pathogens or other foreign bodies (9, 47). During tissue injury, the local cells which are infected by pathogens and undergo necrosis or pyroptosis could release PAMPs or damage-associated molecular patterns (DAMPs) that activate inflammatory signaling in macrophages and other resident cell populations. Activated cells recruit neutrophils, monocytes, and other inflammation-related cells into the tissue by a release series of cytokines. Once the acute injury is under control, macrophages supply nutrition to the tissues where they are located by decomposing remnants and secreting growth factors and mediators, exerting their function effectively in inhibiting inflammation (47). Some macrophages, characterized by producing of growth factors, including platelet-derived growth factor (PDGF), insulin-like growth factor 1 (IGF-1), and vascular endothelial growth factor-α (VEGF-α), are associated with tissue repair and help in promoting cell proliferation and vascular development and thus alleviating local hypoxia that occurs after injury (47). They also produce soluble mediators, such as transforming growth factor-β1 (TGF-β1) that induce local and recruited fibroblasts to differentiate into myofibroblasts, thereby synthesizing extracellular matrix components and promoting wound closure (69). In the final phase of tissue repairment, monocytes and macrophages present an anti-inflammatory phenotype (47, 70). It was found that these macrophages

responded to inhibitory mediators such as IL-10 in the local microenvironment, eventually leading to relieving inflammation (71, 72).

Phagocytosis mainly belongs to the function of M1 macrophages, which goes along with the proinflammatory process, although M2 macrophages also demonstrate a weak function in phagocytosis (73, 74). Stimulated by the serum from Behçet's disease (BD) patients, monocyte-derived macrophages (MDMs) could differentiate into M1 macrophages with enhanced phagocytic capacity (75). Subsequently, M1 macrophages display an enhanced capacity for the elimination of pathogens, which largely results from their increased production of superoxide, NO, and their derivatives (76). M2 MDMs also demonstrate the ability to phagocytose escherichia coli and cancer cells. Further research found that the phagocytosis in M2 macrophages mainly owes to their surface markers, such as CD14, CD206, and CD163 (77). However, compared with M0 and M2 macrophages, LPS-treated M1 macrophages exhibited an obviously higher ability for phagocytic activity (78).

3.3.2 Autophagy

Both autophagy and phagocytosis in macrophages are lysosomal-dependent catabolic processes, by which cells can engulf and deliver cargo to the lysosomes for digestion *via* forming transient vesicular structures (autophagosome and phagosome) (79). Acting as scavenger cells, macrophages could phagocytize cellular debris, invading pathogens, and other apoptotic cells (80, 81). Phagocytizing dead cells in macrophages contribute to diverse immune and inflammatory signals that could also trigger intracellular autophagy in macrophages (82, 83). Other studies have revealed more relations between autophagy and phagocytosis. Autophagy promotes phagocytosis and the clearance of pathogens *via* the NOD-like receptor family pyrin domain containing 3 (NLRP3) inflammasome in macrophages (84). As a novel function for autophagy proteins, the LC3-associated phagocytosis pathway (LAP) is closely associated with phagocytosis in macrophages, which exerts its role in blocking proinflammatory signals upon phagocytosis of dying cells and preventing the presentation of autoantigen to other cells (85, 86). Interestingly, autophagy-deficient macrophages may boost phagocytosis through increased scavenger receptor expression (87).

Regarding the functional changes in activated macrophages, vitamin D could restore anti-inflammatory M2 macrophages in an autophagy-dependent manner (88). Similarly, ubiquitin-specific protease 19 (USP19) could inhibit inflammatory responses and promote M2 polarization by increasing autophagy flux (89). Controversially, another study reported that inhibition of autophagy could drive macrophages to the M2 phenotype (90). In AL, a recent study revealed that by activating LAP, aluminum oxide nanoscale particles (Al-n) attenuated the macrophage M1 polarization and inhibited the secretion of inflammatory factors, leading to the prevention of the AL pathogenesis induced by particles *in vivo* (26). Although autophagy has been shown to be involved in the regulation of macrophage polarization, evidence regarding the regulatory mechanisms is underdeveloped.

3.3.3 Apoptosis

Apoptosis is the sequential death of cells *via* the mechanisms called programmed cell death (PCD) (91), which is characterized by morphological changes in the cellular structures together with a series of enzyme-dependent biochemical processing (92). In the resolution phase of inflammation, the infiltrating leukocytes execute the acute innate response and undergo apoptosis, subsequently cleared by phagocytic macrophages. In this course, macrophages undergo reprogramming from inflammatory to anti-inflammatory, leading to the relief of inflammation (93).

Efficient clearance of early apoptotic cells requires macrophages polarizing into the M2c phenotype (94). The capacity of M2 macrophages to uptake apoptotic cells depends on several necessary molecules, such as Mer tyrosine kinase, Axl receptor tyrosine kinase, growth arrest-specific 6 (Gas-6) (94, 95). In addition, the macrophage itself could also undergo apoptosis induced by wear particles (96). Consequently, the increase in macrophage apoptosis limits the proinflammatory function of macrophages (97, 98), seemly to be another important mechanism regarding the delayed inflammatory response in AL.

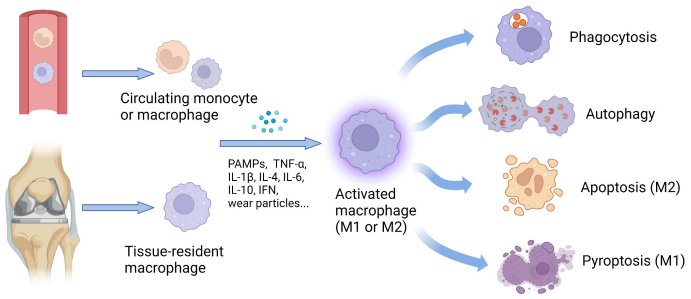

FIGURE 1
Origin and functional changes of macrophages. The number of tissue-resident macrophages can increase exponentially, including locally proliferating macrophages and monocytes recruited from the circulating peripheral blood. Stimulated by various factors, such as cytokines, PAMPs, and wear particles, the macrophages with different origins could be activated and further polarize into M1 or M2 phenotype. According to cellular phenotypes, activated macrophages show diverse functions, including phagocytosis, autophagy, apoptosis, and pyroptosis, to defend against infections and present antigens to other immune cells, thereby regulating the immune responses. IFN, interferon; IL, interleukin; M1, classically activated macrophages; M2, alternatively activated macrophages; PAMPs, pathogen-associated molecular patterns; TNF-α, tumor necrosis factor-alpha.

The caspase-3, a key mediator related to apoptosis, was detected in periprosthetic tissues in a mouse osteolysis model induced by UHMWPE particles (99, 100). Furthermore, apoptosis is associated with phenotypic changes in macrophages. Transcription factor Zhx2 deficiency could enrich the expression of M2 phenotype markers and as well promote the apoptosis of macrophages (101). Likewise, through the inhibition of M2-specific gene expression and apoptotic cell death, Delta-like-ligand 4 (DLL4) may prevent macrophage from polarizing into the M2 phenotype (102).

3.3.4 Pyroptosis

Different from apoptosis, pyroptosis is a proinflammatory type of PCD mediated by the gasdermin family, which usually leads to cell swelling and rapid rupture of plasma membranes, as well as the release of immunogenic cell contents, thereby exaggerating inflammatory status (103). In the aspect of the immune response, pyroptosis induced by the activation of pattern recognition receptors (PRRs) can stimulate inflammatory responses, independent of its effect in promoting cytokine induction (104). Pyroptosis is undoubtedly related to macrophage polarization. On one hand, by secreting exosomal cathepsin S, M1 macrophages induce pyroptosis in pancreatic acinar cells *via* the caspase1-mediated classical pyrolysis pathway, resulting in inflammation and pancreatic tissue damage (105). On the other hand, exosomal Mir-30D-5p of polymorphonuclear neutrophils (PMNs) is reported to induce M1 polarization by upregulating TNF-α, IL-1β, IL-6 and triggering pyroptosis in macrophages, leading to sepsis-associated acute lung injury (106).

Moreover, some mutual signals could mediate both M1 polarization and pyroptosis in macrophage, such as the caspase-1/GSDMD signaling pathway (107) and METTL3/MALAT1/PTBP1/USP8/TAK1 axis (108). The overexpression of brain and muscle Arnt-like protein 1 (BMAL1) also reduces the production of inflammasomes and pyroptosis in macrophages, as well as decreases the proportion of M1 phenotype *via* the TLR2/NF-κB pathway (109). A recent study has found that macrophages can activate the NLRP3 inflammasome and initiate subsequent pyroptosis to affect AL pathogenesis in mice model of cobalt-chromium-molybdenum (CoCrMo) alloy particles-induced osteolysis (110). As a result, wear particles not only induce M1 polarization and production of proinflammatory cytokines, but also boost inflammation by increasing pyroptosis in macrophages and inducing local tissue impairment.

3.4 Bone remodeling and osteoclastogenesis

Bone remodeling is a dynamic and balanced process maintained by osteoblasts (OBs) and osteoclasts (OCs), which is deeply affected by the receptor activator of nuclear factor NF-κB ligand/osteoprotegerin (RANKL/OPG) ratio. Disruption of this homeostasis leads to severe skeletal disorders (111). OBs are a type of bone-forming cells that are derived from bone marrow mesenchymal stem cells (BMSCs) and could respond to anabolic factors, such as bone morphogenic proteins (BMPs) (112). On the other hand, OCs are the unique cells known to absorb bone at or near the bone surface, which originate from bone marrow-derived monocytes/macrophages (BMMs) (113, 114).

Osteoclastogenesis is a complex process involving events of proliferation, differentiation, cell fusion, and multinucleation (111). The primary osteoclastogenic factor is RANKL which triggers a complex network of signaling pathways including NF-κB and mitogen-activated protein kinases (MAPK), *via* the receptor RANK on OC progenitors. By further activating the nuclear factor of activated T cells c1 (NFATc1), the master transcriptional factor of osteoclastogenesis, the fate of OC progenitors is decided by the controlling of key osteoclastogenic genes, such as tartrate-resistant acid phosphatase (TRAP) and cathepsin K (CTSK) (113–115). Calcineurin, a powerful mediator of transcriptional activity of NFATc1, is regulated by cytosolic calcium (Ca^{2+}) downstream of the TEC kinases and phospholipase Cγ (PLCγ), all of which are governed by both RANK and immunoreceptor tyrosine-based activation motif (ITAM)-based signaling. In addition, sustained intracellular Ca^{2+} oscillations are required for OC formation and functions, which will be introduced in the following section 5.5.3 (116). On the opposite side, OPG, as a decoy receptor, blocks RANKL binding to its cellular receptor RANK. An active OC is a highly polarized cell with a distinctive cytoskeletal organization and has the ability to create the sealing zone which is a site of tight membrane apposition to the bone surface, thereby executing its function as a bone-resorbing machine (116).

4 Polarization and phenotype of macrophages

Two major phenotypes of macrophages in response to environmental stimuli are M1 and M2. Usually, the phenotype of macrophages can be transformed by reprogramming (117, 118). Moreover, a recent study based on a spectrum of activated human macrophages revealed that there are continuous intermediate phenotypes between two opposite terminal phenotypes (119). Under such background, researchers use the term "polarization" to define the preference pattern of gene expression and protein synthesis in macrophages after different stimuli (120). "Naive" M0 macrophages, the prototype of M1 and M2 macrophages, are characterized by the expression of CD11b and F4/80, and emerge from committed myeloid progenitors in the presence of macrophage colony-stimulating factor (M-CSF). Although lacking the expression of antigen-presenting molecules (MHC-II) and co-stimulatory molecules (B7), M0 macrophages could readily phagocytose cellular debris or pathogens (78, 121).

The polarization to M1 macrophages has two main inducible sources, either microbial products or the cytokines secreted by TH1 lymphocytes. By recognizing pathogens and presenting antigens to T lymphocytes, M1 macrophages play a critical role in triggering adaptive immunity in the body. During immunization, M1

macrophages produce high amounts of proinflammatory factors (IL-1 β, IL-6, TNF-α, IL-12, and IL-23, among others), which in turn promote Th1 proinflammatory response (8, 10, 12, 122, 123). In contrast, M2 macrophages are mainly responsible for inflammatory relief and tissular repairs. Discovered in the early 1990s, the polarization to M2 macrophages is related to IL-4, IL-10, or IL-13 which are produced by innate and adaptive immune cells, such as mast cells, basophils, and Th2 lymphocytes (9, 122–124). By producing multiple growth factors and cytokines, such as TGF-β, IGF-1, PDGF, VEGF, IL-8, and endothelial growth factor (EGF), M2 macrophages are aided in the suppression of local inflammation and thus beneficial for tissue repairs (8, 10, 12, 122).

4.1 M1 macrophage in AL

4.1.1 Stimulus from wear particles and endotoxin

In the bone-implant interface, macrophage polarized to the M1 phenotype is mainly stimulated by wear particles and endotoxin (55). Upon continuous stimulation, M1 macrophages cause tissue damage by strengthening local inflammation *via* the secretion of TNF-α, IL-1β, IL-6, and IL-8 and the reduction of IL-10 expression (15, 23, 24, 26, 54–58). Besides, other cytokines such as IFN-β (15) and various chemokines, including chemokine (C-X-C motif) ligand 9 (CXCL9), CXCL10, and CXCL11 (56) secreted by M1 macrophages also play a role in AL pathogenesis. These biological reactions are largely affected by the size and type of wear particles (23, 26). Endotoxin also contributes to macrophage differentiation into the M1 phenotype by stimulating TLRs on the cell surface. Particles with PAMPs adhering, such as LTA and LPS, could induce more production of the proinflammatory cytokine than those without endotoxin (30, 32). On the contrary, the removal of endotoxins from particles significantly reduces the cellular activity of macrophages (30) and inhibits OC differentiation (31).

4.1.2 Surface receptor and DAMPs

It is well-established that both polyethylene (PE) and Ti particles can promote the expression of TLRs and various proinflammatory factors in macrophages (43, 125). A recent *in vivo* experiment also confirmed that alloy particles could induce significantly higher numbers of TLR-1, -4, and -6 positive cells in the synovial layer of joints (126). In the downstream of TLRs, NLRP3, ASC, caspase-1, and TNF-α and IL-1β were found to be positive through the colocalization with CD68 in the tissues around the revised prosthesis (43). The NF-κB, MAPK, and TAK1 pathways are involved in mediating signaling transduction downstream of TLRs (61–63, 127–129). In addition to TLRs, macrophages can engulf PMMA debris through macrophage receptors with collagenous structure (MARCO), which is a key pathogenic factor in promoting the phagocytosis of polymethyl methacrylate (PMMA) debris in aging macrophages (130).

As the main alternative hypothesis to PAMPs, DAMPs also activate TLRs during AL. The term "DAMPs" refer to self-molecules released by dying or damaged cells, which are defined as endogenous danger molecules due to they could activate the innate immune system by interacting with pattern recognition receptors (PRRs) (131). DAMPs are recognized by various membrane-bound receptors, including PRRs and non-PRRs, and also by intracellular sensors, notably through inflammasome (132, 133). Through binding to specific receptors, DAMPs activate the inflammatory process and recruit immune cells like neutrophils and monocytes. Therefore, after the clearance of DAMPs, the recruited leukocytes will change from a proinflammatory into a reparative program (133). Cobalt alloy particles could induce macrophage-associated inflammatory responses and bone loss through DAMPs rather than activated TLR4, due to the partially absent of metal-binding histidines in TLR4 (134). However, it has also been thought that the DAMPs generated in response to particles are insufficient to activate TLR2 or TLR4 in these cells (32).

Although DAMPs contribute to the host's immune defense, they also promote pathological inflammatory responses. The DAMPs, such as high-mobility group box 1 (HMGB1), S100 proteins, and heat shock proteins (HSPs), are commonly known as regulatory molecules of inflammatory responses (131). HMGB1 is an ancient DNA-binding nucleoprotein. It can be passively released from dying cells or actively secreted by monocytes, macrophages, and myeloid dendritic cells (135, 136). HMGB1 could induce M1 polarization *via* TLR2, TLR4, and RAGE/NF−κB signaling pathways, leading to LPS–induced acute lung injury (124), meanwhile, it significantly yielded the expression of the M1 marker inducible nitric oxide synthase (iNOS) while decreasing the M2 marker IL-10 in macrophages (137). *In vitro*, HMGB1 silencing down-regulated the secretion of inflammatory cytokines in macrophages, which cannot be reversed by the exogenous HMGB1 (138). Interestingly, HMGB1 could also trigger M2 macrophage polarization *via* the TLR2/NOX2/autophagy axis (139). In the same aspect, loss of HMGB1 in macrophages can increase the differentiation of proinflammatory macrophages and enhance inflammatory response under specific conditions, not the otherwise (140). In this regard, HMGB1 may induce distinct macrophage phenotypes probably due to different redox isoforms (141). Besides HMGB1, the expression level of several members of HSPs is closely related to distinct stages of polarization in macrophages (142). Compared with unpolarized macrophages, a significant up-regulation of members of the HSP70 family (HSPA2 and HSPA8), as well as the HSP90 family (HSP90AA1) can be observed in M1 macrophages. On the other hand, changes in HSP expression were also observed in macrophages during the M2 polarization, although with only five transcripts being significantly modulated. Among them, DNAJB5, HSPA13, HSPBAP1 were upregulated, whereas HSPH1 and HSPB1 were down-regulated (142).

4.1.3 Particles-induced inflammation conduce to osteolysis

Recent studies have found that Ti, CoCrMo particles, and LPS could strongly induce inflammatory responses in macrophages, significantly increasing the production of TNF-α and IL-1β, rising RANKL/OPG ratio, and enhancing the OC activity (143–146). The current paradigm holds the view that the induction of OC

differentiation by inflammatory cytokines is indirectly yielded under RANKL stimulation (147). Proinflammatory cytokines, such as IL-1β, TNF-α, IL-6, soluble IL-6 receptor, and IL-17, could all increase the production of RANKL from OBs. The effects of proinflammatory cytokines could be balanced by anti-inflammatory cytokines, such as IL-4 and IL-13, which could inhibit RANKL expression (147). In addition, a variety of wear particles could conduce to osteolysis *via* elevating M1 polarization (15, 24, 57, 58), since M1 macrophages are an important source of TNF-α production (11).

Although the concrete mechanism of TNF-α on OC differentiation is not fully understood, TNF-α signals promote OC differentiation by upregulating several proinflammatory target genes through the activation and nuclear translocation of NF-κB. One such target is RANK, which increases OC activity by mediating RANKL signaling (148). Interestingly, TNF-α produced by LPS/TLR4 signals can regulate OC generation in LPS-treated macrophages through the activation of RANKL signaling, whereas TNF-α in a RAW264.7 cells-based experiment demonstrates it may act as an autocrine/paracrine factor in promoting osteoclastogenesis, independent of RANKL signaling (149). In addition, the co-culture experiments of macrophages and MSCs (or OBs) revealed that PE and Ti particles could inhibit OB function, meanwhile promoting M1 polarization and osteoclastogenesis (150–152), proposing another mechanism for inflammation-induced osteolysis.

4.2 M2 macrophage in AL

4.2.1 Subtypes of M2 macrophage

The classical M1/M2 system was based on experiments *in vitro* with different stimulation approaches. Subsequent studies revealed that the process of macrophage activation and polarization is much more complex and needed an additional subdivision of the M2 population (153). As a result, the M2 macrophages is further classified into four subtypes: alternative activated macrophages (M2a), type 2 macrophages (M2b), deactivated macrophages (M2c), and M2-like macrophages (M2d) (154). Among them, applied stimuli and the achieved transcriptional changes correspond to particular subtypes: 1) M2a macrophage induced by IL-4 or IL-13 is a profibrotic phenotype, 2) M2b macrophage is stimulated by immune complexes combined with Toll-like receptor or IL-1 receptor agonists, and 3) M2c macrophage is exposure to IL-10, TGF-β, or glucocorticoids, 4) M2d, activated by adenosines or IL-6 (154, 155). For the pathological study, although M2a/c macrophage is found to be beneficial in early inflammatory stages, they have been uncovered to impair tissue remodeling (156). Similarly, M2b macrophages have been thought to be relieving immune responses with minor damage to local tissue (157).

4.2.2 M2 macrophage conduces to inflammatory relief

M2 macrophage has the effect of alleviating inflammation induced by wear particles, through increased expression of IL-10 and decreasing expression of IL-6 and TNF-α (24, 57, 58). In the presence of large amounts of TLR2 ligands, the anti-inflammatory activity of M2 macrophage is inhibited but without evident changes in cell surface markers (158). On the contrary, inhibition of TLR4 caused a shift from inflammatory M1 macrophages toward M2-dominant macrophages (159), suggesting that TLRs act as a switch that plays a role in the regulation of inflammation. In the downstream of TLRs, interleukin-1 receptor-associated kinase (IRAK) -m has been identified as an inhibitor of TLR signaling (160). One study found that knockdown of IRAK-m promoted M1 polarization and inhibited M2 polarization during the mycobacterium tuberculosis infection (161). But the discovery of IRAK-m-mediated local immunosuppression in periprosthetic tissues hints that macrophages have a self-protective mechanism, wherein the wear debris-mediated stimulation is inhibited to prevent overproduction of NK-κB-dependent proinflammatory cytokines and thus suppressing the deleterious host response in AL (162). However, the drawback is that the induction of IRAK-m overexpression triggered by wear debris also appears to conduce to the inhibition of LPS-induced TLR signaling, which leads to low-level biofilm-associated infection and chronic inflammation (162). Therefore, activation of IRAK-m is somehow affected by the local immune environment.

In addition, M2 polarization is regulated by cytokines in the surrounding, especially IL-10 and IL-4. IL-10 is an important anti-inflammatory cytokine (163). Recent studies have verified that IL-10 treatment significantly reduces iNOS expression and promotes CD163 overexpression, suggesting that IL-10 treatment could reprogram bone marrow-derived macrophages (BMDMs) to an M2 phenotype and regulate the process of M1/M2 polarization (164). *In vivo* experiments revealed that the extra addition of IL-10 partially reversed the inhibitory effect of PE particles on bone ingrowth (165). In the aspect of gene regulation, IL-10 not only decreased the activation of signal transducer and activator of transcription 1 (STAT1), NF-κB p65, and c-Jun N-terminal kinase 1 (JNK1) genes but also increased the expression of STAT3 (164). In addition to IL-10, IL-4 also has the ability to switch the M1 phenotype induced by Ti particles into the M2 phenotype (55, 166). Compared with non-activated macrophages, upon IL-4 stimulation, the shift from M1 to the anti-inflammatory M2 phenotype is more thorough (55).

4.2.3 M2 Macrophage in bone remodeling

Macrophages stimulated by cytokines, such as IL-4 and IL-13, have been confirmed to prevent the OC differentiation and inhibit the function of mature OCs (11, 147). In addition, M2 macrophages may promote OB differentiation by producing cytokines that are critical for osteogenesis, including BMP-2, TGF-β, and IGF-1 (11, 167, 168). Also, by interacting with MSCs, M2 macrophages create an anti-inflammatory environment that is conducive to osseointegration (14). A recent study revealed that preconditioning of murine MSCs with IFN-γ and IL-1β highly significant reduction of CD86 and iNOS protein in macrophages under M1 inducers (LPS + IFN-γ) and diminished TNF-α secretion (169). Additionally, CD86 and iNOS protein expression as well as NO and IL-10 secretion were markedly

increased under M2a inducers (IL-4) (169). On the other hand, under the stimulation of IL-4, reduced expression of CD86 and iNOS, as well as increased secretion of nitric oxide (NO) and IL-10 could be discovered in macrophages (169). The secretion of IL-10 could be attributed to the phenotype of M2b macrophages which are generally suggested to be the main subtype of macrophages for inflammatory relief (170). In addition, macrophages stimulated by a conditioned medium from preconditioned MSCs (pre-MSC-CM) may display an overall increased phagocytic capacity (171, 172). Also, M2a macrophages are found to undergo reprogramming to an M2b/M2c phenotype after treatment with the pre-MSC-CM (171, 172), indicating an influence of MSCs behavior on the induction of macrophage polarization.

5 Regulatory mechanisms of macrophages in AL

Several signaling pathways are involved in the process of macrophage polarization (8, 173–179). Various ligands, receptors, transcription factors, and other factors cooperate closely to ensure the precise regulatory capacity of macrophages (8). New research has found that several cytokines can influence M1/M2 polarization through NF-κB, MAPK, and JAK/STAT pathways which are involved in AL (55, 166, 180). Furthermore, depending on the amounts and ratios, molecules in the microenvironment can antagonize or synergistically act, thus in favor of certain macrophage phenotypes (181). Some regulatory mechanisms related to macrophage polarization in the microenvironment of the bone-implant interface are described below (Figure 2).

5.1 Toll-like receptors

5.1.1 Overview of toll-like receptors

TLRs have been intensively studied in innate immunity regarding the recognition of PAMPs (182). It has been reported that TLR2 or TLR4 can recruit MyD88 and further bind to the IRAK to form a signal complex called Myddosome. The Myddosome-complex recruits the ubiquitin ligase TNF receptor-associated factor 6 (TRAF6), which triggers the TAK1 kinase signaling cascade pathway and ultimately leads to NF-κB nuclear translocation through the phosphorylation and activation of IκB kinase α/β (IKKα/β) (63, 183, 184).

5.1.2 Toll-like receptors in macrophage polarization

TLRs are closely related to macrophage polarization (63). HMGB1 is an important mediator that induces M1 polarization through the activation of absent in melanoma 2 (AIM2) inflammasome, TLR2/4 and RAGE/NF-κB signaling pathways in macrophages (124). In addition, LPS can activate downstream TAK1, NF-κB, and MAPK signals through the TLR4/MyD88 pathway, which increases the expression of cyclooxygenase-2

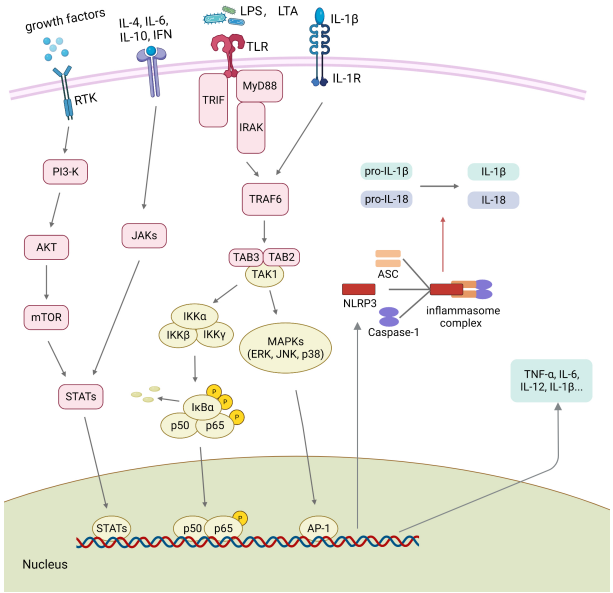

FIGURE 2
Polarization-related signaling transduction in macrophages. The binding of growth factors or cytokines to their receptors activates STATs through JAKs or PI3K/AKT pathway signaling. Activated TLRs and IL-1βR trigger downstream signaling, including the NF-κB and the MAPK signaling pathways. Several transcription factors, such as AP-1, STATs, and p65, are regulated by the upstream signaling pathways and further promote the assembly of NLRP3 inflammasome. Then, the activated NLRP3 inflammasome promotes the maturation of pro-IL-1β and pro-IL-18. ASC, apoptosis-associated speck-like protein containing a CARD; IFN, interferon; IL, interleukin; LPS, lipopolysaccharide; IRAK, Interleukin-1 receptor-associated kinase; LTA, lipoteichoic acid; MyD88, myeloid differentiation primary response protein 88; NLRP3 NOD-like receptor family pyrin domain containing 3; PAMPs, pathogen-associated molecular patterns; RTK, Receptor Tyrosine Kinases; STATs, signal transducers and activators of transcription; TLR, toll-like receptor; TNF-α, tumor necrosis factor-alpha; TRIF, TIR-domain-containing adapter-inducing interferon-beta.

(COX-2) and iNOS, promotes M1 polarization and leads to the up-regulated expression of cytokines TNF-α, IL-1β, IL-6, and PGE2 (61, 63). The particles with LTA adhering could increase the expression of proinflammatory factors by the activation of TLR2/NF-κB and MAPK pathways (32, 185). Previous studies have shown that a variety of TLRs, such as TLR2, which participate in local inflammatory and immune responses, are present in periprosthetic tissues after the revision of total hip arthroplasty (rTHA) (43).

5.1.3 NLRP3 inflammasome

NLRP3 inflammasome widely exists in macrophages, granulocytes, antigen-presenting cells (APC), and other immune cells. It consists of the NLRP3 (sensor protein), ASC (adapter protein), and caspase-1 (186). The initiation of NLRP3 inflammasome could be induced by multiple inflammatory stimuli, such as PAMPs. As the core protein of the NLRP3 inflammasome complex, NLRP3 senses endogenous DAMPs and microbial ligands. The production of ROS, low level of intracellular potassium (K^+), and the release of lysosomal protease into the cytoplasm are all upstream mechanisms that trigger the activation of NLRP3 inflammasome in several conditions (187–189). NLRP3 inflammasome which is activated by pathologically stimulated macrophages could regulate the production of IL-18, IL-1β, and cleavage of caspase-1 (186, 188, 189).

On the other hand, studies have also found that NLRP3 inflammasome participates in macrophage polarization (89, 175, 190, 191). In a co-culture experiment, force-pre-treated human periodontal ligament cells (hPDLCs) promote M1 polarization and increase the secretion of IL-1β in macrophages *via* the activation of NLRP3 inflammasome (191). On the contrary, by inhibiting the activation of NLRP3 inflammasome, metformin induces M2 polarization in macrophages and promotes wound healing in rat dorsal skin (175). Moreover, USP19 could directly promote M2 polarization by suppressing the activation of NLRP3 inflammasome to interferon regulatory factor-4 (IRF-4) (89). Bruton's tyrosine kinase (BTK) is a key factor in TLR4-related pathways, which could activate NF-κB signaling and promote p65 phosphorylation, ASC oligomerization, and caspase-1 activation (192). It has been recently found that BTK could promote TiAl6V4 alloy particles (TiPs)-induced inflammation in BMDMs by positively regulating NF-κB activation, NLRP3 inflammasome formation, and M1 polarization (193). On the contrary, NLRP3 silencing attenuates the promotive effect of conditioned exosomes on M1 polarization in a particles-induced osteolysis model (194).

5.1.4 Syk

Syk is a key component of TLRs in recognizing PAMPs and activating immune responses (195–199). Moreover, Syk plays a critical role in LPS-induced M1 polarization (200). In monocytes, pharmacological inhibition of Syk prevents LPS-induced TLR4 phosphorylation (199), suggesting that Syk may be involved in tyrosine phosphorylation of the TIR domain in TLR4. Recently, PMMA and HA particles were confirmed to augment the expression of CD86, and secretion of cytokines, such as TNF-α and IL-6, in a Syk- and MAPK-dependent (phosphorylation of ERK and p38) manner (56). Also, Syk is reported to be closely associated with the NLRP3 inflammasome-mediated proinflammatory cytokine release (201). In addition, Syk could control NLRP3 activation and IL-1β synthesis in macrophages in response to fungal infections (202).

5.2 NF-κB Signaling Pathway

5.2.1 Overview of NF-κB signaling

In the resting state, NF-κB dimers are sequestered in the cytoplasm in an inactive state by the IκB family of proteins, including IκBα, IκBβ, IκBϵ, and the NF-κB precursors, p105 and p100. The IκB kinase (IKK) complex consists of kinases IKKα, IKKβ, and IKKγ. Upon receiving the activation signals, IκB protein is phosphorylated by IKK complexes, leading to proteasomal degradation of IκB. The released NF-κB dimers are then translocating into the nucleus, where they can bind to specific sites on DNA to regulate gene transcription (75).

5.2.2 NF-κB signaling in macrophage polarization

LPS-induced M1 polarization is dependent on NF-κB p65 activation, and the treatment with IKKβ inhibitors reduces the mRNA expression of M1 markers in macrophages (203). Therefore, IKK inhibitors reduce LPS-induced expressions of IL-1, IL-6, IL-10, TNF-α, and IFN (204). Recent studies have revealed that diverse wear particles (e.g., Ti, TiPs, HA, PE, PMMA) could induce the macrophage to release proinflammatory cytokines and chemokines, which are accomplished by the activation of NF-κB signaling pathways and associated macrophage polarization (15, 26, 54, 205). Qiu et al. found that stimulation of LPS or Ti particles could up-regulate p-IKKβ, p-IκBα, and p-p65 and significantly increase the translocation of p65 into the nucleus in BMDMs. Meanwhile, these particles-induced inflammatory infiltrations increase the number of OCs (TRAP-positive cells) and thereby decrease bone mineral density, eventually leading to PPOL (15). Similarly, Gao et al. found that PMMA particles could up-regulate iNOS and decrease the production of Arginase-1 (Arg-1) and IL-10 by the activation of p65 nuclear translocation in macrophages (54).

5.2.3 NF-κB signaling in osteoclastogenesis

Under the same settings, NF-κB can be activated by RANKL or LPS to augment particles-induced bone loss *via* the enhancement of osteoclastogenesis (206, 207). Upstream stimuli-triggered NF-κB signaling could act on transcription factors (c-fos and NFATc1) and regulate the expression of osteoclastogenesis-related genes, thus promoting OC differentiation and functions (206, 208, 209).

5.3 MAPK signaling pathway

5.3.1 Overview of MAPK signaling

The MAPK signaling pathway takes part in cell differentiation, proliferation, and apoptosis (210). MAPK pathways are organized into three-tiered cascades consisting of three factors: MAPK,

MAPK kinase, and MAPKK kinase. During the phosphorelay process, MAPKKKs which are serine/threonine protein kinases, phosphorylate and activate MAPKKs, and then dually phosphorylate the threonine and tyrosine residues of the conserved TXY motif that belongs to the activation loop of MAPKs, including extracellular signal-regulated kinase (ERK), JNK, and p38 (210, 211).

5.3.2 MAPK signaling in macrophage polarization

MAPK signaling pathway is closely associated with macrophage polarization (61, 212–214). The activation of the MAPK signaling pathway promotes polarization of M1 macrophages, expression of iNOS, and down-regulation of CD206, thereby mediating the secretion of cytokines, such as TNF-α, IL-1β, and IL-6 (214). On the other hand, inhibiting the phosphorylation of JNK, ERK, and p38 in MAPK pathways may switch repolarized M1 to reprogrammed M2 phenotype (213, 214). Studies elucidate that the MAPK signaling pathway is located downstream of TLRs, wherein LPS could activate the MAPK pathway through TLR4/MyD88 pathway to induce M1 polarization and participate in the inflammatory response (61, 62, 215). Further, PMMA and hydroxyapatite (HA) particles are reported to result in M1 polarization by increasing phosphorylation of ERK and p38 (56). Similar to NF-κB signaling, MAPK also mediates wear particles-induced OC differentiation and the following osteolysis (206).

5.4 JAK/STAT Signaling Pathway

5.4.1 Overview of JAK/STAT signaling

STAT proteins are potent cytoplasmic transcription factors wherein several family members have participated in macrophage polarization and OC formation, including STAT1, STAT3, and STAT6 (216, 217). Growing studies reveal the involvement of the JAK/STAT pathway in regulating multiple biological events, such as innate and adaptive immunity, cell growth and differentiation, and programmed cell death (217). In the aspect of functioning, phosphorylated STATs promote monomeric dimerization through their SH2 domains and further translocation into the nucleus, where STATs regulate the transcription of target genes (216, 217).

5.4.2 JAK/STAT signaling in macrophage polarization

Several studies have revealed the mediating role of STATs in macrophage polarization. PARP14 silencing or RBM4 knockdown can promote IFN-γ-induced signaling transduction *via* STAT1 activation, which leads to M1 polarization in macrophages (218, 219). Also, STAT1/6 pathway mediates M1/M2 polarization in macrophages after physalin D stimulation (220). By phosphorylating STAT6, protocatechuic acid (PCA) decreases the activation of NF-κB signaling and gives a bias towards M2 polarization over M1 polarization in macrophages (173). Conclusively, an obvious antagonism between STAT1 and STAT6 has been described to promote M1 and M2 cell polarization, respectively (220). In addition, the activation of JAK/STAT3 signaling facilitates macrophage transformation to M2c polarization (180). In an AL mouse model, compared with the pure stimulation of UHMWPE particles, the extra addition of IL-10 significantly decreases iNOS-positive cells and increases CD163-positive cells *via* reducing the transcription of STAT1, NF-κB p65, and JNK1, and promoting the expression of STAT6 (164).

5.4.3 JAK/STAT signaling in osteoclastogenesis

Compared with STAT1 and STAT6, STAT3 is closely related to osteoclastogenesis. Therefore, inhibition of STAT3 can negatively affect RANKL-mediated OC formation and functions (221). An *in vivo* experiment demonstrated that treatment with TiPs pellet could promote the expression of STAT3 and production of RANKL in OBs, thereby stimulating OCs formation in particles-induced osteolysis models, whereas the activation of STAT3 also mediates nano-particles-induced IL-6-dependent inflammatory response in OBs (222).

5.5 Calcium (Ca^{2+}) signaling

5.5.1 Overview of Ca^{2+} signaling

The centration of Ca^{2+} in the cytoplasm ($[Ca^{2+}]c$) is 20, 000 times lower than that outside the cell. This is achieved by the Ca^{2+}-related transportation and exchange under the dependence on specific proteins. When activated by a variety of external stimuli, cells respond by an increase in the $[Ca^{2+}]c$ and trigger downstream signaling, in the form of Ca^{2+} spikes or oscillations (223). Ca^{2+} signaling participates in various biological processes, resulting from a complex switch between the activation and inactivation of Ca^{2+}-permeable channels (224). The excitability of Ca^{2+} signaling is determined by intracellular Ca^{2+} oscillations, which are attributed by the extracellular Ca^{2+} influx, the effect of ITAM/PLCγ/IP_3 signaling on the release of Ca^{2+} from ER, and the capacity of collecting Ca^{2+} from the cytosol by SERCA. In addition, depending on the depletion of ER Ca^{2+} storage, extracellular Ca^{2+} entry could also be accomplished by the activation of STIM-mediated TRPC channels and Orai1 channels, which is the so-called SOCE mechanism (225, 226) (Figure 3).

5.5.2 Ca^{2+} signaling in macrophage polarization

Ca^{2+} signaling is related to behavior changes in macrophages, such as polarization and phagocytosis, largely depending on Ca^{2+} uptake in mitochondria (227). Many studies have implicated that distinct Ca^{2+} entry channels determine the IFN-induced M1 polarization or IL-4-induced M2 polarization. Naive or M2 macrophages exhibit a robust Ca^{2+} entry that is dependent on the activity of Orai1 channels (228). As a result, blockade of Ca^{2+} entry inhibits NF-κB/STAT1 or STAT6 signaling events and consequently lowers cytokine production that is essential for M1 or M2 polarization in macrophages (228). In detail, Ca^{2+} influx facilitates M1 polarization, enabling the high productivity of proinflammatory mediators, such as cytokines and chemokines (229). Transient receptor canonical ion channel 1 (TRPC1)-

mediated calcium entry seems to play a crucial role in M1 polarization, due to a non-selective TRPC1 current is found in macrophages with M1 phenotype (228, 230). Therefore, knockdown or blockade of the Kir2.1 channel significantly suppresses M1 polarization and promotes M2 polarization (231). Of note, a study found that transient receptor potential vanilloid 1 (TRPV1)-induced Ca^{2+} influx could promote the phosphorylation of Ca^{2+}/calmodulin-dependent protein kinase II (CaMKII), but leads to the inhibition of M1 polarization (232), bringing uncertainty in elucidating regulatory mechanism between Ca^{2+} signaling and macrophage polarization.

5.5.3 Ca^{2+} signaling in osteoclastogenesis

Except for macrophage polarization, Ca^{2+} oscillations are the well-known mechanism in triggering RANKL-induced osteoclastogenesis and bone resorption (233, 234). The increase in the $[Ca^{2+}]c$ is a fundamental process for mediating OC biology, involving in OC proliferation, differentiation, and resorptive function. At the molecular level, cytosolic Ca^{2+} binds to calmodulin and subsequently activates calcineurin, leading to the activation of NFATc1 which is required for OC differentiation (235). Therefore, by blocking the Ca^{2+} entry channels, inhibition of the activity of Ca^{2+}/calmodulin-dependent protein kinase IV (CaMKIV) and calcineurin will lead to a reduction in the nuclear translocation of c-Fos and NFATc1, ultimately resulting in the suppression of osteoclastogenesis (236). Similarly, directly interfering with intracellular Ca^{2+} oscillations would also have the same negative impact on osteoclastogenesis (237). More content associated with Ca^{2+} oscillations in OC biology has been reviewed in the article by Okada H, et al. (234).

6 Future directions

Functional changes of macrophages reflect the intricate and constant regulation of the local environment by the network of cells and cytokines. While macrophage phenotypes have been roughly classified into representative M1 and M2 subtypes, investigating the concrete mechanism for the shift between proinflammatory phenotype and anti-inflammatory state is still challenging, especially in identifying responsible genes and proteins. In this regard, Ca^{2+} signaling based on different stimuli shows bidirectional effects on both macrophage polarization and osteoclast activation, which may be worth further investigation. While it seems clear that the behavior changes of macrophages, such as phagocytosis, pyroptosis, and apoptosis, are closely related to AL pathology, the triggered conditions and signaling events involved have not been

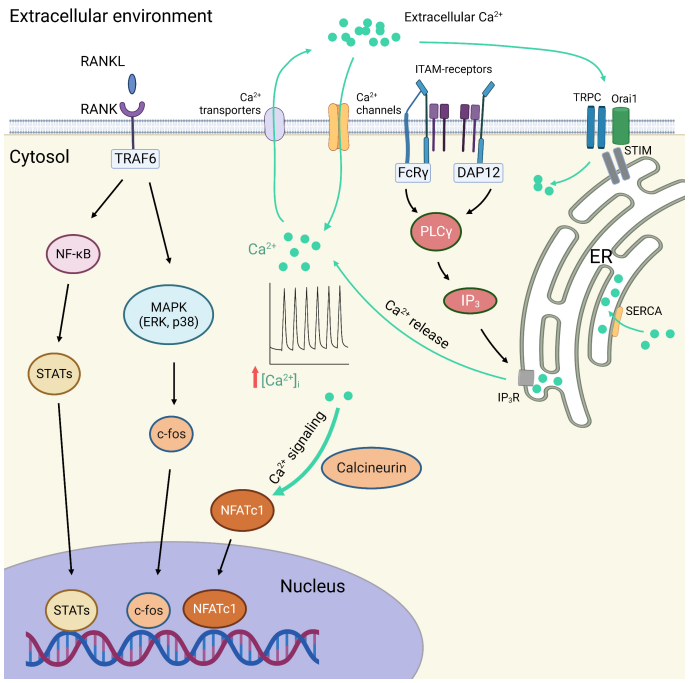

FIGURE 3
RANKL and calcium (Ca^{2+}) signaling in macrophage polarization and osteoclastogenesis. The transcriptional factors responsible for macrophage polarization and osteoclastogenesis are regulated by the NF-κB and MAPK signaling pathways, as well as the Ca^{2+} signaling pathways. The excitability of Ca^{2+} signaling is determined by intracellular Ca^{2+} oscillations, which are attributed by the extracellular Ca^{2+} influx, the effect of ITAM/PLCγ/IP_3 signaling on the release of Ca^{2+} from ER, and the capacity of collecting Ca^{2+} from the cytosol by SERCA. In addition, depending on the depletion of ER Ca^{2+} storage, extracellular Ca^{2+} entry could also be accomplished by the activation of STIM-mediated TRPC channels and Orai1 channels, which is the so-called SOCE mechanism. Ca^{2+}, calcium ions; DAP12, DNAX-activation protein of 12 kDa; ER, endoplasmic reticulum; FcRγ, Fc receptor gamma-chain; IP_3, inositol 1,4,5-trisphosphate; IP_3R, inositol 1,4,5-trisphosphate receptor; ITAM, immunoreceptor tyrosine-based activation motif; MAPK, mitogen-activated protein kinases; NFATc1, nuclear factor of activated T cells c1; PLCγ, phospholipase C-gamma; RANK, receptor activator of nuclear factor-kappa B; RANKL, receptor activator of nuclear factor-kappa B ligand; SERCA, Sarco/endoplasmic reticulum Ca(2+)-ATPase; SOCE, store-operated Ca^{2+} entry; STATs, signal transducers and activators of transcription; STIM, stromal interaction molecule; TRAF6, tumor necrosis factor receptor-associated factor 6; TRPC channels, transient receptor potential canonical channels.

fully elucidated. While PAMPs and DAMPs contribute to the response of macrophages to wear particles *via* TLRs, the main reason for the associated activation of TLRs is still controversial. Likewise, DAMPs affect macrophage programming is also unclear. Therefore, the role of PAMPs and DAMPs in AL still needs to be further elucidated. In addition, the local environment in periprosthetic tissue is complex due to the diversity of involved immune cells, such as dendritic cells and lymphocytes, thus highlighting the importance of intercellular communications *via* different signals. To address unresolved issues, applying CRISPR/Cas9 technology which enables accurate and efficient genome editing, would help in effectively elucidating the underlying mechanisms of macrophages in AL (238).

For the therapeutic strategy of AL, we believe the relief of inflammation and inhibition of bone resorption are keys to success. Through an in-depth study into the mechanisms of interaction between cytokines and macrophages, we may instruct a more accurate regulation of the inflammatory process in order to maintain a balance between immune defense and tissue homeostasis.

Author contributions

YC mainly contributed to the topic determination, literature selection, and draft written. YW (leading), TY, ZZ, JG, and QM screened detailed information from the literature and helped in the manuscript discussion. SS and ZL approved the direction of the topic, revised the manuscript, and supervised the work.

Funding

This work was supported by the National Natural Science Foundation of China (nos. 82100936 and 82272485) and Taishan Scholars Foundation of Shandong Province (no. tsqnz20221170).

Acknowledgments

Draft of Figures 1–3 was created with BioRender.com.

Conflict of interest

The authors declare that the research was conducted in the absence of any commercial or financial relationships that could be construed as a potential conflict of interest.

Publisher's note

References

1. Price AJ, Alvand A, Troelsen A, Katz JN, Hooper G, Gray A, et al. Knee replacement. *Lancet (London England).* (2018) 392(10158):1672–82. doi: 10.1016/S0140-6736(18)32344-4

2. Jiang Y, Jia T, Wooley PH, Yang SY. Current research in the pathogenesis of aseptic implant loosening associated with particulate wear debris. *Acta orthopaedica Belgica.* (2013) 79(1):1–9.

3. Zhang L, Haddouti EM, Welle K, Burger C, Wirtz DC, Schildberg FA, et al. The effects of biomaterial implant Wear debris on osteoblasts. *Front Cell Dev Biol* (2020) 8:352. doi: 10.3389/fcell.2020.00352

4. Abu-Amer Y, Darwech I, Clohisy JC. Aseptic loosening of total joint replacements: Mechanisms underlying osteolysis and potential therapies. *Arthritis Res Ther* (2007) 9(Suppl 1):S6. doi: 10.1186/ar2170

5. Hodges NA, Sussman EM, Stegemann JP. Aseptic and septic prosthetic joint loosening: Impact of biomaterial wear on immune cell function, inflammation, and infection. *Biomaterials* (2021) 278:121127. doi: 10.1016/j.biomaterials.2021.121127

6. Goodman SB, Gallo J. Periprosthetic osteolysis: Mechanisms, prevention and treatment. *J Clin Med* (2019) 8(12). doi: 10.3390/jcm8122091

7. Hirayama D, Iida T, Nakase H. The phagocytic function of macrophage-enforcing innate immunity and tissue homeostasis. *Int J Mol Sci* (2017) 19(1). doi: 10.3390/ijms19010092

8. Juhas U, Ryba-Stanisławowska M, Szargiej P, Myśliwska J. Different pathways of macrophage activation and polarization. *Postepy higieny i medycyny doswiadczalnej* (2015) 69:496–502. doi: 10.5604/17322693.1150133

9. Murray PJ. Macrophage polarization. *Annu Rev Physiol* (2017) 79:541–66. doi: 10.1146/annurev-physiol-022516-034339

10. Funes SC, Rios M, Escobar-Vera J, Kalergis AM. Implications of macrophage polarization in autoimmunity. *Immunology* (2018) 154(2):186–95. doi: 10.1111/imm.12910

11. Muñoz J, Akhavan NS, Mullins AP, Arjmandi BH. Macrophage polarization and osteoporosis: A review. *Nutrients* (2020) 12(10). doi: 10.3390/nu12102999

12. Viola A, Munari F, Sánchez-Rodríguez R, Scolaro T, Castegna A. The metabolic signature of macrophage responses. *Front Immunol* (2019) 10:1462. doi: 10.3389/fimmu.2019.01462

13. Shapouri-Moghaddam A, Mohammadian S, Vazini H, Taghadosi M, Esmaeili SA, Mardani F, et al. Macrophage plasticity, polarization, and function in health and disease. *J Cell Physiol* (2018) 233(9):6425–40. doi: 10.1002/jcp.26429

14. Liu W, Li J, Cheng M, Wang Q, Yeung KWK, Chu PK, et al. Zinc-modified sulfonated polyetheretherketone surface with immunomodulatory function for guiding cell fate and bone regeneration. *Advanced Sci (Weinheim Baden-Wurttemberg Germany).* (2018) 5(10):1800749. doi: 10.1002/advs.201800749

15. Qiu J, Peng P, Xin M, Wen Z, Chen Z, Lin S, et al. ZBTB20-mediated titanium particle-induced peri-implant osteolysis by promoting macrophage inflammatory responses. *Biomaterials science.* (2020) 8(11):3147–63. doi: 10.1039/D0BM00147C

16. Harris WH, Schiller AL, Scholler JM, Freiberg RA, Scott R. Extensive localized bone resorption in the femur following total hip replacement. *J Bone Joint Surg Am volume.* (1976) 58(5):612–8. doi: 10.2106/00004623-197658050-00005

17. Anil U, Singh V, Schwarzkopf R. Diagnosis and detection of subtle aseptic loosening in total hip arthroplasty. *J arthroplasty.* (2022) 37(8):1494–500. doi: 10.1016/j.arth.2022.02.060

18. Delanois RE, Mistry JB, Gwam CU, Mohamed NS, Choksi US, Mont MA. Current epidemiology of revision total knee arthroplasty in the united states. *J arthroplasty.* (2017) 32(9):2663–8. doi: 10.1016/j.arth.2017.03.066

19. Tarazi JM, Chen Z, Scuderi GR, Mont MA. The epidemiology of revision total knee arthroplasty. *J knee surgery.* (2021) 34(13):1396–401. doi: 10.1055/s-0041-1735282

20. Schwartz AM, Farley KX, Guild GN, Bradbury TL Jr. Projections and Epidemiology of Revision Hip and Knee Arthroplasty in the United States to 2030. *J Arthroplasty* (2020) 35(6S):S79–85. doi: 10.1016/j.arth.2020.02.030

21. Sundfeldt M, Carlsson LV, Johansson CB, Thomsen P, Gretzer C. Aseptic loosening, not only a question of wear: A review of different theories. *Acta orthopaedica.* (2006) 77(2):177–97. doi: 10.1080/17453670610045902

22. Wei J, Cai X, Wang Y, Chen H, Zhang B. [Mechanisms, prevention, and treatments of prosthetic aseptic loosening]. *Zhongguo xiu fu chong jian wai ke za zhi = Zhongguo xiufu chongjian waike zazhi = Chin J reparative reconstructive Surg* (2010) 24 (3):296–300.

23. Schoenenberger AD, Schipanski A, Malheiro V, Kucki M, Snedeker JG, Wick P, et al. Macrophage polarization by titanium dioxide (TiO(2)) particles: Size matters. *ACS biomaterials Sci engineering.* (2016) 2(6):908–19. doi: 10.1021/acsbiomaterials.6b00006

24. Li B, Hu Y, Zhao Y, Cheng M, Qin H, Cheng T, et al. Curcumin attenuates titanium particle-induced inflammation by regulating macrophage polarization *In vitro* and in vivo. *Front Immunol* (2017) 8:55. doi: 10.3389/fimmu.2017.00055

25. Li C, Jiang C, Peng M, Li T, Yang Z, Liu Z, et al. Proinflammatory and osteolysis-inducing effects of 3D printing Ti6Al4V particles *in vitro* and in vivo. *RSC Adv* (2018) 8 (4):2229–39. doi: 10.1039/C7RA12677H

26. Hu X, Xu L, Fu X, Huang J, Ji P, Zhang Z, et al. The TiO(2)-μ implant residual is more toxic than the Al(2)O(3)-n implant residual *via* blocking LAP and inducing macrophage polarization. *Nanoscale* (2021) 13(19):8976–90. doi: 10.1039/D1NR00696G

27. Li J, Li Y, Peng X, Li B, Qin H, Chen Y. *In vivo* analysis of the effects of CoCrMo and Ti particles on inflammatory responses and osteolysis. *RSC advances.* (2018) 8 (10):5151–7. doi: 10.1039/C7RA12325F

28. Liu GY, Xu YS, Jiang WL, Leng NN, Chen JM. [Role and mechanism of endoplasmic reticulum stress response induced by wear particles in osteolysis]. *Zhongguo gu shang = China J orthopaedics traumatology* (2020) 33(12):1148–56. doi: 10.12200/j.issn.1003-0034.2020.12.012

29. Longhofer LK, Chong A, Strong NM, Wooley PH, Yang SY. Specific material effects of wear-particle-induced inflammation and osteolysis at the bone-implant interface: A rat model. *J orthopaedic translation.* (2017) 8:5–11. doi: 10.1016/j.jot.2016.06.026

30. Bechtel CP, Gebhart JJ, Tatro JM, Kiss-Toth E, Wilkinson JM, Greenfield EM. Particle-induced osteolysis is mediated by TIRAP/Mal in vitro and in vivo: Dependence on adherent pathogen-associated molecular patterns. *J Bone Joint Surg Am volume* (2016) 98(4):285–94. doi: 10.2106/JBJS.O.00736

31. Bi Y, Seabold JM, Kaar SG, Ragab AA, Goldberg VM, Anderson JM, et al. Adherent endotoxin on orthopedic wear particles stimulates cytokine production and osteoclast differentiation. *J Bone mineral research: Off J Am Soc Bone Mineral Res* (2001) 16(11):2082–91. doi: 10.1359/jbmr.2001.16.11.2082

32. Greenfield EM, Beidelschies MA, Tatro JM, Goldberg VM, Hise AG. Bacterial pathogen-associated molecular patterns stimulate biological activity of orthopaedic wear particles by activating cognate toll-like receptors. *J Biol Chem* (2010) 285 (42):32378–84. doi: 10.1074/jbc.M110.136895

33. Hagman DS, Granade CM, Smith LS, Yakkanti MR, Malkani AL. Results of cemented posterior-stabilized total knee arthroplasty in obese patients with an average 10-year follow-up. *J arthroplasty.* (2020) 35(8):2097–100. doi: 10.1016/j.arth.2020.04.010

34. Koks S, Wood DJ, Reimann E, Awiszus F, Lohmann CH, Bertrand J, et al. The genetic variations associated with time to aseptic loosening after total joint arthroplasty. *J arthroplasty.* (2020) 35(4):981–8. doi: 10.1016/j.arth.2019.11.004

35. Lee SW, Kim WY, Song JH, Kim JH, Lee HH. Factors affecting periprosthetic bone loss after hip arthroplasty. *Hip pelvis.* (2021) 33(2):53–61. doi: 10.5371/hp.2021.33.2.53

36. Levent A, Suero EM, Gehrke T, Citak M. Risk factors for aseptic loosening after total knee arthroplasty with a rotating-hinge implant: A case-control study. *J Bone Joint Surg Am volume.* (2021) 103(6):517–23. doi: 10.2106/JBJS.20.00788

37. Mavčič B, Antolič V, Dolžan V. Association of NLRP3 and CARD8 inflammasome polymorphisms with aseptic loosening after primary total hip arthroplasty. *J orthopaedic research: Off Publ Orthopaedic Res Soc* (2020) 38(2):417–21. doi: 10.1002/jor.24474

38. Schiffner E, Latz D, Thelen S, Grassmann JP, Karbowski A, Windolf J, et al. Aseptic loosening after THA and TKA - do gender, tobacco use and BMI have an impact on implant survival time? *J orthopaedics* (2019) 16(3):269–72. doi: 10.1016/j.jor.2019.03.018

39. Fenelon C, Murphy EP, Fahey EJ, Murphy RP, O'Connell NM, Queally JM. Total knee arthroplasty in hemophilia: Survivorship and outcomes-a systematic review and meta-analysis. *J arthroplasty.* (2022) 37(3):581–92.e1. doi: 10.1016/j.arth.2021.10.015

40. Böhler C, Weimann P, Alasti F, Smolen JS, Windhager R, Aletaha D. Rheumatoid arthritis disease activity and the risk of aseptic arthroplasty loosening. *Semin Arthritis rheumatism.* (2020) 50(2):245–51. doi: 10.1016/j.semarthrit.2019.07.011

41. Christiansen RJ, Münch HJ, Bonefeld CM, Thyssen JP, Sloth JJ, Geisler C, et al. Cytokine profile in patients with aseptic loosening of total hip replacements and its relation to metal release and metal allergy. *J Clin Med* (2019) 8(8). doi: 10.3390/jcm8081259

42. Pajarinen J, Cenni E, Savarino L, Gomez-Barrena E, Tamaki Y, Takagi M, et al. Profile of toll-like receptor-positive cells in septic and aseptic loosening of total hip arthroplasty implants. *J BioMed Mater Res A.* (2010) 94(1):84–92. doi: 10.1002/jbm.a.32674

43. Naganuma Y, Takakubo Y, Hirayama T, Tamaki Y, Pajarinen J, Sasaki K, et al. Lipoteichoic acid modulates inflammatory response in macrophages after phagocytosis of titanium particles through toll-like receptor 2 cascade and inflammasomes. *J BioMed Mater Res A.* (2016) 104(2):435–44. doi: 10.1002/jbm.a.35581

44. Nalepka JL, Lee MJ, Kraay MJ, Marcus RE, Goldberg VM, Chen X, et al. Lipopolysaccharide found in aseptic loosening of patients with inflammatory arthritis. *Clin orthopaedics related Res* (2006) 451:229–35. doi: 10.1097/01.blo.0000224050.94248.38

45. Wasko MK, Goodman SB. Emperor's new clothes: Is particle disease really infected particle disease? *J orthopaedic research: Off Publ Orthopaedic Res Soc* (2016) 34 (9):1497–504. doi: 10.1002/jor.23292

46. Eger M, Hiram-Bab S, Liron T, Sterer N, Carmi Y, Kohavi D, et al. Mechanism and prevention of titanium particle-induced inflammation and osteolysis. *Front Immunol* (2018) 9:2963. doi: 10.3389/fimmu.2018.02963

47. Vannella KM, Wynn TA. Mechanisms of organ injury and repair by macrophages. *Annu Rev Physiol* (2017) 79:593–617. doi: 10.1146/annurev-physiol-022516-034356

48. Wynn TA, Barron L. Macrophages: Master regulators of inflammation and fibrosis. *Semin liver disease.* (2010) 30(3):245–57. doi: 10.1055/s-0030-1255354

49. Duffield JS, Forbes SJ, Constandinou CM, Clay S, Partolina M, Vuthoori S, et al. Selective depletion of macrophages reveals distinct, opposing roles during liver injury and repair. *J Clin Invest* (2005) 115(1):56–65. doi: 10.1172/JCI200522675

50. Jenkins SJ, Ruckerl D, Thomas GD, Hewitson JP, Duncan S, Brombacher F, et al. IL-4 directly signals tissue-resident macrophages to proliferate beyond homeostatic levels controlled by CSF-1. *J Exp Med* (2013) 210(11):2477–91. doi: 10.1084/jem.20121999

51. Jenkins SJ, Ruckerl D, Cook PC, Jones LH, Finkelman FD, van Rooijen N, et al. Local macrophage proliferation, rather than recruitment from the blood, is a signature of TH2 inflammation. *Sci (New York NY).* (2011) 332(6035):1284–8. doi: 10.1126/science.1204351

52. Murray PJ, Wynn TA. Protective and pathogenic functions of macrophage subsets. *Nat Rev Immunol* (2011) 11(11):723–37. doi: 10.1038/nri3073

53. Stratton-Powell AA, Williams S, Tipper JL, Redmond AC, Brockett CL. Mixed material wear particle isolation from periprosthetic tissue surrounding total joint replacements. *J Biomed materials Res Part B Appl biomaterials* (2022) 110(10):2276–89. doi: 10.1002/jbm.b.35076

54. Gao XR, Ge J, Li WY, Zhou WC, Xu L, Geng DQ. NF-κB/let-7f-5p/IL-10 pathway involves in wear particle-induced osteolysis by inducing M1 macrophage polarization. *Cell Cycle (Georgetown Tex).* (2018) 17(17):2134–45. doi: 10.1080/15384101.2018.1515549

55. Rao AJ, Gibon E, Ma T, Yao Z, Smith RL, Goodman SB. Revision joint replacement, wear particles, and macrophage polarization. *Acta biomaterialia.* (2012) 8(7):2815–23. doi: 10.1016/j.actbio.2012.03.042

56. Mahon OR, O'Hanlon S, Cunningham CC, McCarthy GM, Hobbs C, Nicolosi V, et al. Orthopaedic implant materials drive M1 macrophage polarization in a spleen tyrosine kinase- and mitogen-activated protein kinase-dependent manner. *Acta biomaterialia.* (2018) 65:426–35. doi: 10.1016/j.actbio.2017.10.041

57. Liu YW, An SB, Yang T, Xiao YJ, Wang L, Hu YH. Protection effect of curcumin for macrophage-involved polyethylene Wear particle-induced inflammatory osteolysis by increasing the cholesterol efflux. *Med Sci monitor: Int Med J Exp Clin Res* (2019) 25:10–20. doi: 10.12659/MSM.914197

58. Yan Z, Tian X, Zhu J, Lu Z, Yu L, Zhang D, et al. Metformin suppresses UHMWPE particle-induced osteolysis in the mouse calvaria by promoting polarization of macrophages to an anti-inflammatory phenotype. *Mol Med (Cambridge Mass).* (2018) 24(1):20. doi: 10.1186/s10020-018-0013-x

59. Percy MG, Gründling A. Lipoteichoic acid synthesis and function in gram-positive bacteria. *Annu Rev Microbiol* (2014) 68:81–100. doi: 10.1146/annurev-micro-091213-112949

60. Venkataranganayaka Abhilasha K, Kedihithlu Marathe G. Bacterial lipoproteins in sepsis. *Immunobiology* (2021) 226(5):152128. doi: 10.1016/j.imbio.2021.152128

61. Byun EB, Sung NY, Park JN, Yang MS, Park SH, Byun EH. Gamma-irradiated resveratrol negatively regulates LPS-induced MAPK and NF-κB signaling through TLR4 in macrophages. *Int immunopharmacol* (2015) 25(2):249–59. doi: 10.1016/j.intimp.2015.02.015

62. Wu TT, Tai YT, Cherng YG, Chen TG, Lin CJ, Chen TL, et al. GATA-2 transduces LPS-induced il-1β gene expression in macrophages *via* a toll-like receptor 4/MD88/MAPK-dependent mechanism. *PloS One* (2013) 8(8):e72404. doi: 10.1371/journal.pone.0072404

63. Jang HM, Kang GD, Van Le TK, Lim SM, Jang DS, Kim DH. 4-methoxylonchocarpin attenuates inflammation by inhibiting lipopolysaccharide binding to toll-like receptor of macrophages and M1 macrophage polarization. *Int immunopharmacol* (2017) 45:90–7. doi: 10.1016/j.intimp.2017.02.003

64. Neut D, van Horn JR, van Kooten TG, van der Mei HC, Busscher HJ. Detection of biomaterial-associated infections in orthopaedic joint implants. *Clin orthopaedics related Res* (2003) 413):261–8. doi: 10.1097/01.blo.0000073345.50837.84

65. Friedlander AH. Oral cavity staphylococci are a potential source of prosthetic joint infection. *Clin Infect diseases: an Off Publ Infect Dis Soc America* (2010) 50 (12):1682–3. doi: 10.1086/653003

66. Greenfield EM. Do genetic susceptibility, toll-like receptors, and pathogen-associated molecular patterns modulate the effects of wear? *Clin orthopaedics related Res* (2014) 472(12):3709–17. doi: 10.1007/s11999-014-3786-4

67. Wang G, Zhang P, Zhao J. Endotoxin contributes to artificial loosening of prostheses induced by titanium particles. *Med Sci monitor: Int Med J Exp Clin Res* (2018) 24:7001–6. doi: 10.12659/MSM.910039

68. Plüddemann A, Mukhopadhyay S, Gordon S. Innate immunity to intracellular pathogens: Macrophage receptors and responses to microbial entry. *Immunol Rev* (2011) 240(1):11–24. doi: 10.1111/j.1600-065X.2010.00989.x

69. Akhurst RJ, Hata A. Targeting the TGFβ signalling pathway in disease. *Nat Rev Drug discovery.* (2012) 11(10):790–811. doi: 10.1038/nrd3810

70. Ramachandran P, Iredale JP, Fallowfield JA. Resolution of liver fibrosis: basic mechanisms and clinical relevance. *Semin liver disease.* (2015) 35(2):119–31. doi: 10.1055/s-0035-1550057

71. Zigmond E, Bernshtein B, Friedlander G, Walker CR, Yona S, Kim KW, et al. Macrophage-restricted interleukin-10 receptor deficiency, but not IL-10 deficiency, causes severe spontaneous colitis. *Immunity* (2014) 40(5):720–33. doi: 10.1016/j.immuni.2014.03.012

72. Shouval DS, Biswas A, Goettel JA, McCann K, Conaway E, Redhu NS, et al. Interleukin-10 receptor signaling in innate immune cells regulates mucosal immune tolerance and anti-inflammatory macrophage function. *Immunity* (2014) 40(5):706–19. doi: 10.1016/j.immuni.2014.03.011

73. Xia Y, Rao L, Yao H, Wang Z, Ning P, Chen X. Engineering macrophages for cancer immunotherapy and drug delivery. *Advanced materials (Deerfield Beach Fla).* (2020) 32(40):e2002054. doi: 10.1002/adma.202002054

74. Al Haq AT, Tseng HY, Chen LM, Wang CC, Hsu HL. Targeting prooxidant MnSOD effect inhibits triple-negative breast cancer (TNBC) progression and M2 macrophage functions under the oncogenic stress. *Cell Death Dis* (2022) 13(1):49. doi: 10.1038/s41419-021-04486-x

75. Wu X, Wang Z, Shi J, Yu X, Li C, Liu J, et al. Macrophage polarization toward M1 phenotype through NF-κB signaling in patients with behçet's disease. *Arthritis Res Ther* (2022) 24(1):249. doi: 10.1186/s13075-022-02938-z

76. Canton J. Phagosome maturation in polarized macrophages. *J leukocyte Biol* (2014) 96(5):729–38. doi: 10.1189/jlb.1MR0114-021R

77. Schulz D, Severin Y, Zanotelli VRT, Bodenmiller B. In-depth characterization of monocyte-derived macrophages using a mass cytometry-based phagocytosis assay. *Sci Rep* (2019) 9(1):1925. doi: 10.1038/s41598-018-38127-9

78. Tarique AA, Logan J, Thomas E, Holt PG, Sly PD, Fantino E. Phenotypic, functional, and plasticity features of classical and alternatively activated human macrophages. *Am J Respir Cell Mol Biol* (2015) 53(5):676–88. doi: 10.1165/rcmb.2015-0012OC

79. Li G, Sherchan P, Tang Z, Tang J. Autophagy & phagocytosis in neurological disorders and their possible cross-talk. *Curr neuropharmacol* (2021) 19(11):1912–24. doi: 10.2174/1570159X19666210407150632

80. Peiser L, Mukhopadhyay S, Gordon S. Scavenger receptors in innate immunity. *Curr Opin Immunol* (2002) 14(1):123–8. doi: 10.1016/S0952-7915(01)00307-7

81. Gordon S. Phagocytosis: An immunobiologic process. *Immunity* (2016) 44 (3):463–75. doi: 10.1016/j.immuni.2016.02.026

82. Greenlee-Wacker MC. Clearance of apoptotic neutrophils and resolution of inflammation. *Immunol Rev* (2016) 273(1):357–70. doi: 10.1111/imr.12453

83. Lee JW, Nam H, Kim LE, Jeon Y, Min H, Ha S, et al. TLR4 (toll-like receptor 4) activation suppresses autophagy through inhibition of FOXO3 and impairs phagocytic capacity of microglia. *Autophagy* (2019) 15(5):753–70. doi: 10.1080/15548627.2018.1556946

84. Xu SL, Lin Y, Zhu XZ, Liu D, Tong ML, Liu LL, et al. Autophagy promotes phagocytosis and clearance of treponema pallidum *via* the NLRP3 inflammasome in macrophages. *J Eur Acad Dermatol Venereol* (2020) 34(9):2111–9. doi: 10.1111/jdv.16463

85. Heckmann BL, Boada-Romero E, Cunha LD, Magne J, Green DR. LC3-associated phagocytosis and inflammation. *J Mol Biol* (2017) 429(23):3561–76. doi: 10.1016/j.jmb.2017.08.012

86. Heckmann BL, Green DR. LC3-associated phagocytosis at a glance. *J Cell Sci* (2019) 132(5). doi: 10.1242/jcs.222984

87. Bonilla DL, Bhattacharya A, Sha Y, Xu Y, Xiang Q, Kan A, et al. Autophagy regulates phagocytosis by modulating the expression of scavenger receptors. *Immunity* (2013) 39(3):537–47. doi: 10.1016/j.immuni.2013.08.026

88. Das LM, Binko AM, Traylor ZP, Peng H, Lu KQ. Vitamin d improves sunburns by increasing autophagy in M2 macrophages. *Autophagy* (2019) 15(5):813–26. doi: 10.1080/15548627.2019.1569298

89. Liu T, Wang L, Liang P, Wang X, Liu Y, Cai J, et al. USP19 suppresses inflammation and promotes M2-like macrophage polarization by manipulating NLRP3 function *via* autophagy. *Cell Mol Immunol* (2021) 18(10):2431–42. doi: 10.1038/s41423-020-00567-7

90. Chang CP, Su YC, Lee PH, Lei HY. Targeting NFKB by autophagy to polarize hepatoma-associated macrophage differentiation. *Autophagy* (2013) 9(4):619–21. doi: 10.4161/auto.23546

91. D'Arcy MS. Cell death: A review of the major forms of apoptosis, necrosis and autophagy. *Cell Biol Int* (2019) 43(6):582–92. doi: 10.1002/cbin.11137

92. Elmore S. Apoptosis: A review of programmed cell death. *Toxicol pathol* (2007) 35(4):495–516. doi: 10.1080/01926230701320337

93. Maimon N, Zamir ZZ, Kalkar P, Zeytuni-Timor O, Schif-Zuck S, Larisch S, et al. The pro-apoptotic ARTS protein induces neutrophil apoptosis, efferocytosis, and macrophage reprogramming to promote resolution of inflammation. *Apoptosis: an Int J programmed Cell Death* (2020) 25(7-8):558–73. doi: 10.1007/s10495-020-01615-3

94. Zizzo G, Hilliard BA, Monestier M, Cohen PL. Efficient clearance of early apoptotic cells by human macrophages requires M2c polarization and MerTK induction. *J Immunol (Baltimore Md: 1950).* (2012) 189(7):3508–20. doi: 10.4049/jimmunol.1200662

95. Nadella V, Wang Z, Johnson TS, Griffin M, Devitt A. Transglutaminase 2 interacts with syndecan-4 and CD44 at the surface of human macrophages to promote removal of apoptotic cells. *Biochim Biophys Acta* (2015) 1853(1):201–12. doi: 10.1016/j.bbamcr.2014.09.020

96. Catelas I, Petit A, Zukor DJ, Marchand R, Yahia L, Huk OL. Induction of macrophage apoptosis by ceramic and polyethylene particles in vitro. *Biomaterials* (1999) 20(7):625–30. doi: 10.1016/S0142-9612(98)00214-2

97. Wang Q, Ye C, Sun S, Li R, Shi X, Wang S, et al. Curcumin attenuates collagen-induced rat arthritis *via* anti-inflammatory and apoptotic effects. *Int immunopharmacol* (2019) 72:292–300. doi: 10.1016/j.intimp.2019.04.027

98. Schumacher MA, Hedl M, Abraham C, Bernard JK, Lozano PR, Hsieh JJ, et al. ErbB4 signaling stimulates pro-inflammatory macrophage apoptosis and limits colonic inflammation. *Cell Death Dis* (2017) 8(2):e2622. doi: 10.1038/cddis.2017.42

99. Landgraeber S, Putz S, Schlattjan M, Bechmann LP, Totsch M, Grabellus F, et al. Adiponectin attenuates osteolysis in aseptic loosening of total hip replacements. *Acta biomaterialia.* (2014) 10(1):384–93. doi: 10.1016/j.actbio.2013.08.031

100. He J, Wang Y, Xu LH, Qiao J, Ouyang DY, He XH. Cucurbitacin IIa induces caspase-3-dependent apoptosis and enhances autophagy in lipopolysaccharide-stimulated RAW 264.7 macrophages. *Int Immunopharmacol* (2013) 16(1):27–34. doi: 10.1016/j.intimp.2013.03.013

101. Erbilgin A, Seldin MM, Wu X, Mehrabian M, Zhou Z, Qi H, et al. Transcription factor Zhx2 deficiency reduces atherosclerosis and promotes macrophage apoptosis in mice. *Arteriosclerosis thrombosis Vasc Biol* (2018) 38 (9):2016–27. doi: 10.1161/ATVBAHA.118.311266

102. Pagie S, Gérard N, Charreau B. Notch signaling triggered *via* the ligand DLL4 impedes M2 macrophage differentiation and promotes their apoptosis. *Cell communication Signaling* (2018) 16(1):4. doi: 10.1186/s12964-017-0214-x

103. Frank D, Vince JE. Pyroptosis versus necroptosis: Similarities, differences, and crosstalk. *Cell Death differentiation.* (2019) 26(1):99–114. doi: 10.1038/s41418-018-0212-6

104. Shi J, Gao W, Shao F. Pyroptosis: Gasdermin-mediated programmed necrotic cell death. *Trends Biochem Sci* (2017) 42(4):245–54. doi: 10.1016/j.tibs.2016.10.004

105. Xia W, Lu Z, Chen W, Zhou J, Zhao Y. Excess fatty acids induce pancreatic acinar cell pyroptosis through macrophage M1 polarization. *BMC Gastroenterol.* (2022) 22(1):72. doi: 10.1186/s12876-022-02146-8

106. Jiao Y, Zhang T, Zhang C, Ji H, Tong X, Xia R, et al. Exosomal miR-30d-5p of neutrophils induces M1 macrophage polarization and primes macrophage pyroptosis in sepsis-related acute lung injury. *Crit Care (London England).* (2021) 25(1):356. doi: 10.1186/s13054-021-03775-3

107. Li N, Chen J, Geng C, Wang X, Wang Y, Sun N, et al. Myoglobin promotes macrophage polarization to M1 type and pyroptosis *via* the RIG-I/Caspase1/GSDMD signaling pathway in CS-AKI. *Cell Death discovery.* (2022) 8(1):90. doi: 10.1038/s41420-022-00894-w

108. Shu B, Zhou YX, Li H, Zhang RZ, He C, Yang X. The METTL3/MALAT1/PTBP1/USP8/TAK1 axis promotes pyroptosis and M1 polarization of macrophages and contributes to liver fibrosis. *Cell Death discovery.* (2021) 7(1):368. doi: 10.1038/s41420-021-00756-x

109. Chen L, Yu C, Xu W, Xiong Y, Cheng P, Lin Z, et al. Dual-targeted nanodiscs revealing the cross-talk between osteogenic differentiation of mesenchymal stem cells and macrophages. *ACS nano* (2023) 17(3):3153–67. doi: 10.1021/acsnano.2c12440

110. Wu YL, Zhang CH, Teng Y, Pan Y, Liu NC, Liu PX, et al. Propionate and butyrate attenuate macrophage pyroptosis and osteoclastogenesis induced by CoCrMo alloy particles. *Military Med Res* (2022) 9(1):46. doi: 10.1186/s40779-022-00404-0

111. Boyle WJ, Simonet WS, Lacey DL. Osteoclast differentiation and activation. *Nature* (2003) 423(6937):337–42. doi: 10.1038/nature01658

112. Amarasekara DS, Kim S, Rho J. Regulation of osteoblast differentiation by cytokine networks. *Int J Mol Sci* (2021) 22(6). doi: 10.3390/ijms22062851

113. Teitelbaum SL, Ross FP. Genetic regulation of osteoclast development and function. *Nat Rev Genet* (2003) 4(8):638–49. doi: 10.1038/nrg1122

114. Park JH, Lee NK, Lee SY. Current understanding of RANK signaling in osteoclast differentiation and maturation. *Molecules Cells* (2017) 40(10):706–13. doi: 10.14348/molcells.2017.0225

115. Cui Z, Feng C, Chen J, Wang Y, Meng Q, Zhao S, et al. Network pharmacology deciphers the action of bioactive polypeptide in attenuating inflammatory osteolysis *via* the suppression of oxidative stress and restoration of bone remodeling balance. *Oxid Med Cell longevity.* (2022) 2022:4913534. doi: 10.1155/2022/4913534

116. Veis DJ, O'Brien CA. Osteoclasts, master sculptors of bone. *Annu Rev Pathol* (2022) 24(18):257–81. doi: 10.1146/annurev-pathmechdis-031521-040919

117. Davis MJ, Tsang TM, Qiu Y, Dayrit JK, Freij JB, Huffnagle GB, et al. Macrophage M1/M2 polarization dynamically adapts to changes in cytokine microenvironments in cryptococcus neoformans infection. *mBio* (2013) 4(3):e00264–13. doi: 10.1128/mBio.00264-13

118. Cai Y, Wen J, Ma S, Mai Z, Zhan Q, Wang Y, et al. Huang-Lian-Jie-Du decoction attenuates atherosclerosis and increases plaque stability in high-fat diet-induced ApoE(-/-)

mice by inhibiting M1 macrophage polarization and promoting M2 macrophage polarization. *Front Physiol* (2021) 12:666449. doi: 10.3389/fphys.2021.666449

119. Xue J, Schmidt SV, Sander J, Draffehn A, Krebs W, Quester I, et al. Transcriptome-based network analysis reveals a spectrum model of human macrophage activation. *Immunity* (2014) 40(2):274–88. doi: 10.1016/j.immuni.2014.01.006

120. Murray PJ, Allen JE, Biswas SK, Fisher EA, Gilroy DW, Goerdt S, et al. Macrophage activation and polarization: Nomenclature and experimental guidelines. *Immunity* (2014) 41(1):14–20. doi: 10.1016/j.immuni.2014.06.008

121. Wang C, Yu X, Cao Q, Wang Y, Zheng G, Tan TK, et al. Characterization of murine macrophages from bone marrow, spleen and peritoneum. *BMC Immunol* (2013) 14:6. doi: 10.1186/1471-2172-14-6

122. Porta C, Riboldi E, Ippolito A, Sica A. Molecular and epigenetic basis of macrophage polarized activation. *Semin Immunol* (2015) 27(4):237–48. doi: 10.1016/j.smim.2015.10.003

123. Wang N, Liang H, Zen K. Molecular mechanisms that influence the macrophage m1-m2 polarization balance. *Front Immunol* (2014) 5:614. doi: 10.3389/fimmu.2014.00614

124. Wang J, Li R, Peng Z, Hu B, Rao X, Li J. HMGB1 participates in LPS–induced acute lung injury by activating the AIM2 inflammasome in macrophages and inducing polarization of M1 macrophages *via* TLR2, TLR4, and RAGE/NF–κB signaling pathways. *Int J Mol Med* (2020) 45(1):61–80. doi: 10.3892/ijmm.2019.4402

125. Kandahari AM, Yang X, Laroche KA, Dighe AS, Pan D, Cui Q. A review of UHMWPE wear-induced osteolysis: The role for early detection of the immune response. *Bone Res* (2016) 4:16014. doi: 10.1038/boneres.2016.14

126. Cheng X, Jansson V, Kretzer JP, Bader R, Utzschneider S, Paulus AC. The expression levels of toll-like receptors after metallic particle and ion exposition in the synovium of a murine model. *J Clin Med* (2021) 10(16). doi: 10.3390/jcm10163489

127. Zhang C, Li C, Li S, Qin L, Luo M, Fu G, et al. Small heterodimer partner negatively regulates TLR4 signaling pathway of titanium particles-induced osteolysis in mice. *J Biomed nanotechnol* (2018) 14(3):609–18. doi: 10.1166/jbn.2018.2533

128. Vargas-Hernández O, Ventura-Gallegos JL, Ventura-Ayala ML, Torres M, Zentella A, Pedraza-Sánchez S. THP-1 cells increase TNF-α production upon LPS + soluble human IgG co-stimulation supporting evidence for TLR4 and fcγ receptors crosstalk. *Cell Immunol* (2020) 355:104146. doi: 10.1016/j.cellimm.2020.104146

129. Yuan J, Lin F, Chen L, Chen W, Pan X, Bai Y, et al. Lipoxin A4 regulates M1/M2 macrophage polarization *via* FPR2-IRF pathway. *Inflammopharmacology* (2022) 30(2):487–98. doi: 10.1007/s10787-022-00942-y

130. Yamada C, Beron-Pelusso C, Algazzaz N, Heidari A, Luz D, Rawas-Qalaji M, et al. Age-dependent effect between MARCO and TLR4 on PMMA particle phagocytosis by macrophages. *J Cell Mol Med* (2019) 23(8):5827–31. doi: 10.1111/jcmm.14494

131. Roh JS, Sohn DH. Damage-associated molecular patterns in inflammatory diseases. *Immune network.* (2018) 18(4):e27. doi: 10.4110/in.2018.18.e27

132. Galli G, Vacher P, Ryffel B, Blanco P, Legembre P. Fas/CD95 signaling pathway in damage-associated molecular pattern (DAMP)-sensing receptors. *Cells* (2022) 11(9). doi: 10.3390/cells11091438

133. Zindel J, Kubes P. DAMPs, PAMPs, and LAMPs in immunity and sterile inflammation. *Annu Rev pathol* (2020) 15:493–518. doi: 10.1146/annurev-pathmechdis-012419-032847

134. Samelko L, Landgraeber S, McAllister K, Jacobs J, Hallab NJ. Cobalt alloy implant debris induces inflammation and bone loss primarily through danger signaling, not TLR4 activation: Implications for DAMP-ening implant related inflammation. *PloS One* (2016) 11(7):e0160141. doi: 10.1371/journal.pone.0160141

135. Scaffidi P, Misteli T, Bianchi ME. Release of chromatin protein HMGB1 by necrotic cells triggers inflammation. *Nature* (2002) 418(6894):191–5. doi: 10.1038/nature00858

136. Yanai H, Ban T, Wang Z, Choi MK, Kawamura T, Negishi H, et al. HMGB proteins function as universal sentinels for nucleic-acid-mediated innate immune responses. *Nature* (2009) 462(7269):99–103. doi: 10.1038/nature08512

137. Tian S, Zhang L, Tang J, Guo X, Dong K, Chen SY. HMGB1 exacerbates renal tubulointerstitial fibrosis through facilitating M1 macrophage phenotype at the early stage of obstructive injury. *Am J Physiol Renal Physiol* (2015) 308(1):F69–75. doi: 10.1152/ajprenal.00484.2014

138. Jiang Y, Chen R, Shao X, Ji X, Lu H, Zhou S, et al. HMGB1 silencing in macrophages prevented their functional skewing and ameliorated EAM development: Nuclear HMGB1 may be a checkpoint molecule of macrophage reprogramming. *Int immunopharmacol* (2018) 56:277–84. doi: 10.1016/j.intimp.2018.01.013

139. Shiau DJ, Kuo WT, Davuluri GVN, Shieh CC, Tsai PJ, Chen CC, et al. Hepatocellular carcinoma-derived high mobility group box 1 triggers M2 macrophage polarization *via* a TLR2/NOX2/autophagy axis. *Sci Rep* (2020) 10(1):13582. doi: 10.1038/s41598-020-70137-4

140. Yang X, Zhang B, Yu P, Liu M, Zhang C, Su E, et al. HMGB1 in macrophage nucleus protects against pressure overload induced cardiac remodeling *via* regulation of macrophage differentiation and inflammatory response. *Biochem Biophys Res Commun* (2022) 611:91–8. doi: 10.1016/j.bbrc.2022.04.053

141. Qu H, Heinbäck R, Salo H, Ewing E, Espinosa A, Aulin C, et al. Transcriptomic profiling reveals that HMGB1 induces macrophage polarization different from classical M1. *Biomolecules* (2022) 12(6). doi: 10.3390/biom12060779

142. Fagone P, Di Rosa M, Palumbo M, De Gregorio C, Nicoletti F, Malaguarnera L. Modulation of heat shock proteins during macrophage differentiation. *Inflammation research: Off J Eur Histamine Res Soc [et al].* (2012) 61(10):1131–9. doi: 10.1007/s00011-012-0506-y

143. Geng T, Sun S, Chen X, Wang B, Guo H, Zhang S, et al. Strontium ranelate reduces the progression of titanium particle-induced osteolysis by increasing the ratio of osteoprotegerin to receptor activator of nuclear factor-κB ligand in vivo. *Mol Med Rep* (2018) 17(3):3829–36. doi: 10.3892/mmr.2017.8292

144. Hu S, Xue Y, He J, Chen C, Sun J, Jin Y, et al. Irisin recouples osteogenesis and osteoclastogenesis to protect wear-particle-induced osteolysis by suppressing oxidative stress and RANKL production. *Biomaterials science.* (2021) 9(17):5791–801. doi: 10.1039/D1BM00563D

145. Liao L, Lin Y, Liu Q, Zhang Z, Hong Y, Ni J, et al. Cepharanthine ameliorates titanium particle-induced osteolysis by inhibiting osteoclastogenesis and modulating OPG/RANKL ratio in a murine model. *Biochem Biophys Res Commun* (2019) 517(3):407–12. doi: 10.1016/j.bbrc.2019.07.115

146. Wang Q, Ge G, Liang X, Bai J, Wang W, Zhang W, et al. Punicalagin ameliorates wear-particle-induced inflammatory bone destruction by bi-directional regulation of osteoblastic formation and osteoclastic resorption. *Biomaterials science.* (2020) 8(18):5157–71. doi: 10.1039/D0BM00718H

147. Souza PP, Lerner UH. The role of cytokines in inflammatory bone loss. *Immunol investigations.* (2013) 42(7):555–622. doi: 10.3109/08820139.2013.822766

148. Luo G, Li F, Li X, Wang ZG, Zhang B. TNF–α and RANKL promote osteoclastogenesis by upregulating RANK *via* the NF–κB pathway. *Mol Med Rep* (2018) 17(5):6605–11. doi: 10.3892/mmr.2018.8698

149. AlQranei MS, Senbanjo LT, Aljohani H, Hamza T, Chellaiah MA. Lipopolysaccharide- TLR-4 axis regulates osteoclastogenesis independent of RANKL/RANK signaling. *BMC Immunol* (2021) 22(1):23. doi: 10.1186/s12865-021-00409-9

150. Wang L, Wang Q, Wang W, Ge G, Xu N, Zheng D, et al. Harmine alleviates titanium particle-induced inflammatory bone destruction by immunomodulatory effect on the macrophage polarization and subsequent osteogenic differentiation. *Front Immunol* (2021) 12:657687. doi: 10.3389/fimmu.2021.657687

151. Zhu K, Yang C, Dai H, Li J, Liu W, Luo Y, et al. Crocin inhibits titanium particle-induced inflammation and promotes osteogenesis by regulating macrophage polarization. *Int immunopharmacol* (2019) 76:105865. doi: 10.1016/j.intimp.2019.105865

152. Lin T, Kohno Y, Huang JF, Romero-Lopez M, Pajarinen J, Maruyama M, et al. NFκB sensing IL-4 secreting mesenchymal stem cells mitigate the proinflammatory response of macrophages exposed to polyethylene wear particles. *J BioMed Mater Res A.* (2018) 106(10):2744–52. doi: 10.1002/jbm.a.36504

153. Mantovani A, Sica A, Sozzani S, Allavena P, Vecchi A, Locati M. The chemokine system in diverse forms of macrophage activation and polarization. *Trends Immunol* (2004) 25(12):677–86. doi: 10.1016/j.it.2004.09.015

154. Huang X, Li Y, Fu M, Xin HB. Polarizing macrophages in vitro. *Methods Mol Biol (Clifton NJ)* (2018) 1784:119–26. doi: 10.1007/978-1-4939-7837-3_12

155. Das A, Sinha M, Datta S, Abas M, Chaffee S, Sen CK, et al. Monocyte and macrophage plasticity in tissue repair and regeneration. *Am J pathol* (2015) 185(10):2596–606. doi: 10.1016/j.ajpath.2015.06.001

156. Lin CW, Chen CC, Huang WY, Chen YY, Chen ST, Chou HW, et al. Restoring Prohealing/Remodeling-Associated M2a/c Macrophages Using ON101 Accelerates Diabetic Wound Healing. *JID Innov* (2020) 2(5):100138. doi: 10.1016/j.xjidi.2022.100138

157. Yue Y, Yang X, Feng K, Wang L, Hou J, Mei B, et al. M2b macrophages reduce early reperfusion injury after myocardial ischemia in mice: A predominant role of inhibiting apoptosis *via* A20. *Int J Cardiol* (2017) 245:228–35. doi: 10.1016/j.ijcard.2017.07.085

158. Quero L, Hanser E, Manigold T, Tiaden AN, Kyburz D. TLR2 stimulation impairs anti-inflammatory activity of M2-like macrophages, generating a chimeric M1/M2 phenotype. *Arthritis Res Ther* (2017) 19(1):245. doi: 10.1186/s13075-017-1447-1

159. Abdollahi E, Keyhanfar F, Delbandi AA, Falak R, Hajimiresmaiel SJ, Shafiei M. Dapagliflozin exerts anti-inflammatory effects *via* inhibition of LPS-induced TLR-4 overexpression and NF-κB activation in human endothelial cells and differentiated macrophages. *Eur J Pharmacol* (2022) 918:174715. doi: 10.1016/j.ejphar.2021.174715

160. Kobayashi K, Hernandez LD, Galán JE, Janeway CAJr., Medzhitov R, Flavell RA. IRAK-m is a negative regulator of toll-like receptor signaling. *Cell* (2002) 110(2):191–202. doi: 10.1016/S0092-8674(02)00827-9

161. Shen P, Li Q, Ma J, Tian M, Hong F, Zhai X, et al. IRAK-m alters the polarity of macrophages to facilitate the survival of mycobacterium tuberculosis. *BMC Microbiol* (2017) 17(1):185. doi: 10.1186/s12866-017-1095-2

162. Zhang Y, Yu S, Xiao J, Hou C, Li Z, Zhang Z, et al. Wear Particles promote endotoxin tolerance in macrophages by inducing interleukin-1 receptor-associated kinase-m expression. *J BioMed Mater Res A.* (2013) 101(3):733–9. doi: 10.1002/jbm.a.34375

163. Saraiva M, Vieira P, O'Garra A. Biology and therapeutic potential of interleukin-10. *J Exp Med* (2020) 217(1). doi: 10.1084/jem.20190418

164. Jiang J, Jia T, Gong W, Ning B, Wooley PH, Yang SY. Macrophage polarization in IL-10 treatment of particle-induced inflammation and osteolysis. *Am J pathol* (2016) 186(1):57–66. doi: 10.1016/j.ajpath.2015.09.006

165. Goodman S, Trindade M, Ma T, Lee M, Wang N, Ikenou T, et al. Modulation of bone ingrowth and tissue differentiation by local infusion of interleukin-10 in the presence of ultra-high molecular weight polyethylene (UHMWPE) wear particles. *J BioMed Mater Res A.* (2003) 65(1):43–50. doi: 10.1002/jbm.a.10279

166. Antonios JK, Yao Z, Li C, Rao AJ, Goodman SB. Macrophage polarization in response to wear particles in vitro. *Cell Mol Immunol* (2013) 10(6):471–82. doi: 10.1038/cmi.2013.39

167. Gong L, Zhao Y, Zhang Y, Ruan Z. The macrophage polarization regulates MSC osteoblast differentiation in vitro. *Ann Clin Lab Sci* (2016) 46(1):65–71.

168. Zhang Y, Böse T, Unger RE, Jansen JA, Kirkpatrick CJ, van den Beucken J. Macrophage type modulates osteogenic differentiation of adipose tissue MSCs. *Cell Tissue Res* (2017) 369(2):273–86. doi: 10.1007/s00441-017-2598-8

169. Philipp D, Suhr L, Wahlers T, Choi YH, Paunel-Görgülü A. Preconditioning of bone marrow-derived mesenchymal stem cells highly strengthens their potential to promote IL-6-dependent M2b polarization. *Stem Cell Res Ther* (2018) 9(1):286. doi: 10.1186/s13287-018-1039-2

170. MacKenzie KF, Clark K, Naqvi S, McGuire VA, Nöehren G, Kristariyanto Y, et al. PGE(2) induces macrophage IL-10 production and a regulatory-like phenotype *via* a protein kinase a-SIK-CRTC3 pathway. *J Immunol (Baltimore Md: 1950).* (2013) 190(2):565–77. doi: 10.4049/jimmunol.1202462

171. Holthaus M, Santhakumar N, Wahlers T, Paunel-Görgülü A. The secretome of preconditioned mesenchymal stem cells drives polarization and reprogramming of M2a macrophages toward an IL-10-Producing phenotype. *Int J Mol Sci* (2022) 23(8). doi: 10.3390/ijms23084104

172. Rőszer T. Understanding the mysterious M2 macrophage through activation markers and effector mechanisms. *Mediators inflammation.* (2015) 2015:816460. doi: 10.1155/2015/816460

173. Liu Y, Wang X, Pang J, Zhang H, Luo J, Qian X, et al. Attenuation of atherosclerosis by protocatechuic acid *via* inhibition of M1 and promotion of M2 macrophage polarization. *J Agric Food Chem* (2019) 67(3):807–18. doi: 10.1021/acs.jafc.8b05719

174. Li Z, Zhu X, Xu R, Wang Y, Hu R, Xu W. Deacylcynaropicrin inhibits RANKL-induced osteoclastogenesis by inhibiting NF-κB and MAPK and promoting M2 polarization of macrophages. *Front Pharmacol* (2019) 10:599. doi: 10.3389/fphar.2019.00599

175. Qing L, Fu J, Wu P, Zhou Z, Yu F, Tang J. Metformin induces the M2 macrophage polarization to accelerate the wound healing *via* regulating AMPK/mTOR/NLRP3 inflammasome singling pathway. *Am J Trans Res* (2019) 11(2):655–68.

176. Li Y, Zhang Z, Xu K, Du S, Gu X, Cao R, et al. Minocycline alleviates peripheral nerve adhesion by promoting regulatory macrophage polarization *via* the TAK1 and its downstream pathway. *Life Sci* (2021) 276:119422. doi: 10.1016/j.lfs.2021.119422

177. Yu B, Bai J, Shi J, Shen J, Guo X, Liu Y, et al. MiR-106b inhibition suppresses inflammatory bone destruction of wear debris-induced periprosthetic osteolysis in rats. *J Cell Mol Med* (2020) 24(13):7490–503. doi: 10.1111/jcmm.15376

178. Lin Y, Zhao JL, Zheng QJ, Jiang X, Tian J, Liang SQ, et al. Notch signaling modulates macrophage polarization and phagocytosis through direct suppression of signal regulatory protein α expression. *Front Immunol* (2018) 9:1744. doi: 10.3389/fimmu.2018.01744

179. Chen J, Cui Z, Wang Y, Lyu L, Feng C, Feng D, et al. Cyclic polypeptide D7 protects bone marrow mesenchymal cells and promotes chondrogenesis during osteonecrosis of the femoral head *via* growth differentiation factor 15-mediated redox signaling. *Oxid Med Cell longevity.* (2022) 2022:3182368. doi: 10.1155/2022/3182368

180. Miki S, Suzuki JI, Takashima M, Ishida M, Kokubo H, Yoshizumi M. S-1-Propenylcysteine promotes IL-10-induced M2c macrophage polarization through prolonged activation of IL-10R/STAT3 signaling. *Sci Rep* (2021) 11(1):22469. doi: 10.1038/s41598-021-01866-3

181. Mia S, Warnecke A, Zhang XM, Malmström V, Harris RA. An optimized protocol for human M2 macrophages using m-CSF and IL-4/IL-10/TGF-β yields a dominant immunosuppressive phenotype. *Scand J Immunol* (2014) 79(5):305–14. doi: 10.1111/sji.12162

182. Martinon F, Mayor A, Tschopp J. The inflammasomes: Guardians of the body. *Annu Rev Immunol* (2009) 27:229–65. doi: 10.1146/annurev.immunol.021908.132715

183. Gay NJ, Gangloff M, O'Neill LA. What the myddosome structure tells us about the initiation of innate immunity. *Trends Immunol* (2011) 32(3):104–9. doi: 10.1016/j.it.2010.12.005

184. Li H, Yoon JH, Won HJ, Ji HS, Yuk HJ, Park KH, et al. Isotrifoliol inhibits pro-inflammatory mediators by suppression of TLR/NF-κB and TLR/MAPK signaling in LPS-induced RAW264.7 cells. *Int Immunopharmacol* (2017) 45:110–9. doi: 10.1016/j.intimp.2017.01.033

185. Jayakumar T, Yang CM, Yen TL, Hsu CY, Sheu JR, Hsia CW, et al. Anti-inflammatory mechanism of an alkaloid rutaecarpine in LTA-stimulated RAW 264.7 cells: Pivotal role on NF-κB and ERK/p38 signaling molecules. *Int J Mol Sci* (2022) 23(11). doi: 10.3390/ijms23115889

186. Zhen Y, Zhang H. NLRP3 inflammasome and inflammatory bowel disease. *Front Immunol* (2019) 10:276. doi: 10.3389/fimmu.2019.00276

187. Muñoz-Planillo R, Kuffa P, Martínez-Colón G, Smith BL, Rajendiran TM, Núñez G. K^+ efflux is the common trigger of NLRP3 inflammasome activation by bacterial toxins and particulate matter. *Immunity* (2013) 38(6):1142–53. doi: 10.1016/j.immuni.2013.05.016

188. Orlowski GM, Colbert JD, Sharma S, Bogyo M, Robertson SA, Rock KL. Multiple cathepsins promote pro-IL-1β synthesis and NLRP3-mediated IL-1β activation. *J Immunol (Baltimore Md 1950).* (2015) 195(4):1685–97. doi: 10.4049/jimmunol.1500509

189. Kelley N, Jeltema D, Duan Y, He Y. The NLRP3 inflammasome: An overview of mechanisms of activation and regulation. *Int J Mol Sci* (2019) 20(13). doi: 10.3390/ijms20133328

190. Zhang BC, Li Z, Xu W, Xiang CH, Ma YF. Luteolin alleviates NLRP3 inflammasome activation and directs macrophage polarization in lipopolysaccharide-stimulated RAW264.7 cells. *Am J Trans Res* (2018) 10(1):265–73.

191. Zhang J, Liu X, Wan C, Liu Y, Wang Y, Meng C, et al. NLRP3 inflammasome mediates M1 macrophage polarization and IL-1β production in inflammatory root resorption. *J Clin periodontol* (2020) 47(4):451–60. doi: 10.1111/jcpe.13258

192. Ito M, Shichita T, Okada M, Komine R, Noguchi Y, Yoshimura A, et al. Bruton's tyrosine kinase is essential for NLRP3 inflammasome activation and contributes to ischaemic brain injury. *Nat Commun* (2015) 6:7360. doi: 10.1038/ncomms8360

193. Lin S, Wen Z, Li S, Chen Z, Li C, Ouyang Z, et al. LncRNA Neat1 promotes the macrophage inflammatory response and acts as a therapeutic target in titanium particle-induced osteolysis. *Acta biomaterialia.* (2022) 142:345–60. doi: 10.1016/j.actbio.2022.02.007

194. Gao XR, Ge J, Li WY, Zhou WC, Xu L, Geng DQ. miR-34a carried by adipocyte exosomes inhibits the polarization of M1 macrophages in mouse osteolysis model. *J BioMed Mater Res A.* (2021) 109(6):994–1003. doi: 10.1002/jbm.a.37088

195. Mócsai A, Ruland J, Tybulewicz VL. The SYK tyrosine kinase: a crucial player in diverse biological functions. *Nat Rev Immunol* (2010) 10(6):387–402. doi: 10.1038/nri2765

196. Ma P, Yue L, Yang H, Fan Y, Bai J, Li S, et al. Chondroprotective and anti-inflammatory effects of amurensin h by regulating TLR4/Syk/NF-κB signals. *J Cell Mol Med* (2020) 24(2):1958–68. doi: 10.1111/jcmm.14893

197. Slomiany BL, Slomiany A. Helicobacter pylori LPS-induced gastric mucosal spleen tyrosine kinase (Syk) recruitment to TLR4 and activation occurs with the involvement of protein kinase cδ. *Inflammopharmacology* (2018) 26(3):805–15. doi: 10.1007/s10787-017-0430-4

198. Liu L, Lucas RM, Nanson JD, Li Y, Whitfield J, Curson JEB, et al. The transmembrane adapter SCIMP recruits tyrosine kinase syk to phosphorylate toll-like receptors to mediate selective inflammatory outputs. *J Biol Chem* (2022) 298(5):101857. doi: 10.1016/j.jbc.2022.101857

199. Chaudhary A, Fresquez TM, Naranjo MJ. Tyrosine kinase syk associates with toll-like receptor 4 and regulates signaling in human monocytic cells. *Immunol Cell Biol* (2007) 85(3):249–56. doi: 10.1038/sj.icb7100030

200. Li J, Chen YH, Li LZ, Wang F, Song W, Alolga RN, et al. Omics and transgenic analyses reveal that salvianolic acid b exhibits its anti-inflammatory effects through inhibiting the mincle-Syk-Related pathway in macrophages. *J Proteome Res* (2021) 20(7):3734–48. doi: 10.1021/acs.jproteome.1c00325

201. Malik AF, Hoque R, Ouyang X, Ghani A, Hong E, Khan K, et al. Inflammasome components asc and caspase-1 mediate biomaterial-induced inflammation and foreign body response. *Proc Natl Acad Sci United States America.* (2011) 108(50):20095–100. doi: 10.1073/pnas.1105152108

202. Gross O, Poeck H, Bscheider M, Dostert C, Hannesschläger N, Endres S, et al. Syk kinase signalling couples to the Nlrp3 inflammasome for anti-fungal host defence. *Nature* (2009) 459(7245):433–6. doi: 10.1038/nature07965

203. Maehara T, Fujimori K. Contribution of FP receptors in M1 macrophage polarization *via* IL-10-regulated nuclear translocation of NF-κB p65. *Biochim Biophys Acta Mol Cell Biol lipids.* (2020) 1865(5):158654. doi: 10.1016/j.bbalip.2020.158654

204. Glushkova OV, Parfenyuk SB, Khrenov MO, Novoselova TV, Lunin SM, Fesenko EE, et al. Inhibitors of TLR-4, NF-κB, and SAPK/JNK signaling reduce the toxic effect of lipopolysaccharide on RAW 264.7 cells. *J immunotoxicol* (2013) 10(2):133–40. doi: 10.3109/1547691X.2012.700652

205. Guangtao F, Zhenkang W, Zhantao D, Mengyuan L, Qingtian L, Yuanchen M, et al. Icariin alleviates Wear particle-induced periprosthetic osteolysis *via* down-regulation of the estrogen receptor α-mediated NF-κB signaling pathway in macrophages. *Front Pharmacol* (2021) 12:746391. doi: 10.3389/fphar.2021.746391

206. Liu Y, Song FM, Ma ST, Moro A, Feng WY, Liao SJ, et al. Vaccarin prevents titanium particle-induced osteolysis and inhibits RANKL-induced osteoclastogenesis by blocking NF-κB and MAPK signaling pathways. *J Cell Physiol* (2019) 234(8):13832–42. doi: 10.1002/jcp.28063

207. Zhang W, Jiang G, Zhou X, Huang L, Meng J, He B, et al. α-mangostin inhibits LPS-induced bone resorption by restricting osteoclastogenesis *via* NF-κB and MAPK signaling. *Chin Med* (2022) 17(1):34. doi: 10.1186/s13020-021-00555-7

208. An S, Han F, Hu Y, Liu Y, Li J, Wang L. Curcumin inhibits polyethylene-induced osteolysis *via* repressing NF-κB signaling pathway activation. *Cell Physiol Biochem Int J Exp Cell physiol biochem Pharmacol* (2018) 50(3):1100–12. doi: 10.1159/000494537

209. Li X, Lu Y, Li J, Zhou S, Wang Y, Li L, et al. Photoluminescent carbon dots (PCDs) from sour apple: A biocompatible nanomaterial for preventing UHMWPE

wear-particle induced osteolysis *via* modulating Chemerin/ChemR23 and SIRT1 signaling pathway and its bioimaging application. *J nanobiotechnol* (2022) 20(1):301. doi: 10.1186/s12951-022-01498-3

210. Lee K, Seo I, Choi MH, Jeong D. Roles of mitogen-activated protein kinases in osteoclast biology. *Int J Mol Sci* (2018) 19(10). doi: 10.3390/ijms19103004

211. Kyriakis JM, Avruch J. Mammalian mitogen-activated protein kinase signal transduction pathways activated by stress and inflammation. *Physiol Rev* (2001) 81 (2):807–69. doi: 10.1152/physrev.2001.81.2.807

212. Liu L, Guo H, Song A, Huang J, Zhang Y, Jin S, et al. Progranulin inhibits LPS-induced macrophage M1 polarization *via* NF-κB and MAPK pathways. *BMC Immunol* (2020) 21(1):32. doi: 10.1186/s12865-020-00355-y

213. Zhou F, Mei J, Han X, Li H, Yang S, Wang M, et al. Kinsenoside attenuates osteoarthritis by repolarizing macrophages through inactivating NF-κB/MAPK signaling and protecting chondrocytes. *Acta Pharm Sin B* (2019) 9(5):973–85. doi: 10.1016/j.apsb.2019.01.015

214. Lu J, Zhang H, Pan J, Hu Z, Liu L, Liu Y, et al. Fargesin ameliorates osteoarthritis *via* macrophage reprogramming by downregulating MAPK and NF-κB pathways. *Arthritis Res Ther* (2021) 23(1):142. doi: 10.1186/s13075-021-02512-z

215. Lu YC, Yeh WC, Ohashi PS. LPS/TLR4 signal transduction pathway. *Cytokine* (2008) 42(2):145–51. doi: 10.1016/j.cyto.2008.01.006

216. Fan Y, Mao R, Yang J. NF-κB and STAT3 signaling pathways collaboratively link inflammation to cancer. *Protein Cell* (2013) 4(3):176–85. doi: 10.1007/s13238-013-2084-3

217. Hu X, Li J, Fu M, Zhao X, Wang W. The JAK/STAT signaling pathway: from bench to clinic. *Signal transduction targeted Ther* (2021) 6(1):402. doi: 10.1038/s41392-021-00791-1

218. Huangfu N, Zheng W, Xu Z, Wang S, Wang Y, Cheng J, et al. RBM4 regulates M1 macrophages polarization through targeting STAT1-mediated glycolysis. *Int immunopharmacol* (2020) 83:106432. doi: 10.1016/j.intimp.2020.106432

219. Iwata H, Goettsch C, Sharma A, Ricchiuto P, Goh WW, Halu A, et al. PARP9 and PARP14 cross-regulate macrophage activation *via* STAT1 ADP-ribosylation. *Nat Commun* (2016) 7:12849. doi: 10.1038/ncomms12849

220. Ding N, Wang Y, Dou C, Liu F, Guan G, Wei K, et al. Physalin d regulates macrophage M1/M2 polarization *via* the STAT1/6 pathway. *J Cell Physiol* (2019) 234 (6):8788–96. doi: 10.1002/jcp.27537

221. Hu J, Li X, Chen Y, Han X, Li L, Yang Z, et al. The protective effect of WKYMVm peptide on inflammatory osteolysis through regulating NF-κB and CD9/gp130/STAT3 signalling pathway. *J Cell Mol Med* (2020) 24(2):1893–905. doi: 10.1111/jcmm.14885

222. Deng Z, Zhang R, Li M, Wang S, Fu G, Jin J, et al. STAT3/IL-6 dependent induction of inflammatory response in osteoblast and osteoclast formation in nanoscale wear particle-induced aseptic prosthesis loosening. *Biomaterials science.* (2021) 9 (4):1291–300. doi: 10.1039/D0BM01256D

223. Islam MS. Calcium signaling: From basic to bedside. *Adv Exp Med Biol* (2020) 1131:1–6. doi: 10.1007/978-3-030-12457-1_1

224. Dupont G, Combettes L, Bird GS, Putney JW. Calcium oscillations. *Cold Spring Harbor Perspect Biol* (2011) 3(3). doi: 10.1101/cshperspect.a004226

225. Li Z, Liu T, Gilmore A, Gómez NM, Fu C, Lim J, et al. Regulator of G protein signaling protein 12 (Rgs12) controls mouse osteoblast differentiation *via* calcium Channel/Oscillation and gαi-ERK signaling. *J Bone mineral research: Off J Am Soc Bone Mineral Res* (2019) 34(4):752–64. doi: 10.1002/jbmr.3645

226. Di Buduo CA, Abbonante V, Marty C, Moccia F, Rumi E, Pietra D, et al. Defective interaction of mutant calreticulin and SOCE in megakaryocytes from patients with myeloproliferative neoplasms. *Blood* (2020) 135(2):133–44. doi: 10.1182/blood.2019001103

227. Tedesco S, Scattolini V, Albiero M, Bortolozzi M, Avogaro A, Cignarella A, et al. Mitochondrial calcium uptake is instrumental to alternative macrophage polarization and phagocytic activity. *Int J Mol Sci* (2019) 20(19). doi: 10.3390/ijms20194966

228. Nascimento Da Conceicao V, Sun Y, Ramachandran K, Chauhan A, Raveendran A, Venkatesan M, et al. Resolving macrophage polarization through distinct Ca(2+) entry channel that maintains intracellular signaling and mitochondrial bioenergetics. *iScience* (2021) 24(11):103339. doi: 10.1016/j.isci.2021.103339

229. Ji SY, Lee H, Hwangbo H, Hong SH, Cha HJ, Park C, et al. A novel peptide oligomer of bacitracin induces M1 macrophage polarization by facilitating Ca(2+) influx. *Nutrients* (2020) 12(6). doi: 10.3390/nu12061603

230. Chauhan A, Sun Y, Sukumaran P, Quenum Zangbede FO, Jondle CN, Sharma A, et al. M1 macrophage polarization is dependent on TRPC1-mediated calcium entry. *iScience* (2018) 8:85–102. doi: 10.1016/j.isci.2018.09.014

231. Chen K, Man Q, Miao J, Xu W, Zheng Y, Zhou X, et al. Kir2.1 channel regulates macrophage polarization via the Ca2+/CaMK II/ERK/NF-κB signaling pathway. *J Cell Sci* (2022) 135(13). doi: 10.1242/jcs.259544

232. Lv Z, Xu X, Sun Z, Yang YX, Guo H, Li J, et al. TRPV1 alleviates osteoarthritis by inhibiting M1 macrophage polarization *via* Ca(2+)/CaMKII/Nrf2 signaling pathway. *Cell Death Dis* (2021) 12(6):504. doi: 10.1038/s41419-021-03792-8

233. Shi Y, Ye L, Shen S, Qian T, Pan Y, Jiang Y, et al. Morin attenuates osteoclast formation and function by suppressing the NF-κB, MAPK and calcium signalling pathways. *Phytother Res* (2021) 35(10):5694–707. doi: 10.1002/ptr.7229

234. Okada H, Okabe K, Tanaka S. Finely-tuned calcium oscillations in osteoclast differentiation and bone resorption. *Int J Mol Sci* (2020) 22(1). doi: 10.3390/ijms22010180

235. Kang JY, Kang N, Yang YM, Hong JH, Shin DM. The role of Ca(2+)-NFATc1 signaling and its modulation on osteoclastogenesis. *Int J Mol Sci* (2020) 21(10). doi: 10.3390/ijms21103646

236. Kim HJ, Lee J, Lee GR, Kim N, Lee HI, Kwon M, et al. Flunarizine inhibits osteoclastogenesis by regulating calcium signaling and promotes osteogenesis. *J Cell Physiol* (2021) 236(12):8239–52. doi: 10.1002/jcp.30496

237. Okada H, Kajiya H, Omata Y, Matsumoto T, Sato Y, Kobayashi T, et al. CTLA4-ig directly inhibits osteoclastogenesis by interfering with intracellular calcium oscillations in bone marrow macrophages. *J Bone mineral research: Off J Am Soc Bone Mineral Res* (2019) 34(9):1744–52. doi: 10.1002/jbmr.3754

238. Li ZQ, Li CH. CRISPR/Cas9 from bench to bedside: what clinicians need to know before application? *Military Med Res* (2020) 7(1):61. doi: 10.1186/s40779-020-00292-2

frontiers | Frontiers in Immunology

TYPE Original Research
PUBLISHED 06 April 2023
DOI 10.3389/fimmu.2023.1146693

OPEN ACCESS

EDITED BY
Ruoxi Yuan,
Hospital for Special Surgery, United States

REVIEWED BY
Wenhua Wang,
University of Oklahoma, United States
Zhuoyu Wen,
University of Texas Southwestern Medical Center, United States
Yu'e Liu,
Tongji University, China

*CORRESPONDENCE
Qi Yuan
yuanqi@mdjmu.edu.cn

SPECIALTY SECTION
This article was submitted to Inflammation, a section of the journal Frontiers in Immunology

RECEIVED 17 January 2023
ACCEPTED 30 March 2023
PUBLISHED 06 April 2023

CITATION
Hou S, Wang D, Yuan X, Yuan X and Yuan Q (2023) Identification of biomarkers co-associated with M1 macrophages, ferroptosis and cuproptosis in alcoholic hepatitis by bioinformatics and experimental verification. *Front. Immunol.* 14:1146693. doi: 10.3389/fimmu.2023.1146693

Identification of biomarkers co-associated with M1 macrophages, ferroptosis and cuproptosis in alcoholic hepatitis by bioinformatics and experimental verification

Shasha Hou[1], Dan Wang[2], Xiaxia Yuan[1], Xiaohuan Yuan[2] and Qi Yuan[2]*

[1]Department of Life Science and Engineering, Jining University, Jining, China, [2]College of Life Science, Mudanjiang Medical University, Mudanjiang, China

Backgrounds: Alcoholic hepatitis (AH) is a major health problem worldwide. There is increasing evidence that immune cells, iron metabolism and copper metabolism play important roles in the development of AH. We aimed to explore biomarkers that are co-associated with M1 macrophages, ferroptosis and cuproptosis in AH patients.

Methods: GSE28619 and GSE103580 datasets were integrated, CIBERSORT algorithm was used to analyze the infiltration of 22 types of immune cells and GSVA algorithm was used to calculate ferroptosis and cuproptosis scores. Using the "WGCNA" R package, we established a gene co-expression network and analyzed the correlation between M1 macrophages, ferroptosis and cuproptosis scores and module characteristic genes. Subsequently, candidate genes were screened by WGCNA and differential expression gene analysis. The LASSO-SVM analysis was used to identify biomarkers co-associated with M1 macrophages, ferroptosis and cuproptosis. Finally, we validated these potential biomarkers using GEO datasets (GSE155907, GSE142530 and GSE97234) and a mouse model of AH.

Results: The infiltration level of M1 macrophages was significantly increased in AH patients. Ferroptosis and cuproptosis scores were also increased in AH patients. In addition, M1 macrophages, ferroptosis and cuproptosis were positively correlated with each other. Combining bioinformatics analysis with a mouse model of AH, we found that ALDOA, COL3A1, LUM, THBS2 and TIMP1 may be potential biomarkers co-associated with M1 macrophages, ferroptosis and cuproptosis in AH patients.

Conclusion: We identified 5 potential biomarkers that are promising new targets for the treatment and diagnosis of AH patients.

KEYWORDS

alcoholic hepatitis, M1 macrophage, ferroptosis, cuproptosis, WGCNA

Introduction

Alcohol-associated liver disease (ALD) is a serious public health problem worldwide (1). Alcoholic hepatitis (AH) is one of the phenotypes of ALD, which is mainly caused by a long history of excessive alcohol consumption and a recent history of severe alcohol abuse (2). AH presents a clinical syndrome characterized by jaundice and liver injury. In the past 50 years, corticosteroids are still the main therapeutic drugs, and no effective new drugs have been successfully developed (3). Although corticosteroids increase short-term survival in AH patients, approximately 40% of patients do not respond to treatment (4, 5). In recent years, the rapid development of high-throughput sequencing technology has promoted the understanding of AH (6, 7). Therefore, it is urgently needed to identify new biomarkers in AH patients by bioinformatics analysis, which will facilitate the development of new treatment strategies.

The liver plays a major regulatory role in alcohol metabolism and immune monitoring. Hepatocytes exposed to alcohol cause damage and death due to oxidative stress, which in turn produces a variety of inflammatory factors to activate the inflammatory response and immune cells (8). Macrophages are important cells of innate immune system. The complex functional variability and adaptability of macrophages to different infection situations are based on their extensive phenotypic plasticity. naive macrophages (M0) can be polarized into classically activated macrophages (M1 macrophages) and alternately activated macrophages (M2 macrophages), which perform proinflammatory or anti-inflammatory functions, respectively (9). Previous studies have shown that damaged hepatocytes activate the NF-κB signaling pathway under alcohol metabolism, which releases a series of chemokines and inflammatory mediators, ultimately promoting macrophage M1 polarization (10, 11). In addition, Cho et al. revealed that G-CSF improved liver function by promoting macrophage M2 polarization in alcohol-fed mice (12).

Ferroptosis is a unique type of cell death regulation, which is caused by iron accumulation, excessive production of reactive oxygen species (ROS) and excessive lipid peroxidation (13). Cuproptosis is a recently discovered type of cell death caused by the direct binding of copper to the lipidized proteins of the mitochondrial tricarboxylic acid cycle (TCA) (14). Alcohol metabolism in hepatocytes affects mitochondrial function and produces a large number of ROS, leading to elevated lipid peroxidation. Thus, the progression of AH is closely related to ferroptosis and cuproptosis. As recently reported, intestinal sirtuin1 (SIRT1) deficiency protects mice from alcohol-induced inflammation by mitigating hepatic ferroptosis (15). Melatonin inhibits ferroptosis by activating Nrf2-ARE signaling pathway, thus alleviating alcohol-induced liver injury (16). Copper metabolism in the liver is still being explored. Cuproptosis regulates immune cell infiltration and is used to construct risk assessment models for hepatocellular carcinoma (HCC) (17, 18). However, the role of ferroptosis and cuproptosis in AH patients needs to be further explored.

In this study, we downloaded and integrated transcriptome data from AH patients. Potential biomarkers of AH patients were identified based on the M1 macrophages, ferroptosis and cuproptosis scores, and these biomarkers were validated using public datasets and a mouse model of AH. Finally, we identified 5 potential biomarkers: aldolase A (ALDOA), Collagen type III alpha 1 (COL3A1), lumican (LUM), thrombospondin-2 (THBS2) and tissue inhibitor of metalloproteinase-1 (TIMP1). These potential biomarkers could provide new targets for the diagnosis and treatment of AH patients.

Materials and methods

Data set download and evaluation

Gene expression data were downloaded from the Gene Expression Integrated Database (GEO)(http://www.ncbi.nlm.nih.gov/geo/) with accession numbers GSE28619 (19), GSE103580 (20), GSE155907 (21), GSE142530 (7) and GSE97234 (22), the basic information of our selected samples is shown in Supplementary Table S1. The batch effect between GSE28619 and GSE103580 was corrected using the "sva" R package (23). The intersected genes between GSE28619 and GSE103580 were obtained *via* online Venn Diagram analysis (jvenn, http://jvenn.toulouse.inra.fr/app/index.html).

Analysis of immune cells

The CIBERSORT algorithm was used to calculate the proportion of 22 types of immune cells with normalized gene expression data (24). Correlations between immune cells were evaluated using the "corrplot" R package. Based on the characteristics of immune cells, principal component analysis (PCA) was to cluster the normal liver samples and AH samples. Specifically, the "stats" R package was used for PCA analysis. Firstly, z-score was performed on the expression profile, and then prcomp function was used for dimension reduction analysis to obtain the matrix after dimension reduction.

Gene set variation analysis

The "GSVA" R package (25) was used to calculate the scores of ferroptosis gene set and cuproptosis gene set. A total of 64 ferroptosis-related genes were obtained from MigDB (Supplementary Table S2). The 16 cuproptosis-related genes were collected from previous literature (26) (Supplementary Table S3).

Weighted gene co-expression network analysis

WGCNA is an algorithm for constructing gene clustering modules based on similar gene expression patterns. We used the "WGCNA" R package (27) to construct a co-expression network of genes from normal liver samples and AH samples. The concrete

steps are as follows: First, the optimal soft-thresholding power was calculated and selected. Second, the adjacency matrix was constructed based on the selected soft-thresholding power and transformed into a topological overlap matrix. Third, hierarchical clustering tree was established to cluster high-coexpression genes into the same module. Finally, M1 macrophages, ferroptosis and cuproptosis scores were used as characteristics to calculate the correlation between module genes and traits. In this study, we screened hub genes based on threshold weight > 0.2, and Cytoscape software (version 3.9.1) was used to visualize the gene networks.

Functional enrichment analysis

To further clarify biological functions and signaling pathways of candidate genes, we used the "clusterProfiler" R package (28) for functional enrichment analysis, including gene ontology (GO) and Kyoto Encyclopedia of Genes and Genomes (KEGG) analysis. The result of functional enrichment analysis was visualized using the "GOplot" R package (29).

Analysis of differentially expressed genes

We used the "limma" R package (30) to calculate differentially expressed genes (DEGs) between normal liver samples and AH samples. DEGs were obtained by threshold standard $|\log2(FC)| > 1$, p-value < 0.05. The volcano and heatmap plots were visualized *via* the "ggplot2" and "pheatmap" R packages.

Machine learning

By intersecting DEGs and WGCNA hub genes, 27 candidate genes associated with AH patients were identified. For these 27 candidate genes, two machine-learning techniques were used to further screen potential genes in AH patients. The least absolute shrinkage and selection operator (LASSO) is an algorithm used for regularization to improve prediction accuracy and model comprehensibility, and to select variables. We utilized the LASSO algorithm to screen potential biomarkers in AH patients by "glmnet" R package (31). Support vector machines (SVM) is a powerful method whose goal is to establish a threshold between two classes that allows label prediction based on single or multiple feature vectors. We used SVM method to screen potential biomarkers in AH patients by "kernlab" R package (32). The intersection of the results between the two methods were obtained *via* online Venn Diagram analysis (jvenn, http://jvenn.toulouse.inra.fr/app/index.html). To further assess the ability of biomarkers to distinguish AH samples from normal liver samples, we performed receiver operating characteristic (ROC) analysis using the "pROC" R package (33).

A mouse model of AH

As previously mentioned, a mouse model of chronic alcohol plus single binge drinking was established (34). The alcoholic diet was purchased from TROPHIC (Nantong, China). Ten male mice aged 6-8 weeks were fed a liquid control diet for 5 days, then mice were randomly divided into two groups (ethanol-fed group and pair-fed group, n = 5 per group). The ethanol-fed group was fed a Lieber DeCarli liquid diet containing 5% ethanol for 10 days. Then mice were given a single dose of 20% ethanol (5g/kg body weight) by gavage. The pair-fed group was fed with ethanol-free, isocaloric control liquid diet for 10 days. Then mice were given a single dose of dextrin maltose (5g/kg body weight) by gavage. Euthanasia was performed 9 hours after gavage. All animal experiments were performed with the approval of the Experimental Animal Ethics Committee of Mudanjiang Medical University.

Blood biochemical assays

Blood samples of mice were centrifuged at 1000×g for 10 min to obtain serum. Serum alanine aminotransferase (ALT) and aspartate aminotransferase (AST) levels were detected by kits of Nanjing Jiancheng Bioengineering Institute (Nanjing, China).

Content analysis of malondialdehyde (MDA) and glutathione

Liver tissues were homogenized according to the instructions, and MDA and GSH levels were detected by kits of Nanjing Jiancheng Bioengineering Institute (Nanjing, China).

Histology and immunofluorescence

Paraffin or cryostat sections were prepared as described previously (35). Paraffin sections were stained with hematoxylin and eosin (H&E). For fluorescence double staining, cryostat sections were incubated with anti-iNOS antibody (Santa Cruz Biotechnology, Santa Cruz, CA, USA) and anti-F4/80 antibodies (BioLegend, San Diego, CA, USA), followed by incubation with Alexa Fluor 488- or 594-conjugated secondary antibodies (Jackson ImmunoResearch, West Grove, PA, USA). Sections were evaluated under a microscope (DP71, OLYMPUS) of both bright-field and fluorescence microscopy (200 × magnification).

Real-time quantitative PCR

Total RNA was isolated from liver tissues using TRIzol reagent (TransGen Biotech, Beijing, China), and cDNAs were synthesized

using FastKing RT Kit (TIANGEN, Beijing, China). RT-qPCR analysis was performed using SuperReal PreMix Plus (TIANGEN, Beijing, China). The primer sequences were listed in Supplementary Table S4. Data were analyzed using the $2^{-\Delta\Delta CT}$ method and normalized to β-actin (*Actb*) expression.

Western blot

Total protein from liver tissue was extracted using RIPA lysis buffer (Solarbio, Beijing, China) containing protease inhibitor cocktail (MedChemExpress, Princeton, NJ, USA). The samples were incubated at 99°C for 5 min and separated at 115 V by SDS-PAGE for 1 h. The proteins were transferred to PVDF membranes and incubated at 200 mA for 1 h. The membrane was plugged with 5% milk powder for 1 hour and incubated overnight at 4°C with the following primary antibody: anti-FDX1 (Absin, Shanghai, China), anti-GPX4, anti-ACSL4, anti-SLC31A1 and anti-β-actin (Affinity, Cincinnati, OH, USA). HRP-conjugated goat anti-rabbit IgG was used as secondary antibodies. All bands were quantified with an automated digitizing system (ImageJ).

Statistical analysis

All data were presented as mean ± SD and analyzed using GraphPad Prism (version 8.3.0) and R (version 4.2.1). Significant differences in animal experiments were determined by three independent experiments. Differences of continuous variables between two groups were compared using Student's t-test analysis. $P<0.05$ was considered statistically significant.

Results

Overview of study design

The overall design scheme of our current study is shown in Figure 1. First, we combined and normalized data of GSE28619 and GSE103580. Secondly, CIBERSORT method was used to analyze immune cells, GSVA algorithm was used to calculate scores of ferroptosis and cuproptosis, and WGCNA was used to screen hub genes related to M1 macrophages, ferroptosis and cuproptosis. Third, we analyzed DEGs using the "limma" package and intersected DEGs with hub genes. Fourth, we identified biomarkers of AH based on LASSO-SVM algorithm. Finally, we used GEO data (GSE155907, GSE142530 and GSE97234) and a mouse model of AH to validate potential biomarkers.

Normalization of dataset

Both GSE28619 and GSE103580 datasets are chip data. The GSE28619 dataset was based on the GPL570 platform (Affymetrix Human Genome U133 Plus 2.0 Array) and included 7 normal liver samples and 15 AH samples. The GSE103580 dataset was based on the GPL13667 platform (Affymetrix Human Genome U219 Array) from which 13 AH samples were selected. The two datasets were merged and batch removed. The results before and after normalization are shown in Supplementary Figure S1A. As shown in the Venn Diagram (Supplementary Figure S1B), 22,878 and 19,469 probes were identified in GSE28619 and GSE103580, respectively, and 16,510 intersected genes were selected from two datasets for subsequent bioinformatics analysis.

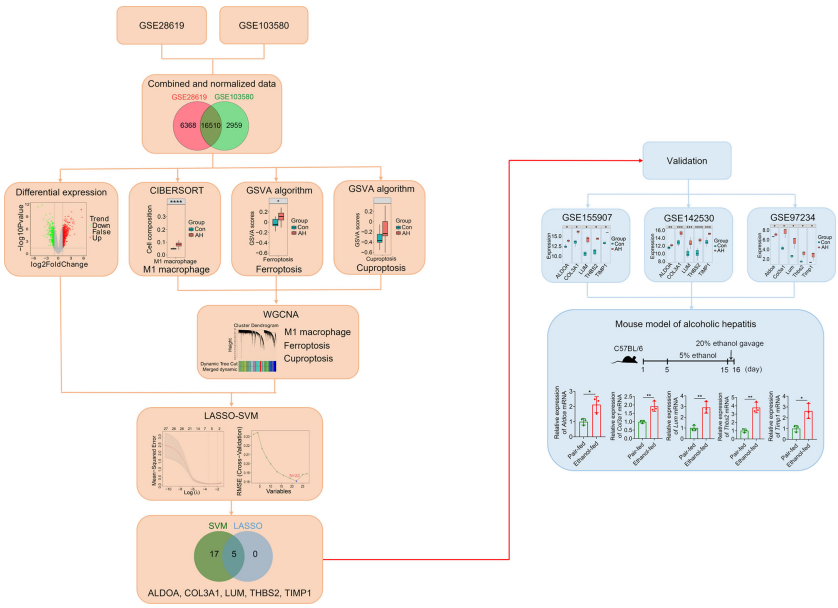

FIGURE 1
Overall schematic diagram of the study design. *p < 0.05, **p < 0.01, ***p < 0.001, ****p < 0.0001.

10.3389/fimmu.2023.1146693

Analysis of immune infiltration in normal liver and AH samples

CIBERSORT, the deconvolution algorithm reported by Newman et al., characterizes cell composition in complex tissues based on normalized gene expression profiles (24). Based on this algorithm, we calculated the infiltration of 22 types of immune cells in normal liver samples and AH samples. The bar chart shows the abundance of different immune cell subsets in each sample (Figure 2A). We further analyzed the correlation between 22 immune cell subsets. As shown in the correlation heatmap (Figure 2B), activated mast cells showed the most significant positive correlation with eosinophils (r = 0.75), while CD8 T cells showed the most significant negative correlation with CD4 memory resting T cells (r = -0.61). Next, we analyzed the difference in immune cells between normal liver samples (control group) and AH samples (AH group). Compared with control group, M0 macrophages, M1 macrophages and resting mast cells were significantly increased in AH group, while plasma cells, helper follicular T cells, gamma delta T cells, activated mast cells and eosinophils were significantly decreased in AH group (Figure 2C). PCA analysis of control group and AH group and performed based on 22 types of immune cells. As shown in Figure 2D, AH group was completely separated from control group, suggesting that activation of immune cells could be a significant feature of AH patients.

Co-expression modules of M1 macrophages, ferroptosis and cuproptosis in AH patients

We found that M1 macrophages were the most differentiated immune cells between control and AH groups (Figure 2C). At the same time, the GSVA algorithm was used to calculate scores of ferroptosis and cuproptosis. Compared with the control group, ferroptosis scores of the AH group were significantly increased. Although there was no statistical difference in GSVA scores of cuproptosis, there was a increasing trend (Figure 3A). In addition, correlation analysis showed that M1 macrophages, ferroptosis and cuproptosis were positively correlated with each other (Figure 3B). To further explore the role of genes co-associated with M1 macrophages, ferroptosis and cuproptosis in AH patients, we used CIBERSORT's M1 macrophage results, ferroptosis and cuproptosis scores as characteristic data for WGCNA analysis. The power value is set as β value when the correlation coefficient between connectivity K and logarithm logarithm (P(k)) reaches

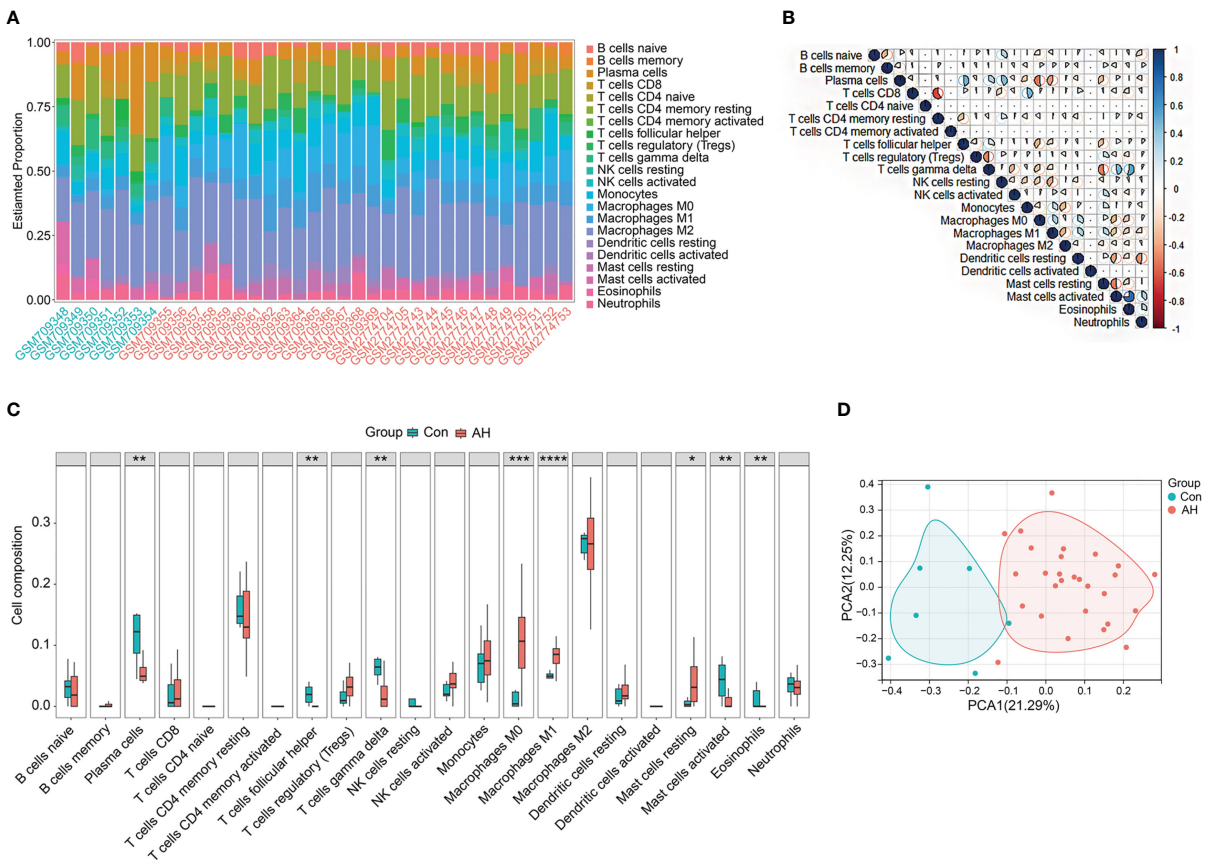

FIGURE 2
Immune infiltration in control group and AH group. **(A)** Bar charts of 22 types of immune cells in selected samples. Green name is normal liver sample, red name is AH sample. **(B)** Correlation heatmap of 22 types of immune cells, blue is positive correlation, red is negative correlation, color intensity represents the degree of correlation. **(C)** Boxplot of difference analysis of immune cells between control group (Con) and AH group (AH). **(D)** Scatter plot of PCA results. *p < 0.05, **p < 0.01, ***p < 0.001, ****p < 0.0001.

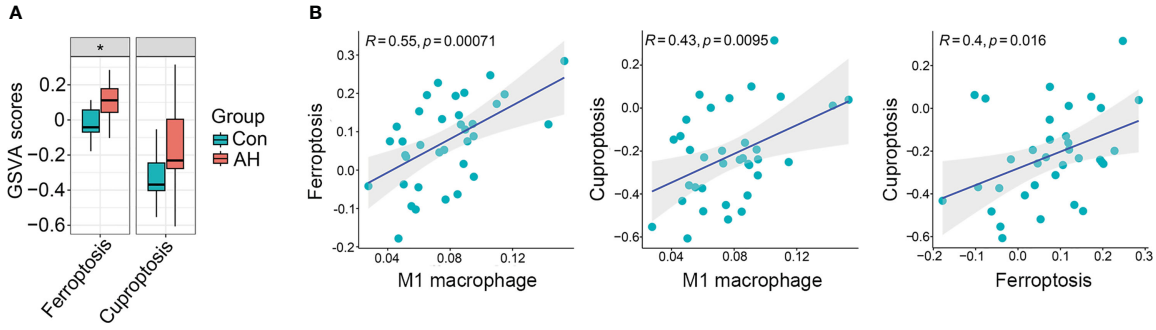

FIGURE 3
M1 macrophages, ferroptosis and cuproptosis were positively correlated with each other. **(A)** Boxplot of difference analysis of ferroptosis and cuproptosis GSVA scores between control group (Con) and AH group (AH). **(B)** Correlation analysis of M1 macrophage, ferroptosis and cuproptosis. *p < 0.05.

0.83. A scale-free topological network (β = 6) was established (Figure 4A). Based on selected soft-thresholding power, a hierarchical clustering tree was established to cluster high-coexpression genes into same module and color code them (Figure 4B). Next, Spearman correlation analysis was used to draw module-trait relationship heatmap for 13 transcription modules identified and evaluate relationship between modules (Figure 4C). We found that red module was closely correlated with M1 macrophages, ferroptosis and cuproptosis, and was also highly correlated with AH traits. Therefore, this module was identified as hub module (Figures 4C, D). The module contains 834 genes, including 33 genes and 41 edges with threshold weight > 0.2 (Figure 4E). These genes are considered as hub genes.

Candidate genes co-associated with M1 macrophages, ferroptosis and cuproptosis in AH patients

To further identify biomarkers associated with AH patients, DEGs analysis was performed on gene expression data from control and AH groups. There were a total of 877 DEGs, including 519 up-regulated genes and 358 down-regulated genes (Figure 5A) (Supplementary Table S5). The intersection of DEGs with hub genes related to M1 macrophages, ferroptosis and cuproptosis was performed to obtain 27 candidate genes (Figure 5B). The heatmap shows expression of these candidate genes in each sample (Figure 5C). Functional enrichment analysis was conducted for the above 27 candidate genes. The top 10 significantly enriched GO terms and KEGG pathways are shown separately in Figures 5D, E (see Supplementary Table S6 for details). AGE-RAGE and PI3K-AKT signaling pathway are associated with inflammation and oxidative stress. This suggests that M1 macrophages, ferroptosis and cuproptosis may be related to each other through the above signaling pathways. In addition, the results of functional enrichment analysis showed that the common high expression of M1 macrophages, ferroptosis and cuproptosis may activate extracellular matrix (ECM)-related signaling pathways.

Identification of biomarkers co-associated with M1 macrophages, ferroptosis and cuproptosis *via* machine learning

For the above 27 candidate genes, SVM and LASSO regression algorithms were used to screen potential biomarkers co-associated with M1 macrophages, ferroptosis and cuproptosis. According to the results of ten fold cross-validation in SVM algorithm, 22 feature genes were identified (Figure 6A, Table 1). The coefficients of LASSO versus log (λ) are shown in Figure 6B that 5 feature genes were obtained (Table 1 and Supplementary Table S7). Finally, 5 genes selected by two machine learning algorithms were overlapped, including ALDOA, COL3A1, LUM, THBS2 and TIMP1 (Figure 6C). To assess predictive accuracy of these biomarkers, ROC curves of 5 genes were analyzed (Figure 6D). The AUC values indicated that 5 biomarkers co-associated with M1 macrophages, ferroptosis and cuproptosis had excellent diagnostic values. Next, we analyzed the correlation between 5 potential biomarkers and M1 macrophage, ferroptosis and cuproptosis. The analysis results showed that 5 potential biomarkers were positively correlated with M1 macrophage, ferroptosis and cuproptosis (Figures 7A–C), and 5 potential biomarkers were also positively correlated with each other (Supplementary Figure S2). In addition, we validated 5 potential biomarkers using GSE155907 and GSE142530 datasets. In two validation datasets, consistent with training dataset, all 5 genes in AH group were up-regulated, with statistical significance (Figures 7D, E). Combined with the above results, 5 genes co-associated with M1 macrophages, ferroptosis and cuproptosis can be used as potential biomarkers in AH patients.

Potential biomarkers were validated in a mouse model of AH

To verify 5 potential biomarkers, we first analyzed mouse dataset (GSE97234) and found that the expression levels of 5 genes were significantly up-regulated in AH group (Figure 8A). Based on the above analysis, we conducted experimental

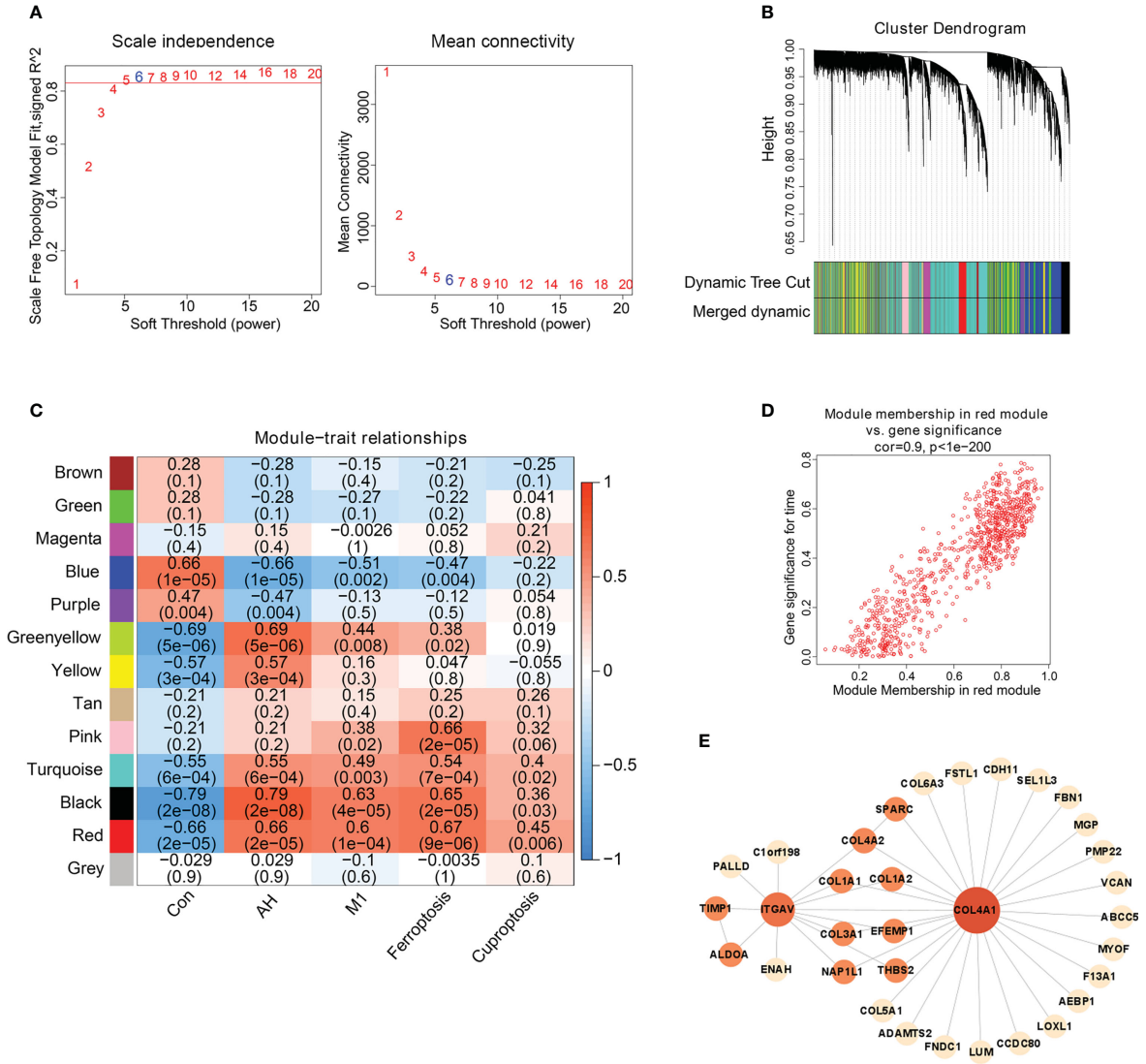

FIGURE 4
Hub gene screening based on WGCNA. **(A)** Scale-free fitting index analysis of soft-thresholding powers. **(B)** Cluster dendrogram. **(C)** Module-trait correlation heatmap, red is positive correlation, blue is negative correlation. **(D)** Scatter plot of red module. Horizontal axis (MM) represented the correlation between genes and modules, and vertical axis (GS) represented the absolute value of correlation between genes and phenotypic characteristics. **(E)** The network of hub genes.

verification in mice. We established a chronic plus single binge alcohol model, which has been widely used to study the pathogenesis of AH (Figure 8B). Compared with pair-fed mice, ethanol-fed mice had a significant decrease in body weight (Figure 8C) and a significant increase in liver weight/body weight ratio (mean, 0.056 vs. 0.048, $P = 0.028$) (Figure 8D). ALT and AST, important indicators of liver injury, were significantly elevated in ethanol-fed mice than in pair-fed mice (ALT, mean, 112.7 vs. 69.1, $P = 0.001$) (AST, mean, 464.0 vs. 269.7, $P = 0.0003$) (Figures 8E, F). H&E staining showed that ethanol feeding resulted in necrosis of hepatocytes and morphological changes of liver tissues, suggesting more severe liver injury in ethanol-fed mice than in pair-fed mice (Figure 8G).

Macrophages play a crucial role in regulating liver homeostasis and hepatic injury. By double immunofluorescence staining of liver tissues with F4/80 (a marker of macrophage) and iNOS (a marker of M1 macrophage), we found that M1 macrophages (F4/80 and iNOS double positive cells) were almost not expressed in pair-fed mice, while the expression of M1 macrophage marker protein was increased in ethanol-fed mice, suggesting the infiltration of more M1 macrophages (Figure 8H). Lipid peroxide and GSH are crucial markers of ferroptosis. MDA is considered to be the end product of the lipid peroxidation process. The MDA and GSH levels of liver tissues were detected by kits. Compared with pair-fed mice, MDA levels (mean, 2.26 vs. 1.17, $P = 0.021$) were significantly increased and GSH levels (mean, 2.24 vs. 5.41, $P = 0.014$) were significantly decreased in ethanol-fed mice (Figures 9A, B). In addition, the well-identified markers of ferroptosis, GPX4 and ACSL4, were detected in liver tissues by western blot. As shown in Figure 9C, the protein expression levels of GPX4 (mean, 0.40 vs. 0.85, $P = 0.048$) were

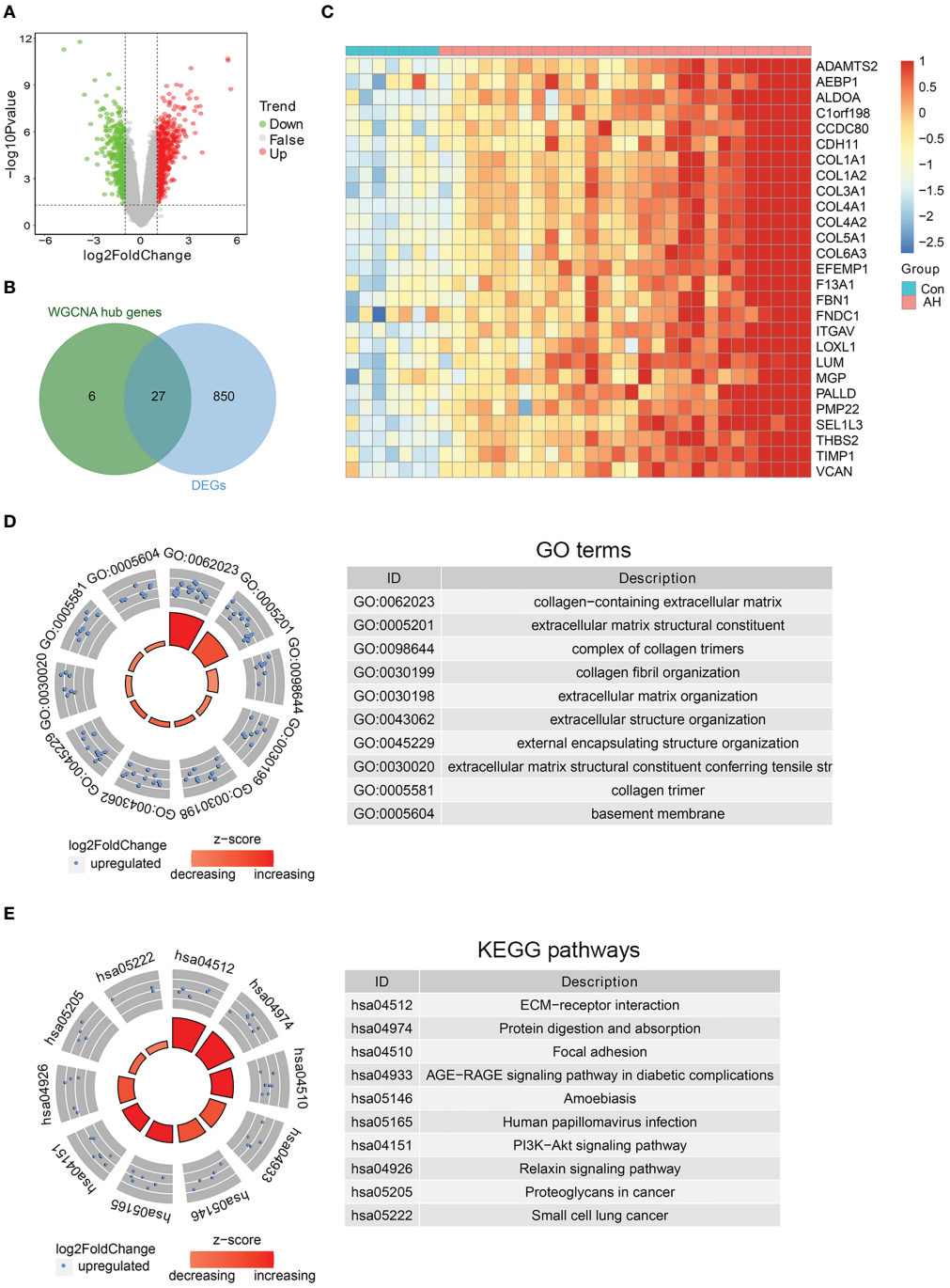

GO terms	
ID	Description
GO:0062023	collagen−containing extracellular matrix
GO:0005201	extracellular matrix structural constituent
GO:0098644	complex of collagen trimers
GO:0030199	collagen fibril organization
GO:0030198	extracellular matrix organization
GO:0043062	extracellular structure organization
GO:0045229	external encapsulating structure organization
GO:0030020	extracellular matrix structural constituent conferring tensile str
GO:0005581	collagen trimer
GO:0005604	basement membrane

KEGG pathways	
ID	Description
hsa04512	ECM−receptor interaction
hsa04974	Protein digestion and absorption
hsa04510	Focal adhesion
hsa04933	AGE−RAGE signaling pathway in diabetic complications
hsa05146	Amoebiasis
hsa05165	Human papillomavirus infection
hsa04151	PI3K−Akt signaling pathway
hsa04926	Relaxin signaling pathway
hsa05205	Proteoglycans in cancer
hsa05222	Small cell lung cancer

FIGURE 5
Identification of biomarkers co-associated with M1 macrophages, ferroptosis and cuproptosis. **(A)** Volcano plot of DEGs between control and AH groups. **(B)** Venn diagram of intersection genes between DEGs and hub genes. **(C)** The heatmap of 27 candidate genes. **(D)** GO enrichment analysis. **(E)** KEGG enrichment analysis.

significantly down-regulated and the protein expression levels of ACSL4 (mean, 2.29 vs. 0.50, P = 0.004) were significantly up-regulated in ethanol-fed mice compared with pair-fed mice. Known biomarkers of cuproptosis, including FDX1 and SLC31A1 were determined. We also detected the expression levels of FDX1 and SLC31A1 in liver tissues by western blot. the protein expression levels of FDX1 (mean, 0.45 vs. 1.25, P = 0.031) were significantly down-regulated and the protein expression levels of SLC31A1 (mean, 2.68 vs. 0.75, P = 0.022) were significantly up-regulated in ethanol-fed mice compared with pair-fed mice (Figure 9D). Combined with the above results, alcohol consumption significantly promoted the infiltration of M1 macrophages, the expression of ferroptosis and cuproptosis.

The expression levels of *Aldoa*, *Col3a1*, *Lum*, *Thbs2* and *Timp1* mRNA were detected by RT-qPCR. As shown in Figure 9E, compared with pair-fed mice, the expression levels of *Aldoa*

10.3389/fimmu.2023.1146693

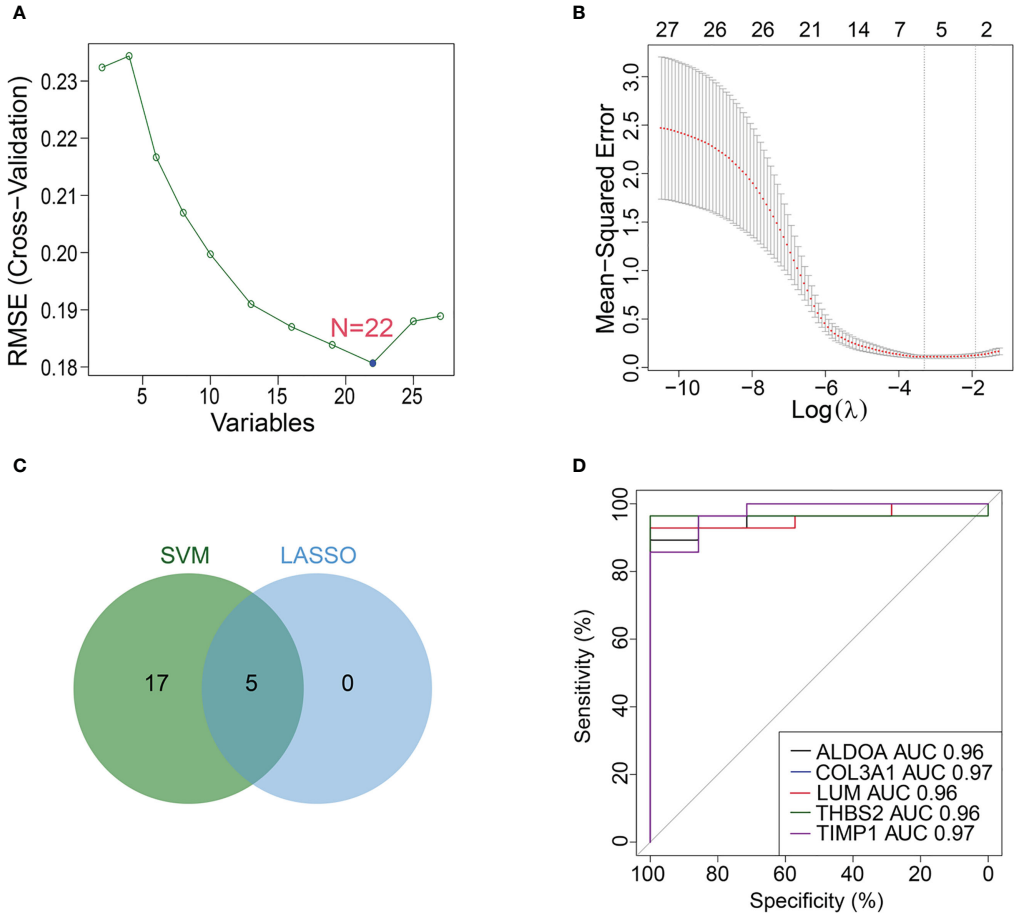

FIGURE 6
Machine learning identifies potential biomarkers. **(A, B)** Biomarkers were analyzed using LASSO regression and SVM algorithm. **(C)** Venn diagram of overlapping biomarkers between LASSO regression and SVM algorithm. **(D)** ROC curve of 5 potential biomarkers.

(mean, 2.12 vs. 1.00, P = 0.027), *Col3a1* (mean, 1.92 vs. 1.00, P = 0.007), *Lum* (mean, 2.92 vs. 1.00, P = 0.005), *Thbs2* (mean, 3.79 vs. 1.00, P = 0.002) and *Timp1* (mean, 2.62 vs. 1.00, P = 0.021) in liver tissues of ethanol-fed mice were significantly increased. These experimental results further support that 5 genes as potential biomarkers for AH patients.

Discussion

In this study, biomarkers co-associated with M1 macrophages, ferroptosis and cuproptosis were identified in AH patients. The CIBERSORT algorithm was used to calculate infiltration of 22 types of immune cells. Ferroptosis and cuproptosis scores were calculated using GSVA algorithm. By WGCNA and LASSO-SVM analysis, we found that ALDOA, COL3A1, LUM, THBS2 and TIMP1 were potential biomarkers in AH patients. These biomarkers were validated in GEO datasets and a mouse model of AH.

Excessive alcohol consumption directly damages hepatocytes, which in turn induces immune cell infiltration and secretion of inflammatory factors, ultimately leading to overactivation of inflammatory cascade (36, 37). For example, neutrophil infiltration and high expression of pro-inflammatory factors (TNF-α and IL-1β) promote the progression of alcohol-related inflammatory response (38). In addition, chronic alcohol consumption leads to upregulation of M1 macrophage-related markers (39). In this study, we used the CIBERSORT algorithm to assess the difference in immune cells between normal liver and AH samples. We found that M1 macrophages were significantly increased in AH patients. These findings provide new insights into immune cell infiltration in AH patients based on transcriptomic analysis.

Clinical calculators such as the Model of End-stage Liver Disease (MELD) score can predict patient mortality and guide clinical treatment strategies (40). However, MELD score is not specifically designed to predict AH. Clinically, biomarkers for AH prediction have not been identified. Therefore, the discovery of new biomarkers for AH prediction is an urgent area of research. In recent years, with the development of high-throughput sequencing technology, the identification of disease-related biomarkers based

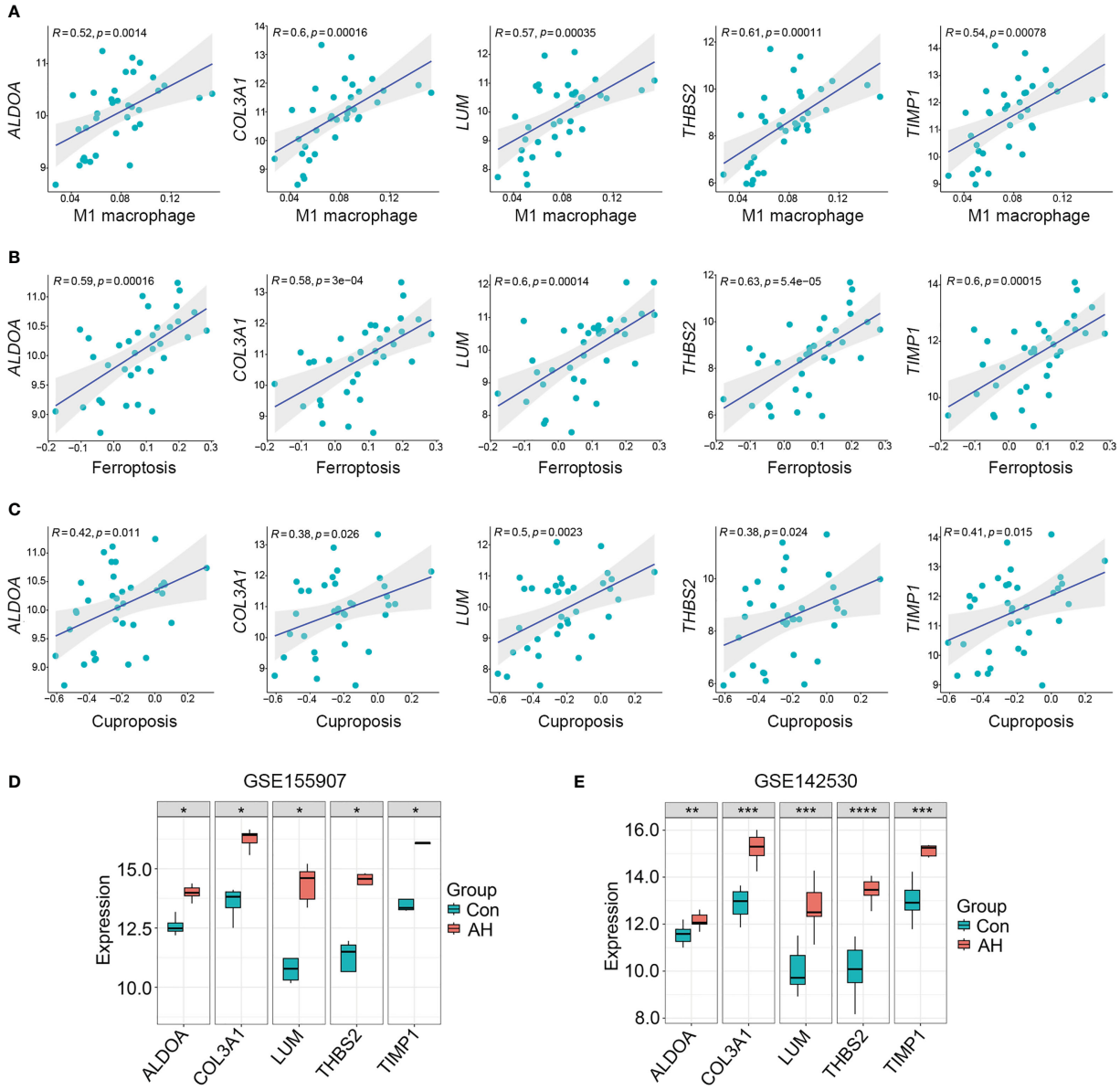

FIGURE 7
5 potential biomarkers were positively correlated with M1 macrophage, ferroptosis and cuproptosis. **(A–C)** Correlation analysis of 5 potential biomarkers with M1 macrophage, ferroptosis and cuproptosis. **(D)** Expression levels of 5 potential biomarkers in GSE155907 dataset. **(E)** Expression levels of 5 potential biomarkers in GSE142530 dataset. *p < 0.05, **p < 0.01, ***p < 0.001, ****p < 0.0001.

on transcriptomic analysis has been widely studied. In previous studies, a prognostic model of hepatocellular carcinoma was established using WGCNA analysis of macrophage-related genes (41). The prognostic model based on ferroptosis and epithelial-mesenchymal transition state helps predict overall survival of hepatocellular carcinoma (42). Cuproptosis-related subtypes predict tumor microenvironments and drug candidates in hepatocellular carcinoma (43). However, biomarkers for AH

TABLE 1 Feature genes obtained by machine learning.

Machine learning	Feature genes
SVM	CCDC80, COL5A1, ITGAV, CDH11, VCAN, THBS2, COL4A2, COL4A1, SEL1L3, PMP22, C1orf198, FBN1, PALLD, COL1A2, COL3A1, EFEMP1, TIMP1, ALDOA, LUM, ADAMTS2, COL6A3, COL1A1
LASSO	ALDOA, COL3A1, LUM, THBS2, TIMP1

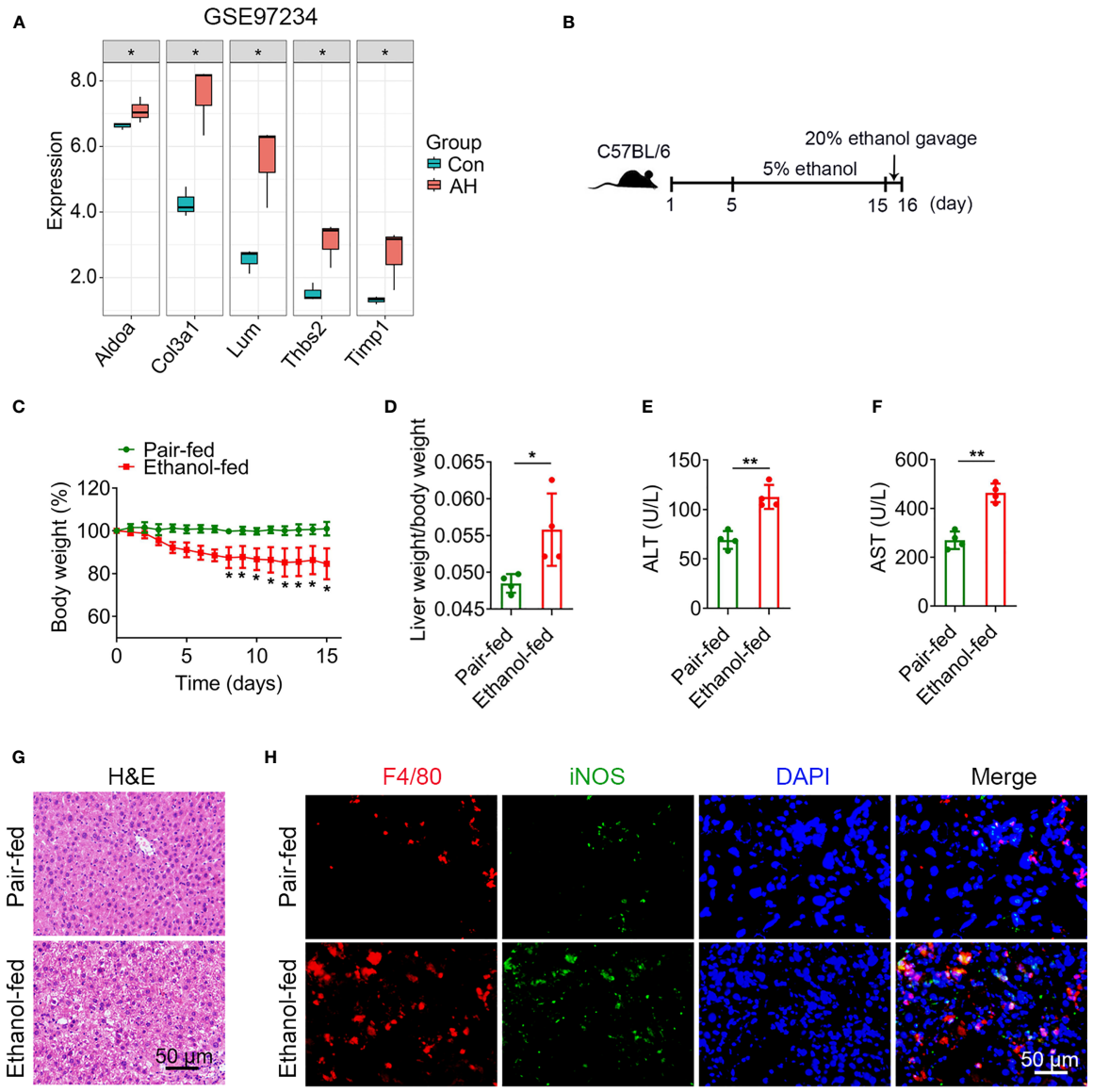

FIGURE 8
Alcohol exposure promotes infiltration of M1 macrophages. **(A)** Expression levels of 5 potential biomarkers in GSE97234 dataset. **(B–H)** Groups of C57BL/6 mice (n = 5 per group) were fed ethanol liquid diet or ethanol free control liquid diet. **(B)** Schematic diagram of a chronic binge eating model. **(C)** Changes in body weight. **(D)** Liver weight/body weight change ratio. **(E, F)** Serum ALT and AST levels. **(G)** Representative H&E staining of liver tissues. Scale bar, 50 μm. **(H)** Double immunofluorescence staining of F4/80 and iNOS in liver tissues. Nuclei were stained with DAPI. Scale bar, 50 μm. $^{*}P < 0.05$, $^{**}P < 0.01$.

prediction still need further analysis. In this study, we used WGCAN and LASSO-SVM analysis to identify 5 AH biomarkers co-associated with M1 macrophages, ferroptosis and cuproptosis in AH patients.

ALDOA is a key metabolic enzyme in glycolysis pathway. High expression of ALDOA is associated with poor prognosis in hepatocellular carcinoma (44). COL3A1 is a fibrous collagen found in connective tissue. Previous studies have shown that COL3A1 is involved in the progression of liver fibrosis (45). The levels of type III collagen formation and degradation were significantly increased in ALD patients compared to healthy individuals (46). In addition, LUM has been identified as a biomarker for advanced fibrosis in non-alcoholic fatty liver disease (47). THBS2 is a novel biomarker for predicting the prognosis of metastatic pancreatic ductal adenocarcinoma (48). Manzardo et al. analyzed miRNA expression in alcoholics to further characterize the genetic influence of alcoholism and the influence of alcohol consumption on predicted target mRNA expression, which involved THBS2 (49). In mice treated with ethanol and CCl_4, down-regulation of TIMP1 effectively inhibited hepatic fibrosis and activation of hepatic stellate cell (50). Clinical studies have found that alcohol consumption in adolescents leads to

10.3389/fimmu.2023.1146693

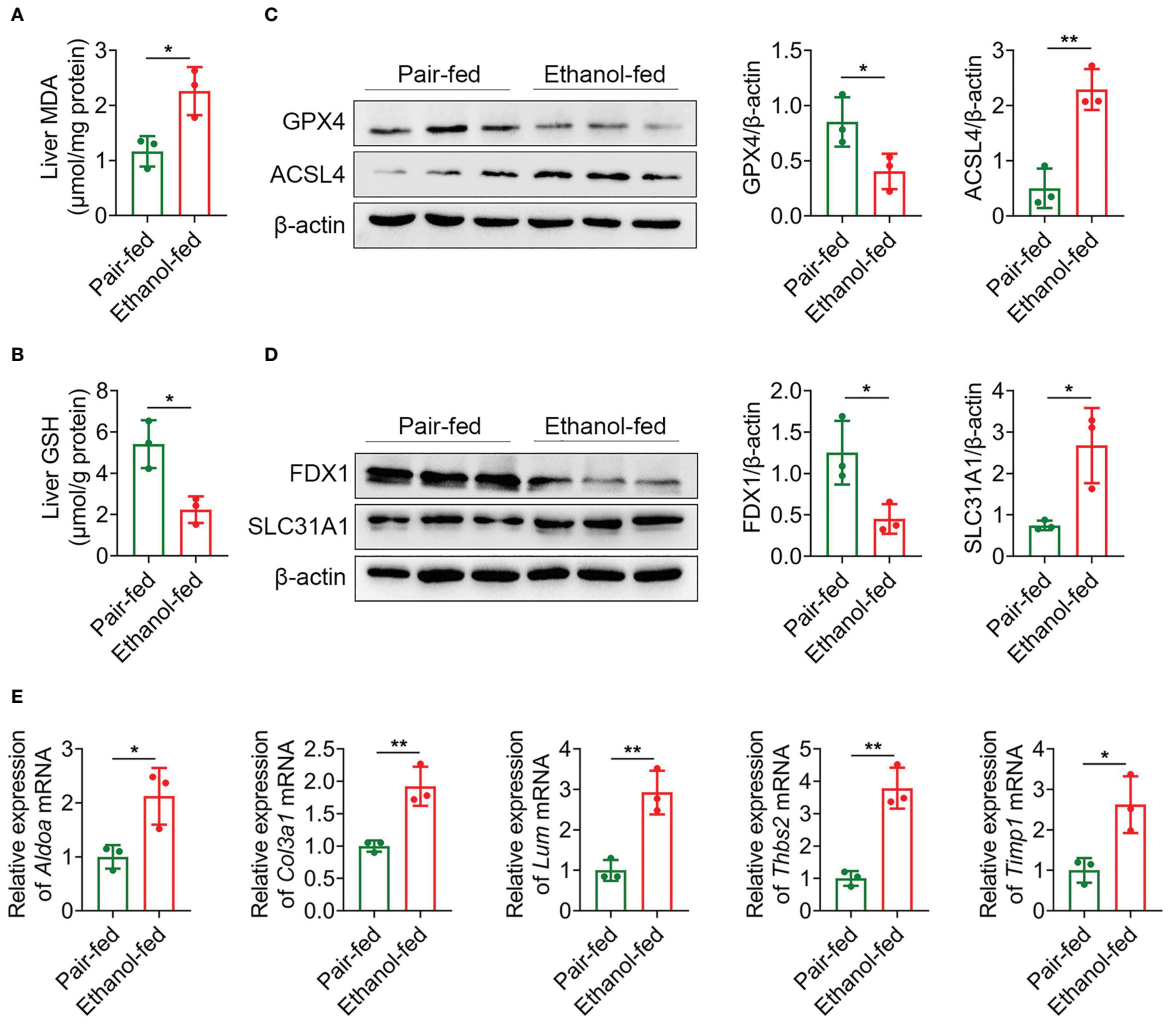

FIGURE 9
Alcohol exposure promotes the expression of ferroptosis, cuproptosis and potential biomarkers. **(A–E)** Groups of C57BL/6 mice (n = 5 per group) were fed ethanol liquid diet or ethanol free control liquid diet. **(A)** Content of MDA in liver tissues. **(B)** Content of GSH in liver tissues. **(C)** The protein expression levels of GPX4 and ACSL4 in liver tissues were determined using western blot analysis. The densities of protein were quantified using densitometry. GPX4 and ACSL4 were normalized to β-actin. **(D)** The protein expression levels of FDX1 and SLC31A1 in liver tissues were determined using western blot analysis. The densities of protein were quantified using densitometry. FDX1 and SLC31A1 were normalized to β-actin. **(E)** The mRNA levels of *Aldoa*, *Col3a1*, *Lum*, *Thbs2* and *Timp1* in liver tissues were measured using RT-qPCR analysis. The results were normalized to *Actb*. $^{*}P < 0.05$, $^{**}P < 0.01$.

elevated serum TIMP1 concentrations (51). We first reported that ALDOA, COL3A1, LUM, THBS2 and TIMP1 were highly expressed in AH and associated with M1 macrophages, ferroptosis and cuproptosis. Further studies with larger clinical cohorts and basic studies are needed to confirm these biomarkers.

Conclusion

In summary, we used CIBERSORT algorithm to analyze 22 types of immune cells, and M1 macrophages were the most significantly increased immune cells in AH patients. By combining bioinformatics analysis with a mouse model of AH, we identified 5 potential biomarkers co-associated with M1 macrophages, ferroptosis and cuproptosis. Further study of these biomarkers can provide new ideas and basis for understanding the disease progression and targeted therapy of AH patients.

Data availability statement

The original contributions presented in the study are included in the article/Supplementary Material. Further inquiries can be directed to the corresponding author.

Ethics statement

The animal study was reviewed and approved by The Experimental Animal Ethics Committee of Mudanjiang Medical University.

Author contributions

Conception and design: QY. Data collection and analysis: SH, DW and QY. Manuscript writing: SH and XXY. Manuscript revising: XHY. All authors contributed to the article and approved the submitted version.

Funding

This work was supported by the Doctoral starting fund of Mudanjiang Medical University, the Key Research and Development Plan Project of Jining (2022YXNS163) and the National Natural Science Foundation of China (82103345).

Acknowledgments

We thank authors of GEO datasets for providing their data freely available to the public, as well as the developers of the R package.

Conflict of interest

The authors declare that the research was conducted in the absence of any commercial or financial relationships that could be construed as a potential conflict of interest.

Publisher's note

Supplementary material

The Supplementary Material for this article can be found online at: https://www.frontiersin.org/articles/10.3389/fimmu.2023.1146693/full#supplementary-material

References

1. Singal AK, Mathurin P. Diagnosis and treatment of alcohol-associated liver disease: A review. *JAMA* (2021) 326(2):165–76. doi: 10.1001/jama.2021.7683

2. Ventura-Cots M, Argemi J, Jones P, Lackner C, El Hag M, Abraldes J, et al. Clinical, histological and molecular profiling of different stages of alcohol-related liver disease. *Gut* (2022) 71(9):1856–66. doi: 10.1136/gutjnl-2021-324295

3. Sehrawat TS, Liu M, Shah VH. The knowns and unknowns of treatment for alcoholic hepatitis. *Lancet Gastroenterol Hepatol* (2020) 5(5):494–506. doi: 10.1016/S2468-1253(19)30326-7

4. Rattan P, Shah VH. Review article: current and emerging therapies for acute alcohol-associated hepatitis. *Aliment Pharmacol Ther* (2022) 56(1):28–40. doi: 10.1111/apt.16969

5. Arab JP, Diaz LA, Baeza N, Idalsoaga F, Fuentes-Lopez E, Arnold J, et al. Identification of optimal therapeutic window for steroid use in severe alcohol-associated hepatitis: A worldwide study. *J Hepatol* (2021) 75(5):1026–33. doi: 10.1016/j.jhep.2021.06.019

6. Furuya S, Argemi J, Uehara T, Katou Y, Fouts DE, Schnabl B, et al. A novel mouse model of acute-on-Chronic cholestatic alcoholic liver disease: A systems biology comparison with human alcoholic hepatitis. *Alcohol Clin Exp Res* (2020) 44(1):87–101. doi: 10.1111/acer.14234

7. Massey V, Parrish A, Argemi J, Moreno M, Mello A, Garcia-Rocha M, et al. Integrated multiomics reveals glucose use reprogramming and identifies a novel hexokinase in alcoholic hepatitis. *Gastroenterology* (2021) 160(5):1725–1740 e1722. doi: 10.1053/j.gastro.2020.12.008

8. Cho YE, Yu LR, Abdelmegeed MA, Yoo SH, Song BJ. Apoptosis of enterocytes and nitration of junctional complex proteins promote alcohol-induced gut leakiness and liver injury. *J Hepatol* (2018) 69(1):142–53. doi: 10.1016/j.jhep.2018.02.005

9. Wang C, Ma C, Gong L, Guo Y, Fu K, Zhang Y, et al. Macrophage polarization and its role in liver disease. *Front Immunol* (2021) 12:803037. doi: 10.3389/fimmu.2021.803037

10. Nowak AJ, Relja B. The impact of acute or chronic alcohol intake on the NF-kappaB signaling pathway in alcohol-related liver disease. *Int J Mol Sci* (2020) 21(24):9407. doi: 10.3390/ijms21249407

11. Zhao N, Xia G, Cai J, Li Z, Lv XW. Adenosine receptor A2B mediates alcoholic hepatitis by regulating cAMP levels and the NF-KB pathway. *Toxicol Lett* (2022) 359:84–95. doi: 10.1016/j.toxlet.2022.01.012

12. Cho Y, Joshi R, Lowe P, Copeland C, Ribeiro M, Morel C, et al. Granulocyte colony-stimulating factor attenuates liver damage by M2 macrophage polarization and hepatocyte proliferation in alcoholic hepatitis in mice. *Hepatol Commun* (2022) 6(9):2322–39. doi: 10.1002/hep4.1925

13. Santana-Codina N, Mancias JD. The role of NCOA4-mediated ferritinophagy in health and disease. *Pharm (Basel)* (2018) 11(4):114. doi: 10.3390/ph11040114

14. Tsvetkov P, Coy S, Petrova B, Dreishpoon M, Verma A, Abdusamad M, et al. Copper induces cell death by targeting lipoylated TCA cycle proteins. *Science* (2022) 375(6586):1254–61. doi: 10.1126/science.abf0529

15. Zhou Z, Ye TJ, DeCaro E, Buehler B, Stahl Z, Bonavita G, et al. Intestinal SIRT1 deficiency protects mice from ethanol-induced liver injury by mitigating ferroptosis. *Am J Pathol* (2020) 190(1):82–92. doi: 10.1016/j.ajpath.2019.09.012

16. Zhao Y, Zhang R, Wang Z, Chen Z, Wang G, Guan S, et al. Melatonin prevents against ethanol-induced liver injury by mitigating ferroptosis *via* targeting brain and muscle ARNT-like 1 in mice liver and HepG2 cells. *J Agric Food Chem* (2022) 70(40):12953–67. doi: 10.1021/acs.jafc.2c04337

17. Zhang Z, Zeng X, Wu Y, Liu Y, Zhang X, Song Z. Cuproptosis-related risk score predicts prognosis and characterizes the tumor microenvironment in hepatocellular carcinoma. *Front Immunol* (2022) 13:925618. doi: 10.3389/fimmu.2022.925618

18. Wang G, Xiao R, Zhao S, Sun L, Guo J, Li W, et al. Cuproptosis regulator-mediated patterns associated with immune infiltration features and construction of cuproptosis-related signatures to guide immunotherapy. *Front Immunol* (2022) 13:945516. doi: 10.3389/fimmu.2022.945516

19. Affo S, Dominguez M, Lozano JJ, Sancho-Bru P, Rodrigo-Torres D, Morales-Ibanez O, et al. Transcriptome analysis identifies TNF superfamily receptors as potential therapeutic targets in alcoholic hepatitis. *Gut* (2013) 62(3):452–60. doi: 10.1136/gutjnl-2011-301146

20. Trepo E, Goossens N, Fujiwara N, Song WM, Colaprico A, Marot A, et al. Combination of gene expression signature and model for end-stage liver disease score predicts survival of patients with severe alcoholic hepatitis. *Gastroenterology* (2018) 154(4):965–75. doi: 10.1053/j.gastro.2017.10.048

21. Liu M, Cao S, He L, Gao J, Arab JP, Cui H, et al. Super enhancer regulation of cytokine-induced chemokine production in alcoholic hepatitis. *Nat Commun* (2021) 12(1):4560. doi: 10.1038/s41467-021-24843-w

22. Khanova E, Wu R, Wang W, Yan R, Chen Y, French SW, et al. Pyroptosis by caspase11/4-gasdermin-D pathway in alcoholic hepatitis in mice and patients. *Hepatology* (2018) 67(5):1737–53. doi: 10.1002/hep.29645

23. Johnson WE, Li C, Rabinovic A. Adjusting batch effects in microarray expression data using empirical bayes methods. *Biostatistics* (2007) 8(1):118–27. doi: 10.1093/biostatistics/kxj037

24. Newman AM, Liu CL, Green MR, Gentles AJ, Feng W, Xu Y, et al. Robust enumeration of cell subsets from tissue expression profiles. *Nat Methods* (2015) 12(5):453–7. doi: 10.1038/nmeth.3337

25. Hänzelmann S, Castelo R, Guinney J. GSVA: gene set variation analysis for microarray and RNA-seq data. *BMC Bioinf* (2013) 17:7. doi: 10.1186/1471-2105-14-7

26. Fu J, Wang S, Li Z, Qin W, Tong Q, Liu C, et al. Comprehensive multiomics analysis of cuproptosis-related gene characteristics in hepatocellular carcinoma. *Front Genet* (2022) 13:942387. doi: 10.3389/fgene.2022.942387

27. Langfelder P, Horvath S. WGCNA: an r package for weighted correlation network analysis. *BMC Bioinf* (2008) 9:559. doi: 10.1186/1471-2105-9-559

28. Yu G, Wang LG, Han Y, He QY. clusterProfiler: an r package for comparing biological themes among gene clusters. *OMICS* (2012) 16(5):284–7. doi: 10.1089/omi.2011.0118

29. Walter W, Sanchez-Cabo F, Ricote M. GOplot: an r package for visually combining expression data with functional analysis. *Bioinformatics* (2015) 31 (17):2912–4. doi: 10.1093/bioinformatics/btv300

30. Ritchie ME, Phipson B, Wu D, Hu Y, Law CW, Shi W, et al. Limma powers differential expression analyses for RNA-sequencing and microarray studies. *Nucleic Acids Res* (2015) 43(7):e47. doi: 10.1093/nar/gkv007

31. Friedman J, Hastie T, Tibshirani R. Regularization paths for generalized linear models *via* coordinate descent. *J Stat Softw* (2010) 33(1):1–22. doi: 10.18637/jss.v033.i01

32. Karatzoglou A, Smola A, Hornik K, Zeileis A. Kernlab - an S4 package for kernel methods in r. *J Stat Software* (2004) 11(9):1–20. doi: 10.18637/jss.v011.i09

33. Robin X, Turck N, Hainard A, Tiberti N, Lisacek F, Sanchez J-C, et al. Proc: An open-source package for r and s+ to analyze and compare roc curves. *BMC Bioinf* (2011) 12:77. doi: 10.1186/1471-2105-12-77

34. Yuan Q, Hou S, Zhai J, Tian T, Wu Y, Wu Z, et al. S100A4 promotes inflammation but suppresses lipid accumulation *via* the STAT3 pathway in chronic ethanol-induced fatty liver. *J Mol Med (Berl)* (2019) 97(10):1399–412. doi: 10.1007/s00109-019-01808-7

35. Yuan Q, Zhang J, Liu Y, Chen H, Liu H, Wang J, et al. MyD88 in myofibroblasts regulates aerobic glycolysis-driven hepatocarcinogenesis *via* ERK-dependent PKM2 nuclear relocalization and activation. *J Pathol* (2022) 256(4):414–26. doi: 10.1002/path.5856

36. Szabo G, Petrasek J. Gut-liver axis and sterile signals in the development of alcoholic liver disease. *Alcohol Alcohol* (2017) 52(4):414–24. doi: 10.1093/alcalc/agx025

37. Hosseini N, Shor J, Szabo G. Alcoholic hepatitis: A review. *Alcohol Alcohol* (2019) 54(4):408–16. doi: 10.1093/alcalc/agz036

38. Enomoto N, Ikejima K, Bradford B, Rivera C, Kono H, Goto M, et al. Role of kupffer cells and gut-derived endotoxins in alcoholic liver injury. *J Gastroenterol Hepatol* (2000) Suppl:D20–25. doi: 10.1046/j.1440-1746.2000.02179.x

39. Ju C, Mandrekar P. Macrophages and alcohol-related liver inflammation. *Alcohol Res* (2015) 37(2):251–62.

40. Forrest E. Use of MELD scores in alcoholic hepatitis. *Lancet Gastroenterol Hepatol* (2020) 5(8):720. doi: 10.1016/S2468-1253(20)30194-1

41. Wang T, Dai L, Shen S, Yang Y, Yang M, Yang X, et al. Comprehensive molecular analyses of a macrophage-related gene signature with regard to prognosis, immune features, and biomarkers for immunotherapy in hepatocellular carcinoma based on WGCNA and the LASSO algorithm. *Front Immunol* (2022) 13:843408. doi: 10.3389/fimmu.2022.843408

42. Liu Z, Wang J, Li S, Li L, Li L, Li D, et al. Prognostic prediction and immune infiltration analysis based on ferroptosis and EMT state in hepatocellular carcinoma. *Front Immunol* (2022) 13:1076045. doi: 10.3389/fimmu.2022.1076045

43. Liu X, Sun B, Yao Y, Lai L, Wang X, Xiong J, et al. Identification of copper metabolism and cuproptosis-related subtypes for predicting prognosis tumor microenvironment and drug candidates in hepatocellular carcinoma. *Front Immunol* (2022) 13:996308. doi: 10.3389/fimmu.2022.996308

44. Wang J, Zhang HM, Dai ZT, Huang Y, Liu H, Chen Z, et al. MKL-1-induced PINK1-AS overexpression contributes to the malignant progression of hepatocellular carcinoma *via* ALDOA-mediated glycolysis. *Sci Rep* (2022) 12(1):21283. doi: 10.1038/s41598-022-24023-w

45. Tao R, Fan XX, Yu HJ, Ai G, Zhang HY, Kong HY, et al. MicroRNA-29b-3p prevents schistosoma japonicum-induced liver fibrosis by targeting COL1A1 and COL3A1. *J Cell Biochem* (2018) 119(4):3199–209. doi: 10.1002/jcb.26475

46. Thiele M, Johansen S, Gudmann NS, Madsen B, Kjaergaard M, Nielsen MJ, et al. Progressive alcohol-related liver fibrosis is characterised by imbalanced collagen formation and degradation. *Aliment Pharmacol Ther* (2021) 54(8):1070–80. doi: 10.1111/apt.16567

47. Chang Y, He J, Xiang X, Li H. LUM is the hub gene of advanced fibrosis in nonalcoholic fatty liver disease patients. *Clin Res Hepatol Gastroenterol* (2021) 45 (1):101435. doi: 10.1016/j.clinre.2020.04.006

48. Gimotty PA, Till JE, Udgata S, Takenaka N, Yee SS, LaRiviere MJ, et al. THSB2 as a prognostic biomarker for patients diagnosed with metastatic pancreatic ductal adenocarcinoma. *Oncotarget* (2021) 12(22):2266–72. doi: 10.18632/oncotarget.28099

49. Manzardo AM, Gunewardena S, Butler MG. Over-expression of the miRNA cluster at chromosome 14q32 in the alcoholic brain correlates with suppression of predicted target mRNA required for oligodendrocyte proliferation. *Gene* (2013) 526 (2):356–63. doi: 10.1016/j.gene.2013.05.052

50. Fujimoto Y, Kaji K, Nishimura N, Enomoto M, Murata K, Takeda S, et al. Dual therapy with zinc acetate and rifaximin prevents from ethanol-induced liver fibrosis by maintaining intestinal barrier integrity. *World J Gastroenterol* (2021) 27(48):8323–42. doi: 10.3748/wjg.v27.i48.8323

51. Zdanowicz K, Kowalczuk-Kryston M, Olanski W, Werpachowska I, Mielech W, Lebensztejn DM. Increase in serum MMP-9 and TIMP-1 concentrations during alcohol intoxication in adolescents-a preliminary study. *Biomolecules* (2022) 12 (5):710. doi: 10.3390/biom12050710

frontiers | Frontiers in Immunology

TYPE Review
PUBLISHED 17 April 2023
DOI 10.3389/fimmu.2023.1147710

OPEN ACCESS

EDITED BY
Chao Yang,
Zhejiang University, China

REVIEWED BY
Tara E. Sutherland,
University of Aberdeen, United Kingdom
Xin Li,
Houston Methodist Research Institute, United States

*CORRESPONDENCE
Xiaoting Zou
xiaotzou2008@163.com
Quan Gong
gongquan1998@163.com
Bing Zheng
hxzheng@yangtzeu.edu.cn

†These authors have contributed equally to this work

SPECIALTY SECTION
This article was submitted to Inflammation, a section of the journal Frontiers in Immunology

RECEIVED 19 January 2023
ACCEPTED 03 April 2023
PUBLISHED 17 April 2023

CITATION
Yu W, Wang S, Wang Y, Chen H, Nie H, Liu L, Zou X, Gong Q and Zheng B (2023) MicroRNA: role in macrophage polarization and the pathogenesis of the liver fibrosis. *Front. Immunol.* 14:1147710. doi: 10.3389/fimmu.2023.1147710

MicroRNA: role in macrophage polarization and the pathogenesis of the liver fibrosis

Wen Yu[1†], Shu Wang[1†], Yangyang Wang[1], Hui Chen[2], Hao Nie[1,3], Lian Liu[3], Xiaoting Zou[1,3*], Quan Gong[1,3*] and Bing Zheng[1,3*]

[1]Department of Immunology, School of Medicine, Yangtze University, Jingzhou, China, [2]Department of Laboratory Medicine, First Affiliated Hospital of Yangtze University, Jingzhou, China, [3]Clinical Molecular Immunology Center, School of Medicine, Yangtze University, Jingzhou, China

Macrophages, as central components of innate immunity, feature significant heterogeneity. Numerus studies have revealed the pivotal roles of macrophages in the pathogenesis of liver fibrosis induced by various factors. Hepatic macrophages function to trigger inflammation in response to injury. They induce liver fibrosis by activating hepatic stellate cells (HSCs), and then inflammation and fibrosis are alleviated by the degradation of the extracellular matrix and release of anti-inflammatory cytokines. MicroRNAs (miRNAs), a class of small non-coding endogenous RNA molecules that regulate gene expression through translation repression or mRNA degradation, have distinct roles in modulating macrophage activation, polarization, tissue infiltration, and inflammation regression. Considering the complex etiology and pathogenesis of liver diseases, the role and mechanism of miRNAs and macrophages in liver fibrosis need to be further clarified. We first summarized the origin, phenotypes and functions of hepatic macrophages, then clarified the role of miRNAs in the polarization of macrophages. Finally, we comprehensively discussed the role of miRNAs and macrophages in the pathogenesis of liver fibrotic disease. Understanding the mechanism of hepatic macrophage heterogeneity in various types of liver fibrosis and the role of miRNAs on macrophage polarization provides a useful reference for further research on miRNA-mediated macrophage polarization in liver fibrosis, and also contributes to the development of new therapies targeting miRNA and macrophage subsets for liver fibrosis.

KEYWORDS

microRNA, macrophage polarization, HSC, liver fibrosis, M1 macrophage, M2 macrophage

1 Introduction

Liver fibrosis is an abnormal wound-healing response that develops in response to liver injury caused by various factors. The activation of hepatic stellate cells (HSCs) is recognized as a central event in liver fibrosis, in which activated HSCs transdifferentiate into myofibroblasts and secrete large amounts of extracellular matrix (ECM) that is deposited

among the cells, leading to liver fibrosis (1). Liver fibrosis is among the common sequelae of chronic damage induced by toxic agents, viral infections, autoimmune diseases, metabolic and genetic diseases (2). Without effective intervention and treatment, it can progress into cirrhosis, hepatocellular carcinoma (HCC), liver failure, and concurrent infection leading to death (3). Although HSCs are major contributors to the pathogenesis of liver fibrosis, certain immune cells such as T and B lymphocytes, NK cells, and macrophages also play important roles (4). Among them, macrophages are the most abundant liver immune cells and are critical in the process of liver injury and subsequent liver fibrosis (5). MicroRNAs (miRNAs) are about 22-26 nucleotides long endogenous non-coding RNAs expressed in animals, plants and some viruses. They participate in post-transcriptional gene regulation through a combination of translational repression and mRNA destabilization (6). Some studies have shown that miRNAs can regulate the activation of HSCs and are involved in various types of chronic liver diseases, such as viral hepatitis, nonalcoholic fatty liver disease and autoimmune liver disease, and play an indispensable role in the occurrence and development of liver fibrosis (7). Furthermore, in the pathological process of liver fibrosis, miRNAs may serve as key regulators of macrophage polarization, where macrophages can differentiate into the M1 phenotype with pro-inflammatory and anti-infective functions or the M2 phenotype with pro-fibrogenic and tissue remodeling roles (8). In this review, we summarize the characteristics of hepatic macrophages and their roles in liver fibrosis. Importantly, we focus on how miRNAs regulate the polarization of macrophages, thus affecting the eventual progression of liver fibrosis. Our study aims to provide new therapeutic ideas for improving liver fibrosis based on miRNAs and macrophages.

2 MicroRNAs

MicroRNAs (miRNAs) are endogenous, small non-coding RNA molecules widely expressed in all types of human cells. They predominantly function to negatively regulate gene expression at the post-transcriptional level and play important roles in various biological functions, such as immune response, cell proliferation and apoptosis (9–11). MicroRNAs are first transcribed in the nucleus by RNA polymerase II to generate primary miRNAs (pri-miRNAs), which are then cleaved by RNase III enzyme Drosha to generate precursor miRNAs (pre-miRNAs). These are translocated from the nucleus to the cytoplasm and then further processed by Dicer to produce double-stranded miRNAs containing mature miRNAs (11, 12). Mature miRNAs are directed to the 3' end of the untranslated region (UTR) of their specific target mRNAs by base-pairing, which represses protein expression by destabilizing the mRNA and translational silencing (10, 13). However, in some cases, miRNAs can also upregulate gene expression by activating the translation of target mRNAs. Generally, a single miRNA can regulate multiple mRNAs simultaneously, and one mRNA can also be regulated by several miRNAs (13). MiRNA dysregulation has been implicated in the pathogenesis of a variety of human diseases, including cancer, cardiovascular disease, metabolic disease, diabetes, and virus-induced diseases (14). Due to their stable presence in body fluids such as blood, urine and saliva, miRNAs might be promising biomarkers for the early diagnosis and potential therapeutic targets of some diseases (15).

3 Liver fibrosis and macrophages

3.1 The origin, phenotype and function of hepatic macrophages

Macrophages are an important component of innate immunity and act as the host's first line of defense against external infection or internal damage (16). According to their origin, intrahepatic macrophages are mainly divided into two types: resident Kupffer cells (KCs) and monocyte-derived macrophages (MoMϕs). KCs originate from yolk sac-derived colony-stimulating factor 1 receptor $(CSF1R)^+$ erythroid progenitors (EMPs), and develop further from EMPs into fetal liver mononuclear cells, which give rise to KCs (17). Kupffer cells, as the liver-resident macrophages, are located only in the intravascular compartment and are mainly located in the hepatic sinusoids. KCs function to remove cellular debris and metabolic waste (18, 19), maintain liver homeostasis, promote tissue repair and regeneration, and initiate the innate and adaptive immune responses (20). During homeostasis, KC replenishment is independent of BM-derived progenitors, and occurs predominantly by the self-renewal of resident stem cells (21, 22). Various pattern recognition receptors (PRRs) are highly expressed on the surface of KCs including Toll-like receptors (TLRs) and nucleotide binding oligomerization domain-like receptors (NLRs), which leads to the rapid response of KCs to various stimuli and activation signals during liver injury (23). The main stimuli recognized by KCs include reactive oxygen species (ROS); damage-associated molecular patterns (DAMPs) such as high mobility group box protein 1 (HMGB1), mitochondrial DNA and ATP; pathogen-associated molecular patterns (PAMPs) such as lipopolysaccharide (LPS), lipoteichoic acid (LTA) and β-glucan (24); hypoxia inducible factor 1α (HIF-1α); multiple metabolites; cell extracellular vesicles and microRNAs (25). KCs and MoMϕs in the liver can be distinguished from each other by their cell surface markers; however, no single marker is available to discriminate these populations. In mouse models, the main surface markers of KCs are $CD11b^{low}$, $F4/80^{high}$, $Clec4F^+$and $CX3CR1^-$ (5, 26). The surface markers of MoMϕs in mice are $CD11b^+$, $F4/80^{int}$, $Ly6C^+$, and $CX3CR1^{hi}$ (5). MoMϕs develop from lineage-negative (LIN^-) hematopoietic stem cells in the bone marrow, can be mainly found at the portal triad in the healthy liver, and function to maintain the iron and cholesterol homeostasis (27). Under pathological conditions, KCs secrete cytokines and chemokines, including TNF-α, IL-1β and CCL2, to recruit circulating monocytes migrating and infiltrating into the liver (28). The liver-infiltrating monocytes then differentiate into MoMϕs. MoMϕs in the murine liver can be further divided into two subgroups according to the expression level of Ly6C: $Ly6C^{hi}$ and $Ly6C^{lo}$ monocyte/macrophages (25). $CD11b^{hi}F4/80^{int}Ly6C^{hi}$ macrophages ($Ly6C^{hi}$ macrophages in short) are derived from recruited

$CCR2^{+}CX3CR1^{lo}Ly6C^{hi}$ monocytes and exert proinflammatory and profibrotic functions, while $CD11b^{hi}F4/80^{hi}Ly6C^{lo}$ macrophages ($Ly6C^{lo}$ macrophages in short) are converted from $Ly6C^{hi}$ macrophages induced by phagocytosis and are involved in anti-inflammatory and antifibrotic processes (29, 30). It should be noted that the $Ly6C^{hi}$ and $Ly6C^{lo}$ phenotypes comprise a new system for macrophage classification based on cell origin and surface makers. Conventionally, macrophages with different functions are classified as M1 and M2 macrophage subsets. M1 macrophages are known as classically activated macrophages with pro-inflammatory properties and participate in tissue damage and inflammation, whereas M2 macrophages are known as alternatively activated macrophages with anti-inflammatory properties and function to promote tissue repair and regeneration. M1 macrophages are mainly stimulated by IFN-γ or LPS, characterized by high expression of CD80, CD86, major histocompatibility complex II (MHC II), Toll-like receptor 4 (TLR4), and inducible nitric oxide synthase (iNOS) (31). Meanwhile, M2 macrophages can be stimulated by T helper 2 (Th2) cytokines such as interleukin 4 (IL-4) and IL-13 (32), with high expression of mannose receptor 1 (MRC1/CD206), CD163, arginase-1 (Arg1), chitinase 3-like 3 (Chil3/Ym1), found in inflammatory zone 1 (FIZZ1) (33). Among them, Chil3 and Fizz1 are the markers only expressed by M2 macrophages in mouse. In addition, M2 macrophages can be further subdivided into M2a, M2b, M2c, and M2d subtypes by distinct stimuli. M2a is induced by IL-4 and IL-13, M2b is induced by immune complex (IC), the M2c type is stimulated by IL-10, transforming growth factor-β (TGF-β) and glucocorticoids, and the M2d type is activated by IL-6, TLR ligands and adenosine (34). Macrophages can be polarized into different subsets in response to different local microenvironments and play essential roles in the initiation, progression and resolution of tissue inflammation and injury in various liver diseases (35).

3.2 The regulatory role of intrahepatic macrophages in liver fibrosis

In hepatic fibrosis, the activated macrophages secrete pro-inflammatory cytokines and chemokines and stimulate HSCs to transdifferentiate into myofibroblasts, which proliferate and produce ECM proteins (36). Although the activation of HSCs is thought to be a central driver of hepatic fibrogenesis (37, 38), hepatic macrophages have emerged as essential in the pathogenesis of liver fibrosis. Moreover, due to their heterogeneity and plasticity, macrophages can exert both pro- or anti-fibrotic effects by regulating the activation or the cell death of HSCs and the formation and degradation of matrix collagen (39, 40). In human and mouse models of diet-induced nonalcoholic steatohepatitis (NASH), the impaired macrophage-mediated clearance of necroptotic hepatocytes (necHCs) and increased activation of HSCs are responsible for liver fibrogenesis; hence, the reduced accumulation of necHCs in NASH liver could be a therapeutic strategy to treat hepatic fibrosis (41). Cai et al. further reported that c-mer tyrosine kinase (MerTK) signaling in macrophages activates HSCs to promote collagen synthesis and induces liver fibrosis through the ERK-TGFβ1 pathway (40). In bile duct ligation (BDL)-induced and carbon tetrachloride (CCl4)-induced liver fibrosis mouse models, the FGF12-mediated proinflammatory activation of hepatic macrophages could induce HSC activation mainly through the monocyte chemoattractant protein-1/chemokine (C-C motif) receptor 2 axis (42). The roles of MoMϕs in liver fibrosis were also investigated. For instance, the proportion of resident macrophages decreases during the process of inflammation and fibrogenesis, while that of the recruited MoMϕs ($CD11b^{high}F4/80^{mid}$ subsets) gradually increases during fibrogenesis (9), suggesting an important function of MoMϕs in liver fibrosis. De Souza et al. further demonstrated that the transplantation of bone marrow-derived $CD11b^{+}CD14^{+}$ monocytes caused the significant improvement of liver fibrosis by inhibiting oxidative stress and inflammation in a murine model of CCl4-induced chronic liver damage (43). In addition, liver fibrosis was attenuated by the transplantation of bone marrow-derived MSCs (BM-MSCs), and the therapeutic effect of BM-MSCs was attributed to promoting the $Ly6C^{hi}/Ly6C^{lo}$ subset conversion and $Ly6C^{lo}$ macrophage restoration through activating the antifibrogenic cytokine and apoptotic pathways (44). Similarly, prepolarized BMDMs also exhibit a therapeutic effect on liver fibrosis. For example, M1 BMDMs significantly ameliorated liver fibrosis by modulating the hepatic microenvironment to recruit endogenous macrophages into fibrotic liver, which showed the phenotype of $Ly6C^{lo}$ restorative macrophages (39). Compared with $Ly6C^{lo}$ macrophages, $Ly6C^{hi}$ macrophages exerted a pro-fibrogenic effect by activating HSCs through secreting various cytokines including TGF-β, platelet-derived growth factor (PDGF), TNF-α, IL-1β, monocyte chemotactic protein 1 (MCP1), CCL3, and CCL5 (36).

Taken together, hepatic macrophages play an important role in the initiation and progression of liver fibrosis. During this process, however, the function, metabolism and polarization of macrophages are regulated by various factors such as miRNAs, which ultimately affect the onset of liver disease. For instance, exosomal miR-690 derived from KCs inhibited inflammation in recruited hepatic macrophages in a mouse model of NASH (45). MiR-206 drove KCs toward M1 polarization, and promoted the recruitment of CD8+ T cells in HCC (46). In addition, miR-26a overexpression extensively inhibited the inflammation in both hepatocytes and KCs therefore attenuated HCC (47). MiR-155 knockdown in KCs could positively regulate the immunosuppressive function of KCs and prolong the survival of liver allografts. MiR-148a-enriched mesenchymal stem cell-derived exosomes (MSC-EXOs) modulated macrophages towards the anti-inflammatory phenotype and exerted ameliorative effects on liver fibrosis (48). In a mouse model of *Schistosomiasis japonicum*, miR-130a-3p promoted the differentiation of macrophages toward the Ly6Clo phenotype and alleviated liver granulomatous inflammation (49). The above studies demonstrate the diverse roles of miRNAs in

hepatic macrophages, influencing the pathology of liver diseases. The regulatory effect of miRNAs on macrophage polarization in other models and tissues will be discussed in more detail below.

4 The regulatory effect of miRNAs on macrophages

4.1 MiRNAs regulate the M1 phenotype polarization of macrophages

Extracellular vesicles (EVs) such as exosomes are cell-derived, membrane-bound organelles involved in intercellular communication. Exosomes play an important regulatory role in the progression of various liver diseases, delivering various biological components such as miRNAs, proteins and lipids to neighboring or distant cells (50). In a rat model of nonalcoholic fatty liver disease (NAFLD) induced by high-fat and high-cholesterol diet, the lipotoxic injury-induced release of miR-192-5p-enriched hepatocyte exosomes played a critical role in M1 macrophage activation; miR-192-5p drove macrophages to polarize towards the proinflammatory M1 phenotype through modulating the Rictor/Akt/FoxO1 signaling pathway, which resulted in hepatic inflammatory response, demonstrating that exosomal miR-192-5p is a key player in the NAFLD-mediated activation of M1 macrophages (51). However, miR-192-5p exhibited an inhibitory role in M1 macrophage polarization in a monosodium urate (MSU) crystal-induced mouse gouty arthritis (GA) model (52). Under the IFN-γ plus LPS-stimulated M1 polarization condition, the MiR-192-5p mimic stimulated RAW264.7 macrophages and resulted in a reduced expression of inflammatory cytokines TNF-α and IL-1β, decreased iNOS expression, and inhibited CD16/32 (M1 marker) expression; miR-192-5p blocked M1 macrophage activation by inhibiting epiregulin, thereby improving GA inflammatory response (52). It is highly likely that the opposite effect of miR-192-5p on the macrophage program in the two disease models is due to the difference in the origin of miRNA and the macrophages. MiR-199a-5p derived from EVs from human serum albumin (HSA)-induced HK-2 cells promoted M1 phenotype polarization by targeting the Klotho/TLR4 pathway, and contributed to the progression of diabetic nephropathy (53). Similarly, in high-fat diet-induced mouse models of NALFD, miR-9-5p was upregulated in lipotoxic extracellular vesicles and promoted M1 polarization by targeting glutaminyl transferase 2 (TGM2) (54). In addition, Ma et al. found that miR-9-5p promotes M1-type polarization by targeting NAD-dependent deacetylase sirtuin-1 (SIRT1) in a cecal ligation and puncture (CLP)-induced sepsis mouse model (55). Likewise, in a mouse model of osteoarthritis (OA), miR-9-5p could promote the progression of OA and M1 polarization by inhibiting SIRT1 expression *via* the NF-κB and AMPK signaling pathways (56). Recently, miR-146a-5p has been recognized as a key player in the field of cardiovascular research. Exosomes enriched with miR-146a-5p obtained from newborn mouse cardiomyocytes were used to treat macrophages, and the results showed that exosomal miR-146a-5p encouraged M1 macrophage polarization, while it inhibited M2 macrophage polarization by targeting TNF receptor-associated factor 6 (TRAF6) (57). In a mouse model of sepsis-related acute lung injury, exosomal miR-30d-5p of TNF-α-stimulated neutrophils promoted M1 macrophage polarization and induced macrophage pyroptosis through activating NF-κB signaling by targeting the suppressor of cytokine signaling (SOCS-1) and SIRT1 both *in vivo* and *in vitro* (58). However, miR-30d-5p-enriched exosomes from adipose-derived stem cells reversed acute ischemic stroke-induced, autophagy-mediated brain injury by suppressing M1 microglial polarization (59). EVs from adipose tissue-derived stem cells were found to attenuate LPS induced inflammation and sepsis by inhibiting M1 macrophage polarization, accompanied by the reduced expression of miR-148a-3p (60). MiR-148a-3p, as a novel downstream molecule of Notch signaling, could enhance M1 polarization through the PTEN/AKT pathway and thus induce pro-inflammatory responses *via* the activation of NF-κB signaling (60). MiR-33a is a lipid regulator of cholesterol and fatty acid metabolism in the cell. MiR-33 enriched in exosomes secreted by endothelin 1-stimulated human umbilical cord vein endothelial cells is transported to macrophages and directly targets NR4A transcription factors to activate M1 macrophages, which has therapeutic implications for atherosclerosis (61). In addition, miR-34a expression in lung macrophages was increased in a model of LPS-induced acute lung injury (ALI); miR-34a overexpression could promote the polarization of pro-inflammatory M1 phenotype and exacerbated ALI and inflammation by targeting kruppel-like factor 4 (KLF4) (62). MiR-34a expression was increased in mice treated with PD-1 inhibitor along with enhanced M1 polarization and cardiac injury, whereas treatment with miR-34a inhibitor reversed M1 polarization and cardiac injury through modulating the miR-34a/KLF4-signaling pathway (63). Similarly, in the context of cardiometabolic diseases, miR-34a could promote the development of atherosclerosis by stimulating M1 polarization *via* liver X receptor α (LXRα), while the inhibition of miR-34a could help the regression of atherosclerosis and reversed the diet-induced metabolic disorder (64). However, miR-34a exhibits different roles by inhibiting M1 polarization in some other diseases. For instance, miR-34a derived from adipocyte exosomes reduced the polarization of M1-type macrophages by inhibiting NLRP3 in a Ti particle-induced osteolysis mouse model (65). In addition, in a rat model of liver injury induced by long term co-exposure to DBP and BaP, miR-34a could inhibit the M1 phenotype and attenuate the disorder of inflammatory factors through the Notch signaling pathway (66). MiR-130b-3p has also been shown to block M1 polarization by blocking interferon regulatory factor 1 (IRF1), thus alleviating the inflammation of lung tissues in LPS-treated mice (67).

MiRNAs present in exosomes derived from tumors have also been shown to modulate M1 macrophage polarization, thereby influencing tumorigenesis. Moradiet al. found that overexpression of miR-130 and miR-33 in exosomes can inhibit tumor progression by promoting M2 to M1 macrophage polarization (68). In a co-culture of breast cancer cells and macrophages, treatment with exosomal miR-33 and miR-130 could significantly reduce the proliferation, invasion and migration of cancer cells, thus

suppressing breast cancer progression (69, 70). In addition, miR-200c could enhance granulocyte-macrophage colony-stimulating factor (GM-CSF)-mediated M1 macrophage polarization to inhibit the growth of mouse breast cancer Met-1 cells (71). MiR-125b showed the ability to reprogram tumor-associated macrophages (TAMs) into an antitumor/pro-inflammatory (M1) phenotype in non-small-cell lung cancer (NSCLC) model (72), which has significant implications for anticancer immunotherapy. MiR-125b also exhibited good anti-tumor effects in murine orthotopic breast cancer, which was attributed to its promotive effect on M1 polarization by targeting interferon regulatory factor 4 (IRF4) in macrophages, and suppressed tumor cells by targeting ETS proto-oncogene 1 and cyclin-J (73). The ability of some other miRNAs to regulate the polarization of M1 in other neoplastic diseases has also been shown, such as miR-9 (74), which was enriched in exosomes derived from human papillomavirus (HPV) positive head and neck squamous cell carcinoma (HNSCC). It could be transported into macrophages and induce the polarization of macrophages into the M1 phenotype by inhibiting the expression of PPARδ (74).

To sum up, a variety of miRNAs can regulate M1 polarization. Notably, a specific miRNA may play distinct roles in the polarization of macrophages in different diseases. As summarized in Table 1, miR-199a-5p, miR-9-5p, miR-146a-5p, miR-148a-3p, miR-33, miR-34a, miR-130, miR-200c, and miR-125b have been shown to promote M1, and miR-130b-3p to suppress M1 through inhibiting various factors. However, such as with miR-192-5p, miR-30d-5p, and miR-34a, the effects of miRNAs on macrophage polarization can be contrasting depending on the disease model, the source of miRNAs, and macrophages from different tissues.

4.2 MiRNAs regulate the M2 phenotype polarization of macrophages

It has been previously noted that some miRNAs are involved in modulating the pathogenesis of certain diseases, primarily by affecting the polarization of M1 macrophages. However, there are also miRNAs with a function in modulating disease pathogenesis by

TABLE 1 M1 macrophage polarization by miRNAs in various diseases.

disease	MiRNAs	Levels	Regulation of macrophage phenotype	Targets	references
NAFLD	miR-192-5p	↑ (in serum)	Promotes M1	Rictor	(51)
	miR-9-5p	↑ (in plasma)	Promotes M1	TGM2	(54)
GA	miR-192-5p	↓ (in serum)	Suppresses M1	EREG	(52)
DN	miR-199a-5p	↑ (in unrine)	Promotes M1	Klotho	(53)
OA	miR-9-5p	↑ (in synovial tissue)	Promotes M1	SIRT1	(55, 56)
MI	miR-146a-5p	↓ (in plasma)	Promotes M1, Suppresses M2	TRAF6	(57)
ALI	miR-30d-5p	↑ (in lung tissue)	Promotes M1	SOCS-1, SIRT1	(58)
	miR-34a	↑ (in lung tissue)	Promotes M1, Suppresses M2	KLF4	(62)
	miR-130b-3p	↓ (in lung tissue)	Suppresses M1	IRF1	(67)
AIS	miR-30d-5p	↓ (in serum)	Suppresses M1, Promotes M2	Beclin-1, Atg5	(59)
sepsis	miR-148a-3p	unknown	Promotes M1	PTEN	(60)
AS	miR-33	↑ (in exosome)	Promotes M1, Suppresses M2	NR4A, AMPK	(61)
	miR-34a	↑ (in atherosclerotic plaques)	Promotes M1, Suppresses M2	LXRα	(64)
cardiac injury	miR-34a	↑ (in heart tissue)	Promotes M1	KLF4	(63)
osteolysis	miR-34a	↑ (in macrophage of the osteolysis site)	Suppresses M1	NLRP3	(65)
liver injury	miR-34a	↓ (in liver tissue)	Suppresses M1, Promotes M2	unknown	(66)
breast cancer	miR-130, miR-33	↑ (in exosome)	Promotes M1, Suppresses M2	unknown	(68–70)
	miR-200c	↑ (in cancer cell line)	Promotes M1	ZEB1	(71)
	MiR-125b	unknown	Promotes M1	IRF4	(73)
NSCLC	MiR-125b	↑ (in lung tissue)	Promotes M1	unknown	(72)
HNSCC	miR-9	↑ (in exosome)	Promotes M1	PPARδ	(74)

AIS, acute ischemic stroke; ALI, acute lung injury; AMPK, AMP-activated protein kinase; AS, atherosclerosis; ATG5, autophagy related 5 homolog; DN, diabetic nephropathy; EREG, epiregulin; GA, gouty arthritis; HNSCC, head and neck squamous cell carcinoma; IRF1, interferon regulatory factor 1; IRF4, interferon regulatory factor 4; KLF4, Kruppel like factor 4; KLF6, Kruppel like factor 6; LXRα, Liver X Receptor α; MI, myocardial infarction; NAFLD, nonalcoholic fatty liver disease; NLRP3, NOD-like receptor protein 3; NR4A, Nerve Growth Factor IB-like Receptor; NSCLC, nonsmall cell lung cancer; OA, osteoarthritis; PPARδ, peroxisome proliferators-activated receptor δ; PTEN, phosphatase and tensin homolog; Rictor, rapamycin-insensitive companion of mammalian target of rapamycin; SIRT1, Sirtuin 1; SOCS1, suppressor of cytokine signaling1; TGM2, transglutaminase2; TRAF6, TNF receptor-associated factor 6; ZEB1, zinc finger E-box-binding homeobox 1.
The symbols ↑, ↓means increase and decrease, respectively.

regulating the polarization of macrophages into the M2 phenotype. As previously mentioned, miR-192-5p drives M1 phenotype polarization to exacerbate the hepatic inflammatory response in NAFLD (51). However, miR-192-5p could effectively rescue mice from coxsackievirus B3 (CVB3)-induced viral lethal myocarditis through switching myocardial-infiltrating macrophages to a predominant M2 phenotype by targeting interleukin-1 receptor-associated kinase 1 (IRAK1) (75). In addition, miR-146a was highly expressed in the M2 rather than the M1 macrophage phenotype. The overexpression of miR-146a resulted in decreased production of pro-inflammatory cytokines and increased expression of M2 marker genes (76, 77), which was different from the effects of miR-146a on M1 polarization induced by PM2.5 (78). Similarly, miR-146a acted as an anti-inflammatory miRNA in the pathogenesis of diabetic nephropathy (DN) by promoting the expression of M2 markers (79), while it exerted a protective role *via* regulating the differentiation of macrophages into M2 cells in some other disease models, such as murine hepatic schistosomiasis (80), a cecal ligation and puncture-induced sepsis model (81), or experimental autoimmune encephalomyelitis (EAE) (82). In addition, miR-99a could promote M2 polarization and inhibit allergic airway inflammation by targeting TNF-α (83), and could also be used as a therapeutic agent to reduce adipose tissue inflammation and improve insulin sensitivity in diabetic mice (84). MiR-511-3p, encoded by the Mrc1/CD206 gene, has also been proven to reduce cockroach allergen-induced lung inflammation and promote M2 macrophage polarization by targeting CCL2 *via* the RhoA/ROCK axis or prostaglandin D_2 synthase (Ptgds) (85, 86). MiR-93-5p, which is upregulated in M2 macrophage exosomes, exerts a renoprotective effect on LPS-induced podocyte injury by targeting TLR4 (87). MiR-93 has been shown to promote angiogenesis and reduce tissue loss in experimental models of peripheral arterial disease (PAD), which is because it promotes and sustains M2-like polarization even under M1-like polarizing settings by targeting interferon regulatory factor-9 to diminish IRG1-itaconic acid synthesis (88). MiR-21-5p, originating from MSC-EXOs, enhances macrophage polarization to the M2 phenotype, thereby reducing inflammation and preventing myocardial ischemia-reperfusion (I/R) injury (89). Likewise, MSC-EXOs were also conferred cardioprotective efficacy *via* shuttling miR-182 that modifies the polarization of M1 macrophages to M2 macrophages by targeting TLR4 (90). In addition, miR-21a could enhance miR-200c methylation and inhibit the expression of two tumor suppressor genes, miR-200c and phosphatase and angiotensin homologue (PTEN), thereby promoting M2 macrophage transformation in the tumor microenvironment (91). In a NASH-associated model of hepatic steatosis, the deficiency of miR-141 and miR-200c resulted in reduced hepatic inflammation, as macrophages polarized toward an M2 anti-inflammatory state with increased Arg1 and IL-10 levels and reduced M1 marker iNOS (92).

Similar to the aforementioned miRNAs that regulate M1 phenotype polarization and thus influence tumorigenesis, some miRNAs influence tumorigenesis primarily by affecting M2 macrophage polarization. MiR-195-5p, functioning as an anticancer agent, could inhibit M2-like TAM polarization in colorectal cancer (CRC) by regulating NOTCH2-mediated tumor cell epithelial-mesenchymal transition (EMT) and suppressing GATA3-mediated IL-4 secretion in CRC cells (93). Furthermore, MiR-770 derived from an exosome of NSCLC cell inhibited the migration of NSCLC by blocking M2 macrophage polarization through targeting MAP3K1 (94). MiR-935 also downregulated M2-like TAM by inhibiting C/EBPβ (95). Tumor-derived exosomal miR-934 induced macrophage M2 polarization by regulating PTEN expression and activating the PI3K/AKT signaling pathway, and the polarized M2 macrophages could further induce premetastatic niche formation and CXCL13 secretion, leading to colorectal cancer liver metastasis (CRLM) and secondary hepatocellular carcinoma (96). Similar to miR-934, the miR-25-3p, miR-130b-3p and miR-425-5p, derived from exosomes of CRC cells and upregulated by CXCL12/CXCR4 axis activation, also regulated the M2 polarization of macrophages through the PTEN/PI3K/Akt signaling pathway, and the serum levels of these miRNAs correlated with the progression and metastasis of CRLM (97). MiR-21-5p and miR-200a derived from small extracellular vesicles (sEVs) synergistically induced M2-like TAM polarization through the PTEN/AKT and SCOS1/STAT1 pathways leading to decreased $CD8^+$ T cell activity, and thus contributed to immune escape and CRC tumor growth (98). In addition, miR-21-5p in EVs secreted in esophageal squamous cell carcinoma (ESCC) promoted the activation of M2 macrophages and exacerbated ESCC through the PTEN/AKT/STAT6 pathway (99). MiR-1246 has been detected to be highly expressed in the serum exosomes of colon cancer patients (100); miR-1246-enriched exosomes from TP53 mutant (mutp53) colon cancer cells could trigger the reprogramming of neighboring macrophages to a tumor-supporting and anti-inflammatory state, which was associated with poor survival in colon cancer patients (101). MiR-1246, as the most enriched miRNA in hypoxic glioma-derived exosomes (H-GDEs), induced M2 macrophage polarization by targeting telomeric repeat sequence binding factor 2 interaction protein (TERF2IP) *via* the STAT3 and NF-κB pathways, and the polarized M2 macrophages subsequently promoted glioma proliferation, migration and invasion. Therefore, miR-1246 may be used as a target in anti-glioma immunotherapy (102). Similarly, miR-182 in macrophages induced the M2 polarization of TAMs through the TGFβ/miR-182/TLR4 axis, and the conditional knockout of miR-182 in macrophages impaired M2-like TAMs and breast tumor development (103). Alternatively, the breast cancer cell-derived exosome miR-138-5p was delivered to TAMs in a mouse breast cancer model to stimulate M2 polarization and inhibit M1 polarization, which could also be used as a target for breast cancer therapy (104). Hypoxia-induced lung cancer cell-derived EV miR-103a increased M2-type polarization, which was associated with reduced PTEN and increased activation of STAT3 and AKT. In contrast, the inhibition of miR-103a could effectively block

hypoxic cancer-mediated M2-type polarization, suggesting the potential of EV inhibition in lung cancer immunotherapy (105, 106). Similarly, high miR-301a-3p expression in exosomes from pancreatic cancer cells resulting from a hypoxic microenvironment induced macrophage M2 polarization through the activation of PTEN/PI3Kγ signaling pathway to promote pancreatic cancer progression (107). It has also been reported that endometriosis (EMS)-derived exosomal miR-301a-3p promoted the M2 polarization of macrophages *via* regulating the PTEN-PI3K axis (108).

As discussed above, many types of miRNAs were demonstrated to have the ability to regulate M2 polarization. As summarized in Table 2, the miRNAs with a promotive effect include miR-192-5p, miR-146a, miR-93-5p, miR-146a, miR-99a, miR-511-3p, miR-93, miR-21-5p, miR-182, miR-25-3p, miR-130b-3p, miR-425-5p, miR-21-5p, miR-200a, miR-934, miR-1246, miR-138-5p, miR-103a, and

TABLE 2 M2 macrophage polarization by miRNAs in various diseases.

disease	MiRNAs	Levels	Regulation of macrophage phenotype	Targets	references
VM	miR-192-5p	↑ (in heart tissue)	Promotes M2	IRAK1	(75)
DN	miR-146a	↑ (in spleen tissue)	Promotes M2	Traf6, Irak1	(79)
	miR-93-5p	↑ (in M2 macrophage)	Promotes M2	TLR4	(87)
hepatic schistosomiasis	miR-146a	↑ (in liver tissue)	Promotes M2, Suppresses M1	Notch1, STAT1	(80)
sepsis	miR-146a	↑ (in exosome)	Promotes M2	IRAK1, TRAF6, IRF5	(81)
EAE	miR-146a	↑ (in central nervous system)	Promotes M2	TLR2, IRAK1	(82)
AAI	MiR-99a	↑ (in lung tissue)	Promotes M2, Suppresses M1	TNF-α	(83)
	miR-511-3p	↑ (in lung tissue)	Promotes M2	CCL2, Ptgds	(85, 86)
PAD	miR-93	↑ (in muscle)	Promotes M2	IRF9	(88)
myocardial I/R injury	miR-21-5p	↑ (in heart tissue)	Promotes M2	unknown	(89)
	miR-182	↑ (in heart tissue)	Promotes M2	TLR4	(90)
NASH	miR-141/200c	↑ (in liver tissue)	Suppresses M2, Promotes M1	unknown	(92)
CRC	miR-195-5p	↓ (in CRC tissue)	Suppresses M2	Notch2	(93)
	miR-25-3, miR-130b-3p, miR-425-5p	↑ (in CRC tissue)	Promotes M2	PTEN	(97)
	miR-21-5p, miR-200a	↑ (in CRC tissue)	Promotes M2	PTEN, SOCS1	(98)
NSCLC	miR-770	↓ (in lung tissue)	Suppresses M2	MAP3K1	(94)
solid tumors	miR-935	↓ (in the monocytes)	Suppresses M2	C/EBPβ	(95)
CRLM	miR-934	↑ (in CRC tissue)	Promotes M2	PTEN	(96)
ESCC	miR-21-5p	↑ (in CRC tissue)	Promotes M2	PTEN	(99)
colon cancer	miR-1246	↑ (in serum)	Promotes M2	TERF2IP	(100–102)
breast cancer	miR-182	↑ (in M2 macrophages of breast tissue)	Promotes M2	TLR4	(103)
	miR-138-5p	↑ (in breast tissue)	Promotes M2, Suppresses M1	KDM6B	(104)
lung cancer	miR-103a	↑ (in lung tissue)	Promotes M2	PTEN	(105, 106)
pancreatic cancer	miR-301a-3p	↑ (in pancreatic cancer cells)	Promotes M2	PTEN	(107)
EMS	miR-301a-3p	↑ (in ectopic endometrial tissues)	Promotes M2	PTEN	(108)

AAI, allergic airway inflammation; C/EBPβ, CCAAT enhancer binding protein; Ccl2, C-C motif chemokine ligand 2; CRLM, colorectal cancer liver metastasis; DN, diabetic nephropathy; EAE, experimental autoimmune encephalomyelitis;EMS,endometriosis; ESCC, esophageal squamous cell carcinoma; IRAK1, Interleukin 1 Receptor Associated Kinase 1; IRF9, interferon regulatory factor 9; KDM6B, lysine (K)-specific demethylase 6B; MAP3K1, mitogen activated protein kinase kinase kinase 1; NASH, nonalcoholic steatohepatitis; NSCLC, nonsmall cell lung cancer; PAD, peripheral arterial disease; PTEN, phosphatase and tensin homolog; SOCS1, suppressor of cytokine signaling 1; STAT1, signal transducer and activator of transcription 1; TERF2IP, telomeric repeat binding factor 2 interacting protein; TLR4, Toll-like receptor4; TNF-α, tumor necrosis factor-α; TRAF6, TNF receptor associated factor 6; VM, viral myocarditis.
The symbols ↑, ↓means increase and decrease, respectively.

miR-301a, while those with the ability to suppress M2 through inhibiting various factors are miR-141/200c, miR-195-5p, miR-770, miR-935.

5 The role of miRNAs and macrophages in liver fibrosis

In recent years, the involvement of miRNAs in liver disease has received extensive attention. A large number of studies have shown that the expression level of miRNAs in the serum and liver tissue of patients with liver fibrosis is significantly changed. MiRNAs are implicated in the liver fibrosis process by affecting the proliferation, apoptosis and activation of HSCs, immune cells and hepatocytes (109). EVs such as exosomes represent an important mode of intercellular communication, serving as cargo carriers between cell membranes and cytoplasmic proteins, lipids and RNA. MiRNAs can be packaged into exosomes and secreted from macrophages to affect the process of liver fibrosis. The macrophage-derived exosomal miRNAs regulate the activation and apoptosis of HSCs involved in the pathology of liver fibrosis are summarized in Figure 1. It was reported that the microRNA Csi-let-7a-5p delivered by EVs from *Clonorchis sinensis* can promote the activation of M1-like macrophages and contribute to the biliary injuries and fibrosis by targeting the *Socs1*- and *Clec7a*- modulated NF-κB signaling pathway (110). Chen et al. used a mouse model of CCl4-induced liver fibrosis to demonstrate that the expression of exosomal miR-500 was upregulated in LPS-induced macrophages, and exosomal miR-500 overexpression could promote the proliferation and activation of HSCs and accelerate liver fibrosis by inhibiting mitochondrial fusion protein 2 (MFN2) (111). MiR-103-3p in exosomes secreted by LPS-treated THP-1 macrophages can promote the activation and proliferation of HSCs by targeting KLF4, and is involved in the crosstalk between macrophages and HSCs during the progression of liver fibrosis (112). In patients with NAFLD, myeloid-specific IL-6 signaling enhanced the release of miR-223-enriched exosomes from macrophages, which transferred antifibrotic miR-223 to hepatocytes to reduce the expression of pro-fibrotic transcriptional activator with PDZ-binding motifs (TAZ) in hepatocytes to inhibit liver fibrosis (113). During the development of NASH, miR-690 expression was significantly lower in mouse and human NASH livers compared to controls; the KC-specific KO of miR-690 increased NASH development, whereas miR-690 therapy restored specific KC functions by targeting NADK and led to reduced fibrosis and steatosis (45). Similarly, it was found that serum exosomes from NASH patients contained decreased levels of miRNA-411-5p. Further investigation revealed that exosomal miR-411-5p from M2 macrophages could inhibit the activation of HSCs. Additionally, miR-411-5p was found to directly downregulate the expression of Calmodulin-Regulated Spectrin-Associated Protein 1 (*CAMSAP1*) to inactivate HSCs (114). CCl4-induced liver fibrosis model, exosomes derived from relaxin-treated macrophages exhibited a potent antifibrogenic effect, which was primarily attributed to miR-30a-5p (115). MiR-30a-5p suppressed the activity of the ASK1, which is known to be involved in the activation of HSCs. This in turn led to the restoration of PPAR-γ activity in the activated HSCs (115). Furthermore, restorative $Ly6C^{lo}$ macrophages showed a higher expression of miR-30a-5p compared to $Ly6C^{hi}$ macrophages, and miR-30a-5p synergized with relaxin gene therapy to achieve an enhanced antifibrosis effect (115).

In addition to miRNAs in macrophage-derived exosomes that are involved in liver fibrosis, some miRNAs may mediate the pathology of liver fibrosis by regulating macrophage polarization (summarized in Figure 2). MiR-155 was reported to be involved in high fat-high cholesterol-high sugar (HF-HC-HS) diet-induced steatosis and liver fibrosis, as miR-155 knockout mice showed significantly less liver injury, decreased steatosis, and attenuation in fibrosis under HF-HC-

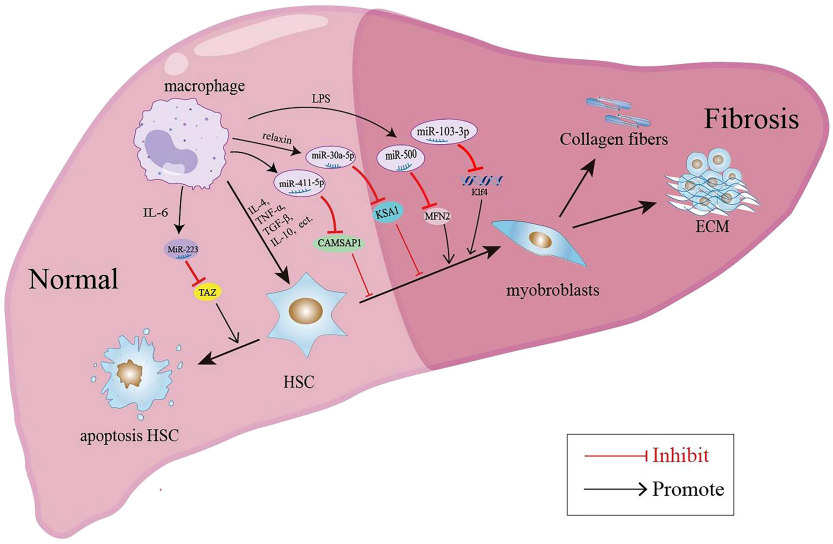

FIGURE 1
Macrophage-derived exosomal miRNAs regulate the activation and apoptosis of HSCs involved in the pathology of liver fibrosis.

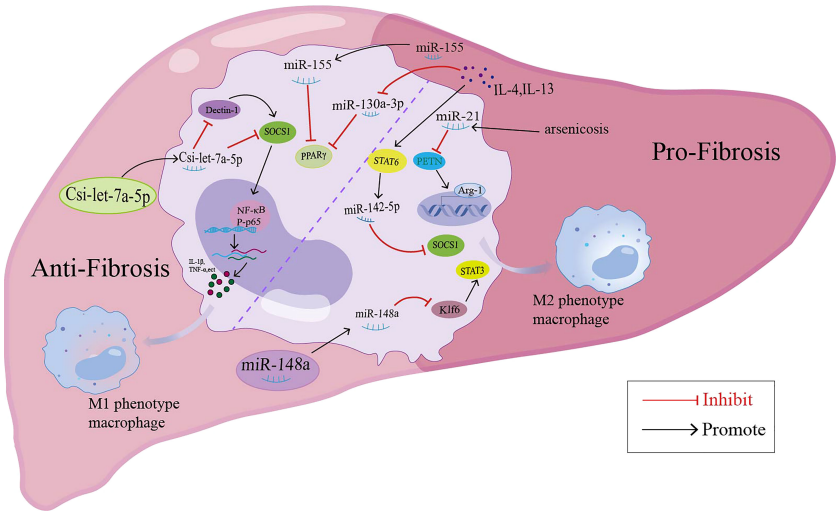

FIGURE 2
miRNAs modulate the macrophage polarization and participate in the liver fibrosis through different signaling pathway.

HS diet or CCl4 treatment, and KCs isolated from miR-155 KO mice displayed the M2 phenotype when exposed to even M1 priming conditions (116, 117). In addition, serum exosomal miR-155 levels in patients with hepatic fibrosis and a hepatic fibrosis rat model were positively correlated with the severity of liver fibrosis, and miR-155 could be used as a biomarker for the diagnosis and progression of liver fibrosis (118). In a murine model of arsenic-induced liver fibrosis, the level of miR-21 and Arg-1 were increased; however, miR-21 deficiency in mice showed attenuated liver fibrosis and M2 polarization compared with WT mice exposed to arsenite (119). MiR-20a-5p was downregulated during liver fibrosis in human and CCl4-induced mouse model samples. Moreover, miR-20a-5p downregulation in liver fibrosis led to the activation of TGF-β signaling pathway by targeting TGFBR2, accompanied by the activation of hepatic macrophages and the production of ECM by HSCs. The reintroduction of miR-20a-5p may be a therapeutic regimen for clinical intervention in hepatic fibrosis (9). MSC-EXOs have been demonstrated to exhibit a protective effect against liver fibrosis. In the CCl4-induced liver fibrosis mouse model, miR-148a enriched MSC-EXOs have been shown to regulate intrahepatic macrophage through KLF6/STAT3 signaling (48). MiR-148a showed the ability to suppress pro-inflammatory macrophages and promote anti-inflammatory macrophages, ultimately helping to reduce the severity of liver fibrosis (48). MiR-130a-3p is an antifibrotic miRNA with decreased expression in the serum of patients with cirrhosis and the liver of mice with schistosomiasis. Overexpression of miR-130a-3p by the lentivirus vector (LV-miR-130a-3p) could alleviate liver granulomatous inflammation and liver fibrosis; moreover, LV-miR-130a-3p promoted the polarization of macrophages towards the restorative Ly6C^{lo} phenotype, inhibited the activation and proliferation of HSCs and also induced the apoptosis of HSCs by inhibiting MAPK1 expression (49). MiR-130a-3p also cooperated with miR-142-5p to control macrophage polarization. The transduction of miR-130a-3p mimics and miR-142-5p anti-sense oligonucleotides (ASO) in IL-4-treated mouse macrophages synergistically inhibited M2 polarization and their profibrogenic activities in both humans and mice, and miR-142-5p and miR-130a-3p mediated M2 macrophages by targeting SOCS1 and PPARγ, respectively (120). During the spontaneous resolution of liver inflammation (SRLI), neutrophil-derived miR-223 downregulated Nlrp3 expression in hepatic proinflammatory macrophages and induced their alternative activation into a restorative phenotype, which released IL-10 thus mitigating fibrogenesis by reducing the activation of HSCs and collagen formation (121). Similarly, in fibrotic NASH induced by long-term administration of a high-fat, fructose and cholesterol (FFC) diet, treatment with synthetic miR-223 analog miR-223-3p significantly alleviated the fibrosis development and activation of HSCs by disrupting the activation of the NLRP3 inflammasome (122).

6 Conclusions

Searching the PubMed database using miRNAs and liver fibrosis as keywords yielded more than 1600 publications, while this number was nearly 3600 when using ‘macrophages’ and ‘liver fibrosis’. Therefore, both miRNAs and macrophages are research hotpots in the field of liver fibrosis. The pathogenesis of liver fibrosis is considered to be a complex, multifactorial process. For instance, activated HSCs are a major contributor to liver fibrosis because they produce excessive amounts of ECM as a result of long-term liver injury. In addition to HSCs, macrophages are also considered a ‘double-edged sword’ in the development of fibrosis. Hepatic macrophages are composed of several heterogeneous subpopulations, which can be classified as ‘pro-inflammatory’ M1 or ‘immunoregulatory’ M2 macrophages according to their function and phenotype. Given that miRNAs epigenetically fine-tune the expression of hundreds of target mRNA, there is growing interest in the regulatory role of miRNAs in macrophage activation, polarization, tissue infiltration, and the mitigation of inflammation.

MiRNAs play different roles in the pathogenesis of multiple diseases; They have the potential as promising biomarkers and therapeutic targets in the treatment of various illnesses. However, the same miRNA may play different or even opposite roles in different pathological processes. For example, miR-192-5p-enriched hepatocyte exosomes promoted M1 phenotype polarization in NAFLD (51); however, miR-192-5p suppressed M1 macrophage polarization in a MSU crystal-induced mouse GA model (52). The exosomal miR-30d-5p of TNF-α-stimulated neutrophils promoted M1 macrophage polarization in a mouse model of sepsis-related acute lung injury (58), whereas miR-30d-5p-enriched exosome from the adipose-derived stem cell suppressed M1 microglial polarization in acute ischemic stroke-induced brain injury (59). These disease-specific functions of miR-192-5p and miR-30d-5p on macrophage polarization may be attributed to the difference in the origin of miRNA-enriched exosome and the disease microenvironment. Although numerous studies have shown that both miRNAs and macrophages are involved in the pathogenesis of liver diseases, the regulatory role of miRNAs in macrophage polarization has also been the focus of research. However, the mechanism of how miRNAs mediate the activation and polarization of macrophages and thus affect the progression of liver fibrosis remains unclear. Some miRNAs (i.e., miR-155, miR-21, miR-20a-5p, miR-148a, miR-130a-3p, and miR-223) can regulate macrophage polarization in liver fibrosis, while relevant studies are mainly limited to animal experiments, so further research is needed to test whether these miRNAs can be applied in clinical liver fibrosis-associated diseases. Due to the dual complexity of macrophage polarization and the pathogenesis of liver fibrosis, it is not feasible to study the pathology of liver fibrosis only based on miRNA or macrophages. A more comprehensive understanding of the cell-specific functions of miRNAs in liver fibrosis through the modulation of macrophage polarization is necessary, which can help identify novel diagnostic targets and design feasible miRNA-based therapies for liver fibrosis.

Author contributions

BZ and QG organized the article. WY and SW wrote the draft. YW, HC, HN, LL and XZ participated in conception and discussion of the article. XZ and BZ supervised the manuscript writing and edited the language, figure and table. WY and SW contributed equally to write the manuscript. All authors contributed to the article and approved the submitted version.

Funding

This work was supported by National Natural Science Foundation of China (Grant no. 82270893), Science and Technology Research Project of Education Department of Hubei Province (Grant no. D20211305), Medical and Health Science and Technology Program of Jingzhou (Grant no. 2022HC75), and Joint Foundation of Medical Research of Yangtze University (Grant no. WJ2019-14).

Conflict of interest

The authors declare that the research was conducted in the absence of any commercial or financial relationships that could be construed as a potential conflict of interest.

Publisher's note

References

1. Koyama Y, Brenner D. Liver inflammation and fibrosis. *J Clin Invest* (2017) 127:55–64. doi: 10.1172/JCI88881

2. George J, Tsuchishima M, Tsutsumi M. Molecular mechanisms in the pathogenesis of n-nitrosodimethylamine induced hepatic fibrosis. *Cell Death Disease* (2019) 10:18. doi: 10.1038/s41419-018-1272-8

3. Roehlen N, Crouchet E, Baumert T. Liver fibrosis: mechanistic concepts and therapeutic perspectives. *Cells* (2020) 9:875. doi: 10.3390/cells9040875

4. Liu M, Hu Y, Yuan Y, Tian Z, Zhang C. γδT cells suppress liver fibrosis *via* strong cytolysis and enhanced NK cell-mediated cytotoxicity against hepatic stellate cells. *Front Immunol* (2019) 10:477. doi: 10.3389/fimmu.2019.00477

5. Krenkel O, Tacke F. Liver macrophages in tissue homeostasis and disease. *Nat Rev Immunol* (2017) 17:306–21. doi: 10.1038/nri.2017.11

6. Kandil R, Merkel O. Recent progress of polymeric nanogels for gene delivery. *Curr Opin Colloid Interface Sci* (2019) 39:11–23. doi: 10.1016/j.cocis.2019.01.005

7. Caviglia J, Yan J, Jang M, Gwak G, Affo S, Yu L, et al. MicroRNA-21 and dicer are dispensable for hepatic stellate cell activation and the development of liver fibrosis. *Hepatol (Baltimore Md)* (2018) 67:2414–29. doi: 10.1002/hep.29627

8. Nelson M, O'Connell R. MicroRNAs: At the interface of metabolic pathways and inflammatory responses by macrophages. *Front Immunol* (2020) 11:1797. doi: 10.3389/fimmu.2020.01797

9. Fu X, Qie J, Fu Q, Chen J, Jin Y, Ding Z. miR-20a-5p/TGFBR2 axis affects pro-inflammatory macrophages and aggravates liver fibrosis. *Front Oncol* (2020) 10:107. doi: 10.3389/fonc.2020.00107

10. Saliminejad K, Khorram Khorshid H, Soleymani Fard S, Ghaffari S. An overview of microRNAs: biology, functions, therapeutics, and analysis methods. *J Cell Physiol* (2019) 234:5451–65. doi: 10.1002/jcp.27486

11. Wang X, He Y, Mackowiak B, Gao B. MicroRNAs as regulators, biomarkers and therapeutic targets in liver diseases. *Gut* (2021) 70:784–95. doi: 10.1136/gutjnl-2020-322526

12. Stavast C, Erkeland S. The non-canonical aspects of MicroRNAs: many roads to gene regulation. *Cells* (2019) 8:1465. doi: 10.3390/cells8111465

13. Tajbakhsh A, Bianconi V, Pirro M, Gheibi Hayat S, Johnston T, Sahebkar A. Efferocytosis and atherosclerosis: regulation of phagocyte function by MicroRNAs. *Trends Endocrinol Metabolism: TEM* (2019) 30:672–83. doi: 10.1016/j.tem.2019.07.006

14. Paul P, Chakraborty A, Sarkar D, Langthasa M, Rahman M, Bari M, et al. Interplay between miRNAs and human diseases. *J Cell Physiol* (2018) 233:2007–18. doi: 10.1002/jcp.25854

15. Tadokoro T, Morishita A, Masaki T. Diagnosis and therapeutic management of liver fibrosis by MicroRNA. *Int J Mol Sci* (2021) 22:8139. doi: 10.3390/ijms22158139

16. Conte E. Targeting monocytes/macrophages in fibrosis and cancer diseases: therapeutic approaches. *Pharmacol Ther* (2021) 234:108031. doi: 10.1016/j.pharmthera.2021.108031

17. Mass E, Ballesteros I, Farlik M, Halbritter F, Günther P, Crozet L, et al. Specification of tissue-resident macrophages during organogenesis. *Sci (New York NY)* (2016) 353:aaf4238. doi: 10.1126/science.aaf4238

18. Deppermann C, Kratofil R, Peiseler M, David B, Zindel J, Castanheira F, et al. Macrophage galactose lectin is critical for kupffer cells to clear aged platelets. *J Exp Med* (2020) 217:e20190723. doi: 10.1084/jem.20190723

19. Scott C, Guilliams M. The role of kupffer cells in hepatic iron and lipid metabolism. *J Hepatol* (2018) 69:1197–9. doi: 10.1016/j.jhep.2018.02.013

20. Abdullah Z, Knolle P. Liver macrophages in healthy and diseased liver. *Pflugers Archiv: Eur J Physiol* (2017) 469:553–60. doi: 10.1007/s00424-017-1954-6

21. Soucie E, Weng Z, Geirsdóttir L, Molawi K, Maurizio J, Fenouil R, et al. Lineage-specific enhancers activate self-renewal genes in macrophages and embryonic stem cells. *Sci (New York NY)* (2016) 351:aad5510. doi: 10.1126/science.aad5510

22. Gomez Perdiguero E, Klapproth K, Schulz C, Busch K, Azzoni E, Crozet L, et al. Tissue-resident macrophages originate from yolk-sac-derived erythro-myeloid progenitors. *Nature* (2015) 518:547–51. doi: 10.1038/nature13989

23. Shim YR, Jeong WI. Recent advances of sterile inflammation and inter-organ cross-talk in alcoholic liver disease. *Exp Mol Med* (2020) 52:772–80. doi: 10.1038/s12276-020-0438-5

24. Lu T, Yang T, Zhong C, Shen C, Lin W, Gu G, et al. Dual effect of hepatic macrophages on liver ischemia and reperfusion injury during liver transplantation. *Immune Netw* (2018) 18:e24. doi: 10.4110/in.2018.18.e24

25. Wen Y, Lambrecht J, Ju C, Tacke F. Hepatic macrophages in liver homeostasis and diseases-diversity, plasticity and therapeutic opportunities. *Cell Mol Immunol* (2021) 18:45–56. doi: 10.1038/s41423-020-00558-8

26. Scott CL, Zheng F, De Baetselier P, Martens L, Saeys Y, De Prijck S, et al. Bone marrow-derived monocytes give rise to self-renewing and fully differentiated kupffer cells. *Nat Commun* (2016) 7:10321. doi: 10.1038/ncomms10321

27. Theurl I, Hilgendorf I, Nairz M, Tymoszuk P, Haschka D, Asshoff M, et al. On-demand erythrocyte disposal and iron recycling requires transient macrophages in the liver. *Nat Med* (2016) 22:945–51. doi: 10.1038/nm.4146

28. Tacke F, Zimmermann H. Macrophage heterogeneity in liver injury and fibrosis. *J Hepatol* (2014) 60:1090–6. doi: 10.1016/j.jhep.2013.12.025

29. Gombozhapova A, Rogovskaya Y, Shurupov V, Rebenkova M, Kzhyshkowska J, Popov S, et al. Macrophage activation and polarization in post-infarction cardiac remodeling. *J Biomed Sci* (2017) 24:13. doi: 10.1186/s12929-017-0322-3

30. Ramachandran P, Pellicoro A, Vernon MA, Boulter L, Aucott RL, Ali A, et al. Differential ly-6C expression identifies the recruited macrophage phenotype, which orchestrates the regression of murine liver fibrosis. *Proc Natl Acad Sci U S A* (2012) 109:E3186–95. doi: 10.1073/pnas.1119964109

31. Saradna A, Do D, Kumar S, Fu Q, Gao P. Macrophage polarization and allergic asthma. *Trans Res: J Lab Clin Med* (2018) 191:1–14. doi: 10.1016/j.trsl.2017.09.002

32. Murray P. Macrophage polarization. *Annu Rev Physiol* (2017) 79:541–66. doi: 10.1146/annurev-physiol-022516-034339

33. Rőszer T. Understanding the mysterious M2 macrophage through activation markers and effector mechanisms. *Mediators Inflamm* (2015) 2015:816460. doi: 10.1155/2015/816460

34. Wang L, Zhang S, Wu H, Rong X, Guo J. M2b macrophage polarization and its roles in diseases. *J Leukoc Biol* (2019) 106:345–58. doi: 10.1002/JLB.3RU1018-378RR

35. van der Heide D, Weiskirchen R, Bansal R. Therapeutic targeting of hepatic macrophages for the treatment of liver diseases. *Front Immunol* (2019) 10:2852. doi: 10.3389/fimmu.2019.02852

36. Tsuchida T, Friedman S. Mechanisms of hepatic stellate cell activation. *Nat Rev Gastroenterol Hepatol* (2017) 14:397–411. doi: 10.1038/nrgastro.2017.38

37. Khomich O, Ivanov A, Bartosch B. Metabolic hallmarks of hepatic stellate cells in liver fibrosis. *Cells* (2019) 9:24. doi: 10.3390/cells9010024

38. Dewidar B, Meyer C, Dooley S, Meindl-Beinker A. TGF-β in hepatic stellate cell activation and liver fibrogenesis-updated 2019. *Cells* (2019) 8:1419. doi: 10.3390/cells8111419

39. Ma P, Gao C, Yi J, Zhao J, Liang S, Zhao Y, et al. Cytotherapy with M1-polarized macrophages ameliorates liver fibrosis by modulating immune microenvironment in mice. *J Hepatol* (2017) 67:770–9. doi: 10.1016/j.jhep.2017.05.022

40. Cai B, Dongiovanni P, Corey KE, Wang X, Shmarakov IO, Zheng Z, et al. Macrophage MerTK promotes liver fibrosis in nonalcoholic steatohepatitis. *Cell Metab* (2020) 31:406–21.e7. doi: 10.1016/j.cmet.2019.11.013

41. Shi H, Wang X, Li F, Gerlach BD, Yurdagul AJr., Moore MP, et al. CD47-SIRPα axis blockade in NASH promotes necroptotic hepatocyte clearance by liver macrophages and decreases hepatic fibrosis. *Sci Transl Med* (2022) 14:eabp8309. doi: 10.1126/scitranslmed.abp8309

42. Li S, Zhou B, Xue M, Zhu J, Tong G, Fan J, et al. Macrophage-specific FGF12 promotes liver fibrosis progression in mice. *Hepatology* (2023) 77:816–33. doi: 10.1002/hep.32640

43. de Souza V, Pereira T, Teixeira V, Carvalho H, de Castro M, D'assunção C, et al. Bone marrow-derived monocyte infusion improves hepatic fibrosis by decreasing osteopontin, TGF-β1, IL-13 and oxidative stress. *World J Gastroenterol* (2017) 23:5146–57. doi: 10.3748/wjg.v23.i28.5146

44. Li Y, Shen S, Shao T, Jin M, Fan D, Lin A, et al. Mesenchymal stem cells attenuate liver fibrosis by targeting Ly6C macrophages through activating the cytokine-paracrine and apoptotic pathways. *Cell Death Discovery* (2021) 7:239. doi: 10.1038/s41420-021-00584-z

45. Gao H, Jin Z, Bandyopadhyay G, Cunha ERK, Liu X, Zhao H, et al. MiR-690 treatment causes decreased fibrosis and steatosis and restores specific kupffer cell functions in NASH. *Cell Metab* (2022) 34:978–90.e4. doi: 10.1016/j.cmet.2022.05.008

46. Liu N, Wang X, Steer CJ, Song G. MicroRNA-206 promotes the recruitment of CD8(+) T cells by driving M1 polarisation of kupffer cells. *Gut* (2022) 71:1642–55. doi: 10.1136/gutjnl-2021-324170

47. Tian Y, Zhang M, Fan M, Xu H, Wu S, Zou S, et al. A miRNA-mediated attenuation of hepatocarcinogenesis in both hepatocytes and kupffer cells. *Mol Ther Nucleic Acids* (2022) 30:1–12. doi: 10.1016/j.omtn.2022.08.036

48. Tian S, Zhou X, Zhang M, Cui L, Li B, Liu Y, et al. Mesenchymal stem cell-derived exosomes protect against liver fibrosis *via* delivering miR-148a to target KLF6/STAT3 pathway in macrophages. *Stem Cell Res Ther* (2022) 13:330. doi: 10.1186/s13287-022-03010-y

49. Liu L, Wang P, Wang Y, Zhang Y, Li C, Yang Z, et al. MiR-130a-3p alleviates liver fibrosis by suppressing HSCs activation and skewing macrophage to Ly6C phenotype. *Front Immunol* (2021) 12:696069. doi: 10.3389/fimmu.2021.696069

50. Devhare P, Ray R. Extracellular vesicles: novel mediator for cell to cell communications in liver pathogenesis. *Mol Aspects Med* (2018) 60:115–22. doi: 10.1016/j.mam.2017.11.001

51. Liu X, Pan Q, Cao H, Xin F, Zhao Z, Yang R, et al. Lipotoxic hepatocyte-derived exosomal MicroRNA 192-5p activates macrophages through Rictor/Akt/Forkhead box transcription factor O1 signaling in nonalcoholic fatty liver disease. *Hepatol (Baltimore Md)* (2020) 72:454–69. doi: 10.1002/hep.31050

52. An L, Yin F. MiR-192-5p suppresses M1 macrophage polarization *via* epiregulin (EREG) downregulation in gouty arthritis. *Tissue Cell* (2021) 73:101669. doi: 10.1016/j.tice.2021.101669

53. Jia Y, Zheng Z, Xue M, Zhang S, Hu F, Li Y, et al. Extracellular vesicles from albumin-induced tubular epithelial cells promote the M1 macrophage phenotype by targeting klotho. *Mol Ther* (2019) 27:1452–66. doi: 10.1016/j.ymthe.2019.05.019

54. Liu H, Niu Q, Wang T, Dong H, Bian C. Lipotoxic hepatocytes promote nonalcoholic fatty liver disease progression by delivering microRNA-9-5p and activating macrophages. *Int J Biol Sci* (2021) 17:3745–59. doi: 10.7150/ijbs.57610

55. Ma W, Zhang W, Cui B, Gao J, Liu Q, Yao M, et al. Functional delivery of lncRNA TUG1 by endothelial progenitor cells derived extracellular vesicles confers anti-inflammatory macrophage polarization in sepsis *via* impairing miR-9-5p-targeted SIRT1 inhibition. *Cell Death Disease* (2021) 12:1056. doi: 10.1038/s41419-021-04117-5

56. Wang J, Ma S, Yu J, Zuo D, He X, Peng H, et al. MiR-9-5p promotes M1 cell polarization in osteoarthritis progression by regulating NF-κB and AMPK signaling pathways by targeting SIRT1. *Int Immunopharmacol* (2021) 101:108207. doi: 10.1016/j.intimp.2021.108207

57. Chen C, Cai S, Wu M, Wang R, Liu M, Cao G, et al. Role of cardiomyocyte-derived exosomal MicroRNA-146a-5p in macrophage polarization and activation. *Dis Markers* (2022) 2022:2948578. doi: 10.1155/2022/2948578

58. Jiao Y, Zhang T, Zhang C, Ji H, Tong X, Xia R, et al. Exosomal miR-30d-5p of neutrophils induces M1 macrophage polarization and primes macrophage pyroptosis in sepsis-related acute lung injury. *Crit Care (London England)* (2021) 25:356. doi: 10.1186/s13054-021-03775-3

59. Jiang M, Wang H, Jin M, Yang X, Ji H, Jiang Y, et al. Exosomes from MiR-30d-5p-ADSCs reverse acute ischemic stroke-induced, autophagy-mediated brain injury by promoting M2 Microglial/Macrophage polarization. *Cell Physiol Biochem* (2018) 47:864–78. doi: 10.1159/000490078

60. Bai X, Li J, Li L, Liu M, Liu Y, Cao M, et al. Extracellular vesicles from adipose tissue-derived stem cells affect notch-miR148a-3p axis to regulate polarization of macrophages and alleviate sepsis in mice. *Front Immunol* (2020) 11:1391. doi: 10.3389/fimmu.2020.01391

61. Zhang J, Zhao W, Xu L, Wang X, Li X, Yang X. Endothelium-specific endothelin-1 expression promotes pro-inflammatory macrophage activation by regulating miR-33/NR4A axis. *Exp Cell Res* (2021) 399:112443. doi: 10.1016/j.yexcr.2020.112443

62. Khan M, Singh P, Dohare R, Jha R, Rahmani A, Almatroodi S, et al. Inhibition of miRNA-34a promotes M2 macrophage polarization and improves LPS-induced lung injury by targeting Klf4. *Genes* (2020) 11:966. doi: 10.3390/genes11090966

63. Xia W, Zou C, Chen H, Xie C, Hou M. Immune checkpoint inhibitor induces cardiac injury through polarizing macrophages *via* modulating microRNA-34a/Kruppel-like factor 4 signaling. *Cell Death Disease* (2020) 11:575. doi: 10.1038/s41419-020-02778-2

64. Xu Y, Xu Y, Zhu Y, Sun H, Juguilon C, Li F, et al. Macrophage miR-34a is a key regulator of cholesterol efflux and atherosclerosis. *Mol Ther* (2020) 28:202–16. doi: 10.1016/j.ymthe.2019.09.008

65. Gao X, Ge J, Li W, Zhou W, Xu L, Geng D. miR-34a carried by adipocyte exosomes inhibits the polarization of M1 macrophages in mouse osteolysis model. *J Biomed Mater Res Part A* (2021) 109:994–1003. doi: 10.1002/jbm.a.37088

66. Chen W, Liu Y, Chen J, Song Y, You M, Yang G. Long-term co-exposure DBP and BaP causes imbalance in liver macrophages polarization *via* activation of notch

signaling regulated by miR-34a-5p in rats. *Chemico-biol Interactions* (2022) 359:109919. doi: 10.1016/j.cbi.2022.109919

67. Guo Q, Zhu X, Wei R, Zhao L, Zhang Z, Yin X, et al. miR-130b-3p regulates M1 macrophage polarization *via* targeting IRF1. *J Cell Physiol* (2021) 236:2008–22. doi: 10.1002/jcp.29987

68. Moradi-Chaleshtori M, Bandehpour M, Soudi S, Mohammadi-Yeganeh S, Hashemi S. *In vitro* and *in vivo* evaluation of anti-tumoral effect of M1 phenotype induction in macrophages by miR-130 and miR-33 containing exosomes. *Cancer Immunol Immunother: CII* (2021) 70:1323–39. doi: 10.1007/s00262-020-02762-x

69. Moradi-Chaleshtori M, Bandehpour M, Heidari N, Mohammadi-Yeganeh S, Mahmoud Hashemi S. Exosome-mediated miR-33 transfer induces M1 polarization in mouse macrophages and exerts antitumor effect in 4T1 breast cancer cell line. *Int Immunopharmacol* (2021) 90:107198. doi: 10.1016/j.intimp.2020.107198

70. Moradi-Chaleshtori M, Shojaei S, Mohammadi-Yeganeh S, Hashemi S. Transfer of miRNA in tumor-derived exosomes suppresses breast tumor cell invasion and migration by inducing M1 polarization in macrophages. *Life Sci* (2021) 282:119800. doi: 10.1016/j.lfs.2021.119800

71. Williams M, Christenson J, O'Neill K, Hafeez S, Ihle C, Spoelstra N, et al. MicroRNA-200c restoration reveals a cytokine profile to enhance M1 macrophage polarization in breast cancer. *NPJ Breast Cancer* (2021) 7:64. doi: 10.1038/s41523-021-00273-1

72. Parayath N, Parikh A, Amiji M. Repolarization of tumor-associated macrophages in a genetically engineered nonsmall cell lung cancer model by intraperitoneal administration of hyaluronic acid-based nanoparticles encapsulating MicroRNA-125b. *Nano Lett* (2018) 18:3571–9. doi: 10.1021/acs.nanolett.8b00689

73. Hu A, Chen X, Bi Q, Xiang Y, Jin R, Ai H, et al. A parallel and cascade control system: magnetofection of miR125b for synergistic tumor-association macrophage polarization regulation and tumor cell suppression in breast cancer treatment. *Nanoscale* (2020) 12:22615–27. doi: 10.1039/D0NR06060G

74. Tong F, Mao X, Zhang S, Xie H, Yan B, Wang B, et al. HPV + HNSCC-derived exosomal miR-9 induces macrophage M1 polarization and increases tumor radiosensitivity. *Cancer Lett* (2020) 478:34–44. doi: 10.1016/j.canlet.2020.02.037

75. Zhang Y, Li X, Wang C, Zhang M, Yang H, Lv K. lncRNA AK085865 promotes macrophage M2 polarization in CVB3-induced VM by regulating ILF2-ILF3 complex-mediated miRNA-192 biogenesis. *Mol Ther Nucleic Acids* (2020) 21:441–51. doi: 10.1016/j.omtn.2020.06.017

76. Zhou Y, Zhao W, Mao L, Wang Y, Xia L, Cao M, et al. Long non-coding RNA NIFK-AS1 inhibits M2 polarization of macrophages in endometrial cancer through targeting miR-146a. *Int J Biochem Cell Biol* (2018) 104:25–33. doi: 10.1016/j.biocel.2018.08.017

77. Huang C, Liu X, QunZhou, Xie J, Ma T, Meng X, et al. MiR-146a modulates macrophage polarization by inhibiting Notch1 pathway in RAW264.7 macrophages. *Int Immunopharmacol* (2016) 32:46–54. doi: 10.1016/j.intimp.2016.01.009

78. Zhong Y, Liao J, Hu Y, Wang Y, Sun C, Zhang C, et al. PM(2.5) upregulates MicroRNA-146a-3p and induces M1 polarization in RAW264.7 cells by targeting Sirtuin1. *Int J Med Sci* (2019) 16:384–93. doi: 10.7150/ijms.30084

79. Bhatt K, Lanting L, Jia Y, Yadav S, Reddy M, Magilnick N, et al. Anti-inflammatory role of MicroRNA-146a in the pathogenesis of diabetic nephropathy. *J Am Soc Nephrol: JASN* (2016) 27:2277–88. doi: 10.1681/ASN.2015010111

80. He X, Tang R, Sun Y, Wang Y, Zhen K, Zhang D, et al. MicroR-146 blocks the activation of M1 macrophage by targeting signal transducer and activator of transcription 1 in hepatic schistosomiasis. *EBioMedicine* (2016) 13:339–47. doi: 10.1016/j.ebiom.2016.10.024

81. Song Y, Dou H, Li X, Zhao X, Li Y, Liu D, et al. Exosomal miR-146a contributes to the enhanced therapeutic efficacy of interleukin-1β-Primed mesenchymal stem cells against sepsis. *Stem Cells (Dayton Ohio)* (2017) 35:1208–21. doi: 10.1002/stem.2564

82. Zhang J, Zhang Z, Lu M, Zhang Y, Shang X, Chopp M. MiR-146a promotes oligodendrocyte progenitor cell differentiation and enhances remyelination in a model of experimental autoimmune encephalomyelitis. *Neurobiol Disease* (2019) 125:154–62. doi: 10.1016/j.nbd.2019.01.019

83. Jaiswal A, Maurya M, Maurya P, Barthwal M. Lin28B regulates angiotensin II-mediated let-7c/miR-99a MicroRNA formation consequently affecting macrophage polarization and allergic inflammation. *Inflammation* (2020) 43:1846–61. doi: 10.1007/s10753-020-01258-1

84. Jaiswal A, Reddy S, Maurya M, Maurya P, Barthwal M. MicroRNA-99a mimics inhibit M1 macrophage phenotype and adipose tissue inflammation by targeting TNFα. *Cell Mol Immunol* (2019) 16:495–507. doi: 10.1038/s41423-018-0038-7

85. Do D, Mu J, Ke X, Sachdeva K, Qin Z, Wan M, et al. miR-511-3p protects against cockroach allergen-induced lung inflammation by antagonizing CCL2. *JCI Insight* (2019) 4:e126832. doi: 10.1172/jci.insight.126832

86. Zhou Y, Do D, Ishmael F, Squadrito M, Tang H, Tang H, et al. Mannose receptor modulates macrophage polarization and allergic inflammation through miR-511-3p. *J Allergy Clin Immunol* (2018) 141:350–64.e8. doi: 10.1016/j.jaci.2017.04.049

87. Wang Z, Sun W, Li R, Liu Y. miRNA-93-5p in exosomes derived from M2 macrophages improves lipopolysaccharide-induced podocyte apoptosis by targeting toll-like receptor 4. *Bioengineered* (2022) 13:7683–96. doi: 10.1080/21655979.2021.2023794

88. Ganta V, Choi M, Kutateladze A, Fox T, Farber C, Annex B. A MicroRNA93-interferon regulatory factor-9-Immunoresponsive gene-1-Itaconic acid pathway modulates M2-like macrophage polarization to revascularize ischemic muscle. *Circulation* (2017) 135:2403–25. doi: 10.1161/CIRCULATIONAHA.116.025490

89. Shen D, He Z. Mesenchymal stem cell-derived exosomes regulate the polarization and inflammatory response of macrophages *via* miR-21-5p to promote repair after myocardial reperfusion injury. *Ann Trans Med* (2021) 9:1323. doi: 10.21037/atm-21-3557

90. Zhao J, Li X, Hu J, Chen F, Qiao S, Sun X, et al. Mesenchymal stromal cell-derived exosomes attenuate myocardial ischaemia-reperfusion injury through miR-182-regulated macrophage polarization. *Cardiovasc Res* (2019) 115:1205–16. doi: 10.1093/cvr/cvz040

91. Li N, Qin J, Han X, Jin F, Zhang J, Lan L, et al. miR-21a negatively modulates tumor suppressor genes PTEN and miR-200c and further promotes the transformation of M2 macrophages. *Immunol Cell Biol* (2018) 96:68–80. doi: 10.1111/imcb.1016

92. Tran M, Lee S, Shin D, Wang L. Loss of miR-141/200c ameliorates hepatic steatosis and inflammation by reprogramming multiple signaling pathways in NASH. *JCI Insight* (2017) 2:e96094. doi: 10.1172/jci.insight.96094

93. Lin X, Wang S, Sun M, Zhang C, Wei C, Yang C, et al. miR-195-5p/NOTCH2-mediated EMT modulates IL-4 secretion in colorectal cancer to affect M2-like TAM polarization. *J Hematol Oncol* (2019) 12:20. doi: 10.1186/s13045-019-0708-7

94. Liu J, Luo R, Wang J, Luan X, Wu D, Chen H, et al. viaTumor cell-derived exosomal miR-770 inhibits M2 macrophage polarization targeting MAP3K1 to inhibit the invasion of non-small cell lung cancer cells. *Front Cell Dev Biol* (2021) 9:679658. doi: 10.3389/fcell.2021.679658

95. Zhang B, Du Y, He Y, Liu Y, Zhang G, Yang C, et al. INT-HA induces M2-like macrophage differentiation of human monocytes *via* TLR4-miR-935 pathway. *Cancer Immunol Immunother: CII* (2019) 68:189–200. doi: 10.1007/s00262-018-2261-6

96. Zhao S, Mi Y, Guan B, Zheng B, Wei P, Gu Y, et al. Tumor-derived exosomal miR-934 induces macrophage M2 polarization to promote liver metastasis of colorectal cancer. *J Hematol Oncol* (2020) 13:156. doi: 10.1186/s13045-020-00991-2

97. Wang D, Wang X, Si M, Yang J, Sun S, Wu H, et al. Exosome-encapsulated miRNAs contribute to CXCL12/CXCR4-induced liver metastasis of colorectal cancer by enhancing M2 polarization of macrophages. *Cancer Lett* (2020) 474:36–52. doi: 10.1016/j.canlet.2020.01.005

98. Yin Y, Liu B, Cao Y, Yao S, Liu Y, Jin G, et al. Colorectal cancer-derived small extracellular vesicles promote tumor immune evasion by upregulating PD-L1 expression in tumor-associated macrophages. *Advanced Sci (Weinheim Baden-Wurttemberg Germany)* (2022) 9:2102620. doi: 10.1002/advs.202102620

99. Song J, Yang P, Li X, Zhu X, Liu M, Duan X, et al. Esophageal cancer-derived extracellular vesicle miR-21-5p contributes to EMT of ESCC cells by disorganizing macrophage polarization. *Cancers* (2021) 13:4122. doi: 10.3390/cancers13164122

100. Huang Y, Huang T, Yadav V, Sumitra M, Tzeng D, Wei P, et al. Preclinical investigation of ovatodiolide as a potential inhibitor of colon cancer stem cells *via* downregulating sphere-derived exosomal β-catenin/STAT3/miR-1246 cargoes. *Am J Cancer Res* (2020) 10:2337–54. eCollection 2020

101. Cooks T, Pateras I, Jenkins L, Patel K, Robles A, Morris J, et al. Mutant p53 cancers reprogram macrophages to tumor supporting macrophages *via* exosomal miR-1246. *Nat Commun* (2018) 9:771. doi: 10.1038/s41467-018-03224-w

102. Qian M, Wang S, Guo X, Wang J, Zhang Z, Qiu W, et al. Hypoxic glioma-derived exosomes deliver microRNA-1246 to induce M2 macrophage polarization by targeting TERF2IP *via* the STAT3 and NF-κB pathways. *Oncogene* (2020) 39:428–42. doi: 10.1038/s41388-019-0996-y

103. Ma C, He D, Tian P, Wang Y, He Y, Wu Q, et al. miR-182 targeting reprograms tumor-associated macrophages and limits breast cancer progression. *Proc Natl Acad Sci* (2022) 119:e2114006119. doi: 10.1073/pnas.2114006119

104. Xun J, Du L, Gao R, Shen L, Wang D, Kang L, et al. Cancer-derived exosomal miR-138-5p modulates polarization of tumor-associated macrophages through inhibition of KDM6B. *Theranostics* (2021) 11:6847–59. doi: 10.7150/thno.51864

105. Hsu Y, Hung J, Chang W, Jian S, Lin Y, Pan Y, et al. Hypoxic lung-Cancer-Derived extracellular vesicle MicroRNA-103a increases the oncogenic effects of macrophages by targeting PTEN. *Mol Ther* (2018) 26:568–81. doi: 10.1016/j.ymthe.2017.11.016

106. Ren W, Hou J, Yang C, Wang H, Wu S, Wu Y, et al. Extracellular vesicles secreted by hypoxia pre-challenged mesenchymal stem cells promote non-small cell lung cancer cell growth and mobility as well as macrophage M2 polarization *via* miR-21-5p delivery. *J Exp Clin Cancer Res: CR* (2019) 38:62. doi: 10.1186/s13046-019-1027-0

107. Wang X, Luo G, Zhang K, Cao J, Huang C, Jiang T, et al. Hypoxic tumor-derived exosomal miR-301a mediates M2 macrophage polarization *via* PTEN/PI3Kγ to promote pancreatic cancer metastasis. *Cancer Res* (2018) 78:4586–98. doi: 10.1158/0008-5472.CAN-17-3841

108. Huang Y, Zhu L, Li H, Ye J, Lin N, Chen M, et al. Endometriosis derived exosomal miR-301a-3p mediates macrophage polarization *via* regulating PTEN-PI3K axis. *Biomed. Pharmacother = Biomedecine pharmacotherapie* (2022) 147:112680. doi: 10.1016/j.biopha.2022.112680

109. Tian X-F, Ji F-J, Zang H-L, Cao H. Activation of the miR-34a/SIRT1/p53 signaling pathway contributes to the progress of liver fibrosis *via* inducing apoptosis in hepatocytes but not in HSCs. *PloS One* (2016) 11:e0158657. doi: 10.1371/journal.pone.0158657

110. Yan C, Zhou Q-Y, Wu J, Xu N, Du Y, Li J, et al. Csi-let-7a-5p delivered by extracellular vesicles from a liver fluke activates M1-like macrophages and exacerbates biliary injuries. *Proc Natl Acad Sci* (2021) 118:e2102206118. doi: 10.1073/pnas.2102206118

111. Chen L, Huang Y, Duan Z, Huang P, Yao H, Zhou Y, et al. Exosomal miR-500 derived from lipopolysaccharide-treated macrophage accelerates liver fibrosis by suppressing MFN2. *Front Cell Dev Biol* (2021) 9:716209. doi: 10.3389/fcell.2021.716209

112. Chen L, Yao X, Yao H, Ji Q, Ding G, Liu X. Exosomal miR-103-3p from LPS-activated THP-1 macrophage contributes to the activation of hepatic stellate cells. *FASEB J* (2020) 34:5178–92. doi: 10.1096/fj.201902307RRR

113. Hou X, Yin S, Ren R, Liu S, Yong L, Liu Y, et al. Myeloid-Cell-Specific IL-6 signaling promotes MicroRNA-223-Enriched exosome production to attenuate NAFLD-associated fibrosis. *Hepatol (Baltimore Md)* (2021) 74:116–32. doi: 10.1002/hep.31658

114. Wan Z, Yang X, Liu X, Sun Y, Yu P, Xu F, et al. M2 macrophage-derived exosomal microRNA-411-5p impedes the activation of hepatic stellate cells by targeting CAMSAP1 in NASH model. *iScience* (2022) 25:104597. doi: 10.1016/j.isci.2022.104597

115. Hu M, Wang Y, Liu Z, Yu Z, Guan K, Liu M, et al. Hepatic macrophages act as a central hub for relaxin-mediated alleviation of liver fibrosis. *Nat Nanotechnol* (2021) 16:466–77. doi: 10.1038/s41565-020-00836-6

116. Bala S, Ganz M, Babuta M, Zhuang Y, Csak T, Calenda C, et al. Steatosis, inflammasome upregulation, and fibrosis are attenuated in miR-155 deficient mice in a high fat-cholesterol-sugar diet-induced model of NASH. *Lab Invest* (2021) 101:1540–9. doi: 10.1038/s41374-021-00626-1

117. Bala S, Csak T, Saha B, Zatsiorsky J, Kodys K, Catalano D, et al. The pro-inflammatory effects of miR-155 promote liver fibrosis and alcohol-induced steatohepatitis. *J Hepatol* (2016) 64:1378–87. doi: 10.1016/j.jhep.2016.01.035

118. Niu L, Zhang Y, Huang T, Sun X, Luo S. Exosomal microRNA-155 as a biomarker for hepatic fibrosis diagnosis and progression. *Ann Trans Med* (2021) 9:137. doi: 10.21037/atm-20-7787

119. Xue J, Xiao T, Wei S, Sun J, Zou Z, Shi M, et al. miR-21-regulated M2 polarization of macrophage is involved in arsenicosis-induced hepatic fibrosis through the activation of hepatic stellate cells. *J Cell Physiol* (2021) 236:6025–41. doi: 10.1002/jcp.30288

120. Su S, Zhao Q, He C, Huang D, Liu J, Chen F, et al. miR-142-5p and miR-130a-3p are regulated by IL-4 and IL-13 and control profibrogenic macrophage program. *Nat Commun* (2015) 6:8523. doi: 10.1038/ncomms9523

121. Calvente C, Tameda M, Johnson C, Del Pilar H, Lin Y, Adronikou N, et al. Neutrophils contribute to spontaneous resolution of liver inflammation and fibrosis *via* microRNA-223. *J Clin Invest* (2019) 129:4091–109. doi: 10.1172/JCI122258

122. Jimenez Calvente C, Del Pilar H, Tameda M, Johnson CD, Feldstein AE. MicroRNA 223 3p negatively regulates the NLRP3 inflammasome in acute and chronic liver injury. *Mol Ther* (2020) 28:653–63. doi: 10.1016/j.ymthe.2019.09.013

frontiers | Frontiers in Immunology

TYPE Review
PUBLISHED 18 April 2023
DOI 10.3389/fimmu.2023.1178337

OPEN ACCESS

EDITED BY
Ruoxi Yuan,
Hospital for Special Surgery, United States

REVIEWED BY
Maria Grazia Totaro,
IFOM - The FIRC Institute of Molecular Oncology, Italy
María José Ruiz Magaña,
University of Granada, Spain

*CORRESPONDENCE
Arnaud Jacquel
jacquel@unice.fr
Patrick Auberger
Patrick.AUBERGER@univ-cotedazur.fr

†These authors have contributed equally to this work

SPECIALTY SECTION
This article was submitted to Cancer Immunity and Immunotherapy, a section of the journal Frontiers in Immunology

RECEIVED 02 March 2023
ACCEPTED 04 April 2023
PUBLISHED 18 April 2023

CITATION
Chaintreuil P, Kerreneur E, Bourgoin M, Savy C, Favreau C, Robert G, Jacquel A and Auberger P (2023) The generation, activation, and polarization of monocyte-derived macrophages in human malignancies.
Front. Immunol. 14:1178337.
doi: 10.3389/fimmu.2023.1178337

The generation, activation, and polarization of monocyte-derived macrophages in human malignancies

Paul Chaintreuil[1,2], Emeline Kerreneur[1,2], Maxence Bourgoin[1,2], Coline Savy[1,2], Cécile Favreau[1,2], Guillaume Robert[1,2†], Arnaud Jacquel[1,2*†] and Patrick Auberger[1,2*†]

[1]Université Côte d'Azur, Institut National de la Santé et de la Recherche Médicale, Nice, France, [2]Inserm U1065, Centre Méditerranéen de Médecine Moléculaire (C3M), Nice, France

Macrophages are immune cells that originate from embryogenesis or from the differentiation of monocytes. They can adopt numerous phenotypes depending on their origin, tissue distribution and in response to different stimuli and tissue environment. Thus, *in vivo*, macrophages are endowed with a continuum of phenotypes that are rarely strictly pro-inflammatory or anti-inflammatory and exhibit a broad expression profile that sweeps over the whole polarization spectrum. Schematically, three main macrophage subpopulations coexist in human tissues: naïve macrophages also called M0, pro-inflammatory macrophages referred as M1 macrophages, and anti-inflammatory macrophages also known as M2 macrophages. Naïve macrophages display phagocytic functions, recognize pathogenic agents, and rapidly undergo polarization towards pro or anti-inflammatory macrophages to acquire their full panel of functions. Pro-inflammatory macrophages are widely involved in inflammatory response, during which they exert anti-microbial and anti-tumoral functions. By contrast, anti-inflammatory macrophages are implicated in the resolution of inflammation, the phagocytosis of cell debris and tissue reparation following injuries. Macrophages also play important deleterious or beneficial roles in the initiation and progression of different pathophysiological settings including solid and hematopoietic cancers. A better understanding of the molecular mechanisms involved in the generation, activation and polarization of macrophages is a prerequisite for the development of new therapeutic strategies to modulate macrophages functions in pathological situations.

KEYWORDS

monocyte-derived macrophages, CSF-1, differentiation, polarization, TAM, LAM, targeting macrophages

1 Introduction

Monocytes are circulating immune cells produced in the bone marrow (BM) during hematopoiesis. This process is responsible for the generation of all blood cells in the bloodstream and ensures their continuous renewal. Hematopoietic stem cells differentiate first into myeloid progenitors that ultimately generate erythrocytes, thrombocytes, granulocytes, and monocytes. Myeloid progenitors give rise to granulomonocytic progenitors and then monoblasts in response to IL-3, GM-CSF (Granulocyte Macrophage Colony Stimulating Factor) or G-CSF (Granulocyte Colony Stimulating Factor). The continuous presence of these cytokines leads to the differentiation of monoblasts into promonocytes and promotes their differentiation into mature monocytes, that leave the BM to enter the bloodstream. The half-life of monocytes in blood circulation is only three days, due to their rapid migration into tissues, their differentiation into macrophages or dendritic cells and their rate of cell death. Detailed analysis of the markers present on the surface of monocytes has revealed different populations of monocytes, mainly characterized by the level of expression of CD14 and CD16 (1, 2). Three distinct monocyte populations coexist in the bloodstream: classical $CD14^{++}$ $CD16^{-}$ monocytes, representing 85% of circulating monocytes, intermediate $CD14^{+}$ $CD16^{+}$ monocytes, accounting for 5% of circulating monocytes, and non-classical $CD14^{+}$ $CD16^{++}$ monocytes, corresponding to the 10% remaining monocytes. Intermediate and non-classical monocytes are derived from classical monocytes and each population is unique in its migration ability, adhesion molecule, cytokine/chemokine, and receptor expression (3, 4). Thus, classical monocytes express CCR2 and CD64, conversely to intermediate and non-classical monocytes, which strongly express CD32 and MHC-II. All these specificities confer these monocyte populations different functions (5–8). Despite these discrepancies, the different monocyte populations share certain functions in common. Monocytes are primarily involved in phagocytosis of cellular debris and circulating pathogens in the blood (9). They all express scavenger receptors that allow them to detect many pathogen-associated molecular patterns (PAMPs) and damaged-associated molecular patterns (DAMPs), including CD14 that recognizes LPS. When a PAMP or DAMP binds to one of these receptors, monocytes become activated and produce various cytokines such as IL-1β, CXCL8 (IL-8) and TNFα as well as reactive oxygen species such as NO (nitric oxide) to eliminate the pathogen or defective self-cells. Monocytes are also capable of presenting antigenic peptides on their surface, although they are much less efficient than specialized antigen-presenting cells such as dendritic cells. Because intermediate and nonclassical monocytes express MHC-II, they can present antigenic peptides more efficiently than classical monocytes and can activate lymphocytes in the bloodstream. One notable difference is that $CD16^{+}$ monocytes express more pro-inflammatory cytokines, such as TNFα, than conventional $CD16^{-}$ monocytes (10). An increase in the CD16+ monocyte population at the expense of $CD16^{-}$ monocytes has also been observed during inflammatory episodes and in pathologies such as atherosclerosis or asthma (11, 12). Conversely, in CMML (Chronic Myelomonocytic Leukemia), classical monocytes accumulate in the blood, show severe activation defects in response to infection or stress and are characterized by alterations in their differentiation into macrophages (13). In addition to their immune functions, monocytes also differentiate into other cell types (macrophages or dendritic cells) in response to different stimuli during their passage through tissues.

Depending on their tissue location, macrophages may endorse a wide heterogeneity of names and functions. Thus, macrophages are called microglia in the brain, osteoclasts and chondroblasts in the bone, Langerhans cells in the skin, Kupffer cells in the liver, alveolar and interstitial macrophages in the lungs (5, 14). However, two types of macrophages are found in the body depending on their origin: resident macrophages derived from embryogenesis such as microglia and macrophages produced from the differentiation of blood monocytes, called monocyte-derived macrophages. Importantly, as the body grows and ages, resident macrophages of embryonic origin are gradually replaced by monocyte-derived macrophages in several tissues, such as in the intestines, kidneys, or the heart (15–17). In addition, resident macrophages can also be replaced, temporarily or permanently, by monocyte-derived macrophages during an inflammatory episode such as a microbial infection (18). This ability of monocyte-derived macrophages to replace and mimic resident macrophages of embryonic origin depends not only on cytokines and growth factors present in the local environment but also on the spatial availability of niches present within the tissue itself. These niches control the number of macrophages present in the tissue and the tissue-specific activity of these macrophages. By regulating the number and functions of resident macrophages, whatever their origins, embryonic and monocyte-derived, these niches play a cardinal function in the regulation of tissue homeostasis of diverse organs (19, 20). Thus, resident macrophages are present in virtually every tissue in the body, where they perform an immune surveillance function and help maintain tissue homeostasis by phagocytosing apoptotic buds and cellular debris. They also perform non-inflammatory functions such as protection of neuronal synapses for microglia or bone destruction by osteoclasts during bone remodeling (21–23). Overall, the role of macrophages, whether of embryonic origin or derived from monocytes, is first to ensure homeostasis in tissues by eliminating dying cells and repairing tissue damage. They also serve to defend the body against pathogens by secreting pro-inflammatory cytokines and by presenting antigenic peptides on their surface.

2 The process of differentiation of monocytes into macrophages

2.1 From blood circulation to tissues

The differentiation of monocytes into macrophages required signals triggered by cytokines and chemokines secreted by both the injured tissue and the endothelial cells of the blood vessels located in the vicinity of the lesion. The main cytokines and chemokines that

allow the recruitment of monocytes are MCP-1 (or CCL2) and MCP-3 (or CCL7), that both recognized the CCR2 receptor expressed on the surface of monocytes. When MCP-1 and/or MCP-3 bind to CCR2, interactions between monocytes and endothelial cells lead to monocyte diapedesis, a process during which monocytes differentiate into macrophages (24). When monocytes are about endothelial cells of blood vessels, they engage interactions through cell surface glycoproteins and selectins expressed on the surface of endothelial cells. Interactions of glycoproteins with E-selectin and P-selectin allow the slowing down of monocytes in the bloodstream. This interaction is strengthened during the process of diapedesis thanks to the expression by monocytes of the integrin receptors LFA-1, Mac-1, or VLA-4. Integrin receptors can strongly bind ICAM1 and VCAM1 integrins, present on the surface of endothelial cells. This interaction eventually leads to the immobilization of the monocyte on the endothelial cells, which consequently remodel their cytoskeleton resulting in the creation of a space between the endothelial cells consecutive to the opening of the cellular junctions. Monocytes thus transit through the blood vessel wall to the tissue via the newly created inter-cellular space (25). It is during diapedesis that monocytes differentiate into macrophages. Indeed, in response to stimuli generated by injured tissue, endothelial cells secrete several cytokines promoting the differentiation of monocytes into macrophages or dendritic cells. Among these cytokines, CSF-1 (M-CSF), CSF-2 (GM-CSF), and IL-34 are all able to induce the differentiation of monocytes into macrophages *ex vivo*, each of them generating macrophages with different functions (26–28). *In vivo*, monocyte differentiation cannot be restricted to the action of these cytokines because the microenvironment around monocytes includes many other cytokines generating monocyte differentiation into different types of macrophages.

2.2 Signaling pathways activated downstream of the CSF-1 receptor

CSF-1 produced by endothelial cells can bind to the CSF1R. CSF1R is a transmembrane receptor with tyrosine kinase activity, expressed weakly in hematopoietic stem cells but much more strongly in monocytes and cells of monocytic origin (macrophages, dendritic cells) (29). It should be noted that the CSF1R can also bind IL-34, another cytokine able to induce the differentiation of monocytes into macrophages (28, 30). CSF-1 binding to its receptor, triggers dimerization and auto-phosphorylation of its intracellular tyrosine residues, resulting in several signaling cascades. Among the activated signaling pathways, some will ensure the survival of the monocyte/macrophage by inducing proliferation and/or inhibiting apoptosis, while others will allow monocytes to differentiate into macrophages (31) (Figure 1).

2.2.1 The MAPK/ERK pathway

Activation of the MAPK/ERK pathway occurs via the phosphorylation of tyrosine 697 of the CSF1R (32). This phosphorylation allows the recruitment of two adaptor molecules, Grb2 which recruits RAS and SOS which increases the activity of RAS and then RAF, leading to the activation of the MAPK/ERK pathway (33). This activation which is effective only a few seconds after the binding of CSF-1 to its receptor results in a first phase of transient activation followed by a second phase of continuous activation of ERK (34). However, this second phase is independent of Grb2-SOS and the signaling leading to the activation of the MAPK/ERK pathway under these settings is currently unknown (35). The MAPK/ERK pathway is required for the expression of several proteins including CD33 (Siglec-3), a membrane receptor expressed in cells of myeloid origin that also regulates the expression of Dusp5, a natural inhibitor of the MAPK/ERK pathway that acts as a negative feedback loop of the activation of this pathway (36). CSF-1 also induced expression of VEGF mRNA and protein expression through the MAPK/ERK signaling pathway. Furthermore, CSF-1 triggered nuclear translocation of the transcription factor Sp1 and inhibition of ERK1/2 led to sequestration of Sp1 in the cytoplasm (37). In addition, inhibition of either ERK1/2 or Sp1 leads to a decrease in transcription of the gene encoding VEGF, demonstrating the importance of the MAPK/ERK/Sp1 axis in CSF-1-mediated increase in VEGF expression. Nevertheless, the activation of the MAPK/ERK pathway and its consequences upon CSF-1 binding to its receptor are still largely unknown. Although necessary for monocyte/macrophage survival the roles and cellular targets of the MAPK/ERK pathway during monocyte to macrophage differentiation remains elusive.

2.2.2 The SRC kinase pathway

Activation of the SRC kinase pathway occurs via phosphorylation of tyrosine 559 of the CSF1R (38). This phosphorylation allows the recruitment and direct activation of SRC kinases, that next phosphorylate and activate the kinase PYK2 (39). Following phosphorylation by SRC kinases, Pyk2 is relocated to focal adhesion complexes to phosphorylate paxillin (40). SRC kinases also regulate integrins, particularly the α5 and β1 subunits. Inhibition of SRC kinases results in a significant loss of macrophage motility through their inability to form filipodia, which are required for movement. This loss of movement capacity is partly related to the inactivation of paxillin, which no longer form focal adhesion complexes (41). SRC kinases also activate phospholipase Cγ2 (PLCγ2) and the MAPK pathway in a delayed manner. Indeed, both PLCγ2 and MAPKs exhibit a first transient activation phase quickly after CSF1R activation and then a second persistent activation phase several hours later. Inhibition of SRC kinases at the onset of CSF1R activation leads to a loss of PLCγ2 and MAPK phosphorylation only during the persistent activation phase but does not affect the phosphorylation that occurs during the transient phase. SRC kinase inhibition next leads to an abrogation of the differentiation of monocytes into macrophages (42). Furthermore, Lyn and Hck, two members of the SRC kinase family, are involved in caspase activation during differentiation, their inhibition leading to a decrease in Nucleophosmin (NPM) substrate protein cleavage (please refer to the caspase activation cascade below). However, the mechanism of action of Lyn and Hck during caspase activation is

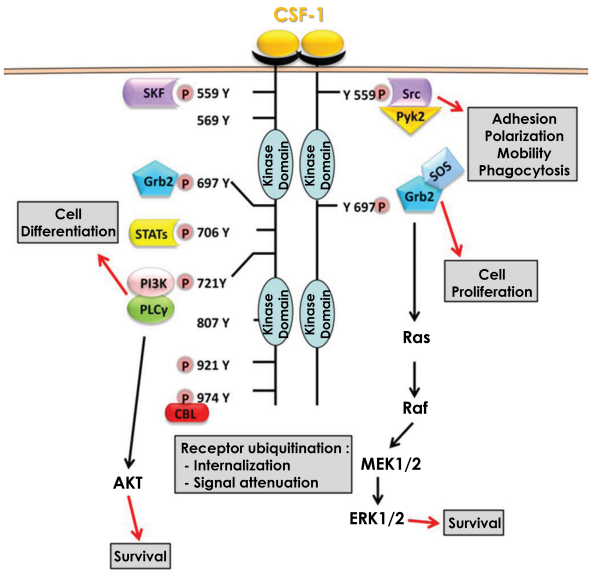

FIGURE 1
Signaling pathways downstream of CSF1R. Binding of CSF-1 to its receptor CSF1R leads to dimerization and subsequent auto-phosphorylation of several tyrosine residues in the intracellular domain. These phosphorylation reactions are then responsible for the activation of multiple signaling pathways that promote cell differentiation and monocyte survival.

not yet determined, although it is hypothesized that Hck regulates the activation of the PI3K/AKT waves (43).

2.2.3 The PI3K/AKT pathway

Activation of the PI3K/AKT pathway occurs via the phosphorylation of tyrosine 721 of the CSF1R (44). This phosphorylation allows the recruitment and direct activation of PI3K, which then associates with and activates PLCγ2 (45). At the same time, PI3K triggers AKT activation and downstream signaling pathways (46). Inhibition of the PI3K/AKT pathway leads to death of differentiating monocytes by apoptosis, suggesting that the PI3K/AKT pathway is responsible for cell survival during macrophage differentiation. This cell death pathway, which is also dependent on caspases-8, -3 and -9, is blocked during differentiation by the increased expression of anti-apoptotic proteins such as Bcl-xL and Mcl-1 (47). Increased expression of Bcl-xl and Mcl-1 depends on PI3K/AKT activity as its inhibition reduces Bcl-xL and Mcl-1 levels and increases expression of the pro-apoptotic protein Bax. Similarly, inhibition of NF-κB leads to a reduction in Bcl-xL expression and death by apoptosis of differentiating monocytes. The induction of NF-κB, and in turn of Bcl-xL during differentiation is dependent on the ability of PI3K/AKT to degrade IκB, the natural inhibitor of NF-κB. Indeed, when PI3K/AKT is inhibited, IκB is no longer degraded and thus can repress NF-κB, leading to cell apoptosis. Thus, the PI3K/AKT/NF-κB axis ensures cell differentiation by protecting monocytes from apoptosis partly through Bcl-xL (48). AKT activation occurs in successive waves and is concomitant with the phosphorylation/dephosphorylation process of the CSF1R tyrosine 721. These waves of activation, which increase in duration and strength with each wave, are necessary for the differentiation of monocytes into macrophages and promote the activation of non-apoptotic caspases, another major pathway of macrophage differentiation (43).

2.2.4 The caspase cascade pathway

The activation of non-apoptotic caspases during the differentiation of monocytes into macrophages was first demonstrated in primary human monocytes. Indeed, in response to CSF-1, caspases-3 and -9 are activated without inducing apoptosis. Using the human cell line U937 as a model, and phorbol esters as a differentiating agent, it was reported that caspase inhibition impaired monocyte differentiation and triggered caspase-independent cell death (49). Later, caspase-8 was shown to be important for differentiation using caspase-8 deficient mice. Indeed, *ex vivo* stimulation of myeloid progenitors from caspase 8 knock-out mice with CSF-1 resulted in a significant decrease in the number of differentiated macrophages compared to the one of wild-type mice (50). These results highlighted the important role played by caspases during the differentiation of monocytes into macrophages, but their mechanisms of activation and action has remained unknown for a long time. Only recently, data from our group underscored an original mode of caspase activation during the differentiation of monocytes into macrophages. Indeed, in response to CSF-1, caspase-8 is activated, generating a 34 kDa cleavage fragment, different from the fragments detected following induction of apoptosis suggesting different functions for caspase-8 during differentiation and apoptosis. During monocyte differentiation, activation of caspase-8 occurs within a multimolecular complex, we called Non-Apoptotic Differentiation Inducing Complex (NADIC) composed of the long isoform of FLIP (FLIP-L), FADD and RIP1. This complex is reminiscent of the DISC that assembles during

apoptosis but unlike the later does not include a death receptor (Figure 2). In NADIC complex, caspase-8 cleaves FLIP and RIP1, generating cleavage fragments of 43 kDa (found in other contexts) and 42 kDa (only found during the differentiation of monocytes into macrophages) respectively, giving them new functions. The cleavage fragment of FLIP allows a more efficient recruitment of RIP1 into the complex while the cleavage fragment of RIP1 negatively regulates the activation of NF-κB, which is transient during the differentiation of monocytes into macrophages. Caspase-8 activation leads to the cleavage of caspase-3 in an original 26 kDa fragment that is absent during the completion of apoptosis. The importance of caspase-8 in the cleavage of caspase-3 has been demonstrated using siRNAs directed against this protease (43, 51). Next, to identify the substrates of caspases during the differentiation of monocytes into macrophages, U937 cells were stably transfected with an empty vector or with a vector containing the p35 protein a natural and irreversible inhibitor of caspases. Following phorbol ester stimulation of U937 cells to induce differentiation, 2D-gel electrophoresis and mass spectrometry analyses were performed. By comparing the proteomes of control and phorbol ester-treated cells, dozen proteins were identified as potential targets of caspases.

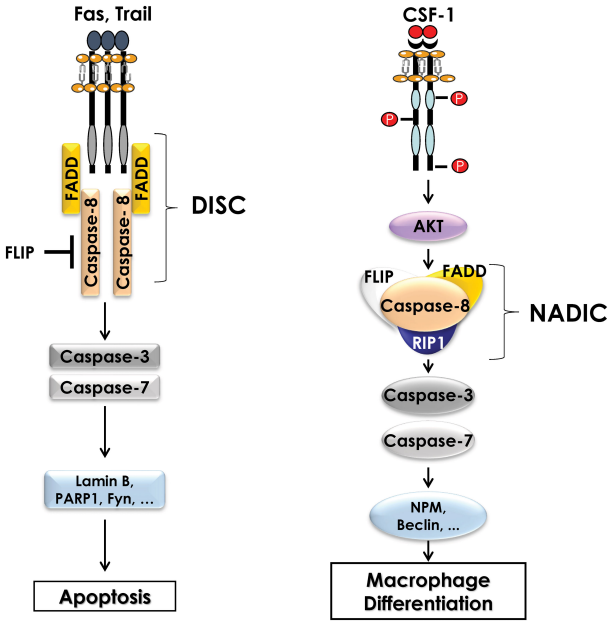

FIGURE 2
Comparison of the Death Inducing Signaling Complex (DISC) and the complex formed during differentiation of monocytes (NADIC). During induction of extrinsic apoptosis, caspase-8 interacts with a death receptor (FAS, TRAIL) and FADD to form the DISC (Death-inducing signaling complex) at the cell membrane. The FLIP protein may also be present in the DISC to inhibit caspase-8 activity. Activation of caspase-8 leads to the cleavage of caspases-3 and -7 and then to the cleavage of numerous substrate proteins, ultimately inducing apoptosis of the cell. During the differentiation of monocytes into macrophages, CSF1R triggering leads to the activation of the AKT pathway, which is involved in the formation of an intracellular multimolecular complex including caspase-8, FLIP, FADD and RIP1 called non-apoptotic differentiation-inducing complex (NADIC). Within this complex, caspase-8 is activated and then cleaves caspases-3 and -7 to allow the cleavage of substrate proteins that are required for differentiation of monocytes into macrophages.

Among these proteins, some were cytoplasmic, such as RIP1, while others were nuclear, such as (NPM). Most of these proteins are cleaved by caspase-3 but some of them are cleaved by caspase-8 (RIP1, FLIP) (52).

Although the function of the cleavage fragments of RIP1, FLIP and NPM during the differentiation of monocytes into macrophages has been investigated, the role of other caspase substrate proteins is still under investigation. The function of RIP1 and FLIP having been discussed previously, we will only mention here the role of the NPM protein. NPM is a protein expressed ubiquitously in the body and has several functions, including centrosome duplication and ribosome regulation. NPM is also a chaperone protein belonging to the NF-κB complex where it plays a co-activator or co-repressor role depending on the transcriptional targets. During differentiation, NPM is cleaved by caspases, generating a 30 kDa cleavage fragment and then by cathepsins to yield a 20 kDa cleavage fragment. Our recent data established that the cleavage site of NPM by caspases during differentiation of monocytes occurs in a specific sequence, different from the apoptotic consensus sites of apoptotic caspases (Chaintreuil et al., unpublished observation). NPM cleavage is not necessary for the differentiation of monocytes into macrophages but is required for the functionality of the generated macrophages. Indeed, overexpression of NPM cleavage fragments results in a reduction of the phagocytic capacity and motility of macrophages (53). $P47^{PHOX}$ is another substrate of caspases during differentiation of human macrophages. Our recent results established that $P47^{PHOX}$ cleavage by caspase-7 promotes the formation of the NAPDH complex NOX2 and the production of cytosolic superoxide anions (54).

2.2.5 The autophagy pathway

In monocytes stimulated with CSF-1, electron microscopy analysis has revealed a drastic increased in the number of phagosomes and auto-phagolysosomes and characteristic images of mitophagy in differentiating monocytes. Accordingly, we found that LC3-I was lipidated, and cleaved to LC3-II, a hallmark of autophagy induction, while cathepsin B activity and LAMP2 protein expression were drastically increased. In addition, ULK1, a kinase involved in the initiation phase of autophagy, was phosphorylated by CAMKK2, leading to an increase in its activity. Accordingly, pharmacological, or genetic inhibition of CAMKK2 and ULK1 resulted in a defect of monocyte differentiation into macrophages. Moreover, pharmacological inhibition of cathepsins or genetic inhibition of different ATG genes including Beclin-1 (ATG6) or ATG7 also impaired macrophage differentiation, demonstrating the essential role of autophagy in this process (55). Interestingly, in CMML, monocytes exhibit significant differentiation defects, due in part to the presence of α-defensins in the blood of patients. This observation led to the identification of the receptor responsible for autophagy induction in CSF-1-stimulated monocytes. Indeed, the purinergic receptor P2RY6 is inhibited by α-defensins, leading to a defect in the differentiation of monocytes into macrophages. We established that CSF-1 increased P2RY6 expression and activity at the cell surface, leading to activation of a PLCβ3 - CAMKK2β -

AMPK - ULK1 signaling pathway responsible for the induction of autophagy. Accordingly, genetic inhibition of each of these proteins individually results in an impairment of autophagy induction and macrophage differentiation (55, 56)(Figure 3).

3 The process of macrophage polarization

Ex vivo, macrophages stimulated with CSF-1 are considered naïve (also called M0 macrophages) and, although they possess phagocytic activity and pathogen detection ability, they must undergo a polarization process to acquire their full functions, whether pro- or anti-inflammatory. *In vivo*, the recruited monocytes are differentiated and polarized simultaneously according to the extracellular environment and the secretion of cytokines by the different cell types present at the site of monocyte recruitment. This cytokine environment controls the functions of macrophages, whatever their origin, so that they can respond spatially and temporally to the tissue conditions they are confronted with. Thus, *in vivo*, macrophages encompassed a broad diversity of cells with different roles (anti-inflammatory or pro-inflammatory) and functional states that are determined by microenvironmental signals (14, 57, 58). This balanced phenotype applies to both resident and monocyte-derived macrophages. However, *ex vivo*, it is difficult to mimic the complex extracellular environment that allows monocyte-derived macrophages to exhibit a large spectrum of profiles between pro- and anti-inflammatory and a plethora of different functions. Thus, to specifically study monocyte/macrophage differentiation or polarization, it is possible *ex vivo* to dissociate monocyte differentiation from macrophage polarization by sequentially adding the cytokine(s) that promote differentiation of monocytes into macrophages and the ones that trigger specialization/polarization of macrophages. Thus, the polarization of macrophages *ex vivo* allows the generation of macrophages with a pro-inflammatory profile (M1 macrophages) or, conversely, with an anti-inflammatory profile (M2 macrophages) depending on the cytokines used (Figure 4). Although the dichotomy between pro- and anti-inflammatory macrophages is increasingly being challenged *in vivo*, *ex vivo* experiments that use simplified models of pro- or anti-inflammatory macrophage polarization, remain pertinent at least to decipher the molecular mechanisms involved in macrophage polarization. The following sub-sections, therefore, encompass the knowledge acquired on macrophage polarization *ex vivo* and *in vivo*.

3.1 Pro-inflammatory polarization

Several stimuli allow naïve macrophages to display a pro-inflammatory climate, among which the co-stimulation with LPS and IFNγ or TNFα. *In vivo*, IFNγ and TNFα are mostly secreted by Th1 T cells that condition a pro-inflammatory environment. Pro-inflammatory macrophages also express and secrete numerous pro-inflammatory cytokines including TNFα, IL-1β, IL-6, IL-12, GM-CSF, which amplify inflammation. Secretion of CCL20, CXCL10 and CXCL11 by pro-inflammatory macrophages increases the

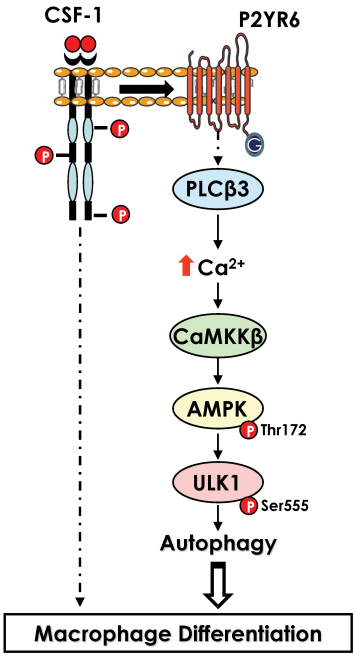

FIGURE 3
Activation of autophagy during macrophage differentiation. Activation of CSF1R leads to an increase in level of the purinergic receptor P2RY6 at the surface of differentiating monocytes. P2RY6 triggers PLCβ activation, increase in calcium level and a cascade of kinase activation CAMKK2>ULK1 that culminate in the induction of autophagy.

10.3389/fimmu.2023.1178337

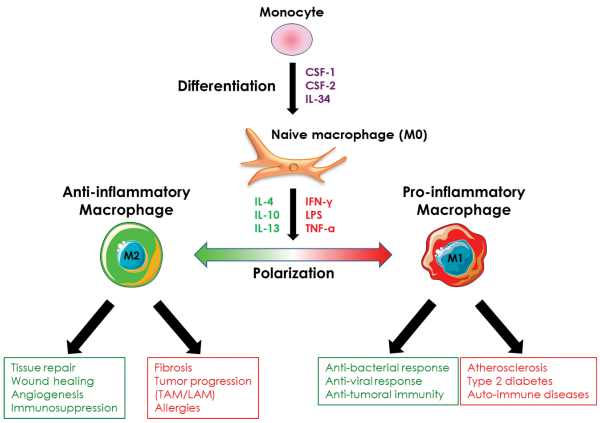

FIGURE 4
Macrophage polarization. Monocyte-derived-macrophages can be polarized *ex vivo* and *in vivo* into pro- or anti-inflammatory macrophages in response to different stimuli. Pro-inflammatory macrophages are involved in the anti-microbial and anti-tumor response and are implicated in the evolution of several pathologies such as atherosclerosis or type 2 diabetes. Anti-inflammatory macrophages exhibit an immunosuppressive activity, are involved in tissue repair, and promote angiogenesis. They are also involved in the evolution of various pathologies including fibrosis and tumor progression.

recruitment of certain immune cells including Th1 T cells, neutrophils, and NK cells (59). Pro-inflammatory macrophages also express on their surface specific markers such as MHC-II or CD80 and CD86, which are co-stimulatory proteins that participate in T cell activation. Pro-inflammatory macrophages have mainly bactericidal, virucidal and anti-tumor activity. In addition to their ability to secrete various cytokines and chemokines, they also generate ROS via activation of the NADPH oxidase complex and phagocytose pathogenic organisms via the complement cascade. Phagocytosis removes bacteria and viruses from the extracellular environment, while ROS generation leads to tissue degradation. This is an extremely efficient process that allows the elimination of infectious elements (bacteria, viruses) or cancerous cells present at the expense of tissue integrity. To prevent too much tissue damage, the pro-inflammatory response is inhibited by specific immune cells, including Th2 T cells and anti-inflammatory macrophages (60).

3.2 Anti-inflammatory polarization

Anti-inflammatory macrophages are subdivided into four main subtypes: M2a, M2b, M2c, and M2d. Each expresses specific markers, produces distinct cytokines, and exerts different functions. Their polarization status is heavily dependent on different cytokines secreted by Th2 T cells (Figure 5).

3.2.1 M2a macrophages

M2a macrophages are generated following the stimulation of naive macrophages with IL-4 and/or IL-13. These macrophages express on their surface receptors such as CD163, CD206 or CD209 which bind cellular debris, giving them a strong phagocytic potential. They express and secrete anti-inflammatory cytokines and chemokines such as IL-10, TGF-β, CCL17, CCL24 and CSF-1 which limit inflammation by inhibiting pro-inflammatory immune cells and recruiting more anti-inflammatory cells such as Th2 and Treg (regulatory T lymphocytes) (61). During the generation of M2a anti-inflammatory macrophages, IL-33 potentiates IL-13-induced polarization by increasing the expression of arginase-1, CCL17 and CCL24 (62). M2a macrophages have mainly immunosuppressive activity and are involved in tissue repair. Their phagocytic potential allows them to remove cellular debris following inflammation, thus favoring injured tissue repair. Arginase-1 plays an important role in this process as it catalyzes the modification of L-arginine to L-ornithine, which then yields polyamines and proline, two compounds necessary for tissue healing and repair (63). They also secrete proteases (mainly MMPs) that degrade necrotic tissue before replacement with healthy tissue (64).

3.2.2 M2b macrophages

M2b macrophages are derived from naive macrophages co-stimulated with an immune complex (a complex formed by an immunogenic epitope and an antibody) and an agonist of TLRs (LPS) or IL-1 receptor (IL-1β) (65). M2b macrophages exhibits a balanced profile between pro- and anti-inflammatory and express various pro-inflammatory (TNFα, IL-6, IL-1β…) and anti-inflammatory (IL-10, CCL1, CCL17….) cytokines. They express CD86 and participate in T cell activation (66). Despite a strong phagocytic activity, M2b macrophages are not involved in bacterial clearance, this role going to M1 macrophages. By contrast, they can inhibit the polarization of naive macrophages into pro-inflammatory macrophages, thus promoting the survival of bacteria, viruses, or cancer cells (67). CCL1 expression by M2b macrophages is essential because it not only maintains M2b macrophage functions but also preferentially recruits Th2 and Treg T cells over Th1 T cells to mediate an anti-inflammatory response (68, 69).

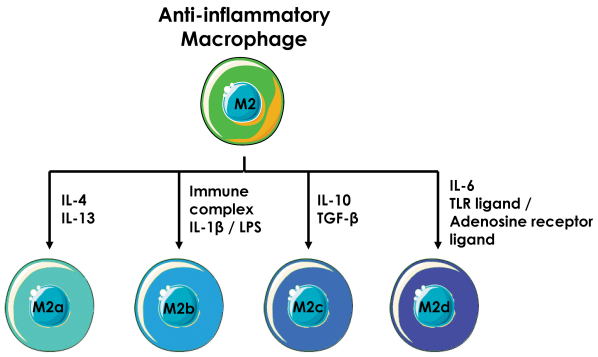

FIGURE 5
Anti-inflammatory macrophage polarization. Anti-inflammatory macrophages are divided into four subpopulations, each of which is generated by different stimuli.

3.2.3 M2c macrophages

When naive macrophages are stimulated with IL-10, they polarize into M2c macrophages and express extracellular receptors such as CD206, CD163 or MerTK (Mer Tyrosine Kinase) on their surface. They secrete anti-inflammatory cytokines and chemokines (IL-10, CCL18, CXCL13, TGFβ, etc.) that help limit the development of inflammation (70). M2c macrophages are primarily involved in tissue homeostasis. They have a strong anti-inflammatory activity mediated by cytokines and chemokines as well as the ability to phagocytose apoptotic cells via the MerTK receptor. This receptor can bind two ligands: Gas6 and Protein S. Gas6 and Protein S bind to negatively charged phospholipids such as phosphatidylserine which is exposed at the level of the outer leaflet of the plasma membrane of the cell during apoptosis. Thus, when the cell enters apoptosis, Gas6 and protein S are exposed outside of the cell and bind to MerTK, leading to phagocytosis of the apoptotic cell by the M2c macrophage (71, 72). This phagocytic ability is important to maintain cellular homeostasis by rapidly removing apoptotic buds (73).

3.2.4 M2d macrophages

M2d macrophages have been identified recently and correspond to the population of immunosuppressive macrophages found in cancers. They are more generally known as TAM (Tumor-Associated Macrophages) or LAM (Leukemia-Associated Macrophages) (74–76). However, this designation is not perfectly accurate as TAMs and LAMs does not define a homogeneous macrophage population, some of them exhibiting pro-inflammatory functions, although the majority corresponds to anti-inflammatory macrophages (77, 78). M2d macrophages are induced by stimulation of naive macrophages with IL-6 or by co-stimulation with an agonist of TLRs and of adenosine receptors (79, 80). M2d macrophages secrete significant amounts of anti-inflammatory cytokines and chemokines (IL-10, CCL18, CCL22…) that participate in shaping an anti-inflammatory environment. M2d macrophages bear the strongest immunosuppressive ability and promote angiogenesis and tumor progression. Indeed, activation of the adenosine receptor impairs the expression of pro-inflammatory and strongly increases the expression of anti-inflammatory cytokines such as CCL18 and CCL22 that induce the recruitment of naive T cells and Treg and the activation of T cells into Treg (81). M2d macrophages also express the ILT3 receptor on their surface, that can dimerize with a stimulatory receptor such as MHC-II or CD16 and thus acts as a natural inhibitor of these receptors (82). Ultimately, ILT3 expression strongly reduces the ability of macrophage to adopt a pro-inflammatory profile despite the presence of pro-inflammatory signals. In addition, M2d macrophages express VEGF, conferring pro-angiogenic properties that promote cancer cell growth (83).

3.3 The plasticity of macrophages

Once polarized, macrophages can still undergo profound adaptation of their phenotype. Thus, polarized macrophages can be reprogrammed *ex vivo* in response to different stimuli. For instance, repolarization of anti-inflammatory macrophages by LPS+INFγ increases the expression of pro-inflammatory markers and cytokines, while decreasing the expression of their anti-inflammatory counterparts. Conversely, repolarization of pro-inflammatory macrophages using IL-4 increases the expression of anti-inflammatory markers and cytokines (84, 85). *In vivo*, most studies have focused on the repolarization of TAMs into pro-inflammatory macrophages. For example, in a mouse model of breast cancer, metformin triggers repolarization of TAMs into pro-inflammatory macrophages (86). Therefore, the plasticity of polarized macrophages has paved the way for therapeutic intervention aiming at modifying their phenotype and function in different pathological settings. While a given subtype of anti-inflammatory macrophages can be repolarized into another type of macrophage, M2b macrophages cannot be repolarized into M1 macrophages under any conditions. The molecular mechanism blocking this repolarization is, at present, unknown (66).

3.4 Role of macrophages in cancer

In many, if not all, solid cancers and in hematological malignancies, pro-tumor macrophages (TAMs and LAMs

respectively) play a deleterious role for the organism and contribute strongly to tumor growth via different processes (Figure 6). In contrast, macrophages with a rather pro-inflammatory profile represent major players in the elimination of cancer cells. $CD169^+$ macrophages (Siglec-1) can phagocytose dead cancer cells during the initial phases of tumor progression. They also present tumor antigens on their surface that activate $CD8^+$ T cells involved in the mediation of an anti-tumor response by targeting and killing cancer cells. When the $CD169^+$ macrophage population is depleted, $CD8^+$ T cell activation is greatly reduced, as is the overall anti-tumor response. Thus, these $CD169^+$ specific macrophages act as antigen-presenting cells and are of paramount importance to the $CD8^+$ T cell anti-tumor response (87). More generally, pro-inflammatory macrophages, by producing nitric oxide or TRAIL, a ligand for DR4 and DR5 may induce tumor cell death. This anti-tumor effect mainly occurs during the early stages of tumor development, as pro-inflammatory macrophages are rapidly reprogrammed by cancer cells to promote their growth and expansion (88). For a long time, it was accepted that pro-tumor macrophages were exclusively derived from monocytes following their recruitment by cancer cells. However, over the last decade, a growing number of evidence have pointed to the role played by resident macrophages in tumor growth. Thus, in cancers, TAMs and LAMs constitute a highly heterogeneous population, with different functions and origins (89). Using mouse models, it has been established that the proportion of resident macrophages in TAMs and LAMs can be different depending on the cancer location. In a mouse model of glioma, microglia which are the resident macrophages in the brain was the main source of TAMs (90). In humans, the proportion of microglia composing TAMs population differs according to the type of glioma and seems less deleterious than monocyte-derived TAMs which display a greater immunosuppressive signature and are associated with higher mortality (91). The same picture could be drawn in pancreatic cancer, where most TAMs derived from resident macrophages of embryonic origin. These TAMs can proliferate, thus ensuring a constant increase in their number as well as their renewal. Their profile is also different from that of monocyte-derived TAMs, with a strong capacity to remodel the extracellular matrix, suggesting a role for these embryonic-derived TAMs in the metastatic capabilities of cancer cells. Furthermore, in a CCR2-deficient mouse model, inhibition of monocyte-derived macrophage recruitment is not sufficient to inhibit tumor progression while deletion of resident macrophages significantly reduces tumor progression, demonstrating the impact of resident macrophages in pancreatic cancer progression (92). In a mouse model of lung cancer, it was reported that monocyte-derived TAMs as well as interstitial macrophages of embryonic origin were present in the tumor while alveolar macrophages (the resident macrophages of the lung), were absent, suggesting either their progressive elimination during tumor development or a drastic change in their phenotype. It has been suggested that the various macrophage subpopulations found in the tumor displayed different functions, with monocyte-derived TAMs impacting cancer cell dissemination while TAMs of embryonic origin being involved in tumor growth (93). In a mouse model of breast cancer, characterization of TAM populations as well as their spatial localization demonstrated that TAM niches present within the tumor are modified throughout tumor development, exhibiting different macrophage populations depending on the stage of tumor evolution. For example, ductal macrophages, present in the ductal epithelium, accumulate in the tumor at the expense of stromal macrophages, which are confined to the healthy tissues surrounding the tumor. This contributes to the establishment of different macrophage niches within the breast tumor and surrounding tissue that support the generation of specific subpopulations of macrophages, with different functions and polarization status. In a model where the macrophage niches show little diversity, the profile of macrophages tends to be the same, indicating the importance of niches in the establishment of the heterogeneity of macrophages. Finally, it has been shown that in humans, TAMs also exhibit some heterogeneity suggesting the establishment of different macrophage niches during human breast cancer development (94).

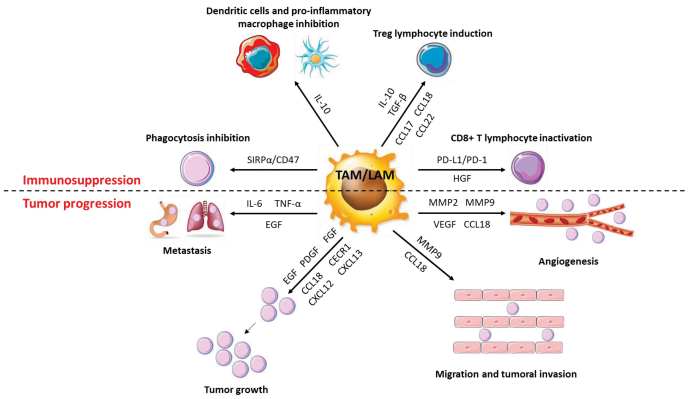

FIGURE 6
Role of macrophages in cancer progression. TAMs have a very diverse activity profile to promote cancer cells. They promote the growth and metastatic potential of cancer cells by secreting numerous molecules (cytokines, chemokines, growth factors, etc.) that act directly or indirectly on them. Thus, TAMs disrupt the anti-tumor response and promote angiogenesis, tumor growth and metastatic potential.

Anti-inflammatory macrophages are likely the most represented immune cells in the extracellular environment of solid tumors. They are recruited by cancer cells and the environment of the tumor shapes their functions. Indeed, co-culture of macrophages with ovarian tumor cells leads to their polarization into TAMs and is accompanied by overexpression of anti-inflammatory cytokines and chemokines and angiogenesis-promoting growth factors like VEGF (95). In the TME, exosomes are produced by a wide variety of cell types including tumor cells, whose components cause the differentiation and polarization of monocytes into TAMs (96). These exosomes also block the differentiation of monocytes into dendritic cells to ensure a significant presence of anti-inflammatory macrophages and to limit immune response. These TAMs are strongly immunosuppressive and secrete high amounts of IL-10 and TGFβ and fail to express MHC-II, thus preventing the activation of T lymphocytes. In addition, they dampen T cell proliferation in a TGF-β-dependent manner (97). CSF-1 is a poor prognostic marker in multiple cancers, including pancreatic cancer and breast cancer. Indeed, CSF-1 primes the differentiation of monocytes into macrophages with an anti-inflammatory profile and favors the anti-inflammatory polarization of macrophages (98–100). MCP-1 which is involved in monocyte recruitment to the tumor is secreted by cancer cells and leads to the massive recruitment of monocytes that, once in the tumor microenvironment can differentiate and polarize into TAMs. Once polarized, TAMs are also able to secrete MCP-1 to amplify the recruitment of new monocytes, thus forming a permanent recruitment loop (101, 102). Finally, VEGF or Placental Growth Factor (PlGF) are also able to induce the recruitment and survival of monocytes in the tumor micro-environment (103, 104).

3.5 Functions of TAMs

TAMs exert numerous pro-tumoral effects among which immunosuppression, tumor growth, angiogenesis, and improvement of the metastatic potential of cancerous cells.

3.5.1 Immunosuppressive functions

TAMs secrete huge amounts of IL-10 and TGFβ that promote the activation of T cells into Th2 or Treg at the expense of pro-inflammatory Th1 T cells (105). Within the tumor, Tregs inhibit other types of T cells and in particular cytotoxic T cells whose main function is to eliminate cancer cells. TAMs also secrete various chemokines allowing the recruitment of immune cells with immunosuppressive functions. Thus, CCL17 and CCL22 induce the recruitment of Th2 and Treg lymphocytes while CCL18 promotes the recruitment of naive T lymphocytes. Naïve T lymphocytes, while being able to be activated as Th2 or Treg, promote cell anergy when they are in a particularly anti-inflammatory and immunosuppressive environment as is the case within a tumor (106). In ovarian cancers, Tregs are recruited by TAMs via CCL22 and presence of Tregs is a marker of poor prognosis (107). The secretion of IL-10 by TAMs inhibits the expression of pro-inflammatory cytokines such as IL-12 or TNFα by macrophages and dendritic cells and reduces IFNγ expression by NK cells, thus contributing to make the tumor microenvironment anti-inflammatory and to limit the pro-tumor response of the immune cells. IL-10 also reduces the expression of CD80 and CD86 co-stimulatory receptors on the surface of macrophages and dendritic cells, decreasing their ability to activate cytotoxic T cells (108). Finally, TAMs express co-inhibitory molecules such as PD-L1 (b7-h1) or b7-h4 on their surface, which function to block T cell activation. PD-L1 is known to bind to the PD-1 receptor of active T cells, resulting in the abolition of their activity by suppressing the pro-inflammatory action of T cells. The co-inhibitory molecule b7-h4 has a similar mechanism of action to PD-L1 but, unlike PD-L1, the receptor for b7-h4 has not yet been identified. However, it has been determined that b7-h4 can block cytotoxic T-cell activity, like PD-L1. The expression of b7-h4 by TAMs is increased by IL-10 secreted by Treg lymphocytes (109–112).

3.5.2 Function as promoter of tumor growth

TAMs express and secrete numerous factors that promote tumor growth, such as EGF (Epithelial Growth Factor), PDGF (Platelet-Derived Growth Factor), FGF (Fibroblast Growth Factor) or HGF (Hepatocyte Growth Factor) (113). In ovarian cancers, expression by TAMs of the EGF-R triggers cancer cell proliferation and promotes their migration (114). In phyllodes tumors, a rare form of breast cancer, a positive feedback loop is established between TAMs and myofibroblasts and promotes tumor progression. Myofibroblasts secrete the chemokine CCL5 which binds to the CCR5 receptor expressed on the surface of macrophages, stimulates the AKT pathway and induces the polarization of macrophages into TAMs. TAMs then secrete the chemokine CCL18, which promotes phyllodes tumor proliferation by inducing the differentiation of fibroblasts into myofibroblasts, which in turn secrete CCL5 (115).

3.5.3 Functions in neo-angiogenesis

One of the main characteristics of solid tumors is the generation of new blood vessels to sustain their development according to increased supply of nutrients. TAMs promote angiogenesis by expressing numerous pro-angiogenic factors such as VEGF, BFGF (Basic Fibroblast Growth Factor), TNFα or metalloproteinases such as MMP2 and MMP9. The expression of these different molecules leads to the proliferation of endothelial cells, the remodeling of the extracellular matrix and the neo-vascularization of tissues in cancers (116, 117). Moreover, VEGF production is greatly increased when TAMs are stimulated with CSF-1 or CCL2, inducing increased angiogenesis when these two cytokines/chemokines are present in large amounts within the tumor (118). CCL18 secretion by TAMs, in association with VEGF, also promotes angiogenesis. Nevertheless, the mode of action of the chemokine CCL18 on VEGF production, and more generally on the induction of angiogenesis, has not yet been determined (119).

3.5.4 Functions in promoting metastatic potential

The dissemination of cancer cells in the body (metastasis) is a marker of very poor prognosis in all types of cancers. An epithelial-mesenchymal transition (EMT) stage is necessary for cancer cells to spread in the body. During this step, cancer cells lose their cell-cell adhesion, acquire migratory properties, invade the extracellular matrix before transiting through blood vessels to form metastases (120, 121). TAMs are important players in the dissemination of cancer cells as they contribute to the degradation of the extracellular matrix by secreting proteases into the extracellular environment, including cathepsins or metalloproteinases (122). For example, the production of MMP9 by TAMs contributes to the metastatic potential of melanoma by restructuring the extracellular matrix (123). In lung cancers, TAMs secrete IL-6 and TNFα in response to TLR2 activation by versicane, a proteoglycan produced by cancer cells. Both cytokines are required for cancer cell dissemination by inducing low-grade inflammation that promotes extracellular matrix destruction (124). Excessive production of CCL18 by TAMs is correlated with increased aggressiveness of cancer cells. Indeed, CCL18 can bind to the PITPNM3 receptor of cancer cells to induce integrin clustering that enhances the invasion of the extracellular matrix by cancer cells leading to their migration and metastasis (125). Finally, TAMs can directly promote EMT by secreting EGF. EGF binds to the EGFR, resulting in activation of the ERK1/2 pathway and expression of various markers of EMT including vimentin and Slug (126).

3.6 LAMs in leukemia

The presence of macrophages within hematopoietic stem cell niches in the BM has only been recently documented (127–129). In this line, the presence of leukemia-associated macrophages (LAMs) within the BM was demonstrated in a mouse model of T-ALL (T Acute Lymphoblastic Leukemia). In this model, LAMs display unique characteristics that differ significantly from TAMs, including both a pro- and anti-inflammatory gene expression profile. LAMs produce lower amounts of CSF-1, TGFβ, and VEGF than TAMs but exhibit higher amounts of IL-1β, IL-6, and CXCL11 (76). Despite these differences, LAMs share the same functions and mechanism of action as TAMs, i.e., pro-tumor effects such as immunosuppression or cancer cell proliferation. Nevertheless, the role of LAMs in the metastatic potential of hematologic cancer cells is still poorly established (80). In Acute Myeloid Leukemia (AML), cancer cells induce the differentiation and polarization of monocytes into LAMs via Gfi1, a transcription factor involved in macrophage development (130). Moreover, it was established that LAMs are associated with an unfavorable prognosis in AML patients (131). In T-ALL and chronic lymphocytic leukemia (CLL), the generation of LAMs is dependent on M-CSF. Indeed, inhibition of CSF1R leads to a defect in anti-inflammatory macrophage infiltration in BM as well as reduced leukemia progression (132–135). In CLL, LAMs, also known as CLL-nurse like cells (NLCs), promote the survival and proliferation of cancer cells via the expression of the chemokines CXCL12 and CXCL13 and impairs treatment-mediated apoptosis (136).

4 Targeting macrophages in cancer

4.1 In solid tumors

The identification of the deleterious role of TAMs in cancer has paved the way for the development of therapeutic strategies to modulate their functions. These strategies aim at limiting their recruitment or/and depleting, modulating, or reprogramming them within the tumor (Figure 7). In this section, we will essentially present the different results obtained in recent years in pre-clinical models and in clinical studies.

4.1.1 Recruitment, generation, and depletion of TAMs

The CCL2-CCR2 axis is the main pathway for the recruitment of TAMs within the tumor. Targeting this pathway allows to reduce the number of TAMs recruited and to promote a pro-inflammatory

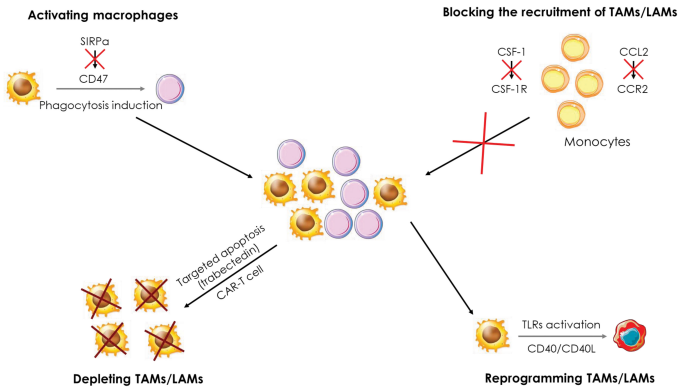

FIGURE 7
Therapeutic strategies targeting macrophages in cancer. Several therapeutic strategies targeting TAMs/LAMs are being developed to treat cancers. i) Blockade of monocyte recruitment by inhibiting the CCL2/CCR2 and CSF-1/CSFR1 axes, ii) Depletion of TAMs/LAMs using apoptosis inducers and CAR-T cells, iii) Activation of macrophages through the inhibition of the SIRPα/CD47 axis to induce phagocytosis of cancer cells and iv) reprogramming of TAMs/LAMs by activation of the CD40/CD40L axis and TLRs.

response and a reduction of tumor growth. CCL2 deletion in many types of cancers (lung, endometrial, breast, etc.) leads to a drastic decrease in the number of TAMs infiltrating the tumors because of defects in monocyte recruitment (137–139). The use of CCL2 neutralizing antibodies in a mouse model of xenografted human renal cancer strongly reduces the presence of TAMs, xenograft growth and blood vessel density (140). In parallel to the pre-clinical trials, clinical studies were conducted targeting either CCL2 or CCR2 and CCR5 receptors. For example, a phase II study in prostate cancer patients was managed to investigate the efficacy of Carlumab, an antibody directed against CCL2. Although Carlumab was well tolerated by patients, it only resulted in transient suppression of chemokine effects, did not block the CCL2/CCR2 pathway, and exhibit no anti-tumor effect (141). Two phase 1b/2 studies in patients with pancreatic cancer were launched to test the tolerability and efficacy of a CCR2 antagonist, PF-04136309. The first one showed that PF-04136309, in combination with Folforinox chemotherapy, was well tolerated by patients and induced a decrease in the number of TAMs in tumors (142). The second study established first that PF-04136309 in combination with nab-paclitaxel and gemcitabine exhibits some lung toxicity in patients. In addition, the decrease in the number of TAMs in tumors was observed in only 2 of the 21 patients enrolled in the study (143), two observations that preclude further utilization of this combo in the clinic. By contrast, the PF-04136309/Folforinox combination which shows acceptable results in phase 1b/2 would warrant further investigation. Finally, a recent phase I study in patients with colorectal cancer showed no benefit of the anti-PD-1 drug Pembrolizumab and the CCR5 antagonist Maraviroc combination (144). Nevertheless, additional phase I and II studies involving blockade of the CCL2/CCR2 pathway are underway in various types of cancers (145).

CSF-1 is another cytokine that allows the recruitment of TAMs to the tumor and several therapeutic strategies aiming at blocking the activation of the CSF-1/CSF1R pathway are currently investigated. For instance, CSF1R inhibition was shown to exhibit anti-tumor activity in AML by blocking paracrine signals from support cells (146) and disruption of CSF-1 receptor signaling by BLZ945 inhibits growth of AML cells with inversion of the chromosome 16 (147). Emactuzumab is a human monoclonal antibody to CSF1R that blocks its dimerization and activation that was found to trigger the specific depletion of anti-inflammatory CSF1R+ macrophages *in vitro* and *in vivo* in the primate Macaca Fascicularis. However, macrophages generated following stimulation with CSF-2, which exhibit a global pro-inflammatory profile, are not affected by Emactuzumab. In mice, a murine antibody against CSF1R, named 2G2, was generated to mimic the action of Emactuzumab. In colorectal cancer and fibrosarcoma models, 2G2 induced a drastic reduction in the number of TAMs in the tumors associated to a greater infiltration of neutrophils and cytotoxic T lymphocytes, impeding tumor development. Finally, a phase I study was conducted in patients with pigmented villonodular synovitis (SVN or diffuse-type giant cell tumor (Dt-GCT)), a rare type of tumor. The administration of Emactuzumab improves the clinical status of patients inducing partial responses. This study was completed by administering Emactuzumab to patients with various other types of solid tumors (lung cancer, liver cancer, …) with similar results. Thus, targeting the CSF-1/CSF1R pathway appears to represent an attractive therapeutic strategy in the treatment of cancers (148, 149). A phase I study in glioblastoma patients evaluated the toxicity and efficacy of BLZ945, in combination with PDR001, an anti-PD1 antibody. A good tolerance of the combination was established combined with encouraging anti-tumor activity, which led to the initiation of a phase II study that is currently underway (150). In a mouse model of lung cancer, BLZ945 fails to induce depletion of CSF1R+ TAMs but causes remodeling of the tumor microenvironment in which immune cells present within the tumor, such as NK or T cells, secrete large amounts of IFN-γ. In addition, dendritic cells were found to express high level of IL-12, together promoting an effective anti-tumor response (151). PLX3397 is a CSF1R inhibitor that induces TAMs depletion in a mouse model of osteosarcoma. This depletion results in a slowdown of tumor growth and a decrease in the number of metastases, while reducing the number of Treg and improving tumor infiltration by cytotoxic T lymphocytes (152). A phase I study in patients with sarcoma established that PLX3397 in combination with Sirolimus an mTOR pathway inhibitor, was well-tolerated. In these patients, the number of TAMs was decreased in the tumors, supporting an advancement of this combination into phase II (153). In a phase II study, the combination of AMG820, an antibody to CSF1R and Pembrolizumab showed no significant effect since no treated patients exceeded the predefined efficacy threshold and only one-third of patients experienced stable disease progression or partial response (154). Other phase I and II studies involving blockade of the CSF-1/CSF1R pathway are underway in different types of cancers (145). Trabectedin, a pro-apoptotic molecule, is currently used in many clinical trials because it specifically induces apoptotic death in macrophages, including TAMs. This apoptotic effect is due to the activation of the TRAIL signaling pathway which leads to the activation of caspase-8 and ultimately to macrophage apoptosis. This apoptosis is necessary for the anti-tumor activity of trabectedin (155). Recently, a CAR-T cell (Chimeric Antigen Receptor T cell) possessing a CAR recognizing the folate receptor in mouse models of ovarian, colon or melanoma cancers showed promising results. Indeed, the folate receptor is mainly expressed by anti-inflammatory TAMs and its targeting via CAR-T cells allows to specifically suppress this macrophage population and increase the infiltration of immune cells such as cytotoxic T lymphocytes and pro-inflammatory monocytes. In addition, tumor progression was significantly slowed down, and survival of mice was improved. In conclusion, this new type of treatment could be very effective in specifically targeting TAMs while preserving other macrophage populations (156).

4.1.2 Activation/inactivation and reprogramming of TAMs

The CD40/CD40L axis is a pathway involved in the activation of pro-inflammatory macrophages. When CD40L, expressed on the surface of activated T cells, binds to the CD40 receptor, it triggers the production of various factors such as TNFα or ROS. Thus, the CD40/CD40L pathway participates in the anti-microbial and anti-

tumor activity of macrophages. In addition, it also stimulates T-cell induced immunity, thus initiating a positive feedback loop. Different strategies have been developed to trigger the activation of this pathway and to force macrophages to exert anti-tumor activity. A first phase I study with a CD40 agonist monoclonal antibody (CP-870,893) in patients with pancreatic cancer in combination with gemcitabine gave appreciable results. Indeed, the combination was well tolerated by the patients and showed promising anti-tumor effects, justifying its progression to phase II (157). In a mouse model of pancreatic cancer, the use of a CD40 agonist, FGK.45, induces T-cell infiltration into the tumor. In combination with an anti-PD1, the tumor even shows regression, dependent on the infiltration of $CD8^+$ and $CD4^+$ T cells. CD40 activation leads to an increase in CCL5 expression by TAMs allowing the recruitment of $CD4^+$ T cells into the tumor, which are essential for tumor regression. In addition, macrophages transiently express CD86 and MHC-II after treatment with a CD40 agonist, promoting pro-inflammatory T cell activation (158). The combination of 2G2 and FGK.45 not only efficiently depletes TAMs, but also induces their pro-inflammatory activation prior to their death. These results, obtained in a mouse model of colon cancer, highlighted the transient hyperactivation of TAMs that leads to the recruitment and activation of cytotoxic T cells and ultimately to tumor regression (159). In addition, a phase I clinical trial was conducted combining Emactuzumab with the CD40 agonist antibody Selicrelumab. This treatment administered to patients with various types of solid tumors showed an acceptable safety profile and an increase in the number of cytotoxic T lymphocytes in the tumors. However, no strong clinical response was achieved, 40% of patients showing stabilization of the pathology but no patient exhibiting improvement (160). In patients with metastatic pancreatic cancer, the combination of APX005M, a CD40 agonist antibody, with the reference treatment gemcitabine + nab-paclitaxel, with or without immunotherapy (using nivolumab, an anti-PD1), was well tolerated by patients. This treatment induced a clinical response in more than half of the patients (14 of 24). A phase II study is underway and if the results observed in phase I are confirmed in phase II and III assays, this combination could replace the current chemotherapy used for patients with metastatic pancreatic cancer (161). In addition, numerous phase I studies are underway in a variety of solid tumor types to determine the effects of CD40 agonists on tumor growth progression (145).

Another way to activate macrophages is to target TLRs, which, upon activation, promote the pro-inflammatory activity of macrophages and suppress their immunosuppressive activities. The gold standard treatment for bladder cancer patients is BCG (bacillus Calmette-Guérin) which stimulates TLR2 and TLR4 to induce a pro-inflammatory response in macrophages. Nevertheless, relapses are frequent, and some patients do not respond to BCG treatment. Therefore, there is a need to improve this treatment to trigger a better response in patients (162). Recently, a phase I study tested the efficacy of a percutaneous BCG primo-injection 21 days prior to intravesicular injection, with the goal of "priming" TAMs. The primary injection was well tolerated but some patients failed to respond to treatment, suggesting a mechanism of resistance to BCG (163). In a mouse model of breast cancer, the combination of IFN-γ and MPLA (Monophosphoryl Lipid A), a TLR4 ligand, results in the reduction of tumor growth and metastatic potential of cancer cells via reprogramming of TAMs into pro-inflammatory macrophages expressing TNFα and IL-12. The secretion of these two factors by the reprogrammed macrophages activates cytotoxic T lymphocytes that participate in the elimination of cancer cells. Furthermore, in a mouse model of ovarian cancer, the combination of IFN-γ and MPLA increases the sensitivity of cancer cells to chemotherapies. Currently, IFN-γ and MPLA are used separately in clinical studies and their combination could lead to a new therapeutic approach to induce reprogramming of TAMs in cancers (164). Another pre-clinical study shows an anti-tumor effect after treatment of mice with lung cancer or fibrosarcoma with the combination of a TLR3 agonist poly(I:C) and TLR8 agonists, R837 or R848. This study was motivated by the fact that these agonists are used in clinical studies individually. The combination of a TLR3 and TLR8 agonist repolarizes TAMs into pro-inflammatory macrophages, reduces tumor growth and increases T cell infiltration into tumors. Thus, combining these two agonists represents a new therapeutic opportunity and a phase I study would be interesting to conduct (165). A phase I study in patients with various types of cancers including melanoma and kidney cancer refractory to anti-PD1 showed that a nanoplexed form of poly(I:C), BO-112, in combination with an anti-PD resulted in an anti-tumor response with partial responses in 10% of patients and stabilization of the pathology in more than one third of patients. BO-112, in combination with an anti-PD1, could therefore represent a new therapeutic strategy to combat anti-PD1 resistance (165). Similarly, the use of a TLR9 agonist, CMP-001, in combination with an anti-PD1 in patients with metastatic melanoma overcomes resistance to anti-PD1. The TAMs are reprogrammed and secrete IFN-γ which allows the recruitment of T lymphocytes and a reduction of the tumor in 25% of the patients in this study. Considering these promising results, a phase II study is underway (166). Numerous other phase I to III studies involving TLR agonists are underway as monotherapy or in combination with other molecules. Overall, these treatments are well tolerated by patients and show interesting clinical effects, in particular stabilization of diverse pathologies. Currently, none of these treatments has been approved to treat cancer, but it is not excluded that some of them will complete the arsenal of cancer treatment in the coming years (145, 167–169).

Specific markers can be expressed on the cell surface that are referred to as "don't eat me" signals. One of these signals is CD47, which is overexpressed in many cancers. Expression of CD47 prevents cancer cells from being phagocytosed and thus promotes tumor growth. CD47 is recognized by the SIRPα protein expressed on the surface of monocytes/macrophages and neutrophils and multiple pre-clinical and clinical trials are underway to overcome the inhibition of phagocytosis induced by the CD47/SIRPα axis. The use of an anti-CD47 antibody not only enhances phagocytosis of cancer cells by macrophages but also facilitates antigen presentation by macrophages to ultimately activate cytotoxic T cells (170). *In vitro*, the use of an anti-CD47 antibody, Hu5F9-G4, increases the phagocytic capacities of pro-inflammatory as well

as anti-inflammatory macrophages. *In vivo*, CD47 blockade results in significant pro-inflammatory polarization of macrophages in mice xenografted with human glioblastoma and enhanced phagocytosis of tumor cells. A clinical study is underway regarding the use of Hu5F9-G4 in colorectal cancer patients (171). Two other preclinical studies in mouse models of lung cancer and breast cancer show similar results. In the lung cancer model, Hu5F9-G4 inhibited tumor growth by promoting the phagocytic abilities of macrophages (172). In the breast cancer model, Hu5F9-G4 was used in combination with trastuzumab, an anti-HER2 antibody. Indeed, nearly 30% of breast cancer patients have HER2 overexpression, and trastuzumab is one of the gold standard treatments for HER2-overexpressing breast cancers. However, relapses are frequent and new therapeutic strategies must be developed to fight these relapses more effectively. The combination of Hu5F9-G4 and trastuzumab was shown to reduce tumor growth and overcome the resistance of cancer cells to trastuzumab. This combination holds great promise, particularly for patients with trastuzumab resistance (173). Currently, results of phase I and II studies investigating the efficacy of anti-CD47 in different types of cancer show promising results, particularly in combination with reference treatments where they lead to a decrease in toxicity (145).

4.1.3 Chimeric antigen receptor macrophages

CAR-M represents a new weapon in the armamentarium of therapeutic strategies available to fight solid and hematopoietic cancers. Based on the principle of CAR-T cells, it is assumed that CAR-M cells would be more effective than CAR-T cells in patients with solid tumors. Indeed, CAR-T cells are very effective in hematological cancers but show limited results in solid tumors. In a mouse model of breast cancer, the administration of CAR-M cells expressing an anti-HER2 antibody and the transmembrane and intracellular domain of CD147 allows to specifically target cancer cells expressing HER2. The presence of CAR-M cells inhibits tumor growth and is associated with a massive infiltration of T cells in the tumor. Activation of CD147 also promotes the production of MMPs that degrade the extracellular matrix and participate in the destabilization of the tumor microenvironment (174). Injection of another CAR-M targeting HER2 into mice carrying lung metastases significantly reduced tumor burden and increased mouse survival. In addition, CAR-M can remodel the tumor microenvironment to create a pro-inflammatory climate that promotes T cell recruitment and activity. *In vitro*, CAR-M modify the phenotype of anti-inflammatory macrophages by reprogramming them into pro-inflammatory macrophages. This observation suggests that the same phenomenon takes place *in vivo*, with TAMs reprogrammed into pro-inflammatory macrophages (175). A clinical study is underway to test the efficacy of this CAR-M in patients. This new strategy seems promising and, although the number of pre-clinical and clinical studies is still very low, it would be of cardinal interest if CAR-M cells prove to be as effective in solid tumors as CAR-T cells in hematopoietic malignancies (176).

4.2 In leukemia

Many of the treatments targeting LAMs in leukemia involve the use of an anti-CD47 antibody. Bispecific antibodies have been developed to be more effective against cancer cells. RTX-CD47 is a bispecific antibody targeting CD20, a molecule overexpressed on the surface of leukemic B lymphocytes, and CD47. *In vitro*, RTX-CD47 induces phagocytosis by macrophages of B lymphocytes from different malignant B lymphocyte cell lines in a co-culture system. Moreover, the use of this bi-specific antibody on healthy donor cells does induce their phagocytosis by macrophages, demonstrating a strict specificity of this antibody for CD20 overexpressing cells. In combination with three anti-cancer therapies, daratumumab (anti-CD38), alemtuzumab (anti-CD54), and obinutuzumab (anti-CD20), TRX-CD47 synergistically increases the phagocytic potential of macrophages and allows for more efficient elimination of malignant B cells (177). CD33 is expressed on the surface of all myeloid cells but its expression significantly increased in leukemic blasts. This is why MBD004, a CD33/CD47 bi-specific antibody was used in a mouse model of AML. This bispecific antibody was shown to induce a reduction in the number of blasts. HMBDOO4 in addition to acting at the level of blasts, also reduced the hemagglutination of erythrocytes observed when using an anti-CD47 alone and therefore increases tolerability in patients. HMBD004 facilitates the specific phagocytosis of blasts by macrophages, thus leading to a decrease in tumor mass. A phase I clinical trial is underway to determine the toxicity of HMBD004 in patients with AML (178). The development of a bi-specific B-cell-targeting antibody, NI-1701, was conducted to allow targeting of CD20-resistant malignant B cells in B-CLL (B-Chronic Lymphocytic Leukemia) and B-ALL (B-Acute Lymphoblastic Leukemia). NI-1701 combines an anti-CD47 and an anti-CD19 antibody (specific marker for B lymphocytes). The use of NI-1701 in several mouse models of B-cell lymphoma and leukemia significantly reduced the growth of blasts by facilitating their phagocytosis by macrophages. Furthermore, in a primate model, NI-1701 was found to be well tolerated and could therefore entered clinical trials (179). In a phase I study, the lack of efficacy of CC-90002, an anti-CD47 antibody led to the discontinuation of the clinical trial that targeted patients with refractory or relapsed AML or high-risk myelodysplastic syndromes. Indeed, although treatment was well-tolerated, CC-90002 failed to induce a strong and durable response (180). Nevertheless, the use of anti-CD47 antibodies in combination with standard of care for different diseases has shown globally promising results. A phase I-b study combining Magrolimab, an anti-CD47, with azacitidine in patients with myelodysplastic syndromes or AML shows very promising results with a percentage objective response rate of 100% in MDS and 69% in AML. The treatment was also well tolerated by patients and was characterized by the complete loss of blast cells in the BM, particularly in TP53-mutated patients (181, 182). A phase III study is currently enrolling patients to investigate the efficacy of Magrolimab + azacitidine treatment in patients with high-risk

MDS (183). A phase Ib study in patients with mutated TP53 MDS treated with Magrolimab + Azacitidine has also been initiated and preliminary results show a durable response and increased overall survival (184). A phase III study comparing this treatment to the current standard of care is also underway (181). Other phase I, II or III clinical trials have been initiated to test the efficacy and toxicity of different anti-CD47 antibodies as a single agent or in combination with different reference treatments (185). Finally, a phase I study in patients with pediatric leukemia showed that GNKG168, a TLR9 agonist, could be an interesting therapeutic approach. Indeed, the expression of genes involved in the regulation of blasts was decreased, suggesting a beneficial role of GNKG168 in tumor progression. However, further research needs to be conducted to determine whether TLR9 activation is beneficial for pediatric leukemia patients (186).

5 Future perspectives

The versatility of macrophages can be envisioned as a promising opportunity to design novel therapies. In this line, targeting and/or reprogramming immunosuppressive macrophages during cancer progression could be of utmost importance to improve current treatments and in particular immunotherapies. To achieve this goal, a better knowledge of the molecular mechanisms of macrophage generation, activation and polarization will undoubtedly help identifying signaling pathways and vulnerabilities for TAMs or LAMs targeting and elimination/reprogramming in solid and hematopoietic tumors. In this context, several strategies to prevent anti-inflammatory macrophage-mediated immunosuppression are currently being tested in different clinical trials. These clinical strategies aimed at limiting TAMs or LAMs recruitment and/or depleting, modulating, or reprogramming them within the tumor. Finally, the identification by our group of a protease cascade CTSB>Caspase-8>Caspase-3/7>Substrates required for the differentiation of monocytes and the persistence of this pathway during M2 macrophage polarization may open new avenues to manipulate macrophage plasticity to promote solid and hematopoietic tumor elimination.

Author contributions

PC, EK, MB, CS, CF and GR were all involved in the concept, design, and critical review of the content of this article. PC makes the figures. AJ and PA write the paper. All authors agree to the accuracy and integrity of this work as presented. All authors contributed to the article and approved the submitted version.

Funding

This work was supported by INSERM, the "Investments for the Future" Labex Signalife (ANR-11-LABX-0028-01), ITMO cancer (2019–2023), the ARC Foundation. EK is supported by a fellowship from Ligue Nationale Contre le Cancer. PA team is also supported by grants from ARC Foundation (Equipe labellisée 2022-2025), the ALF association (2021–2022), and INCA (PLBIO-2019-133). PA, AJ and GR are member of the OPALE Carnot institute.

Conflict of interest

The authors declare that the research was conducted in the absence of any commercial or financial relationships that could be construed as a potential conflict of interest.

Publisher's note

References

1. Ziegler-Heitbrock HW, Ulevitch RJ. Cd14: Cell surface receptor and differentiation marker. *Immunol Today* (1993) 14(3):121–5. doi: 10.1016/0167-5699(93)90212-4

2. Wong KL, Yeap WH, Tai JJ, Ong SM, Dang TM, Wong SC. The three human monocyte subsets: Implications for health and disease. *Immunol Res* (2012) 53(1-3):41–57. doi: 10.1007/s12026-012-8297-3

3. Yona S, Kim KW, Wolf Y, Mildner A, Varol D, Breker M, et al. Fate mapping reveals origins and dynamics of monocytes and tissue macrophages under homeostasis. *Immunity* (2013) 38(1):79–91. doi: 10.1016/j.immuni.2012.12.001

4. Frankenberger M, Sternsdorf T, Pechumer H, Pforte A, Ziegler-Heitbrock HW. Differential cytokine expression in human blood monocyte subpopulations: A polymerase chain reaction analysis. *Blood* (1996) 87(1):373–7. doi: 10.1182/blood.V87.1.373.373

5. Gordon S, Taylor PR. Monocyte and macrophage heterogeneity. *Nat Rev Immunol* (2005) 5(12):953–64. doi: 10.1038/nri1733

6. Tacke F, Randolph GJ. Migratory fate and differentiation of blood monocyte subsets. *Immunobiology* (2006) 211(6-8):609–18. doi: 10.1016/j.imbio.2006.05.025

7. Anbazhagan K, Duroux-Richard I, Jorgensen C, Apparailly F. Transcriptomic network support distinct roles of classical and non-classical monocytes in human. *Int Rev Immunol* (2014) 33(6):470–89. doi: 10.3109/08830185.2014.902453

8. Duroux-Richard I, Robin M, Peillex C, Apparailly F. Micrornas: Fine tuners of monocyte heterogeneity. *Front Immunol* (2019) 10:2145. doi: 10.3389/fimmu.2019.02145

9. van Furth R, Cohn ZA, Hirsch JG, Humphrey JH, Spector WG, Langevoort HL. The mononuclear phagocyte system: A new classification of macrophages, monocytes, and their precursor cells. *Bull World Health Organ* (1972) 46(6):845–52.

10. Belge KU, Dayyani F, Horelt A, Siedlar M, Frankenberger M, Frankenberger B, et al. The proinflammatory Cd14+Cd16+Dr++ monocytes are a major source of tnf. *J Immunol* (2002) 168(7):3536–42. doi: 10.4049/jimmunol.168.7.3536

11. Schlitt A, Heine GH, Blankenberg S, Espinola-Klein C, Dopheide JF, Bickel C, et al. Cd14+Cd16+ monocytes in coronary artery disease and their relationship to serum tnf-alpha levels. *Thromb Haemost* (2004) 92(2):419–24. doi: 10.1160/TH04-02-0095

12. Moniuszko M, Bodzenta-Lukaszyk A, Kowal K, Lenczewska D, Dabrowska M. Enhanced frequencies of Cd14++Cd16+, but not Cd14+Cd16+, peripheral blood

monocytes in severe asthmatic patients. *Clin Immunol* (2009) 130(3):338–46. doi: 10.1016/j.clim.2008.09.011

13. Selimoglu-Buet D, Wagner-Ballon O, Saada V, Bardet V, Itzykson R, Bencheikh L, et al. Characteristic repartition of monocyte subsets as a diagnostic signature of chronic myelomonocytic leukemia. *Blood* (2015) 125(23):3618–26. doi: 10.1182/blood-2015-01-620781

14. Davies LC, Jenkins SJ, Allen JE, Taylor PR. Tissue-resident macrophages. *Nat Immunol* (2013) 14(10):986–95. doi: 10.1038/ni.2705

15. Epelman S, Lavine KJ, Beaudin AE, Sojka DK, Carrero JA, Calderon B, et al. Embryonic and adult-derived resident cardiac macrophages are maintained through distinct mechanisms at steady state and during inflammation. *Immunity* (2014) 40 (1):91–104. doi: 10.1016/j.immuni.2013.11.019

16. Molawi K, Wolf Y, Kandalla PK, Favret J, Hagemeyer N, Frenzel K, et al. Progressive replacement of embryo-derived cardiac macrophages with age. *J Exp Med* (2014) 211(11):2151–8. doi: 10.1084/jem.20140639

17. Ginhoux F, Guilliams M. Tissue-resident macrophage ontogeny and homeostasis. *Immunity* (2016) 44(3):439–49. doi: 10.1016/j.immuni.2016.02.024

18. Hoeffel G, Ginhoux F. Fetal monocytes and the origins of tissue-resident macrophages. *Cell Immunol* (2018) 330:5–15. doi: 10.1016/j.cellimm.2018.01.001

19. Guilliams M, Scott CL. Does niche competition determine the origin of tissue-resident macrophages? *Nat Rev Immunol* (2017) 17(7):451–60. doi: 10.1038/nri.2017.42

20. Guilliams M, Thierry GR, Bonnardel J, Bajenoff M. Establishment and maintenance of the macrophage niche. *Immunity* (2020) 52(3):434–51. doi: 10.1016/j.immuni.2020.02.015

21. Bessis A, Bechade C, Bernard D, Roumier A. Microglial control of neuronal death and synaptic properties. *Glia* (2007) 55(3):233–8. doi: 10.1002/glia.20459

22. Boyce BF, Yao Z, Xing L. Osteoclasts have multiple roles in bone in addition to bone resorption. *Crit Rev Eukaryot Gene Expr* (2009) 19(3):171–80. doi: 10.1615/critreveukargeneexpr.v19.i3.10

23. Park MD, Silvin A, Ginhoux F, Merad M. Macrophages in health and disease. *Cell* (2022) 185(23):4259–79. doi: 10.1016/j.cell.2022.10.007

24. Imhof BA, Aurrand-Lions M. Adhesion mechanisms regulating the migration of monocytes. *Nat Rev Immunol* (2004) 4(6):432–44. doi: 10.1038/nri1375

25. Nourshargh S, Alon R. Leukocyte migration into inflamed tissues. *Immunity* (2014) 41(5):694–707. doi: 10.1016/j.immuni.2014.10.008

26. Italiani P, Boraschi D. From monocytes to M1/M2 macrophages: Phenotypical vs. functional differentiation. *Front Immunol* (2014) 5:514. doi: 10.3389/fimmu.2014.00514

27. Stanley ER, Chen DM, Lin HS. Induction of macrophage production and proliferation by a purified colony stimulating factor. *Nature* (1978) 274(5667):168–70. doi: 10.1038/274168a0

28. Boulakirba S, Pfeifer A, Mhaidly R, Obba S, Goulard M, Schmitt T, et al. Il-34 and csf-1 display an equivalent macrophage differentiation ability but a different polarization potential. *Sci Rep* (2018) 8(1):256. doi: 10.1038/s41598-017-18433-4

29. Yeung YG, Jubinsky PT, Sengupta A, Yeung DC, Stanley ER. Purification of the colony-stimulating factor 1 receptor and demonstration of its tyrosine kinase activity. *Proc Natl Acad Sci U.S.A.* (1987) 84(5):1268–71. doi: 10.1073/pnas.84.5.1268

30. Lin H, Lee E, Hestir K, Leo C, Huang M, Bosch E, et al. Discovery of a cytokine and its receptor by functional screening of the extracellular proteome. *Science* (2008) 320(5877):807–11. doi: 10.1126/science.1154370

31. Stanley ER, Chitu V. Csf-1 receptor signaling in myeloid cells. *Cold Spring Harb Perspect Biol* (2014) 6(6). doi: 10.1101/cshperspect.a021857

32. van der Geer P, Hunter T. Tyrosine 706 and 807 phosphorylation site mutants in the murine colony-stimulating factor-1 receptor are unaffected in their ability to bind or phosphorylate phosphatidylinositol-3 kinase but show differential defects in their ability to induce early response gene transcription. *Mol Cell Biol* (1991) 11(9):4698–709. doi: 10.1128/mcb.11.9.4698-4709.1991

33. Pawson T, Schlessingert J. Sh2 and Sh3 domains. *Curr Biol* (1993) 3(7):434–42. doi: 10.1016/0960-9822(93)90350-w

34. Suzu S, Hiyoshi M, Yoshidomi Y, Harada H, Takeya M, Kimura F, et al. M-Csf-Mediated macrophage differentiation but not proliferation is correlated with increased and prolonged erk activation. *J Cell Physiol* (2007) 212(2):519–25. doi: 10.1002/jcp.21045

35. Gobert Gosse S, Bourgin C, Liu WQ, Garbay C, Mouchiroud G. M-csf stimulated differentiation requires persistent mek activity and mapk phosphorylation independent of Grb2-sos association and phosphatidylinositol 3-kinase activity. *Cell Signal* (2005) 17(11):1352–62. doi: 10.1016/j.cellsig.2005.02.002

36. Richardson ET, Shukla S, Nagy N, Boom WH, Beck RC, Zhou L, et al. Erk signaling is essential for macrophage development. *PloS One* (2015) 10(10):e0140064. doi: 10.1371/journal.pone.0140064

37. Curry JM, Eubank TD, Roberts RD, Wang Y, Pore N, Maity A, et al. M-csf signals through the Mapk/Erk pathway Via Sp1 to induce vegf production and induces angiogenesis in vivo. *PloS One* (2008) 3(10):e3405. doi: 10.1371/journal.pone.0003405

38. Marks DC, Csar XF, Wilson NJ, Novak U, Ward AC, Kanagasundarum V, et al. Expression of a Y559f mutant csf-1 receptor in M1 myeloid cells: A role for src kinases in csf-1 receptor-mediated differentiation. *Mol Cell Biol Res Commun* (1999) 1(2):144–52. doi: 10.1006/mcbr.1999.0123

39. Pixley FJ, Stanley ER. Csf-1 regulation of the wandering macrophage: Complexity in action. *Trends Cell Biol* (2004) 14(11):628–38. doi: 10.1016/j.tcb.2004.09.016

40. Schlaepfer DD, Hauck CR, Sieg DJ. Signaling through focal adhesion kinase. *Prog Biophys Mol Biol* (1999) 71(3-4):435–78. doi: 10.1016/s0079-6107(98)00052-2

41. Suen PW, Ilic D, Caveggion E, Berton G, Damsky CH, Lowell CA. Impaired integrin-mediated signal transduction, altered cytoskeletal structure and reduced motility in Hck/Fgr deficient macrophages. *J Cell Sci* (1999) 112(Pt 22):4067–78. doi: 10.1242/jcs.112.22.4067

42. Bourgin-Hierle C, Gobert-Gosse S, Therier J, Grasset MF, Mouchiroud G. Src-family kinases play an essential role in differentiation signaling downstream of macrophage colony-stimulating factor receptors mediating persistent phosphorylation of phospholipase c-Gamma2 and map kinases Erk1 and Erk2. *Leukemia* (2008) 22(1):161–9. doi: 10.1038/sj.leu.2404986

43. Jacquel A, Benikhlef N, Paggetti J, Lalaoui N, Guery L, Dufour EK, et al. Colony-stimulating factor-1-Induced oscillations in phosphatidylinositol-3 Kinase/Akt are required for caspase activation in monocytes undergoing differentiation into macrophages. *Blood* (2009) 114(17):3633–41. doi: 10.1182/blood-2009-03-208843

44. Reedijk M, Liu X, van der Geer P, Letwin K, Waterfield MD, Hunter T, et al. Tyr721 regulates specific binding of the csf-1 receptor kinase insert to pi 3'-kinase Sh2 domains: A model for Sh2-mediated receptor-target interactions. *EMBO J* (1992) 11 (4):1365–72. doi: 10.1002/j.1460-2075.1992.tb05181.x

45. Bourette RP, Myles GM, Choi JL, Rohrschneider LR. Sequential activation of phoshatidylinositol 3-kinase and phospholipase c-Gamma2 by the m-csf receptor is necessary for differentiation signaling. *EMBO J* (1997) 16(19):5880–93. doi: 10.1093/emboj/16.19.5880

46. Kelley TW, Graham MM, Doseff AI, Pomerantz RW, Lau SM, Ostrowski MC, et al. Macrophage colony-stimulating factor promotes cell survival through Akt/Protein kinase b. *J Biol Chem* (1999) 274(37):26393–8. doi: 10.1074/jbc.274.37.26393

47. Busca A, Saxena M, Kumar A. Critical role for antiapoptotic bcl-xl and mcl-1 in human macrophage survival and cellular Iap1/2 (Ciap1/2) in resistance to hiv-Vpr-Induced apoptosis. *J Biol Chem* (2012) 287(18):15118–33. doi: 10.1074/jbc.M111.312660

48. Busca A, Saxena M, Iqbal S, Angel J, Kumar A. Pi3k/Akt regulates survival during differentiation of human macrophages by maintaining nf-Kappab-Dependent expression of antiapoptotic bcl-xl. *J Leukoc Biol* (2014) 96(6):1011–22. doi: 10.1189/jlb.1A0414-212R

49. Sordet O, Rebe C, Plenchette S, Zermati Y, Hermine O, Vainchenker W, et al. Specific involvement of caspases in the differentiation of monocytes into macrophages. *Blood* (2002) 100(13):4446–53. doi: 10.1182/blood-2002-06-1778

50. Kang TB, Ben-Moshe T, Varfolomeev EE, Pewzner-Jung Y, Yogev N, Jurewicz A, et al. Caspase-8 serves both apoptotic and nonapoptotic roles. *J Immunol* (2004) 173 (5):2976–84. doi: 10.4049/jimmunol.173.5.2976

51. Rebe C, Cathelin S, Launay S, Filomenko R, Prevotat L, L'Ollivier C, et al. Caspase-8 prevents sustained activation of nf-kappab in monocytes undergoing macrophagic differentiation. *Blood* (2007) 109(4):1442–50. doi: 10.1182/blood-2006-03-011585

52. Cathelin S, Rebe C, Haddaoui L, Simioni N, Verdier F, Fontenay M, et al. Identification of proteins cleaved downstream of caspase activation in monocytes undergoing macrophage differentiation. *J Biol Chem* (2006) 281(26):17779–88. doi: 10.1074/jbc.M600537200

53. Guery L, Benikhlef N, Gautier T, Paul C, Jego G, Dufour E, et al. Fine-tuning nucleophosmin in macrophage differentiation and activation. *Blood* (2011) 118 (17):4694–704. doi: 10.1182/blood-2011-03-341255

54. Solier S, Mondini M, Meziani L, Jacquel A, Lacout C, Berghe TV, et al. Caspase inhibition modulates monocyte-derived macrophage polarization in damaged tissues. *Int J Mol Sci* (2023) 24(4). doi: 10.3390/ijms24044151

55. Jacquel A, Obba S, Boyer L, Dufies M, Robert G, Gounon P, et al. Autophagy is required for csf-1-Induced macrophagic differentiation and acquisition of phagocytic functions. *Blood* (2012) 119(19):4527–31. doi: 10.1182/blood-2011-11-392167

56. Obba S, Hizir Z, Boyer L, Selimoglu-Buet D, Pfeifer A, Michel G, et al. The Prkaa1/Ampkalpha1 pathway triggers autophagy during Csf1-induced human monocyte differentiation and is a potential target in cmml. *Autophagy* (2015) 11 (7):1114–29. doi: 10.1080/15548627.2015.1034406

57. Lawrence T, Natoli G. Transcriptional regulation of macrophage polarization: Enabling diversity with identity. *Nat Rev Immunol* (2011) 11(11):750–61. doi: 10.1038/nri3088

58. Xue J, Schmidt SV, Sander J, Draffehn A, Krebs W, Quester I, et al. Transcriptome-based network analysis reveals a spectrum model of human macrophage activation. *Immunity* (2014) 40(2):274–88. doi: 10.1016/j.immuni.2014.01.006

59. Mantovani A, Sica A, Sozzani S, Allavena P, Vecchi A, Locati M. The chemokine system in diverse forms of macrophage activation and polarization. *Trends Immunol* (2004) 25(12):677–86. doi: 10.1016/j.it.2004.09.015

60. Shapouri-Moghaddam A, Mohammadian S, Vazini H, Taghadosi M, Esmaeili SA, Mardani F, et al. Macrophage plasticity, polarization, and function in health and disease. *J Cell Physiol* (2018) 233(9):6425–40. doi: 10.1002/jcp.26429

61. Porta C, Riboldi E, Ippolito A, Sica A. Molecular and epigenetic basis of macrophage polarized activation. *Semin Immunol* (2015) 27(4):237–48. doi: 10.1016/j.smim.2015.10.003

62. Kurowska-Stolarska M, Stolarski B, Kewin P, Murphy G, Corrigan CJ, Ying S, et al. Il-33 amplifies the polarization of alternatively activated macrophages that contribute to airway inflammation. *J Immunol* (2009) 183(10):6469–77. doi: 10.4049/jimmunol.0901575

63. Albina JE, Mills CD, Henry WLJr., Caldwell MD. Temporal expression of different pathways of 1-arginine metabolism in healing wounds. *J Immunol* (1990) 144 (10):3877–80. doi: 10.4049/jimmunol.144.10.3877

64. Wynn TA, Vannella KM. Macrophages in tissue repair, regeneration, and fibrosis. *Immunity* (2016) 44(3):450–62. doi: 10.1016/j.immuni.2016.02.015

65. Ambarus CA, Santegoets KC, van Bon L, Wenink MH, Tak PP, Radstake TR, et al. Soluble immune complexes shift the tlr-induced cytokine production of distinct polarized human macrophage subsets towards il-10. *PloS One* (2012) 7(4):e35994. doi: 10.1371/journal.pone.0035994

66. Wang LX, Zhang SX, Wu HJ, Rong XL, Guo J. M2b macrophage polarization and its roles in diseases. *J Leukoc Biol* (2019) 106(2):345–58. doi: 10.1002/JLB.3RU1018-378RR

67. Nakamura K, Ito I, Kobayashi M, Herndon DN, Suzuki F. Orosomucoid 1 drives opportunistic infections through the polarization of monocytes to the M2b phenotype. *Cytokine* (2015) 73(1):8–15. doi: 10.1016/j.cyto.2015.01.017

68. Asai A, Nakamura K, Kobayashi M, Herndon DN, Suzuki F. Ccl1 released from M2b macrophages is essentially required for the maintenance of their properties. *J Leukoc Biol* (2012) 92(4):859–67. doi: 10.1189/jlb.0212107

69. Zingoni A, Soto H, Hedrick JA, Stoppacciaro A, Storlazzi CT, Sinigaglia F, et al. The chemokine receptor Ccr8 is preferentially expressed in Th2 but not Th1 cells. *J Immunol* (1998) 161(2):547–51. doi: 10.4049/jimmunol.161.2.547

70. Tang L, Zhang H, Wang C, Li H, Zhang Q, Bai J. M2a and M2c macrophage subsets ameliorate inflammation and fibroproliferation in acute lung injury through interleukin 10 pathway. *Shock* (2017) 48(1):119–29. doi: 10.1097/SHK.0000000000000820

71. Stitt TN, Conn G, Gore M, Lai C, Bruno J, Radziejewski C, et al. The anticoagulation factor protein s and its relative, Gas6, are ligands for the tyro 3/Axl family of receptor tyrosine kinases. *Cell* (1995) 80(4):661–70. doi: 10.1016/0092-8674(95)90520-0

72. Scott RS, McMahon EJ, Pop SM, Reap EA, Caricchio R, Cohen PL, et al. Phagocytosis and clearance of apoptotic cells is mediated by mer. *Nature* (2001) 411 (6834):207–11. doi: 10.1038/35075603

73. Zizzo G, Hilliard BA, Monestier M, Cohen PL. Efficient clearance of early apoptotic cells by human macrophages requires M2c polarization and mertk induction. *J Immunol* (2012) 189(7):3508–20. doi: 10.4049/jimmunol.1200662

74. Duluc D, Delneste Y, Tan F, Moles MP, Grimaud L, Lenoir J, et al. Tumor-associated leukemia inhibitory factor and il-6 skew monocyte differentiation into tumor-associated macrophage-like cells. *Blood* (2007) 110(13):4319–30. doi: 10.1182/blood-2007-02-072587

75. Duluc D, Corvaisier M, Blanchard S, Catala L, Descamps P, Gamelin E, et al. Interferon-gamma reverses the immunosuppressive and protumoral properties and prevents the generation of human tumor-associated macrophages. *Int J Cancer* (2009) 125(2):367–73. doi: 10.1002/ijc.24401

76. Chen SY, Yang X, Feng WL, Liao JF, Wang LN, Feng L, et al. Organ-specific microenvironment modifies diverse functional and phenotypic characteristics of leukemia-associated macrophages in mouse T cell acute lymphoblastic leukemia. *J Immunol* (2015) 194(6):2919–29. doi: 10.4049/jimmunol.1400451

77. Mantovani A, Schioppa T, Porta C, Allavena P, Sica A. Role of tumor-associated macrophages in tumor progression and invasion. *Cancer Metastasis Rev* (2006) 25 (3):315–22. doi: 10.1007/s10555-006-9001-7

78. Yang X, Feng W, Wang R, Yang F, Wang L, Chen S, et al. Hepatic leukemia-associated macrophages exhibit a pro-inflammatory phenotype in Notch1-induced acute T cell leukemia. *Immunobiology* (2018) 223(1):73–80. doi: 10.1016/j.imbio.2017.10.009

79. Wang Q, Ni H, Lan L, Wei X, Xiang R, Wang Y. Fra-1 protooncogene regulates il-6 expression in macrophages and promotes the generation of M2d macrophages. *Cell Res* (2010) 20(6):701–12. doi: 10.1038/cr.2010.52

80. Wang L, Zheng G. Macrophages in leukemia microenvironment. *Blood Sci* (2019) 1(1):29–33. doi: 10.1097/BS9.0000000000000014

81. Hoves S, Krause SW, Schutz C, Halbritter D, Scholmerich J, Herfarth H, et al. Monocyte-derived human macrophages mediate anergy in allogeneic T cells and induce regulatory T cells. *J Immunol* (2006) 177(4):2691–8. doi: 10.4049/jimmunol.177.4.2691

82. Cella M, Dohring C, Samaridis J, Dessing M, Brockhaus M, Lanzavecchia A, et al. A novel inhibitory receptor (Ilt3) expressed on monocytes, macrophages, and dendritic cells involved in antigen processing. *J Exp Med* (1997) 185(10):1743–51. doi: 10.1084/jem.185.10.1743

83. Pinhal-Enfield G, Ramanathan M, Hasko G, Vogel SN, Salzman AL, Boons GJ, et al. An angiogenic switch in macrophages involving synergy between toll-like receptors 2, 4, 7, and 9 and adenosine a(2a) receptors. *Am J Pathol* (2003) 163 (2):711–21. doi: 10.1016/S0002-9440(10)63698-X

84. Porcheray F, Viaud S, Rimaniol AC, Leone C, Samah B, Dereuddre-Bosquet N, et al. Macrophage activation switching: An asset for the resolution of inflammation. *Clin Exp Immunol* (2005) 142(3):481–9. doi: 10.1111/j.1365-2249.2005.02934.x

85. Davis MJ, Tsang TM, Qiu Y, Dayrit JK, Freij JB, Huffnagle GB, et al. Macrophage M1/M2 polarization dynamically adapts to changes in cytokine microenvironments in cryptococcus neoformans infection. *mBio* (2013) 4(3):e00264–13. doi: 10.1128/mBio.00264-13

86. Ma Q, Gu JT, Wang B, Feng J, Yang L, Kang XW, et al. Plgf signaling and macrophage repolarization contribute to the anti-neoplastic effect of metformin. *Eur J Pharmacol* (2019) 863:172696. doi: 10.1016/j.ejphar.2019.172696

87. Asano K, Nabeyama A, Miyake Y, Qiu CH, Kurita A, Tomura M, et al. Cd169-positive macrophages dominate antitumor immunity by crosspresenting dead cell-associated antigens. *Immunity* (2011) 34(1):85–95. doi: 10.1016/j.immuni.2010.12.011

88. Klimp AH, de Vries EG, Scherphof GL, Daemen T. A potential role of macrophage activation in the treatment of cancer. *Crit Rev Oncol Hematol* (2002) 44 (2):143–61. doi: 10.1016/s1040-8428(01)00203-7

89. Laviron M, Boissonnas A. Ontogeny of tumor-associated macrophages. *Front Immunol* (2019) 10:1799. doi: 10.3389/fimmu.2019.01799

90. Muller A, Brandenburg S, Turkowski K, Muller S, Vajkoczy P. Resident microglia, and not peripheral macrophages, are the main source of brain tumor mononuclear cells. *Int J Cancer* (2015) 137(2):278–88. doi: 10.1002/ijc.29379

91. Muller S, Kohanbash G, Liu SJ, Alvarado B, Carrera D, Bhaduri A, et al. Single-cell profiling of human gliomas reveals macrophage ontogeny as a basis for regional differences in macrophage activation in the tumor microenvironment. *Genome Biol* (2017) 18(1):234. doi: 10.1186/s13059-017-1362-4

92. Nywening TM, Belt BA, Cullinan DR, Panni RZ, Han BJ, Sanford DE, et al. Targeting both tumour-associated Cxcr2(+) neutrophils and Ccr2(+) macrophages disrupts myeloid recruitment and improves chemotherapeutic responses in pancreatic ductal adenocarcinoma. *Gut* (2018) 67(6):1112–23. doi: 10.1136/gutjnl-2017-313738

93. Loyher PL, Hamon P, Laviron M, Meghraoui-Kheddar A, Goncalves E, Deng Z, et al. Macrophages of distinct origins contribute to tumor development in the lung. *J Exp Med* (2018) 215(10):2536–53. doi: 10.1084/jem.20180534

94. Laviron M, Petit M, Weber-Delacroix E, Combes AJ, Arkal AR, Barthelemy S, et al. Tumor-associated macrophage heterogeneity is driven by tissue territories in breast cancer. *Cell Rep* (2022) 39(8):110865. doi: 10.1016/j.celrep.2022.110865

95. Hagemann T, Wilson J, Burke F, Kulbe H, Li NF, Pluddemann A, et al. Ovarian cancer cells polarize macrophages toward a tumor-associated phenotype. *J Immunol* (2006) 176(8):5023–32. doi: 10.4049/jimmunol.176.8.5023

96. Han C, Zhang C, Wang H, Zhao L. Exosome-mediated communication between tumor cells and tumor-associated macrophages: Implications for tumor microenvironment. *Oncoimmunology* (2021) 10(1):1887552. doi: 10.1080/2162402X.2021.1887552

97. Valenti R, Huber V, Filipazzi P, Pilla L, Sovena G, Villa A, et al. Human tumor-released microvesicles promote the differentiation of myeloid cells with transforming growth factor-Beta-Mediated suppressive activity on T lymphocytes. *Cancer Res* (2006) 66(18):9290–8. doi: 10.1158/0008-5472.CAN-06-1819

98. Lin EY, Gouon-Evans V, Nguyen AV, Pollard JW. The macrophage growth factor csf-1 in mammary gland development and tumor progression. *J Mammary Gland Biol Neoplasia* (2002) 7(2):147–62. doi: 10.1023/a:1020399802795

99. Pyonteck SM, Akkari L, Schuhmacher AJ, Bowman RL, Sevenich L, Quail DF, et al. Csf-1r inhibition alters macrophage polarization and blocks glioma progression. *Nat Med* (2013) 19(10):1264–72. doi: 10.1038/nm.3337

100. Laoui D, Van Overmeire E, De Baetselier P, Van Ginderachter JA, Raes G. Functional relationship between tumor-associated macrophages and macrophage colony-stimulating factor as contributors to cancer progression. *Front Immunol* (2014) 5:489. doi: 10.3389/fimmu.2014.00489

101. Saji H, Koike M, Yamori T, Saji S, Seiki M, Matsushima K, et al. Significant correlation of monocyte chemoattractant protein-1 expression with neovascularization and progression of breast carcinoma. *Cancer* (2001) 92(5):1085–91. doi: 10.1002/1097-0142(20010901)92:5<1085::aid-cncr1424>3.0.co;2-k

102. Sica A, Schioppa T, Mantovani A, Allavena P. Tumour-associated macrophages are a distinct M2 polarised population promoting tumour progression: Potential targets of anti-cancer therapy. *Eur J Cancer* (2006) 42(6):717–27. doi: 10.1016/j.ejca.2006.01.003

103. Duyndam MC, Hilhorst MC, Schluper HM, Verheul HM, van Diest PJ, Kraal G, et al. Vascular endothelial growth factor-165 overexpression stimulates angiogenesis and induces cyst formation and macrophage infiltration in human ovarian cancer xenografts. *Am J Pathol* (2002) 160(2):537–48. doi: 10.1016/s0002-9440(10)64873-0

104. Adini A, Kornaga T, Firoozbakht F, Benjamin LE. Placental growth factor is a survival factor for tumor endothelial cells and macrophages. *Cancer Res* (2002) 62 (10):2749–52.

105. Biswas SK, Gangi L, Paul S, Schioppa T, Saccani A, Sironi M, et al. A distinct and unique transcriptional program expressed by tumor-associated macrophages

(Defective nf-kappab and enhanced irf-3/Stat1 activation). *Blood* (2006) 107(5):2112–22. doi: 10.1182/blood-2005-01-0428

106. Mantovani A, Sozzani S, Locati M, Allavena P, Sica A. Macrophage polarization: Tumor-associated macrophages as a paradigm for polarized M2 mononuclear phagocytes. *Trends Immunol* (2002) 23(11):549–55. doi: 10.1016/s1471-4906(02)02302-5

107. Curiel TJ, Coukos G, Zou L, Alvarez X, Cheng P, Mottram P, et al. Specific recruitment of regulatory T cells in ovarian carcinoma fosters immune privilege and predicts reduced survival. *Nat Med* (2004) 10(9):942–9. doi: 10.1038/nm1093

108. Moore KW, de Waal Malefyt R, Coffman RL, O'Garra A. Interleukin-10 and the interleukin-10 receptor. *Annu Rev Immunol* (2001) 19:683–765. doi: 10.1146/annurev.immunol.19.1.683

109. Kryczek I, Wei S, Zou L, Zhu G, Mottram P, Xu H, et al. Cutting edge: Induction of B7-H4 on apcs through il-10: Novel suppressive mode for regulatory T cells. *J Immunol* (2006) 177(1):40–4. doi: 10.4049/jimmunol.177.1.40

110. Kryczek I, Zou L, Rodriguez P, Zhu G, Wei S, Mottram P, et al. B7-H4 expression identifies a novel suppressive macrophage population in human ovarian carcinoma. *J Exp Med* (2006) 203(4):871–81. doi: 10.1084/jem.20050930

111. Kuang DM, Zhao Q, Peng C, Xu J, Zhang JP, Wu C, et al. Activated monocytes in peritumoral stroma of hepatocellular carcinoma foster immune privilege and disease progression through pd-L1. *J Exp Med* (2009) 206(6):1327–37. doi: 10.1084/jem.20082173

112. Bloch O, Crane CA, Kaur R, Safaee M, Rutkowski MJ, Parsa AT. Gliomas promote immunosuppression through induction of B7-H1 expression in tumor-associated macrophages. *Clin Cancer Res* (2013) 19(12):3165–75. doi: 10.1158/1078-0432.CCR-12-3314

113. Pollard JW. Tumour-educated macrophages promote tumour progression and metastasis. *Nat Rev Cancer* (2004) 4(1):71–8. doi: 10.1038/nrc1256

114. Yin M, Li X, Tan S, Zhou HJ, Ji W, Bellone S, et al. Tumor-associated macrophages drive spheroid formation during early transcoelomic metastasis of ovarian cancer. *J Clin Invest* (2016) 126(11):4157–73. doi: 10.1172/JCI87252

115. Nie Y, Huang H, Guo M, Chen J, Wu W, Li W, et al. Breast phyllodes tumors recruit and repolarize tumor-associated macrophages Via secreting Ccl5 to promote malignant progression, which can be inhibited by Ccr5 inhibition therapy. *Clin Cancer Res* (2019) 25(13):3873–86. doi: 10.1158/1078-0432.CCR-18-3421

116. Lin EY, Pollard JW. Tumor-associated macrophages press the angiogenic switch in breast cancer. *Cancer Res* (2007) 67(11):5064–6. doi: 10.1158/0008-5472.CAN-07-0912

117. Carmeliet P, Jain RK. Angiogenesis in cancer and other diseases. *Nature* (2000) 407(6801):249–57. doi: 10.1038/35025220

118. Varney ML, Olsen KJ, Mosley RL, Singh RK. Paracrine regulation of vascular endothelial growth factor–a expression during macrophage-melanoma cell interaction: Role of monocyte chemotactic protein-1 and macrophage colony-stimulating factor. *J Interferon Cytokine Res* (2005) 25(11):674–83. doi: 10.1089/jir.2005.25.674

119. Lin L, Chen YS, Yao YD, Chen JQ, Chen JN, Huang SY, et al. Ccl18 from tumor-associated macrophages promotes angiogenesis in breast cancer. *Oncotarget* (2015) 6(33):34758–73. doi: 10.18632/oncotarget.5325

120. Geiger TR, Peeper DS. Metastasis mechanisms. *Biochim Biophys Acta* (2009) 1796(2):293–308. doi: 10.1016/j.bbcan.2009.07.006

121. Dongre A, Weinberg RA. New insights into the mechanisms of epithelial-mesenchymal transition and implications for cancer. *Nat Rev Mol Cell Biol* (2019) 20 (2):69–84. doi: 10.1038/s41580-018-0080-4

122. Wang R, Zhang J, Chen S, Lu M, Luo X, Yao S, et al. Tumor-associated macrophages provide a suitable microenvironment for non-small lung cancer invasion and progression. *Lung Cancer* (2011) 74(2):188–96. doi: 10.1016/j.lungcan.2011.04.009

123. Marconi C, Bianchini F, Mannini A, Mugnai G, Ruggieri S, Calorini L. Tumoral and macrophage upar and mmp-9 contribute to the invasiveness of B16 murine melanoma cells. *Clin Exp Metastasis* (2008) 25(3):225–31. doi: 10.1007/s10585-007-9136-0

124. Kim S, Takahashi H, Lin WW, Descargues P, Grivennikov S, Kim Y, et al. Carcinoma-produced factors activate myeloid cells through Tlr2 to stimulate metastasis. *Nature* (2009) 457(7225):102–6. doi: 10.1038/nature07623

125. Chen J, Yao Y, Gong C, Yu F, Su S, Chen J, et al. Ccl18 from tumor-associated macrophages promotes breast cancer metastasis Via Pitpnm3. *Cancer Cell* (2011) 19 (4):541–55. doi: 10.1016/j.ccr.2011.02.006

126. Gao L, Zhang W, Zhong WQ, Liu ZJ, Li HM, Yu ZL, et al. Tumor associated macrophages induce epithelial to mesenchymal transition Via the Egfr/Erk1/2 pathway in head and neck squamous cell carcinoma. *Oncol Rep* (2018) 40(5):2558–72. doi: 10.3892/or.2018.6657

127. Winkler IG, Sims NA, Pettit AR, Barbier V, Nowlan B, Helwani F, et al. Bone marrow macrophages maintain hematopoietic stem cell (Hsc) niches and their depletion mobilizes hscs. *Blood* (2010) 116(23):4815–28. doi: 10.1182/blood-2009-11-253534

128. Ehninger A, Trumpp A. The bone marrow stem cell niche grows up: Mesenchymal stem cells and macrophages move in. *J Exp Med* (2011) 208(3):421–8. doi: 10.1084/jem.20110132

129. Wattrus SJ, Smith ML, Rodrigues CP, Hagedorn EJ, Kim JW, Budnik B, et al. Quality assurance of hematopoietic stem cells by macrophages determines stem cell clonality. *Science* (2022) 377(6613):1413–9. doi: 10.1126/science.abo4837

130. Al-Matary YS, Botezatu L, Opalka B, Hones JM, Lams RF, Thivakaran A, et al. Acute myeloid leukemia cells polarize macrophages towards a leukemia supporting state in a growth factor independence 1 dependent manner. *Haematologica* (2016) 101 (10):1216–27. doi: 10.3324/haematol.2016.143180

131. Brauneck F, Fischer B, Witt M, Muschhammer J, Oelrich J, da Costa Avelar PH, et al. Tigit blockade repolarizes aml-associated tigit(+) M2 macrophages to an M1 phenotype and increases Cd47-mediated phagocytosis. *J Immunother Cancer* (2022) 10 (12). doi: 10.1136/jitc-2022-004794

132. Liao J, Feng W, Wang R, Ma S, Wang L, Yang X, et al. Diverse in vivo effects of soluble and membrane-bound m-csf on tumor-associated macrophages in lymphoma xenograft model. *Oncotarget* (2016) 7(2):1354–66. doi: 10.18632/oncotarget.6362

133. Komohara Y, Noyori O, Saito Y, Takeya H, Baghdadi M, Kitagawa F, et al. Potential anti-lymphoma effect of m-csfr inhibitor in adult T-cell Leukemia/Lymphoma. *J Clin Exp Hematop* (2018) 58(4):152–60. doi: 10.3960/jslrt.18034

134. Polk A, Lu Y, Wang T, Seymour E, Bailey NG, Singer JW, et al. Colony-stimulating factor-1 receptor is required for nurse-like cell survival in chronic lymphocytic leukemia. *Clin Cancer Res* (2016) 22(24):6118–28. doi: 10.1158/1078-0432.CCR-15-3099

135. Edwards VD, Sweeney DT, Ho H, Eide CA, Rofelty A, Agarwal A, et al. Targeting of colony-stimulating factor 1 receptor (Csf1r) in the cll microenvironment yields antineoplastic activity in primary patient samples. *Oncotarget* (2018) 9 (37):24576–89. doi: 10.18632/oncotarget.25191

136. Burger JA, Gribben JG. The microenvironment in chronic lymphocytic leukemia (Cll) and other b cell malignancies: Insight into disease biology and new targeted therapies. *Semin Cancer Biol* (2014) 24:71–81. doi: 10.1016/j.semcancer.2013.08.011

137. Fujimoto H, Sangai T, Ishii G, Ikehara A, Nagashima T, Miyazaki M, et al. Stromal mcp-1 in mammary tumors induces tumor-associated macrophage infiltration and contributes to tumor progression. *Int J Cancer* (2009) 125(6):1276–84. doi: 10.1002/ijc.24378

138. Pena CG, Nakada Y, Saatcioglu HD, Aloisio GM, Cuevas I, Zhang S, et al. Lkb1 loss promotes endometrial cancer progression Via Ccl2-dependent macrophage recruitment. *J Clin Invest* (2015) 125(11):4063–76. doi: 10.1172/JCI82152

139. Nakatsumi H, Matsumoto M, Nakayama KI. Noncanonical pathway for regulation of Ccl2 expression by an Mtorc1-Foxk1 axis promotes recruitment of tumor-associated macrophages. *Cell Rep* (2017) 21(9):2471–86. doi: 10.1016/j.celrep.2017.11.014

140. Arakaki R, Yamasaki T, Kanno T, Shibasaki N, Sakamoto H, Utsunomiya N, et al. Ccl2 as a potential therapeutic target for clear cell renal cell carcinoma. *Cancer Med* (2016) 5(10):2920–33. doi: 10.1002/cam4.886

141. Pienta KJ, Machiels JP, Schrijvers D, Alekseev B, Shkolnik M, Crabb SJ, et al. Phase 2 study of carlumab (Cnto 888), a human monoclonal antibody against cc-chemokine ligand 2 (Ccl2), in metastatic castration-resistant prostate cancer. *Invest New Drugs* (2013) 31(3):760–8. doi: 10.1007/s10637-012-9869-8

142. Nywening TM, Wang-Gillam A, Sanford DE, Belt BA, Panni RZ, Cusworth BM, et al. Targeting tumour-associated macrophages with Ccr2 inhibition in combination with folfirinox in patients with borderline resectable and locally advanced pancreatic cancer: A single-centre, open-label, dose-finding, non-randomised, phase 1b trial. *Lancet Oncol* (2016) 17(5):651–62. doi: 10.1016/S1470-2045(16)00078-4

143. Noel M, O'Reilly EM, Wolpin BM, Ryan DP, Bullock AJ, Britten CD, et al. Phase 1b study of a small molecule antagonist of human chemokine (C-c motif) receptor 2 (Pf-04136309) in combination with nab-Paclitaxel/Gemcitabine in first-line treatment of metastatic pancreatic ductal adenocarcinoma. *Invest New Drugs* (2020) 38 (3):800–11. doi: 10.1007/s10637-019-00830-3

144. Haag GM, Springfeld C, Grun B, Apostolidis L, Zschabitz S, Dietrich M, et al. Pembrolizumab and maraviroc in refractory mismatch repair Proficient/Microsatellite-stable metastatic colorectal cancer - the piccasso phase I trial. *Eur J Cancer* (2022) 167:112–22. doi: 10.1016/j.ejca.2022.03.017

145. Mantovani A, Allavena P, Marchesi F, Garlanda C. Macrophages as tools and targets in cancer therapy. *Nat Rev Drug Discovery* (2022) 21(11):799–820. doi: 10.1038/s41573-022-00520-5

146. Edwards DK, Watanabe-Smith K, Rofelty A, Damnernsawad A, Laderas T, Lamble A, et al. Csf1r inhibitors exhibit antitumor activity in acute myeloid leukemia by blocking paracrine signals from support cells. *Blood* (2019) 133(6):588–99. doi: 10.1182/blood-2018-03-838946

147. Simonis A, Russkamp NF, Mueller J, Wilk CM, Wildschut MHE, Myburgh R, et al. Disruption of csf-1r signaling inhibits growth of aml with Inv(16). *Blood Adv* (2021) 5(5):1273–7. doi: 10.1182/bloodadvances.2020003125

148. Ries CH, Cannarile MA, Hoves S, Benz J, Wartha K, Runza V, et al. Targeting tumor-associated macrophages with anti-Csf-1r antibody reveals a strategy for cancer therapy. *Cancer Cell* (2014) 25(6):846–59. doi: 10.1016/j.ccr.2014.05.016

149. Cassier PA, Italiano A, Gomez-Roca C, Le Tourneau C, Toulmonde M, D'Angelo SP, et al. Long-term clinical activity, safety and patient-reported quality of life for emactuzumab-treated patients with diffuse-type tenosynovial giant-cell tumour. *Eur J Cancer* (2020) 141:162–70. doi: 10.1016/j.ejca.2020.09.038

150. Lin C-C, Gil-Martin M, Bauer TM, Naing A, Lim DW-T, Sarantopoulos J, et al. Abstract Ct171: Phase I study of Blz945 alone and with spartalizumab (Pdr001) in

patients (Pts) with advanced solid tumors. *Cancer Res* (2020) 80(16_Supplement): CT171–CT. doi: 10.1158/1538-7445.am2020-ct171

151. Pfirschke C, Zilionis R, Engblom C, Messemaker M, Zou AE, Rickelt S, et al. Macrophage-targeted therapy unlocks antitumoral cross-talk between ifngamma-secreting lymphocytes and Il12-producing dendritic cells. *Cancer Immunol Res* (2022) 10(1):40–55. doi: 10.1158/2326-6066.CIR-21-0326

152. Fujiwara T, Yakoub MA, Chandler A, Christ AB, Yang G, Ouerfelli O, et al. Csf1/Csf1r signaling inhibitor pexidartinib (Plx3397) reprograms tumor-associated macrophages and stimulates T-cell infiltration in the sarcoma microenvironment. *Mol Cancer Ther* (2021) 20(8):1388–99. doi: 10.1158/1535-7163.MCT-20-0591

153. Manji GA, Van Tine BA, Lee SM, Raufi AG, Pellicciotta I, Hirbe AC, et al. A phase I study of the combination of pexidartinib and sirolimus to target tumor-associated macrophages in unresectable sarcoma and malignant peripheral nerve sheath tumors. *Clin Cancer Res* (2021) 27(20):5519–27. doi: 10.1158/1078-0432.CCR-21-1779

154. Razak AR, Cleary JM, Moreno V, Boyer M, Calvo Aller E, Edenfield W, et al. Safety and efficacy of amg 820, an anti-Colony-Stimulating factor 1 receptor antibody, in combination with pembrolizumab in adults with advanced solid tumors. *J Immunother Cancer* (2020) 8(2). doi: 10.1136/jitc-2020-001006

155. Germano G, Frapolli R, Belgiovine C, Anselmo A, Pesce S, Liguori M, et al. Role of macrophage targeting in the antitumor activity of trabectedin. *Cancer Cell* (2013) 23(2):249–62. doi: 10.1016/j.ccr.2013.01.008

156. Rodriguez-Garcia A, Lynn RC, Poussin M, Eiva MA, Shaw LC, O'Connor RS, et al. Car-T cell-mediated depletion of immunosuppressive tumor-associated macrophages promotes endogenous antitumor immunity and augments adoptive immunotherapy. *Nat Commun* (2021) 12(1):877. doi: 10.1038/s41467-021-20893-2

157. Beatty GL, Torigian DA, Chiorean EG, Saboury B, Brothers A, Alavi A, et al. A phase I study of an agonist Cd40 monoclonal antibody (Cp-870,893) in combination with gemcitabine in patients with advanced pancreatic ductal adenocarcinoma. *Clin Cancer Res* (2013) 19(22):6286–95. doi: 10.1158/1078-0432.CCR-13-1320

158. Huffman AP, Lin JH, Kim SI, Byrne KT, Vonderheide RH. Ccl5 mediates Cd40-driven Cd4+ T cell tumor infiltration and immunity. *JCI Insight* (2020) 5(10). doi: 10.1172/jci.insight.137263

159. Hoves S, Ooi CH, Wolter C, Sade H, Bissinger S, Schmittnaegel M, et al. Rapid activation of tumor-associated macrophages boosts preexisting tumor immunity. *J Exp Med* (2018) 215(3):859–76. doi: 10.1084/jem.20171440

160. Machiels JP, Gomez-Roca C, Michot JM, Zamarin D, Mitchell T, Catala G, et al. Phase ib study of anti-Csf-1r antibody emactuzumab in combination with Cd40 agonist selicrelumab in advanced solid tumor patients. *J Immunother Cancer* (2020) 8 (2). doi: 10.1136/jitc-2020-001153

161. O'Hara MH, O'Reilly EM, Varadhachary G, Wolff RA, Wainberg ZA, Ko AH, et al. Cd40 agonistic monoclonal antibody Apx005m (Sotigalimab) and chemotherapy, with or without nivolumab, for the treatment of metastatic pancreatic adenocarcinoma: An open-label, multicentre, phase 1b study. *Lancet Oncol* (2021) 22(1):118–31. doi: 10.1016/S1470-2045(20)30532-5

162. Pettenati C, Ingersoll MA. Mechanisms of bcg immunotherapy and its outlook for bladder cancer. *Nat Rev Urol* (2018) 15(10):615–25. doi: 10.1038/s41585-018-0055-4

163. Ji N, Mukherjee N, Morales EE, Tomasini ME, Hurez V, Curiel TJ, et al. Percutaneous bcg enhances innate effector antitumor cytotoxicity during treatment of bladder cancer: A translational clinical trial. *Oncoimmunology* (2019) 8(8):1614857. doi: 10.1080/2162402X.2019.1614857

164. Sun L, Kees T, Almeida AS, Liu B, He XY, Ng D, et al. Activating a collaborative innate-adaptive immune response to control metastasis. *Cancer Cell* (2021) 39 (10):1361–74 e9. doi: 10.1016/j.ccell.2021.08.005

165. Anfray C, Mainini F, Digifico E, Maeda A, Sironi M, Erreni M, et al. Intratumoral combination therapy with Poly(I:C) and resiquimod synergistically triggers tumor-associated macrophages for effective systemic antitumoral immunity. *J Immunother Cancer* (2021) 9(9). doi: 10.1136/jitc-2021-002408

166. Ribas A, Medina T, Kirkwood JM, Zakharia Y, Gonzalez R, Davar D, et al. Overcoming pd-1 blockade resistance with cpg-a toll-like receptor 9 agonist vidutolimod in patients with metastatic melanoma. *Cancer Discovery* (2021) 11 (12):2998–3007. doi: 10.1158/2159-8290.CD-21-0425

167. Chow LQM, Morishima C, Eaton KD, Baik CS, Goulart BH, Anderson LN, et al. Phase ib trial of the toll-like receptor 8 agonist, motolimod (Vtx-2337), combined with cetuximab in patients with recurrent or metastatic scchn. *Clin Cancer Res* (2017) 23(10):2442–50. doi: 10.1158/1078-0432.CCR-16-1934

168. Ferris RL, Saba NF, Gitlitz BJ, Haddad R, Sukari A, Neupane P, et al. Effect of adding motolimod to standard combination chemotherapy and cetuximab treatment of patients with squamous cell carcinoma of the head and neck: The Active8 randomized clinical trial. *JAMA Oncol* (2018) 4(11):1583–8. doi: 10.1001/jamaoncol.2018.1888

169. Karapetyan L, Luke JJ, Davar D. Toll-like receptor 9 agonists in cancer. *Onco Targets Ther* (2020) 13:10039–60. doi: 10.2147/OTT.S247050

170. Tseng D, Volkmer JP, Willingham SB, Contreras-Trujillo H, Fathman JW, Fernhoff NB, et al. Anti-Cd47 antibody-mediated phagocytosis of cancer by macrophages primes an effective antitumor T-cell response. *Proc Natl Acad Sci U.S.A.* (2013) 110(27):11103–8. doi: 10.1073/pnas.1305569110

171. Zhang M, Hutter G, Kahn SA, Azad TD, Gholamin S, Xu CY, et al. Anti-Cd47 treatment stimulates phagocytosis of glioblastoma by M1 and M2 polarized macrophages and promotes M1 polarized macrophages in vivo. *PloS One* (2016) 11 (4):e0153550. doi: 10.1371/journal.pone.0153550

172. Weiskopf K, Jahchan NS, Schnorr PJ, Cristea S, Ring AM, Maute RL, et al. Cd47-blocking immunotherapies stimulate macrophage-mediated destruction of small-cell lung cancer. *J Clin Invest* (2016) 126(7):2610–20. doi: 10.1172/JCI81603

173. Upton R, Banuelos A, Feng D, Biswas T, Kao K, McKenna K, et al. Combining Cd47 blockade with trastuzumab eliminates Her2-positive breast cancer cells and overcomes trastuzumab tolerance. *Proc Natl Acad Sci U.S.A.* (2021) 118(29). doi: 10.1073/pnas.2026849118

174. Zhang W, Liu L, Su H, Liu Q, Shen J, Dai H, et al. Chimeric antigen receptor macrophage therapy for breast tumours mediated by targeting the tumour extracellular matrix. *Br J Cancer* (2019) 121(10):837–45. doi: 10.1038/s41416-019-0578-3

175. Klichinsky M, Ruella M, Shestova O, Lu XM, Best A, Zeeman M, et al. Human chimeric antigen receptor macrophages for cancer immunotherapy. *Nat Biotechnol* (2020) 38(8):947–53. doi: 10.1038/s41587-020-0462-y

176. Chen Y, Yu Z, Tan X, Jiang H, Xu Z, Fang Y, et al. Car-macrophage: A new immunotherapy candidate against solid tumors. *BioMed Pharmacother* (2021) 139:111605. doi: 10.1016/j.biopha.2021.111605

177. van Bommel PE, He Y, Schepel I, Hendriks M, Wiersma VR, van Ginkel RJ, et al. Cd20-selective inhibition of Cd47-sirpalpha "Don't eat me" signaling with a bispecific antibody-derivative enhances the anticancer activity of daratumumab, alemtuzumab and obinutuzumab. *Oncoimmunology* (2018) 7(2):e1386361. doi: 10.1080/2162402X.2017.1386361

178. Douglas B, Thakkar D, Peter B, Zhou J, Chng WJ, Piers I. Hmbd004, a novel anti-Cd47xcd33 bispecific antibody displays potent anti-tumor effects in pre-clinical models of aml. *Blood* (2017) 130:1378–.

179. Buatois V, Johnson Z, Salgado-Pires S, Papaioannou A, Hatterer E, Chauchet X, et al. Preclinical development of a bispecific antibody that safely and effectively targets Cd19 and Cd47 for the treatment of b-cell lymphoma and leukemia. *Mol Cancer Ther* (2018) 17(8):1739–51. doi: 10.1158/1535-7163.MCT-17-1095

180. Zeidan AM, DeAngelo DJ, Palmer J, Seet CS, Tallman MS, Wei X, et al. Phase 1 study of anti-Cd47 monoclonal antibody cc-90002 in patients with Relapsed/Refractory acute myeloid leukemia and high-risk myelodysplastic syndromes. *Ann Hematol* (2022) 101(3):557–69. doi: 10.1007/s00277-021-04734-2

181. Daver NG, Vyas P, Kambhampati S, Malki MMA, Larson RA, Asch AS, et al. Tolerability and efficacy of the first-in-Class anti-Cd47 antibody magrolimab combined with azacitidine in frontline Tp53m aml patients: Phase 1b results. *J Clin Oncol* (2022) 40(16_suppl):7020. doi: 10.1200/JCO.2022.40.16_suppl.7020

182. Sallman DA, Asch AS, Al Malki MM, Lee DJ, Donnellan WB, Marcucci G, et al. The first-in-Class anti-Cd47 antibody magrolimab (5f9) in combination with azacitidine is effective in mds and aml patients: Ongoing phase 1b results. *Blood* (2019) 134(Supplement_1):569. doi: 10.1182/blood-2019-126271

183. Garcia-Manero G, Daver NG, Xu J, Chao M, Chung T, Tan A, et al. Magrolimab + azacitidine versus azacitidine + placebo in untreated higher risk (Hr) myelodysplastic syndrome (Mds): The phase 3, randomized, enhance study. *J Clin Oncol* (2021) 39 (15_suppl):TPS7055–TPS. doi: 10.1200/JCO.2021.39.15_suppl.TPS7055

184. Sallman DA, Malki MMA, Asch AS, Wang ES, Jurcic JG, Bradley TJ, et al. Magrolimab in combination with azacitidine for untreated higher-risk myelodysplastic syndromes (Hr-mds): 5f9005 phase 1b study results. *J Clin Oncol* (2022) 40 (16_suppl):7017. doi: 10.1200/JCO.2022.40.16_suppl.7017

185. Li W, Wang F, Guo R, Bian Z, Song Y. Targeting macrophages in hematological malignancies: Recent advances and future directions. *J Hematol Oncol* (2022) 15(1):110. doi: 10.1186/s13045-022-01328-x

186. Ronsley R, Kariminia A, Ng B, Mostafavi S, Reid G, Subrt P, et al. The Tlr9 agonist (Gnkg168) induces a unique immune activation pattern in vivo in children with minimal residual disease positive acute leukemia: Results of the tacl T2009-008 phase I study. *Pediatr Hematol Oncol* (2019) 36(8):468–81. doi: 10.1080/08880018.2019.1667461

frontiers | Frontiers in Immunology

TYPE Review
PUBLISHED 01 May 2023
DOI 10.3389/fimmu.2023.1155077

OPEN ACCESS

EDITED BY
Yanan Ma,
Memorial Sloan Kettering Cancer Center, United States

REVIEWED BY
Lili Qu,
UCHC, United States
Jingkai Zhou,
City of Hope National Medical Center, United States
Guolong Zuo,
University of California, San Francisco, United States
Xinhe Shan,
Penn Medicine, United States

*CORRESPONDENCE
Junxiang Li
lijunxiang1226@163.com
Rui Shi
shiai588@163.com

†These authors have contributed equally to this work

RECEIVED 31 January 2023
ACCEPTED 20 March 2023
PUBLISHED 01 May 2023

CITATION
Wang K, Mao T, Lu X, Wang M, Yun Y, Jia Z, Shi L, Jiang H, Li J and Shi R (2023) A potential therapeutic approach for ulcerative colitis: targeted regulation of macrophage polarization through phytochemicals. *Front. Immunol.* 14:1155077. doi: 10.3389/fimmu.2023.1155077

A potential therapeutic approach for ulcerative colitis: targeted regulation of macrophage polarization through phytochemicals

Ke Wang[1,2†], Tangyou Mao[2†], Xinyu Lu[1,2], Muyuan Wang[1,2], Yifei Yun[1,2], Zeyu Jia[1,2], Lei Shi[2], Haoxi Jiang[1,2], Junxiang Li[2*] and Rui Shi[2*]

[1]Graduate School, Beijing University of Chinese Medicine, Beijing, China, [2]Dongfang Hospital, Beijing University of Chinese Medicine, Beijing, China

Ulcerative colitis (UC), a type of inflammatory bowel disease characterized by recurring and incurable symptoms, causes immense suffering and economic burden for patients due to the limited treatment options available. Therefore, it is imperative to develop novel and promising strategies, as well as safe and effective drugs, for the clinical management of UC. Macrophages play a critical role as the initial line of defense in maintaining intestinal immune homeostasis, and their phenotypic transformation significantly influences the progression of UC. Scientific studies have demonstrated that directing macrophage polarization toward the M2 phenotype is an effective strategy for the prevention and treatment of UC. Phytochemicals derived from botanical sources have garnered the interest of the scientific community owing to their distinct bioactivity and nutritional value, which have been shown to confer beneficial protective effects against colonic inflammation. In this review, we explicated the influence of macrophage polarization on the development of UC and collated data on the significant potential of natural substances that can target the macrophage phenotype and elucidate the possible mechanism of action for its treatment. These findings may provide novel directions and references for the clinical management of UC.

KEYWORDS

macrophage, phenotype, polarization, phytochemicals, therapeutic effects, ulcerative colitis

1 Introduction

Ulcerative colitis (UC) is a chronic, idiopathic inflammatory disorder that affects the mucosa of the colon and rectum consecutively. It is listed by the World Health Organization as a modern refractory disease, with typical clinical symptoms including recurrent abdominal pain, diarrhea, and hematochezia. Over recent decades, the incidence

rate of UC has surged globally, ranging from 0.5 to 31.5 per 100,000 individuals annually across various populations, according to relevant statistics. An escalating body of evidence has indicated that UC typically manifests in individuals aged 30 to 40 years, with no sex predominance (1–3). Despite significant advancements made in the past decades, the precise etiology of UC largely remains an enigma. Pathogenic factors, including genetic predisposition, environmental factors, intestinal dysbiosis, and immune dysregulation, are widely acknowledged as being involved in the development of UC (3, 4).

Lifelong treatment is almost imperative for patients diagnosed with UC due to the dearth of known preventive or fundamentally curative interventions. The current therapeutic goal is persistent remission, mucosal healing, and mitigation of the risk of colorectal neoplasia. As the major treatment option for UC, typical drugs used in the clinic mainly include aminosalicylates, corticosteroids, immunosuppressants, biological agents, and microecologics (5, 6), which have not achieved satisfactory results on account of the various adverse effects, drug tolerance, and the high rate of recrudescence, among others (7, 8). Hence, there is an urgent need to explore and develop novel safe and effective medications for UC.

Macrophages, as the sentinels of intestinal immune homeostasis, can manifest diverse functional phenotypes in response to various environmental cues and stimuli, thereby either promoting or resolving intestinal inflammation, which play an essential role in the development of UC. Based on the *in vitro* model of monocyte-derived macrophages, the macrophage population can be divided into the classically activated M1 macrophages with pro-inflammatory activity and the alternatively activated M2 macrophages with anti-inflammatory characteristics. In intestinal homeostasis, resident macrophages usually present an M2 phenotype with low reactivity to Toll-like receptor (TLR) ligands to maintain tolerance to the different antigens from food and symbiotic microflora (9). On the contrary, in the colon of patients with UC, M1 macrophages play a dominant role with the excessive accumulation of pro-inflammatory factors, leading to the damage of the intestinal epithelial barrier and the imbalance of immune homeostasis (10, 11). Furthermore, there is compelling evidence that macrophage polarization tends to be a severe imbalanced condition in the intestinal tissues of patients with UC who are non-responsive to conventional treatments (12, 13). Therefore, targeting macrophage polarization is often an attractive aspect for UC therapy.

2 Macrophage

Evidence indicates that intestinal resident cells are derived from embryonic precursors that undergo continuous *in situ* proliferation during the neonatal period and are subsequently replaced by macrophages originating from peripheral blood with advancing age (14, 15). Due to their constant exposure to gut pathogens and their high energy consumption, lamina propria (LP) macrophages have a short life span and necessitate continuous replenishment by bone marrow-derived peripheral blood monocytes, which subsequently differentiate into mature macrophages in the gut (16). The most abundant macrophage population in the body is distributed in the gastrointestinal mucosa, especially in the LP near the epithelium, while a small proportion exists in the smooth muscle layer of the intestinal wall (16). Maintaining gut immune homeostasis is a cooperative and an elaborately dynamic process that requires moderate tolerance for the beneficial commensal microorganisms colonizing the gastrointestinal tract and the innocuous antigens from food substances. At the same time, it is vital to respond promptly to invading pathogens for host protection (17). As a crucial component of innate immunity, intestinal macrophages are polarized to different phenotypes by environmental cues, with the heterogeneous functions of identifying pathogens, phagocytosing microorganisms and debris, remodeling impaired tissues, supporting regulatory T cells, and regulating inflammation, which are considered as the main factors contributing to and maintaining intestinal homeostasis (18–20). Throughout the construction of monocyte-derived macrophage models *in vitro*, the macrophage population can be classified into two categories with opposing functions: the classically activated macrophages (M1 macrophages) that represent pro-inflammatory conditions and the alternatively activated macrophages (M2 macrophages) that represent anti-inflammatory conditions (21–25). Once the balance of macrophage polarization is broken, dysfunction will occur, impairing the ability to maintain homeostasis and sense signals of tissue damage in the body, which may lead to inflammatory diseases (26). It is worth noting that, while this taxonomic approach substantially contributes to the comprehension of the metabolic programming of the different macrophage functions, it may not fully reflect the *in vivo* condition of macrophages, which are influenced by complex environmental cues and may display features of both phenotypes (9, 16). Research in this area has shown that when this occurs to certain cytokines or complexes such as transforming growth factor beta (TGF-β), glucocorticoids, or the immune complex, macrophages become a continuum of activation forms alongside the M1/M2 axis, with similar but different transcription and functions (9, 27). However, categorization into either M1 or M2 brings benefits in macrophage polarization to understand their heterogeneous functions and their transformation.

2.1 M1 macrophages

Generally, M1 macrophages could be activated by tumor necrosis factor alpha (TNF-α) and TLR ligands such as lipopolysaccharides (LPS) or interferon gamma (IFN-γ); overexpress CD64, CD86, and CD16/32; and secrete high levels of the pro-inflammatory cytokines TNF-α, IL-1α, IL-1β, IL-6, IL-12, and IL-23, among others. In terms of function, the M1 phenotype possesses antigen presentation, pathogen elimination, and antitumor abilities. These macrophages synthesize nitric oxide (NO), which can mediate protection against infection and reactive oxygen species (ROS)-induced tissue damage, as well as impair tissue regeneration and wound healing. Moreover, a large amount of inducible nitric oxide synthase (iNOS) is excreted by M1

macrophages, which is regarded as an antimicrobial cytokine (28, 29).

2.2 M2 macrophages

Representing anti-inflammatory activity, M2 macrophages are identified by distinct markers including IL-10, CD206, and CD163 (30) and are polarized by stimulating the Th2 cytokines IL-4 and IL-13 *via* the activation of STAT6 through IL-4 receptor alpha (IL-4Rα). In addition, IL-10 can also induce the M2 phenotype by activating STAT3 *via* the IL-10 receptor (IL-10R). Functionally, M2 macrophages have the potent capacity of phagocytosis, obliterate the debris of apoptotic cells, accelerate tissue repair and wound healing, and possess pro-angiogenic and pro-fibrotic properties. In addition, these macrophages produce higher levels of IL-10 and arginase 1 (Arg-1), an effector enzyme in urea metabolism that inhibits immune responses (29, 31).

3 The origination of intestinal macrophages

Intestinal resident macrophages are mainly supplemented by circulating monocytes recruited to the mucosa, which express lymphocyte antigen 6C-high (LY6C^{hi}), CC-chemokine receptor 2-high (CCR2^{hi}), and CX3C-chemokine receptor 1-low (CX3CR1^{low}) in a mouse model. Subsequently, after entering the intestinal mucosa and encountering special intestinal signals such as TGF-β, macrophage colony-stimulating factor 1 (CSF-1 or M-CSF), and IL-10, as well as some environmental cues including short-chain fatty acids (SCFAs) produced by the gut microbiota (32), LY6C^{hi} monocytes begin to differentiate locally to mature resident macrophages. During this process, the monocyte population first occurs in major histocompatibility complex class II (MHCII) before increasing F4/80 with a decline in LY6C throughout a series of short-lived CX3CR1^{int} intermediates (33). Mature intestinal macrophages can be distinguished by F4/80^{+}, CD11b^{+}, CD11c^{+}, and CD64^{+} with a high expression of CX3CR1 (34). Previous research has shown that, in intestinal homeostasis, the majority of resident macrophages exhibit weak reactivity for the stimulation of TLR, increased production of anti-inflammatory cytokines such as IL-10, and suppression of pro-inflammatory cytokines such as iNOS and IL-6 (32), which express CD163 and CD206 (35), characterized more like an M2 macrophage. These macrophages play a pivotal role in the regulation of gut homeostasis *via* the clearance of harmful bacteria and adventive substances, IL-10, and the excretion of prostaglandin E2 to stimulate epithelial stem cell renewal and survival to promote the integrity of the epithelial barrier (36).

Circulating monocyte differentiation in the context of inflammation occurrence has been changed and disrupted compared with the above description, which is switched to polarize into a pro-inflammatory condition, M1 macrophage. During this period, the terminal differentiation process of LY6C^{hi} monocytes into mature intestinal macrophages is disrupted, leading to the accumulation of LY6C^{hi} monocytes, LY6C^{int} population, MHCII-positive and CX3CR1^{int} immature macrophages. LY6C^{int}CX3CR1^{int} cells retain their pro-inflammatory capacity through the secretion of inflammatory cytokines, including IL-12, IL-23, and IL-1β, thereby promoting type 1 T helper (Th1) and Th17 immune responses and aggravating tissue damage (32). There is evidence that the proportion and the number of CX3CR1^{int} macrophages obviously increase in mice after management with dextran sulfate sodium (DSS) (35).

Consequently, to some degree, Ly6C^{lo} monocytes could be regarded as the macrophages of the circulatory system. Monocytes gradually undergo differentiation into resident macrophages in intestinal homeostasis. When the colon is inflamed, resident macrophages are still replenished from monocytes in blood circulation. However, the phenotype changes from tolerant to sensitive to ambient and pro-inflammatory, with high TLR expression, and the balance of macrophage polarization is deflected to M1 macrophages. More interestingly, research has revealed that Ly6C^{hi} monocytes can also be transformed into Ly6C^{lo} monocytes and subsequently returned to the bone marrow to replenish the local macrophage population (9, 37). Nevertheless, the reasons underlying the dysregulation of macrophage polarization are not yet fully understood and may be related to the exceptional accumulation of monocytes and their response to local alterations or repolarization between M1 and M2 macrophages. Of course, it cannot be ruled out that both scenarios may act in concert (9, 35).

4 Macrophage polarization affects the development of UC

The origination of macrophages posits that M1 and M2 macrophages are distinct subsets polarized from a common precursor, displaying diversity in phenotype and function, which can be polarized into various phenotypes in response to multiple environmental cues, consequently acquiring different abilities and transforming into each other under specific conditions (19, 35). CCR2^{+}L6Cy^{hi} monocytes can replenish macrophages in all phenotypes during intestinal homeostasis and inflammation, which differentiate as a continuum of CX3CR1^{int} pool. UC is a chronic inflammatory disease driven initially by the disruption of the epithelial barrier, which is composed of a single layer of intestinal cells that connect with adjacent cells to form a continuous physical barrier, controlling the permeability of the luminal content (38). When foreign pathogens invade intestinal by crossing the injured epithelial layer, the balance of macrophages is deflected as M1 macrophages presenting a pro-inflammatory condition to engulf foreign materials and secrete pro-inflammatory cytokines such as TNF-α, IL-6, IL12, and IL-23, which promote immune responses mediated *via* Th1 and Th17 cells to protect the host from invasion (26). Under ideal conditions,

the protective inflammatory response is self-limited and would completely resolve after the pathogens were eliminated, without causing tissue damage or impairment of wound healing due to excessive immune response. Generally, it is an active process controlled by the recruitment of M1 macrophages and the accumulation of M2 macrophages (32). However, the balance of macrophage polarization is destroyed gradually by the infiltration of more and more M1 macrophages, inflammatory cytokines are overexpressed, and a high level of iNOS is induced, which directly or indirectly affect intestinal epithelial cells, leading to their injury or necrosis, which elevates the occurrence and development of UC (9). The alteration of macrophage polarization in inflammation and homeostasis is shown in Figure 1. Furthermore, Lissner et al. revealed that M1 macrophages invaded intestinal deregulated tight junction proteins and induced epithelial cell apoptosis to disrupt the epithelial barrier directly (39). Correspondingly, there is evidence that the polarization of macrophages gives priority to the M1 phenotype in the intestinal mucosa of patients with inflammatory bowel disease (IBD) and in experimental colitis mice (11, 39, 40). It should be noted that, although colonic M1 macrophages predominate during colitis, M2-like resident macrophages are also present to combat inflammation and to facilitate wound healing, which helps resolve the inflammation (36). Indeed, promoting the phenotype of anti-inflammatory M2 macrophages has been considered a promising treatment for IBD. M2 macrophages play an important role in the alleviation of colitis.

5 Targeting macrophage polarization as an effective strategy for UC treatment

Given the significant impact of macrophage polarization on the development of UC, targeting the skewed axis represents a promising strategy for its prevention and treatment and has spurred extensive research. In recent years, studies have revealed that M1 macrophage enrichment in the colon biopsies of patients with IBD was positively correlated with disease severity (41). In addition, there is evidence that vedolizumab-induced reduction in

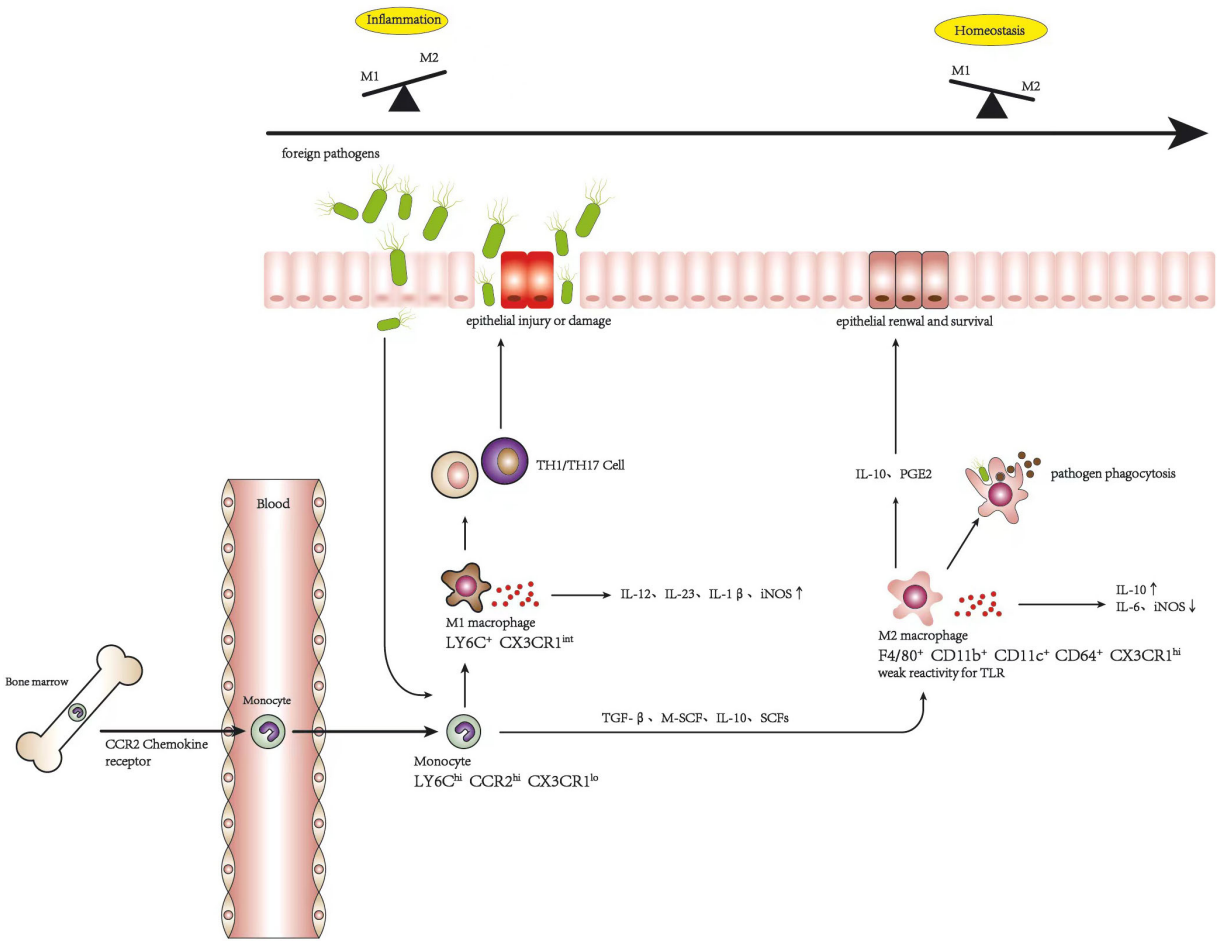

FIGURE 1
Alteration of macrophage polarization in inflammation and homeostasis.

the ratio of M1/M2 macrophages does contribute to the resolution of intestinal inflammation (42). It has been demonstrated that intraperitoneal or intravenous injection of exogenous bone marrow-derived M2 macrophages could effectively reduce the severity of colitis in mice caused by dinitrobenzene sulfonic acid (DNBS) (43, 44). Furthermore, it was evidenced that mice with deficient M2 macrophage polarization were more vulnerable to colitis induced by DSS (45). Caprioli et al. demonstrated that the downregulation of M1 macrophage pathway genes was connected to the mucosal healing of patients with IBD through treatment with infliximab, and M1 macrophages were significantly decreased, which was associated with the increased rate of macrophage apoptosis, representing a key mechanism for the therapeutic success of antitumor necrosis factor antibodies (46). Parallel results exist showing a prominent increase of the proportion of M2 macrophages in patients with IBD responding to infliximab therapy, but not in non-responders (30, 47). Eissa et al. have provided proof that the intestinal mucosa of patients diagnosed with UC is characterized by abundant infiltration of pro-inflammatory macrophages, producing a significant number of inflammatory mediators (e.g., TNF-α, IL-1β, and IL-6) through the activation of the nuclear factor kappa B (NF-κB) signaling pathway, which is negatively correlated with chromofungin (CHR), a short peptide with antimicrobial effects encoded from chromogranin A exon IV that is downregulated in UC. Moreover, exogenous CHR administration significantly mitigates colitis associated with a reduction of M1 macrophage markers (48). In addition, it has been revealed that intracolonic administration of CHR can increase M2 macrophage polarization, which decrease colonic collagen deposition and sustain the homeostasis of intestinal epithelial cells, thus protecting against colitis induced by DSS (49). Follistatin-like protein 1 (FSTL1), a pleiotropic cytokine that participates in a comprehensive spectrum of physiological and pathogenic processes, exhibits a highly expressional acitivity in human and mouse UC. It facilitates pro-inflammatory M1 phenotype macrophages and inhibits the M2 anti-inflammatory phenotype, leading to the excessive production of various inflammatory cytokines *in vitro* and *in vivo*. Li et al. found that the inhibition of FSTL1 could lead to UC remission, and the phenomenon disappears with the depletion of macrophages (50). Park et al. showed that adipose tissue-derived mesenchymal stem cells (ASCs) reduced the large amount of macrophages and the M1 macrophage population to mitigate UC in a model of DSS-induced mice. In the cell culture experiment, it was indicated that ASCs take effect by promoting the phenotype transition from M1 to M2, leading to anti-inflammatory cytokine proliferation (51). Cao et al. also reported that extracellular vesicles (EVs) secreted by bone marrow mesenchymal stem cells (BMSCs) could reinforce M2 macrophage polarization, supported by increased level of CD163 as the M2 marker, to effectively lessen the severity of UC. This result appeared to be associated with the JAK1/STAT1/STAT6 signaling pathway (52). These discoveries presume that the polarization of macrophages may be connected to mucosal healing in patients with IBD and could be an effective therapy for this disease.

6 Multiple phytochemicals show therapeutic prospects in UC treatment by targeting macrophage polarization

The first-line therapy currently used in the clinic for mild to moderate UC is mainly 5-aminosalicylic acid (5-ASA) drugs, which can be administered as suppositories, enemas, or oral preparations (53). Patients who do not respond to or do not achieve remission with 5-ASA drugs can be treated with corticosteroids (54), but glucocorticoids should not be used to maintain remission because of their lack of long-term efficacy and the risk of side effects (55). Thiopurines or biologic drugs, or both, should be used in patients with moderate to severe colitis, but long-term use must be carefully monitored for associated adverse effects, such as lymphoproliferative disorders (56, 57). Surgical treatment is usually indicated for uncontrollable massive bleeding, perforation, or endoscopically unresectable UC-associated adverse lesions (58). Phytochemicals, which are extracted from nature and with widely available sources, have been confirmed to possess abundant biological activities, as well as relatively low toxicity and high efficacy, which are particularly prominent in antitumor applications (59–61). The utilization of natural products in the management and prevention of various ailments can be traced back to ancient times, owing to their remarkable and indisputable effectiveness. The wealth of active compounds and diverse agent functions in natural products has always been an appealing prospect for researchers to explore and investigate novel phytochemical entity drugs with fewer adverse effects, thereby leading to more effective clinical application. In recent decades, a wealth of data has emerged indicating that numerous active ingredients sourced from plants and natural products hold immense potential in the management of IBD. This article aimed to present recent research focused on the treatment of UC using natural product-derived drugs that have been experimentally confirmed to be beneficial *in vitro* or *in vivo* based on online search protocols including PubMed, Web of Science, and Elsevier SD. The following key search terms were used: 'ulcerative colitis,' 'Inflammatory bowel disease,' 'colitis,' 'Intestinal inflammation,' 'macrophage,' 'polarization,' and 'natural products,' 'compound,' 'phytochemical.' The phytochemicals targeting macrophage polarization in UC treatment are listed in Table 1.

Dictyophora indusiata polysaccharide (DIP)

Dictyophora indusiata polysaccharide (DIP) isolated from dictyophora indusiate one of the most popular edible mushrooms due to its daintiness and multi-nutrition, was reported to possess potent antioxidant and anti-inflammatory activities *in vitro* (74, 75). Recent evidence has shown that DIP could conspicuously alleviate the severity of colitis in DSS-induced mice, and this mitigation is associated with the restoration of gut microbiota function and gut epithelial integrity, improvement of oxidative stress, and regulation of macrophage polarization balance (62, 76, 77). Wang et al. found that treatment with DIP significantly reduced M1 macrophage

TABLE 1 Phytochemicals targeting macrophage polarization in ulcerative colitis (UC) treatment.

Phytochemicals	*In vitro/in vivo* model	Effective dose/ concentration	Related clinical symptoms of UC	Macrophage phenotype-related indicators	Related molecular mechanisms in the regulation of macrophage phenotype in UC	Reference
Dictyophora indusiata polysaccharide	DSS-induced C57BL/6 mice	25, 50, and 100 mg/kg	Body weight loss↓ Colon length shortened↓ Histopathological damage↓ DAI↓ MPO↓ Spleen *vs.* body mass ratio↓	$F4/80^+CD11b^+$ cells in the spleen↓ $F4/80^+TNF\text{-}\alpha^+$ cells in the spleen↓ $F4/80^+CD206^+$ cells in the spleen↑ TNF-α, IL-1β, and IL-6 levels and mRNA expression in the colon↓ IL-10 evel and mRNA expression in the colon↑	NLRP3, Bax, and IRF5 protein in the colon↓ p-STAT3/STAT3 in the colon↓ p-IκBα/IκBα in the colon↓ Bcl-2 and IRF4 protein↑ CD86 in the colon↓	(52)
Didymin	DSS-induced C57BL/6 mice	2 and 4 mg/kg	DAI↓ MPO↓ Histological scores↓ Colon length shortened↓ Infiltration of neutrophils in the colon↓	$F4/80^+Nos2^+$ cells in the colon↓ $F4/80^+CD206^+$ cells in the colon↑ Colonic TNF, IL-1β, IL-6, and Nos2 mRNA expression↓ Arg-1, Chil3, Retnla, and IL-10 mRNA expression↑		(55)
	LPS- and IFN-γ-induced BMDMs	3, 10, and 30 μM		$F4/80^+Nos2^+$ cells ↓ $F4/80^+CD206^+$ cells ↑ TNF, IL-1β, IL-6, and Nos2 mRNA expression↓ Arg-1, Chil3, and Retnla mRNA expression↑	OCR level↓ Acetyl-CoA level↑ Hadhb mRNA expression↑ Hadhb mRNA reverse $F4/80^+Nos2^+$ cells decreased, $F4/80^+CD206^+$ cells increased Hadhb mRNA inhibited the reduction of TNF, IL-1β, IL-6, and Nos2 mRNA expression and promoted Arg-1, Chil3, and Retnla mRNA expression	
	M2: IL-4- and IL13-induced BMDMs	3, 10, and 30 μM		No alteration in Arg-1, Chil3, and Retnla mRNA expression↑ IL-10 mRNA expression↑		
Genistein	DSS-induced C57BL/6 mice	10 mg/kg	Body weight loss↓ Colon length↑ Inflammation scores↓ Glandular cell architecture recovery CD4% in the spleen, cLP↓ CD4% in MLNs↑ DCs in the spleen, MLNs, cLP↑ $CD4^+IL\text{-}10^+$ T cells↑ in the cLP	$CD11b^+CD11C^+$ cells in the spleen, MLNs, cLP↓ $F4/80^+CD206^+$ cells in the spleen, MLNs, cLP↑		(60)
	$F4/80^+CD206^+$ cells sorted from the spleen			Arg1 and IL-10 levels↑		
Loganin	DSS-induced BALB/c mice	50 and 100 mg/kg	Body weight loss↓ DAI↓ Colon length ↑ MPO↓	$F4/80^+iNOS^+$ cells in the colon↓ IL-6, TNF-α, and IL-1β mRNA expression and protein in the colon↓	Sirt1 mRNA expression in the colon↑ NF-κB p65 acetylation in the colon↓	(62)

(Continued)

TABLE 1 Continued

Phytochemicals	*In vitro/in vivo* model	Effective dose/ concentration	Related clinical symptoms of UC	Macrophage phenotype-related indicators	Related molecular mechanisms in the regulation of macrophage phenotype in UC	Reference
			Histological alterations↓ Inflammation infiltration↓	MCP-1, CXCL10, and COX-2 mRNA expression in colon↓		
Dioscin	DSS-induced BALB/c mice	40, 80, and 160 mg/kg	Body weight loss↓ DAI↓ Colon length↑ Histological scores↓ MPO↓	$F4/80^+CD86^+$ cells in the colon↓ $F4/80^+CD206^+$ cells in the colon↑ TNF-α, IFN-γ, and IL-6 levels in the colon↓ IL-10 level in the colon↑ CD86 protein in the colon↓ CD206 protein in the colon↑		(63)
	LPS- and IFN-γ-induced RAW264.7	0.625, 1.25, and 2.5 μM		$F4/80^+CD86^+$ cells↓ Expression of iNOS, TNF-α, and IL-6↓ Secretion of NO, TNF-α, IL-6, and IL-1β↓	Glucose, lactic acid↓ Protein of Raptor, HIF-1α, CD86, HK-2, PKM2, LDHA↓	
	RAW264.7	0.625, 1.25, and 2.5 μM		$F4/80^+CD206^+$ cells↑ Secretion of IL-10↑ Expression of Arg-1, IL-10, and Ym1↑	Uptake of free fatty acids↑ Protein of CD206, ACSL1, CPT-1A, CPT-2, Rictor, PPAR-γ↑	
Lupeol	LPS- and IFN-γ-induced peripheral blood mononuclear $CD14^+$ cells in the presence of GM-CSF	5 and 10 μM		$CD86^+$ cells↓ $CD206^+$ cells↑ TNF-α and IL-1β levels↓ IL-12 and IL-10 levels↑	IRF5 protein↓ p-p38 protein↓ SB203580 (specific inhibitor of p38 MAPK) reduced IRF5 expression	(64)
	IL-4-induced peripheral blood mononuclear $CD14^+$ cells in the presence of M-CSF	5 and 10 μM		No significant change in $CD206^+$ cells and the IL-10 and IL13 levels in the colon	No significant change in IRF5 and p-p38 protein SB203580 (specific inhibitor of p38 MAPK) affected little in IRF5 protein	
	DSS-induced C57BL/6 mice	50 mg/kg	Histological scores ↓ Colon length↑ Body weight loss↓ Survival rate↑	mRNA expression of IL-12, IL-6, IL-1β, TNF-α, iNOS, and CD86 in the colon↓ mRNA expression of IL-10, IGF-1, and Arg-1 in the colon↑		
Berberine	DSS-induced C57BL/6 mice	40 mg/kg	Colon length↑ DAI↓ Inflammatory cell infiltration↓	$F4/80^+CD11b^+CD16/32^+$ cells in the colon↓ TNF-α, IL-1β, and IL-6 levels in serum and mRNA expression the colon↓ IL-10 level in serum and mRNA expression the colon↑	AKT1 protein and mRNA expression in the colon↑ AKT2 mRNA expression in the colon↓	(65)
	LPS-induced RAW264.7	10 and 20 nM		CD16/32+cells↓ TNF-α, IL-12, IL-6 level and mRNA expression↓	AKT1 protein and mRNA expression↑ AKT2 mRNA expression in the colon↓ p-p65/NF-kB protein↓ SOCS1 protein↑ siAKT1 reduced CD16/32^+ cells and SOCS1 promotion and p-p65/NF-kB decline by berberine siSOCS1 inhibited the reduction of p-p65/NF-kB by berberine	

(Continued)

TABLE 1 Continued

Phytochemicals	*In vitro/in vivo* model	Effective dose/ concentration	Related clinical symptoms of UC	Macrophage phenotype-related indicators	Related molecular mechanisms in the regulation of macrophage phenotype in UC	Reference
Ginsenoside Rg1	DSS-induced BALB/c mice	200 mg/kg	Body weight loss↓ Colon length↑ Colon weight↓ Inflammatory cell infiltration↓	$CD11b^+F4/80^+iNOS^+$ cells in the colon↓ $CD11b^+F4/80^+CD206^+$ cells and $CD11b^+F4/80^+CD163^+$cells in the colon↑ Arg1 protein in the colon↑ MIF-1 and PIM-1 protein in the colon↓	Rock1, RhoA, and Nogo-B proteins in the colon↓	(37)
Baicalin	LPS-induced mouse peritoneal macrophages	50 μM		TNF-α and IL-23 mRNA expression↓ Arg-1 and Fizz-1 mRNA expression↑	IRF4 siRNA inhibited iNOS/CD206 decliine by baicalin	(66)
	DSS-induced C57BL/6 mice	100 mg/kg	DAI↓ Inflammatory cell infiltration↓	iNOS/CD206 in the colon↓ TNF-α and IL-23 mRNA expression in the colon↓ Arg-1 and Fizz-1 mRNA expression in the colon↑ IRF4 protein in the colon↓ IRF5 protein in the colon↑		
Toosendanin	DSS-induced C57BL/6 mice	0.5 and 1 mg/kg	Colon length↑ Body weight loss↓ DAI↓ Weight of spleen↓ MPO↓ Histological score↓	$CD11b^+CD11c^+$ cells in the colon↓ $F4/80^+CD206^+$ cells in the colon↑ TNF-α, IL-6, and IL-1β levels and mRNA expression in the colon↓	NLRP3 protein↓ Nrf2 and HO-1 protein↑	(67)
Artemisinin	DSS-induced C57BL/6 mice	20 and 80 mg/kg	Body weight loss↓ Colon length↑ MPO↓ Inflammatory cell infiltration↓ DAI↓ Spleen index↓	TNF-α, IL-1β, and IL-6 levels in the colon↓ iNOS protein↓ Arg-1 protein↑	ERK phosphorylation↓ MyD88 activation↓	(68)
	PBMCs of CD patients	10 and 100 μM		$CD11b^+CD206^+$ cells↑ TNF-α, IL-1β, and IL-6 levels and mRNA expression↓		
Tiliroside	DSS-induced C57BL/6 mice	12.5, 25, and 50 mg/kg	Body weight loss↓ Diarrhea, rectal bleeding↓ Colon length↑ MPO↓ Inflammatory cell infiltration↓	$CD68^+iNOS^+$ cells in the colon $CD68^+CD206^+$ cells in the colon TNF-α, IL-1β, and IL-6 mRNA expression in the colon↓ Arg-1, Chil3, and CD206 mRNA expression in the colon↑		(69)
	TNBS-induced C57BL/6 mice	25 and 50 mg/kg	Survival rate↑ Colon length↑ MPO↓			
	LPS- and IFN-γ-induced BMDMs	10, 20, and 40 μM		TNF-α, IL-1β, and iNOS mRNA expression↓ Arg-1, Chil3, and CD206 mRNA expression↑	HIF-1α protein and mRNA expression↓	
	IL-4-induced BMDMs	10, 20, and 40 μM		No significant impact on Arg-1, Chil3, and CD206 mRNA expression		
Platycodin D	DSS-induced C57BL/J mice	10 mg/kg	Body weight loss↓ Colon length↑ DAI↓	$F4/80^+iNOS^+$ cells in the colon↓ $F4/80^+CD206^+$ cells in the colon↑		(70)

(Continued)

TABLE 1 Continued

Phytochemicals	*In vitro/in vivo* model	Effective dose/ concentration	Related clinical symptoms of UC	Macrophage phenotype-related indicators	Related molecular mechanisms in the regulation of macrophage phenotype in UC	Reference
			Histological scores↓	TNF-α, IL-1β, and IL-6 levels and mRNA expression in the colon↓ IL-10 level and mRNA expression in the colon↑		
	LPS induced RAW264.7	2.5 and 5 μM		$F4/80^+iNOS^+$ cells↓ $F4/80^+CD206^+$ cells↑ TNF-α, IL-1β, and IL-6 levels and mRNA expression↓ IL-10 level and mRNA expression↑	p-PI3K and p-Akt protein↑ p-p65 protein↓	
Sulforaphane		DSS-induced C57BL/6JNifdc	10, 20, and 40 mg/kg	Body weight loss↓ Colon length↑ DAI↓ Histological scores↓	$F4/80^+CD68^+$ cells in the colon↓ $F4/80^+CD206^+$ cells in the colon↑	(71)
Rhein	M1:LPS + IFN-γ induced BMDMs	10, 1, and 0.1 μM		IL-1β and iNOS mRNA expression↓ IL-10 and CD206 mRNA expression↑ TNF-α, IL-1β, and IL-6 levels↓	p-STAT3 protein↓	(72)
Rosmarinic acid	DSS-induced ICR mice	100 mg/kg	Body weight loss↓ Inflammatory cell infiltration↓ DAI↓	TNF-α, IL-1β, IL-12, NOS2, and CD16/32 mRNA expression in the colon↓ Arg, Mrc, Mgl1, and CD206 mRNA expression in the colon↑		(73)
	LPS-induced PBMs	10 μM		TNF-α, IL-1β, IL-12, NOS2, and CCL4 mRNA expression↓	HO-1 protein↑	
	IL-4-induced PBM	10 μM		Arg, Mrc, Mgl1, and Dectin-1 mRNA expression in the colon↑		

PBMCs, peripheral blood mononuclear cells; BMDMs, bone marrow-derived macrophages; PBMs, peripheral blood macrophages; LPS, lipopolysaccharides; DSS, dextran sulfate sodium; DAI, Disease Activity Index; MPO, myeloperoxidase; cLP, colon lamina propria; MLNs, mesenteric lymph nodes; DCs, dendritic cells; iNOS, inducible nitric oxide synthase. '↑' means increase, '↓' means decrease.

polarization and promoted the M2 phenotype in the spleen of mice orally administered DSS, and the macrophages marked by CD86 in the colon were also inhibited, which were consistent with the deregulation of the expression of TNF-α, IL-6, and IL-1β and the high secretion of IL-10 after DIP administration. In addition, DIP downregulated the activation of the NF-κB, STAT3, and NLRP3 signaling pathways in the colon of mice treated with DSS, which may be associated with the mechanism of macrophage polarization balance (62). Significantly, the biological activity of polysaccharides is highly correlated to their conformation of space, which means that their efficacy would greatly weaken or even vanish once they are degraded into monosaccharides or oligosaccharides.

Didymin

Didymin, a dietary glycoside widely distributed in citrus fruits such as mandarin, bergamot, orange, *Origanum*, and Vulgare Duanxueliu, has attracted attention due to its antioxidant capacity (63). Recently, Lv et al. have found that didymin can effectively reduce colitis in mice by targeting macrophage polarization to the M2 phenotype. Their experiment results showed that didymin decreased the proportion of M1 and increased M2 in the colon of mice induced by DSS, and mice injected with exogenous M1 macrophages after being administered with clodronate liposomes to deplete autologous macrophages exhibited more sensitivity to DSS; however, the severity of colitis was declined by didymin management before exogenous M1 macrophages injection. Interestingly, didymin resisted M1 macrophage polarization, but there was no alteration on M2 macrophages and on the expression of Arg-1, Chil3, and Retnla, indicating that the effect of didymin on ameliorating colitis is dependent on the transformation of M1 macrophages toward M2. A further study suggested that the macrophage phenotype modulation of didymin is presented through the improvement of fatty acid oxidation (FAO) by fortifying the expression of Hadhb (60).

Genistein

Genistein, an isoflavonoid compound widely distributed in soy-based products (78), also called phytoestrogen owing to a pattern resembling estradiol, shows high anti-inflammatory, anticancer, antioxidant, and antidiabetic properties and has attracted interest in medical research (64, 79, 80). Recently, it has been revealed that genistein could conspicuously mitigate experimental colitis, which is associated with targeting macrophage polarization. The results of the experiment indicated that the administration of genistein resulted in the decline of M1 and the elevation of M2 macrophages in the spleen, mesenteric lymph nodes (MLNs), and colon lamina propria (cLP) of DSS-induced mice. Apart from this, the M2 macrophages sorted from colitis mice induced by genistein highly expressed Arg-1 and IL-10 compared with those managed using phosphate-buffered saline (PBS). However, the detailed mechanism of how genistein shifts M1 macrophages toward the M2 phenotype still remains unclear (81).

Loganin

Loganin, a type of bioactive iridoid glycoside extracted from traditional Chinese medicine, commonly called *Cornus officinalis*, was established to have potent anti-depression, neuropathic protection, and anti-inflammation effects (82–84). Yuan et al. reported that loganin could prominently alleviate the pathologic alterations of DSS-induced colitis, increase the tight junction proteins to protect the intestinal epithelial barrier, and inhibit the expression of colonic pro-inflammatory cytokines such as IL-1β, IL-6, and TNF-α (85). Another study demonstrated the high expression of Sirt1, inhibition of the acetylation of NF-κB p65, and the suppression of loganin in the M1 macrophages of colitis mice, which was counteracted after using the Sirt1 inhibitor Ex527. These findings suggest that the therapeutic potential may have involved the inhibition of M1 macrophages regulated by the Sirt1/NF-κB pathway (65).

Dioscin

Dioscin is a steroid saponin isolated from *Dioscorea nipponica* (86), which has been reported to be a potential therapeutic component for colitis. It showed high availability in suppressing glycolysis and promoting FAO to predispose macrophage polarization from M1 toward M2. Interestingly, the agonist of the mTORC1 signal could reverse the effects of dioscin on the downregulation of glycolysis and the counteraction of the HIF-1α protein expression, which is indispensable for the transcription of the inflammatory cytokines and metabolic genes associated with glycolysis, resulting in the abortion of M1 macrophage decline. In addition, after administration of the mammalian target of rapamycin complex 2 (mTORC2) inhibitor, the enhancement of dioscin on the peroxisome proliferator-activated receptor gamma (PPAR-γ) protein and FAO-related enzymes was prominently impaired, and the promotion of M2 macrophages was counteracted as well. These findings demonstrated that dioscin modulated the polarization and metabolism of macrophages by regulating the mTORC1/HIF-1α and mTORC2/PPAR-γ signaling pathways to mitigate the severity of colitis, which was further confirmed in experimental colitis mice (87). Similarly, Shi et al. showed that dioscin catalyzed the expression of miR-125a-5p to shift macrophages toward the M2 phenotype, thereby restoring the intestinal epithelial barrier function and facilitating experimental colitis (88).

Lupeol

Lupeol is a triterpenoid compound with exclusive bioactivity found in numerous natural plants including *Albizia lebbeck* and *Alnus glutinosa* (89). It has been reported that lupeol exhibited protective effects against colitis in experimental animals, and this involved blocking the NF-κB signaling of intestinal epithelial cells and modulating macrophages leaning toward the M2 phenotype to relieve inflammatory responses (66, 90). Zhu et al. observed that *IRF5*, a key transcription factor associated with M1 macrophages, was remarkably reduced after lupeol incubation of M1 macrophages induced by LPS and IFN-γ with exposure to granulocyte-macrophage colony-stimulating factor (GM-CSF), but the same results were not detected in M2 macrophages, which were inferred to be bound with the modulation of a specific signaling pathway. This hypothesis was subsequently confirmed as studies showed that the p38 mitogen-activated protein kinase (MAPK) phosphorylation of M1 macrophages was reduced by lupeol, which was counteracted by the use of the p38 MAPK inhibitor (90). Therefore, lupeol possibly inhibits *IRF5* through a specific receptor and downstream signaling pathway, such as p38 MAPK, to switch M1 macrophages toward M2.

Berberine

Berberine, a plant isoquinoline alkaloid largely found in the root of *Coptis chinensis* (91), has been proven to be beneficial in colitis treatment through various mechanisms, such as inhibiting the IFN-γ and JAK2/STAT3 signaling pathways to attenuate inflammatory responses (67, 92), regulating the intestinal mucosal immune homeostasis through the Wnt/β-catenin pathway (93), and reducing the activation of the MAPK and NF-κB signaling pathways to decrease pro-inflammatory cytokine production (68). Recently, Yunxin et al. have reported that berberine could correct macrophage polarization imbalance by inhibiting differentiation of the M1 phenotype to prevent colitis development directly by upregulating the AKT1 pathway and the protein expression of *SOCS1*, one of the target genes of AKT1, and decreasing the level of NF-κB phosphorylation. In addition, it was observed that knocking out the AKT1 gene reversed the effect of berberine on the modulation of SOCS1 and NF-κB phosphorylation protein expression. The downregulation of berberine on M1 macrophage polarization and related pro-inflammatory cytokines, such as IL-6 and TNF-α, was also neutralized on account of *AKT1* small

interfering RNA (siRNA) transfection, suggesting that the inhibitory activity of berberine on M1 polarization is dependent on the AKT1/SOCS1/NF-κB signaling pathway (94).

Ginsenoside Rg1

Ginsenoside Rg1 is a major active constituent of *Panax ginseng* and has been reported to be an anti-inflammatory treatment for various diseases (69). Recent evidence has shown that ginsenoside Rg1 could conspicuously ameliorate the severity of symptoms and reduce the inflammatory response by downregulating the expression of TNF-α, IL-33, IL-6, and CCL-2 in a DSS-induced colitis mouse model (40, 95). Ginsenoside Rg1 has been reported to be a good regulator of macrophage polarization, which increased the M2 phenotype and inhibited the M1 phenotype, similar to Y27632, a specific inhibitor of Rock1. Furthermore, it is worth noting that the increase in the expression of the Rock1, RhoA, and Nogo-B proteins in the colonic tissues of colitis mice was attenuated by ginsenoside Rg1 and Y27632, demonstrating that the trends of Nogo signaling in the regulation of the macrophage phenotype in colitis mice were largely consistent with ginsenoside Rg1. These results may imply that regulation by ginsenoside Rg1 of the phenotype of macrophages in colitis mice may be associated with the Nogo-B signaling pathway (40).

Baicalin

Baicalin, one of the active ingredients of *Scutellaria baicalensis* Georgi, was proven to be therapeutic in IBD (70, 96). Zhu et al. investigated the anti-inflammatory effect of baicalin against LPS-induced mouse peritoneal macrophages and found that it could effectively inhibit the LPS-induced promotion of the inflammatory macrophage subset of M1, reducing the ratio of M1/M2. Consistently, they found that baicalin treatment obviously mitigated the severity of DSS-induced colitis in mice (97). The related mechanism may involve the regulation of the IRF4/IRF5 protein expression of baicalin, as the results showed that baicalin could directly facilitate the protein expression of *IRF4* and block that of *IRF5*, and the decline of the M1/M2 of baicalin was reversed after *IRF4* siRNA transfection (97).

Toosendanin (TSN)

Toosendanin (TSN) is a triterpenoid distributed in the bark or fruits of a type of commonly used Chinese herbal medicine, known as *Melia toosendan* Sieb et Zucc (59). Fan et al. determined that TSN could alleviate the symptoms of DSS-induced mice by reducing the inflammatory responses and macrophage polarization, as the experiment results showed that TSN could downregulate the percentage of the M1 phenotype and the expression of pro-inflammatory cytokines such as TNF-α, IL-6, and IL-1β, but promoted M2 macrophages. A further study revealed that the activation of NLRP3 induced by DSS in the colonic macrophage of colitis mice was reversed by TSN, which influenced the composition of IL-1β. Interestingly, TSN acted as an activator of the NFE-related factor 2 (*Nrf2*) signaling pathway, a key transcription factor facilitating the antioxidant response *via* the synthesis of heme oxygenase-1 (HO-1), which modulated IL-10 production to affect the macrophage phenotype (71). The results showed that the decline of the colonic expression of *Nrf2* and HO-1 in mice induced by DSS was counteracted by TSN management (98). This evidence implied that TSN regulation of macrophage alteration attenuating DSS-induced colitis is associated with the NLRP3 and Nrf2/HO-1 pathways, but the specificity of the relationship needs further validation.

Artemisinin

Artemisinin is the main active compound isolated from *Artemisia annua* L, which was initially popular for its strong antimalarial properties, but which has also been revealed in recent years to exert various activities such as antivirus, anti-parasite, tumor suppression, and inflammation prevention (72). Previous evidence showed the protective function of artemisinin against DSS-induced colitis in mice, which involved the induction of CYP3A expression through the activation of the pregnane X receptor (PXR) (99). A study by Huai et al. provided proof that the inflammatory colonic tissues of patients with Crohn's disease (CD) presented significantly increased M2 macrophages marked by $CD11b^{+}CD206^{+}$ and reduction of the pro-inflammatory cytokine expression after the administration of artemisinin *in vitro*. In addition, it has been suggested that artemisinin could mitigate the symptoms of colitis *via* upregulating the macrophages of murine colitis tissues polarized to the M2 phenotype, which may be associated with inhibiting the MYD88 and ERK signaling pathways owing to evidence showing that artemisinin significantly suppressed MyD88 activation and ERK phosphorylation in the colon tissue of a DSS-induced mouse model (100). However, the specific mechanism of artemisinin on the MYD88 and ERK signaling pathways affecting the regulation of macrophage phenotype remains to be further studied.

Tiliroside

Tiliroside, a natural flavonoid derived from several medicinal and dietary plants, such as linden, rosehip, and strawberry, was revealed to exhibit anti-inflammatory, antioxidant, anticarcinogenic, and hepatoprotective activities (73). Zhuang et al. reported that the protective function of tiliroside in UC was related to the blocking of M1 macrophage polarization, and this effect was mainly achieved by accelerating the proteasomal degradation of HIF-1α, consequently attenuating glycolysis. This was validated in the experiments showing that tiliroside could significantly decrease the extraction of 2-NBDG, a fluorescent deoxyglucose analog widely used in detecting cellular glucose uptake; the gene expression of glycolytic enzymes such as glucose transporter 1 (Glut1), enolase 1 (Eno1), and pyruvate kinase M (Pkm); and the production of lactate in bone marrow-derived macrophages (BMDMs) induced by LPS and IFN-γ. Another evidence exhibited tiliroside prominently downregulating the protein

level of HIF-1α, but had no effect on the mRNA expression. In addition, tiliroside ceased to be effective after using clodronate liposomes, which can significantly deplete macrophages *in vivo*, suggesting that tiliroside inhibited colitis through a macrophage-dependent mechanism (101). In a word, the findings above showed the potential of tiliroside as a therapeutic strategy for UC through targeting the HIF-1a/glycolysis pathway to mediate M1 macrophage reduction.

Platycodin D (PLD)

Platycodin D (PLD) is a triterpenoid saponin extracted from the root of the *Platycodon grandiflorum* plant (102). Guo et al. studied the anti-inflammatory effects of PLD on DSS-induced colitis in mice, as well as on LPS-induced RAW264.7, and found that PLD was effective in mitigating colitis through shifting macrophage polarization to deflect the M2 phenotype. Further examination showed that the property of PLD on the regulation of macrophage polarization involved the activation of the PI3K/Akt pathway and the inhibition of the NF-κB pathway, as data revealed the upregulation of p-PI3K and p-Akt proteins with a decline of the nuclear translocation of the p65 subunit after PLD administration in LPS-stimulated RAW264.7 cells, which was further confirmed to be or at least partly dependent on adenosine 5′-monophosphate-activated protein kinase (AMPK) due to the effect of PLD on PI3K/Akt and NF-κB pathway modulation being reduced after the knockdown of AMPK. It is noteworthy that a higher dose of PLD exerted a lower anti-inflammatory effect on the macrophages managed by LPS compared to a lower dose, which may be associated with the modest suppression of cell activity (103).

Sulforaphane

Sulforaphane is a dietary isothiocyanate widely distributed in cruciferous vegetables such as broccoli, cabbage, and Brussels sprouts. It possesses great antioxidant and anti-inflammatory activities (104). Studies on DSS-induced colitis in mice found that management with sulforaphane could conspicuously improve the clinical symptoms of colitis and the damaged epithelial integrity (105). Sun et al. reported that sulforaphane elevated the IL-10 production of LPS- and IFN-γ-induced BMDMs and switched the macrophages from the M1 to the M2 phenotype with the activation of STAT3. Moreover, after the neutralization of IL-10, the effect of sulforaphane on the M2 phenotype priority was suppressed, as well as the level of STAT3 phosphorylation, implying the modulation of sulforaphane on macrophage polarization mediating the phenotype switch from M1 to M2 in murine colitis caused by DSS, and this effect was closely related to the activation of the IL-10/STAT3 signaling pathways (106).

Rhein

Rhein is a natural flavonoid compound derived from rhubarb that is widely used as a traditional Chinese medicine to treat edema, constipation, and inflammation (107). It has been reported that rhein has potential in alleviating DSS-induced colitis through regulating macrophage polarization toward the M2 phenotype, i.e., toward the anti-inflammatory condition. Experimental data from RAW264.7 cells showed that the relative expression of M1 markers and pro-inflammation mediators were significantly inhibited after the administration of rhein, but the results for M2 were totally reversed. In addition, researchers found that rhein could prevent the activation of the Nox2 redox-mediated NLRP3 inflammasome and modulate the Nrf2-dependent redox balance to block the maturation and secretion of IL-1β in macrophages, one of the key pro-inflammatory cytokines (108).

Rosmarinic acid (RA)

Rosmarinic acid (RA) is a natural compound extracted from plants of the Lamiaceae family, including rosemary, lemon balm, and mint (109). Some studies have investigated the protective effects of RA against colitis in mice induced by DSS and found that it is a potential anti-inflammatory candidate for UC treatment (110, 111). Mai et al. reported that RA could inhibit M1 macrophages with the promotion of M2 in both the colonic tissues of DSS-induced mice and in peripheral blood macrophages cultured *in vitro* and upregulate the protein level of HO-1. In addition, the inhibition of RA of the LPS-mediated NF-κB p65 translocation into the nucleus was shortened by interdicting HO-1; moreover, the administration of the NF-κB inhibitor BAY11-7082 had no significant effect on the modulation of macrophage differentiation by RA. These results indicated that RA dampened M1 macrophage polarization *via* promoting HO-1 to impede the NF-κB pathway in ameliorating experimental colitis (111).

7 Conclusion and future perspectives

As a modern refractory disease, UC has negatively impacted the quality of life of patients due to its recurrence and obstinacy, with intolerable symptoms such as frequent hematochezia and abdominal pain (58). A series of studies have demonstrated the great importance of the imbalance of macrophage polarization in the development of UC; therefore, targeting macrophage polarization tendency to the anti-inflammatory phenotype, i.e., of M2, is a potential therapeutic option for UC (21, 30, 36, 112). As the hotspot of new drug development, natural products exhibit abundant bioactivities and nutritional value. In this paper, we summarized more than a dozen investigated phytochemicals extracted from diverse plants, including didymin, genistein, loganin, etc., which could ameliorate experimental colitis by modulating macrophage polarization (60, 65, 81). Their chemical

structures include flavonoid, polyphenol, alkaloid, and terpenoid derivatives, and the related modulatory mechanisms involved regulating Hadhb-mediated FAO, the Sirt1/NF-κB signaling pathway, and mTORC2/PPAR-γ signaling, among others (60, 65, 87). The aforementioned findings demonstrated that phytochemicals have promising prospects in mitigating the symptoms of UC by modulating macrophage polarization. However, investigations pertaining to their therapeutic efficacy in patients with UC are yet to be conducted, as all current research has been limited to experimental animal models. Furthermore, the underlying regulatory mechanisms and the potential toxicity of these phytochemicals, which act as regulators of macrophage polarization, require further elucidation. Consequently, further research should concentrate on the toxicity and safety of phytochemicals with effects on the regulation of macrophage polarization, as well as on particular mechanisms that are needed to promote natural regulators of macrophage polarization as UC therapy.

Author contributions

RS, JL, and TM provided direction and guidance for this manuscript. KW wrote the whole manuscript. XL, MW, YY, LS, ZJ, and HJ were responsible for the collation of the paper. RS and TM made significant revisions to the manuscript. All authors contributed to the article and approved the submitted version.

Funding

This work was supported by the National Natural Science Foundation of China (No. 81874386), Chinese Medicine Inheritance and Innovation "OneHundred Million" Talent Project Qihuang Scholar (to JL) and Capital's Funds for Health Improvement and Research (shoufa 2022-4-4205).

Conflict of interest

The authors declare that the research was conducted in the absence of any commercial or financial relationships that could be construed as a potential conflict of interest.

Publisher's note

References

1. da Silva BC, Lyra AC, Rocha R, Santana GO. Epidemiology, demographic characteristics and prognostic predictors of ulcerative colitis. *World J Gastroenterol* (2014) 20(28):9458–67. doi: 10.3748/wjg.v20.i28.9458

2. Torres J, Halfvarson J, Rodriguez-Lago I, Hedin CRH, Jess T, Dubinsky M, et al. Results of the seventh scientific workshop of ECCO: precision medicine in IBD-prediction and prevention of inflammatory bowel disease. *J Crohns Colitis* (2021) 15 (9):1443–54. doi: 10.1093/ecco-jcc/jjab048

3. Ungaro R, Mehandru S, Allen PB, Peyrin-Biroulet L, Colombel J-F. Ulcerative colitis. *Lancet* (2017) 389(10080):1756–70. doi: 10.1016/S0140-6736(16)32126-2

4. Younis N, Zarif R, Mahfouz R. Inflammatory bowel disease: between genetics and microbiota. *Mol Biol Rep* (2020) 47(4):3053–63. doi: 10.1007/s11033-020-05318-5

5. Bhattacharya S, Cross RK. Medical treatment of ulcerative colitis. *Semin Colon Rectal Surg* (2022) 33. doi: 10.1016/j.scrs.2022.100863

6. Kayal M, Shah S. Ulcerative colitis: current and emerging treatment strategies. *J Clin Med* (2019) 9(1):94. doi: 10.3390/jcm9010094

7. Li C, Wang J, Ma R, Li L, Wu W, Cai D, et al. Natural-derived alkaloids exhibit great potential in the treatment of ulcerative colitis. *Pharmacol Res* (2022) 175:105972. doi: 10.1016/j.phrs.2021.105972

8. Weisshof R, El Jurdi K, Zmeter N, Rubin DT. Emerging therapies for inflammatory bowel disease. *Adv Ther* (2018) 35(11):1746–62. doi: 10.1007/s12325-018-0795-9

9. Han X, Ding S, Jiang H, Liu G. Roles of macrophages in the development and treatment of gut inflammation. *Front Cell Dev Biol* (2021) 9:625423. doi: 10.3389/fcell.2021.625423

10. Li M, Xue Q, Yang X, Aung LHH, Yang Y, Yu T. The pathophysiological role of macrophages in colitis and their treatment. *Recent Adv Microb Diversity* (2022), 277–97. doi: 10.1016/B978-0-12-822368-0.00013-X

11. Grimm MC, Pullman WE, Bennett GM, Sullivan PJ, Pavli P, Doe WF. Direct evidence of monocyte recruitment to inflammatory bowel disease mucosa. *J Gastroenterol Hepatol* (1995) 10(4):387–95. doi: 10.1111/j.1440-1746.1995.tb01589.x

12. Koelink PJ, Bloemendaal FM, Li B, Westera L, Vogels EWM, van Roest M, et al. Anti-TNF therapy in IBD exerts its therapeutic effect through macrophage IL-10 signalling. *Gut* (2020) 69(6):1053–63. doi: 10.1136/gutjnl-2019-318264

13. Vos ACW, Wildenberg ME, Arijs I, Duijvestein M, Verhaar AP, de Hertogh G, et al. Regulatory macrophages induced by infliximab are involved in healing *in vivo* and in vitro. *Inflammatory Bowel Dis* (2012) 18(3):401–8. doi: 10.1002/ibd.21818

14. Locati M, Curtale G, Mantovani A. Diversity, mechanisms, and significance of macrophage plasticity. *Annu Rev Pathol* (2020) 15:123–47. doi: 10.1146/annurev-pathmechdis-012418-012718

15. Bain CC, Bravo-Blas A, Scott CL, Perdiguero EG, Geissmann F, Henri S, et al. Constant replenishment from circulating monocytes maintains the macrophage pool in the intestine of adult mice. *Nat Immunol* (2014) 15(10):929–37. doi: 10.1038/ni.2967

16. Delfini M, Stakenborg N, Viola MF, Boeckxstaens G. Macrophages in the gut: masters in multitasking. *Immunity* (2022) 55(9):1530–48. doi: 10.1016/j.immuni.2022.08.005

17. Moreira Lopes TC, Mosser DM, Gonçalves R. Macrophage polarization in intestinal inflammation and gut homeostasis. *Inflamm Res* (2020) 69(12):1163–72. doi: 10.1007/s00011-020-01398-y

18. Wang S, Ye Q, Zeng X, Qiao S. Functions of macrophages in the maintenance of intestinal homeostasis. *J Immunol Res* (2019) 2019:1512969. doi: 10.1155/2019/1512969

19. Kuhl AA, Erben U, Kredel LI, Siegmund B. Diversity of intestinal macrophages in inflammatory bowel diseases. *Front Immunol* (2015) 6:613. doi: 10.3389/fimmu.2015.00613

20. Mantovani A, Biswas SK, Galdiero MR, Sica A, Locati M. Macrophage plasticity and polarization in tissue repair and remodelling. *J Pathol* (2013) 229(2):176–85. doi: 10.1002/path.4133

21. Seyedizade SS, Afshari K, Bayat S, Rahmani F, Momtaz S, Rezaei N, et al. Current status of M1 and M2 macrophages pathway as drug targets for inflammatory bowel disease. *Arch Immunol Ther Exp (Warsz)* (2020) 68(2):10. doi: 10.1007/s00005-020-00576-4

22. Mosser DM, Edwards JP. Exploring the full spectrum of macrophage activation. *Nat Rev Immunol* (2008) 8(12):958–69. doi: 10.1038/nri2448

23. Mackaness GB. Cellular resistance to infection. *J Exp Med* (1962) 116(3):381–406. doi: 10.1084/jem.116.3.381

24. Gordon S. Alternative activation of macrophages. *Nat Rev Immunol* (2003) 3 (1):23–35. doi: 10.1038/nri978

25. Mills CD, Kincaid K, Alt JM, Heilman MJ, Hill AM. M-1/M-2 macrophages and the Th1/Th2 paradigm. *J Immunol* (2000) 164(12):6166–73. doi: 10.4049/jimmunol.164.12.6166

26. Yang Z, Lin S, Feng W, Liu Y, Song Z, Pan G, et al. A potential therapeutic target in traditional Chinese medicine for ulcerative colitis: macrophage polarization. *Front Pharmacol* (2022) 13:999179. doi: 10.3389/fphar.2022.999179

27. Murray PJ. Macrophage polarization. *Annu Rev Physiol* (2017) 79:541–66. doi: 10.1146/annurev-physiol-022516-034339

28. Zhang J, Zhou X, Hao H. Macrophage phenotype-switching in cancer. *Eur J Pharmacol* (2022) 931:175229. doi: 10.1016/j.ejphar.2022.175229

29. Shapouri-Moghaddam A, Mohammadian S, Vazini H, Taghadosi M, Esmaeili SA, Mardani F, et al. Macrophage plasticity, polarization, and function in health and disease. *J Cell Physiol* (2018) 233(9):6425–40. doi: 10.1002/jcp.26429

30. Du Y, Rong L, Cong Y, Shen L, Zhang N, Wang B. Macrophage polarization: an effective approach to targeted therapy of inflammatory bowel disease. *Expert Opin Ther Targets* (2021) 25(3):191–209. doi: 10.1080/14728222.2021.1901079

31. Yunna C, Mengru H, Lei W, Weidong C. Macrophage M1/M2 polarization. *Eur J Pharmacol* (2020) 877:173090. doi: 10.1016/j.ejphar.2020.173090

32. Na YR, Stakenborg M, Seok SH, Matteoli G. Macrophages in intestinal inflammation and resolution: a potential therapeutic target in IBD. *Nat Rev Gastroenterol Hepatol* (2019) 16(9):531–43. doi: 10.1038/s41575-019-0172-4

33. Bain CC, Mowat AM. The monocyte-macrophage axis in the intestine. *Cell Immunol* (2014) 291(1-2):41–8. doi: 10.1016/j.cellimm.2014.03.012

34. Davies LC, Jenkins SJ, Allen JE, Taylor PR. Tissue-resident macrophages. *Nat Immunol* (2013) 14(10):986–95. doi: 10.1038/ni.2705

35. Bain CC, Scott CL, Uronen-Hansson H, Gudjonsson S, Jansson O, Grip O, et al. Resident and pro-inflammatory macrophages in the colon represent alternative context-dependent fates of the same Ly6Chi monocyte precursors. *Mucosal Immunol* (2013) 6(3):498–510. doi: 10.1038/mi.2012.89

36. Pan X, Zhu Q, Pan LL, Sun J. Macrophage immunometabolism in inflammatory bowel diseases: from pathogenesis to therapy. *Pharmacol Ther* (2022) 238:108176. doi: 10.1016/j.pharmthera.2022.108176

37. Gren ST, Grip O. Role of monocytes and intestinal macrophages in crohn's disease and ulcerative colitis. *Inflamm Bowel Dis* (2016) 22(8):1992–8. doi: 10.1097/MIB.0000000000000824

38. Okumura R, Takeda K. Roles of intestinal epithelial cells in the maintenance of gut homeostasis. *Exp Mol Med* (2017) 49(5):e338. doi: 10.1038/emm.2017.20

39. Lissner D, Schumann M, Batra A, Kredel LI, Kuhl AA, Erben U, et al. Monocyte and M1 macrophage-induced barrier defect contributes to chronic intestinal inflammation in IBD. *Inflamm Bowel Dis* (2015) 21(6):1297–305. doi: 10.1097/MIB.0000000000000384

40. Long J, Liu XK, Kang ZP, Wang MX, Zhao HM, Huang JQ, et al. Ginsenoside Rg1 ameliorated experimental colitis by regulating the balance of M1/M2 macrophage polarization and the homeostasis of intestinal flora. *Eur J Pharmacol* (2022) 917:174742. doi: 10.1016/j.ejphar.2022.174742

41. Liu H, Dasgupta S, Fu Y, Bailey B, Roy C, Lightcap E, et al. Subsets of mononuclear phagocytes are enriched in the inflamed colons of patients with IBD. *BMC Immunol* (2019) 20(1):42. doi: 10.1186/s12865-019-0322-z

42. Zeissig S, Rosati E, Dowds CM, Aden K, Bethge J, Schulte B, et al. Vedolizumab is associated with changes in innate rather than adaptive immunity in patients with inflammatory bowel disease. *Gut* (2019) 68(1):25–39. doi: 10.1136/gutjnl-2018-316023

43. Ackermann M, Mucci A, McCabe A, Frei S, Wright K, Snapper SB, et al. Restored macrophage function ameliorates disease pathophysiology in a mouse model for IL10 receptor-deficient very early onset inflammatory bowel disease. *J Crohns Colitis* (2021) 15(9):1588–95. doi: 10.1093/ecco-jcc/jjab031

44. Hunter MM, Wang A, Parhar KS, Johnston MJ, Van Rooijen N, Beck PL, et al. *In vitro*-derived alternatively activated macrophages reduce colonic inflammation in mice. *Gastroenterology* (2010) 138(4):1395–405. doi: 10.1053/j.gastro.2009.12.041

45. Takada Y, Hisamatsu T, Kamada N, Kitazume MT, Honda H, Oshima Y, et al. Monocyte chemoattractant protein-1 contributes to gut homeostasis and intestinal inflammation by composition of IL-10-producing regulatory macrophage subset. *J Immunol* (2010) 184(5):2671–6. doi: 10.4049/jimmunol.0804012

46. Caprioli F, Bose F, Rossi RL, Petti L, Vigano C, Ciafardini C, et al. Reduction of CD68+ macrophages and decreased IL-17 expression in intestinal mucosa of patients with inflammatory bowel disease strongly correlate with endoscopic response and mucosal healing following infliximab therapy. *Inflamm Bowel Dis* (2013) 19(4):729–39. doi: 10.1097/MIB.0b013e318280292b

47. Vos AC, Wildenberg ME, Duijvestein M, Verhaar AP, van den Brink GR, Hommes DW. Anti-tumor necrosis factor-alpha antibodies induce regulatory macrophages in an fc region-dependent manner. *Gastroenterology* (2011) 140(1):221–30. doi: 10.1053/j.gastro.2010.10.008

48. Eissa N, Hussein H, Kermarrec L, Elgazzar O, Metz-Boutigue MH, Bernstein CN, et al. Chromofungin (CHR: CHGA47-66) is downregulated in persons with active ulcerative colitis and suppresses pro-inflammatory macrophage function through the inhibition of NF-kappaB signaling. *Biochem Pharmacol* (2017) 145:102–13. doi: 10.1016/j.bcp.2017.08.013

49. Eissa N, Hussein H, Kermarrec L, Grover J, Metz-Boutigue ME, Bernstein CN, et al. Chromofungin ameliorates the progression of colitis by regulating alternatively activated macrophages. *Front Immunol* (2017) 8:1131. doi: 10.3389/fimmu.2017.01131

50. Li G, Ren H, Wu X, Hu Q, Hong Z, Wang G, et al. Follistatin like protein-1 modulates macrophage polarization and aggravates dextran sodium sulfate-induced colitis. *Int Immunopharmacol* (2020) 83:106456. doi: 10.1016/j.intimp.2020.106456

51. Park HJ, Kim J, Saima FT, Rhee KJ, Hwang S, Kim MY, et al. Adipose-derived stem cells ameliorate colitis by suppression of inflammasome formation and regulation of M1-macrophage population through prostaglandin E2. *Biochem Biophys Res Commun* (2018) 498(4):988–95. doi: 10.1016/j.bbrc.2018.03.096

52. Cao L, Xu H, Wang G, Liu M, Tian D, Yuan Z. Extracellular vesicles derived from bone marrow mesenchymal stem cells attenuate dextran sodium sulfate-induced ulcerative colitis by promoting M2 macrophage polarization. *Int Immunopharmacol* (2019) 72:264–74. doi: 10.1016/j.intimp.2019.04.020

53. Feagan BG, Chande N, MacDonald JK. Are there any differences in the efficacy and safety of different formulations of oral 5-ASA used for induction and maintenance of remission in ulcerative colitis? evidence from cochrane reviews. *Inflamm Bowel Dis* (2013) 19(9):2031–40. doi: 10.1097/MIB.0b013e3182920108

54. Kornbluth A, Sachar DB. Practice parameters committee of the American college of g. ulcerative colitis practice guidelines in adults: American college of gastroenterology, practice parameters committee. *Am J Gastroenterol* (2010) 105(3):501–23. doi: 10.1038/ajg.2009.727

55. Chotiyarnwong P, McCloskey EV. Pathogenesis of glucocorticoid-induced osteoporosis and options for treatment. *Nat Rev Endocrinol* (2020) 16(8):437–47. doi: 10.1038/s41574-020-0341-0

56. Beigel F, Steinborn A, Schnitzler F, Tillack C, Breiteneicher S, John JM, et al. Risk of malignancies in patients with inflammatory bowel disease treated with thiopurines or anti-TNF alpha antibodies. *Pharmacoepidemiol Drug Saf* (2014) 23(7):735–44. doi: 10.1002/pds.3621

57. Fukata N, Okazaki K, Omiya M, Matsushita M, Watanabe MMembers of the Ministry of H, et al. Hematologic malignancies in the Japanese patients with inflammatory bowel disease. *J Gastroenterol* (2014) 49(9):1299–306. doi: 10.1007/s00535-013-0873-3

58. Kobayashi T, Siegmund B, Le Berre C, Wei SC, Ferrante M, Shen B, et al. Ulcerative colitis. *Nat Rev Dis Primers* (2020) 6(1):74. doi: 10.1038/s41572-020-0205-x

59. He X, Wang N, Zhang Y, Huang X, Wang Y. The therapeutic potential of natural products for treating pancreatic cancer. *Front Pharmacol* (2022) 13:1051952. doi: 10.3389/fphar.2022.1051952

60. Lv Q, Xing Y, Liu Y, Chen Q, Xu J, Hu L, et al. Didymin switches M1-like toward M2-like macrophage to ameliorate ulcerative colitis *via* fatty acid oxidation. *Pharmacol Res* (2021) 169:105613. doi: 10.1016/j.phrs.2021.105613

61. Slezakova S, Ruda-Kucerova J. Anticancer activity of artemisinin and its derivatives. *Anticancer Res* (2017) 37(11):5995–6003. doi: 10.21873/anticanres.12046

62. Wang Y, Ji X, Yan M, Chen X, Kang M, Teng L, et al. Protective effect and mechanism of polysaccharide from dictyophora indusiata on dextran sodium sulfate-induced colitis in C57BL/6 mice. *Int J Biol Macromol* (2019) 140:973–84.

63. Yao Q, Lin MT, Zhu YD, Xu HL, Zhao YZ. Recent trends in potential therapeutic applications of the dietary flavonoid didymin. *Molecules* (2018) 23(10):2547. doi: 10.3390/molecules23102547

64. Khan FB, Singh P, Jamous YF, Ali SA, Abdullah, Uddin S, et al. Multifaceted pharmacological potentials of curcumin, genistein, and tanshinone IIA through proteomic approaches: an in-depth review. *Cancers (Basel)* (2022) 15(1):249. doi: 10.3390/cancers15010249

65. Liu S, Shen H, Li J, Gong Y, Bao H, Zhang J, et al. Loganin inhibits macrophage M1 polarization and modulates sirt1/NF-kappaB signaling pathway to attenuate ulcerative colitis. *Bioengineered* (2020) 11(1):628–39. doi: 10.1080/21655979.2020.1774992

66. Lee C, Lee JW, Seo JY, Hwang SW, Im JP, Kim JS. Lupeol inhibits LPS-induced NF-kappa b signaling in intestinal epithelial cells and macrophages, and attenuates acute and chronic murine colitis. *Life Sci* (2016) 146:100–8. doi: 10.1016/j.lfs.2016.01.001

67. Li X, Xu S, Zhang Y, Li K, Gao XJ, Guo MY. Berberine depresses inflammation and adjusts smooth muscle to ameliorate ulcerative colitis of cats by regulating gut microbiota. *Microbiol Spectr* (2022) 10(6):e0320722. doi: 10.1128/spectrum.03207-22

68. Yan F, Wang L, Shi Y, Cao H, Liu L, Washington MK, et al. Berberine promotes recovery of colitis and inhibits inflammatory responses in colonic macrophages and epithelial cells in DSS-treated mice. *Am J Physiol Gastrointest Liver Physiol* (2012) 302(5):G504–14. doi: 10.1152/ajpgi.00312.2011

69. Jin J, Zhong Y, Long J, Wu T, Jiang Q, Wang H, et al. Ginsenoside Rg1 relieves experimental colitis by regulating balanced differentiation of Tfh/Treg cells. *Int Immunopharmacol* (2021) 100:108133. doi: 10.1016/j.intimp.2021.108133

70. Wang X, Xie L, Long J, Liu K, Lu J, Liang Y, et al. Therapeutic effect of baicalin on inflammatory bowel disease: a review. *J Ethnopharmacol* (2022) 283:114749. doi: 10.1016/j.jep.2021.114749

71. Song S, An J, Li Y, Liu S. Electroacupuncture at ST-36 ameliorates DSS-induced acute colitis *via* regulating macrophage polarization induced by suppressing NLRP3/IL-1beta and promoting Nrf2/HO-1. *Mol Immunol* (2019) 106:143–52. doi: 10.1016/j.molimm.2018.12.023

72. Ho WE, Peh HY, Chan TK, Wong WS. Artemisinins: pharmacological actions beyond anti-malarial. *Pharmacol Ther* (2014) 142(1):126–39. doi: 10.1016/j.pharmthera.2013.12.001

73. Velagapudi R, Aderogba M, Olajide OA. Tiliroside, a dietary glycosidic flavonoid, inhibits TRAF-6/NF-kappaB/p38-mediated neuroinflammation in activated BV2 microglia. *Biochim Biophys Acta* (2014) 1840(12):3311–9. doi: 10.1016/j.bbagen.2014.08.008

74. Deng C, Hu Z, Fu H, Hu M, Xu X, Chen J. Chemical analysis and antioxidant activity in vitro of a beta-d-glucan isolated from dictyophora indusiata. *Int J Biol Macromol* (2012) 51(1-2):70–5. doi: 10.1016/j.ijbiomac.2012.05.001

75. Wang Y, Lai L, Teng L, Li Y, Cheng J, Chen J, et al. Mechanism of the anti-inflammatory activity by a polysaccharide from dictyophora indusiata in lipopolysaccharide-stimulated macrophages. *Int J Biol Macromol* (2019) 126:1158–66. doi: 10.1016/j.ijbiomac.2019.01.022

76. Kanwal S, Joseph TP, Owusu L, Xiaomeng R, Meiqi L, Yi X. A polysaccharide isolated from dictyophora indusiata promotes recovery from antibiotic-driven intestinal dysbiosis and improves gut epithelial barrier function in a mouse model. *Nutrients* (2018) 10(8):1003. doi: 10.3390/nu10081003

77. Kanwal S, Joseph TP, Aliya S, Song S, Saleem MZ, Nisar MA, et al. Attenuation of DSS induced colitis by dictyophora indusiata polysaccharide (DIP) via modulation of gut microbiota and inflammatory related signaling pathways. *J Funct Foods* (2020) 64:103641. doi: 10.1016/j.jff.2019.103641

78. Shete VS, Telange DR, Mahajan NM, Pethe AM, Mahapatra DK. Development of phospholipon(R)90H complex nanocarrier with enhanced oral bioavailability and anti-inflammatory potential of genistein. *Drug Deliv* (2023) 30(1):2162158. doi: 10.1080/10717544.2022.2162158

79. Geng Y, Chen S, Yang Y, Miao H, Li X, Li G, et al. Long-term exposure to genistein inhibits the proliferation of gallbladder cancer by downregulating the MCM complex. *Sci Bull (Beijing)* (2022) 67(8):813–24. doi: 10.1016/j.scib.2022.01.011

80. Zhang N, Zhang W, Guo X, Liu J, Li S, Zhang H, et al. Genistein protects against hyperglycemia and fatty liver disease in diet-induced prediabetes mice *via* activating hepatic insulin signaling pathway. *Front Nutr* (2022) 9:1072044. doi: 10.3389/fnut.2022.1072044

81. Abron JD, Singh NP, Price RL, Nagarkatti M, Nagarkatti PS, Singh UP. Genistein induces macrophage polarization and systemic cytokine to ameliorate experimental colitis. *PloS One* (2018) 13(7):e0199631. doi: 10.1371/journal.pone.0199631

82. Kou Y, Li Z, Yang T, Shen X, Wang X, Li H, et al. Therapeutic potential of plant iridoids in depression: a review. *Pharm Biol* (2022) 60(1):2167–81. doi: 10.1080/13880209.2022.2136206

83. Jang JH, Yang G, Seok JK, Kang HC, Cho YY, Lee HS, et al. Loganin prevents hepatic steatosis by blocking NLRP3 inflammasome activation. *Biomol Ther (Seoul)* (2023) 31(1):40–7. doi: 10.4062/biomolther.2022.077

84. Cheng KI, Chang YC, Chu LW, Hsieh SL, An LM, Dai ZK, et al. The iridoid glycoside loganin modulates autophagic flux following chronic constriction injury-induced neuropathic pain. *Int J Mol Sci* (2022) 23(24). doi: 10.3390/ijms232415873

85. Yuan J, Cheng W, Zhang G, Ma Q, Li X, Zhang B, et al. Protective effects of iridoid glycosides on acute colitis *via* inhibition of the inflammatory response mediated by the STAT3/NF-small ka, CyrillicB pathway. *Int Immunopharmacol* (2020) 81:106240. doi: 10.1016/j.intimp.2020.106240

86. Kou Y, Sun Q, Zhu R, Lin Z, Li Z, Xu H, et al. Dioscin induces M1 macrophage polarization through connexin-43 channels in tumor-associated-macrophages-mediated melanoma metastasis. *Phytomedicine* (2023) 109:154559. doi: 10.1016/j.phymed.2022.154559

87. Wu MM, Wang QM, Huang BY, Mai CT, Wang CL, Wang TT, et al. Dioscin ameliorates murine ulcerative colitis by regulating macrophage polarization. *Pharmacol Res* (2021) 172:105796. doi: 10.1016/j.phrs.2021.105796

88. Shi L, Zhang P, Jin R, Chen X, Dong L, Chen W. Dioscin ameliorates inflammatory bowel disease by up-regulating miR-125a-5p to regulate macrophage polarization. *J Clin Lab Anal* (2022) 36(6):e24455. doi: 10.1002/jcla.24455

89. Sohag AAM, Hossain MT, Rahaman MA, Rahman P, Hasan MS, Das RC, et al. Molecular pharmacology and therapeutic advances of the pentacyclic triterpene lupeol. *Phytomedicine* (2022) 99:154012. doi: 10.1016/j.phymed.2022.154012

90. Zhu Y, Li X, Chen J, Chen T, Shi Z, Lei M, et al. The pentacyclic triterpene lupeol switches M1 macrophages to M2 and ameliorates experimental inflammatory bowel disease. *Int Immunopharmacol* (2016) 30:74–84. doi: 10.1016/j.intimp.2015.11.031

91. Li YH, Xiao HT, Hu DD, Fatima S, Lin CY, Mu HX, et al. Berberine ameliorates chronic relapsing dextran sulfate sodium-induced colitis in C57BL/6 mice by suppressing Th17 responses. *Pharmacol Res* (2016) 110:227–39. doi: 10.1016/j.phrs.2016.02.010

92. Yang T, Ma X, Wang R, Liu H, Wei S, Jing M, et al. Berberine inhibits IFN-gamma signaling pathway in DSS-induced ulcerative colitis. *Saudi Pharm J* (2022) 30(6):764–78. doi: 10.1016/j.jsps.2022.03.015

93. Dong Y, Fan H, Zhang Z, Jiang F, Li M, Zhou H, et al. Berberine ameliorates DSS-induced intestinal mucosal barrier dysfunction through microbiota-dependence and wnt/beta-catenin pathway. *Int J Biol Sci* (2022) 18(4):1381–97. doi: 10.7150/ijbs.65476

94. Liu Y, Liu X, Hua W, Wei Q, Fang X, Zhao Z, et al. Berberine inhibits macrophage M1 polarization *via* AKT1/SOCS1/NF-kappaB signaling pathway to protect against DSS-induced colitis. *Int Immunopharmacol* (2018) 57:121–31. doi: 10.1016/j.intimp.2018.01.049

95. Zhu G, Wang H, Wang T, Shi F. Ginsenoside Rg1 attenuates the inflammatory response in DSS-induced mice colitis. *Int Immunopharmacol* (2017) 50:1–5. doi: 10.1016/j.intimp.2017.06.002

96. Shen J, Cheng J, Zhu S, Zhao J, Ye Q, Xu Y, et al. Regulating effect of baicalin on IKK/IKB/NF-kB signaling pathway and apoptosis-related proteins in rats with ulcerative colitis. *Int Immunopharmacol* (2019) 73:193–200. doi: 10.1016/j.intimp.2019.04.052

97. Zhu W, Jin Z, Yu J, Liang J, Yang Q, Li F, et al. Baicalin ameliorates experimental inflammatory bowel disease through polarization of macrophages to an M2 phenotype. *Int Immunopharmacol* (2016) 35:119–26. doi: 10.1016/j.intimp.2016.03.030

98. Fan H, Chen W, Zhu J, Zhang J, Peng S. Toosendanin alleviates dextran sulfate sodium-induced colitis by inhibiting M1 macrophage polarization and regulating NLRP3 inflammasome and Nrf2/HO-1 signaling. *Int Immunopharmacol* (2019) 76:105909. doi: 10.1016/j.intimp.2019.105909

99. Hu D, Wang Y, Chen Z, Ma Z, You Q, Zhang X, et al. Artemisinin protects against dextran sulfate-sodium-induced inflammatory bowel disease, which is associated with activation of the pregnane X receptor. *Eur J Pharmacol* (2014) 738:273–84. doi: 10.1016/j.ejphar.2014.04.050

100. Huai M, Zeng J, Ge W. Artemisinin ameliorates intestinal inflammation by skewing macrophages to the M2 phenotype and inhibiting epithelial-mesenchymal transition. *Int Immunopharmacol* (2021) 91:107284. doi: 10.1016/j.intimp.2020.107284

101. Zhuang H, Lv Q, Zhong C, Cui Y, He L, Zhang C, et al. Tiliroside ameliorates ulcerative colitis by restoring the M1/M2 macrophage balance *via* the HIF-1alpha/glycolysis pathway. *Front Immunol* (2021) 12:649463. doi: 10.3389/fimmu.2021.649463

102. Wu Y, Huang D, Wang X, Pei C, Xiao W, Wang F, et al. Suppression of NLRP3 inflammasome by platycodin d *via* the TLR4/MyD88/NF-kappaB pathway contributes to attenuation of lipopolysaccharide induced acute lung injury in rats. *Int Immunopharmacol* (2021) 96:107621. doi: 10.1016/j.intimp.2021.107621

103. Guo R, Meng Q, Wang B, Li F. Anti-inflammatory effects of platycodin d on dextran sulfate sodium (DSS) induced colitis and e. coli lipopolysaccharide (LPS) induced inflammation. *Int Immunopharmacol* (2021) 94:107474. doi: 10.1016/j.intimp.2021.107474

104. Williams EJ, Guilleminault L, Berthon BS, Eslick S, Wright T, Karihaloo C, et al. Sulforaphane reduces pro-inflammatory response to palmitic acid in monocytes and adipose tissue macrophages. *J Nutr Biochem* (2022) 104:108978. doi: 10.1016/j.jnutbio.2022.108978

105. Zhang Y, Tan L, Li C, Wu H, Ran D, Zhang Z. Sulforaphane alter the microbiota and mitigate colitis severity on mice ulcerative colitis induced by DSS. *AMB Express* (2020) 10(1):119. doi: 10.1186/s13568-020-0948-5

106. Sun Y, Tang J, Li C, Liu J, Liu H. Sulforaphane attenuates dextran sodium sulphate induced intestinal inflammation *via* IL-10/STAT3 signaling mediated macrophage phenotype switching. *Food Sci Hum Wellness* (2022) 11(1):129–42. doi: 10.1016/j.fshw.2021.07.014

107. Zhuang S, Zhong J, Zhou Q, Zhong Y, Liu P, Liu Z. Rhein protects against barrier disruption and inhibits inflammation in intestinal epithelial cells. *Int Immunopharmacol* (2019) 71:321–7. doi: 10.1016/j.intimp.2019.03.030

108. Zhou Y, Gao C, Vong CT, Tao H, Li H, Wang S, et al. Rhein regulates redox-mediated activation of NLRP3 inflammasomes in intestinal inflammation through macrophage-activated crosstalk. *Br J Pharmacol* (2022) 179(9):1978–97. doi: 10.1111/bph.15773

109. Hassanzadeh-Taheri M, Ahmadi-Zohan A, Mohammadifard M, Hosseini M. Rosmarinic acid attenuates lipopolysaccharide-induced neuroinflammation and cognitive impairment in rats. *J Chem Neuroanat* (2021) 117:102008. doi: 10.1016/j.jchemneu.2021.102008

110. Jin BR, Chung KS, Hwang S, Hwang SN, Rhee KJ, Lee M, et al. Rosmarinic acid represses colitis-associated colon cancer: a pivotal involvement of the TLR4-mediated NF-kappaB-STAT3 axis. *Neoplasia* (2021) 23(6):561–73. doi: 10.1016/j.neo.2021.05.002

111. Mai P, Chen C, Xiao X, Ma X, Shi Y, Miao G, et al. Rosmarinic acid protects against ulcerative colitis by regulating macrophage polarization depending on heme oxygenase-1 in mice. *Eur J Inflamm* (2020) 18. doi: 10.1177/2058739220959916

112. Wang Y, Smith W, Hao D, He B, Kong L. M1 and M2 macrophage polarization and potentially therapeutic naturally occurring compounds. *Int Immunopharmacol* (2019) 70:459–66. doi: 10.1016/j.intimp.2019.02.050

frontiers | Frontiers in Immunology

TYPE Original Research
PUBLISHED 21 June 2023
DOI 10.3389/fimmu.2023.1181823

OPEN ACCESS

EDITED BY
Ruoxi Yuan,
Hospital for Special Surgery, United States

REVIEWED BY
Yang Zhao,
Chinese Academy of Sciences (CAS), China
Erika M. Palmieri,
National Institutes of Health (NIH),
United States

*CORRESPONDENCE
Mathias Chamaillard
mathias.chamaillard@inserm.fr
Lionel F. Poulin
lionel.poulin@cnrs.fr

†These authors have contributed equally to this work

‡These authors share senior authorship

RECEIVED 07 March 2023
ACCEPTED 23 May 2023
PUBLISHED 21 June 2023

CITATION
Chauvin C, Alvarez-Simon D, Radulovic K, Boulard O, Laine W, Delacre M, Waldschmitt N, Segura E, Kluza J, Chamaillard M and Poulin LF (2023) NOD2 in monocytes negatively regulates macrophage development through TNFalpha.
Front. Immunol. 14:1181823.
doi: 10.3389/fimmu.2023.1181823

NOD2 in monocytes negatively regulates macrophage development through TNFalpha

Camille Chauvin[1,2†], Daniel Alvarez-Simon[1†], Katarina Radulovic[3], Olivier Boulard[4], William Laine[5], Myriam Delacre[1], Nadine Waldschmitt[6], Elodie Segura[7], Jérome Kluza[5], Mathias Chamaillard[4*‡] and Lionel F. Poulin[4*‡]

[1]U1019, Institut Pasteur de Lille, Univ. Lille, Centre National de la Recherche Scientifique, Inserm, Centre Hospitalo- Universitaire Lille, Lille, France, [2]INSERM U1138, Centre de Recherche des Cordeliers, Paris, France, [3]Unité de Recherche Clinique, Centre Hospitalier de Valenciennes, Valenciennes CEDEX, France, [4]U1003, Univ. Lille Inserm, Lille, France, [5]UMR9020-U1277 - CANTHER - Cancer Heterogeneity Plasticity and Resistance to Therapies, University Lille, Lille, France, [6]Chair of Nutrition and Immunology, School of Life Sciences, Technische Universität München, Freising-Weihenstephan, Germany, [7]INSERM U932, Institut Curie, Paris Sciences et Lettres Research University, Paris, France

Objective: It is believed that intestinal recruitment of monocytes from Crohn's Disease (CD) patients who carry NOD2 risk alleles may repeatedly give rise to recruitment of pathogenic macrophages. We investigated an alternative possibility that NOD2 may rather inhibit their differentiation from intravasating monocytes.

Design: The monocyte fate decision was examined by using germ-free mice, mixed bone marrow chimeras and a culture system yielding macrophages and monocyte-derived dendritic cells (mo-DCs).

Results: We observed a decrease in the frequency of mo-DCs in the colon of *Nod2*-deficient mice, despite a similar abundance of monocytes. This decrease was independent of the changes in the gut microbiota and dysbiosis caused by Nod2 deficiency. Similarly, the pool of mo-DCs was poorly reconstituted in a *Nod2*-deficient mixed bone marrow (BM) chimera. The use of pharmacological inhibitors revealed that activation of NOD2 during monocyte-derived cell development, dominantly inhibits mTOR-mediated macrophage differentiation in a TNFα-dependent manner. These observations were supported by the identification of a TNFα-dependent response to muramyl dipeptide (MDP) that is specifically lost when CD14-expressing blood cells bear a frameshift mutation in NOD2.

Conclusion: NOD2 negatively regulates a macrophage developmental program through a feed-forward loop that could be exploited for overcoming resistance to anti-TNF therapy in CD.

KEYWORDS

NOD2, monocytes, macrophages, mo-DCs, TNF-α, colitis, microbiota, mTOR

Introduction

Monocytes and macrophages play an essential role in the immune system due to their ability to convert from a homeostatic to a pro-inflammatory phenotype in response to immune invasion. Circulating monocytes continuously replenish the intestinal populations of macrophages during homeostasis. The intestine is particularly enriched in phagocytes that ensure robustness in the steady state and play a role in processes of remodeling upon tissue injury. Among those, some macrophages have been seeded embryonically and self-renewed from yolk sac-derived precursor cells in mice. Under healthy conditions, intestinal macrophages have an estimated half-life of three weeks. In human and mouse, subsets of macrophages have been characterized based on a differential expression of CD11c (1, 2). In mice, the pool of Ly6C^{low} CX3CR1^{int} macrophages that share some features of monocyte-derived dendritic cells (mo-DCs) is then continually replenished by the emigration of short-lived Ly6C^{high} monocytes from the bloodstream (3). Activation of the C-C chemokine receptor type 2 (CCR2) is a prerequisite for such leukocytes to exit from the bone marrow at steady state (4). Along a continuum of differentiation stages, Ly6C^{high} monocytes may then give rise to nascent phagocytes with ascribed different functions and distinct bioenergetic programs (5). Whereas mature macrophages are largely immotile with phagocytic capacity (6), mo-DCs are believed to migrate for presenting protein antigens on major histocompatibility complexes class I and II (MHCI and MHCII) molecules to T cells (7–9). The community of circulating Ly6C^{high} monocytes that are rapidly mobilized upon injury is then thought to seemingly serve as a reservoir of mo-DCs that can be distinguished from CD11c-expressing macrophages on the basis of ontogenetic, morphological, and gene expression criteria (10).

In humans, the equivalent of inflammatory monocytes is classical monocytes CD14^{+}CD16^{-} which represent up to 80-95% of the large reservoir of monocytes. They can be distinguished from intermediate and non-classical subsets by their expression of well-characterized surface proteins, including CD16 (also referred as Fc gamma receptor IIIa) and the glycoprotein CD14 that acts as a co-receptor for toll-like receptor 4. While the intermediate monocytes CD14^{+}CD16^{+} regulate angiogenesis and modulate effector T cell activity (11), the nonclassical monocytes CD14^{-}CD16^{+} are mobile and involved in the maintenance of vascular homeostasis (12). Recent studies demonstrated that the molecular ontogeny of human monocyte-derived cells is orchestrated by distinct transcription factors that are specifically activated by environmental cues. Comparative transcriptomic analysis revealed that the monocyte fate specification into mo-DC and monocyte-derived macrophages (mo-Mac) is at least partially coordinated by Interferon Regulatory Factor 4 (IRF4) and MAF BZIP Transcription Factor B (MAFB) (8) respectively.

As monocyte-derived cells display high plasticity to their environment, they can express high susceptibility to the chronic inflammatory stimulations arising in the intestine during inflammatory bowel diseases (IBD). The inflammatory microenvironment, including increasing levels of CCL2 and IL-8, promotes the recruitment of monocytes in the intestine of IBD patients (13, 14). While an increase of immature macrophages has been correlated with the endoscopic severity score of the disease (15), a defect of mo-DCs function, including a decrease in TH17 activation and IL-12 production in response to NOD2 stimulation has been observed in Crohn's disease (CD) patients (16, 17). In IBD, macrophages have been associated with inflammation and fibrosis while (cDCs) express a more pro-inflammatory phenotype (18). Of particular importance, it has now been elegantly demonstrated that the monocyte fate toward mo-DCs is orchestrated by the aryl hydrocarbon receptor (8), which defect is associated with a susceptibility to several common diseases, including CD (19). Likewise, monocytes may give rise to mo-DCs upon inhibition of the mammalian target of rapamycin (mTOR) pathway (20) for which the sustained activation in CD is likely a consequence of a genetically predisposed defect in autophagy (21). Interestingly, an increased number of inflammatory macrophages is observed within the intestinal mucosa of CD patients at the expense of their pro-resolving counterpart (22). Those data were supported by a recent single-cell analysis of inflamed tissues from CD, which revealed the presence of a discrete subset of pathogenic macrophages within the diseased intestine of CD patients that fail to respond to anti-TNF therapy (23). It is thereby tempting to speculate that a defect in the development of monocyte-derived phagocytes may allow the expansion of pathogenic macrophages that maintain a TH1-biased CD4 T cell response through the production of inflammatory and fibrogenic effectors.

Genetic variants in the *NOD2* gene confer an increased susceptibility to CD, likely due to the loss of NOD2 function. Furthermore, patients who carry NOD2 risk alleles are at greater risk of developing stricturing disease, that corresponds to a narrowing of the intestine due to continued inflammation (23). The Nucleotide-binding Oligomerization Domain (NOD)-like receptor NOD2 is a cytosolic sensor of bacterial muramyl dipeptide (MDP). MDP is an active component in Freund's complete adjuvant and derivatives have been synthesized for improving their pharmacological properties. The recognition of MDP by NOD2 has been associated with autophagy induction, bacterial destruction, and antigen presentation in DC. Indeed, while NOD2-mediated autophagosome formation was necessary for MHC II upregulation, mo-DCs from CD–variant NOD2 patients were unable to kill and localize intact *Escherichia coli* into the lysosomal compartment; however, this defect was reversible with rapamycin (24). Furthermore, probiotics induce an anti-inflammatory phenotype on bone marrow-derived DC with an increase of IL-10 production in a Nod2- and a strain-specific

Abbreviations: AMPK, AMP-activated protein kinase; BM, bone marrow; CD, Crohn's disease; cDC, conventional dendritic cells; DSS, Dextran sodium sulfate; ECAR, Extracellular acidification rate; GF, germ-free; GM-CSF, Granulocyte-macrophage colony-stimulating factor; GSEA, Geneset enrichment analysis; IL, interleukin; IRF, Interferon Regulatory Factor; LPMC, Lamina Propria Mononuclear Cells; LPS, Lipopolysaccharide; MDP, muramyl dipeptide; MHCI and MHCII, major histocompatibility complexes class I and II; mo-DCs, monocyte-derived dendritic cells; mo-Mac, monocyte-derived macrophages; mTOR, mammalian target of rapamycin; NOD2, Nucleotide binding Oligomerization Domain; RAPTOR, Regulatory-associated protein of mTOR; SPF, specific pathogen-free; TNF-α, Tumor necrosis factor-alpha; WT, wild-type.

manner in a mouse model of TNBS-mediated colon inflammation (25). While peptidoglycan derived from the *L. salivarius* Ls33 strain only partially activated DC *in vitro*, it induced protection associated with an increase of IL-10 production and of regulatory $CD11c^+CD103^+$ DCs and $CD4^+FoxP3^+$ Treg cells in the mesenteric lymph nodes of colitic mice.

Despite substantial efforts that were made in studying how the homeostatic trafficking of monocytes is controlled by NOD2, it remains unclear whether NOD2 may orchestrate their differentiation into a developmentally distinct subset of cells that are specialized for the maintenance of immune surveillance. After stimulating their exit from the bone marrow, classical monocytes have the capacity of being converted into non-classical cells in a NOD2-dependent manner (26). It has been proposed that MDP might increase the exit of monocytes from bone marrow and the yield of $Ly6C^{lo}$ in the blood of WT but not *Nod2*$^{-/-}$ mice (26). In addition, NOD2 has been involved in the CCL2 production by colonic stromal cells in *Citrobacter rodentium* infection (27). Besides this phenomenon, it is now well established that sensing of bacterial endotoxin promotes the mobilization of inflammatory monocytes, which can develop into cells with a typical probing morphology and with critical features of mo-DCs including cross-priming capacities of cell-associated antigens to $CD8^+$ T cells (7). It suggests the likelihood that loss of NOD2 may directly inhibit the development of potentially reprogrammable cells of monocytic origin into inflammatory macrophages. NOD2 has been involved in the induction of immune tolerance *via* the generation of immature $CD103^+$ classical dendritic cells (cDC1) associated with tolerogenic DC, in a GM-CSF-dependent manner in mice (28). In addition, the cross-tolerization to multiple TLRs has been observed after chronic stimulation of NOD2 with MDP (29), and as a result, increased activation of TLR signaling has been proposed in the process of NOD2 deficiency-induced intestinal epithelium inflammation. In parallel, this concept reminds the one of "trained immunity" upon parasite infection where chromatin remodeling leads to the induction of instructed immune responses by monocytes or macrophages (30). The context-dependence of differentiation has already been observed in monocytic cells. In another setting, programmable cells of monocytic origin (PCMOs) with plastic properties have been described to give rise to two subsets of DC in the presence of IL-3 or TNF-α (31). While mo-DCs are markedly less abundant within the healthy intestine than macrophages, it does not exclude the possibility that mo-DCs may play an essential role in intestinal homeostasis. Indeed, DCs have been shown to play a crucial role in gut homeostasis by interacting with the gut microbiome and by regulating the balance between TH1/TH17 and Tregs (32). Mononuclear phagocytes (MNPs), including monocytes, macrophages, and dendritic cells (DCs), are present in large numbers in the colonic lamina propria and fulfill a variety of overlapping functions that are critical to the maintenance of gut homeostasis. Disruption of the intestinal MNP system leads to infection and inflammation (33–39). In general, mo-DCs can enhance the ability of classical DCs to elicit adaptive responses by presenting antigens to T cells directly in tissues to increase their effector functions (40–42). Distinct tolerogenic DCs have been identified in different anatomic parts of the intestine suggesting region-specific mechanisms of homeostasis (32). It is yet unclear whether mo-DCs and conventional DCs are complementary or redundant in the maintenance of gut homeostasis (43). The recognition of Pattern Recognition Receptors (PRR) and C-type lectin receptors by DCs has been shown to influence their metabolic reprogramming toward glycolysis, and eventually to shape their contribution to immune responses or tolerance (43). MDP has been reported to induce rapid metabolic reprogramming in human macrophages (44). Murabutide, a NOD2 ligand, and TNF-α have been reported to promote the differentiation of mo-DCs while the TLR2 agonist Pam3Csk4 assisted mo-Macs development in a culture of human monocytes with M-CSF, IL-4, and TNF-α, and in mouse skin *in vivo* (9). The involvement of the mTOR pathway has been described in the differentiation of mo-DCs. However, while the differentiation and the survival of human mo-DCs are conditioned by mTORC1 and are specifically inhibited by the mTOR inhibitor, rapamycin (45), another study reported that the mTORC1 inhibitor, temsirolimus, increased the differentiation of mo-DCs (20). Given these findings, one may then consider that NOD2 might influence the differentiation of bone marrow precursors into tissue phagocytes in a context-dependent manner.

In this study, we provide experimental evidence that NOD2-dependent bacterial sensing by monocytes inhibits their differentiation in macrophages. Indeed, monocytes' fate can be influenced by the context. Such developmental switch occurs even in a context where their development from circulating monocytes is promoted into macrophages, upon activation of the metabolic signaling node mTORC1, which controls terminal differentiation of myeloid progenitors (46). We observed that this transition in the early steps of phenotypic developmental stages relied on the glycolytic-mediated control of monocytes/macrophages by the bacterial sensor NOD2 (47). We demonstrated that recognition of the gut microbiota by NOD2 is required for *de novo* reconstitution of mo-DCs that occupy the lamina propria of the murine intestine while having minimal effect on the mobilization of their precursors to the intestinal mucosa. Given that MDP is physiologically present in high concentrations within the intestinal lumen, our study set the stage to modulate NOD2-dependent signaling at the monocytic stage to avoid the activation of default developmental pathways, including mTORC1. These alternative developmental switches are probably leading to anti-TNF failure through an accumulation of inflammatory macrophages in the intestine of CD patients.

Results

Lack of NOD2 results in a competitive disadvantage for the mo-DCs pool within the colon and the peritoneal cavity in mice at steady-state that re-equilibrates during inflammation

Since Nod2 has been shown to regulate monocyte-derived cell differentiation in different contexts, we aimed to investigate whether in the colon this phenomenon is additionally a consequence of an

10.3389/fimmu.2023.1181823

impaired mobilization of monocytes from the BM as it was observed in C3H/HeJ Tlr4 mutant mice (7). Alternatively, maturation of Ly6C^{high} monocytes can follow different paths such as mo-DCs or CD11c^{+} macrophages which are considered as an intermediate between monocytes and macrophages (1). If NOD2 is intrinsically required for the development of Ly6C^{high} monocytes into mo-DCs in mice, inappropriate conversion of Ly6C^{high} monocytes into mo-DCs would be expected to promote the accumulation of macrophages. To this end, we realized mixed BM chimera mice. *Nod2*-deficient animals were lethally irradiated, and 24h later reconstituted with equal amounts (eg. 50:50) of BM cells from wild-type (WT) (CD45.1) and *Nod2*-deficient mice (CD45.2) (Figure 1A). CCL2 production and subsequent CD11b^{+}Gr1^{+}F4/80^{+} phagocytic cells' recruitment to the colon have been shown to be reduced during *C. rodentium* infection in *Nod2*$^{-/-}$ mice (27), however, we did not expect a defect in monocyte recruitment in *Nod2*$^{-/-}$ mice at steady state. Peritoneal content of mo-DCs and mo-Macs within the peritoneum (8) and colonic tissue were analyzed 8 weeks after BM reconstitution as

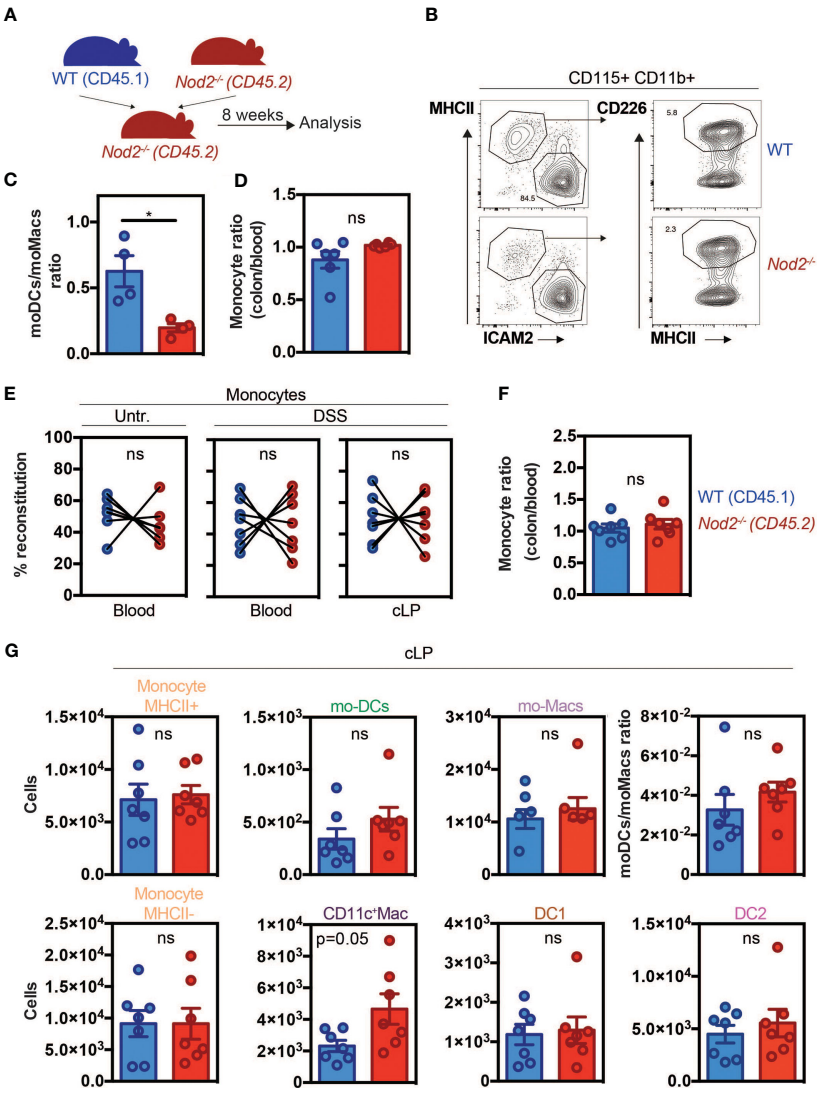

FIGURE 1
Nod2 signaling is required in BM cells to reconstitute the mo-DCs pool in the peritoneal cavity despite similar monocyte recruitment. **(A)** Experimental protocol. Mixed BM chimeras were generated by transferring WT (expressing CD45.1)(blue) and Nod2$^{-/-}$ (expressing CD45.2) (red) cells in a 1:1 ratio into lethally irradiated Nod2-deficient recipients. Cells were isolated from the blood and the peritoneum 8 weeks after reconstitution. **(B)** Peritoneal cells were harvested and the proportion of mo-Mac (MHCII^{-}ICAM2^{+}) and mo-DCs (MHCII^{+}CD226^{+}) was determined by flow cytometry by gating within the CD115^{+}CD11b^{+} cells. The frequency of the CD226^{+} DC is calculated within the CD115^{+} CD11b^{+} cells. **(C)** The ratio of mo-DCs/mo-Macs from frequencies obtained in B (n=4 mice). **(D)** Reconstitution index of Ly6C^{+} monocytes in the colon (CD11c^{-}CD11b^{+}Ly6C^{+}CCR2^{+} gate) divided by the same ratio in the blood (n=6 mice). **(E)** 8 weeks after reconstitution, mixed chimera mice were treated with a 5-day course of 2% DSS (n=7 mice) **(E-G)**. **(E)** Monocytes content (in the blood: CD11b^{+} Ly6hi^{+}, in the colon: CD11c^{-}CD11b^{+}Ly6C^{+}CCR2^{+}MHCII^{-}) in the blood (CD11b^{+} Ly6hi^{+}) of untreated and blood and colonic lamina propria cells (cLP) in DSS-treated mice. **(F)** Ratio of WT and Nod2-/- monocyte frequencies (colon/blood). **(G)** Colonic cells were analyzed as described in Supplementary Figure 2A. Numbers per million of monocytes MHCII^{+} (CD11c^{-}CD11b^{+}Ly6C^{+}CCR2^{+}MHCII^{+}), mo-DCs (CD11c^{+}CD11b^{+}Ly6C^{+}CCR2^{+}MHCII^{+}), mo-Macs (CD11c^{-}CD11b^{+}Ly6C^{-}CCR2^{-}MHCII^{+}), monocytes MHCII^{-} (CD11c-CD11b^{+}Ly6C^{+}CCR2^{+}MHCII^{-}), CD11c^{+}Macs (CD11c^{+}CD11b^{+}Ly6C^{+}CCR2^{-}MHCII^{+}), DC1 (CD11c^{+}CD11b^{-}) and DC2 (CD11c^{+}CD11b^{+}Ly6C^{-}CCR2^{-}MHCII^{+}) in the cLP (number of cells per million of live cells). The ratio of mo-DCs/mo-Mac from total cell number. Bars indicate mean ± SEM. Statistical significance was assessed by the non-parametric Mann-Whitney U test. ns, non significant.

previously described (48) (Figure 1). Peritoneal cells express both CD115 and CD11b, they can be further subdivided into large MHC II$^-$ CD102$^+$ (ICAM2$^+$) F4/80$^+$ macrophages and MHC II$^+$ CD226$^+$ F4/80^{lo} subsets that differ in function and origin. The MHC II$^+$ CD226$^+$ F4/80^{lo} subset is Irf4-dependent and is continuously renewed by blood monocytes (49). These cells selectively express CD226, which is a marker of human mo-DCs, both *in vitro* and in ascites, and display a typical DC morphology profile (8). In our model, while the total numbers of mo-DCs and mo-Macs were increased in the *Nod2*-deficient competitive BM chimeras, no differences in frequencies were observed as compared to WT cells. However, within the peritoneum of these *Nod2*-deficient competitive BM chimeras, we observed a lowered relative proportion of mo-DCs when compared to mo-Macs in the CD45.2 cells as compared to the CD45.1 cells (Figures 1B, C; Supplementary Figures 1A, B). At steady-state, resident macrophage subsets have been shown to arise from Ly6C^{hi} monocytes in the intestine (10). In the colon, macrophages can be segregated into CD11c$^+$CD11b$^+$MHCII$^+$Ly6C$^+$ macrophages related to the CX3CR1^{int} inflammatory macrophages, and CD11c$^-$CD11b$^+$Ly6C^{lo}MHCII$^+$ monocyte-derived macrophages corresponding to the CX3CR1^{hi} tissue-resident macrophages (10, 50). Likewise what was observed in the peritoneal cavity, similar results were obtained in their colon in which the number of macrophages was significantly heightened (Supplementary Figures 1A, B) (Supplementary Figures 2A, B (gating strategy)). As *Nod2*-deficient mice are known to develop dysbiosis, we next assessed whether the capacity of blood monocytes to be recruited, to survive, and to expand into the colon may depend on the recognition of the gut microbiota by NOD2. Gut dysbiosis is responsible for decreased numbers of Ly6C^{high} monocytes in the spleen of mice at steady-state, however, MDP stimulation could restore splenic Ly6C^{high} cell frequency (51). In our settings, monocytes from either WT or *Nod2*$^{-/-}$ BM were similarly recruited in the colon of *Nod2*-deficient mice at steady-state (Figure 1D). We next assessed how inflammation may differentially alter the proportion of BM-derived phagocytes in the colon of *Nod2*-deficient chimeras. Colonic recruitment of CD11b$^+$Ly6C$^+$CD11c$^-$ MHCII$^-$ monocytes has been shown to be a feature of murine colitis (52). While the segregation between CD11b$^+$ DCs and macrophages could be arduous due to the appearance of a CD64-expressing population of mo-DCs, a subset of CD11c$^+$ monocytes/macrophages has been shown to be involved in intestinal inflammation (39). Dextran sodium sulfate (DSS) was then administered in the drinking water of mixed-BM chimera mice to induce acute colitis (Figures 1E–G; Supplementary Figure 2A, B (gating strategy)). Such an established preclinical model of colitis is characterized by epithelial erosion, crypt loss, ulceration, and infiltration of immune cells. Similar reconstitution of WT and *Nod2*$^{-/-}$ Ly6C^{high} monocytes was observed in the blood and in the colon under DSS, as compared to untreated BM chimeras (Figure 1E). In agreement, the ratios of colonic and blood monocytes were equivalent between WT and *Nod2*$^{-/-}$(Figure 1F). Likewise, the number of colonic Ly6C^{high} MHCII$^+$ activated monocytes was not affected by Nod2 deficiency in response to inflammation (Supplementary Figure 2C). Furthermore, no difference in body weight loss was noticed at the time of the autopsy (data not shown). Upon inflammation, while the numbers of Ly6C^{high} monocytes, cDC, and the mo-DCs/mo-Macs ratio were equivalent in the colon of mixed BM chimera mice, CD11c-expressing macrophages were present in a greater number in *Nod2*$^{-/-}$ as compared to WT donor cells (p=0.05) (Figure 1G). These results show that NOD2 does not regulate the proportion of colonic mo-Macs at steady state *in vivo*, whereas it did alter mo-Mac and mo-DC ratios upon inflammation.

Recognition of the gut microbiota by NOD2 regulates the reconstitution of intestinal mo-DCs from mobilized monocytes

As the recognition of gut microbiota by NOD2 has been shown to be essential for the homeostasis of immune cells, we investigated more precisely whether it may impact the mononuclear phagocyte composition of the colonic lamina propria. The phagocytes composition was analyzed by flow cytometry in the colon of WT and *Nod2*$^{-/-}$ specific pathogen-free (SPF) and germ-free (GF) mice at steady-state using the markers CD11c, CD11b, CCR2, Ly6C, and MHCII (Figure 2A; Supplementary Figure 3). In the WT mice, the frequency of activated MHCII$^+$ monocytes (Figure 2B) and of the proportion of mature tissue macrophages (Figure 2C) were reduced within the lamina propria of the colon of GF as compared to SPF WT mice, as observed in a series of studies (3, 53). By contrast, the expression level of MHCII on the classical subset of monocytes was similar within the colon of SPF *Nod2*-deficient mice as what was observed in the GF condition (Figure 2B, lower part). However, while the mo-DCs-like cells (CD11b$^+$CD11c$^+$Ly6C$^+$CCR2$^+$MHCII$^+$) (54) proportions were decreased in GF WT mice as compared to SPF mice (Figure 2C), this difference was lost in *Nod2*$^{-/-}$ mice, highlighting the role of microbiota recognition and NOD2 in the accumulation of mo-DCs in the colon. As NOD2 has been shown to shape the recruitment of CD103$^+$ DCs in the gut lamina propria (28), we reasoned that the loss of NOD2 signaling may have impaired either the trafficking or the development of some discrete subsets of cDC. To our surprise, only minor fluctuations were detected in the proportions of cDC1 and cDC2 that co-express or not CD11b respectively (Figure 2D). These results could be explained by the fact that cDC arise from a specific precursor. In addition, these cells were used as a control and we did not expect them to be affected in this context. Given that the gut microbiota does not regulate the abundance of cDC1, the decreased abundance of mo-DCs was not likely due to competition with cDC1 to occupy the colonic niche under homeostatic conditions. In addition, the moderate increase in cDC2 frequency observed in GF *Nod2*$^{-/-}$ mice was not observed in bone marrow chimera mice (Figure 1). This said, the number of CD11c-expressing macrophages was too low to conclusively apprehend potential differences in our experimental setting. Altogether, our data indicate that the Nod2-dependent recognition of the gut microbiota by monocytes when entering the colon from the blood is an important means by which NOD2 could facilitate the on-demand accumulation of intestinal mo-DCs from mobilized monocytes and subsequently may prevent the replenishment of macrophages. To exclude the potential influence of opportunistic pathobionts that may

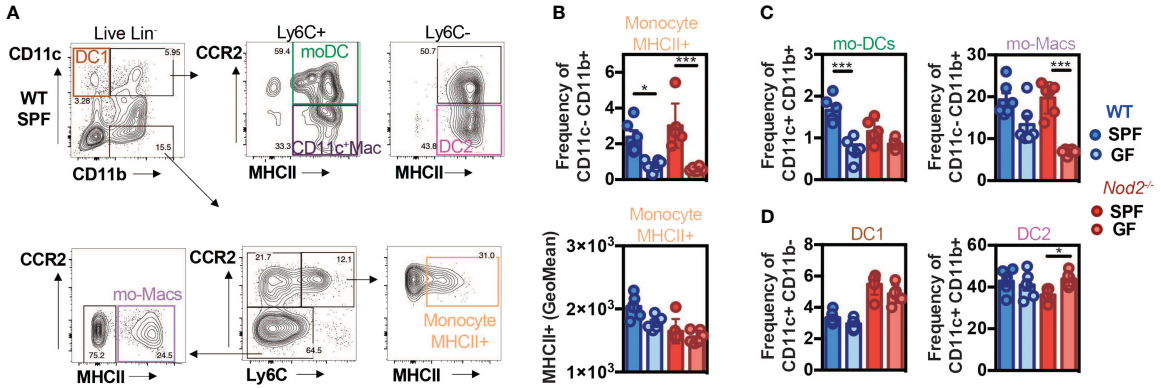

FIGURE 2
Default of conventional DCs and monocytes-derived cells recruitment in NOD2$^{-/-}$ mice under microbiota deprivation. Colon Lamina Propria Mononuclear Cells (LPMC) frequency analysis in Wild-type (WT) (blue) and NOD2$^{-/-}$ (red) mice raised under Specific-Pathogen Free (SPF)(sharp color) and Germ-Free (GF)(light color) conditions. **(A)** Gating strategy to determine the frequency of conventional DC1 (CD11c$^+$CD11b$^-$), of mo-DCs (CD11c$^+$CD11b$^+$Ly6C$^+$CCR2$^+$MHCII$^+$), of CD11c$^+$ Macs (CD11c$^+$CD11b$^+$Ly6C$^+$CCR2$^-$MHCII$^+$), of conventional DC2 (CD11c$^+$CD11b$^+$Ly6C$^-$CCR2$^-$MHCII$^+$), and the frequencies of mo-Macs (CD11c$^-$CD11b$^+$Ly6C$^-$CCR2$^-$MHCII$^+$), and Mo$^-$MHCII$^+$ (CD11c$^-$CD11b$^+$Ly6C$^+$CCR2$^+$MHCII$^+$), based on their CCR2, Ly6C and MHC levels, after exclusion of Lineage and doublet cells. **(B)** The frequency and MHCII GeoMean of CCR2$^+$Ly6C$^+$MHCII$^+$ activated monocytes were evaluated in the monocyte-derived cells CD11c$^-$CD11b$^+$. **(C)** The frequency of mo-DCs was evaluated in the Ly6C$^+$ cells. The frequency of CCR2$^-$Ly6C$^-$ mo-Macs was evaluated in the CD11c$^-$CD11b$^+$ monocyte-derived cells. **(D)** Frequency of DC1 cells (CD11c$^+$CD11b$^-$ gate) and DC2 cells (Ly6C$^-$ gate). Bars indicate mean ± SEM (n=4-6/group). Statistical significance was assessed by two-way ANOVA. *P<0.05; ***P<0.001.

have been present in *Nod2*-deficient mice, the faecal microbiota from WT SPF mice was transplanted in GF recipients that are either deficient for NOD2 or not (Supplementary Figure 4A). The composition of mononuclear phagocytes was analyzed in the colon four weeks after transplantation such that their gut microbiota becomes similar to the one of the control mice (Supplementary Figure 4B). The frequency and absolute numbers of CD11c$^+$MHCII$^+$ and CD11c$^-$MHCII$^+$ mononuclear phagocytes were not significantly different in the GF *Nod2*$^{-/-}$ recipients as compared to GF WT recipients when exposed to WT microbiota (Supplementary Figure 4B). These results suggest that changes in the gut microbiota composition, that are pre-existing in the *Nod2*-deficient mice, could not be sufficient to influence the frequency of mononuclear phagocytes within the colonic lamina propria in mice. Altogether, our results indicate that recognition of the gut microbiota by Nod2 regulates the reconstitution of intestinal mo-DCs from mobilized monocytes.

NOD2 signaling enhances the yield of mo-DCs from monocytes by inhibiting their differentiation in macrophages

In order to establish whether activation of NOD2 signaling may regulate mo-DCs development and therefore inhibit the differentiation of recruited monocytes toward macrophages, MDP was added at the start of the culture of mouse BM cells with a conditioning medium containing GM-CSF. When monocytes were cultured with murabutide, a NOD2 agonist, they exhibited enhanced TNF-α secretion as early as 6hours post-induction, which diminished at 24hours (9), suggesting that the effect of NOD2 stimulation is observable over a narrow window of time. The culture of mouse BM cells with the growth factor GM-CSF is a widely used protocol to generate either mo-Macs or mo-DCs within the CD11c$^+$MHCII$^+$ fraction (Figure 3A) (55). The percentage of CD115$^+$CD64$^+$ mo-Macs was significantly diminished while the frequency of mo-DCs significantly increased when BM cells were cultured in the presence of MDP as compared with the medium alone (Figures 3B, C). We then verified if similar results could be observed in *in vitro* culture of human monocytes. To this end, CD14$^+$ monocytes were differentiated for 5 days in the presence of GM-CSF and interleukin-4 (IL-4), a well-established cocktail of conditioning soluble factors (56, 57), giving rise to both mo-DCs and mo-Macs (58). Light microscopy revealed that monocytes acquired an elongated shape as early as 24 hours after being exposed to MDP (Figure 3D). After 5 days of stimulation, we noticed the formation of a homotypic cluster of adherent cells with a probing morphology (Figure 3D). To support this, both adherent and non-adherent cells were harvested and stained at their surface for CD14, CD16, CD1a, and HLA-DR. Live and singlet cells were gated on HLA-DR-expressing cells and were systematically analyzed on day 6 (Figures 3E–G). Similarly to what is observed in *in vitro* cultures with M-CSF, TNF-α and IL-4 (9), early presence of MDP into such a culture system reduced the frequency of mo-Macs and their CD16 expression by five-fold (Figures 3F, G, lower part), while enhancing the yield of mo-DCs and their expression of CD1a (Figure 3G, upper part). Conversely, addition of LPS drastically diminished the frequency of mo-DCs in favor of mo-Macs that are expressing higher levels of CD16 (Figures 3E–G, lower part). By contrast, the yield of mo-Macs was similar between GM-CSF and IL-4 culture of monocytes that are treated or not with MDP for the last two days of culture (data not shown), suggesting an early involvement of NOD2 in shaping the development of mo-DCs in the disadvantage of mo-Macs *in vitro*. This observation is in agreement with the time-restricted ability of soluble factors such as IL-4 or TNF-α to induce the monocyte differentiation process

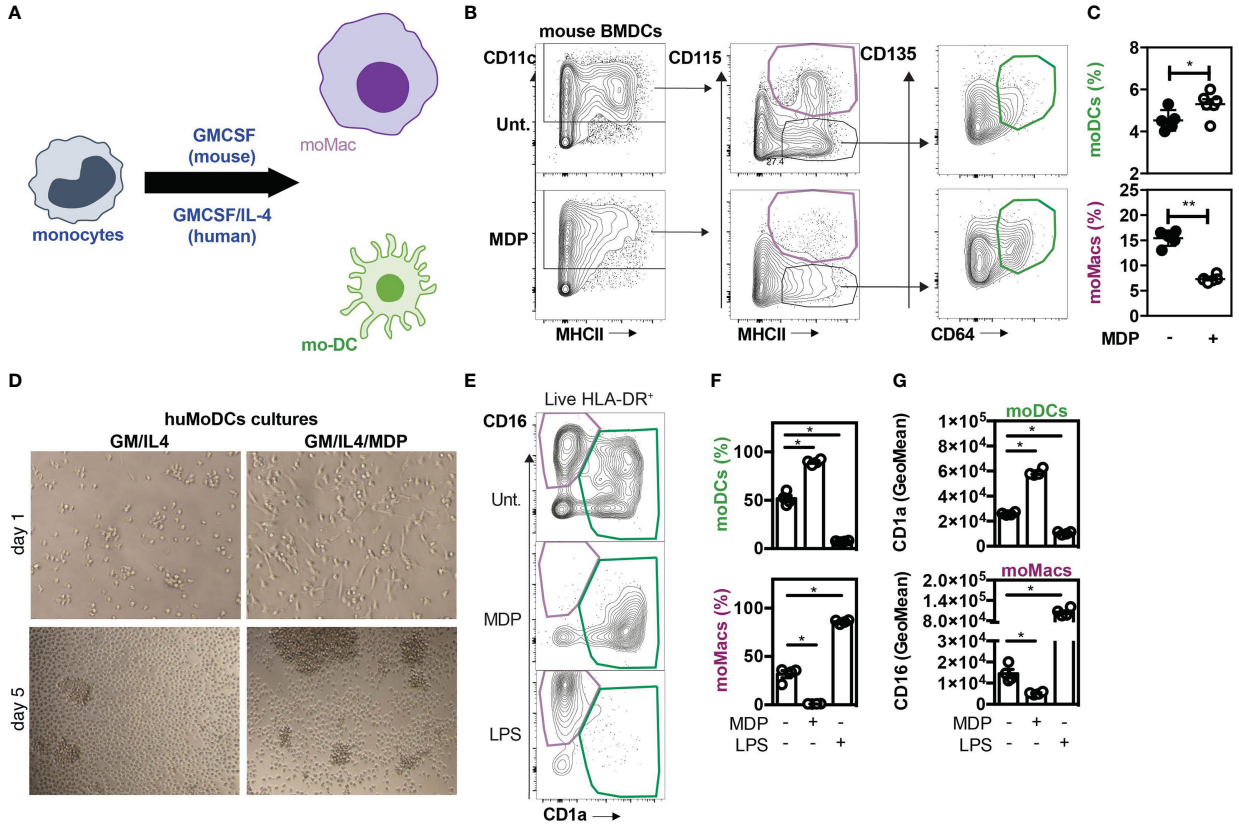

FIGURE 3
NOD2 stimulation is responsible for a mo-Macs/mo-DCs switch. **(A)** Experimental protocol. **(B)** Gating strategy for flow cytometry analysis of BMDCs upon MDP treatment. Mouse BM-derived cells were generated *in vitro* for 7 days in GM-CSF in the presence or not of MDP (10ug/ml). Mo-DCs were gated as $CD11c^+$ $MHCII^+$ $CD115^-$ $CD135^+$ $CD64^+$ (green) and mo-Macs were gated as $CD11c^+$ $MHCII^+$ $CD115^+$ (purple). Frequencies are calculated from the $CD11c^+$ gate. **(C)** Frequencies of mo-DCs and mo-Macs in the mouse BMDC culture stimulated or not with MDP at the start of the culture. **(D)** Mo-DCs were generated by culturing $CD14^+$ circulating human monocytes with GM-CSF and IL-4. MDP was added at the beginning of the 5 day-culture. Morphology of the differentiating cells at day 1 and day 5 of culture in the presence or not of MDP. **(E)** The impact of MDP or LPS stimulation at the start of the culture on mo-Macs ($CD16^+CD1a^-$) and mo-DCs ($CD16^-CD1a^+$) differentiation was evaluated by flow cytometry at day 6, after gating on live HLA^-DR^+ cells. **(F)** mo-DCs and mo-Macs frequencies. **(G)** CD1a and CD16 fluorescent mean intensity (GeoMeans) (n=5). These data are representative of at least 4 independent experiments with different mice **(B-C)** or donors **(D-G)**. Bars indicate mean ± SEM. Statistical significance was assessed by the non-parametric Mann-Whitney test. *P<0.05; **P<0.01.

toward mo-DCs in the first 72h of development (59, 60). This result is consistent with the steadily decline of NOD2 expression during the first 72h of the monocyte culture in the presence of GM-CSF and IL-4 (60). Indeed, monocytes differentiated for 72h with M-CSF, GM-CSF or $GM\text{-}CSF^+IL^-4$ have been described to exhibit transcriptomic, phenotypic, and functional divergences (60). While highly expressed in $CD14^+$ monocytes, transcriptomic analysis determined that *NOD2* expression was maintained only by monocytes differentiated with GM-CSF but was rather decreased in monocytes differentiated with M-CSF and GM-CSF+IL-4. Accordingly, qRT-PCR analysis revealed a lowered expression of *NOD2* in terminally differentiated mo-DCs when compared to naïve monocytes (Supplementary Figure 5), indicating that the expression of *NOD2* is temporally regulated during monocyte differentiation. These results suggest that early NOD2 signaling conditions the differentiation of nascent phagocytes into mo-DCs that promote inflammatory responses. Consequently, those findings suggested that early NOD2 signaling may progressively promote the differentiation of rapidly mobilized monocytes into ontogenetically related cells with specific features of mo-DCs by inhibiting their conversion into mo-Macs within the lamina propria (61). Overall, our data indicate that MDP sensing by monocytes promotes *in vitro* their conversion into mo-DCs.

NOD2 signaling acts through the mTORC1 pathway to license bifurcation of monocytes commitment

We next asked how NOD2 signaling in monocytes modulates the unique property of monocytes to differentiate into macrophages or mo-DCs that are phenotypically and functionally different. To this end, we investigated the signaling events after NOD2 stimulation with a focus on the components of the mechanistic target of rapamycin (mTOR), mTORC1, and mTORC2, signaling pathways that are both involved in the generation and activity of tissue-resident peritoneal macrophages *in vivo* (62, 63), and of human mo-Macs *in vitro* (9). As we have previously shown with human monocytes

(Figures 3E, F), the addition of MDP increased the yield of mo-DCs while decreasing the mo-Macs frequency (Figures 4A, B). However, the proportion of macrophages increased after the addition of MHY1485, which is a cell permeable activator that targets the ATP domain of mTORC1 but not mTORC2, used to promote the activation of mTORC1 (Figures 4A, B). These results highlighting the role of mTORC1 in the conversion of monocytes in macrophages are in agreement with what was observed with GM-CSF culture of mouse myeloid progenitors (64). Interestingly, MDP addition led to a significant decrease in macrophage frequency and an increase of mo-DCs yield, during the MHY1485 treatment, suggesting that NOD2 may act through mTORC1 during monocyte differentiation (Figures 4A, B). In line with our hypothesis, the proportion of mo-DCs was enhanced upon treatment of monocytes with wortmannin that acts upstream of the mTOR pathway similarly to what was observed with MDP alone (Figures 4A, B). Wortmannin is a selective inhibitor of phosphoinositide 3-kinases (PI3K), that can also block autophagy and has been described to irreversibly inhibit the serine-specific auto-kinase activity of mTOR (65). The PI3K/AKT pathway has been shown to negatively regulate the NOD2-mediated NF-κB pathway (66). As a result, the mo-Macs differentiation was completely inhibited. The addition of MDP to wortmannin, which is a non-specific, covalent inhibitor of PI3K that is also used for suppressing autophagy by interfering with autophagosome formation, did not increase mo-DCs frequencies. Cell toxicity was avoided as much as possible by treating cells for only 24 hours (data not shown). Similar results were obtained with rapamycin, the prototypic mTORC1 inhibitor, able to induce autophagy by potentiating LC3 lipidation (Figures 4A, B). These data are in agreement with the greater proportion of mo-DCs that is observed upon treatment with the mTORC1 inhibitor temsirolimus (20). These results suggest that NOD2 activation might negatively regulate the ability of the PI3K pathway to licensing the metabolic reprogramming of monocytes at an early stage of development.

NOD2 activates mTORC2 pathway and promotes anaerobic glycolysis

In an effort to further understand how NOD2 activation may impair mTORC1-dependent macrophage differentiation, we cultured the human monocytic cell line THP1 that express NOD2 (67), which

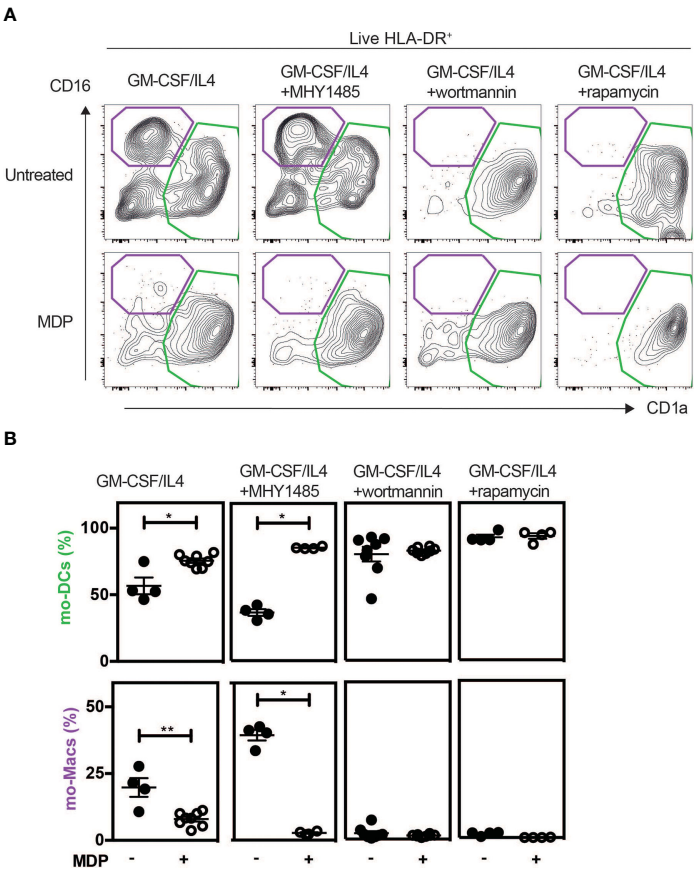

FIGURE 4
MDP enhances the differentiation of Mo-DCs in a mTORC1 independent manner. As described in Figure 3D, human CD14$^+$ monocytes were treated or not with MDP, the mTOR activator MHY1485, the PI3K inhibitor wortmannin, or the mTOR inhibitor Rapamycin for 5 days at the same timepoint. Mo-DCs (CD1a$^+$) and mo-Macs (CD16$^+$) frequencies were assessed by flow cytometry using the HLA-DR, CD16 and CD1a markers. **(A)** Contour representing the mo-DCs (green) and mo-Macs (purple). **(B)** The frequency of mo-Macs and mo-DCs in the four conditions are depicted. Representative of 2 experiments with at least 3 biological replicates. Bars indicate mean ± SEM. Statistical significance was assessed by the non-parametric Mann-Whitney test. *P<0.05; **P<0.01.

has been extensively used to study the development and function of human monocyte-derived phagocytes. THP1 cells were stimulated for 30 minutes with MDP, and the phosphorylation state of the Regulatory-associated protein of mTOR (also known as RAPTOR) at serine 792 (S792), which is mediated by AMP-activated protein kinase (AMPK), was quantified. This S792-phosphorylation of RAPTOR has been shown to reduce mTORC1 activity (68) and to act as a metabolic checkpoint that coordinates the energy status of each cell (68). In this experimental setting, activation of NOD2 signaling seemed to induce S792 phosphorylation of RAPTOR (Supplementary Figure 6A), suggesting that NOD2 could inhibit lipid uptake and foam cell formation through negative feedback on mTORC1 activity. At a time point of 24hours of stimulation, immunoblot analysis expectedly revealed that treatment with MDP did not increase the phosphorylation of S6K, which is a surrogate marker of mTORC1 activation (Supplementary Figure 6B). We next measured the phosphorylation of AKT at serine 473, as a surrogate marker of mTORC2 activation (64). In agreement with our hypothesis, we observed that a short treatment for 24 hours of THP1 cells with MDP increased this specific phosphorylation of the residue S473 (Supplementary Figure 6B). This phosphorylation was not observed in THP1 cells that lack the expression of NOD2. LPS also induced S473 phosphorylation, however, the phosphorylation of S473 was reduced when MDP treatment was followed by LPS stimulation (Supplementary Figure 6B). Consistent with that observation, MDP-treated THP1 monocytic cells were characterized by a NOD2-dependent upregulation of *IRF4* expression (Supplementary Figure 6C), which is a target gene of mTORC2 (69). Interestingly, LPS and Pam3 stimulations have been reported to decrease IRF4 expression in monocytes in a mTORC1-independent manner (9), suggesting that NOD2-mediated induction of IRF4 may be independent of this phenomenon. In line with the ability of NOD2 signaling to activate the Signal transducer and activator of transcription 5 (STAT5) (70), the treatment of THP1 cells with MDP significantly lowered the expression of IRF8 that is inhibited by STAT5 (71) (Supplementary Figure 6C). These results suggest that stimulation of monocytes with MDP induces mTORC2 activation and may act as a negative feedback loop on mTORC1, *via* the phosphorylation of AKTS473 and RAPTORS792 respectively. It has been postulated that GM-CSF may regulate *irf4* expression *via* STAT5 expression in monocytes and in macrophages (72). We could speculate that Nod2 may act in the same way and control IRF4 and IRF8 expression in monocytes *via* STAT5 activation. Metabolism changes, including in glycolysis and oxidative phosphorylation sustains energy needs of macrophages and dendritic cells, but also rewires their activation, polarization and differentiation as pro-inflammatory and anti-inflammatory cells (73–75). As the mTORC2 pathway plays a key role in the glycolytic reprogramming of monocytes that are rapidly mobilized on demand (76, 77), we next investigated if MDP treatment of monocytes is associated with changes in mTORC2-mediated metabolic cascade. To this end, previously published RNAseq data for MDP-treated vs untreated Ly6C^{hi} mouse monocytes (GEO accession number GSE101496) were mined for candidate genes encoding for enzymes involved in glycolysis. We observed an MDP-induced upregulation of several glycolytic genes such as the enzyme Gapdh that regulates the conversion of D-glyceraldehyde 3-phosphate into 1,3-bisphosphoglycerate (Supplementary Figure 7A) (26). To get further insights on how NOD2 may provide energy for monocytes, we next quantified the glycolytic capacity and reserve of THP1 cells that were deficient or not for NOD2. As THP1 cells mainly rely on glycolysis as a source of ATP for survival (78), these cells represent a suitable model. The oxygen consumption rate (OCR) was measured in NOD2-deficient and WT THP1 cells. We could observe that the lack of NOD2 could affect the OCR, a measurement of oxidative phosphorylation (OXPHOS) and extracellular acidification rate (ECAR), a surrogate measurement of glycolytic activity. Indeed, the extracellular acidification rate (ECAR) was measured by using a Seahorse bioanalyser. During the first step of glycolysis, we noticed a similar basal glycolytic rate between NOD2-deficient and parental THP1 cells (Supplementary Figure 7B). Upon blockade of oxidative phosphorylation of ADP to ATP by oligomycin, the basal glycolytic capacity of WT cells was similar to the one of THP1 *NOD2*$^{-/-}$ cells. By contrast, the inhibition of glycolytic H+ production by the competitive inhibitor of glycolysis, 2-Deoxy-D-glucose (2-DG), revealed a trend to a lower glycolytic reserve in the absence of NOD2. These results suggest that NOD2 may promote a lower pH, by sustaining a higher glycolytic demand, which is required for mo-DCs differentiation (20). TNF-α or IFNγ stimulations have been shown to induce a metabolic reprogramming of macrophages toward a pro-inflammatory M1 phenotype (79). NOD2 triggering may favor a switch in glycolysis to influence monocyte differentiation *via* cytokine production. Altogether, these results indicate that NOD2 signaling of monocytes may interfere with the PI3K/mTORC1 pathway through the mTORC2/AKT complex, which might inhibit the diversion of monocyte differentiation to macrophages *via* metabolic reprogramming (76). In other words, these data suggest that MDP may induce a transient negative regulation of the mTOR pathway to limit the accumulation of macrophages, leading to an unrepressed generation of mo-DCs.

The inhibition of the mTORC1 pathway by NOD2 promotes the secretion of TNF-α

We previously observed that early MDP treatment can condition and activate the metabolic pathways of monocyte-derived cells and also promote the differentiation of mo-DCs to the detriment of mo-Macs. Since bacteria are able to stimulate multiple PRRs, and chronic stimulation with MDP has been shown to down-regulate TLR4-induced TNF-α secretion by human monocyte-derived macrophages (80), we next experimentally addressed the functional impact of early NOD2 signaling on the ability of nascent phagocytes to respond to LPS when synergizing with MDP (81). Of note, while a short pre-incubation with MDP has been shown to act synergistically with LPS to induce the synthesis of TNF-α in monocytes (82), a decrease of TNF-α secretion and other pro-inflammatory cytokines, referred to as tolerance to TLR4 restimulation, appears after 24hours of pre-treatment with MDP in human monocyte-derived macrophages (80). Furthermore, mice injected with MDP were protected against

TNBS- or DSS-induced colitis by the suppression of multiple TLR pathways (29) suggesting a cross-tolerization of TLRs by chronic NOD2 stimulation (83). To evaluate the LPS responsiveness of MDP-treated cells, THP1 and THP1 cells that do not express NOD2 (THP1 *NOD2*$^{-/-}$) were incubated sequentially with MDP and then LPS or LPS alone. As expected, the cells pre-treated with MDP enhanced their subsequent cytokine response upon LPS treatment (Figure 5A, left upper part). This synergistic effect on the production of TNF-α to subsequent treatment with LPS was blunted with THP1 *NOD2*$^{-/-}$ (Figure 5A, lower part). In order to confirm our data with primary cells, mouse BM monocytes were cultured in the presence of MDP. The responsiveness to LPS was next analyzed by measuring the release of Tnf-α by specific ELISA. An apparent synergistic effect on the secretion of Tnf-α was retained in those cells that were primed with MDP (Supplementary Figure 8A). This synergistic effect on the production of Tnf-α to subsequent treatment with LPS was absent in monocytes that were isolated from the BM of *Nod2*-deficient mice (Supplementary Figure 8B). Such a functional model of hierarchy could be of particular importance in the context of loss of bacterial tolerance or the need for the replenishment of tissue mo-DCs following injury or infection. We then hypothesized that activation of NOD2 signaling may influence the bioenergetic needs of nascent mo-DCs by interfering with the mTOR pathway. In agreement with the autocrine role of NOD2-mediated TNF-α secretion on the development of mo-DCs (9), the PI3K inhibitor wortmannin increased by 3-fold the secretion of TNF-α upon stimulation of MDP-primed THP1 cells with LPS when compared to control cells (Figure 5A, blue, upper part). This effect of wortmannin on the monocyte responsiveness to LPS is lost with MDP-primed THP1 cells that do not express NOD2 (Figure 5A, red, lower part). In agreement with what was observed with wortmannin, rapamycin treatment, which inhibits mTOR, did not impair the secretion of TNF-α by THP1 cells when stimulated with MDP (Figure 5A). On another hand, bafilomycin treatment, which inhibits autophagy at the final step of fusion of lysosome with autophagosome, blunted the synergistic effect of MDP (data not shown). Interestingly, we found that the activation of mTORC1 with MHY1485, which is supposed to promote a macrophage phenotype (Figure 4B), inhibited the MDP-induced secretion of TNF-α by THP1 cells (Figure 5B). However, no TNF-α secretion was observed in *NOD2*-deficient THP1 even in the presence of MHY1485, suggesting that in our settings, MDP was not able to impair the effect of the macrophage prone drug MHY1485 on TNF-α production. Altogether, these results suggest that MDP, in synergy with LPS, can induce TNF-α secretion that may influence the differentiation of monocyte-derived cells toward mo-DCs. Given the effect of mTOR pathway inhibition on TNF-α secretion, we can speculate

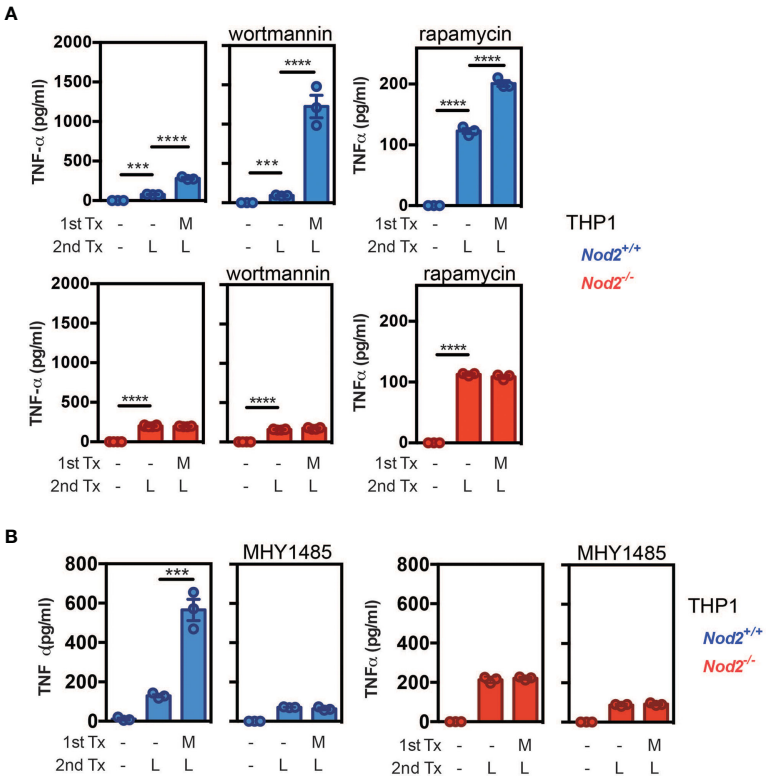

FIGURE 5
NOD2 signaling is hierarchically dominant over mTORC1 activation to condition monocyte differentiation into mo-DCs. **(A)** THP1 (blue) and THP1 *NOD2*-deficient cells (red) were treated as described in the material and method section to evaluate the LPS responsiveness of MDP-treated cells. In addition, the PI3K inhibitor wortmannin or the mTOR inhibitor rapamycin were added or not for 24h. TNF-α production was measured by ELISA. **(B)** LPS responsiveness was evaluated by measuring TNF-α production in THP1 WT or *Nod2*$^{-/-}$ cells treated with MDP, MHY1485, or both for 24h. Bars indicate mean ± SEM at least three biological replicates and data are representative of 2 independent experiments. Statistical significance was assessed by ordinary one-way multiple comparisons. ***P<0.005 ****P<0.001.

that NOD2 signaling influences monocyte fate decision over the activation of mTORC1 for conditioning their differentiation into mo-DCs *via* TNF-α induction.

NOD2 loss-of-function mutation impairs the phenotypic switch of monocytes in CD patients in a TNF-α dependent manner

To evaluate the importance of a monocyte phenotypic switch in CD patients with NOD2 mutations, we used a published RNA-seq data set from an exploratory cohort that is deposited in the GEO database (GSE69446) (84). Given that CD14-expressing cells are obligate precursors of discrete subsets of phagocytes that play a role in CD pathogenesis, the monocytes were isolated from peripheral blood of healthy controls (n=2) and CD patients in complete remission for at least 4 weeks prior to inclusion. Among those five patients, three carried the loss-of-function mutation in the *NOD2* gene, referred to as 1007fs mutation. As depicted in the Venn-diagram (Figure 6A), MDP treatment of monocytes from healthy donors and CD patients significantly modified the expression of up to 362 and 1,660 genes, respectively. Among those, a list of 306 genes was commonly regulated by MDP in blood monocytes from both control and CD patients. Geneset enrichment analysis (GSEA) indicated that the pathway "TNF-alpha signaling *via* NF-kB" (24/200)(adjusted p-value 3.12E-20) was significantly induced among the 156 commonly differentially upregulated genes that are induced by MDP in CD14-expressing cells from either control or CD patients (Figure 6B; Supplementary Data Set 1). In addition, the "mTORC1 signaling" pathway (4/200) (adjusted p-value 0.13) tended to be upregulated by MDP. The pathway "Wnt-beta Catenin Signalling" (3/42)(adjusted p-value 0.019) was also significantly induced among the 156 common genes induced by MDP in control and CD cells (Supplementary Data Set 1). Moreover, we noticed an enrichment of up-regulated genes related to dendritic cells (9/199)(adjusted p-value 7.8E-3) (Supplementary Data Set 2), among those *NR4A3* is involved in the proper differentiation of Mo-DCs (85). Furthermore, a list of down-regulated genes that are related to diverse subsets of tissue macrophages was identified by using GSEA (11/204)(adjusted p-value 1.1E-5) (Supplementary Data Set 3). Among the CD patients, we next assessed whether cells bearing an unfunctional NOD2 (n=3), as homozygous for the 1007fs NOD2 mutation, may differentially respond to MDP. This led us to identify a specific loss of MDP-induced expression of 10 genes, including *IL12B* and *miR-155* in mutated patients as compared to the patients who did not bear this mutation (n=2) (Supplementary Data Set 4). Inhibition of miR-155 in human monocytes by an antagomir during 6h increased significantly MAFB (9), a transcription factor implicated in the molecular control of monocyte-macrophage differentiation (86). Pathway enrichment analysis identified a set of genes among the 17 that were implicated in TNF-α signaling *via* NF-kB (5/200)(adjusted p-value 2.53E-7) (Supplementary Data Set 5) and TNF-α effects on cytokine activity, cell motility, and apoptosis (4/135) (adjusted p-value 1.75E-4) (Supplementary Data Set 6). Accordingly, the Kyoto Encyclopedia of Genes and Genomes (KEGG) database analysis of the 941 up-regulated genes in CD cells which are not present in control cells after MDP treatment identified a set of genes related to "TNF signaling pathway" (28/112)(adjusted p-value 5.6E-11) (Supplementary Data Set 7). These results extracted from transcriptomic data suggest that MDP might regulate and affect the differentiation of monocytes into the macrophage pathway by the induction of DC-inducing soluble factors, such as TNF-α. We then evaluated whether the formation of mo-DCs, which is initiated by NOD2 signaling, is inhibited upon neutralization of TNF-α with adalimumab, which is a fully human anti-TNF-α monoclonal antibody. Interestingly, it has been shown that the percentage of classical monocytes was higher in patients responding to adalimumab than in patients not responding to the same drug (87). CD14-expressing cells have been cultured for 5 days in a medium with GM-CSF, IL-4, MDP, and/or adalimumab (Figures 6C, D) and/or isotype control (data not shown). In contrast with the isotype control, the addition of adalimumab in the medium together with GM-CSF and IL-4 significantly increased the frequency of mo-Macs (Figures 6C, D). Among those, it has been noticed that some co-express the macrophage marker CD14 (88). Interestingly, in the presence of MDP, mo-DCs did not express the marker CD14 (Figure 6C). Monocytes in the presence of MDP produced higher levels of TNF-α (Supplementary Figure 9). In conclusion, NOD2 may molecularly define an education process that subsequently prevents the accumulation of monocyte-derived macrophages.

Discussion

We report herein experimental evidence that monocytes fail to differentiate into mo-Macs when the NOD2-mediated signaling is activated. By using competitive BM chimera, we did not observe a lack of recruitment of Ly6C^{hi} monocytes in the colon, suggesting that systemic MDP does not affect the number of recruited colonic monocytic cells at baseline, but may rather trigger early changes in epigenetic regulation of mo-DCs development (89). Besides the Nod2-dependent regulation of GM-CSF secretion by stromal cells in mice (28), our data highlighted a Nod2-dependent regulation of a developmental process of mo-DCs by the gut microbiota that is likely solicited when the DCs population must be replenished after fecal transplantation. This is particularly true within the first years of life, in which the immunological tolerance is not yet fully operational. One may anticipate that such demand-driven generation of mo-DCs is likely dependent on several mechanisms governing tolerance to MDP that are programmed in time for keeping a fine balance between each discrete subsets of phagocytes with context-dependent functions. Overall, our data suggest that MDP sensing by monocytes could promote *in vivo* their early conversion into mo-DCs for the maintenance of intestinal homeostasis at the expense of inflammatory macrophages.

Chronic stimulation of monocytes with MDP causes what is often called NOD2-induced tolerance which consists of tolerance to MDP and other bacterial signals such as LPS (90). On another hand, MDP can restore cytokine production, including TNF-α production, in LPS-

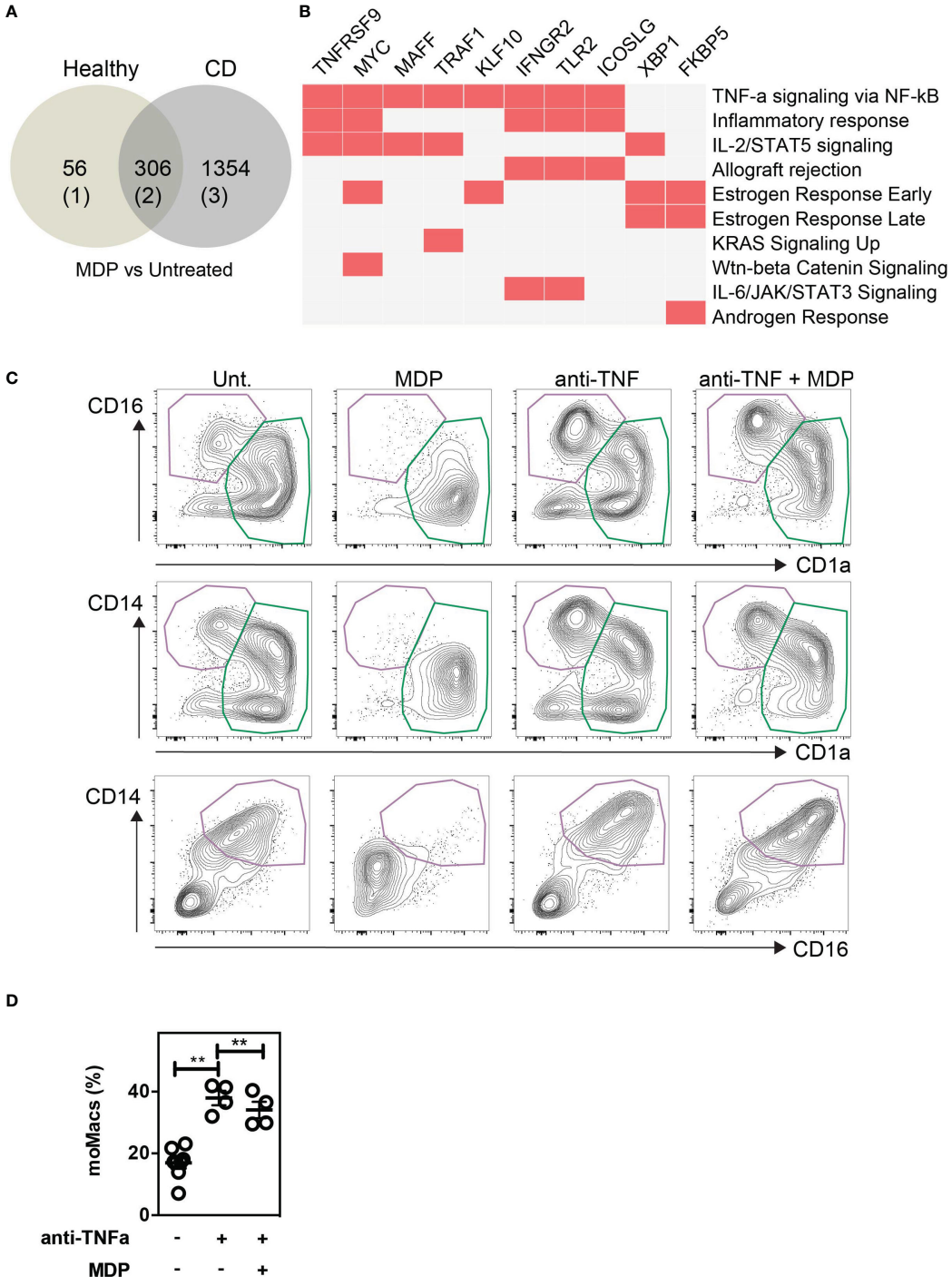

FIGURE 6
NOD2-induced decrease of macrophages is dependent on TNF-α production. Public RNA-seq data set of untreated or MDP-stimulated monocytes isolated from peripheral blood of healthy controls (n=2) and CD patients in complete remission were analyzed. Among the CD patients, 3 are bearing and 2 are not bearing the loss of function mutation in the *NOD2* gene. **(A)** Venn diagram comparing the Differentially Expressed Genes (DEG) between MDP-treated and untreated in healthy controls and CD patients. **(B)** Geneset enrichment analysis (GSEA) among the 156 commonly differentially upregulated genes that are induced by MDP in CD14-expressing cells from either control or CD patients. **(C)** Monocytes were treated or not with MDP, anti-TNFα (Adalimumab), or both during GM/IL4 cultures. Isotype was used as a control. Mo-DCs and mo-Macs frequencies were assessed by flow cytometry using the CD14, CD16 and CD1a markers on day 6 of the culture. Contour plot representing the mo-DCs (green) and mo-Macs (purple). Representative of at least 2 independent experiments with different donors and with at least 4 biological replicates. **(D)** The frequency of mo-Macs upon anti-TNFα and MDP treatment is depicted. Bars indicate mean ± SEM. Statistical significance was assessed by the non-parametric Mann-Whitney. **, P<0.001.

tolerized macrophages (91). Proteosomal degradation of NOD2 protein confers rapid induction of refractoriness to MDP that protects the host from tissue damage or even death (90, 92). Such negative feedback regulatory mechanism fails to occur when human primary monocytes or transfected cell lines are defective in either the E3 Ubiquitin ligase ZNRF4 or the protein NLRP12 (48, 93). Consequently, treatment with MDP of monocyte-derived cells that are deficient for the aforementioned molecules led to an excessive inflammation with a sustained NF-κB activation. We have observed NOD2-mediated induction of IRF4. A proteo-analysis of HEK response to MDP highlighted that the Crk-like protein and the phosphoglycerate kinase 1 (PGK1) are upregulated in the NOD2-WT as compared to controls. Crk-like protein is an oncogene and an adaptor protein that has been shown to associate with STAT5, while PGK1 protein has been shown to be an enzyme of the glycolytic pathway (94). According to the ability of NOD2 signaling to activate STAT5, we observed a decrease in IRF8 expression with MDP (Supplementary Figure 6C).

One may infer that blood monocytes deficient for Nod2 may develop into inflammatory macrophages in the gut and lead to an increased inflammatory response in colitis for instance. Different studies have shown that most of the immune cells, particularly myeloid cells, may actually have dual activity, pro-inflammatory or immunosuppressive, depending on the signals received from the microenvironment (95). As this dual display of antagonizing functions exists also in conventional dendritic cells (96), we anticipated that similar dual properties of mo-DCs would likely exist and be influenced by microbial-derived products in their microenvironment.

The notion that metabolic control is upstream of inflammatory function has been proposed recently (97). Indeed, circulating monocytes and monocyte-derived macrophages from patients with fibroinflammatory vasculopathy are highly efficient in glucose import and are expressing higher glycolysis-associated genes (GLUT1, HK2, PKM2, LDH, c-myc, and HIF-1α) in comparison to healthy individuals. Consistently, the expression of the Aldoa and Aldoc that are converting F1,6BP into GADP and of the Gadph that is converting GADP into 1,3BPG were significantly upregulated in Ly6C^{hi} mouse monocytes that were treated by MDP as compared to untreated (Supplementary Figure 7A) (26). Similarly, MDP stimulation enhanced the expression of the Pgk1 converting 1,3BPG into 3-P-G and the Pagm1 that is involved in the conversion of the latter into 2PG. Aside from these enzymes, the Ldhb which is converting the Lactate into Pyruvate was downregulated, as well as the HK-II which is converting the glucose into glucose 6-phosphate (G6P). In addition, to confirm in human the MDP-mediated metabolic switch toward glycolysis observed in mouse monocytes, we analyzed the RNA-seq data set from an exploratory cohort of CD patients carrying a loss-of-function mutation in the *NOD2* gene and in complete remission vs healthy controls (as described in Figure 6B). Among the common 156 up-regulated genes induced by MDP either in control and CD monocytes as compared to untreated, analysis of MSigDB database indicated also the pathway "mTORC1 signaling" and containing SLC7A5, XBP1, HSPA5, PPA1, AK4, and CFP (Supplementary Data Set 1). Further studies will be needed to better understand the MDP-induced regulation of glycolysis enzymes and their regulation of mTORC1 signaling (98). Additionally, among the genes having a loss of MDP-induced expression in monocytes from SNP13 CD patients, *AK4* is involved in the positive regulation of mouse myeloid cells glycolysis and inflammatory cytokine production such as Tnf-α and Il-6 (99). In addition, we observed a decline of oxidative phosphorylation and glycolytic activity in NOD2-deficient THP1 cells suggesting a metabolic switch after NOD2 stimulation. As the induction of metabolic enzymes seems to appear rapidly after MDP stimulation (Supplementary Figure 7), glycolysis may precede the production of inflammatory cytokines during mo-DCs/mo-Macs differentiation (97). MDP has been shown to induce a metabolic reprogramming of human Monocyte-derived Macrophages (MDM) and a lower level of glycolysis than MDM, but comparable OXPHOS in MoDC at basal conditions (44). Moreover, a NOD2 agonist injected *in vivo* increased both glucose consumption and lactate release in mouse peritoneal macrophages and increased TNF and IL-6 production. While the effect of the addition of MDP can be detected very rapidly on glycolysis and OXPHOS (e.g. 10min), cytokine production can be detected after 3h of culture of human mo-Macs or mo-DCs (44). In addition, it has been suggested that the increase of glycolysis may take place without *de novo* gene synthesis in MDM upon treatment with NOD1 or NOD2 agonists due to the fact that it occurs after 1h of stimulation (44). However, while IRF5 has been shown to be necessary for NOD2-induced glycolysis, TNF-α, IL-1β or IL-12 could promote glycolytic gene expression and glycolysis in an IRF5-dependent manner in macrophages (47). Moreover, the autocrine pro-inflammatory cytokines were required for glycolysis suggesting a positive regulation of TNF-α and IL-1β on NOD2-mediated glycolysis in polarized and unpolarized macrophages. Of note, the knock-down of glycolytic genes induced the decrease of cytokine release, highlighting the double feedback regulation of cytokines and glycolytic genes. It has been mentioned that 2-DG partially prevented mo-DC differentiation, without affecting cell viability (20). Moreover, 2-DG appeared to block NOD1 agonist– or LPS-induced elevation of ECAR in mo-Macs and to inhibit LPS-induced TNF-α, IL-6, and IL-12 production by mo-DCs (44). Treatment with 2-DG has also been shown to inhibit Flt3L-induced proliferation of mouse precursors in a dose-dependent manner, indicating that aerobic glycolysis is involved in DC development (75). The NOD2/Ataxin-3 axis has been described in the regulation of myeloid cell metabolism (100). Indeed, ataxin-3 depletion led to a significant reduction in the oxidative phosphorylation of THP1. 2DG treatment has also been involved in the decrease of TNF, IL-1β, and IL-10 secretion and the reduction of the expression of genes involved in innate immune signaling pathways, cytokines secretion, and ROS production in LPS-stimulated human monocytes (101) suggesting a rewiring of monocyte function after glycolysis blockade. In addition, 2-DG treatment increased IL-23 secretion in GM-DCs *in vitro* and *in vivo* after imiquimod stimulation and promoted an increase of Ddit3 and Xbp1s expression in imiquimod-treated GM-DCs (102). XBP1s, a transcription factor that has been associated with CD (103), is proposed to play a major role in the development, differentiation, survival, and immune responses of various immune cells, including dendritic cells and

macrophages (104), suggesting that glycolysis inhibition by 2-DG could affect monocyte-derived cell differentiation after PRR activation. As microbiota-derived circulating peptidoglycan is found in the mouse blood (105), one can propose that MDP can induce a metabolic reprogramming of circulating monocytes leading to a higher glucose consumption which regulates their mitochondrial activity, such as ROS production and effector molecules expression such as TNF-α. Here, we demonstrated that blocking TNF-α with adalimumab, which has been described to bind to membrane TNF-α with relatively higher affinity than etanercept (106), limits the development of MDP-induced mo-DCs. Similarly to our observations with the *in vitro* generated human mo-DCs with GM-CSF and IL-4, it was recently shown that MDP stimulation of human monocytes in *in vitro* culture with IL-4, M-CSF, and TNF-α promotes the generation of mo-DCs and limits the one of macrophages. In addition, intradermal injection of TNF-α into the ear of mice increases mo-DC numbers (9).

Interestingly, DC obtained from either *Tnfr1*$^{-/-}$ mice or patients treated with anti-TNF-α showed an unusual mixed immature/mature phenotype (107, 108) suggesting the development of macrophages in these cultures (55, 109). While TNF-α is a weak stimulator of CCR7 expression (110), it counterbalances the emergence of M2-like tumor macrophages (111). Such cytokine is sharply induced by microbiota, in Nod2-dependent and –independent pathways, during weaning for lowering the risk of developing colorectal cancer later in life (112). Conversely, an impaired dendritic cell function has been reported in most CD patients with NOD2 1007fs mutation (113). While TNF-α can upregulate NOD2 expression in myelomonocytic cell lines (67), anti-TNF therapy could alter the Nod2-induced equilibrium between discrete subsets of intestinal phagocytes with different properties. Additional analysis of published RNAseq data of the CD patients' cohort in remission and healthy controls, while comparing to untreated, indicated that the pathway "Wnt-beta Catenin Signalling" was also significantly induced among the 156 common genes induced by MDP either in CD14-expressing control and CD cells including MYC, HEY1, JAG1 and A Disintegrin And Metalloproteinase 17 (ADAM17) (Supplementary Data Set 1). Wnt-beta catenin signaling pathway limits the differentiation into macrophages of BM cells cultured with GM-CSF (69). It is worth noting that A Disintegrin And Metalloproteinase 17 (ADAM17 (also known as TNF-alpha converting enzyme (TACE)) is a sheddase with a broad range of substrates such as membrane-bound TNF-α (114) and M-CSF receptor (59). ADAM17-dependent cleavage of M-CSF receptor is the mechanism by which GM-CSF and IL-4 block M-CSF- and RANKL-induced osteoclast differentiation from monocytes (59). Modulating the NOD2/TNF-α signaling axis to balance the induction of mo-DCs and repression of mo-Macs appears to be a promising new target for immunotherapy of colorectal cancer and to treat stricturing complications of CD patients.

Additionally, among the 17 genes losing MDP-induced expression in monocytes from CD patients with the homozygous SNP13 mutation, *NR4A3* is involved in the proper differentiation of Mo-DCs (FC 1.72, adjusted p-value 0.00206) (Supplementary Data Set 4) (85). One may suggest that inhibition of M-CSF receptor signaling by MDP on monocytes is required to impair macrophage differentiation in certain circumstances. For instance, type 1 cysteinyl leukotriene receptor (CYSLTR1) was significantly down-regulated from healthy controls or CD patients under MDP treatment (84). Inhibition of CYSLTR1 prevents M-CSF- and RANKL-induced osteoclast differentiation of BM precursors (115). Additionally, the ETS variant transcription factor 3 (ETV3) was significantly up-regulated within the MDP-treated monocytes from healthy controls or CD patients. It is induced by the anti-inflammatory cytokine IL-10 (116), and blocks M-CSF-induced macrophage proliferation (117). In CD patients, a unique response to MDP was observed with 941 and 413 up-regulated and down-regulated genes respectively (84). Analysis of Azimuth Cell Type database showed enrichment of up-regulated genes that are related to "Myeloid Dendritic Type 1" among which CCR7 is a hallmark of DC as it is critically required for their migration to lymph nodes (118). Equally of importance, the transcription factor *NRA43*, which is involved in the proper differentiation of mo-DCs (85), is less induced by MDP treatment in monocytes from CD patients than in cells from healthy controls (FC 1.6 and FC 1.71, respectively) as compared to untreated.

Thus, by using BM chimera and fecal transplantation models, our study highlights the role of NOD2 and the microbiota in the reconstitution of monocyte-derived cells in the colon of mice at steady state while not affecting mo-Macs during colitis. NOD2 promotes mo-DCs development by interfering with mouse BM and human monocyte differentiation in macrophages. In addition, we observed that NOD2 impacts mo-DCs/mo-Macs differentiation through activation of the mTORC2 pathway and a metabolic switch in NOD2 transfected THP1 involving TNF-α. The involvement of TNF-α signaling pathway has been confirmed in transcriptomic data of CD patients. Here, we provided a better understanding of macrophage-differentiation inhibition by NOD2-mediated signaling, which may offer new therapeutic strategies aiming at limiting the detrimental effects of pathogenic macrophages in gut pathologies such as CD.

Materials and methods

Mice

All animal studies were approved by the local investigational review board of the Institut Pasteur of Lille (N°28010-2016012820187595). Animal experiments were performed in an accredited establishment (N° B59-108) according to governmental guidelines N°86/609/CEE. Age-matched and gender-matched C57BL/6J WT, Nod2-deficient mice (Nod2$^{-/-}$), have free access to a standard laboratory chow diet in a temperature-controlled SPF environment and a half-daylight cycle exposure. C57BL/6J WT GF, Nod2$^{-/-}$ GF mice were bred at TAAM-CNRS and were transferred into autoclaved sterile micro-isolator cages. C57BL/6J WT mice were purchased from Janvier Laboratories, France. Ly5.1 WT mice (CD45.1) were purchased from Charles Rivers Laboratories, France.

Nod2$^{-/-}$ mice were provided by R.A. Flavell (Yale University School of Medicine, Howard Hughes Medical Institute).

Induction of acute colitis

A single cycle of acute colitis was induced by giving mice 2% (wt/vol) DSS (TdB Consultancy) for a period of 4 to 5 days followed by normal drinking water for the indicated period of time with a threshold of the maximal lost weight of 20% of the initial weight. DSS was dissolved in drinking water and changed every 3 days. Signs of morbidity, including body weight, stool consistency, occult blood, or the presence of macroscopic rectal bleeding, were checked daily. At specific time points throughout the course of the challenge, mice were autopsied to assess the severity of the disease by measurement of colon lengths and cell composition by flow cytometry.

Bone marrow transplantation experiments

Recipient mice underwent a lethal total-body irradiation (2X 5.5Gy, 4h between each dose). Twenty-four hours post-irradiation, mice received intravenously 2×10^6 fresh BM cells. *Nod2*-deficient animals were irradiated and reconstituted in a 1:1 ratio with bone marrow cells from WT (CD45.1) and *Nod2*-deficient mice (CD45.2). Blood was collected in heparin-containing tubes 7–8 weeks after BM transplantation and reconstitution efficiency was checked by flow cytometry (119). Cellular content within the colon, the blood, and the peritoneum of chimeric mice were analyzed 8 weeks after BM reconstitution by flow cytometry. In some experiments, DSS was administered for 5 days in the drinking water of mixed-BM chimera mice to induce acute colitis.

Fecal transplantation

Fecal microbiota from WT mice was transplanted by gavage in GF mice that are deficient or not for Nod2 (120). The mice were used after four weeks of colonization with feces from WT mice.

Isolation of mouse colonic lamina propria cells

Lamina Propria Mononuclear Cells (LPMC) were prepared from murine intestines by enzymatic digestion as previously described (3). Briefly, cells were isolated from colons, after removal of epithelial cells, by enzymatic digestion with 1.25 mg/ml collagenase D (Roche Diagnostics), 0.85 mg/ml collagenase V (Sigma-Aldrich), 1 mg/ml dispase (Life Technologies), and 30 U/ml DNaseI (Roche Diagnostics) in complete RPMI 1640 for 30–40 min in a shaking incubator until complete digestion of the tissue. After isolation, cells were passed through a 40µm cell strainer before use (BD biosciences). Colonic cell numbers were determined by counting beads and following the manufacturer's instructions (AccuCheck counting beads, Invitrogen).

Generation of bone marrow-derived dendritic cells

Bone marrow cells were flushed out of the mouse bones with complete RPMI 1640 (Gibco). A single-cell suspension was then prepared by repeated pipetting. Bone marrow-derived dendritic cells (BMDCs) were generated for 7 days in respectively RPMI-1640 medium (Gibco), supplemented with glutamine, penicillin, streptomycin, 2-mercaptoethanol (all from Gibco), and 10% heat-inactivated fetal calf serum (GE Healthcare). The medium was supplemented with 20 ng/ml GM-CSF of J558 cells (GM-CSF-producing cells). Half of the medium was removed at day 3 and new medium supplemented with GM-CSF supernatant (2x, 40 ng/ml) was added (55). When mentioned, muramyl dipeptide (MDP) (10µg/ml; Invitrogen) was added from the beginning of a 6-day culture with GM-CSF (day 0).

Human monocyte-derived dendritic cell generation

Human Peripheral Blood Mononuclear Cells were prepared from buffy coats (Etablissement Francais du Sang (EFS), Lille, France) using Ficoll Paque (Lymphoprep, StemCell). The use of human samples was approved by the French Ministry of Education and Research under the agreement DC 2013-2575. According to French Public Health Law (art L 1121–1-1, art L 1121–1-2), Institutional Review Board and written consent approval are not required for human non-interventional studies. Monocytes were positively isolated using $CD14^+$ microbeads (Miltenyi Biotec) according to the manufacturer's recommendations. Cells were cultured for 6 days with rhGM-CSF (20ng/ml; Peprotech) and rhIL-4 (5ng/ml; Peprotech). When mentioned, muramyl dipeptide (MDP) (10µg/ml; Invitrogen) was added from the beginning of a 5-day culture with GM-CSF and IL-4 (day 0). The mTOR activator MYH1485 (2µM, Sigma), wortmannin (1µM, Sigma) or rapamycin (100nM, Sigma) were added at the start of the culture (day 0). Adalimumab (Humira M02-497) was a gift from Abbott (Abbott Park, IL, USA).

Cytokine measurement

Cytokine levels were determined by ELISA kits (DuoSet), according to protocols provided by R&D Systems.

Western blot

Protein extraction was performed using RIPA buffer in the presence of a complete Mini EDTA-free protease inhibitor (Roche)

and PhosSTOPTM phosphatase inhibitor (Roche). Protein separation was performed by SDS-page using Bolt 4 to 12% Bis-Tris protein gels (Invitrogen). Transferences were done in an iBlot 2 gel transfer device using iBlot 2 transfer nitrocellulose stacks (Invitrogen). Membranes were blotted against phospho-AKT (Ser473) (Cell Signaling), phospho-RAPTOR (Ser792) (Cell Signaling), phospho-p70 S6 Kinase (Thr389) (Cell Signaling), β-ACTIN (Cell Signaling) and their correspondent HRP-conjugated secondary antibodies. The revelation was performed using the SuperSignal West Femto Maximum Sensitivity Substrate (Thermo Scientific) and images were acquired using an ImageQuant LAS 4000 (GE Healthcare).

Flow cytometry

Single-cell suspensions were stained and analyzed using a FACS LSR Fortessa^{TM} system (BD Biosciences). Dead cells were excluded with the LIVE/DEAD Fixable Violet Dead Cell staining kit (Life technologies). The cells were then incubated for 10 minutes with purified rat anti-mouse CD16/CD32 (Biolegend, 93 clone)(only for mouse cells) and normal mouse serum (Interchim) before being stained with various monoclonal antibodies for 20 minutes in the dark on ice. For mouse cells, lineage-positive cells were excluded using the PerCP5.5-conjugated anti-CD3 (17A2), anti-NK1.1 (PK136), anti-CD19 (6D5), anti-Ly6G (1A8) (Biolegend). PerCP-conjugated anti-CCR3 (83103) added to the lineage staining to exclude eosinophils was from R&D. Alexa Fluor 700-conjugated anti-Ly6C (AL21) was from BD Pharmingen. PECF594-conjugated anti-CD11c (HL3) was from BD Horizon. Allophycocyanin-Cy7-conjugated anti-CD11b (M1/70), Brilliant violet 510-conjugated anti-MHC Class II (I-A/I-E) (M5/114.15.2), Brilliant violet 650-conjugated anti-CD45.2 (104), Brilliant violet 711-conjugated anti-CD45.1 (A20), PE-conjugated anti-CD135 (A2F10), APC-conjugated anti-CD115 (AFS98), PE-conjugated anti-CD226 (10E5), FITC-conjugated anti-CD102 (3C4) were all from Biolegend. PE-conjugated anti-CCR2 (475301) was from R&D systems. The data were analyzed with Flowjo software V10.1 (TreeStar). For human cells, a similar procedure was used with anti-HLA-DR FITC (eBioscience, clone LN3), anti-CD1a APC (Biolegend, clone HI149), anti-CD16 PE-Cy7 (BD Pharmingen, clone 3G8), anti-CD14 PE (Miltenyi Biotec, clone REA599).

THP1 cell culture and stimulation

The THP1 monocytic cell line was cultured in RPMI 1640 medium (Gibco) supplemented with 10% heat-inactivated FBS (Gibco), L-glutamine (Thermo Fisher), Penicillin and Streptomycin (Thermo Fisher), MEM non-essential amino acids (Thermo Fisher), sodium pyruvate (Thermo Fisher), HEPES (Thermo Fisher) and 0.05mM of 2-mercaptoethanol (Thermo Fisher). Cells were kept in the culture at cell concentrations ranging from $2x10^5$ cells/mL to $8x10^5$ cells/mL and routinely verified negatively for mycoplasma contamination by PCR analysis. THP1 stimulation was performed in 96-well flat bottom plates at $1x10^5$ cells per well in a final volume of 200 µl. Cells were stimulated with two sequential treatments of 24 hours each. For the first 24 hours of treatment, cells were cultured in RPMI complete medium or RPMI medium with MDP at 100µg/ml. The second 24-hour treatment consisted of LPS (Invivogen) at 50ng/ml or RPMI medium. In selected experiments, the first treatment was MHY1485 (Sigma) at 2µM, rapamycin (Sigma) at 100nM, or wortmannin (Sigma) at 1µM. In some conditions, THP-1 macrophages were generated by adding PMA (5ng/ml) for 48h, followed by at least 2 days without PMA (121, 122). Culture supernatants were collected after the second treatment and TNF-α levels were quantified by ELISA using the Human TNF-alpha DuoSet ELISA (R&D systems) following manufacturer recommendations.

Generation of BM-derived dendritic cells

BM cells were flushed out of the mouse bones with complete RPMI 1640 (Gibco). A single-cell suspension was then prepared by repeated pipetting. BM-derived dendritic cells (BMDCs) were generated for 7 days in respectively RPMI-1640 medium (Gibco), supplemented with glutamine, penicillin, streptomycin, 2-mercaptoethanol ([all from Gibco)], and 10% heat-inactivated fetal calf serum (GE Healthcare). The medium was supplemented with 20 ng/ml GM-CSF of J558 cells (GM-CSF-producing cells). Half of the medium was removed on day 3 and a new medium supplemented with GM-CSF supernatant (2x, 40 ng/ml) was added (55).

Extracellular acidification rate (ECAR)

ECAR was measured under basal conditions and in response to glucose (10mM) using the Seahorse Glycolysis Stress Test Kit by using a Seahorse bioanalyser.

Gene expression

RNAs were extracted using the RNEasy mini kit (Qiagen). According to the manufacturer's instructions, isolated RNA was reverse-transcribed with the cDNA synthesis kit (Agilent Technologies). The resulting cDNA (equivalent to 500ng of total RNA) was amplified using the SYBR Green real-time PCR kit and detected on a Stratagene Mx3005 P (Agilent Technologies). qPCR was conducted using forward and reverse primers (sequences available upon request). The relative abundance of gene expression was assessed using the $2^{-\Delta\Delta Ct}$ method. Actb was used as an internal reference gene in order to normalize the transcript levels.

Statistics

Data were analyzed using Prism6.0 (GraphPad Software, San Diego, CA). Statistical significance was assessed by non-parametric Mann-Whitney test or two-way ANOVA for multiple comparisons.

Values represent the mean of normalized data ± SEM. *, P<0.05; **, P<0.01; ***, P<0.001; ****, P<0.0001.

Data availability statement

Publicly available datasets were analyzed in this study. This data can be found here: https://www.ncbi.nlm.nih.gov/geo/query/acc.cgi?acc=GSE69446: GEO database (accession number GSE69446).

Ethics statement

All animal studies were approved by the local investigational review board of the Institut Pasteur of Lille (N°28010-2016012820187595).

Author contributions

Conceptualization: CC, DAS, ES, MC, and LP. Methodology: CC, DAS, KR, OB, WL, MD, NW, ES, JK, MC, and LP. Formal analysis: CC, DAS, KR, OB, WL, NW, ES, JK, MC, and LP. Investigation: CC, DAS, KR, OB, WL, MD, NW, JK, MC, and LP. Writing – original draft: MC and LP. Writing – review and editing: all authors. Visualization: CC, DAS, MC, and LP. Supervision: LP and MC. Funding acquisition: MC and LP. All authors contributed to the article and approved the submitted version.

Funding

This work was funded by the French government's ATIP-Avenir program and by the Fondation Recherche Médicale" (grant number EQU202103012718). LP also received a fellowship from the ATIP-Avenir program, funding support by the French national IBD patients' association (Association François Aupetit (AFA) and by "Comité du Nord de La Ligue contre le cancer ". CC received a fellowship funded by the cancer charity "La Ligue contre le cancer". ES received funding support from the Agence Nationale de la Recherche (grant number ANR-17-CE15-0011-01). This work is supported by a grant from Contrat de Plan Etat-Région CPER Cancer 2015-2020.

Acknowledgments

We thank the staff at the animal and cytometry facility at the Pasteur Institute of Lille. Pathway analysis has been realized with Enrichr (123–125). We thank the ONCOLille institute.

Conflict of interest

The authors declare that the research was conducted in the absence of any commercial or financial relationships that could be construed as a potential conflict of interest.

Publisher's note

Supplementary material

The Supplementary Material for this article can be found online at: https://www.frontiersin.org/articles/10.3389/fimmu.2023.1181823/full#supplementary-material

SUPPLEMENTARY FIGURE 1
Mixed BM chimera mice were generated as described in . Absolute numbers **(A)** and frequency **(B)** and their relative ratios of total WT and Nod2$^{-/-}$ mo-DCs and mo-Macs in the colon of recipients are depicted and the ratio of mo-DCs vs mo-Macs (n=4). Bars indicate mean ± SEM. Statistical significance was assessed by non-parametric Mann-Whitney test. * P<0.05.

SUPPLEMENTARY FIGURE 2
Gating strategy of the mixed BM chimera mice generated as described in . **(A)** Contour plots of conventional DC1, DC2, mo-DCs, CD11c^{+} Macs, mo-Macs, Monocyte MHCII^{+} and Monocyte MHCII^{-} are depicted. **(B)** Each subset is represented according to CD45.1 and CD45.2. **(C)** MHCII GeoMean in Monocyte MHCII^{+}.

SUPPLEMENTARY FIGURE 3
Gating strategy in WT GF **(A)**, in *Nod2*$^{-/-}$ SPF **(B)**, and in *Nod2*$^{-/-}$ GF (C) as explained in . Contour plots and frequency of conventional DC1, DC2, of mo-DCs, mo-Macs, and Monocyte MHCII+ are depicted.

SUPPLEMENTARY FIGURE 4
Fecal microbiota from WT mice was transplanted in GF mice that are deficient or not for *Nod2*. Four weeks after colonization, the proportions of mononuclear phagocytes were evaluated in the transplanted mice. **(A)** Experimental set-up. **(B)** Frequency and absolute number of CD11c^{-} MHCII^{+} and CD11c^{+} MHCII+ cells (n=3/group).

SUPPLEMENTARY FIGURE 5
Expression of *NOD2* in mo-DCs upon differentiation for 5 days with GM-CSF and IL-4. Bars indicate mean ± SEM from three biological replicates. The statistical significance was assessed by multi-comparison non-parametric Friedman paired test, with Dunn's post-test. *, P<0.05, **, P<0.01.

SUPPLEMENTARY FIGURE 6
(A) THP1 (left part) and THP1 *NOD2*-deficient cells (right part) were stimulated for the indicated time with MDP and the presence of phosphorylated RAPTOR (Ser792) was measured at 0, 30min, and 60min by western blot. β-ACTIN was measured as a control. **(B)** THP1 (left part) and THP1 *NOD2*-deficient cells (right part) were stimulated for the indicated time with MDP, LPS, or both sequentially for 24 hours each and the presence of phosphorylated AKT (Ser473), and phospho-p70 S6 Kinase (Thr389) was measured at different timepoints by western blot. β-ACTIN was measured as a control. Quantification of the western-blots **(C)** *IRF4* and *IRF8* mRNA expression in THP1 (blue) and THP1 NOD2$^{-/-}$ (red) monocytic cell lines was measured by RT-qPCR at the beginning of the culture or 24h and 48h after MDP treatment. Data are representative of 2 independent experiments with at least three biological replicates. Bars indicate mean ± SEM. Statistical significance was assessed by ordinary one-way multiple comparisons **(A)**. ***, P<0.005.

SUPPLEMENTARY FIGURE 7
MDP enhances the differentiation of Mo-DCs in a glycolytic and MTORC1-independent manner. **(A)** Overexpressed enzymes involved in glycolysis in MDP-treated mouse monocytes in published RNA-seq data sets (GEO

accession number GSE101496). **(B)** Mitochondrial respiration calculated as OCR (B, upper part), glycolysis activity calculated as ECAR (B, lower part), before and after Glc (glucose) administration. (Oligo, oligomycin; 2DG, 2-deoxyglucose; AA, antimycin A; Rot, rotenone). Extracellular acidification rate (ECAR) was measured in the MDP-treated *Nod2*$^{+/+}$ (blue) and *Nod2*$^{-/-}$ THP1 (red) cells. Data are representative of 2 independent experiments with at least four biological replicates. **(C)** Measure of the ECAR non glycolytic, ECAR basal and ECAR maximal between the THP1 *NOD2*$^{+/+}$ and *NOD2*$^{-/-}$.

SUPPLEMENTARY FIGURE 8

Mouse BM monocytes from WT **(A)** and *Nod2*$^{-/-}$ mice **(B)** were treated with MDP or LPS for 24h (1st Tx), and washed before a second treatment with MDP or LPS (2nd Tx). mTNF-α was measured 24h after the last treatment in the supernatant. Data are representative of 2 independent experiments with at least three biological replicates. Bars indicate mean ± SEM. Statistical significance was assessed by the non-parametric Mann-Whitney test. **, P<0.01.

SUPPLEMENTARY FIGURE 9

Mo-DCs were differentiated in the presence of MDP, and hTNF-α was measured at 24h. Bars indicate the mean ± SEM of four biological replicates. Statistical significance was assessed by the non-parametric Mann-Whitney test. *, P<0.05.

References

1. Bujko A, Atlasy N, Landsverk OJB, Richter L, Yaqub S, Horneland R. Transcriptional and functional profiling defines human small intestinal macrophage subsets. *J Exp Med* (2018) 215(2):441–58. doi: 10.1084/jem.20170057

2. Seo SU, Kuffa P, Kitamoto S, Nagao-Kitamoto H, Rousseau J, Kim YG, et al. Intestinal macrophages arising from CCR2(+) monocytes control pathogen infection by activating innate lymphoid cells. *Nat Commun* (2015) 6:8010. doi: 10.1038/ncomms9010

3. Bain CC, Bravo-Blas A, Scott CL, Perdiguero EG, Geissmann F, Henri S, et al. Constant replenishment from circulating monocytes maintains the macrophage pool in the intestine of adult mice. *Nat Immunol* (2014) 15(10):929–37. doi: 10.1038/ni.2967

4. Zigmond E, Bernshtein B, Friedlander G, Walker CR, Yona S, Kim KW, et al. Macrophage-restricted interleukin-10 receptor deficiency, but not IL-10 deficiency, causes severe spontaneous colitis. *Immunity* (2014) 40(5):720–33. doi: 10.1016/j.immuni.2014.03.012

5. Menezes S, Melandri D, Anselmi G, Perchet T, Loschko J, Dubrot J, et al. The heterogeneity of Ly6C(hi) monocytes controls their differentiation into iNOS(+) macrophages or monocyte-derived dendritic cells. *Immunity* (2016) 45(6):1205–18. doi: 10.1016/j.immuni.2016.12.001

6. Guilliams M, Ginhoux F, Jakubzick C, Naik SH, Onai N, Schraml BU, et al. Dendritic cells, monocytes and macrophages: a unified nomenclature based on ontogeny. *Nat Rev Immunol* (2014) 14(8):571–8. doi: 10.1038/nri3712

7. Cheong C, Matos I, Choi JH, Dandamudi DB, Shrestha E, Longhi MP, et al. Microbial stimulation fully differentiates monocytes to DC-SIGN/CD209(+) dendritic cells for immune T cell areas. *Cell* (2010) 143(3):416–29. doi: 10.1016/j.cell.2010.09.039

8. Goudot C, Coillard A, Villani AC, Gueguen P, Cros A, Sarkizova S, et al. Aryl hydrocarbon receptor controls monocyte differentiation into dendritic cells versus macrophages. *Immunity* (2017) 47(3):582–596.e6. doi: 10.1016/j.immuni.2017.08.016

9. Coillard A, Guyonnet L, De Juan A, Cros A, Segura E. TLR or NOD receptor signaling skews monocyte fate decision via distinct mechanisms driven by mTOR and miR-155. *Proc Natl Acad Sci U.S.A.* (2021), 118(43). doi: 10.1073/pnas.2109225118

10. Bain CC, Scott CL, Uronen-Hansson H, Gudjonsson S, Jansson O, Grip O, et al. Resident and pro-inflammatory macrophages in the colon represent alternative context-dependent fates of the same Ly6Chi monocyte precursors. *Mucosal Immunol* (2013) 6(3):498–510. doi: 10.1038/mi.2012.89

11. Sidibe A, Ropraz P, Jemelin S, Emre Y, Poittevin M, Pocard M, et al. Angiogenic factor-driven inflammation promotes extravasation of human proangiogenic monocytes to tumours. *Nat Commun* (2018) 9(1):355. doi: 10.1038/s41467-017-02610-0

12. Auffray C, Fogg D, Garfa M, Elain G, Join-Lambert O, Kayal S, et al. Monitoring of blood vessels and tissues by a population of monocytes with patrolling behavior. *Science* (2007) 317(5838):666–70. doi: 10.1126/science.1142883

13. Thiesen S, Janciauskiene S, Uronen-Hansson H, Agace W, Högerkorp CM, Spee P, et al. CD14(hi)HLA-DR(dim) macrophages, with a resemblance to classical blood monocytes, dominate inflamed mucosa in crohn's disease. *J Leukoc Biol* (2014) 95 (3):531–41.

14. Smythies LE, Maheshwari A, Clements R, Eckhoff D, Novak L, Vu HL, et al. Mucosal IL-8 and TGF-beta recruit blood monocytes: evidence for cross-talk between the lamina propria stroma and myeloid cells. *J Leukoc Biol* (2006) 80(3):492–9. doi: 10.1189/jlb.1005566

15. Chapuy L, Bsat M, Sarkizova S, Rubio M, Therrien A, Wassef E, et al. Two distinct colonic CD14(+) subsets characterized by single-cell RNA profiling in crohn's disease. *Mucosal Immunol* (2019) 12(3):703–19. doi: 10.1038/s41385-018-0126-0

16. Nieminen JK, Sipponen T, Färkkilä M, Vaarala O. Monocyte-derived dendritic cells from crohn's disease patients exhibit decreased ability to activate T helper type 17 responses in memory cells. *Clin Exp Immunol* (2014) 177(1):190–202. doi: 10.1111/cei.12326

17. Salucci V, Rimoldi M, Penati C, Sampietro GM, van Duist MM, Matteoli G, et al. Monocyte-derived dendritic cells from crohn patients show differential NOD2/CARD15-dependent immune responses to bacteria. *Inflammation Bowel Dis* (2008) 14(6):812–8. doi: 10.1002/ibd.20390

18. Wick MJ. Human intestinal mononuclear phagocytes in health and inflammatory bowel disease. *Front Immunol* (2020) 11:410. doi: 10.3389/fimmu.2020.00410

19. Lamas B, Richard ML, Leducq V, Pham HP, Michel ML, Da Costa G, et al. CARD9 impacts colitis by altering gut microbiota metabolism of tryptophan into aryl hydrocarbon receptor ligands. *Nat Med* (2016) 22(6):598–605. doi: 10.1038/nm.4102

20. Erra Díaz F, Ochoa V, Merlotti A, Dantas E, Mazzitelli I, Gonzalez Polo V, et al. Extracellular acidosis and mTOR inhibition drive the differentiation of human monocyte-derived dendritic cells. *Cell Rep* (2020) 31(5):107613.

21. Cosin-Roger J, Simmen S, Melhem H, Atrott K, Frey-Wagner I, Hausmann M, et al. Hypoxia ameliorates intestinal inflammation through NLRP3/mTOR downregulation and autophagy activation. *Nat Commun* (2017) 8(1):98. doi: 10.1038/s41467-017-00213-3

22. Bernardo D, Marin AC, Fernández-Tomé S., Montalban-Arques A, Carrasco A, Tristán E, et al. Human intestinal pro-inflammatory CD11c(high)CCR2(+)CX3CR1(+) macrophages, but not their tolerogenic CD11c(-)CCR2(-)CX3CR1(-) counterparts, are expanded in inflammatory bowel disease. *Mucosal Immunol* (2018) 11(4):1114–26. doi: 10.1038/s41385-018-0030-7

23. Martin JC, Chang C, Boschetti G, Ungaro R, Giri M, Grout JA, et al. Single-cell analysis of crohn's disease lesions identifies a pathogenic cellular module associated with resistance to anti-TNF therapy. *Cell* (2019) 178(6):1493–1508.e20. doi: 10.1016/j.cell.2019.08.008

24. Cooney R, Baker J, Brain O, Danis B, Pichulik T, Allan P, et al. NOD2 stimulation induces autophagy in dendritic cells influencing bacterial handling and antigen presentation. *Nat Med* (2010) 16(1):90–7. doi: 10.1038/nm.2069

25. Macho Fernandez E, Valenti V, Rockel C, Hermann C, Pot B, Boneca IG, et al. Anti-inflammatory capacity of selected lactobacilli in experimental colitis is driven by NOD2-mediated recognition of a specific peptidoglycan-derived muropeptide. *Gut* (2011) 60(8):1050–9. doi: 10.1136/gut.2010.232918

26. Lessard AJ, LeBel M, Egarnes B, Prefontaine P, Theriault P, Droit A, et al. Triggering of NOD2 receptor converts inflammatory Ly6C(high) into Ly6C(low) monocytes with patrolling properties. *Cell Rep* (2017) 20(8):1830–43. doi: 10.1016/j.celrep.2017.08.009

27. Kim YG, Kamada N, Shaw MH, Warner N, Chen GY, Franchi L, et al. The Nod2 sensor promotes intestinal pathogen eradication via the chemokine CCL2-dependent recruitment of inflammatory monocytes. *Immunity* (2011) 34(5):769–80. doi: 10.1016/j.immuni.2011.04.013

28. Prescott D, Maisonneuve C, Yadav J, Rubino SJ, Girardin SE, Philpott DJ. NOD2 modulates immune tolerance via the GM-CSF-dependent generation of CD103(+) dendritic cells. *Proc Natl Acad Sci U.S.A.* (2020) 117(20):10946–57. doi: 10.1073/pnas.1912866117

29. Watanabe T, Asano N, Murray PJ, Ozato K, Tailor P, Fuss IJ, et al. Muramyl dipeptide activation of nucleotide-binding oligomerization domain 2 protects mice from experimental colitis. *J Clin Invest* (2008) 118(2):545–59.

30. Netea MG, Domínguez-Andrés J, Barreiro LB, Chavakis T, Divangahi M, Fuchs E, et al. Defining trained immunity and its role in health and disease. *Nat Rev Immunol* (2020) 20(6):375–88. doi: 10.1038/s41577-020-0285-6

31. Beikzadeh B, Delirezh N. Phenotypic and functional comparison of two distinct subsets of programmable cell of monocytic origin (PCMOs)-derived dendritic cells with conventional monocyte-derived dendritic cells. *Cell Mol Immunol* (2016) 13 (2):160–9. doi: 10.1038/cmi.2014.135

32. Moreira TG, Mangani D, Cox LM, Leibowitz J, Lobo ELC, Oliveira MA, et al. PD-L1(+) and XCR1(+) dendritic cells are region-specific regulators of gut homeostasis. *Nat Commun* (2021) 12(1):4907. doi: 10.1038/s41467-021-25115-3

33. Meuret G, Bitzi A, Hammer B. Macrophage turnover in crohn's disease and ulcerative colitis. *Gastroenterology* (1978) 74(3):501–3. doi: 10.1016/0016-5085(78)90285-8

34. Bune AJ, Hayman AR, Evans MJ, Cox TM. Mice lacking tartrate-resistant acid phosphatase (Acp 5) have disordered macrophage inflammatory responses and reduced clearance of the pathogen, staphylococcus aureus. *Immunology* (2001) 102 (1):103–13. doi: 10.1046/j.1365-2567.2001.01145.x

35. Niess JH, Brand S, Gu X, Landsman L, Jung S, McCormick BA, et al. CX3CR1-mediated dendritic cell access to the intestinal lumen and bacterial clearance. *Science* (2005) 307(5707):254–8. doi: 10.1126/science.1102901

36. Schulz O, Jaensson E, Persson EK, Liu X, Worbs T, Agace WW, et al. Intestinal CD103+, but not CX3CR1+, antigen sampling cells migrate in lymph and serve classical dendritic cell functions. *J Exp Med* (2009) 206(13):3101–14. doi: 10.1084/jem.20091925

37. Worthington JJ, Czajkowska BI, Melton AC, Travis MA. Intestinal dendritic cells specialize to activate transforming growth factor-β and induce Foxp3+ regulatory T cells via integrin αvβ8. *Gastroenterology* (2011) 141(5):1802–12. doi: 10.1053/j.gastro.2011.06.057

38. Cosín-Roger J, Ortiz-Masiá D, Calatayud S, Hernández C, Esplugues JV, Barrachina MD. The activation of wnt signaling by a STAT6-dependent macrophage phenotype promotes mucosal repair in murine IBD. *Mucosal Immunol* (2016) 9 (4):986–98. doi: 10.1038/mi.2015.123

39. Arnold IC, Mathisen S, Schulthess J, Danne C, Hegazy AN, Powrie F. CD11c(+) monocyte/macrophages promote chronic helicobacter hepaticus-induced intestinal inflammation through the production of IL-23. *Mucosal Immunol* (2016) 9(2):352–63. doi: 10.1038/mi.2015.65

40. Honda T, Egen JG, Lämmermann T, Kastenmüller W, Torabi-Parizi P, Germain RN. Tuning of antigen sensitivity by T cell receptor-dependent negative feedback controls T cell effector function in inflamed tissues. *Immunity* (2014) 40(2):235–47. doi: 10.1016/j.immuni.2013.11.017

41. Ma Y, Adjemian S, Mattarollo SR, Yamazaki T, Aymeric L, Yang H, et al. Anticancer chemotherapy-induced intratumoral recruitment and differentiation of antigen-presenting cells. *Immunity* (2013) 38(4):729–41. doi: 10.1016/j.immuni.2013.03.003

42. Wakim LM, Waithman J, van Rooijen N, Heath WR, Carbone FR. Dendritic cell-induced memory T cell activation in nonlymphoid tissues. *Science* (2008) 319 (5860):198–202. doi: 10.1126/science.1151869

43. Møller SH, Wang L, Ho PC. Metabolic programming in dendritic cells tailors immune responses and homeostasis. *Cell Mol Immunol* (2022) 19(3):370–83. doi: 10.1038/s41423-021-00753-1

44. Murugina NE, Budikhina AS, Dagil YA, Maximchik PV, Balyasova LS, Murugin VV, et al. Glycolytic reprogramming of macrophages activated by NOD1 and TLR4 agonists: no association with proinflammatory cytokine production in normoxia. *J Biol Chem* (2020) 295(10):3099–114. doi: 10.1074/jbc.RA119.010589

45. Wculek SK, Khouili SC, Priego E, Heras-Murillo I, Sancho D. Metabolic control of dendritic cell functions: digesting information. *Front Immunol* (2019) 10:775. doi: 10.3389/fimmu.2019.00775

46. Lee PY, Sykes DB, Ameri S, Kalaitzidis D, Charles JF, Nelson-Maney N, et al. The metabolic regulator mTORC1 controls terminal myeloid differentiation. *Sci Immunol* (2017) 2(11). doi: 10.1126/sciimmunol.aam6641

47. Hedl M, Yan J, Abraham C. IRF5 and IRF5 disease-risk variants increase glycolysis and human M1 macrophage polarization by regulating proximal signaling and Akt2 activation. *Cell Rep* (2016) 16(9):2442–55. doi: 10.1016/j.celrep.2016.07.060

48. Normand S, Waldschmitt N, Neerincx A, Martinez-Torres RJ, Chauvin C, Couturier- Maillard A, et al. Proteasomal degradation of NOD2 by NLRP12 in monocytes promotes bacterial tolerance and colonization by enteropathogens. *Nat Commun* (2018) 9(1):5338. doi: 10.1038/s41467-018-07750-5

49. Kim KW, Williams JW, Wang YT, Ivanov S, Gilfillan S, Colonna M, et al. MHC II+ resident peritoneal and pleural macrophages rely on IRF4 for development from circulating monocytes. *J Exp Med* (2016) 213(10):1951–9. doi: 10.1084/jem.20160486

50. Tamoutounour S, Henri S, Lelouard H, de Bovis B, de Haar C, van der Woude CJ, et al. CD64 distinguishes macrophages from dendritic cells in the gut and reveals the Th1-inducing role of mesenteric lymph node macrophages during colitis. *Eur J Immunol* (2012) 42(12):3150–66. doi: 10.1002/eji.201242847

51. Kolypetri P, Liu S, Cox LM, Fujiwara M, Raheja R, Ghitza D, et al. Regulation of splenic monocyte homeostasis and function by gut microbial products. *iScience* (2021) 24(4):102356. doi: 10.1016/j.isci.2021.102356

52. Jones GR, Bain CC, Fenton TM, Kelly A, Brown SL, Ivens AC, et al. Dynamics of colon monocyte and macrophage activation during colitis. *Front Immunol* (2018) 9:2764. doi: 10.3389/fimmu.2018.02764

53. Niess JH, Adler G. Enteric flora expands gut lamina propria CX3CR1+ dendritic cells supporting inflammatory immune responses under normal and inflammatory conditions. *J Immunol* (2010) 184(4):2026–37. doi: 10.4049/jimmunol.0901936

54. Laoui D, Keirsse J, Morias Y, Van Overmeire E, Geeraerts X, Elkrim Y, et al. The tumour microenvironment harbours ontogenically distinct dendritic cell populations with opposing effects on tumour immunity. *Nat Commun* (2016) 7:13720. doi: 10.1038/ncomms13720

55. Helft J, Bottcher J, Chakravarty P, Zelenay S, Huotari J, Schraml BU, et al. GM-CSF mouse bone marrow cultures comprise a heterogeneous population of CD11c(+) MHCII(+) macrophages and dendritic cells. *Immunity* (2015) 42(6):1197–211. doi: 10.1016/j.immuni.2015.05.018

56. Sallusto F, Lanzavecchia A. Efficient presentation of soluble antigen by cultured human dendritic cells is maintained by granulocyte/macrophage colony-stimulating factor plus interleukin 4 and downregulated by tumor necrosis factor alpha. *J Exp Med* (1994) 179(4):1109–18. doi: 10.1084/jem.179.4.1109

57. Romani N, Gruner S, Brang D, Kämpgen E, Lenz A, Trockenbacher B, et al. Proliferating dendritic cell progenitors in human blood. *J Exp Med* (1994) 180(1):83–93. doi: 10.1084/jem.180.1.83

58. Chapuis F, Rosenzwajg M, Yagello M, Ekman M, Biberfeld P, Gluckman JC. Differentiation of human dendritic cells from monocytes in vitro. *Eur J Immunol* (1997) 27(2):431–41. doi: 10.1002/eji.1830270213

59. Hiasa M, Abe M, Nakano A, Oda A, Amou H, Kido S, et al. GM-CSF and IL-4 induce dendritic cell differentiation and disrupt osteoclastogenesis through m-CSF receptor shedding by up-regulation of TNF-alpha converting enzyme (TACE). *Blood* (2009) 114(20):4517–26. doi: 10.1182/blood-2009-04-215020

60. Sander J, Schmidt SV, Cirovic B, McGovern N, Papantonopoulou O, Hardt AL, et al. Cellular differentiation of human monocytes is regulated by time-dependent interleukin-4 signaling and the transcriptional regulator NCOR2. *Immunity* (2017) 47 (6):1051–1066.e12. doi: 10.1016/j.immuni.2017.11.024

61. Smythies LE, Sellers M, Clements RH, Mosteller-Barnum M, Meng G, Benjamin WH, et al. Human intestinal macrophages display profound inflammatory anergy despite avid phagocytic and bacteriocidal activity. *J Clin Invest* (2005) 115(1):66–75. doi: 10.1172/JCI200519229

62. Byles V, Covarrubias AJ, Ben-Sahra I, Lamming DW, Sabatini DM, Manning B, et al. The TSC-mTOR pathway regulates macrophage polarization. *Nat Commun* (2013) 4:2834. doi: 10.1038/ncomms3834

63. Deng W, Yang J, Lin X, Shin J, Gao J, Zhong XP. Essential role of mTORC1 in self-renewal of murine alveolar macrophages. *J Immunol* (2017) 198(1):492–504. doi: 10.4049/jimmunol.1501845

64. Zhang M, Liu F, Zhou P, Wang Q, Xu C, Li Y, et al. The MTOR signaling pathway regulates macrophage differentiation from mouse myeloid progenitors by inhibiting autophagy. *Autophagy* (2019) 15(7):1150–62. doi: 10.1080/15548627.2019.1578040

65. Brunn GJ, Williams J, Sabers C, Wiederrecht G, Lawrence JC Jr, Abraham RT. Direct inhibition of the signaling functions of the mammalian target of rapamycin by the phosphoinositide 3-kinase inhibitors, wortmannin and LY294002. *EMBO J* (1996) 15(19):5256–67. doi: 10.1002/j.1460-2075.1996.tb00911.x

66. Tokuhira N, Kitagishi Y, Suzuki M, Minami A, Nakanishi A, Ono Y, et al. PI3K/AKT/PTEN pathway as a target for crohn's disease therapy (Review). *Int J Mol Med* (2015) 35(1):10–6. doi: 10.3892/ijmm.2014.1981

67. Gutierrez O, Pipaon C, Inohara N, Fontalba A, Ogura Y, Prosper F, et al. Induction of Nod2 in myelomonocytic and intestinal epithelial cells via nuclear factor-kappa b activation. *J Biol Chem* (2002) 277(44):41701–5. doi: 10.1074/jbc.M206473200

68. Gwinn DM, Shackelford DB, Egan DF, Mihaylova MM, Mery A, Vasquez DS, et al. AMPK phosphorylation of raptor mediates a metabolic checkpoint. *Mol Cell* (2008) 30(2):214–26. doi: 10.1016/j.molcel.2008.03.003

69. Sheng Y, Ju W, Huang Y, Li J, Ozer H, Qiao X, et al. Activation of wnt/β-catenin signaling blocks monocyte-macrophage differentiation through antagonizing PU.1-targeted gene transcription. *Leukemia* (2016) 30(10):2106–9.

70. Hedl M, Sun R, Huang C, Abraham C. STAT3 and STAT5 signaling thresholds determine distinct regulation for innate receptor-induced inflammatory cytokines, and STAT3/STAT5 disease variants modulate these outcomes. *J Immunol* (2019) 203 (12):3325–38. doi: 10.4049/jimmunol.1900031

71. Zhao Y, Shen X, Na N, Chu Z, Su H, Chao S, et al. mTOR masters monocyte development in bone marrow by decreasing the inhibition of STAT5 on IRF8. *Blood* (2018) 131(14):1587–99. doi: 10.1182/blood-2017-04-777128

72. Achuthan A, Cook AD, Lee MC, Saleh R, Khiew HW, Chang MW, et al. Granulocyte macrophage colony-stimulating factor induces CCL17 production via IRF4 to mediate inflammation. *J Clin Invest* (2016) 126(9):3453–66. doi: 10.1172/JCI87828

73. Jha AK, Huang SC, Sergushichev A, Lampropoulou V, Ivanova Y, Loginicheva E, et al. Network integration of parallel metabolic and transcriptional data reveals metabolic modules that regulate macrophage polarization. *Immunity* (2015) 42(3):419–30. doi: 10.1016/j.immuni.2015.02.005

74. He Z, Zhu X, Shi Z, Wu T, Wu L. Metabolic regulation of dendritic cell differentiation. *Front Immunol* (2019) 10:410. doi: 10.3389/fimmu.2019.00410

75. Kratchmarov R, Viragova S, Kim MJ, Rothman NJ, Liu K, Reizis B, et al. Metabolic control of cell fate bifurcations in a hematopoietic progenitor population. *Immunol Cell Biol* (2018) 96(8):863–71. doi: 10.1111/imcb.12040

76. Jangani M, Vuononvirta J, Yamani L, Ward E, Capasso M, Nadkarni S, et al. Loss of mTORC2-induced metabolic reprogramming in monocytes uncouples migration and maturation from production of proinflammatory mediators. *J Leukoc Biol* (2022) 111(5):967–80. doi: 10.1002/JLB.1A0920-588R

77. Cheng SC, Quintin J, Cramer RA, Shepardson KM, Saeed S, Kumar V, et al. mTOR- and HIF-1α-mediated aerobic glycolysis as metabolic basis for trained immunity. *Science* (2014) 345(6204):1250684.

78. Mehrotra P, Jamwal SV, Saquib N, Sinha N, Siddiqui Z, Manivel V, et al. Pathogenicity of mycobacterium tuberculosis is expressed by regulating metabolic

thresholds of the host macrophage. *PloS Pathog* (2014) 10(7):e1004265. doi: 10.1371/journal.ppat.1004265

79. Guo C, Islam R, Zhang S, Fang J. Metabolic reprogramming of macrophages and its involvement in inflammatory diseases. *Excli J* (2021) 20:628–41.

80. Hedl M, Li J, Cho JH, Abraham C. Chronic stimulation of Nod2 mediates tolerance to bacterial products. *Proc Natl Acad Sci U.S.A.* (2007) 104(49):19440–5. doi: 10.1073/pnas.0706097104

81. Yang S, Tamai R, Akashi S, Takeuchi O, Akira S, Sugawara S, et al. Synergistic effect of muramyldipeptide with lipopolysaccharide or lipoteichoic acid to induce inflammatory cytokines in human monocytic cells in culture. *Infect Immun* (2001) 69 (4):2045–53. doi: 10.1128/IAI.69.4.2045-2053.2001

82. Wolfert MA, Murray TF, Boons GJ, Moore JN. The origin of the synergistic effect of muramyl dipeptide with endotoxin and peptidoglycan. *J Biol Chem* (2002) 277 (42):39179–86. doi: 10.1074/jbc.M204885200

83. Biswas A, Petnicki-Ocwieja T, Kobayashi KS. Nod2: a key regulator linking microbiota to intestinal mucosal immunity. *J Mol Med (Berl)* (2012) 90(1):15–24. doi: 10.1007/s00109-011-0802-y

84. Chen Y, Salem M, Boyd M, Bornholdt J, Li Y, Coskun M, et al. Relation between NOD2 genotype and changes in innate signaling in crohn's disease on mRNA and miRNA levels. *NPJ Genom Med* (2017) 2:3. doi: 10.1038/s41525-016-0001-4

85. Boulet S, Daudelin JF, Odagiu L, Pelletier AN, Yun TJ, Lesage S, et al. The orphan nuclear receptor NR4A3 controls the differentiation of monocyte-derived dendritic cells following microbial stimulation. *Proc Natl Acad Sci U.S.A.* (2019) 116 (30):15150–9. doi: 10.1073/pnas.1821296116

86. Aziz A, Soucie E, Sarrazin S, Sieweke MH. MafB/c-maf deficiency enables self-renewal of differentiated functional macrophages. *Science* (2009) 326(5954):867–71. doi: 10.1126/science.1176056

87. Gibellini L, De Biasi S, Bianchini E, Bartolomeo R, Fabiano A, Manfredini M, et al. Anti-TNF-α drugs differently affect the TNFα-sTNFR system and monocyte subsets in patients with psoriasis. *PloS One* (2016) 11(12):e0167757.

88. Chomarat P, Banchereau J, Davoust J, Palucka AK. IL-6 switches the differentiation of monocytes from dendritic cells to macrophages. *Nat Immunol* (2000) 1(6):510–4. doi: 10.1038/82763

89. Yarilina A, Park-Min KH, Antoniv T, Hu X, Ivashkiv LB. TNF activates an IRF1-dependent autocrine loop leading to sustained expression of chemokines and STAT1-dependent type I interferon-response genes. *Nat Immunol* (2008) 9(4):378–87. doi: 10.1038/ni1576

90. Hedl M, Abraham C. Secretory mediators regulate Nod2-induced tolerance in human macrophages. *Gastroenterology* (2011) 140(1):231–41. doi: 10.1053/j.gastro.2010.09.009

91. Guzmán-Beltrán S, Torres M, Arellano M, Juárez E. Human macrophages chronically exposed to LPS can be reactivated by stimulation with MDP to acquire an antimicrobial phenotype. *Cell Immunol* (2017) 315:45–55. doi: 10.1016/j.cellimm.2017.02.004

92. Lee KH, Biswas A, Liu YJ, Kobayashi KS. Proteasomal degradation of Nod2 protein mediates tolerance to bacterial cell wall components. *J Biol Chem* (2012) 287 (47):39800–11. doi: 10.1074/jbc.M112.410027

93. Bist P, Cheong WS, Ng A, Dikshit N, Kim BH, Pulloor NK, et al. E3 ubiquitin ligase ZNRF4 negatively regulates NOD2 signalling and induces tolerance to MDP. *Nat Commun* (2017) 8:15865. doi: 10.1038/ncomms15865

94. Weichart D, Gobom J, Klopfleisch S, Häsler R, Gustavsson N, Billmann S, et al. Analysis of NOD2-mediated proteome response to muramyl dipeptide in HEK293 cells. *J Biol Chem* (2006) 281(4):2380–9. doi: 10.1074/jbc.M505986200

95. Sieminska I, Baran J. Myeloid-derived suppressor cells in colorectal cancer. *Front Immunol* (2020) 11:1526. doi: 10.3389/fimmu.2020.01526

96. Maier B, Leader AM, Chen ST, Tung N, Chang C, LeBerichel J, et al. A conserved dendritic-cell regulatory program limits antitumour immunity. *Nature* (2020) 580(7802):257–62. doi: 10.1038/s41586-020-2134-y

97. Watanabe R, Hilhorst M, Zhang H, Zeisbrich M, Berry GJ, Wallis BB, et al. Glucose metabolism controls disease-specific signatures of macrophage effector functions. *JCI Insight* (2018) 3(20). doi: 10.1172/jci.insight.123047

98. Roberts DJ, Tan-Sah VP, Ding EY, Smith JM, Miyamoto S. Hexokinase-II positively regulates glucose starvation-induced autophagy through TORC1 inhibition. *Mol Cell* (2014) 53(4):521–33. doi: 10.1016/j.molcel.2013.12.019

99. Chin WY, He CY, Chow TW, Yu QY, Lai LC, Miaw SC. Adenylate kinase 4 promotes inflammatory gene expression via Hif1α and AMPK in macrophages. *Front Immunol* (2021) 12:630318. doi: 10.3389/fimmu.2021.630318

100. Chapman TP, Corridoni D, Shiraishi S, Pandey S, Aulicino A, Wigfield S, et al. Ataxin-3 links NOD2 and TLR2 mediated innate immune sensing and metabolism in myeloid cells. *Front Immunol* (2019) 10:1495. doi: 10.3389/fimmu.2019.01495

101. Otto NA, Butler JM, Ramirez-Moral I, van Weeghel M, van Heijst JWJ, Scicluna BP, et al. Adherence affects monocyte innate immune function and metabolic reprogramming after lipopolysaccharide stimulation in vitro. *J Immunol* (2021) 206(4):827–38. doi: 10.4049/jimmunol.2000702

102. Mogilenko DA, Haas JT, L'Homme L, Fleury S, Quemener S, Levavasseur M, et al. Metabolic and innate immune cues merge into a specific inflammatory response via the UPR. *Cell* (2019) 177(5):1201–1216.e19.

103. Fritz T, Niederreiter L, Adolph T, Blumberg RS, Kaser A. Crohn's disease: NOD2, autophagy and ER stress converge. *Gut* (2011) 60(11):1580–8. doi: 10.1136/gut.2009.206466

104. Park SM, Kang TI, So JS. Roles of XBP1s in transcriptional regulation of target genes. *Biomedicines* (2021) 9(7). doi: 10.3390/biomedicines9070791

105. Huang Z, Wang J, Xu X, Wang H, Qiao Y, Chu WC, et al. Antibody neutralization of microbiota-derived circulating peptidoglycan dampens inflammation and ameliorates autoimmunity. *Nat Microbiol* (2019) 4(5):766–73. doi: 10.1038/s41564-019-0381-1

106. Nguyen DX, Ehrenstein MR. Anti-TNF drives regulatory T cell expansion by paradoxically promoting membrane TNF-TNF-RII binding in rheumatoid arthritis. *J Exp Med* (2016) 213(7):1241–53. doi: 10.1084/jem.20151255

107. Baldwin HM, Ito-Ihara T, Isaacs JD, Hilkens CM. Tumour necrosis factor alpha blockade impairs dendritic cell survival and function in rheumatoid arthritis. *Ann Rheum Dis* (2010) 69(6):1200–7. doi: 10.1136/ard.2009.110502

108. Funk JO, Walczak H, Voigtländer C, Berchtold S, Baumeister T, Rauch P, et al. Cutting edge: resistance to apoptosis and continuous proliferation of dendritic cells deficient for TNF receptor-1. *J Immunol* (2000) 165(9):4792–6. doi: 10.4049/jimmunol.165.9.4792

109. Erlich Z, Shlomovitz I, Edry-Botzer L, Cohen H, Frank D, Wang H, et al. Macrophages, rather than DCs, are responsible for inflammasome activity in the GM-CSF BMDC model. *Nat Immunol* (2019) 20(4):397–406. doi: 10.1038/s41590-019-0313-5

110. Spörri R, Reis e Sousa C. Inflammatory mediators are insufficient for full dendritic cell activation and promote expansion of CD4+ T cell populations lacking helper function. *Nat Immunol* (2005) 6(2):163–70. doi: 10.1038/ni1162

111. Kratochvill F, Neale G, Haverkamp JM, Van de Velde LA, Smith AM, Kawauchi D, et al. TNF counterbalances the emergence of M2 tumor macrophages. *Cell Rep* (2015) 12(11):1902–14. doi: 10.1016/j.celrep.2015.08.033

112. Al Nabhani Z, Dulauroy S, Marques R, Cousu C, Al Bounny S, Déjardin F, et al. A weaning reaction to microbiota is required for resistance to immunopathologies in the adult. *Immunity* (2019) 50(5):1276–1288.e5. doi: 10.1016/j.immuni.2019.02.014

113. Kramer M, Netea MG, de Jong DJ, Kullberg BJ, Adema GJ. Impaired dendritic cell function in crohn's disease patients with NOD2 3020insC mutation. *J Leukoc Biol* (2006) 79(4):860–6. doi: 10.1189/jlb.0805484

114. Horiuchi K, Kimura T, Miyamoto T, Takaishi H, Okada Y, Toyama Y, et al. Cutting edge: TNF-alpha-converting enzyme (TACE/ADAM17) inactivation in mouse myeloid cells prevents lethality from endotoxin shock. *J Immunol* (2007) 179(5):2686–9. doi: 10.4049/jimmunol.179.5.2686

115. Zheng C, Shi X. Cysteinyl leukotriene receptor 1 (cysLT1R) regulates osteoclast differentiation and bone resorption. *Artif Cells Nanomed Biotechnol* (2018) 46(sup3): S64–s70. doi: 10.1080/21691401.2018.1489264

116. El Kasmi KC, Smith AM, Williams L, Neale G, Panopoulos AD, Watowich SS, et al. Cutting edge: a transcriptional repressor and corepressor induced by the STAT3-regulated anti-inflammatory signaling pathway. *J Immunol* (2007) 179(11):7215–9. doi: 10.4049/jimmunol.179.11.7215

117. Klappacher GW, Lunyak VV, Sykes DB, Sawka-Verhelle D, Sage J, Brard G, et al. An induced ets repressor complex regulates growth arrest during terminal macrophage differentiation. *Cell* (2002) 109(2):169–80. doi: 10.1016/S0092-8674(02)00714-6

118. Jang MH, Sougawa N, Tanaka T, Hirata T, Hiroi T, Tohya K, et al. CCR7 is critically important for migration of dendritic cells in intestinal lamina propria to mesenteric lymph nodes. *J Immunol* (2006) 176(2):803–10. doi: 10.4049/jimmunol.176.2.803

119. Poulin LF, Henri S, de Bovis B, Devilard E, Kissenpfennig A, Malissen B. The dermis contains langerin+ dendritic cells that develop and function independently of epidermal langerhans cells. *J Exp Med* (2007) 204(13):3119–31. doi: 10.1084/jem.20071724

120. Couturier-Maillard A, Secher T, Rehman A, Normand S, De Arcangelis A, Haesler R, et al. NOD2-mediated dysbiosis predisposes mice to transmissible colitis and colorectal cancer. *J Clin Invest* (2013) 123(2):700–11. doi: 10.1172/JCI62236

121. Park EK, Jung HS, Yang HI, Yoo MC, Kim C, Kim KS. Optimized THP-1 differentiation is required for the detection of responses to weak stimuli. *Inflammation Res* (2007) 56(1):45–50. doi: 10.1007/s00011-007-6115-5

122. Maeß MB, Wittig B, Cignarella A, Lorkowski S. Reduced PMA enhances the responsiveness of transfected THP-1 macrophages to polarizing stimuli. *J Immunol Methods* (2014) 402(1-2):76–81.

123. Chen EY, Tan CM, Kou Y, Duan Q, Wang Z, Meirelles GV, et al. Enrichr: interactive and collaborative HTML5 gene list enrichment analysis tool. *BMC Bioinf* (2013) 14:128. doi: 10.1186/1471-2105-14-128

124. Kuleshov MV, Jones MR, Rouillard AD, Fernandez NF, Duan Q, Wang Z, et al. Enrichr: a comprehensive gene set enrichment analysis web server 2016 update. *Nucleic Acids Res* (2016) 44(W1):W90–7. doi: 10.1093/nar/gkw377

125. Xie Z, Bailey A, Kuleshov MV, Clarke DJB, Evangelista JE, Jenkins SL, et al. Gene set knowledge discovery with enrichr. *Curr Protoc* (2021) 1(3):e90. doi: 10.1002/cpz1.90

frontiers | Frontiers in Immunology

TYPE Review
PUBLISHED 06 October 2023
DOI 10.3389/fimmu.2023.1194988

OPEN ACCESS

EDITED BY
Yanan Ma,
Memorial Sloan Kettering Cancer Center, United States

REVIEWED BY
Vidyanath Chaudhary,
Hospital for Special Surgery, United States
Xin Li,
Houston Methodist Research Institute, United States

*CORRESPONDENCE
Hans-Joachim Anders
hjanders@med.uni-muenchen.de

RECEIVED 27 March 2023
ACCEPTED 22 September 2023
PUBLISHED 06 October 2023

CITATION
Long H, Lichtnekert J, Andrassy J, Schraml BU, Romagnani P and Anders H-J (2023) Macrophages and fibrosis: how resident and infiltrating mononuclear phagocytes account for organ injury, regeneration or atrophy.
Front. Immunol. 14:1194988.
doi: 10.3389/fimmu.2023.1194988

Macrophages and fibrosis: how resident and infiltrating mononuclear phagocytes account for organ injury, regeneration or atrophy

Hao Long[1,2,3], Julia Lichtnekert[1], Joachim Andrassy[4], Barbara U. Schraml[5,6], Paola Romagnani[7] and Hans-Joachim Anders[1*]

[1]Division of Nephrology, Department of Medicine IV, University Hospital, Ludwig-Maximilians-University (LMU), Munich, Germany, [2]Department of Urology, The Affiliated Hospital of Southwest Medical University, Luzhou, China, [3]Sichuan Clinical Research Center for Nephropathy, Luzhou, China, [4]Department of General, Visceral and Transplant Surgery, University Hospital of Ludwig-Maximilians-University (LMU) Munich, Munich, Germany, [5]Institute for Cardiovascular Physiology and Pathophysiology, Biomedical Center, Ludwig-Maximilians-University (LMU), Munich, Germany, [6]Walter-Brendel-Centre of Experimental Medicine, University Hospital, Ludwig-Maximilians-University (LMU), Munich, Germany, [7]Department of Biomedical, Experimental and Clinical Sciences "Mario Serio", University of Firenze, Nephrology and Dialysis Unit, Meyer Children's Hospital, Firenze, Italy

Mononuclear phagocytes (MP), i.e., monocytes, macrophages, and dendritic cells (DCs), are essential for immune homeostasis via their capacities to clear pathogens, pathogen components, and non-infectious particles. However, tissue injury-related changes in local microenvironments activate resident and infiltrating MP towards pro-inflammatory phenotypes that contribute to inflammation by secreting additional inflammatory mediators. Efficient control of injurious factors leads to a switch of MP phenotype, which changes the microenvironment towards the resolution of inflammation. In the same way, MP endorses adaptive structural responses leading to either compensatory hypertrophy of surviving cells, tissue regeneration from local tissue progenitor cells, or tissue fibrosis and atrophy. Under certain circumstances, MP contribute to the reversal of tissue fibrosis by clearance of the extracellular matrix. Here we give an update on the tissue microenvironment-related factors that, upon tissue injury, instruct resident and infiltrating MP how to support host defense and recover tissue function and integrity. We propose that MP are not intrinsically active drivers of organ injury and dysfunction but dynamic amplifiers (and biomarkers) of specific tissue microenvironments that vary across spatial and temporal contexts. Therefore, MP receptors are frequently redundant and suboptimal targets for specific therapeutic interventions compared to molecular targets upstream in adaptive humoral or cellular stress response pathways that influence tissue milieus at a contextual level.

KEYWORDS

dendritic cells, macrophages, inflammation, necrosis, fibrosis, polyploidy

1 Introduction

Tissue fibrosis is defined by an excess of extracellular matrix (ECM) and characterized by tissue stiffness (sclerosis), which can impair the function of elastic organs such as the heart, lungs, or skin (1). In addition, excess ECM can impair transepithelial transport functions, e.g., in the lungs (air-blood-air) and the kidneys (urine-blood-urine) (2). Apart from progressive scleroderma, where autoimmunity directly triggers fibrosis in otherwise healthy organs, in most cases, fibrosis does not spread into healthy tissue, e.g., in dermal wound healing (3). Generally, fibrosis instead serves as a marker for adaptive mechanisms responding to focal or diffuse parenchymal injury. For example, in the heart, liver, and kidney, interstitial fibrosis is a typical result of ischemic or toxic parenchymal damage leading to compensatory parenchymal cell hypertrophy, a process involving cell cycle entry, polyploidization, and a hypersecretory cell state involving the secretion of pro-fibrotic mediators (4). In this context, tissue-resident or infiltrating MP amplify the pro-fibrotic microenvironment, fibroblasts, and downstream ECM producers (5, 6). Here we focus on the role of MP in tissue injury and repair to understand better their role in fibrogenesis. We briefly summarize the spectrum of tissue-resident and infiltrating MP and the recent progress in their role in the different phases of injury, repair, and progressive and reversible fibrosis.

2 Development and definition of mononuclear phagocytes

MP comprising macrophages, monocytes, and DCs can be found in all lymphoid and non-lymphoid tissues (7). Macrophages develop from two distinct haematopoetic lineages and can therefore be divided in fetal-derived and monocyte derived macrophages. Fetal-derived macrophages arise from erythro-myeloid progenitors from the yolk sac and colonize the fetal liver before birth. Some of these macrophages persist into adulthood as resident cells in various tissues and are able to self-renew (Figure 1) (8). The expression of macrophage colony-stimulating factor 1 receptor (CSF-1R) plays a pivotal role in regulating the development of macrophages. In mice lacking CSF-1 tissue-resident macrophages in most organs are absent (9).

In contrast, monocytes and DCs derive from bone marrow progenitors. In the bone marrow, hematopoietic stem cells (HSCs) can differentiate into common myeloid progenitor cells (CMPs). When stimulated by FMS-like tyrosine kinase 3 ligand (Flt3L), some of these CMPs can further develop into macrophage and dendritic cell progenitor cells (MDPs). MDPs represent a specific precursor for both common dendritic cell progenitor cells (CDPs) and monocyte progenitor cells (CMoPs). CMoPs can differentiate into monocytes under the stimulation of CSF 1/2. During inflammation, macrophages can derive from monocytes, called

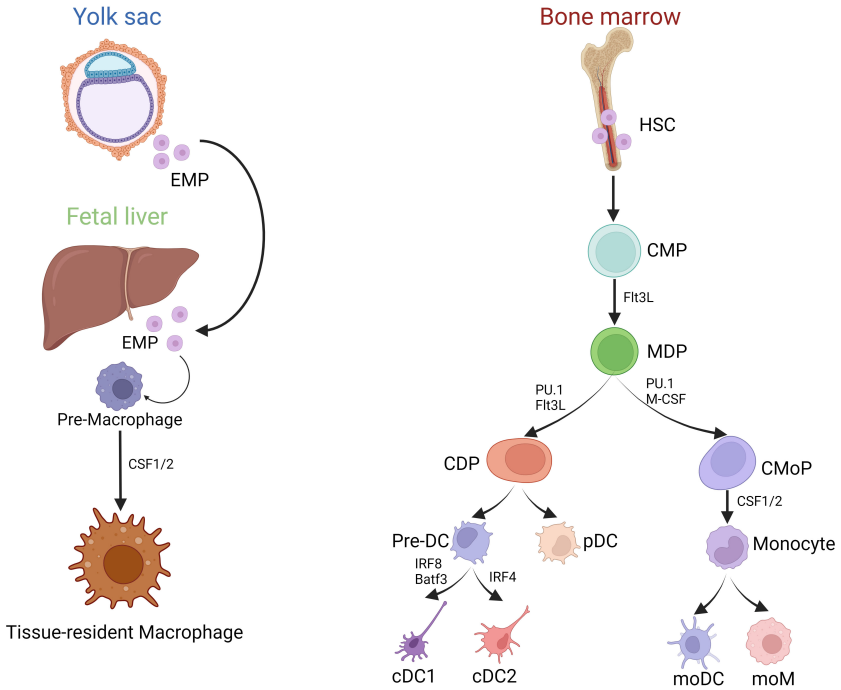

FIGURE 1
Development of MP. (Created with BioRender.com) Development of MP mainly includes two sources: (1) Yolk sac and Fetal liver erythrocyte-myeloid progenitor (EMP)-derived way; (2) Bone marrow HSC derived way. Tissue-resident macrophages primarily originate from embryonic yolk sac EMPs and fetal liver EMPs, whereas bone marrow-derived monocytes enter the tissues during inflammatory conditions as infiltrating cells, and then differentiate into moDC and moM. However, bone marrow HSCs can evolve into CMPs, and part of them can differentiate into MDPs under the stimulation of Flt3L. MDPs are directed precursors of CDPs and CMoPs. After evolving, CDPs can produce each subgroup of the DCs series, including precursor DC (pre-DC) and pDC. IRF8 is required for the lineage development of cDC1s, helping to define distinct cDC1 subsets. IRF4, a nuclear factor interacting with PU.1, is essential for many aspects of cDC2 function.

monocyte-derived macrophages (moM) (Figure 1). CDPs, derived from MDPs, can be further categorized into plasmacytoid dendritic cells (pDCs) and conventional dendritic cells (cDCs). pDCs are particularly known for their capacity to secrete alpha interferons (IFN), while cDCs are considered highly effective in activating T-cell responses (7). cDCs further divide into IRF8 and Batf3-dependent type I conventional dendritic cells (cDC1s) that excel at cross-presentation and IRF4-expressing type II conventional dendritic cells (cDC2s), best known for their ability to drive T helper (Th) cell differentiation (10, 11). cDC2s are heterogeneous, with subpopulations with non-redundant functions in Th17 and Th2 responses regulated by NOTCH2 and KLF4, respectively (12). In addition, the development of cDCs and pDCs relies mainly on the hematopoietic cytokine Flt3L.

Historically, macrophages were defined by positivity for F4/80 and DCs by positivity for CD11c and major histocompatibility complex (MHC) II. However, macrophages, monocytes, and DCs may overlap in phenotype and function (7, 13), and this is particularly prominent for example in the kidney, which is why macrophages and DCs in the kidney are referred to as renal MP (14). In addition, surface marker expression profiles are dynamic and depend on cell maturation and activation status (15), which makes it difficult to attribute specific functions to specific subtypes of cells.

Flt3L stimulates the differentiation of both populations of dendritic cells *in vitro*, providing an accurate reflection of the physiological process. On the other hand, culturing bone marrow (BM) cells in the presence of granulocyte-macrophage colony-stimulating factor (GM-CSF) results in DCs resembling those derived from monocytes (moDC). However, when BM cells are cultured with a combination of GM-CSF and Flt3L, generating a significant quantity of $CD103^+$ DCs is possible, which is a promising target for tolerance induction or vaccination (16).

A way of classifying macrophages has been assessed by *in vitro* assays where, under the influence of various cytokines representing distinct tissue microenvironments, macrophages turn into individual phenotypes with specific secretome and functional capacities (Table 1). Nevertheless, the spectrum of different techniques used to describe MP to distinct cell populations is one of the reasons for some uncertainty in the nomenclature (17).

Refined lineage-tracing technologies of macrophages, monocytes, and DCs have facilitated the distinction of these cells (13, 15, 18–20). Therefore, a classification of MP subtypes based on cell origin has been suggested (21). Such a definition has limitations and may not be tenable in the dynamics of acute disorders with changing microenvironments when cell types exhibit phenotypic plasticity, and lineage tracing-related definitions are less valuable. However, it has become clear that MP subtypes have specific functions in pathology (22, 23). Defining cell types by lineage-specific transcription factors is a powerful tool to establish the functions of MP in immunity. Recently, lineage-specific transcription factors have been used to determine the functions of different MP lineages, such as MAFB for macrophages and ZBTB46 for DCs (24). Likewise, IRF4, a nuclear factor that interacts with PU.1, is essential for the many aspects of cDC2s function but also mediates macrophage polarization to the M2 phenotype (21). However, such models have limitations, e.g., expression by other immune cell lineages (25) (Table 2).

3 Mononuclear phagocytes in tissue injury and repair

These highly phagocytic cells sense their environment for signs of damage or pathogens and initiate immune responses. MP are present in different organs, e.g. in the bone, where the turnover process requires osteoclasts, while in the liver, Kupffer cells are in charge of eliminating pathogens and pathogen components from the blood in the portal vein, clearing old red blood cells, and recovering iron ions (26). MP reside in different compartments in the same organ. For example, macrophages located in the alveolar space are called alveolar macrophages, while macrophages found in

TABLE 1 Types of macrophages and their related phenotypes.

M0	M1	M2a	M2b	M2c
Tissue-resident macrophages, highly plastic, multifunctional cells	Classic activation phenotype, Pro-inflammatory macrophages, Support the development of Th1	Alternative activation phenotype and anti-inflammatory/pro-fibrotic macrophages, Support the development of Th2		
	Pro-inflammatory and host defense phenotype	Anti-inflammatory Phenotype, promote Wound healing and tissue fibrosis	Anti-inflammatory phenotype, immunoregulation	Pro-regenerative and healing phenotype
	Induced by LPS, IFN-γ	Mainly induced by IL-4	Induced by immune compound and IL-1R and/or TLR ligands	Induced by IL-10, TGF-β, glucocorticoids
	Secrete TNF-α, IL-1, IL-6, IL-12, IL-23, iNOS, MMP12, MINCLE	Secrete significant amounts of IL-10 and IL-1R antagonists	Contribute to Th2-like activation, produce IL-10	Secrete TGF-β, IL-10, ARG1
	Upregulate MHC-II, CD16, CD32, CD80, CD86	Down-regulate IL-1β, IL-12, NO	Downregulate TNF-α, IL-1β, IL-12, IL-6	Downregulate TNF-α, IL-1β, IL-12, IL-6

Th1(T helper cells type 1), LPS (Lopopolysaccharides), IFN-γ (Interferon γ), TNF-α (Tumor Necrosis Factor α), IL (Interleukin), iNOS (Inducible Nitric Oxide Synthase), MMP12(Matrix Metalloproteinase 12), MINCLE (Macrophage-inducible C-type Lectin), MHC-II (Major Histocompatibility Complex Class II), Th2(T helper cells type 2), NO (Nitrogen Oxide), IL-1R (Interleukin 1 Receptor), TLR (Toll-like Receptor), TGF-β (Transforming Growth Factor β), ARG1 (Arginase 1).

TABLE 2 Different lineages of mouse MP.

MP	Subsets	Surface Markers	Transcription factors	Functions
Monocytes	Ly6C high inflammatory	Ly6C high, CCR2 high	KLF4	Differentiate into DCs and tissue macrophages during inflammation
Macrophages	Ly6C low patrolling	Ly6C low, CCR2 low, Cx3CR1	MAFB	Endothelial integrality
	Tissue-specific	F4/80, MERTK, CD64, CD11b	MAFB	Tissue-specific: Lungs (Alveolar macrophages), Bone (osteoclasts), Liver (Kupffer cells), etc.
Dendritic cells	pDCs	SIGLEC H, BST2, CD123, BDCA2, AXL, CD45RA, CD33	TCF4(E2-2), ZEB2	Production of type I IFNs
	cDC1s	XCR1, CD103, Clec9a, CD11c, MHC-II, CD205	ZBTB46, IRF8	Th1 and CTL immune, cross-presentation, IL-12 production
	cDC2s	CD11b, CD11c, SIRP-α, MHC-ii, CD205	ZBTB46, IRF4, NOTCH2, KLF4	Th2 and Th17 immune, IL-23 and IL-6 production

MP (Mononuclear Phagocytes), pDCs (plasmacytoid dendritic cells), cDC1s (Type I conventional dendritic cells), cDC2s (Type II conventional dendritic cells), CCR2 (C-C motif Chemokine Receptor 2), CX3CR1 (C-X3-C motif Chemokine Receptor 1), MERTK (MER Proto Oncogene, Tyrosine Kinase), SIGLEC-H (Sialic acid binding Ig-like Lectin H), BST2 (Bone Marrow Stromal Cell Antigen 2), BDCA2 (Blood Dendritic Cell Antigen 2), XCR1 (X-C motif Chemokine Receptor 1), Clec9a (C-type Lectin Domain Containing 9A), MHC-II (Major Histocompatibility Complex Class II), SIRP-α (Signal Regulatory Protein α), KLF4 (Kruppel-like factor 4), MAFB (MAF BZIP Transcription Factor B), TCF4 (Transcription factor 4), ZEB2 (Zinc Finger E-Box Binding Homeobox 2), ZBTB46 (Zinc finger and BTB domain containing 46), IRF8 (Interferon Regulatory Factor 8), IRF4 (Interferon Regulatory Factor 4), NOTCH2 (Neurogenic locus notch homolog protein 2), IFNs (Interferons), Th1(T helper cells type 1), CTL (Cytotoxic T cell), IL (Interleukin), Th2(T helper cells type 2), Th17(T helper cells type 17).

interstitial compartments are referred to as interstitial macrophages (27). Here, we describe the different microenvironments along tissue injury and repair and discuss the respective contribution of MP in these contexts.

3.1 Tissue injury and necroinflammation

Invasion of pathogens, exposure to toxins, metabolic stress, ischemia, trauma, or the presence of malignant cells are triggers of cell injury and the release of Danger-Associated Molecular Patterns (DAMPs) or Pathogen-Associated Molecular Patterns (PAMPs), respectively. These molecules trigger immune responses and hence promote further tissue damage. PAMPs occur on the surface of pathogens, including lipopolysaccharide (LPS) and bacterial or viral nucleic acids. DAMPs are released from damaged or dying cells, including intracellular molecules, such as S100A9 proteins, HMGB1, uric acid, and histones. PAMPs and DAMPs have the identical ability to activate pattern recognition receptors (PRRs) of the innate immune system, such as Toll-like receptors (TLRs), NOD-like receptors (NLRs), C-type lectin receptors (CLRs) or inflammasomes to secrete multiple pro-inflammatory mediators that induce local inflammation (9, 28–30). Parenchymal cells and resident MP are the first cell types that sense danger and initiate evolutionarily conserved defense mechanisms that create a barrier to intruding pathogens. Histamine and other vasoactive mediators induce endothelial leakage, allowing serum components such as immunoglobulins and other opsonin to reach the injury site. Local chemokine release and upregulation of adhesion molecules on the luminal endothelial surface facilitate the transmigration of first neutrophils and subsequently CC-chemokine receptor 2^+ ($CCR2^+$) monocytes to limit pathogen spreading by direct killing and phagocytic clearance (31, 32). Upon arrival, such monocytes encounter a microenvironment characterized by DAMPs (in case of infection also PAMPs), chemokines such as C-chemokine ligand-2 (CCL2), chemokine fractalkine (CX3CL1), etc., which specifically attract monocytes. Once at the injury site, monocytes can serve as effectors or further differentiate into moM or moDC (33, 34). Meanwhile, pro-inflammatory cytokines and lipid mediators induce a pro-inflammatory macrophage phenotype, which is difficult to distinguish from activated resident macrophage populations by surface markers. Such pro-inflammatory macrophage phenotypes share similarities with cultured macrophages stimulated with IFN-γ and LPS, referred to as the M1 phenotype which supports the development of Th1. M1 macrophages are characterized by activation markers on the cell surface and molecules involved in antigen presentation, including MHC-II, CD16, CD32, CD80, and CD86 (35–38). Meanwhile, M1 macrophages enhance the inflammatory microenvironment by producing pro-inflammatory mediators, such as TNF-α, IL-1, IL-6, IL-12, IL-23, and other molecules such as inducible nitric oxide synthase (iNOS), matrix metalloproteinase 12 (MMP-12), and macrophage-induced C-type lectin (MINCLE) (Table 1). This contribution to the inflammatory milieu leads to the initiation of various forms of regulated cell death, like necrosis, apoptosis, and pyroptosis. Moreover, when cells undergo necrosis, they release additional DAMPs, further activating neighboring MP. The auto-amplification loop is called necroinflammation (39, 40).

Furthermore, different subsets of DCs accelerate tissue inflammation in a complementary manner. pDCs release large amounts of type I IFNs essential for antiviral immune defense (41, 42). Tissue-resident cDC1s and cDC2s detect immunogenic substances and further recognize and release pro-inflammatory mediators such as CXCL2, IL-12, and IL-6 (14). Significantly

CXCL2 changes the microenvironment by recruiting neutrophils, which promote necroinflammation (43). In addition to cytokine production, cDC1s, and cDC2s enter regional lymph nodes to initiate adaptive immune responses. Among them, a unique feature of cDC1s is the ability to cross-present antigens to $CD8^+$ T cells, whereas cDC2s cross-present antigens to $CD4^+$ T cells (44, 45).

Recently, the multifaceted role of the adaptive immune system in the pro-inflammatory environment of the damaged heart after acute myocardial infarction has been elucidated (46). Under the stress of chronic overload, DCs accumulate potent γ-ketoaldehydes, which activate the pro-inflammatory program of reactive oxygen species (ROS) and the secretion of IL-1β, IL-6, and IL-23 (47). DCs can also increase the expression of T-cell co-stimulatory proteins. In a hypertensive state, heart DCs promote the proliferation of T cells, particularly $CD8^+$ T cells, and contribute to their polarization towards a pro-inflammatory phenotype (47–49). So, DCs play a pro-inflammatory role in cardiac injury by sustaining oxidative stress, releasing pro-inflammatory factors, and activating T cells.

3.2 Resolution of inflammation

In vitro studies dissect three subsets of M2 macrophages based on their phenotypes and functions (Table 1). M2a macrophages respond to IL-4 and IL-13 and show a predominantly anti-inflammatory phenotype. They secrete high levels of IL-10 and IL-1 receptor antagonists, and growth factors that aid tissue healing by stabilizing angiogenesis, such as platelet-derived growth factor (PDGF), transforming growth factor β (TGF-β), etc. which help to suppress the inflammatory response (50, 51). Additionally, M2a macrophages can induce an anti-inflammatory Th2-like immune response, promote wound healing, and contribute to tissue fibrosis. On the other hand, M2b macrophages can participate in immunoregulation and contribute to Th2-like activation induced by immune complexes and TLR and/or IL-1R ligands. They produce IL-10, which further contributes to the anti-inflammatory response. M2c macrophages are activated by various factors such as IL-10, TGF-β, and glucocorticoids. These stimuli induce a specific phenotype in M2c macrophages characterized by their ability to promote tissue repair and inhibit tissue inflammation (52–54).. Control of inflammation is essential to limit immunopathology. Therefore, the activation of pro-inflammatory signaling pathways precedes their deactivation via the subsequent induction of anti-inflammatory signaling pathways. Well-known phenomena of endotoxin tolerance or ischemic preconditioning represent this process. For example, macrophages participate in efferocytosis, a process in which they engulf apoptotic neutrophils (31, 55). Efferocytosis initiates the resolution of inflammation, which prevents further neutrophil recruitment and eliminates neutrophils silently before they may undergo secondary necrosis (56, 57). Efferocytosis induces a shift to an "alternately activated" macrophage phenotype, also known as the M2 type (Table 1). The interaction between M2 macrophages and the adaptive immune system is critical for resolving inflammatory responses in multiple tissues, especially with Th2 cells (58) and regulatory T cells (Tregs) (59–61). M2 macrophages stimulate epicardial progenitor cell proliferation (62) and promote the secretion of ECM molecules and tissue remodeling (63). In contrast to M1 macrophages, M2 macrophages express the enzyme arginase 1 (ARG1) constitutively. ARG1 is responsible for hydrolyzing L-arginine into L-ornithine, a crucial precursor for producing polyamines necessary for cell survival. Additionally, L-ornithine can generate proline and hydroxyproline, essential amino acids required for collagen synthesis. Collagen is vital in maintaining the structural integrity of non-injured tissue parenchyma (64, 65).

DCs exhibit their contributions to the innate and adaptive immune systems as gatekeepers for the induction of adaptive immunity. Harmless foreign proteins circulating in the bloodstream get filtered in the kidney, transported across proximal tubular epithelial cells, and can reach the kidney lymph nodes independent of DC uptake and processing. Once in the lymph node, local tolerogenic DCs process these proteins. This mechanism helps preventing immune responses against harmless foreign or self-proteins in the serum (66). $Batf3^+$ DCs in the kidney lymph nodes present filtered antigens along with programmed cell death ligand 1(PD-L1) to cytotoxic T lymphocytes (CTLs), resulting in cross-tolerance development (67).

3.3 Tissue adaptation to injury: hypertrophy, regeneration, fibrosis

3.3.1 Hypertrophy

The tissue response to injury differs across cell lineages and stages of differentiation. For example, upon injury and loss of organ function, surviving differentiated parenchymal cells respond with polyploidization to support organ function recovery by undergoing cell hypertrophy (Figure 2) (4). The Hippo/Yes-associated protein (Yap) signaling pathway is the primary regulator of polyploidization. Yap accelerates the growth of polyploid cells by regulating Skp2, an E3 ligase that targets p27 for proteolytic degradation. This mechanism occurs in various types of parenchymal cells, such as polyploid differentiated hepatocytes that drive functional recovery by increasing the output of the metabolic function and hepatocyte progenitors that drive the restoration of liver mass through proliferation and differentiation. Similarly, in the early phase of heart injury, polyploidization of cardiomyocytes and regeneration driven by cardiomyocyte progenitors are critical for maintaining heart function and restoring tissue integrity. However, polyploidization can have negative consequences in the long term, as it is associated with scarring and chronic heart failure (4). Although it has been demonstrated that macrophages can promote hypertension-induced cardiac hypertrophy and failure through miR-155-dependent paracrine signaling, and the absence of miR-155 can reduce pressure overload-induced cardiac hypertrophy and inflammation, the role of MP in this context is still uncertain (68).

In the kidney, both podocytes and tubular cells exhibit similar responses to injury, which include undergoing polyploidization-induced hypertrophy and progenitor cell proliferation (4). After

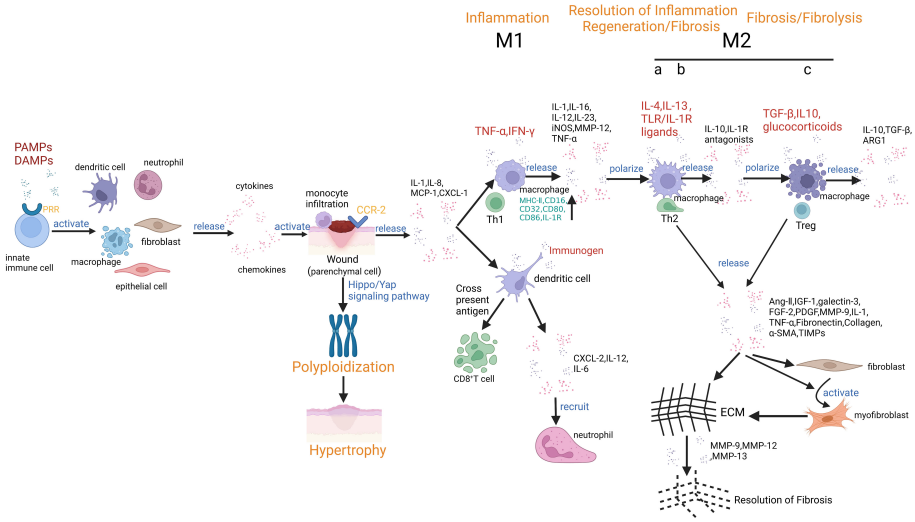

FIGURE 2
Mononuclear phagocytes and tissue fibrosis (Created with BioRender.com). The PRRs on innate immune cells recognize DAMPs or PAMPs and activate TRMs, neutrophils, DCs, fibroblasts, and endothelial cells, which release various pro-inflammatory chemokines and cytokines. Monocytes are abundantly recruited from the blood to sites of inflammation, secrete pro-inflammatory cytokines and chemokines, and differentiate into moM or moDC. Meanwhile, following injury, surviving differentiated parenchymal cells can increase their functional capacity by undergoing hypertrophy through polyploidization, all while maintaining their functional performance. One of the regulators of polyploidization is the Hippo/Yap signaling pathway. During tissue injury and early stages of inflammation, macrophages initially assume the M1 type. M1 macrophages are characterized by their role in host defense and production of pro-inflammatory cytokines. Meanwhile, distinct DC subsets promote tissue inflammation in a complementary manner. cDC1s and cDC2s are tissue-resident and recognize, activate, and release cytokines upon detection of immunogenic substances. The resulting changes in the microenvironment promote the recruitment of neutrophils. In addition, a unique feature of cDC1s is the ability to cross-present antigens to $CD8^+$ T cells. Once the acute inflammatory phase is resolved, there is a shift in the predominant macrophage population towards the M2 type. M2 macrophages are characterized by the secretion of anti-inflammatory mediators and growth factors that aid tissue healing by stabilizing angiogenesis. It stimulates and promotes ECM assembly and remodeling. M2 macrophages are known to secrete numerous pro-fibrotic factors that contribute to the proliferation of fibroblasts, activation, and survival of myofibroblasts, as well as the excessive production of ECM. After removing the injury stimulus, macrophages will transition from a phenotype driven by the uptake of cellular debris to an anti-fibrotic phenotype and secrete multiple fibrinolytic MMPs, which enhance the degradation of fibrotic ECM.

acute kidney injury (AKI), most tubular epithelial cells (TECs) undergo endocycle-mediated hypertrophy, which supports function but not tissue regeneration. These endocyclic TECs can indicate irreversible TEC loss and may be a prognostic indicator of the risk of developing chronic kidney injury (CKD). TEC progenitors have a limited clonal response, and targeting tubular $Pax2^+$ progenitors has been considered a potential treatment strategy for AKI (69). A recent study by De Chiara and colleagues showed that Yap1-driven polyploidization of tubular cells is a compensatory mechanism to enhance residual kidney function and prevent premature death in kidney failure resulting from AKI. However, tubular cell polyploidy promotes tubular cell senescence, progressive interstitial fibrosis, and AKI-CKD transition. On the other hand, blocking Yap1-driven polyploidization at a later stage can prevent the development of CKD and improve the GFR-loss who survive the early injury phase (70). Polyploidization is the result of an alternative cell cycle process known as endoreplication. Endoreplication can lead to the formation of mononucleated polyploid cells through the endocycle or mono/multinucleated polyploid cells through endomitosis (71, 72).

3.3.2 Regeneration

Immature tissue progenitors respond with cell proliferation and differentiation to replace lost cells, i.e., regeneration (Figure 2). Regeneration refers to the replacement and complete reconstruction of damaged or lost tissue structures through the proliferation of cells and tissues. Repair may restore part of the original structure, but reconstruction is incomplete and leads to structural remodeling (73). Injuries are categorized based on the ability of the tissue to regenerate. For example, skeletal muscle, epithelial tissues, liver, etc., can recover from mild injuries quickly after the inflammation subsides. When scars form, they can regress over a few weeks as myofibroblasts, ECM, and inflammatory macrophage infiltrate resolve, allowing regeneration of the parenchyma, resulting in the restoration of normal tissue (74–76). Immune mediators support this process. For example, IL-22 is a cytokine with evident pro-regenerative characteristics. In the colon, $CD11c^+$ DCs secrete IL-22, which signals through the transducer and activator of the STAT3 pathway to promote re-epithelialization. Similarly, following ischemia, tubules release DAMPs that activate TLR4 on renal DCs, producing IL-22 to expedite tubule recovery. Additionally, M2 macrophages in healing kidneys secrete Wingless and Int (Wnt) ligands, including Wnt7b, which activate the Wnt signaling pathway and encourage tubule recovery, and this demonstrates how the immune systems' resident and infiltrating cells play an active role in supporting the regeneration process (77).

3.3.3 Fibrosis

Interstitial fibroblasts respond with increased secretion of ECM to stabilize the integrity of the remaining parenchyma, leading to

tissue fibrosis (Figure 2). Fibrosis occurs for example in response to acute kidney injury and contributes to the transition to chronic kidney disease, and is commonly associated with repetitive injuries or chronic wounds with inadequate vascular supply. The persistence of damaging factors, such as hepatitis C in the liver, or a prolonged inflammatory response that is insufficient in replacing damaged cells, can lead to prolonged damage (78–80). When tissues cannot fully restore tissue architecture, scarring occurs. Severe injury implies scarring even in tissues with high regenerative capacity, such as skin (68). Tissues with limited regenerative potential, such as the brain and heart, undergo rapid healing via the formation of a scar, but this comes at the cost of organ function (81). Over several months, the scar undergoes a maturation process, forming clusters of ECM, myofibroblasts, and macrophages (82). The canonical Wnt pathway regulates myofibroblast activity in various tissues. In a sustained high Wnt activity model, myofibroblasts' persistent activation and proliferation lead to severe tissue fibrosis (83–89). M2 macrophages play a critical role in promoting fibrotic processes across various tissues. They actively secrete a range of pro-fibrotic factors, including TGF-β1, Fibroblast growth factor 2(FGF2), PDGF, and galectin 3. These factors serve to stimulate myofibroblast proliferation, enhance their survival, activate them, and lead to the overproduction of ECM components. Additionally, macrophages produce cytokines such as IL-1, MMP-9, angiotensin (Ang)-II, and IGF-1, which trigger processes like epithelial-mesenchymal transition (EMT) and endothelial-mesenchymal transition (EndoMT) in various cell types, including tubular epithelial cells, endothelial cells, pericytes, local fibroblasts, and mesangial cells. This, in turn, leads to the transdifferentiation or activation of myofibroblasts (90, 91). Furthermore, recent research suggests that monocytes/macrophages can differentiate into collagen-producing fibroblasts or directly into myofibroblasts (92). Activated macrophages can also disrupt glomerular and peritubular capillaries, promoting hypoxia-driven fibrosis (90).

Classical TGF-β signaling via TGF-βR1 and TGF-βR2 operates the complexes containing Smad2, Smad3, and Smad4. Smad3 deficiency in mice leads to a significant decrease in myofibroblast accumulation in the kidney. It protects against renal fibrosis in different disease models, indicating a crucial role for Smad3 in the macrophage-myofibroblast transition (MMT) process. Conversely, Th2 cytokines, such as IL-4 and IL-13, can promote fibrosis in various organ-based diseases by inducing macrophage M2 polarization through the JAK-STAT pathway. In the kidney, $CD4^+$ T cells promote kidney fibrosis by producing high levels of IL-4 and IL-13 and exhibiting a Th2 phenotype. Mice lacking the IL-4 receptor α-chain are protected from kidney fibrosis induced by unilateral ureteral obstruction (UUO) and folic acid, with reduced STAT6 signaling in the kidney and lower numbers of both $CD206^+$ M2 macrophages and $CD206^+PDGFR\beta^+$ bone marrow-derived fibroblasts (52).

In the context of studying MMT in human diseases, researchers commonly identify intermediate cells exhibiting both macrophage markers, such as CD68, and myofibroblast markers, like α-smooth muscle actin (αSMA). In a biopsy-based investigation involving patients with various native kidney diseases, researchers observed the presence of $CD68^+\alpha SMA^+$ cells exclusively in patients with active fibrotic lesions. These dual-marker cells were not found in samples characterized by acute inflammation without fibrosis or in tissues with inactive fibrosis. Furthermore, there was a positive correlation between the number of $CD68^+\alpha SMA^+$ cells and the total count of myofibroblasts in tissues exhibiting active fibrosis. Notably, the majority of $CD68^+\alpha SMA^+$ cells co-expressed CD206, suggesting that macrophages undergoing MMT were predominantly of the M2 subtype (93).

In addition, injecting activated DCs into the injured heart can improve myocardial fibrosis, remodeling, and cardiac function, and this is believed to occur through the modulation of Tregs and the shift of macrophage polarization toward the M2 phenotype (94).

3.4 The resolution of tissue fibrosis

The formation and degradation of ECM counterbalance each other, and tissue fibrosis can be reversible whenever ECM breakdown predominates. The outcome of wound healing is determined by a delicate equilibrium between pro-fibrotic and anti-fibrotic factors (95). Macrophages secrete MMPs, a family of proteases involved in the degradation of different types of ECM proteins, e.g., during the resolution of fibrosis (96). In cases of liver injury, myofibroblasts and activated hepatic stellate cells produce tissue inhibitors of MMPs (TIMPs), inhibiting macrophage-secreted MMPs' activity. This inhibition contributes to the progressive deposition of ECM and the accumulation of scar tissue in the liver (97, 98). Following the cessation of the injury stimulus, macrophages undergo a phenotype transition towards an anti-fibrotic phenotype (99, 100). Apart from clearing cellular debris, such macrophages secrete several fibrinolytic MMPs, such as MMP9, MMP12, and MMP13, which facilitate the degradation of fibrotic ECM (101–103). In addition, macrophages also can generate additional mediators that offer protection against kidney fibrosis. These include collagenases, nitric oxide (NO), and bone morphogenic protein-7 (BMP-7) (104).

Due to recent technical advances, single-cell RNA sequencing (scRNA-seq) discovered macrophage populations with abundant heterogeneity, functionality, and subtle differences in their *in vivo* phenotypes. Sommerfeld et al. employed a platform that combined single-cell technology and functional assessment to elucidate how macrophages reacted to diverse microenvironments and demonstrated that controlling M1/M2 macrophage populations can determine the outcome of tissues in fibrosis (105).

4 Summary, knowledge gaps, and research opportunities

Focal fibrosis is an essential element in tissue repair and stabilizes the surrounding parenchyma. The presence of fibrotic tissue during the healing process can be transient or accumulate over an extended

period. The duration of fibrosis ultimately determines the formation of scar tissue or parenchymal reconstitution. The degree and duration of injury, the body response to invading microorganisms, and changes in inflammation over time modulate the outcome.

Over the years, studies revealed that the MP system is involved in all phases of this process. During homeostasis, circulating monocytes migrate into tissues to become tissue-resident macrophages or DCs. Upon tissue injury, the surviving differentiated parenchymal cells can enhance their functional capacity by undergoing hypertrophy through polyploidization, and the changing tissue environment primes different mononuclear phagocyte phenotypes and determines their function in changing spatial and temporal contexts. During injury-related necroinflammation, macrophages polarize to the M1 type, performing host defense and pro-inflammatory functions, and secrete pro-inflammatory cytokines that support Th1 cells to function. cDC2s contribute to tissue inflammation in a complementary manner, activate and release cytokines after recognizing immunogenic substances, promote the recruitment of neutrophils, and function as innate immune response inducers. During the inflammation subsidence period, macrophages polarize to the M2 type, which mainly plays an anti-inflammatory function, produces anti-inflammatory mediators, promotes angiogenesis, and secrete growth factors beneficial to tissue healing. In contrast, cDC1s regulate inflammatory processes by sustaining Tregs. Furthermore, cDC1s can limit the activity of cytotoxic T cells through the signal from PD-L1. In the post-injury repair and fibrosis phase, M2 macrophages generate substantial quantities of pro-fibrotic factors that enhance myofibroblasts' proliferation, survival, and activation. Conversely, macrophages play a crucial role in promoting ECM degradation during the final stage of fibrotic regression by secreting MMPs.

In recent years, scRNAseq has enabled the characterization of the functions of macrophages, particularly in various microenvironments. The tissue fate during inflammation and fibrosis might be determined by manipulating functional changes of these cells, which is a potential and promising therapeutic target for post-injury repair. For example, various cells of the MP lineage express macrophage colony-stimulating factor receptors (M-CSFR), including tumor-associated macrophages. As a result, chimeric antigen receptor T-cell immunotherapy (CAR-T) targeting M-CSFR has been used in tumor treatment (106). Besides, the therapeutic effect also can be forecasted by scRNAseq (107). However, the relationship between MP and fibrosis presents numerous unsolved questions and challenges, offering valuable research opportunities for further investigation and understanding (Table 3).

TABLE 3 Research opportunities for further investigation and understanding.

The single-cell analysis offers new research opportunities.
The functional roles of different MP lineages remain to be dissected, which requires lineage-specific tools, such as the Cre-lox system.
The roles of MP in tissue polyploidization and cell hypertrophy remain largely unknown. As compensatory hypertrophy is an essential adaption mechanism, MP likely support this process by secreting specific ligands or modulators.
Whether specifically reducing tissue fibrosis improves organ function is unclear and may differ in various organs. While anti-fibrotic therapy appears to benefit lung function, there is a lack of evidence supporting its effectiveness in treating liver, kidney, and heart fibrosis. As the enthusiasm for targeting fibrosis as a potential treatment continues, there is a growing need for further interventional evidence to understand its therapeutic potential better.
Whether manipulating MP is a way to improve tissue regeneration after injury needs more exploration. We show that MP can benefit tissue responses in multiple directions, suggesting that targeting MP to enhance tissue recovery could be a viable option.

MP (Mononuclear Phagocytes).

Author contributions

H-JA generated the concept. HL wrote the first draft. The manuscript was further modified and edited by all authors. All authors contributed to the article and approved the submitted version.

Funding

The authors declare financial support was received for the research, authorship, and/or publication of this article. The Chinese Scholarship Council supported HL. The Deutsche Forschungsgemeinschaft supported JA (AN391/41), HJA (AN372/14-4, 20-2, 29-1, 30-1, 32-1), BS (Deutsche Forschungsgemeinschaft, (322359157-FOR2599, 360372040-SFB 1335). The European Research Council supported BS (ERC-2016-STG-715182).

Acknowledgments

We are grateful for the drawing materials provided by BioRender.

Conflict of interest

H-JA received either honoraries or project support from Bayer, Boehringer-Ingelheim, Novartis, Kezar, Astra-Zeneca, Novartis, GSK, Previpharma, VariantBio, Sanofi, and Vifor.

The remaining authors declare that the research was conducted in the absence of any commercial or financial relationships that could be construed as a potential conflict of interest.

Publisher's note

References

1. Wynn TA, Ramalingam TR. Mechanisms of fibrosis: therapeutic translation for fibrotic disease. *Nat Med* (2012) 18(7):1028–40. doi: 10.1038/nm.2807

2. Jandl K, Mutgan AC, Eller K, Schaefer L, Kwapiszewska G. The basement membrane in the cross-roads between the lung and kidney. *Matrix Biol* (2022) 105:31–52. doi: 10.1016/j.matbio.2021.11.003

3. Abedi M, Alavi-Moghadam S, Payab M, Goodarzi P, Mohamadi-Jahani F, Sayahpour FA, et al. Mesenchymal stem cell as a novel approach to systemic sclerosis; current status and future perspectives. *Cell Regener* (2020) 9(1):20. doi: 10.1186/s13619-020-00058-0

4. Lazzeri E, Angelotti ML, Conte C, Anders H-J, Romagnani P. Surviving acute organ failure: cell polyploidization and progenitor proliferation. *Trends Mol Med* (2019) 25(5):366–81. doi: 10.1016/j.molmed.2019.02.006

5. Vasse GF, Nizamoglu M, Heijink IH, Schlepütz M, van Rijn P, Thomas MJ, et al. Macrophage-stroma interactions in fibrosis: biochemical, biophysical, and cellular perspectives. *J Pathol* (2021) 254(4):344–57. doi: 10.1002/path.5632

6. Henderson NC, Rieder F, Wynn TA. Fibrosis: from mechanisms to medicines. *Nature* (2020) 587(7835):555–66. doi: 10.1038/s41586-020-2938-9

7. Guilliams M, Ginhoux F, Jakubzick C, Naik SH, Onai N, Schraml BU, et al. Dendritic cells, monocytes and macrophages: A unified nomenclature based on ontogeny. *Nat Rev Immunol* (2014) 14(8):571–8. doi: 10.1038/nri3712

8. Lazarov T, Juarez-Carreño S, Cox N, Geissmann F. Physiology and diseases of tissue-resident macrophages. *Nature* (2023) 618(7966):698–707. doi: 10.1038/s41586-023-06002-x

9. Lech M, Anders H-J. Macrophages and fibrosis: how resident and infiltrating mononuclear phagocytes orchestrate all phases of tissue injury and repair. *Biochim Biophys Acta* (2013) 1832(7):989–97. doi: 10.1016/j.bbadis.2012.12.001

10. Pakalniškytė D, Schraml BU. Tissue-specific diversity and functions of conventional dendritic cell S. *Adv Immunol* (2017) 134:89–135. doi: 10.1016/bs.ai.2017.01.003

11. Cabeza-Cabrerizo M, Cardoso A, Minutti CM, Pereira da Costa M, Reis e Sousa C. Dendritic cells revisited. *Annu Rev Immunol* (2021) 39:131–66. doi: 10.1146/annurev-immunol-061020-053707

12. Guermonprez P, Gerber-Ferder Y, Vaivode K, Bourdely P, Helft J. Origin and development of classical dendritic cells. *Int Rev Cell Mol Biol* (2019) 349:1–54. doi: 10.1016/bs.ircmb.2019.08.002

13. Poltorak MP, Schraml BU. Fate mapping of dendritic cells. *Front Immunol* (2015) 6:199. doi: 10.3389/fimmu.2015.00199

14. Rogers NM, Ferenbach DA, Isenberg JS, Thomson AW, Hughes J. Dendritic cells and macrophages in the kidney: A spectrum of good and evil. *Nat Rev Nephrol* (2014) 10(11):625–43. doi: 10.1038/nrneph.2014.170

15. Salei N, Rambichler S, Salvermoser J, Papaioannou NE, Schuchert R, Pakalniškytė D, et al. The kidney contains ontogenetically distinct dendritic cell and macrop hage subtypes throughout development that differ in their inflammatory properties. *J Am Soc Nephrol* (2020) 31(2):257–78. doi: 10.1681/ASN.2019040419

16. Mayer CT, Ghorbani P, Nandan A, Dudek M, Arnold-Schrauf C, Hesse C, et al. Selective and efficient generation of functional batf3-dependent cd103 + Dendritic cells from mouse bone marrow. *Blood* (2014) 124(20):3081–91. doi: 10.1182/blood-2013-12-545772

17. Lamy R, Wolf M, Bispo C, Clay SM, Zheng S, Wolfreys F, et al. Characterization of recruited mononuclear phagocytes following corneal chemical injury. *Int J Mol Sci* (2022) 23(5):2574. doi: 10.3390/ijms23052574

18. Schraml BU, van Blijswijk J, Zelenay S, Whitney PG, Filby A, Acton SE, et al. Genetic tracing via dngr-1 expression history defines dendritic cells as a hematopoietic lineage. *Cell* (2013) 154(4):843–58. doi: 10.1016/j.cell.2013.07.014

19. Schulz C, Gomez Perdiguero E, Chorro L, Szabo-Rogers H, Cagnard N, Kierdorf K, et al. A lineage of myeloid cells independent of myb and hematopoietic stem cells. *Science* (2012) 336(6077):86–90. doi: 10.1126/science.1219179

20. Hoeffel G, Chen J, Lavin Y, Low D, Almeida FF, See P, et al. C-myb(+) erythro-myeloid progenitor-derived fetal monocytes give rise to adult tissue-resident macrophages. *Immunity* (2015) 42(4):665–78. doi: 10.1016/j.immuni.2015.03.011

21. Günthner R, Anders H-J. Interferon-regulatory factors determine macrophage phenotype polarization. *Mediators Inflammation* (2013) 2013:731023. doi: 10.1155/2013/731023

22. Salei N, Ji X, Pakalniškytė D, Kuentzel V, Rambichler S, Li N, et al. Selective depletion of a cd64-expressing phagocyte subset mediates pro tection against toxic kidney injury and failure. *Proc Natl Acad Sci U.S.A.* (2021) 118(39):e2022311118. doi: 10.1073/pnas.2022311118

23. Li N, Steiger S, Fei L, Li C, Shi C, Salei N, et al. Irf8-dependent type I conventional dendritic cells (Cdc1s) control post-ischemic inflammation and mildly protect against post-ischemic acute kidney injury and disease. *Front Immunol* (2021) 12:685559. doi: 10.3389/fimmu.2021.685559

24. Brähler S, Zinselmeyer BH, Raju S, Nitschke M, Suleiman H, Saunders BT, et al. Opposing roles of dendritic cell subsets in experimental gn. *J Am Soc Nephrol* (2018) 29 (1):138–54. doi: 10.1681/ASN.2017030270

25. Zhou W, Zhou L, Zhou J, Bank JRILC, Chu C, Zhang C, et al. Zbtb46 defines and regulates ilc3s that protect the intestine. *Nature* (2022) 609(7925):159–65. doi: 10.1038/s41586-022-04934-4

26. Kierdorf K, Prinz M, Geissmann F, Gomez Perdiguero E. Development and function of tissue resident macrophages in mice. *Semin Immunol* (2015) 27(6):369–78. doi: 10.1016/j.smim.2016.03.017

27. Garbi N, Lambrecht BN. Location, function, and ontogeny of pulmonary macrophages during the steady state. *Pflugers Arch* (2017) 469(3-4):561–72. doi: 10.1007/s00424-017-1965-3

28. Kalish SV, Lyamina SV, Usanova EA, Manukhina EB, Larionov NP, Malyshev IY. Macrophages reprogrammed in vitro towards the M1 phenotype and activated with lps extend lifespan of mice with ehrlich ascites carcinoma. *Med Sci Monit Basic Res* (2015) 21:226–34. doi: 10.12659/msmbr.895563

29. Ishizuka EK, Ferreira MJ, Grund LZ, Coutinho EMM, Komegae EN, Cassado AA, et al. Role of interplay between il-4 and ifn-Γ in the in regulating M1 macrophage polarization induced by nattectin. *Int Immunopharmacol* (2012) 14(4):513–22. doi: 10.1016/j.intimp.2012.08.009

30. Venturin GL, Chiku VM, Silva KLO, de Almeida BFM, de Lima VMF. M1 polarization and the effect of Pge_2 on tnf-A Production by lymph node cells from dogs with visceral leishmaniasis. *Parasite Immunol* (2016) 38(11):698–704. doi: 10.1111/pim.12353

31. Ortega-Gómez A, Perretti M, Soehnlein O. Resolution of inflammation: an integrated view. *EMBO Mol Med* (2013) 5(5):661–74. doi: 10.1002/emmm.201202382

32. Serhan CN, Brain SD, Buckley CD, Gilroy DW, Haslett C, O'Neill LAJ, et al. Resolution of inflammation: state of the art, definitions and terms. *FASEB J* (2007) 21 (2):325–32. doi: 10.1096/fj.06-7227rev

33. Menezes S, Melandri D, Anselmi G, Perchet T, Loschko J, Dubrot J, et al. The heterogeneity of $ly6c^{Hi}$ monocytes controls their differ entiation into $inos^{+}$ Macrophages or monocyte-derived dendritic cells. *Immunity* (2016) 45(6):1205–18. doi: 10.1016/j.immuni.2016.12.001

34. Olingy CE, San Emeterio CL, Ogle ME, Krieger JR, Bruce AC, Pfau DD, et al. Non-classical monocytes are biased progenitors of wound healing macrophages during soft tissue injury. *Sci Rep* (2017) 7(1):447. doi: 10.1038/s41598-017-00477-1

35. Wojtan P, Mierzejewski M, Osińska I, Domagała-Kulawik J. Macrophage polarization in interstitial lung diseases. *Cent Eur J Immunol* (2016) 41(2):159–64. doi: 10.5114/ceji.2016.60990

36. Karuppagounder V, Arumugam S, Thandavarayan RA, Sreedhar R, Giridharan VV, Afrin R, et al. Curcumin alleviates renal dysfunction and suppresses inflammation by S hifting from M1 to M2 macrophage polarization in daunorubicin induced nephrotoxicity in rats. *Cytokine* (2016) 84:1–9. doi: 10.1016/j.cyto.2016.05.001

37. Lv LL, Tang PM-K, Li CJ, You YK, Li J, Huang X-R, et al. The pattern recognition receptor, mincle, is essential for maintaining the M1 macrophage phenotype in acute renal inflammation. *Kidney Int* (2017) 91(3):587–602. doi: 10.1016/j.kint.2016.10.020

38. Onore CE, Careaga M, Babineau BA, Schwartzer JJ, Berman RF, Ashwood P. Inflammatory macrophage phenotype in btbr T+Tf/J mice. *Front Neurosci* (2013) 7:158. doi: 10.3389/fnins.2013.00158

39. Linkermann A, Stockwell BR, Krautwald S, Anders H-J. Regulated cell death and inflammation: an auto-amplification loop causes organ failure. *Nat Rev Immunol* (2014) 14(11):759–67. doi: 10.1038/nri3743

40. Cremers NAJ, van den Bosch MHJ, van Dalen S, Di Ceglie I, Ascone G, van de Loo F, et al. S100a8/A9 increases the mobilization of pro-inflammatory $ly6c^{High}$ monocytes to the synovium during experimental osteoarthritis. *Arthritis Res Ther* (2017) 19(1):217. doi: 10.1186/s13075-017-1426-6

41. Kadowaki N, Antonenko S, Lau JY, Liu YJ. Natural interferon alpha/beta-producing cells link innate and adaptive immunity. *J Exp Med* (2000) 192(2):219–26. doi: 10.1084/jem.192.2.219

42. Smit JJ, Rudd BD, Lukacs NW. Plasmacytoid dendritic cells inhibit pulmonary immunopathology and promote clearance of respiratory syncytial virus. *J Exp Med* (2006) 203(5):1153–9. doi: 10.1084/jem.20052359

43. Tittel AP, Heuser C, Ohliger C, Knolle PA, Engel DR, Kurts C. Kidney dendritic cells induce innate immunity against bacterial pyelon ephritis. *J Am Soc Nephrol* (2011) 22(8):1435–41. doi: 10.1681/ASN.2010101072

44. Kurts C, Cannarile M, Klebba I, Brocker T. Dendritic cells are sufficient to cross-present self-antigens to cd8 T cells in vivo. *J Immunol* (2001) 166(3):1439–42. doi: 10.4049/jimmunol.166.3.1439

45. Hildner K, Edelson BT, Purtha WE, Diamond M, Matsushita H, Kohyama M, et al. Batf3 deficiency reveals a critical role for cd8alpha+ Dendritic cells in cytotoxic T cell immunity. *Science* (2008) 322(5904):1097–100. doi: 10.1126/science.1164206

46. Forte E, Panahi M, Baxan N, Ng FS, Boyle JJ, Branca J, et al. Type 2 mi induced by a single high dose of isoproterenol in C57bl/6j M ice triggers a persistent adaptive immune response against the heart. *J Cell Mol Med* (2021) 25(1):229–43. doi: 10.1111/jcmm.15937

47. Kirabo A, Fontana V, de Faria APC, Loperena R, Galindo CL, Wu J, et al. Dc isoketal-modified proteins activate T cells and promote hypertensio N. *J Clin Invest* (2014) 124(10):4642–56. doi: 10.1172/JCI74084

48. Forte E, Perkins B, Sintou A, Kalkat HS, Papanikolaou A, Jenkins C, et al. Cross-priming dendritic cells exacerbate immunopathology after ischemi C tissue damage in the heart. *Circulation* (2021) 143(8):821–36. doi: 10.1161/CIRCULATIONAHA.120.044581

49. Ngwenyama N, Kirabo A, Aronovitz M, Velázquez F, Carrillo-Salinas F, Salvador AM, et al. Isolevuglandin-modified cardiac proteins drive cd4+ T-cell activation in the heart and promote cardiac dysfunction. *Circulation* (2021) 143(12):1242–55. doi: 10.1161/CIRCULATIONAHA.120.051889

50. Spiller KL, Anfang RR, Spiller KJ, Ng J, Nakazawa KR, Daulton JW, et al. The role of macrophage phenotype in vascularization of tissue engineering scaffolds. *Biomaterials* (2014) 35(15):4477–88. doi: 10.1016/j.biomaterials.2014.02.012

51. Jetten N, Verbruggen S, Gijbels MJ, Post MJ, De Winther MPJ, Donners MMPC. Anti-inflammatory M2, but not pro-inflammatory M1 macrophages promote angiogenesis in vivo. *Angiogenesis* (2014) 17(1):109–18. doi: 10.1007/s10456-013-9381-6

52. Tang PM-K, Nikolic-Paterson DJ, Lan H-Y. Macrophages: versatile players in renal inflammation and fibrosis. *Nat Rev Nephrol* (2019) 15(3):144–58. doi: 10.1038/s41581-019-0110-2

53. Cao Q, Harris DCH, Wang Y. Macrophages in kidney injury, inflammation, and fibrosis. *Physiol (Bethesda)* (2015) 30(3):183–94. doi: 10.1152/physiol.00046.2014

54. Murray PJ, Allen JE, Biswas SK, Fisher EA, Gilroy DW, Goerdt S, et al. Macrophage activation and polarization: nomenclature and experimental guidelines. *Immunity* (2014) 41(1):14–20. doi: 10.1016/j.immuni.2014.06.008

55. Headland SE, Norling LV. The resolution of inflammation: principles and challenges. *Semin Immunol* (2015) 27(3):149–60. doi: 10.1016/j.smim.2015.03.014

56. Elliott MR, Ravichandran KS. The dynamics of apoptotic cell clearance. *Dev Cell* (2016) 38(2):147–60. doi: 10.1016/j.devcel.2016.06.029

57. Uderhardt S, Herrmann M, Oskolkova OV, Aschermann S, Bicker W, Ipseiz N, et al. 12/15-lipoxygenase orchestrates the clearance of apoptotic cells and maintains immunologic tolerance. *Immunity* (2012) 36(5):834–46. doi: 10.1016/j.immuni.2012.03.010

58. Sadtler K, Estrellas K, Allen BW, Wolf MT, Fan H, Tam AJ, et al. Developing a pro-regenerative biomaterial scaffold microenvironment requires T helper 2 cells. *Science* (2016) 352(6283):366–70. doi: 10.1126/science.aad9272

59. Cao Q, Wang Y, Zheng D, Sun Y, Wang Y, Lee VWS, et al. Il-10/tgf-beta-modified macrophages induce regulatory T cells and protect against adriamycin nephrosis. *J Am Soc Nephrol* (2010) 21(6):933–42. doi: 10.1681/ASN.2009060592

60. Soroosh P, Doherty TA, Duan W, Mehta AK, Choi H, Adams YF, et al. Lung-resident tissue macrophages generate foxp3+ Regulatory T cells and promote airway tolerance. *J Exp Med* (2013) 210(4):775–88. doi: 10.1084/jem.20121849

61. Haribhai D, Ziegelbauer J, Jia S, Upchurch K, Yan K, Schmitt EG, et al. Alternatively activated macrophages boost induced regulatory T and th1 7 cell responses during immunotherapy for colitis. *J Immunol* (2016) 196(8):3305–17. doi: 10.4049/jimmunol.1501956

62. Pinto AR, Godwin JW, Rosenthal NA. Macrophages in cardiac homeostasis, injury responses and progenitor cell mobilisation. *Stem Cell Res* (2014) 13(3 Pt B):705–14. doi: 10.1016/j.scr.2014.06.004

63. Madsen DH, Leonard D, Masedunskas A, Moyer A, Jürgensen HJ, Peters DE, et al. M2-like macrophages are responsible for collagen degradation through a mannose receptor-mediated pathway. *J Cell Biol* (2013) 202(6):951–66. doi: 10.1083/jcb.201301081

64. Morris SM Jr. Arginine metabolism: boundaries of our knowledge. *J Nutr* (2007) 137(6 Suppl 2):1602S–9S. doi: 10.1093/jn/137.6.1602S

65. Yang Z, Ming X-F. Functions of arginase isoforms in macrophage inflammatory responses: impact on cardiovascular diseases and metabolic disorders. *Front Immunol* (2014) 5:533. doi: 10.3389/fimmu.2014.00533

66. Lukacs-Kornek V, Burgdorf S, Diehl L, Specht S, Kornek M, Kurts C. The kidney-renal lymph node-system contributes to cross-tolerance against innocuous circulating antigen. *J Immunol* (2008) 180(2):706–15. doi: 10.4049/jimmunol.180.2.706

67. Gottschalk C, Damuzzo V, Gotot J, Kroczek RA, Yagita H, Murphy KM, et al. Batf3-dependent dendritic cells in the renal lymph node induce tolerance against circulating antigens. *J Am Soc Nephrol* (2013) 24(4):543–9. doi: 10.1681/ASN.2012101022

68. Heymans S, Corsten MF, Verhesen W, Carai P, van Leeuwen REW, Custers K, et al. Macrophage microrna-155 promotes cardiac hypertrophy and failure. *Circulation* (2013) 128(13):1420–32. doi: 10.1161/CIRCULATIONAHA.112.001357

69. Lazzeri E, Angelotti ML, Peired A, Conte C, Marschner JA, Maggi L, et al. Endocycle-related tubular cell hypertrophy and progenitor proliferation recover renal function after acute kidney injury. *Nat Commun* (2018) 9(1):1344. doi: 10.1038/s41467-018-03753-4

70. De Chiara L, Conte C, Semeraro R, Diaz-Bulnes P, Angelotti ML, Mazzinghi B, et al. Tubular cell polyploidy protects from lethal acute kidney injury but promotes consequent chronic kidney disease. *Nat Commun* (2022) 13(1):5805. doi: 10.1038/s41467-022-33110-5

71. Edgar BA, Zielke N, Gutierrez C. Endocycles: A recurrent evolutionary innovation for post-mitotic cell growth. *Nat Rev Mol Cell Biol* (2014) 15(3):197–210. doi: 10.1038/nrm3756

72. Orr-Weaver TL. When bigger is better: the role of polyploidy in organogenesis. *Trends Genet* (2015) 31(6):307–15. doi: 10.1016/j.tig.2015.03.011

73. Gonzalez A, Costa TF, Andrade Z, Medrado ARAP. Wound healing - a literature review. *Bras Dermatol* (2016) 91(5):614–20. doi: 10.1590/abd1806-4841.20164741

74. Duffield JS, Lupher M, Thannickal VJ, Wynn TA. Host responses in tissue repair and fibrosis. *Annu Rev Pathol* (2013) 8:241–76. doi: 10.1146/annurev-pathol-020712-163930

75. Mann CJ, Perdiguero E, Kharraz Y, Aguilar S, Pessina P, Serrano AL, et al. Aberrant repair and fibrosis development in skeletal muscle. *Skelet Muscle* (2011) 1(1):21. doi: 10.1186/2044-5040-1-21

76. Gurtner GC, Werner S, Barrandon Y, Longaker MT. Wound repair and regeneration. *Nature* (2008) 453(7193):314–21. doi: 10.1038/nature07039

77. Anders H-J. Immune system modulation of kidney regeneration–mechanisms and implications. *Nat Rev Nephrol* (2014) 10(6):347–58. doi: 10.1038/nrneph.2014.68

78. Cao Z, Lis R, Ginsberg M, Chavez D, Shido K, Rabbany SY, et al. Targeting of the pulmonary capillary vascular niche promotes lung alveolar repair and ameliorates fibrosis. *Nat Med* (2016) 22(2):154–62. doi: 10.1038/nm.4035

79. Degryse AL, Tanjore H, Xu XC, Polosukhin VV, Jones BR, McMahon FB, et al. Repetitive intratracheal bleomycin models several features of idiopathic pulmonary fibrosis. *Am J Physiol Lung Cell Mol Physiol* (2010) 299(4):L442–52. doi: 10.1152/ajplung.00026.2010

80. Mouratis MA, Aidinis V. Modeling pulmonary fibrosis with bleomycin. *Curr Opin Pulm Med* (2011) 17(5):355–61. doi: 10.1097/MCP.0b013e328349ac2b

81. Aurora AB, Olson EN. Immune modulation of stem cells and regeneration. *Cell Stem Cell* (2014) 15(1):14–25. doi: 10.1016/j.stem.2014.06.009

82. Wynn TA. Cellular and molecular mechanisms of fibrosis. *J Pathol* (2008) 214(2):199–210. doi: 10.1002/path.2277

83. Guo Y, Xiao L, Sun L, Liu F. Wnt/beta-catenin signaling: A promising new target for fibrosis diseases. *Physiol Res* (2012) 61(4):337–46. doi: 10.33549/physiolres.932289

84. Akhmetshina A, Palumbo K, Dees C, Bergmann C, Venalis P, Zerr P, et al. Activation of canonical Wnt signalling is required for tgf-B-mediated fibrosis. *Nat Commun* (2012) 3:735. doi: 10.1038/ncomms1734

85. Bastakoty D, Saraswati S, Cates J, Lee E, Nanney LB, Young PP. Inhibition of Wnt/B-catenin pathway promotes regenerative repair of cutaneous and cartilage injury. *FASEB J* (2015) 29(12):4881–92. doi: 10.1096/fj.15-275941

86. Piersma B, Bank RA, Boersema M. Signaling in fibrosis: tgf-B, Wnt, and yap/taz converge. *Front Med (Lausanne)* (2015) 2:59. doi: 10.3389/fmed.2015.00059

87. Hamburg EJ, Atit RP. Sustained B-catenin activity in dermal fibroblasts is sufficient for skin fibrosis. *J Invest Dermatol* (2012) 132(10):2469–72. doi: 10.1038/jid.2012.155

88. Hamburg-Shields E, DiNuoscio GJ, Mullin NK, Lafyatis R, Atit RP. Sustained B-catenin activity in dermal fibroblasts promotes fibrosis B Y up-regulating expression of extracellular matrix protein-coding genes. *J Pathol* (2015) 235(5):686–97. doi: 10.1002/path.4481

89. Mastrogiannaki M, Lichtenberger BM, Reimer A, Collins CA, Driskell RR, Watt FM. B-catenin stabilization in skin fibroblasts causes fibrotic lesions by preventing adipocyte differentiation of the reticular dermis. *J Invest Dermatol* (2016) 136(6):1130–42. doi: 10.1016/j.jid.2016.01.036

90. Meng X-M, Tang PM-K, Li J, Lan HY. Macrophage phenotype in kidney injury and repair. *Kidney Dis (Basel)* (2015) 1(2):138–46. doi: 10.1159/000431214

91. Braga TT, Agudelo JSH, Camara NOS. Macrophages during the fibrotic process: M2 as friend and foe. *Front Immunol* (2015) 6:602. doi: 10.3389/fimmu.2015.00602

92. LeBleu VS, Taduri G, O'Connell J, Teng Y, Cooke VG, Woda C, et al. Origin and function of myofibroblasts in kidney fibrosis. *Nat Med* (2013) 19(8):1047–53. doi: 10.1038/nm.3218

93. Meng X-M, Wang S, Huang X-R, Yang C, Xiao J, Zhang Y, et al. Inflammatory macrophages can transdifferentiate into myofibroblasts during renal fibrosis. *Cell Death Dis* (2016) 7(12):e2495. doi: 10.1038/cddis.2016.402

94. Choo EH, Lee J-H, Park E-H, Park HE, Jung N-C, Kim T-H, et al. Infarcted myocardium-primed dendritic cells improve remodeling and cardiac function after myocardial infarction by modulating the regulatory T cell and macrophage polarization. *Circulation* (2017) 135(15):1444–57. doi: 10.1161/CIRCULATIONAHA.116.023106

95. Huen SC, Moeckel GW, Cantley LG. Macrophage-specific deletion of transforming growth factor-B1 does not prevent renal fibrosis after severe ischemia-reperfusion or obstructive injury. *Am J Physiol Renal Physiol* (2013) 305(4):F477–84. doi: 10.1152/ajprenal.00624.2012

96. Geervliet E, Bansal R. Matrix metalloproteinases as potential biomarkers and therapeutic targets in liver diseases. *Cells* (2020) 9(5):1212. doi: 10.3390/cells9051212

97. Roderfeld M. Matrix metalloproteinase functions in hepatic injury and fibrosis. *Matrix Biol* (2018) 68-69:452–62. doi: 10.1016/j.matbio.2017.11.011

98. Ruiz V, Ordóñez RM, Berumen J, Ramírez R, Uhal B, Becerril C, et al. Unbalanced collagenases/timp-1 expression and epithelial apoptosis in experimental lung fibrosis. *Am J Physiol Lung Cell Mol Physiol* (2003) 285(5):L1026–36. doi: 10.1152/ajplung.00183.2003

99. Popov Y, Sverdlov DY, Bhaskar KR, Sharma AK, Millonig G, Patsenker E, et al. Macrophage-mediated phagocytosis of apoptotic cholangiocytes contributes to reversal of experimental biliary fibrosis. *Am J Physiol Gastrointest Liver Physiol* (2010) 298(3):G323–34. doi: 10.1152/ajpgi.00394.2009

100. Ramachandran P, Pellicoro A, Vernon MA, Boulter L, Aucott RL, Ali A, et al. Differential ly-6c expression identifies the recruited macrophage phenotype, which orchestrates the regression of murine liver fibrosis. *Proc Natl Acad Sci U.S.A.* (2012) 109 (46):E3186–95. doi: 10.1073/pnas.1119964109

101. Fallowfield JA, Mizuno M, Kendall TJ, Constandinou CM, Benyon RC, Duffield JS, et al. Scar-associated macrophages are a major source of hepatic matrix metal loproteinase-13 and facilitate the resolution of murine hepatic fibrosis. *J Immunol* (2007) 178(8):5288–95. doi: 10.4049/jimmunol.178.8.5288

102. Hironaka K, Sakaida I, Matsumura Y, Kaino S, Miyamoto K, Okita K. Enhanced interstitial collagenase (Matrix metalloproteinase-13) production of kupffer cell by gadolinium chloride prevents pig serum-induced rat liver fibrosis. *Biochem Biophys Res Commun* (2000) 267(1):290–5. doi: 10.1006/bbrc.1999.1910

103. Kwan PO, Tredget EE. Biological principles of scar and contracture. *Handb Clin* (2017) 33(2):277–92. doi: 10.1016/j.hcl.2016.12.004

104. Wang X, Chen J, Xu J, Xie J, Harris DCH, Zheng G. The role of macrophages in kidney fibrosis. *Front Physiol* (2021) 12:705838. doi: 10.3389/fphys.2021.705838

105. Sommerfeld SD, Cherry C, Schwab RM, Chung L, Maestas DR Jr., Laffont P, et al. Interleukin-36γ-producing macrophages drive il-17-mediated fibrosis. *Sci Immunol* (2019) 4(40):eaax4783. doi: 10.1126/sciimmunol.aax4783

106. Zhang P, Zhao S, Wu C, Li J, Li Z, Wen C, et al. Effects of csf1r-targeted chimeric antigen receptor-modified nk92mi & T cells on tumor-associated macrophages. *Immunotherapy* (2018) 10(11):935–49. doi: 10.2217/imt-2018-0012

107. Achkova DY, Beatson RE, Maher J. Car T-cell targeting of macrophage colony-stimulating factor receptor. *Cells* (2022) 11(14):2190. doi: 10.3390/cells11142190

frontiers | Frontiers in Immunology

TYPE Review
PUBLISHED 10 October 2023
DOI 10.3389/fimmu.2023.1193053

OPEN ACCESS

EDITED BY
Ruoxi Yuan,
Hospital for Special Surgery, United States

REVIEWED BY
Nanshan Song,
Nanjing University of Chinese Medicine, China
Yuan Lin,
Memorial Sloan Kettering Cancer Center, United States

*CORRESPONDENCE
Lili Fan
fanlili@jnu.edu.cn
Xiaojuan Li
lixiaojuan@jnu.edu.cn
Jiaxu Chen
chenjiaxu@hotmail.com

†These authors have contributed equally to this work

RECEIVED 24 March 2023
ACCEPTED 20 September 2023
PUBLISHED 10 October 2023

CITATION
Fang S, Wu Z, Guo Y, Zhu W, Wan C, Yuan N, Chen J, Hao W, Mo X, Guo X, Fan L, Li X and Chen J (2023) Roles of microglia in adult hippocampal neurogenesis in depression and their therapeutics.
Front. Immunol. 14:1193053.
doi: 10.3389/fimmu.2023.1193053

Roles of microglia in adult hippocampal neurogenesis in depression and their therapeutics

Shaoyi Fang[1†], Zhibin Wu[1†], Yali Guo[1], Wenjun Zhu[1], Chunmiao Wan[1], Naijun Yuan[1,2], Jianbei Chen[3], Wenzhi Hao[1], Xiaowei Mo[1], Xiaofang Guo[1], Lili Fan[1*], Xiaojuan Li[1*] and Jiaxu Chen[1,3*]

[1]Formula-Pattern of Traditional Chinese Medicine, School of Traditional Chinese Medicine, Jinan University, Guangzhou, China, [2]Shenzhen People's Hospital, 2nd Clinical Medical College, Jinan University, Shenzhen, China, [3]School of Traditional Chinese Medicine, Beijing University of Chinese Medicine, Beijing, China

Adult hippocampal neurogenesis generates functional neurons from neural progenitor cells in the hippocampal dentate gyrus (DG) to complement and repair neurons and neural circuits, thus benefiting the treatment of depression. Increasing evidence has shown that aberrant microglial activity can disrupt the appropriate formation and development of functional properties of neurogenesis, which will play a crucial role in the occurrence and development of depression. However, the mechanisms of the crosstalk between microglia and adult hippocampal neurogenesis in depression are not yet fully understood. Therefore, in this review, we first introduce recent discoveries regarding the roles of microglia and adult hippocampal neurogenesis in the etiology of depression. Then, we systematically discuss the possible mechanisms of how microglia regulate adult hippocampal neurogenesis in depression according to recent studies, which involve toll-like receptors, microglial polarization, fractalkine-C-X3-C motif chemokine receptor 1, hypothalamic-pituitary-adrenal axis, cytokines, brain-derived neurotrophic factor, and the microbiota-gut-brain axis, etc. In addition, we summarize the promising drugs that could improve the adult hippocampal neurogenesis by regulating the microglia. These findings will help us understand the complicated pathological mechanisms of depression and shed light on the development of new treatment strategies for this disease.

KEYWORDS

depression, microglia, adult hippocampal neurogenesis, antidepressant, neurogenesis

1 Introduction

Depression is one of the most common psychiatric disorders affecting humans. Its clinical symptoms include impaired sociability, anhedonia, behavioral despair, loss of appetite, sleep problems, suicidal tendencies, and anxiety, which lead to a severe decline in quality of life (1). Depression is considered a common mental disorder with a complex and multifactorial etiology. At present, the prognosis of clinical antidepressant treatment is poor, and drug development for depression has shown high failure rates in clinical trials (2). Therefore, the underlying mechanisms of depression remain to be further explored.

The pathogenesis mechanisms associated with depression have been reported including monoamine neurotransmission, dysregulation of the hypothalamic-pituitary-adrenal axis (HPA axis), synaptic remodeling, inflammation, neurogenesis, etc (3), among which neurogenesis is one of the most important aspects. Neurogenesis is the process by which value-added neural precursor cells differentiate to produce new mature neurons and integrate into an established neural network to function (4). There are two major reservoirs of neurogenesis: the subventricular zone (SVZ) of the lateral ventricle and the dentate gyrus (DG) of the hippocampus (5). Accumulating evidence has shown that impaired hippocampal neurogenesis is a critical factor in the pathogenesis of depression in rodents (6–8). In addition, promoting effective neurogenesis is emerging as an important strategy for the treatment of depression, as dead and lost neurons in the lesion require replacement by newborn neurons to replenish and reestablish neuronal connections. For instance, first-line antidepressants on the market, such as fluoxetine and paroxetine, can promote the value-added and survival of hippocampal precursor cells in rodents, which in turn can have antidepressant effects (9). Although significantly reduced hippocampal volume has been found in the brains of depressed patients using MRI (10), evidence for impaired hippocampal neurogenesis in depression patients is lacking. Particularly, single-cell technologies, mainly single-cell RNA sequencing, are novel technologies to analyze the genome sequence in a single cell, which enables comprehensive and high-resolution cell type determination and identifying new cell markers, offering new possibilities to address biological and medical questions (11). In a recent study, hippocampal immature neurons in human present across the entire human lifespan have been found using the new single-cell technologies (12), suggesting that the damage to adult hippocampal neurogenesis in depression patients will one day be visible with technological innovations in the neurological field. The present study suggests that the mechanism of impaired adult neurogenesis in depression is related to the abnormal activation of microglia.

Evidence indicates that immunoreactions can directly or indirectly affect the neurobiological processes of mental disorders (13–15). Accumulating evidence indicates that neuroinflammation plays a leading role in depression. For example, it has been demonstrated that there is a strong association between the levels of inflammatory factors in the peripheral blood and cerebrospinal fluid (CSF) in depression patients (16). Studies in rodents have also shown that immune challenges can induce depressive-like behaviors (17, 18). Microglia serve as immune cells in the central nervous system (CNS) and play dominant roles in monitoring the microenvironment for any stimuli or injury that may be harmful. When pro-inflammatory cytokines are consistently increased in the circulatory system of patients with depression, microglia are quickly activated and subsequently secrete a variety of non-discriminative harmful factors, finally leading to neuronal damage and the pathogenesis of depression. Importantly, neuroinflammation, mainly triggered by microglia, contributes to reduced hippocampal neurogenesis, which is important for the development of depression. However, the mechanism of the reduction in neuroinflammation-induced hippocampal neurogenesis in depression remains to be further elucidated, according to recent discoveries.

Therefore, in order to review the roles and mechanisms of microglia in the neurogenesis of depression, we first introduce neurogenesis, microglia, and the role of both in depression. Then, we systematically discussed the possible mechanisms of how microglia modulate the adult hippocampal neurogenesis in depression and summarized the promising drugs targeting microglia to alter neurogenesis for treating depression and their potential regulation mechanism, which will help in understanding the pathogenesis of depression and promoting the development of new and exciting treatments for depression.

2 Neurogenesis

2.1 Introduction of neurogenesis

Neurogenesis is the process by which new neurons be generated by neural stem cells (NSCs), promoting the structural plasticity of the brain (19). Although neurons in the adult brain do not regenerate or replenish in the traditional view, recent decades have seen the publication of numerous studies demonstrating that a large majority of mammalian species retain the capacity for neurogenesis in the CNS into adult life. It is currently understood that the adult mammalian brain has two major reservoirs of neural stem cells (NSCs), called “neurogenic niches” in the SVZ of the lateral wall of the lateral ventricle and the subgranular zone (SGZ) of the DG of the hippocampus (20). Under resting conditions, neurogenesis is restricted in the above two neurogenic niches, while under pathological conditions, neural precursor cells generated in the SGZ and SVZ need to migrate to the olfactory bulb and the subgranular zone of the DG of the hippocampus to compensate for neuronal loss in the brain to maintain hippocampal structural and functional plasticity (21). Although the process of neurogenesis is sophisticated, it can be summarized in four phases: In the first stage, NSCs divide and proliferate to form a pool of NSCs, which can differentiate to produce neuroblasts and further differentiate into immature neurons. In the second stage, neuroblasts and immature neurons located in the subgranular region migrate to the granular cell layer. However, due to the mature neuronal structures not yet being formed, the axons and dendrites of immature neurons are short. In the third stage, in order to establish correct synapses with other neurons, immature neurons differentiate into mature neurons

with intact neuronal structures and neurites. Meanwhile, dendrites extend into the molecular layer and axons extend to the CA3 subfield. Finally, the dendrites and axons of mature neurons establish synaptic connections with other neurons, and these synaptic connections integrate with pre-existing circuits to ensure the normal functioning of the CNS (22). Since the hippocampus is an important structure involving humans' learning, memory, and mood regulation (23, 24), and the DG is one of the core regions for neurogenesis, neurogenesis in the hippocampus has been implicated in the process of cognitive functions and emotion. Indeed, it has been found that adult-born neurons in the DG contribute to learning and memory, including cognitive flexibility, emotional memory, spatial navigation, novelty detection, pattern separation, stress response, and emotion (25). Thus, the regulation of adult neurogenesis has a vital impact on the treatment of some neuropsychiatric diseases.

2.2 Adult hippocampal neurogenesis and depression

Abnormalities in different stages of neurogenesis can lead to the development of depression (26). First, in patients with depression, the number and differentiation capacity of NSCs in the hippocampus decrease, which may lead to a decrease in neurons and dysfunction, which affects emotion regulation and cognitive function in patients with depression (27, 28). The antidepressant fluoxetine can increase the proliferative capacity of NSCs and the expression of Bcl-2, thereby preventing apoptosis through the activation of Bcl-2, promoting the development of synapses and the differentiation of serotonin neurons (29). This study reveals a new antidepressant drug treatment mechanism that promotes the development and differentiation of NSCs by stimulating Bcl-2 expression, thereby helping to treat depression. Secondly, when there are problems with the maturity of newborn neurons in the hippocampus, it may negatively affect behavioral functions such as learning, memory, and emotional control (30). Previous studies have shown that antidepressants can promote the increase of new neurons. For instance, many studies have shown that antidepressants including fluoxetine, paroxetine, tranylcypromine, and reboxetine reverse hippocampal volume loss in patients with depression as well as depression in rodents (8, 31, 32). Furthermore, the proliferation rate of newborn neurons, which is promoted by fluoxetine in the hippocampus, is synchronized with the clinically observed delay time of the therapeutic effect (33). It has been shown that newborn cell proliferation in the adult hippocampus decreases when exposed to chronic stress (34). Interestingly, the presence of newborn neurons was sufficient to cause anti-reversal and remission in mouse models of depression (35, 36). In addition, previous studies have shown that in the early neuronal development stage, neurons with deletion of the TLR7 gene show downregulation of gene expression related to neurodevelopment, synaptic organization, and activity, while mice with deletion of the TLR7 gene show significant behavioral changes in anxiety, aggression, smell, and situational fear memory. The electrophysiological analysis further revealed that loss of *TLR7* led to impaired hippocampal long-term enhancement (37). What's more, recent studies showed that if the newborn granule cells are damaged, it causes damage to neurons connected to CA3 in the DG network, which affects the information coding in the downstream hippocampal region, which may lead to the onset and progression of depression (38, 39). The above implies that impaired neuronal maturity can also lead to depression. Therefore, this current research has indicated that diminished adult hippocampal neurogenesis may be associated with the development of depression, and that it might be one of the ways to reverse or prevent diminished hippocampal neurogenesis in adults with antidepressants (Figure 1).

3 Microglia

3.1 Introduction of microglia

Microglial originate from the embryonic mesoderm, primarily derived from myeloid progenitors within the yolk sac (40). During early embryonic development, these cells persistently proliferate in the brain and are regulated by various molecular factors, including but not limited to transcription factors, growth factors, chemokines, MMPs, and microRNAs (41). The exact numbers or proportions of microglia in the hippocampus can vary, influenced by factors such as age and health (42). Generally, the hippocampus exhibits a relatively high microglial density compared to other brain regions, reflecting its vital role in cognitive function (43). In the hippocampus, microglia constitute a slightly higher proportion, accounting for approximately 10 to 15 percent of the total cell population, whereas in other brain regions, this proportion typically ranges from 5 to 10 percent (43). Microglia are the leading type of immune cells in the CNS and are in charge of modulating inflammation. Originally, microglia were thought to exist in a quiescent or resting state when characterized by small stationary soma, with smaller cell bodies and highly branched protrusions (44). Normally, the highly branched resting state of microglia provides a highly dynamic and efficient monitoring system for the brain (Physiology of Microglia) (45, 46). Conversely, when pathological stimulation occurs, microglia are rapidly activated. There are three main activated microglial morphotypes in current reports: hyper-ramified, phagocytic, and amoeboid types (47–49). When the brain microenvironment changes, the resting microglia react by transitioning into "hyper-ramified" morphotypes, which are often defined by longer, thicker, more abundant processes that attach to larger, lobular, and irregularly shaped cell bodies (50, 51). Once the changes or stimuli intensify, the hyper-ramified microglia shift into phagocytic and even amoeboid types, which show much fewer, albeit thicker and shorter, processes, and much rounder, larger, and more regularly shaped cells with no processes, respectively (52). Alternatively, the activated microglia, similar to peripheral macrophages, have two primary polarization phenotypes: M1 (classical activation) and M2 (alternative activation) (53). M1-phenotype microglia are classically activated microglia that can express surface markers such as cluster of differentiation 86 (CD86) and inducible nitric oxide synthase (iNOS) (54, 55). M1-phenotype microglia mainly play a pro-inflammatory role and promote the synthesis of inflammatory

10.3389/fimmu.2023.1193053

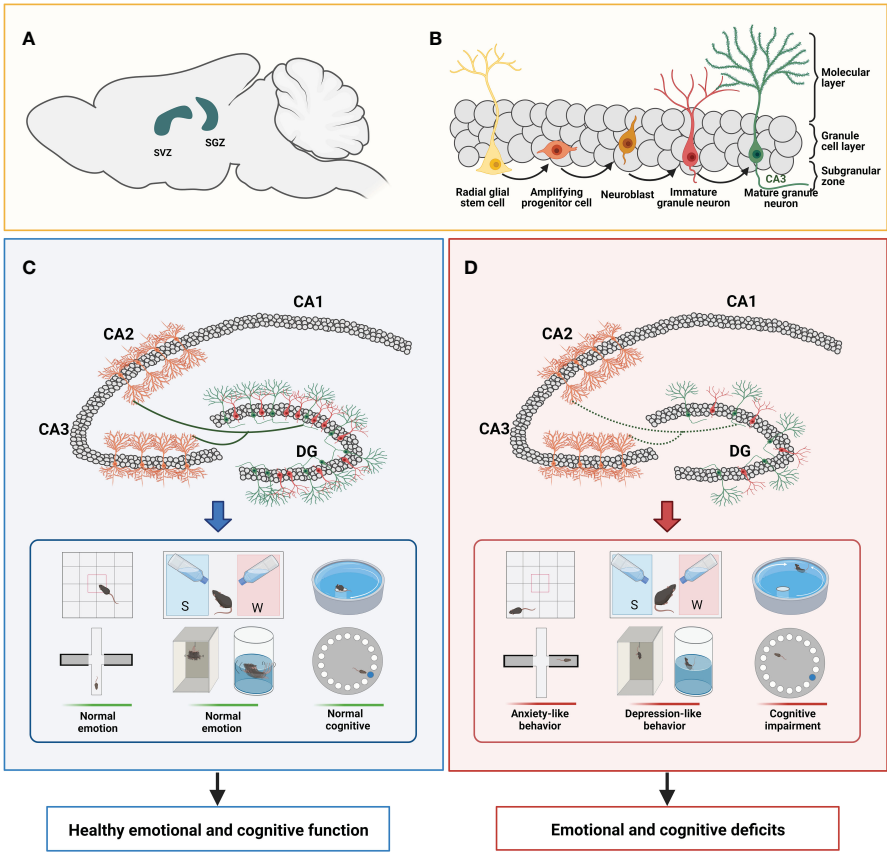

FIGURE 1
Neurogenesis and its role in learning and memory, cognitive function, and emotion. **(A)** The area of neurogenesis is limited to the SVZ of the lateral ventricle and the SGZ of the hippocampus. **(B)** Radial glial stem cells in the subgranular zone produce neural stem cells (NSCs). Amplifying progenitor cells located in the subgranular zone arise from the asymmetric division of NSCs and differentiate into neuroblasts. Neuroblasts migrate into the granule cell layer to develop into immature granule neurons. Immature neurons grow into mature neurons, and their dendritic trees gradually extend to the molecular layer and axons extend to the CA3 subfields. **(C)** Under normal conditions, the axons of new granule neurons located in the DG area will extend to the CA3 and CA2 subfields to establish synaptic contacts with pyramidal neurons and integrate the pre-existing circuits, playing an important role in behaviors associated with the hippocampus. Rodents with normal neurogenesis have typical responses in some emotional tests (such as OFT, EPM, SPT, TST, and FST) and cognitive tests (such as MWM and Barnes maze). **(D)** In some neuropsychiatric diseases, hippocampal neurogenesis is impaired, manifested by decreased newborn neurons and impaired synaptic connections with pyramidal neurons in the CA3 and CA2 subfields. Compared to normal rodents, rodents with impaired neurogenesis exhibit anxiety-like behaviors (such as reduced entry times and residence times in the central zone in the OFT; reduced the number and frequency of exploring the open arm, and prefer to stay in the closed arm in the EPM) or depression-like behaviors on certain mood tests (such as inactive behaviors in the FST and TST; anhedonia in SPT), and impaired social cognition on some cognitive tests (such as unable to locate the location of the hidden platform in the MWM and the location of the markers in the Barnes maze). SVZ subventricular zone, SGZ subgranular zone, DG dentate gyrus, OFT open field test, EPM Elevated Plus Maze, SPT Sucrose Preference Test, TST Tail Suspension Test, FST Forced Swimming Test, MWM Morris Water Maze.

mediators such as tumor necrosis factor-alpha (TNF-α), interleukin-1β (IL-1β), and iNOS, which can promote chronic neuroinflammation, phagocytosis, oxidative stress, and neurodegeneration and inhibit regeneration (56). Therefore, M1 microglia often have obvious neurotoxic effects (57). In contrast, the M2-phenotype microglia are alternatively activated microglia that can express surface markers such as cluster of differentiation 206 (CD206) and cluster of differentiation 163 (CD163), which release neuroprotective and anti-inflammatory cytokines, such as interleukin-10 (IL-10) and transforming growth factor-β (TGF-β), to exert anti-inflammatory effects, promote wound healing, neuroprotection, and tissue repair (58). Therefore, M2 microglia often have neuroprotective effects (59). Furthermore, many studies have reported three main sub-phenotypes (M2a, M2b, and M2c) in M2 microglia, corresponding to different stimulations and functions (42). The M2a phenotype can be activated by interleukin-4 (IL-4) and interleukin-13 (IL-13), resulting in the secretion of IL-10, chemoattractant cytokine ligand 17 (CCL17), and chemoattractant cytokine ligand 18 (CCL18) to clear apoptotic cells, promote cell debris removal, and contribute to neuroprotection (56, 60, 61). The M2b phenotype can be activated by toll-like receptor (TLR) ligands and immune complexes, which secrete TNF-α, interleukin 1 (IL-1), and interleukin 6 (IL-6). These cytokines support immune regulation, inflammation inhibition, B cell conversion and antibody production, and recruitment of regulatory T cells (62, 63). The M2c phenotype can be activated by anti-inflammatory IL-10 and corticosteroids, which in turn release many more anti-inflammatory cytokines, such as IL-4, and increase growth factors, such as TGF-β, to promote nerve regeneration (64, 65). Usually, an imbalance of M1 and M2 polarization occurs in neurodegenerative

or neuro-damaged illnesses, such as depression, stroke, and Alzheimer's disease, and therapeutic candidates that target modulating the activation of M1 and M2 polarization appear promising for these diseases (66).

3.2 Microglial activation and depression

In many clinical reports, microglial activation in the insula, anterior cingulate cortex, and prefrontal cortex (PFC) have been found in patients with depression and those with suicidal ideation (67). These results suggest that the degree of microglial activation is positively correlated with depression severity (68). In rodents, chronic stress, including chronic unpredictable mild stress (CUMS), chronic social defeat stress (CSDS), and chronic restraint stress (CRS), commonly used to induce depression, results in elevated peripheral cytokines and the activation of microglia in stress-sensitive brain regions, such as the hippocampus, PFC, and amygdala (69). In contrast, minocycline, a potential anti-inflammatory agent, significantly blocks microglial activation and has been shown to contribute to improving depressive-like behaviors (70–72). Similarly, a previous study found that lipopolysaccharide (LPS)-induced inflammation, a classical microglia activation pathway that acts via the TLR4/nuclear factor-k-gene binding signaling pathway, increased the risk of depression in mice, which could be improved by the microglial depletion of PLX5622 or minocycline (70, 73). This indicates that microglial activation is strongly associated with the development of depression (Figure 2).

Many studies have revealed how the activation of microglia leads to the occurrence and development of depression. Firstly, it involves inflammation and polarization of microglia. Reassuringly, some preclinical studies have conducted more in-depth investigations in this area (74). Tang et al. found that CSDS mice showed higher M1 microglia markers, including iNOS, cluster of differentiation 16 (CD16), CD86, and C-X-C motif chemokine ligand 10, and no significant changes in M2 markers such as arginase-1 (Arg-1) and CD206 in the hippocampus at the transcriptional and protein levels, suggesting that M1 polarization plays a vital role in depression pathogenesis (75). Another study revealed that although no change in the total microglia number in CUMS-induced depressive mice was observed, much more activated microglia expressing M1-marker CD68 and less M2-marker CD206 was detected throughout the DG, CA1, and CA2 regions in the hippocampus (76). Taken together, the activation of microglia in susceptible brain regions towards the classical M1 polarization state instead of the M2 polarization state results in an increase in the production of toxic substances that harm neurons, which factors are crucial in the development and progression of depression (77).

Secondly, the phagocytic function of microglia in depression. The phagocytic function of microglia is considered an important factor affecting the occurrence and development of depression. Synapses interconnect neurons into networks that transmit neurotransmitters and mediate neuronal signaling, which contains pre-and postsynaptic separated by the synaptic cleft. Preclinical and clinical evidence suggests activated microglia in depressed animals and humans may aberrantly phagocytose neuronal synapses, resulting in synaptic dysfunction and depressive symptoms (78, 79). Preclinical studies in mouse models of depression have reported increased microglial phagocytosis of synapses in microglia-neuron contact areas (80). For example, there was a notable increase in the presence of phagocytic microglia actively engulfing puncta containing Postsynaptic density protein 95 (PSD95) in the DG of CSDS mice when compared with normal mice (81). Similar findings have been observed in other models, including decreased hippocampal expression of PSD95, synapses, and growth associated protein-43 and enhanced microglial phagocytosis in maternally separated rats. The hippocampus of chronic unpredictable mild stress mice also showed comparable results. Interestingly, intraperitoneal LPS injection in mice at postnatal day 50 to model early-life inflammation resulted in long-term phagocytosis of glutamatergic spines on neurons of the anterior cingulate cortex (82). The H3-receptor inverse agonist JNJ10181457 prevented abnormal LPS-induced microglial phagocytosis, decreased neuronal loss, improved neurotransmitter transmission, and had antidepressant effects in mice (83). Positron emission tomography revealed significantly increased translocator protein, a microglial marker, in the hippocampus, prefrontal cortex, and temporal cortex of depressed patients, suggesting microglial activation may contribute to depression pathophysiology. Functional imaging studies have also shown depressed patients exhibit decreased synaptic connectivity and neuronal circuitry in the prefrontal cortex and hippocampus (84). Together, these findings suggest aberrant phagocytosis of synapses by activated microglia in the hippocampus may underlie decreased synapses observed in depression. Therefore, in addition to modulating neuroinflammation, regulating microglial phagocytosis of synapses may provide novel insights into the mechanisms and therapeutic approaches for depression.

Finally, the trophic support function of microglia and endogenous microglial reduction is closely related to depression. Microglia support neuronal plasticity, neurogenesis, neural circuits and synaptic integrity through neuroimmune mechanisms including phagocytosis and cytokine secretion under baseline physiological conditions (85–87). Microglia also produce and respond to trophic factors like brain derived neurotrophic factor (BDNF) (88). BDNF was first isolated from the porcine brain in 1982 and found to support the survival of cultured embryonic sensory neurons (89). Considerable clinical evidence over subsequent decades has demonstrated BDNF plays an important role in depression (90). Regulating the C-X3-C motif chemokine receptor 1 (CX3CR1) in horses with phytoestrogens such as genistein increases BDNF and TGF-β secretion, promoting neuron-microglia interactions and synaptic remodeling. Endogenous microglial reduction or impairment may deprive neurons of adequate nutrition and energy, disrupting their function and contributing to depression (91). Kreisel et al. first reported the chronic unpredictable stress-induced microglial loss in the hippocampus, which could worsen severe depression (92). Administering innate immune stimulants like LPS and macrophage colony-stimulating factors to increase microglial

10.3389/fimmu.2023.1193053

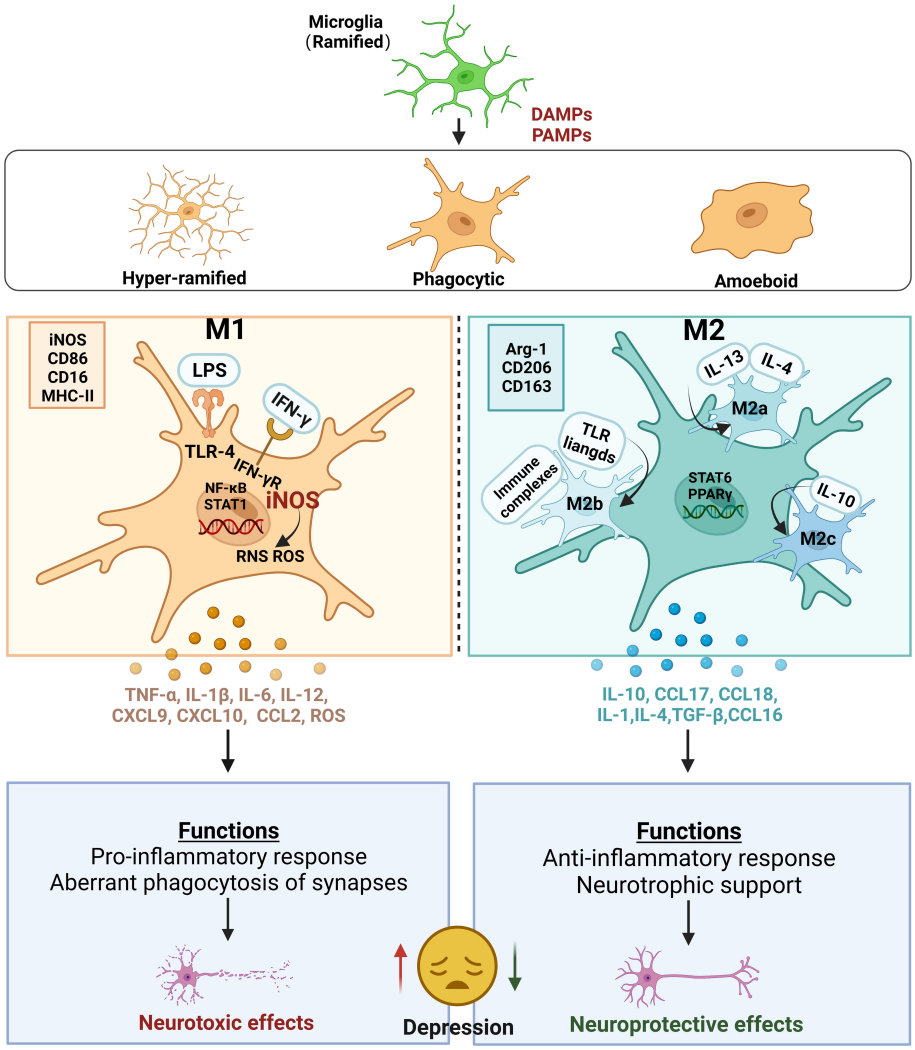

FIGURE 2
Microglial activation and their roles in depression. Ramified microglia stimulated by PAMPs or DAMPs are activated into three main microglial morphotypes, including hyper-ramified, activated, and amoeboid types. Alternatively, two main polarization states are defined in activated microglia: M1 and M2 phenotypes. The classic M1 polarization microglia is usually marked with iNOS, CD86, CD16 and MHC-II. Under the M1 state, exposure to LPS and/or IFN-γ stimulates and binds to TLR-4 or IFN-γ receptors, respectively, leading to the activation of NF-κB and STAT1. Meanwhile, the increase in iNOS produces a burst of ROS and RNS. All these lead to the excessive release of pro-inflammatory cytokines, such as TNF-α, IL-1β, IL-6, IL-12, and chemokines, such as CXCL9, CXCL10, CCL2, and ROS, which produce neurotoxic effects on the neurons in CNS. The alternative M2 polarization microglia is usually marked with ARG-1, CD206 and CD163. M2 microglia can also be divided into three subtypes including M2a, M2b and M2c, because of the different stimulis. Upon stimulation with IL-4/IL-13, the cells transform into the M2a-phenotype microglia with an increase in IL-10, CCL17 and CCL18. Exposed to TLR ligands and immune complexes, the cells transform into the M2b-phenotype microglia with an expression of IL-6. Upon stimulation with IL-10, the cells transform into the M2c-phenotype microglia with an increase in IL-4, TGF-β and CCL16. The phenotypes of M1 microglia perform functions that aberrant phagocytosis of synapses leading to produce neurotoxic effects on the neurons in CNS. The phenotypes of M2 microglia perform functions that neurotrophic support leading to produce neuroprotective effects on the neurons in CNS. Thus, the imbalance of M1 and M2 polarization induces increased excessive neurotoxicity and decreased neuroprotection, leading to depression. PAMPs pathogen-associated molecular patterns, DAMPs danger-associated molecular patterns, iNOS inducible nitric oxide synthase, CD86 cluster of differentiation 86, CD16 cluster of differentiation 16, MHC-II major histocompatibility complex II, LPS lipopolysaccharide, IFN-γ interferon gamma, TLR-4 toll-like receptor 4, NF-κB transcription factors nuclear factor kappa-B, STAT1 signal transducer and activator of transcription 1, ROS reactive oxygen species, RNS reactive nitrogen species, TNF-α tumor necrosis factor α, IL-1β Interleukin-1β, Interleukin-6 IL-6, Interleukin-12 IL-12, CXCL9 chemokine (C-X-C motif) ligand 9, CXCL10 chemokine (C-X-C motif) ligand 10, CCL2 chemokines chemoattractant cytokine ligand 2, CNS central nervous system, ARG-1 arginase-1, CD206 cluster of differentiation 206, CD163 cluster of differentiation 163, IL-4 interleukin-4, IL-13 interleukin-13, IL-10 interleukin-10, CCL17 chemoattractant cytokine ligand 17, CCL18 chemoattractant cytokine ligand 18, IL-1 interleukin-1, Interleukin-10, IL-10 Interleukin-4 IL-4, TGF-β transforming growth factor-β, CCL16 chemoattractant cytokine ligand 16

numbers in the DG has reversed depressive behaviors in chronic stress mice. For instance, a single intraperitoneal 75 or 100 μg/kg dose of LPS reversed depressive behaviors of chronic unpredictable stress mice within 5 hours, as demonstrated by behavioral testing (93). The antidepressant effect of low-dose LPS depends on microglial activation regulating extracellular signal-regulated kinase (ERK) 1/2 signaling to increase BDNF synthesis. These findings suggest restoring endogenous microglial levels and function may benefit severe depression treatment, in addition to modulating microglia directly.

4 The function of microglia in adult hippocampal neurogenesis and its molecular mechanism in depression

Microglia are actively involved in the modulation of adult neurogenesis. Under physiological conditions, each of the individual components of adult neurogenesis, including the proliferation of NSCs, the migration of adult neuronal cells and immature neurons, their differentiation to mature neurons, and the extension of neuronal synapses, and integration of immature neurons into an existing circuit, is influenced by microglia (94, 95). First, microglia, as brain-resident immune cells, play a "housekeeping" role during neural development; that is, the proliferation of NSCs is controlled by microglia, and excess apoptotic proliferating cells are engulfed by microglia (49, 95, 96). Microglia release soluble factors that promote different stages of neurogenesis. It has been shown that nutrient factors such as insulin-like growth factor-1 (IGF-1) and brain-derived neurotrophic factor (BDNF), which are secreted by microglia, help the neural stem cell proliferation and the differentiation and guide the migration of neural precursor cells (97, 98). In addition, microglia modulate the integration of new neurons into existing neuronal circuits and refine neural circuits during development by pruning neuronal synapses (99). Therefore, microglia can participate in multiple stages of adult neurogenesis and play key roles in supporting adult neurogenesis.

There are many existing models of depression, and different models simulate different types of depression with distinct internal mechanisms. Currently, reports have focused on models involving the microglia mechanisms, neurogenesis mechanisms, or microglia-neuron regulation of neurogenesis mechanisms. These models focus on early life stress (maternal separation (MS), maternal sleep deprivation, and adult stress (CUMS and chronic mild stress (CMS)), as well as toxic infection (LPS) models. Additionally, genetic mutations have also been reported to cause depression (Table 1). Under pathological conditions, microglia can contribute to depression through a variety of mechanisms, including toll-like receptors (TLRs), nod-like receptor protein 3 (NLRP3) inflammasome, lesion of the HPA axis, metabolism of 5-hydroxytryptamine (5-HT), inflammatory cytokines, and their mediated inflammatory signal pathways, imbalance of M1/M2 polarization, gut microbiota, and microRNA. These mechanisms are described in further detail below (Figure 3).

4.1 TLRs activate microglia to reduce neurogenesis

TLRs, expressed on microglia are a subfamily of pattern recognition receptors (PRRs) that identify endogenous noxious stimuli and invading pathogens, thereby inducing induction of innate and adaptive immune responses (109, 110). Experimental results demonstrated that social avoidance and anxiety induced by repeated social defeat stress (R-SDS) were abolished in mice lacking Toll-like receptors 2 and 4 (TLR2/4). Transcriptome analysis further revealed that microglia in the brains of R-SDS mice induced the expression of IL-1α and TNF-α via the TLR2/4 signaling pathway. Treatment capable of blocking microglial-mediated cytokine release was able to attenuate R-SDS-induced social avoidance. These results suggest a crucial role of TLR2/4 in microglial activation and cytokine release in response to R-SDS-induced stress (111). Research has revealed that Toll-like receptor 5 (TLR5) expression in mouse embryonic stem cells promotes neurodifferentiation and enhances it through the nuclear factor-κB and interleukin 6/CREB pathways. Furthermore, TLR5 expression was also observed in the SGZ of the hippocampus in rat, where it governs the proliferation of adult hippocampal NSCs by regulating the cell cycle, and promotes neural differentiation through the JNK pathway. These findings provide evidence of TLR5's significant modulatory role in neurogenesis from embryonic stem cells and adult hippocampal NSCs, and suggest it is a promising therapeutic target for Brain-related diseases (112). In contrast, promising immunosuppressive drugs, such as icariin, can improve neuroinflammation in the hippocampus by inhibiting the activation of the TLR4-NF-κB signaling pathway to exert protective effects on neurogenesis, thereby improving depressive behavior in mice (113). These results provide a new understanding of depression pathology, wherein inflammation can be triggered by activating TLRs in microglia, resulting in a reduction in neurogenesis, and ultimately playing a crucial role in the development of depression.

4.2 NLRP3 inflammasome triggers microglia to regulate neurogenesis

Inflammasomes are cytosolic immune signaling complexes that lead to inflammation and pyroptosis. They are composed of pattern recognition receptors, adapter structural domains and enzymatic caspase-1 structural domains. Inflammasome initiation sensors are PRRs, including nucleotide-binding oligomerization domains leucine-rich repeat-containing protein receptors (NLRs), which are not present in melanoma-2-like receptors, and proteins with tripartite motifs (114). NLRs consist of NLRP1, NLRP2, NLRP3, NLRP6, NLRC4, and NLRP12, of which NLRP3 has received the most attention in studies of the pathological mechanism of depression (115, 116). Male C57BL/6 mice were subjected to CUMS for a period of 6 weeks. A comprehensive assessment of negative emotional behaviors was carried out to determine the susceptibility of the mice. Various parameters such as microglial activation, transcription of endogenous retroviral sequences, intrinsic nucleic acid sensing response, and immune inflammation were evaluated in the Basolateral Amygdala. The findings of the study revealed that chronically stressed mice exhibited significant depressive and anxious-like behaviors, accompanied by notable microglial cell morphological activation, transcription of MuERV-L, MusD, and IAP genes, activation of the cGAS-IFI16-STING pathway, initiation of the NF-κB signaling pathway, and activation of the NLRP3 inflammasome in the Basolateral Amygdala (115). However, these abnormal indicators were gradually reversed after antidepressant administration, suggesting a close link between

TABLE 1 Expression patterns of depression-like behaviors, microglia, inflammatory molecules, and molecular markers of neurogenesis in rodent models of depression.

Depression model	Stress	Animal	Test/ Score	Behavioral Effects	Microglia	Pro-inflam-mation	Antiinflammation	Proliferation	Differentiation	Reference
Early-life stress	MS for 14 days	♂ C57BL/6 J mice(baby)	SPT FST OFT	control and immobility time >mean of control The SPT and OFT showed no significant differences between maternal-separated or control mice in terms of the number of spontaneous movements	↑Activated microglia ↓The average number and length of microglial processes ↓Expression of the microglial marker CX3CR1	↑iNOS ↑TNF-α ↑IFN-γ ↑IL-6 ↑IL-1β	↓IL-4 ↓TGF-β ↓IL-1rα ↓Ym-1 ↓Arg-1	↓$BrdU^+$	↓$BrdU^+/DCX^+$	(100)
Adult stress	CUMS for 4 weeks	♂ Sprague Dawley rats (3 weeks)	SPT OFT MWM	↓sucrose preference ↓Time in the center of the open field ↑escape distance	↑the number of Iba-1^+ microglia ↓the mean number of intersections and surface area ↓ramification length ↑soma volume	——	——	——	↓DCX^+	(101)
	CUMS for 21 days	Cx3cr1CreERT2 mice and Nr3c1fl/fl mice (6.5 to 8.5 weeks)	Saccharin preference PR	↓Body weight ↓Saccharin preference	↑arborization area ↑Cell body areaTrem2 ↑Cx3cr1 ↑Mertk	↑CD68 ↑TNF-α ↑IL-1β	↓Arg-1 ↓Fizz-1	↓Ki-67	↓DCX	(102)
	CUS for 5 weeks	♂ C57BL/6 mice (3-4 months)	SPT NOR	↓Exploration time Sucrose preference	↓Microglia number ↓Processes length ↑Soma area	——	——	——	↓DCX^+	(103)
	CUS for 6 weeks	♀ Sprague-Dawley rats (10 months)	SPT NSF FST	↑immobility and swimming and struggling behavior in FST ↑anxiety-like behavior in NSF ↑anhedonia-like behavior in the SPT ↓Body weight	the number and length of Iba-1^+ microglia are equal in OVX and sham surgery	——	——	——	——	(104)
	CMS for 3 weeks	♂ C57BL/6J mice (8-10 weeks)	TST FST	↑immobility and swimming and struggling behavior in FST ↓sucrose preference	↓Microgia number ↓Processes length ↑Soma area ↑iba -1^+	↑iNOS ↑CD86 ↑CD45 ↑CD11b	↓IL-4 ↓Arg-1 ↓CD206	↓$BrdU^+$	↓$BrdU^+/DCX^+$	(105)

(Continued)

10.3389/fimmu.2023.1193053

TABLE 1 Continued

Depression model	Stress	Animal	Test/ Score	Behavioral Effects	Microglia	Pro-inflam-mation	Antiinflammation	Proliferation	Differentiation	Reference
Infectious organisms	0.83 mg/kg LPS (I.p.)	♂ ICR mice (8 weeks)	SPT OFT TST FST	↑immobility time in the FST and TST ↓sucrose preference	↑the number of Iba-1$^+$ microglia ↓the number of ramifications	↑IL-6 ↑TNF-α ↑IL-18	↑IL-4 ↑IL-10	——	↓DCX$^+$	(106)
	0.83 mg/kg LPS (I.p.)	♂ ICR mice	SPT OFT TST FST	↓the total distance traveled ↓the time spent in the central area ↓the inner area distance traveled ↓sucrose preference in the SPT ↑immobility time in the TST and FST	↑the number of Iba-1$^+$ microglia ↓the number of ramifications	↑CD68 ↑CD16 ↑CXCL10 ↑iNOS ↑IL-1β ↑TNF-α ↑IL-18	↑Arg-1 ↑CD206	——	↓DCX$^+$	(107)
Gene mutation	——	♂ Arid1afl/fl mouse(1-2 weeks)	OFT LDB EPM MWM FC MBT Self-grooming test	↓Body weight ↓the time in the center of the open field ↓the time In the light region The open arm is less significant in the elevated crypto,did not cause any difference in Y maze experiment and MWM	↑Soma area ↑iba-1	——	↑Arg-1	↓BrdU$^+$	↓NeuN$^+$BrdU$^+$ ↓DCX$^+$Brdu$^+$	(108)

BrdU, 5-Bromo-2-deoxyuridine; CD, Cluster of differentiation; CMS, Chronic mild stress; CUMS, Chronic unpredictable mild stress; CUS, Chronic unpredictable stress; CX3CR1, C-X3-C motif chemokine receptor 1; EPM, Elevated plus maze; FC, Fear conditioning; FST, Forced swimming test; Iba-1, Ionized calcium binding adapter molecule 1; IL, Interleukin; IFN-γ, Interferon-γ; I.P., Intraperitoneal injections; iNOS, Inducible nitric oxide synthase; LDB, The light–dark box; MBT, Marble burying test; MS, Maternal separation; MWM, Morris water maze; NOR, Novel object recognition; NSF, Novelty-suppressed feeding test; OFT, Open field test; PR, Progressive ratio schedule; SPT, Sucrose preference test; TGF-β, Transforming growth factor-β; TNF-α, Tumor necrosis factor α; TST, Tail suspension test.

10.3389/fimmu.2023.1193053

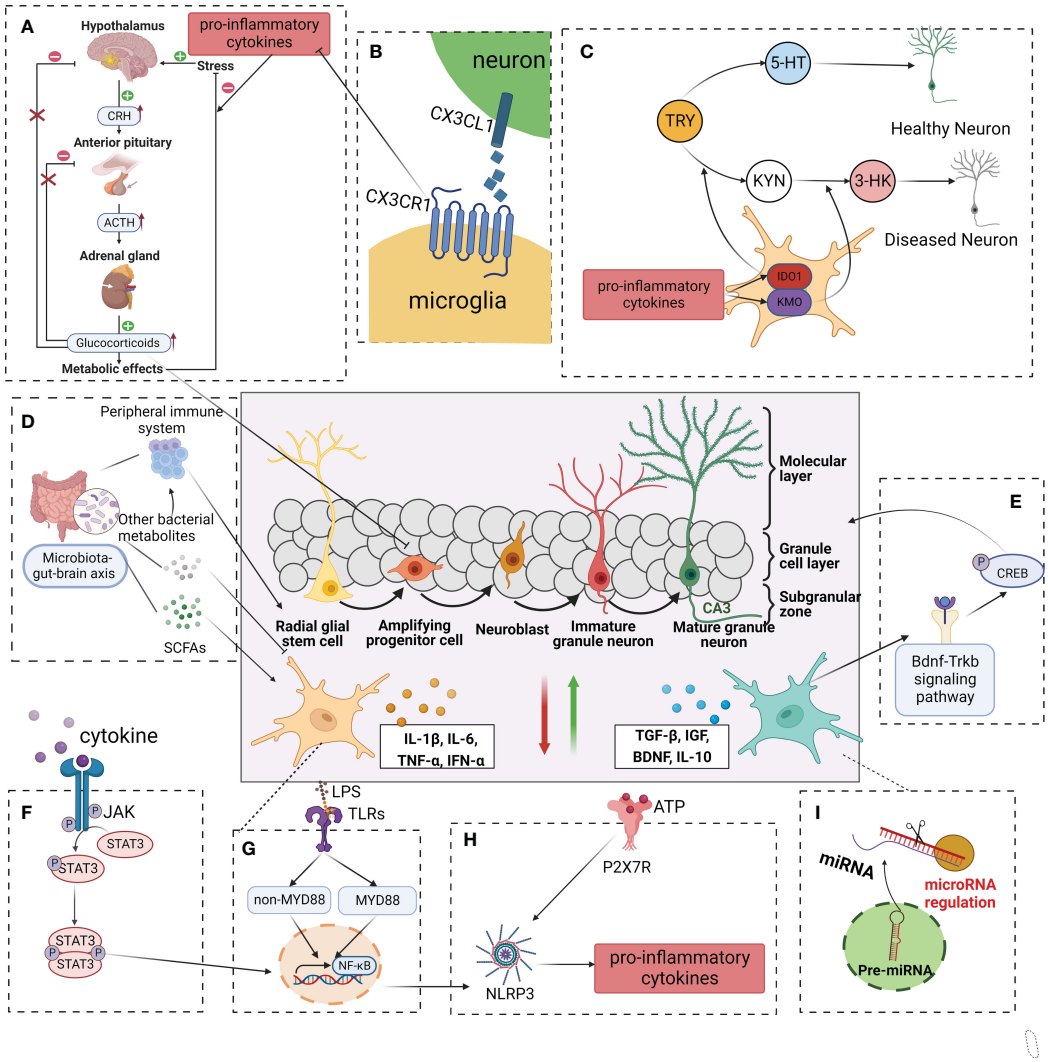

FIGURE 3
Modulation of adult neurogenesis by microglia in depressive. In a healthy central nervous system, microglia produce neurotrophic factors, phagocyte redundant neurons, and connections, remove cell debris, and control stem cell proliferation, in this way regulating synaptogenesis and neuronal pruning. In a pathological state, exogenous and endogenous factors such as infections(LPS), stress, and systemic inflammation/metabolic deregulation can induce microglial activation and impaired neurogenesis. **(A)** Cytokines such as IL-1β, IL-6, and TNF-α, with negative consequences to the HPA axis. **(B)** CX3CR1 is involved in interactions between microglia and neurons, which may reduce to pro-inflammation cytokine. **(C)** Inflammatory microglia(M1) also exhibit upregulated IDO, reducing serotonin availability and possibly contributing to neurogenesis in depression. **(D)** SCFAs、other bacterial metabolites and components of the immune system can affect microglial maturation, activation and function. **(E)** A neuroprotective microglial phenotype (classically referred to as "M2-like") activated the BDNF-TrkB-CREB signaling pathway, enhanced neurogenesis, diminished synapse loss in the hippocampus, and contribute to an overall lower level of neuroinflammation. **(F–H)** Intracellularly, several pathways become activated including the TLR, JAK, and STAT, which will trigger the activation of the NF-κB, downregulate NLRP3, and consequent induction of first-line cytokine production, such as IL-1β, IL-6, and TNF-α. **(I)** MicroRNAs have been associated with multiple pathways of depression pathophysiology. LPS lipopolysaccharide, TLR toll-like receptor, JAK Janus kinase, STAT signal transducer and activator of transcription, NF-κB nuclear transcription factor-kappa B, NLRP3 nod-like receptor protein 3, IL-1β interleukin-1β, IL-6 interleukin 6, TNF-α tumor necrosis factor-alpha, HPA hypothalamic-pituitary-adrenal, IDO indoleamine 2,3-dioxygenase, CX3CR1 C-X3-C motif chemokine receptor 1, BDNF-TrkB-CREB brain derived neurotrophic factor- tyrosine kinase receptor B- cyclic adenosine monophosphate response element binding protein, SCFAs short chain fatty acids.

depression and the NLRP3 inflammasome. For example, Du et al. found that fluoxetine, a classical antidepressant, can remarkably suppress the activation of NLRP3 inflammasome, followed by reduced caspase-1 cleavage and IL-1β which were secreted in peripheral macrophages and central microglia (117). Recent studies have demonstrated that they can diminish the expression of NLRP3 inflammasome and lower the levels of inflammatory factors that are regulated by microglia, ultimately providing anti-depressant effects. NLRP3 is also involved in the regulation of neurogenesis. Many studies have shown that microglia triggered by NLRP3 inflammasome activation secrete many more pro-inflammatory cytokines, such as IL-1β, thus resulting in the reduction of hippocampal neurogenesis (118). Conversely, mice were exposed to CMS for three weeks, and the results revealed that CMS exposure altered the morphology of microglia in the hippocampus and increased the number of $TUNEL^+$ and $GSDMD^+$

microglia in the dentate gyrus (119). Furthermore, the CMS exposure led to a decrease in the number of 5-ethynyl-2-deoxyuridine (BrdU) $^{+}$, BrdU-DCX^{+}, and BrdU-NeuN^{+} cells in the hippocampal dentate gyrus, as well as a reduction in the percentage of NeuN^{+} cells among BrdU^{+} cells. Additionally, the expression of pyroptosis-related molecules, such as NLRP3, caspase-1, GSDMD-N, and IL-1β, was significantly upregulated in the hippocampus of CMS-exposed mice (119). These findings indicate that CMS exposure impairs hippocampal neurogenesis and induces microglial pyroptosis. The study found that porphyran suppressed the NF-κB/NLRP3 signaling pathway in the hippocampus and activated the BDNF/TrkB/ERK/CREB signaling pathway in CUMS mice, thereby inhibiting the activation of microglia and reducing the release of pro-inflammatory cytokines mediated by microglia (120). It also increased the expression of DCX in the hippocampal DG area, promoted neurogenesis, and maintained synaptic plasticity, ultimately exerting an antidepressant effect (120). These data have shown that NLRP3 plays a key role in the regulation of neurogenesis, a key molecular mechanism in the pathogenesis of depression.

4.3 Imbalance of polarization of microglia affect neurogenesis

The M1 and M2 polarization of microglia differentially regulates neurogenesis in physiological and pathological states (121). M1 polarization of microglia is negatively correlated with neurogenesis (117). The M1 phenotype of microglia secretes excessive inflammatory mediators that lead to impaired neurogenesis and promote the onset and progression of depression. Additionally, pro-inflammatory mediators such as macrophage inflammatory protein-2 (MIP2), IL-1β, iNOS, and TNF-α activate M1 microglia, which then produce many more damaging factors that reduce hippocampal neurogenesis and induce depression (121). The activation of microglia into the M1 state affects neurogenesis by inhibiting the proliferation of NSCs, increasing the apoptosis of neural progenitors, and reducing the survival of newborn neurons and their integration into existing neural circuits (122). In contrast, M2 polarization of microglia, an alternative subtype of microglial activation, is positively correlated with neurogenesis. A recent study found that the alternatively activated microglial phenotype (M2), which is activated by IL-4, enhances neurogenesis and thus ameliorates depression-like behaviors (123). Therefore, modulating the microglial phenotype to regulate neuroinflammation and neurogenesis appears to be a possible mechanism for the development of depression.

4.4 Transcription (STAT) family members activate microglia to regulate neurogenesis

The Janus kinase (JAK)/STAT pathway is engaged in the modulation of a number of CNS functions, involving neurogenesis, synaptic plasticity and microglia activation, all of which are implicated in the pathophysiology of depression (124, 125). First, JAK/STAT signaling is important for regulating inflammatory responses and microglial polarization (125). Studies have shown that inhibition of the JAK/STAT1 pathway can block microglial activation and suppress microglia-mediated neuroinflammation. Kwon et al. found that microglia-specific STAT3 KO mice showed antidepressive-like behavior in the animal model of chronic stress procedures, suggesting that suppression of microglia STAT3 may be a new treatment tactic for depression (126). Furthermore, recent studies have indicated that JAKs may have a role in hippocampal neurogenesis. For instance, research has demonstrated that pharmacologically inhibiting JAK3 in cultured neurons can stimulate neurogenesis (127). Other studies have shown that JAK3 is involved in inhibiting neurogenesis and causing depressive symptoms in animal models under stress (128, 129). As a result, JAK3 inhibition has the potential to improve depressive and anxious behavior and restore normal levels of hippocampal neurogenesis in mice subjected to stress (130). However, microglia modulate the mechanisms of microglia as well as neurogenesis in response to depression via the JAK/STAT signaling pathway is unclear. Therefore, it is important to concentrate on the JAK/STAT signaling pathway in microglia and elucidate its relationship with depression. Such research may provide new insights for future studies on depression.

4.5 Activation of Fractalkine-CX3CR1 in microglia suppresses neurogenesis

The signaling pathway of Fractalkine-CX3CR1 is essential for regulating of interactions between microglia and neurons (131). Fractalkines, also called CX3CL1, are transmembrane chemokines expressed by neurons in the brain. It reduces migration and increases neuronal adhesion (132). A combination of CX3CR1 and CX3CL1, which is only expressed by microglia, maintains microglia in a quiescent state, and hence inhibits the release of pro-inflammatory cytokines (133). CX3CR1 is significantly upregulated in depression (134). The character of microglia in modulating neurogenesis in depression via the CX3CL1-CX3CR1 signal is complex and controversial. Evidence has shown that CX3CL1-CX3CR1 signaling participates in the control of microglial activation, and thus influences adult neurogenesis. For instance, there are reports indicating that compared with wild-type mice, the number of DCX^{+} positive cells and BrdU^{+} labeled cells in the hippocampus of CXCR1 deficient mice is reduced, indicating that neurogenesis is inhibited due to CX3CR1 deficiency (135). Similarly, studies have shown that the deficiency of the CX3CR1 of microglial damages synaptic integration in hippocampal granule neurons in adult neurogenesis, promotes the activation of microglia in the DG of CXCR1 deficient mice, and induces a pro-inflammatory phenotype in this area of DG (136). These results suggest that microglia regulate adult hippocampal neurogenesis via CX3CL1-CX3CR1 signaling. However, many contradictory reports have been published. For example, Mattison et al. found that the freeing of pro-inflammatory factors such as IL-6 was significantly reduced by LPS administration in CX3CR1 knockout mice, suggesting an obvious suppression of the inflammatory response in CX3CR1 knockout mice (137). Moreover, Liu et al. found that deficiency of CX3CR1

might promote alternative activation of microglia (M2 polarization) and attenuate their ability to synthesize and release inflammatory cytokines, thus benefiting adult neurogenesis (138). Therefore, the role of CX3CL1/CX3CL1 signaling in microglial activation and subsequent regulation of neurogenesis in depression is an intricate and controversial topic of research, which is further complicated as new studies have revealed inconsistent results.

4.6 Abnormalities in the HPA axis inhibit adult neurogenesis involving pro-inflammatory cytokines released by microglia

The HPA axis is a complicated combination of interactions concerning the pituitary, hypothalamus gland, and adrenal gland. The HPA axis is an essential component of the neuroendocrine system and is related to the control of stressful responses and the pathophysiology of a lot of neuropsychiatric disorders (139). Inflammation and stress stimulate the hypothalamus to secrete corticotropin-releasing hormone, which further stimulates the pituitary to release corticotropin. The adrenal gland releases glucocorticoids, which can act on the hypothalamus for negative feedback regulation. The HPA axis is hyperactive during depression (140). Abnormalities in the HPA axis are observed in a substantial proportion of patients with depression and are primarily characterized by glucocorticoid dysregulation (141). Studies have shown that excessive glucocorticoids reduce the proliferation of nerve cells, thereby inhibiting adult neurogenesis (142). Moreover, adult hippocampal neurogenesis can mediate negative feedback through the HPA axis. Snyder et al. used the spatial specificity of X-ray irradiation to reduce hippocampal neurogenesis, resulting in excessive secretion of glucocorticoids (135). Taken together, glucocorticoids reduce adult hippocampal neurogenesis, resulting in the failure of negative feedback that is critical for the HPA axis, which leads to a persistent elevation of glucocorticoids and reduces adult hippocampal neurogenesis. This vicious cycle may play an essential character in depression pathophysiology. Interestingly, regulation of the HPA axis is also influenced by cytokines released by microglia. For example, microglia-discharged pro-inflammatory cytokines, such as IL-1 and IL-6, can effectively induce glucocorticoid secretion during chronic and acute stress (143). Therefore, microglia may regulate the HPA axis by releasing pro-inflammatory factors and elevating glucocorticoids to reduce adult hippocampal neurogenesis, thereby playing a crucial role in depression.

4.7 Reduction of 5-HT suppresses neurogenesis relates to the activation of microglia

TRY metabolism involves two important metabolic pathways: 5-HT synthesis and kynurenine synthesis. The 5-HT synthesis is initiated by tryptophan hydroxylase, which converts TRY to hypoxanthine, which in turn is converted to 5-HT by serotonin synthetase (144). It is currently known that 5-HT strongly correlates with the pathogenesis of depression. Selective serotonin reuptake inhibitors (SSRIs), the most common clinical antidepressants, improve depressive mood by adding the 5-HT levels of the synaptic cleft (145). Studies have reported that 5-HT is synthesized by 5-HT neurons located in the raphe nucleus, and has significant implications in the regulation of neurogenesis. Removal of 5-HT neurons in the dorsal raphe and median raphe has been found to decrease neurogenesis, which is recovered by 5-HT reinnervation. Increased 5-HT levels have been shown to promote neurogenesis, thereby improving depressive behavior (146). Thus, the depletion of 5-HT suppresses neurogenesis in the DG, which is a hypothesis for the pathogenesis of depression. Another catabolic pathway of TRY contains indoleamine 2,3-dioxygenase (IDO) and TRY 2,3-dioxygenase (TDO), which produce by metabolism from TRY to kynurenine (KYN) (147). When the KYN metabolic pathway is enhanced, it deprives TRY of 5-HT synthesis, resulting in reduced serotonin production (148). Increased activation of the KYN pathway has been observed in depressed patients, and the level of activation is relevant to the level of depression (149). KYN can be further metabolized into several neurotoxins such as 3-hydroxykynurenine (3-HK), which is catalyzed by kynurenine monooxygenase (KMO) (150). Numerous studies have shown that pro-inflammatory cytokines stimulate IDO and KMO, which are mainly expressed in microglia, thereby increasing neurotoxins, which is one of the potential mechanisms by which inflammation is mediated by microglia and induces depression (150). However, the mechanism by which microglial activity interacts with KYN metabolites has not been definitively determined, though we can infer that under stress conditions, pro-inflammatory factors released by activated microglia activate the kynurenine pathway, resulting in a decrease in the synthesis of 5-HT and an increase in neurotoxins such as 3-HK, which may inhibit neurogenesis and lead to depression.

4.8 Cytokines secreted by microglia participate in neurogenesis

Cytokines are redundant secreted proteins with growth, differentiation, and activation functions that regulate and determine the nature of immune responses and control immune cell trafficking and cellular arrangement of immune organs (151). Inflammatory cytokines consist of pro-inflammatory and anti-inflammatory cytokines, the balance of which determines whether the body produces an inflammatory response. The role of cytokines in neurogenesis is reflected in the fact that pro-inflammatory cytokines impair neurogenesis, whereas anti-inflammatory cytokines protect or promote neurogenesis. Excessive pro-inflammatory cytokines induce an inflammatory response, which can induce the expression and release of cathepsin C in microglia to promote an inflammatory response and reduce neurogenesis (152). For example, IL-1β, IL-6, TNF-α, and IFN-α are currently the broadest studied inflammatory cytokines (153). Multiple studies have suggested that TNF-α and IL-6 levels are increased remarkably in the peripheral blood of depressed patients than in healthy controls, suggesting a strong association between inflammatory

cytokines and depression (153). This mechanism may be related to the activated M1 microglial phenotype (154, 155). Conversely, anti-inflammatory cytokines, including TGF-β and IL-10, secreted by M2 phenotype microglia, exerted anti-inflammatory effects. Furthermore, existing evidence suggests that inflammatory cytokines are strong relativity of neurogenesis. For instance, CMS exposure in mice was found to upregulate inflammatory factors and inhibit neuronal growth in the dentate gyrus region of the hippocampus, leading to depression-like behavior (156). Surprisingly, drug treatment reprogrammed Arg-1$^+$ microglial cell phenotypes in the dentate gyrus region, suppressed neuronal inflammation, increased the quantification of hippocampal newborn neurons (BrdU$^+$ - DCX$^+$ cells), and improved depression-like behavior in CMS-exposed mice (156). Thus, the balance of cytokines participates in neurogenesis, thus influencing the occurrence of depression.

4.9 BDNF and its cascade signaling promote neurogenesis associated with microglia

BDNF, a protein synthesized in the brain and are widespread in the CNS, has critical function in the survival, differentiation, growth, and development of neurons (157). Tyrosine kinase receptor B (TrkB) acts as a BDNF specific receptor. Binding to the TrkB receptor activates intracellular signaling pathways that play an important role in sustaining neural growth, neuronal differentiation, and neuronal survival, as well as in maintaining synaptic plasticity and neuronal structure and function in adults (158). Wen et al. found that BDNF and TrkB were significantly reduced in the brain, especially in the hippocampus of mice, with significantly increased depressive and anxiety-like behaviors, suggesting a strong link between depression and the BDNF-TrkB signaling pathway (159). This mechanism may be related to the function of the BDNF-TrKB signaling pathway in neurogenesis. For example, Sonoyama et al. demonstrated that BDNF variants and variants of the TrkB kinase domain can lead to damaged processing and secretion of mature peptides in the BDNF-TrKB signaling pathway, resulting in impaired neurite growth and inhibition of hippocampal neurogenesis (160). Notably, Li et al. have shown that upregulation of the BDNF-TrkB signaling pathway can promote neuronal plasticity and thus increase the antidepressant response (161). In addition, some studies have found that the BDNF-TrkB signaling pathway is associated with microglia. Bagheri et al. found that high activation of M2 microglia and decreased activation of M1 microglia resulted in increased BDNF secretion (162). Ding found that BDNF can accelerate the activation of microglia to free TNF-α and IL-1β, aggravating the neuroinflammatory response through the BDNF-TrkB signaling pathway (162). The microglial subset with high expression of Arg-1 driven by IL-4 is crucial for maintaining hippocampal neurogenesis and stress resilience. In a mouse model, reducing Arg-1$^+$ microglia led to decreased secretion of BDNF from Arg-1$^+$ microglia in the DG region of the hippocampus, resulting in reduced survival and maturation of NSPCs and inhibition of hippocampal neurogenesis, as well as increased susceptibility to stress-induced depression. Conversely, enhancing IL-4 signaling to increase Arg-1$^+$ microglia restored hippocampal neurogenesis and resistance to stress-induced depression (105). Therefore, microglia can promote neurogenesis and reduce depressive symptoms by acting on the BDNF or BDNF-TrkB signaling pathway.

4.10 Microbial gut-brain axis regulates the crosstalk between microglia and neurogenesis

The gut-brain axis is a two-way relationship between the gut and CNS connected by neurons of the sympathetic and parasympathetic nervous systems, that has been shown to induce stress-related gastrointestinal and mental symptoms. The gut microbiome is strongly connected to the gut, and by extension the brain, thus extending the gut-brain axis to the gut-brain-microbiota axis (163). Recently, dysregulation of the gut-brain-microbiota axis has been emerged as one of the leading hypotheses for explaining the pathogenesis of depression (164). Yu Du. found that mouse treated with antibiotics demonstrated a reduction in saccharin preference due to more than 90% of the gut microbiota being killed by antibiotics, which may indicate the key function of the gut microbiota in depressive-like behaviors (164). The underlying mechanism may be related to the significant role of gut microbiota in regulating the maturation and activation of microglia. Sun et al. found that changes in gut microbiota led to systemic inflammation that differentially activated inflammatory regulatory pathways in the brain, especially those associated with microglia, leading to the occurrence of depression (165). Carlessi et al. found that gut microbes secrete substantial amounts of microglia-activated amyloid and LPS to induce depression (166). Furthermore, several clinical and experimental studies have indicated that gut microbiota may be both a pathogenic determinant of neurogenesis-related diseases and a novel therapeutic target. For example, Sarubbo et al. found that germ-free (GF) and GF-colonized mice exhibited a trend of cell proliferation with elevated expression of BrdU in the dorsal hippocampus (167). Notably, Cerdó et al. found that using a strain-specific combination of probiotics restores neurogenesis defects in adult patients, which further confirms the link between gut microbiota and hippocampal neurogenesis (168). Previously, literature reported that regulating short-chain fatty acids, which are widely present in intestinal endocrine and immune cells and are important mediators for regulating body function through the gut microbiota, can decrease the ratio of Iba-1$^+$/CD68$^+$ cells in the hippocampal DG area of CUMS mice while increasing Ki67/NeuN, granular cell layer width, and dendritic spine density and quantity of neurons, thereby promoting neurogenesis and exerting an anti-depressant effect (101). In addition, Hanna Karakuła-Juchnowicz et al. found that gut dysbiosis and irritation may dysregulate the immune system near the brain, causing neurodegeneration (169). These results suggest that the microbial gut-brain axis may influence microglial activation and neurogenesis in depression. However, the function of the microbial-gut-brain axis in microglial regulation of neurogenesis requires further study.

4.11 MicroRNA regulates the link between microglia and neurogenesis

MicroRNA (miRNA) is a non-coding RNA (ncRNA) that consists of 18-24 nucleotides, which is highly conserved in species that modulate gene expression, mainly by destabilizing the target mRNA and inhibiting the translation of the target mRNA to regulate target mRNAs (170). Microglia utilize exosomes to transfer microRNAs, specifically miR-146a-5p, to inhibit neurogenesis in cases of depression. Overexpression of miR-146a-5p in the hippocampal DG leads to a suppression of excitatory neuron spontaneous discharge and neurogenesis via direct targeting of Krüppel-like factor 4 (KLF4). Downregulation of miR-146a-5p expression results in improved adult neurogenesis in the DG and alleviates depression-like behaviors in rats. Notably, circular RNA ANKS1B acts as a miRNA sponge for miR-146a-5p and mediates post-transcriptional regulation of KLF4 expression. These findings demonstrate the critical role of miR-146a-5p in regulating neurogenesis during pathological processes related to depression and indicate that exosomes from microglia provide a new communication pathway between glial cells and neurons (171). These data demonstrate that multiple miRNA genes in the human body have different effects on depression and neurogenesis, which will be further clarified. It was also found that different miRNAs also have different effects on the polarization of microglia (172). For example, neuron-derived exosomes with high miR-21-5p expression promote M1 polarization of microglia. In contrast, MiR-124-enriched exosomes promoted M2 polarization of microglia (173). Currently, there are few studies on the roles of miRNAs in the regulation of microglia and neurogenesis, despite the complex link between neurogenesis and microglia in depression. Thus, elucidating the regulatory mechanisms of miRNAs in depression from the perspective of the regulation of microglia in neurogenesis may provide new insights into depression.

5 Drugs targeting microglia to alter neurogenesis for treating depression

According to the above summary, microglia play a significant role in modulating neurogenesis and, thus, play a key function in the pathogenesis of depression. Therefore, here we introduced some drugs that act on this mechanism, some of which are already in clinical use, such as tricyclic antidepressants (TCAs) and SSRI, and some are under development, such as minocycline, ketamine, and natural products derived from plants (Table 2).

5.1 First-line antidepressant drugs in clinical practice

5.1.1 TCAs

TCAs comprise the main category of antidepressant drugs commonly prescribed to treat depression (198). TCAs can inhibit the presynaptic reuptake of 5-HT and norepinephrine, increase the density of monoamine transmitters in the synaptic cleft, and clinically improve depressive symptoms (199). The commonly available TCAs include imipramine, clomipramine, and amitriptyline. Recently, TCAs have been demonstrated to have therapeutic effects of anti-inflammatory and neuroprotection by inhibiting the activation of microglia and promoting neurogenesis in the hippocampus in depression (174, 200). For example, imipramine was found to reduce stress-induced inflammation and depression-like behavior by modulating microglia activation (175). In addition, imipramine inhibits the activation of M1 microglia and the freeing of pro-inflammatory factors to reduce neuronal damage and upregulate BDNF expression to promote neurogenesis (177). However, it is important to note that imipramine is a tricyclic antidepressant known to lower seizure threshold, so caution should be exercised when prescribing it to individuals with epilepsy or those at risk of seizures. Anthor study found that Imipramine has the potential to exacerbate suicidal thoughts during the early stages of administration in patients under the age of 24 (201). Furthermore, Imipramine, along with other types of antidepressants, can potentially trigger the onset of manic or mixed episodes in individuals diagnosed with bipolar disorder (202, 203). Similarly, clomipramine has demonstrated the ability to reduce depressive behavior and neuroinflammation by modulating the microglial NLRP3 inflammasome (176). In another study, Zhang et al. found that clomipramine modulated the microglial NLRP3 inflammasome to reduce depressive behavior and increase hippocampal volume in exposure to CUMS model of rats (204). Meanwhile, amitriptyline was found to inhibit LPS-induced microglial expression of pro-inflammatory factors (205) and increase BDNF expression in microglia (206). It is crucial to recognize that while these TCAs offer potential benefits in treating depression, there are associated risks. For instance, the use of clomipramine during pregnancy has been linked to adverse effects in fetuses, including lethargy and the potential for congenital heart defects, as well as withdrawal symptoms in newborns (207). Additionally, clomipramine may be detected in breast milk, necessitating careful consideration in breastfeeding mothers (207, 208). Amitriptyline, another TCA, has also shown promise by inhibiting microglial expression of pro-inflammatory factors and increasing BDNF expression in microglia (209). However, it's crucial to note that Amitriptyline should never be combined with alcohol or other central nervous system depressants, as this may significantly potentiate their effects. Additionally, caution must be exercised when transitioning from monoamine oxidase inhibitors to Amitriptyline, as doing so within a two-week timeframe can lead to a potentially life-threatening condition known as serotonin syndrome (41). While TCAs come with various risks and potential side effects, these data suggest that some TCAs hold the potential to not only regulate microglial functions for anti-inflammatory effects but also to promote neurogenesis. As discussed earlier, TCAs can inhibit the presynaptic reuptake of serotonin and norepinephrine, leading to an increased concentration of monoamine transmitters in the synaptic cleft. However, it's important to note that the precise mechanisms governing microglial activation and neurogenesis promotion remain unclear and warrant further investigation.

10.3389/fimmu.2023.1193053

TABLE 2 Drugs targeting microglia to alter neurogenesis for treating depression.

Reference	Type	Drug	Model	Modeling method	Dosing	Mechanism: microglia/ Neurogenesis/ microglia -mediated regulation of neurogenesis.
(174)	First-line antidepressant drugs in clinical practice	clomipramine and imipramine	BV2 cells/ primary microglia	treated with or without LPS (100 ng/ml) for 24 h	pretreated with Clomipramine (15 μM) and imipramine(10 μM) for 24h	activation microglia (indirectly)
(175)		imipramine	mice	RSD	oral (15 mg/kg) for 1 week	activation microglia (indirectly)
(176)		clomipramine	mice	injected with LPS (1 mg/ kg)	I. p (20 mg/kg) for 1 week	activation.microglia (indirectly)
(177)		imipramine	mice	CUS for 5 weeks	oral (20 mg/kg)	microglia -mediated regulation of neurogenesis(directly)
		sertraline	mice	CUMS for 5 weeks	oral (5 mg/kg) for 5 weeks	activation microglia (indirectly)
(178)		fluoxetine	mice	UCMS for 6 weeks	oral (15 mg/kg) for 6 weeks	microglia -mediated regulation of neurogenesis(directly)
(100)	Potential anti-inflammatory candidate drugs	minocycline	mice	MS	I. p (20 mg/kg) for 2 weeks	microglia -mediated regulation of neurogenesis(directly)
(179)		ketamine	mice	Genetically engineered mouse	I. p (7 mg/kg)	regulating neurogenesis (indirectly)
(180)		ketamine	rat	treated with long-term corticosterone administration for 4 weeks	I. p (2.5, 5, 10 mg/kg)	regulating neurogenesis (indirectly)
(181)	Natural compounds	Xanthoceraside	mice	CUMS	I. p (0.02, 0.32 mg/kg)	regulating neurogenesis (indirectly)
(182)		Xanthoceraside	microglia	induction with Ab25–35 (10 mM)/IFN-g (10 U/ mL) for 24-h	pretreatment (0, 0.001, 0.01, or 0.1 mM) for 16h	regulating neurogenesis (indirectly)
(183)		Curcumin	BV2 cells	treated with or without LPS (1 μg/mL) for 24 h	pretreatment (1,5, 10, 20, and 40 μM) for 2 h	regulating microglia (indirectly)
(184)		Paeoniflorin	mice	I. p of RESP (1 mg/kg) for 3 days	I. g (10, 20, 40mg/kg) for 3 days	regulating microglia (indirectly)
(185)		Paeoniflorin	mice	CUMS for 5 weeks	I. p (20 mg/kg) for 3 weeks	regulating neurogenesis (indirectly)
(186)		Paeoniflorin	rat	MCAO procedures	I. p (5, 10 mg/kg) for 2 weeks	microglia -mediated regulation of neurogenesis(directly)
(187)		Paeoniflorin	rat	permanent four-vessel occlusion	oral (40 mg/kg) for 4 weeks	microglia -mediated regulation of neurogenesis(directly)
(188)		Resveratrol	mice	I. p of LPS (1 mg/kg)	oral (30 mg/kg) for 7 days	regulating microglia (indirectly)
(189)		Resveratrol	microglia	treated with LPS (1 μg/ ml) for 4 h and ATP (5 mM) for 1 h	pretreatment (10 μM) for 1h	regulating microglia (indirectly)
(190)		Resveratrol	mice	CLP	I. p (10, 30 mg/kg) at 1 hour prior to surgery and again at 6 h, 12 h, and 18 h after surgery	regulating microglia (indirectly)
(191)		Resveratrol	mice	I. p of LPS (5 mg/kg)	I. p (20 mg/kg) for 2 weeks	microglia -mediated regulation of neurogenesis(directly)
(192)		Resveratrol	mice			

(Continued)

TABLE 2 Continued

Reference	Type	Drug	Model	Modeling method	Dosing	Mechanism: microglia/ Neurogenesis/ microglia -mediated regulation of neurogenesis.
				injected with 120 mg kg-1 of D-galactose (0.2 mL per 10/d) for 62 days	oral (functional fermented milk: 0.9% NaCl = 1: 3, functional fermented milk: 0.9% NaCl = 1: 1, functional fermented milk) for 62 days	regulating neurogenesis (indirectly)
(193)	Others	Melatonin	mice	I. p of LPS (5 mg/kg)	I. p (30 mg/kg) for 4 times	regulating microglia (indirectly)
(194)		Melatonin	rat	exposed to pyridostigmine bromide, DEET, and permethrin, and 15 min of restraint stress for 4 weeks	oral (5, 10, 20, 40, or 80 mg/kg) for 8 weeks (5 days/week)	microglia -mediated regulation of neurogenesis(directly)
(195)		Melatonin	mice	CMS for 7 weeks	I. p (2.5mg/kg) for 4 weeks	microglia -mediated regulation of neurogenesis(directly)
(196)		Omega-3 fatty acids	hippocampal progenitor cell	bilateral oophorectomy	PUFA treatment (approximately 340 mg/g for EPA, 240 mg/g for DHA) for 10 weeks	microglia -mediated regulation of neurogenesis(directly)
(197)		Omega-3 fatty acids	mice	I. p of LPS (1 mg/kg)	feed with n-3 PUFA balanced	microglia -mediated regulation of neurogenesis(directly)

CLP, Cecal ligation and puncture; CMS, Chronic mild stress; CUMS, Chronic unpredictable mild stress; CUS, Chronic unpredictable stress; I. g, intragastric administration; I. p, intraperitoneal injection; MS, Maternal separation; RSD, Repeated social defeat; UCMS, Unpredictable chronic mild stress.

5.1.2 SSRIs

Currently, SSRIs are the first line of antidepressants used in clinical practice. This category includes sertraline, paroxetine, fluvoxamine, fluoxetine, citalopram, and escitalopram, which selectively inhibit 5-HT reuptake by antagonistically binding presynaptic membrane 5-HT transporters in neurons, thus increasing the concentration of 5-HT in the synaptic cleft (204, 210). Previous studies have shown that adult neurogenesis and olfactory memory are positively regulated by fluoxetine. It is reported that increased release of pro-inflammatory cytokines by microglia and activation of M1 microglia may lead to elevated expression of serotonin transporter (SERT) (211). Interestingly, SSRIs not only target SERT by inhibiting serotonin reuptake but also centrally act on microglial cells that respond to various signals of inflammatory factors (212). Similarly, fluoxetine cannot improve behavior by inhibiting SERT, which is observed that the increasing the deprivation of dopaminergic neurons and the hurtful activation of microglia in the substantia nigra pars compacta during LPS-induced neurotoxicity (213). These findings support the notion that SSRIs reduce microglial activation by modulating SERT and improving depressive symptoms (214–216). The protective role of SSRIs in neurogenesis has been found to be closely related to the 5H-T and BDNF signaling pathways in schizophrenic models (217). There are no existing studies showing that SSRIs modulate 5-HT to further modulate microglial activation, improve neurogenesis, or alleviate depression. Interestingly, it has been shown that escitalopram before and after treatment can prevent CA1 neuronal death induced by cerebral ischemia by increasing BDNF and thereby reducing microglia activation and oxidative stress (218). Troubat et al. found that the administration of fluoxetine to CUMS mice effectively reduced the activation of microglia in the DG area of the hippocampus of CUMS mice, alleviated neurogenesis damage in the hippocampus, and reduced Depression-like phenotype in CUMS animal model (178). Silvia Alboni et al. obtained the same results (219). SSRIs often recommended as first-line antidepressants, typically take 2 to 4 weeks to initiate therapeutic effects, reaching their maximum efficacy within 4 to 8 weeks (220). However, these benefits come with a range of potential side effects, including gastrointestinal symptoms, hepatotoxicity, weight gain, and metabolic irregularities, as well as the possibility of cardiovascular complications (221). What's noteworthy is that fewer than 50% of patients do not experience complete relief from their depressive symptoms when treated with initial SSRI therapy (222). This limitation necessitates a transition to second-line treatment options. Furthermore, it's essential to recognize that the use of antidepressants carries an elevated risk, especially in individuals predisposed to bipolar disorder, of experiencing manic or hypomanic episodes (223). In the future, the promising potential of SSRIs to foster adult hippocampal neurogenesis through their modulation of microglial cells holds great significance. While this avenue shows considerable therapeutic promise, it is essential to address and mitigate the potential side effects associated with SSRIs. As we continue to delve into the intricate mechanisms of neurogenesis and microglial activation, the path forward involves refining the use of SSRIs to maximize their benefits in alleviating depression while

minimizing adverse effects. Additionally, ongoing research endeavors aim to uncover novel approaches that harness the neurogenic advantages of SSRIs, ultimately paving the way for more effective and safer antidepressant treatments.

5.2 Potential anti-inflammatory candidate drugs

5.2.1 Minocycline

A recent meta-analysis of clinical trials assessed t antidepressant effects and side effects of pharmacological anti-inflammatory interventions in depression or depressive symptoms, revealing that anti-inflammatory agents could enhance the treatment effects of minocycline (224)Minocycline, one of the most studied anti-inflammatory agents, is a second-generation semi-synthetic tetracycline derivative that exhibits efficient spectrum antibacterial effects (70) Further research has found that minocycline exerts its antidepressant effect mainly by inhibiting the activation of microglia, thus protecting hippocampal neurogenesis. For instance, Laumet et al. showed that inflammatory cytokines, including IL-6 and TNF-α, released by hyperproliferative microglia in the hippocampus with peripheral nerve injury could induce secondary changes in hippocampal neurons, thus leading to depression-like phenotype. These effects were reversed by administration of minocycline (225). More importantly, minocycline could alleviate depression-like behaviors induced by early stress in adolescent mice by inhibiting microglial activation and restoring neurogenesis in the hippocampus (100). Additionally, Wadhwa et al. found that minocycline promotes different stages of neurogenesis, such as proliferation (BrdU, Ki-67), differentiation (DCX) cells, and growth factor (BDNF), by inhibiting microglial activation (226). Another study further showed that minocycline decreased M1 microglial marker protein (CD68 and CD16) expression and increased M2 microglial marker protein (CD206 and Arg-1 protein) expression, resulting in a significant increase in neuronal proliferation via the BDNF/TrkB signaling pathway (227). While these findings are promising, it's important to acknowledge that the current body of evidence is based on a limited number of studies with relatively small sample sizes (70). Therefore, while Minocycline offers a proof-of-concept for treating depression through anti-inflammatory mechanisms, further large-scale clinical trials are necessary to establish its efficacy and safety definitively. These future studies can also explore which subgroups of patients are most likely to benefit from Minocycline-based treatment, possibly based on their microglial markers, inflammatory markers regulating by microglial and neurogenesis markers. In summary, Minocycline presents a compelling candidate for depression treatment due to its anti-inflammatory properties, microglial modulation, and promotion of neurogenesis. Continued research in this direction holds the potential to refine its role in depression therapy and provide tailored solutions for individuals struggling with this debilitating condition.

5.2.2 Ketamine

Ketamine, an N-methyl-d-aspartate receptor antagonist, is considered one of the most promising new agents for antidepression because of its fast and long-lasting antidepressant effects (228, 229). Nonetheless, the antidepressant mechanisms of ketamine remain unclear. Recently, our group found that (R)-ketamine exerts an antidepressant effect by inhibiting microglial ERK-NRBP1-CREB-BDNF signaling in the mPFC of CSDS mice, suggesting that the regulation of ketamine involves microglia and BDNF (230). However, it is unclear whether ketamine affects neurogenesis in the hippocampus. A previous study showed that treatment with ketamine or its metabolite hydroxynorketamine could increase the immune-related protein STAT, after which STAT3 enters the nucleus to regulate downstream transcription, upregulates BDNF, PSD95, and syn1, and alter neuronal plasticity (231, 232). This indicates that ketamine, or its metabolite, plays a crucial function in the modulating of immune-related neuronal plasticity. Notably, another study found that ketamine rapidly relieved depressive-like behaviors by increasing the differentiation of neural progenitor cells and promoting the maturation of new neurons in the DG of the hippocampus (179, 180). Interestingly, another study indicated that ketamine significantly increased the proliferation of NSCs in the DG of model mouse and thus exerted an antidepressant effect but had no effect on synaptic plasticity or hippocampal function (226, 233). While ketamine does offer antidepressant effects, its potential for addiction raises concerns (234). So, the necessity for healthcare supervision in the administration of intravenous ketamine or intranasal esketamine creates a clinical challenge, limiting access for many healthcare providers and their patients. Together, these studies indicate that the antidepressant effect of ketamine may act through a mechanism that modulates microglia and neurogenesis in the hippocampus; however, this mechanism remains to be further studied.

5.3 Natural compounds

5.3.1 Xanthoceraside

Xanthoceraside, a triterpenoid saponin monomer, was extracted from the husk of *Xanthoceras sorbifolia Bunge*. Xanthoceraside has been demonstrated to have a broad protective effect against spatial memory impairment, oxidative stress, and inflammatory reactions (235). Guan et al. demonstrated that xanthoceraside could exert antidepressant effects in several depression models of mice by reversing the CUMS-induced inhibition of the hippocampal BDNF signaling pathway and neurogenesis (181), suggesting that the effect of xanthoceraside on depression is related to the protection of neurogenesis. Moreover, xanthoceraside, a triterpenoid saponin monomer compound, has excellent anti-inflammatory effects by regulating the microglia phenotype. It has also been shown that xanthoceraside can inhibit pro-inflammatory cytokine expression in Aβ25-35/IFN-γ-stimulated, and thus has a good effect on the inhibition of

microglial activation (182). In summary, while there is currently limited information on specific mechanisms in xanthoceraside in regulating neurogenesis via microglia, existing research suggests that xanthoceraside may be a potential drug candidate for depression because of its actions in promoting neurogenesis and enhancing neuroplasticity, and reducing neuroinflammatory reactions mediated by microglia that contribute to depressive symptoms. However, further research is needed to fully understand its efficacy and underlying mechanisms.

5.3.2 Curcumin

Curcumin is a natural substance extracted from the spice turmeric (*Curcuma longa*), a member of the ginger family (Zingiberaceae). Curcumin exhibits various pharmacological properties, such as antioxidant, regulating microglial phenotype, antineoplastic, hypoglycemic, immunomodulatory, and antimicrobial effects (236, 237). Numerous studies have shown that curcumin administration has an obvious antidepressant effect. The mechanism underlying the antidepressant activity of curcumin may involve the regulation of the serotonin and dopamine system, anti-inflammatory effects, and neuroprotection (219, 238). Previous studies have speculated that neurogenesis and neuroprotection in susceptible brain areas may have a critical function in psychiatric and neurological disorders, including anxiety depression, and Alzheimer's disease (239). Recently, it has been shown that treatment with curcumin could reverse hippocampal neuron damage in response to chronic stress and increase cell proliferation and NSCs populations, suggesting that curcumin relieves impaired hippocampal neurogenesis (240). Curcumin also exerts a regulatory effect on microglial phenotypes. For example, curcumin has been shown to significantly alleviate LPS-induced inflammation by switching from the M1 pro-inflammatory phenotype to the M2 anti-inflammatory phenotype by downregulating the TLR4/NF-κB pathway (183, 241). Current research suggests that curcumin has the potential in improving depression by regulating microglia. Moreover, it also promotes neurogenesis, which further alleviates depressive symptoms. However, there is currently no direct evidence to prove that curcumin promotes neurogenesis by modulating microglia. Therefore, more in-depth research is needed to explore the mechanism of curcumin in regulating microglia and promoting neurogenesis, and to further demonstrate it as a drug candidate for treating depression.

5.3.3 Paeoniflorin

Paeoniflorin is a water-soluble monoterpenoid glycoside derived from multiple herbaceous plants such as *Radix Paeoniae Rubra*, *Radix Paeoniae Alba*, *Paeonia suffruticosa*, and *Cimicifugae Foetidae*. Many studies have demonstrated that paeoniflorin possesses multiple pharmacological properties including improving microglial-mediated inflammatory factors, antidepressant, neuroprotective, and anti-apoptotic effects (184, 242). A systematic review and meta-analysis revealed that paeoniflorin can significantly improve depressive-like behaviors in animals, suggesting that paeoniflorin can be a potential treatment for patients with depression (243). First, the antidepressant effects of paeoniflorin may be related to its neuroprotective effects. For example, Sicheng et al. found that paeoniflorin reversed the loss of dendritic spine density and the decline of the expression of BDNF and PSD95 in the hippocampus of CUMS model mouse, thus exerting an antidepressant effect (185). More importantly, paeoniflorin inhibited microglial proliferation by suppressing the JNK and NF-κB signaling pathways, leading to significant reductions in the pro-inflammatory cytokines IL-1β, IL-6, and TNF-α mediated by microglia (186). Compared to the control group, paeoniflorin promoted the expression of von Willebrand factor and doublecortin, suggesting that Paeonia extract contributes to neurogenesis and angiogenesis in rats (186). Paeoniflorin has excellent anti-inflammatory effects. The data indicate that paeoniflorin exerts antidepressant effects and prevents neuroinflammation by inhibiting the CASP-11-mediated pyroptosis signaling pathway activated in overactivated small glial cells in the hippocampus of reserpine-treated mice, resulting in synaptic plasticity abnormalities (184). *In vitro* experiments with N9 microglial cells of mice show that paeoniflorin can also prevent LPS and adenosine triphosphate (ATP)-induced pyroptosis and has an effective and selective CASP-1 activator inhibitor VX-765 to promote the inhibitory effect of paeoniflorin on pyroptosis (184). This reveals a previously unrecognized inflammatory mechanism of antidepressant action, and proposes a unique treatment opportunity to relieve depression through paeoniflorin therapy. Interestingly, there is direct evidence that paeoniflorin can protect neurogenesis by regulating the activation of microglia, modulating M1/M2 subset polarization in the hippocampus, and inhibiting the freeing of inflammatory cytokines (187). These results indicated that the regulation of microglia and hippocampal neurogenesis is an important mechanism underlying the antidepressant effects of paeoniflorin.

5.3.4 Resveratrol

Resveratrol is a polyphenol and phytoalexin derived from the skin of grapes, red wine, Japanese knotweeds, and peanuts. It has been shown that resveratrol has extensive properties including antioxidant, improving microglial-mediated inflammatory factor, and neuroprotective properties (244–246). Resveratrol showed excellent anti-depressive activity with an obvious improvement in depressive-like behavior tests. Alyssa et al. identified three main biological mechanisms of resveratrol, including modulating the HPA axis, microglia, and BDNF and neurogenesis, based on results from 22 preclinical studies (244). In terms of anti-inflammatory properties, resveratrol can inhibit the M1 microglial activation that induced by LPS stimulation, which involves the balance of M1/M2 polarization and the NLRP3 inflammasome (188–190). In terms of neurogenesis, resveratrol could exhibit neuroprotective and hippocampal neurogenesis properties (247). For example, pretreatment with resveratrol was found to activate the Sirt1 pathway, inhibit microglial activation, promote neurogenesis indicated by $BrdU^+DCX^+$ markers, and improve depressive-like behaviors in LPS-treated mice (191). Similarly, Wu et al. found that functional fermented milk rich in resveratrol

significantly enhanced neurogenesis in a D-galactose mouse model (192). It can be concluded that resveratrol could prevent mood dysfunction by increasing hippocampal neurogenesis and reducing glial activation, but the detailed mechanisms remain to be elucidated.

While short-term animal experiments have provided strong support for the potential of natural compounds such as xanthoceraside, curcumin, paeoniflorin, and resveratrol in promoting adult hippocampal neurogenesis mediated by microglial cells as a strategy against depression, there is currently a lack of additional data revealing the potential toxic side effects of these drugs. To gain a more comprehensive understanding of the potential value of these compounds, further animal experiments are needed. Furthermore, these studies should place particular emphasis on investigating the effects of repeated long-term administration of these compounds, including in-depth research into organ toxicity, immune responses, and tolerance. This collective effort aims to ensure the success and safety of these natural compounds in the treatment of depression, providing a more reliable foundation for future clinical practices.

5.4 Others

5.4.1 Glycogen synthase kinase 3 inhibitor

Glycogen synthase kinase 3 (GSK-3) is a serine/threonine kinase enzyme, which has two subunits, including GSK-3α and GSK-3β, the dysregulation of which could lead to mental disorders, including depression and cognitive impairment (248, 249). It has been showed that a significant increase in the activation of GSK-3β has been found in postmortem brain regions of depression patients (249). As a critical regulator of cognitive function, GSK-3β plays a significant role in cognitive processes, including synaptic plasticity, neurogenesis, and neural cell survival (250). *In vitro* and *in vivo* studies have shown that GSK-3 inhibits neurogenesis in the adult hippocampus. In contrast, adult hippocampal neurogenesis is promoted by the inhibition of GSK-3 (251). These results demonstrate that the development of a GSK-3 inhibitor will be beneficial for adult hippocampal neurogenesis. Furthermore, it has been found that the mechanism by which GSK-3 regulates cognitive functions involving neurogenesis, synaptic plasticity, and neural cell survival is related to neuroinflammation. Microglia-mediated inflammatory responses are highly dependent on GSK-3 activity. Studies have shown that GSK-3 has pro-inflammatory effects (252), whereas GSK-3 inhibitors exhibit anti-inflammatory effects by upregulating the release of IL-10 from microglia (253). Therefore, based on the effect of GSK-3 on neurogenesis and microglia, we propose GSK-3 inhibitor as a potential therapeutic agent for depression.

5.4.2 Melatonin

Melatonin, called N-Acetyl-5-methoxytryptamine, is a hormone primarily synthesized and secreted by the pineal gland, and has various biological activities, which contain the modulating of the biological clock, anti-inflammatory, analgesic, anti-depressive, and neuroprotective effects (254). Melatonin exhibits antidepressant effects in multiple animal models, but its mechanism remains unclear (255). Inhibition of neuroinflammation and promotion of neuroplasticity may be the most important mechanisms by which melatonin maintains antidepressant-like effects (256). Melatonin can improve LPS-induced acute depression-like phenotype by suppressing the activation of the microglial NLRP3 inflammasome, thus reducing the pro-inflammatory factors released by microglia (193). In another study, melatonin was found to not only inhibit the M1 microglial activation as well as the NLRP3 inflammasome, but also unregulate the BDNF-ERK-CREB pathway to promote neurogenesis and reduce synaptic loss in the hippocampus (194). Similarly, in CMS rats, melatonin has been found to inhibit inflammatory cytokine production and protect neurogenesis, thus ameliorating depressive symptoms (195). These results suggest that the antidepressant mechanism of melatonin may be engaged in microglial activation and neurogenesis. Although the correlation between melatonin and depression is complex, exploring the effects of melatonin on microglia and neurogenesis in depression may facilitate the development of new antidepressant candidates.

5.4.3 Omega-3 fatty acids

Omega-3 fatty acids are derived from α-linolenic acid, which is mainly obtained from the diet because of its failure to be synthesized by humans. Omega-3 fatty acids, including eicosapentaenoic acid (EPA) and docosahexaenoic acid (DHA), are incorporated into cell membranes and play a significant role in anti-inflammatory processes and the viscosity of cell membranes (257). A meta-analysis verified that low levels of omega-3 fatty acids are strongly associated with the development of mood disorders, while omega-3 fatty acid ingest is related to alleviated depressive symptoms (258). The ovariectomy procedure induces anxiety and depression-like behaviors, accompanied by increased neurodegeneration in the hippocampal region and activation of microglia in rats (196). Additionally, ovariectomy enhances the expression of pro-inflammatory cytokines and suppresses the expression of anti-inflammatory cytokine IL-10 (196). Correspondingly, ovariectomy strengthens the NFκB signaling pathway and shifts microglia polarization from the anti-inflammatory M2 to the pro-inflammatory M1 phenotype (196). However, daily supplementation with omega-3 polyunsaturated fatty acids can inhibit the M1 polarization of microglia in ovariectomy rats and increase the M2 polarization (196). Moreover, omega-3 fatty acids also show a preventive effect on glucocorticoid-induced reduction in hippocampal neurogenesis and increase apoptosis (259). Maternal intake of omega-3 fatty acids can affect hippocampal neurogenesis during development, and this effect may persist into adulthood through alterations in adult hippocampal neurogenesis. Injection of bacterial endotoxin LPS in mice reduced the number of neural progenitor cells, and this effect was exacerbated by a diet deficient in omega-3 fatty acids. A diet deficient in omega-3 fatty acids also reduced DG volume, decreased adult hippocampal neurogenesis ($BrdU^+$ DCX^+ positive cells), and decreased the number of microglia Administration of

omega-3 fatty acids reversed these effects (197). These findings suggest that a diet deficient in omega-3 fatty acids has negative effects on the cellular composition of the adult DG, reduces adult hippocampal neurogenesis, and impairs the monitoring of microglia. It is reported that omega-3 fatty acids significantly reduce the excretion of pro-inflammatory cytokines, including IL-6, IL-1β, and TNF-α, via microglia and have an enhanced anti-inflammatory effect (260). The influence of omega-3 fatty acids on microglia may be a mechanism underlying its antidepressant effects. Therefore, according to the multiple effects on hippocampal neurogenesis and anti-inflammatory effects on microglia, omega-3 fatty acids will be a valuable and safe dietary product in the development of antidepressant agents.

Considering the research on GSK-3 inhibitors, melatonin, and Ω-3 fatty acids in animal models of depression, these therapeutic approaches presently encounter various mysteries and knowledge gaps within the field of depression. Although some potential therapeutic mechanisms have been demonstrated at the cellular and molecular levels, further exploration is essential to fully uncover their potential and the associated risks within the context of the whole organism.

Currently, there are relatively few antidepressant mechanisms and drug candidates that focus on regulating adult hippocampal neurogenesis through the modulation of microglia. The aforementioned pre-clinical and clinical studies provide important ideas and insights for the treatment of depression, particularly in cases related to impaired neurogenesis. Further investigation of specific targets that regulate hippocampal microglia may offer more effective options for drug therapy. These research findings reveal the important role of microglia in hippocampal neurogenesis, providing new avenues for the development of novel drug candidate treatments for depression. Future research should focus on optimizing these drugs and determining their mechanisms of action, in order to more effectively translate these therapeutic methods into clinical practice.

6 Conclusions and perspectives

Depression is a common psychiatric disorder with high morbidity and suicidality that adversely affects an individual's life and is closely related to a decreased life span and impaired quality of life (121). Although decades of research have largely focused on serotonergic dysfunctions in the synaptic cleft, first-line antidepressants designed for the target have not yet received satisfactory results due to the deficiency in patients' responses and serious side effects (261). The main reason for this might be the incomplete understanding of the pathogenesis of this disease.

Adult hippocampal neurogenesis is capable of producing new functional neurons to form supplementary neural connections with other regions of the hippocampus, supporting spatial cognitive function and emotion under physiological conditions. Altered adult hippocampal neurogenesis plays an important role in the development and treatment of depression (262). Microglia, the predominant resident immune cells in the brain, constitute the brain microenvironment that mainly regulates adult hippocampal neurogenesis. The important role of microglia in adult hippocampal neurogenesis under physiological conditions has been demonstrated in several studies. For instance, microglia maintain the neurogenic niche environment through their phagocytic capacity and interaction with neurons through fractalkine-CX3CR1 signaling (263). In addition, microglia secrete growth factors and cytokines to support the development of new neurons in the hippocampus (264). However, the exact molecular mechanisms by which microglia regulate adult hippocampal neurogenesis and contribute to depression remain to be elucidated.

In this review, we illustrate the roles of microglia and adult hippocampal neurogenesis in depression, as well as the possible mechanism of crosstalk between the two. Finally, we summarize potential therapeutic approaches that focus on this mechanism. To draw a conclusion upon the review, when depression occurs, the function of microglial activation in adult hippocampal neurogenesis is similar to a double-edged sword, exerting both protective and detrimental effects. This depends on how the pathological environment determines the fate of microglial phenotypes. In line with this, promising therapies have reversed the shift in microglial phenotypes to those that contribute to the improvement of depression. In clinical trials, heterogeneity among patients with depression is common due to factors such as age, gender, medical history, and severity of symptoms (265). For example, in approximately 52% of untreated patients with depression, a single intervention such as antidepressant medication or evidence-based psychological therapy is insufficient for full remission, with most patients only experiencing partial symptom relief due to patient heterogeneity (266). Among patients participating in "real-world" clinical trials, the combination of patient heterogeneity was 28% (267). In addition, patients with increased inflammatory markers are more likely to be treatment-resistant to commonly used antidepressants. Patients with autoimmune disorders have a high prevalence of depression, and are at increased risk for subsequent autoimmune disorders such as rheumatoid arthritis, multiple sclerosis, inflammatory bowel disease, and systemic lupus erythematosus (268–270). Therefore, this is why about 50% of patients with depression respond to first-line treatment with SSRIs (271). Here, although other candidate drugs can improve microglia function to combat depression, we believe that minocycline, ketamine, and natural compounds paeoniflorin have the most potential, as they can directly regulate microglia function across the blood-brain barrier to enhance neurogenesis and exert antidepressant effects. We expect that our research will have positive implications for the development of future drugs for depression treatment. Therefore, newer genetic, epigenetic, and high-throughput omics technologies are expected to be applied to explore the molecular, cellular, and circuits involved in depression, and to discover novel therapeutic strategies aimed at promoting mechanisms in the future.

Author contributions

SYF, ZBW wrote the manuscript, and they contributed equally to this work. YLG, WJZ, CMW, NJY, JBC, WZH, XWM and XFG

helped to collect and modify this manuscript. JXC and XJL conceived, designed and revised the manuscript. LLF prepared figures and tables, and revised the manuscript. All authors read and approved the final manuscript.

Funding

This work was financially supported by the National Natural Science Foundation of China (No. 82274410), the National Natural Science Foundation of China (No. 81973748; 82174278), Huang Zhendong Research Fund for Traditional Chinese Medicine of Jinan University, Key-Area Research and Development Program of Guangdong Province (No. 2020B1111100001), Guangzhou Key Laboratory of Formula-Pattern of Traditional Chinese Medicine, the Fundamental Research Funds for the Central Universities of Jinan University (116210004), China Postdoctoral Science Foundation (55350600), Guangdong Basic and Applied Basic Research Foundation (32221265), and National Innovation and Entrepreneurship Training Program for Undergraduate (202210559065).

Conflict of interest

The authors declare that the research was conducted in the absence of any commercial or financial relationships that could be construed as a potential conflict of interest.

Publisher's note

References

1. Schramm E, Klein DN, Elsaesser M, Furukawa TA, Domschke K. Review of dysthymia and persistent depressive disorder: history, correlates, and clinical implications. *Lancet Psychiatry* (2020) 7(9):801–12. doi: 10.1016/s2215-0366(20)30099-7

2. Wong CH, Siah KW, Lo AW. Corrigendum: estimation of clinical trial success rates and related parameters. *Biostatistics (Oxford England)* (2019) 20(2):366. doi: 10.1093/biostatistics/kxy072

3. Dean J, Keshavan M. The neurobiology of depression: an integrated view. *Asian J Psychiatry* (2017) 27:101–11. doi: 10.1016/j.ajp.2017.01.025

4. Sorrells SF, Paredes MF, Cebrian-Silla A, Sandoval K, Qi D, Kelley KW, et al. Human hippocampal neurogenesis drops sharply in children to undetectable levels in adults. *Nature* (2018) 555(7696):377–81. doi: 10.1038/nature25975

5. Kempermann G, Gage FH, Aigner L, Song H, Curtis MA, Thuret S, et al. Human adult neurogenesis: evidence and remaining questions. *Cell Stem Cell* (2018) 23(1):25–30. doi: 10.1016/j.stem.2018.04.004

6. Toda T, Gage FH. Review: adult neurogenesis contributes to hippocampal plasticity. *Cell Tissue Res* (2018) 373(3):693–709. doi: 10.1007/s00441-017-2735-4

7. Dranovsky A, Hen R. Hippocampal neurogenesis: regulation by stress and antidepressants. *Biol Psychiatry* (2006) 59(12):1136–43. doi: 10.1016/j.biopsych.2006.03.082

8. Malberg JE, Eisch AJ, Nestler EJ, Duman RS. Chronic antidepressant treatment increases neurogenesis in adult rat hippocampus. *J Neurosci* (2000) 20(24):9104–10. doi: 10.1523/JNEUROSCI.20-24-09104.2000

9. Toda T, Parylak SL, Linker SB, Gage FH. The role of adult hippocampal neurogenesis in brain health and disease. *Mol Psychiatry* (2019) 24(1):67–87. doi: 10.1038/s41380-018-0036-2

10. Gorham LS, Jernigan T, Hudziak J, Barch DM. Involvement in sports, hippocampal volume, and depressive symptoms in children. *Biol Psychiatry Cognit Neurosci Neuroimaging* (2019) 4(5):484–92. doi: 10.1016/j.bpsc.2019.01.011

11. Sardoo AM, Zhang S, Ferraro TN, Keck TM, Chen Y. Decoding brain memory formation by single-cell rna sequencing. *Briefings Bioinf* (2022) 23(6):bbac412. doi: 10.1093/bib/bbac412

12. Zhou Y, Su Y, Li S, Kennedy BC, Zhang DY, Bond AM, et al. Molecular landscapes of human hippocampal immature neurons across lifespan. *Nature* (2022) 607(7919):527–33. doi: 10.1038/s41586-022-04912-w

13. Garcia-Bueno B, Caso JR, Leza JC. Stress as a neuroinflammatory condition in brain: damaging and protective mechanisms. *Neurosci Biobehav Rev* (2008) 32(6):1136–51. doi: 10.1016/j.neubiorev.2008.04.001

14. Maes M, Yirmyia R, Noraberg J, Brene S, Hibbeln J, Perini G, et al. The inflammatory & Neurodegenerative (I&Nd) hypothesis of depression: leads for future research and new drug developments in depression. *Metab Brain Dis* (2009) 24(1):27–53. doi: 10.1007/s11011-008-9118-1

15. Cazareth J, Guyon A, Heurteaux C, Chabry J, Petit-Paitel A. Molecular and cellular neuroinflammatory status of mouse brain after systemic lipopolysaccharide challenge: importance of ccr2/ccl2 signaling. *J Neuroinflamm* (2014) 11:132. doi: 10.1186/1742-2094-11-132

16. Chai Y, Cai Y, Fu Y, Wang Y, Zhang Y, Zhang X, et al. Salidroside ameliorates depression by suppressing nlrp3-mediated pyroptosis via P2x7/Nf-Kappab/Nlrp3 signaling pathway. *Front Pharmacol* (2022) 13:812362. doi: 10.3389/fphar.2022.812362

17. Dantzer R, O'Connor JC, Freund GG, Johnson RW, Kelley KW. From inflammation to sickness and depression: when the immune system subjugates the brain. *Nat Rev Neurosci* (2008) 9(1):46–56. doi: 10.1038/nrn2297

18. Zheng LS, Kaneko N, Sawamoto K. Minocycline treatment ameliorates interferon-alpha- induced neurogenic defects and depression-like behaviors in mice. *Front Cell Neurosci* (2015) 9:5. doi: 10.3389/fncel.2015.00005

19. Cameron HA, Glover LR. Adult neurogenesis: beyond learning and memory. *Annu Rev Psychol* (2015) 66:53–81. doi: 10.1146/annurev-psych-010814-015006

20. Gage FH. Mammalian neural stem cells. *Science* (2000) 287(5457):1433–8. doi: 10.1126/science.287.5457.1433

21. Schmidt-Hieber C, Jonas P, Bischofberger J. Enhanced synaptic plasticity in newly generated granule cells of the adult hippocampus. *Nature* (2004) 429(6988):184–7. doi: 10.1038/nature02553

22. Goncalves JT, Schafer ST, Gage FH. Adult neurogenesis in the hippocampus: from stem cells to behavior. *Cell* (2016) 167(4):897–914. doi: 10.1016/j.cell.2016.10.021

23. Burgess N, Maguire EA, O'Keefe J. The human hippocampus and spatial and episodic memory. *Neuron* (2002) 35(4):625–41. doi: 10.1016/s0896-6273(02)00830-9

24. Davidson RJ, Lewis DA, Alloy LB, Amaral DG, Bush G, Cohen JD, et al. Neural and behavioral substrates of mood and mood regulation. *Biol Psychiatry* (2002) 52(6):478–502. doi: 10.1016/s0006-3223(02)01458-0

25. Kang E, Wen Z, Song H, Christian KM, Ming GL. Adult neurogenesis and psychiatric disorders. *Cold Spring Harbor Perspect Biol* (2016) 8(9):a019026. doi: 10.1101/cshperspect.a019026

26. Siopi E, Denizet M, Gabellec MM, de Chaumont F, Olivo-Marin JC, Guilloux JP, et al. Anxiety- and depression-like states lead to pronounced olfactory deficits and impaired adult neurogenesis in mice. *J Neurosci* (2016) 36(2):518–31. doi: 10.1523/jneurosci.2817-15.2016

27. Duman RS, Aghajanian GK. Synaptic dysfunction in depression: potential therapeutic targets. *Sci (New York NY)* (2012) 338(6103):68–72. doi: 10.1126/science.1222939

28. Borsini A, Merrick B, Edgeworth J, Mandal G, Srivastava DP, Vernon AC, et al. Neurogenesis is disrupted in human hippocampal progenitor cells upon exposure to serum samples from hospitalized covid-19 patients with neurological symptoms. *Mol Psychiatry* (2022) 27(12):5049–61. doi: 10.1038/s41380-022-01741-1

29. Chen SJ, Kao CL, Chang YL, Yen CJ, Shui JW, Chien CS, et al. Antidepressant administration modulates neural stem cell survival and serotoninergic differentiation through Bcl-2. *Curr Neurovascular Res* (2007) 4(1):19–29. doi: 10.2174/156720207779940707

30. Gage FH. Adult neurogenesis in neurological diseases. *Sci (New York NY)* (2021) 374(6571):1049–50. doi: 10.1126/science.abm7468

31. MacQueen GM, Campbell S, McEwen BS, Macdonald K, Amano S, Joffe RT, et al. Course of illness, hippocampal function, and hippocampal volume in major

depression. *Proc Natl Acad Sci U.S.A.* (2003) 100(3):1387–92. doi: 10.1073/pnas.0337481100

32. Vermetten E, Vythilingam M, Southwick SM, Charney DS, Bremner JD. Long-term treatment with paroxetine increases verbal declarative memory and hippocampal volume in posttraumatic stress disorder. *Biol Psychiatry* (2003) 54(7):693–702. doi: 10.1016/s0006-3223(03)00634-6

33. Santarelli L, Saxe M, Gross C, Surget A, Battaglia F, Dulawa S, et al. Requirement of hippocampal neurogenesis for the behavioral effects of antidepressants. *Science* (2003) 301(5634):805–9. doi: 10.1126/science.1083328

34. Námestková K, Simonová Z, Syková E. Decreased proliferation in the adult rat hippocampus after exposure to the morris water maze and its reversal by fluoxetine. *Behav Brain Res* (2005) 163(1):26–32. doi: 10.1016/j.bbr.2005.04.013

35. Tunc-Ozcan E, Peng CY, Zhu Y, Dunlop SR, Contractor A, Kessler JA. Activating newborn neurons suppresses depression and anxiety-like behaviors. *Nat Commun* (2019) 10(1):3768. doi: 10.1038/s41467-019-11641-8

36. Abbott LC, Nigussie F. Adult neurogenesis in the mammalian dentate gyrus. *Anatomia Histol Embryol* (2020) 49(1):3–16. doi: 10.1111/ahe.12496

37. Hung YF, Chen CY, Li WC, Wang TF, Hsueh YP. Tlr7 deletion alters expression profiles of genes related to neural function and regulates mouse behaviors and contextual memory. *Brain Behav Immun* (2018) 72:101–13. doi: 10.1016/j.bbi.2018.06.006

38. Saral S, Topçu A, Alkanat M, Mercantepe T, Şahin Z, Akyıldız K, et al. Agomelatine attenuates cisplatin-induced cognitive impairment via modulation of Bdnf/Trkb signaling in rat hippocampus. *J Chem Neuroanat* (2023) 130:102269. doi: 10.1016/j.jchemneu.2023.102269

39. Hong N, Kim HJ, Kang K, Park JO, Mun S, Kim HG, et al. Photobiomodulation improves the synapses and cognitive function and ameliorates epileptic seizure by inhibiting downregulation of nlgn3. *Cell Biosci* (2023) 13(1):8. doi: 10.1186/s13578-022-00949-6

40. Martin E, El-Behi M, Fontaine B, Delarasse C. Analysis of microglia and monocyte-derived macrophages from the central nervous system by flow cytometry. *J Visualized Experiments: JoVE* (2017) 124:55781. doi: 10.3791/55781

41. Bianchin MM, Snow Z. Primary microglia dysfunction or microgliopathy: A cause of dementias and other neurological or psychiatric disorders. *Neuroscience* (2022) 497:324–39. doi: 10.1016/j.neuroscience.2022.06.032

42. Zhang L, Zhang J, You Z. Switching of the microglial activation phenotype is a possible treatment for depression disorder. *Front Cell Neurosci* (2018) 12:306. doi: 10.3389/fncel.2018.00306

43. Lawson LJ, Perry VH, Dri P, Gordon S. Heterogeneity in the distribution and morphology of microglia in the normal adult mouse brain. *Neuroscience* (1990) 39 (1):151–70. doi: 10.1016/0306-4522(90)90229-w

44. Colonna M, Butovsky O. Microglia function in the central nervous system during health and neurodegeneration. *Annu Rev Immunol* (2017) 35:441–68. doi: 10.1146/annurev-immunol-051116-052358

45. Yin N, Yan E, Duan W, Mao C, Fei Q, Yang C, et al. The role of microglia in chronic pain and depression: innocent bystander or culprit? *Psychopharmacology* (2021) 238(4):949–58. doi: 10.1007/s00213-021-05780-4

46. Garaschuk O, Verkhratsky A. Physiology of microglia. *Methods Mol Biol* (2019) 2034:27–40. doi: 10.1007/978-1-4939-9658-2_3

47. Holloway OG, Canty AJ, King AE, Ziebell JM. Rod microglia and their role in neurological diseases. *Semin Cell Dev Biol* (2019) 94:96–103. doi: 10.1016/j.semcdb.2019.02.005

48. Prinz M, Jung S, Priller J. Microglia biology: one century of evolving concepts. *Cell* (2019) 179(2):292–311. doi: 10.1016/j.cell.2019.08.053

49. Lier J, Streit WJ, Bechmann I. Beyond activation: characterizing microglial functional phenotypes. *Cells* (2021) 10(9):2236. doi: 10.3390/cells10092236

50. Yirmiya R, Rimmerman N, Reshef R. Depression as a microglial disease. *Trends Neurosci* (2015) 38(10):637–58. doi: 10.1016/j.tins.2015.08.001

51. Ransohoff RM. A polarizing question: do M1 and M2 microglia exist? *Nat Neurosci* (2016) 19(8):987–91. doi: 10.1038/nn.4338

52. Jia X, Gao Z, Hu H. Microglia in depression: current perspectives. *Sci China Life Sci* (2021) 64(6):911–25. doi: 10.1007/s11427-020-1815-6

53. Wolf SA, Boddeke HW, Kettenmann H. Microglia in physiology and disease. *Annu Rev Physiol* (2017) 79:619–43. doi: 10.1146/annurev-physiol-022516-034406

54. Lisi L, Ciotti GM, Braun D, Kalinin S, Currò D, Dello Russo C, et al. Expression of inos, cd163 and arg-1 taken as M1 and M2 markers of microglial polarization in human glioblastoma and the surrounding normal parenchyma. *Neurosci Lett* (2017) 645:106–12. doi: 10.1016/j.neulet.2017.02.076

55. Zhou T, Huang Z, Sun X, Zhu X, Zhou L, Li M, et al. Microglia polarization with M1/M2 phenotype changes in Rd1 mouse model of retinal degeneration. *Front Neuroanat* (2017) 11:77. doi: 10.3389/fnana.2017.00077

56. Orihuela R, McPherson CA, Harry GJ. Microglial M1/M2 polarization and metabolic states. *Br J Pharmacol* (2016) 173(4):649–65. doi: 10.1111/bph.13139

57. Kwon HS, Koh SH. Neuroinflammation in neurodegenerative disorders: the roles of microglia and astrocytes. *Transl Neurodegener* (2020) 9(1):42. doi: 10.1186/s40035-020-00221-2

58. Liu LR, Liu JC, Bao JS, Bai QQ, Wang GQ. Interaction of microglia and astrocytes in the neurovascular unit. *Front Immunol* (2020) 11:1024. doi: 10.3389/fimmu.2020.01024

59. Tang Y, Le W. Differential roles of M1 and M2 microglia in neurodegenerative diseases. *Mol Neurobiol* (2016) 53(2):1181–94. doi: 10.1007/s12035-014-9070-5

60. Kalkman HO, Feuerbach D. Microglia M2a polarization as potential link between food allergy and autism spectrum disorders. *Pharm (Basel)* (2017) 10(4):95. doi: 10.3390/ph10040095

61. Walker DG, Lue LF. Immune phenotypes of microglia in human neurodegenerative disease: challenges to detecting microglial polarization in human brains. *Alzheimers Res Ther* (2015) 7(1):56. doi: 10.1186/s13195-015-0139-9

62. Chhor V, Le Charpentier T, Lebon S, Ore MV, Celador IL, Josserand J, et al. Characterization of phenotype markers and neuronotoxic potential of polarised primary microglia in vitro. *Brain Behav Immun* (2013) 32:70–85. doi: 10.1016/j.bbi.2013.02.005

63. Varnum MM, Ikezu T. The classification of microglial activation phenotypes on neurodegeneration and regeneration in alzheimer's disease brain. *Arch Immunol Ther Exp (Warsz)* (2012) 60(4):251–66. doi: 10.1007/s00005-012-0181-2

64. Kisucká A, Bimbová K, Bačová M, Gálik J, Lukáčová N. Activation of Neuroprotective Microglia and Astrocytes at the Lesion Site and in the Adjacent Segments Is Crucial for Spontaneous Locomotor Recovery after Spinal Cord Injury. *Cells* (2021) 10(8):1943. doi: 10.3390/cells10081943

65. Lam D, Lively S, Schlichter LC. Responses of rat and mouse primary microglia to pro- and anti-inflammatory stimuli: molecular profiles, K(+) channels and migration. *J Neuroinflamm* (2017) 14(1):166. doi: 10.1186/s12974-017-0941-3

66. Nakagawa Y, Chiba K. Diversity and plasticity of microglial cells in psychiatric and neurological disorders. *Pharmacol Ther* (2015) 154:21–35. doi: 10.1016/j.pharmthera.2015.06.010

67. Zhang L, Verwer RWH, Lucassen PJ, Huitinga I, Swaab DF. Prefrontal cortex alterations in glia gene expression in schizophrenia with and without suicide. *J Psychiatr Res* (2020) 121:31–8. doi: 10.1016/j.jpsychires.2019.11.002

68. Suzuki H, Ohgidani M, Kuwano N, Chretien F, Lorin de la Grandmaison G, Onaya M, et al. Suicide and microglia: recent findings and future perspectives based on human studies. *Front Cell Neurosci* (2019) 13:31. doi: 10.3389/fncel.2019.00031

69. Hayley S, Hakim AM, Albert PR. Depression, dementia and immune dysregulation. *Brain* (2021) 144(3):746–60. doi: 10.1093/brain/awaa405

70. Rosenblat JD, McIntyre RS. Efficacy and tolerability of minocycline for depression: A systematic review and meta-analysis of clinical trials. *J Affect Disord* (2018) 227:219–25. doi: 10.1016/j.jad.2017.10.042

71. Kobayashi K, Imagama S, Ohgomori T, Hirano K, Uchimura K, Sakamoto K, et al. Minocycline selectively inhibits M1 polarization of microglia. *Cell Death Dis* (2013) 4(3):e525. doi: 10.1038/cddis.2013.54

72. Ahmed A, Misrani A, Tabassum S, Yang L, Long C. Minocycline inhibits sleep deprivation-induced aberrant microglial activation and keap1-Nrf2 expression in mouse hippocampus. *Brain Res Bull* (2021) 174:41–52. doi: 10.1016/j.brainresbull.2021.05.028

73. Witcher KG, Bray CE, Chunchai T, Zhao F, O'Neil SM, Gordillo AJ, et al. Traumatic brain injury causes chronic cortical inflammation and neuronal dysfunction mediated by microglia. *J Neurosci* (2021) 41(7):1597–616. doi: 10.1523/jneurosci.2469-20.2020

74. Mechawar N, Savitz J. Neuropathology of mood disorders: do we see the stigmata of inflammation? *Transl Psychiatry* (2016) 6(11):e946. doi: 10.1038/tp.2016.212

75. Tang J, Yu W, Chen S, Gao Z, Xiao B. Microglia polarization and endoplasmic reticulum stress in chronic social defeat stress induced depression mouse. *Neurochem Res* (2018) 43(5):985–94. doi: 10.1007/s11064-018-2504-0

76. Bassett B, Subramaniyam S, Fan Y, Varney S, Pan H, Carneiro AMD, et al. Minocycline alleviates depression-like symptoms by rescuing decrease in neurogenesis in dorsal hippocampus via blocking microglia activation/phagocytosis. *Brain Behav Immun* (2021) 91:519–30. doi: 10.1016/j.bbi.2020.11.009

77. Hickman S, Izzy S, Sen P, Morsett L, El Khoury J. Microglia in neurodegeneration. *Nat Neurosci* (2018) 21(10):1359–69. doi: 10.1038/s41593-018-0242-x

78. Jang DY, Yang B, You MJ, Rim C, Kim HJ, Sung S, et al. Fluoxetine decreases phagocytic function via rev-Erbα in microglia. *Neurochem Res* (2023) 48(1):196–209. doi: 10.1007/s11064-022-03733-7

79. Szepesi Z, Manouchehrian O, Bachiller S, Deierborg T. Bidirectional microglia-neuron communication in health and disease. *Front Cell Neurosci* (2018) 12:323. doi: 10.3389/fncel.2018.00323

80. Györffy BA, Kun J, Török G, Bulyáki É, Borhegyi Z, Gulyássy P, et al. Local apoptotic-like mechanisms underlie complement-mediated synaptic pruning. *Proc Natl Acad Sci United States America* (2018) 115(24):6303–8. doi: 10.1073/pnas.1722613115

81. Han QQ, Shen SY, Chen XR, Pilot A, Liang LF, Zhang JR, et al. Minocycline alleviates abnormal microglial phagocytosis of synapses in a mouse model of depression. *Neuropharmacology* (2022) 220:109249. doi: 10.1016/j.neuropharm.2022.109249

82. Cao P, Chen C, Liu A, Shan Q, Zhu X, Jia C, et al. Early-life inflammation promotes depressive symptoms in adolescence via microglial engulfment of dendritic spines. *Neuron* (2021) 109(16):2573–89.e9. doi: 10.1016/j.neuron.2021.06.012

83. Iida T, Yoshikawa T, Kárpáti A, Matsuzawa T, Kitano H, Mogi A, et al. Jnj10181457, a histamine H3 receptor inverse agonist, regulates *in vivo* microglial functions and improves depression-like behaviours in mice. *Biochem Biophys Res Commun* (2017) 488(3):534–40. doi: 10.1016/j.bbrc.2017.05.081

84. Perlman G, Simmons AN, Wu J, Hahn KS, Tapert SF, Max JE, et al. Amygdala response and functional connectivity during emotion regulation: A study of 14 depressed adolescents. *J Affect Disord* (2012) 139(1):75–84. doi: 10.1016/j.jad.2012.01.044

85. Bar E, Barak B. Microglia roles in synaptic plasticity and myelination in homeostatic conditions and neurodevelopmental disorders. *Glia* (2019) 67(11):2125–41. doi: 10.1002/glia.23637

86. Lorenzen K, Mathy NW, Whiteford ER, Eischeid A, Chen J, Behrens M, et al. Microglia induce neurogenic protein expression in primary cortical cells by stimulating Pi3k/Akt intracellular signaling in vitro. *Mol Biol Rep* (2021) 48(1):563–84. doi: 10.1007/s11033-020-06092-0

87. Paolicelli RC, Ferretti MT. Function and dysfunction of microglia during brain development: consequences for synapses and neural circuits. *Front Synaptic Neurosci* (2017) 9:9. doi: 10.3389/fnsyn.2017.00009

88. Glanzer JG, Enose Y, Wang T, Kadiu I, Gong N, Rozek W, et al. Genomic and proteomic microglial profiling: pathways for neuroprotective inflammatory responses following nerve fragment clearance and activation. *J Neurochem* (2007) 102(3):627–45. doi: 10.1111/j.1471-4159.2007.04568.x

89. Barde YA, Edgar D, Thoenen H. Purification of a new neurotrophic factor from mammalian brain. *EMBO J* (1982) 1(5):549–53. doi: 10.1002/j.1460-2075.1982.tb01207.x

90. Hashimoto K. Brain-derived neurotrophic factor as a biomarker for mood disorders: an historical overview and future directions. *Psychiatry and clinical neurosciences* (2010) 64(4):341–57. doi: 10.1111/j.1440-1819.2010.02113.x

91. Fujikawa R, Yamada J, Iinuma KM, Jinno S. Phytoestrogen genistein modulates neuron-microglia signaling in a mouse model of chronic social defeat stress. *Neuropharmacology* (2022) 206:108941. doi: 10.1016/j.neuropharm.2021.108941

92. Tong L, Gong Y, Wang P, Hu W, Wang J, Chen Z, et al. Microglia loss contributes to the development of major depression induced by different types of chronic stresses. *Neurochem Res* (2017) 42(10):2698–711. doi: 10.1007/s11064-017-2270-4

93. Cai Z, Ye T, Xu X, Gao M, Zhang Y, Wang D, et al. Antidepressive properties of microglial stimulation in a mouse model of depression induced by chronic unpredictable stress. *Prog Neuropsychopharmacol Biol Psychiatry* (2020) 101:109931. doi: 10.1016/j.pnpbp.2020.109931

94. Walton NM, Sutter BM, Laywell ED, Levkoff LH, Kearns SM, Marshall GP 2nd, et al. Microglia instruct subventricular zone neurogenesis. *Glia* (2006) 54(8):815–25. doi: 10.1002/glia.20419

95. Willis EF, MacDonald KPA, Nguyen QH, Garrido AL, Gillespie ER, Harley SBR, et al. Repopulating microglia promote brain repair in an il-6-dependent manner. *Cell* (2020) 180(5):833–46 e16. doi: 10.1016/j.cell.2020.02.013

96. Thored P, Heldmann U, Gomes-Leal W, Gisler R, Darsalia V, Taneera J, et al. Long-term accumulation of microglia with proneurogenic phenotype concomitant with persistent neurogenesis in adult subventricular zone after stroke. *Glia* (2009) 57 (8):835–49. doi: 10.1002/glia.20810

97. Diaz-Aparicio I, Paris I, Sierra-Torre V, Plaza-Zabala A, Rodriguez-Iglesias N, Marquez-Ropero M, et al. Microglia actively remodel adult hippocampal neurogenesis through the phagocytosis secretome. *J Neurosci* (2020) 40(7):1453–82. doi: 10.1523/JNEUROSCI.0993-19.2019

98. Beccari S, Valero J, Maletic-Savatic M, Sierra A. A simulation model of neuroprogenitor proliferation dynamics predicts age-related loss of hippocampal neurogenesis but not astrogenesis. *Sci Rep* (2017) 7(1):16528. doi: 10.1038/s41598-017-16466-3

99. Butovsky O, Ziv Y, Schwartz A, Landa G, Talpalar AE, Pluchino S, et al. Microglia activated by il-4 or ifn-gamma differentially induce neurogenesis and oligodendrogenesis from adult stem/progenitor cells. *Mol Cell Neurosci* (2006) 31 (1):149–60. doi: 10.1016/j.mcn.2005.10.006

100. Han Y, Zhang L, Wang Q, Zhang D, Zhao Q, Zhang J, et al. Minocycline inhibits microglial activation and alleviates depressive-like behaviors in male adolescent mice subjected to maternal separation. *Psychoneuroendocrinology* (2019) 107:37–45. doi: 10.1016/j.psyneuen.2019.04.021

101. Li H, Xiang Y, Zhu Z, Wang W, Jiang Z, Zhao M, et al. Rifaximin-mediated gut microbiota regulation modulates the function of microglia and protects against cums-induced depression-like behaviors in adolescent rat. *J Neuroinflamm* (2021) 18(1):254. doi: 10.1186/s12974-021-02303-y

102. Picard K, Bisht K, Poggini S, Garofalo S, Golia MT, Basilico B, et al. Microglial-glucocorticoid receptor depletion alters the response of hippocampal microglia and neurons in a chronic unpredictable mild stress paradigm in female mice. *Brain Behav Immun* (2021) 97:423–39. doi: 10.1016/j.bbi.2021.07.022

103. Rimmerman N, Schottlender N, Reshef R, Dan-Goor N, Yirmiya R. The hippocampal transcriptomic signature of stress resilience in mice with microglial fractalkine receptor (Cx3cr1) deficiency. *Brain Behav Immun* (2017) 61:184–96. doi: 10.1016/j.bbi.2016.11.023

104. Mahmoud R, Wainwright SR, Chaiton JA, Lieblich SE, Galea LAM. Ovarian Hormones, but Not Fluoxetine, Impart Resilience within a Chronic Unpredictable Stress Model in Middle-Aged Female Rats. *Neuropharmacology* (2016) 107:278–93. doi: 10.1016/j.neuropharm.2016.01.033

105. Zhang J, Rong P, Zhang L, He H, Zhou T, Fan Y, et al. Il4-driven microglia modulate stress resilience through Bdnf-dependent neurogenesis. *Sci Adv* (2021) 7(12): eabb9888. doi: 10.1126/sciadv.abb9888

106. Xu XF, Shi MM, Luo MY, Liu DD, Guo DM, Ling C, et al. Targeting perk mediated endoplasmic reticulum stress attenuates neuroinflammation and alleviates lipopolysaccharide-induced depressive-like behavior in male mice. *Int Immunopharmacol* (2022) 111:109092. doi: 10.1016/j.intimp.2022.109092

107. Guo D, Xu Y, Liu Z, Wang Y, Xu X, Li C, et al. Igf2 inhibits hippocampal over-activated microglia and alleviates depression-like behavior in Lps- treated male mice. *Brain Res Bull* (2023) 194:1–12. doi: 10.1016/j.brainresbull.2023.01.001

108. Gong M, Shi R, Liu Y, Ke J, Liu X, Du HZ, et al. Abnormal microglial polarization induced by arid1a deletion leads to neuronal differentiation deficits. *Cell Proliferation* (2022) 55(11):e13314. doi: 10.1111/cpr.13314

109. Ciesielska A, Matyjek M, Kwiatkowska K. Tlr4 and cd14 trafficking and its influence on Lps-induced pro-inflammatory signaling. *Cell Mol Life Sci* (2021) 78 (4):1233–61. doi: 10.1007/s00018-020-03656-y

110. Lu YC, Yeh WC, Ohashi PS. Lps/tlr4 signal transduction pathway. *Cytokine* (2008) 42(2):145–51. doi: 10.1016/j.cyto.2008.01.006

111. Nie X, Kitaoka S, Tanaka K, Segi-Nishida E, Imoto Y, Ogawa A, et al. The innate immune receptors Tlr2/4 mediate repeated social defeat stress-induced social avoidance through prefrontal microglial activation. *Neuron* (2018) 99(3):464–79.e7. doi: 10.1016/j.neuron.2018.06.035

112. Rolls A, Shechter R, London A, Ziv Y, Ronen A, Levy R, et al. Toll-like receptors modulate adult hippocampal neurogenesis. *Nat Cell Biol* (2007) 9(9):1081–8. doi: 10.1038/ncb1629

113. Seong KJ, Choi S, Lee HG, Rhee JH, Lee JH, Koh JT, et al. Toll-like receptor 5 promotes the neurogenesis from embryonic stem cells and adult hippocampal neural stem cells in mice. *Stem Cells (Dayton Ohio)* (2022) 40(3):303–17. doi: 10.1093/stmcls/sxab025

114. Chen M, Rong R, Xia X. Spotlight on pyroptosis: role in pathogenesis and therapeutic potential of ocular diseases. *J Neuroinflamm* (2022) 19(1):183. doi: 10.1186/s12974-022-02547-2

115. Alcocer-Gómez E, Ulecia-Morón C, Marín-Aguilar F, Rybkina T, Casas-Barquero N, Ruiz-Cabello J, et al. Stress-induced depressive behaviors require a functional nlrp3 inflammasome. *Mol Neurobiol* (2016) 53(7):4874–82. doi: 10.1007/s12035-015-9408-7

116. Li J, Shui X, Sun R, Wan L, Zhang B, Xiao B, et al. Microglial phenotypic transition: signaling pathways and influencing modulators involved in regulation in central nervous system diseases. *Front Cell Neurosci* (2021) 15:736310. doi: 10.3389/fncel.2021.736310

117. Du RH, Tan J, Sun XY, Lu M, Ding JH, Hu G. Fluoxetine inhibits nlrp3 inflammasome activation: implication in depression. *Int J Neuropsychopharmacol* (2016) 19(9):pyw037. doi: 10.1093/ijnp/pyw037

118. Komleva YK, Lopatina OL, Gorina IV, Shuvaev AN, Chernykh A, Potapenko IV, et al. Nlrp3 deficiency-induced hippocampal dysfunction and anxiety-like behavior in mice. *Brain Res* (2021) 1752:147220. doi: 10.1016/j.brainres.2020.147220

119. Su D, Jiang W, Yuan Q, Guo L, Liu Q, Zhang M, et al. Chronic exposure to aflatoxin B1 increases hippocampal microglial pyroptosis and vulnerability to stress in mice. *Ecotoxicol Environ Saf* (2023) 258:114991. doi: 10.1016/j.ecoenv.2023.114991

120. Yi LT, Zhang MM, Cheng J, Wan HQ, Li CF, Zhu JX, et al. Antidepressant-like effects of degraded porphyran isolated from porphyra haitanensis. *Mol Nutr Food Res* (2021) 65(9):e2000869. doi: 10.1002/mnfr.202000869

121. Singhal G, Baune BT. Microglia: an interface between the loss of neuroplasticity and depression. *Front Cell Neurosci* (2017) 11:270. doi: 10.3389/fncel.2017.00270

122. Chugh D, Nilsson P, Afjei SA, Bakochi A, Ekdahl CT. Brain inflammation induces post-synaptic changes during early synapse formation in adult-born hippocampal neurons. *Exp Neurol* (2013) 250:176–88. doi: 10.1016/j.expneurol.2013.09.005

123. Zhang L, Tang M, Xie X, Zhao Q, Hu N, He H, et al. Ginsenoside rb1 induces a pro-neurogenic microglial phenotype via pparγ Activation in male mice exposed to chronic mild stress. *J Neuroinflamm* (2021) 18(1):171. doi: 10.1186/s12974-021-02185-0

124. Shariq AS, Brietzke E, Rosenblat JD, Pan Z, Rong C, Ragguett RM, et al. Therapeutic potential of jak/stat pathway modulation in mood disorders. *Rev Neurosci* (2018) 30(1):1–7. doi: 10.1515/revneuro-2018-0027

125. Yan Z, Gibson SA, Buckley JA, Qin H, Benveniste EN. Role of the jak/stat signaling pathway in regulation of innate immunity in neuroinflammatory diseases. *Clin Immunol* (2018) 189:4–13. doi: 10.1016/j.clim.2016.09.014

126. Kwon SH, Han JK, Choi M, Kwon YJ, Kim SJ, Yi EH, et al. Dysfunction of microglial stat3 alleviates depressive behavior via neuron-microglia interactions. *Neuropsychopharmacology* (2017) 42(10):2072–86. doi: 10.1038/npp.2017.93

127. Pansri P, Phanthong P, Suthprasertporn N, Kitiyanant Y, Tubsuwan A, Dinnyes A, et al. Brain-derived neurotrophic factor increases cell number of neural progenitor cells derived from human induced pluripotent stem cells. *PeerJ* (2021) 9: e11388. doi: 10.7717/peerj.11388

128. Gulbins A, Grassmé H, Hoehn R, Kohnen M, Edwards MJ, Kornhuber J, et al. Role of janus-kinases in major depressive disorder. *Neuro-Signals* (2016) 24(1):71–80. doi: 10.1159/000442613

129. Kumar S, Mehan S, Narula AS. Therapeutic modulation of jak-Stat, Mtor, and Ppar-Γ Signaling in neurological dysfunctions. *J Mol Med (Berlin Germany)* (2023) 101 (1-2):9–49. doi: 10.1007/s00109-022-02272-6

130. Wang JQ, Derges JD, Bodepudi A, Pokala N, Mao LM. Roles of non-receptor tyrosine kinases in pathogenesis and treatment of depression. *J Integr Neurosci* (2022) 21(1):25. doi: 10.31083/j.jin2101025

131. Harrison JK, Jiang Y, Chen S, Xia Y, Maciejewski D, McNamara RK, et al. Role for neuronally derived fractalkine in mediating interactions between neurons and Cx3cr1-expressing microglia. *Proc Natl Acad Sci U.S.A.* (1998) 95(18):10896–901. doi: 10.1073/pnas.95.18.10896

132. Lauro C, Catalano M, Trettel F, Mainiero F, Ciotti MT, Eusebi F, et al. The chemokine Cx3cl1 reduces migration and increases adhesion of neurons with mechanisms dependent on the beta1 integrin subunit. *J Immunol* (2006) 177 (11):7599–606. doi: 10.4049/jimmunol.177.11.7599

133. Biber K, Neumann H, Inoue K, Boddeke HW. Neuronal 'on' and 'Off' Signals control microglia. *Trends Neurosci* (2007) 30(11):596–602. doi: 10.1016/j.tins.2007.08.007

134. Snijders G, Sneeboer MAM, Fernandez-Andreu A, Udine EPsychiatric donor program of the Netherlands Brain B, , Boks MP, et al. Distinct non-inflammatory signature of microglia in post-mortem brain tissue of patients with major depressive disorder. *Mol Psychiatry* (2021) 26(7):3336–49. doi: 10.1038/s41380-020-00896-z

135. Bachstetter AD, Morganti JM, Jernberg J, Schlunk A, Mitchell SH, Brewster KW, et al. Fractalkine and cx 3 cr1 regulate hippocampal neurogenesis in adult and aged rats. *Neurobiol Aging* (2011) 32(11):2030–44. doi: 10.1016/j.neurobiolaging.2009.11.022

136. Bolos M, Perea JR, Terreros-Roncal J, Pallas-Bazarra N, Jurado-Arjona J, Avila J, et al. Absence of microglial Cx3cr1 impairs the synaptic integration of adult-born hippocampal granule neurons. *Brain Behav Immun* (2018) 68:76–89. doi: 10.1016/j.bbi.2017.10.002

137. Mattison HA, Nie H, Gao H, Zhou H, Hong JS, Zhang J. Suppressed pro-inflammatory response of microglia in Cx3cr1 knockout mice. *J Neuroimmunol* (2013) 257(1-2):110–5. doi: 10.1016/j.jneuroim.2013.02.008

138. Liu Y, Zhang T, Meng D, Sun L, Yang G, He Y, et al. Involvement of cx3cl1/Cx3cr1 in depression and cognitive impairment induced by chronic unpredictable stress and relevant underlying mechanism. *Behav Brain Res* (2020) 381:112371. doi: 10.1016/j.bbr.2019.112371

139. Mikulska J, Juszczyk G, Gawrońska-Grzywacz M, Herbet M. Hpa axis in the pathomechanism of depression and schizophrenia: new therapeutic strategies based on its participation. *Brain Sci* (2021) 11(10):1298. doi: 10.3390/brainsci11101298

140. Vreeburg SA, Hoogendijk WJ, van Pelt J, Derijk RH, Verhagen JC, van Dyck R, et al. Major depressive disorder and hypothalamic-pituitary-adrenal axis activity: results from a large cohort study. *Arch Gen Psychiatry* (2009) 66(6):617–26. doi: 10.1001/archgenpsychiatry.2009.50

141. Swaab DF, Bao AM, Lucassen PJ. The stress system in the human brain in depression and neurodegeneration. *Ageing Res Rev* (2005) 4(2):141–94. doi: 10.1016/j.arr.2005.03.003

142. David DJ, Samuels BA, Rainer Q, Wang JW, Marsteller D, Mendez I, et al. Neurogenesis-dependent and -independent effects of fluoxetine in an animal model of anxiety/depression. *Neuron* (2009) 62(4):479–93. doi: 10.1016/j.neuron.2009.04.017

143. Felger JC, Lotrich FE. Inflammatory cytokines in depression: neurobiological mechanisms and therapeutic implications. *Neuroscience* (2013) 246:199–229. doi: 10.1016/j.neuroscience.2013.04.060

144. Ichiyama A, Nakamura S, Nishizuka Y, Hayaishi O. Enzymic studies on the biosynthesis of serotonin in mammalian brain. *J Biol Chem* (1970) 245(7):1699–709. doi: 10.1016/S0021-9258(19)77149-X

145. Lochmann D, Richardson T. Selective serotonin reuptake inhibitors. *Handb Exp Pharmacol* (2019) 250:135–44. doi: 10.1007/164_2018_172

146. Cao Y, Liu J, Wang Q, Liu M, Cheng Y, Zhang X, et al. Antidepressive-like effect of imperatorin from angelica dahurica in prenatally stressed offspring rats through 5-hydroxytryptamine system. *Neuroreport* (2017) 28(8):426–33. doi: 10.1097/wnr.0000000000000778

147. Hirata F, Hayaishi O, Tokuyama T, Seno S. *In vitro* and in vivo formation of two new metabolites of melatonin. *J Biol Chem* (1974) 249(4):1311–3. doi: 10.1016/S0021-9258(19)42976-1

148. Karu N, McKercher C, Nichols DS, Davies N, Shellie RA, Hilder EF, et al. Tryptophan metabolism, its relation to inflammation and stress markers and association with psychological and cognitive functioning: tasmanian chronic kidney disease pilot study. *BMC Nephrol* (2016) 17(1):171. doi: 10.1186/s12882-016-0387-3

149. Raison CL, Dantzer R, Kelley KW, Lawson MA, Woolwine BJ, Vogt G, et al. Csf concentrations of brain tryptophan and kynurenines during immune stimulation with Ifn-alpha: relationship to Cns immune responses and depression. *Mol Psychiatry* (2010) 15(4):393–403. doi: 10.1038/mp.2009.116

150. Arnone D, Saraykar S, Salem H, Teixeira AL, Dantzer R, Selvaraj S. Role of kynurenine pathway and its metabolites in mood disorders: A systematic review and meta-analysis of clinical studies. *Neurosci Biobehav Rev* (2018) 92:477–85. doi: 10.1016/j.neubiorev.2018.05.031

151. Borish LC, Steinke JW. 2. Cytokines and chemokines. *J Allergy Clin Immunol* (2003) 111(2 Suppl):S460–75. doi: 10.1067/mai.2003.108

152. Lowry JR, Klegeris A. Emerging roles of microglial cathepsins in neurodegenerative disease. *Brain Res Bull* (2018) 139:144–56. doi: 10.1016/j.brainresbull.2018.02.014

153. Kim YK, Na KS, Myint AM, Leonard BE. The role of pro-inflammatory cytokines in neuroinflammation, neurogenesis and the neuroendocrine system in major depression. *Prog Neuropsychopharmacol Biol Psychiatry* (2016) 64:277–84. doi: 10.1016/j.pnpbp.2015.06.008

154. Pozzo ED, Tremolanti C, Costa B, Giacomelli C, Milenkovic VM, Bader S, et al. Microglial pro-inflammatory and anti-inflammatory phenotypes are modulated by translocator protein activation. *Int J Mol Sci* (2019) 20(18):4467. doi: 10.3390/ijms20184467

155. Smith JA, Das A, Ray SK, Banik NL. Role of pro-inflammatory cytokines released from microglia in neurodegenerative diseases. *Brain Res Bull* (2012) 87(1):10–20. doi: 10.1016/j.brainresbull.2011.10.004

156. Zhang J, Liu Q, Su D, Li L, Xiao C, He H, et al. Akebia saponin D acts via the ppar-gamma pathway to reprogramme a pro-neurogenic microglia that can restore hippocampal neurogenesis in mice exposed to chronic mild stress. *CNS Neurosci Ther* (2023) 29(9):2555–71. doi: 10.1111/cns.14196

157. Zhang JC, Yao W, Hashimoto K. Brain-derived neurotrophic factor (Bdnf)-Trkb signaling in inflammation-related depression and potential therapeutic targets. *Curr Neuropharmacol* (2016) 14(7):721–31. doi: 10.2174/1570159x14666160119094646

158. Jin W. Regulation of bdnf-Trkb signaling and potential therapeutic strategies for parkinson's disease. *J Clin Med* (2020) 9(1):257. doi: 10.3390/jcm9010257

159. JiaWen W, Hong S, ShengXiang X, Jing L. Depression- and anxiety-like behaviour is related to Bdnf/Trkb signalling in a mouse model of psoriasis. *Clin Exp Dermatol* (2018) 43(3):254–61. doi: 10.1111/ced.13378

160. Sonoyama T, Stadler LKJ, Zhu M, Keogh JM, Henning E, Hisama F, et al. Human Bdnf/Trkb variants impair hippocampal synaptogenesis and associate with neurobehavioural abnormalities. *Sci Rep* (2020) 10(1):9028. doi: 10.1038/s41598-020-65531-x

161. Li YJ, Li YJ, Yang LD, Zhang K, Zheng KY, Wei XM, et al. Silibinin exerts antidepressant effects by improving neurogenesis through Bdnf/Trkb pathway. *Behav Brain Res* (2018) 348:184–91. doi: 10.1016/j.bbr.2018.04.025

162. Bagheri S, Moradi K, Ehghaghi E, Badripour A, Keykhaei M, Ashraf-Ganjouei A, et al. Melatonin improves learning and memory of mice with chronic social isolation stress via an interaction between microglia polarization and Bdnf/Trkb/Creb signaling pathway. *Eur J Pharmacol* (2021) 908:174358. doi: 10.1016/j.ejphar.2021.174358

163. Quigley EMM. Microbiota-brain-gut axis and neurodegenerative diseases. *Curr Neurol Neurosci Rep* (2017) 17(12):94. doi: 10.1007/s11910-017-0802-6

164. Du Y, Gao XR, Peng L, Ge JF. Crosstalk between the microbiota-gut-brain axis and depression. *Heliyon* (2020) 6(6):e04097. doi: 10.1016/j.heliyon.2020.e04097

165. Sun J, Xu J, Yang B, Chen K, Kong Y, Fang N, et al. Effect of clostridium butyricum against microglia-mediated neuroinflammation in alzheimer's disease via regulating gut microbiota and metabolites butyrate. *Mol Nutr Food Res* (2020) 64(2):e1900636. doi: 10.1002/mnfr.201900636

166. Carlessi AS, Borba LA, Zugno AI, Quevedo J, Réus GZ. Gut microbiota-brain axis in depression: the role of neuroinflammation. *Eur J Neurosci* (2021) 53(1):222–35. doi: 10.1111/ejn.14631

167. Sarubbo F, Cavallucci V, Pani G. The influence of gut microbiota on neurogenesis: evidence and hopes. *Cells* (2022) 11(3):382. doi: 10.3390/cells11030382

168. Cerdó T, Diéguez E, Campoy C. Impact of gut microbiota on neurogenesis and neurological diseases during infancy. *Curr Opin Pharmacol* (2020) 50:33–7. doi: 10.1016/j.coph.2019.11.006

169. Karakuła-Juchnowicz H, Szachta P, Opolska A, Morylowska-Topolska J, Gałęcka M, Juchnowicz D, et al. The role of igg hypersensitivity in the pathogenesis and therapy of depressive disorders. *Nutr Neurosci* (2017) 20(2):110–8. doi: 10.1179/1476830514y.0000000158

170. Bartel DP. Micrornas: genomics, biogenesis, mechanism, and function. *Cell* (2004) 116(2):281–97. doi: 10.1016/s0092-8674(04)00045-5

171. Fan C, Li Y, Lan T, Wang W, Long Y, Yu SY. Microglia secrete mir-146a-5p-containing exosomes to regulate neurogenesis in depression. *Mol Ther* (2022) 30 (3):1300–14. doi: 10.1016/j.ymthe.2021.11.006

172. Brites D, Fernandes A. Neuroinflammation and depression: microglia activation, extracellular microvesicles and microrna dysregulation. *Front Cell Neurosci* (2015) 9:476. doi: 10.3389/fncel.2015.00476

173. Yang Y, Ye Y, Kong C, Su X, Zhang X, Bai W, et al. Mir-124 enriched exosomes promoted the M2 polarization of microglia and enhanced hippocampus neurogenesis after traumatic brain injury by inhibiting Tlr4 pathway. *Neurochem Res* (2019) 44 (4):811–28. doi: 10.1007/s11064-018-02714-z

174. Hwang J, Zheng LT, Ock J, Lee MG, Kim SH, Lee HW, et al. Inhibition of glial inflammatory activation and neurotoxicity by tricyclic antidepressants. *Neuropharmacology* (2008) 55(5):826–34. doi: 10.1016/j.neuropharm.2008.06.045

175. Ramirez K, Sheridan JF. Antidepressant imipramine diminishes stress-induced inflammation in the periphery and central nervous system and related anxiety- and depressive- like behaviors. *Brain Behav Immun* (2016) 57:293–303. doi: 10.1016/j.bbi.2016.05.008

176. Gong W, Zhang S, Zong Y, Halim M, Ren Z, Wang Y, et al. Involvement of the microglial Nlrp3 inflammasome in the anti-inflammatory effect of the antidepressant clomipramine. *J Affect Disord* (2019) 254:15–25. doi: 10.1016/j.jad.2019.05.009

177. Kreisel T, Frank MG, Licht T, Reshef R, Ben-Menachem-Zidon O, Baratta MV, et al. Dynamic microglial alterations underlie stress-induced depressive-like behavior and suppressed neurogenesis. *Mol Psychiatry* (2014) 19(6):699–709. doi: 10.1038/mp.2013.155

178. Troubat R, Leman S, Pinchaud K, Surget A, Barone P, Roger S, et al. Brain immune cells characterization in Ucms exposed P2x7 knock-out mouse. *Brain Behav Immun* (2021) 94:159–74. doi: 10.1016/j.bbi.2021.02.012

179. Ma Z, Zang T, Birnbaum SG, Wang Z, Johnson JE, Zhang CL, et al. Trkb dependent adult hippocampal progenitor differentiation mediates sustained ketamine antidepressant response. *Nat Commun* (2017) 8(1):1668. doi: 10.1038/s41467-017-01709-8

180. Soumier A, Carter RM, Schoenfeld TJ, Cameron HA. New hippocampal neurons mature rapidly in response to ketamine but are not required for its acute antidepressant effects on neophagia in rats. *eNeuro* (2016) 3(2):ENEURO.0116-15. doi: 10.1523/eneuro.0116-15.2016

181. Guan W, Gu JH, Ji CH, Liu Y, Tang WQ, Wang Y, et al. Xanthoceraside administration produces significant antidepressant effects in mice through activation of the hippocampal bdnf signaling pathway. *Neurosci Lett* (2021) 757:135994. doi: 10.1016/j.neulet.2021.135994

182. Qi Y, Zou LB, Wang LH, Jin G, Pan JJ, Chi TY, et al. Xanthoceraside inhibits pro-inflammatory cytokine expression in Aβ25-35/Ifn-Γ-stimulated microglia through the tlr2 receptor, myd88, nuclear factor-Kb, and mitogen-activated protein kinase signaling pathways. *J Pharmacol Sci* (2013) 122(4):305–17. doi: 10.1254/jphs.13031fp

183. Zhang J, Zheng Y, Luo Y, Du Y, Zhang X, Fu J. Curcumin inhibits lps-induced neuroinflammation by promoting microglial M2 polarization via Trem2/Tlr4/Nf-Kb pathways in bv2 cells. *Mol Immunol* (2019) 116:29–37. doi: 10.1016/j.molimm.2019.09.020

184. Tian DD, Wang M, Liu A, Gao MR, Qiu C, Yu W, et al. Antidepressant effect of paeoniflorin is through inhibiting pyroptosis Casp-11/Gsdmd pathway. *Mol Neurobiol* (2021) 58(2):761–76. doi: 10.1007/s12035-020-02144-5

185. Liu SC, Hu WY, Zhang WY, Yang L, Li Y, Xiao ZC, et al. Paeoniflorin attenuates impairment of spatial learning and hippocampal long-term potentiation in mice subjected to chronic unpredictable mild stress. *Psychopharmacology* (2019) 236 (9):2823–34. doi: 10.1007/s00213-019-05257-5

186. Tang H, Wu L, Chen X, Li H, Huang B, Huang Z, et al. Paeoniflorin improves functional recovery through repressing neuroinflammation and facilitating neurogenesis in rat stroke model. *PeerJ* (2021) 9:e10921. doi: 10.7717/peerj.10921

187. Luo XQ, Li A, Yang X, Xiao X, Hu R, Wang TW, et al. Paeoniflorin exerts neuroprotective effects by modulating the M1/M2 subset polarization of microglia/macrophages in the hippocampal ca1 region of vascular dementia rats via cannabinoid receptor 2. *Chin Med* (2018) 13:14. doi: 10.1186/s13020-018-0173-1

188. Yang X, Xu S, Qian Y, Xiao Q. Resveratrol regulates microglia M1/M2 polarization via Pgc-1α in conditions of neuroinflammatory injury. *Brain Behav Immun* (2017) 64:162–72. doi: 10.1016/j.bbi.2017.03.003

189. Tufekci KU, Eltutan BI, Isci KB, Genc S. Resveratrol inhibits nlrp3 inflammasome-induced pyroptosis and mir-155 expression in microglia through sirt1/ampk pathway. *Neurotoxicity Res* (2021) 39(6):1812–29. doi: 10.1007/s12640-021-00435-w

190. Sui DM, Xie Q, Yi WJ, Gupta S, Yu XY, Li JB, et al. Resveratrol protects against sepsis-associated encephalopathy and inhibits the Nlrp3/Il-1β Axis in microglia. *Mediators Inflammation* (2016) 2016:1045657. doi: 10.1155/2016/1045657

191. Liu L, Zhang Q, Cai Y, Sun D, He X, Wang L, et al. Resveratrol counteracts lipopolysaccharide-induced depressive-like behaviors via enhanced hippocampal neurogenesis. *Oncotarget* (2016) 7(35):56045–59. doi: 10.18632/oncotarget.11178

192. Wu Z, Chen T, Pan D, Zeng X, Guo Y, Zhao G. Resveratrol and organic selenium-rich fermented milk reduces D-galactose-induced cognitive dysfunction in mice. *Food Funct* (2021) 12(3):1318–26. doi: 10.1039/d0fo02029j

193. Arioz BI, Tastan B, Tarakcioglu E, Tufekci KU, Olcum M, Ersoy N, et al. Melatonin attenuates lps-induced acute depressive-like behaviors and microglial nlrp3 inflammasome activation through the Sirt1/Nrf2 pathway. *Front Immunol* (2019) 10:1511. doi: 10.3389/fimmu.2019.01511

194. Madhu LN, Kodali M, Attaluri S, Shuai B, Melissari L, Rao X, et al. Melatonin improves brain function in a model of chronic gulf war illness with modulation of oxidative stress, Nlrp3 inflammasomes, and bdnf-erk-creb pathway in the hippocampus. *Redox Biol* (2021) 43:101973. doi: 10.1016/j.redox.2021.101973

195. Vega-Rivera NM, Ortiz-López L, Granados-Juárez A, Estrada-Camarena EM, Ramírez-Rodríguez GB. Melatonin reverses the depression-associated behaviour and regulates microglia, fractalkine expression and neurogenesis in adult mice exposed to chronic mild stress. *Neuroscience* (2020) 440:316–36. doi: 10.1016/j.neuroscience.2020.05.014

196. Wu B, Song Q, Zhang Y, Wang C, Yang M, Zhang J, et al. Antidepressant activity of Ω-3 polyunsaturated fatty acids in ovariectomized rats: role of neuroinflammation and microglial polarization. *Lipids Health Dis* (2020) 19(1):4. doi: 10.1186/s12944-020-1185-2

197. Rodríguez-Iglesias N, Nadjar A, Sierra A, Valero J. Susceptibility of female mice to the dietary omega-3/Omega-6 fatty-acid ratio: effects on adult hippocampal neurogenesis and glia. *Int J Mol Sci* (2022) 23(6):3399. doi: 10.3390/ijms23063399

198. Manousi N, Samanidou VF. Recent advances in the hplc analysis of tricyclic antidepressants in bio-samples. *Mini Rev Med Chem* (2020) 20(1):24–38. doi: 10.2174/1389557519666190617150518

199. Licinio J. Research and treatment approaches to depression. *Nature reviews Neuroscience* (2001) 2(5):343–51. doi: 10.1038/35072566

200. Boldrini M, Hen R, Underwood MD, Rosoklija GB, Dwork AJ, Mann JJ, et al. Hippocampal angiogenesis and progenitor cell proliferation are increased with antidepressant use in major depression. *Biol Psychiatry* (2012) 72(7):562–71. doi: 10.1016/j.biopsych.2012.04.024

201. Naguy A. Imipramine-precipitated status epilepticus. *World J Pediatrics: WJP* (2021) 17(2):218–9. doi: 10.1007/s12519-020-00409-6

202. Antidepressant Agents. *Livertox: clinical and research information on drug-induced liver injury*. Bethesda (MD: National Institute of Diabetes and Digestive and Kidney Diseases (2012).

203. Imipramine. *Livertox: clinical and research information on drug-induced liver injury*. Bethesda (MD: National Institute of Diabetes and Digestive and Kidney Diseases (2012).

204. Zhang S, Hu J, Liu G, Wu H, Li M, Shi C, et al. Chronic clomipramine treatment increases hippocampal volume in rats exposed to chronic unpredictable mild stress. *Transl Psychiatry* (2022) 12(1):245. doi: 10.1038/s41398-022-02006-9

205. Park BK, Kim YH, Kim YR, Choi JJ, Yang C, Jang IS, et al. Antineuroinflammatory and neuroprotective effects of gyejibokryeong-hwan in lipopolysaccharide-stimulated bv2 microglia. *Evid Based Complement Alternat Med* (2019) 2019:7585896. doi: 10.1155/2019/7585896

206. Hisaoka-Nakashima K, Kajitani N, Kaneko M, Shigetou T, Kasai M, Matsumoto C, et al. Amitriptyline induces brain-derived neurotrophic factor (Bdnf) Mrna expression through Erk-dependent modulation of multiple bdnf Mrna variants in primary cultured rat cortical astrocytes and microglia. *Brain Res* (2016) 1634:57–67. doi: 10.1016/j.brainres.2015.12.057

207. Källén B, Otterblad Olausson P. Antidepressant drugs during pregnancy and infant congenital heart defect. *Reprod Toxicol (Elmsford NY)* (2006) 21(3):221–2. doi: 10.1016/j.reprotox.2005.11.006

208. Bloem BR, Lammers GJ, Roofthooft DW, De Beaufort AJ, Brouwer OF. Clomipramine withdrawal in newborns. *Arch Dis Childhood Fetal Neonatal Edition* (1999) 81(1):F77. doi: 10.1136/fn.81.1.f77a

209. Chadwick W, Mitchell N, Caroll J, Zhou Y, Park SS, Wang L, et al. Amitriptyline-mediated cognitive enhancement in aged 3xtg alzheimer's disease mice is associated with neurogenesis and neurotrophic activity. *PloS One* (2011) 6(6):e21660. doi: 10.1371/journal.pone.0021660

210. Hofmann SG, Curtiss J, Carpenter JK, Kind S. Effect of treatments for depression on quality of life: A meta-analysis. *Cognit Behav Ther* (2017) 46(4):265–86. doi: 10.1080/16506073.2017.1304445

211. Xu W, Yao X, Zhao F, Zhao H, Cheng Z, Yang W, et al. Changes in hippocampal plasticity in depression and therapeutic approaches influencing these changes. *Neural Plast* (2020) 2020:8861903. doi: 10.1155/2020/8861903

212. Tynan RJ, Weidenhofer J, Hinwood M, Cairns MJ, Day TA, Walker FR. A comparative examination of the anti-inflammatory effects of Ssri and Snri antidepressants on lps stimulated microglia. *Brain Behav Immun* (2012) 26(3):469–79. doi: 10.1016/j.bbi.2011.12.011

213. Turkin A, TuChina O, Klempin F. Microglia function on precursor cells in the adult hippocampus and their responsiveness to serotonin signaling. *Front Cell Dev Biol* (2021) 9:665739. doi: 10.3389/fcell.2021.665739

214. Domingues RR, Wiltbank MC, Hernandez LL. Pregnancy complications and neonatal mortality in a serotonin transporter null mouse model: insight into the use of selective serotonin reuptake inhibitor during pregnancy. *Front Med (Lausanne)* (2022) 9:848581. doi: 10.3389/fmed.2022.848581

215. Lu Y, Xu X, Jiang T, Jin L, Zhao XD, Cheng JH, et al. Sertraline ameliorates inflammation in cums mice and inhibits Tnf-Alpha-induced inflammation in microglia cells. *Int Immunopharmacol* (2019) 67:119–28. doi: 10.1016/j.intimp.2018.12.011

216. Houwing DJ, Esquivel-Franco DC, Ramsteijn AS, Schuttel K, Struik EL, Arling C, et al. Perinatal fluoxetine treatment and dams' Early life stress history have opposite effects on aggressive behavior while having little impact on sexual behavior of male rat offspring. *Psychopharmacol (Berl)* (2020) 237(9):2589–600. doi: 10.1007/s00213-020-05535-7

217. Alenina N, Klempin F. The role of serotonin in adult hippocampal neurogenesis. *Behav Brain Res* (2015) 277:49–57. doi: 10.1016/j.bbr.2014.07.038

218. Lee CH, Park JH, Yoo KY, Choi JH, Hwang IK, Ryu PD, et al. Pre- and post-treatments with escitalopram protect against experimental ischemic neuronal damage via regulation of bdnf expression and oxidative stress. *Exp Neurol* (2011) 229(2):450–9. doi: 10.1016/j.expneurol.2011.03.015

219. Alboni S, Poggini S, Garofalo S, Milior G, El Hajj H, Lecours C, et al. Fluoxetine treatment affects the inflammatory response and microglial function according to the quality of the living environment. *Brain Behav Immun* (2016) 58:261–71. doi: 10.1016/j.bbi.2016.07.155

220. Zisook S, Trivedi MH, Warden D, Lebowitz B, Thase ME, Stewart JW, et al. Clinical correlates of the worsening or emergence of suicidal ideation during Ssri treatment of depression: an examination of citalopram in the star*D study. *J Affect Disord* (2009) 117(1-2):63–73. doi: 10.1016/j.jad.2009.01.002

221. Carvalho AF, Sharma MS, Brunoni AR, Vieta E, Fava GA. The safety, tolerability and risks associated with the use of newer generation antidepressant drugs: A critical review of the literature. *Psychother Psychosomatics* (2016) 85 (5):270–88. doi: 10.1159/000447034

222. Trivedi MH, Rush AJ, Wisniewski SR, Nierenberg AA, Warden D, Ritz L, et al. Evaluation of outcomes with citalopram for depression using measurement-based care in star*D: implications for clinical practice. *Am J Psychiatry* (2006) 163(1):28–40. doi: 10.1176/appi.ajp.163.1.28

223. Connolly KR, Thase ME. If at first you don't succeed: A review of the evidence for antidepressant augmentation, combination and switching strategies. *Drugs* (2011) 71(1):43–64. doi: 10.2165/11587620-000000000-00000

224. Köhler-Forsberg O, NL C, Hjorthøj C, Nordentoft M, Mors O, Benros ME. Efficacy of anti-inflammatory treatment on major depressive disorder or depressive symptoms: meta-analysis of clinical trials. *Acta Psychiatr Scand* (2019) 139(5):404–19. doi: 10.1111/acps.13016

225. Laumet G, Zhou W, Dantzer R, Edralin JD, Huo X, Budac DP, et al. Upregulation of neuronal kynurenine 3-monooxygenase mediates depression-like behavior in a mouse model of neuropathic pain. *Brain Behav Immun* (2017) 66:94–102. doi: 10.1016/j.bbi.2017.07.008

226. Wadhwa M, Prabhakar A, Ray K, Roy K, Kumari P, Jha PK, et al. Inhibiting the microglia activation improves the spatial memory and adult neurogenesis in rat hippocampus during 48 H of sleep deprivation. *J Neuroinflamm* (2017) 14(1):222. doi: 10.1186/s12974-017-0998-z

227. Miao H, Li R, Han C, Lu X, Zhang H. Minocycline promotes posthemorrhagic neurogenesis via M2 microglia polarization via upregulation of the trkb/bdnf pathway in rats. *J Neurophysiol* (2018) 120(3):1307–17. doi: 10.1152/jn.00234.2018

228. Berman RM, Cappiello A, Anand A, Oren DA, Heninger GR, Charney DS, et al. Antidepressant effects of ketamine in depressed patients. *Biol Psychiatry* (2000) 47 (4):351–4. doi: 10.1016/s0006-3223(99)00230-9

229. Murrough JW, Iosifescu DV, Chang LC, Al Jurdi RK, Green CE, Perez AM, et al. Antidepressant efficacy of ketamine in treatment-resistant major depression: A two-site randomized controlled trial. *Am J Psychiatry* (2013) 170(10):1134–42. doi: 10.1176/appi.ajp.2013.13030392

230. Yao W, Cao Q, Luo S, He L, Yang C, Chen J, et al. Microglial erk-nrbp1-Creb-Bdnf signaling in sustained antidepressant actions of (R)-ketamine. *Mol Psychiatry* (2022) 27(3):1618–29. doi: 10.1038/s41380-021-01377-7

231. Miller AH, Maletic V, Raison CL. Inflammation and its discontents: the role of cytokines in the pathophysiology of major depression. *Biol Psychiatry* (2009) 65 (9):732–41. doi: 10.1016/j.biopsych.2008.11.029

232. Moda-Sava RN, Murdock MH, Parekh PK, Fetcho RN, Huang BS, Huynh TN, et al. Sustained rescue of prefrontal circuit dysfunction by antidepressant-induced spine formation. *Science* (2019) 364(6436):eaat8078. doi: 10.1126/science.aat8078

233. Michaëlsson H, Andersson M, Svensson J, Karlsson L, Ehn J, Culley G, et al. The novel antidepressant ketamine enhances dentate gyrus proliferation with no effects on synaptic plasticity or hippocampal function in depressive-like rats. *Acta Physiol (Oxf)* (2019) 225(4):e13211. doi: 10.1111/apha.13211

234. Swainson J, Klassen LJ, Brennan S, Chokka P, Katzman MA, Tanguay RL, et al. Non-parenteral ketamine for depression: A practical discussion on addiction potential and recommendations for judicious prescribing. *CNS Drugs* (2022) 36(3):239–51. doi: 10.1007/s40263-022-00897-2

235. Chen Q, Liu Y, Zhang Y, Jiang X, Zhang Y, Asakawa T. An in vitro verification of the effects of paeoniflorin on lipopolysaccharide-exposed microglia. *Evid Based Complement Alternat Med* (2020) 2020:5801453. doi: 10.1155/2020/5801453

236. Gupta SC, Patchva S, Aggarwal BB. Therapeutic roles of curcumin: lessons learned from clinical trials. *AAPS J* (2013) 15(1):195–218. doi: 10.1208/s12248-012-9432-8

237. He GL, Liu Y, Li M, Chen CH, Gao P, Yu ZP, et al. The amelioration of phagocytic ability in microglial cells by curcumin through the inhibition of emf-induced pro-inflammatory responses. *J Neuroinflamm* (2014) 11:49. doi: 10.1186/1742-2094-11-49

238. Kulkarni SK, Bhutani MK, Bishnoi M. Antidepressant activity of curcumin: involvement of serotonin and dopamine system. *Psychopharmacol (Berl)* (2008) 201 (3):435–42. doi: 10.1007/s00213-008-1300-y

239. Pluta R, Bogucka-Kocka A, Ułamek-Kozioł M, Furmaga-Jabłońska W, Januszewski S, Brzozowska J, et al. Neurogenesis and neuroprotection in postischemic brain neurodegeneration with alzheimer phenotype: is there a role for curcumin? *Folia Neuropathol* (2015) 53(2):89–99. doi: 10.5114/fn.2015.52405

240. Xu Y, Ku B, Cui L, Li X, Barish PA, Foster TC, et al. Curcumin reverses impaired hippocampal neurogenesis and increases serotonin receptor 1a mrna and brain-derived neurotrophic factor expression in chronically stressed rats. *Brain Res* (2007) 1162:9–18. doi: 10.1016/j.brainres.2007.05.071

241. Kulkarni S, Dhir A, Akula KK. Potentials of curcumin as an antidepressant. *ScientificWorldJournal* (2009) 9:1233–41. doi: 10.1100/tsw.2009.137

242. Wang XL, Feng ST, Wang YT, Chen NH, Wang ZZ, Zhang Y. Paeoniflorin: A neuroprotective monoterpenoid glycoside with promising anti-depressive properties. *Phytomedicine* (2021) 90:153669. doi: 10.1016/j.phymed.2021.153669

243. Wang XL, Wang YT, Guo ZY, Zhang NN, Wang YY, Hu D, et al. Efficacy of paeoniflorin on models of depression: A systematic review and meta-analysis of rodent studies. *J Ethnopharmacol* (2022) 290:115067. doi: 10.1016/j.jep.2022.115067

244. Moore A, Beidler J, Hong MY. Resveratrol and depression in animal models: A systematic review of the biological mechanisms. *Molecules* (2018) 23(9):2197. doi: 10.3390/molecules23092197

245. Nabavi SM, Daglia M, Braidy N, Nabavi SF. Natural products, micronutrients, and nutraceuticals for the treatment of depression: A short review. *Nutr Neurosci* (2017) 20(3):180–94. doi: 10.1080/1028415x.2015.1103461

246. Schlotterose L, Cossais F, Lucius R, Hattermann K. Breaking the circulus vitiosus of neuroinflammation: resveratrol attenuates the human glial cell response to cytokines. *Biomed Pharmacother = Biomed Pharmacother* (2023) 163:114814. doi: 10.1016/j.biopha.2023.114814

247. Park HR, Kong KH, Yu BP, Mattson MP, Lee J. Resveratrol inhibits the proliferation of neural progenitor cells and hippocampal neurogenesis. *J Biol Chem* (2012) 287(51):42588–600. doi: 10.1074/jbc.M112.406413

248. Fan X, Zhao Z, Wang D, Xiao J. Glycogen synthase kinase-3 as a key regulator of cognitive function. *Acta Biochim Biophys Sin (Shanghai)* (2020) 52(3):219–30. doi: 10.1093/abbs/gmz156

249. Inkster B, Zai G, Lewis G, Miskowiak KW. Gsk3β: A plausible mechanism of cognitive and hippocampal changes induced by erythropoietin treatment in mood disorders? *Transl Psychiatry* (2018) 8(1):216. doi: 10.1038/s41398-018-0270-z

250. Grimes CA, Jope RS. The multifaceted roles of glycogen synthase kinase 3beta in cellular signaling. *Prog Neurobiol* (2001) 65(4):391–426. doi: 10.1016/s0301-0082 (01)00011-9

251. Morales-Garcia JA, Luna-Medina R, Alonso-Gil S, Sanz-Sancristobal M, Palomo V, Gil C, et al. Glycogen synthase kinase 3 inhibition promotes adult hippocampal neurogenesis in vitro and in vivo. *ACS Chem Neurosci* (2012) 3 (11):963–71. doi: 10.1021/cn300110c

252. Martin M, Rehani K, Jope RS, Michalek SM. Toll-like receptor-mediated cytokine production is differentially regulated by glycogen synthase kinase 3. *Nat Immunol* (2005) 6(8):777–84. doi: 10.1038/ni1221

253. Huang WC, Lin YS, Wang CY, Tsai CC, Tseng HC, Chen CL, et al. Glycogen synthase kinase-3 negatively regulates anti-inflammatory interleukin-10 for lipopolysaccharide-induced Inos/No biosynthesis and rantes production in microglial cells. *Immunology* (2009) 128(1 Suppl):e275–86. doi: 10.1111/j.1365-2567.2008.02959.x

254. Asefy Z, Khusro A, Mammadova S, Hoseinnejhad S, Eftekhari A, Alghamdi S, et al. Melatonin hormone as a therapeutic weapon against neurodegenerative diseases. *Cell Mol Biol (Noisy-le-grand)* (2021) 67(3):99–106. doi: 10.14715/cmb/2021.67.3.13

255. Won E, Na KS, Kim YK. Associations between melatonin, neuroinflammation, and brain alterations in depression. *Int J Mol Sci* (2021) 23(1):305. doi: 10.3390/ijms23010305

256. Wang YQ, Jiang YJ, Zou MS, Liu J, Zhao HQ, Wang YH. Antidepressant actions of melatonin and melatonin receptor agonist: focus on pathophysiology and treatment. *Behav Brain Res* (2022) 420:113724. doi: 10.1016/j.bbr.2021.113724

257. Luchtman DW, Song C. Cognitive enhancement by omega-3 fatty acids from child-hood to old age: findings from animal and clinical studies. *Neuropharmacology* (2013) 64:550–65. doi: 10.1016/j.neuropharm.2012.07.019

258. Su KP, Yang HT, Chang JP, Shih YH, Guu TW, Kumaran SS, et al. Eicosapentaenoic and docosahexaenoic acids have different effects on peripheral phospholipase A2 gene expressions in acute depressed patients. *Prog Neuropsychopharmacol Biol Psychiatry* (2018) 80(Pt C):227–33. doi: 10.1016/j.pnpbp.2017.06.020

259. Borsini A, Stangl D, Jeffries AR, Pariante CM, Thuret S. The role of omega-3 fatty acids in preventing glucocorticoid-induced reduction in human hippocampal neurogenesis and increase in apoptosis. *Transl Psychiatry* (2020) 10(1):219. doi: 10.1038/s41398-020-00908-0

260. Layé S, Nadjar A, Joffre C, Bazinet RP. Anti-inflammatory effects of omega-3 fatty acids in the brain: physiological mechanisms and relevance to pharmacology. *Pharmacol Rev* (2018) 70(1):12–38. doi: 10.1124/pr.117.014092

261. Carnevali L, Montano N, Tobaldini E, Thayer JF, Sgoifo A. The contagion of social defeat stress: insights from rodent studies. *Neurosci Biobehav Rev* (2020) 111:12–8. doi: 10.1016/j.neubiorev.2020.01.011

262. Anacker C, Hen R. Adult hippocampal neurogenesis and cognitive flexibility - linking memory and mood. *Nat Rev Neurosci* (2017) 18(6):335–46. doi: 10.1038/nrn.2017.45

263. Araki T, Ikegaya Y, Koyama R. The effects of microglia- and astrocyte-derived factors on neurogenesis in health and disease. *Eur J Neurosci* (2021) 54(5):5880–901. doi: 10.1111/ejn.14969

264. Cope EC, Gould E. Adult neurogenesis, glia, and the extracellular matrix. *Cell Stem Cell* (2019) 24(5):690–705. doi: 10.1016/j.stem.2019.03.023

265. Tomasetti C, Montemitro C, Fiengo ALC, Santone C, Orsolini L, Valchera A, et al. Novel pathways in the treatment of major depression: focus on the glutamatergic system. *Curr Pharm Design* (2019) 25(4):381–7. doi: 10.2174/1381612825666190312102444

266. Drevets WC, Wittenberg GM, Bullmore ET, Manji HK. Immune targets for therapeutic development in depression: towards precision medicine. *Nat Rev Drug Discovery* (2022) 21(3):224–44. doi: 10.1038/s41573-021-00368-1

267. Leuchter AF, Husain MM, Cook IA, Trivedi MH, Wisniewski SR, Gilmer WS, et al. Painful physical symptoms and treatment outcome in major depressive disorder: A star*D (Sequenced treatment alternatives to relieve depression) report. *psychol Med* (2010) 40(2):239–51. doi: 10.1017/s0033291709006035

268. Ananthakrishnan AN, Khalili H, Pan A, Higuchi LM, de Silva P, Richter JM, et al. Association between depressive symptoms and incidence of crohn's disease and ulcerative colitis: results from the nurses' Health study. *Clin Gastroenterol Hepatol* (2013) 11(1):57–62. doi: 10.1016/j.cgh.2012.08.032

269. Matcham F, Rayner L, Steer S, Hotopf M. The prevalence of depression in rheumatoid arthritis: A systematic review and meta-analysis. *Rheumatol (Oxford England)* (2013) 52(12):2136–48. doi: 10.1093/rheumatology/ket169

270. Bachen EA, Chesney MA, Criswell LA. Prevalence of mood and anxiety disorders in women with systemic lupus erythematosus. *Arthritis Rheum* (2009) 61 (6):822–9. doi: 10.1002/art.24519

271. Arteaga-Henríquez G, Simon MS, Burger B, Weidinger E, Wijkhuijs A, Arolt V, et al. Low-grade inflammation as a predictor of antidepressant and anti-inflammatory therapy response in Mdd patients: A systematic review of the literature in combination with an analysis of experimental data collected in the Eu-Moodinflame consortium. *Front Psychiatry* (2019) 10:458. doi: 10.3389/fpsyt.2019.00458

10.3389/fimmu.2023.1193053

Glossary

HPA axis	Hypothalamic-pituitary-adrenal axis
CSF	Cerebrospinal fluid
CNS	Central nervous system
NLRP3	Nod-like receptor protein 3
NLR	Nucleotide-binding oligomerization
IL-1β	Interleukin-1β
IL-6	Interleukin-6
TGF-β	Transforming growth factor-β
IL-10	Interleukin-10
IL-4	Interleukin-4
IL-13	Interleukin-13
IFN-α	Interferon-α
IFN-γ	Interferon-γ
CD163	Cluster of differentiation 163
CD206	Cluster of differentiation 206
M1 microglia	M1-phenotype microglia
INOS	Inducible nitric oxide synthase
CD86	Cluster of differentiation 86
MS	maternal separation
CUMS	Chronic unpredictable mild stress
CMS	Chronic mild stress
CSDS	chronic social defeat stress
CUS	Chronic mild stress
CRS	Chronic restraint stress
LPS	Lipopolysaccharide
TLR4	Toll-like receptor 4
AD	Alzheimer's disease
PFC	Prefrontal cortex
DG	Dentate gyrus
NSC	Neural stem cell
SVZ	Subventricular zone
SGZ	Subgranular zone
5-HT	5-hydroxytryptamine
NF-κB	Nuclear transcription factor-kappa B
MyD88	Myeloid differentiation factor 88
PRRs	Pattern recognition receptors
NLRs	Nucleotide-binding oligomerization domains leucine-rich repeat-containing protein receptors
R-SDS	Repeated social defeat stress

(Continued)

Continued

TLR2/4	Toll-like receptor 2 and 4
TNF-α	Tumor necrosis factor α
BDNF	Brain derived neurotrophic Factor
ERF	Extracellular signal-regulated kinase
CREB	cAMP-response element binding protein
MIP2	Macrophage inflammatory protein-2
CX3CR1	C-X3-C motif chemokine receptor 1
BrdU	5-ethynyl-2-deoxyuridine
TRY	Tryptophan
SSRIs	Selective serotonin reuptake inhibitors
DCX	Doublecortin
IDO	Indoleamine 2,3-dioxygenase
TDO	Tryptophan 2,3-dioxygenase
JAK	Janus kinase
STAT	Signal transducer and activator of transcription
KYN	Kynurenine; TrkB: Tyrosine kinase receptor B
KLF4	Kruppel like factor 4
CDKL5	Cyclin dependent kinase like 5
Brdu	5-Bromo-2-deoxyuridine
CAMP	Cyclic adenosine monophosphate
Tnfr1	Tumor necrosis factor receptor 1
GR	Glucocorticoid receptor
PD	Parkinson disease
QUIN	Quinolinic acid
miRNA	MicroRNA
ncRNA	non-coding RNA
KLF4	Kruppel like factor 4
HNK	Hydroxynorketamine
ALA	α-linolenic acid
EPA	Eicosapentaenoic acid
DHA	Docosahexaenoic acid
Aβ25–35	Amyloid b-Protein Fragment 25-35
GSK-3	Glycogen synthase kinase 3
NO	Nitric oxide
HD	Huntington's disease
GCS	Glucocorticoid
DST	DEX inhibition test
ACTH	Adrenocorticotropic hormone
SGK	Serum and glucocorticoid induced kinase
NSCs	Neural stem cells

(Continued)

Continued

Arg-1	Arginase-1
GF	Germ-free
IGF-1	Insulin-like growth factor-1
CCL17	Chemoattractant cytokine ligand 17
CCL18	Chemoattractant cytokine ligand 18
PSD95	Postsynaptic density protein 95
ERK	Extracellular signal-regulated kinase
TCAs	Tricyclic antidepressants
SERT	serotonin transporter

Frontiers in Immunology

Explores novel approaches and diagnoses to treat immune disorders.

The official journal of the International Union of Immunological Societies (IUIS) and the most cited in its field, leading the way for research across basic, translational and clinical immunology.

Discover the latest Research Topics

See more →

Frontiers

Avenue du Tribunal-Fédéral 34
1005 Lausanne, Switzerland
frontiersin.org

Contact us

+41 (0)21 510 17 00
frontiersin.org/about/contact